APPENDIX B.1.1

Downhole Data

Appendix B.1.1
Downhole Data

The following data reports were prepared for the SR 710 Tunnel Technical Study Final Geotechnical Summary Report (CH2M HILL, 2010). However, only data relevant to the SR 710 North Study are provided herein. To view the reports in their entirety, refer to the Technical Study (CH2M HILL, 2010).

GEOVision
geophysical services

SR-710 TUNNEL TECHNICAL STUDY
BORING GEOPHYSICS

BORINGS Z1-B3, Z1-B5, Z1-B6, Z1-B7, Z2-B1, Z2-B4, Z3-B1, Z3-B3, Z3-B4, Z3-B6, Z3-B8, Z3-B12 AND Z4-B4

Report 9014-01 rev 0

October 5, 2009

SR-710 TUNNEL TECHNICAL STUDY
BORING GEOPHYSICS

BORINGS Z1-B3, Z1-B5, Z1-B6, Z1-B7, Z2-B1, Z2-B4, Z3-B1, Z3-B3, Z3-B4, Z3-B6, Z3-B8, Z3-B12 AND Z4-B4

Report 9014-01 rev 0

October 5, 2009

Prepared for:

Cascade Drilling, Inc.
555 South Harbor Boulevard
La Habra, California 90631
562-929-8176

Prepared by

GEOVision Geophysical Services
1124 Olympic Drive
Corona, California 92881
(951) 549-1234

TABLE OF CONTENTS

TABLE OF CONTENTS **3**

TABLE OF FIGURES **4**

TABLE OF TABLES **5**

APPENDICES **6**

INTRODUCTION **7**

SCOPE OF WORK **7**

INSTRUMENTATION **9**

SUSPENSION VELOCITY INSTRUMENTATION 9
CALIPER / NATURAL GAMMA INSTRUMENTATION 12
ACOUSTIC TELEVIEWER / BORING DEVIATION INSTRUMENTATION 14

MEASUREMENT PROCEDURES **16**

SUSPENSION VELOCITY MEASUREMENT PROCEDURES 16
CALIPER / NATURAL GAMMA PROCEDURES 17
ACOUSTIC TELEVIEWER / BORING DEVIATION MEASUREMENT PROCEDURES 19

DATA ANALYSIS **20**

SUSPENSION VELOCITY ANALYSIS 20
CALIPER / NATURAL GAMMA ANALYSIS 22
ACOUSTIC TELEVIEWER / BORING DEVIATION ANALYSIS 23

RESULTS **24**

SUSPENSION VELOCITY RESULTS 24
CALIPER / NATURAL GAMMA RESULTS 25
ACOUSTIC TELEVIEWER / BORING DEVIATION RESULTS 25

SUMMARY **26**

DISCUSSION OF SUSPENSION VELOCITY RESULTS 26
DISCUSSION OF CALIPER / NATURAL GAMMA RESULTS 26
DISCUSSION OF ACOUSTIC TELEVIEWER / BORING DEVIATION RESULTS 27
QUALITY ASSURANCE 28
SUSPENSION VELOCITY DATA RELIABILITY 28

CERTIFICATION **29**

Table of Figures

Figure 1: Concept illustration of Suspension P S logging system 34
Figure 2: Example of filtered (1400 Hz lowpass) suspension record 35
Figure 3. Example of unfiltered suspension record 36
Figure 4: Boring Z1-B3, Suspension R1-R2 P- and S_H-wave velocities 37
Figure 5. Boring Z1-B3, Caliper and Natural Gamma logs 39
Figure 6. Boring Z1-B3, Stereonet Plot 40
Figure 7. Boring Z1-B3, Deviation Projection 43
Figure 8: Boring Z1-B5, Suspension R1-R2 P- and S_H-wave velocities 44
Figure 9. Boring Z1-B5, Caliper and Natural Gamma logs 47
Figure 10. Boring Z1-B5, Stereonet Plot 48
Figure 11. Boring Z1-B5, Deviation Projection 52
Figure 12: Boring Z1-B6, Suspension R1-R2 P- and S_H-wave velocities 53
Figure 13. Boring Z1-B6 Caliper and Natural Gamma logs 56
Figure 14. Boring Z1-B6, Stereonet Plot 57
Figure 15. Boring Z1-B6, Deviation Projection 63
Figure 16: Boring Z1-B7, Suspension R1-R2 P- and S_H-wave velocities 64
Figure 17. Boring Z1-B7, Caliper and Natural Gamma logs 67
Figure 18. Boring Z1-B7, Stereonet Plot 68
Figure 19. Boring Z1-B7, Deviation Projection 70
Figure 20: Boring Z2-B1, Suspension R1-R2 P- and S_H-wave velocities 71
Figure 21. Boring Z2-B1, Caliper and Natural Gamma logs 73
Figure 22. Boring Z2-B1, Stereonet Plot 74
Figure 23. Boring Z2-B1, Deviation Projection 76
Figure 24: Boring Z2-B4, Suspension R1-R2 P- and S_H-wave velocities 77
Figure 25. Boring Z2-B4, Caliper and Natural Gamma logs 80
Figure 26. Boring Z2-B4, Stereonet Plot 81
Figure 27. Boring Z2-B4, Deviation Projection 85
Figure 28: Boring Z3-B1, Suspension R1-R2 P- and S_H-wave velocities 86
Figure 29. Boring Z3-B1, Caliper and Natural Gamma logs 89
Figure 30. Boring Z3-B1, Stereonet Plot 90
Figure 31. Boring Z3-B1, Deviation Projection 92
Figure 32: Boring Z3-B3, Suspension R1-R2 P- and S_H-wave velocities 93
Figure 33. Boring Z3-B3, Caliper and Natural Gamma logs 95
Figure 34. Boring Z3-B3, Stereonet Plot 96
Figure 35. Boring Z3-B3, Deviation Projection 98
Figure 36: Boring Z3-B4, Suspension R1-R2 P- and S_H-wave velocities 99
Figure 37. Boring Z3-B4, Caliper and Natural Gamma logs 102
Figure 38. Boring Z3-B4, Stereonet Plot 103
Figure 39. Boring Z3-B4, Deviation Projection 105
Figure 40: Boring Z3-B6, Suspension R1-R2 P- and S_H-wave velocities 106
Figure 41. Boring Z3-B6, Caliper and Natural Gamma logs 109
Figure 42. Boring Z3-B6, Stereonet Plot 110
Figure 43. Boring Z3-B6, Deviation Projection 112
Figure 44. Boring Z3-B8, Caliper and Natural Gamma logs 113
Figure 45: Boring Z3-B12, Suspension R1-R2 P- and S_H-wave velocities 114
Figure 46. Boring Z3-B12, Caliper and Natural Gamma logs 116
Figure 47. Boring Z3-B12, Stereonet Plot 117
Figure 48. Boring Z3-B12, Deviation Projection 119
Figure 49: Boring Z4-B4, Suspension R1-R2 P- and S_H-wave velocities 120
Figure 50. Boring Z4-B4, Caliper and Natural Gamma logs 123
Figure 51. Boring Z4-B4, Stereonet Plot 124
Figure 52. Boring Z4-B4, Deviation Projection 126

Table of Tables

Table 1. Boring locations and logging dates....30
Table 2. Logging dates and depth ranges....31
Table 3. Boring Deviation Data Summary....33
Table 4. Boring Z1-B3, Suspension R1-R2 depths and P- and S_H-wave velocities....38
Table 5. Boring Z1-B3, Structure depth, dip azimuth, dip and description....41
Table 6. Boring Z1-B5, Suspension R1-R2 depths and P- and S_H-wave velocities....45
Table 7. Boring Z1-B5, Structure depth, dip azimuth, dip and description....49
Table 8. Boring Z1-B6, Suspension R1-R2 depths and P- and S_H-wave velocities....54
Table 9. Boring Z1-B6, Structure depth, dip azimuth, dip and description....58
Table 10. Boring Z1-B7, Suspension R1-R2 depths and P- and S_H-wave velocities....65
Table 11. Boring Z1-B7, Structure depth, dip azimuth, dip and description....69
Table 12. Boring Z2-B1, Suspension R1-R2 depths and P- and S_H-wave velocities....72
Table 13. Boring Z2-B1, Structure depth, dip azimuth, dip and description....75
Table 14. Boring Z2-B4, Suspension R1-R2 depths and P- and S_H-wave velocities....78
Table 15. Boring Z2-B4, Structure depth, dip azimuth, dip and description....82
Table 16. Boring Z3-B1, Suspension R1-R2 depths and P- and S_H-wave velocities....87
Table 17. Boring Z3-B1, Structure depth, dip azimuth, dip and description....91
Table 18. Boring Z3-B3, Suspension R1-R2 depths and P- and S_H-wave velocities....94
Table 19. Boring Z3-B3, Structure depth, dip azimuth, dip and description....97
Table 20. Boring Z3-B4, Suspension R1-R2 depths and P- and S_H-wave velocities....100
Table 21. Boring Z3-B4, Structure depth, dip azimuth, dip and description....104
Table 22. Boring Z3-B6, Suspension R1-R2 depths and P- and S_H-wave velocities....107
Table 23. Boring Z3-B6, Structure depth, dip azimuth, dip and description....111
Table 24. Boring Z3-B12, Suspension R1-R2 depths and P- and S_H-wave velocities....115
Table 25. Boring Z3-B12, Structure depth, dip azimuth, dip and description....118
Table 26. Boring Z4-B4, Suspension R1-R2 depths and P- and S_H-wave velocities....121
Table 27. Boring Z4-B4, Structure depth, dip azimuth, dip and description....125

APPENDICES

APPENDIX A SUSPENSION VELOCITY MEASUREMENT QUALITY ASSURANCE SUSPENSION SOURCE TO RECEIVER ANALYSIS RESULTS……129

APPENDIX B CALIPER AND NATURAL GAMMA LOGS……..162

APPENDIX C ACOUSTIC TELEVIEWER DIPS LOGS……..214

APPENDIX D GEOPHYSICAL LOGGING SYSTEMS - NIST TRACEABLE CALIBRATION PROCEDURES AND CALIBRATION RECORDS……634

APPENDIX E BORING GEOPHYSICAL LOGGING FIELD MEASUREMENT PROCEDURES……..……648

INTRODUCTION

Boring geophysical measurements were collected in thirteen uncased borings located within four zones of the SR-710 tunnel technical study. Geophysical data acquisition was performed between January 14 and March 31, 2009 by Robert Steller, Charles Carter and Lauren Annis of **GEO***Vision*. Data analysis was performed by Robert Steller and reviewed by John Diehl of **GEO***Vision*. Report preparation was performed by Robert Steller and reviewed by John Diehl of **GEO***Vision*. The work was performed under subcontract with Cascade Drilling for CH2M Hill, Inc. (CH2M) with Ravee Raveendra serving as the point of contact for CH2M.

This report describes the field measurements, data analysis, and results of this work.

SCOPE OF WORK

This report presents the results of boring geophysical measurements collected between January 14 and March 31, 2009, in thirteen borings, as detailed in Table 1. The purpose of these studies was to supplement stratigraphic information obtained during CH2M's soil and rock sampling program and to acquire shear wave velocities and compressional wave velocities as a function of depth, as a component of the SR-710 tunnel study.

The OYO/Robertson Suspension PS Logging System (Suspension System) was used to obtain in-situ horizontal shear (S_H) and compressional (P) wave velocity measurements in all borings, except Z3-B8, at 1.6-foot intervals. Measurements followed **GEO***Vision* Procedure for P-S Suspension Seismic Velocity Logging, revision 1.3. The acquired data was analyzed and a profile of velocity versus depth was produced for both compressional and horizontally polarized shear waves.

A detailed reference for the suspension PS velocity measurement techniques used in this study is:

> Guidelines for Determining Design Basis Ground Motions, Report TR-102293, Electric Power Research Institute, Palo Alto, California, November 1993, Sections 7 and 8.

The Robertson 3ACS probe was used to collect 3-arm mechanical caliper and natural gamma data at 0.05-foot intervals in all borings to aid in identification of stratagraphic transitions. Measurement procedures followed these ASTM standards:

- ASTM D5753, "Planning and Conducting Borehole Geophysical Surveys
- ASTM D6274, "Conducting Borehole Geophysical Logging – Gamma ASTM D6274-98 (Re-approved 2004), Conducting Borehole Geophysical Logging - Gamma"
- ASTM D6167-97 (Re-approved 2004) "Conducting Borehole Geophysical Logging – Mechanical Caliper"

The acquired data was combined and a profile of these parameters versus depth was produced.

The Robertson High Resolution Acoustic Televiewer (HiRAT) was used to collect deviation data and acoustic televiewer images of the rock at 0.008-foot intervals in all borings except Z3-B8. Measurements followed the **GEO***Vision* HiRAT Field Procedure, revision 1.0. In addition, the boring images were analyzed and planar features such as bedding planes and fractures were identified for dip, azimuth and stereonet processing to identify dominant fracture and bedding planes.

INSTRUMENTATION

Suspension Velocity Instrumentation

Suspension velocity measurements were performed using the suspension PS logging system, manufactured by OYO Corporation, and their subsidiary, Robertson Geologging. This system directly determines the average velocity of a 3.28-foot high segment of the soil column surrounding the boring of interest by measuring the elapsed time between arrivals of a wave propagating upward through the soil column. The receivers that detect the wave, and the source that generates the wave, are moved as a unit in the boring producing relatively constant amplitude signals at all depths.

The suspension system probe consists of a combined reversible polarity solenoid horizontal shear-wave source (S_H) and compressional-wave source (P), joined to two biaxial receivers by a flexible isolation cylinder, as shown in Figure 1. The separation of the two receivers is 3.28 feet, allowing average wave velocity in the region between the receivers to be determined by inversion of the wave travel time between the two receivers. The total length of the probe as used in these surveys is 19 feet, with the center point of the receiver pair 12.1 feet above the bottom end of the probe.

The probe receives control signals from, and sends the digitized receiver signals to, instrumentation on the surface via an armored 4 conductor cable. The cable is wound onto the drum of a winch and is used to support the probe. Cable travel is measured to provide probe depth data, using a 3.28-foot circumference sheave fitted with a digital rotary encoder.

The entire probe is suspended in the boring by the cable, therefore, source motion is not coupled directly to the boring walls; rather, the source motion creates a horizontally propagating impulsive pressure wave in the fluid filling the boring and surrounding the source. This pressure wave is converted to P and S_H-waves in the surrounding soil and rock as it passes through the casing and grout annulus and impinges upon the wall of the boring. These waves propagate

through the soil and rock surrounding the boring, in turn causing a pressure wave to be generated in the fluid surrounding the receivers as the soil waves pass their location. Separation of the P and S_H-waves at the receivers is performed using the following steps:

1. Orientation of the horizontal receivers is maintained parallel to the axis of the source, maximizing the amplitude of the recorded S_H -wave signals.
2. At each depth, S_H-wave signals are recorded with the source actuated in opposite directions, producing S_H-wave signals of opposite polarity, providing a characteristic S_H-wave signature distinct from the P-wave signal.
3. The 7.0-foot separation of source and receiver 1 permits the P-wave signal to pass and damp significantly before the slower S_H-wave signal arrives at the receiver. In faster soils or rock, the isolation cylinder is extended to allow greater separation of the P- and S_H-wave signals.
4. In saturated soils, the received P-wave signal is typically of much higher frequency than the received S_H-wave signal, permitting additional separation of the two signals by low pass filtering.
5. Direct arrival of the original pressure pulse in the fluid is not detected at the receivers because the wavelength of the pressure pulse in fluid is significantly greater than the dimension of the fluid annulus surrounding the probe (foot versus inch scale), preventing significant energy transmission through the fluid medium.

In operation, a distinct, repeatable pattern of impulses is generated at each depth as follows:

1. The source is fired in one direction producing dominantly horizontal shear with some vertical compression, and the signals from the horizontal receivers situated parallel to the axis of motion of the source are recorded.
2. The source is fired again in the opposite direction and the horizontal receiver signals are recorded.
3. The source is fired again and the vertical receiver signals are recorded. The repeated source pattern facilitates the picking of the P and S_H-wave arrivals; reversal of the source changes the polarity of the S_H-wave pattern but not the P-wave pattern.

The data from each receiver during each source activation is recorded as a different channel on the recording system. The Suspension PS system has six channels (two simultaneous recording channels), each with a 1024 sample record. The recorded data are displayed as six channels with a common time scale. Data are stored on disk for further processing. Up to 8 sampling sequences can be summed to improve the signal to noise ratio of the signals.

Review of the displayed data on the recorder or computer screen allows the operator to set the gains, filters, delay time, pulse length (energy), sample rate, and summing number to optimize the quality of the data before recording. Verification of the calibration of the Suspension PS digital recorder is performed every twelve months using a NIST traceable frequency source and counter, as outlined in Appendix D.

Caliper / Natural Gamma Instrumentation

Caliper and natural gamma data were collected using a Model 3ACS 3-arm caliper probe, serial number 5368, manufactured by Robertson Geologging, Ltd. With the short arm configuration used in these surveys, the probe permitted measurement of boring diameters between 1.6 and 16 inches. With this tool, caliper measurements were collected concurrent with measurement of natural gamma emission from the boring walls. The probe is 6.82 feet long, and 1.5 inches in diameter.

This probe is useful in the following studies:

- Measurement of boring diameter and volume
- Location of hard and soft formations
- Location of fissures, caving, pinching and casing damage
- Bed boundary identification
- Strata correlation between borings

The probe receives control signals from, and sends the digitized measurement values to, a Robertson Micrologger II on the surface via an armored 4 conductor cable. The cable is wound onto the drum of a winch and is used to support the probe. Cable travel is measured to provide probe depth data, using a 3.28-foot circumference sheave fitted with a digital rotary encoder. The probe and depth data are transmitted by USB link from the Micrologger unit to a laptop computer where it is displayed and stored on hard disk.

The caliper consists of three arms, each with a toothed quadrant at their base, pivoted in the lower probe body. A toothed rack engages with each quadrant, thus constraining the arms to move together. Linear movement of the rack is converted to opening and closing of the arms. Springs hold the arms open in the operating position. A motor drive is provided to retract the arms, allowing the probe to be lowered into the boring. The rack is coupled to a potentiometer which converts movement into a voltage sensed by the probe's microprocessor.

Natural gamma measurements rely upon small quantities of radioactive material contained in all soil and rocks to emit gamma radiation as they decay. Trace amounts of Uranium and Thorium are present in a few minerals, where potassium-bearing minerals such as feldspar, mica and clays will include traces of a radioactive isotope of Potassium. These emit gamma radiation as they decay with an extremely long half-life. This radiation is detected by scintillation - the production of a tiny flash of light when gamma rays strike a crystal of sodium iodide. The light is converted into an electrical pulse by a photomultiplier tube. Pulses above a threshold value of 60 thousand electron Volts (KeV) are counted by the probe's microprocessor. The measurement is useful because the radioactive elements are concentrated in certain soil and rock types e.g. clay or shale, and depleted in others e.g. sandstone or coal.

Acoustic Televiewer / Boring Deviation Instrumentation

An acoustic image and boring deviation data were collected using a High Resolution Acoustic Televiewer probe (HiRAT), serial number 5174, manufactured by Robertson Geologging, Ltd. The probe is 5.2 feet long, 1.6 inches in diameter, and may be fitted with upper and lower four-band centralizers.

In this application, this probe is useful in the following studies:

- Measurement of boring inclination and deviation from vertical
- Determination of need to correct soil and geophysical log depths to true vertical depths
- Acoustic imaging of the boring wall to identify fractures, dikes, and weathered zones, and determine dip and azimuth of these features

The probe receives control signals from, and sends the digitized measurement values to, a Robertson Micrologger II on the surface via an armored 4 conductor cable. The cable is wound onto the drum of a winch and is used to support the probe. Cable travel is measured to provide probe depth data, using a 3.28-foot circumference sheave fitted with a digital rotary encoder. The probe and depth data are transmitted by USB link from the Micrologger unit to a laptop computer where it is displayed and stored on hard disk.

This system produces images of the boring wall based upon the amplitude and travel time of an ultrasonic beam reflected from the formation wall. The ultrasonic energy is generated by a piezoelectric transducer at a frequency of 1.4 MHz. A periodic acoustic energy wave is emitted by the transducer and travels through the acoustic head and boring fluid until it reaches the interface between the boring fluid and the boring wall. Here a portion of the energy is reflected back to the transducer, the remainder continuing on into the formation. By careful time sequencing, the piezoelectric transducer acts as both the transmitter of the ultrasonic pulse and receiver of the reflected wave. The travel time of the energy wave is the period between transmission of the source energy pulse and the return of the reflected wave measured at the point of maximum wave amplitude. The magnitude of the wave energy is measured in dB, a

unit-less ratio of the detected echo wave amplitude divided by the amplitude of the transmitted wave. The strength of the reflected signal depends primarily upon the impedance contrast of the boring fluid and the boring wall formation. In a number of these borings, there was significant clay "wall cake" which attenuated the acoustic signal, and created a low impedance contrast at the boring wall.

The acoustic wave propagates along the axis of the probe and then is reflected perpendicular to this axis by a reflector that focuses the beam to a 0.1-inch diameter spot about 2 inches from the central axis of the probe. This reflector is mounted on the shaft of a stepper motor enabling the position of the measurement to be rotated through 360°. Sampling rates of 90, 180 and 360 measured points per revolution are available. During these surveys, data were collected at 360 samples per revolution, providing an equivalent horizontal pixel size of approximately 0.05 inches on the boring wall. It should be noted that during logging the probe is moving in the boring, so that the measured points describe a very fine pitch spiral.

The probe contains a fluxgate magnetometer to monitor magnetic north, and all raw televiewer data are referenced to magnetic north. The processed data is referenced to true north, using a declination of 12.9 degrees east for these sites and dates, obtained from the NOAA declination web site (http://www.ngdc.noaa.gov/geomagmodels/Declination.jsp). Also, a three-axis accelerometer is enclosed in the probe, and boring deviation data are recorded during the logging runs, to permit correction of structure dip angle from apparent dip, (referenced to boring axis), to true dip (referenced to a vertical axis) in non-vertical borings.

The data are presented on a computer screen for operator review during the logging run, and stored on hard disk for later processing.

MEASUREMENT PROCEDURES

Suspension Velocity Measurement Procedures

Twelve borings (excluding Z3-B8) were logged while filled with bentonite or polymer based drilling mud. Measurements followed the **GEO***Vision* Procedure for P-S Suspension Seismic Velocity Logging, revision 1.31, as presented in Appendix E. These procedures were supplied and approved in advance of the work. Prior to each logging run, the probe was positioned with the top of the probe at the top of the surface casing, and the electronic depth counter was set to 8.2 feet, the distance between the mid-point of the receiver and the top of the probe, minus the height of the casing stick-up, as verified with a tape measure, and recorded on the field logs. The probe was lowered to the bottom of the boring, stopping at 1.6-foot intervals to collect data, as summarized in Table 2.

At each measurement depth the measurement sequence of two opposite horizontal records and one vertical record was performed, and the gains were adjusted as required. The data from each depth were viewed on the computer display, checked, and recorded on disk before moving to the next depth.

Upon completion of the measurements, the probe zero depth indication at the depth reference point was verified prior to removal from the boring, and after survey depth error (ASDE) was calculated, as listed in Table 3.

Caliper / Natural Gamma Procedures

The borings were filled with bentonite or polymer based drilling mud and logged from the bottom of the boring up until the caliper entered the bottom of the surface casing or reached the surface, as listed in Table 2. Measurements followed ASTM D6167-97 (Re-approved 2004) Conducting Borehole Geophysical Logging – Mechanical Caliper.

Prior to and following each logging run, the caliper tool was verified, using the manufacturer's supplied three point calibration jig. The three point jig is a circular plate with a series of holes in the top surface into which the tips of the caliper arms fit. This has circles of diameters from 2 to 12 inches. The calibration jig is placed over a bucket with the probe standing upright with its nose section passing through the jig's central hole. The caliper probe arms are opened under program control, and a log is recorded as the tips of the arms are placed in the holes on the calibration jig. The measured dimensions, as displayed on the recording computer screen was recorded on the field log sheet, as well as in the digital files, and compared with the calibration jig dimensions. These files are presented in LAS 2.0 format in the boring specific sub-directories of the data directory on the data disk (CD-R) labeled Report 9014-02 that accompanies this report. If the verification records did not fall within +/- 0.05 inches of the calibration jig values, the caliper tool was re-calibrated, using the three point calibration jig, and the log repeated. As with the verification, the tips of the caliper arms are placed in the holes marked with the required diameter. During calibration, the value of the current calibration point, as stamped on the jig, is entered via the control computer. The system counts for 15 seconds to make an average of the response. The procedure is repeated for the second and third required openings. The computation and generation of the calibration coefficient file is entirely automatic. The calibration file is simply the set of coefficients of a quadratic curve which fits the three data points.

Natural gamma was not calibrated in the field, as it is a qualitative measurement, not a quantitative value, and is used only to assist in picking transitions between stratigraphic units, as described in ASTM D6274-98 (Re-approved 2004), Conducting Borehole Geophysical Logging - Gamma.

In each boring, the probe was positioned with the top of the probe at the top of the casing, and the electronic depth counter was set to the specified length of the probe, minus the height of the casing stick-up, as verified with a tape measure, and recorded on the field logs. The probe was lowered to the bottom of the boring, where the caliper legs were opened, and data collection begun. The probe was then returned to the surface at 10 feet/minute, collecting data continuously at 0.05-foot spacing, as summarized in Table 2.

Upon completion of the measurements, the probe zero depth indication at the depth reference point was verified prior to removal from the boring, and after survey depth error (ASDE) was calculated, as listed in Table 3.

Acoustic Televiewer / Boring Deviation Measurement Procedures

Twelve borings (excluding Z3-B8) were logged while filled with bentonite or polymer based drilling mud. Measurements followed the **GEO***Vision* standard field procedures, as presented in Appendix E.

Prior to use, the HiRAT probe tiltmeter and compass functions were checked by comparison with a Brunton surveyors' compass, and the results recorded on the field logs.

In each boring, the HiRAT probe was positioned with the top of the probe at the top of the casing, and the electronic depth counter was set to the specified length of the probe, minus the height of the casing stick-up, as verified with a tape measure, and recorded on the field logs. The probe was lowered to the bottom of the boring, and data collection begun. The rotational scan resolution was set to 360 samples per revolution, giving a horizontal pixel size of approximately 0.05 inches. The probe was returned to the surface at a nominal rate of 3 feet/minute, with an acquisition rate of 125 samples/foot, giving an equivalent vertical pixel size of 0.008 feet (approximately 0.1 inches).

Upon completion of the measurements, the probe zero depth indication at grade was verified prior to removal from the boring, and after survey depth error (ASDE) was calculated, as listed in Table 3.

DATA ANALYSIS

Suspension Velocity Analysis

Using the proprietary OYO program PSLOG.EXE version 1.0, the recorded digital waveforms were analyzed to locate the most prominent first minima, first maxima, or first break on the vertical axis records, indicating the arrival of P-wave energy.

The difference in travel time between receiver 1 and receiver 2 (R1-R2) arrivals was used to calculate the P-wave velocity for that 3.28-foot segment of the soil column. When observable, P-wave arrivals on the horizontal axis records were used to verify the velocities determined from the vertical axis data. The time picks were then transferred into an EXCEL template (EXCEL version 2003 SP2) to complete the velocity calculations based upon the arrival time picks made in PSLOG. The EXCEL analysis files are included in the boring specific directories on the data disk (CD-R) labeled Report 9014-02 that accompanies this report.

The P-wave velocity over the 7.0-foot interval from source to receiver 1 (S-R1) was also picked using PSLOG, and calculated and plotted in EXCEL, for quality assurance of the velocity derived from the travel time between receivers. In this analysis, the depth values as recorded were increased by 5.2 feet to correspond to the mid-point of the7.0-foot S-R1 interval. Travel times were obtained by picking the first break of the P-wave signal at receiver 1 and subtracting 0.3 milliseconds, the calculated and experimentally verified delay from source trigger pulse (beginning of record) to source impact. This delay corresponds to the duration of acceleration of the solenoid before impact.

As with the P-wave records, the recorded digital waveforms were analyzed to locate clear S_H-wave pulses, as indicated by the presence of opposite polarity pulses on each pair of horizontal records. Ideally, the S_H-wave signals from the 'normal' and 'reverse' source pulses are very nearly inverted images of each other. Digital Fast Fourier Transform – Inverse Fast Fourier Transform (FFT – IFFT) lowpass filtering was used to remove the higher frequency P-wave

signal from the S_H-wave signal. Different filter cutoffs were used to separate P- and S_H-waves at different depths, ranging from 600 Hz in the slowest zones to 3000 Hz in the regions of highest velocity. At each depth, the filter frequency was selected to be at least twice the fundamental frequency of the S_H-wave signal being filtered.

Generally, the first maxima were picked for the 'normal' signals and the first minima for the 'reverse' signals, although other points on the waveform were used if the first pulse was distorted. The absolute arrival time of the 'normal' and 'reverse' signals may vary by +/- 0.2 milliseconds, due to differences in the actuation time of the solenoid source caused by constant mechanical bias in the source or by boring inclination. This variation does not affect the R1-R2 velocity determinations, as the differential time is measured between arrivals of waves created by the same source actuation. The final velocity value is the average of the values obtained from the 'normal' and 'reverse' source actuations.

As with the P-wave data, S_H-wave velocity calculated from the travel time over the 7.0-foot interval from source to receiver 1 was calculated and plotted for verification of the velocity derived from the travel time between receivers. In this analysis, the depth values were increased by 5.2 feet to correspond to the mid-point of the 7.0-foot S-R1 interval. Travel times were obtained by picking the first break of the S_H-wave signal at the near receiver and subtracting 0.3 milliseconds, the calculated and experimentally verified delay from the beginning of the record at the source trigger pulse to source impact.

These data and analysis were reviewed by John Diehl as a component of **GEO***Vision*'s in-house Quality assurance program.

Figure 2 shows an example of R1 - R2 measurements on a sample filtered suspension record. In Figure 2, the time difference over the 3.28-foot interval of 1.88 milliseconds for the horizontal signals is equivalent to an S_H-wave velocity of 1745 feet/second. Whenever possible, time differences were determined from several phase points on the S_H-waveform records to verify the data obtained from the first arrival of the S_H-wave pulse. Figure 3 displays the same record before filtering of the S_H-waveform record with a 1400 Hz FFT - IFFT digital lowpass filter,

illustrating the presence of higher frequency P-wave energy at the beginning of the record, and distortion of the lower frequency S_H-wave by residual P-wave signal.

Caliper / Natural Gamma Analysis

No analysis is required with the caliper or natural gamma data; however depths to identifiable boring features on the acoustic televiewer and suspension logs were compared to verify compatible depth readings on all logs. Using Robertson Geologging Winlogger software version 1.5, build 401J, these data were converted to LAS 2.0 and PDF formats for transmittal to the client.

Acoustic Televiewer / Boring Deviation Analysis

The acoustic televiewer data were processed using Robertson's RGLDIP software, version 6.2. Sinusoidal projections of fractures observed in the boring walls were interactively picked on the un-wrapped televiewer image, and are presented on the logs as red sinusoids superimposed over the televiewer image. Bedding features, where identifiable, were picked on the same images, and are presented on the logs as green sinusoids. The sinusoidal projections were processed using the mechanical caliper diameter data to calculate apparent dip angle. True dip was calculated, correcting for the plunge of the borings using the recorded data from the accelerometer located in the probes, and presented in arrow format, with true dip indicated by the arrow position across the plot. Azimuth of dip (not strike), is indicated by the direction of the arrow tail, with true north being "up". These values are presented with the comments to the right of the arrow plots, as dip azimuth followed by dip angle.

The televiewer images were also processed to create a simulated core image of the borings. It must be noted that the simulated core image represents a core that would have the full diameter of the boring, not the diameter of the cores removed during drilling, so that direct comparison between the two is not possible. Also, the unwrapped image is viewed from the perspective of an observer in the center of the boring looking outward. The simulated core image is viewed form the "outside" of the boring looking inward, so there is a reversal of the position of east and west relative to north between the two images.

The televiewer data were also processed to extract the deviation data and produce an ASCII file and plots of boring deviation. Stereonet analysis of the identified features was performed with Robertson's RGLDIP software, version 6.2, to assist in identifying dominant fracture and bedding planes in the borings. Concentrations of similarly oriented features were enclosed in three to five small circles on the stereonet image, and the vector mean dip and azimuth for each small circle was calculated.

RESULTS

Suspension Velocity Results

Suspension R1-R2 P- and S_H-wave velocities are plotted in Figures 4, 8, 12, 16, 20, 24, 28, 32, 36, 40, 45, and 49. The suspension velocity data presented in these figures are presented in Tables 5, 7, 9, 11, 13, 15, 17, 19, 21, 23, 25, and 27. The EXCEL analysis file for each boring are included in the boring specific directories on the data disk (CD-R) labeled Report 9014-02 that accompanies this report.

P- and S_H-wave velocity data from R1-R2 analysis and quality assurance analysis of S-R1 data are plotted together in Figures A-1 through A-12 to aid in visual comparison. It should be noted that R1-R2 data are an average velocity over a 3.28-foot segment of the soil column; S-R1 data are an average over 7.0 feet, creating a significant smoothing relative to the R1-R2 plots. S-R1 data are presented in Tables A-1 through A-12, and included in the EXCEL analysis files for each boring on the data disk (CD-R) labeled Report 9014-02 that accompanies this report. The EXCEL analysis files include Poisson's Ratio calculations, tabulated data and plots.

Calibration procedures and records for the suspension PS measurement system are presented in Appendix D.

The **GEO***Vision* standard field procedures, as provided to CH2M for approval prior to field work, are reproduced in Appendix E.

Caliper / Natural Gamma Results

Caliper and natural gamma data are presented as single page logs in Figures 5, 9, 13, 17, 21, 25, 29, 33, 37, 41, 44, 46 and 50, as well as multi-page logs in Appendix B. LAS 2.0 data and Acrobat files for each boring are included in the boring specific sub-directories in the data directory on the data disk (CD-R) labeled Report 9014-02 that accompanies this report.

Acoustic Televiewer / Boring Deviation Results

Acoustic televiewer amplitude images and picked sinusoids are presented in Appendix C. The same logs are presented in .pdf format in the boring specific sub-directories of the data disk (CD-R) labeled Report 9014-02 that accompanies this report. Fracture and bedding depth, dip and azimuth of dip data are provided on the multi-page log sheets in Appendix C, and in Tables 6, 8, 10, 12, 14, 16, 18, 20, 22, 24, 26 and 28 as well as in .txt and EXCEL format.

Upper hemisphere stereonet plots are presented in Figures 6, 10, 14, 18, 22, 26, 30, 34, 38, 42, 47, and 51, as well as in PDF format. These borings did not exhibit different zones of feature orientation; the feature orientations appeared to be fairly evenly distributed over the boring depths, so they were processed as single zone models.

The mean dips for each of the stereonet small circles are presented in Figures 6, 10, 14, 18, 22, 26, 30, 34, 38, 42, 47, and 51, and in ASCII format. Feature distribution histograms and Rose diagrams are presented in the boring specific sub-directories of the data disk (CD-R).

Boring deviation data is presented graphically in Figures 7, 11, 15, 19, 23, 27, 31, 35, 39, 43, 48 and 52, and summarized in Table 4. Deviation data plots in Acrobat format and deviation data at 1.0-foot stations are presented in text format in the boring specific sub-directories of the data disk (CD-R).

SUMMARY

Discussion of Suspension Velocity Results

Suspension PS velocity data are ideally collected in an uncased fluid filled boring, drilled with rotary mud (rotary wash) methods. The borings at these sites were well suited for collection of suspension PS velocity data, though in some cases the shallow portions of the borings were eroded out to large diameters, which degraded the quality of the velocity data.

Suspension PS velocity data quality is judged based upon 5 criteria:

1. Consistent data between receiver to receiver (R1 – R2) and source to receiver (S – R1) data.
2. Consistent relationship between P-wave and S_H -wave (excluding transition to saturated soils)
3. Consistency between data from adjacent depth intervals.
4. Clarity of P-wave and S_H-wave onset, as well as damping of later oscillations.
5. Consistency of profile between adjacent borings, if available.

Generally, these data show excellent correlation between R1 – R2 and S – R1 data, as well as excellent correlation between P-wave and S_H-wave velocities. P-wave and S_H-wave onsets are very clear, and later oscillations are well damped, with the exception of the borings that showed larger diameters due to erosion, Z1-B6, Z1-B7, Z2-B1 and Z3-B12, some which had diameters approaching 12 inches.

Discussion of Caliper / Natural Gamma Results

Caliper and natural gamma data were collected in each boring. The caliper logs for these borings generally show nominal bit diameters of below about 100 feet, with the softer material above 100 feet eroded out to almost 12 inches in some locations. Natural gamma data were collected with this tool in all the borings, and shows a number of thin layers that correspond to

features on the acoustic televiewer logs. One such example is at 361 – 362 feet in Z1-B6, where there is a significant drop in natural gamma, and an apparent hard sandstone layer on the acoustic televiewer image. A significant velocity increase can be seen at the same depth.

Discussion of Acoustic Televiewer / Boring Deviation Results

Despite the large nominal diameter (5.5 inches) of the Cascade Drilling borings, the acoustic televiewer data quality in borings with good diameter control and clean walls, like Z1-B3, Z1-B5 are quite clear, showing contacts between soft and harder rock units, fractures in the rock, and even spiral marks form the coring bit.

Boring Z1-B6 has good diameter control below 100 feet, but the images are not as clear due to a thick wall cake. This is illustrated by the presence of interference patterns caused by standing acoustic waves in the wall cake, similar to optical moiré patterns. These can be seen clearly in Z1-B6 at 333 – 334 feet. Heavy wall cake was a regular problem, with the probe completely covered in clay at the end of logging runs.

Boring Z2-B1 is eroded out to 8 inches or more for the entire depth, and yields almost no acoustic image. Z3-B1 does not show many planar features, but the image quality is good. This boring shows a number of hard inclusions in a softer matrix, but few planar features.

The twelve borings in which deviation data were collected were inclined at 2.0 degrees, or less, from vertical, and the maximum error in depth value was 0.3 feet in 319 feet, or less than 0.1 percent, as presented in Table 4. This error is less than depth errors from other causes, and no adjustment of log depths is indicated.

Quality Assurance

These boring geophysical measurements were performed using industry-standard or better methods for measurements and analyses. All work was performed under **GEO***Vision* quality assurance procedures, which include:

- Use of NIST-traceable calibrations, where applicable, for field and laboratory instrumentation
- Use of standard field data logs
- Use of independent verification of velocity data by comparison of receiver-to-receiver and source-to-receiver velocities
- Independent review of calculations and results by a registered professional engineer, geologist, or geophysicist.

Suspension Velocity Data Reliability

P- and S_H-wave velocity measurement using the Suspension Method gives average velocities over a 3.28-foot interval of depth. This high resolution results in the scatter of values shown in the graphs. Individual measurements are very reliable with estimated precision of +/- 5%. Standardized field procedures and quality assurance checks contribute to the reliability of these data.

CERTIFICATION

All geophysical data, analysis, interpretations, conclusions, and recommendations in this document have been prepared under the supervision of and reviewed by a **GEO***Vision* California Professional Geophysicist.

7/31/09

Antony J. Martin Date
California Professional Geophysicist GP989
GEO*Vision* Geophysical Services

* This geophysical investigation was conducted under the supervision of a California Professional Geophysicist using industry standard methods and equipment. A high degree of professionalism was maintained during all aspects of the project from the field investigation and data acquisition, through data processing interpretation and reporting. All original field data files, field notes and observations, and other pertinent information are maintained in the project files and are available for the client to review for a period of at least one year.

  A professional geophysicist's certification of interpreted geophysical conditions comprises a declaration of his/her professional judgment. It does not constitute a warranty or guarantee, expressed or implied, nor does it relieve any other party of its responsibility to abide by contract documents, applicable codes, standards, regulations or ordinances.

BORING DESIGNATION	DATES LOGGED	COORDINATES (FEET, ZONE 5, NAD83) [1]		ELEVATION [1] (FEET NAVD88)
		NORTH	EAST	
Z1-B3	1/30/2009	1855594.07	6492810.43	343.23
Z1-B5	2/25/2009	1850576.02	6499981.20	442.15
Z1-B6	2/10/2009	1852836.59	6503970.85	447.22
Z1-B7	1/26/2009	1849941.30	6506175.09	480.52
Z2-B1	1/21/2009	1866308.10	6492663.29	451.02
Z2-B4	3/31/2009	1858027.66	6507350.57	558.11
Z3-B1	3/19/2009	1873601.92	6507232.68	885.14
Z3-B3	2/11/2009	1870194.48	6514774.44	801.99
Z3-B4	3/6/2009	1870813.73	6516733.49	768.04
Z3-B6	3/5/2009	1868062.70	6516722.28	750.00
Z3-B8	3/23/2009	1860993.95	6514198.81	594.27
Z3-B12	1/14/2009	1856063.15	6513380.17	501.00
Z4-B4	3/17/2009	1851895.71	6514496.46	454.42

[1] Coordinates and elevation provided by CH2M dated 6/17/09

Table 1. Boring locations and logging dates

BORING NUMBER	TOOL AND RUN NUMBER	DEPTH RANGE (FEET)	BOTTOM OF BOREHOLE CASING	SAMPLE OR MEASUREMENT INTERVAL (FEET)	DATE LOGGED
Z1-B3	CALIPER/GAMMA 1	300.7 – 71.0	86	0.05	1/30/2009
Z1-B3	ACOUSTIC TELEVIEWER 1	300.9 – 82.3	86	0.008	1/30/2009
Z1-B3	SUSPENSION PS 1	88.6 – 288.7	86	1.6	1/30/2009
Z1-B5	CALIPER/GAMMA 1	500.1 – 4.1	8	0.05	2/25/2009
Z1-B5	ACOUSTIC TELEVIEWER 1	499.4 – 35.0	8	0.008	2/25/2009
Z1-B5	SUSPENSION PS 1	11.8 – 487.2	8	1.6	2/25/2009
Z1-B6	CALIPER/GAMMA 1	400.1 – 1.0	4	0.05	2/10/2009
Z1-B6	ACOUSTIC TELEVIEWER 1	400.0 – 65.0	4	0.008	2/10/2009
Z1-B6	SUSPENSION PS 1	6.6 – 390.4	4	1.6	2/10/2009
Z1-B7	CALIPER/GAMMA 1	299.0 - 0	11	0.05	1/26/2009
Z1-B7	ACOUSTIC TELEVIEWER 1	299.0 – 145.0	11	0.008	1/26/2009
Z1-B7	SUSPENSION PS 1	13.1 – 290.4	11	1.6	1/26/2009
Z2-B1	CALIPER/GAMMA 1	149.0 – 1.0	19	0.05	1/21/2009
Z2-B1	ACOUSTIC TELEVIEWER 1	149.0 – 18.5	19	0.008	1/21/2009
Z2-B1	SUSPENSION PS 1	21.3 – 137.8	19	1.6	1/21/2009
Z2-B4	CALIPER/GAMMA 1	358.3 – 6.0	6	0.05	3/31/2009
Z2-B4	CALIPER/GAMMA 2	374.5 – 325.0	6	0.05	3/31/2009
Z2-B4	ACOUSTIC TELEVIEWER 1	358.7 – 1.8	6	0.008	3/31/2009
Z2-B4	ACOUSTIC TELEVIEWER 2	374.2 – 347.0	6	0.008	3/31/2009
Z2-B4	SUSPENSION PS 1	3.3 – 305.1	6	1.6	3/31/2009
Z2-B4	SUSPENSION PS 2	306.8 – 360.9	6	1.6	3/31/2009
Z3-B1	CALIPER/GAMMA 1	300.2 – 14.8	26	0.05	3/19/2009
Z3-B1	ACOUSTIC TELEVIEWER 1	300.2 – 22.2	26	0.008	3/19/2009
Z3-B1	SUSPENSION PS 1	4.0 – 287.1	26	1.6	3/19/2009

- PROBE DID NOT TOUCH BOTTOM OF BORING

Table 2. Logging dates and depth ranges

BORING NUMBER	TOOL AND RUN NUMBER	DEPTH RANGE (FEET)	BOTTOM OF BOREHOLE CASING	SAMPLE OR MEASUREMENT INTERVAL (FEET)	DATE LOGGED
Z3-B3	CALIPER/GAMMA 1	273.0 – 165.1	174.5	0.05	2/11/2009
Z3-B3	CALIPER/GAMMA 2	273.0 – 50.0	55	0.05	2/11/2009
Z3-B3	ACOUSTIC TELEVIEWER 1	274.0 – 173.0	174.5	0.008	2/11/2009
Z3-B3	SUSPENSION PS 1	177.2 – 262.5	174.5	1.6	2/11/2009
Z3-B3	SUSPENSION PS 2	57.4 – 183.7	55	1.6	2/11/2009
Z3-B4	CALIPER/GAMMA 1	274.9 – 2.1	3.5	0.05	3/6/2009
Z3-B4	ACOUSTIC TELEVIEWER 1	275.3 – 2.5	3.5	0.008	3/6/2009
Z3-B4	SUSPENSION PS 1	2.8 – 262.5	3.5	1.6	3/6/2009
Z3-B6	CALIPER/GAMMA 1	325.0 - 5.3	10.5	0.05	3/5/2009
Z3-B6	ACOUSTIC TELEVIEWER 1	320.4 – 308.9	10.5	0.008	3/5/2009
Z3-B6	ACOUSTIC TELEVIEWER 2	318.7 – 28.3	10.5	0.008	3/5/2009
Z3-B6	SUSPENSION PS 1	43.0 – 311.7	10.5	1.6	3/5/2009
Z3-B8	CALIPER/GAMMA 1	275.7 – 4.2	4	0.05	3/23/2009
Z3-B12	CALIPER/GAMMA 1	273.0 – 50.0	57.5	0.05	1/14/2009
Z3-B12	CALIPER/GAMMA 2	273.0 – 245.5	57.5	0.05	1/14/2009
Z3-B12	CALIPER/GAMMA 3	258.0 – 54.0	57.5	0.05	1/14/2009
Z3-B12	ACOUSTIC TELEVIEWER 1	67.5 – 186.8	57.5	0.008	1/14/2009
Z3-B12	ACOUSTIC TELEVIEWER 2	182.6 – 57.0	57.5	0.008	1/14/2009
Z3-B12	SUSPENSION PS 1	59.0 – 185.4	57.5	1.6	1/14/2009
Z3-B12	SUSPENSION PS 2	173.9 – 251.0 8.2 – 62.3	5	1.6	1/14/2009
Z4-B4	CALIPER/GAMMA 1	275.0 – 2.0	7	0.05	3/17/2009
Z4-B4	ACOUSTIC TELEVIEWER 1	275.1 – 270.3	7	0.008	3/17/2009
Z4-B4	ACOUSTIC TELEVIEWER 2	275.1 – 4.7	7	0.008	3/17/2009
Z4-B4	SUSPENSION PS 1	4.7 – 262.5	7	1.6	3/17/2009

- PROBE DID NOT TOUCH BOTTOM OF BORING

Table 2, continued. Logging dates and depth ranges

BORING NUMBER	MEAN DEVIATION AND AZIMUTH (DEGREES TN)	SURVEY DEPTH (FEET)	VERTICAL DEPTH (FEET)	DEPTH ERROR (FEET)	HORIZONTAL OFFSET (FEET)
Z1-B3	0.7 – N213	300.8	300.7	0.1	3.8
Z1-B5	0.5 – N292	499.3	499.3	0	4.7
Z1-B6	1.3 – N031	400.0	399.8	0.2	9.0
Z1-B7	1.5 – N226	299.0	298.9	0.1	7.6
Z2-B1	1.2 – N178	148.9	148.0	0	3.0
Z2-B4	0.9 – N000	374.6	374.5	0.1	6.0
Z3-B1	1.8 – N307	300.2	300.0	0.2	9.3
Z3-B3	0.5 – N265	273.9	273.9	0	2.2
Z3-B4	0.2 – N033	275.2	275.2	0	1.1
Z3-B6	2.0 – N081	318.7	318.4	0.3	11.3
Z3-B12	0.3 – N264	182.5	182.5	0	0.9
Z4-B4	0.6 – N000	275.1	275.0	0.1	2.6

Table 3. Boring Deviation Data Summary

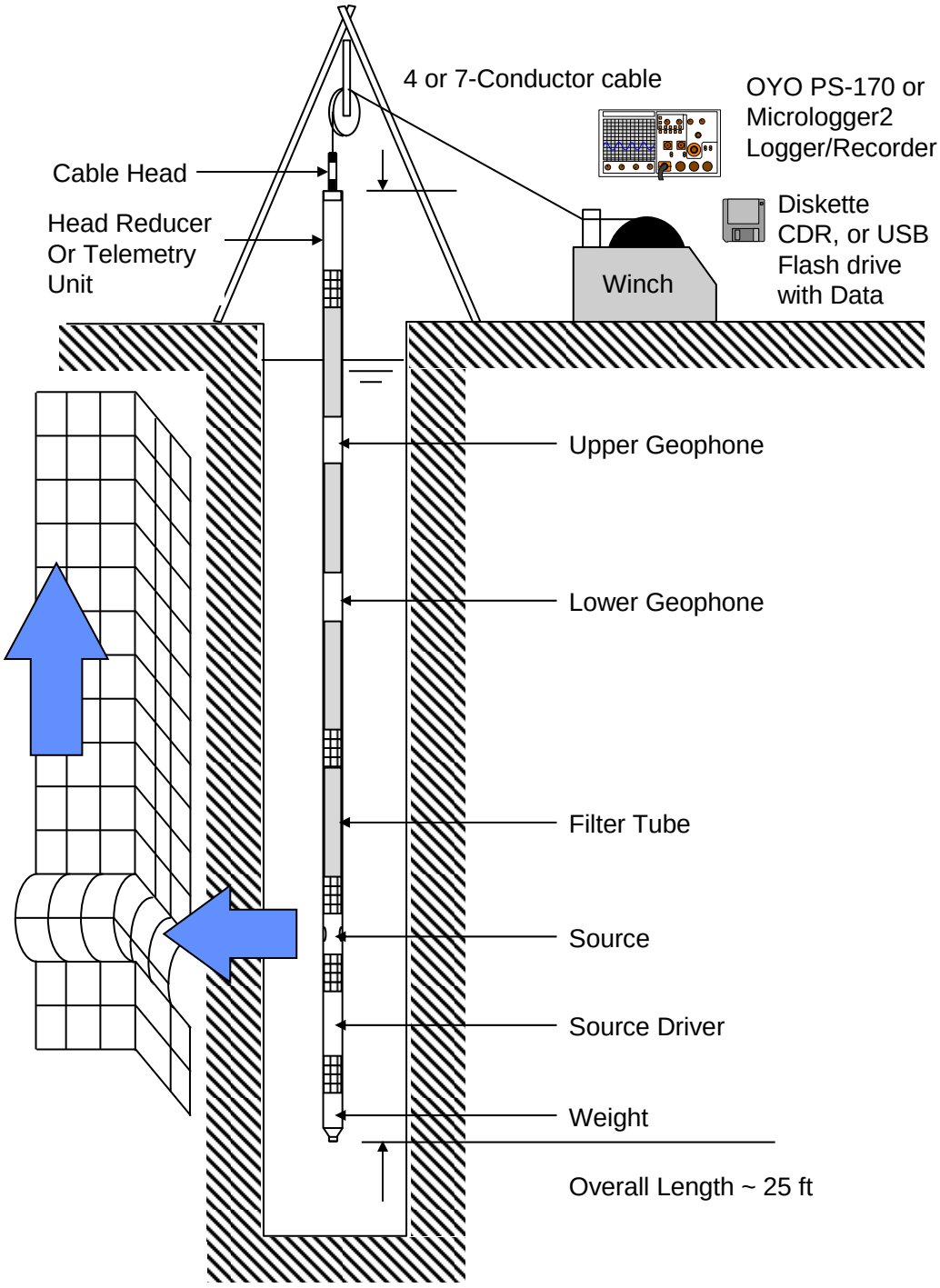

Figure 1: Concept illustration of Suspension P S logging system

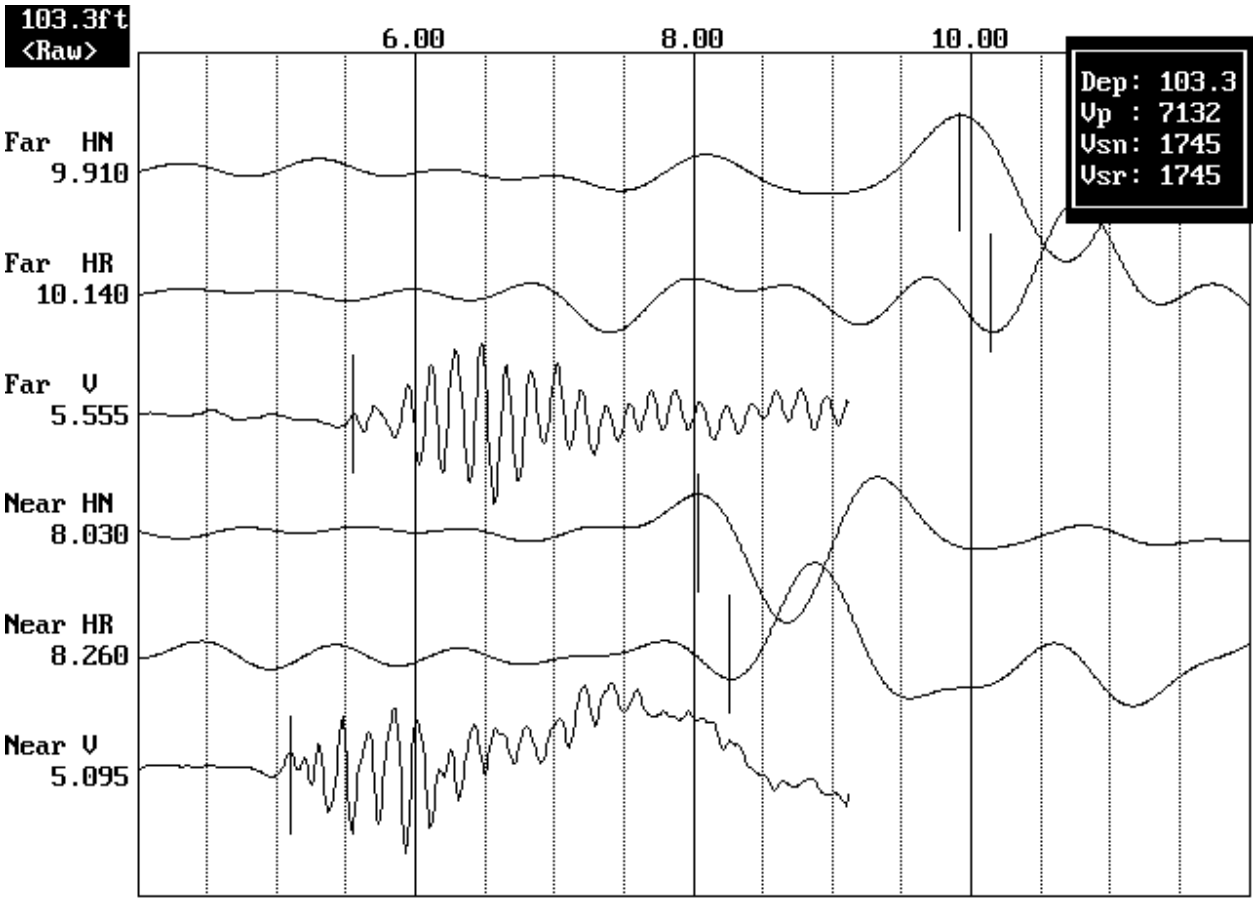

Figure 2: Example of filtered (1400 Hz lowpass) suspension record

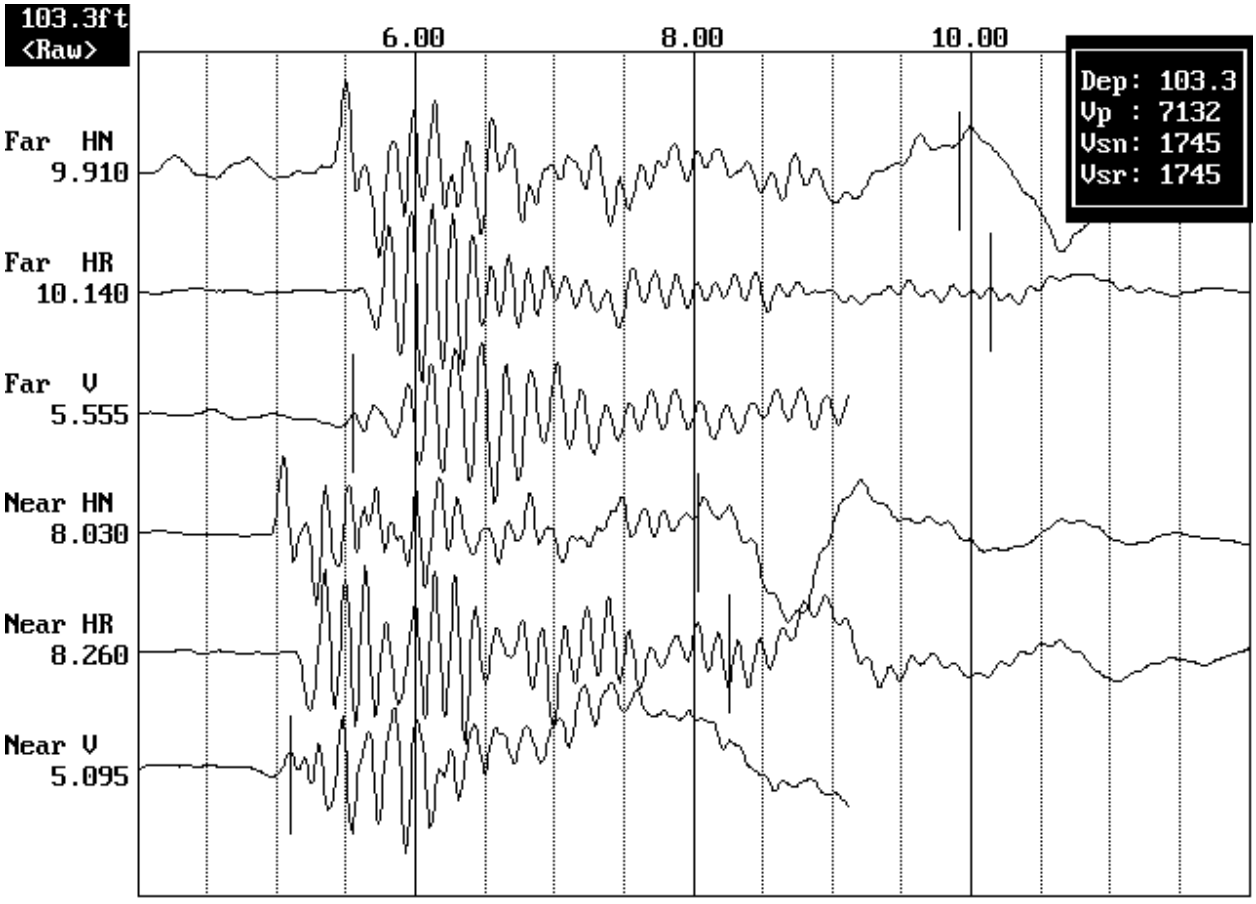

Figure 3. Example of unfiltered suspension record

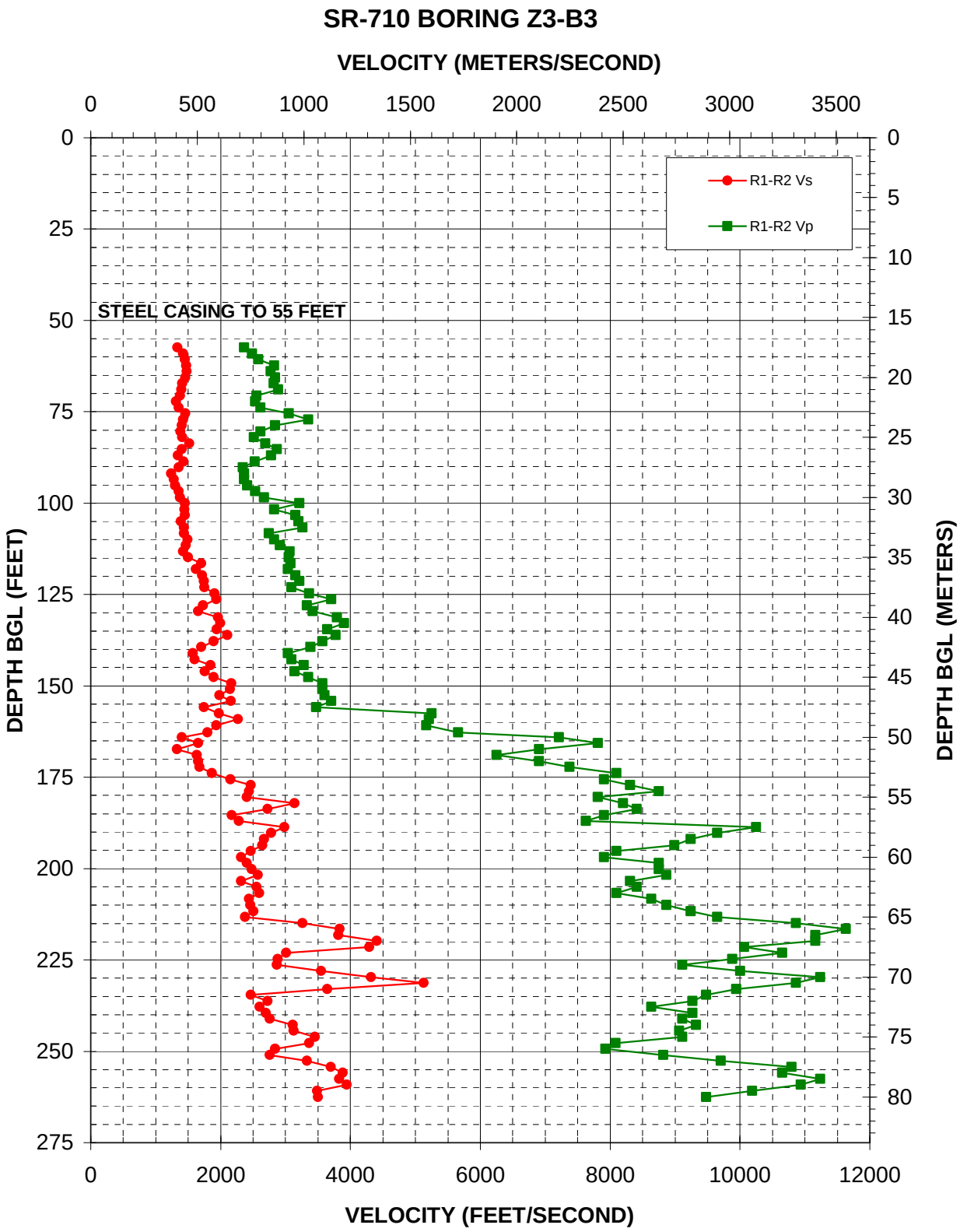

Figure 32: Boring Z3-B3, Suspension R1-R2 P- and S_H-wave velocities

Depth (feet)	V_s (feet/sec)	V_p (feet/sec)
57.41	1334	2360
59.06	1426	2485
60.70	1448	2583
62.34	1468	2828
63.98	1481	2769
65.62	1458	2841
67.26	1408	2816
68.90	1393	2891
70.54	1379	2553
72.18	1312	2533
73.82	1353	2614
75.46	1455	3052
77.10	1423	3348
78.74	1402	2841
80.38	1384	2614
82.02	1411	2514
83.66	1515	2689
85.30	1405	2865
86.94	1345	2780
88.58	1433	2524
90.22	1353	2343
91.86	1240	2360
93.50	1282	2360
95.14	1299	2412
96.78	1356	2533
98.43	1379	2667
100.07	1452	3217
101.71	1445	2828
103.35	1448	3155
104.99	1387	3201
106.63	1439	3265
108.27	1439	2745
109.91	1491	2828
111.55	1465	2916
113.19	1426	3066
114.83	1498	3052
116.47	1704	3081
118.11	1624	3038
119.75	1713	3155
121.39	1740	3217
123.03	1750	3095
124.67	1907	3365
126.31	1936	3707
127.95	1731	3331
129.59	1657	3418
131.23	1959	3793
132.87	1994	3906
134.51	1941	3645
136.15	2103	3771
137.80	1896	3566
139.44	1700	3382
141.08	1574	3038
142.72	1600	3095
144.36	1848	3281
146.00	1759	3140
147.64	1896	3348
149.28	2166	3566
150.92	2144	3566
152.56	1982	3605
154.20	2158	3707
155.84	1745	3472
157.48	1976	5249
159.12	2270	5208
160.76	1936	5167
162.73	1798	5657
164.04	1402	7211
165.68	1657	7812
167.32	1331	6907
168.96	1632	6249
170.60	1657	6907
172.24	1674	7373
173.88	1864	8101
175.52	2151	7906
177.17	2467	8306
178.81	2439	8749
180.45	2404	7812
182.09	3140	8202
183.73	2723	8412
185.37	2173	7906
187.01	2278	7630
188.65	2983	10253
190.29	2780	9650
191.93	2667	9242
193.57	2646	8989
195.21	2467	8101
196.85	2319	7906
198.49	2404	8749
200.13	2476	8749
201.77	2573	8867
203.41	2319	8306
205.05	2553	8412
206.69	2594	8101
208.33	2439	8634
209.97	2458	8867
211.61	2504	9242
213.25	2377	9650
214.90	3265	10864
216.54	3837	11634
218.18	3815	11159
219.82	4404	11159
221.46	4289	10064
223.10	3010	10652
224.74	2878	9882
226.38	2865	9113
228.02	3547	10003
229.66	4317	11236
231.30	5126	10864
232.94	3645	9942
234.58	2467	9482
236.22	2723	9268
237.86	2604	8634
239.50	2700	9268
241.14	2757	9113
242.78	3110	9321
244.42	3125	9063
246.06	3454	9113
247.70	3365	8081
249.34	2841	7925
250.98	2757	8819
252.62	3331	9707
254.27	3697	10792
255.91	3883	10652
257.55	3826	11236
259.19	3941	10936
260.83	3490	10189
262.47	3500	9482

Table 18. Boring Z3-B3, Suspension R1-R2 depths and P- and S_H-wave velocities

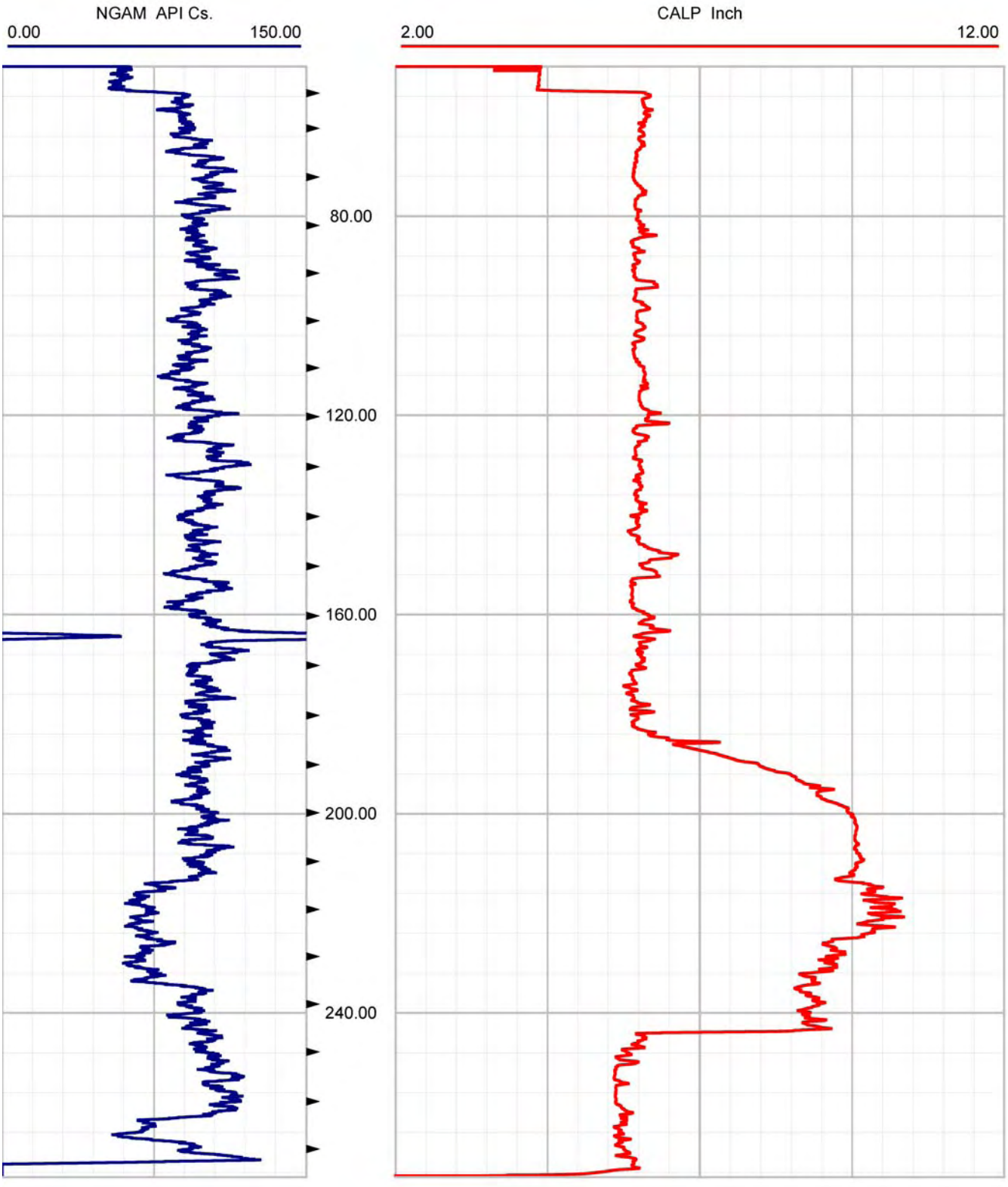

Figure 33. Boring Z3-B3, Caliper and Natural Gamma logs

DIP DATA INTERPRETATION
RGLDIP vsn 6.2
FRACTURE ANALYSIS STEREOGRAMS

CASCADE DRILLING

Borehole: Z3-B3

SR-710 TUNNEL INVESTIGATION

top of borehole.....
East:_
North:_
Elev:_

North ref: true
Depth units are feet

Zone from 273.652 to 271.984ft
Mean dip format: dip-azimuth and dip

Interpretation 1

Dip data sets .....
BHTV dips

Z3-B3
Zone 0. 271.984 - 273.642ft
Deviation 1.60 N308.50

dipdata sets.....
BHTV dips
• Highlighted dips: Fracture Planar Hairline-fracture

	mean dip	n	f
N348 52	N348 52	2	2.04
N123 29	N123 29	1	(0.00)

intersections

	N348 52	N123 29
N348 52		16 N065
N123 29	16 N065	

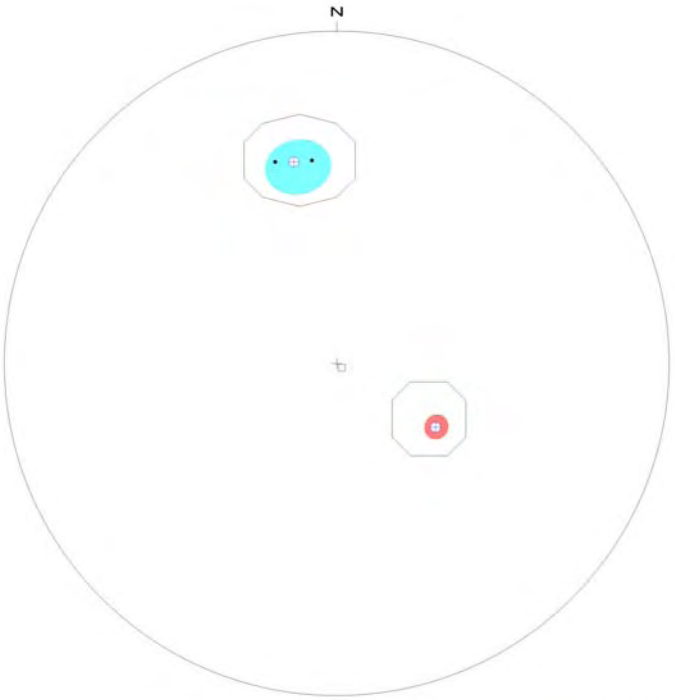

equal-area upper-hemisphere 0-90
contour-levels 1,

Z3-B3, Interpretation 1 273.642 to 271.984ft 1

Figure 34. Boring Z3-B3, Stereonet Plot

Depth (feet)	Dip azimuth	Dip	Structure description
273.15	N343	53	Primary-structure Planar Bedding
272.68	N353	52	Primary-structure Planar Bedding
272.48	N123	29	Fracture Planar Hairline-fracture

Table 19. Boring Z3-B3, Structure depth, dip azimuth, dip and description

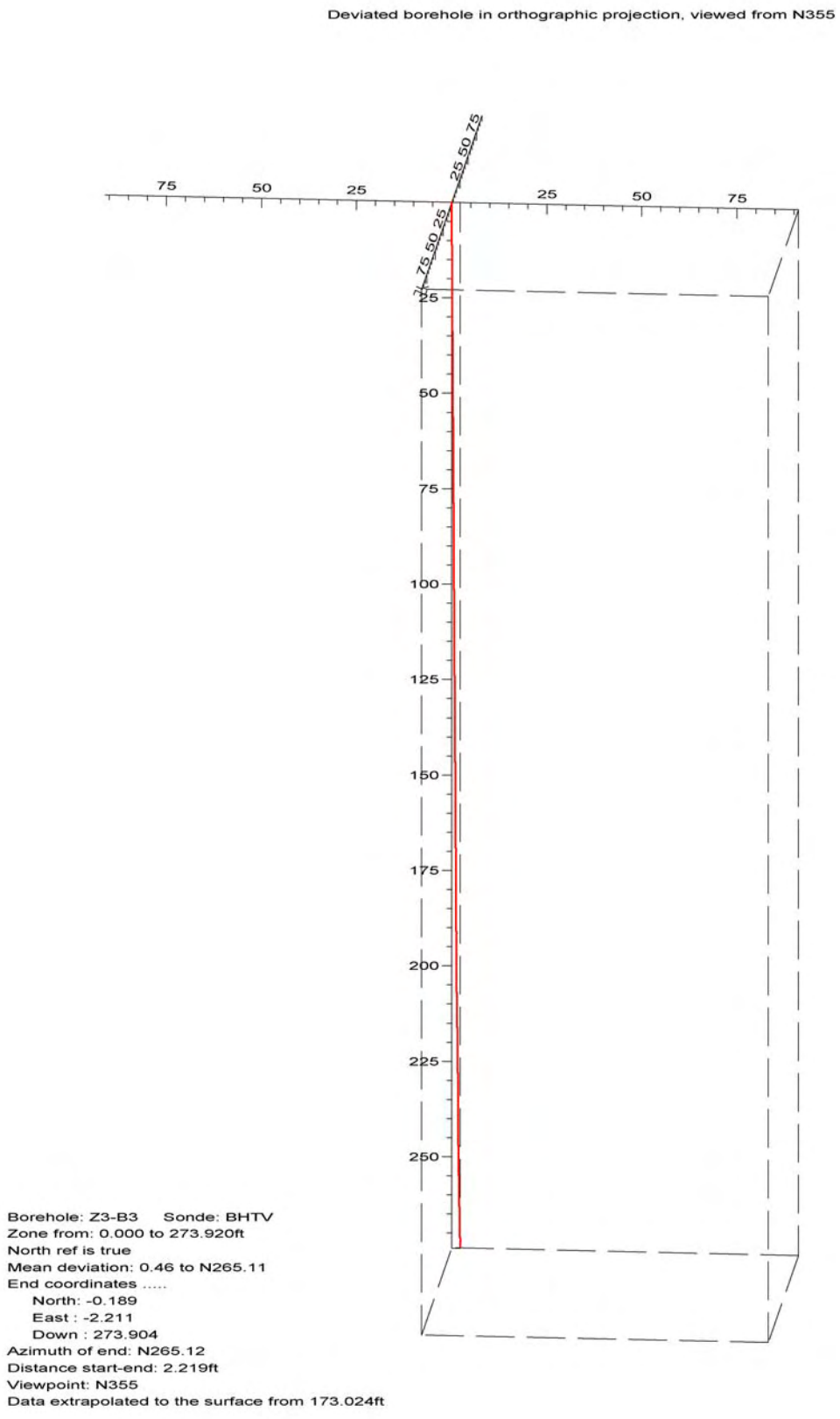

Figure 35. Boring Z3-B3, Deviation Projection

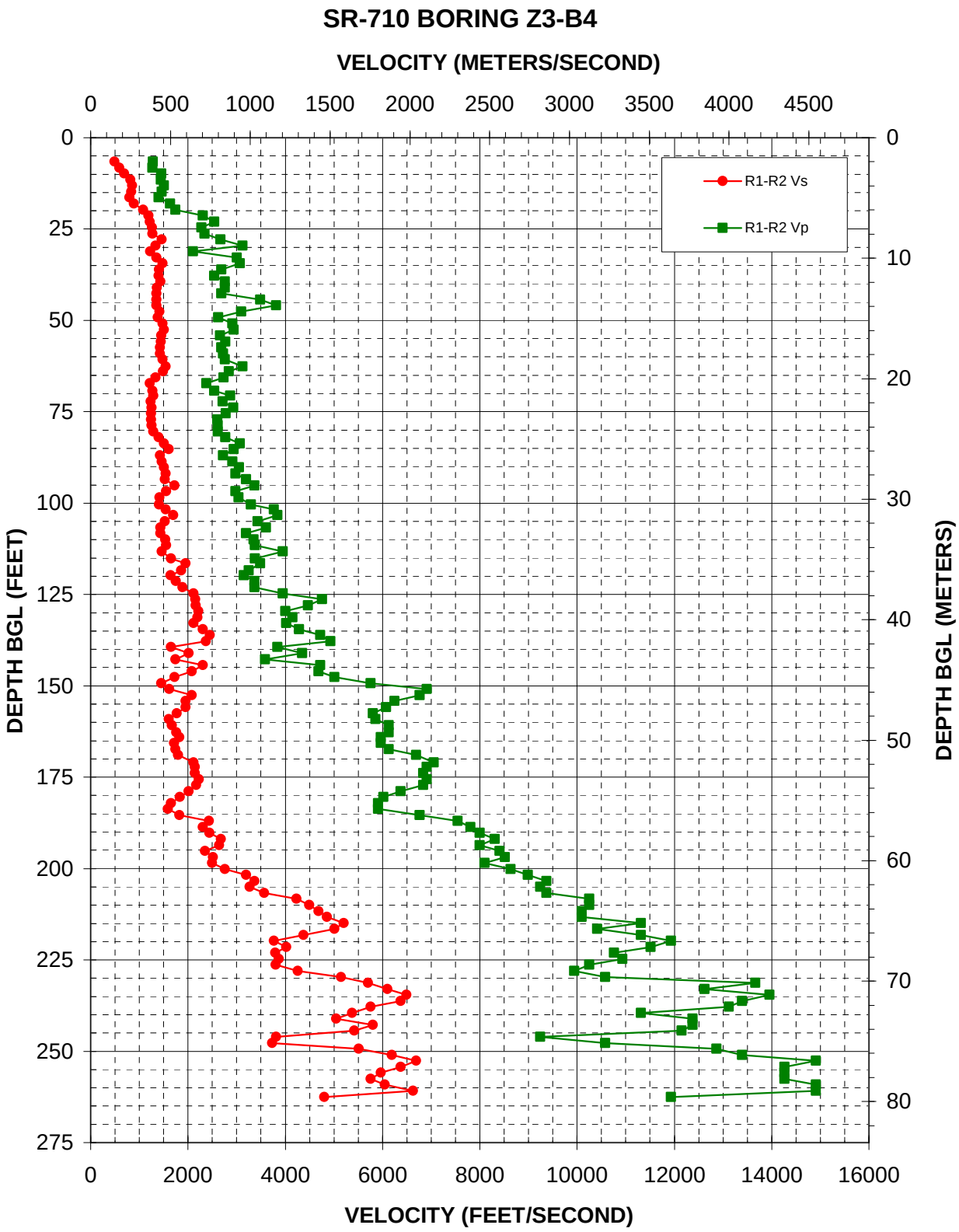

Figure 36: Boring Z3-B4, Suspension R1-R2 P- and S_H-wave velocities

Depth (feet)	V_s (feet/sec)	V_p (feet/sec)
6.56	489	1277
8.20	594	1272
9.84	689	1452
11.48	814	1445
13.12	857	1505
14.76	833	1458
16.40	800	1402
18.04	894	1632
19.69	1079	1745
21.33	1189	2310
22.97	1215	2543
24.61	1267	2278
26.25	1272	2343
27.89	1458	2667
29.53	1334	3125
31.17	1224	2103
32.81	1356	3010
34.45	1485	3066
36.09	1408	2689
37.73	1396	2543
39.37	1433	2757
41.01	1361	2757
42.65	1356	2689
44.29	1350	3490
45.93	1356	3815
47.57	1420	3095
49.21	1384	2625
50.85	1478	2916
52.49	1505	2942
54.13	1452	2657
55.77	1445	2769
57.41	1426	2689
59.06	1426	2723
60.70	1478	2757
62.66	1540	3125
63.98	1491	2841
65.62	1334	2734
67.26	1215	2377
69.23	1272	2543
70.54	1287	2865
72.18	1233	2711
73.82	1252	2929
75.46	1247	2780
77.10	1247	2604
78.74	1252	2614
80.38	1292	2614
82.02	1402	2769
83.66	1512	3066
85.30	1608	2942
86.94	1426	2723
88.58	1465	2916
90.22	1512	3052
91.86	1548	2983
93.50	1526	3201
95.14	1727	3365
96.78	1555	2983
98.43	1414	3038
100.39	1408	3297
101.71	1540	3771
103.35	1700	3837
104.99	1526	3435
106.63	1433	3605
108.27	1433	3201
109.91	1533	3348
111.55	1555	3382
113.19	1458	3953
115.16	1649	3382
116.47	1953	3490
118.44	1864	3248
119.75	1640	3155
121.39	1754	3365
123.03	1886	3365
124.67	2117	3953
126.31	2151	4755
127.95	2158	4464
129.59	2217	4001
131.23	2202	4153
132.87	2117	4026
134.51	2310	4289
136.15	2448	4721
137.80	2369	4934
139.44	1649	3837
141.08	2013	4345
142.72	1745	3586
144.36	2310	4721
146.00	2076	4687
147.64	1727	5009
149.28	1452	5756
150.92	1620	6907
152.56	2083	6765
154.20	1953	6249
155.84	1953	6076
157.48	1773	5807
159.12	1608	5859
160.76	1674	6132
162.73	1759	6132
164.04	1828	5965
165.68	1713	5965
167.32	1745	6132
168.96	1798	6696
170.93	2117	7056
172.24	2144	6907
173.88	2144	6835
175.52	2224	6907
177.17	2173	6835
178.81	2019	6371
180.45	1838	6020
182.09	1657	5911
183.73	1589	5911
185.37	1823	6765
187.01	2430	7542
188.65	2310	7812
190.29	2439	8002
191.93	2678	8306
193.57	2646	8002
195.21	2352	8412
196.85	2514	8522
198.49	2495	8101
200.13	2757	8634
201.77	3201	8989
203.41	3365	9374
205.05	3265	9242
206.69	3566	9374
208.33	4233	10253
209.97	4494	10253
211.61	4687	10095
213.25	4861	10095
214.90	5208	11313
216.54	5009	10415
218.18	4374	11313
219.82	3771	11930
221.46	4026	11512
223.10	3793	10757
224.74	3871	10936
226.38	3804	10253
228.02	4261	9942
229.66	5146	10583
231.30	5706	13670
232.94	6104	12619
234.58	6497	13961
236.22	6371	13391
237.86	5756	13123
239.50	5378	11313
241.14	5047	12381
242.78	5807	12381
244.42	5423	12151
246.06	3815	9242
247.70	3728	10583
249.34	5514	12866
250.98	6190	13391

Table 20. Boring Z3-B4, Suspension R1-R2 depths and P- and S_H-wave velocities

Depth (feet)	V_s (feet/sec)	V_p (feet/sec)
252.62	6696	14913
254.27	6371	14265
255.91	5965	14265
257.55	5756	14265
259.19	6048	14913
260.83	6628	14913
262.47	4807	11930

Table 20, continued. Boring Z3-B4, Suspension R1-R2 depths and P- and S_H-wave velocities

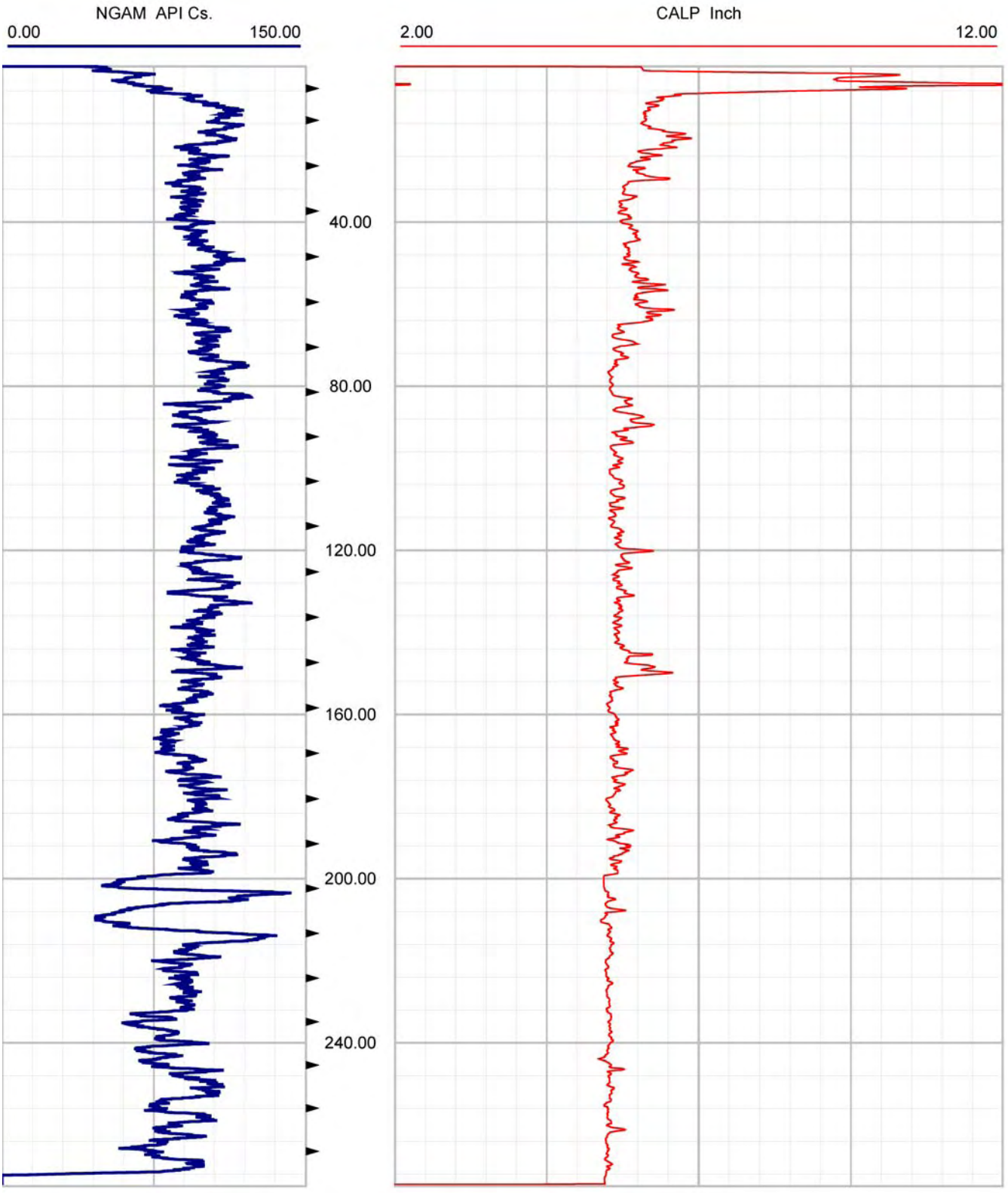

Figure 37. Boring Z3-B4, Caliper and Natural Gamma logs

DIP DATA INTERPRETATION
RGLDIP vsn 6.2
FRACTURE ANALYSIS STEREOGRAMS

CASCADE DRILLING

Borehole: Z3-B4

SR-710 TUNNEL INVESTIGATION

top of borehole.....
East:_
North:_
Elev:_

North ref: true
Depth units are feet

Zone from 275.196 to 64.540ft
Mean dip format: dip-azimuth and dip

Interpretation 1

Dip data sets .....
BHTV dips

Z3-B4
Zone 0. 64.540 - 275.196ft
Deviation 0.30 N 25.80

dipdata sets.....
BHTV dips
• Highlighted dips: Fracture Planar Hairline-fracture

	mean dip	n	f
N334 53	N334 53	7	(0.06)
N072 58	N072 58	3	(0.03)
N157 59	N157 59	7	(0.06)
N181 11	N181 11	10	(0.05)

intersections

	N334 53	N072 58	N157 59	N181 11
N334 53		43 N018	02 N246	04 N247
N072 58	43 N018		50 N113	10 N156
N157 59	02 N246	50 N113		05 N244
N181 11	04 N247	10 N156	05 N244	

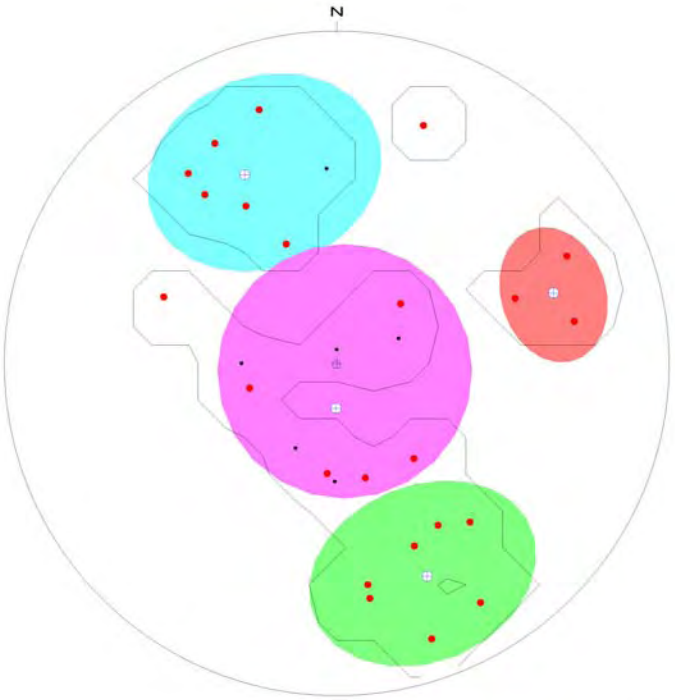

equal-area upper-hemisphere 0-90
contour-levels 1,

Z3-B4, Interpretation 1 275.196 to 64.540ft 1

Figure 38. Boring Z3-B4, Stereonet Plot

Depth (feet)	Dip azimuth	Dip	Structure description
274.74	N141	30	Fracture Planar Hairline-fracture
274.42	N065	65	Fracture Planar Hairline-fracture
274.33	N020	65	Fracture Planar Hairline-fracture
273.39	N331	65	Fracture Planar Hairline-fracture
273.13	N080	62	Fracture Planar Hairline-fracture
271.88	N185	27	Fracture Planar Hairline-fracture
271.42	N157	50	Fracture Planar Hairline-fracture
271.18	N148	48	Fracture Planar Hairline-fracture
270.43	N161	77	Fracture Planar Hairline-fracture
270.26	N181	29	Primary-structure Planar Bedding
267.93	N149	73	Fracture Planar Hairline-fracture
265.43	N166	29	Fracture Planar Hairline-fracture
265.05	N343	69	Fracture Planar Hairline-fracture
259.99	N330	45	Fracture Planar Hairline-fracture
258.86	N322	54	Fracture Planar Hairline-fracture
258.15	N291	47	Fracture Planar Hairline-fracture
257.82	N047	21	Fracture Planar Hairline-fracture
252.67	N070	48	Fracture Planar Hairline-fracture
250.25	N254	22	Fracture Planar Hairline-fracture
248.28	N172	61	Fracture Planar Hairline-fracture
247.64	N359	3	Primary-structure Planar Bedding
245.30	N322	62	Fracture Planar Hairline-fracture
236.66	N172	57	Fracture Planar Hairline-fracture
215.95	N140	52	Fracture Planar Hairline-fracture
199.28	N337	32	Fracture Planar Hairline-fracture
191.94	N357	49	Primary-structure Planar Bedding
190.56	N206	23	Primary-structure Planar Bedding
133.02	N270	23	Primary-structure Planar Bedding
65.04	N068	16	Primary-structure Planar Bedding

Table 21. Boring Z3-B4, Structure depth, dip azimuth, dip and description

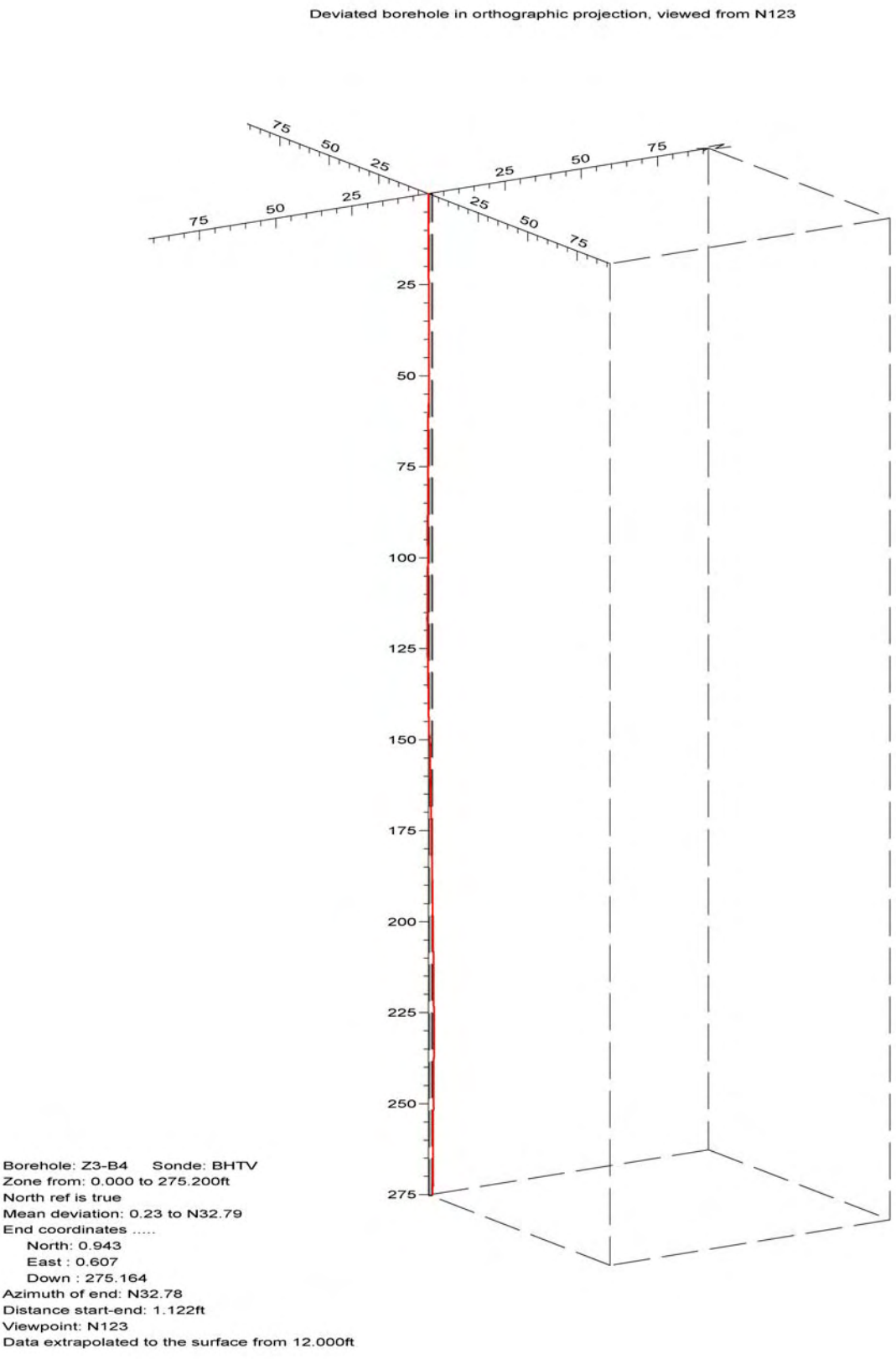

Figure 39. Boring Z3-B4, Deviation Projection

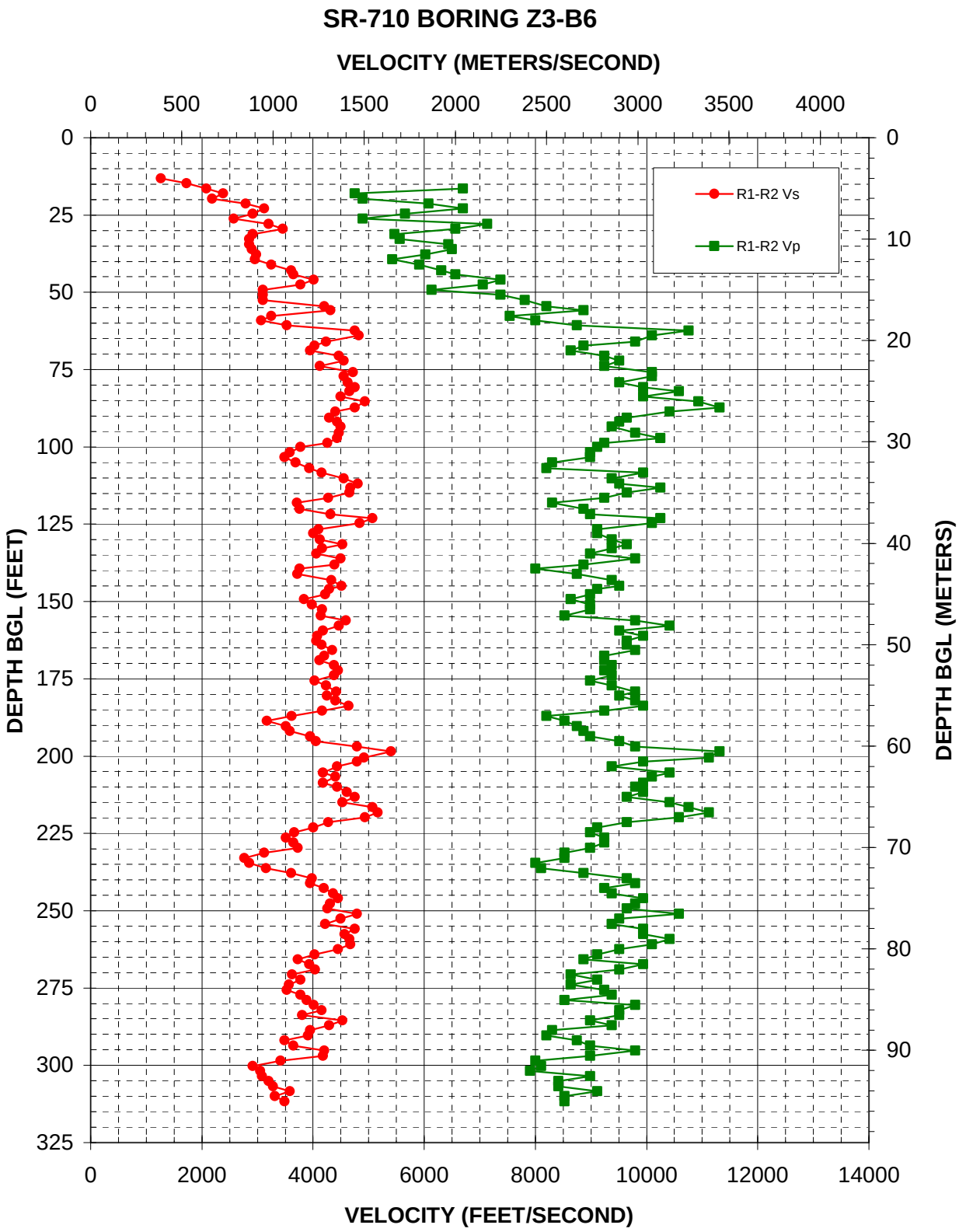

Figure 40: Boring Z3-B6, Suspension R1-R2 P- and S_H-wave velocities

Depth (feet)	V_s (feet/sec)	V_p (feet/sec)
13.12	1262	
14.76	1727	
16.40	2083	6696
18.04	2386	4755
19.69	2187	4897
21.33	2792	6076
22.97	3125	6696
24.61	2916	5657
26.25	2573	4897
27.89	3201	7132
29.53	3454	6562
31.17	2916	5468
32.81	2853	5561
34.45	2853	6433
36.09	2903	6497
37.73	2983	6020
39.37	2956	5423
41.01	3248	5911
42.98	3605	6309
44.29	3645	6562
45.93	4013	7373
47.57	3771	7056
49.21	3095	6132
50.85	3095	7373
52.49	3095	7812
54.46	4206	8202
55.77	4317	8867
57.74	3248	7542
59.06	3066	8002
60.70	3528	8749
62.34	4755	10757
63.98	4825	10095
65.94	4233	9794
67.26	4026	8867
68.90	3953	8634
70.54	4464	9242
72.18	4557	9510
73.82	4127	9242
75.79	4721	10095
77.10	4557	10095
79.07	4621	9510
80.71	4755	9942
82.02	4654	10583
83.66	4494	9942
85.30	4934	10936
87.27	4755	11313
88.58	4404	10415
90.55	4289	9650
91.86	4434	9510
93.50	4494	9374
95.47	4464	9794
97.11	4434	10253
98.75	4261	9242
100.07	3771	9113
101.71	3586	8989
103.35	3490	8989
104.99	3686	8306
106.96	3929	8202
108.27	4153	9942
110.24	4557	9374
111.88	4807	9510
113.19	4670	10253
114.83	4654	9650
116.47	4275	9242
118.11	3707	8306
120.08	3760	8867
121.72	4317	8989
123.03	5067	10253
124.67	4843	10095
126.64	4101	9113
127.95	4001	9113
129.92	4127	9374
131.56	4525	9650
132.87	4166	9374
134.51	4063	8989
136.15	4494	9794
138.12	4389	8867
139.44	3760	8002
141.08	3718	8749
143.04	4331	9374
145.01	4510	9510
146.00	4289	9113
147.64	4220	8989
149.28	3837	8634
150.92	3977	8989
152.56	4166	8989
154.53	4140	8522
156.17	4589	9794
157.81	4464	10415
159.45	4179	9510
161.09	4076	9942
162.73	4063	9650
164.04	4153	9650
165.68	4345	9794
167.65	4206	9242
168.96	4114	9242
170.60	4374	9374
172.24	4449	9242
173.88	4374	9374
175.52	4026	8989
177.17	4233	9374
179.13	4419	9794
180.45	4247	9510
182.09	4404	9794
183.73	4637	9942
185.37	4166	9242
187.01	3615	8202
188.65	3170	8522
190.29	3509	8749
191.93	3586	8867
193.57	3953	8989
195.21	4050	9510
196.85	4790	9794
198.49	5401	11313
200.46	4915	11121
201.77	4790	9942
203.41	4434	9374
205.38	4179	10415
206.69	4404	10095
208.66	4179	9942
209.97	4434	9794
211.61	4605	9942
213.25	4755	9650
214.90	4525	10415
216.54	5067	10757
218.18	5167	11121
219.82	4934	10583
221.46	4275	9650
223.10	4001	9113
224.74	3666	8989
226.38	3509	9242
228.02	3645	9242
229.66	3728	8989
231.30	3125	8522
232.94	2769	8522
234.58	2853	8002
236.22	3155	8101
237.86	3605	8867
239.50	3977	9650
241.14	3953	9794
242.78	4193	9242
244.42	4360	9374
246.06	4449	9942
247.70	4303	9794
249.34	4261	9650
250.98	4790	10583
252.62	4494	9510
254.27	4220	9374
255.91	4755	9942
257.55	4573	9942

Table 22. Boring Z3-B6, Suspension R1-R2 depths and P- and S_H-wave velocities

Depth (feet)	V_s (feet/sec)	V_p (feet/sec)
259.19	4654	10415
260.83	4670	10095
262.47	4449	9510
264.11	4026	9113
265.75	3728	8867
267.39	3929	9942
269.03	4038	9510
270.67	3625	8634
272.31	3771	9113
273.95	3566	8634
275.59	3528	9242
277.23	3771	9374
278.87	3883	8522
280.51	4013	9794
282.15	4153	9510
283.79	3804	9510
285.43	4525	8989
287.07	4289	9374
288.71	3953	8306
290.35	3906	8202
291.99	3490	8749
293.64	3645	8989
295.28	4206	9794
296.92	4179	8989
298.56	3418	8002
300.20	2916	8101
301.84	3052	7906
303.48	3081	8989
305.12	3201	8412
306.76	3281	8412
308.40	3586	9113
310.04	3314	8522
311.68	3490	8522

Table 22, continued. Boring Z3-B6, Suspension R1-R2 depths and P- and S_H-wave velocities

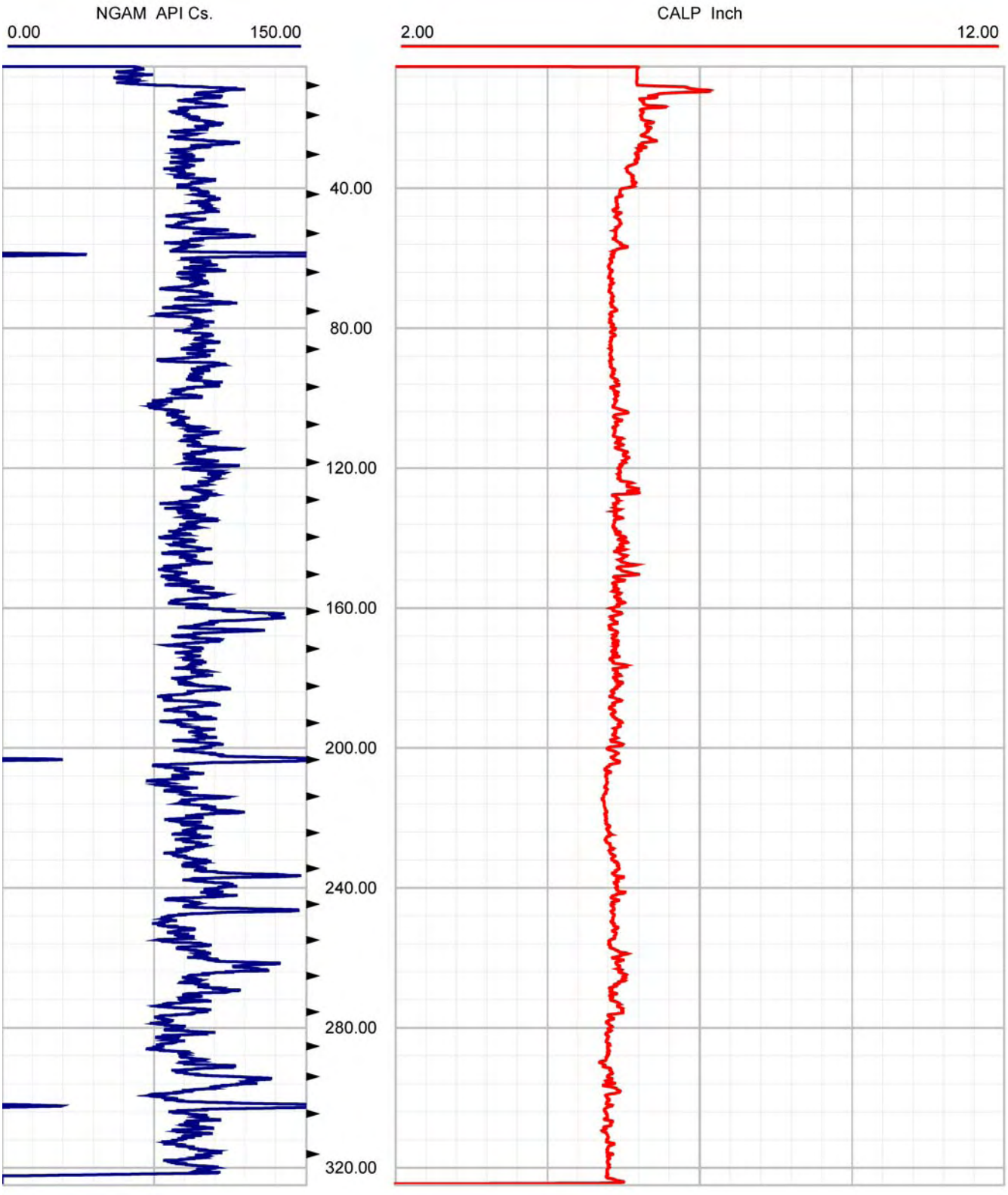

Figure 41. Boring Z3-B6, Caliper and Natural Gamma logs

DIP DATA INTERPRETATION
RGLDIP vsn 6.2
FRACTURE ANALYSIS STEREOGRAMS

CASCADE DRILLING

Borehole: Z3-B6

SR-710 TUNNEL INVESTIGATION

top of borehole.....
East:_
North:_
Elev:_

North ref: true
Depth units are feet

Zone from 285.973 to 45.665ft
Mean dip format: dip-azimuth and dip

Interpretation 1

Dip data sets .....
BHTV dips

Z3-B6
Zone 0. 45.665 - 285.973ft
Deviation 2.10 N 78.30

dipdata sets.....
BHTV dips
• Highlighted dips: Fracture Planar Hairline-fracture

	mean dip	n	f
N293 51	N293 51	7	(0.04)
N347 35	N347 35	4	(0.02)

intersections

	N293 51	N347 35
N293 51		35 N348
N347 35	35 N348	

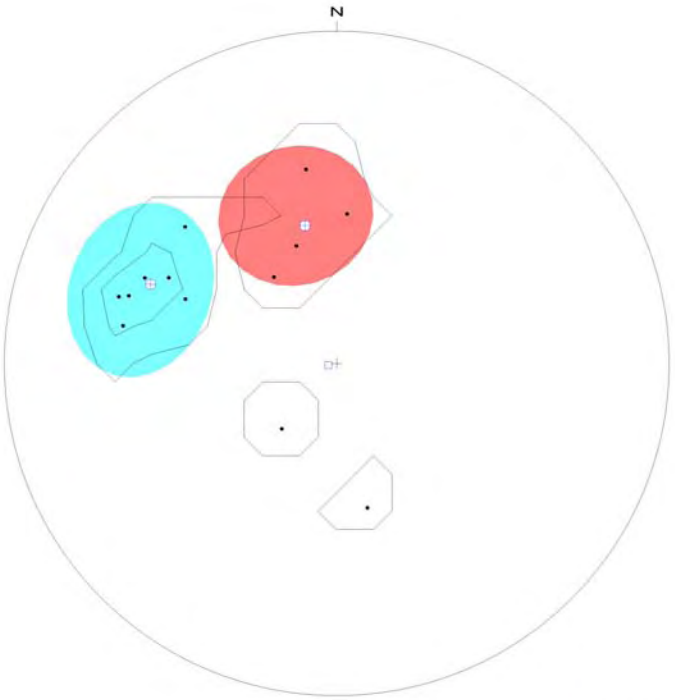

mean dip
well axis

equal-area upper-hemisphere 0-90
contour-levels 1,3,

Z3-B6, Interpretation 1 285.973 to 45.665ft 1

Figure 42. Boring Z3-B6, Stereonet Plot

Depth (feet)	Dip azimuth	Dip	Structure description
285.47	N351	49	Primary-structure Planar Bedding
267.80	N324	26	Primary-structure Planar Bedding
256.46	N004	37	Primary-structure Planar Bedding
255.27	N341	31	Primary-structure Planar Bedding
219.30	N312	52	Primary-structure Planar Bedding
108.50	N280	55	Primary-structure Planar Bedding
108.43	N288	56	Primary-structure Planar Bedding
97.24	N294	53	Primary-structure Planar Bedding
97.13	N287	58	Primary-structure Planar Bedding
63.31	N168	37	Primary-structure Planar Bedding
61.26	N220	21	Primary-structure Planar Bedding
46.68	N293	41	Primary-structure Planar Bedding
46.17	N297	47	Primary-structure Planar Bedding

Table 23. Boring Z3-B6, Structure depth, dip azimuth, dip and description

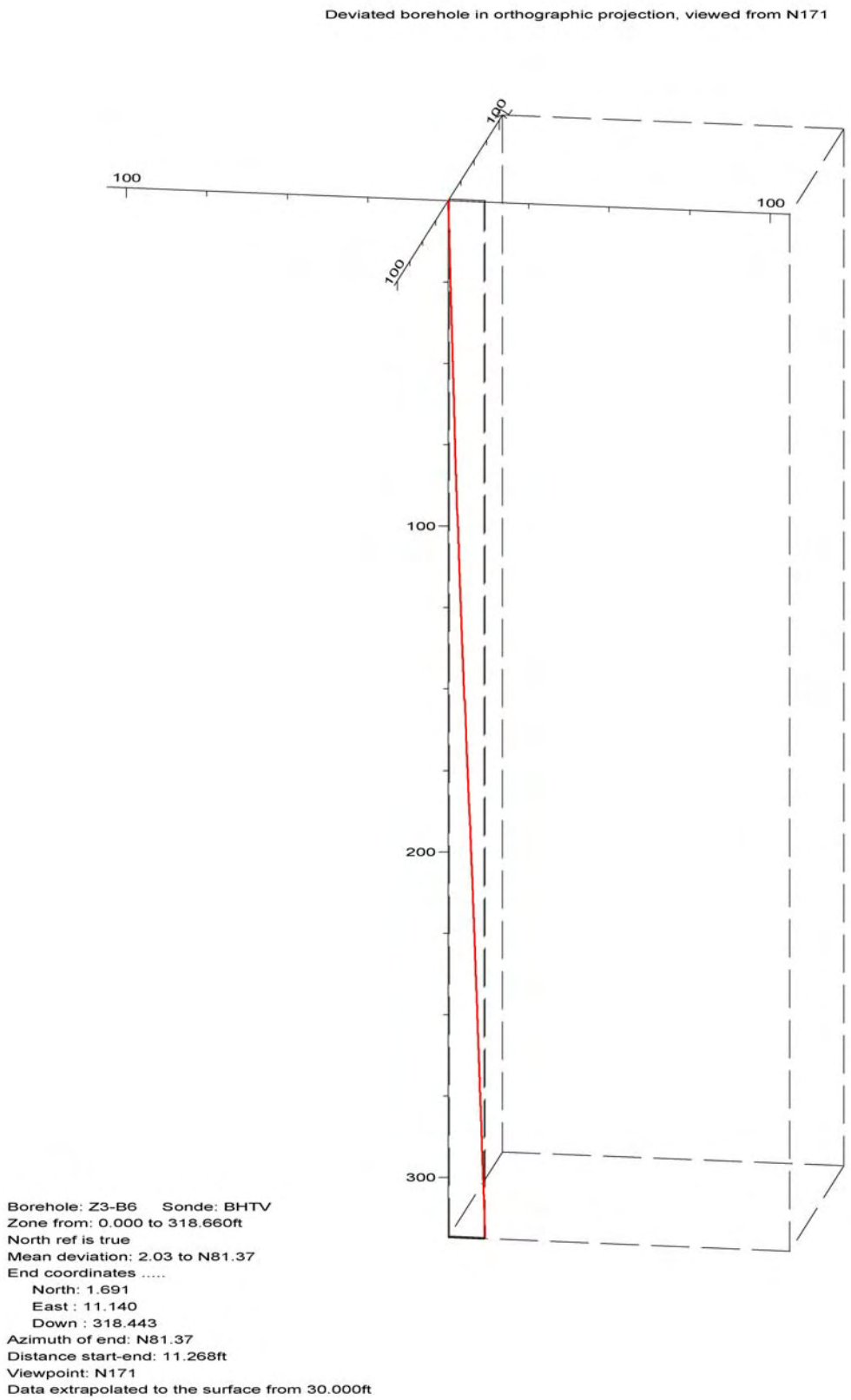

Figure 43. Boring Z3-B6, Deviation Projection

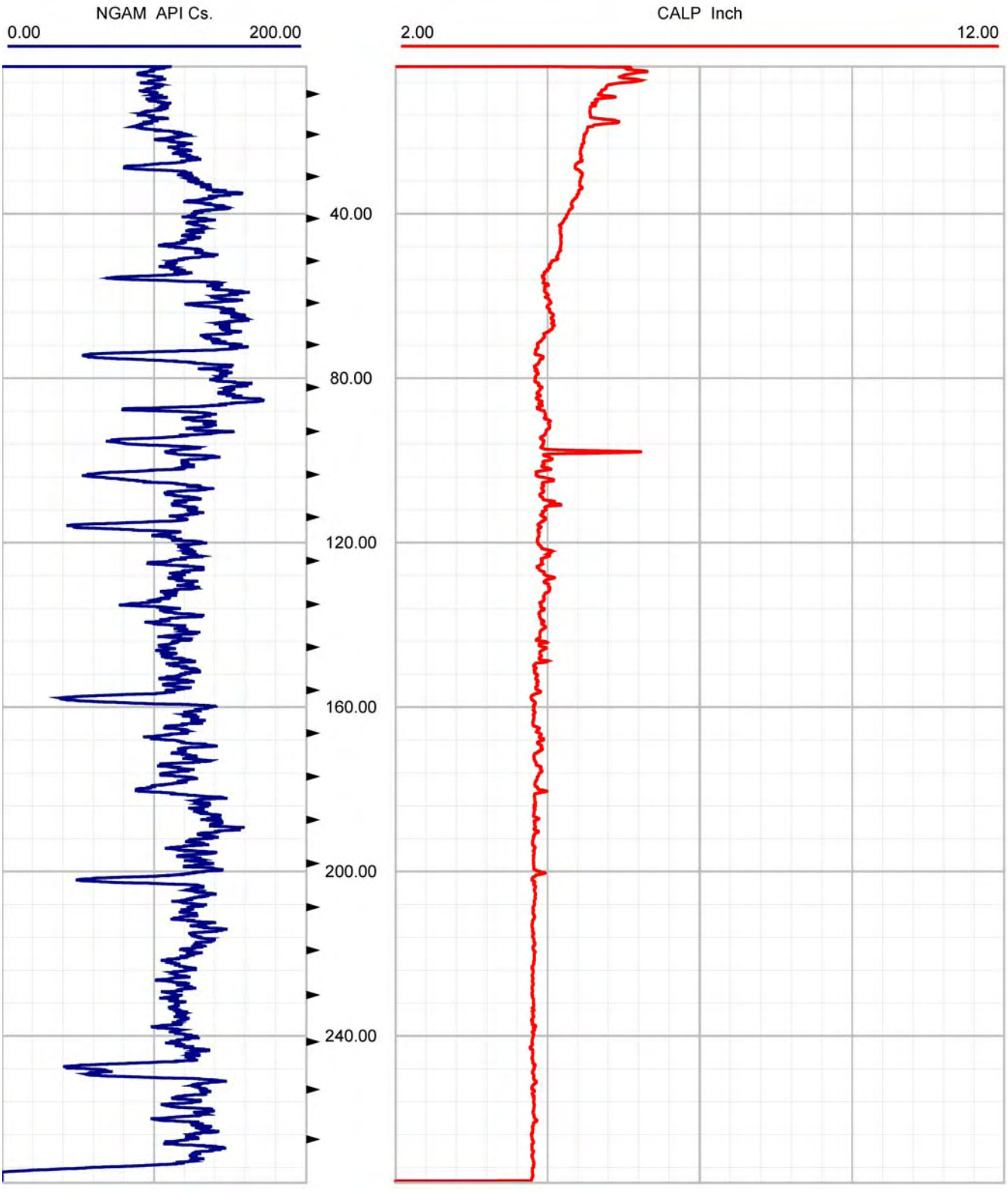

Figure 44. Boring Z3-B8, Caliper and Natural Gamma logs

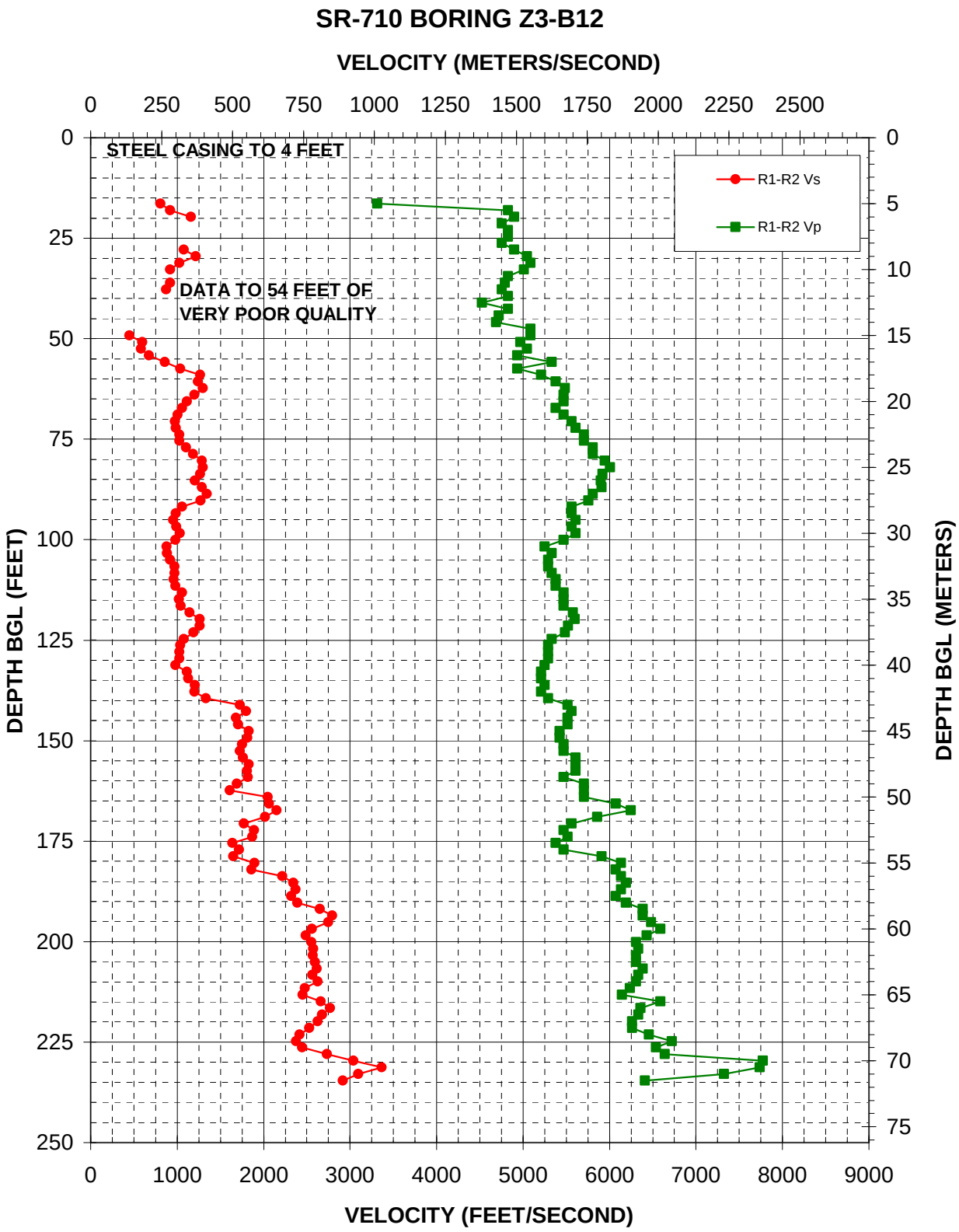

Figure 45: Boring Z3-B12, Suspension R1-R2 P- and S_H-wave velocities

Depth (feet)	V_s (feet/sec)	V_p (feet/sec)
8.20		
16.40	805	3314
18.04	918	4825
19.69	1161	4897
21.33		4755
22.97		4825
24.61		4825
26.25		4755
27.89	1076	4897
29.53	1215	5047
31.17	1025	5087
32.81	918	5009
34.45		4825
36.09	918	4790
37.73	875	4755
39.37		4825
41.01		4525
42.65		4825
44.29		4721
45.93		4687
47.57		5087
49.21	449	5087
50.85	599	4971
52.49	583	5047
54.13	676	4934
55.77	859	5335
57.41	1038	4934
59.06	1267	5208
60.70	1243	5378
62.34	1297	5486
63.98	1202	5468
65.62	1116	5468
67.26	1055	5378
68.90	1006	5468
70.54	976	5561
72.18	988	5608
73.82	1028	5706
75.46	1025	5706
77.10	1105	5807
78.74	1184	5807
80.38	1289	5944
82.02	1299	6009
83.66	1267	5922
85.30	1206	5901
86.94	1287	5911
88.58	1345	5807
90.22	1272	5756
91.86	1058	5561
93.50	988	5561
95.14	954	5608
96.78	991	5561
98.43	1032	5608
100.07	982	5468
101.71	877	5249
103.35	882	5335
104.99	922	5292
106.63	971	5292
108.27	971	5335
109.91	959	5378
111.55	979	5378
113.19	1058	5468
114.83	1020	5468
116.47	1043	5468
118.11	1143	5580
119.75	1262	5599
121.39	1259	5523
123.03	1191	5486
124.67	1079	5335
126.31	1035	5292
127.95	1025	5292
129.59	1028	5292
131.23	982	5249
132.87	1112	5208
134.51	1131	5208
136.15	1206	5249
137.80	1202	5208
139.44	1334	5292
141.08	1727	5514
142.72	1798	5561
144.36	1682	5514
146.00	1704	5514
147.64	1828	5423
149.28	1813	5423
150.92	1750	5468
152.56	1727	5468
154.20	1764	5608
155.84	1828	5608
157.48	1808	5608
159.12	1818	5468
160.76	1691	5706
162.40	1608	5706
164.04	2051	5706
165.68	2063	6076
167.32	2151	6249
168.96	2019	5859
170.60	1773	5561
172.24	1891	5468
173.88	1869	5514
175.52	1640	5378
177.17	1718	5468
178.81	1649	5911
180.45	1896	6132
182.09	1859	6076
183.73	2217	6132
185.37	2343	6190
187.01	2369	6132
188.65	2319	6076
190.29	2390	6190
191.93	2651	6383
193.57	2792	6383
195.21	2745	6484
196.85	2558	6588
198.49	2485	6433
200.13	2553	6309
201.77	2573	6334
203.41	2568	6309
205.05	2594	6309
206.69	2614	6383
208.33	2563	6334
209.97	2625	6309
211.61	2476	6237
213.25	2453	6144
214.90	2662	6588
216.54	2769	6358
218.18	2678	6334
219.82	2625	6261
221.46	2529	6261
223.10	2417	6458
224.74	2377	6723
226.38	2448	6536
228.02	2734	6641
229.66	3038	7774
231.30	3365	7738
232.94	3095	7323
234.58	2916	6408

NOTE: “blank” space indicates data of insufficient quality for good pick. See Appendix A for Source-to-Receiver measurement.

Table 24. Boring Z3-B12, Suspension R1-R2 depths and P- and S_H-wave velocities

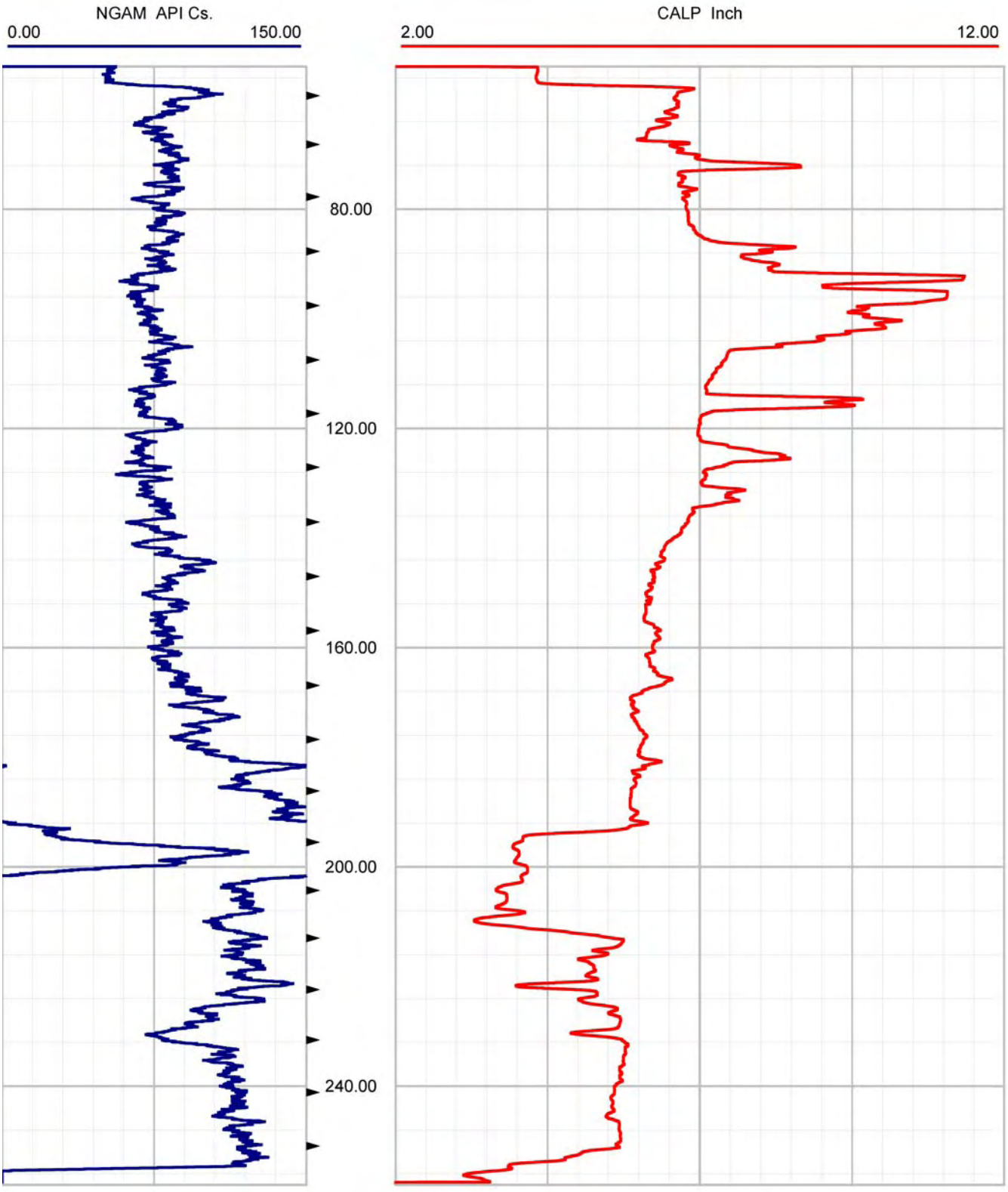

Figure 46. Boring Z3-B12, Caliper and Natural Gamma logs

DIP DATA INTERPRETATION
RGLDIP vsn 6.2
FRACTURE ANALYSIS STEREOGRAMS

CASCADE DRILLING

Borehole: Z3-B12

SR-710 TUNNEL INVESTIGATION

top of borehole.....
East:_
North:_
Elev:_

North ref: true
Depth units are feet

Zone from 179.361 to 113.631ft
Mean dip format: dip-azimuth and dip

Interpretation 1

Dip data sets .....
BHTV dips

Z3-B12
Zone 0. 113.631 - 179.351ft
Deviation 0.20 N234.00

dipdata sets.....
BHTV dips
• Highlighted dips: Fracture Planar Open-fracture

	mean dip	n	f
N175 56	N175 56	17	0.47
N351 26	N351 26	1	(0.00)

intersections

	N175 56	N351 26
N175 56		01 N264
N351 26	01 N264	

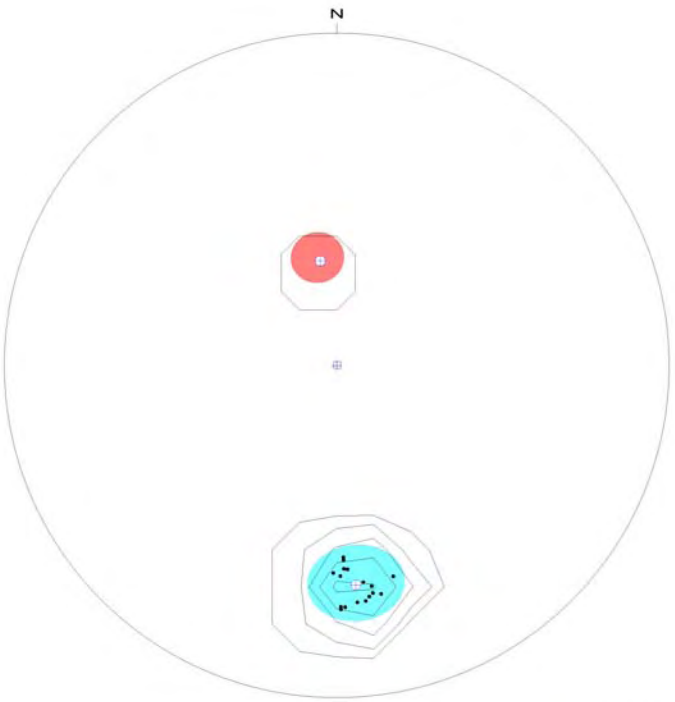

equal-area upper-hemisphere 0-90
contour-levels 1,3,6,10,15,

Z3-B12, Interpretation 1 179.351 to 113.631ft 1

Figure 47. Boring Z3-B12, Stereonet Plot

Depth (feet)	Dip azimuth	Dip	Structure description
178.86	N179	62	Primary-structure Planar Bedding
178.55	N179	63	Primary-structure Planar Bedding
177.99	N178	62	Primary-structure Planar Bedding
176.93	N175	61	Primary-structure Planar Bedding
176.29	N173	61	Primary-structure Planar Bedding
174.71	N172	60	Primary-structure Planar Bedding
162.82	N171	57	Primary-structure Planar Bedding
162.36	N169	59	Primary-structure Planar Bedding
161.74	N165	55	Primary-structure Planar Bedding
159.94	N171	59	Primary-structure Planar Bedding
157.05	N179	53	Primary-structure Planar Bedding
156.16	N173	55	Primary-structure Planar Bedding
152.02	N178	49	Primary-structure Planar Bedding
150.86	N178	48	Primary-structure Planar Bedding
148.50	N178	51	Primary-structure Planar Bedding
146.45	N181	53	Primary-structure Planar Bedding
131.08	N177	52	Primary-structure Planar Bedding
114.13	N351	26	Primary-structure Planar Bedding

Table 25. Boring Z3-B12, Structure depth, dip azimuth, dip and description

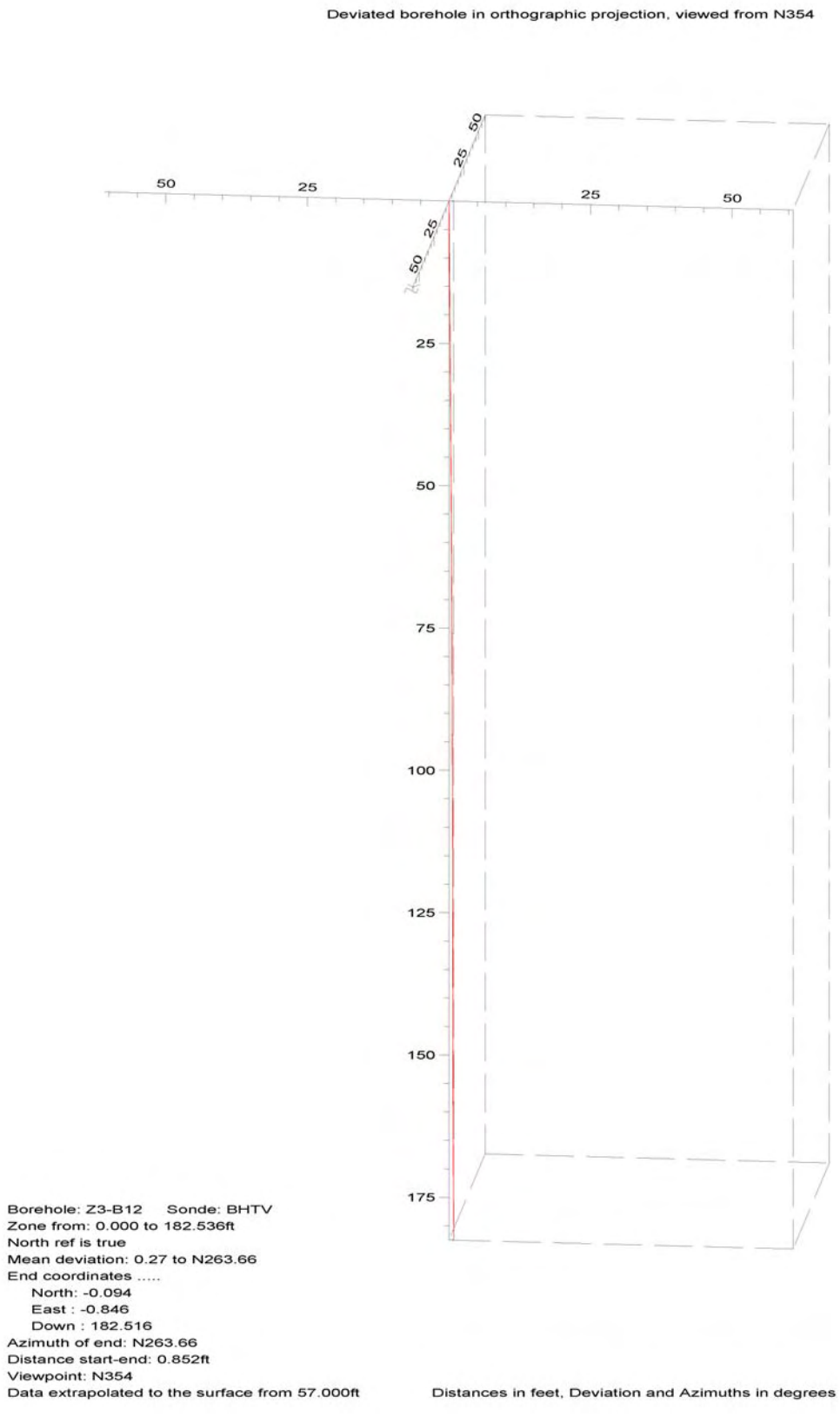

Figure 48. Boring Z3-B12, Deviation Projection

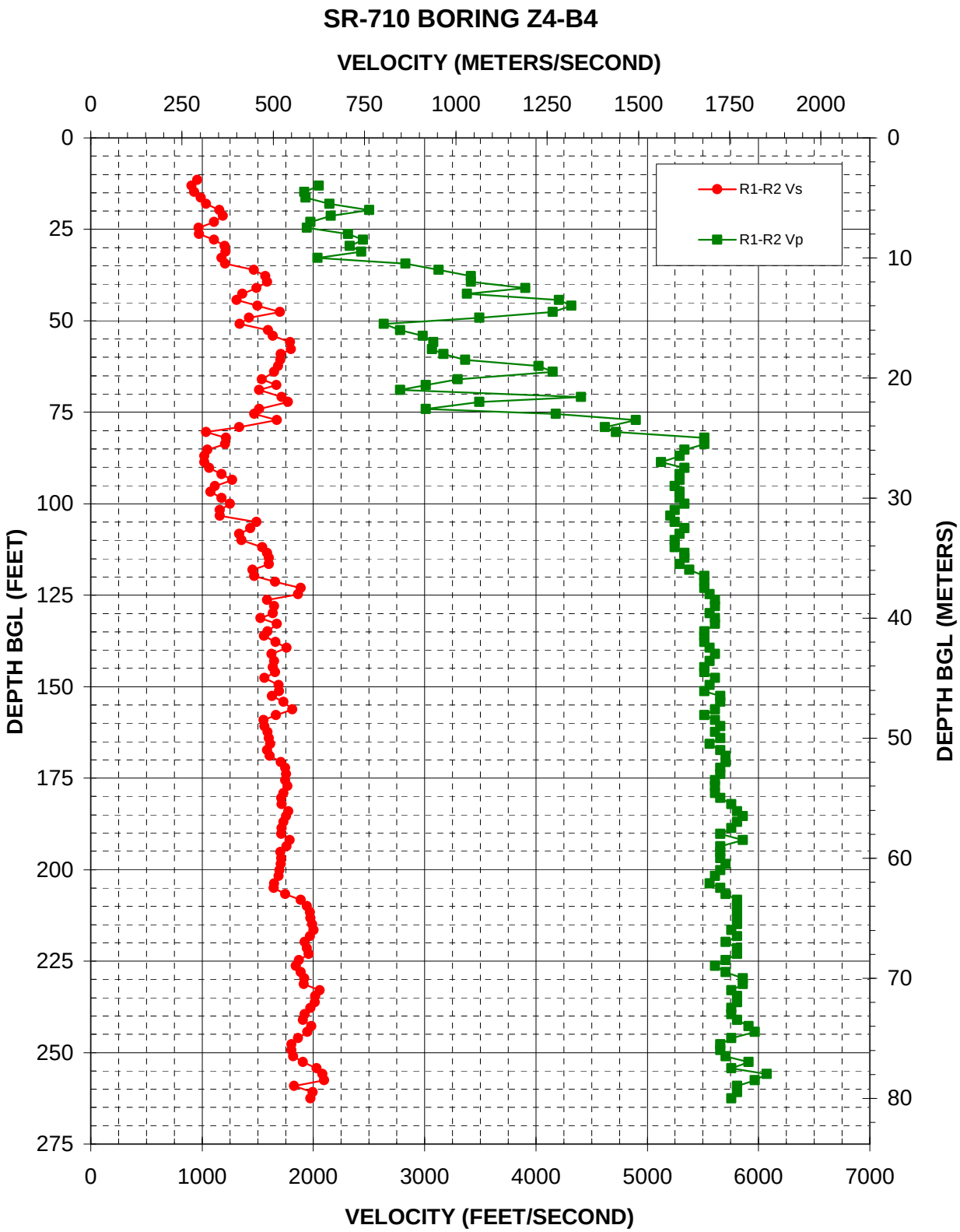

Figure 49: Boring Z4-B4, Suspension R1-R2 P- and S_H-wave velocities

Depth (feet)	V_s (feet/sec)	V_p (feet/sec)
11.48	958	
13.12	904	2051
14.76	929	1919
16.40	991	1930
18.04	1035	2144
19.69	1155	2504
21.33	1189	2158
22.97	1108	1976
24.61	968	1941
26.25	974	2310
27.89	1108	2448
29.53	1202	2327
31.17	1211	2430
32.81	1176	2038
34.45	1206	2828
36.09	1465	3125
37.73	1570	3418
39.37	1585	3418
41.01	1491	3906
42.65	1361	3382
44.29	1312	4206
45.93	1498	4317
47.57	1700	4153
49.21	1420	3490
50.85	1339	2635
52.49	1593	2780
54.13	1636	2983
55.77	1793	3081
57.74	1798	3066
59.06	1709	3170
60.70	1704	3365
62.34	1682	4026
63.98	1649	4153
65.94	1537	3297
67.59	1670	3010
68.90	1512	2780
70.87	1718	4404
72.18	1773	3490
74.15	1512	3010
75.46	1471	4179
77.10	1674	4897
79.07	1334	4621
80.38	1038	4721
82.02	1215	5514
83.66	1206	5514
85.30	1048	5335
86.94	1022	5292
88.58	1022	5126
90.22	1065	5335
91.86	1176	5292
93.50	1272	5292
95.14	1116	5249
96.78	1076	5292
98.43	1176	5292
100.07	1252	5335
101.71	1159	5249
103.35	1159	5208
104.99	1491	5249
106.63	1433	5335
108.27	1334	5292
109.91	1356	5249
111.88	1540	5249
113.52	1585	5335
114.83	1600	5335
116.47	1600	5292
118.11	1455	5378
119.75	1468	5514
121.39	1657	5514
123.03	1886	5514
124.67	1864	5561
126.31	1585	5608
127.95	1649	5608
129.92	1636	5561
131.23	1526	5608
132.87	1674	5608
134.84	1589	5514
136.15	1559	5514
137.80	1661	5514
139.44	1759	5561
141.08	1624	5608
143.04	1649	5561
144.69	1636	5514
146.00	1657	5514
147.64	1562	5608
149.61	1687	5561
151.25	1691	5514
152.56	1628	5657
154.20	1731	5657
156.17	1813	5608
157.81	1665	5514
159.12	1555	5608
160.76	1562	5657
162.40	1589	5608
164.04	1600	5657
165.68	1612	5561
167.32	1585	5657
168.96	1608	5706
170.60	1709	5706
172.24	1750	5657
173.88	1754	5657
175.52	1750	5608
177.17	1769	5608
179.13	1731	5608
180.45	1713	5657
182.09	1718	5756
184.06	1776	5807
185.37	1754	5859
187.01	1731	5807
188.65	1718	5756
190.29	1713	5657
191.93	1788	5859
193.57	1759	5657
195.21	1704	5657
196.85	1713	5657
198.49	1709	5706
200.13	1696	5657
201.77	1687	5608
203.74	1649	5561
205.05	1645	5657
206.69	1750	5706
208.33	1886	5807
209.97	1941	5807
211.61	1970	5807
213.25	1976	5807
214.90	1988	5807
216.54	2001	5756
218.18	1970	5807
219.82	1924	5706
221.46	1941	5807
223.10	1959	5807
224.74	1869	5706
226.38	1843	5608
228.02	1886	5706
229.66	1919	5859
231.30	1913	5859
232.94	2057	5756
234.58	2019	5807
236.22	2013	5807
237.86	1976	5756
239.50	1924	5756
241.14	1907	5807
242.78	1982	5911
244.42	1947	5965
246.06	1864	5756
247.70	1803	5657
249.34	1803	5657
250.98	1818	5706
252.62	1907	5911
254.27	2031	5756
255.91	2083	6076

Table 26. Boring Z4-B4, Suspension R1-R2 depths and P- and S_H-wave velocities

Depth (feet)	V_s (feet/sec)	V_p (feet/sec)
257.55	2096	5965
259.19	1828	5807
260.83	1994	5807
262.47	1976	5756

Table 26, continued. Boring Z4-B4, Suspension R1-R2 depths and P- and S_H-wave velocities

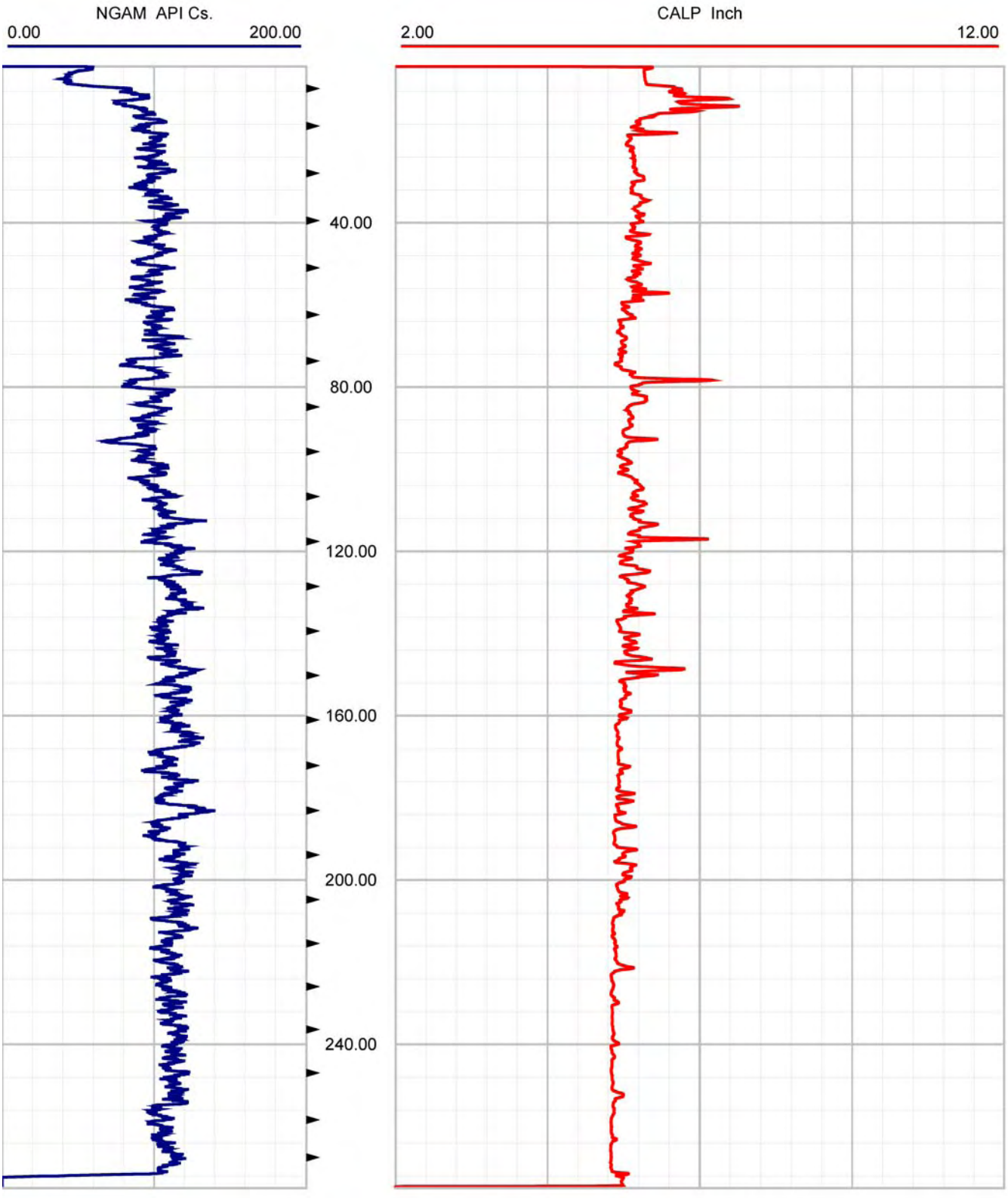

Figure 50. Boring Z4-B4, Caliper and Natural Gamma logs

DIP DATA INTERPRETATION
RGLDIP vsn 6.2
FRACTURE ANALYSIS STEREOGRAMS

CASCADE DRILLING

Borehole: Z4-B4

SR-710 TUNNEL INVESTIGATION

top of borehole.....
East:_
North:_
Elev:_

North ref: true
Depth units are feet

Zone from 274.222 to 17.723ft
Mean dip format: dip-azimuth and dip

Interpretation 1

Dip data sets .....
BHTV dips

Z4-B4
Zone 0. 17.723 - 274.222ft
Deviation 0.60 N356.10

dipdata sets.....
BHTV dips
• Highlighted dips: Fracture Planar Hairline-fracture

	mean dip	n	f
N088 72	N088 72	10	(0.13)
N238 37	N238 37	5	(0.02)
N156 6	N156 6	7	(0.03)
N314 68	N314 68	3	(0.03)

intersections

	N088 72	N238 37	N156 6	N314 68
N088 72		17 N172	06 N176	47 N018
N238 37	17 N172		06 N156	37 N242
N156 6	06 N176	06 N156		02 N225
N314 68	47 N018	37 N242	02 N225	

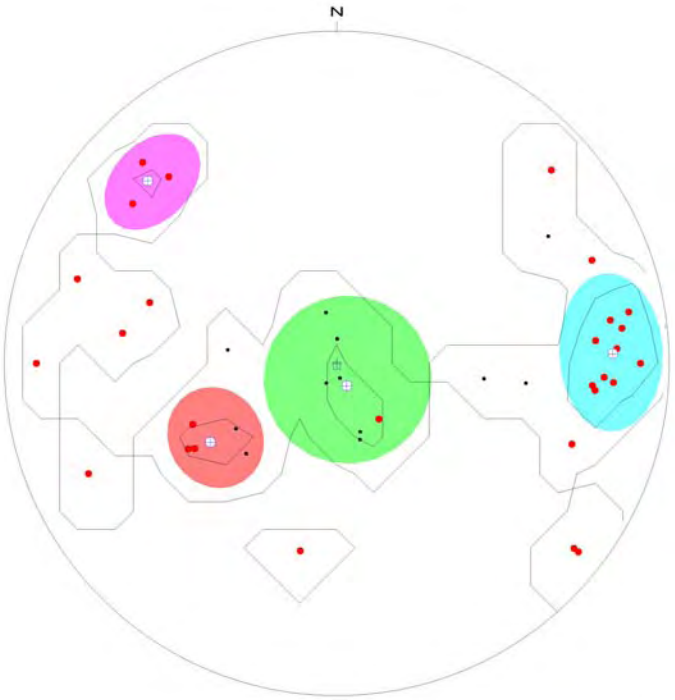

equal-area upper-hemisphere 0-90
contour-levels 1,3,

Z4-B4, Interpretation 1 274.222 to 17.723ft 1

Figure 51. Boring Z4-B4, Stereonet Plot

Depth (feet)	Dip azimuth	Dip	Structure description
273.72	N318	65	Fracture Planar Hairline-fracture
273.28	N316	73	Fracture Planar Hairline-fracture
269.47	N308	67	Fracture Planar Hairline-fracture
257.47	N239	41	Fracture Planar Hairline-fracture
245.93	N109	64	Fracture Planar Hairline-fracture
208.70	N143	17	Fracture Planar Hairline-fracture
187.06	N001	6	Primary-structure Planar Bedding
182.56	N128	81	Fracture Planar Hairline-fracture
173.49	N128	80	Fracture Planar Hairline-fracture
172.05	N068	72	Fracture Planar Hairline-fracture
168.70	N208	6	Primary-structure Planar Bedding
168.04	N168	4	Primary-structure Planar Bedding
159.96	N083	75	Fracture Planar Hairline-fracture
159.55	N240	43	Fracture Planar Hairline-fracture
155.97	N247	39	Fracture Planar Hairline-fracture
152.85	N288	50	Fracture Planar Hairline-fracture
152.03	N191	48	Fracture Planar Hairline-fracture
150.23	N094	72	Fracture Planar Hairline-fracture
146.46	N085	67	Fracture Planar Hairline-fracture
145.99	N081	72	Fracture Planar Hairline-fracture
144.45	N246	71	Fracture Planar Hairline-fracture
142.84	N087	73	Fracture Planar Hairline-fracture
140.85	N288	71	Fracture Planar Hairline-fracture
121.97	N080	78	Fracture Planar Hairline-fracture
121.13	N095	66	Fracture Planar Hairline-fracture
120.84	N096	67	Fracture Planar Hairline-fracture
120.50	N093	69	Fracture Planar Hairline-fracture
118.41	N090	81	Fracture Planar Hairline-fracture
118.05	N278	55	Fracture Planar Hairline-fracture
117.53	N225	32	Primary-structure Planar Bedding
117.11	N096	37	Primary-structure Planar Bedding
114.88	N277	27	Primary-structure Planar Bedding
113.08	N270	80	Fracture Planar Hairline-fracture
112.28	N048	76	Fracture Planar Hairline-fracture
98.48	N059	63	Primary-structure Planar Bedding
78.32	N096	48	Primary-structure Planar Bedding
43.39	N237	30	Primary-structure Planar Bedding
35.14	N348	13	Primary-structure Planar Bedding
18.61	N161	18	Primary-structure Planar Bedding
18.22	N163	20	Primary-structure Planar Bedding

Table 27. Boring Z4-B4, Structure depth, dip azimuth, dip and description

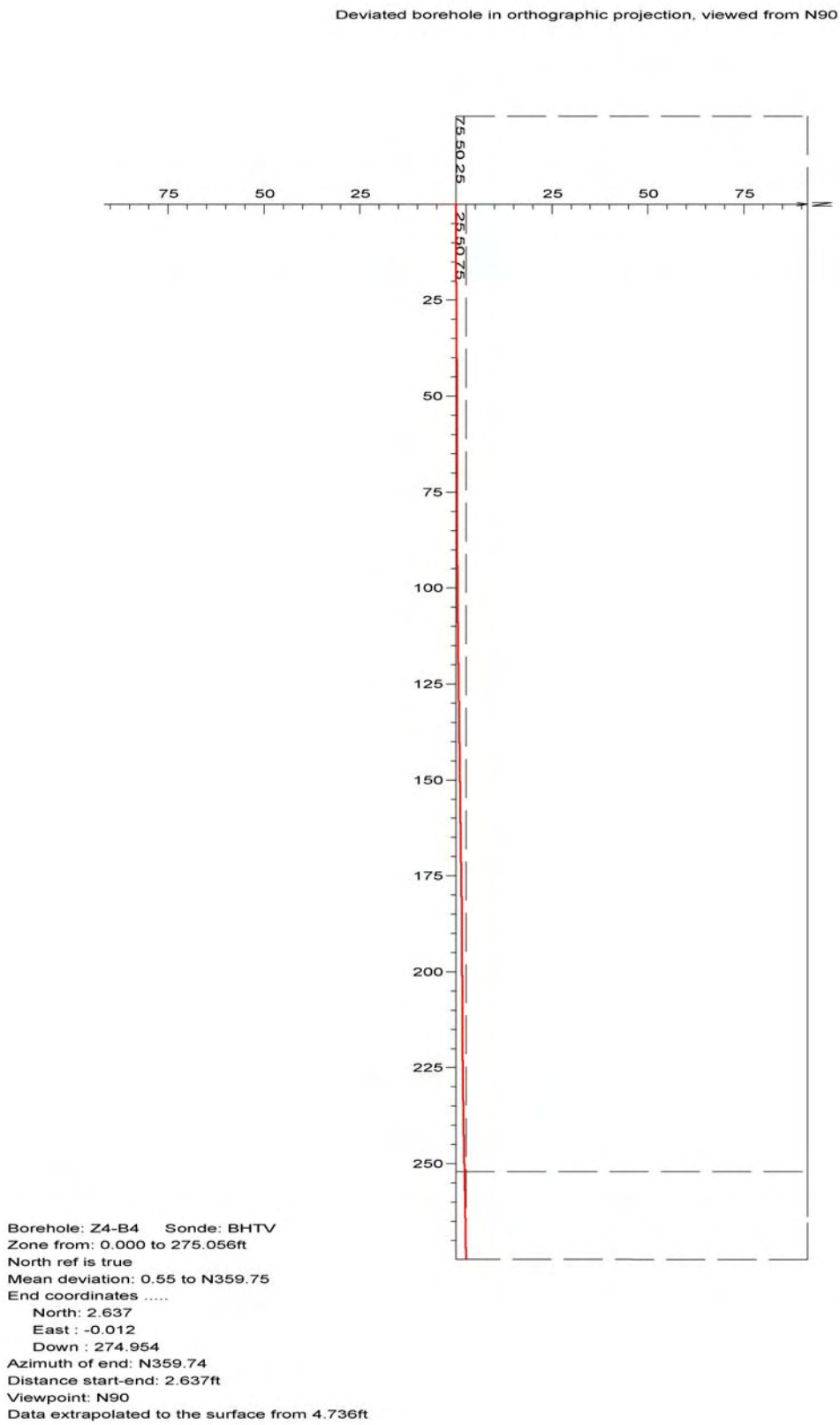

Figure 52. Boring Z4-B4, Deviation Projection

This page left intentionally blank

APPENDIX A

SUSPENSION VELOCITY MEASUREMENT QUALITY ASSURANCE SUSPENSION SOURCE TO RECEIVER ANALYSIS RESULTS

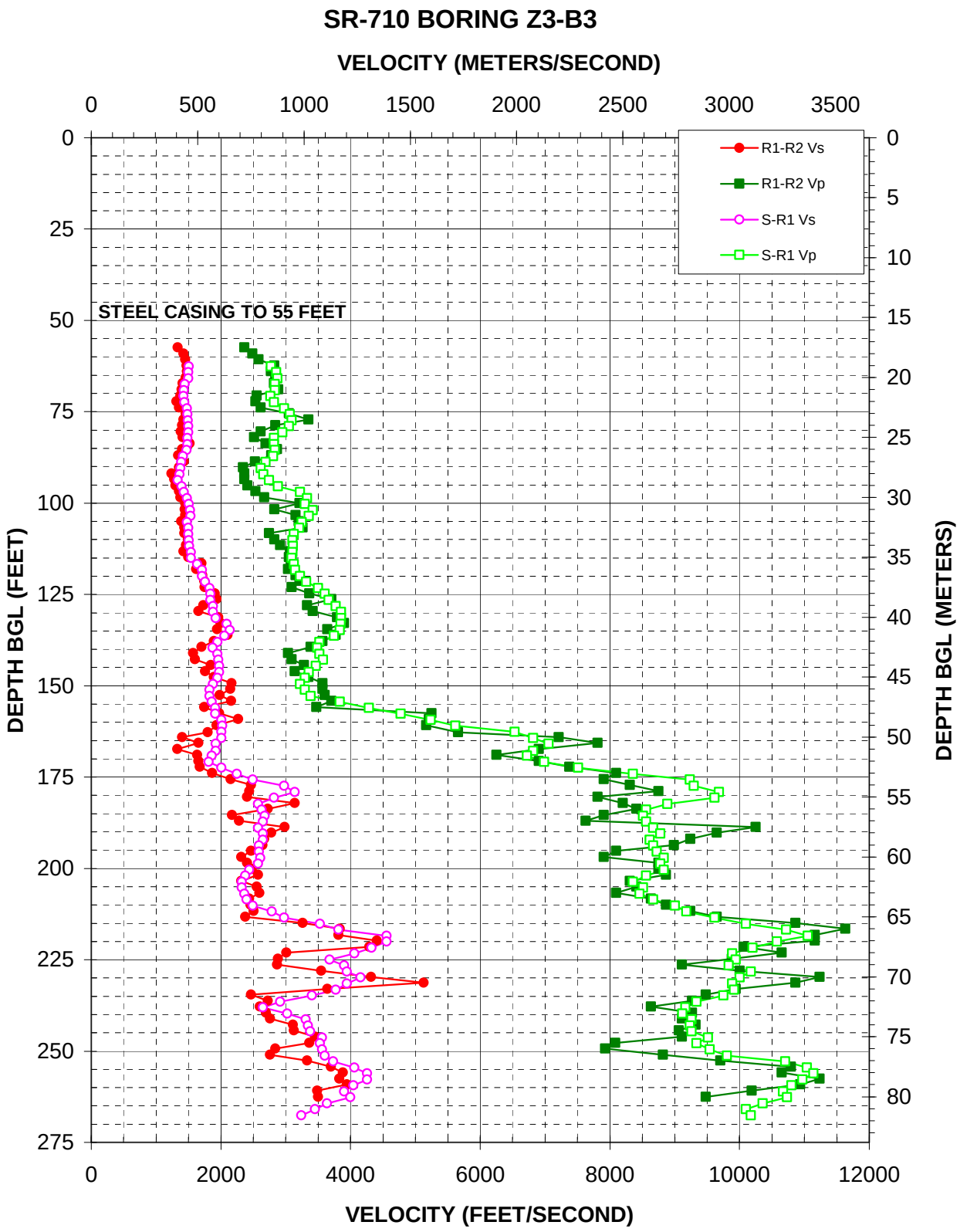

Figure A-8. Boring Z3-B3, R1 - R2 high resolution analysis and S - R1 quality assurance analysis P- and S_H-wave data

Depth (feet)	V_s (feet/sec)	V_p (feet/sec)
62.57	1503	2775
64.21	1497	2854
65.85	1497	2872
67.49	1445	2831
69.13	1430	2831
70.77	1424	2764
72.41	1437	2820
74.05	1478	2975
75.69	1484	3066
77.33	1491	3093
78.97	1497	3053
80.61	1497	2950
82.25	1484	2820
83.89	1484	2820
85.53	1469	2831
87.17	1418	2803
88.81	1388	2690
90.45	1377	2615
92.09	1363	2654
93.73	1337	2743
95.37	1399	2877
97.01	1430	3221
98.65	1478	3327
100.30	1503	3296
101.94	1526	3417
103.58	1533	3359
105.22	1478	3250
106.86	1497	3206
108.50	1497	3127
110.14	1505	3107
111.78	1510	3114
113.42	1540	3107
115.06	1540	3093
116.70	1633	3127
118.34	1712	3148
119.98	1712	3221
121.62	1760	3320
123.26	1828	3502
124.90	1838	3601
126.54	1838	3666
128.18	1882	3775
129.82	1882	3858
131.46	1924	3858
133.10	2090	3847
134.74	2141	3837
136.38	2059	3745
138.02	1950	3519
139.67	1872	3484
141.31	1950	3519
142.95	1961	3573
144.59	1972	3467
146.23	1972	3359
147.87	1950	3296
149.51	1882	3221
151.15	1828	3296
152.79	1828	3384
154.43	1857	3837
156.07	1913	4281
157.71	1913	4776
159.35	2012	5240
160.99	2023	5617
162.63	2012	6531
164.27	2012	6817
165.91	1924	7056
167.88	1924	6817
169.19	1857	6719
170.83	1810	6986
172.47	2012	7509
174.11	2250	8358
175.75	2490	9238
177.40	2975	9299
179.04	3141	9684
180.68	2820	9618
182.32	2572	8887
183.96	2630	8562
185.60	2675	8510
187.24	2649	8562
188.88	2572	8668
190.52	2649	8776
192.16	2649	8615
193.80	2591	8668
195.44	2591	8722
197.08	2610	8831
198.72	2572	8776
200.36	2438	8831
202.00	2380	8562
203.64	2325	8358
205.28	2325	8510
206.92	2364	8459
208.56	2396	8668
210.20	2490	9001
211.84	2786	9178
213.48	2975	9618
215.12	3528	10102
216.77	3816	10719
218.41	4559	11057
220.05	4559	10574
221.69	4323	10205
223.33	4058	9889
224.97	3676	9945
226.61	3901	9833
228.25	3944	10175
229.89	4154	10001
231.53	3944	9889
233.17	3775	9917
234.81	3408	9751
236.45	2913	9336
238.09	2649	9166
239.73	3026	9118
241.37	3312	9263
243.01	3343	9238
244.65	3375	9263
246.29	3564	9514
247.93	3528	9336
249.57	3564	9539
251.21	3601	9806
252.85	3735	10703
254.49	4058	11039
256.14	4255	11144
257.78	4255	10970
259.42	4047	10802
261.06	3901	10670
262.70	4001	10735
264.34	3638	10355
265.98	3450	10102
267.62	3243	10175

Table A-8. Boring Z3-B3, S - R1 quality assurance analysis P- and S_H-wave data

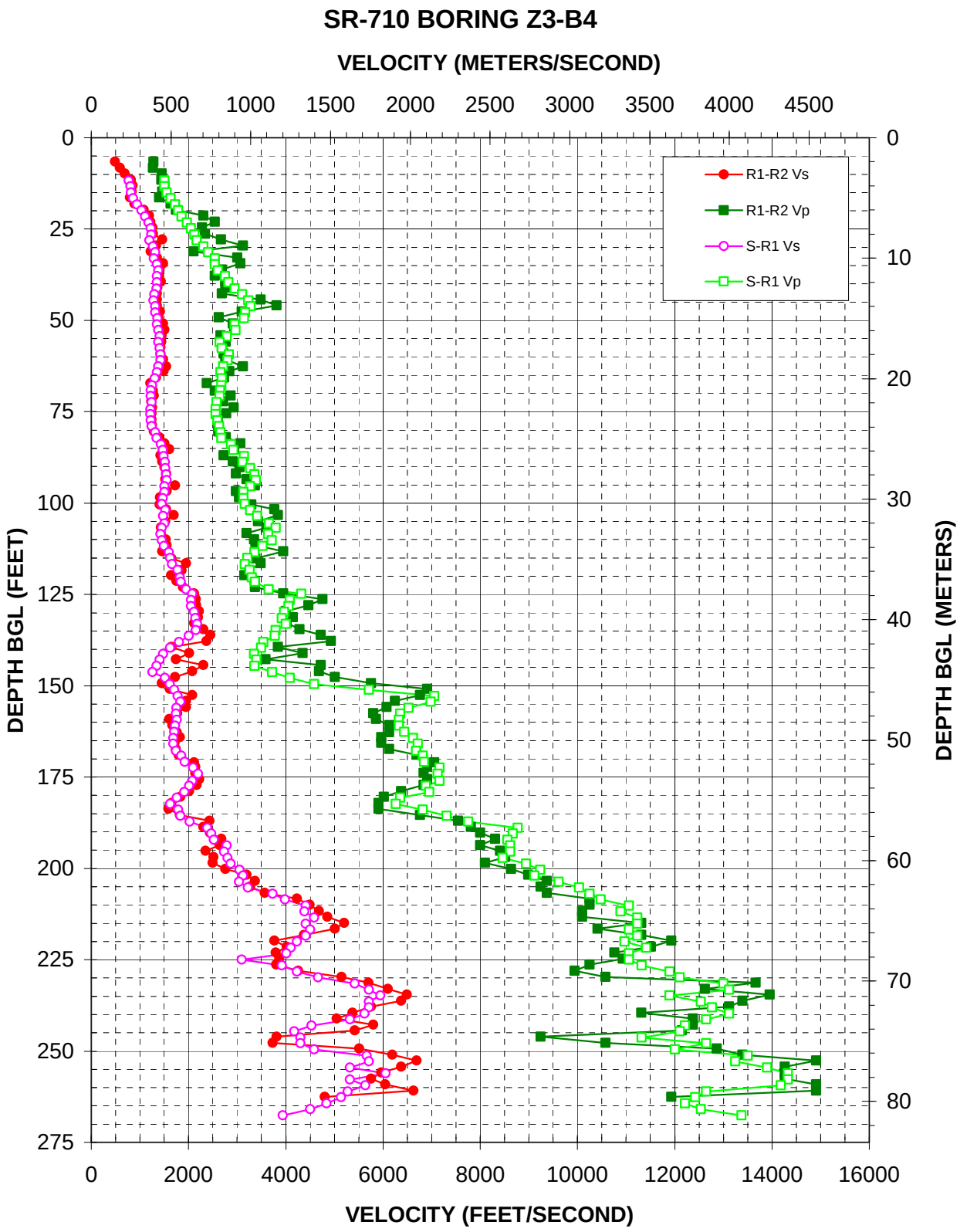

Figure A-9. Boring Z3-B4, R1 - R2 high resolution analysis and S - R1 quality assurance analysis P- and S_H-wave data

Depth (feet)	V_s (feet/sec)	V_p (feet/sec)
11.71	767	1510
13.35	807	1510
14.99	815	1550
16.63	858	1633
18.27	941	1721
19.91	1034	1791
21.56	1111	1862
23.20	1182	1972
24.84	1227	2053
26.48	1236	2128
28.12	1198	2174
29.76	1272	2302
31.40	1315	2404
33.04	1286	2544
34.68	1350	2544
36.32	1382	2610
37.96	1355	2753
39.60	1355	2820
41.24	1340	2950
42.88	1295	3107
44.52	1281	3235
46.16	1315	3281
47.80	1315	3170
49.44	1361	3141
51.08	1355	2950
52.72	1377	2969
54.36	1410	2786
56.00	1377	2644
57.64	1410	2690
59.28	1427	2837
60.93	1427	2803
62.57	1377	2711
64.21	1350	2659
65.85	1305	2690
67.81	1254	2680
69.13	1227	2654
70.77	1227	2639
72.41	1240	2581
74.38	1219	2562
75.69	1219	2562
77.33	1227	2600
78.97	1245	2630
80.61	1315	2659
82.25	1345	2675
83.89	1433	2877
85.53	1469	2925
87.17	1487	3141
88.81	1513	3114
90.45	1526	3273
92.09	1540	3359
93.73	1553	3384
95.37	1507	3273
97.01	1507	3134
98.65	1469	3134
100.30	1451	3163
101.94	1526	3273
103.58	1481	3417
105.54	1507	3657
106.86	1457	3795
108.50	1427	3638
110.14	1451	3715
111.78	1500	3519
113.42	1596	3359
115.06	1625	3213
116.70	1664	3163
118.34	1782	3258
120.31	1828	3304
121.62	1848	3367
123.59	1950	3647
124.90	2077	4321
126.54	2053	4082
128.18	2053	4058
129.82	2115	3967
131.46	2141	3922
133.10	2180	4001
134.74	2154	3795
136.38	2006	3775
138.02	1810	3546
139.67	1625	3493
141.31	1478	3351
142.95	1404	3400
144.59	1348	3359
146.23	1258	3725
147.87	1513	4082
149.51	1618	4589
151.15	1704	5708
152.79	1782	7056
154.43	1838	6986
156.07	1755	6531
157.71	1747	6354
159.35	1760	6325
160.99	1721	6325
162.63	1708	6441
164.27	1688	6624
165.91	1692	6719
167.88	1747	6687
169.19	1853	6817
170.83	1924	6850
172.47	2102	7164
174.11	2194	7128
176.08	2077	7164
177.40	2012	6883
179.04	1918	6951
180.68	1764	6354
182.32	1621	6269
183.96	1791	6817
185.60	1833	7314
187.24	2023	7758
188.88	2388	8776
190.52	2472	8668
192.16	2526	8562
193.80	2786	8615
195.44	2732	8615
197.08	2808	8459
198.72	2866	8944
200.36	3053	9238
202.00	3120	9118
203.64	3039	9618
205.28	3221	10030
206.92	3735	10250
208.56	3989	10479
210.20	4416	11057
211.84	4388	10885
213.48	4589	11234
215.12	4416	11234
216.77	4501	11057
218.41	4416	11234
220.05	4230	10970
221.69	4106	11416
223.33	4012	11057
224.97	3093	11057
226.61	3922	11324
228.25	4230	11900
229.89	4665	12105
231.53	5422	13002
233.17	5708	13123
234.81	5950	11900
236.45	5708	12537
238.09	5708	12765
239.73	5617	13123
241.37	5319	12650
243.01	4530	12210
244.65	4179	12105
246.29	4307	11324
247.93	4307	12650
249.57	4589	12002
251.21	5662	13502
252.85	5708	13247
254.49	5319	13903
256.14	6053	14329

Table A-9. Boring Z3-B4, S - R1 quality assurance analysis P- and S_H-wave data

Depth (feet)	V_s (feet/sec)	V_p (feet/sec)
257.78	5319	14329
259.42	5639	14184
261.06	5279	12650
262.70	5144	12427
264.34	4842	12210
265.98	4501	12537
267.62	3944	13373

Table A-9, continued. Boring Z3-B4, S - R1 quality assurance analysis P- and S_H-wave data

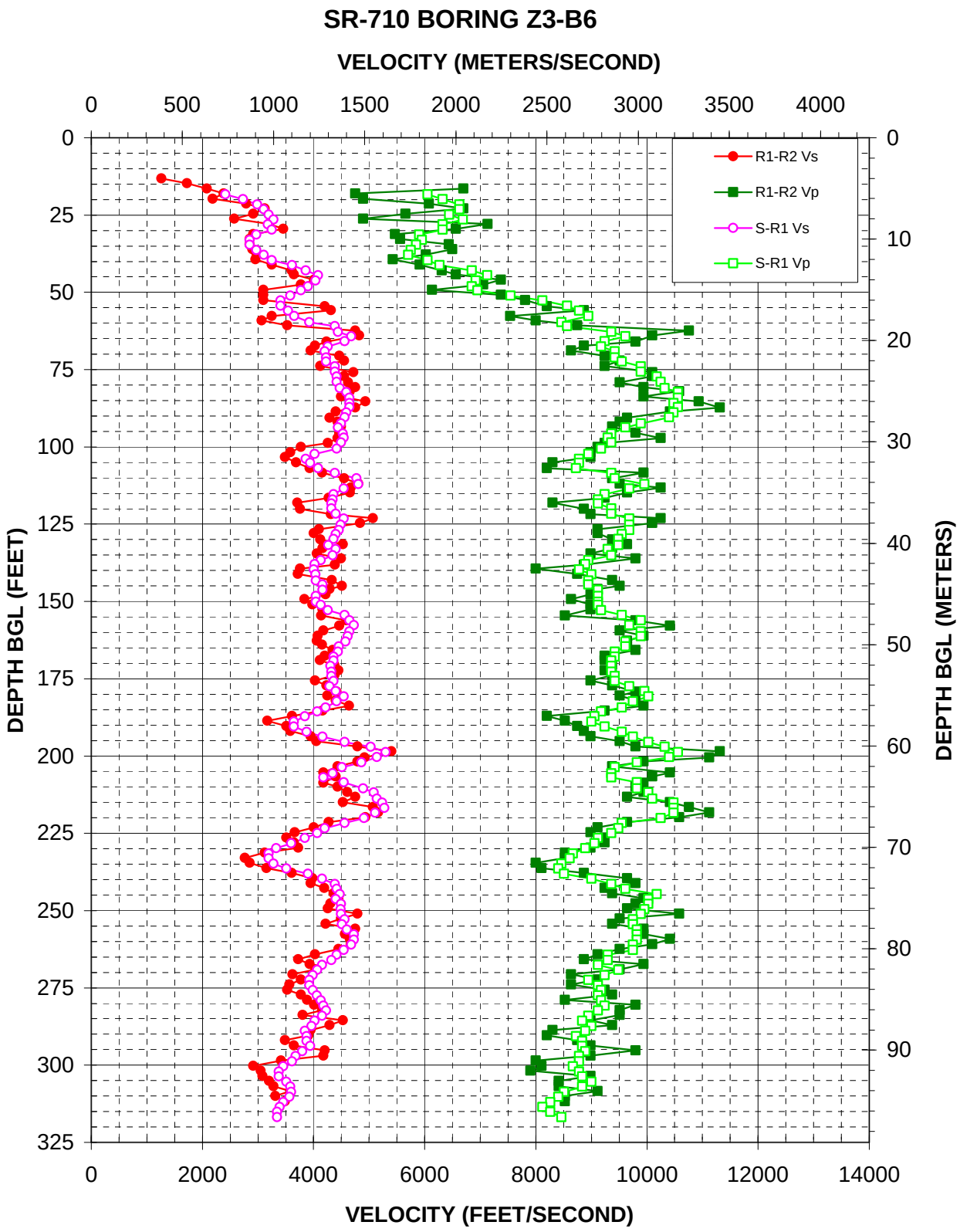

Figure A-10. Boring Z3-B6, R1 - R2 high resolution analysis and S - R1 quality assurance analysis P- and S_H-wave data

Depth (feet)	V_s (feet/sec)	V_p (feet/sec)
18.27	2413	6053
19.91	2732	6325
21.56	2988	6624
23.20	3107	6624
24.84	3191	6441
26.48	3281	6687
28.12	3177	6325
29.76	3250	6325
31.40	2975	5900
33.04	2854	5950
34.68	2854	5851
36.32	2975	5755
37.96	3107	5708
39.60	3250	6053
41.24	3619	6269
42.88	3858	6850
44.52	4082	7128
46.16	4035	6917
48.13	3901	6850
49.44	3775	6951
51.08	3582	7549
52.72	3408	8117
54.36	3408	8562
56.00	3546	8776
57.64	3657	8944
59.61	3922	8459
60.93	4388	8562
62.89	4444	9361
64.21	4681	9618
65.85	4559	9238
67.49	4255	9178
69.13	4204	9424
71.10	4230	9424
72.41	4230	9552
74.05	4388	9889
75.69	4388	9889
77.33	4416	10175
78.97	4416	10250
80.94	4472	10325
82.25	4589	10558
84.22	4650	10558
85.86	4650	10479
87.17	4650	10558
88.81	4589	10479
90.45	4559	10401
92.42	4501	9889
93.73	4444	9618
95.70	4530	9361
97.01	4544	9299
98.65	4501	9361
100.62	4416	9178
102.26	4023	8944
103.90	3858	8776
105.22	3944	8776
106.86	4082	8722
108.50	4388	9361
110.14	4776	9424
112.11	4809	9959
113.42	4544	9684
115.39	4361	9238
117.03	4347	9118
118.34	4321	9118
119.98	4321	9361
121.62	4402	9361
123.26	4544	9684
125.23	4486	9684
126.87	4458	9684
128.18	4402	9552
129.82	4361	9488
131.79	4268	9488
133.10	4402	9299
135.07	4347	9361
136.71	4130	8944
138.02	4023	8887
139.67	4001	8776
141.31	4035	9001
143.27	4047	8944
144.59	4167	8944
146.23	4167	9118
148.20	4047	9118
150.16	4047	9118
151.15	4130	9118
152.79	4255	9178
154.43	4559	9552
156.07	4650	9889
157.71	4728	9684
159.68	4650	9889
161.32	4619	9889
162.96	4574	9618
164.60	4458	9618
166.24	4444	9424
167.88	4361	9424
169.19	4361	9361
170.83	4307	9361
172.80	4321	9361
174.11	4321	9424
175.75	4361	9424
177.40	4294	9684
179.04	4402	9959
180.68	4544	10030
182.32	4416	9751
184.28	4217	9552
185.60	4070	9178
187.24	3847	9059
188.88	3647	9001
190.52	3647	9238
192.16	3879	9552
193.80	4167	9751
195.44	4559	10030
197.08	5033	10325
198.72	5299	10558
200.36	5144	10401
202.00	4859	9820
203.64	4515	9424
205.61	4347	9361
206.92	4179	9361
208.56	4544	9820
210.53	4893	9820
211.84	5088	10030
213.81	5144	10102
215.12	5240	10479
216.77	5279	10479
218.41	5106	10479
220.05	4910	10250
221.69	4559	9552
223.33	4204	9488
224.97	4070	9361
226.61	3847	9118
228.25	3601	9059
229.89	3327	8887
231.53	3191	8668
233.17	3191	8615
234.81	3281	8459
236.45	3510	8408
238.09	3901	8510
239.73	4154	9001
241.37	4388	9361
243.01	4416	9618
244.65	4472	10175
246.29	4402	10030
247.93	4501	10030
249.57	4486	9959
251.21	4501	9889
252.85	4559	9751
254.49	4515	9751
256.14	4604	9820
257.78	4728	9820
259.42	4728	9820
261.06	4681	9751
262.70	4544	9751

Table A-10. Boring Z3-B6, S - R1 quality assurance analysis P- and S_H-wave data

Depth (feet)	V_s (feet/sec)	V_p (feet/sec)
264.34	4416	9299
265.98	4321	9299
267.62	4154	9118
269.26	4070	9488
270.90	3989	9238
272.54	3922	8944
274.18	3922	9118
275.82	3989	9178
277.46	4058	9118
279.10	4130	9178
280.74	4179	9238
282.38	4230	9118
284.02	4154	8944
285.66	4023	8831
287.30	3967	9001
288.94	3847	8887
290.58	3879	8722
292.22	3879	8831
293.86	3944	8831
295.51	3795	8887
297.15	3676	8776
298.79	3619	8776
300.43	3459	8668
302.07	3375	8776
303.71	3375	8831
305.35	3510	9001
306.99	3582	8831
308.63	3601	8510
310.27	3564	8408
311.91	3459	8260
313.55	3392	8117
315.19	3343	8260
316.83	3343	8459

Table A-10, continued. Boring Z3-B6, S - R1 quality assurance analysis
P- and S_H-wave data

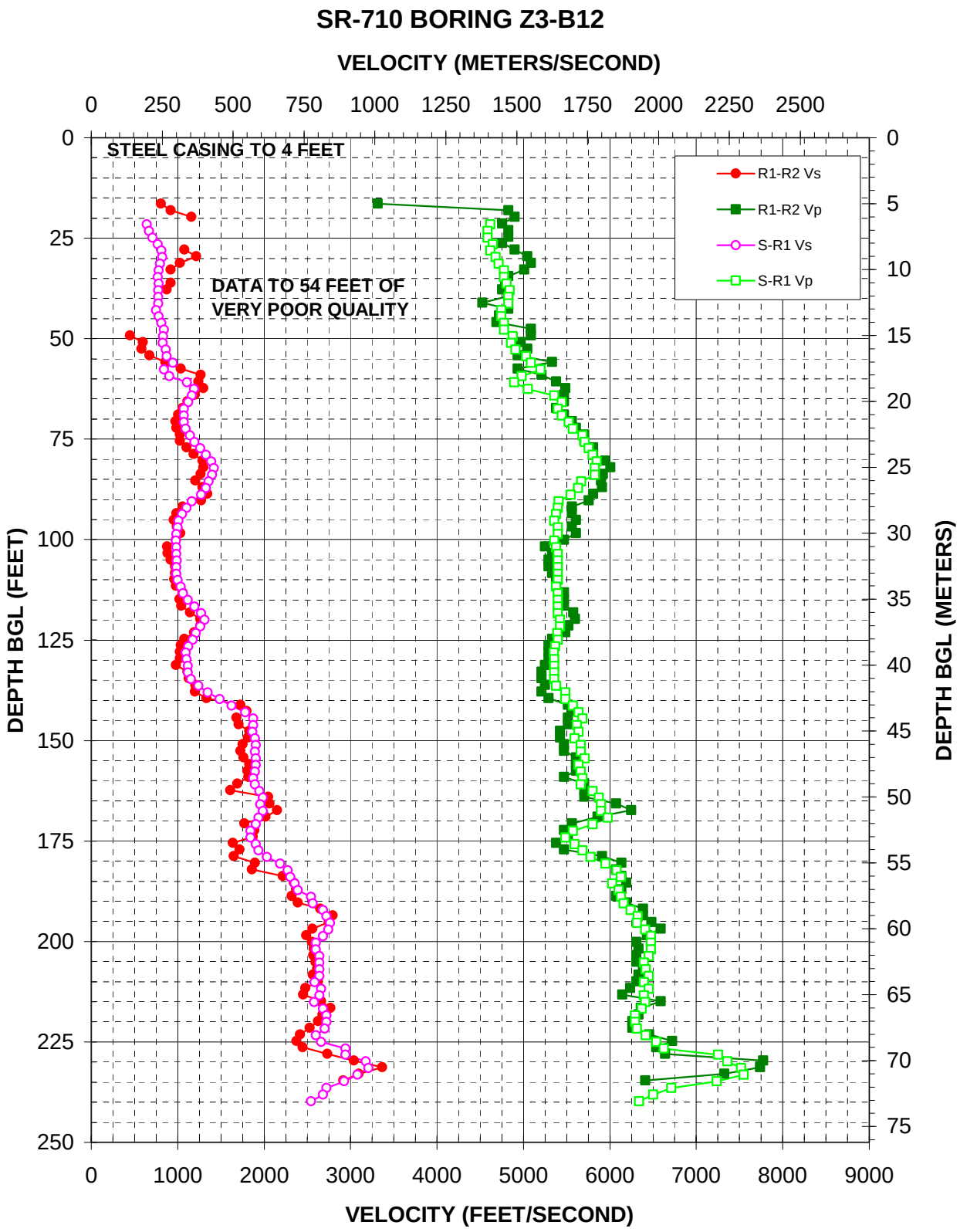

Figure A-11. Boring Z3-B12, R1 - R2 high resolution analysis and S - R1 quality assurance analysis P- and S_H-wave data

Depth (feet)	V_s (feet/sec)	V_p (feet/sec)
13.35		
21.56	645	4619
23.20	669	4589
24.84	711	4589
26.48	769	4650
28.12	814	4619
29.76	823	4681
31.40	795	4712
33.04	782	4776
34.68	773	4776
36.32	782	4809
37.96	778	4842
39.60	778	4825
41.24	778	4825
42.88	749	4744
44.52	782	4744
46.16	814	4776
47.80	843	4776
49.44	833	4876
51.08	828	4859
52.72	864	4910
54.36	874	5033
56.00	945	5088
57.64	843	5201
59.28	906	4979
60.93	1111	4893
62.57	1188	5051
64.21	1164	5360
65.85	1122	5443
67.49	1072	5401
69.13	1072	5443
70.77	1072	5528
72.41	1092	5572
74.05	1142	5685
75.69	1196	5708
77.33	1261	5755
78.97	1327	5802
80.61	1390	5851
82.25	1418	5827
83.89	1401	5827
85.53	1358	5671
87.17	1327	5635
88.81	1272	5546
90.45	1164	5409
92.09	1102	5401
93.73	1053	5380
95.37	1010	5360
97.01	1002	5401
98.65	985	5401
100.30	979	5360
101.94	985	5380
103.58	985	5401
105.22	993	5401
106.86	985	5401
108.50	985	5401
110.14	1002	5401
111.78	1037	5380
113.42	1062	5401
115.06	1120	5401
116.70	1196	5401
118.34	1274	5401
119.98	1312	5426
121.62	1261	5426
123.26	1211	5392
124.90	1174	5401
126.54	1122	5368
128.18	1092	5351
129.82	1102	5360
131.46	1120	5360
133.10	1120	5360
134.74	1153	5360
136.38	1244	5380
138.02	1348	5485
139.67	1484	5485
141.31	1625	5572
142.95	1782	5639
144.59	1872	5685
146.23	1872	5617
147.87	1862	5639
149.51	1892	5594
151.15	1903	5662
152.79	1892	5662
154.43	1903	5708
156.07	1903	5639
157.71	1892	5662
159.35	1872	5685
160.99	1892	5662
162.63	1945	5802
164.27	1989	5875
165.91	1956	5900
167.55	1989	5900
169.19	1934	5975
170.83	1903	5802
172.47	1843	5572
174.11	1845	5485
175.75	1903	5594
177.40	1934	5685
179.04	2035	5779
180.68	2187	5950
182.32	2272	6079
183.96	2302	6132
185.60	2356	6027
187.24	2388	6105
188.88	2544	6132
190.52	2562	6159
192.16	2680	6241
193.80	2721	6325
195.44	2764	6314
197.08	2743	6412
198.72	2680	6477
200.36	2600	6477
202.00	2600	6477
203.64	2639	6453
205.28	2639	6394
206.92	2639	6418
208.56	2639	6453
210.20	2583	6394
211.84	2659	6453
213.48	2639	6394
215.12	2581	6412
216.77	2680	6371
218.41	2721	6291
220.05	2721	6291
221.69	2700	6314
223.33	2600	6418
224.97	2659	6537
226.61	2944	6624
228.25	2944	7253
229.89	3177	7360
231.53	3206	7517
233.17	3079	7549
234.81	2925	7238
236.45	2721	6712
238.09	2680	6501
239.73	2544	6337

Table A-11. Boring Z3-B12, S - R1 quality assurance analysis P- and S_H-wave data

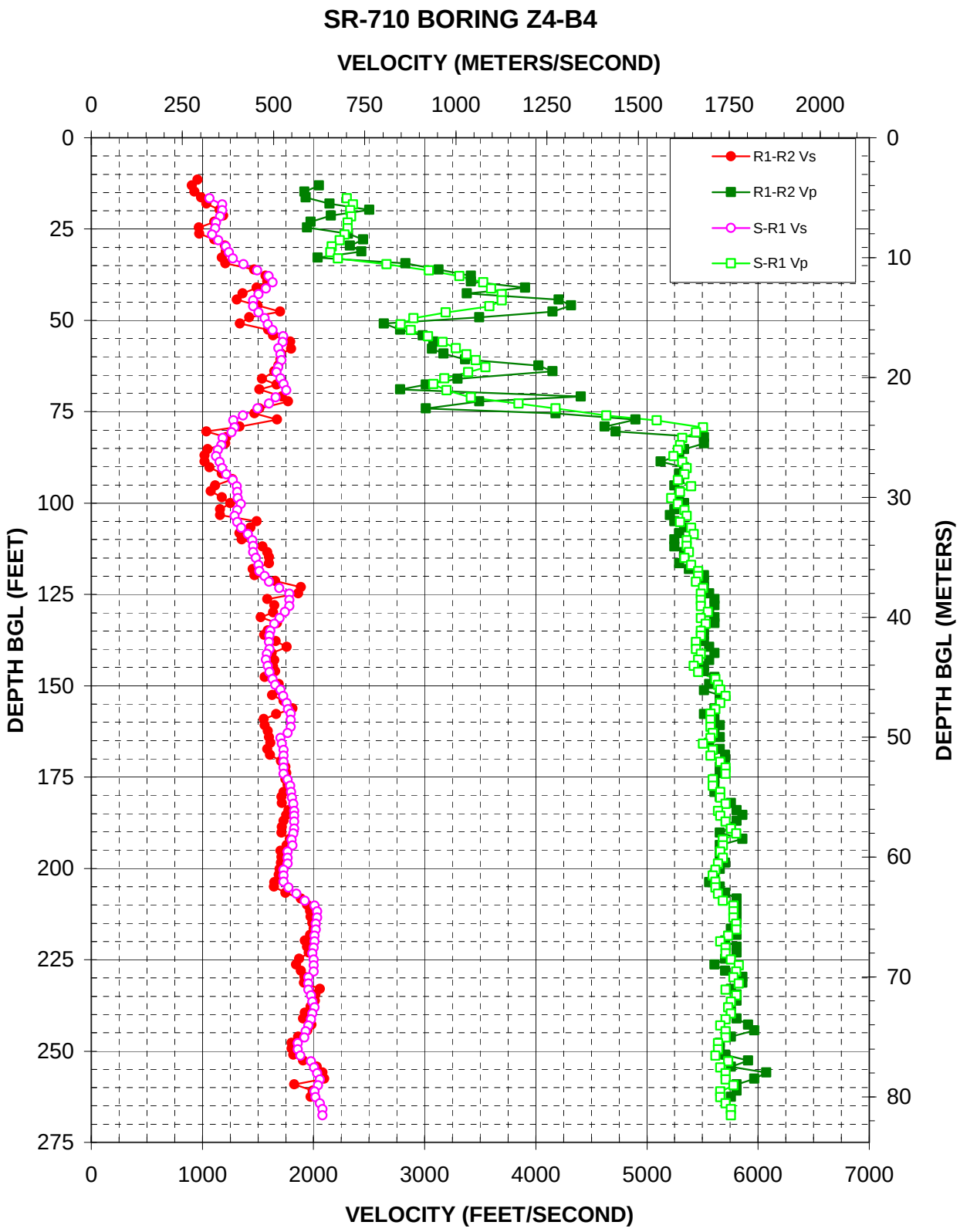

Figure A-12. Boring Z4-B4, R1 - R2 high resolution analysis and S - R1 quality assurance analysis P- and S_H-wave data

Depth (feet)	V_s (feet/sec)	V_p (feet/sec)
16.63	1064	2302
18.27	1178	2356
19.91	1178	2333
21.56	1159	2340
23.20	1125	2310
24.84	1114	2310
26.48	1087	2280
28.12	1143	2236
29.76	1211	2167
31.40	1240	2154
33.04	1277	2222
34.68	1371	2659
36.32	1494	3039
37.96	1596	3312
39.60	1633	3528
41.24	1574	3601
42.88	1507	3695
44.52	1457	3695
46.16	1457	3582
47.80	1507	3191
49.44	1560	2901
51.08	1588	2786
52.72	1633	2877
54.36	1729	3033
56.00	1723	3163
57.64	1686	3281
59.28	1704	3375
60.93	1712	3459
62.89	1686	3546
64.21	1668	3392
65.85	1704	3177
67.49	1734	3079
69.13	1755	3199
71.10	1660	3417
72.74	1599	3847
74.05	1497	4179
76.02	1366	4634
77.33	1281	5088
79.30	1291	5507
80.61	1263	5443
82.25	1182	5319
84.22	1170	5299
85.53	1140	5279
87.17	1125	5240
88.81	1155	5319
90.45	1178	5360
92.09	1215	5339
93.73	1277	5279
95.37	1310	5401
97.01	1314	5299
98.65	1320	5220
100.30	1348	5279
101.94	1315	5339
103.58	1291	5360
105.22	1315	5299
106.86	1350	5401
108.50	1410	5422
110.14	1451	5360
111.78	1457	5360
113.42	1457	5380
115.06	1481	5339
117.03	1507	5401
118.67	1513	5464
119.98	1560	5464
121.62	1599	5443
123.26	1692	5507
124.90	1782	5485
126.54	1782	5485
128.18	1782	5485
129.82	1742	5550
131.46	1696	5485
133.10	1650	5528
135.07	1614	5485
136.38	1607	5485
138.02	1599	5443
139.99	1607	5443
141.31	1583	5485
142.95	1574	5464
144.59	1588	5422
146.23	1607	5464
148.20	1633	5617
149.84	1656	5639
151.15	1704	5662
152.79	1729	5708
154.76	1760	5662
156.40	1773	5617
157.71	1796	5572
159.35	1796	5572
161.32	1796	5572
162.96	1769	5594
164.27	1704	5572
165.91	1717	5507
167.55	1734	5594
169.19	1734	5572
170.83	1734	5662
172.47	1734	5708
174.11	1734	5708
175.75	1769	5594
177.40	1791	5594
179.04	1800	5662
180.68	1810	5662
182.32	1819	5708
184.28	1828	5639
185.60	1828	5662
187.24	1828	5708
189.21	1828	5755
190.52	1819	5802
192.16	1803	5685
193.80	1812	5685
195.44	1769	5662
197.08	1766	5685
198.72	1766	5639
200.36	1734	5617
202.00	1734	5594
203.64	1734	5617
205.28	1777	5617
206.92	1848	5639
208.89	1924	5685
210.20	2012	5779
211.84	2035	5779
213.48	2035	5779
215.12	2023	5802
216.77	2023	5802
218.41	2012	5731
220.05	2012	5662
221.69	2000	5708
223.33	1989	5708
224.97	2000	5755
226.61	2000	5827
228.25	2000	5802
229.89	1956	5779
231.53	1956	5827
233.17	1956	5708
234.81	1978	5802
236.45	1989	5755
238.09	2012	5731
239.73	1989	5755
241.37	1978	5708
243.01	1956	5662
244.65	1929	5708
246.29	1918	5708
247.93	1857	5639
249.57	1857	5639
251.21	1882	5617
252.85	1978	5731
254.49	2006	5662
256.14	2035	5708
257.78	2059	5708
259.42	2041	5779
261.06	2012	5662

Table A-12. Boring Z4-B4, S - R1 quality assurance analysis P- and S_H-wave data

Depth (feet)	V_s (feet/sec)	V_p (feet/sec)
262.70	2018	5662
264.34	2059	5708
265.98	2083	5755
267.62	2083	5755

Table A-12, continued. Boring Z4-B4, S - R1 quality assurance analysis P- and S_H-wave data

APPENDIX B

CALIPER AND
NATURAL GAMMA LOGS

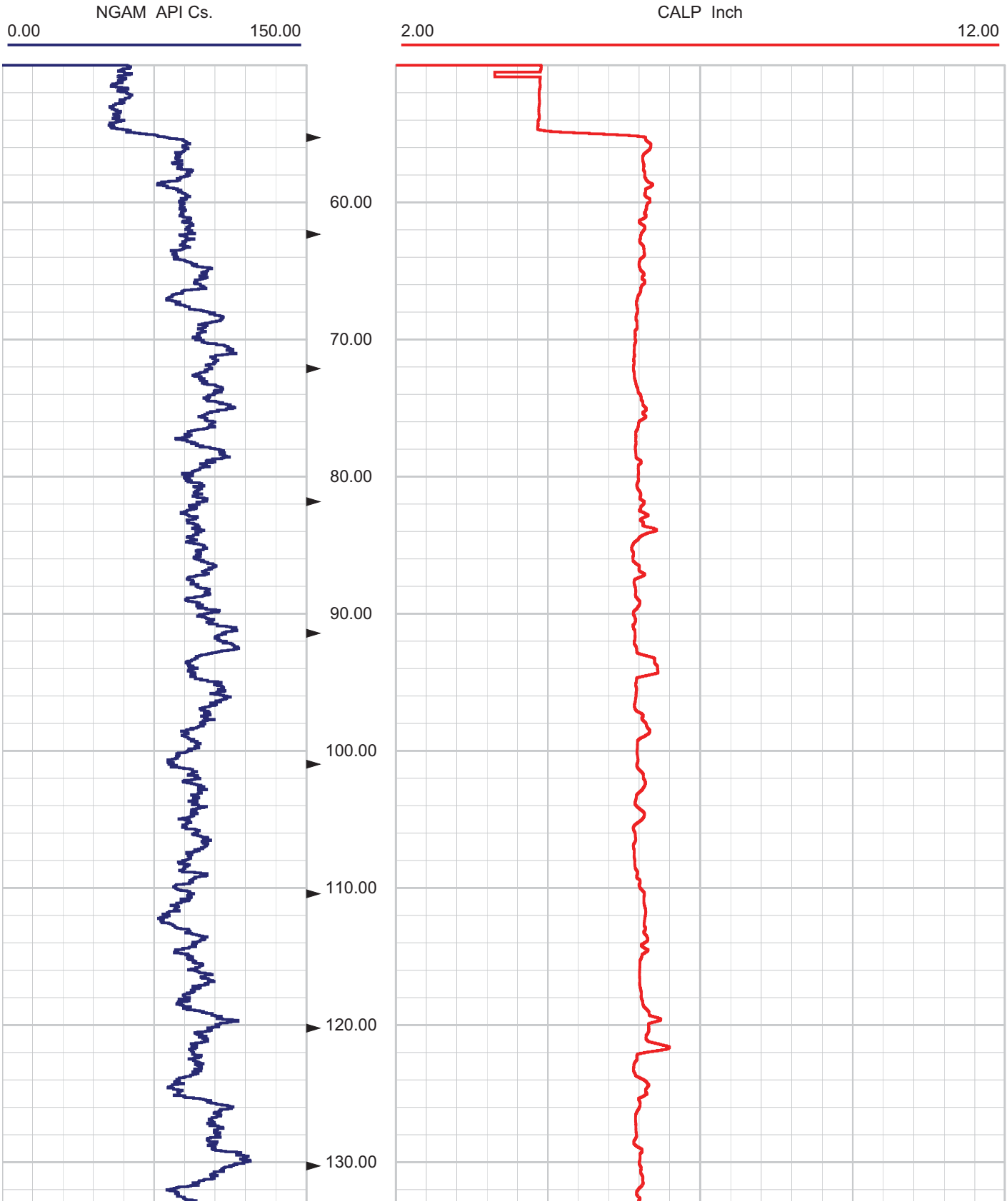

SR-710 Boring Z3-B3 Caliper and Natural Gamma rev 1.1 Sheet 1 of 3

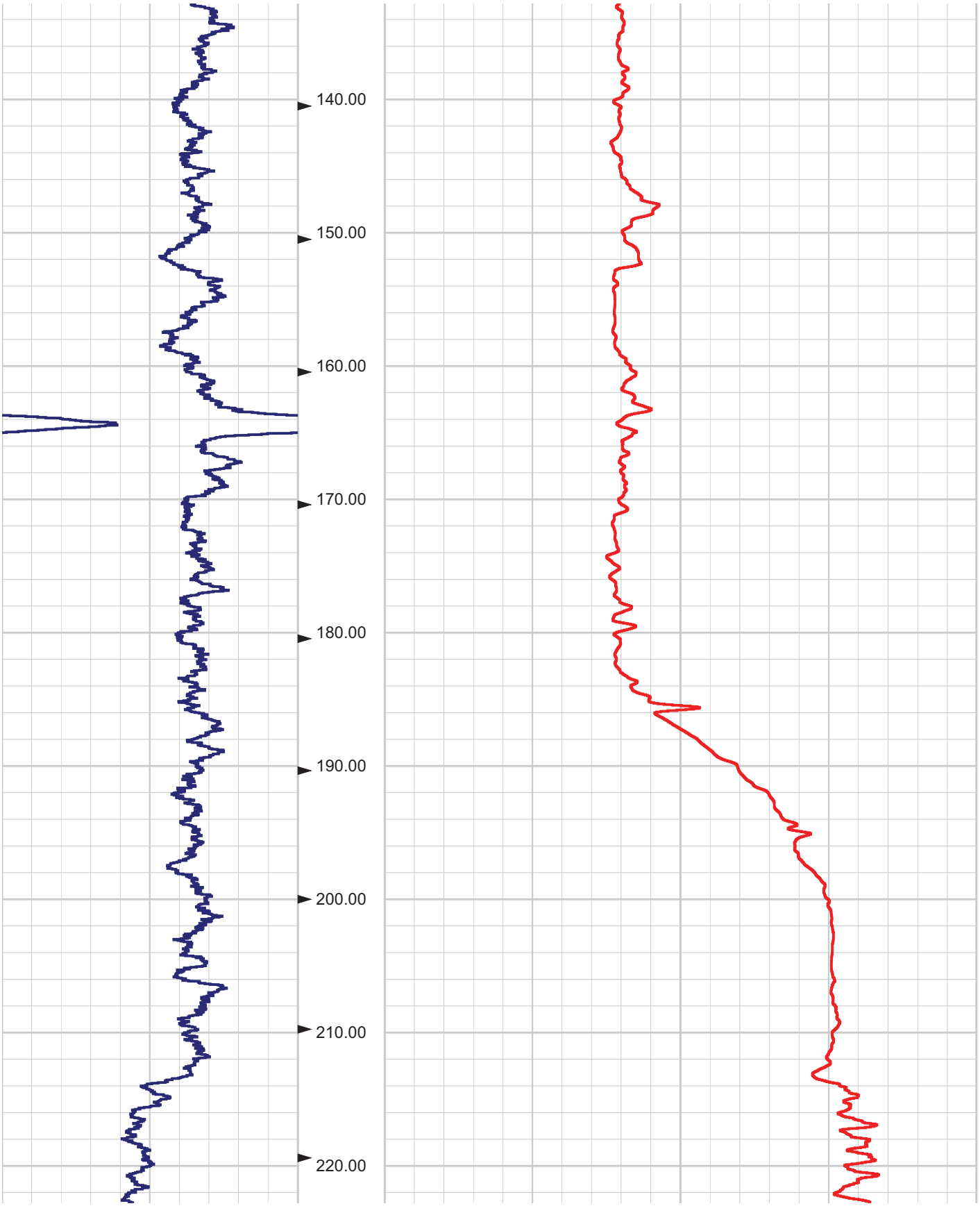

SR-710 Boring Z3-B3 Caliper and Natural Gamma rev 1.1 Sheet 2 of 3

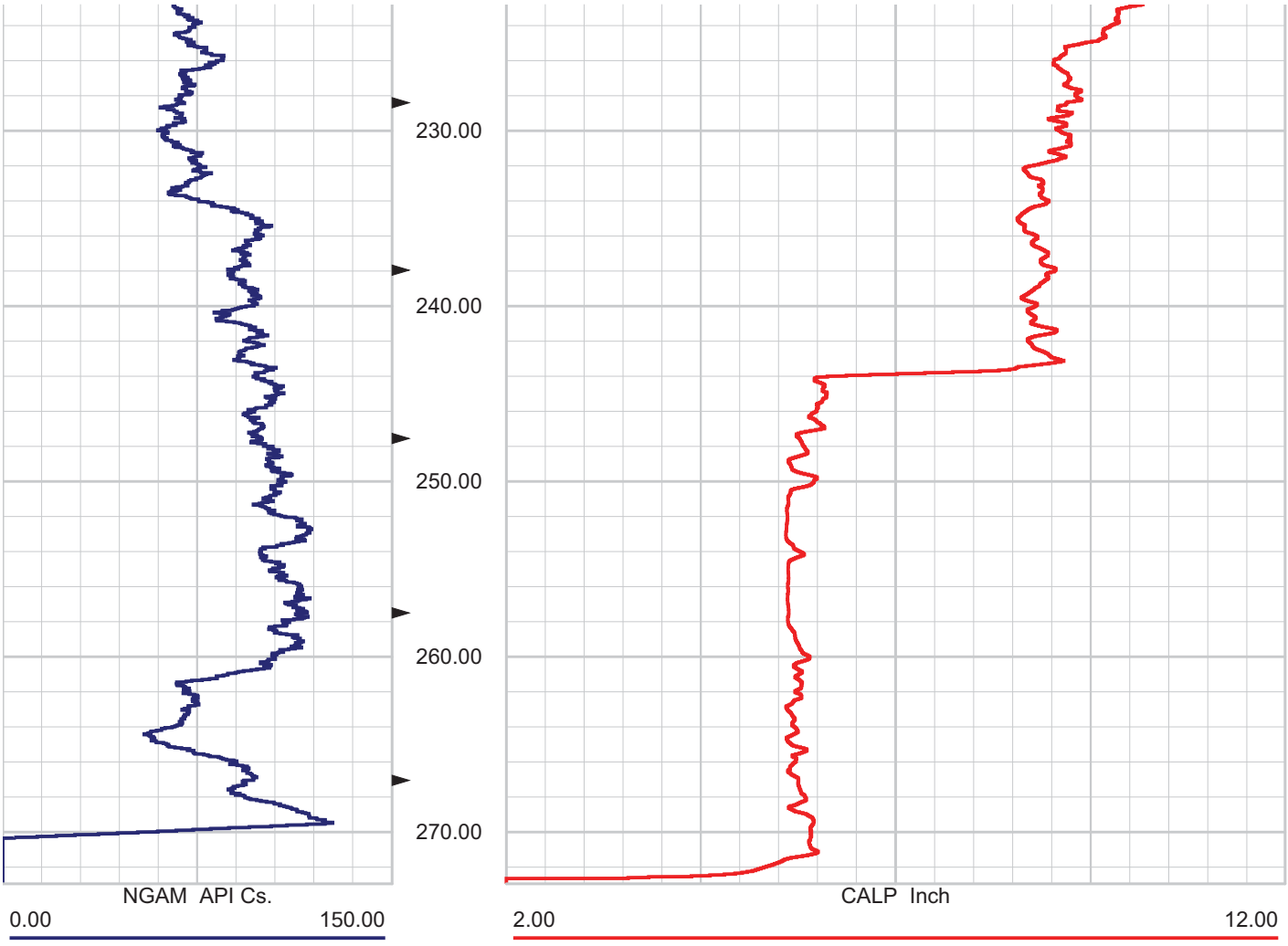
230.00
240.00
250.00
260.00
270.00
NGAM API Cs.
0.00
150.00
CALP Inch
2.00
12.00

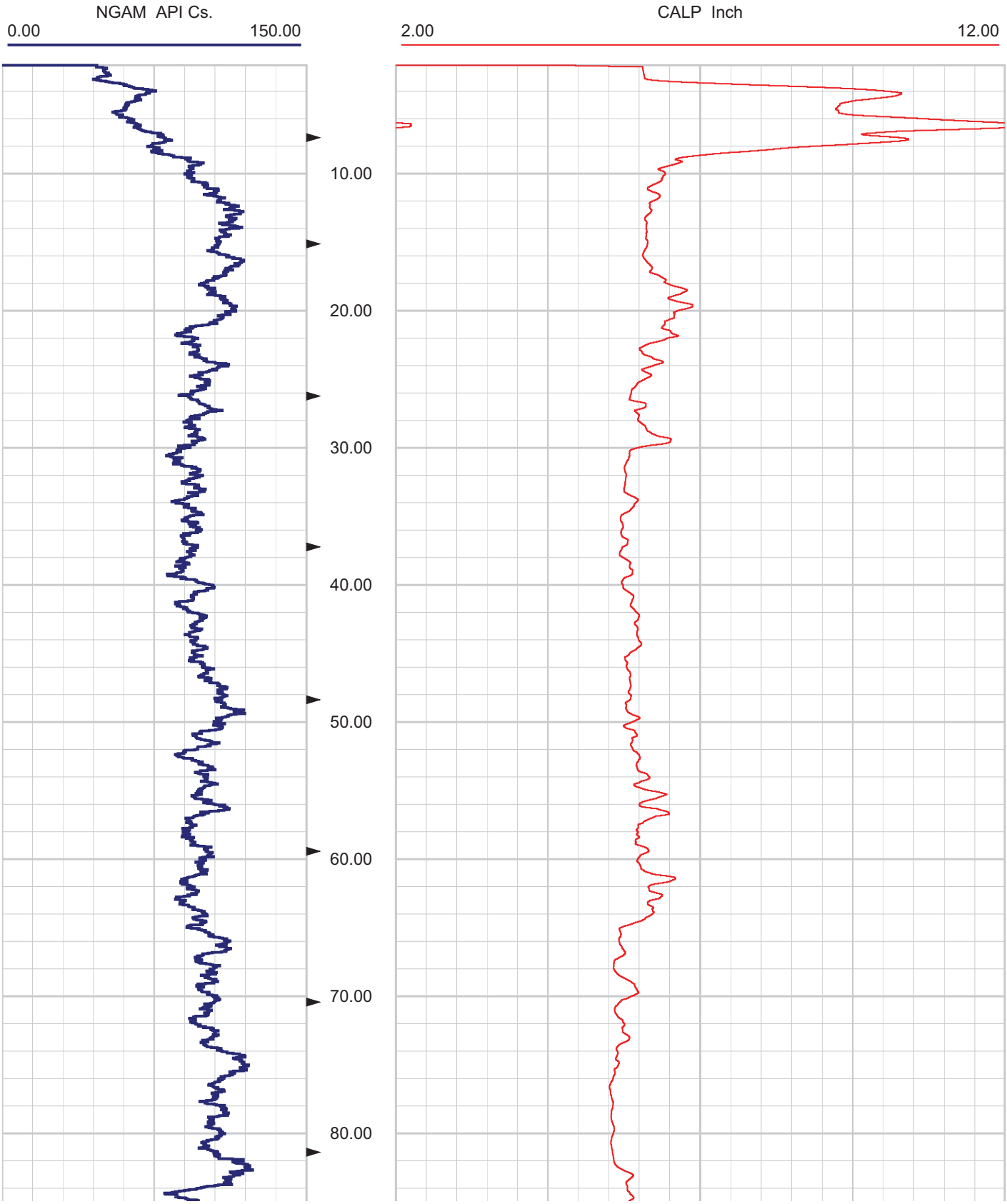

SR-710 Boring Z3-B4 Caliper and Natural Gamma rev 1.1 Sheet 1 of 4

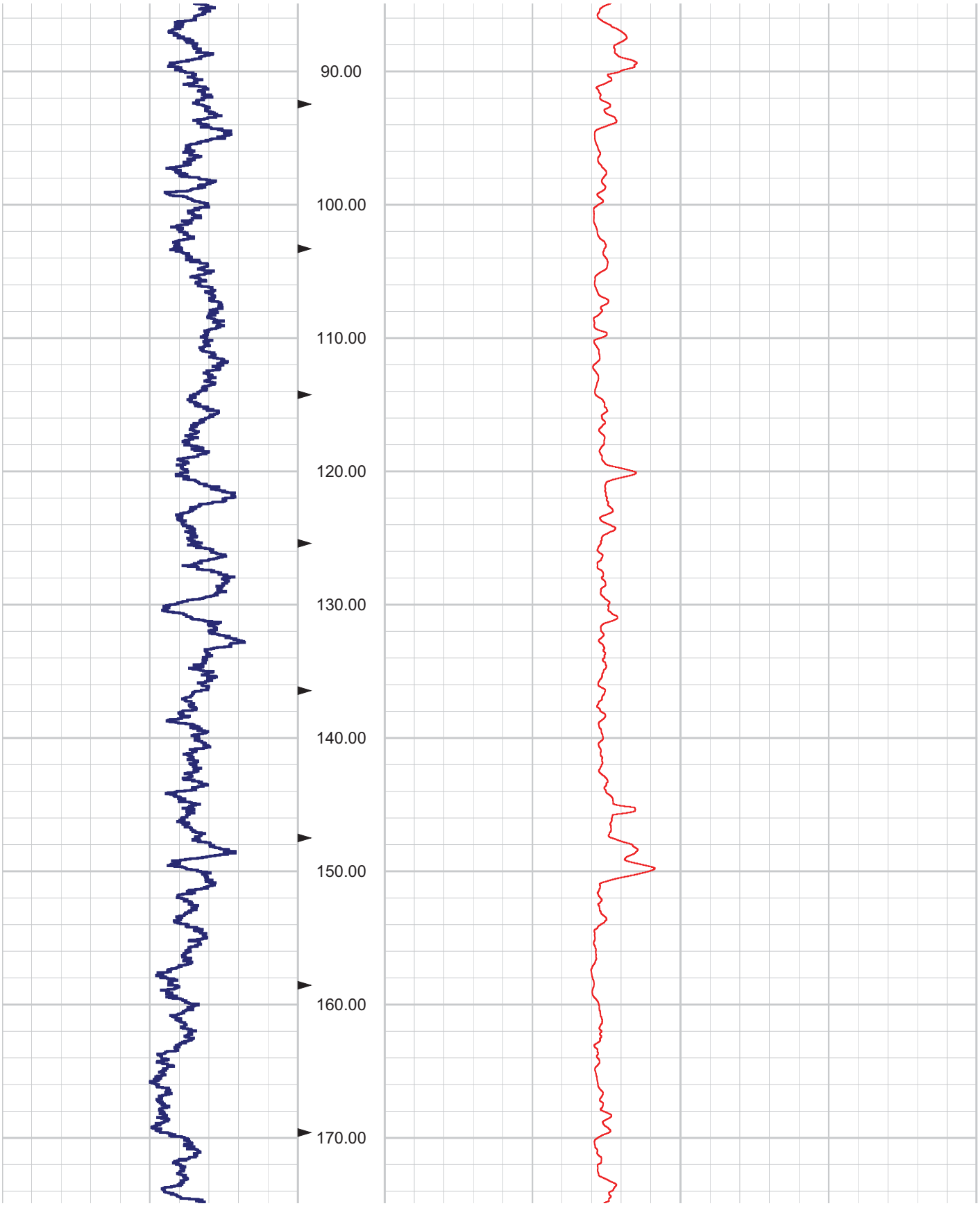

SR-710 Boring Z3-B4 Caliper and Natural Gamma rev 1.1 Sheet 2 of 4

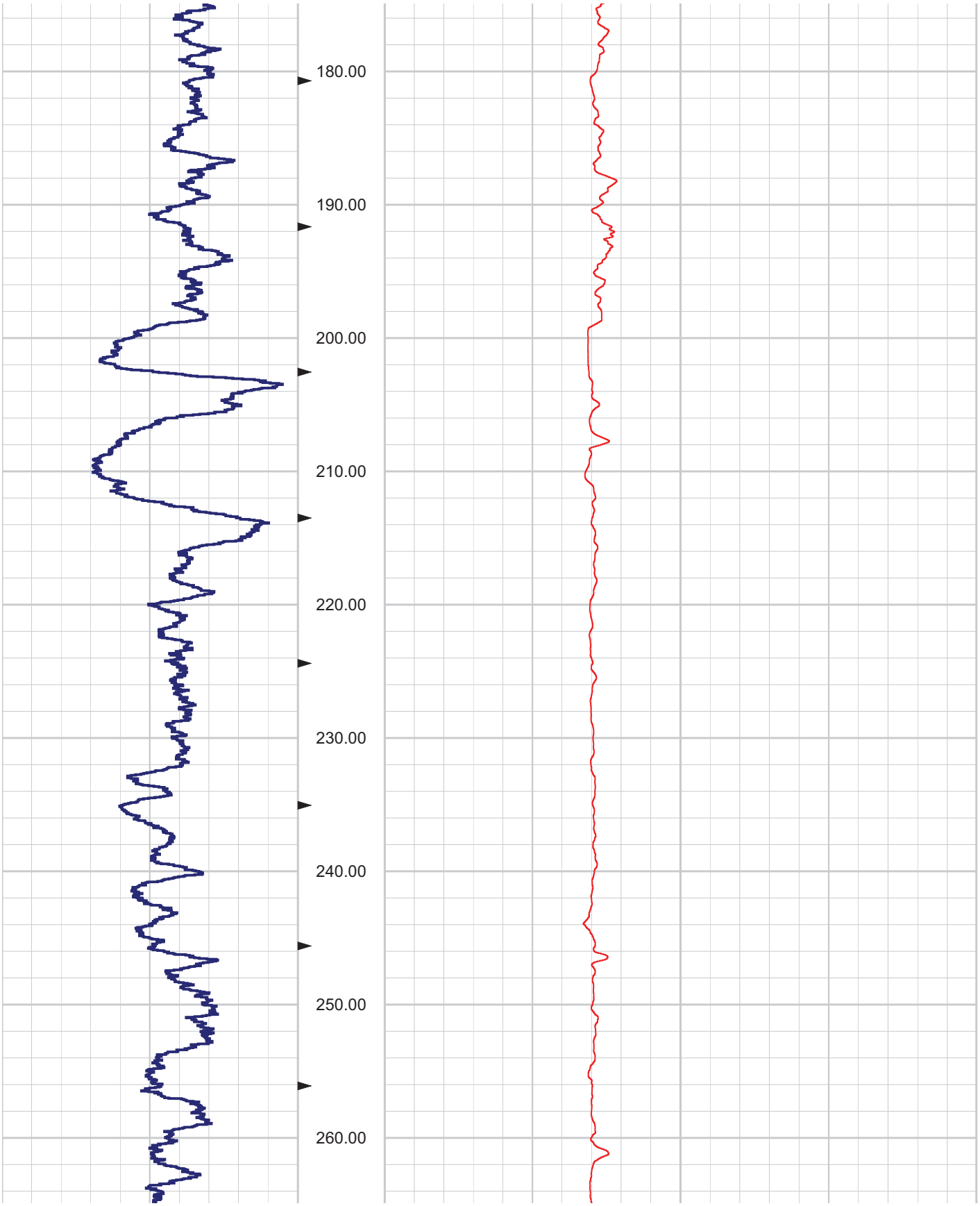

SR-710 Boring Z3-B4 Caliper and Natural Gamma rev 1.1 Sheet 3 of 4

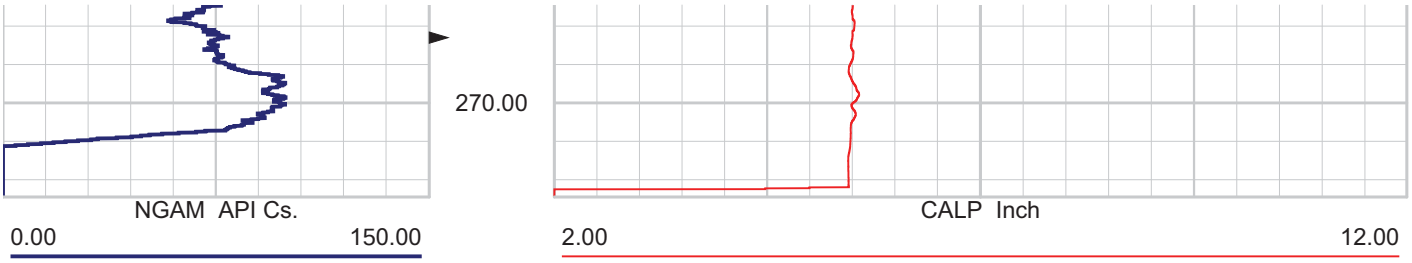
270.00
NGAM API Cs.
0.00
150.00
CALP Inch
2.00
12.00

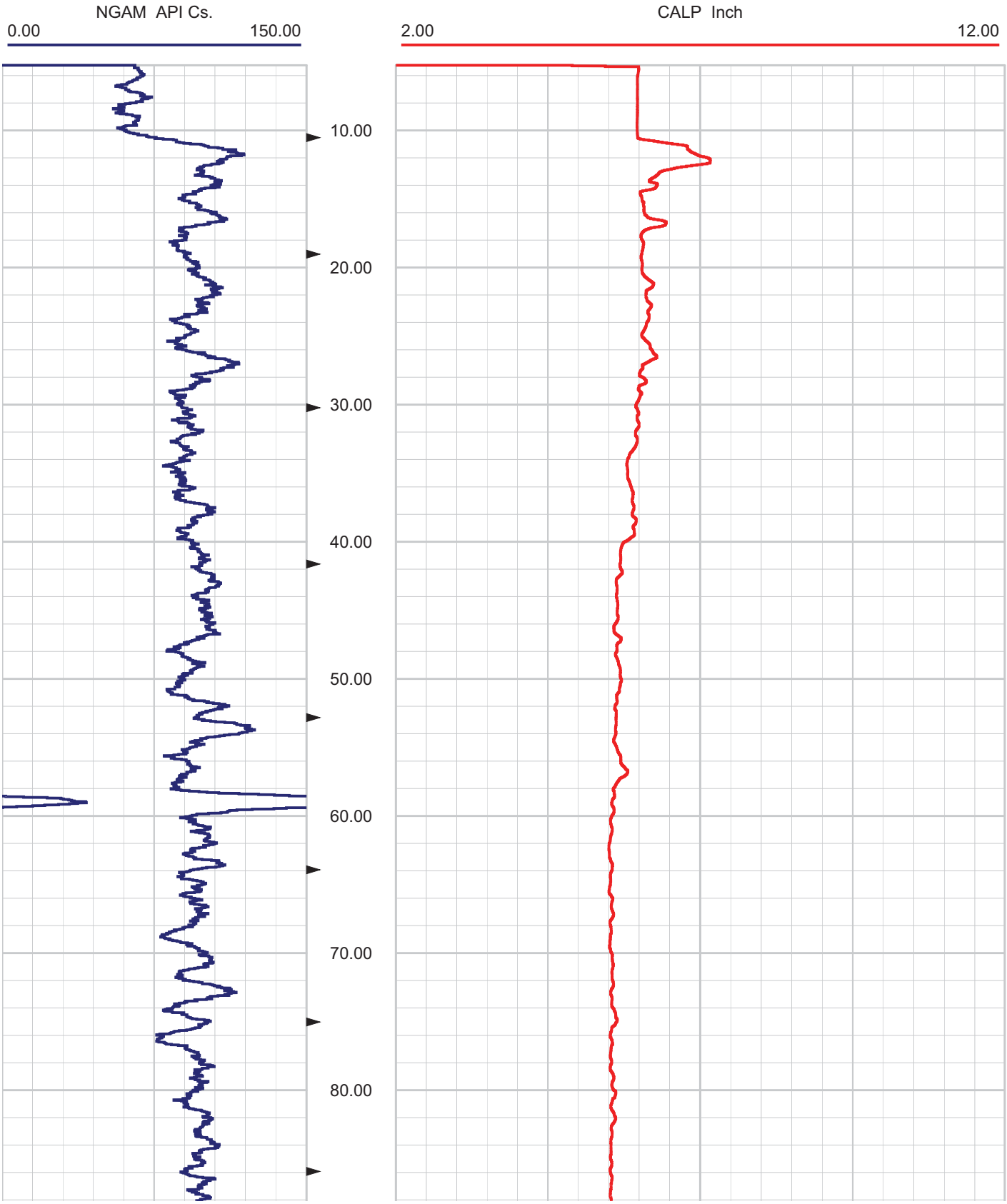

SR-710 Boring Z3-B6 Caliper and Natural Gamma rev 1.1 Sheet 1 of 4

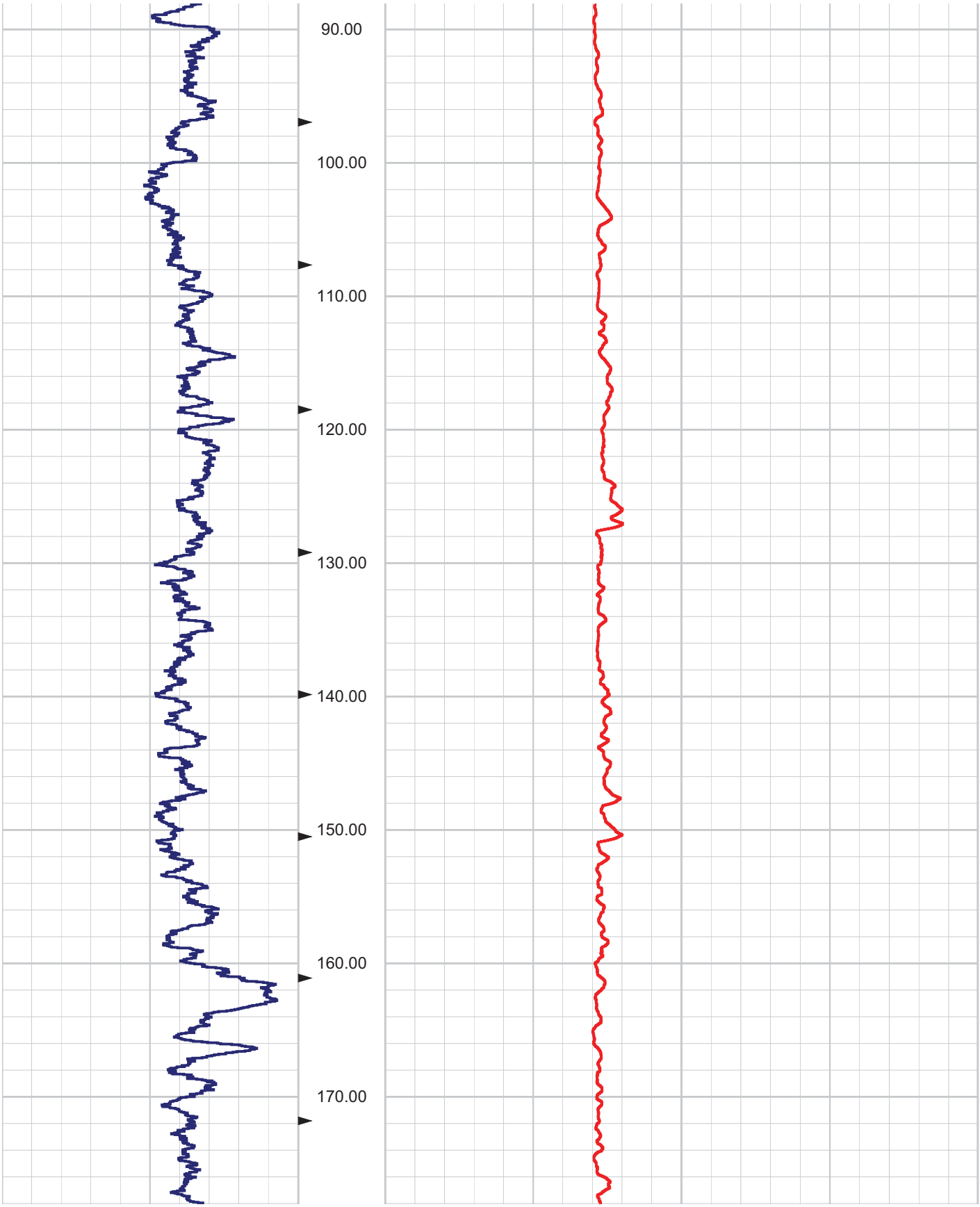

SR-710 Boring Z3-B6 Caliper and Natural Gamma rev 1.1 Sheet 2 of 4

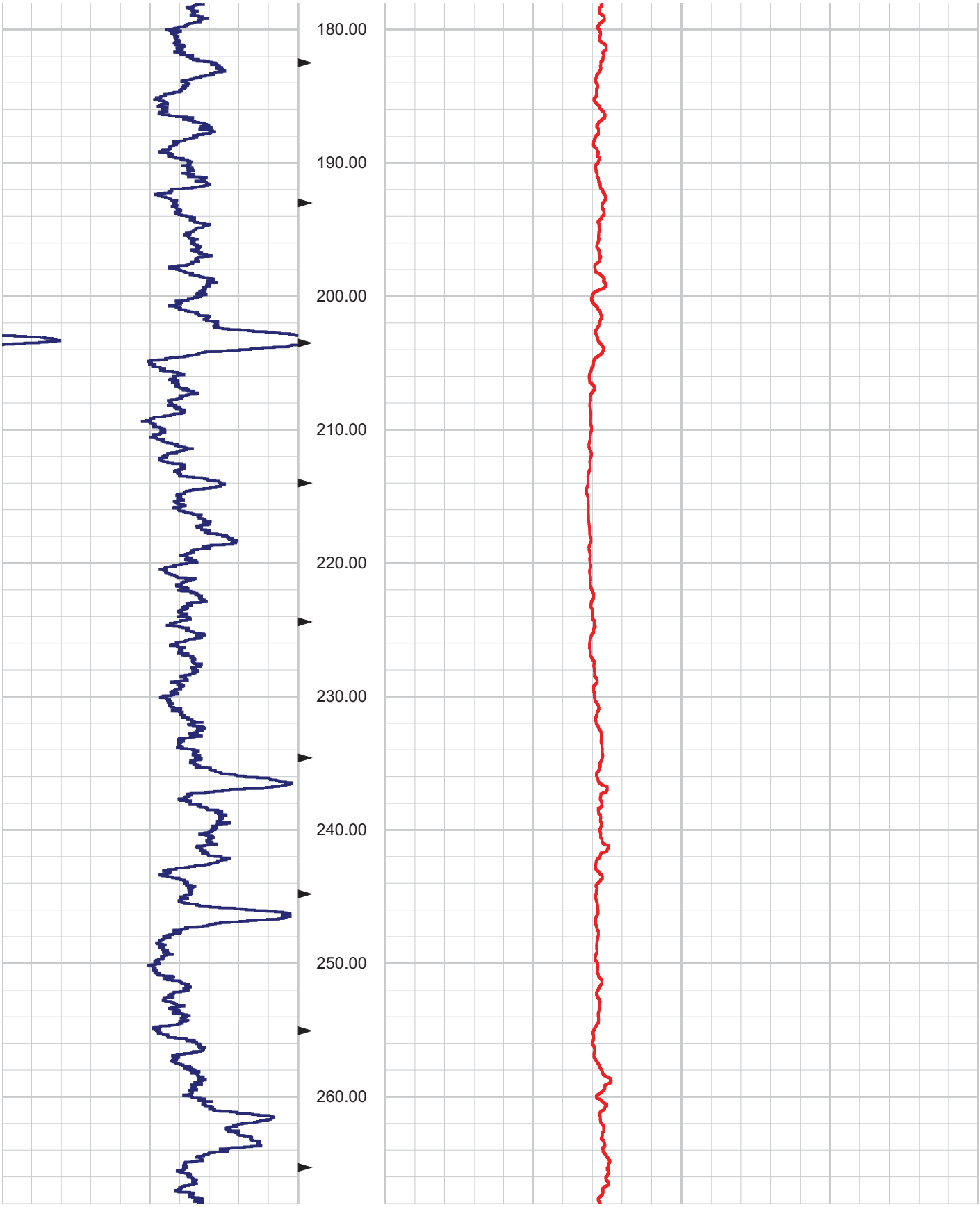

SR-710 Boring Z3-B6 Caliper and Natural Gamma rev 1.1 Sheet 3 of 4

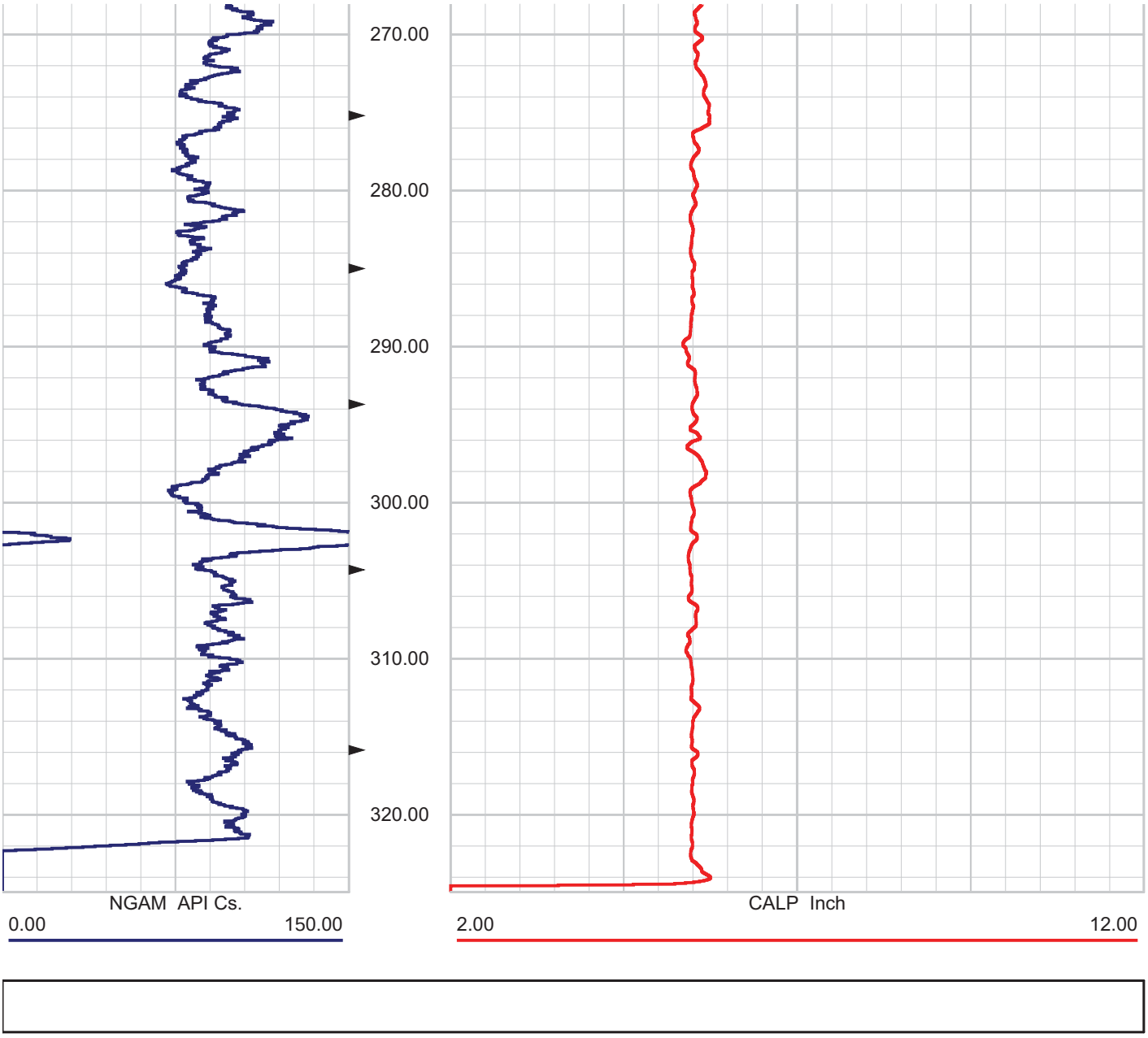
270.00
280.00
290.00
300.00
310.00
320.00
NGAM API Cs.
0.00
150.00
CALP Inch
2.00
12.00

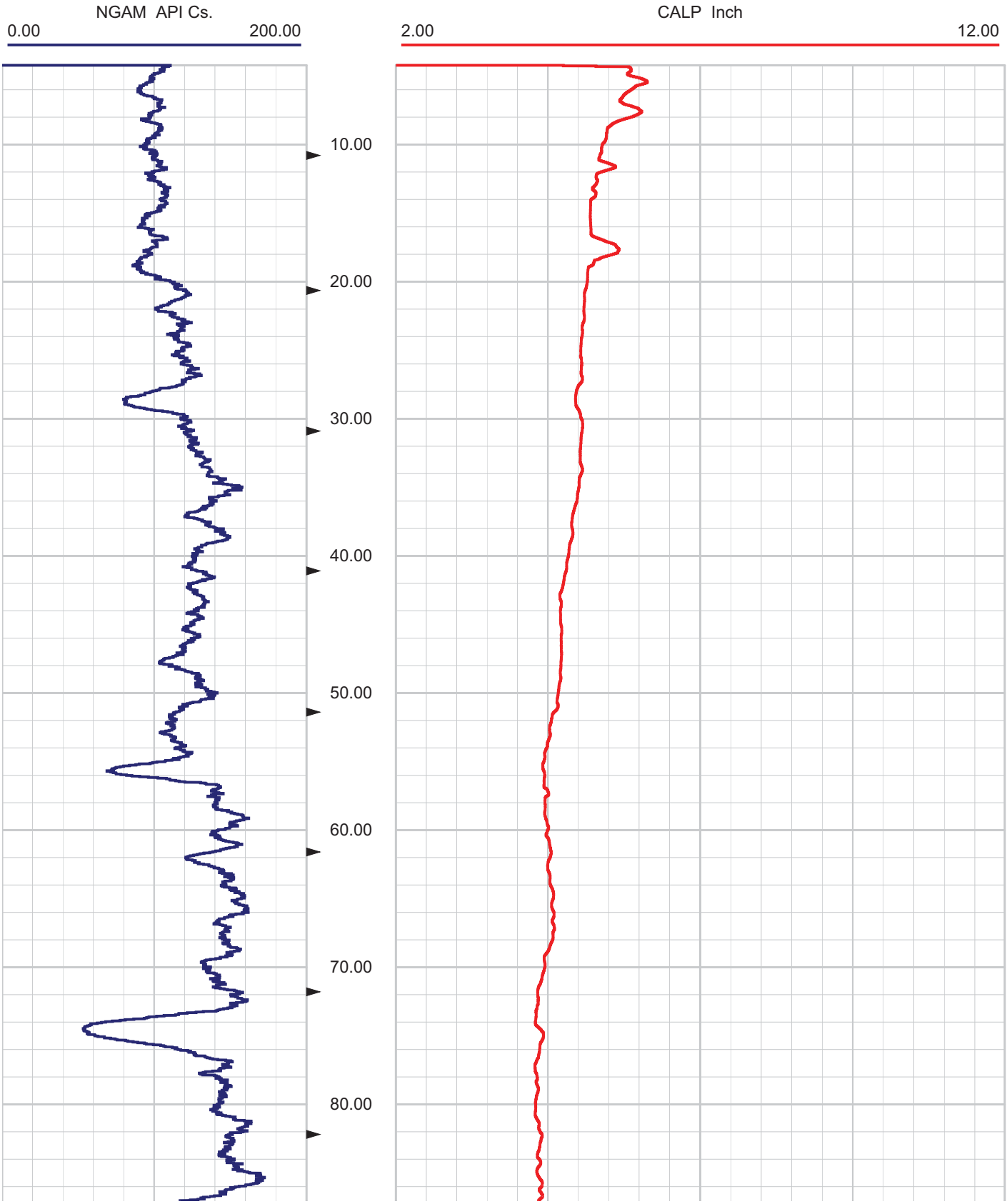

SR-710 Boring Z3-B8 Caliper and Natural Gamma rev 1.1 Sheet 1 of 4

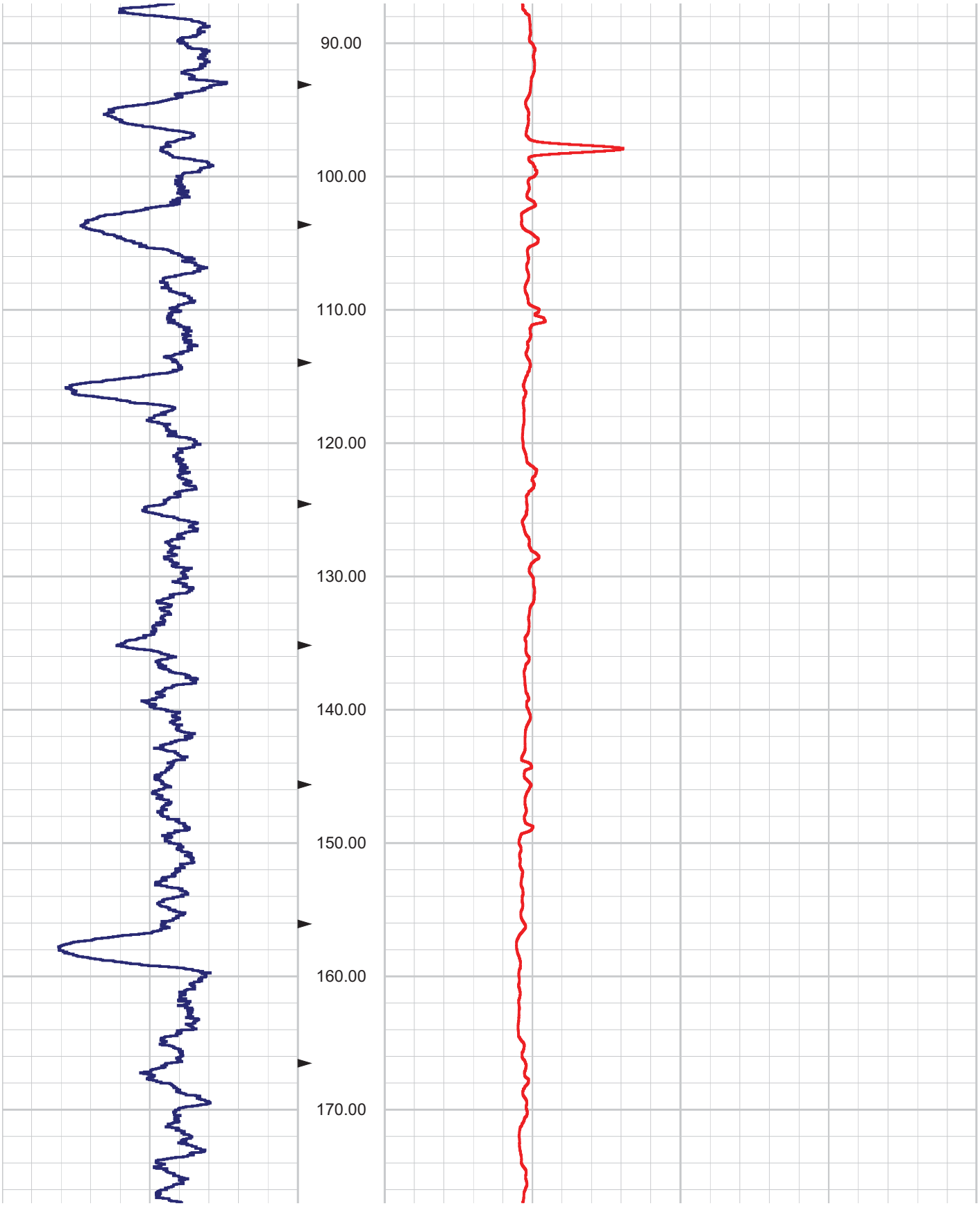

SR-710 Boring Z3-B8 Caliper and Natural Gamma rev 1.1 Sheet 2 of 4

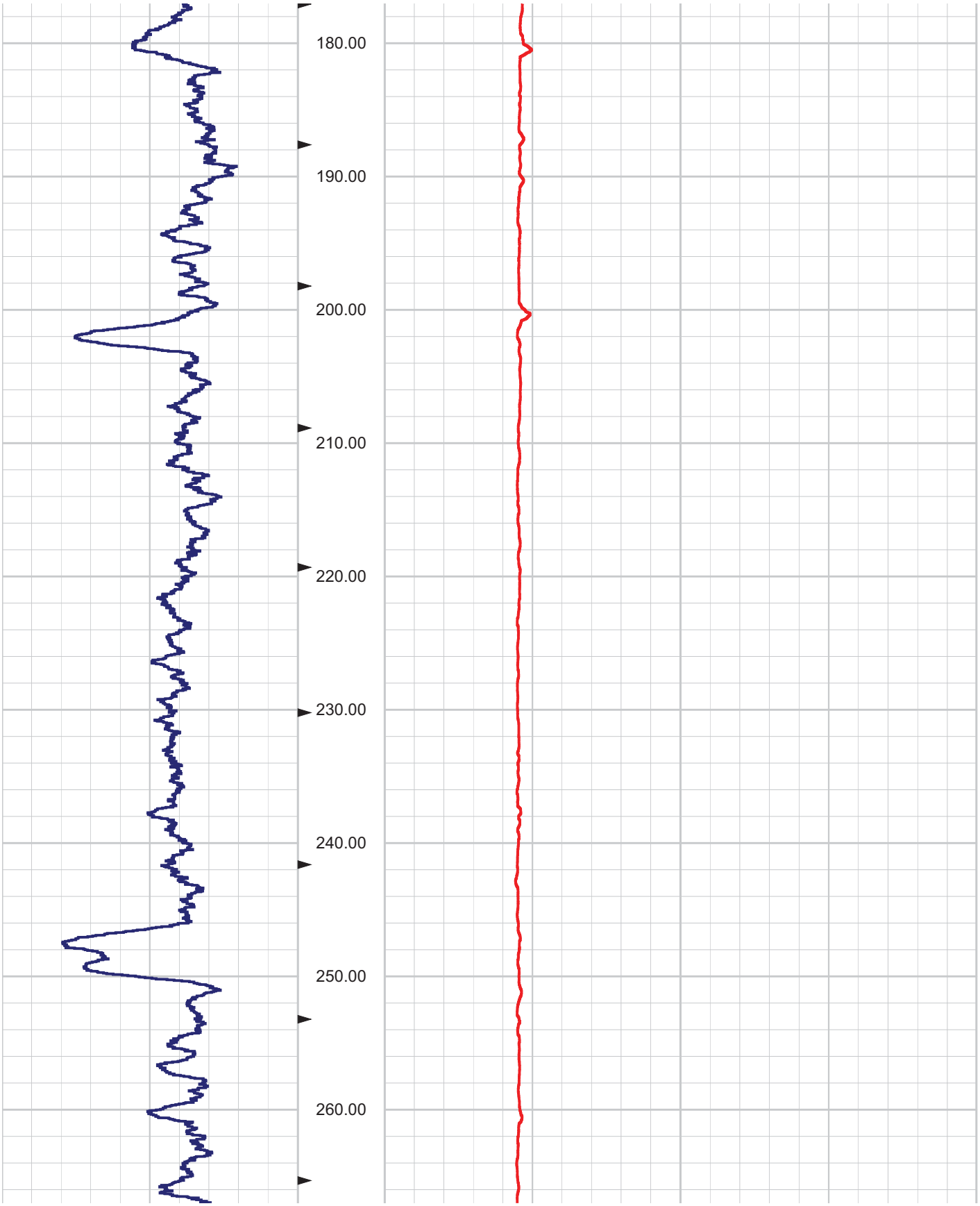

SR-710 Boring Z3-B8 Caliper and Natural Gamma rev 1.1 Sheet 3 of 4

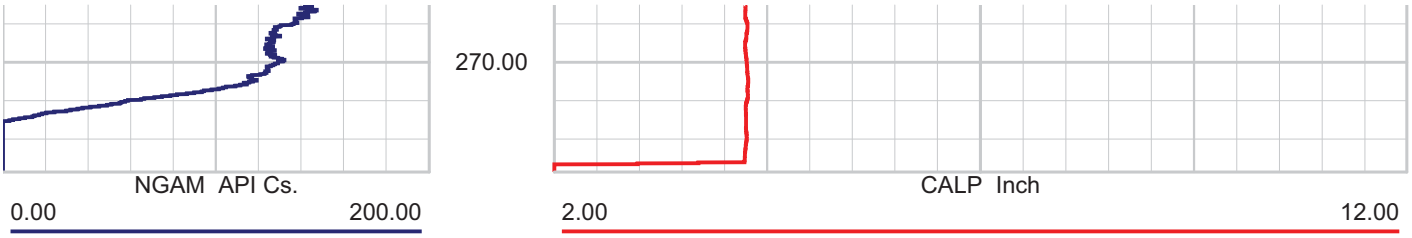

Depth: 3.00 ft Date: 23 Mar 2009 Time: 14:16:54 File: "C:\Winlogger401\Data\SR710\Z3-B8\Z3B8CALUP01.LOG"

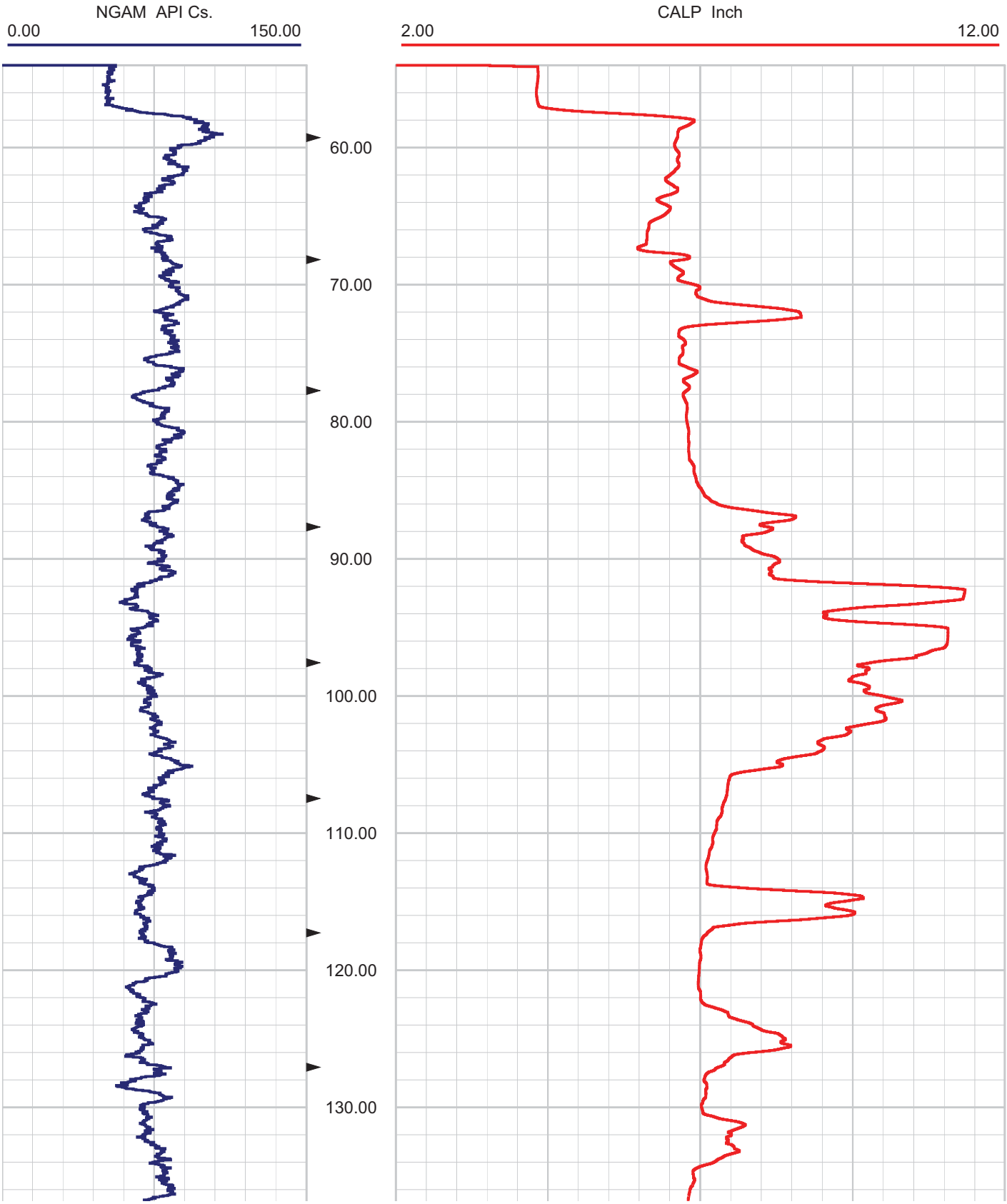

SR-710 Boring Z3-B12 Caliper and Natural Gamma rev 1.1 Sheet 1 of 3

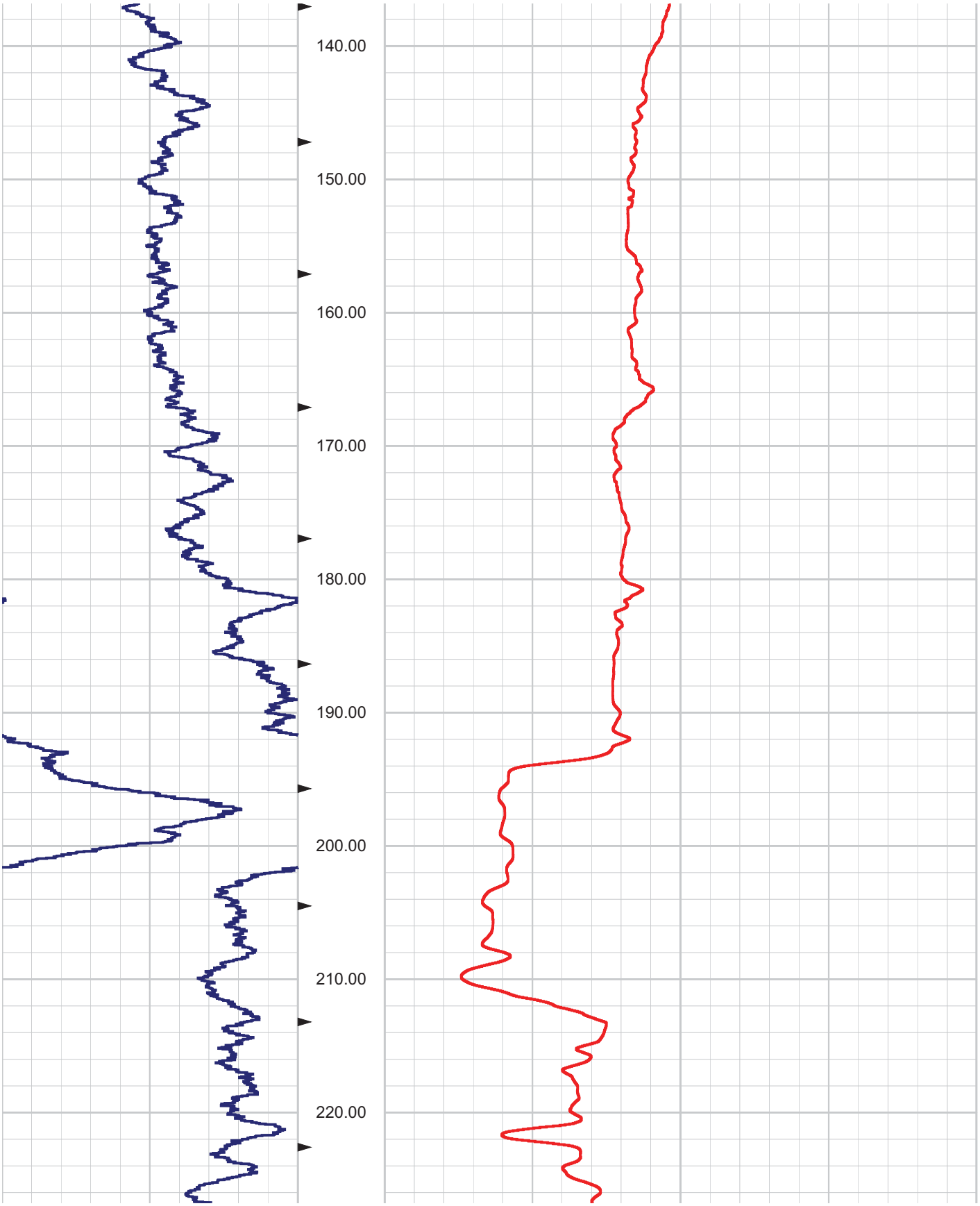

SR-710 Boring Z3-B12 Caliper and Natural Gamma rev 1.1 Sheet 2 of 3

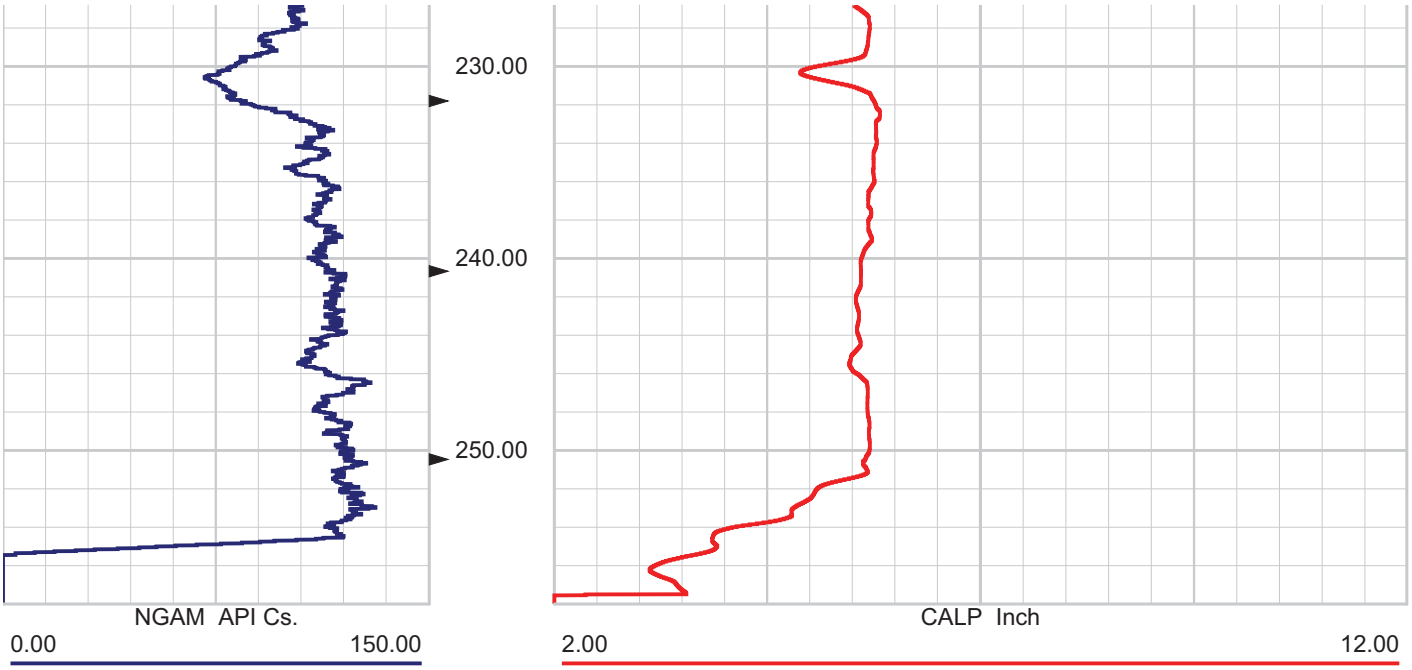
230.00
240.00
250.00
NGAM API Cs.
0.00
150.00
CALP Inch
2.00
12.00

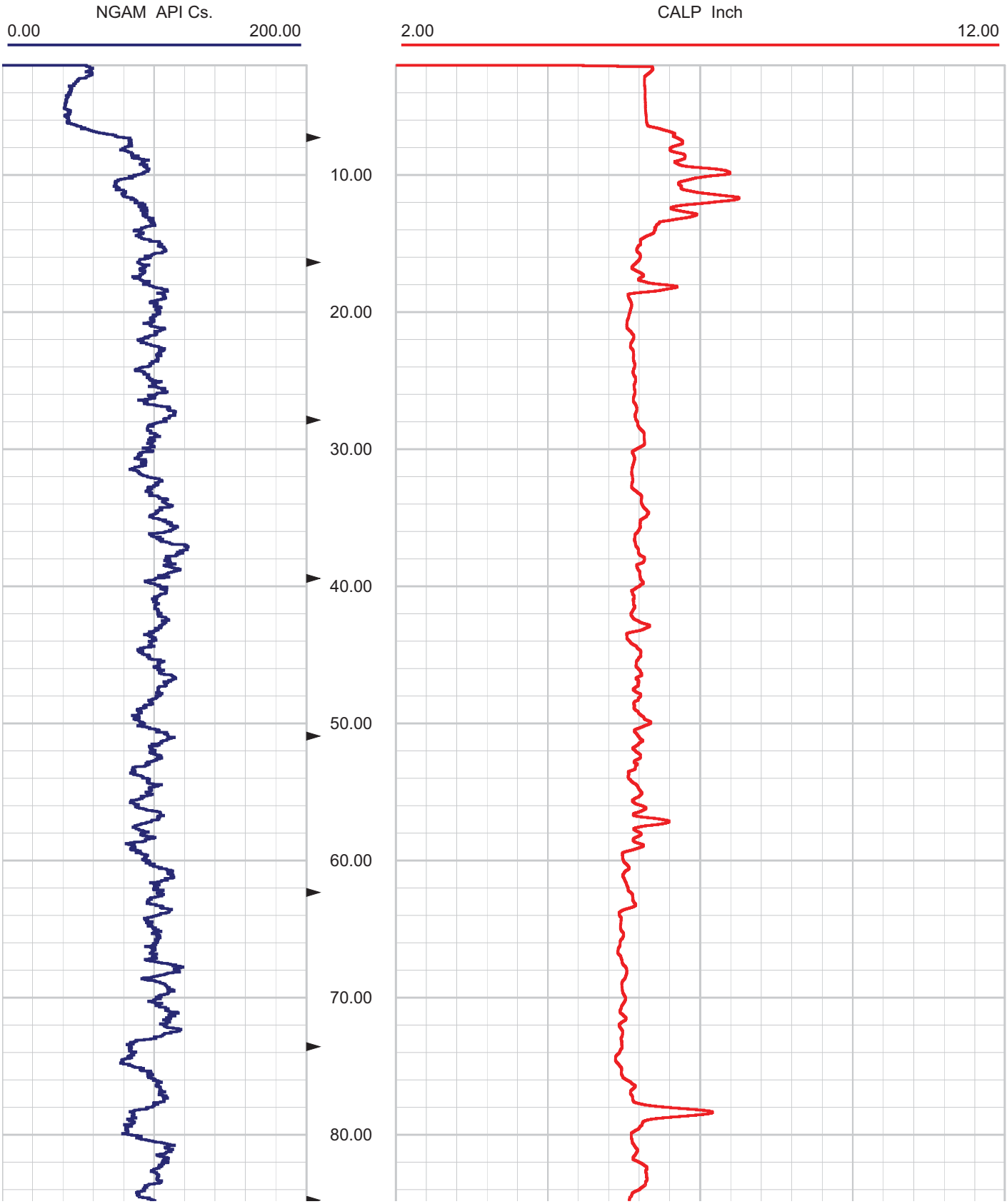

SR-710 Boring Z4-B4 Caliper and Natural Gamma rev 1.1 Sheet 1 of 4

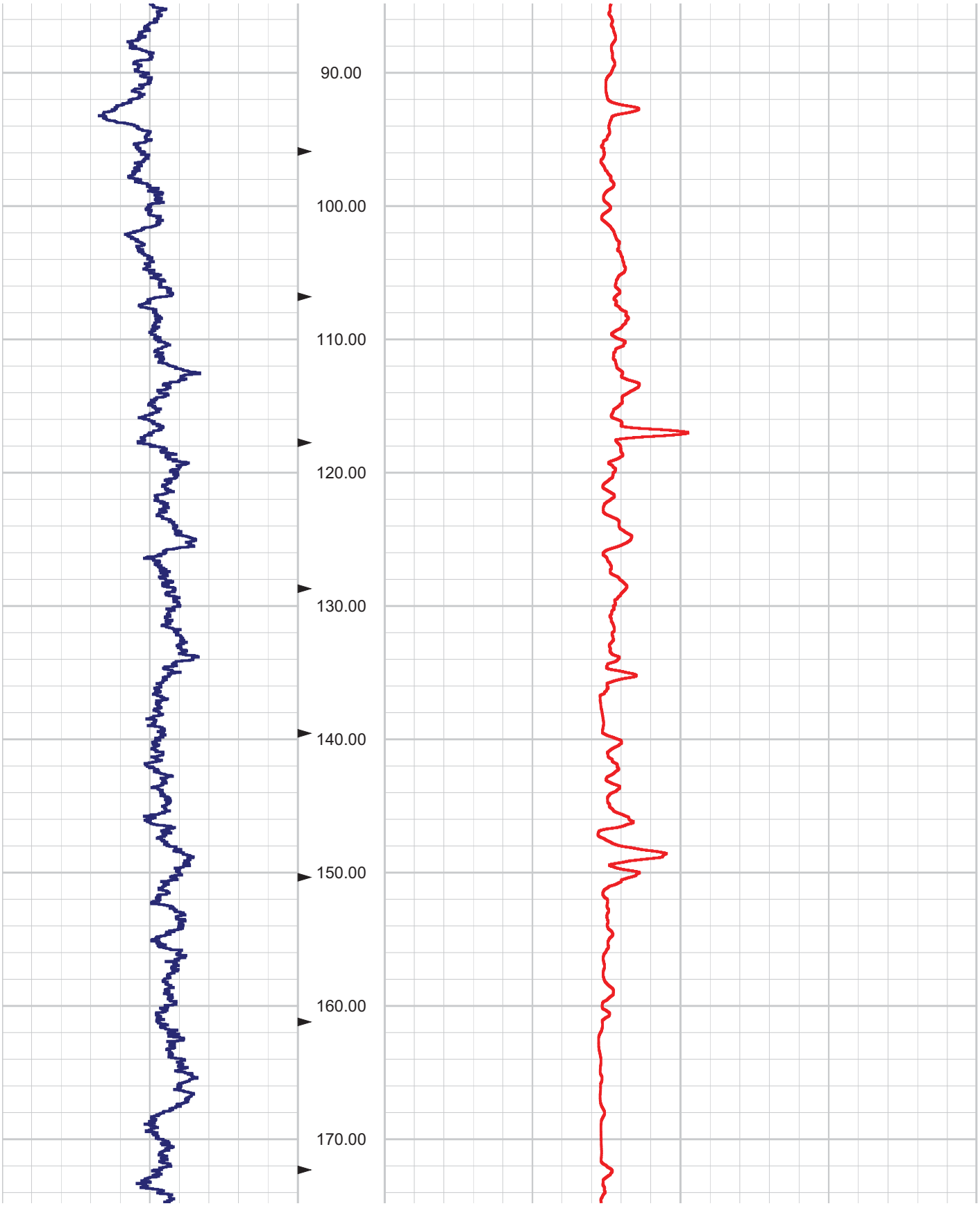

SR-710 Boring Z4-B4 Caliper and Natural Gamma rev 1.1 Sheet 2 of 4

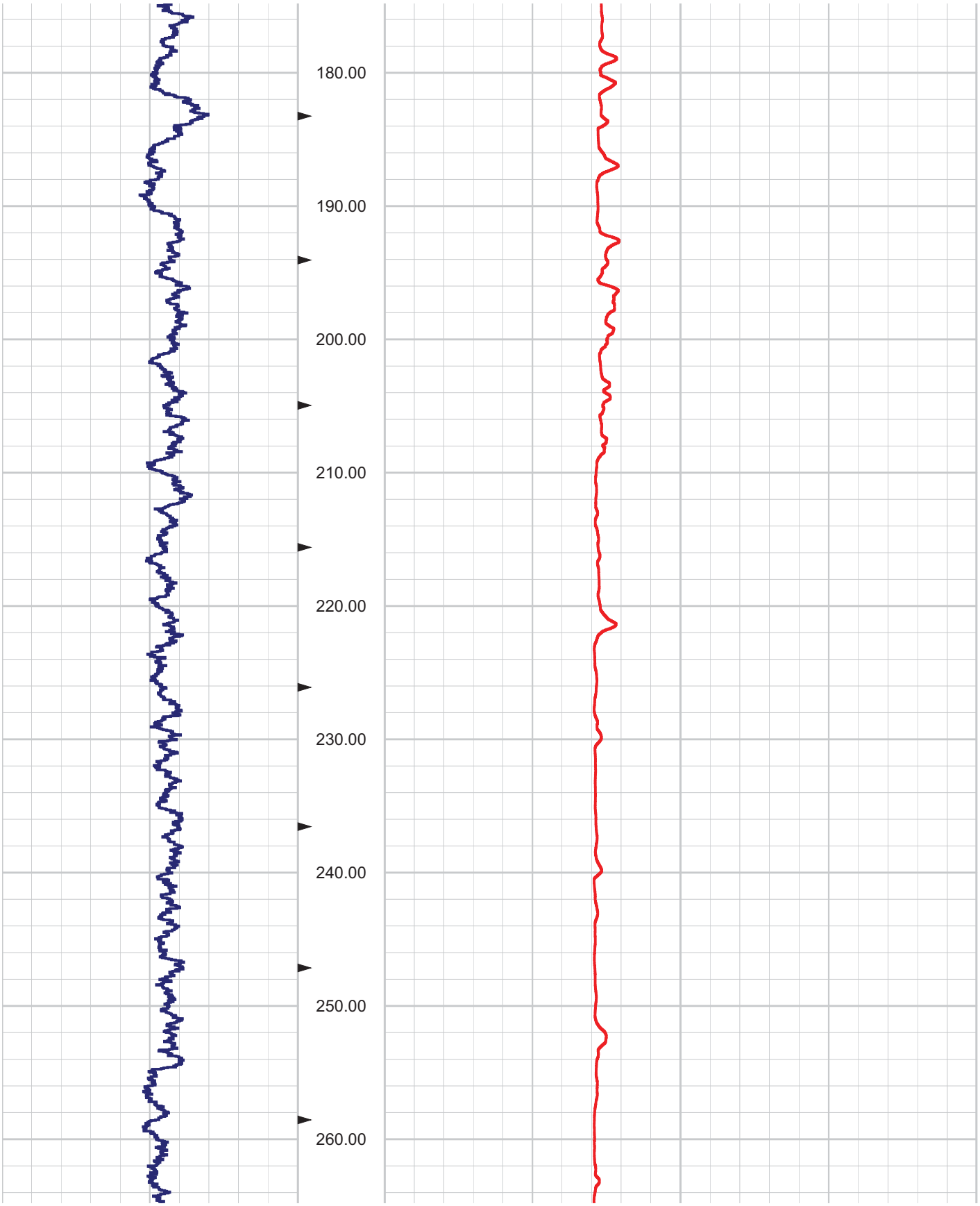

SR-710 Boring Z4-B4 Caliper and Natural Gamma rev 1.1 Sheet 3 of 4

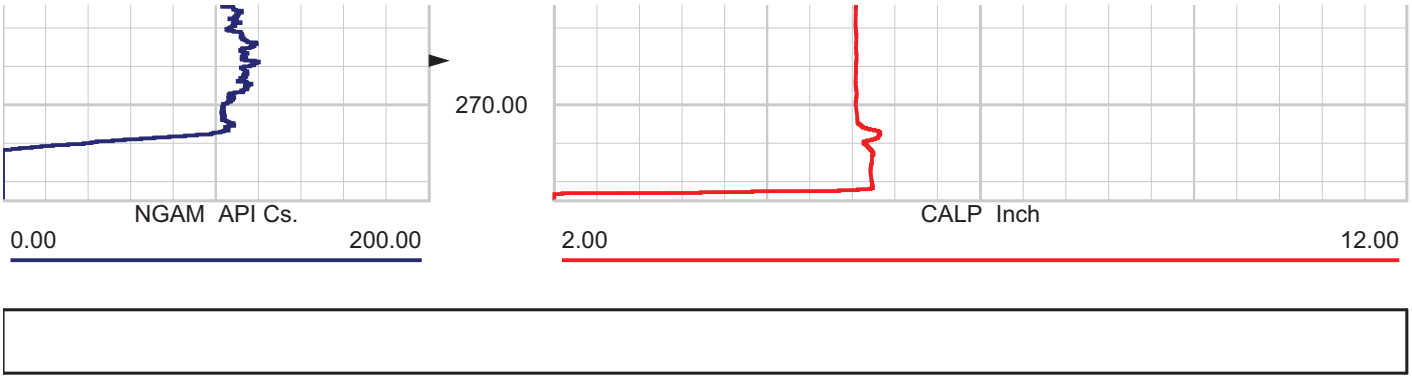
270.00
NGAM API Cs.
0.00
200.00
CALP Inch
2.00
12.00

APPENDIX C

ACOUSTIC TELEVIEWER DIPS LOGS

BHTV DATA PROCESSING
RGLDIP vsn 6.2
INTERPRETED BHTV DIPS LOG

CASCADE DRILLING

Borehole: Z3-B3

SR-710 TUNNEL INVESTIGATION

top of borehole.....
East: _
North: _
Elev: _

North ref. is true
Depth units are feet
Vertical scale: 1/10
Horiz scale = 1.00x Vert scale

Zone from 273.984 to 173.200ft
Format: BHTV-NESWN

Borehole diam: 5.600inch
Vertical = borehole-axis
Image: Amplitude

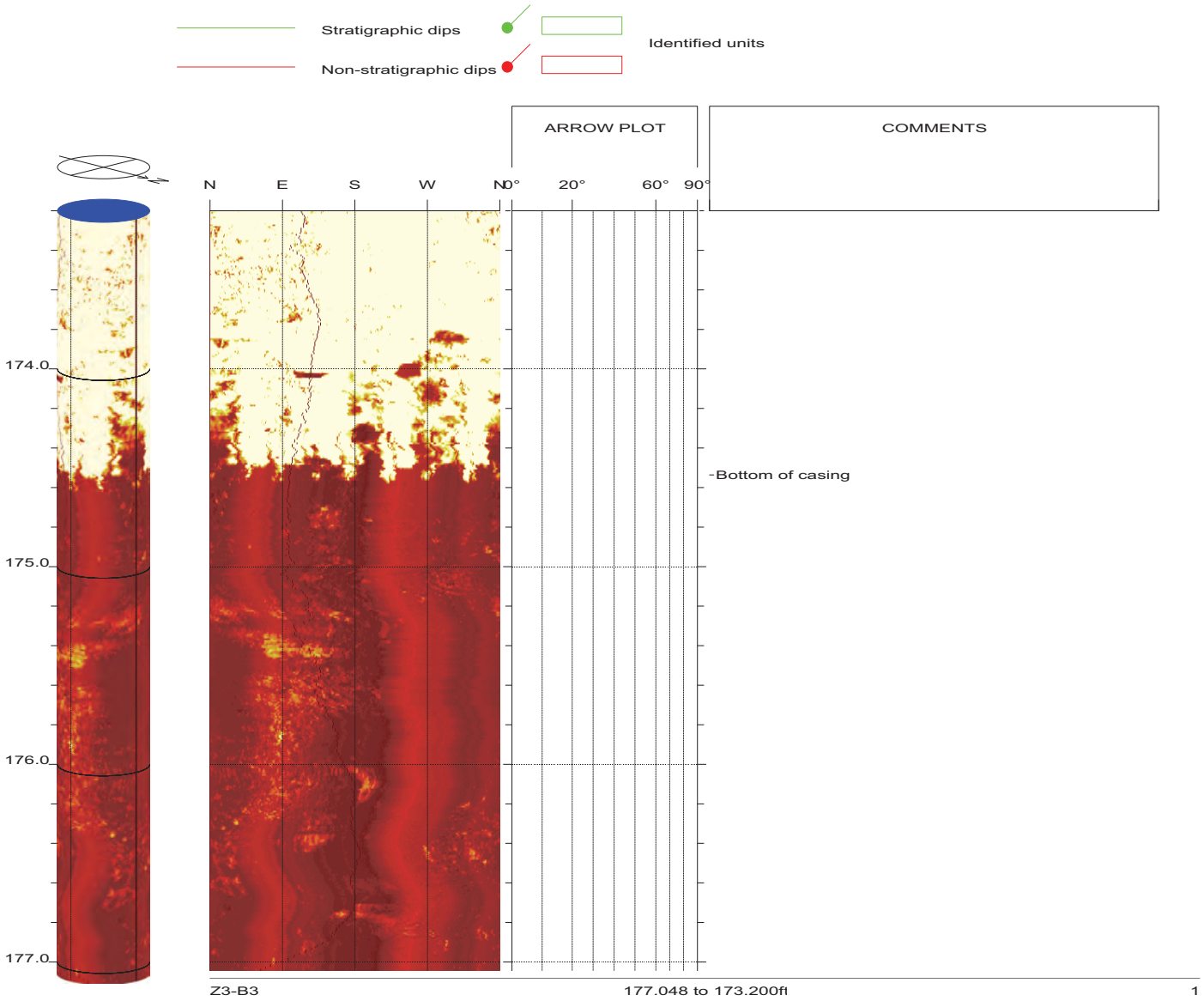

SR-710 Boring Z3-B3 Acoustic Televiewer Dips rev 1 Sheet 1 of 15

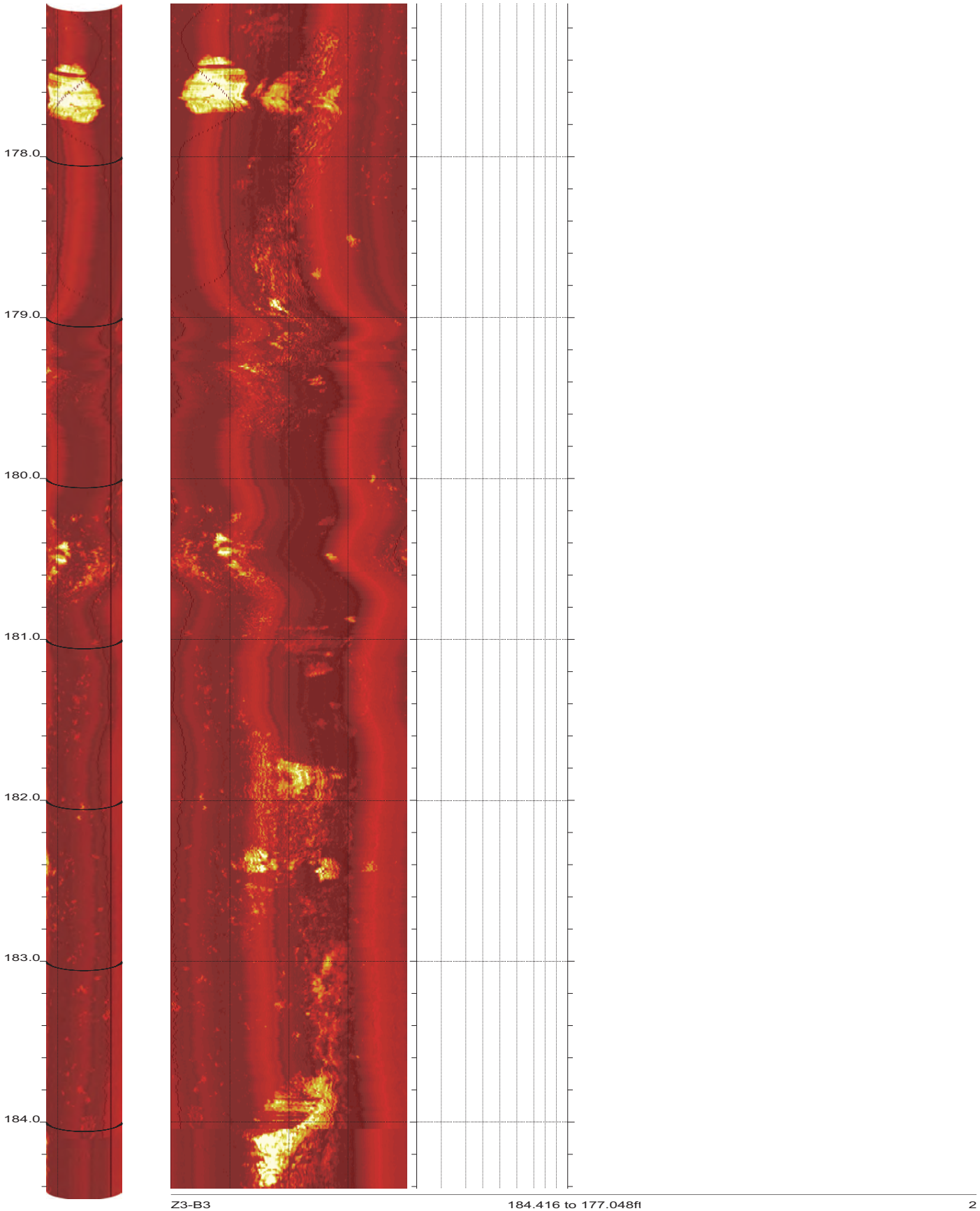

SR-710 Boring Z3-B3 Acoustic Televiewer Dips rev 1 Sheet 2 of 15

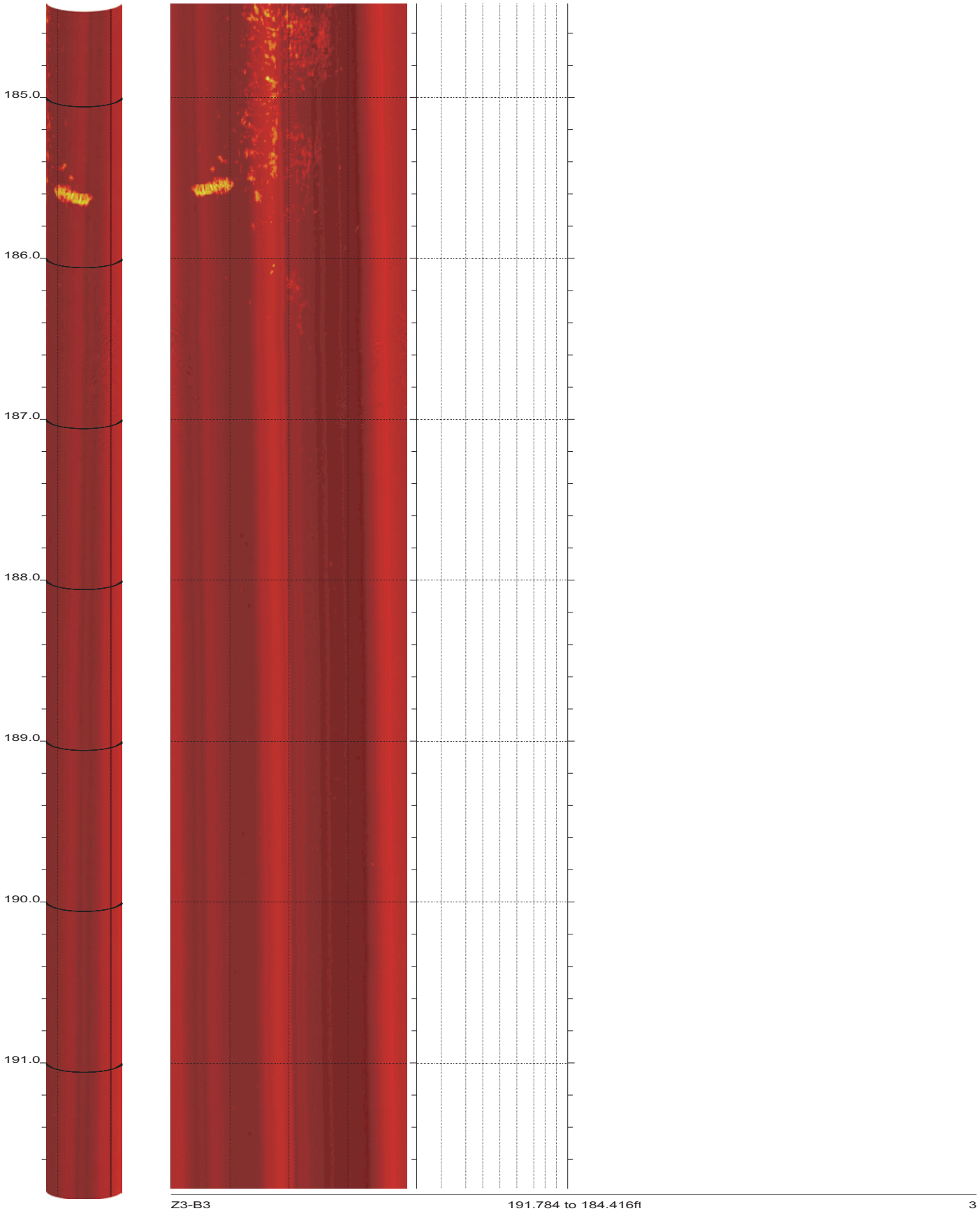

SR-710 Boring Z3-B3 Acoustic Televiewer Dips rev 1 Sheet 3 of 15

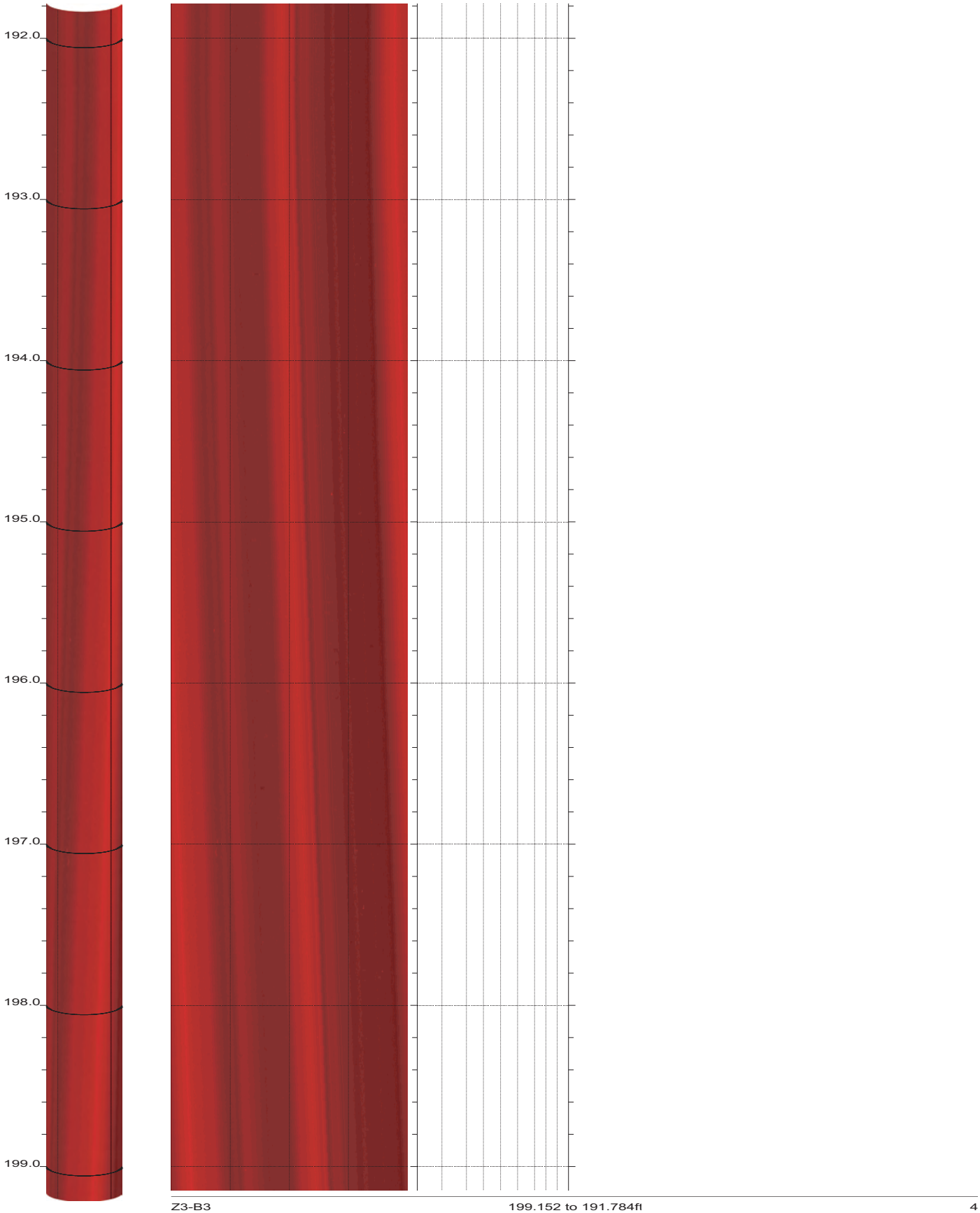

SR-710 Boring Z3-B3 Acoustic Televiewer Dips rev 1 Sheet 4 of 15

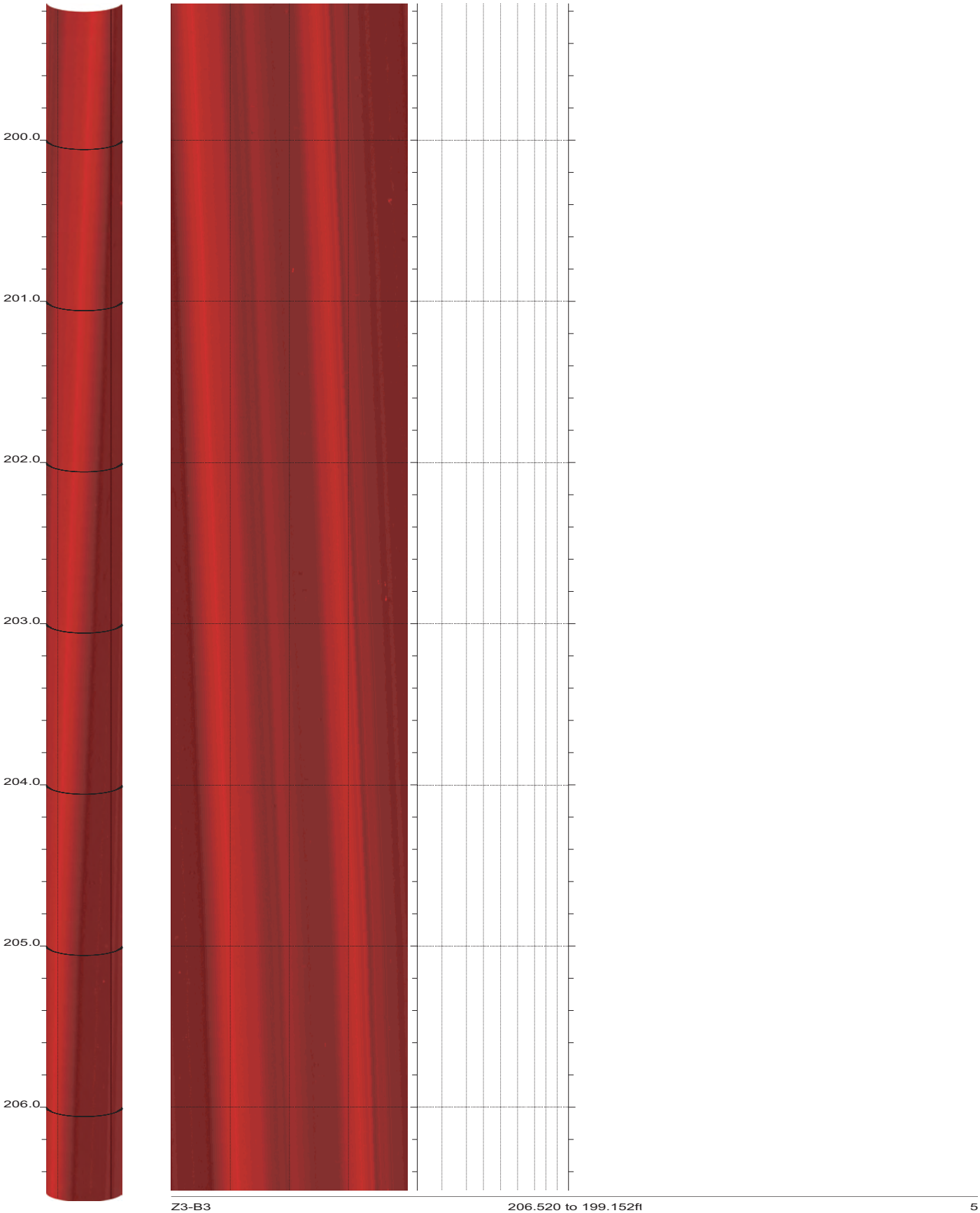

SR-710 Boring Z3-B3 Acoustic Televiewer Dips rev 1 Sheet 5 of 15

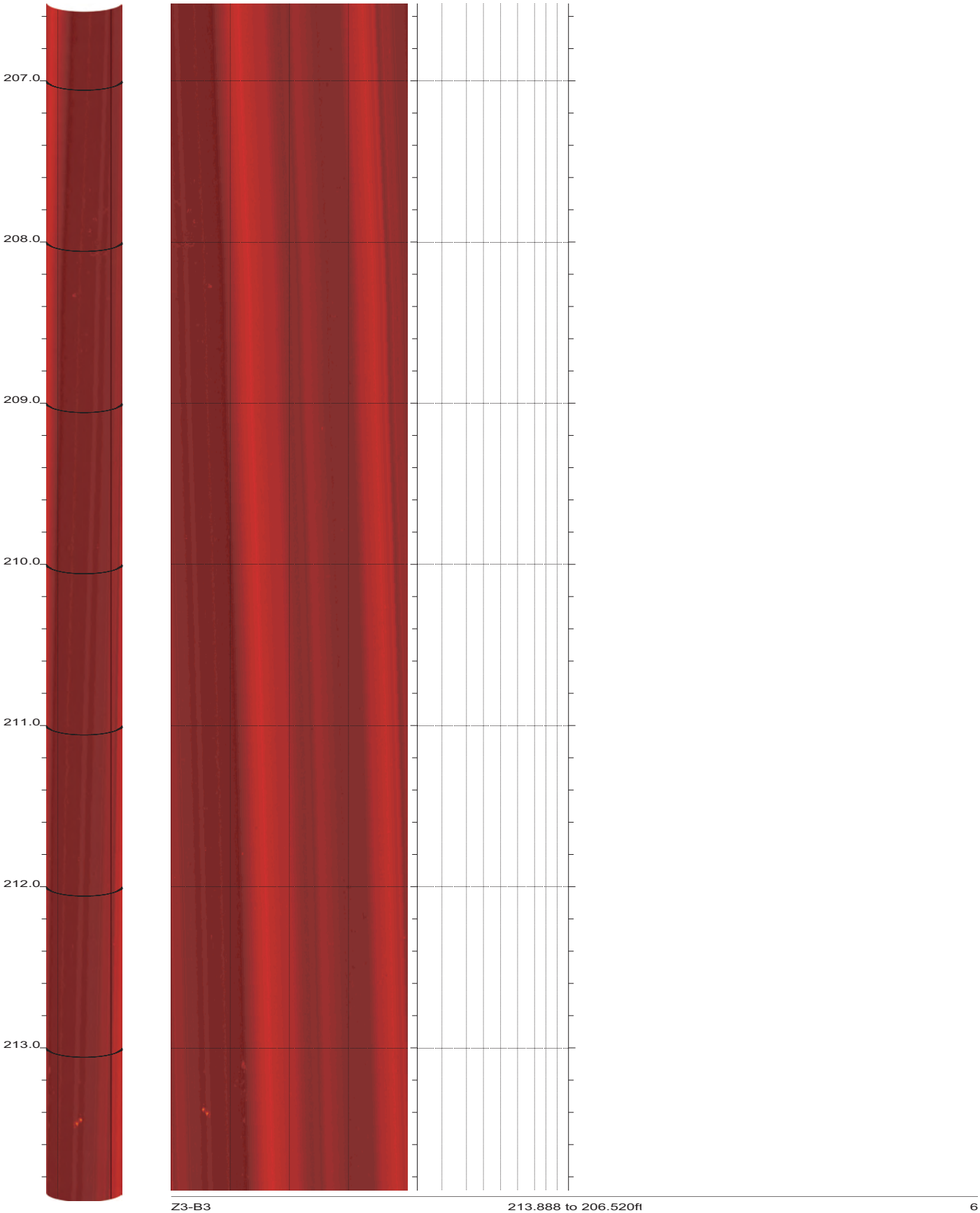

SR-710 Boring Z3-B3 Acoustic Televiewer Dips rev 1 Sheet 6 of 15

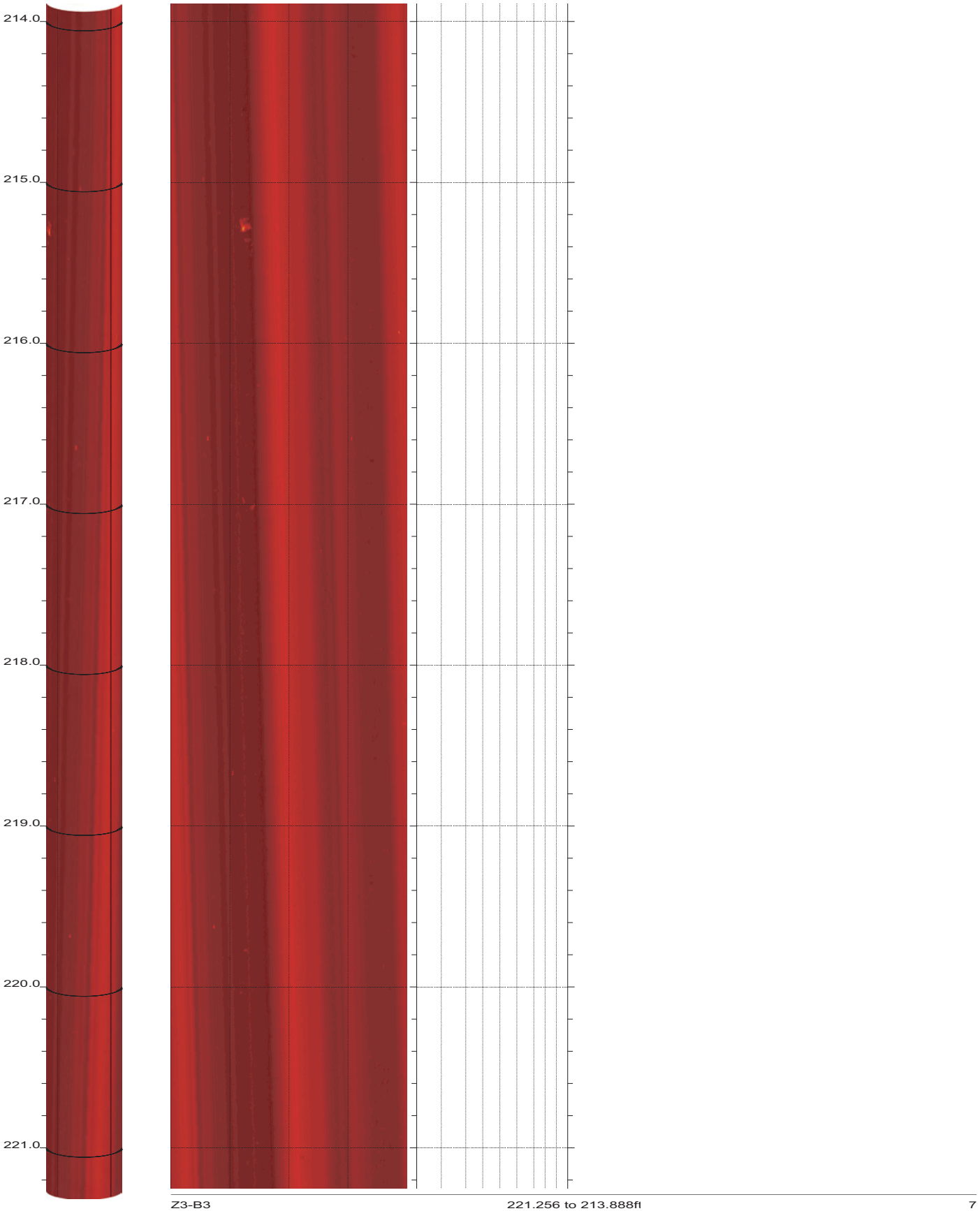

SR-710 Boring Z3-B3 Acoustic Televiewer Dips rev 1 Sheet 7 of 15

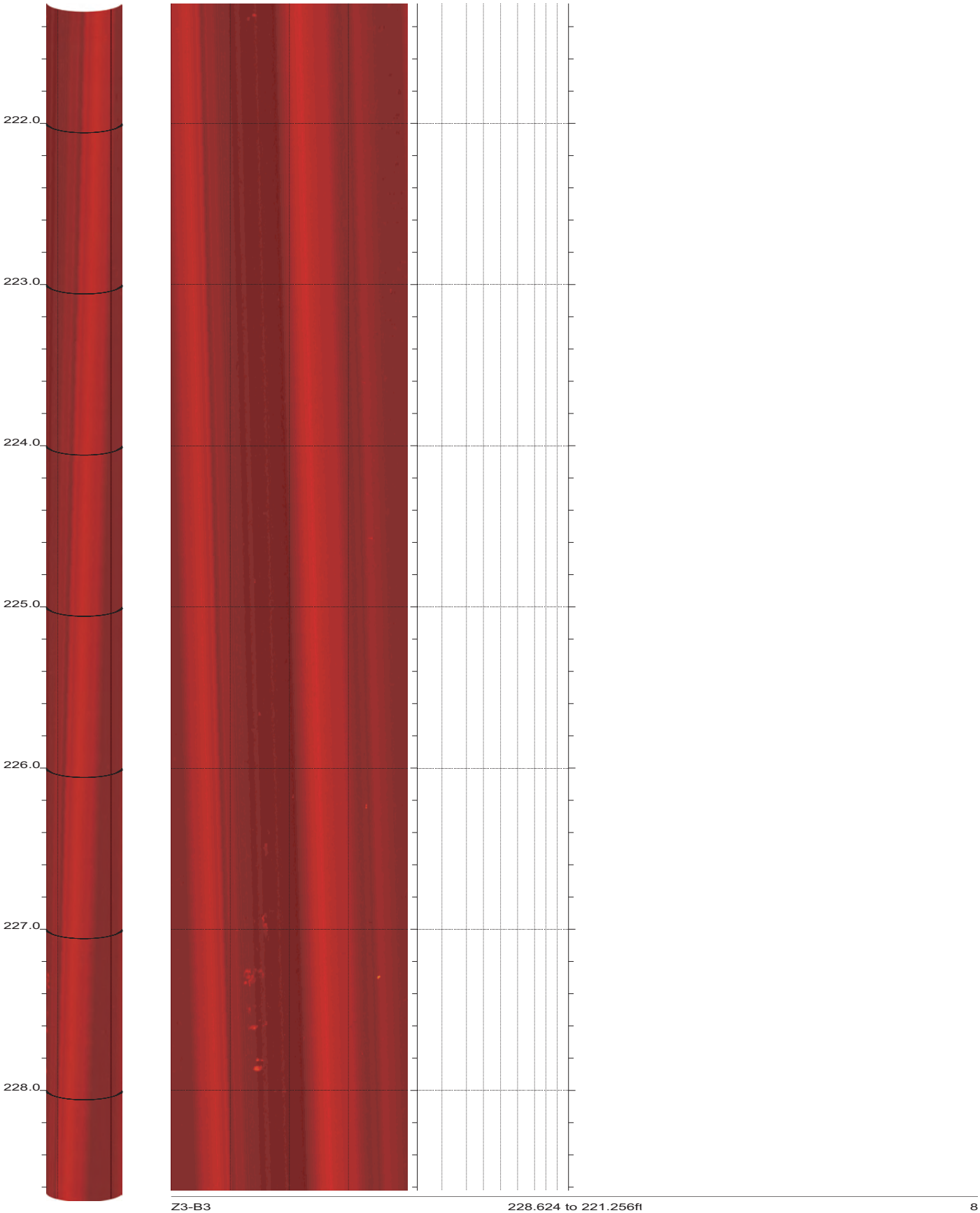

SR-710 Boring Z3-B3 Acoustic Televiewer Dips rev 1 Sheet 8 of 15

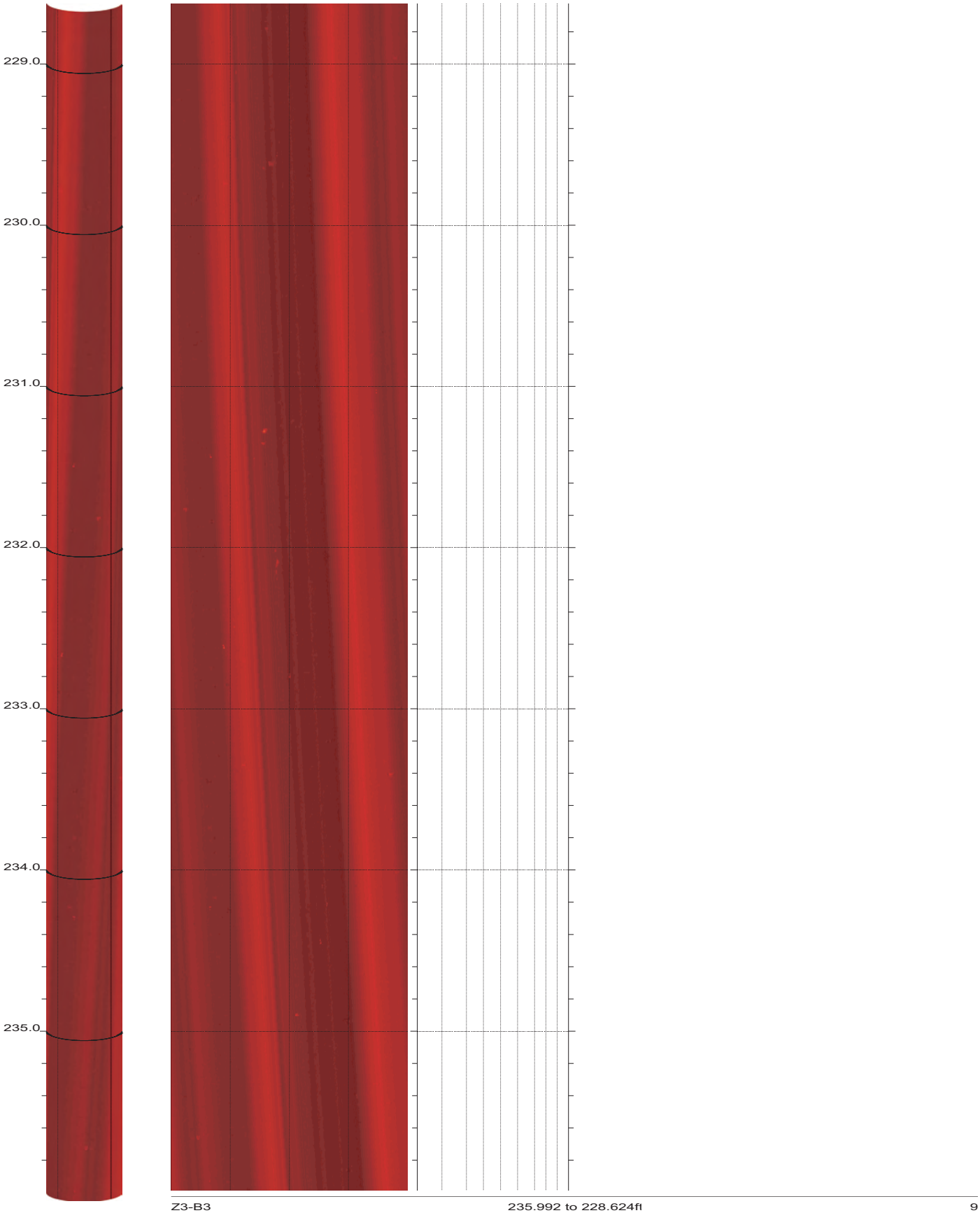

SR-710 Boring Z3-B3 Acoustic Televiewer Dips rev 1 Sheet 9 of 15

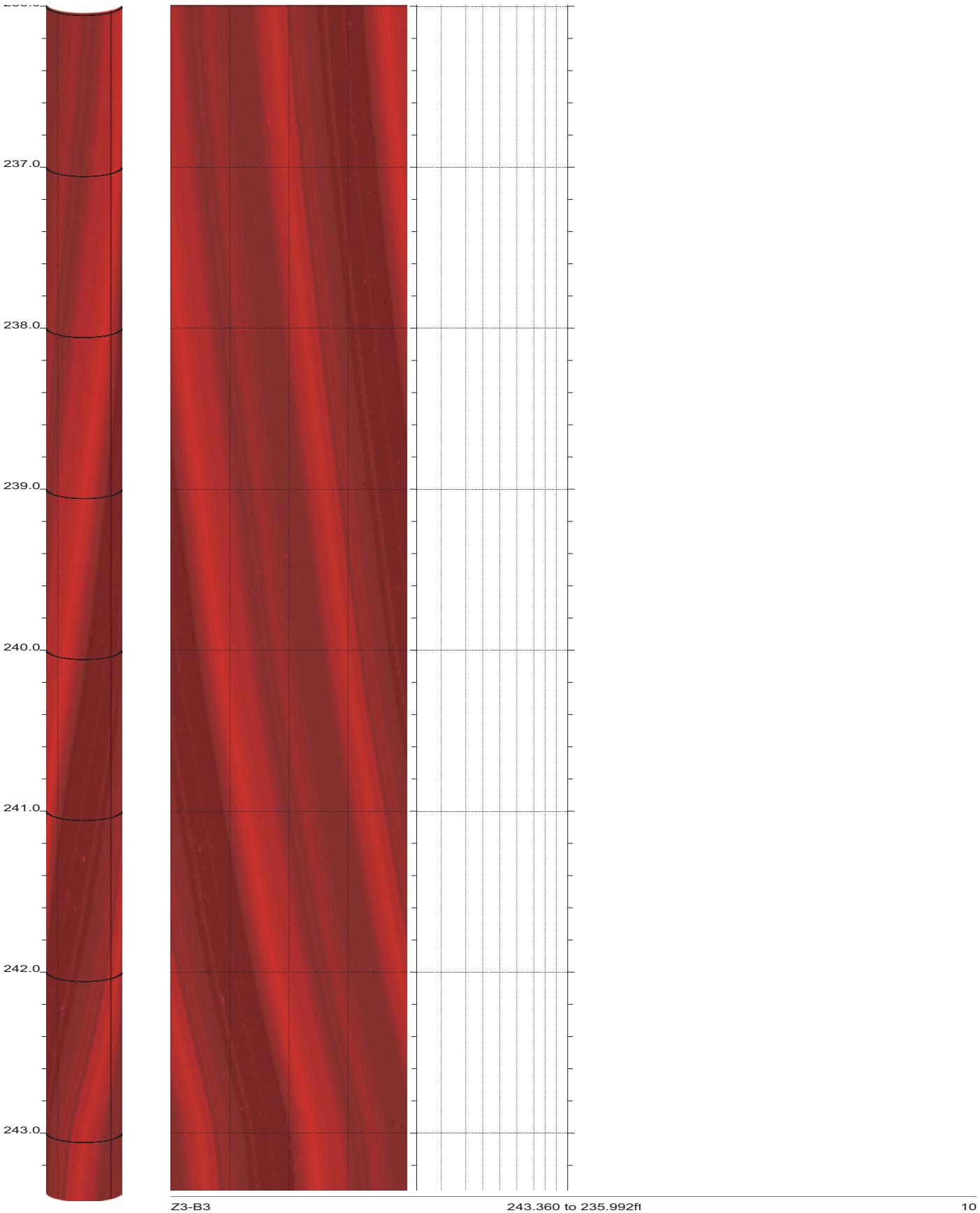

SR-710 Boring Z3-B3 Acoustic Televiewer Dips rev 1 Sheet 10 of 15

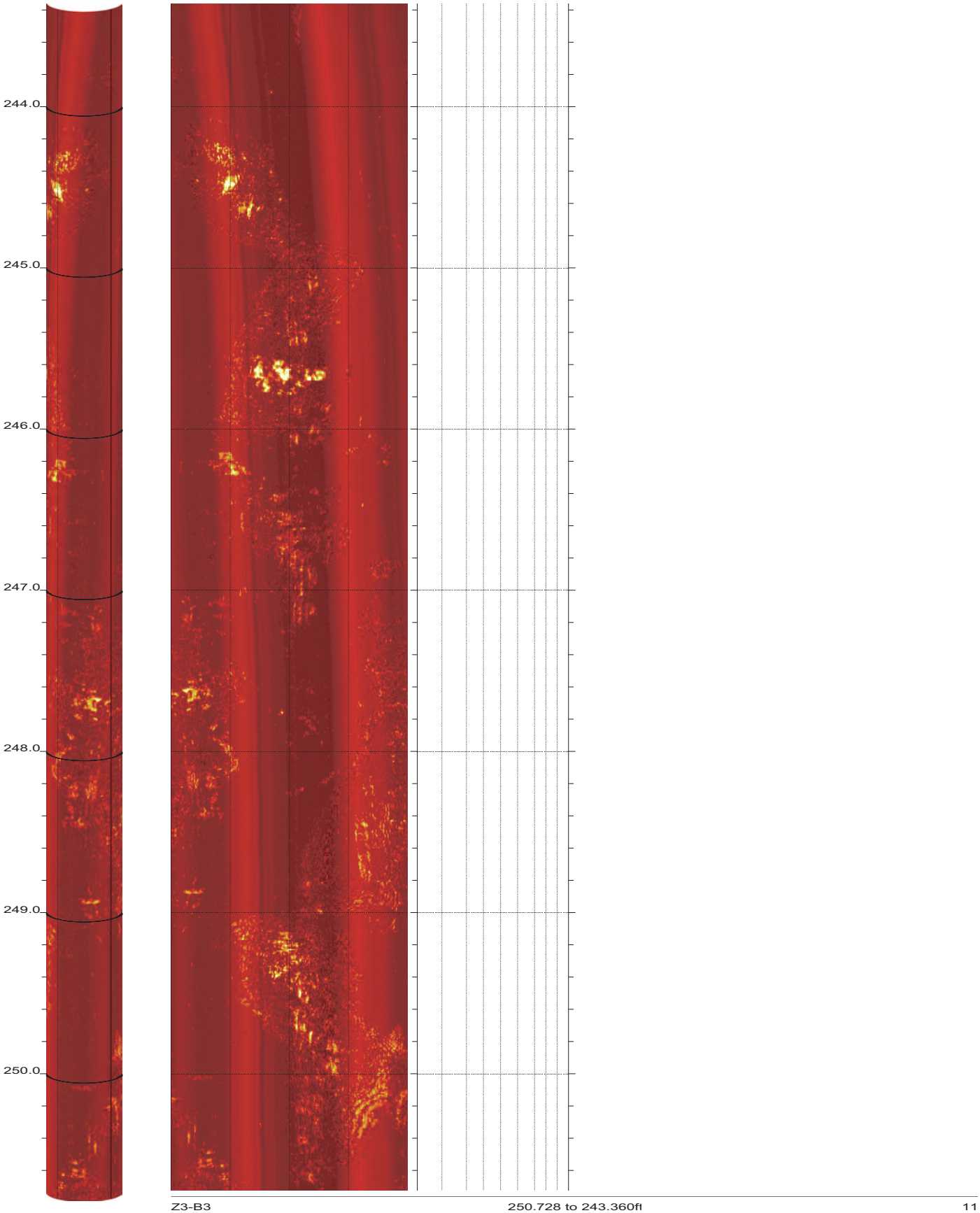

SR-710 Boring Z3-B3 Acoustic Televiewer Dips rev 1 Sheet 11 of 15

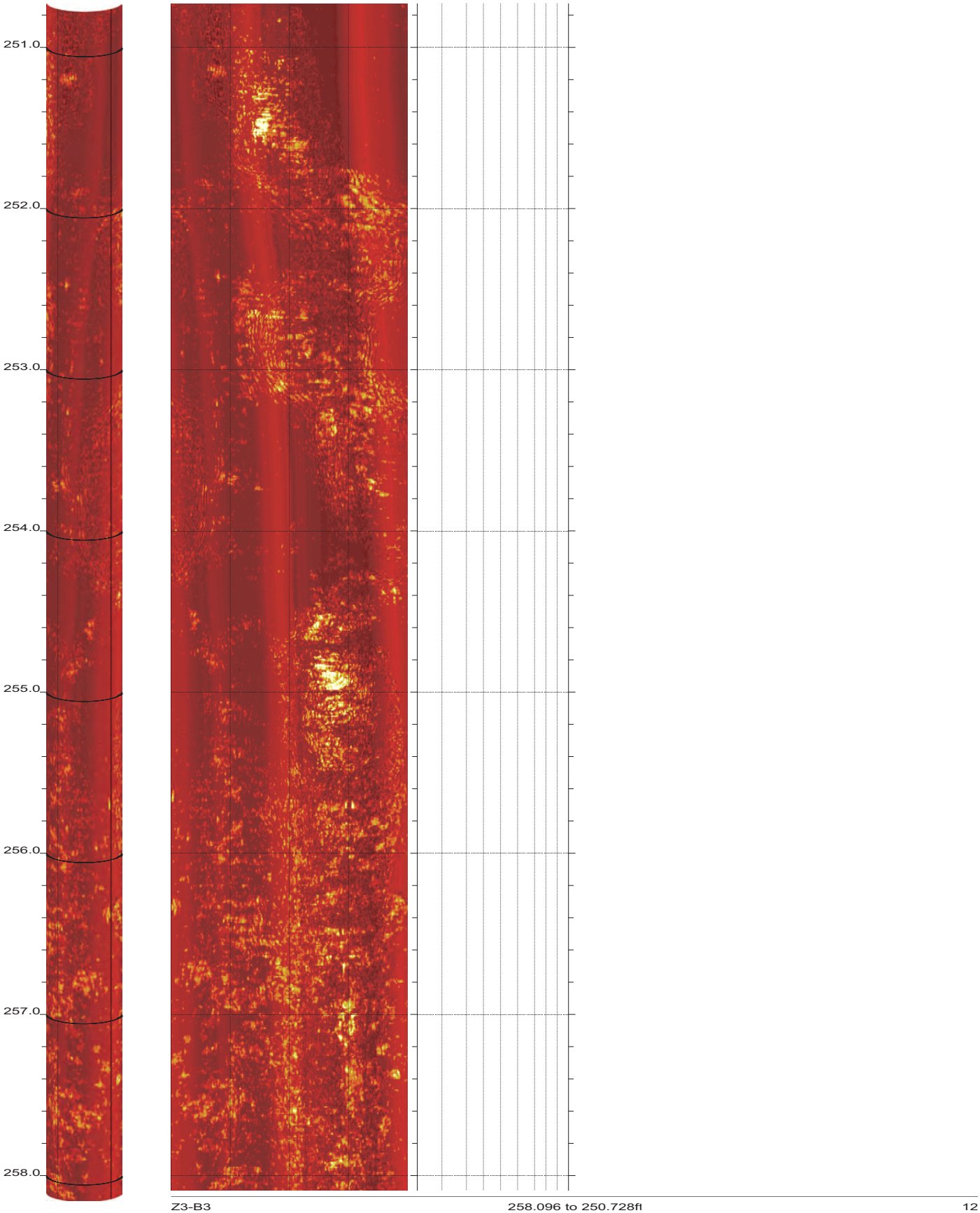

SR-710 Boring Z3-B3 Acoustic Televiewer Dips rev 1 Sheet 12 of 15

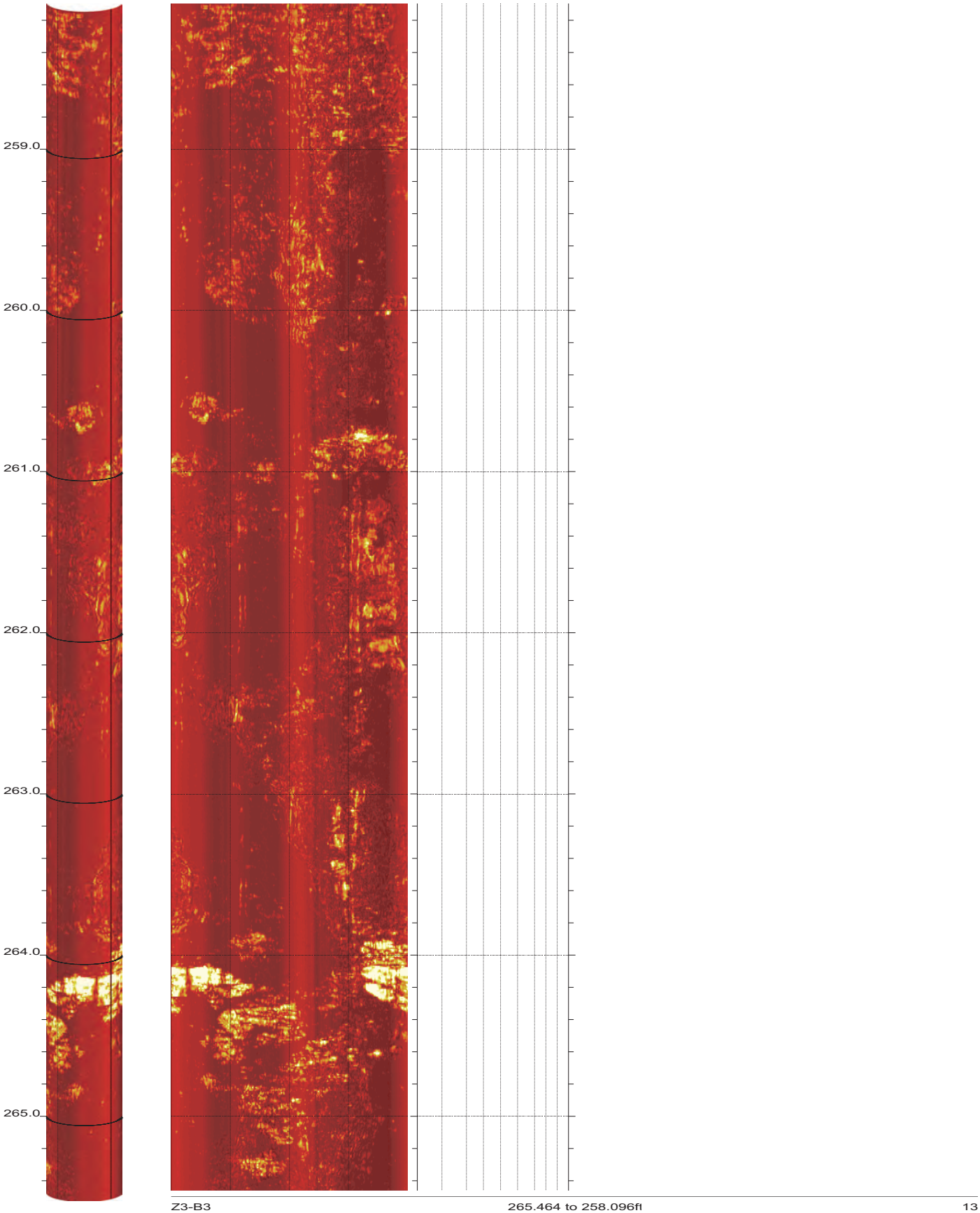

SR-710 Boring Z3-B3 Acoustic Televiewer Dips rev 1 Sheet 13 of 15

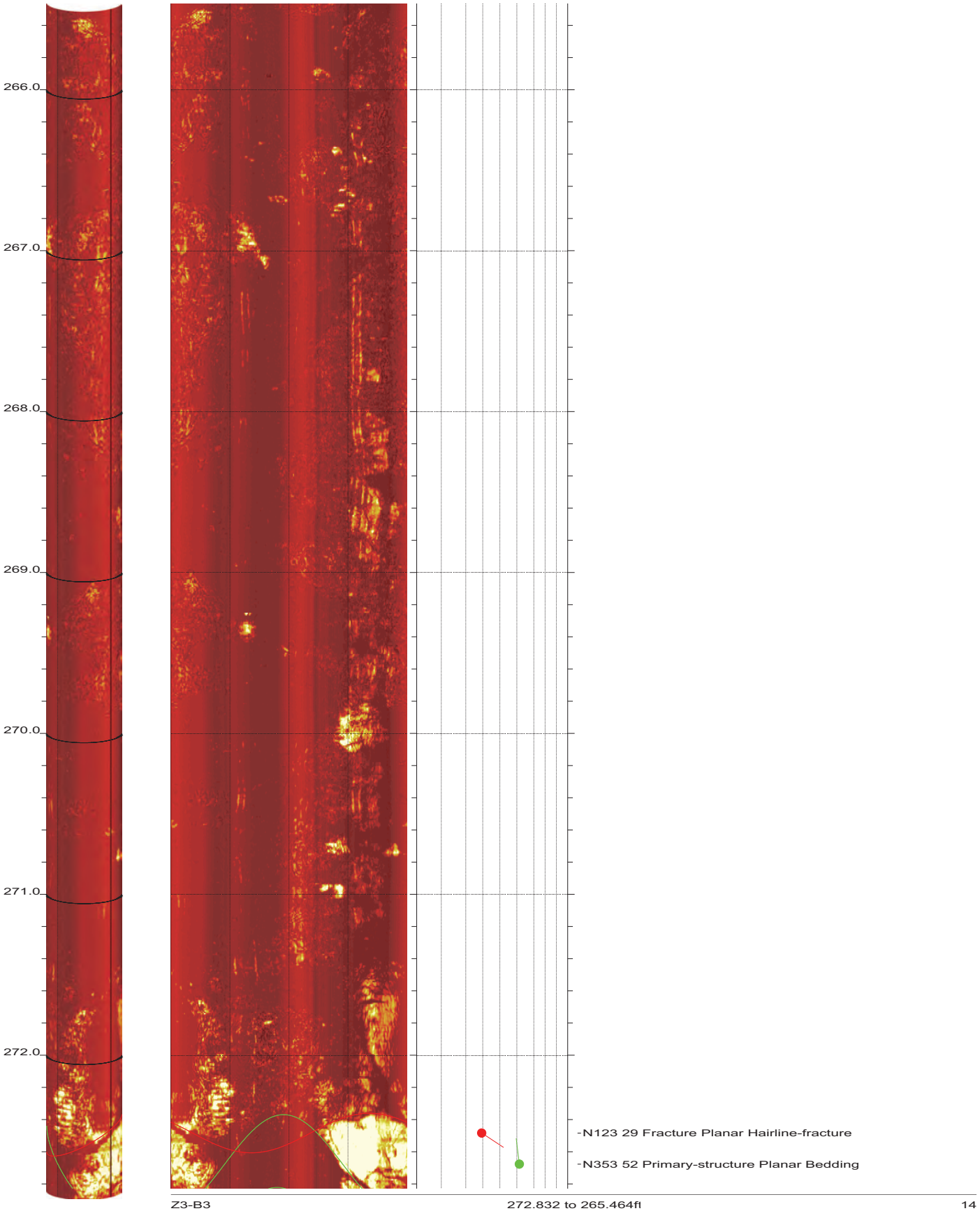

SR-710 Boring Z3-B3 Acoustic Televiewer Dips rev 1 Sheet 14 of 15

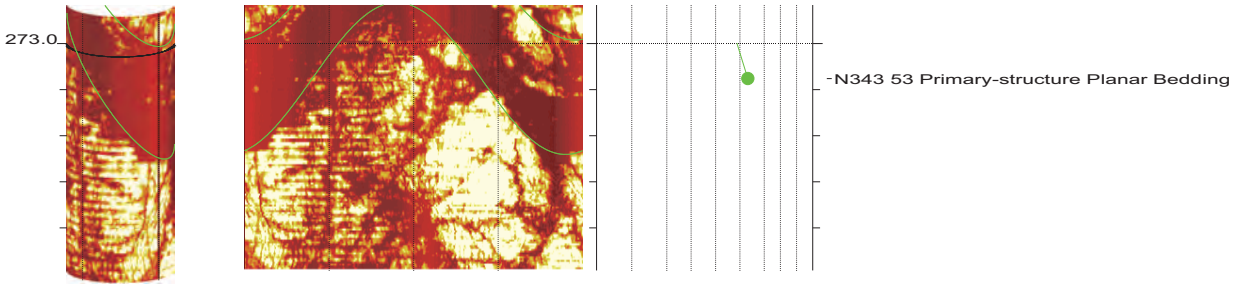
273.0
-N343 53 Primary-structure Planar Bedding

BHTV DATA PROCESSING
RGLDIP vsn 6.2
INTERPRETED BHTV DIPS LOG

CASCADE DRILLING

Borehole: Z3-B4

SR-710 TUNNEL INVESTIGATION

top of borehole.....
East: _
North: _
Elev: _

North ref. is true
Depth units are feet
Vertical scale: 1/10
Horiz scale = 1.00x Vert scale

Zone from 275.000 to 2.600ft
Format: BHTV-NESWN

Borehole diam: 5.600inch
Vertical = borehole-axis
Image: Amplitude

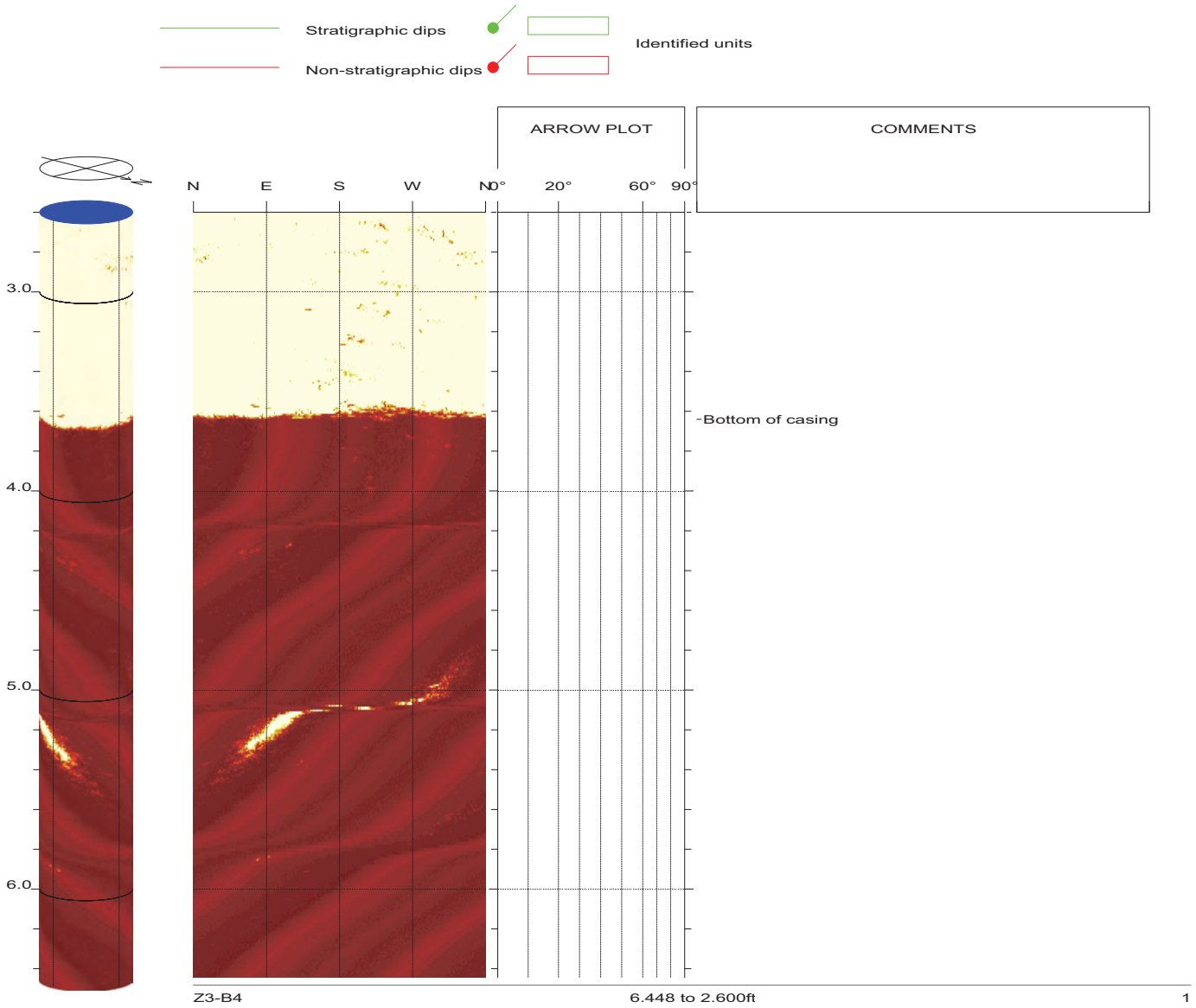

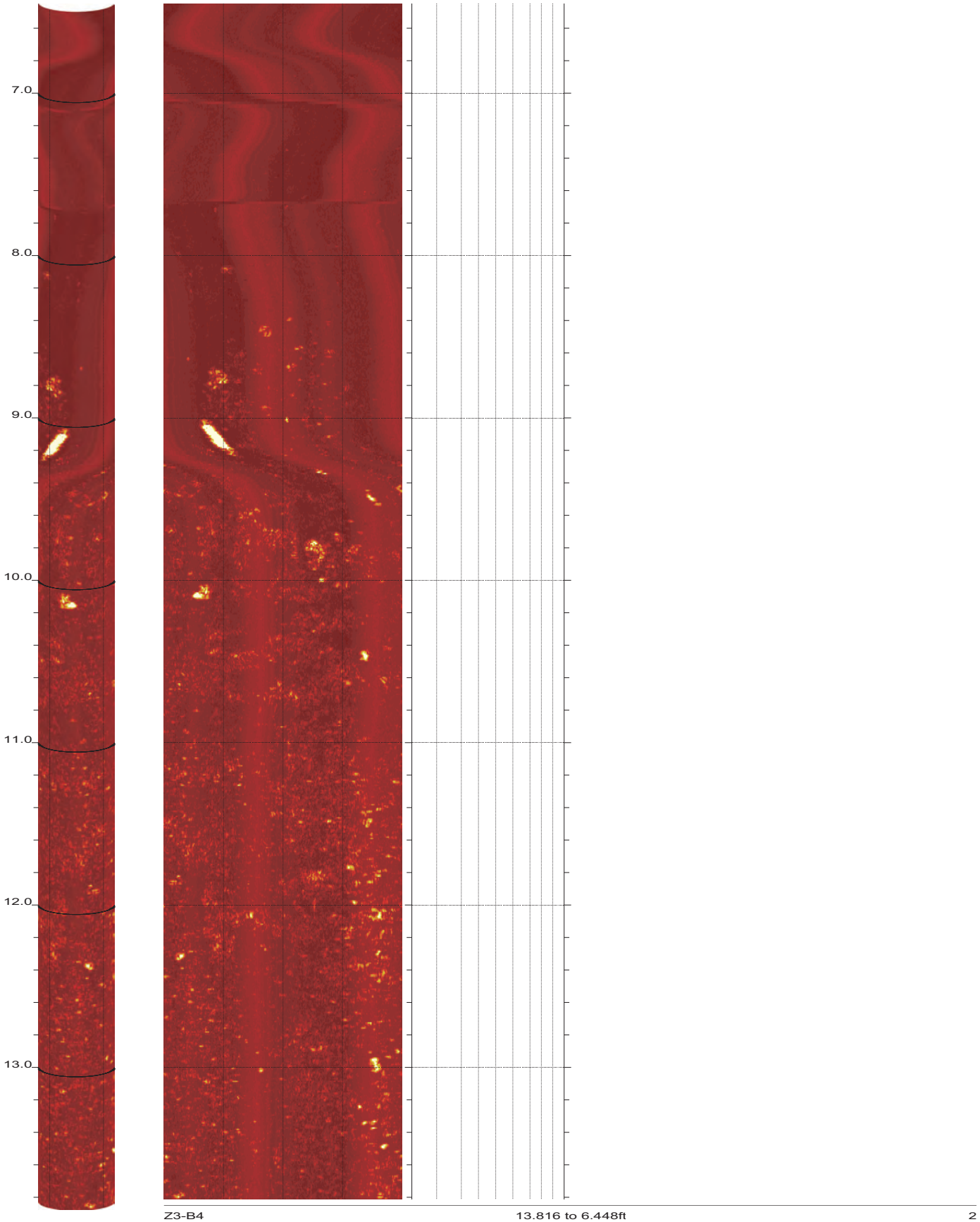
7.0
8.0
9.0
10.0
11.0
12.0
13.0
Z3-B4
13.816 to 6.448ft
2

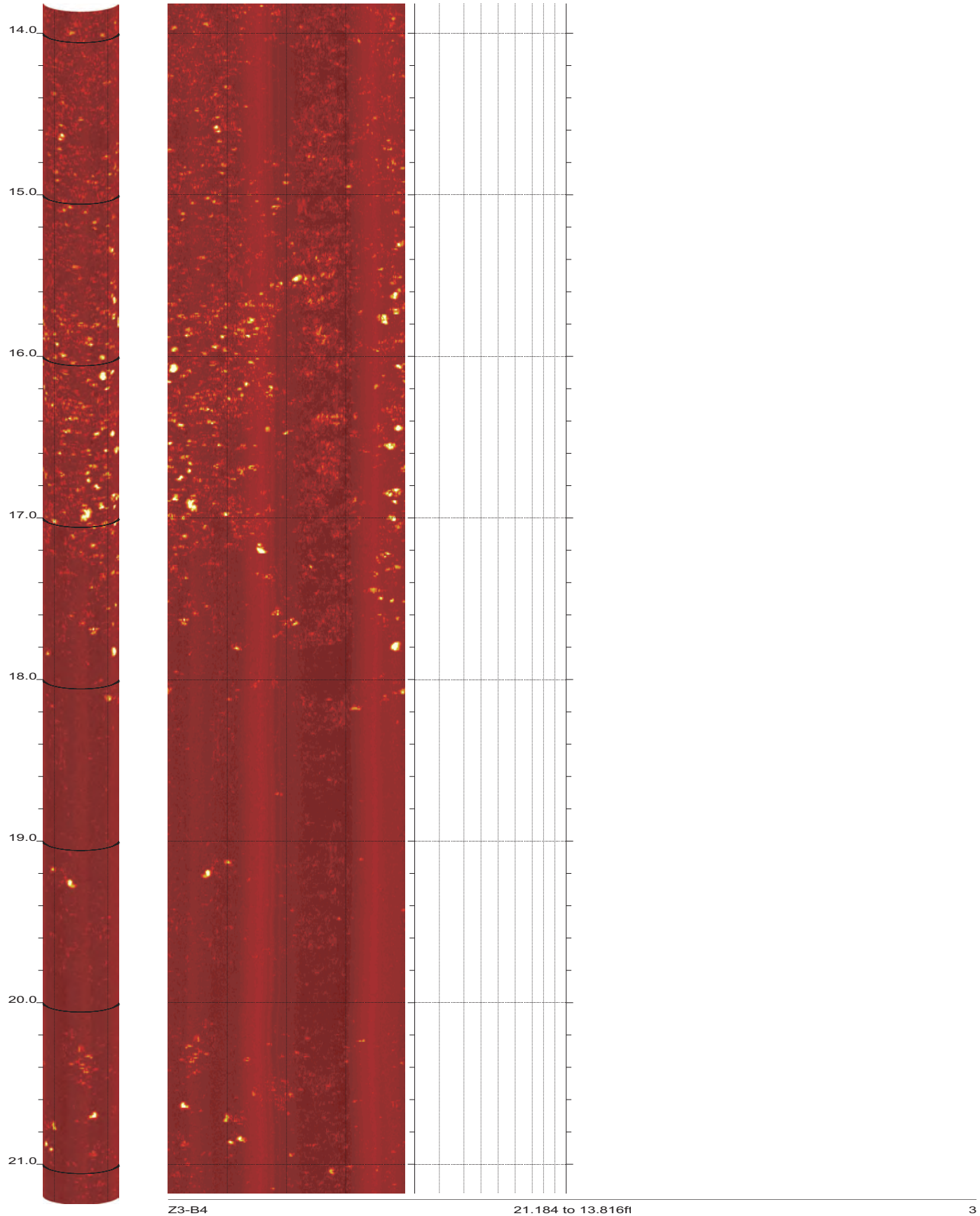

SR-710 Boring Z3-B4 Acoustic Televiewer Dips rev 1 Sheet 3 of 38

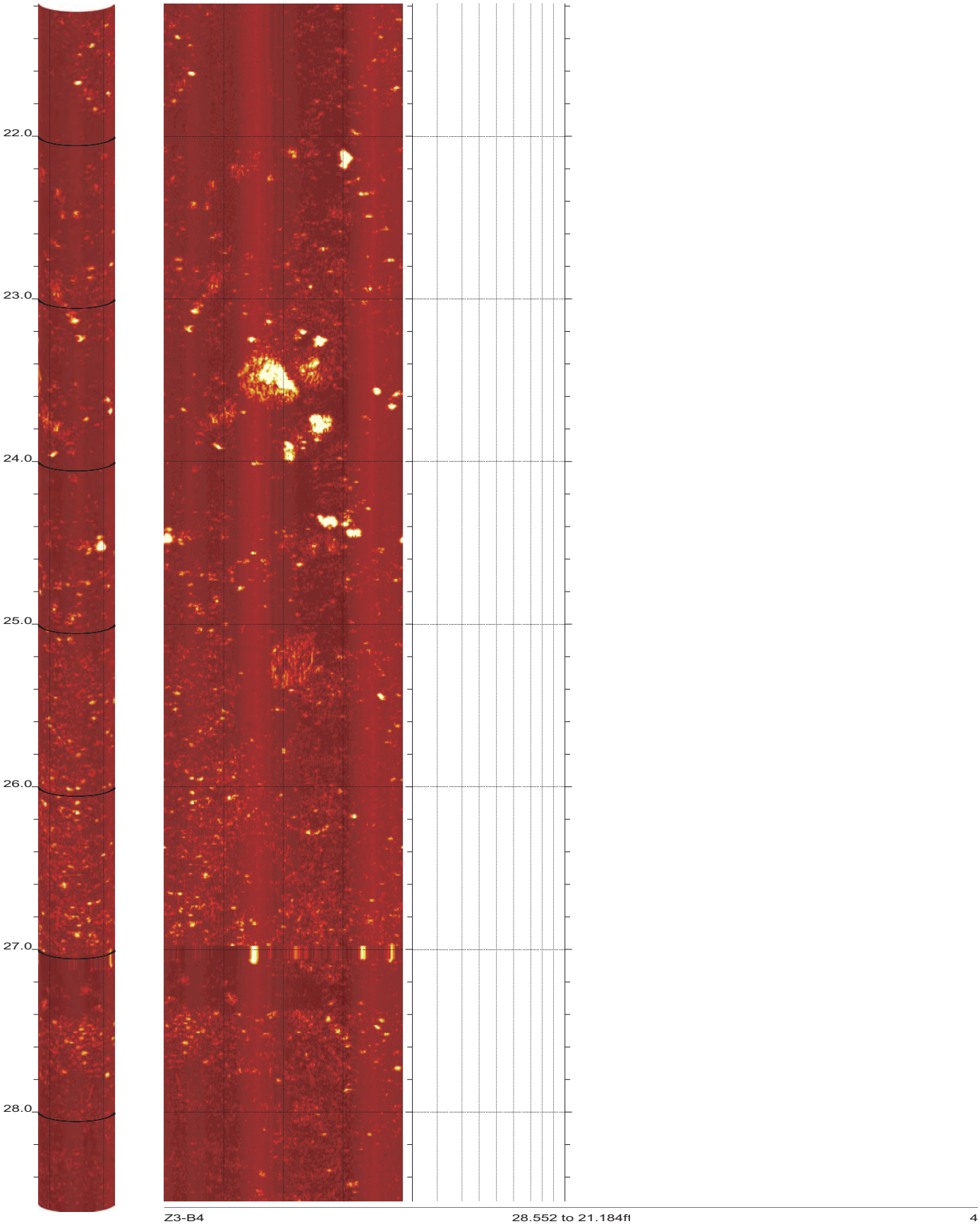

SR-710 Boring Z3-B4 Acoustic Televiewer Dips rev 1 Sheet 4 of 38

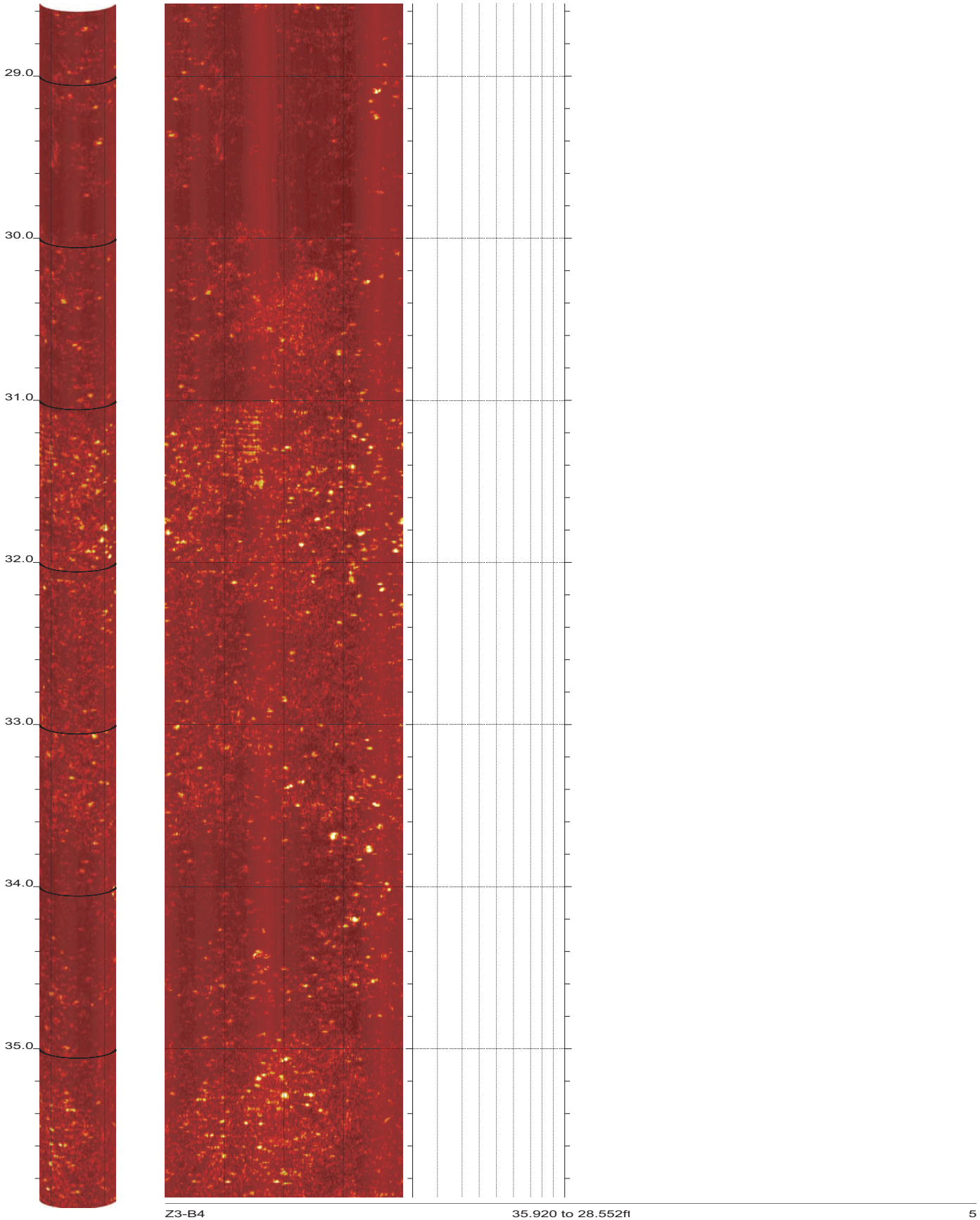
29.0
30.0
31.0
32.0
33.0
34.0
35.0
Z3-B4
35.920 to 28.552fl
5

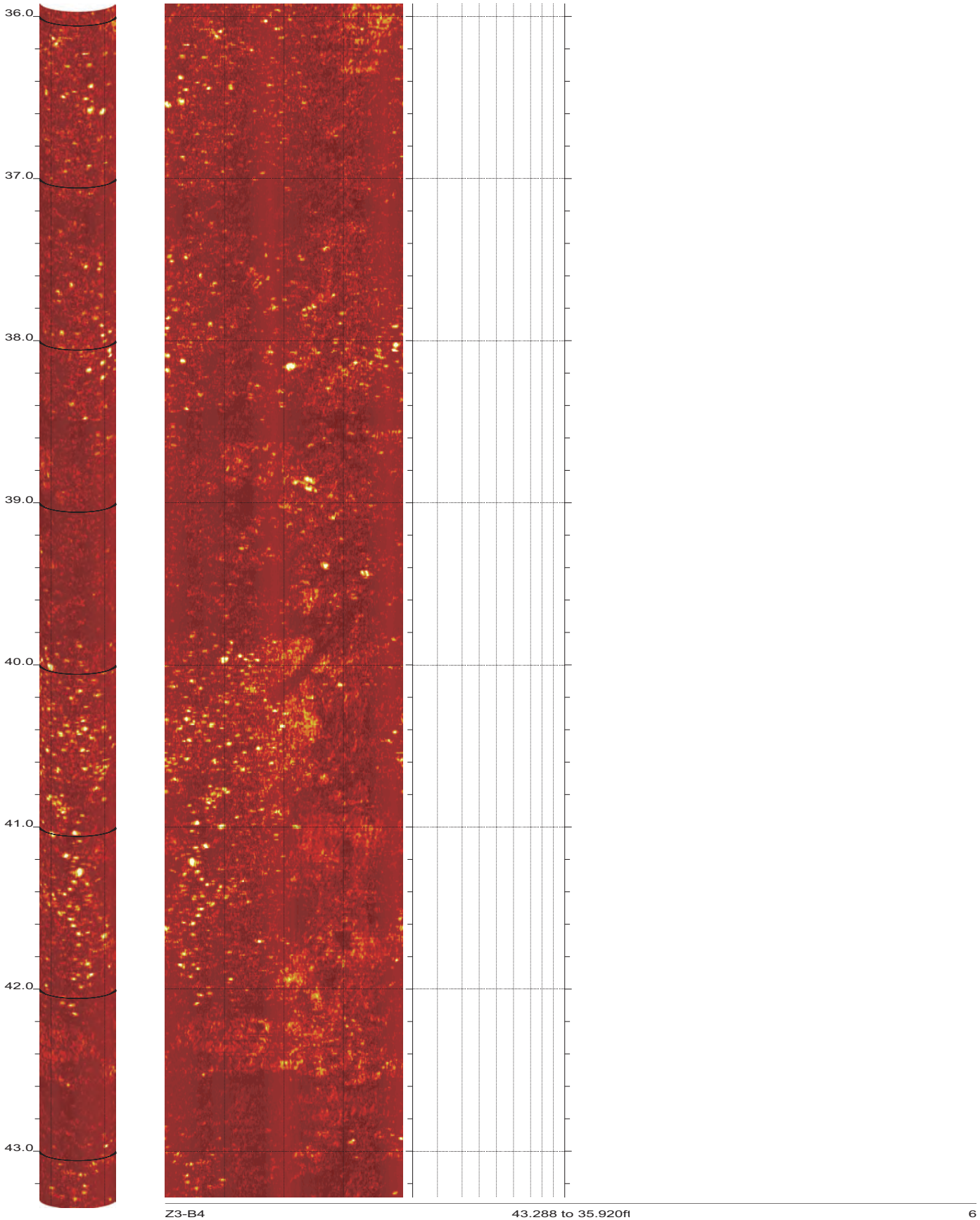

SR-710 Boring Z3-B4 Acoustic Televiewer Dips rev 1 Sheet 6 of 38

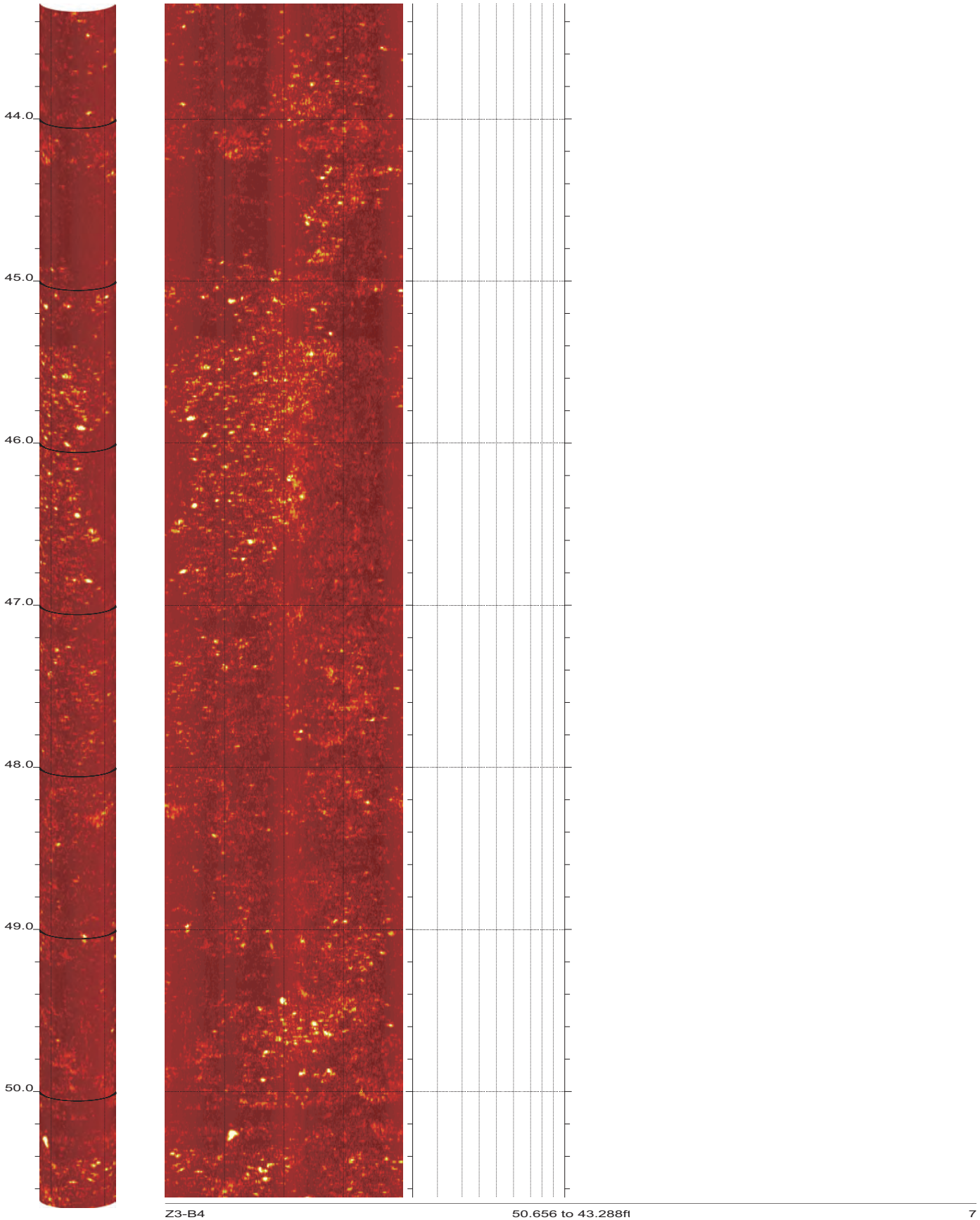
44.0
45.0
46.0
47.0
48.0
49.0
50.0
Z3-B4
50.656 to 43.288ft
7

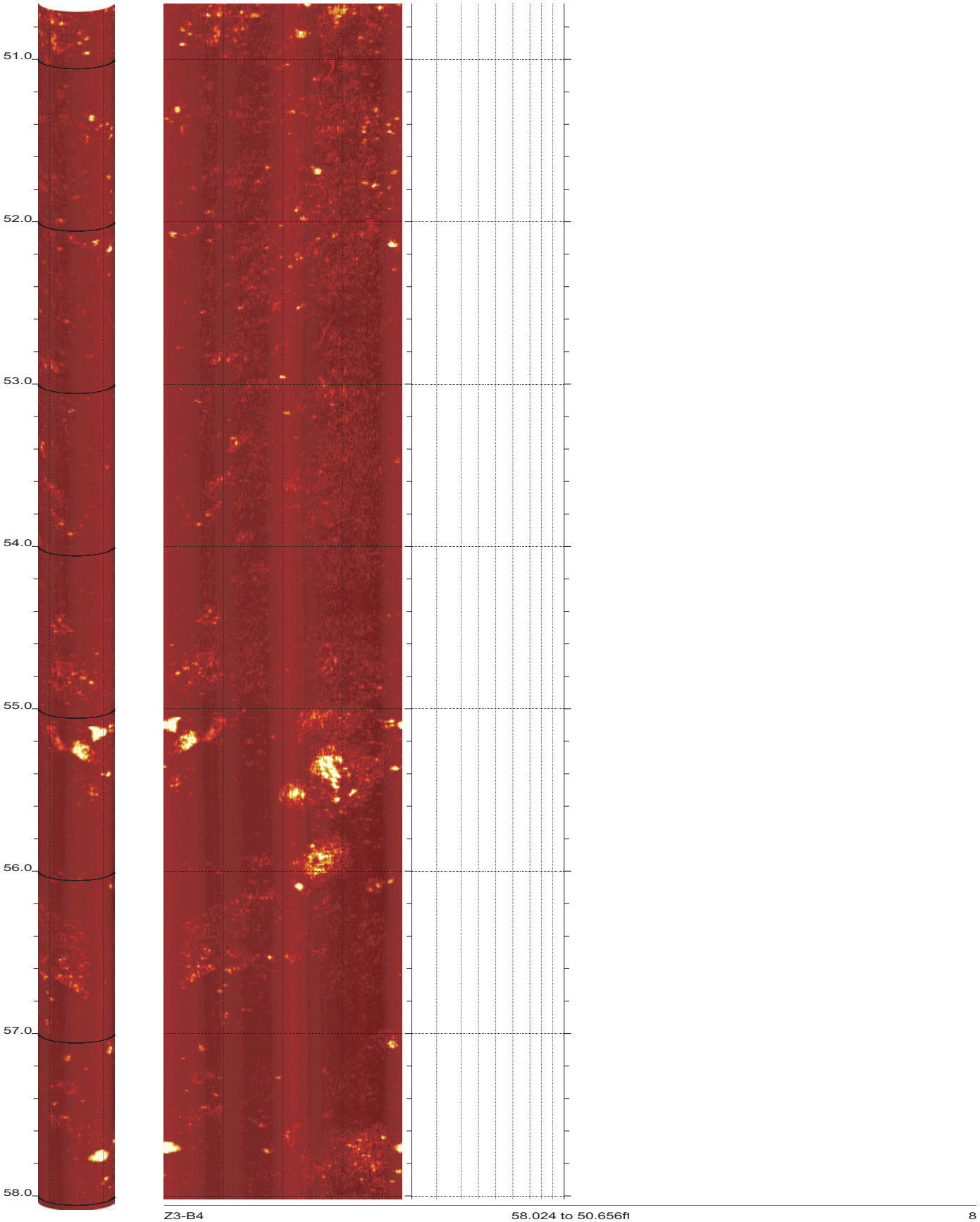

SR-710 Boring Z3-B4 Acoustic Televiewer Dips rev 1 Sheet 8 of 38

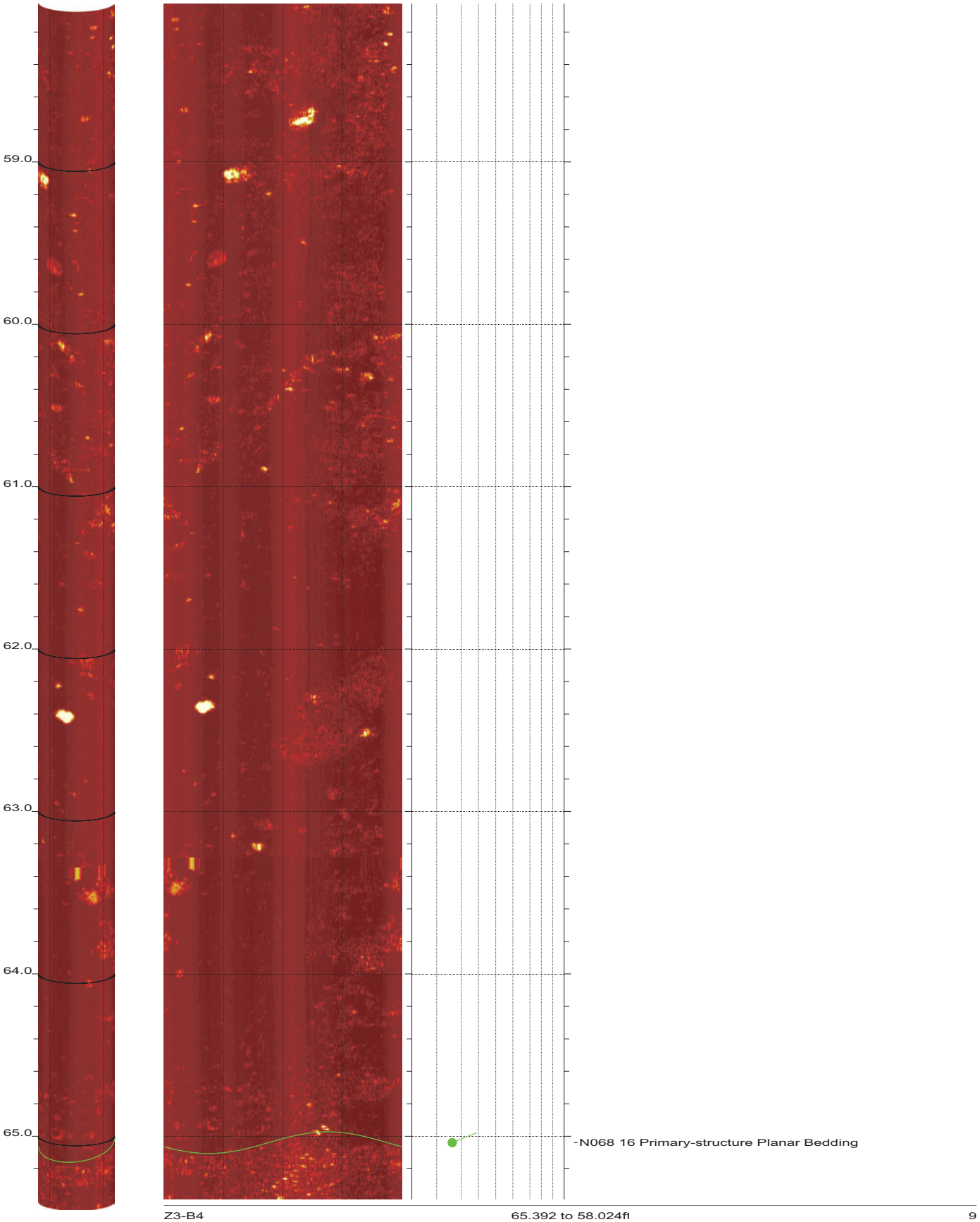

SR-710 Boring Z3-B4 Acoustic Televiewer Dips rev 1 Sheet 9 of 38

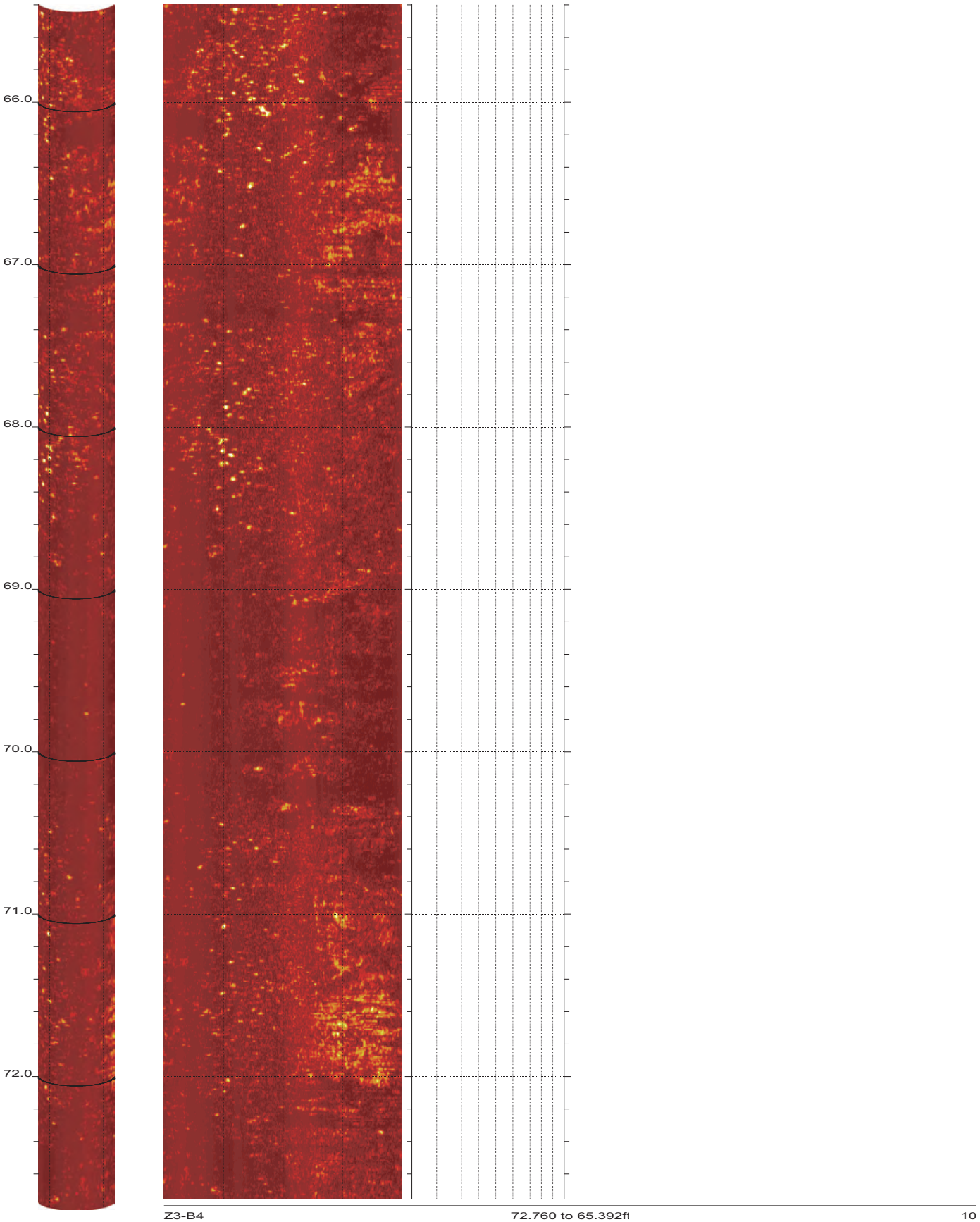
66.0
67.0
68.0
69.0
70.0
71.0
72.0
Z3-B4
72.760 to 65.392fl
10

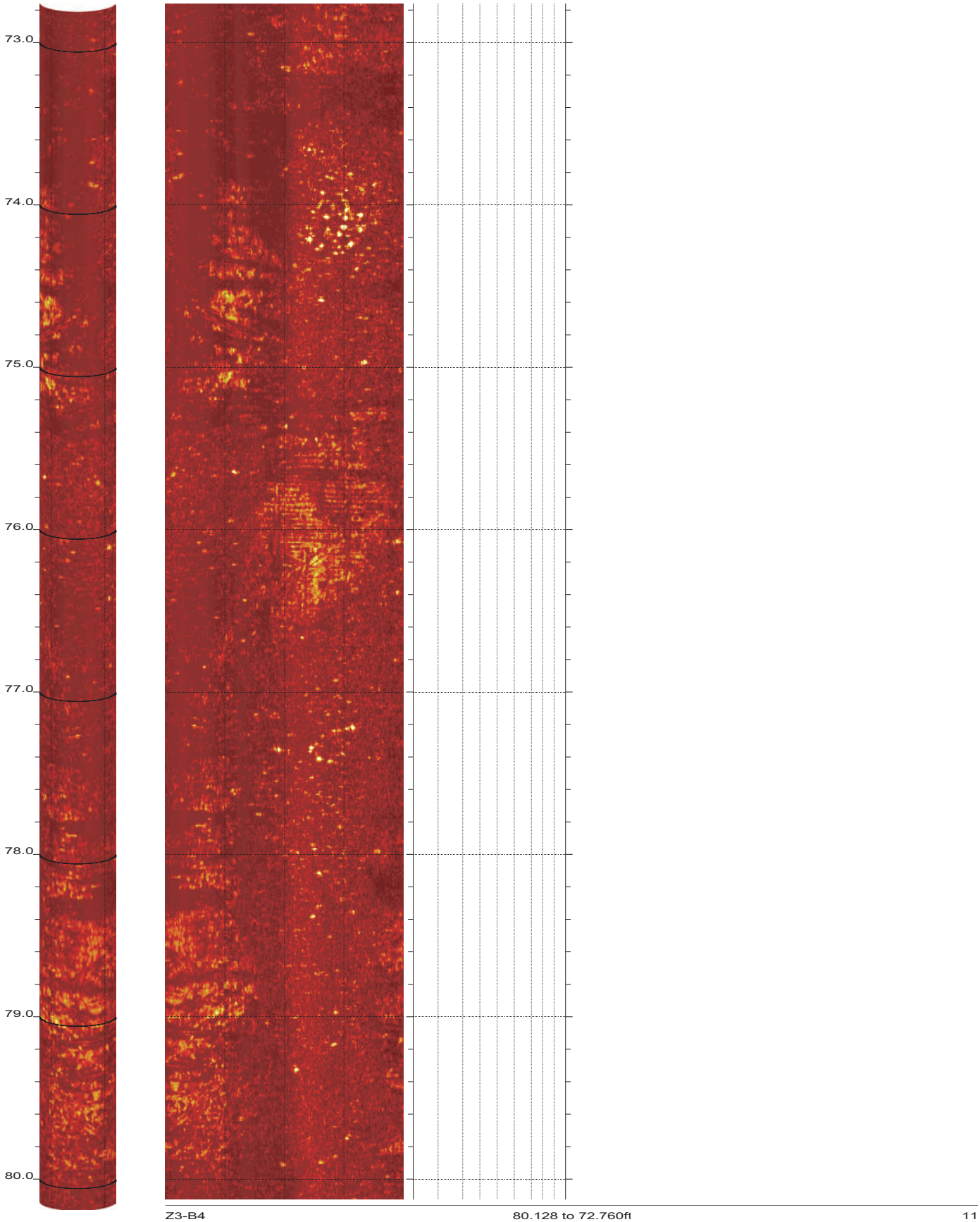
73.0
74.0
75.0
76.0
77.0
78.0
79.0
80.0
Z3-B4
80.128 to 72.760ft
11

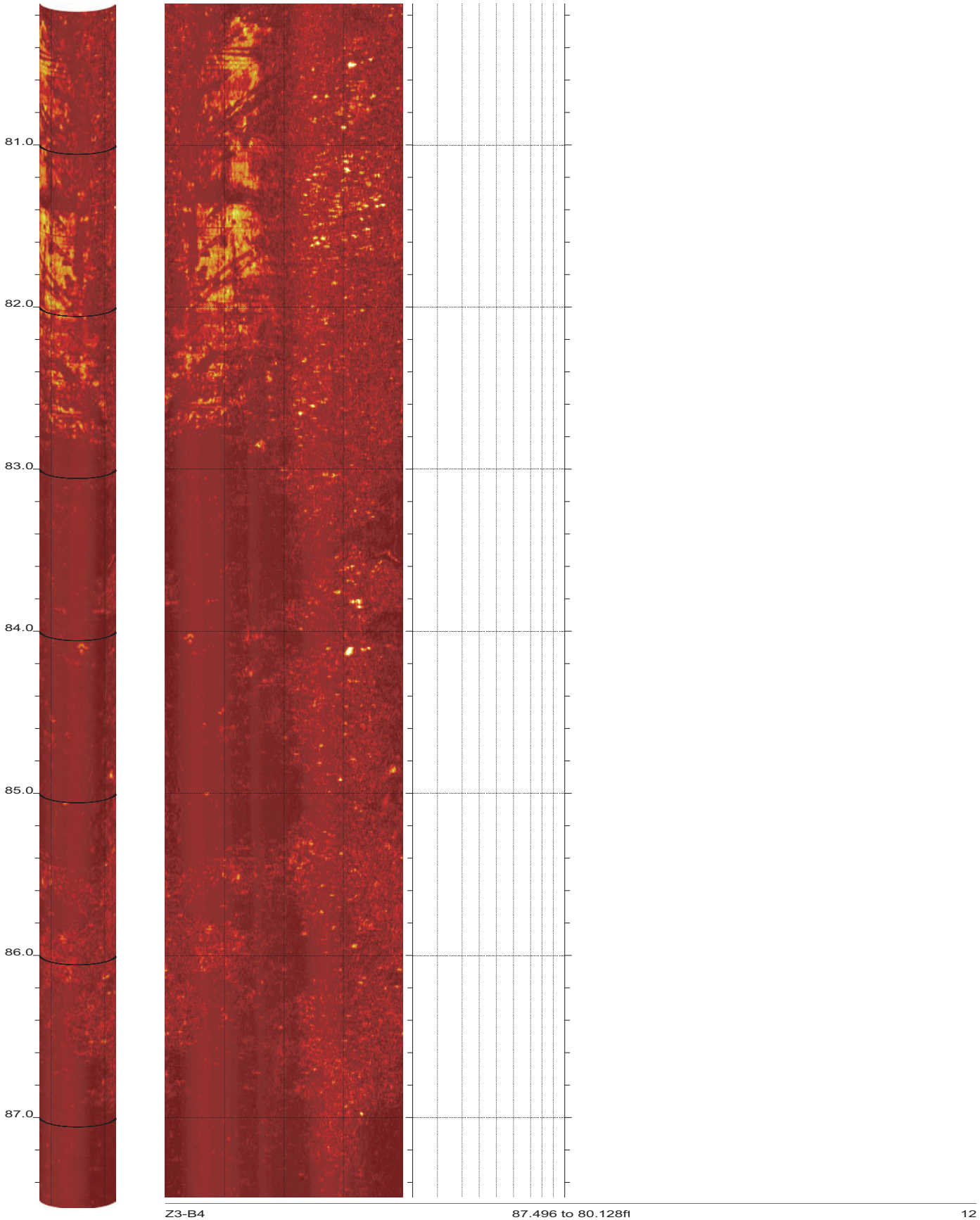
81.0
82.0
83.0
84.0
85.0
86.0
87.0
Z3-B4
87.496 to 80.128ft
12

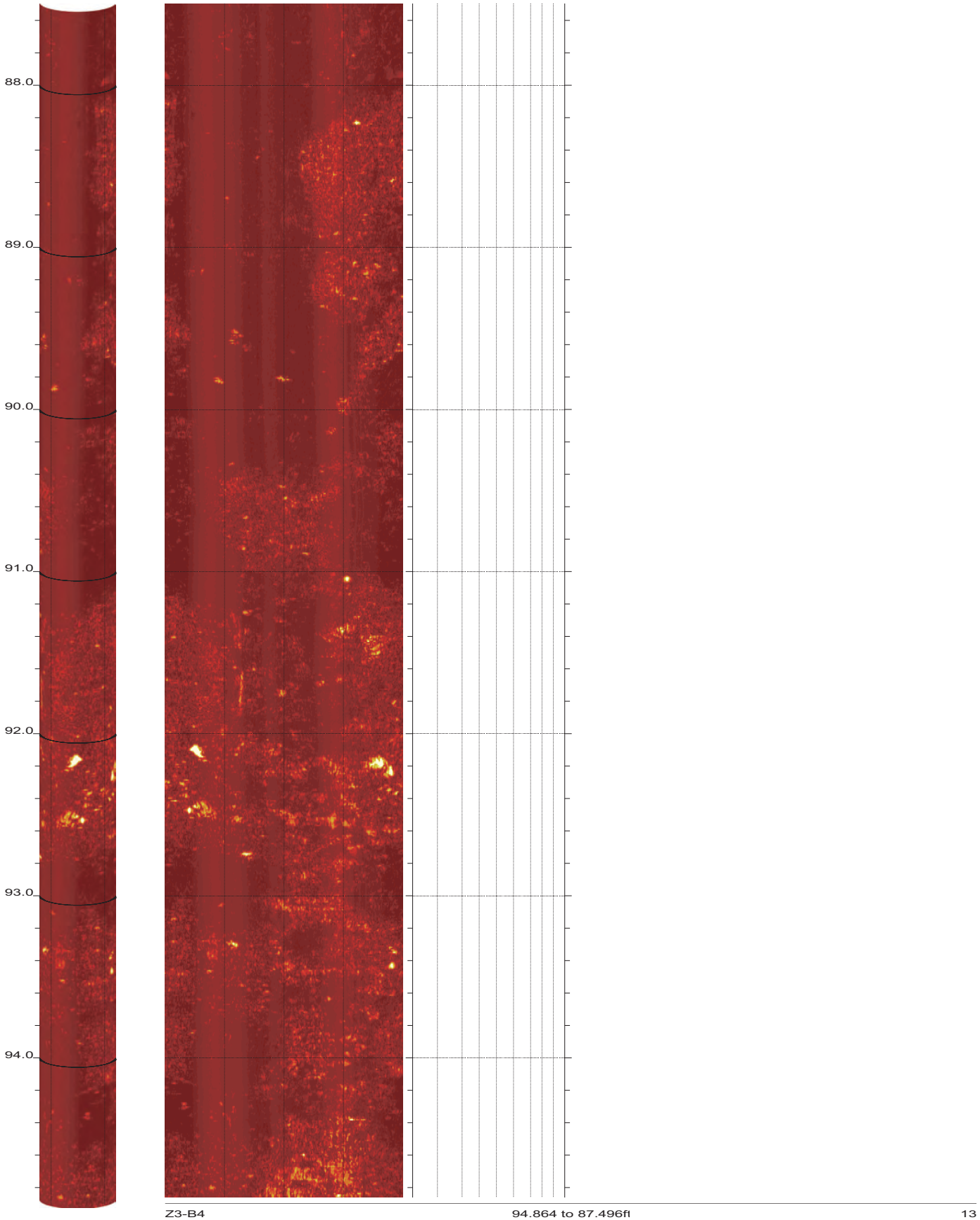
88.0
89.0
90.0
91.0
92.0
93.0
94.0
Z3-B4
94.864 to 87.496ft
13

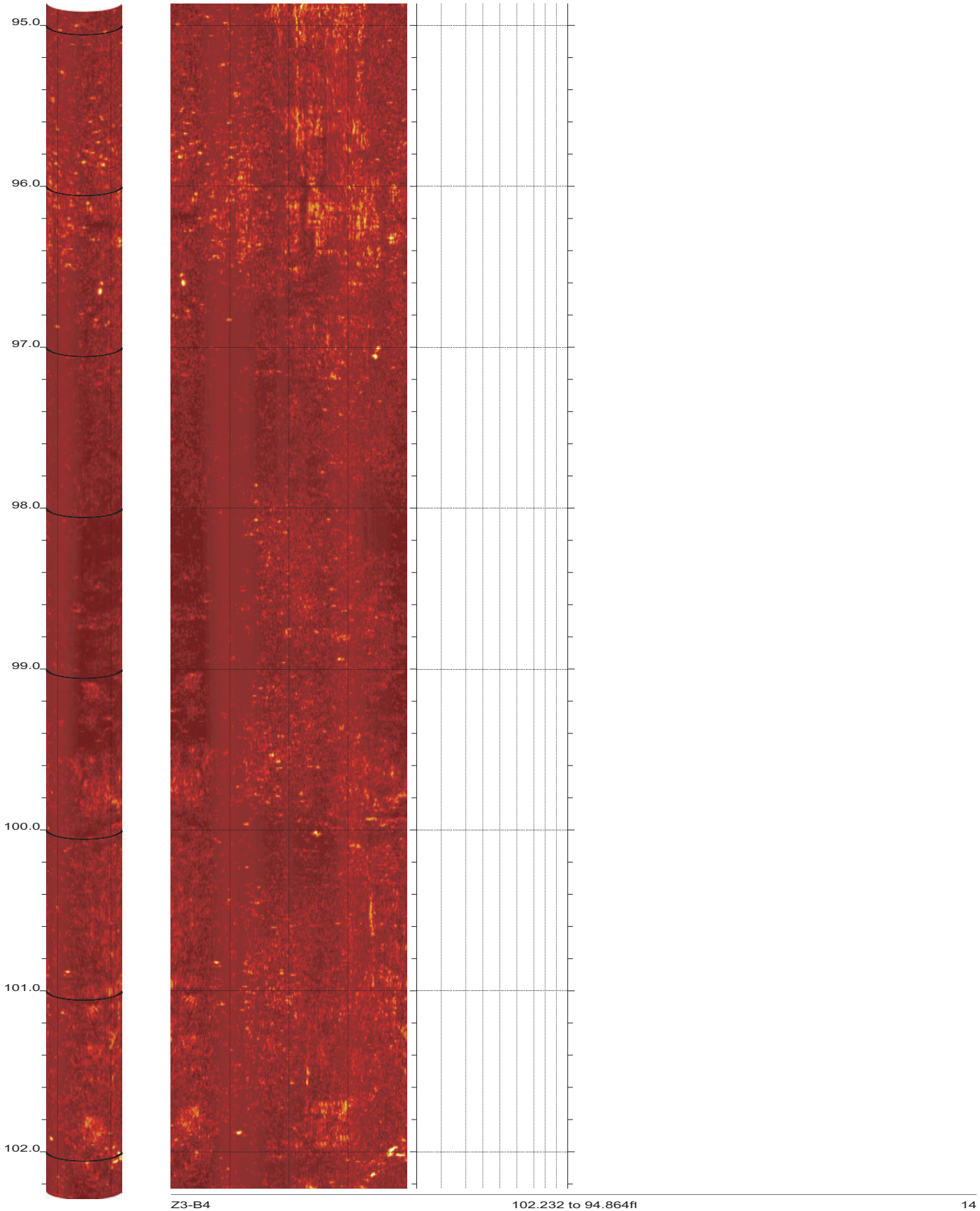
95.0
96.0
97.0
98.0
99.0
100.0
101.0
102.0
Z3-B4
102.232 to 94.864ft
14

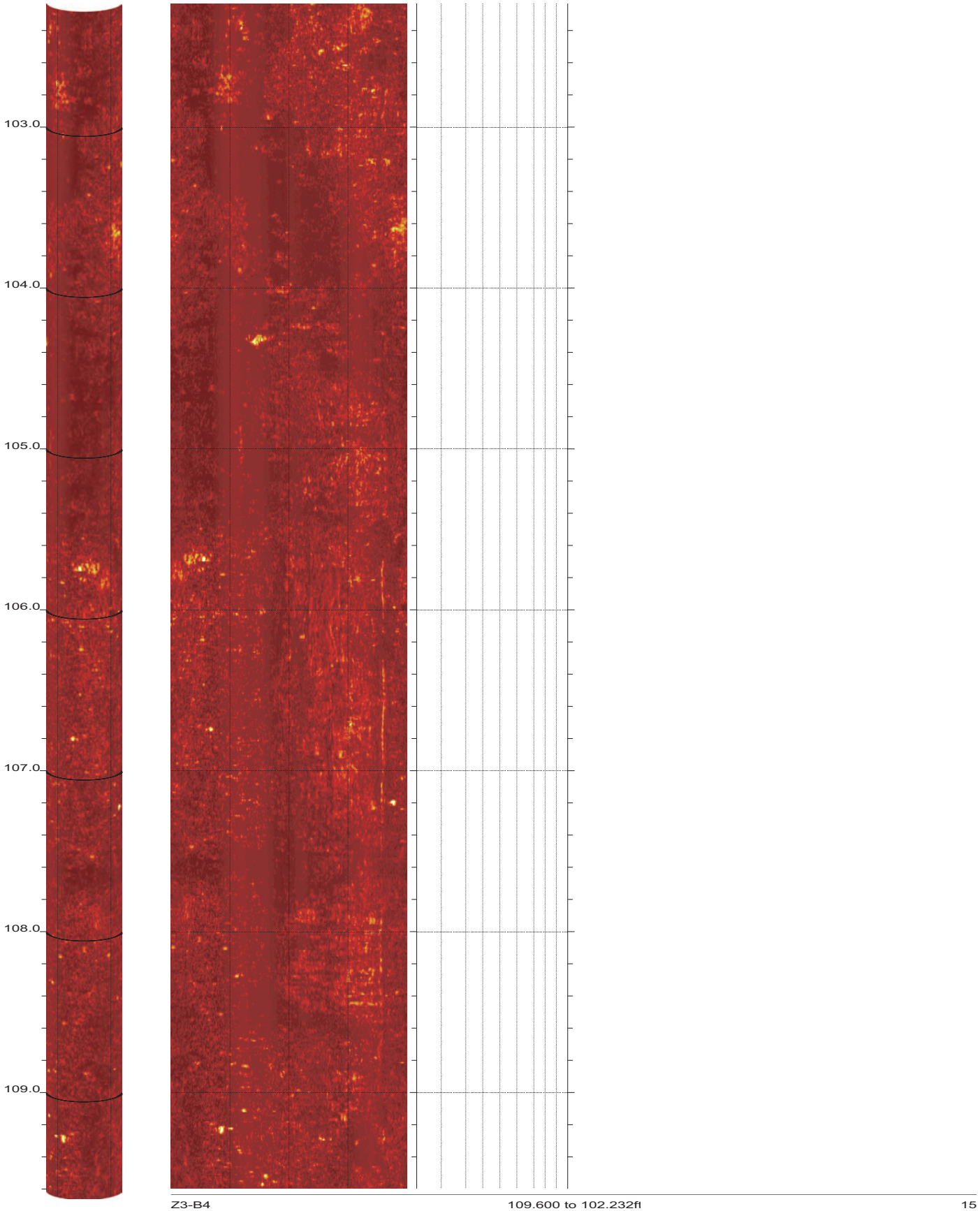

SR-710 Boring Z3-B4 Acoustic Televiewer Dips rev 1 Sheet 15 of 38

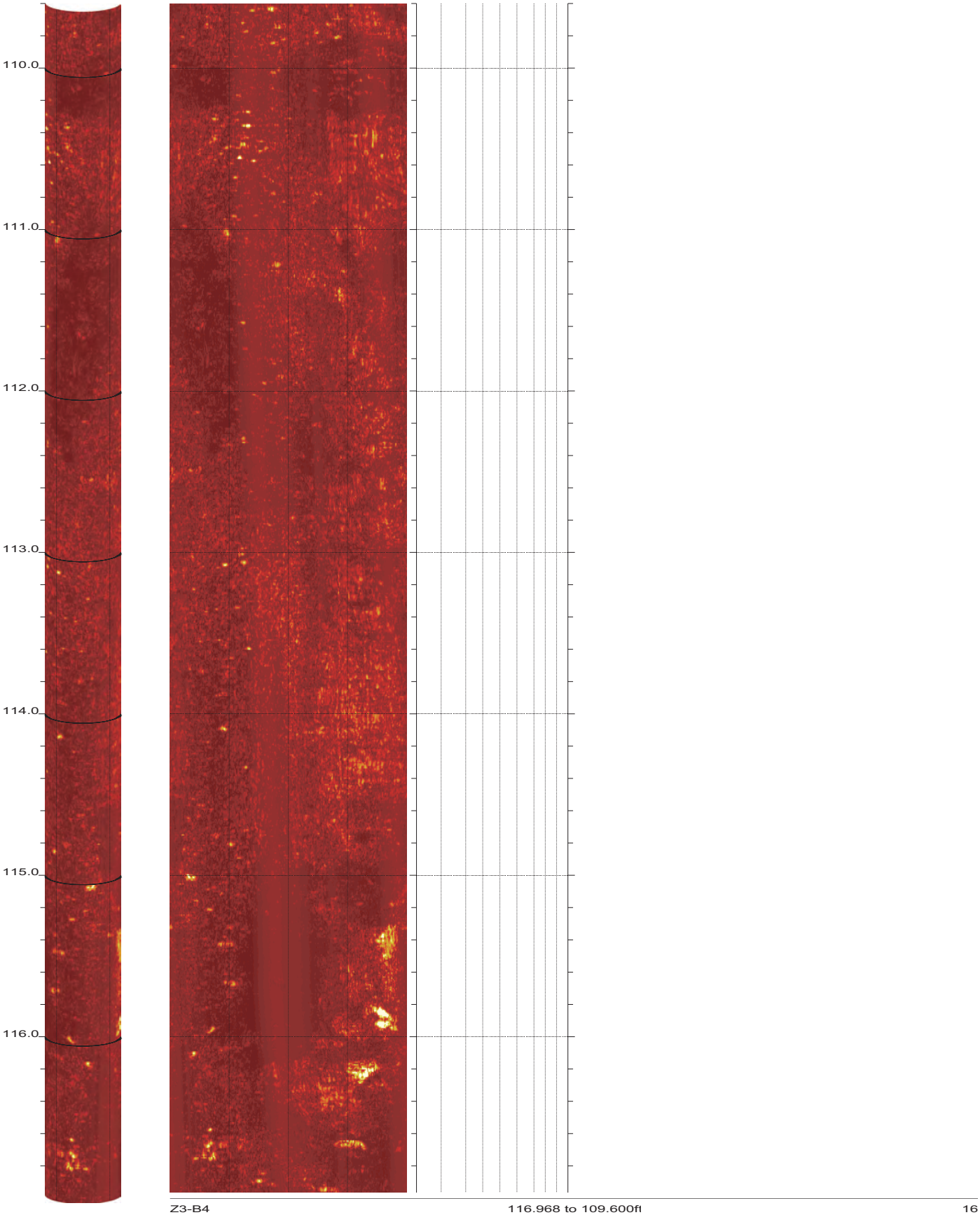
110.0
111.0
112.0
113.0
114.0
115.0
116.0
Z3-B4
116.968 to 109.600ft
16

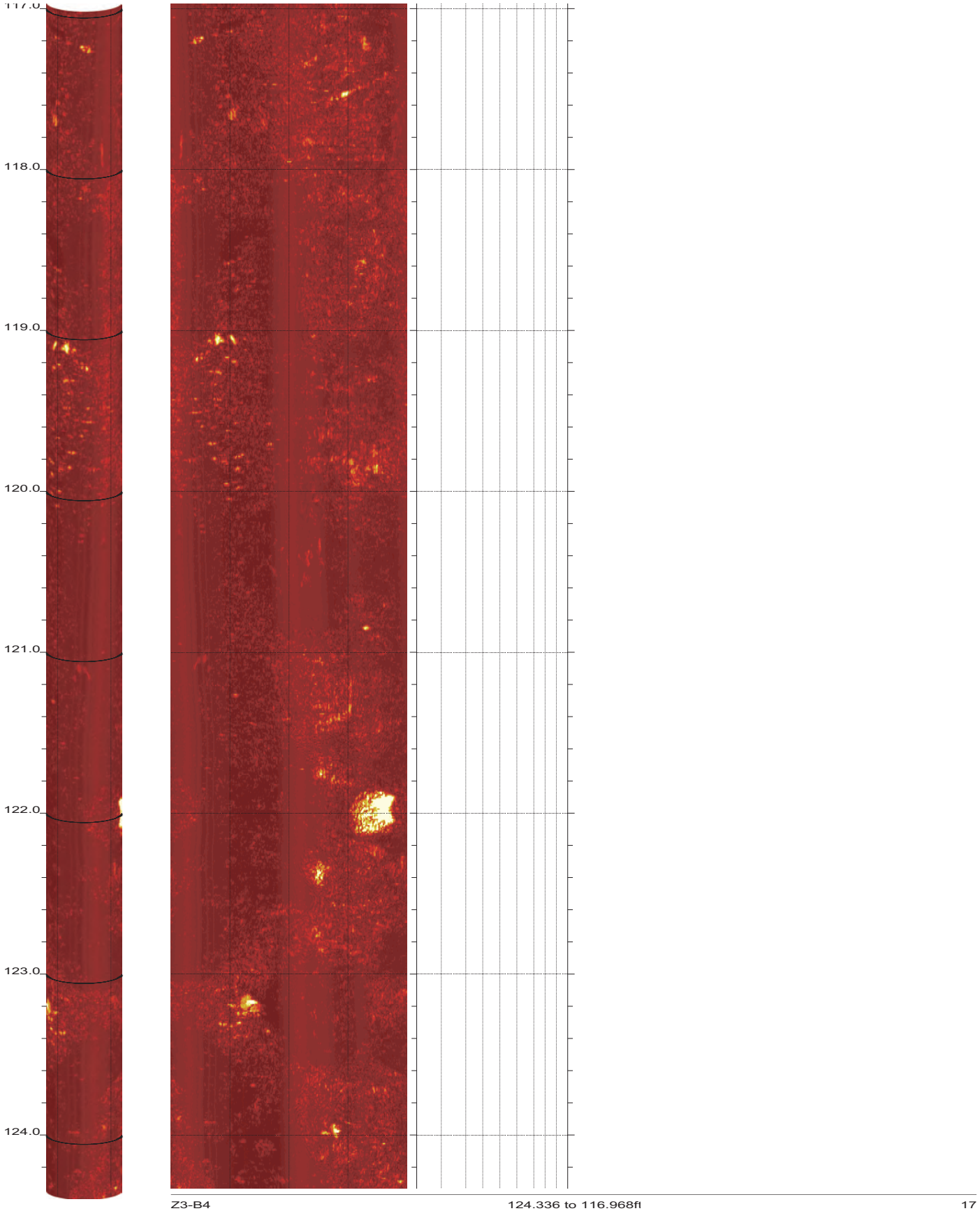
117.0
118.0
119.0
120.0
121.0
122.0
123.0
124.0
Z3-B4
124.336 to 116.968ft
17

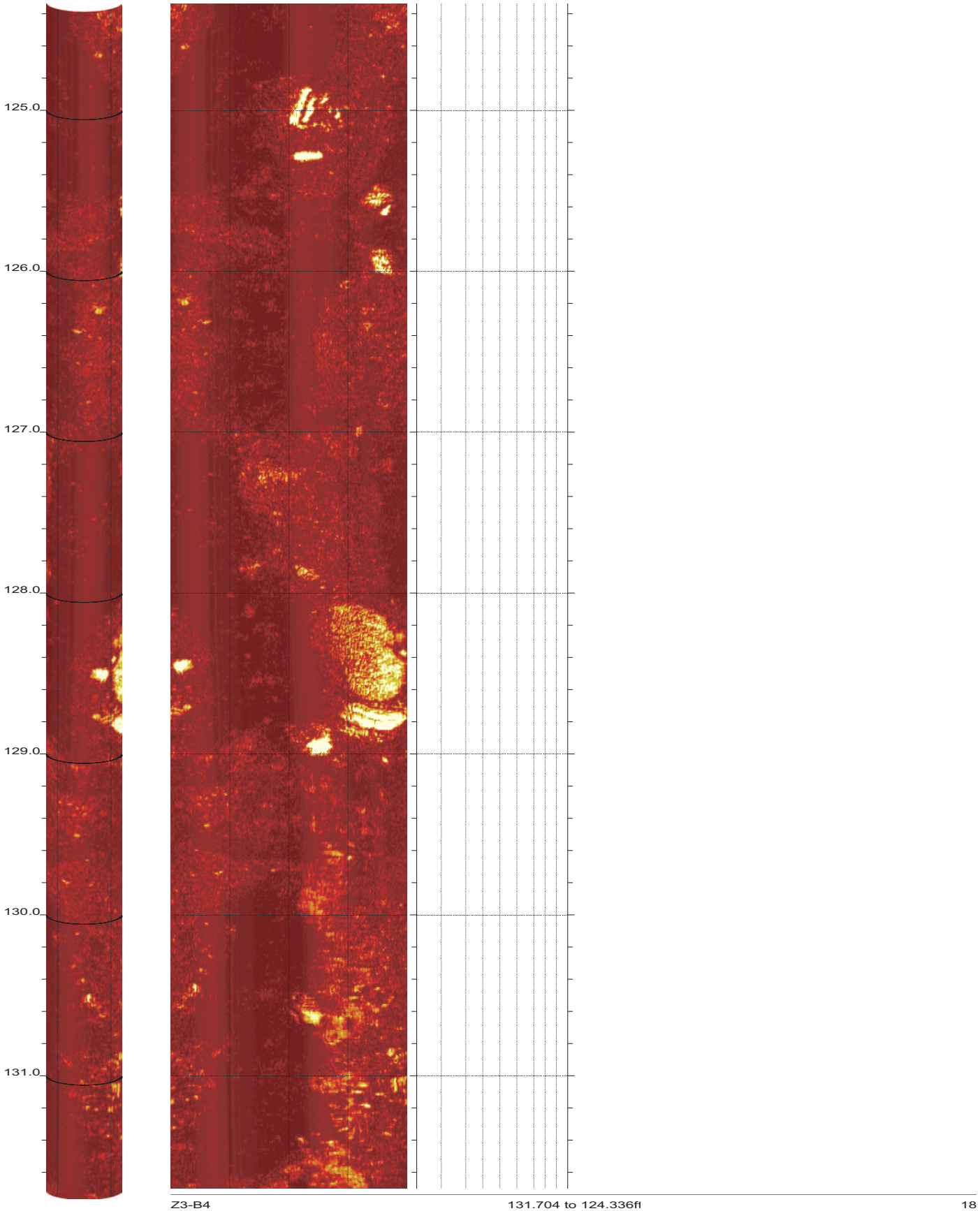

SR-710 Boring Z3-B4 Acoustic Televiewer Dips rev 1 Sheet 18 of 38

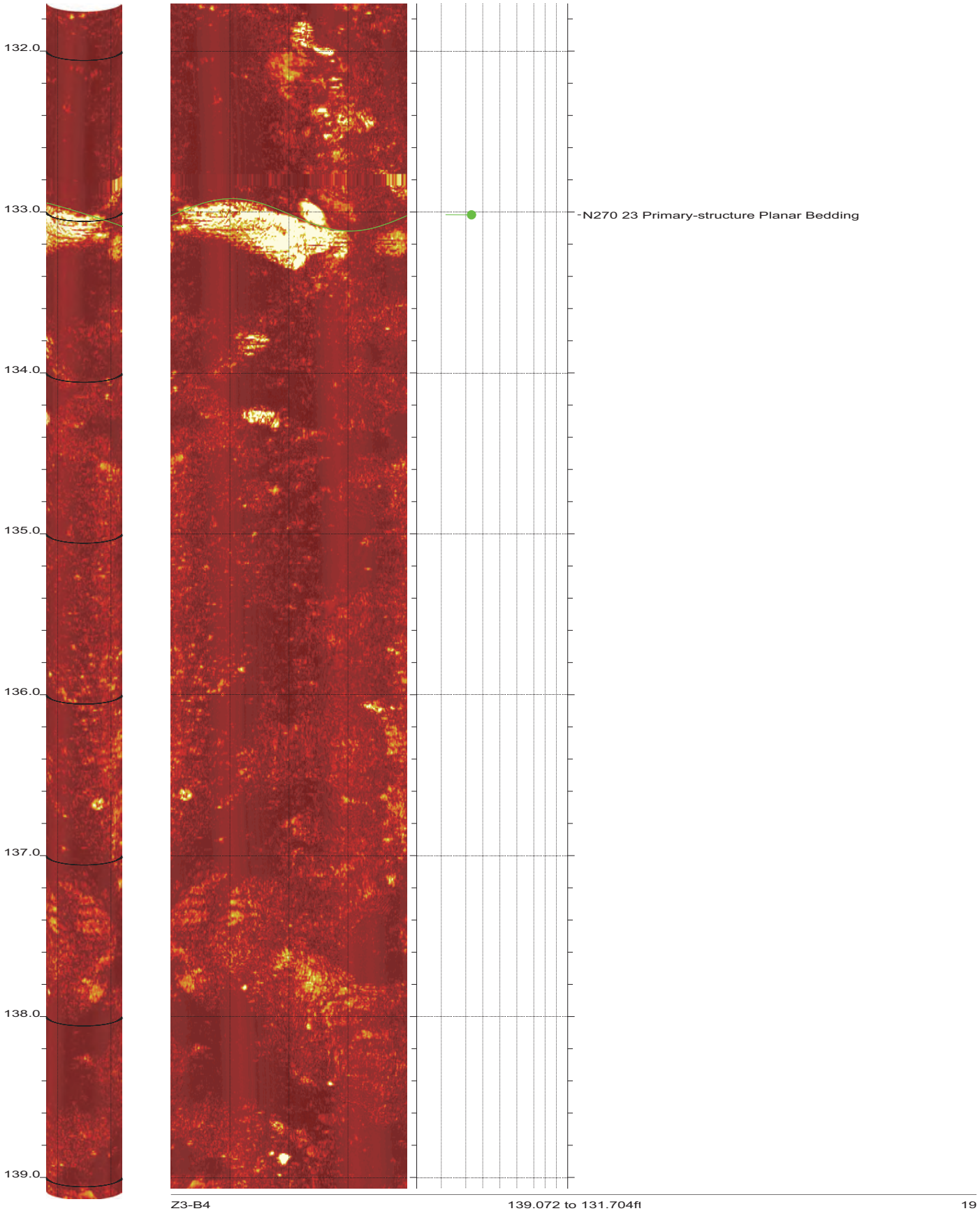

SR-710 Boring Z3-B4 Acoustic Televiewer Dips rev 1 Sheet 19 of 38

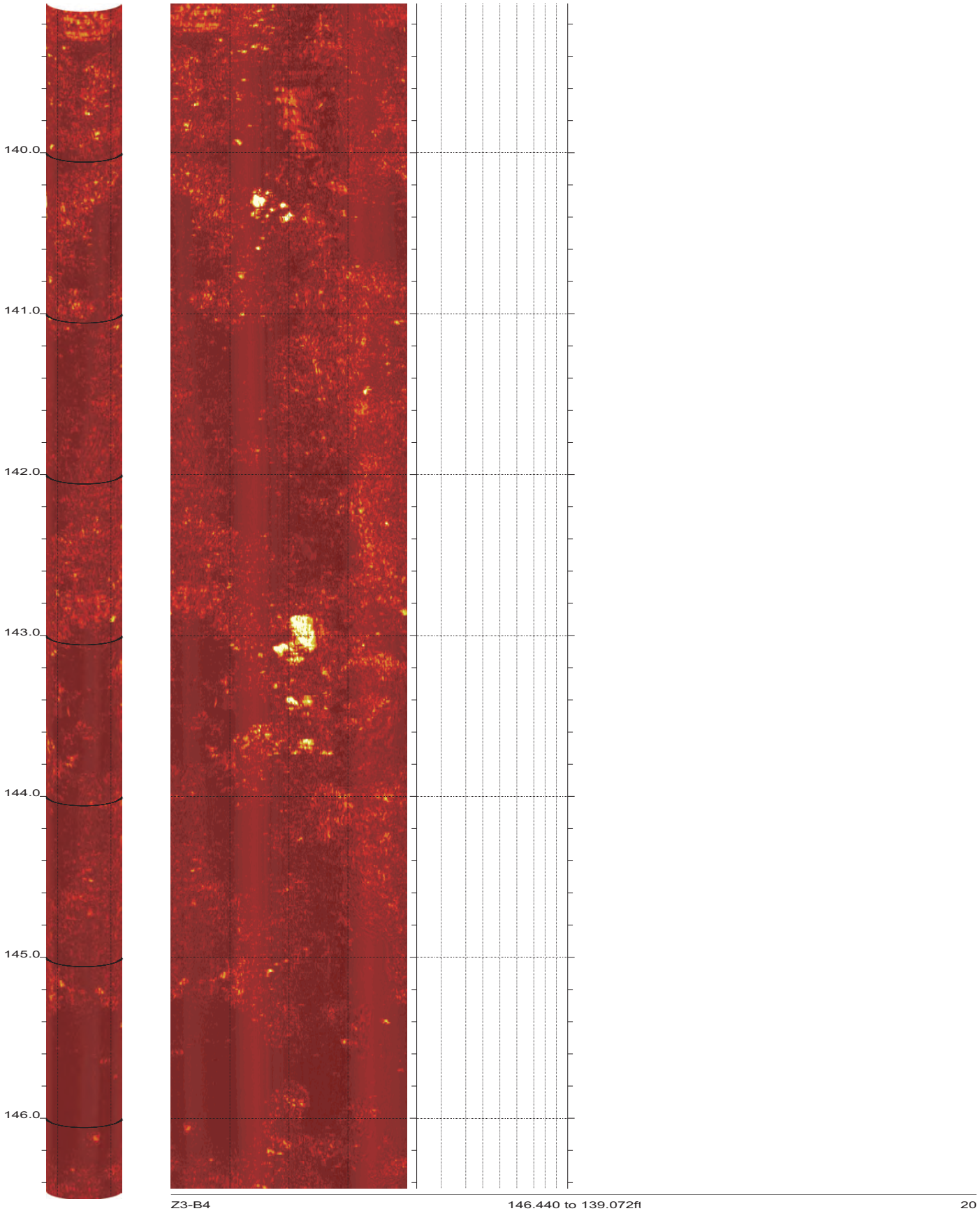

SR-710 Boring Z3-B4 Acoustic Televiewer Dips rev 1 Sheet 20 of 38

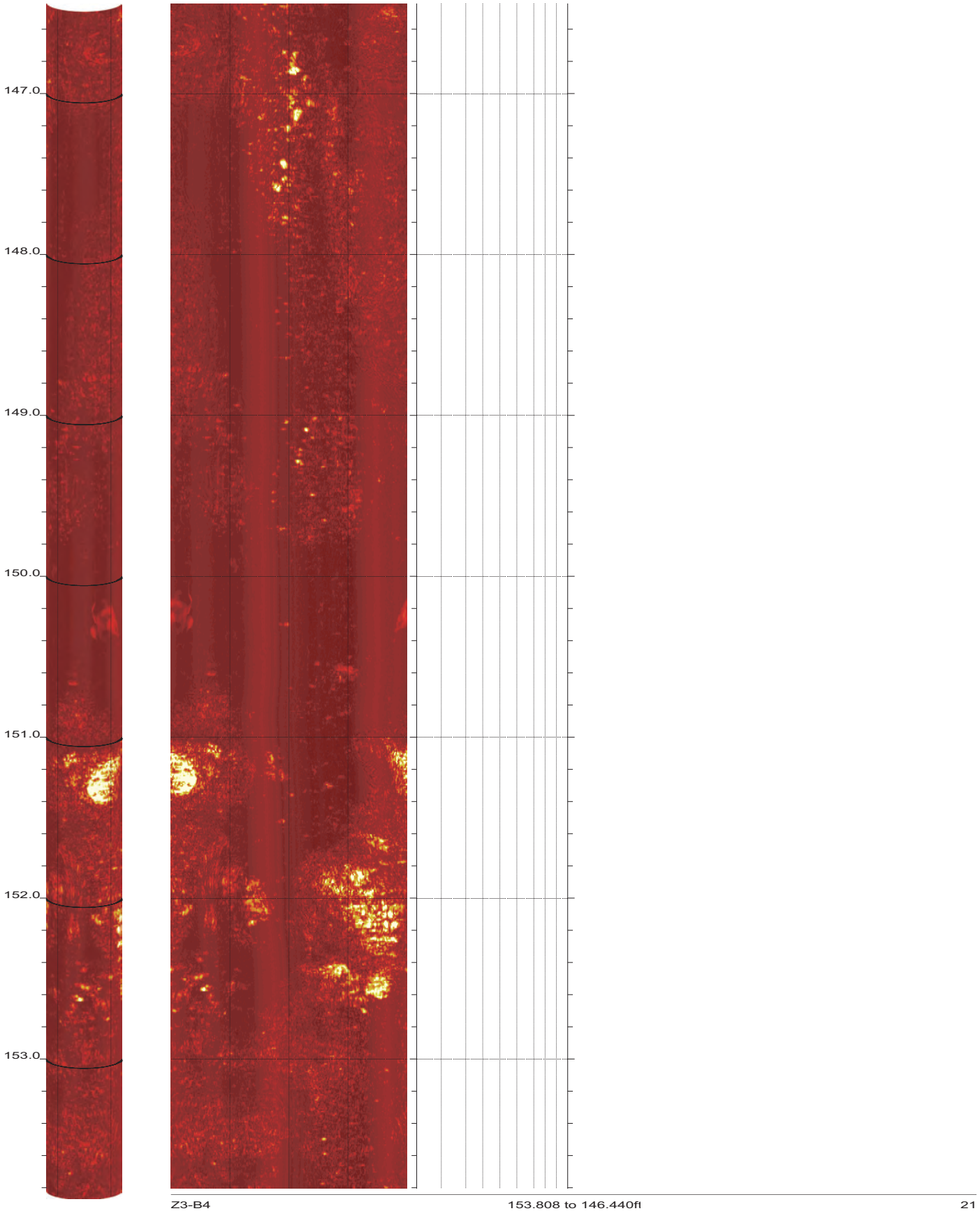

SR-710 Boring Z3-B4 Acoustic Televiewer Dips rev 1 Sheet 21 of 38

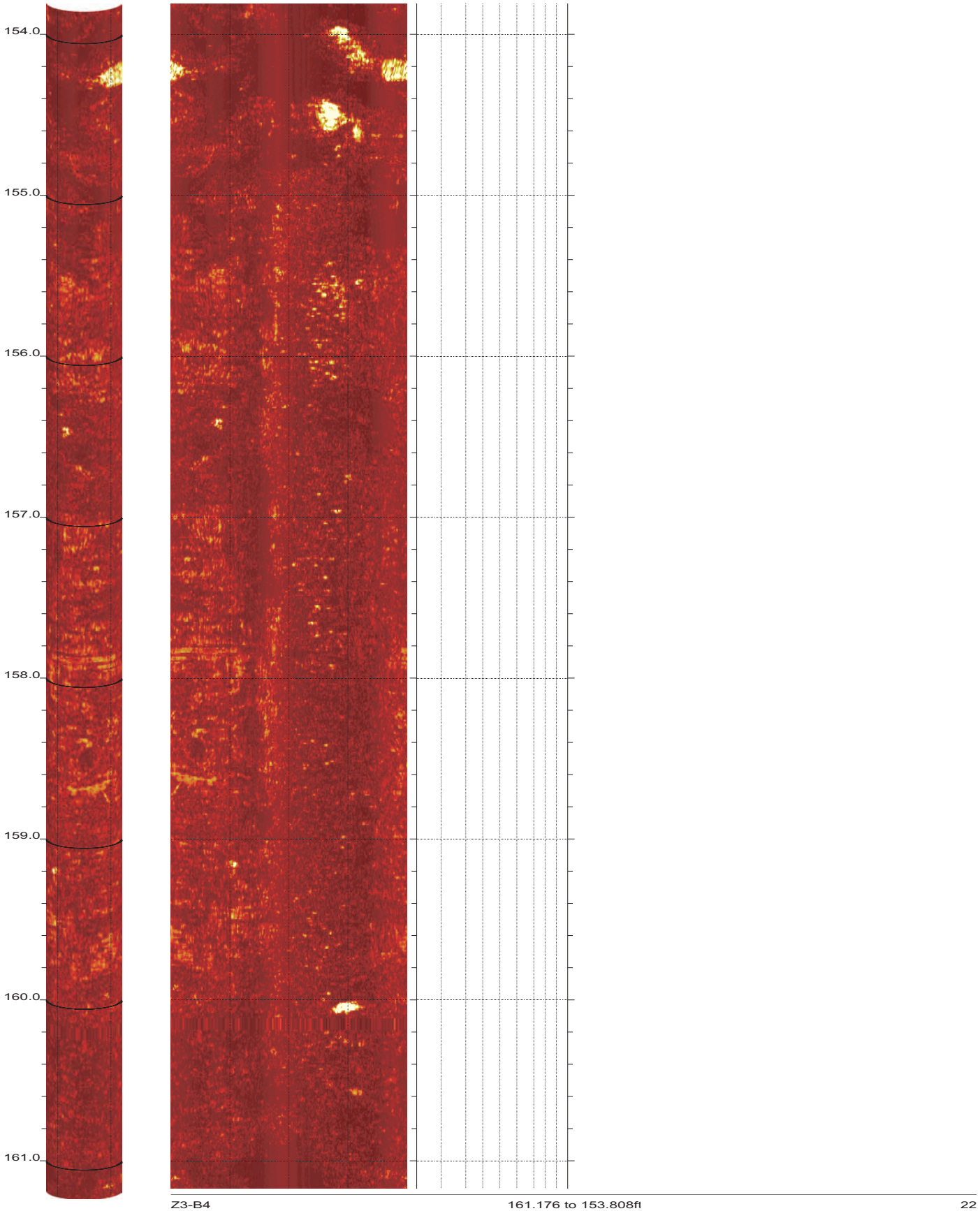
154.0
155.0
156.0
157.0
158.0
159.0
160.0
161.0
Z3-B4
161.176 to 153.808ft
22

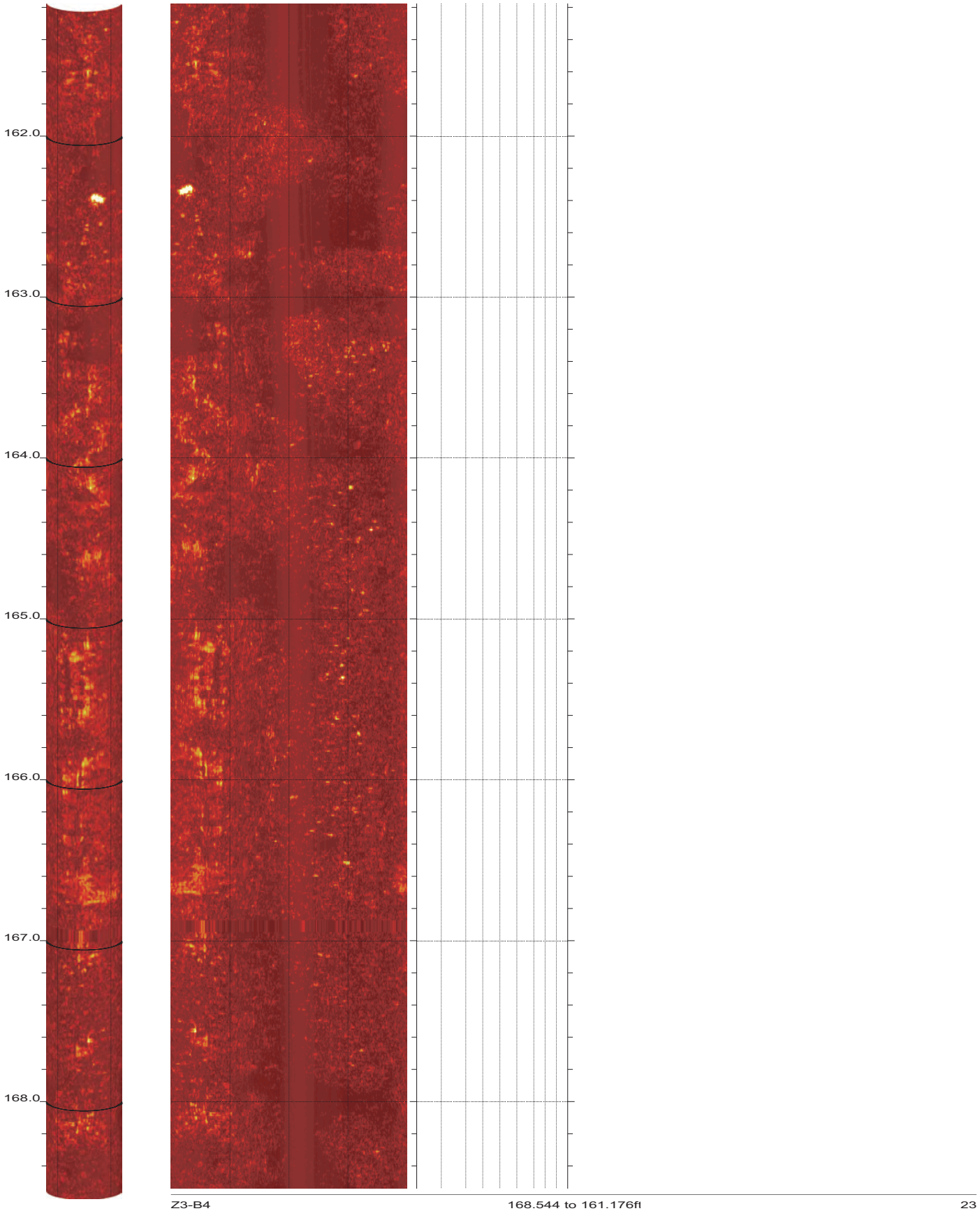

SR-710 Boring Z3-B4 Acoustic Televiewer Dips rev 1 Sheet 23 of 38

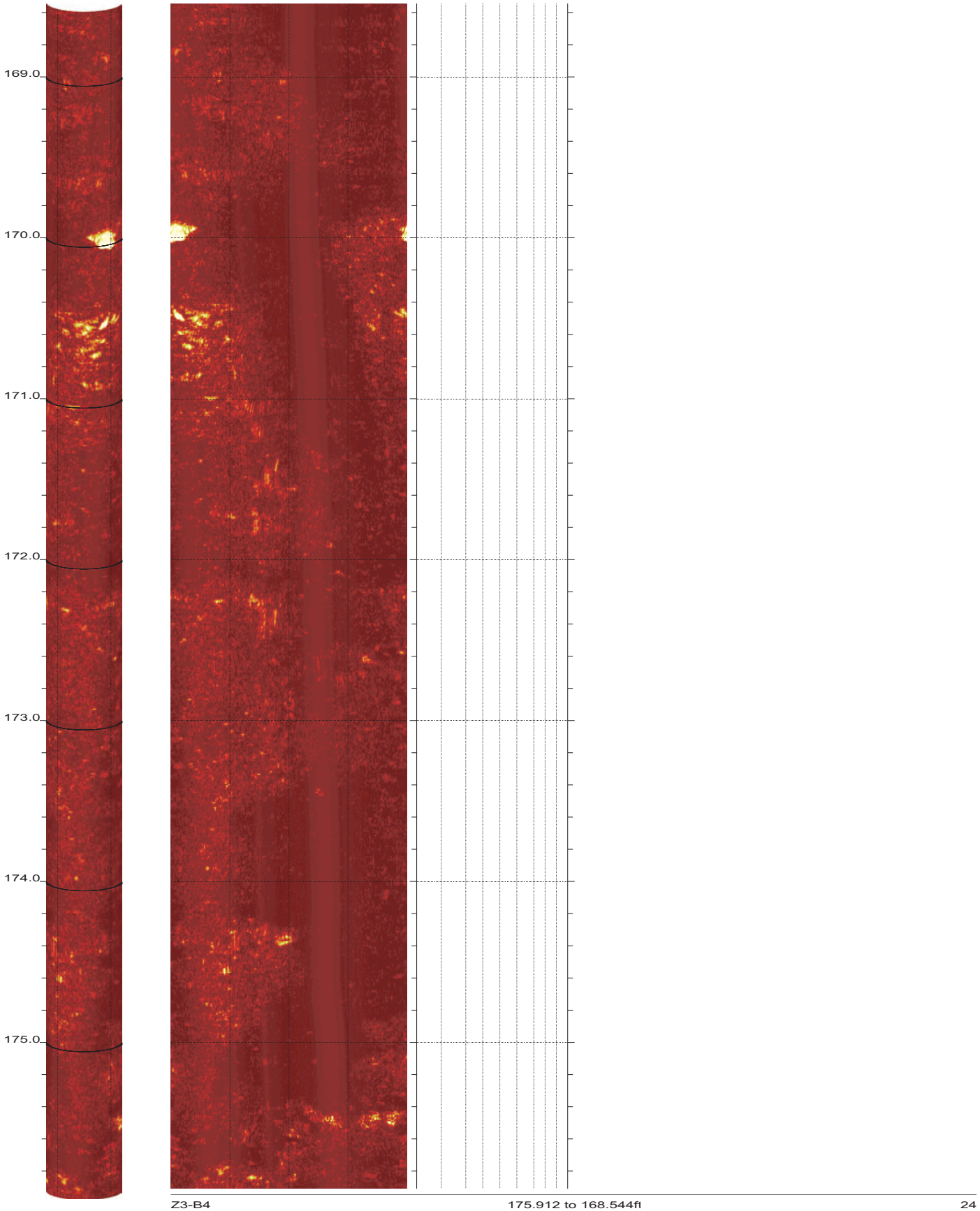

SR-710 Boring Z3-B4 Acoustic Televiewer Dips rev 1 Sheet 24 of 38

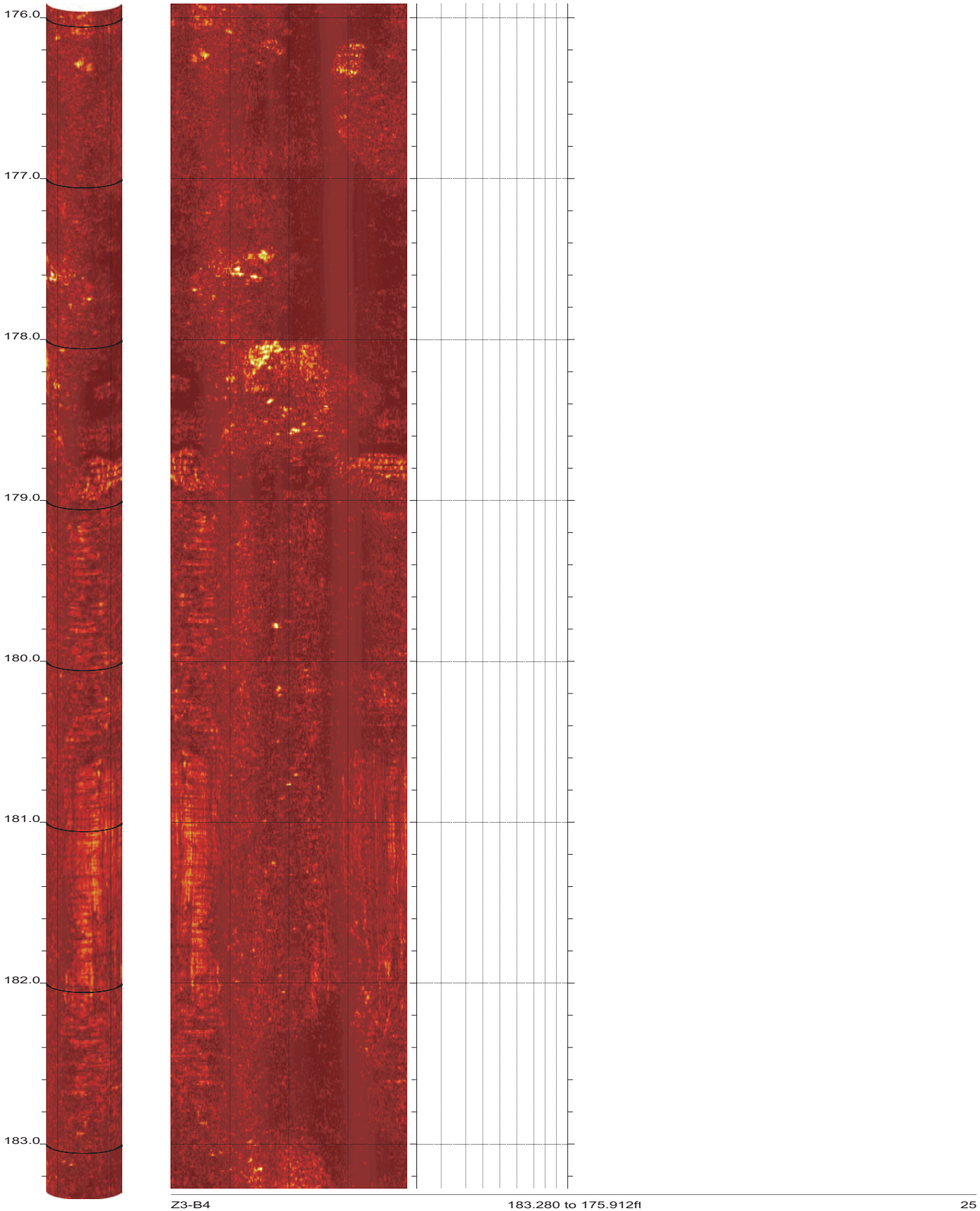

SR-710 Boring Z3-B4 Acoustic Televiewer Dips rev 1 Sheet 25 of 38

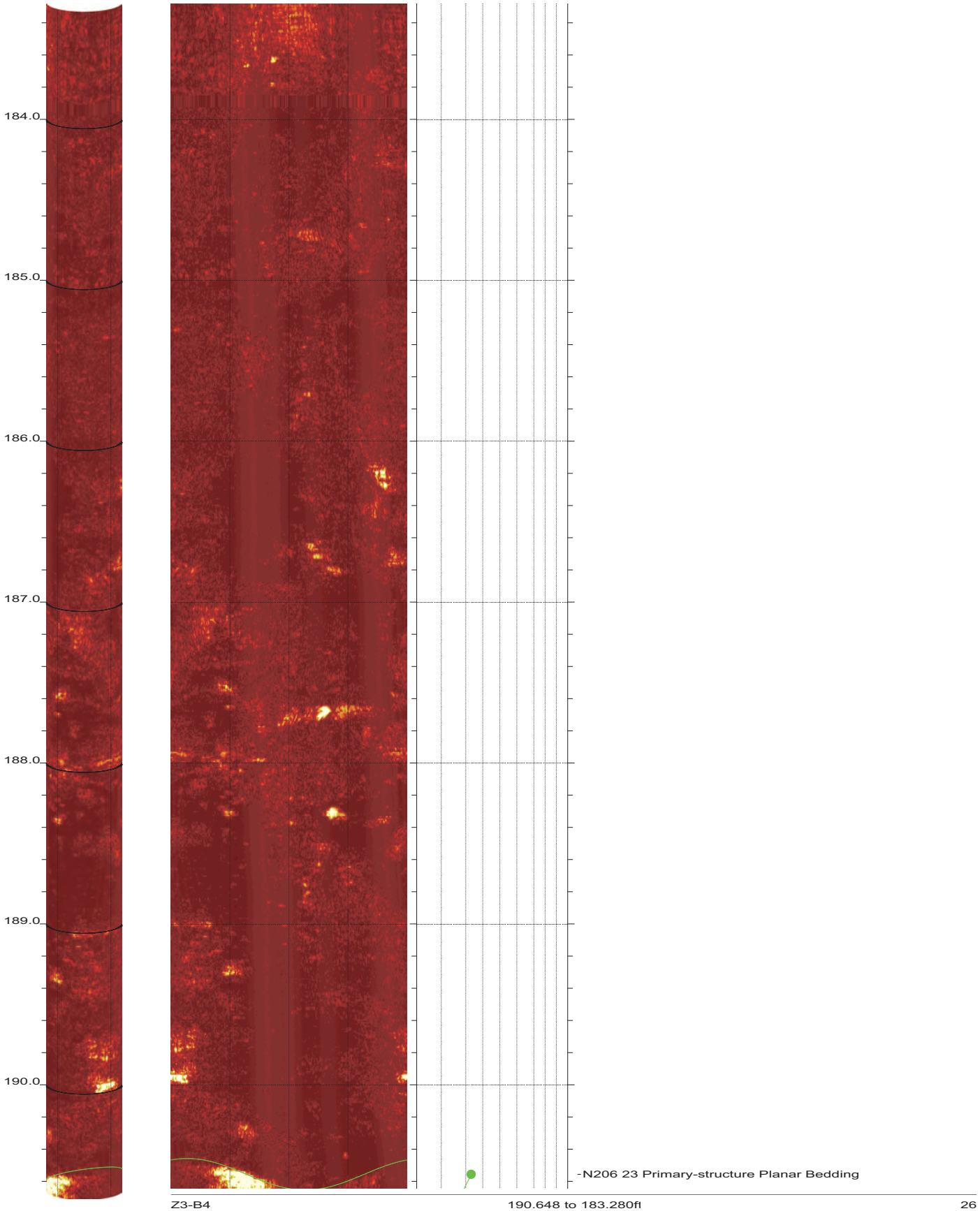

SR-710 Boring Z3-B4 Acoustic Televiewer Dips rev 1 Sheet 26 of 38

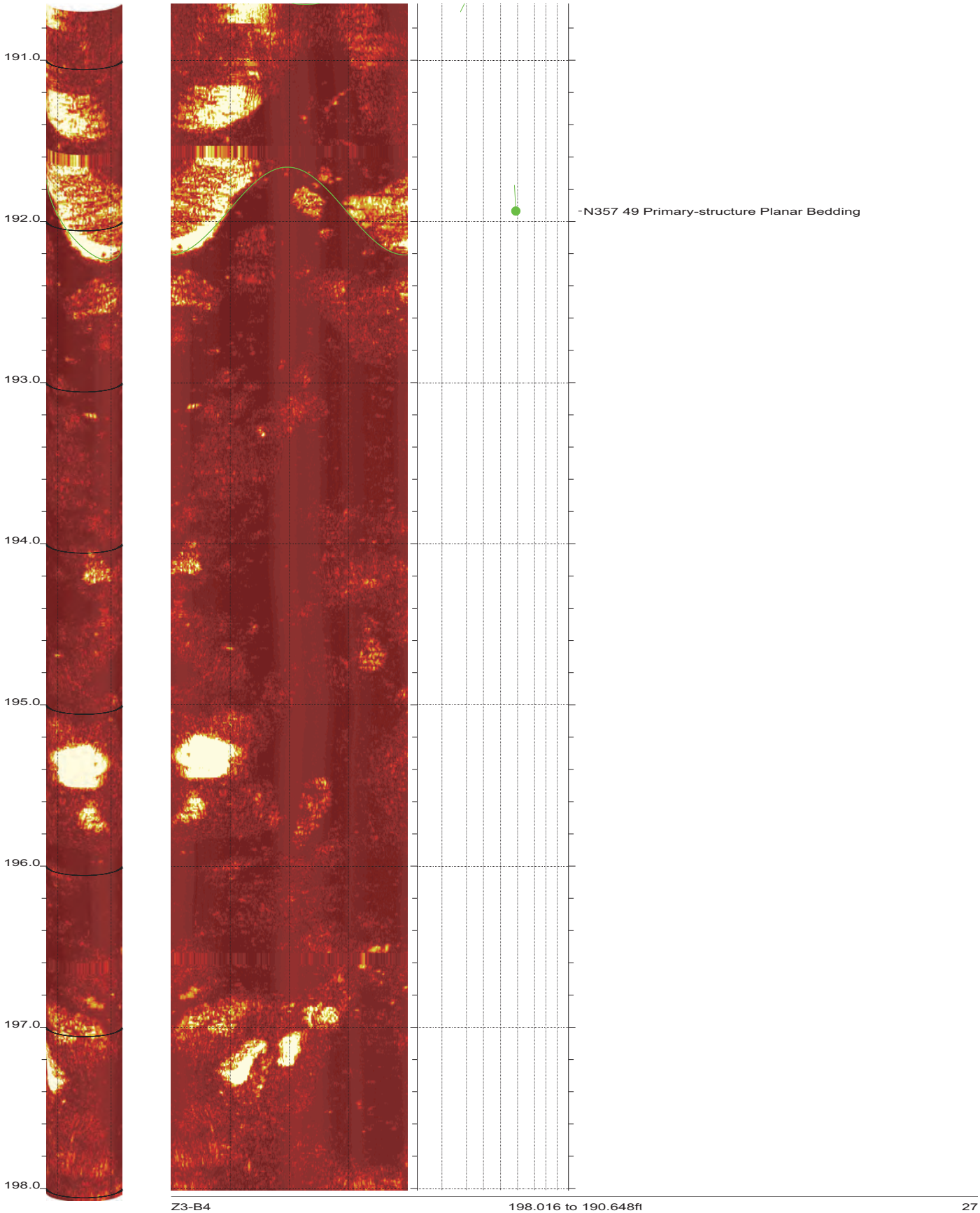

SR-710 Boring Z3-B4 Acoustic Televiewer Dips rev 1 Sheet 27 of 38

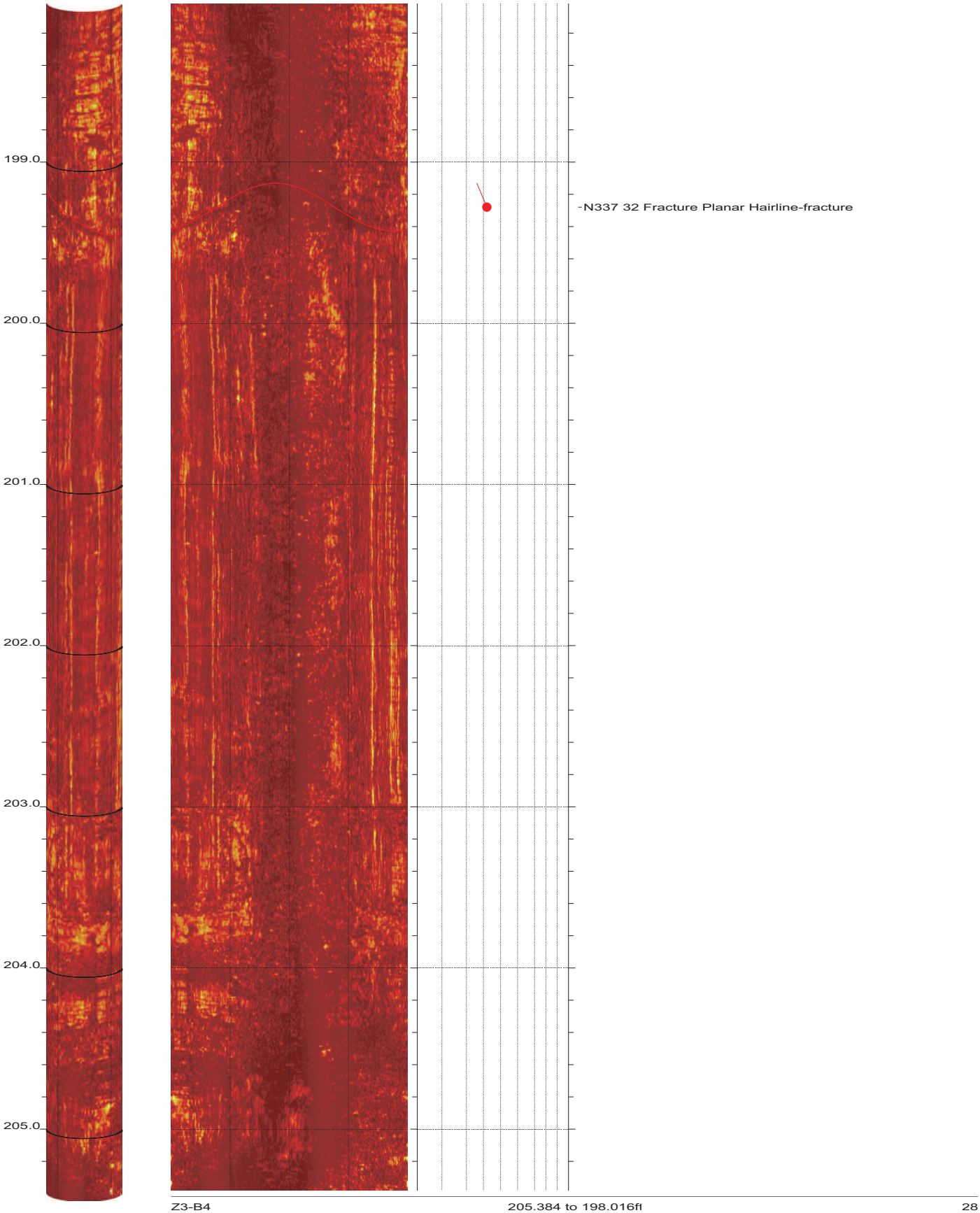

SR-710 Boring Z3-B4 Acoustic Televiewer Dips rev 1 Sheet 28 of 38

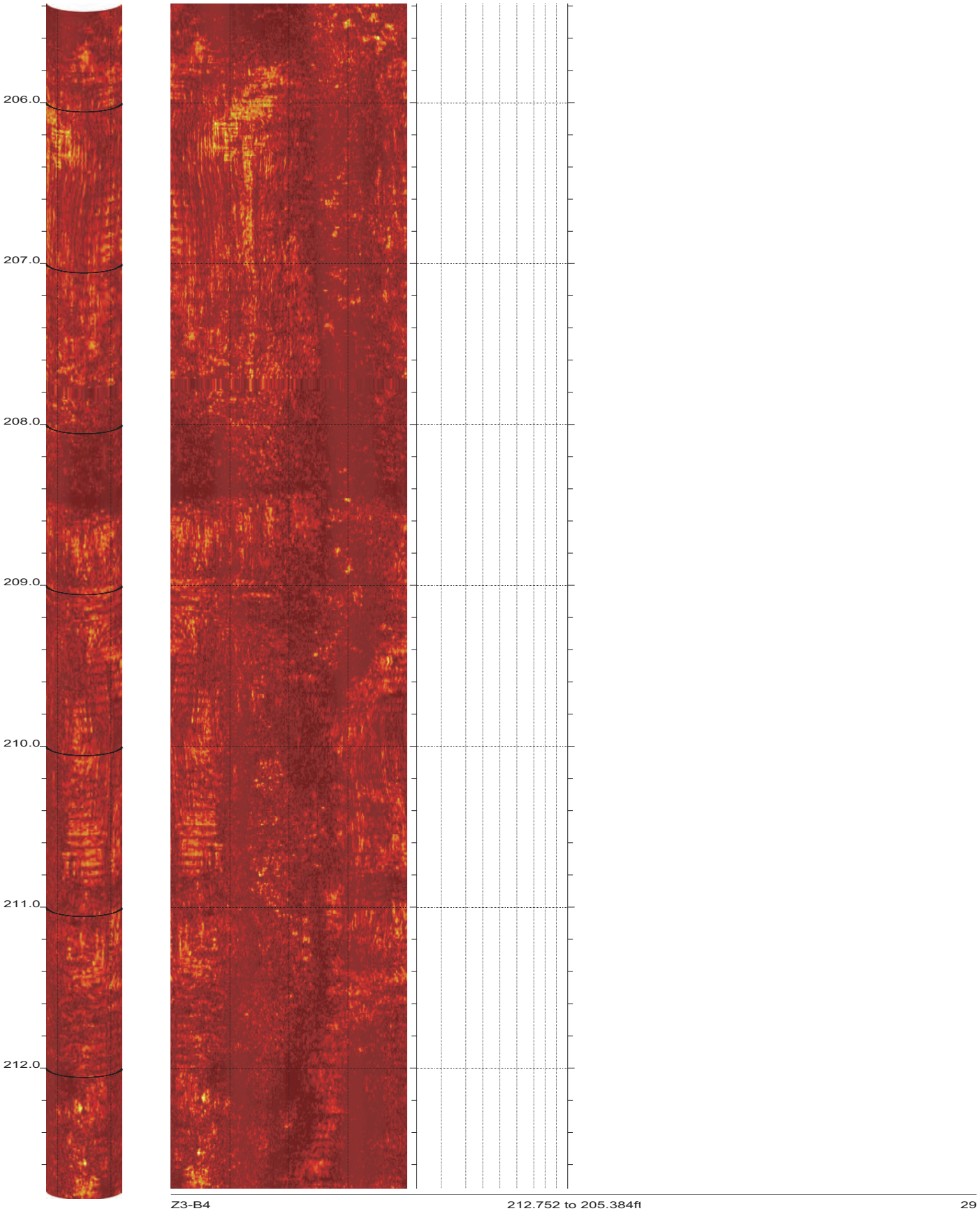

SR-710 Boring Z3-B4 Acoustic Televiewer Dips rev 1 Sheet 29 of 38

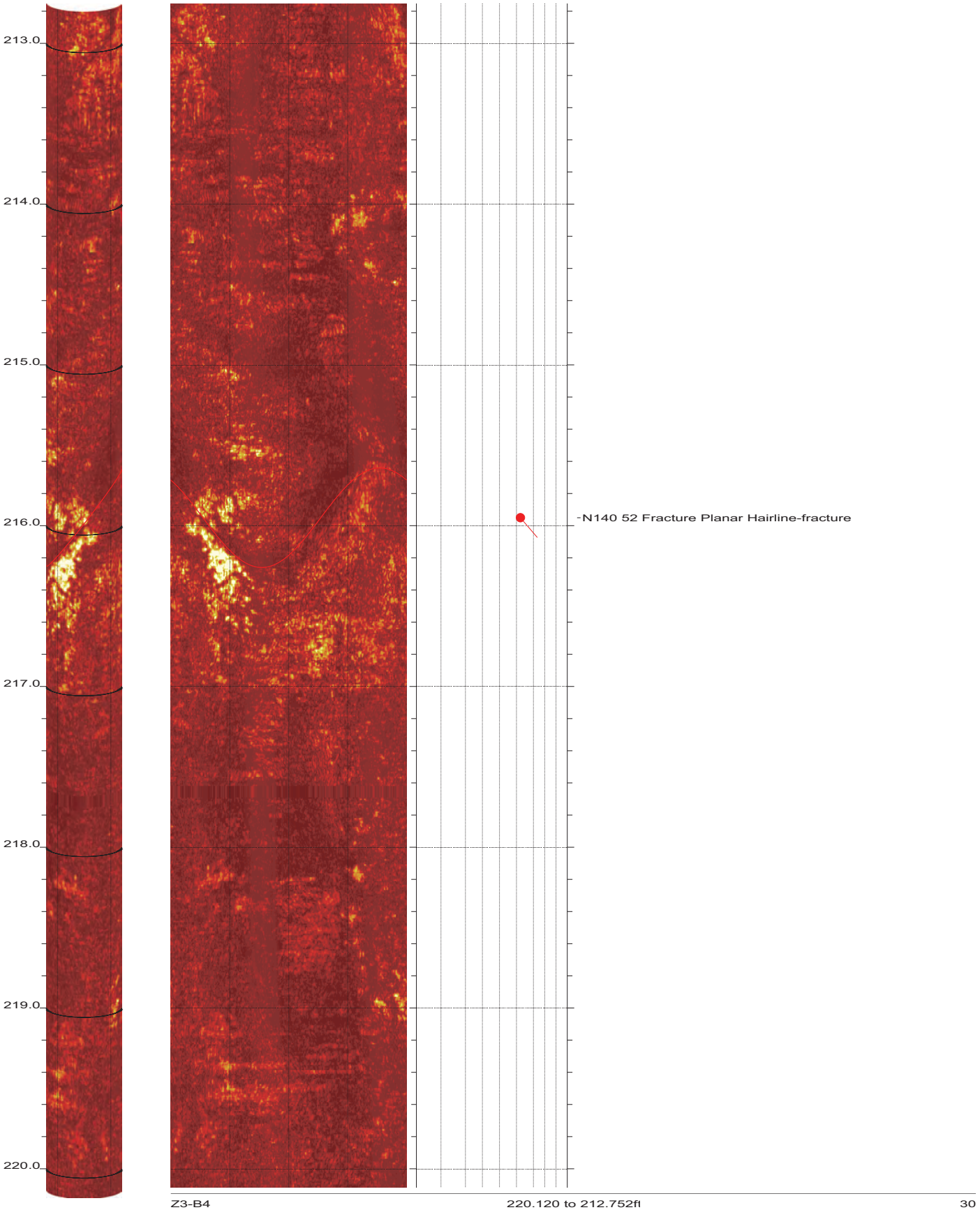

SR-710 Boring Z3-B4 Acoustic Televiewer Dips rev 1 Sheet 30 of 38

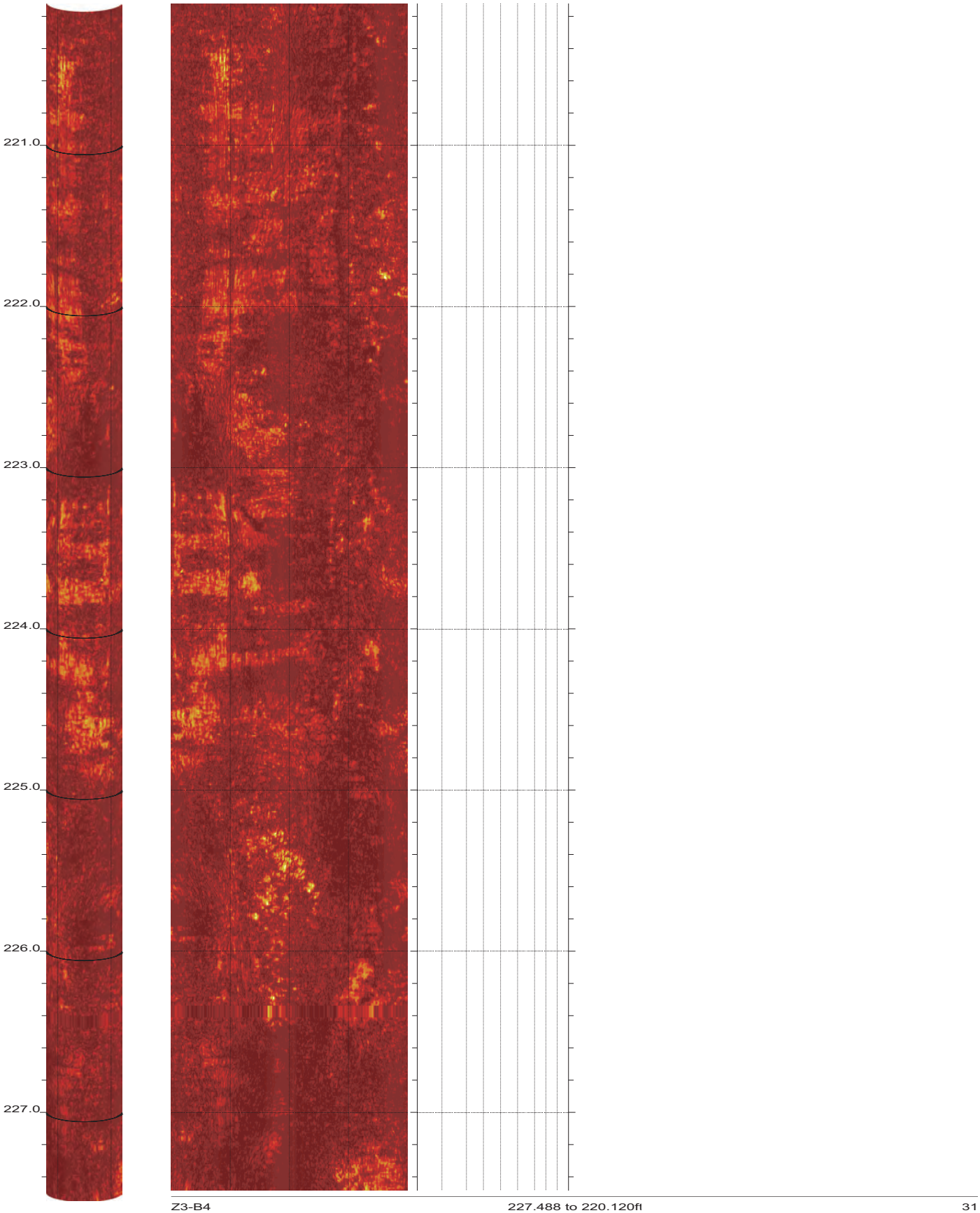

SR-710 Boring Z3-B4 Acoustic Televiewer Dips rev 1 Sheet 31 of 38

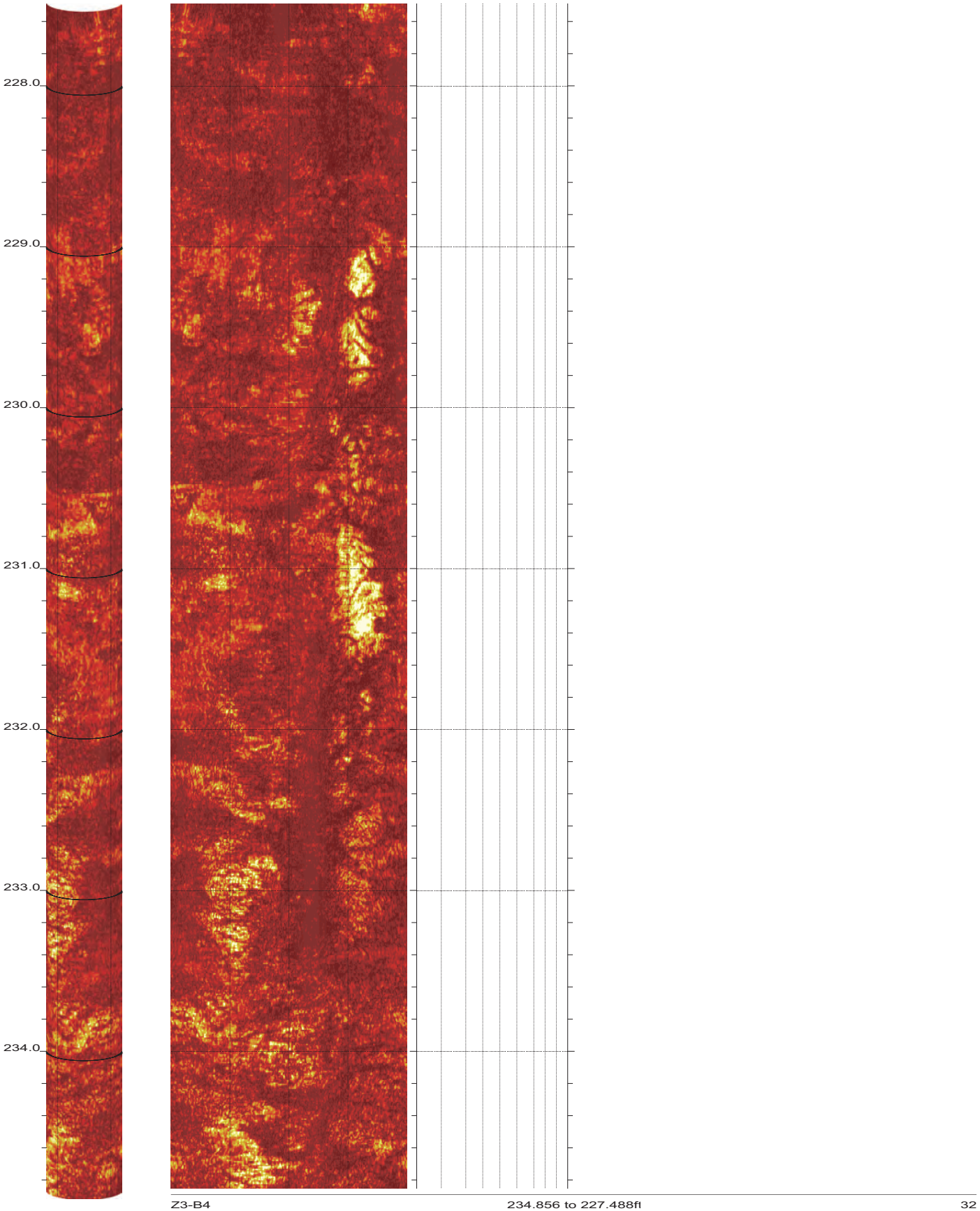

SR-710 Boring Z3-B4 Acoustic Televiewer Dips rev 1 Sheet 32 of 38

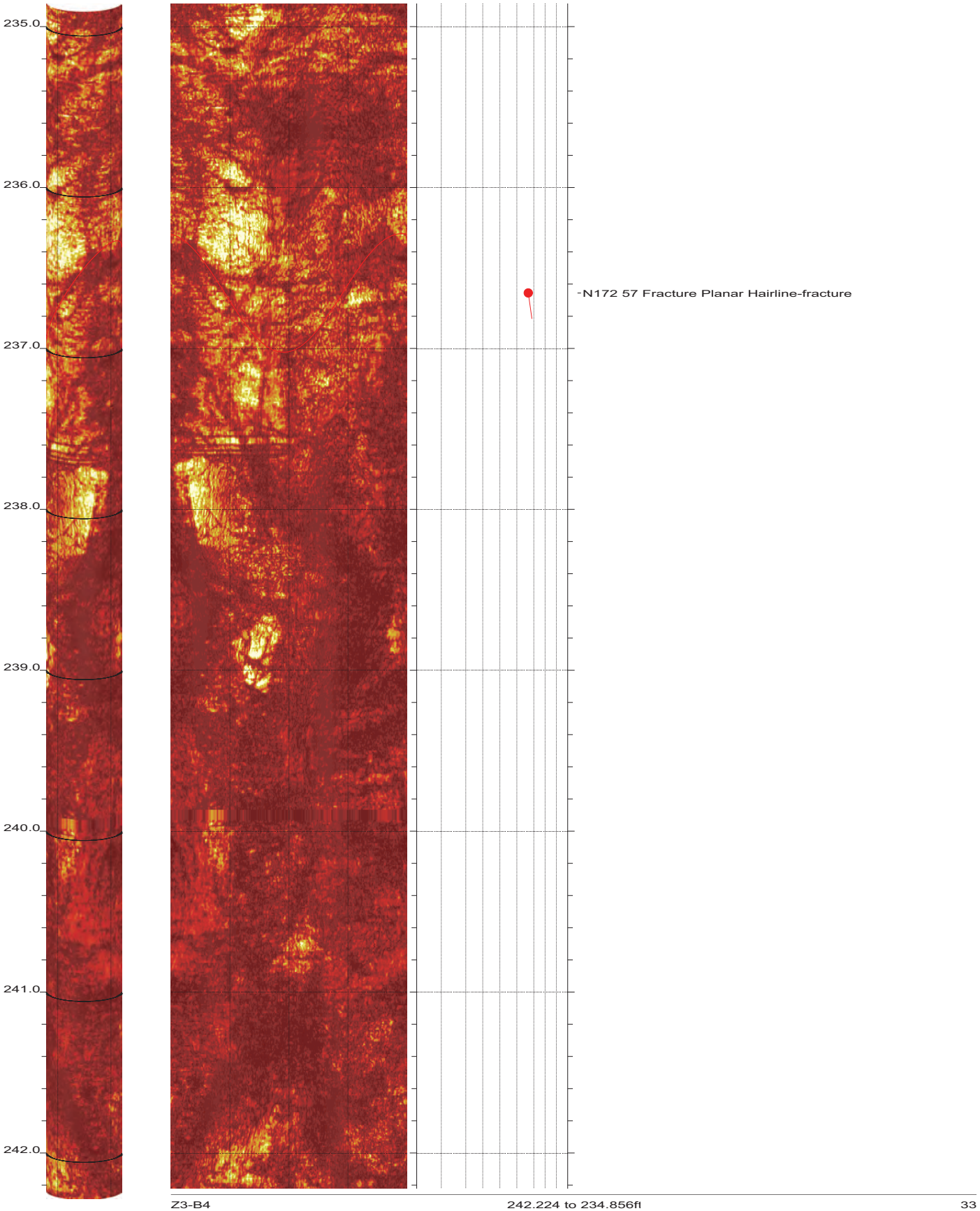

SR-710 Boring Z3-B4 Acoustic Televiewer Dips rev 1 Sheet 33 of 38

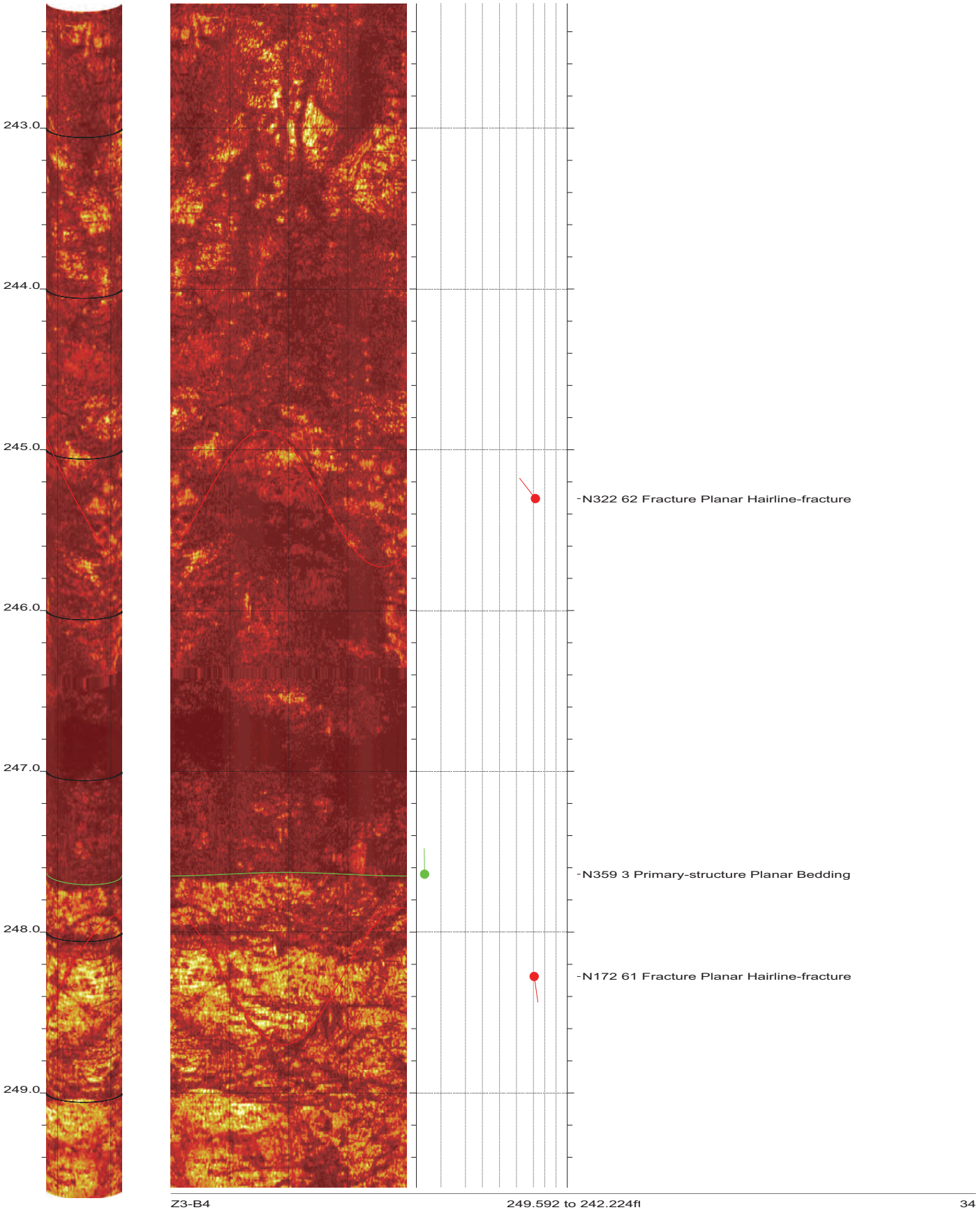

SR-710 Boring Z3-B4 Acoustic Televiewer Dips rev 1 Sheet 34 of 38

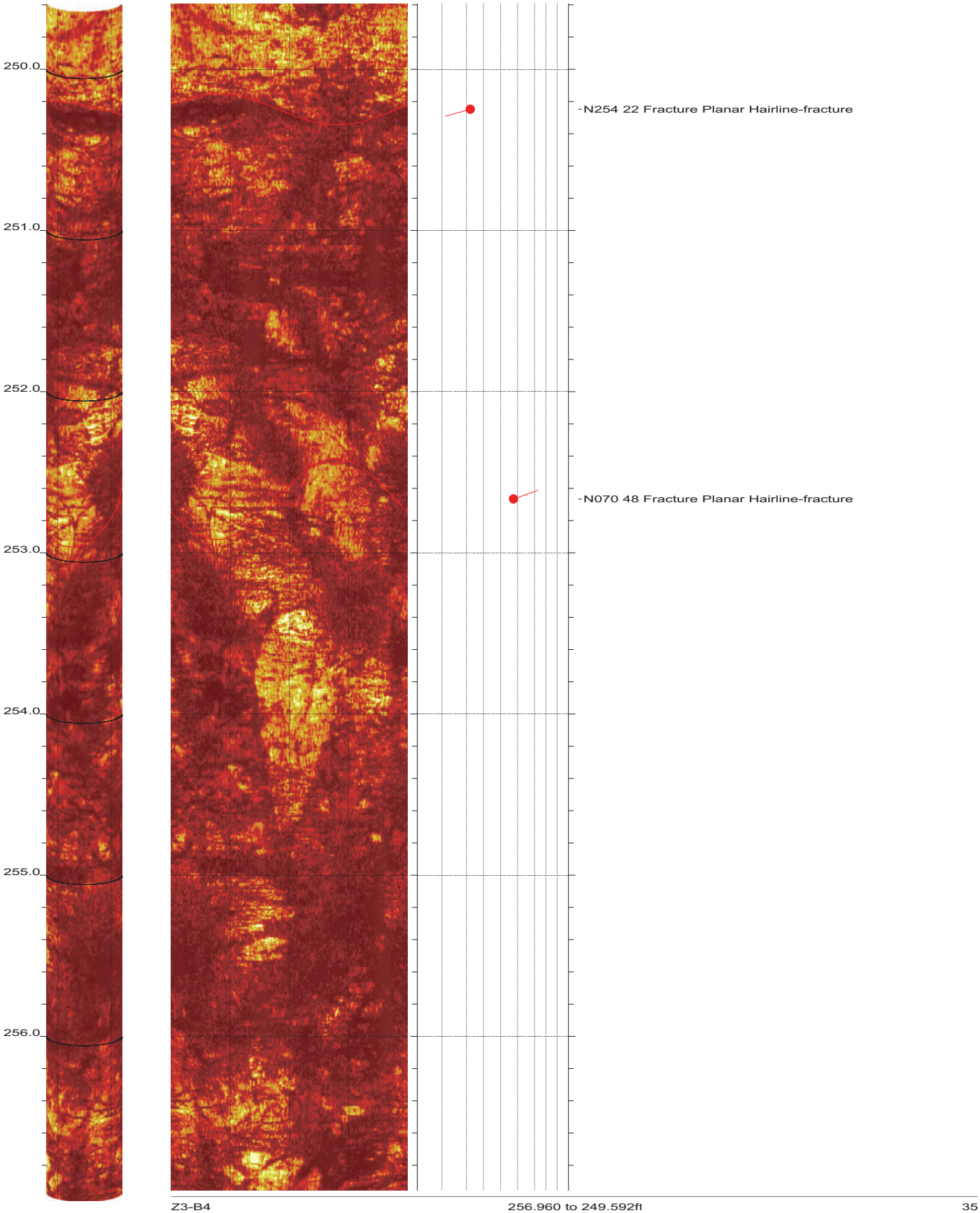

SR-710 Boring Z3-B4 Acoustic Televiewer Dips rev 1 Sheet 35 of 38

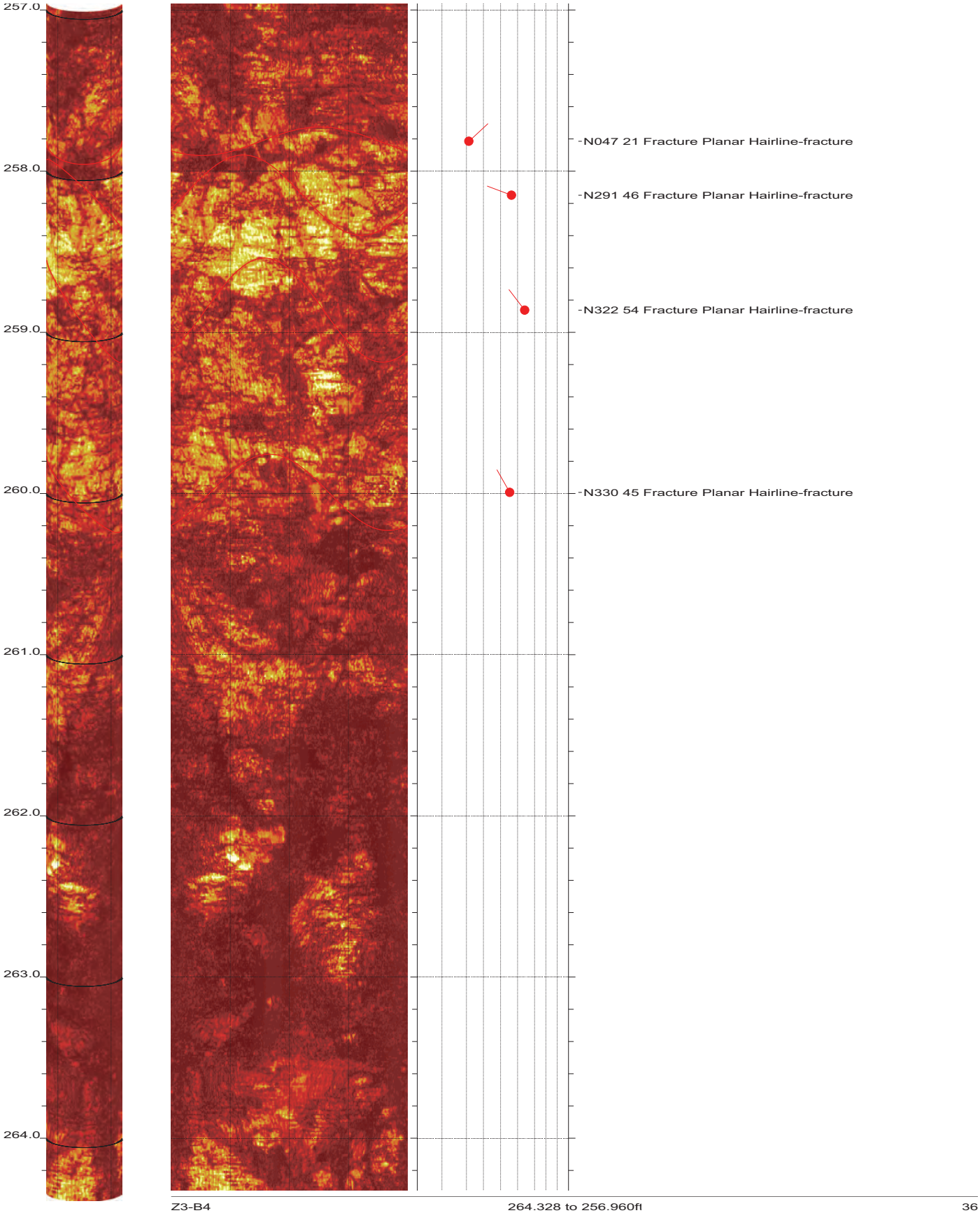

SR-710 Boring Z3-B4 Acoustic Televiewer Dips rev 1 Sheet 36 of 38

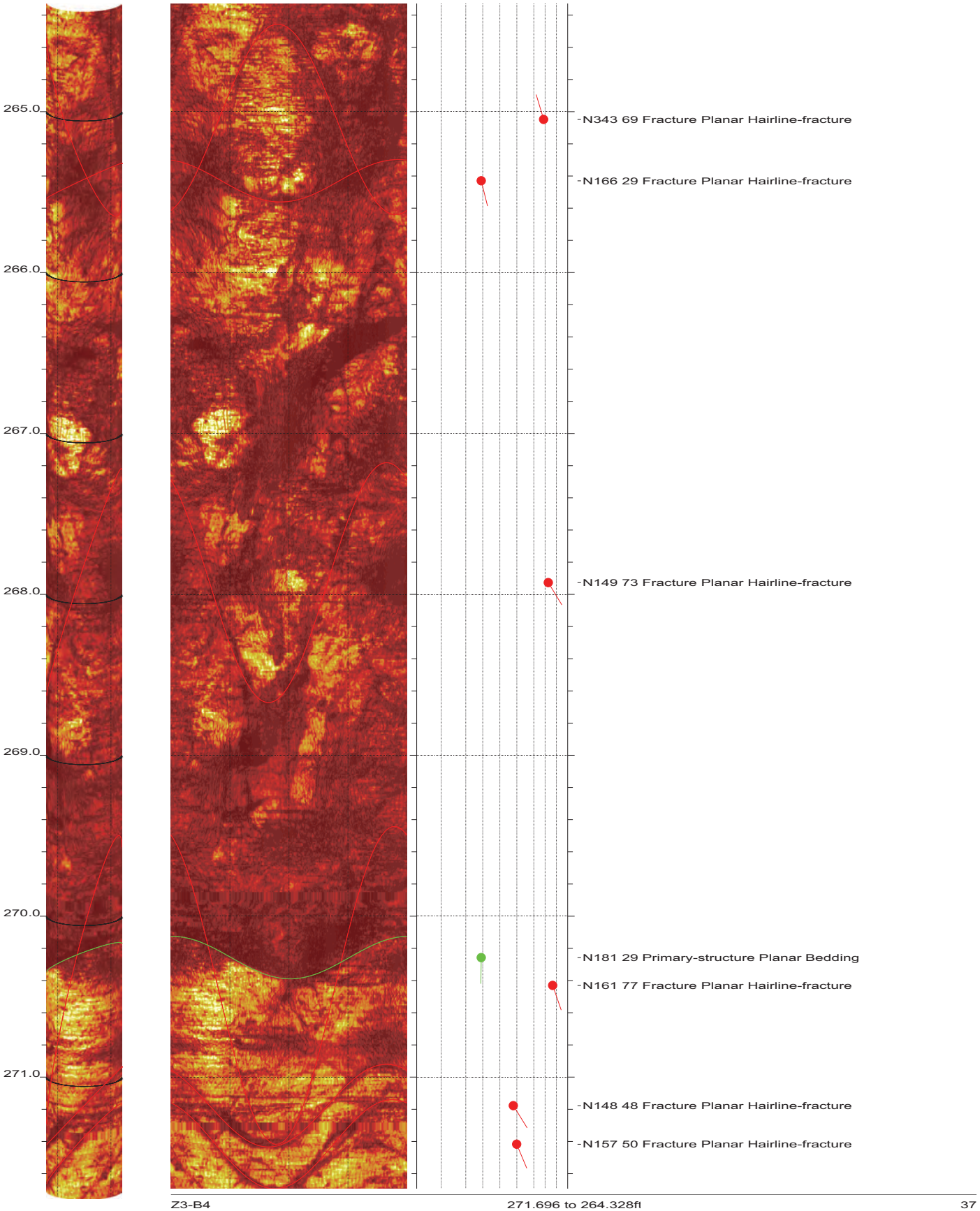

SR-710 Boring Z3-B4 Acoustic Televiewer Dips rev 1 Sheet 37 of 38

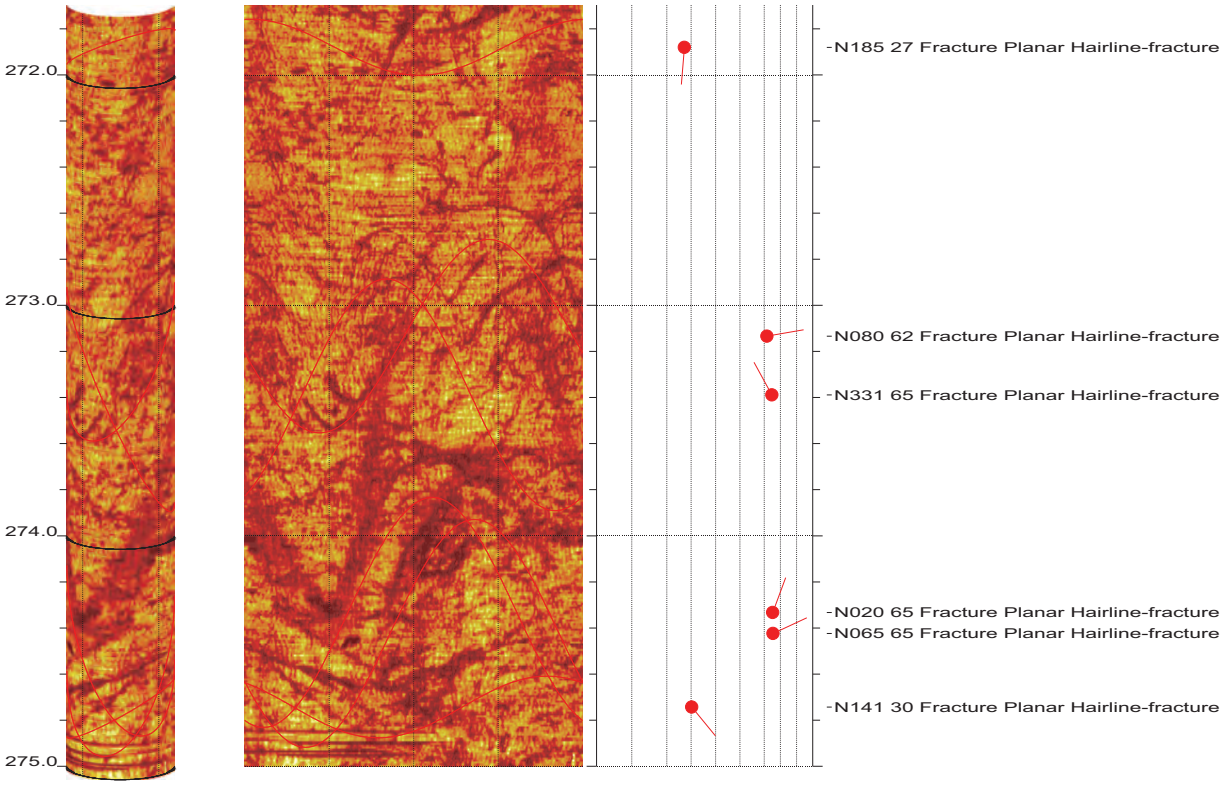
272.0
273.0
274.0
275.0
-N185 27 Fracture Planar Hairline-fracture
-N080 62 Fracture Planar Hairline-fracture
-N331 65 Fracture Planar Hairline-fracture
-N020 65 Fracture Planar Hairline-fracture
-N065 65 Fracture Planar Hairline-fracture
-N141 30 Fracture Planar Hairline-fracture

BHTV DATA PROCESSING
RGLDIP vsn 6.2
INTERPRETED BHTV DIPS LOG

CASCADE DRILLING

Borehole: Z3-B6

SR-710 TUNNEL INVESTIGATION

top of borehole.....
East: _
North: _
Elev: _

North ref. is true
Depth units are feet
Vertical scale: 1/10
Horiz scale = 1.00x Vert scale

Zone from 318.600 to 28.400ft
Format: BHTV-NESWN

Borehole diam: 5.600inch
Vertical = borehole-axis
Image: Amplitude

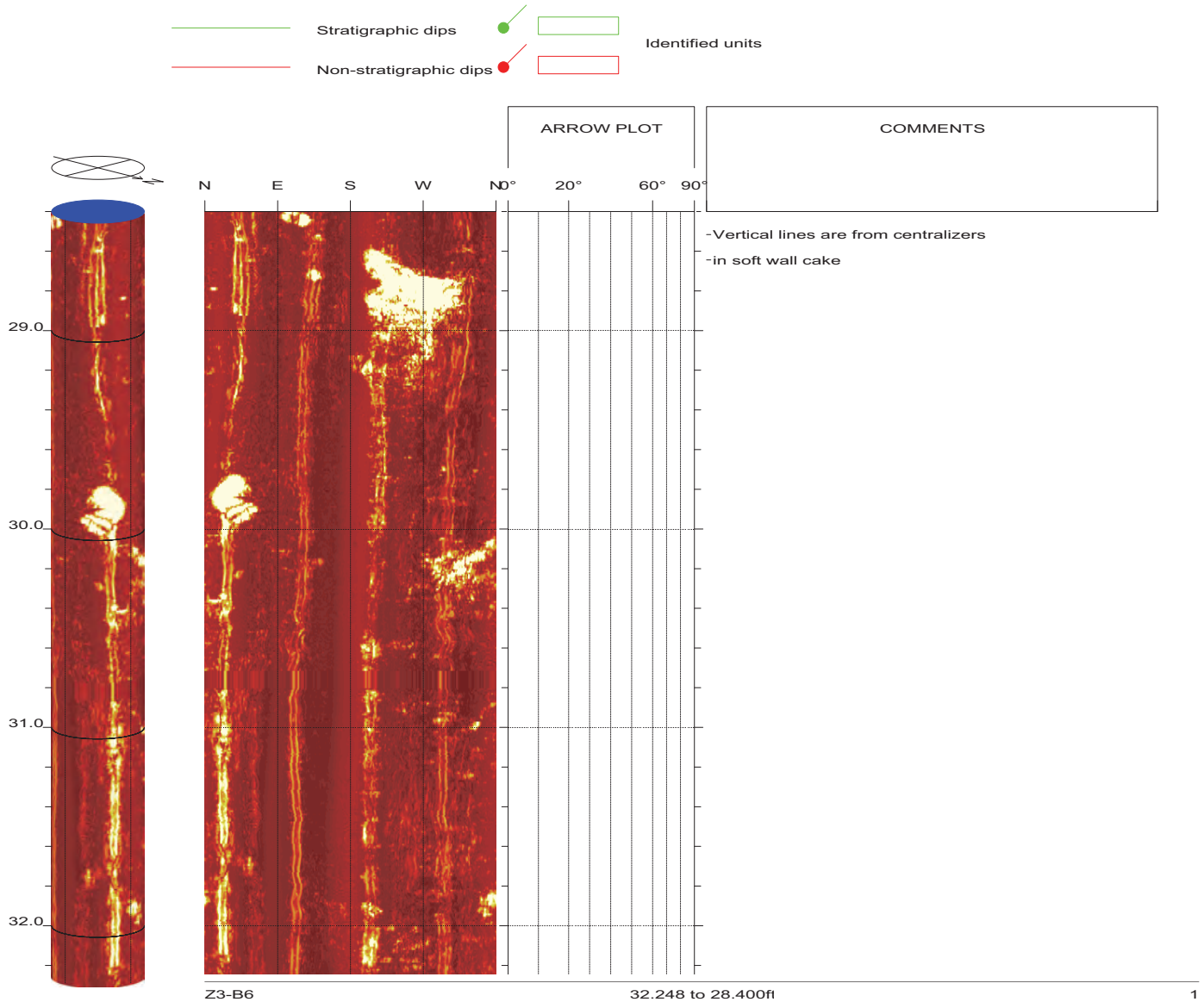

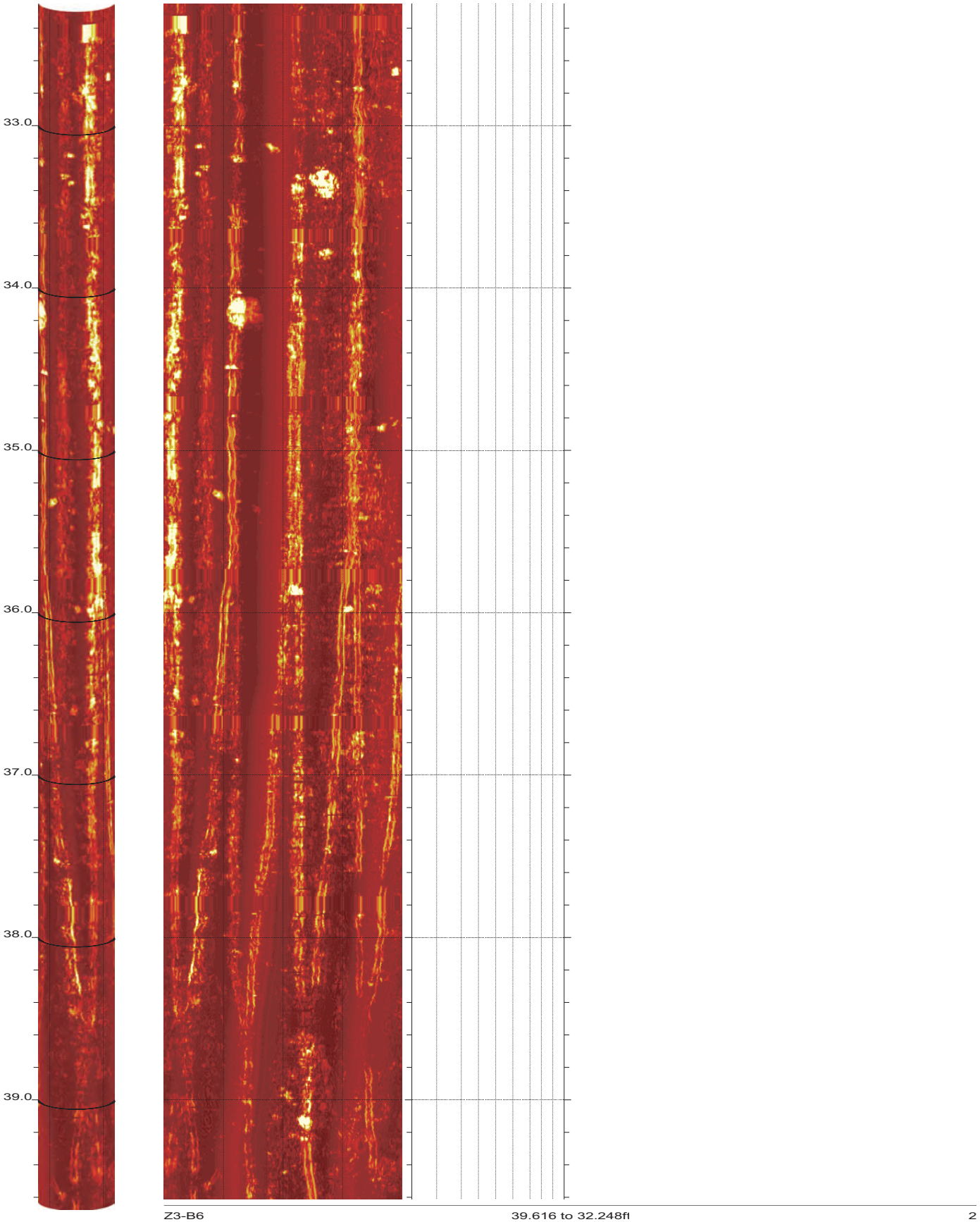

SR-710 Boring Z3-B6 Acoustic Televiewer Dips rev 1 Sheet 2 of 40

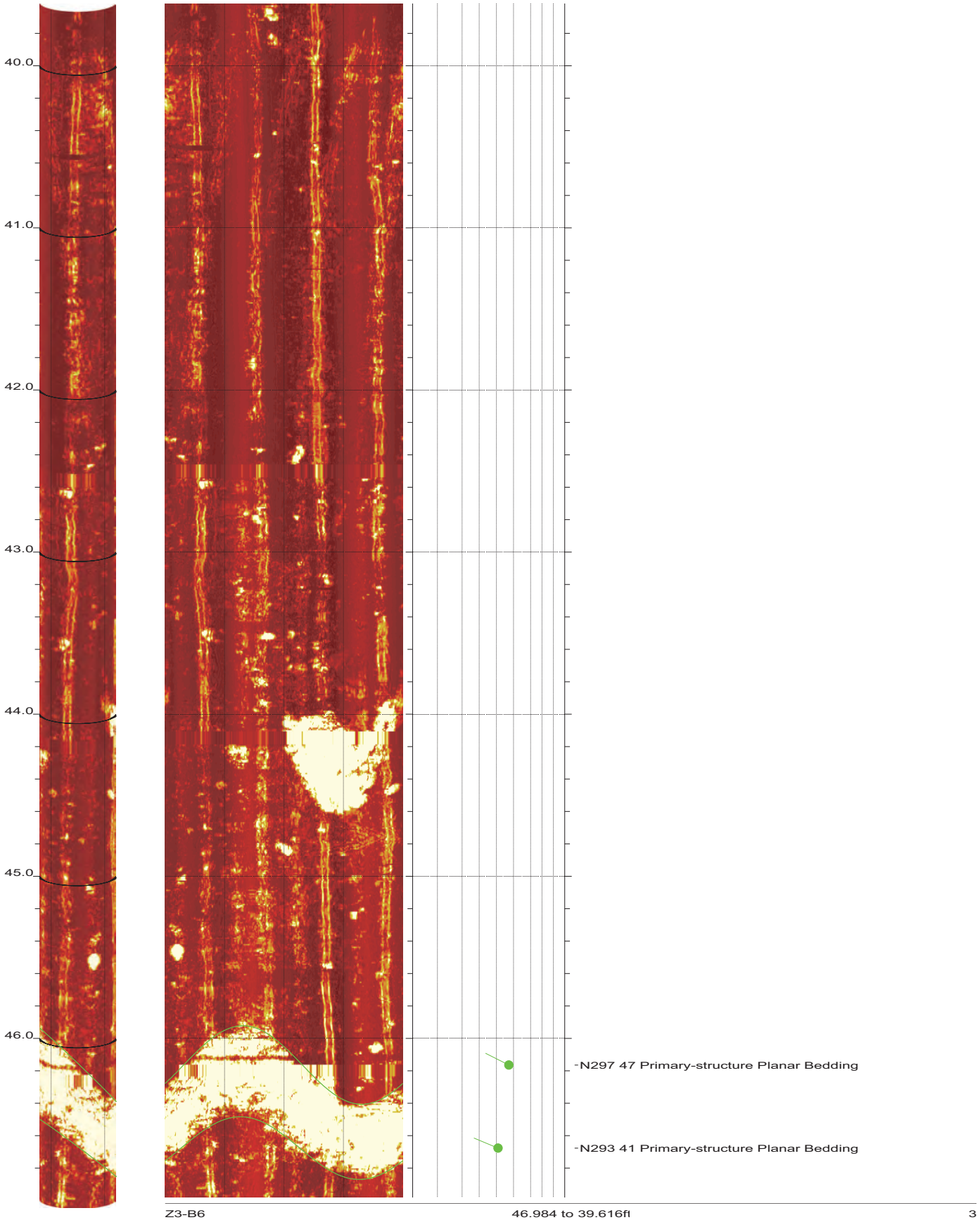

SR-710 Boring Z3-B6 Acoustic Televiewer Dips rev 1 Sheet 3 of 40

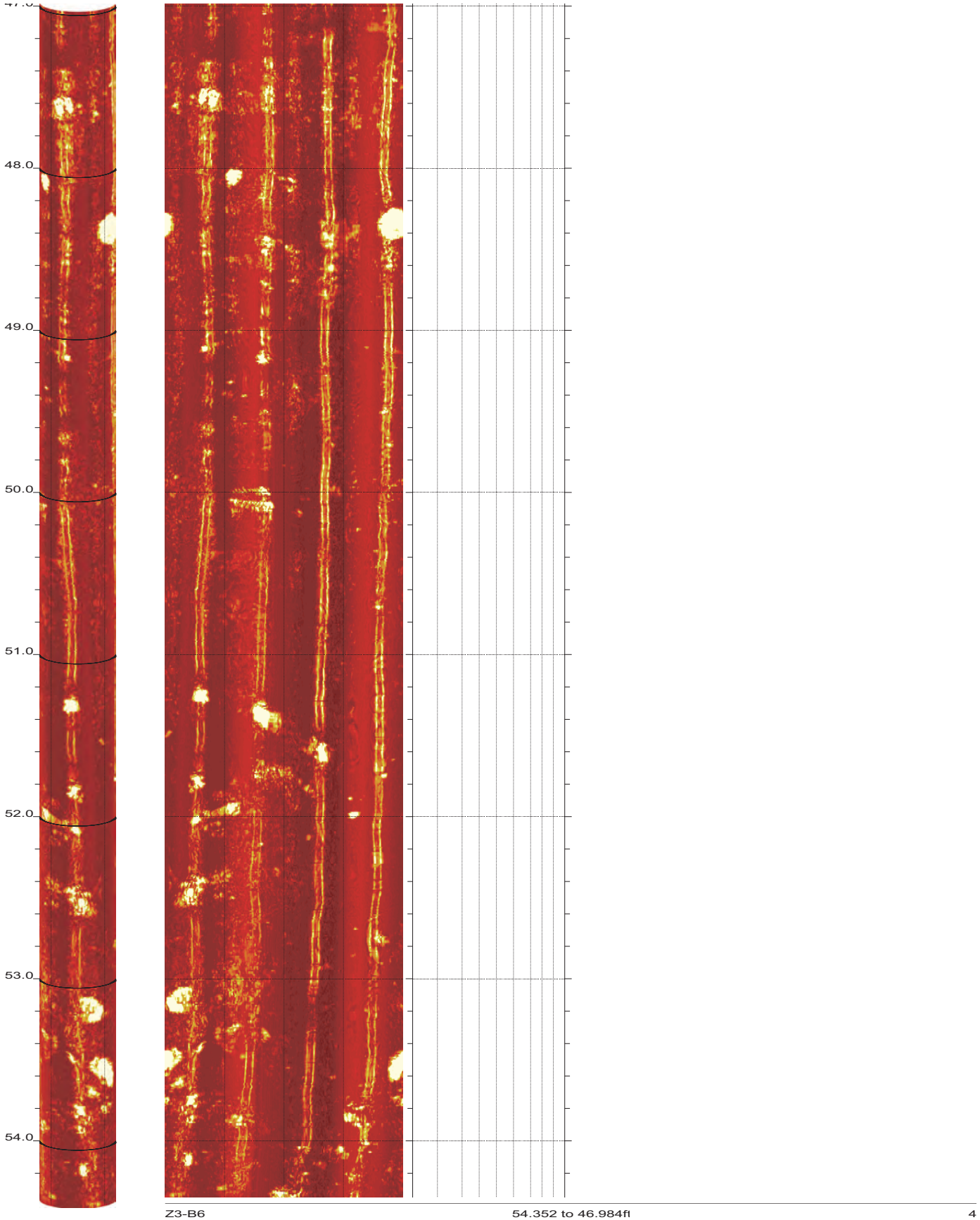

SR-710 Boring Z3-B6 Acoustic Televiewer Dips rev 1 Sheet 4 of 40

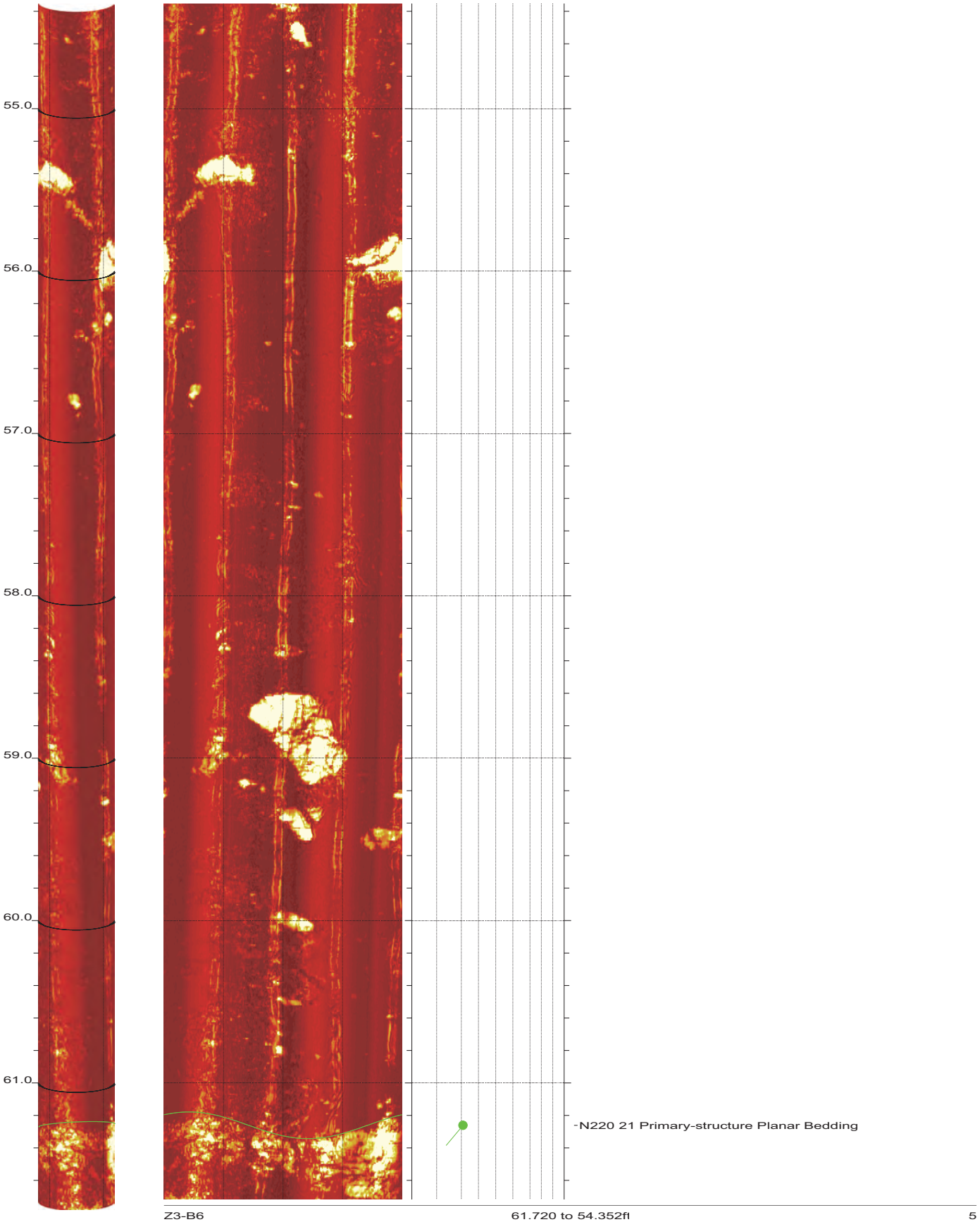

SR-710 Boring Z3-B6 Acoustic Televiewer Dips rev 1 Sheet 5 of 40

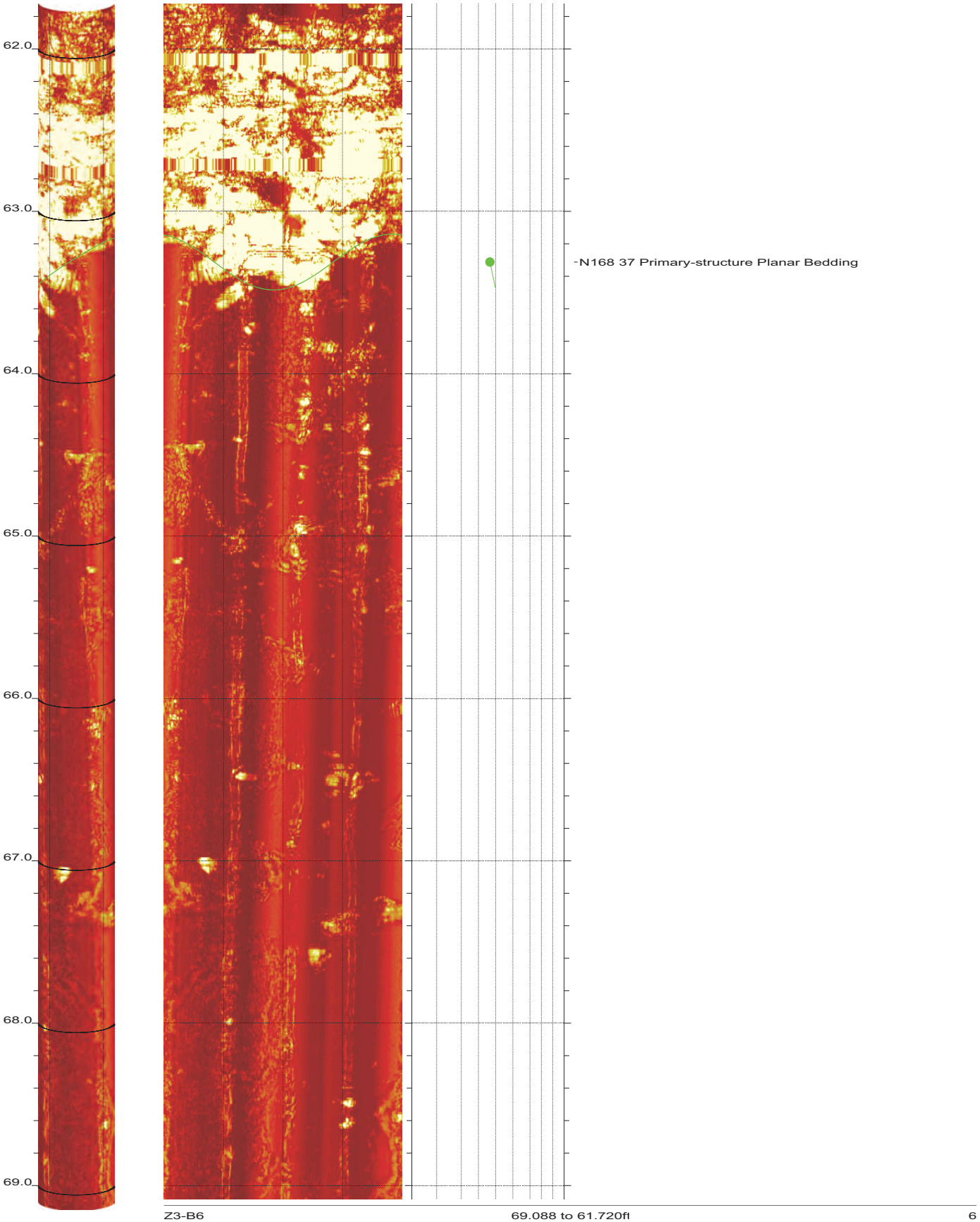

SR-710 Boring Z3-B6 Acoustic Televiewer Dips rev 1 Sheet 6 of 40

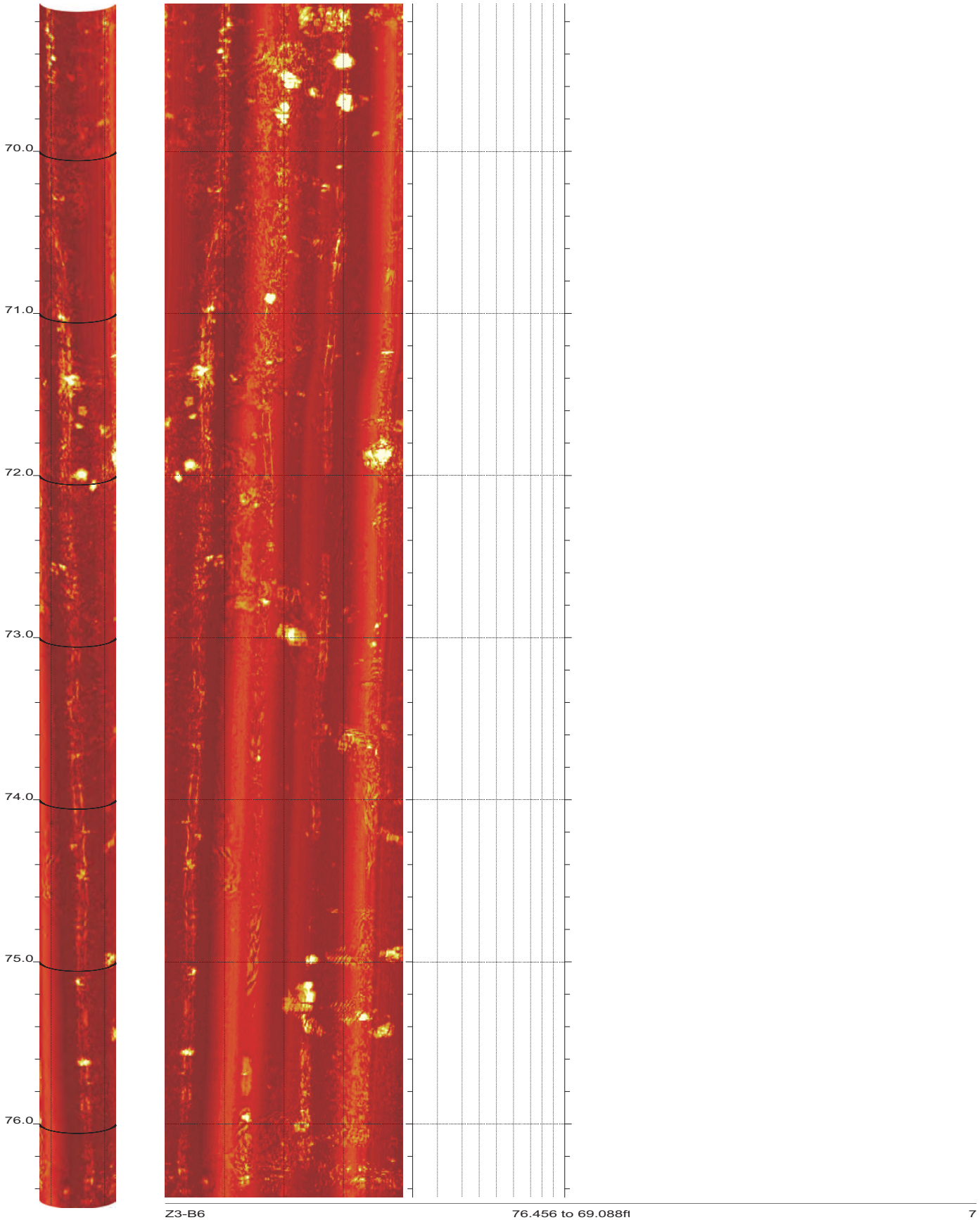

SR-710 Boring Z3-B6 Acoustic Televiewer Dips rev 1 Sheet 7 of 40

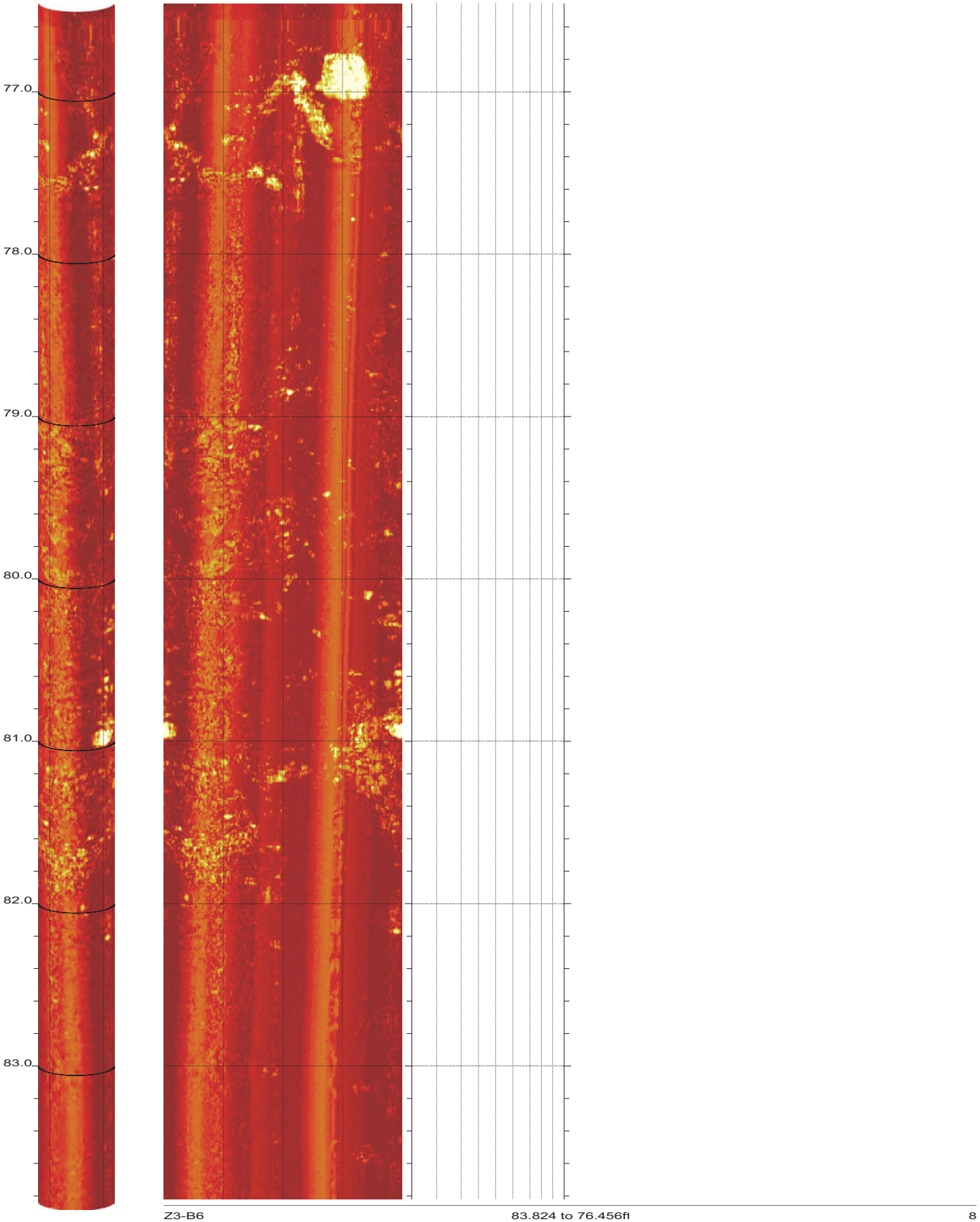

SR-710 Boring Z3-B6 Acoustic Televiewer Dips rev 1 Sheet 8 of 40

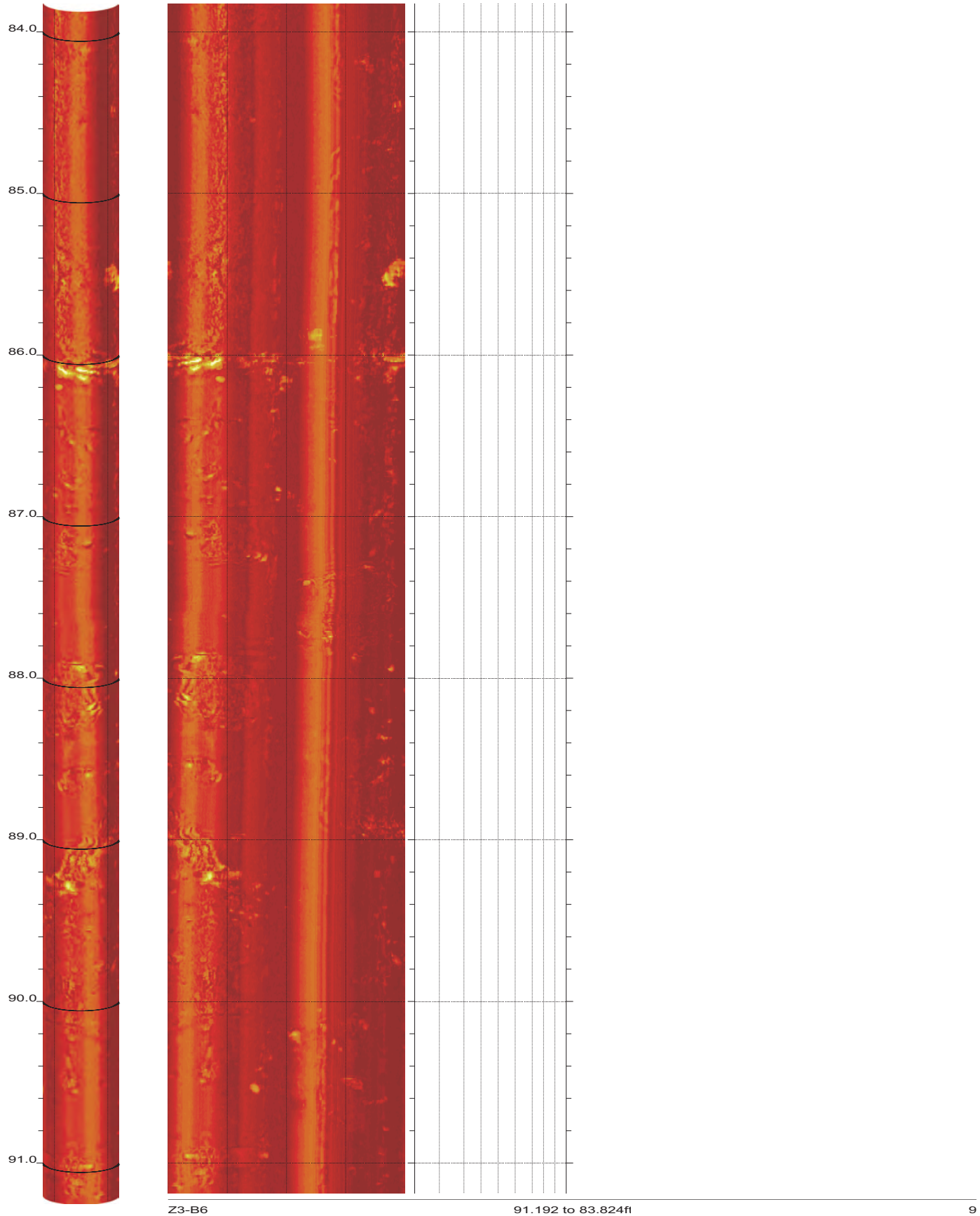

SR-710 Boring Z3-B6 Acoustic Televiewer Dips rev 1 Sheet 9 of 40

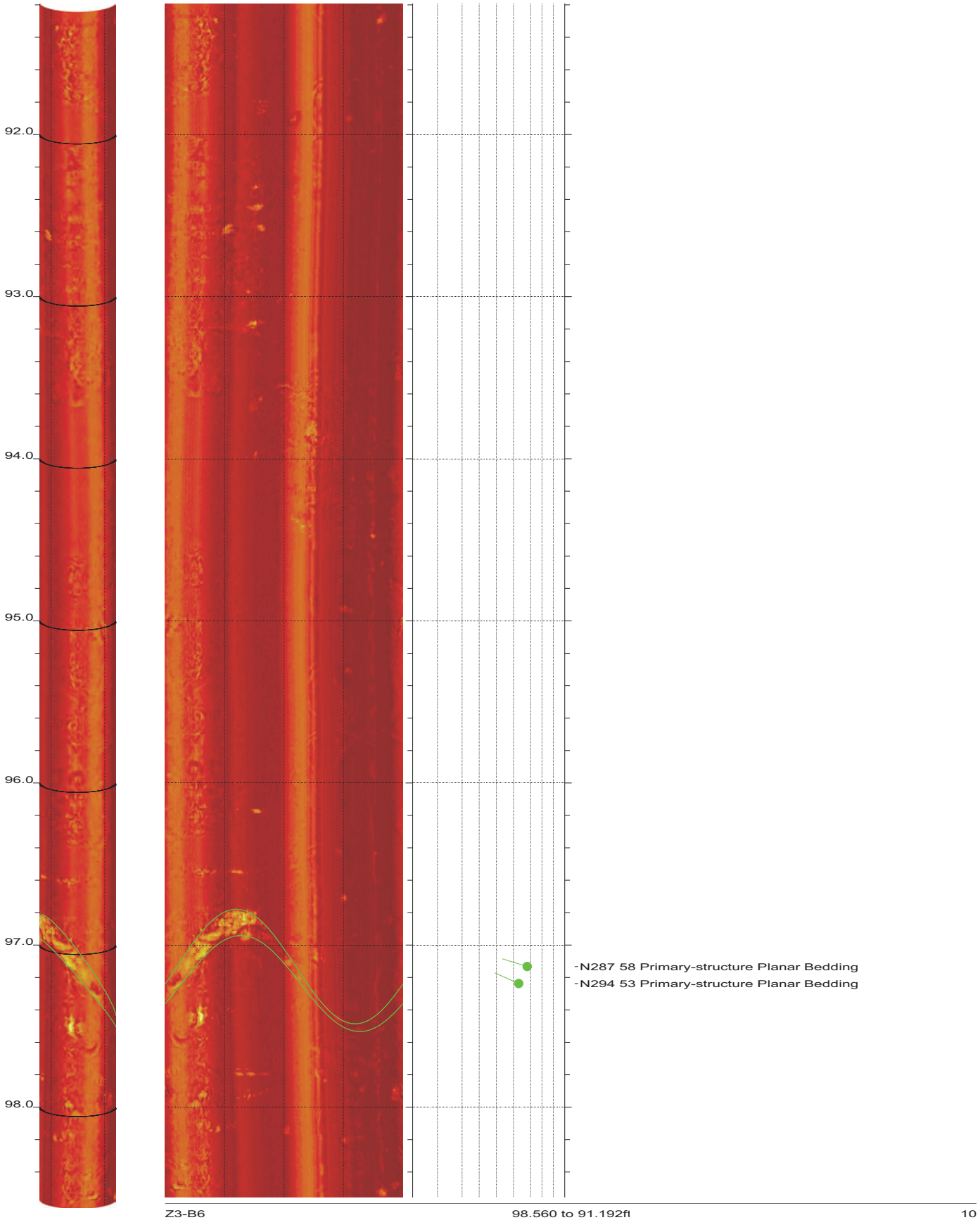

SR-710 Boring Z3-B6 Acoustic Televiewer Dips rev 1 Sheet 10 of 40

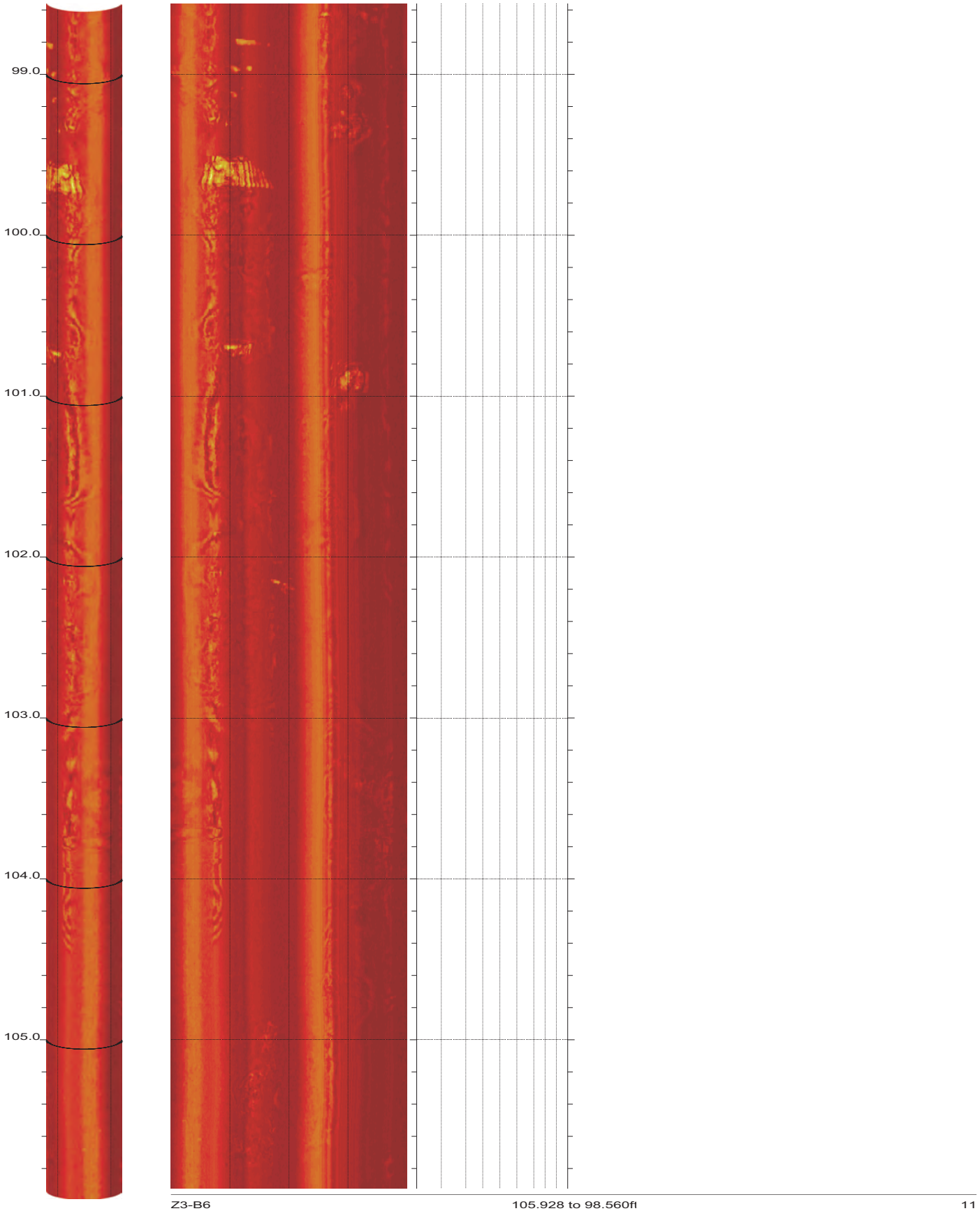
99.0
100.0
101.0
102.0
103.0
104.0
105.0
Z3-B6
105.928 to 98.560ft
11

SR-710 Boring Z3-B6 Acoustic Televiewer Dips rev 1 Sheet 12 of 40

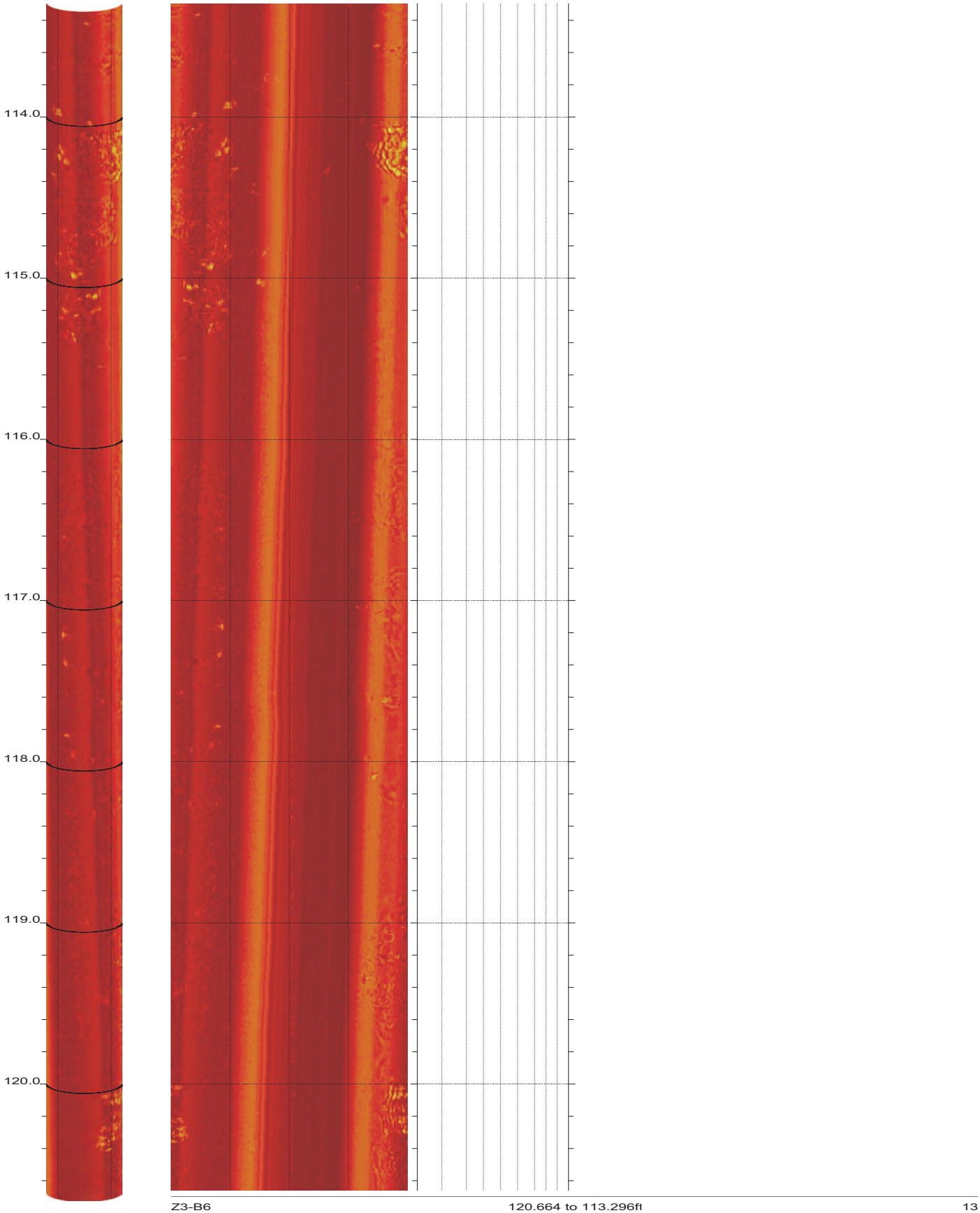
114.0
115.0
116.0
117.0
118.0
119.0
120.0
Z3-B6
120.664 to 113.296fl
13

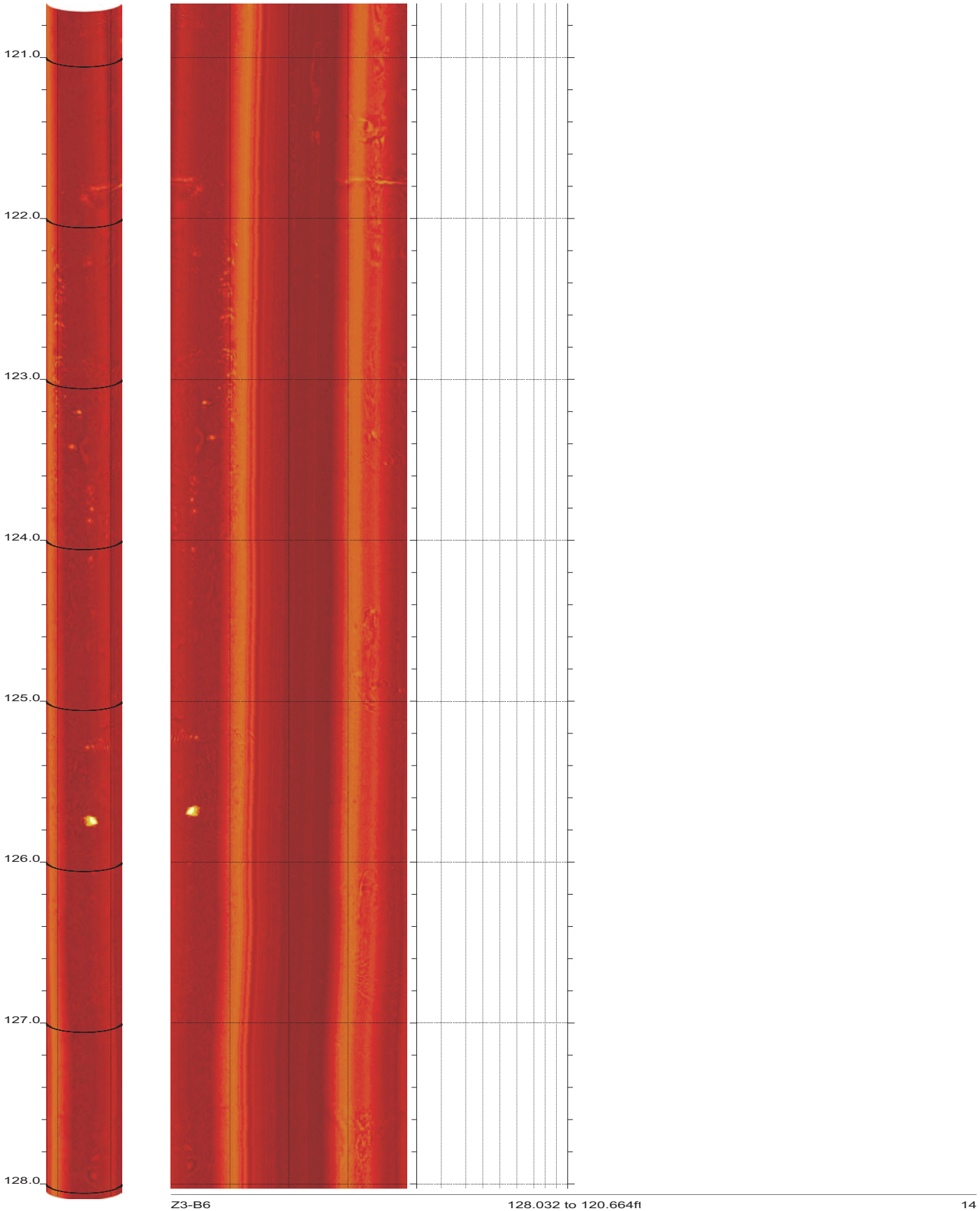
121.0
122.0
123.0
124.0
125.0
126.0
127.0
128.0
Z3-B6
128.032 to 120.664ft
14

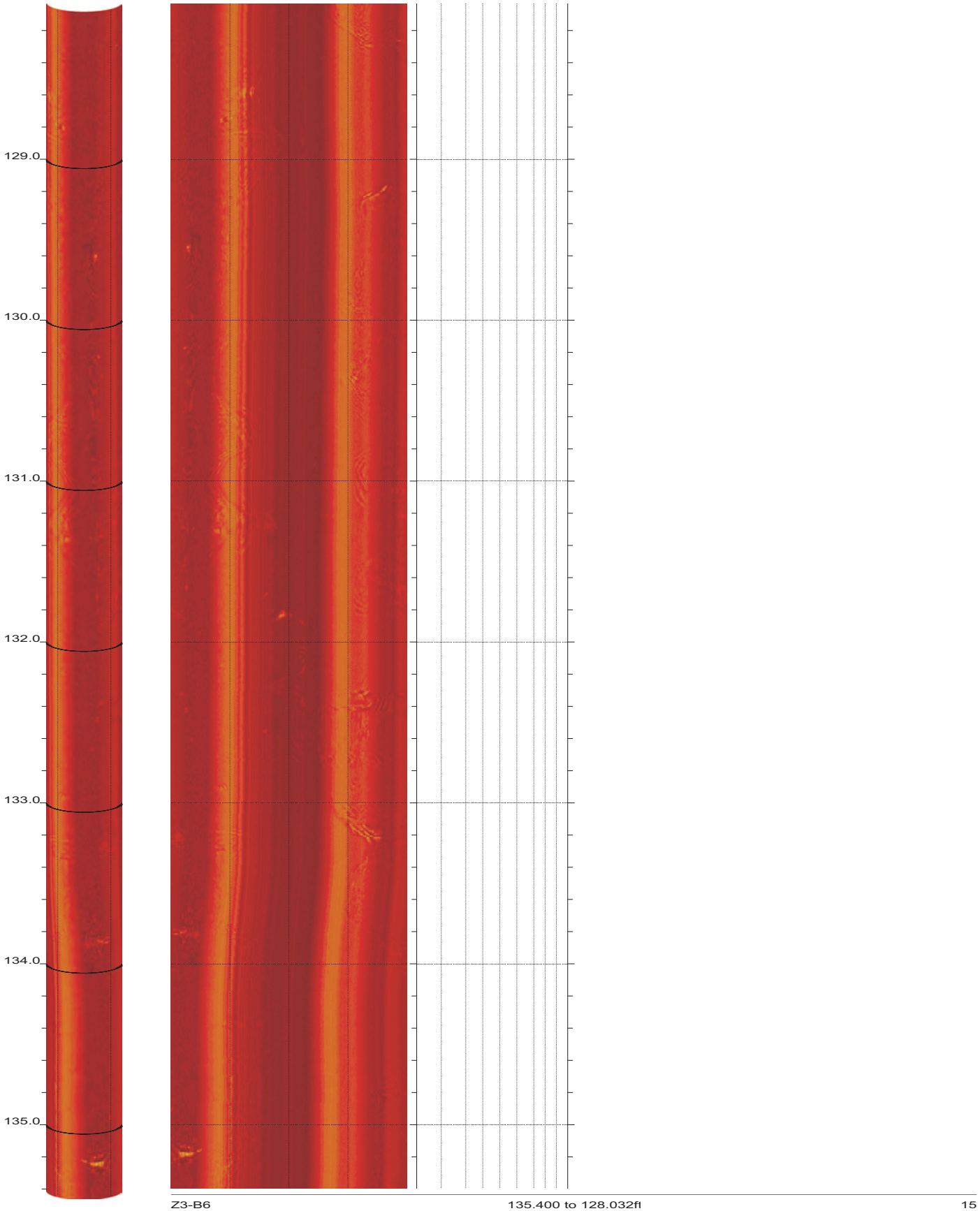

SR-710 Boring Z3-B6 Acoustic Televiewer Dips rev 1 Sheet 15 of 40

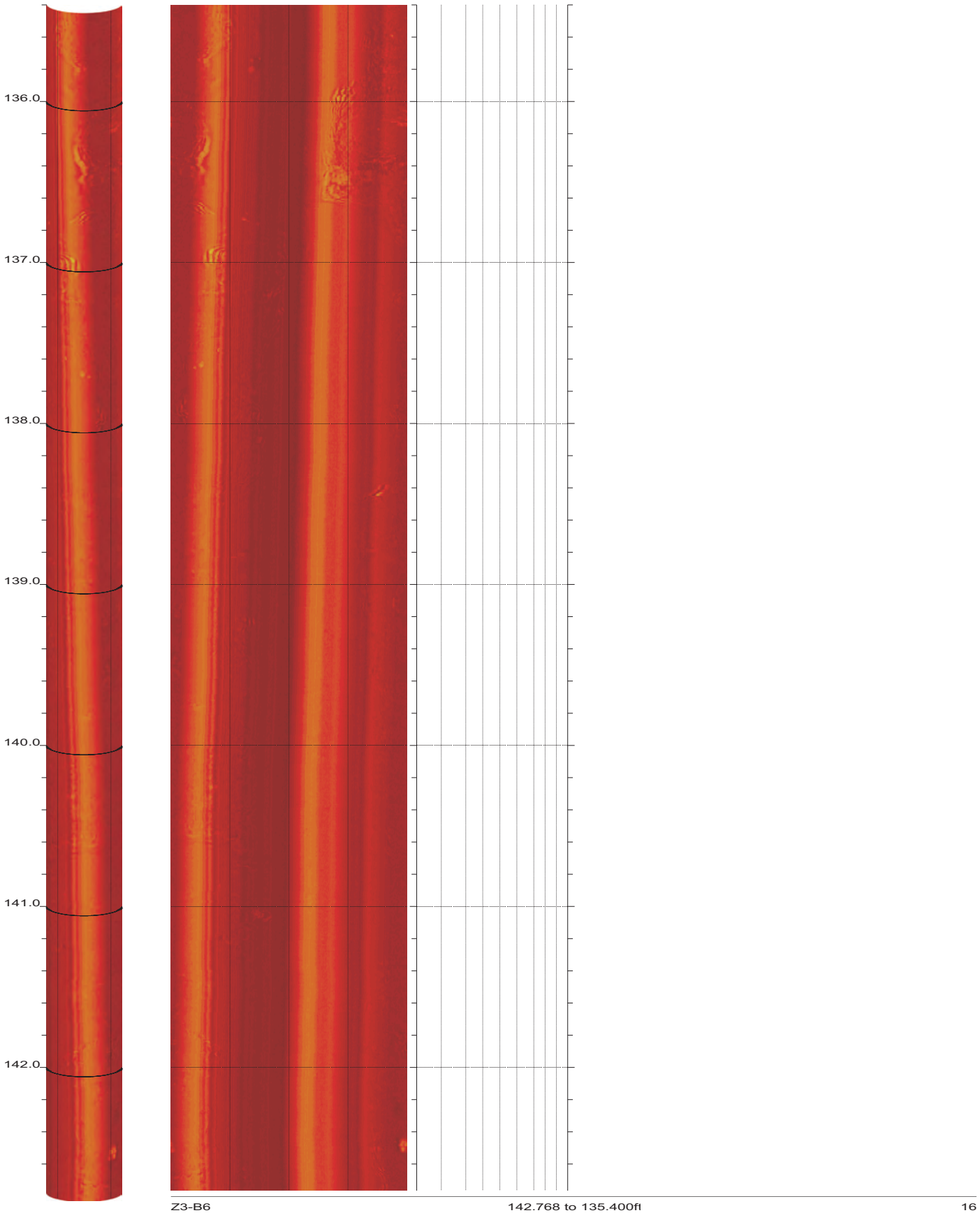

SR-710 Boring Z3-B6 Acoustic Televiewer Dips rev 1 Sheet 16 of 40

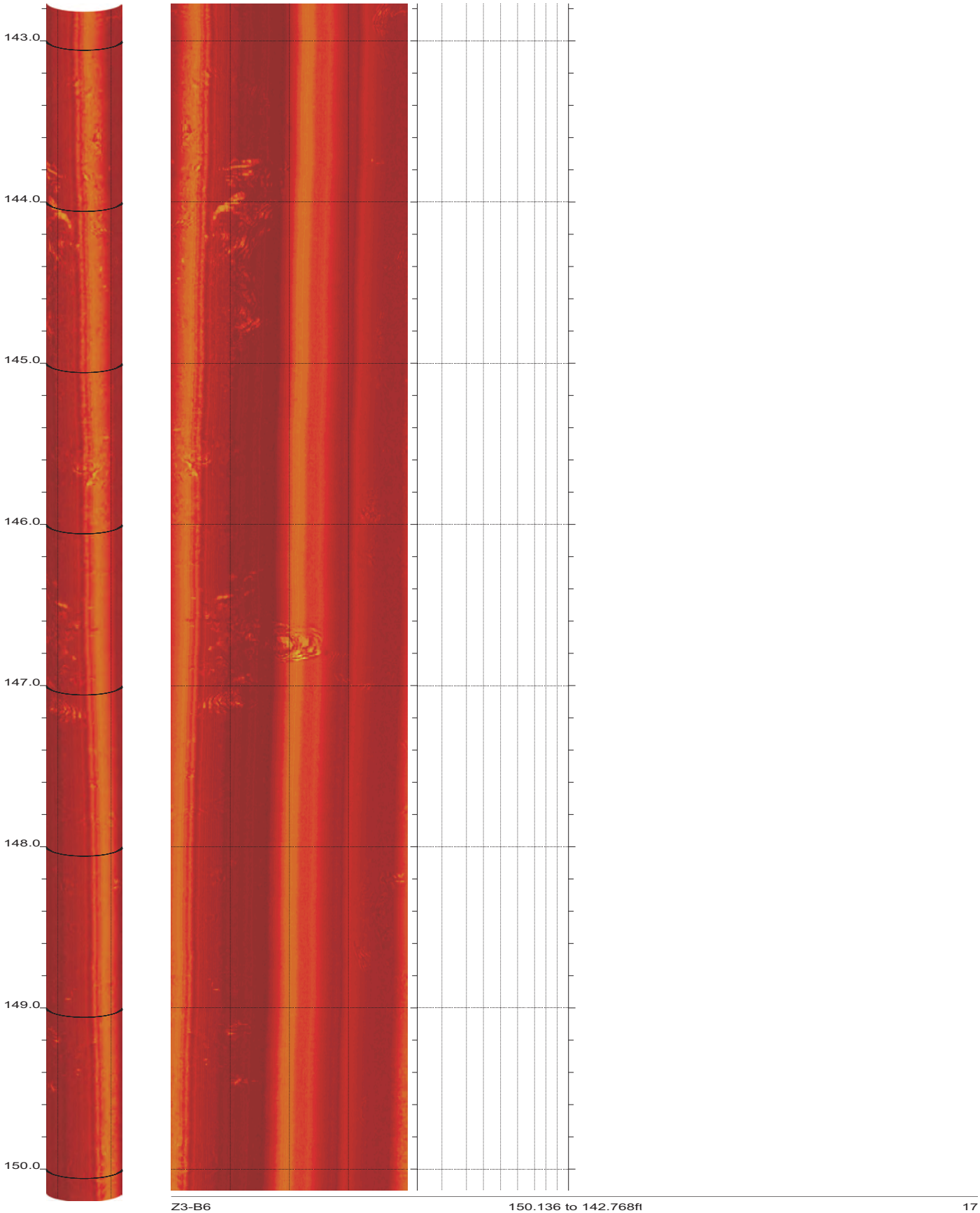
143.0
144.0
145.0
146.0
147.0
148.0
149.0
150.0
Z3-B6
150.136 to 142.768ft
17

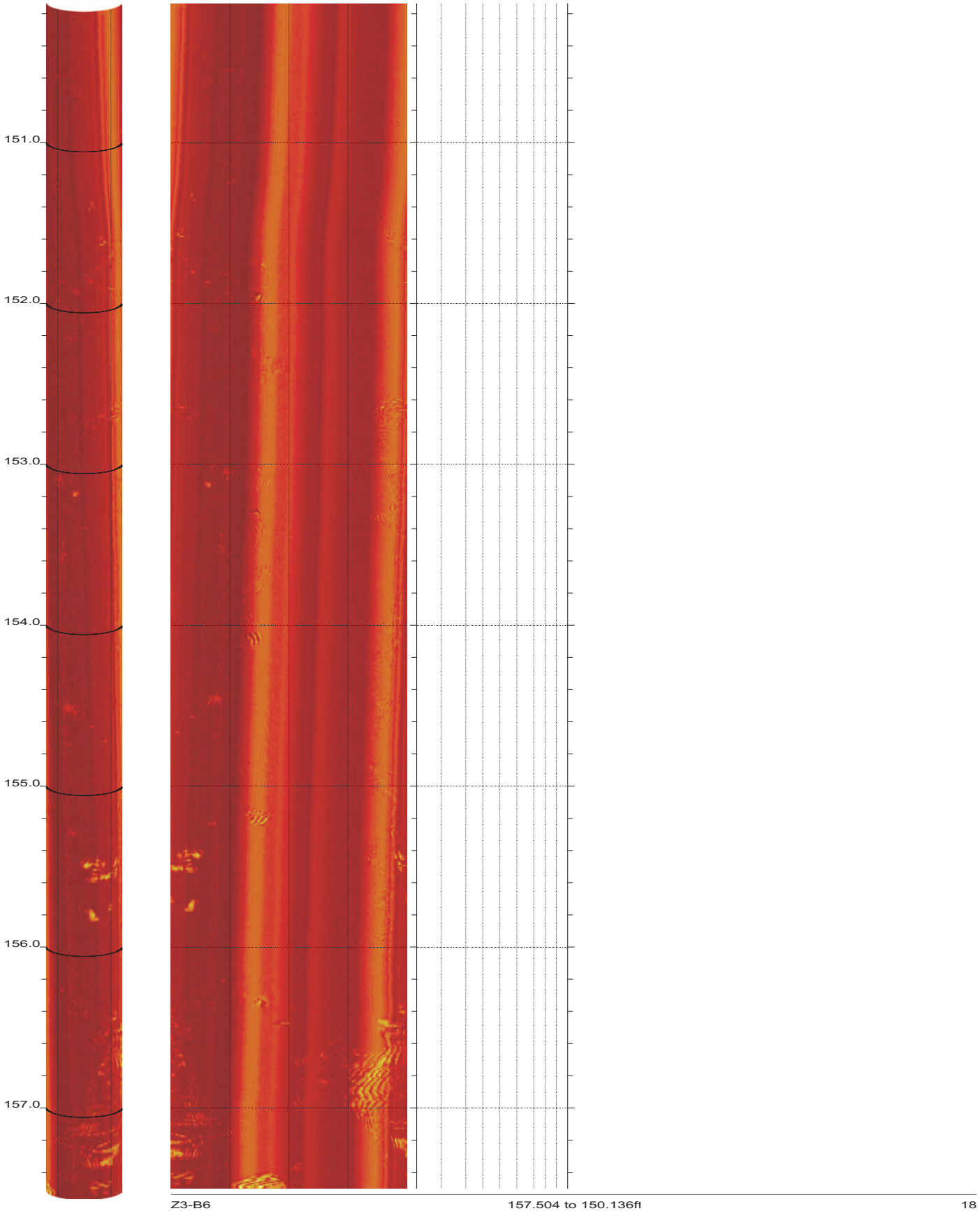

SR-710 Boring Z3-B6 Acoustic Televiewer Dips rev 1 Sheet 18 of 40

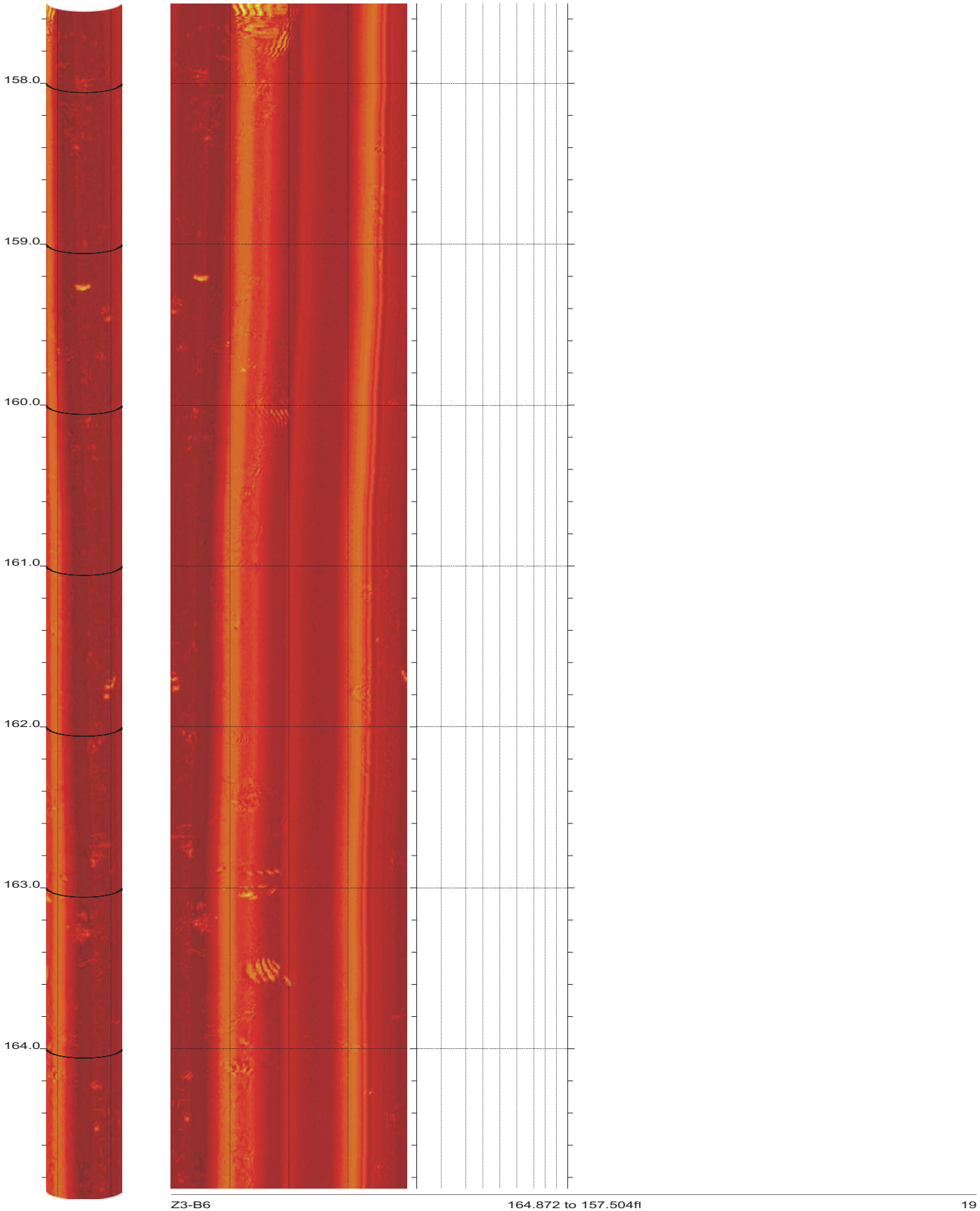
158.0
159.0
160.0
161.0
162.0
163.0
164.0
Z3-B6
164.872 to 157.504ft
19

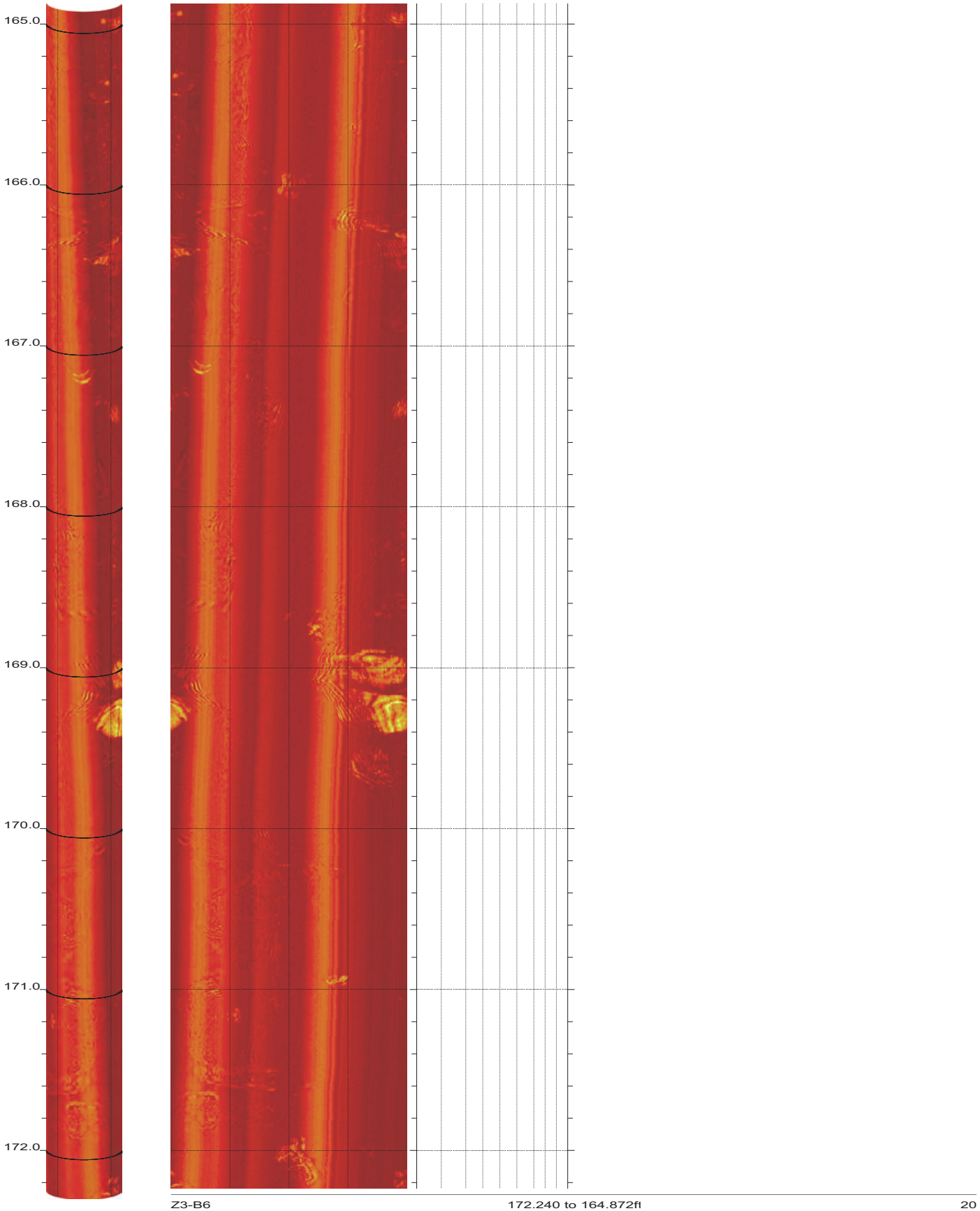

SR-710 Boring Z3-B6 Acoustic Televiewer Dips rev 1 Sheet 20 of 40

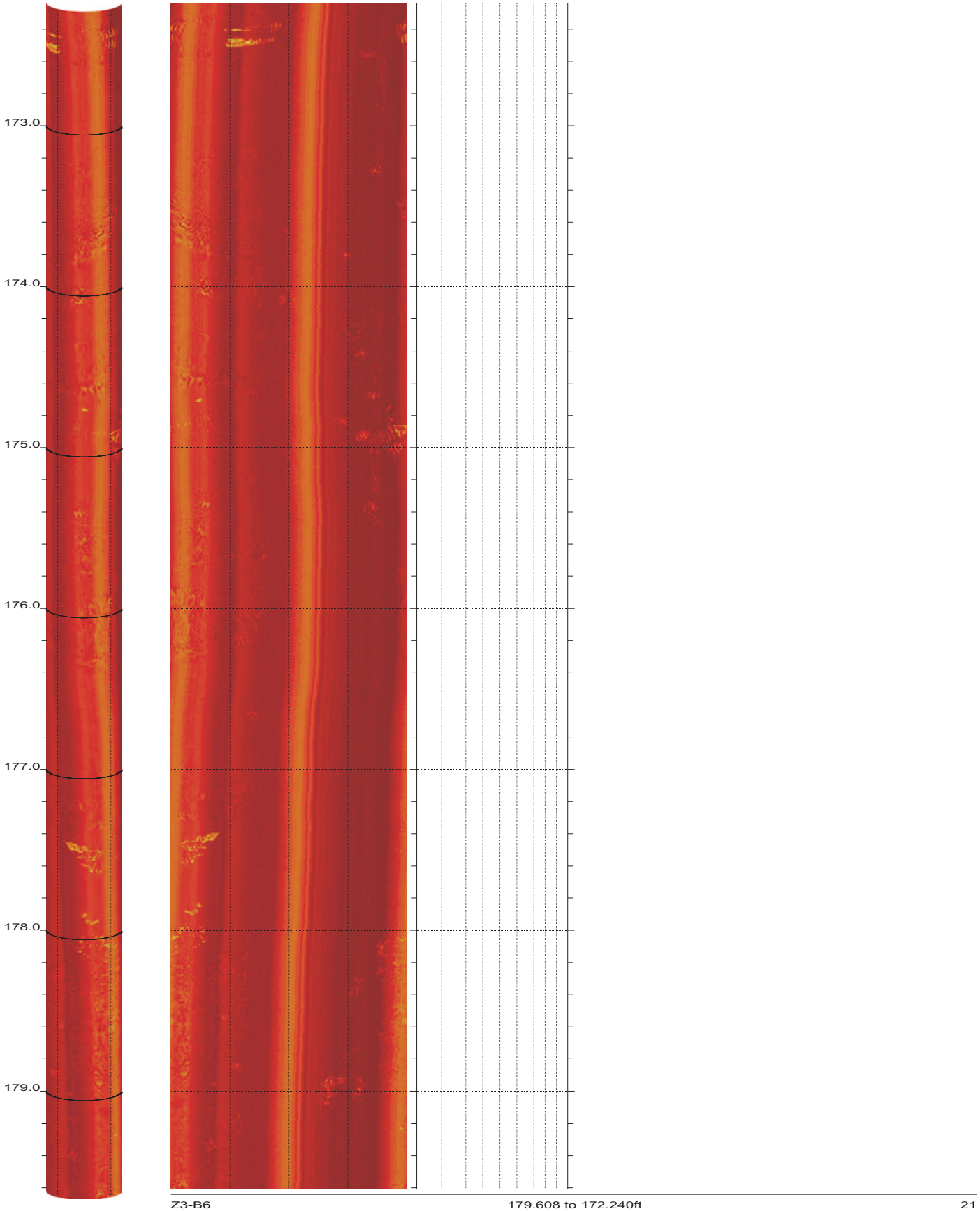

SR-710 Boring Z3-B6 Acoustic Televiewer Dips rev 1 Sheet 21 of 40

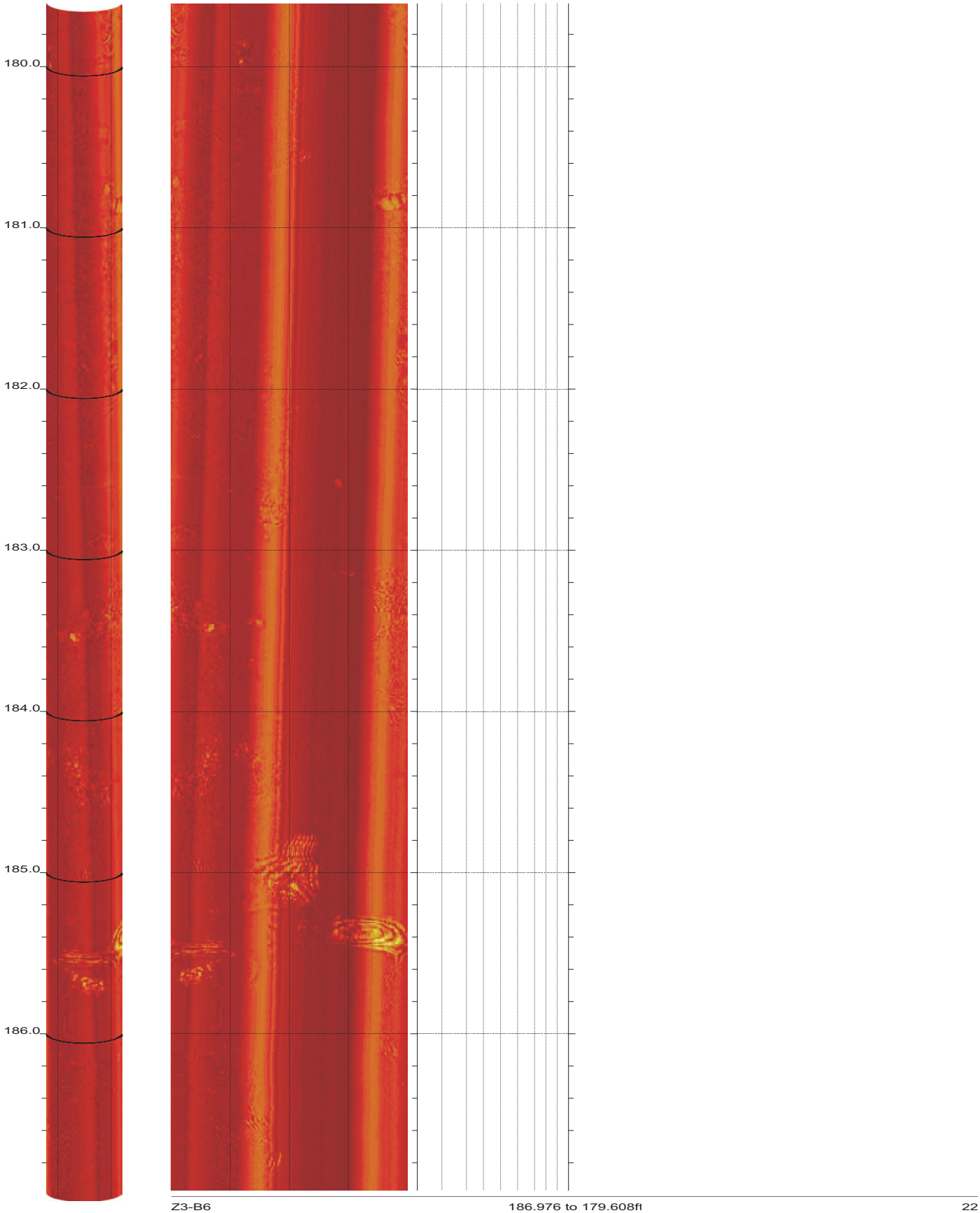
180.0
181.0
182.0
183.0
184.0
185.0
186.0
Z3-B6
186.976 to 179.608ft
22

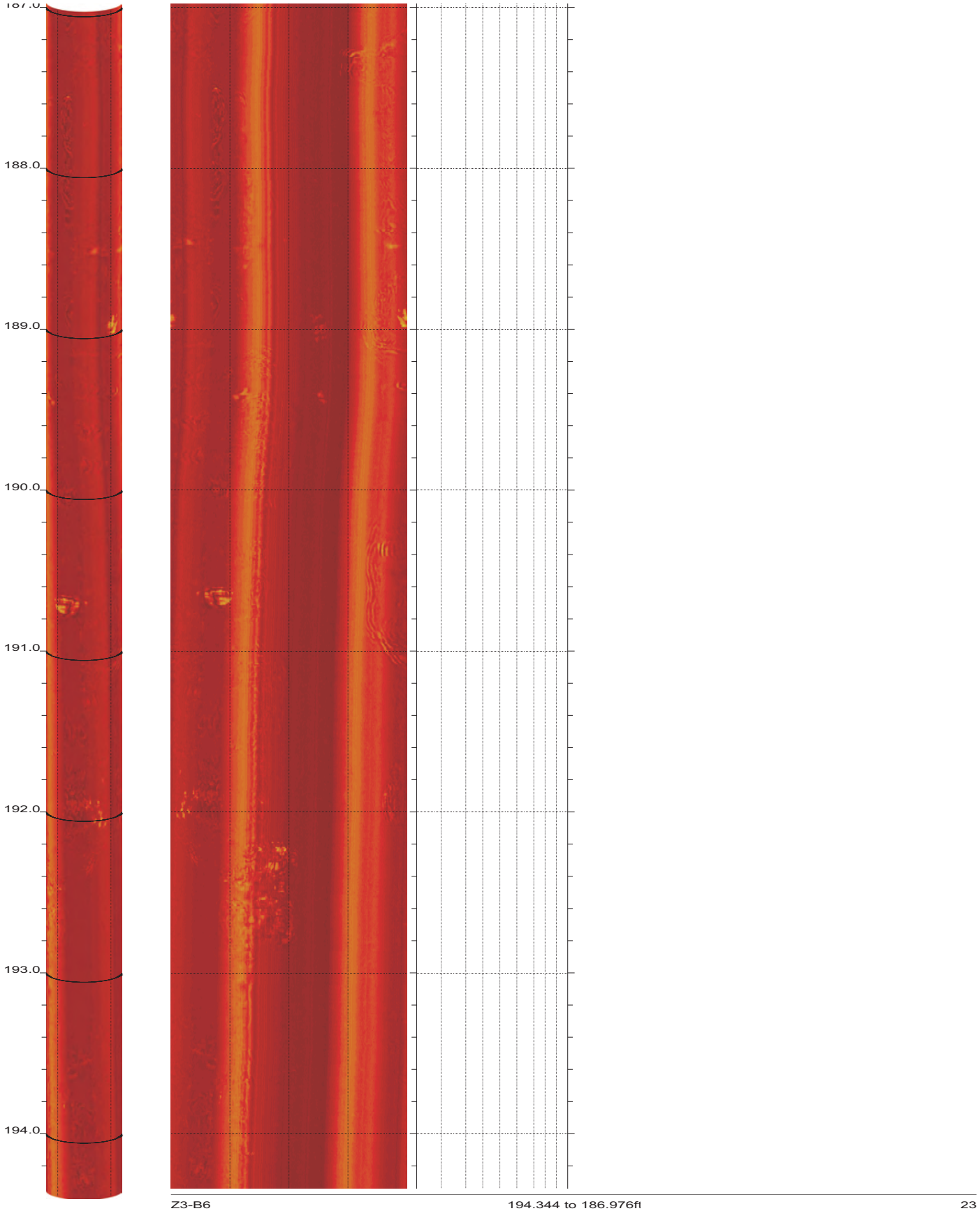
188.0
189.0
190.0
191.0
192.0
193.0
194.0
Z3-B6
194.344 to 186.976fl
23

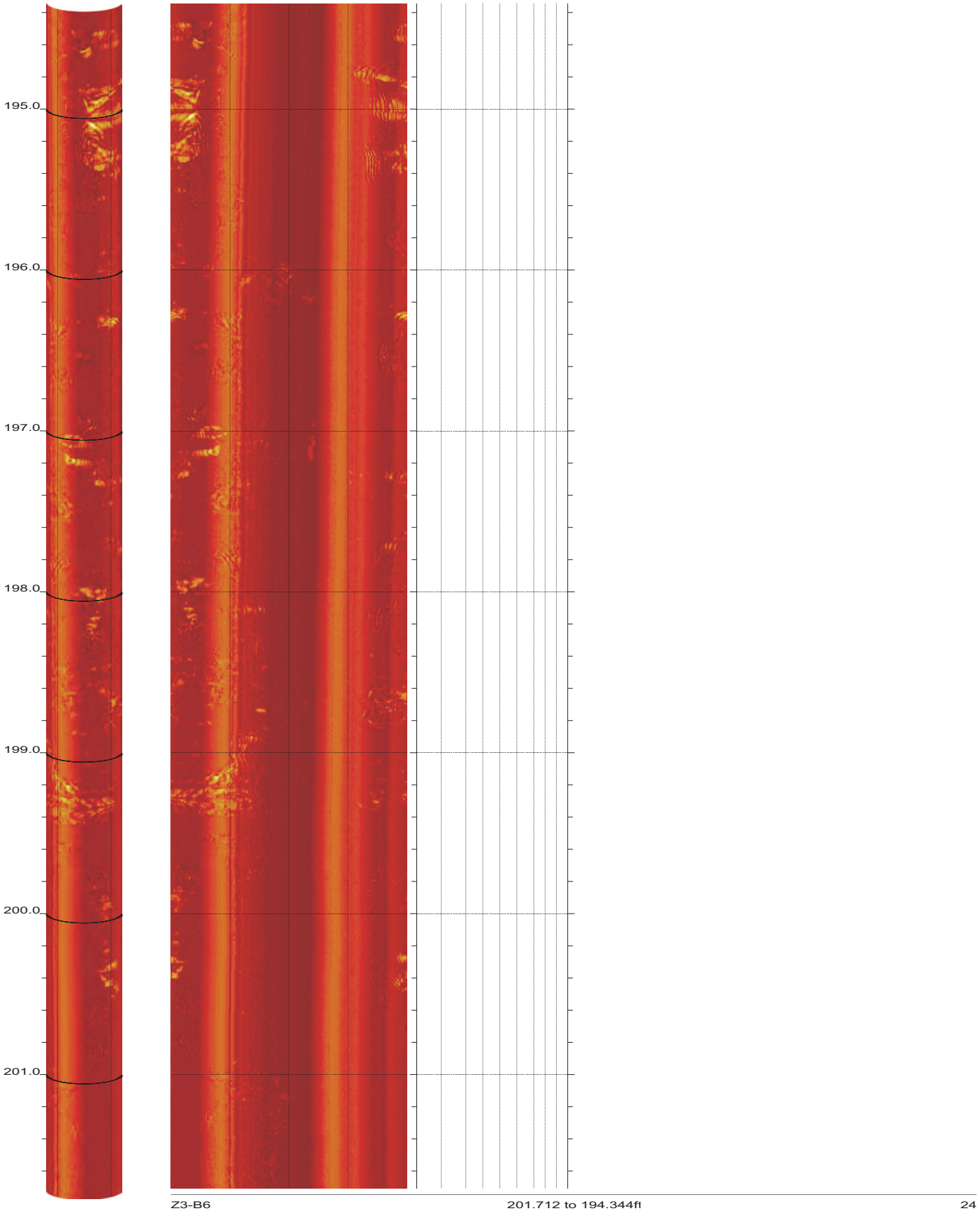

SR-710 Boring Z3-B6 Acoustic Televiewer Dips rev 1 Sheet 24 of 40

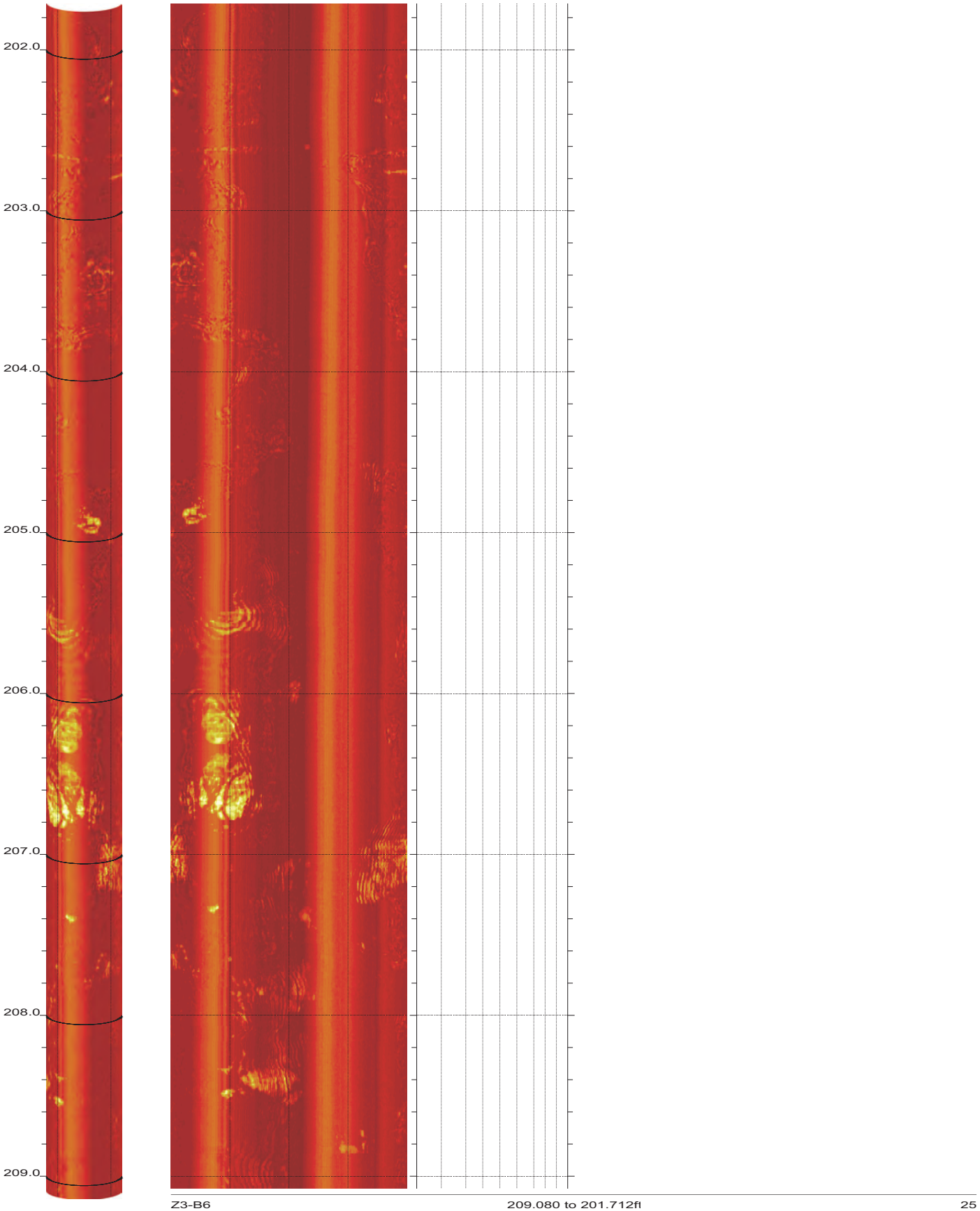
202.0
203.0
204.0
205.0
206.0
207.0
208.0
209.0
Z3-B6
209.080 to 201.712fl
25

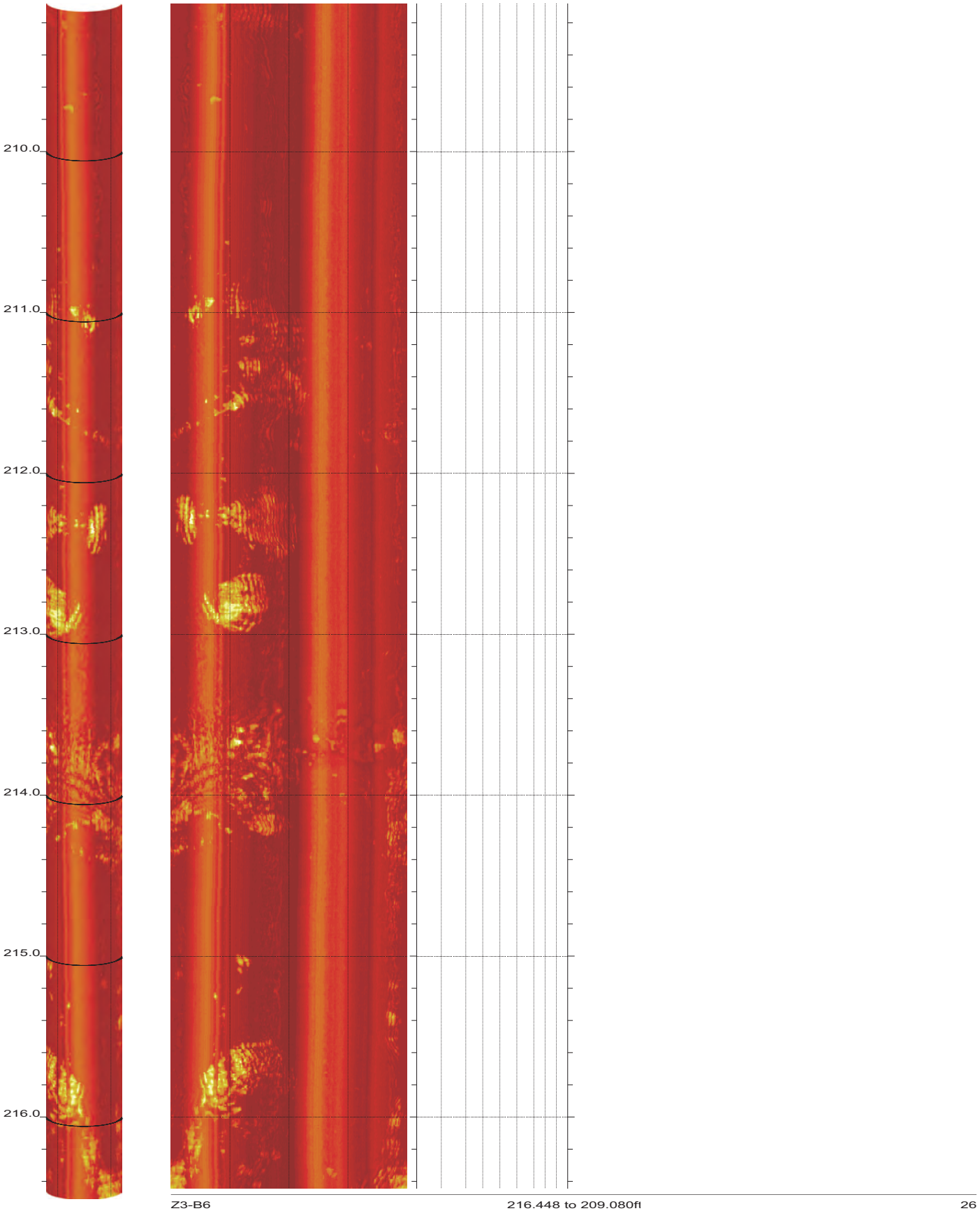
210.0
211.0
212.0
213.0
214.0
215.0
216.0
Z3-B6
216.448 to 209.080ft
26

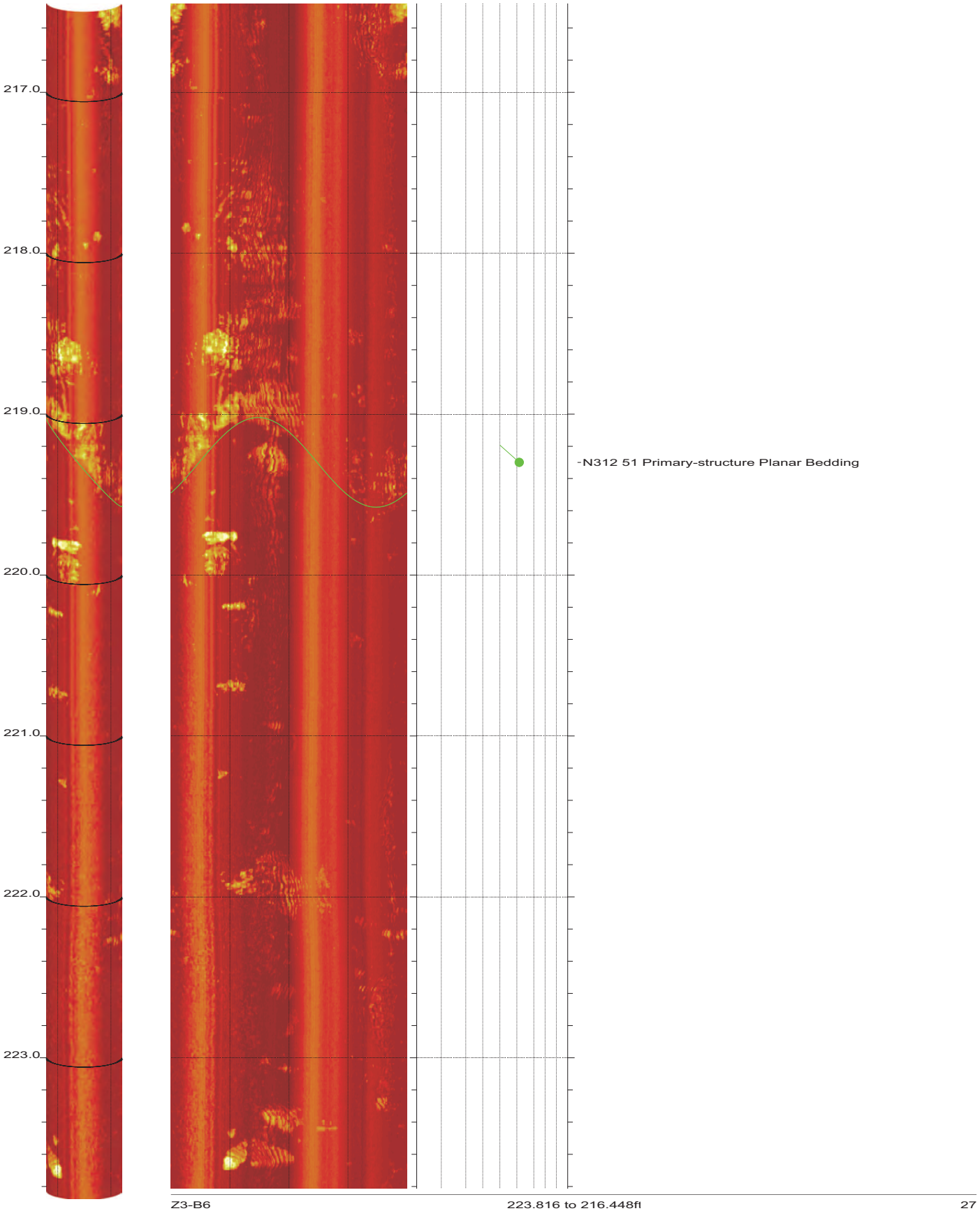

SR-710 Boring Z3-B6 Acoustic Televiewer Dips rev 1 Sheet 27 of 40

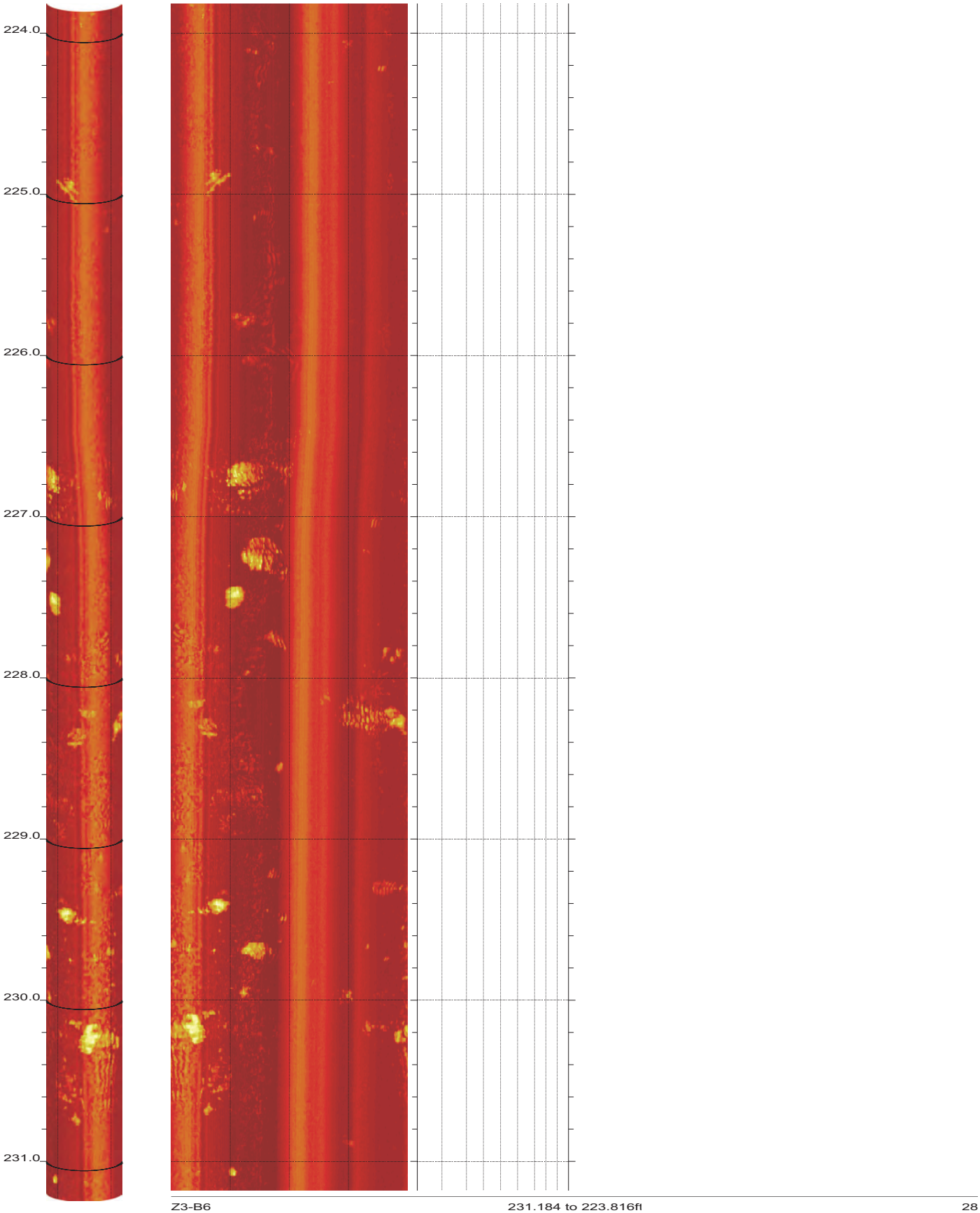

SR-710 Boring Z3-B6 Acoustic Televiewer Dips rev 1 Sheet 28 of 40

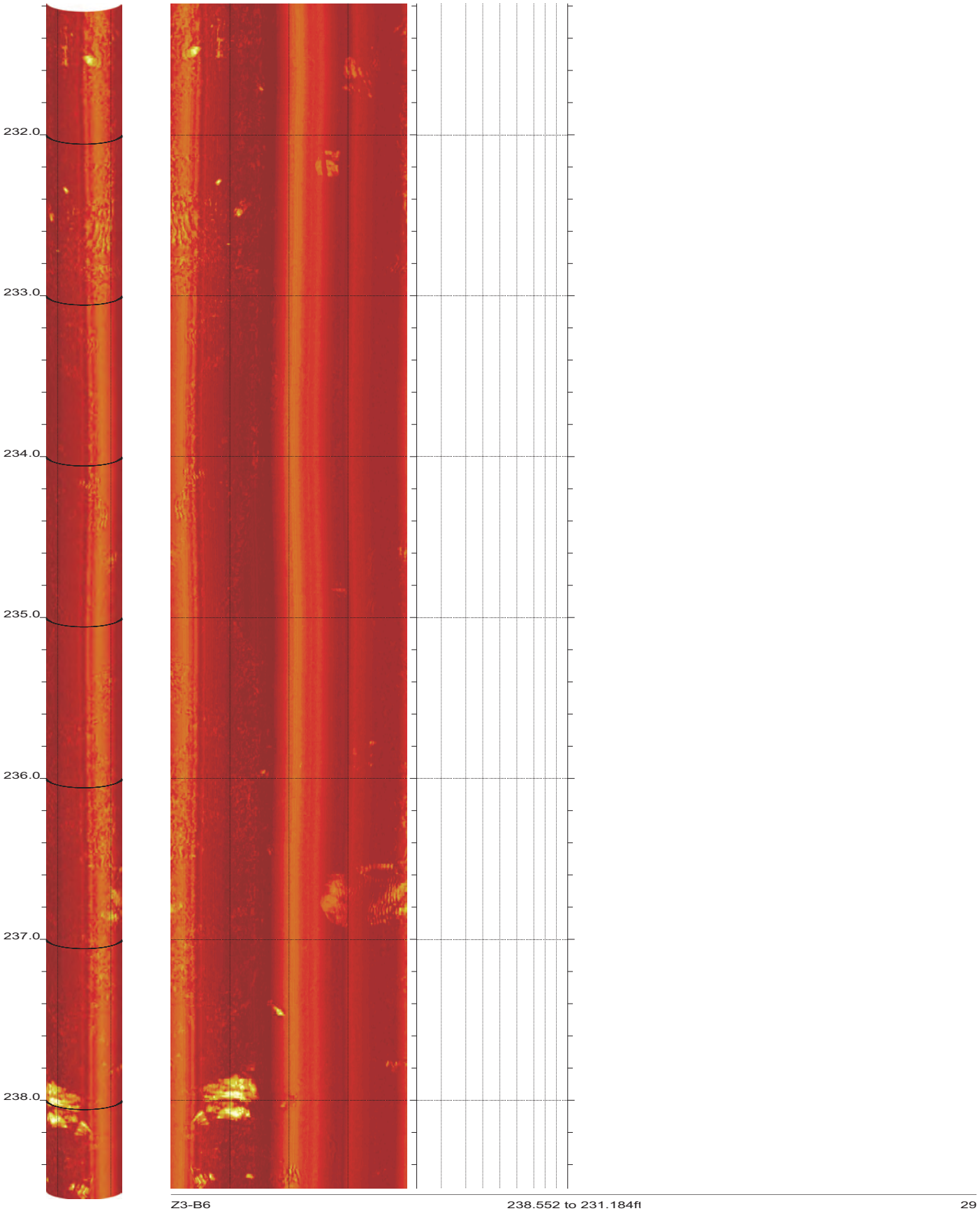

SR-710 Boring Z3-B6 Acoustic Televiewer Dips rev 1 Sheet 29 of 40

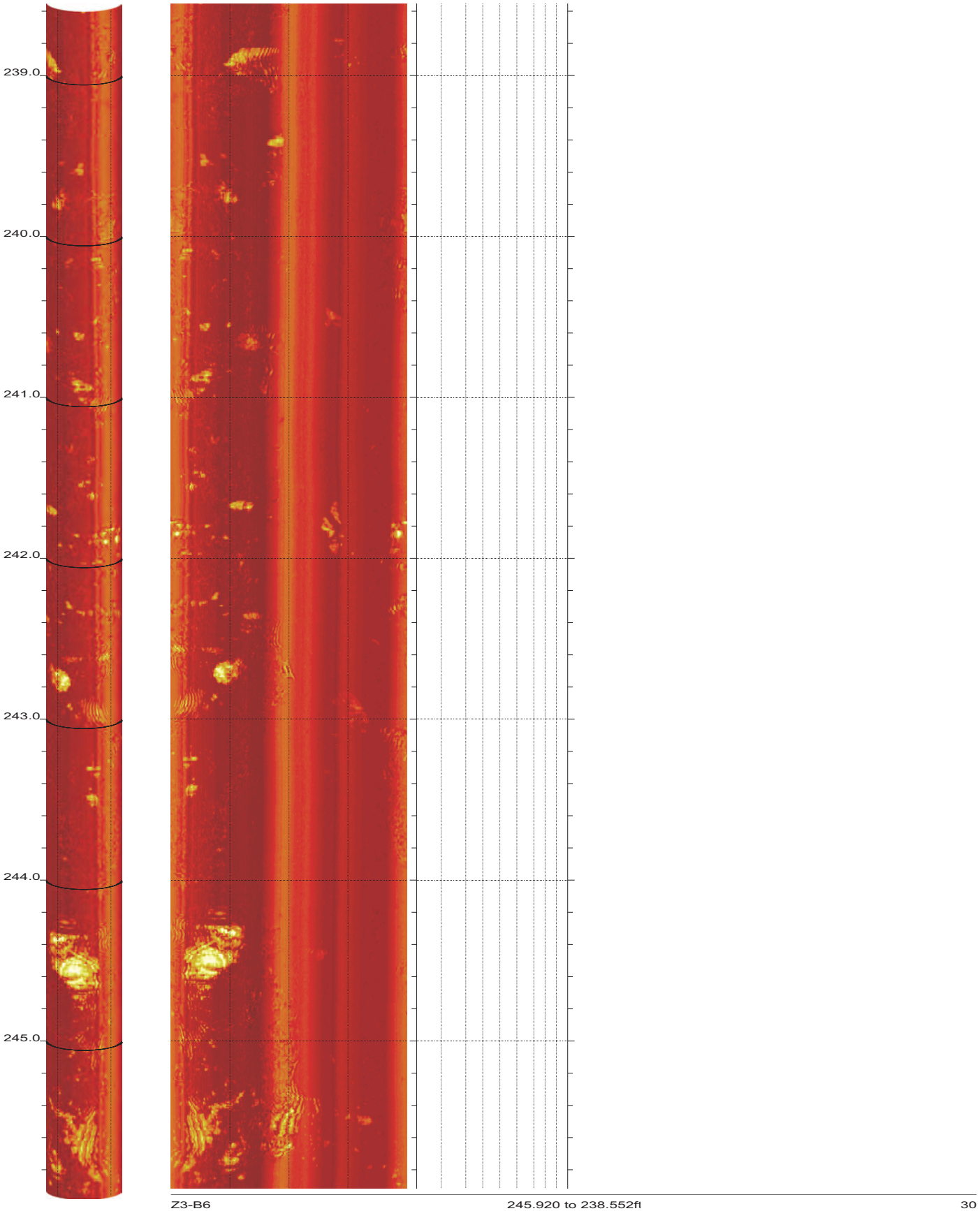

SR-710 Boring Z3-B6 Acoustic Televiewer Dips rev 1 Sheet 30 of 40

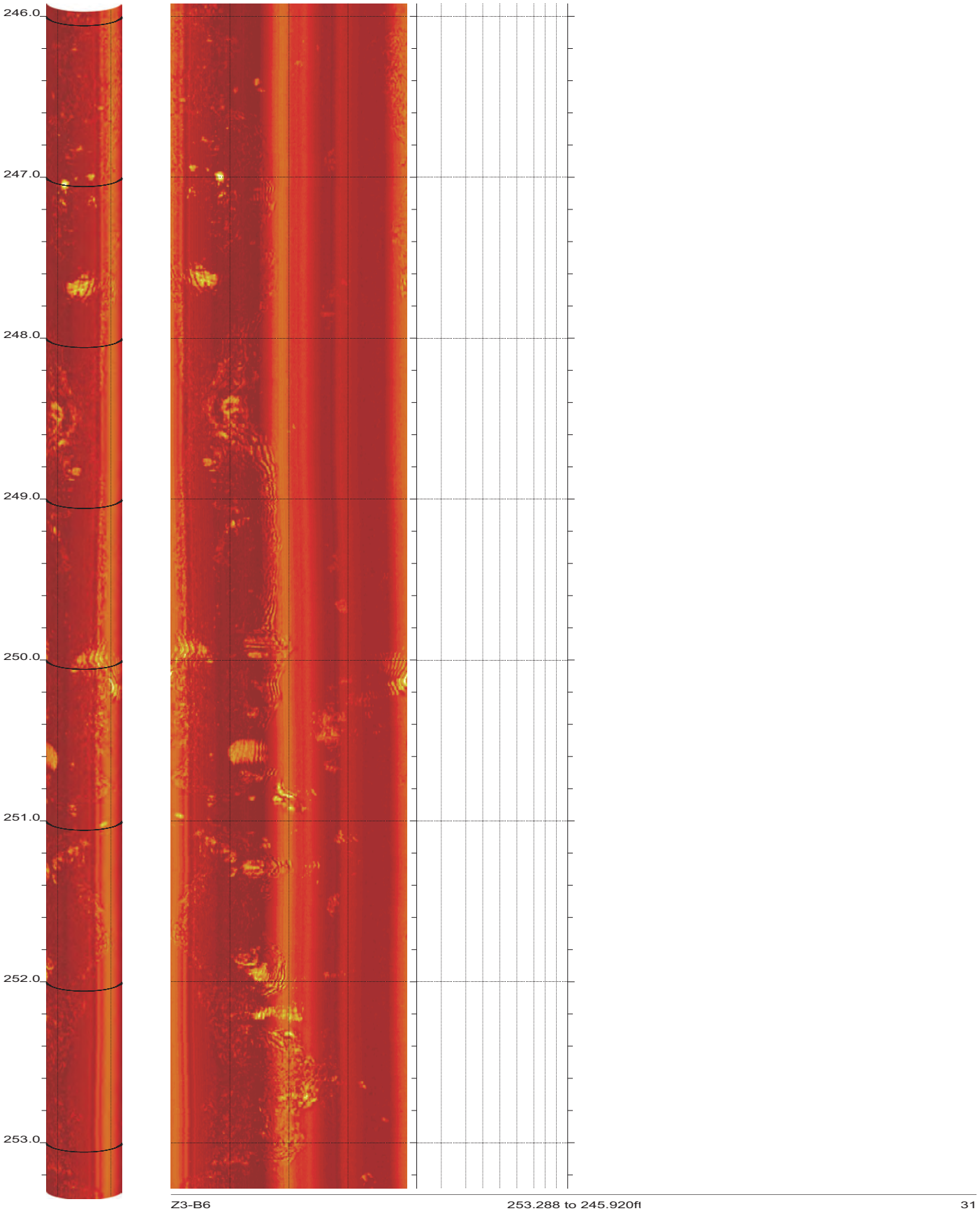

SR-710 Boring Z3-B6 Acoustic Televiewer Dips rev 1 Sheet 31 of 40

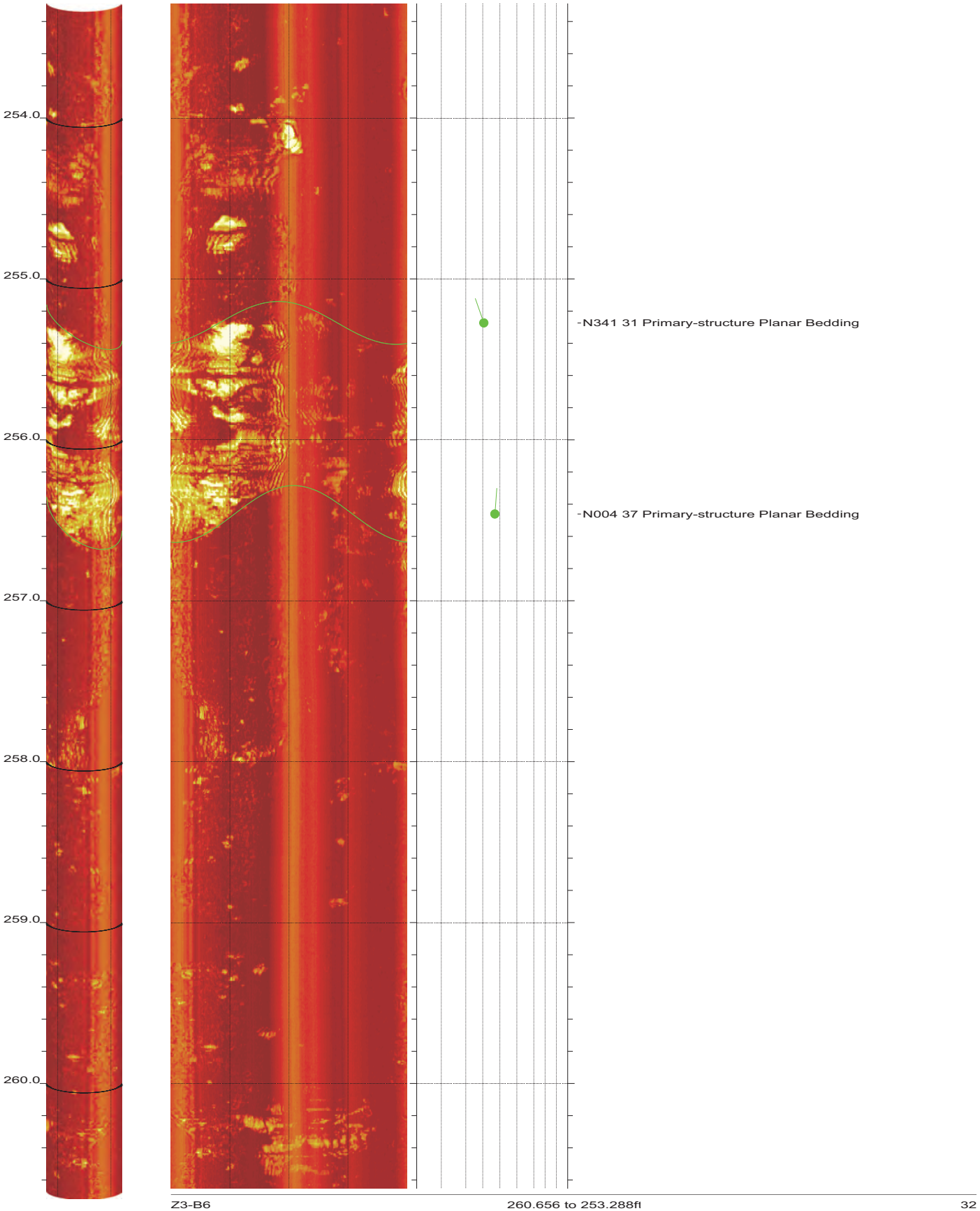

SR-710 Boring Z3-B6 Acoustic Televiewer Dips rev 1 Sheet 32 of 40

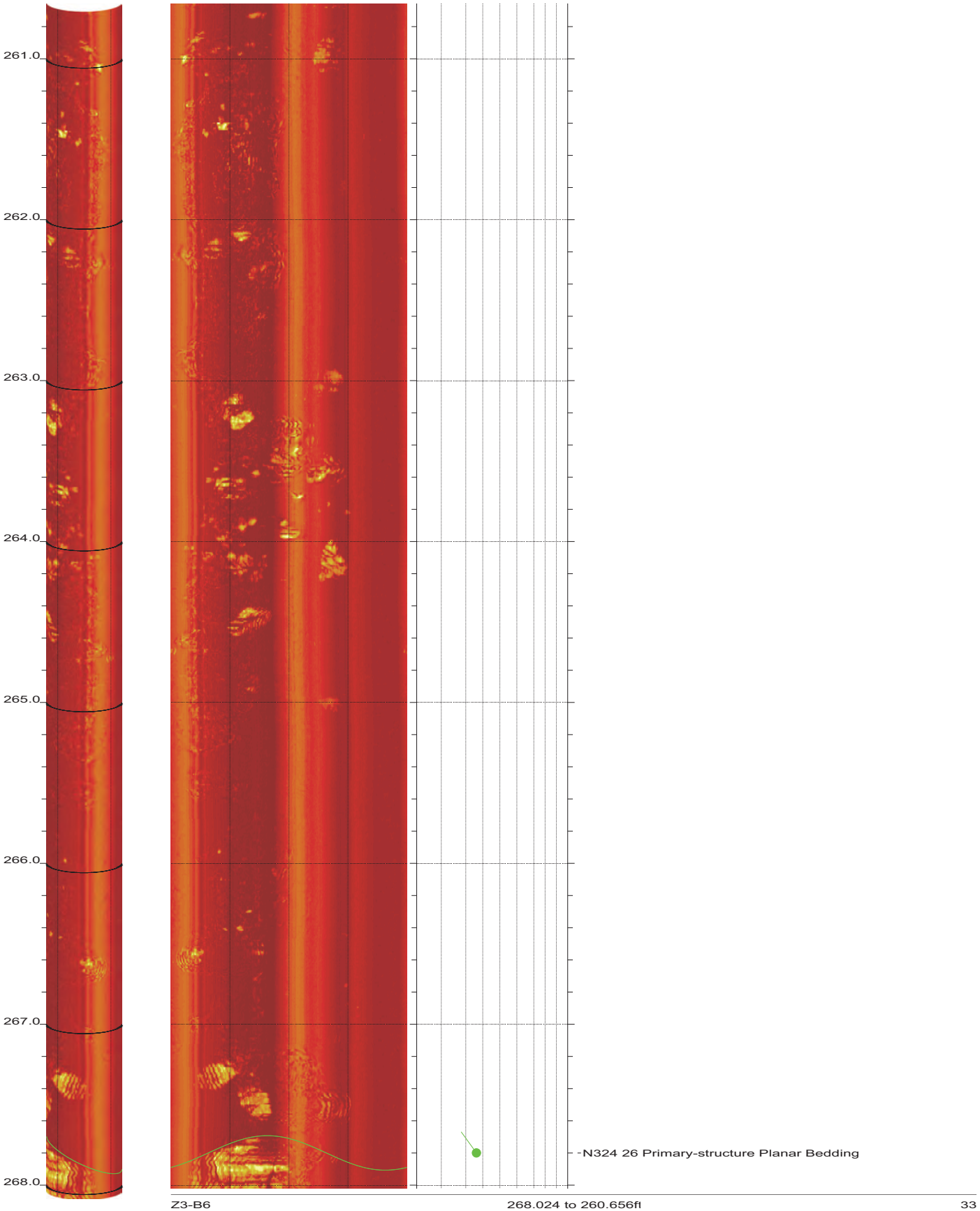

SR-710 Boring Z3-B6 Acoustic Televiewer Dips rev 1 Sheet 33 of 40

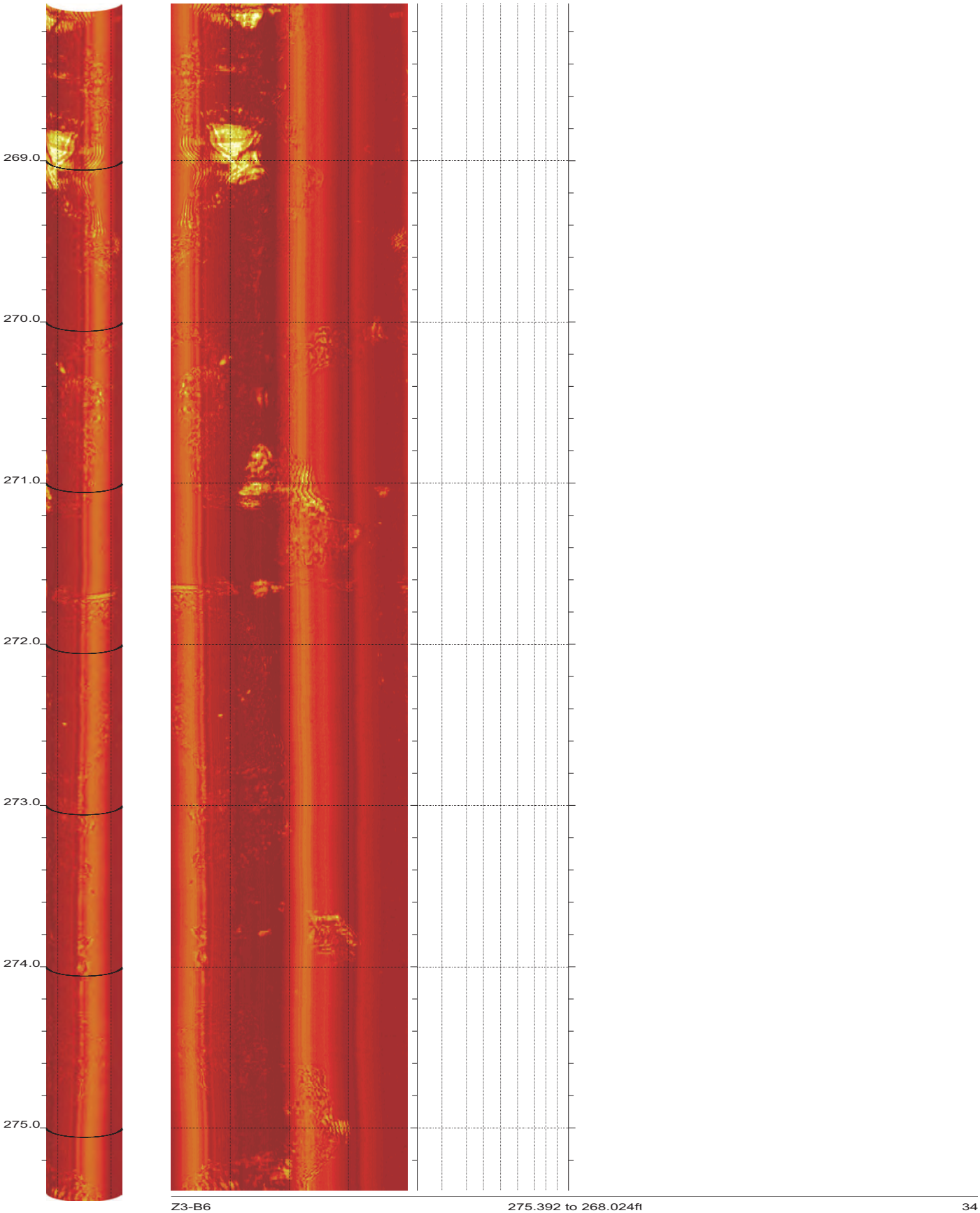

SR-710 Boring Z3-B6 Acoustic Televiewer Dips rev 1 Sheet 34 of 40

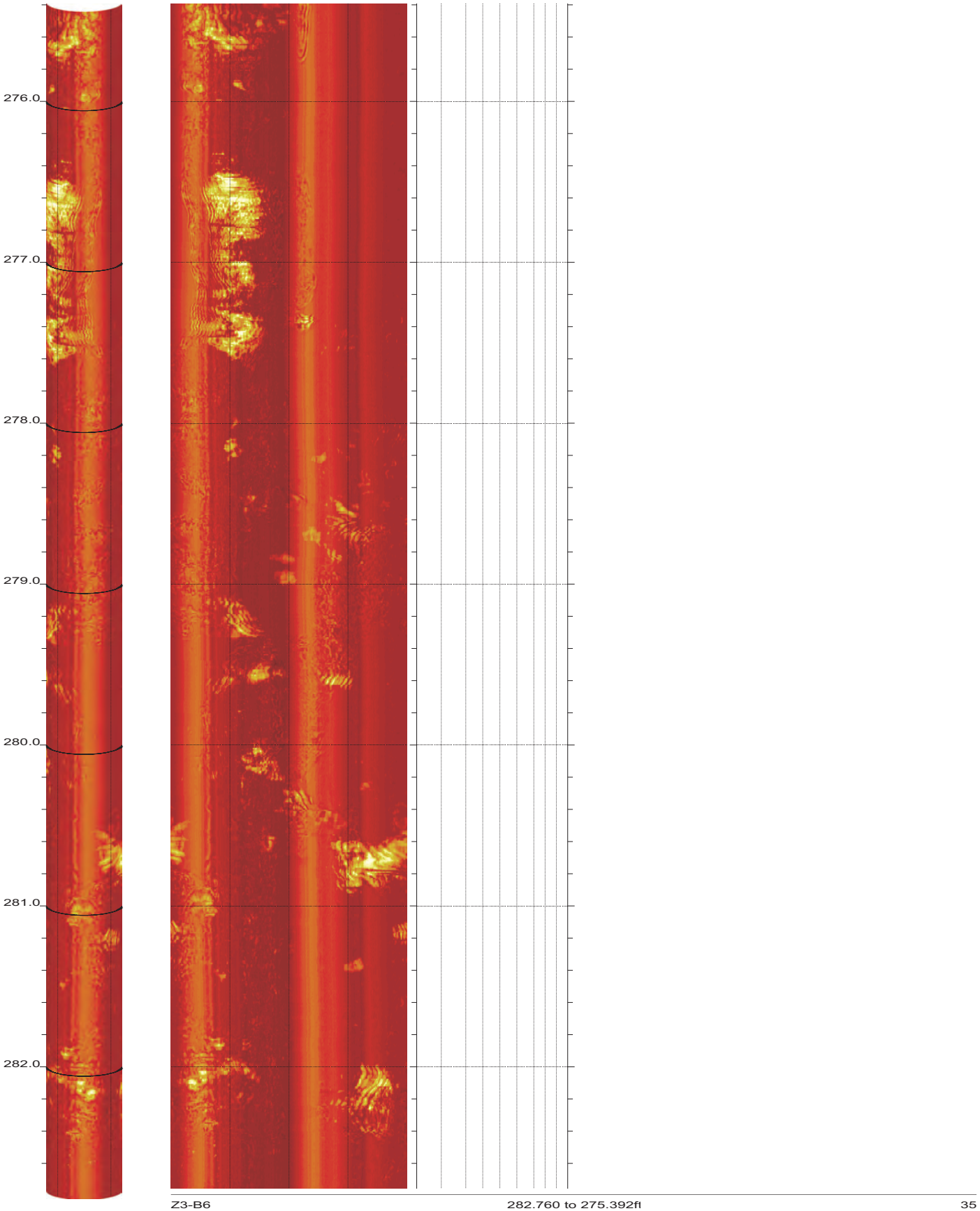

SR-710 Boring Z3-B6 Acoustic Televiewer Dips rev 1 Sheet 35 of 40

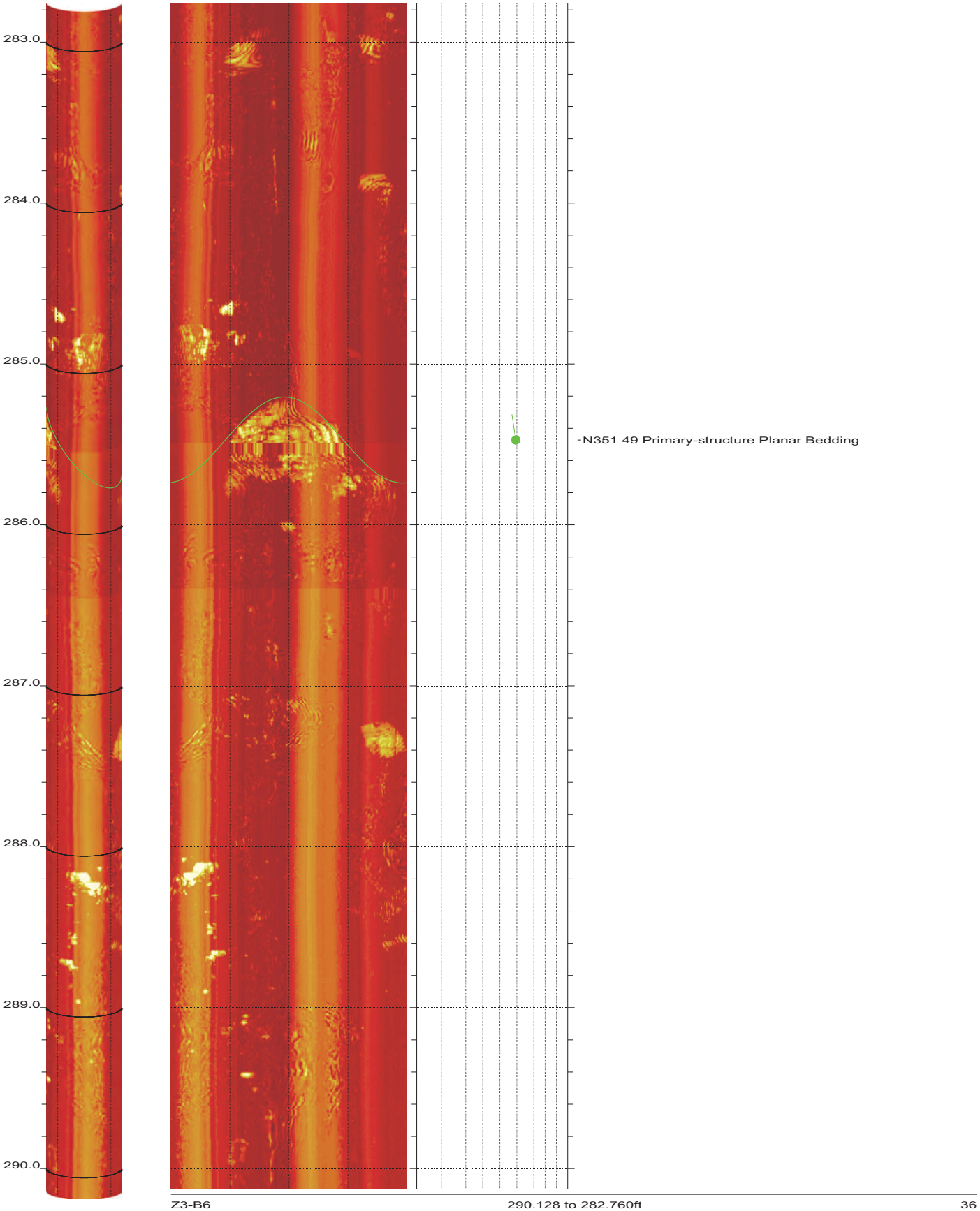

SR-710 Boring Z3-B6 Acoustic Televiewer Dips rev 1 Sheet 36 of 40

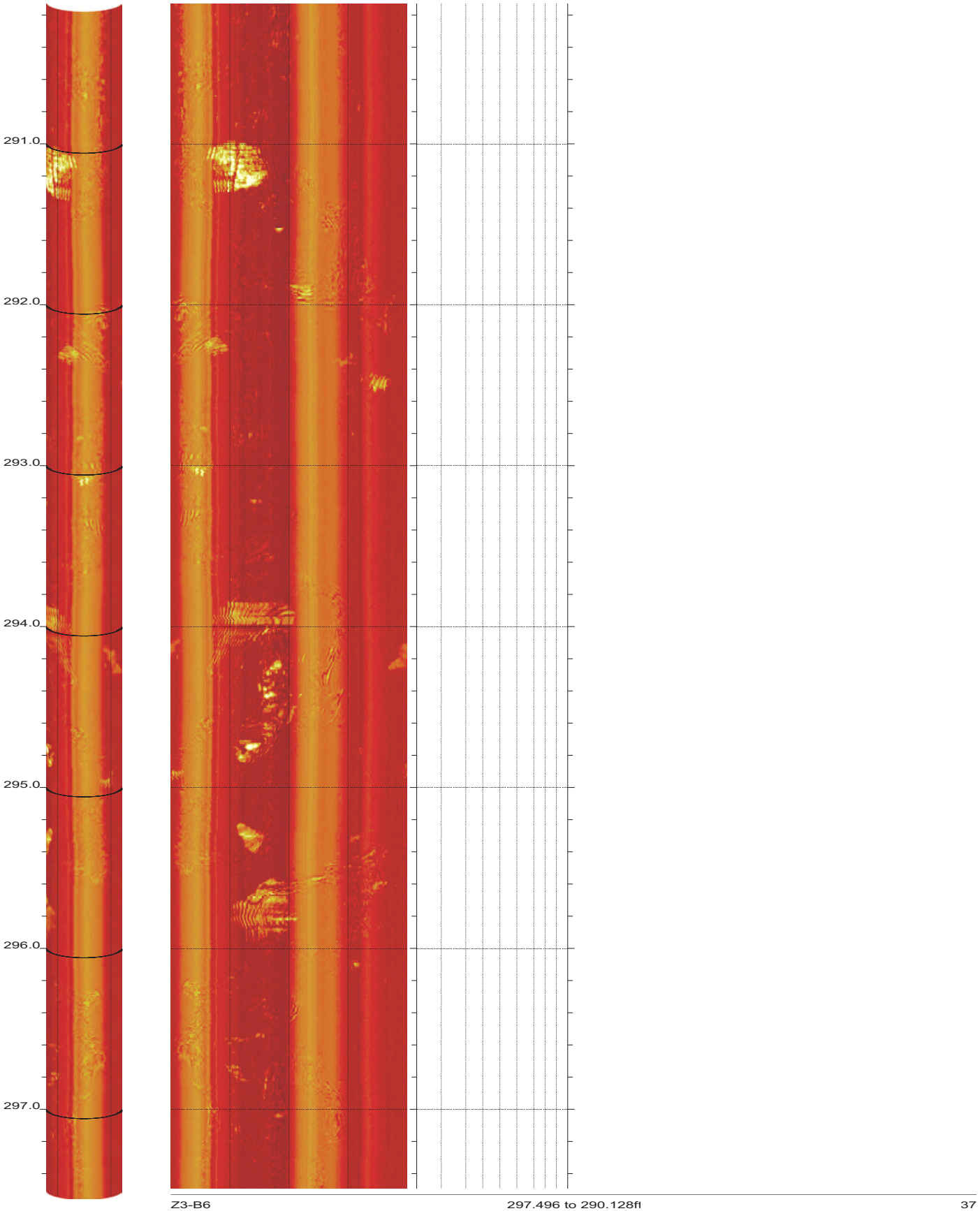

SR-710 Boring Z3-B6 Acoustic Televiewer Dips rev 1 Sheet 37 of 40

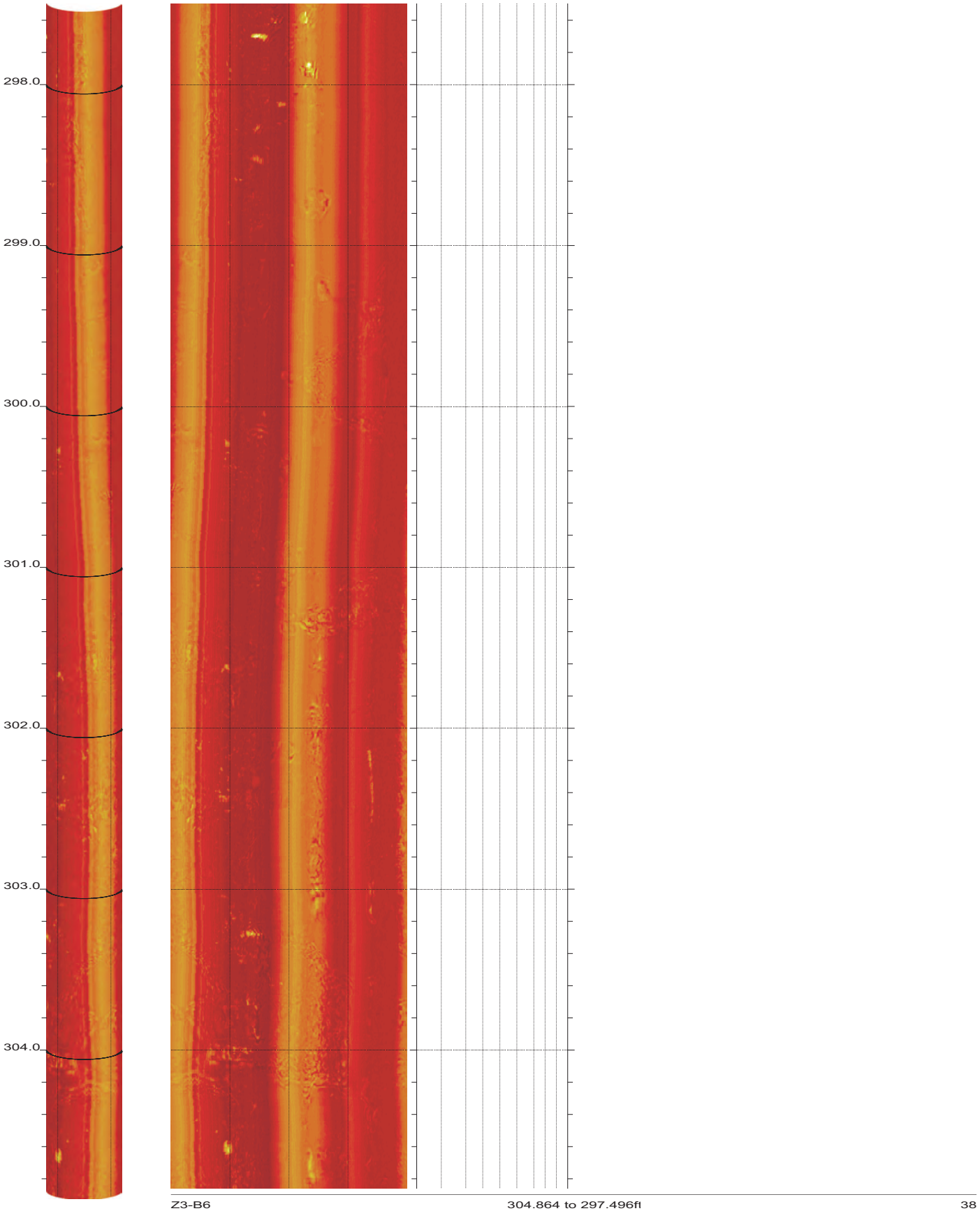
298.0
299.0
300.0
301.0
302.0
303.0
304.0
Z3-B6
304.864 to 297.496fl
38

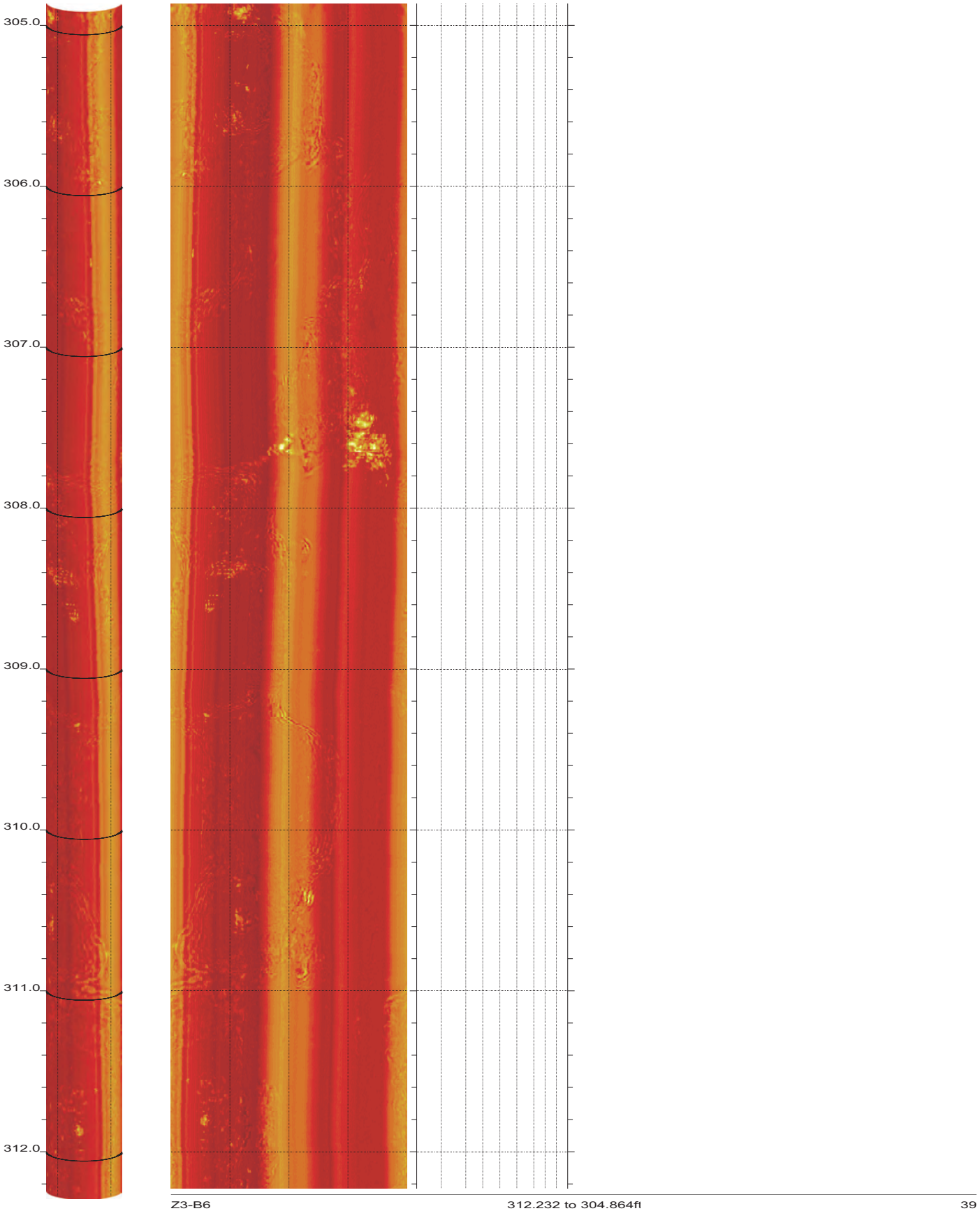

SR-710 Boring Z3-B6 Acoustic Televiewer Dips rev 1 Sheet 39 of 40

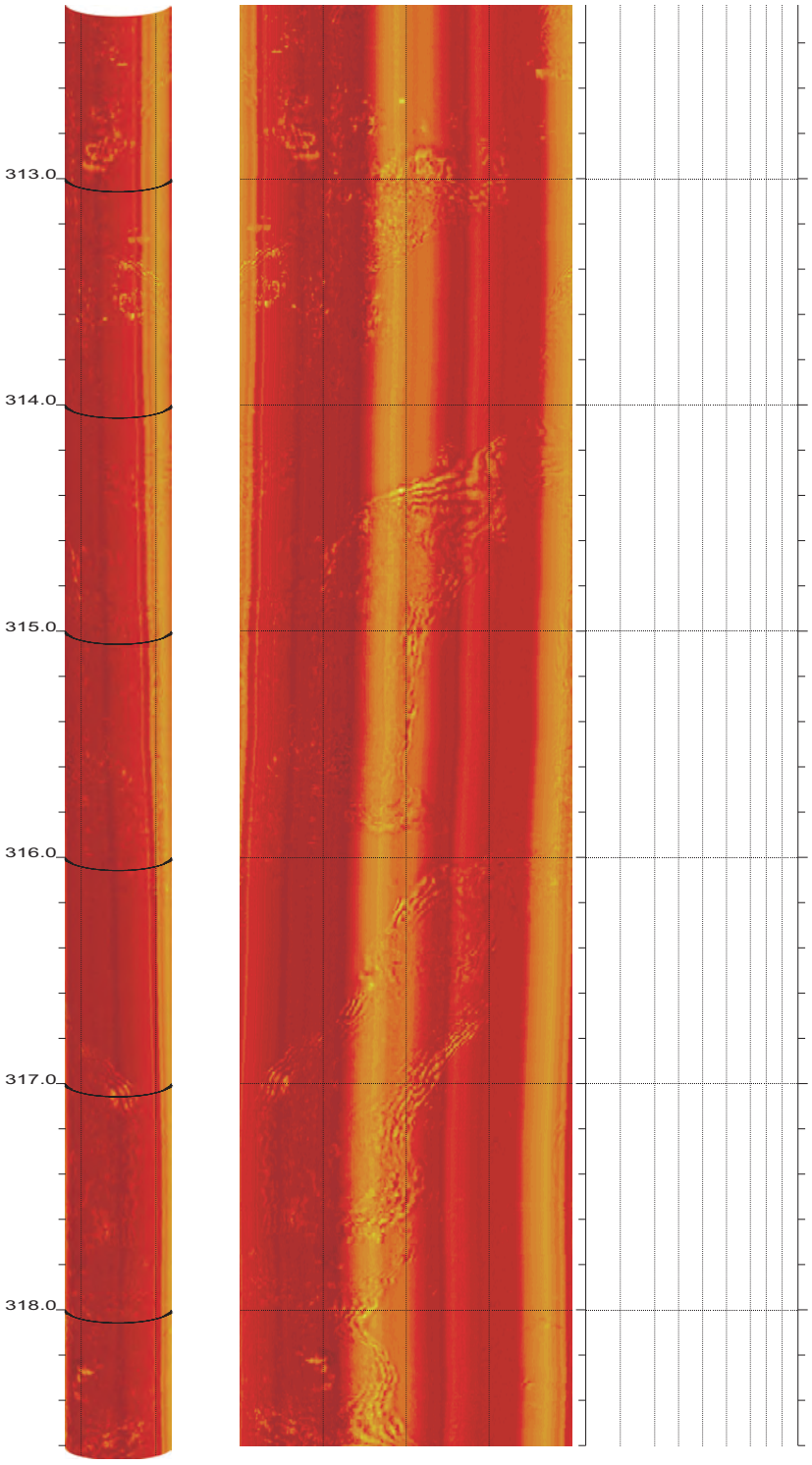

Z3-B6 318.600 to 312.232fl 40

SR-710 Boring Z3-B6 Acoustic Televiewer Dips rev 1 Sheet 40 of 40

BHTV DATA PROCESSING
RGLDIP vsn 6.2
INTERPRETED BHTV DIPS LOG

CASCADE DRILLING

Borehole: Z3-B12

SR-710 TUNNEL INVESTIGATION

top of borehole.....
East: _
North: _
Elev: _

North ref. is true
Depth units are feet
Vertical scale: 1/10
Horiz scale = 1.00x Vert scale

Zone from 182.400 to 57.000ft
Format: BHTV-NESWN

Borehole diam: 7.000inch
Vertical = borehole-axis
Image: Amplitude

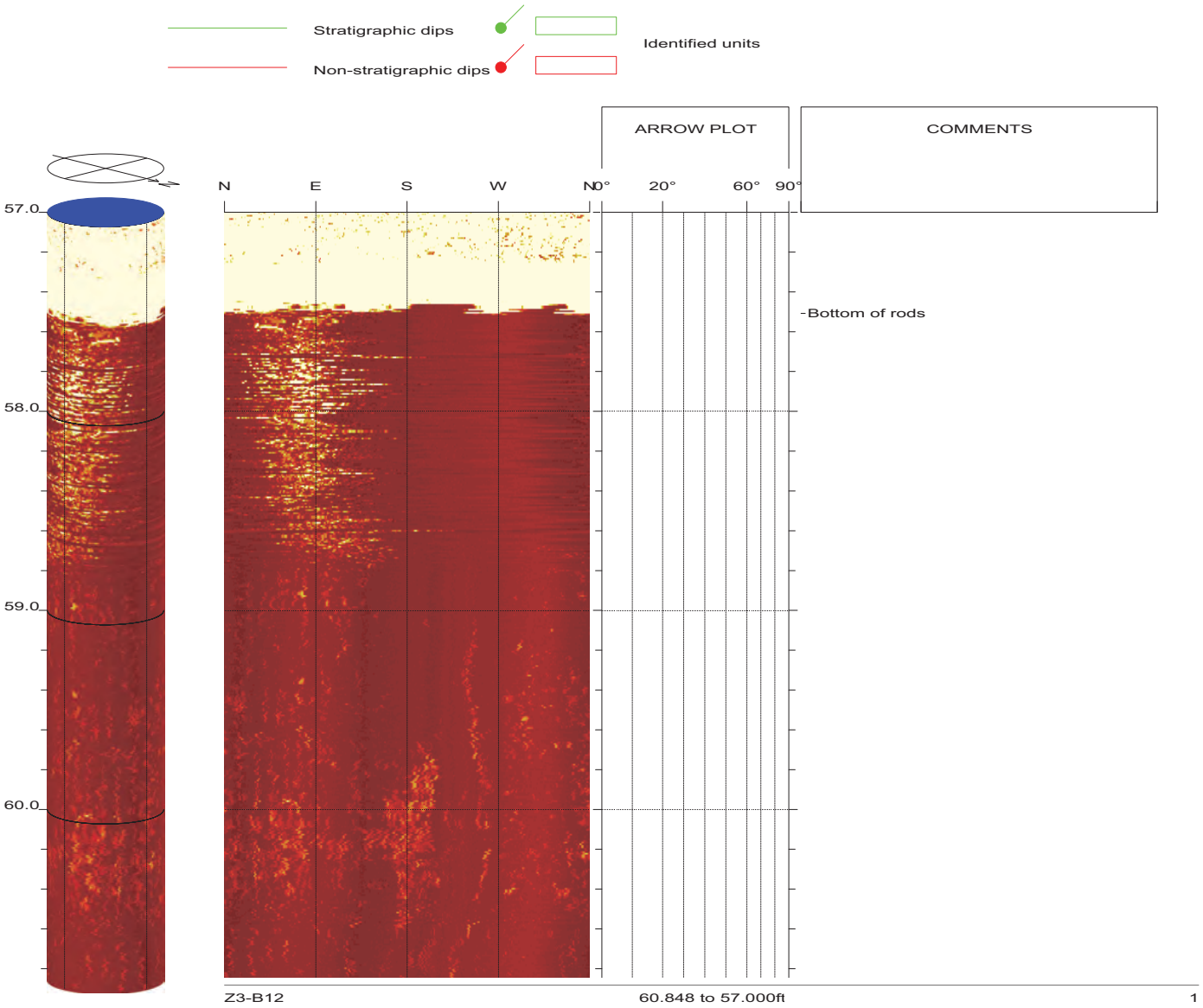

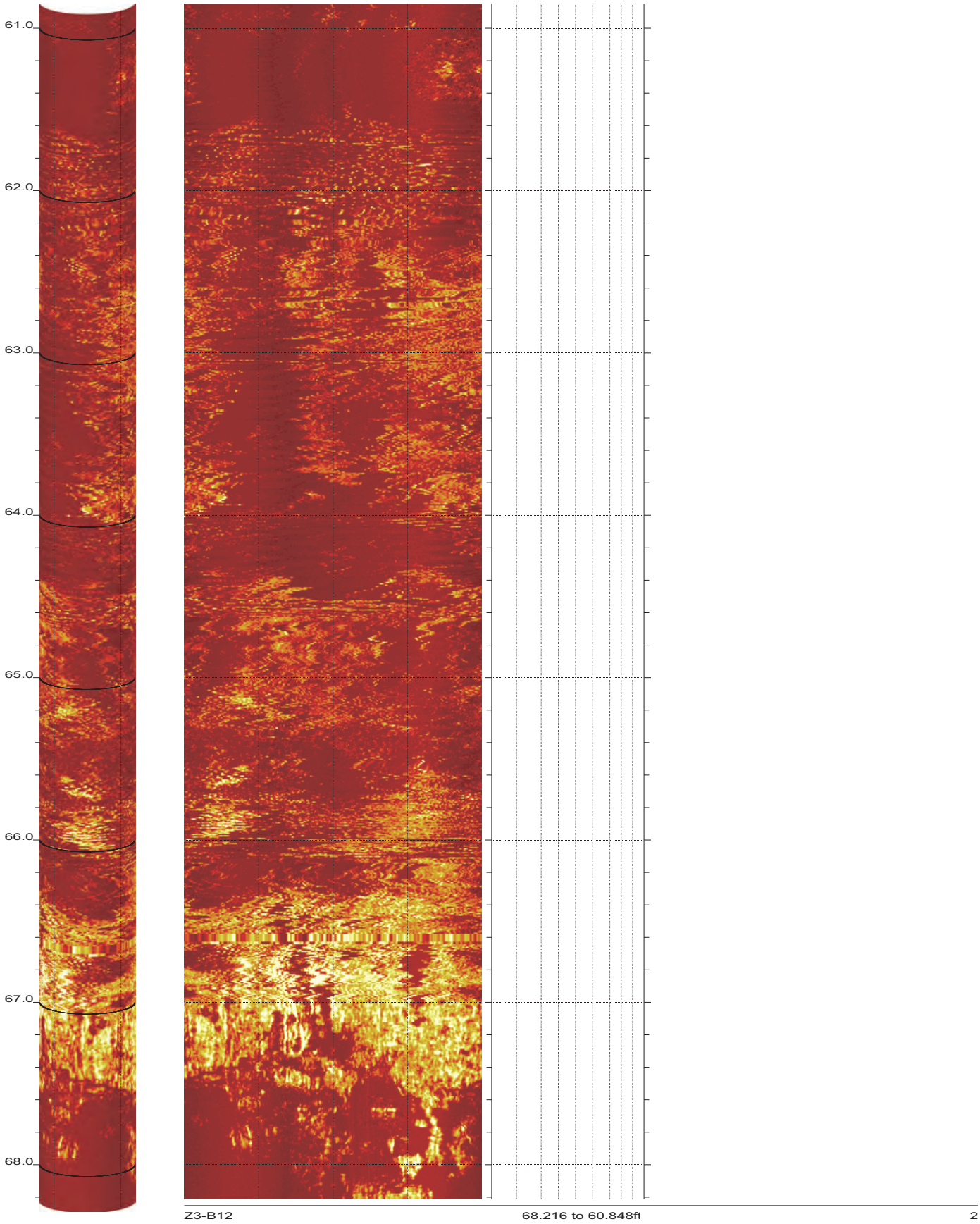
61.0
62.0
63.0
64.0
65.0
66.0
67.0
68.0
Z3-B12
68.216 to 60.848ft
2

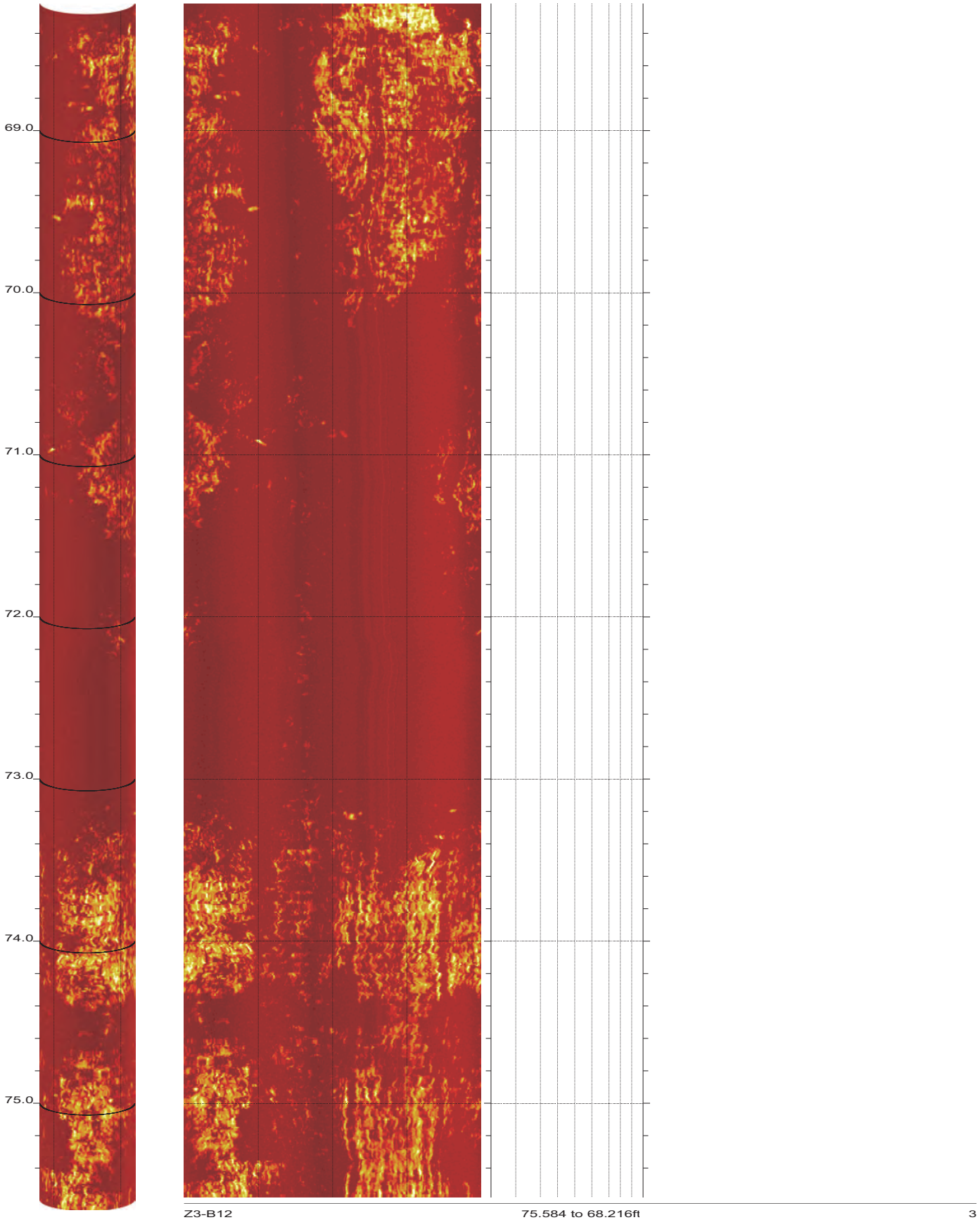

SR-710 Boring Z3-B12 Acoustic Televiewer Dips rev 1 Sheet 3 of 18

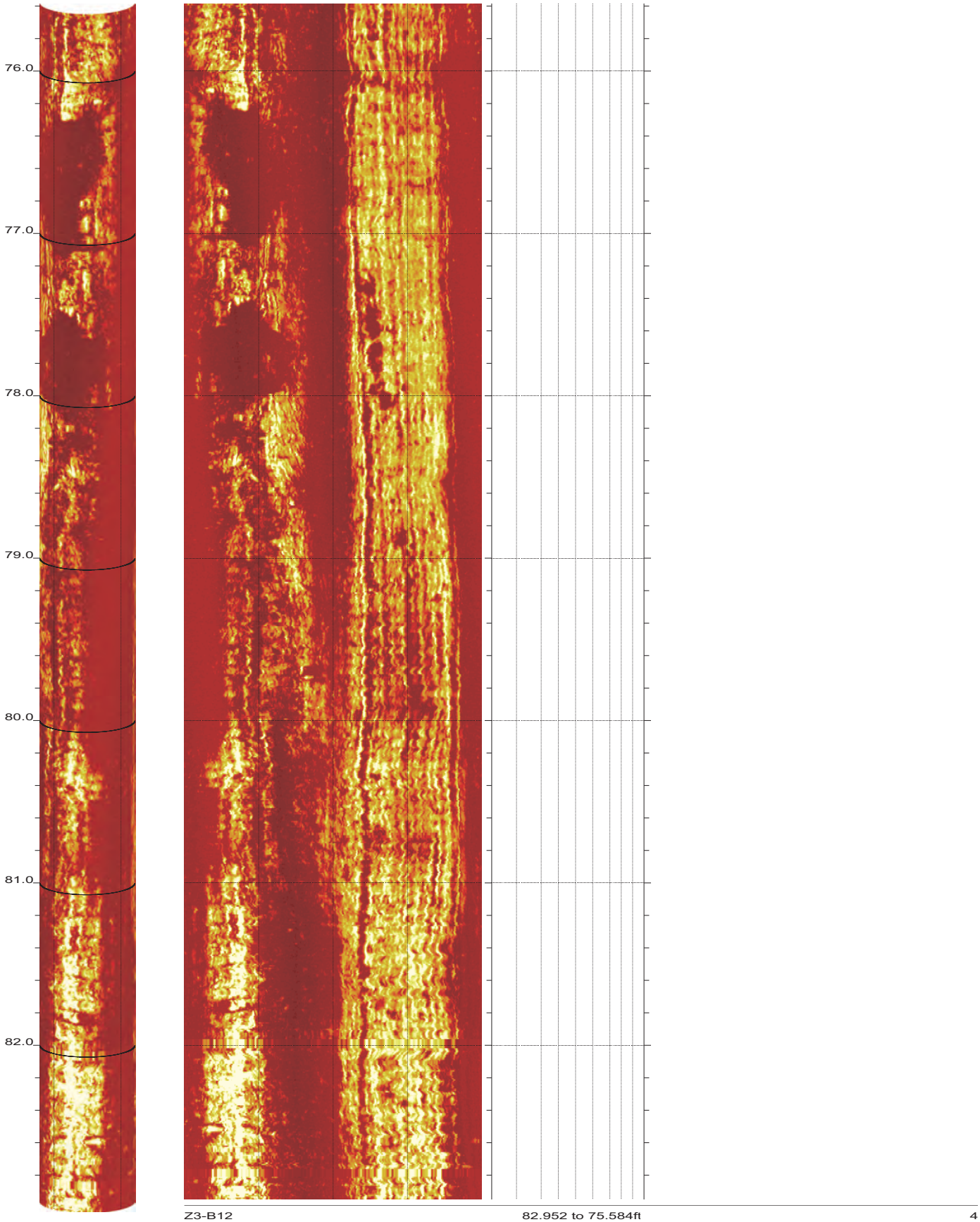

SR-710 Boring Z3-B12 Acoustic Televiewer Dips rev 1 Sheet 4 of 18

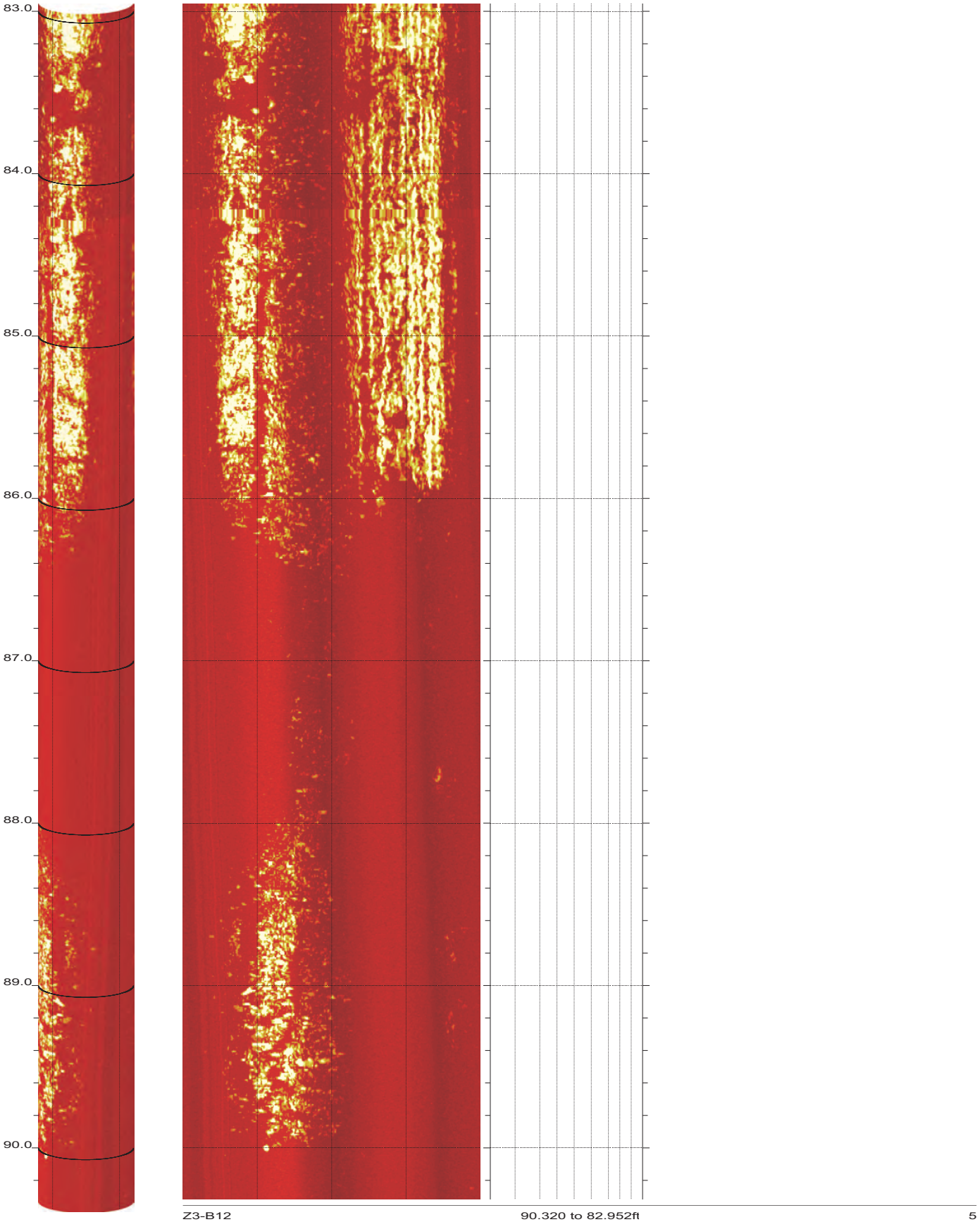

SR-710 Boring Z3-B12 Acoustic Televiewer Dips rev 1 Sheet 5 of 18

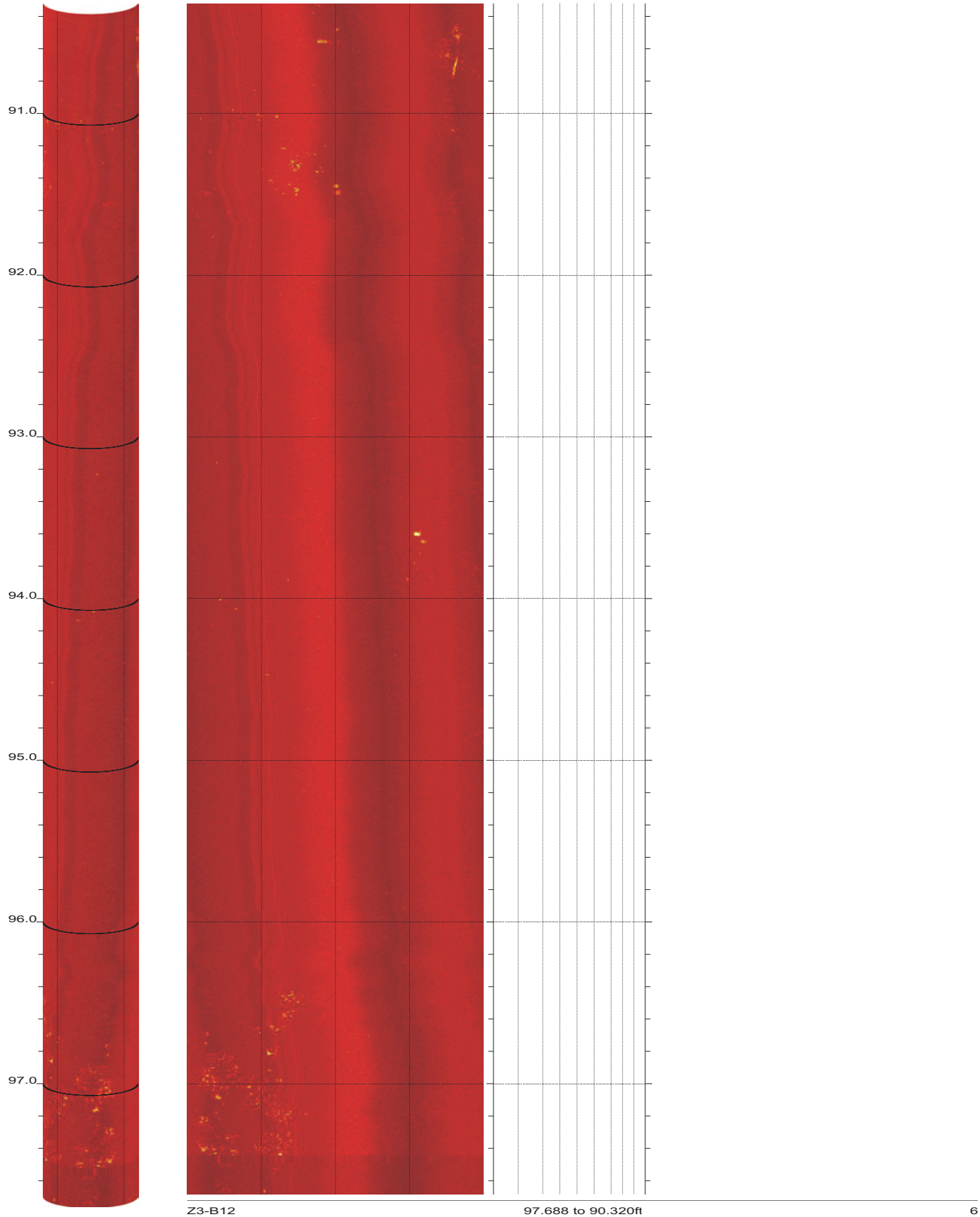
91.0
92.0
93.0
94.0
95.0
96.0
97.0
Z3-B12
97.688 to 90.320ft
6

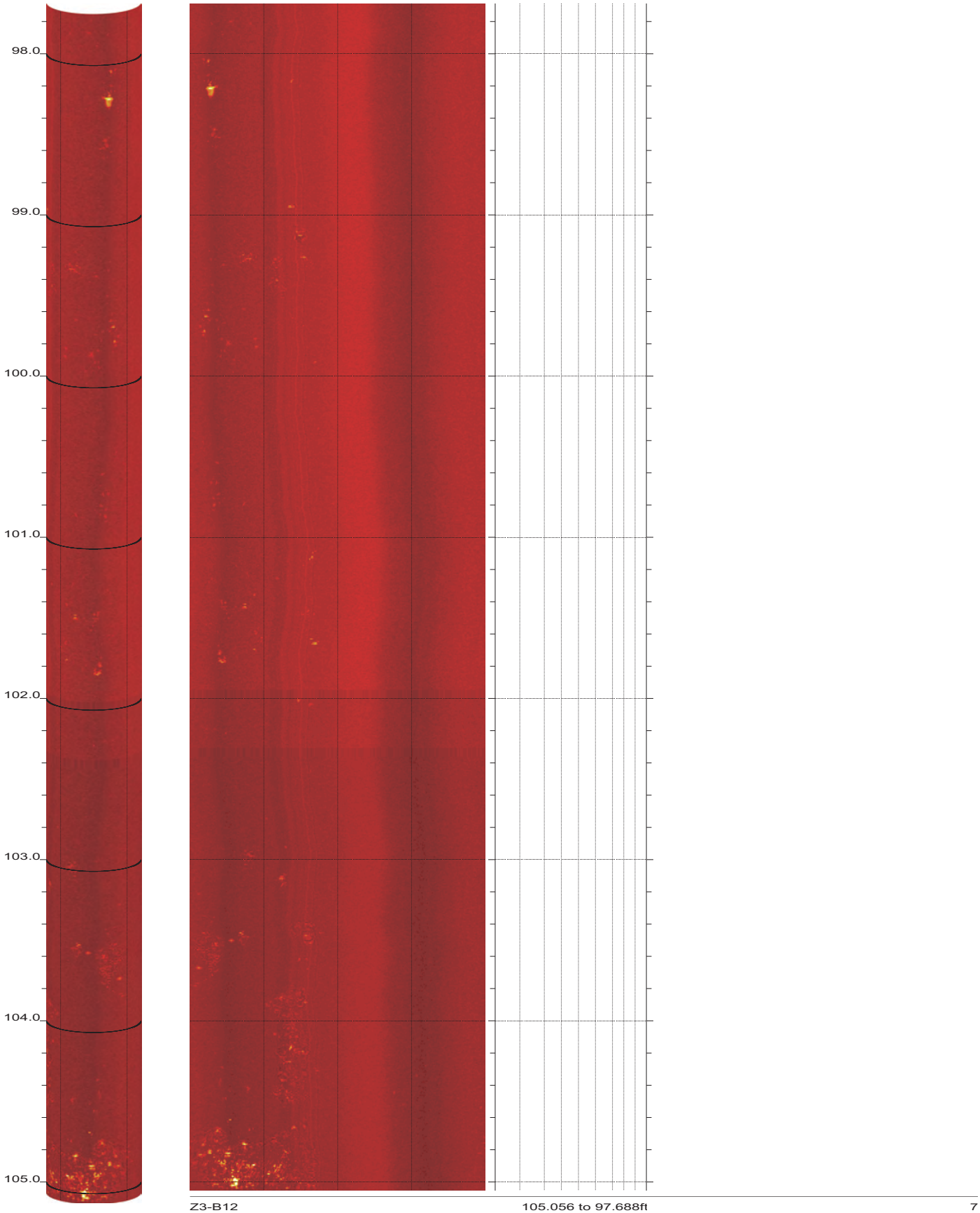

SR-710 Boring Z3-B12 Acoustic Televiewer Dips rev 1 Sheet 7 of 18

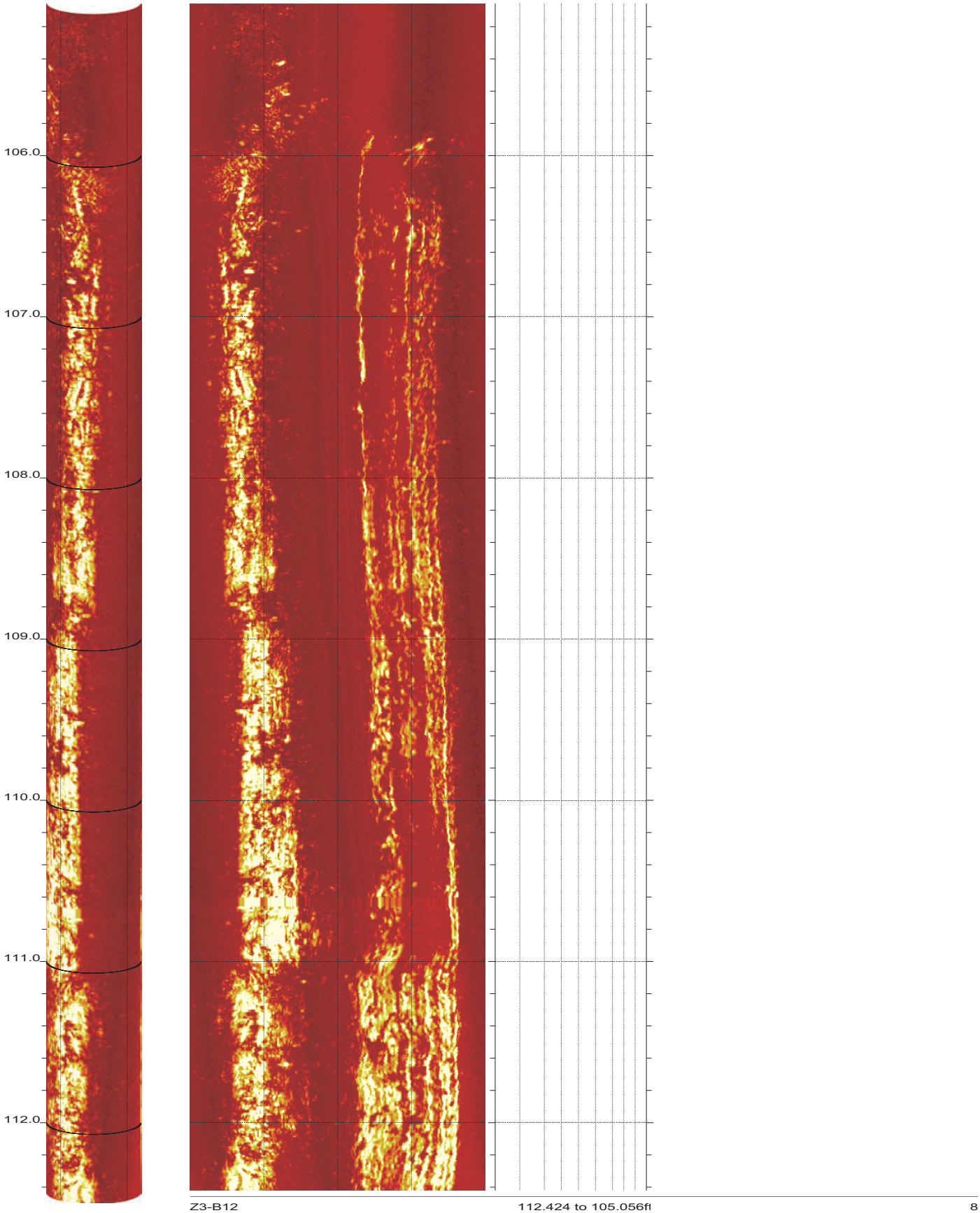

SR-710 Boring Z3-B12 Acoustic Televiewer Dips rev 1 Sheet 8 of 18

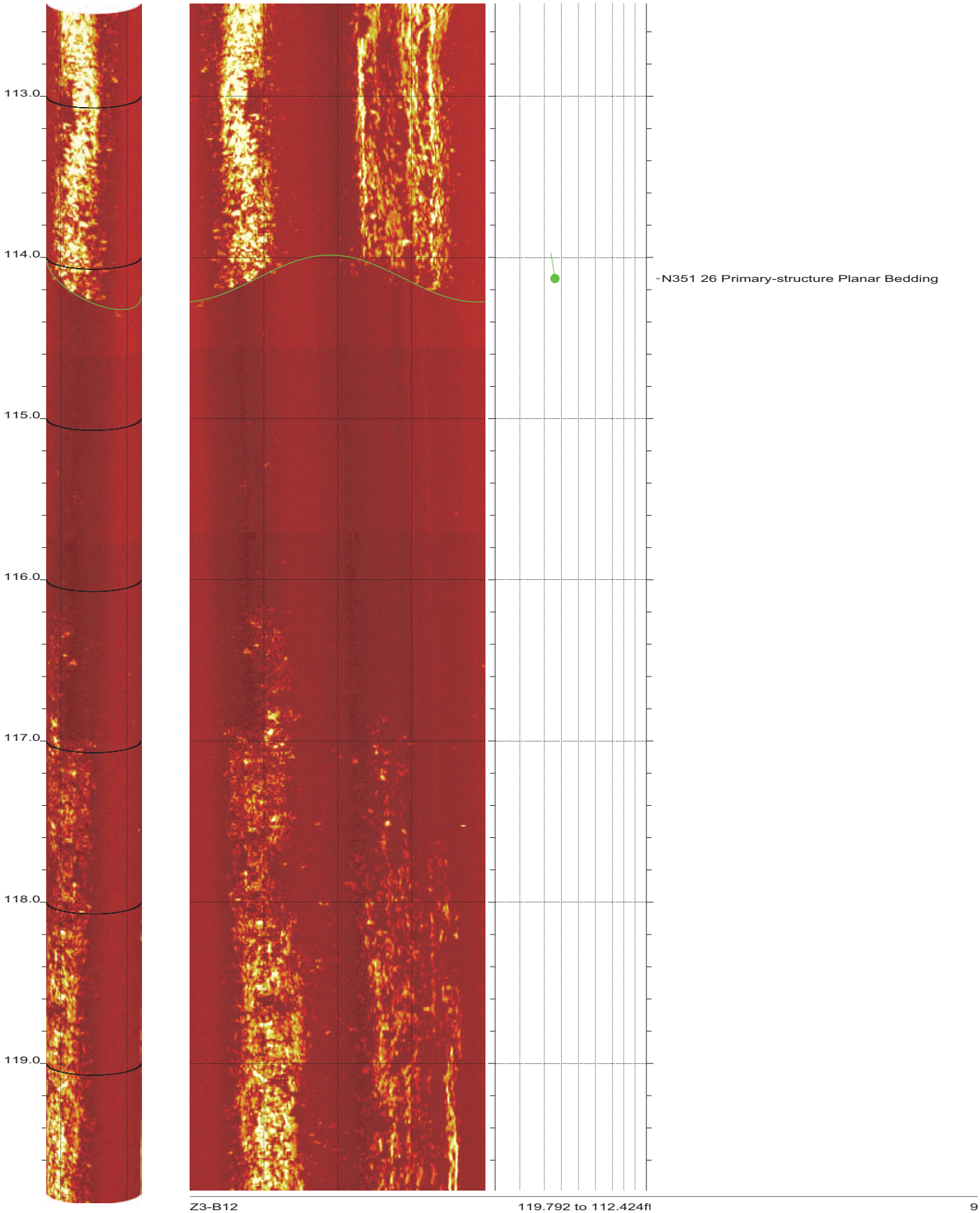
113.0
114.0
115.0
116.0
117.0
118.0
119.0
N351 26 Primary-structure Planar Bedding
Z3-B12
119.792 to 112.424ft
9

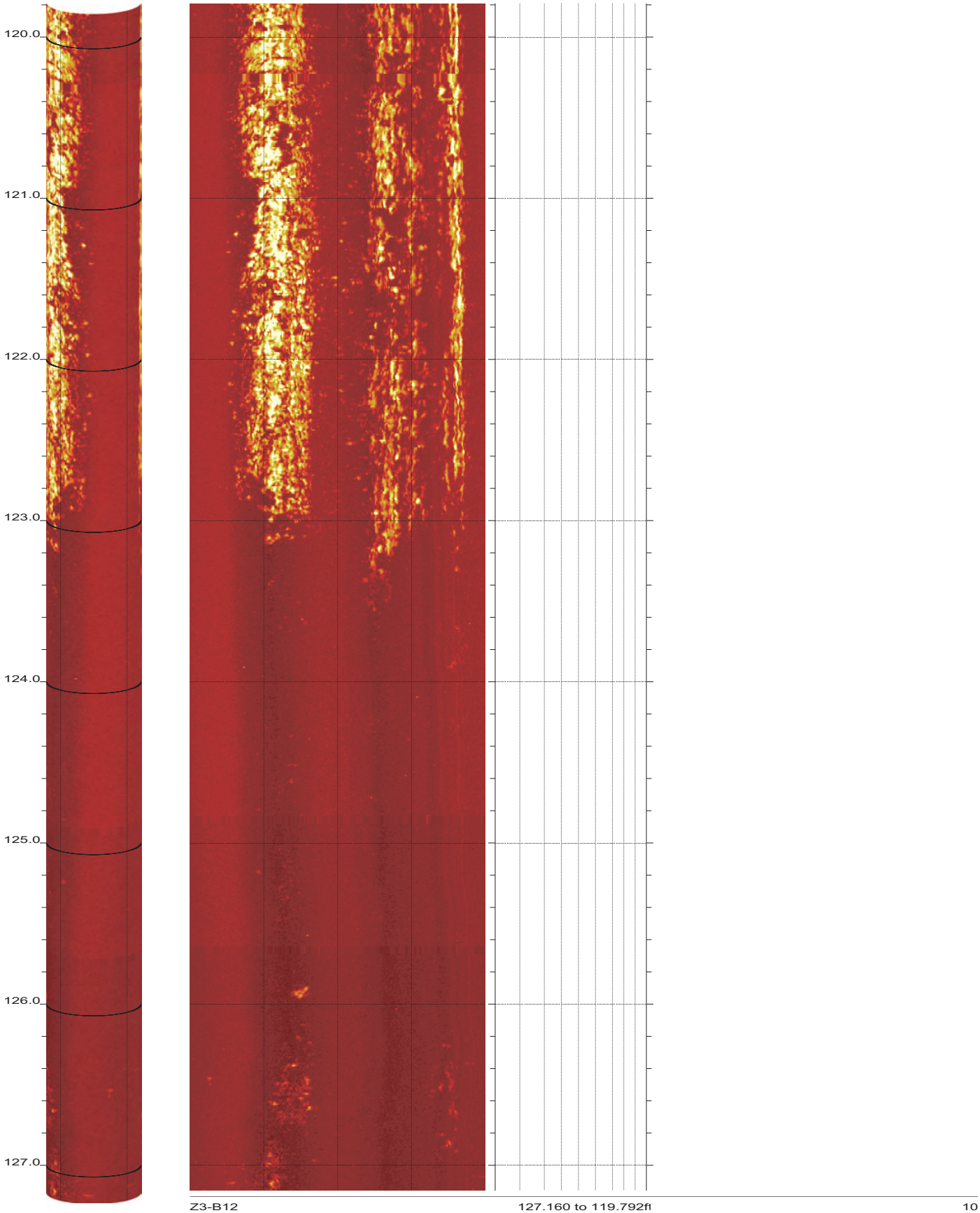
120.0
121.0
122.0
123.0
124.0
125.0
126.0
127.0
Z3-B12
127.160 to 119.792fl
10

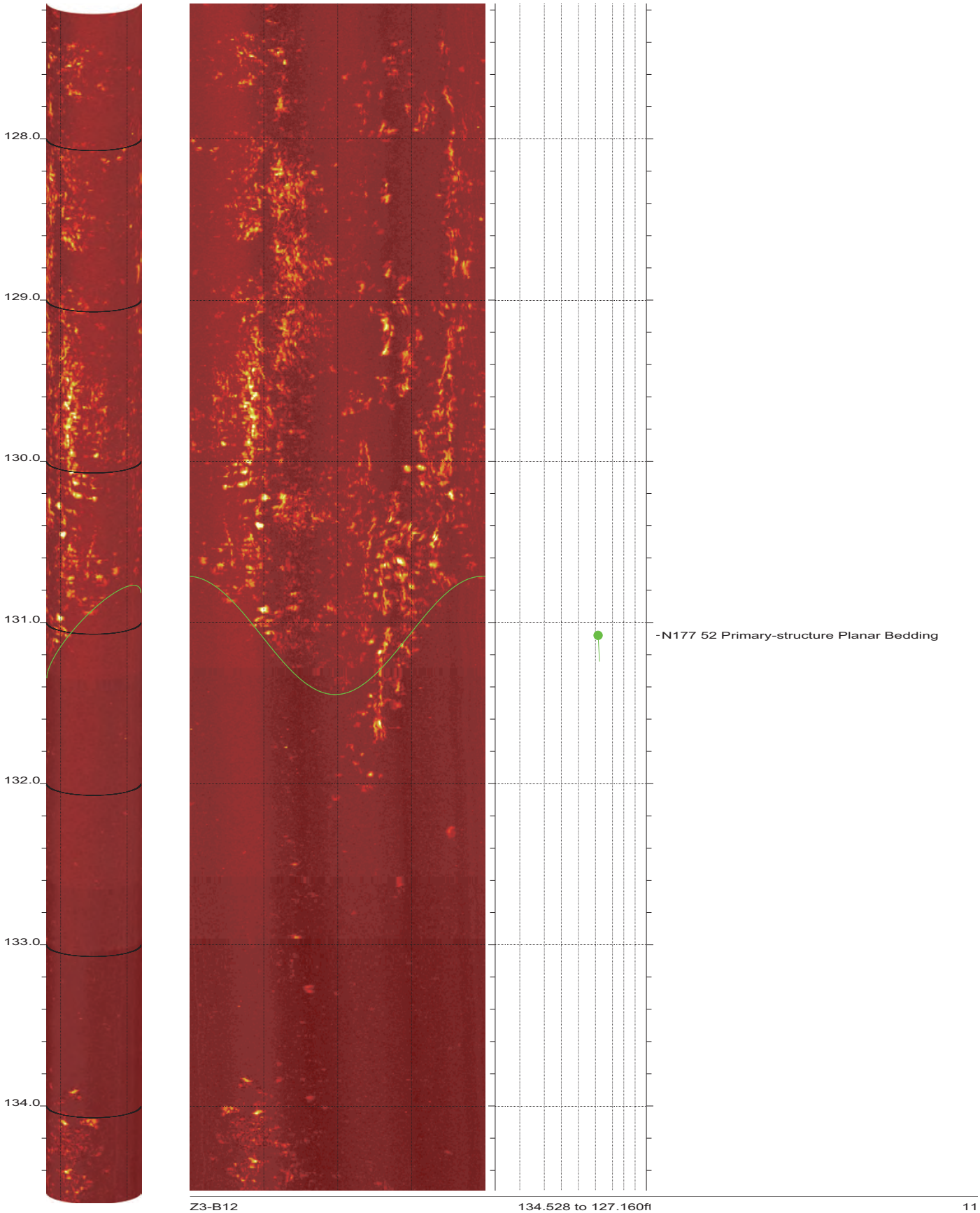
128.0
129.0
130.0
131.0
132.0
133.0
134.0
-N177 52 Primary-structure Planar Bedding
Z3-B12
134.528 to 127.160ft
11

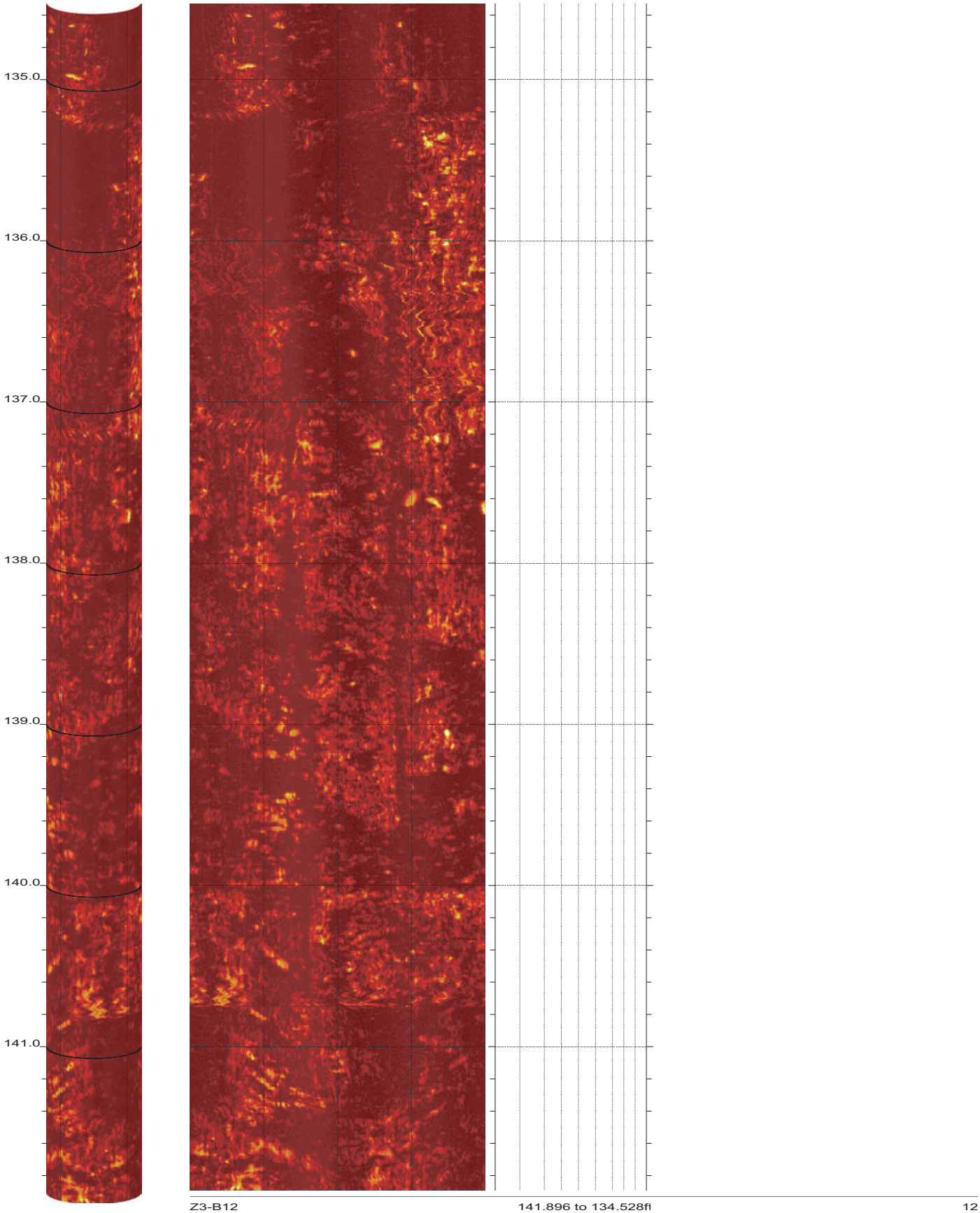
135.0
136.0
137.0
138.0
139.0
140.0
141.0
Z3-B12
141.896 to 134.528fl
12

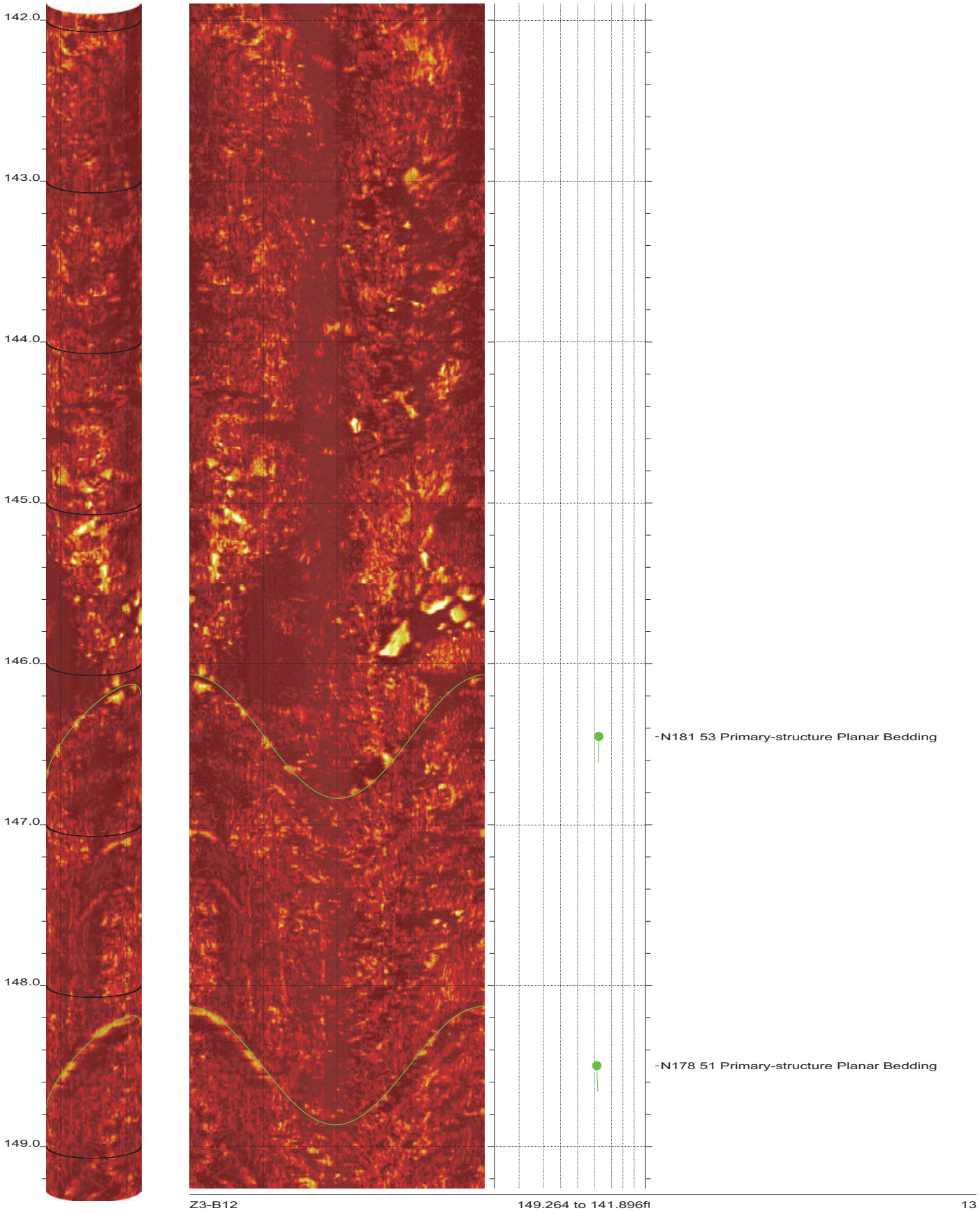
142.0
143.0
144.0
145.0
146.0
147.0
148.0
149.0
N181 53 Primary-structure Planar Bedding
N178 51 Primary-structure Planar Bedding
Z3-B12
149.264 to 141.896fl
13

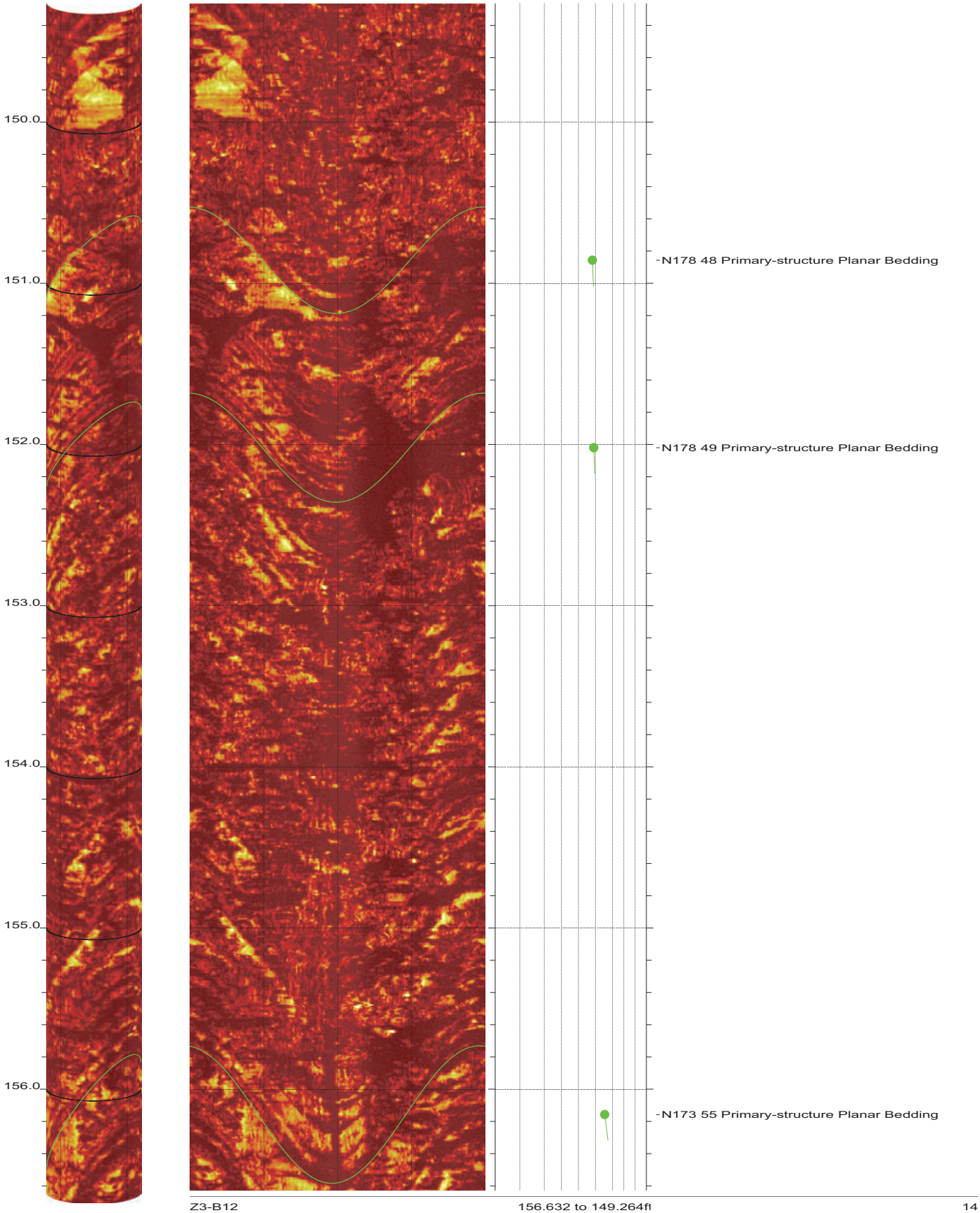
150.0
151.0
152.0
153.0
154.0
155.0
156.0
N178 48 Primary-structure Planar Bedding
N178 49 Primary-structure Planar Bedding
N173 55 Primary-structure Planar Bedding
Z3-B12
156.632 to 149.264fl
14

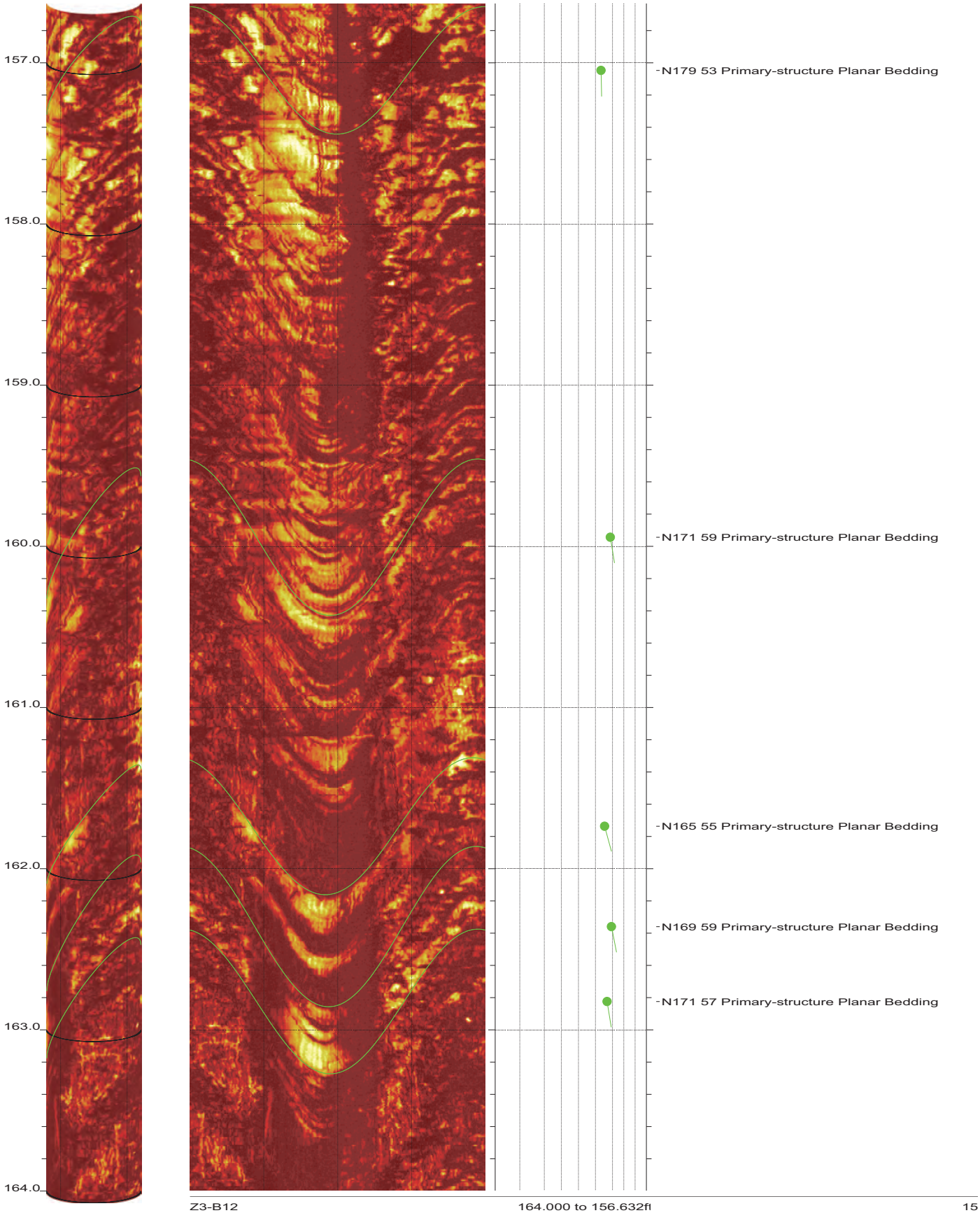
157.0
158.0
159.0
160.0
161.0
162.0
163.0
164.0
N179 53 Primary-structure Planar Bedding
N171 59 Primary-structure Planar Bedding
N165 55 Primary-structure Planar Bedding
N169 59 Primary-structure Planar Bedding
N171 57 Primary-structure Planar Bedding
Z3-B12
164.000 to 156.632ft
15

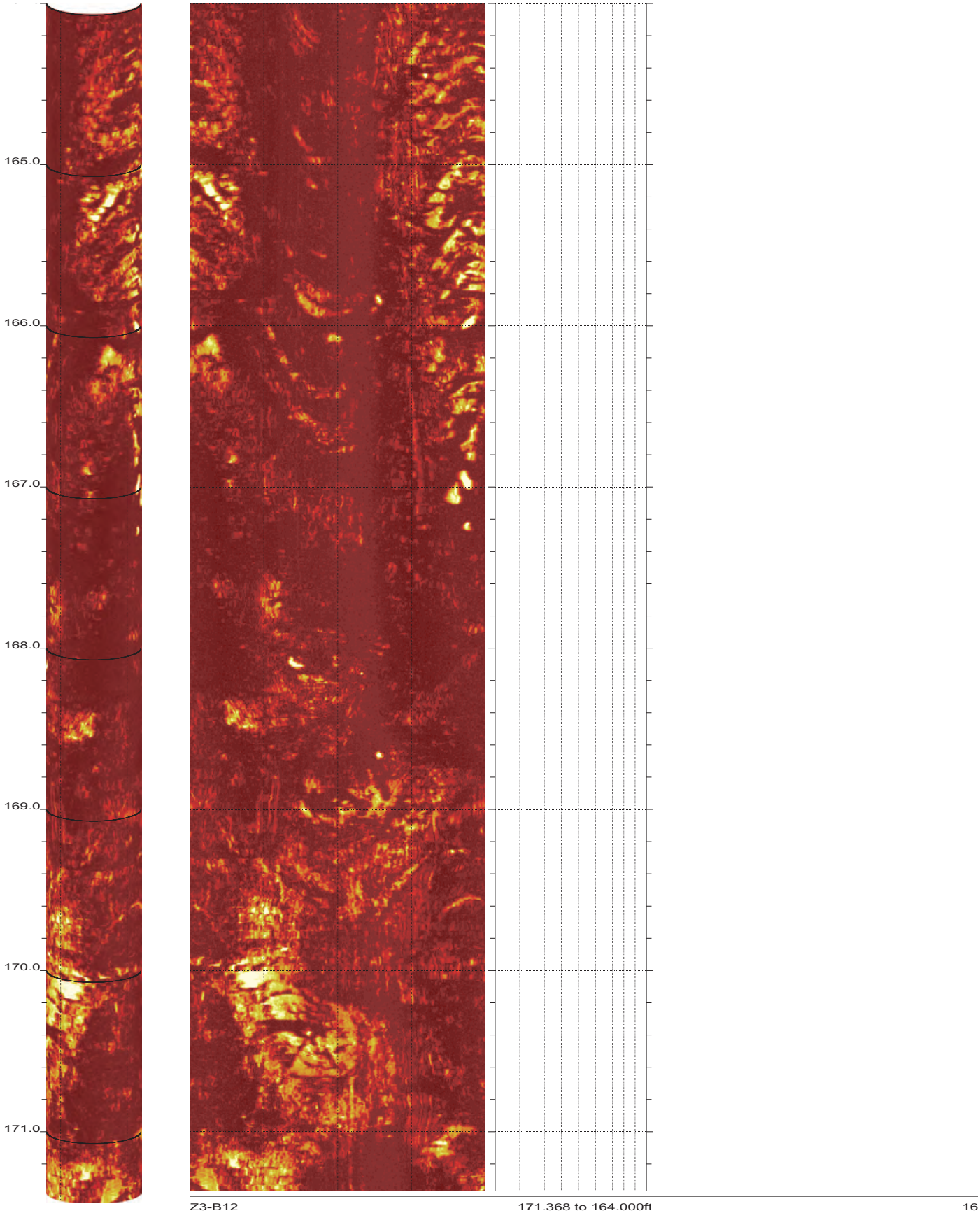
165.0
166.0
167.0
168.0
169.0
170.0
171.0
Z3-B12
171.368 to 164.000ft
16

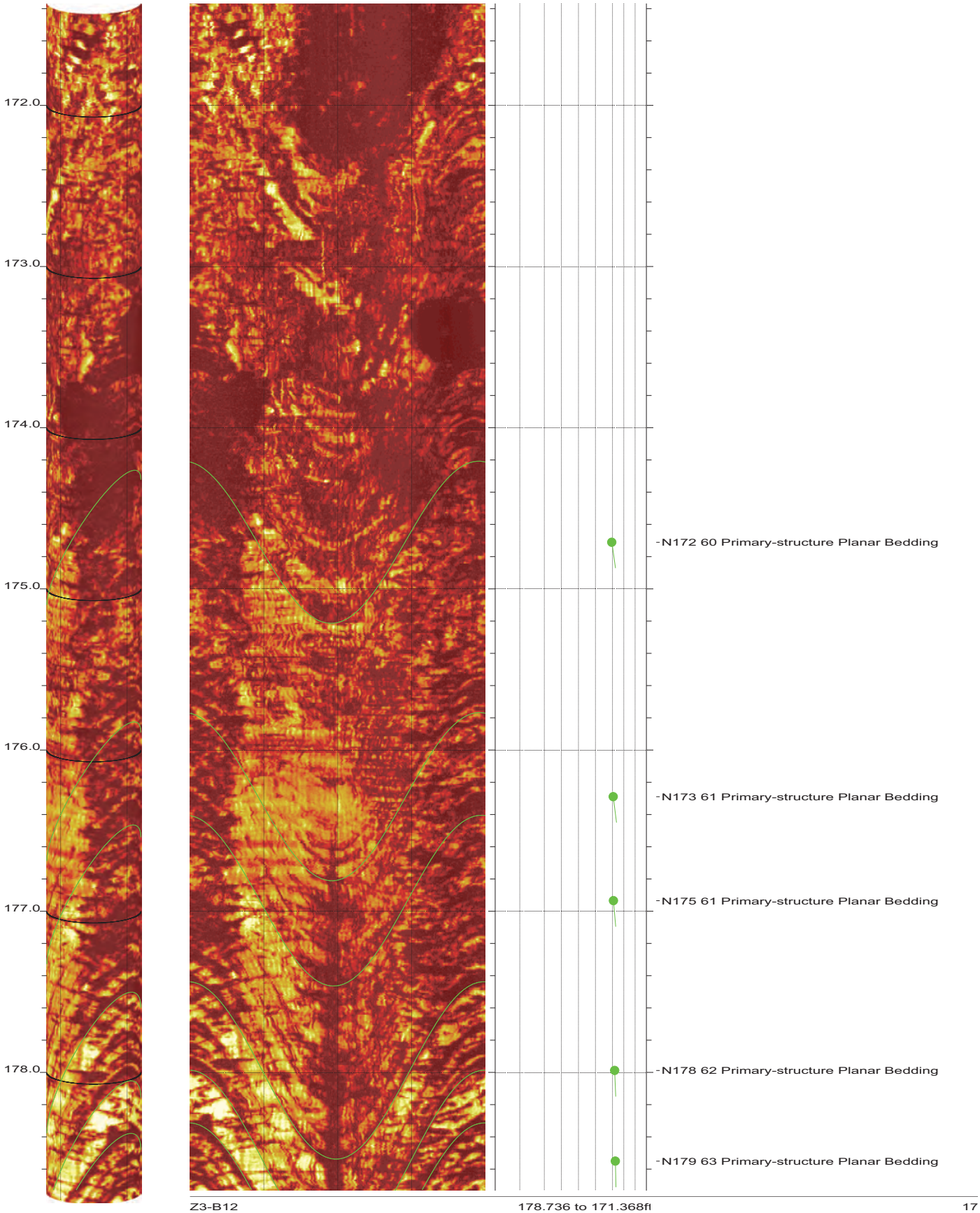
172.0
173.0
174.0
175.0
176.0
177.0
178.0
N172 60 Primary-structure Planar Bedding
N173 61 Primary-structure Planar Bedding
N175 61 Primary-structure Planar Bedding
N178 62 Primary-structure Planar Bedding
N179 63 Primary-structure Planar Bedding
Z3-B12
178.736 to 171.368fl
17

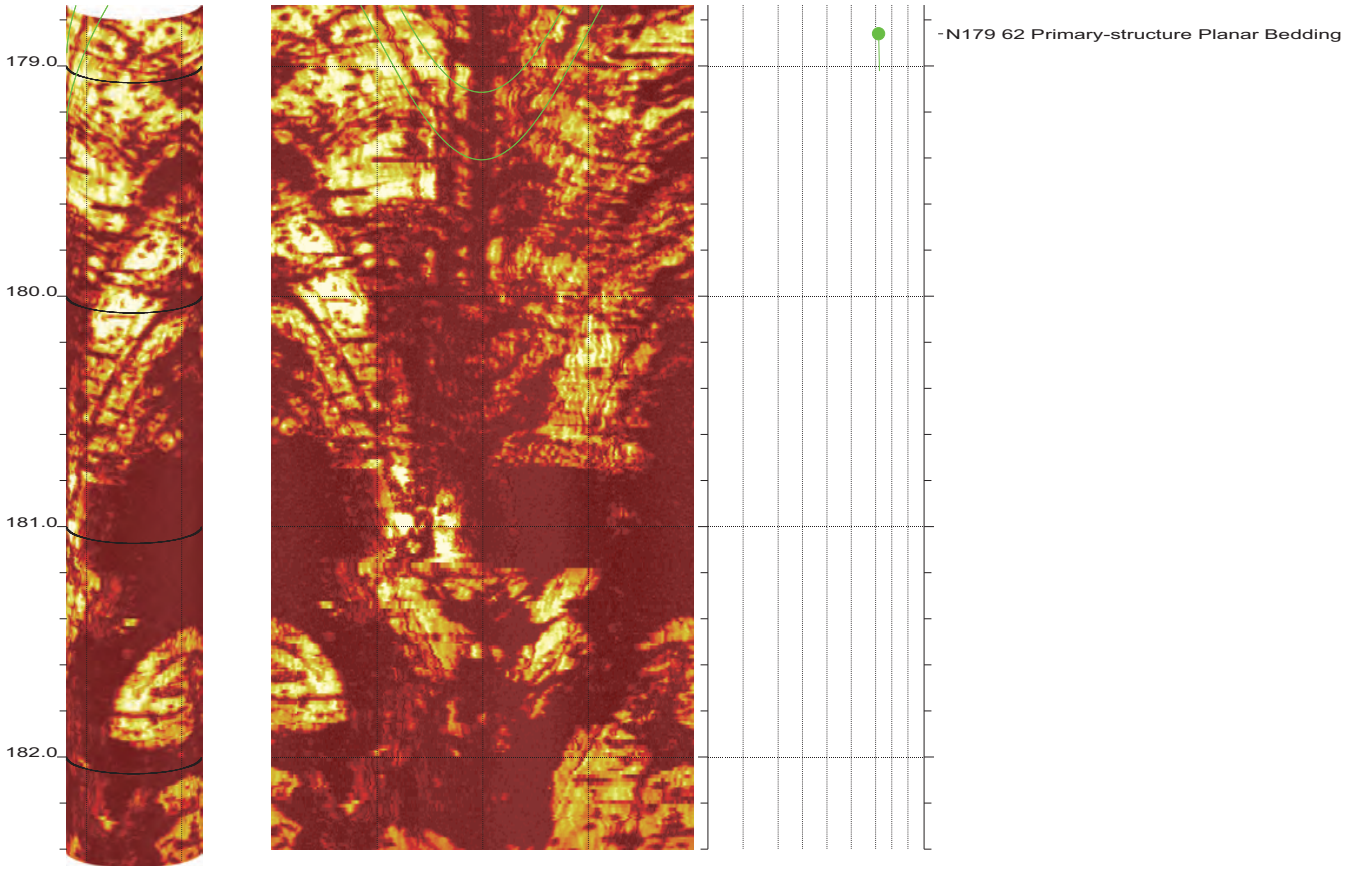
179.0
180.0
181.0
182.0
N179 62 Primary-structure Planar Bedding

BHTV DATA PROCESSING
RGLDIP vsn 6.2
INTERPRETED BHTV DIPS LOG

CASCADE DRILLING

Borehole: Z4-B4

SR-710 TUNNEL INVESTIGATION

top of borehole.....
East: _
North: _
Elev: _

North ref. is true
Depth units are feet
Vertical scale: 1/10
Horiz scale = 1.00x Vert scale

Zone from 275.000 to 6.800ft
Format: BHTV-NESWN

Borehole diam: 5.700inch
Vertical = borehole-axis
Image: Amplitude

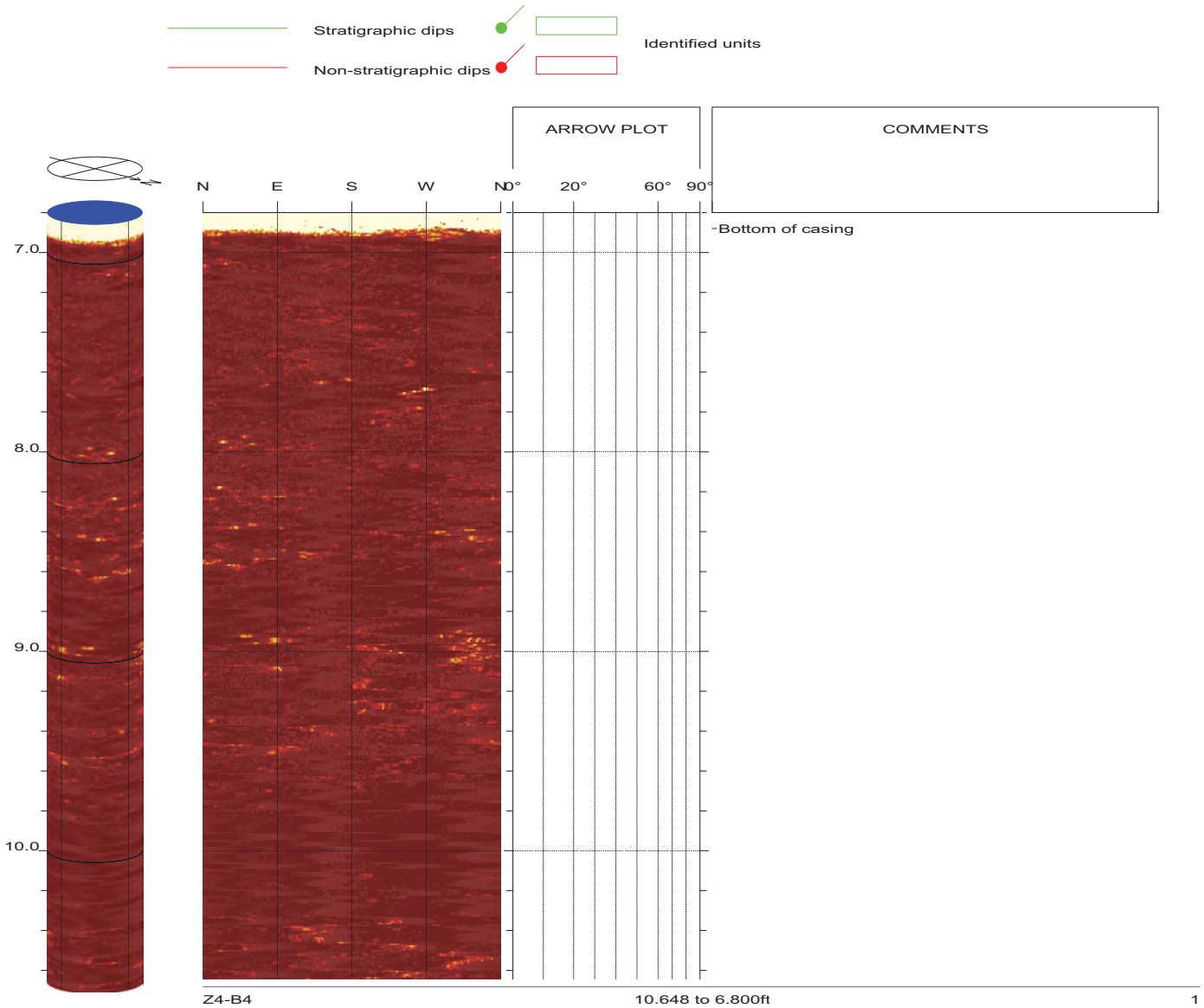

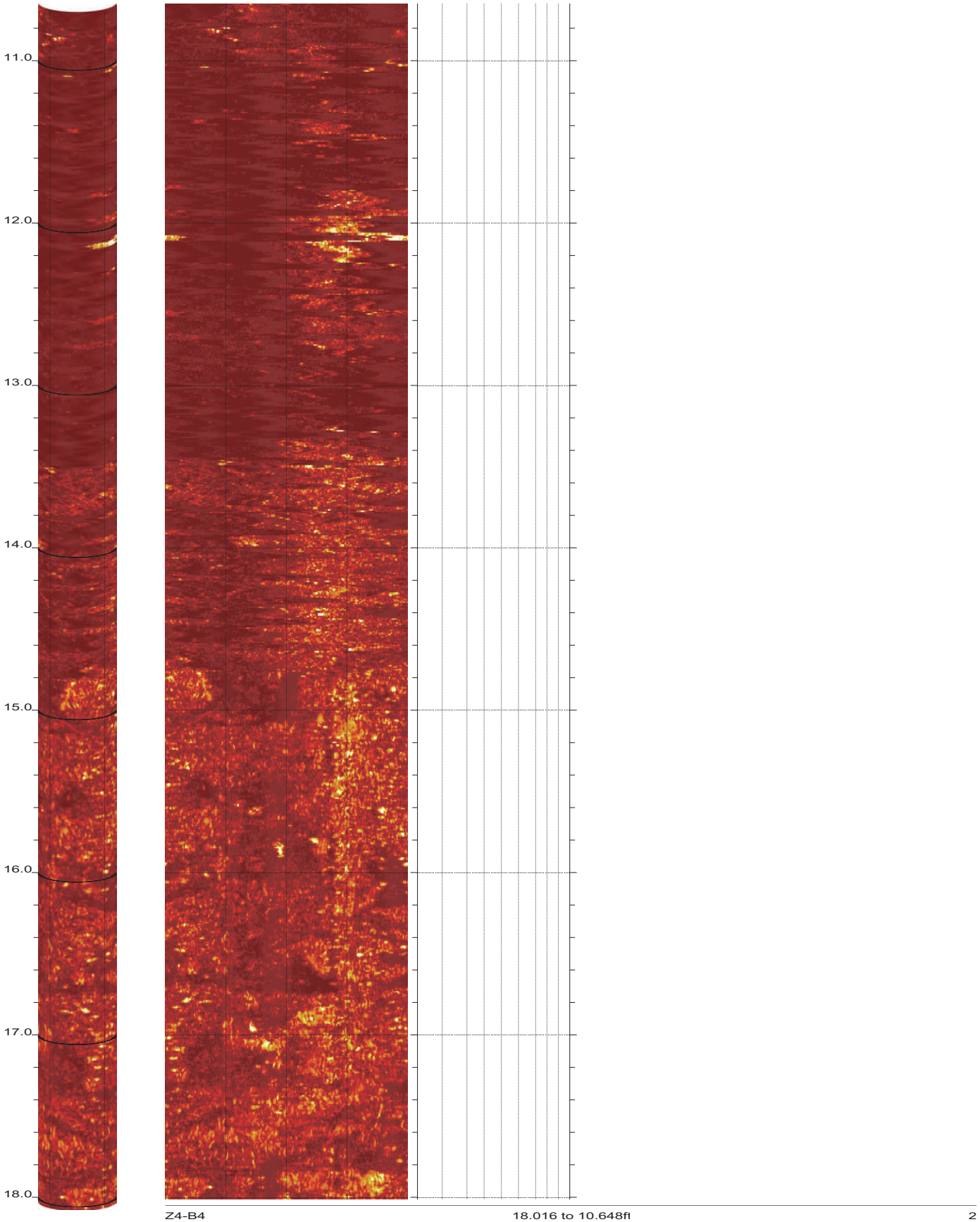

SR-710 Boring Z4-B4 Acoustic Televiewer Dips rev 1 Sheet 2 of 37

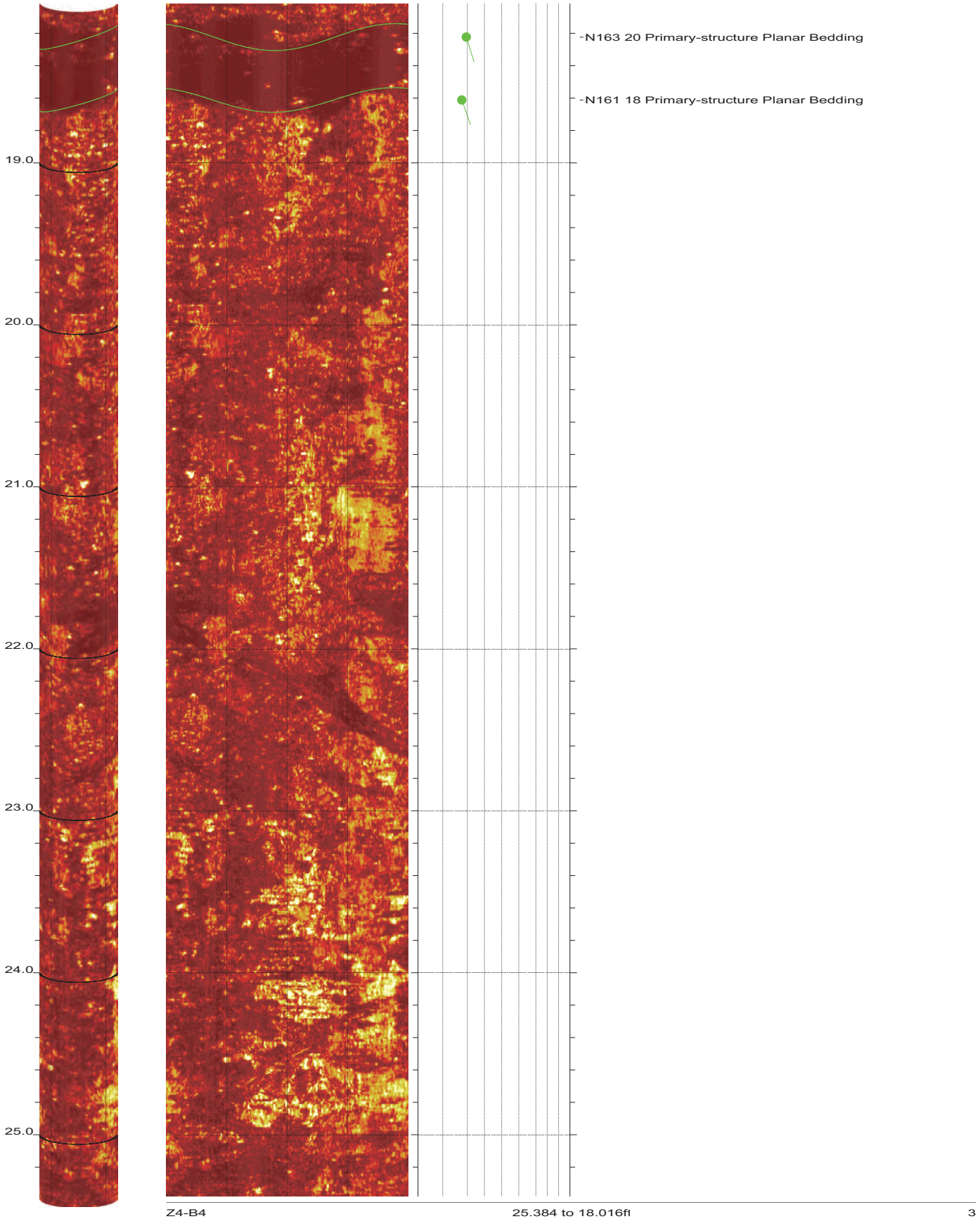

SR-710 Boring Z4-B4 Acoustic Televiewer Dips rev 1 Sheet 3 of 37

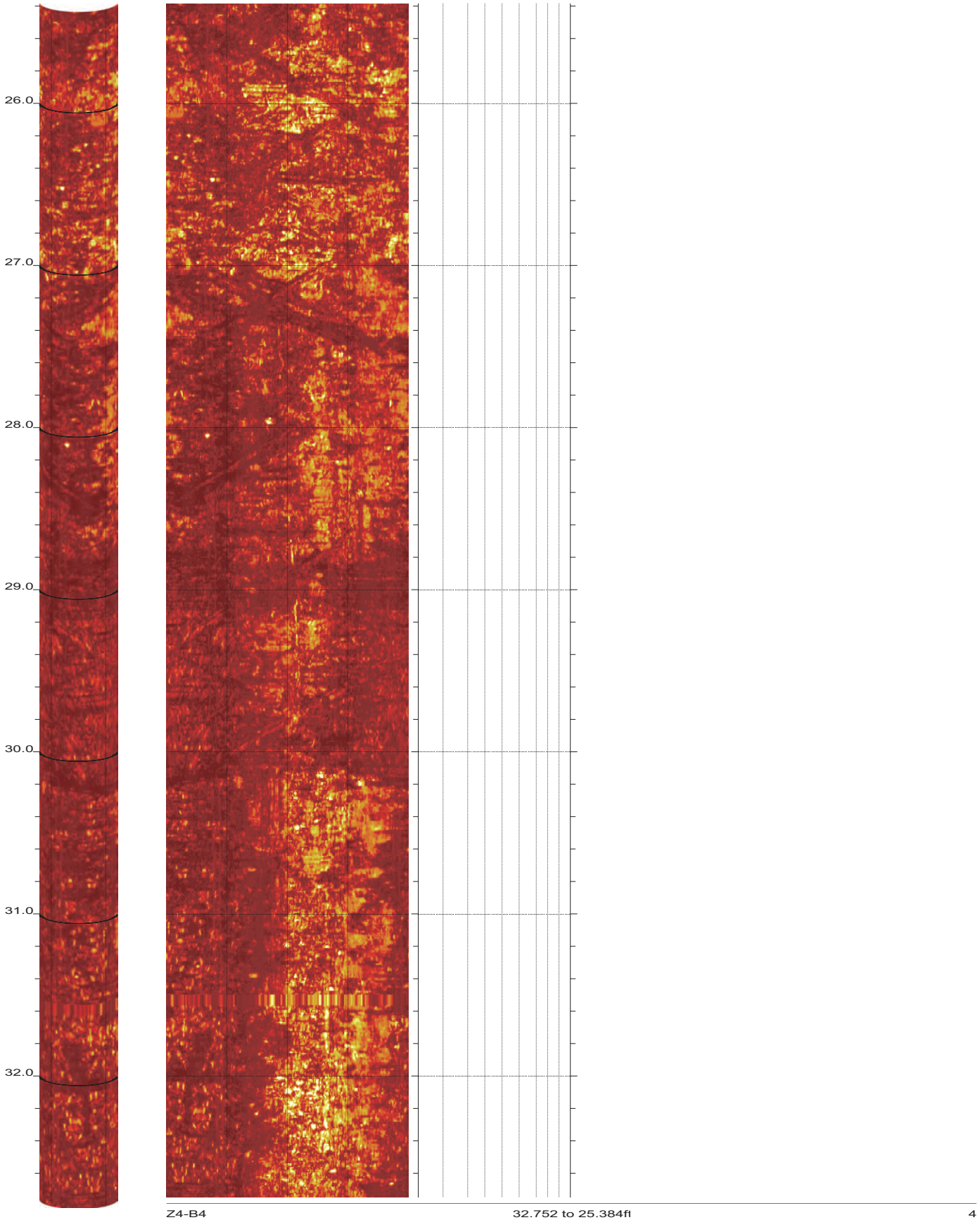

SR-710 Boring Z4-B4 Acoustic Televiewer Dips rev 1 Sheet 4 of 37

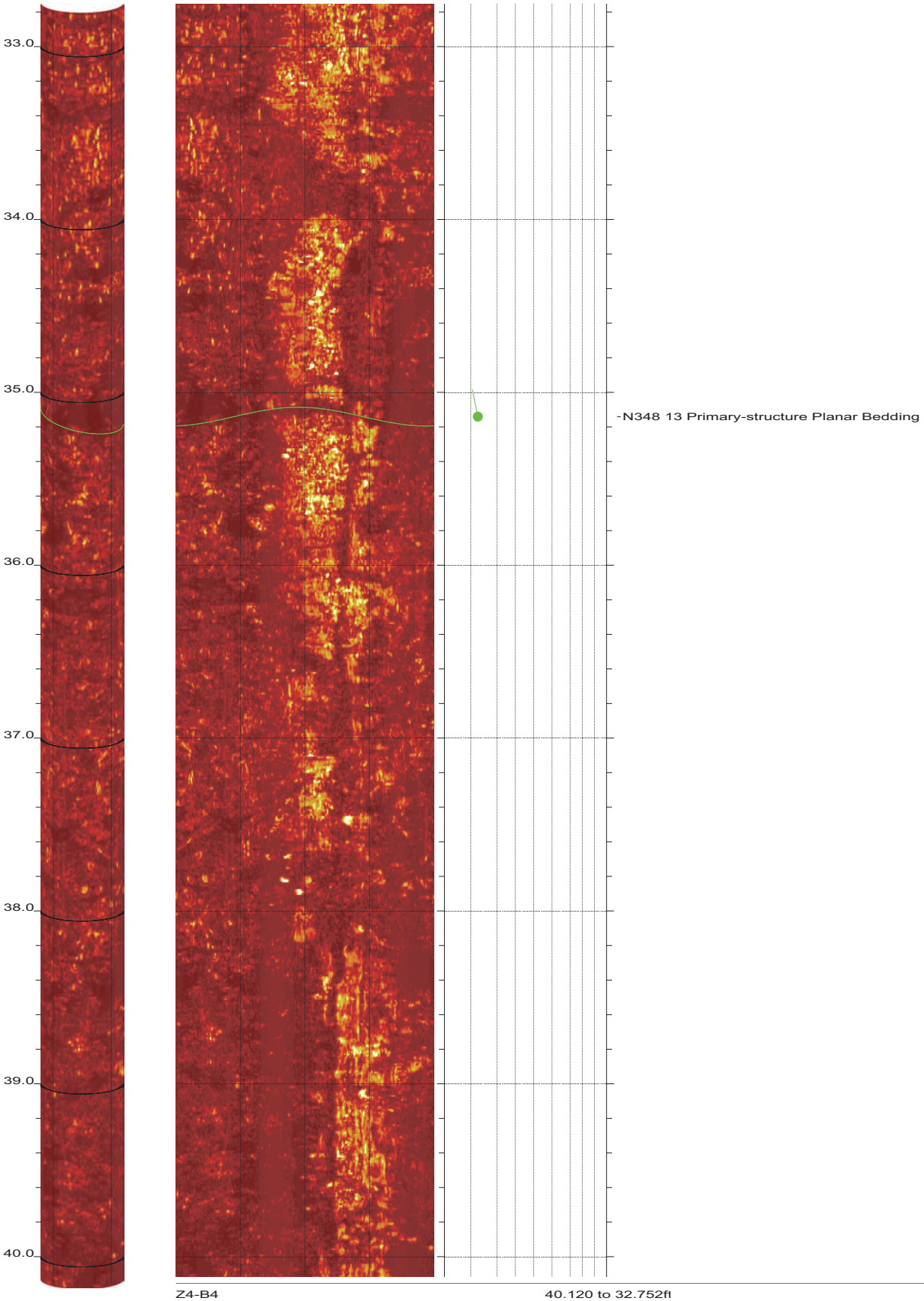

SR-710 Boring Z4-B4 Acoustic Televiewer Dips rev 1 Sheet 5 of 37

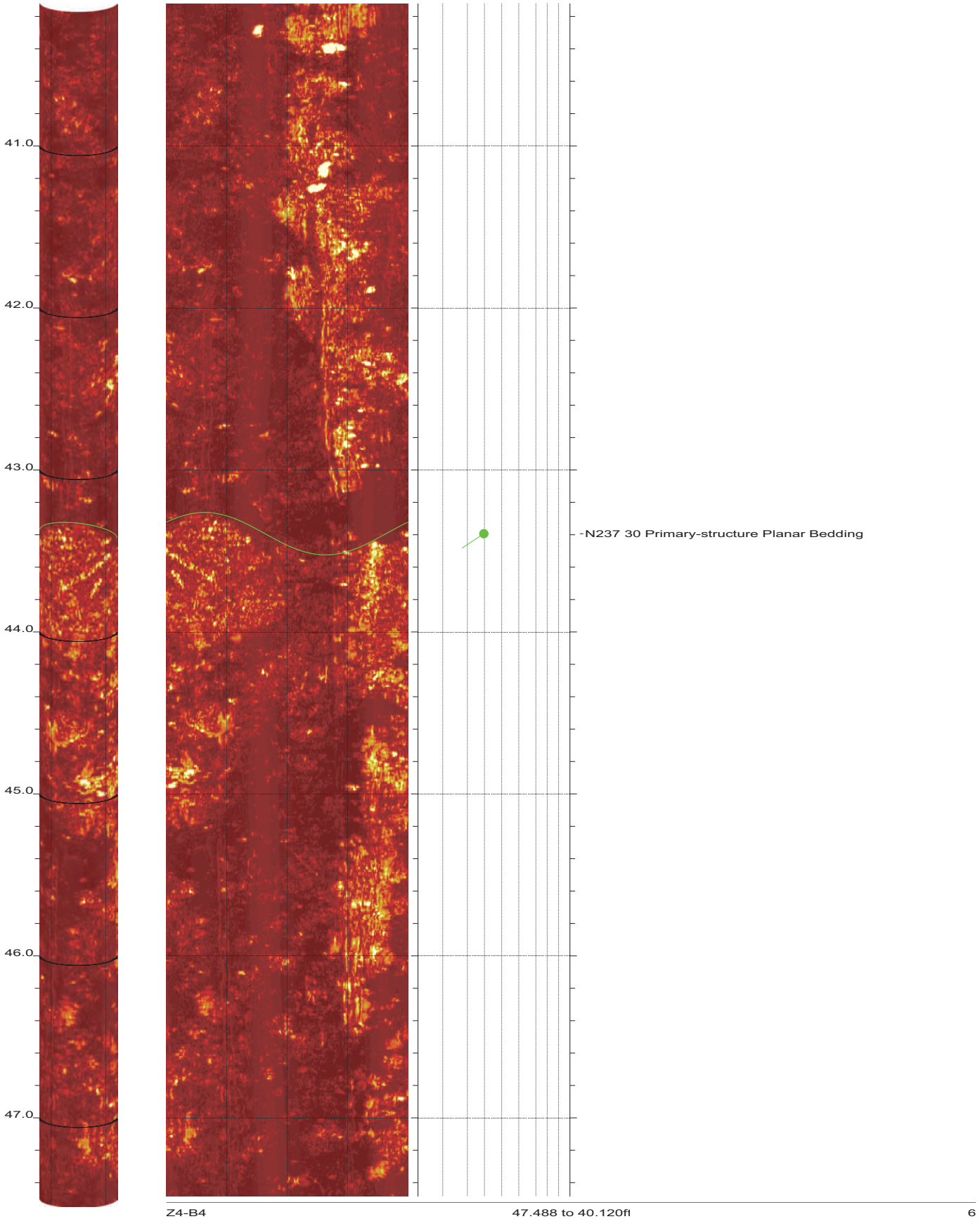

SR-710 Boring Z4-B4 Acoustic Televiewer Dips rev 1 Sheet 6 of 37

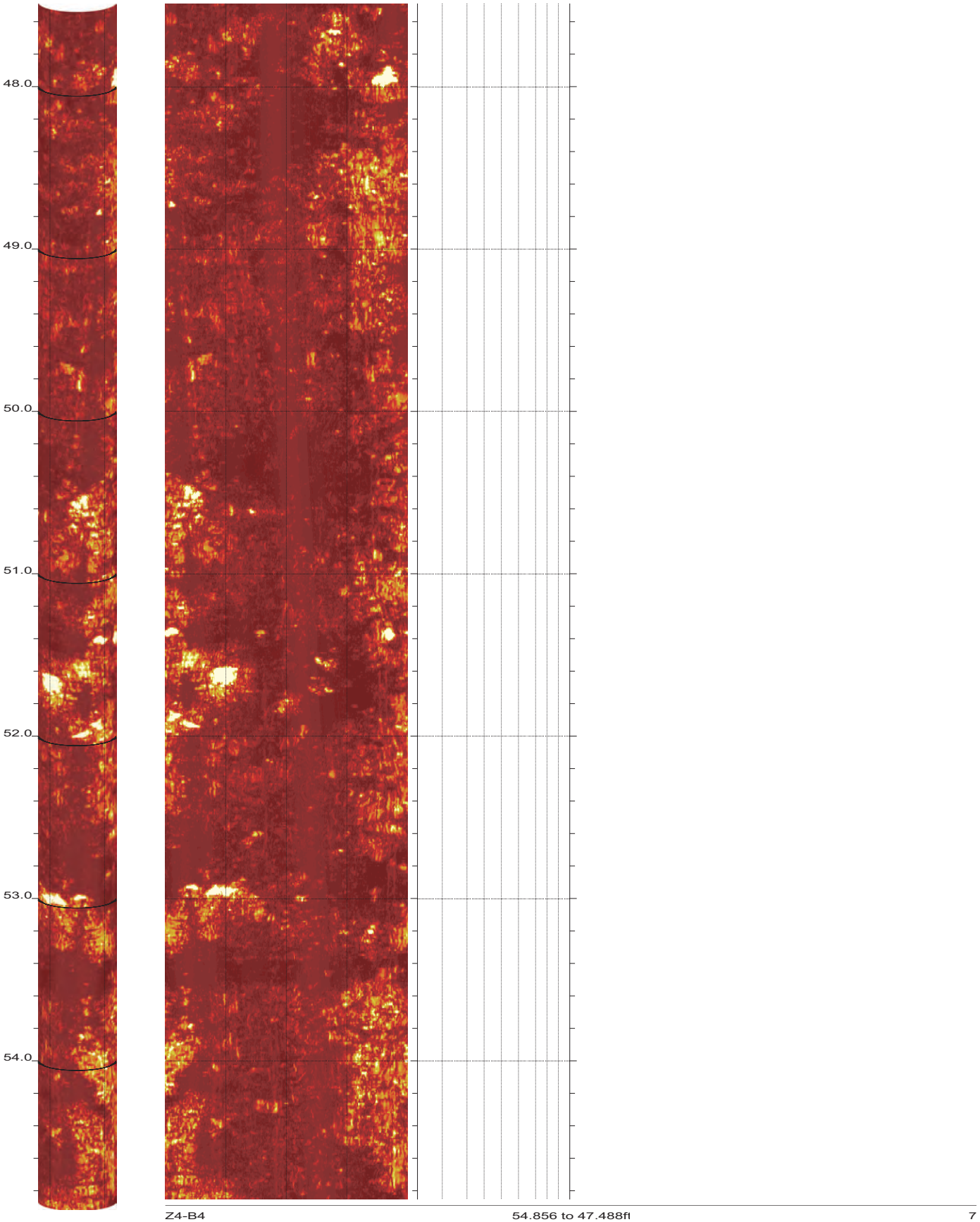

SR-710 Boring Z4-B4 Acoustic Televiewer Dips rev 1 Sheet 7 of 37

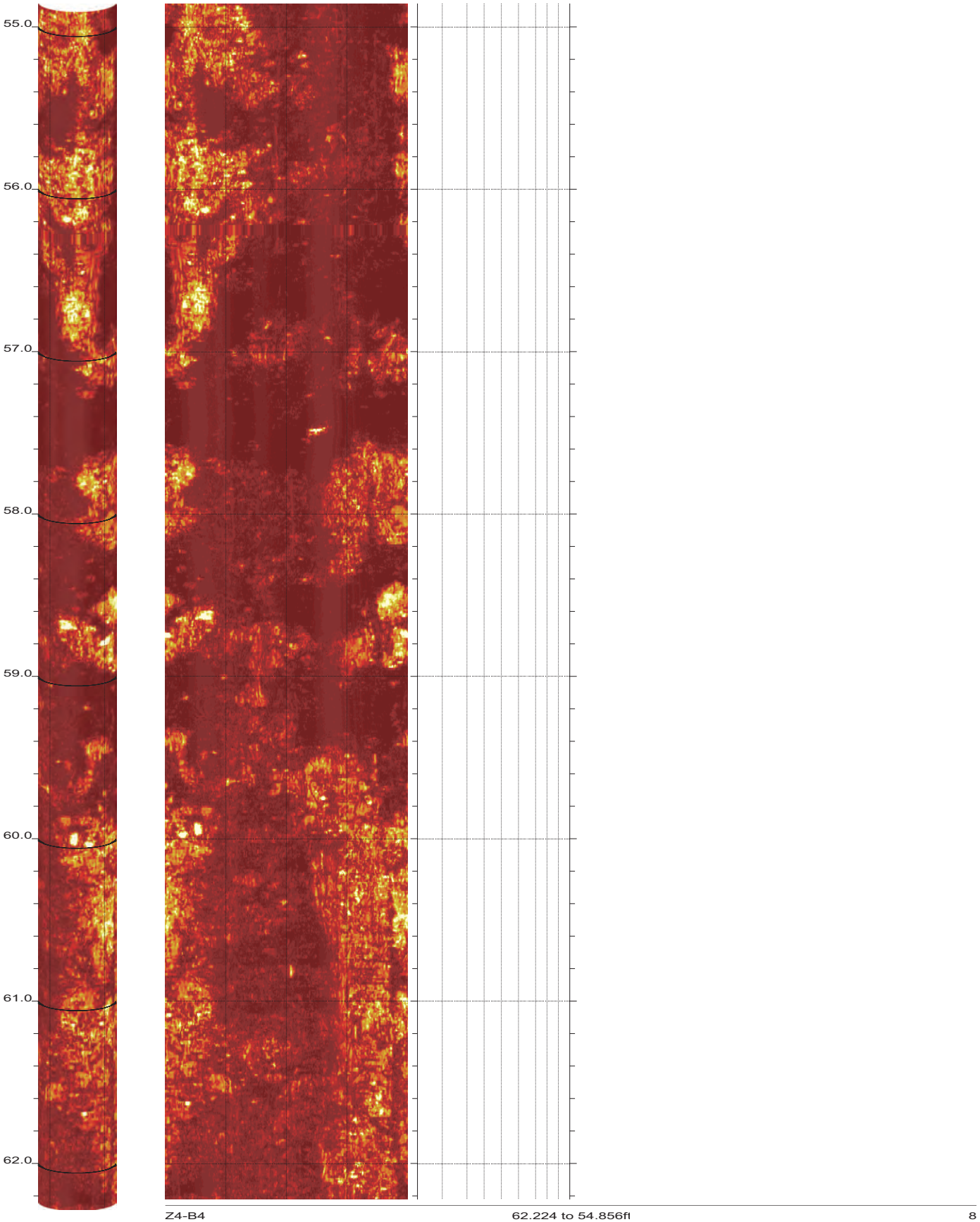

SR-710 Boring Z4-B4 Acoustic Televiewer Dips rev 1 Sheet 8 of 37

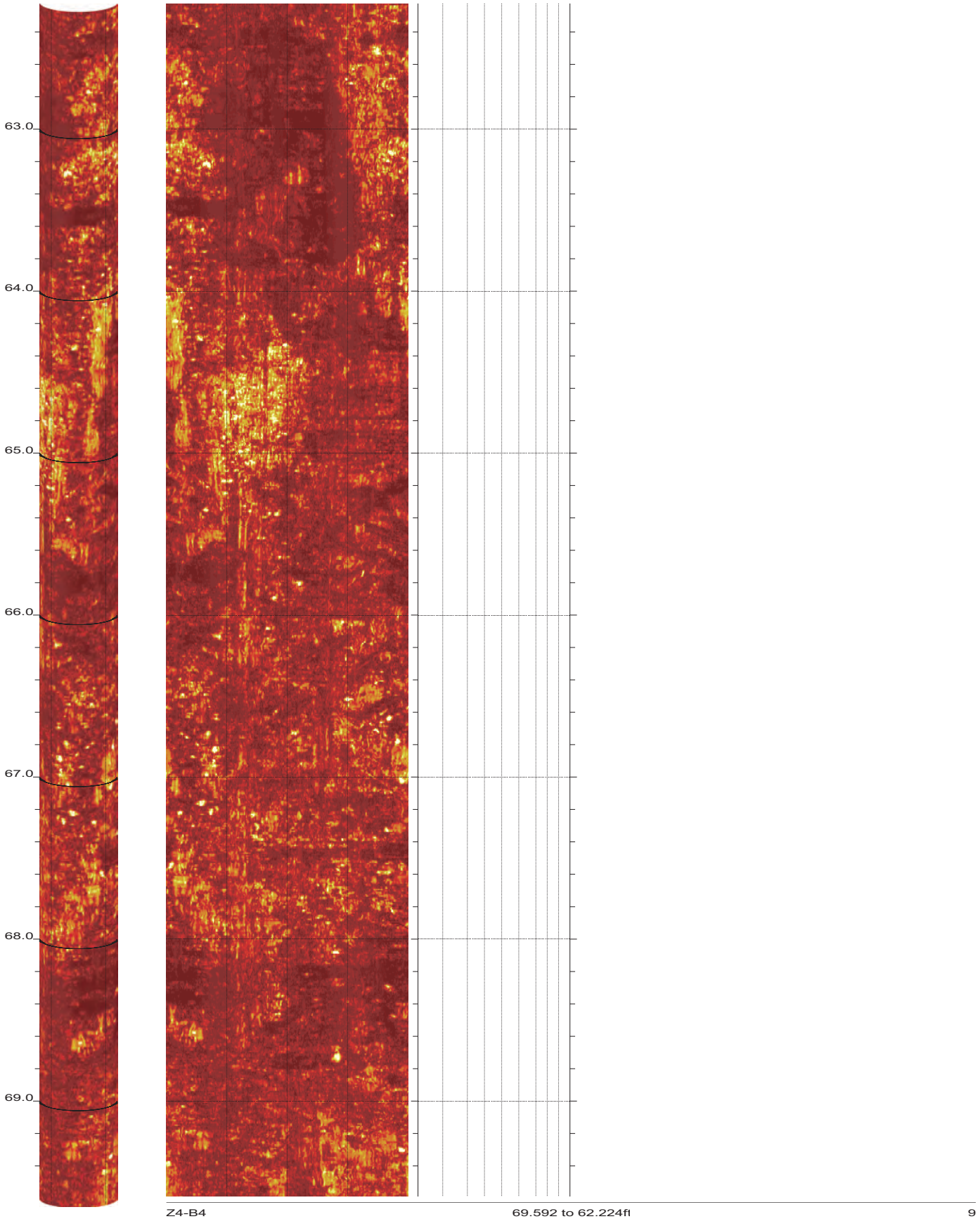

SR-710 Boring Z4-B4 Acoustic Televiewer Dips rev 1 Sheet 9 of 37

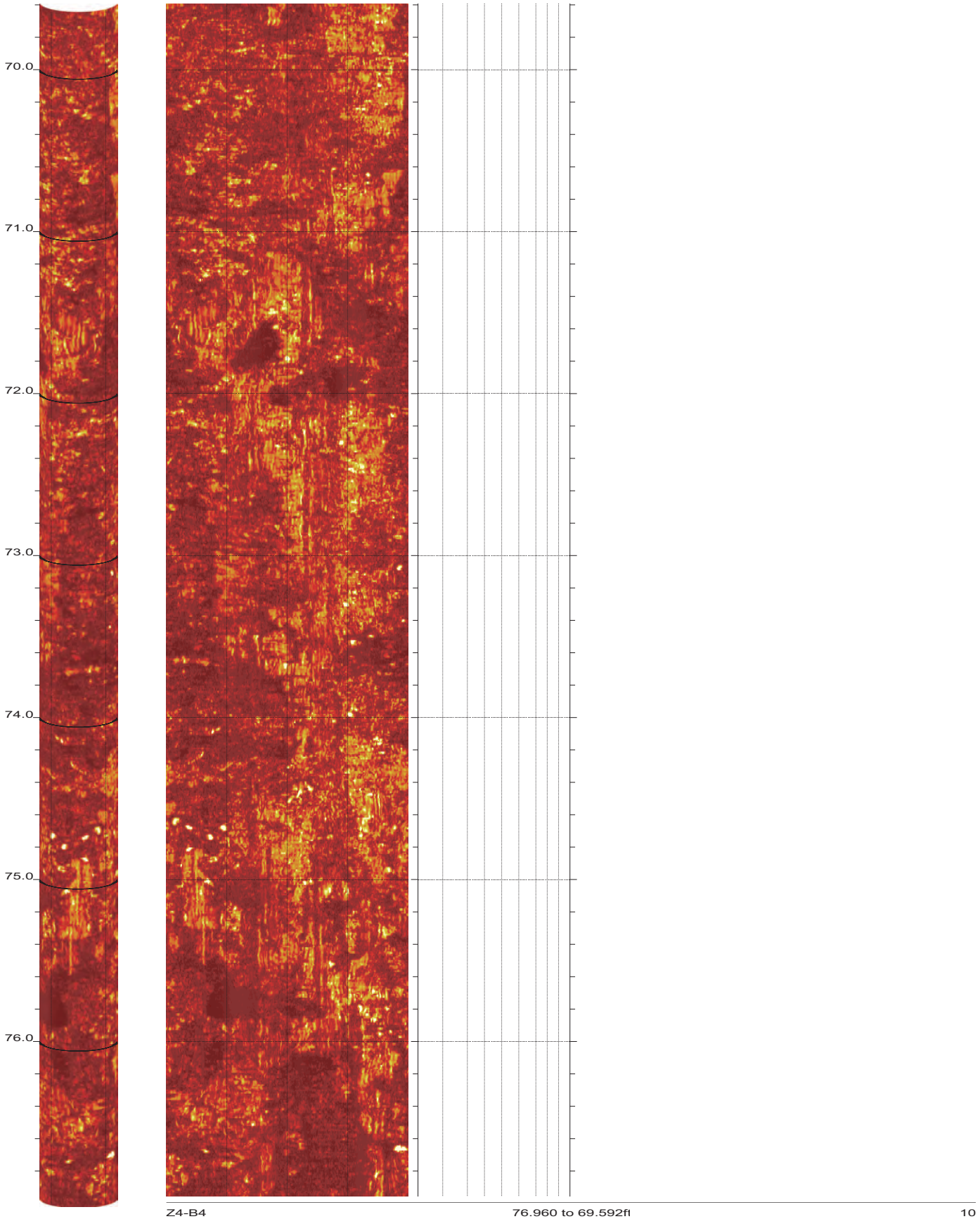

SR-710 Boring Z4-B4 Acoustic Televiewer Dips rev 1 Sheet 10 of 37

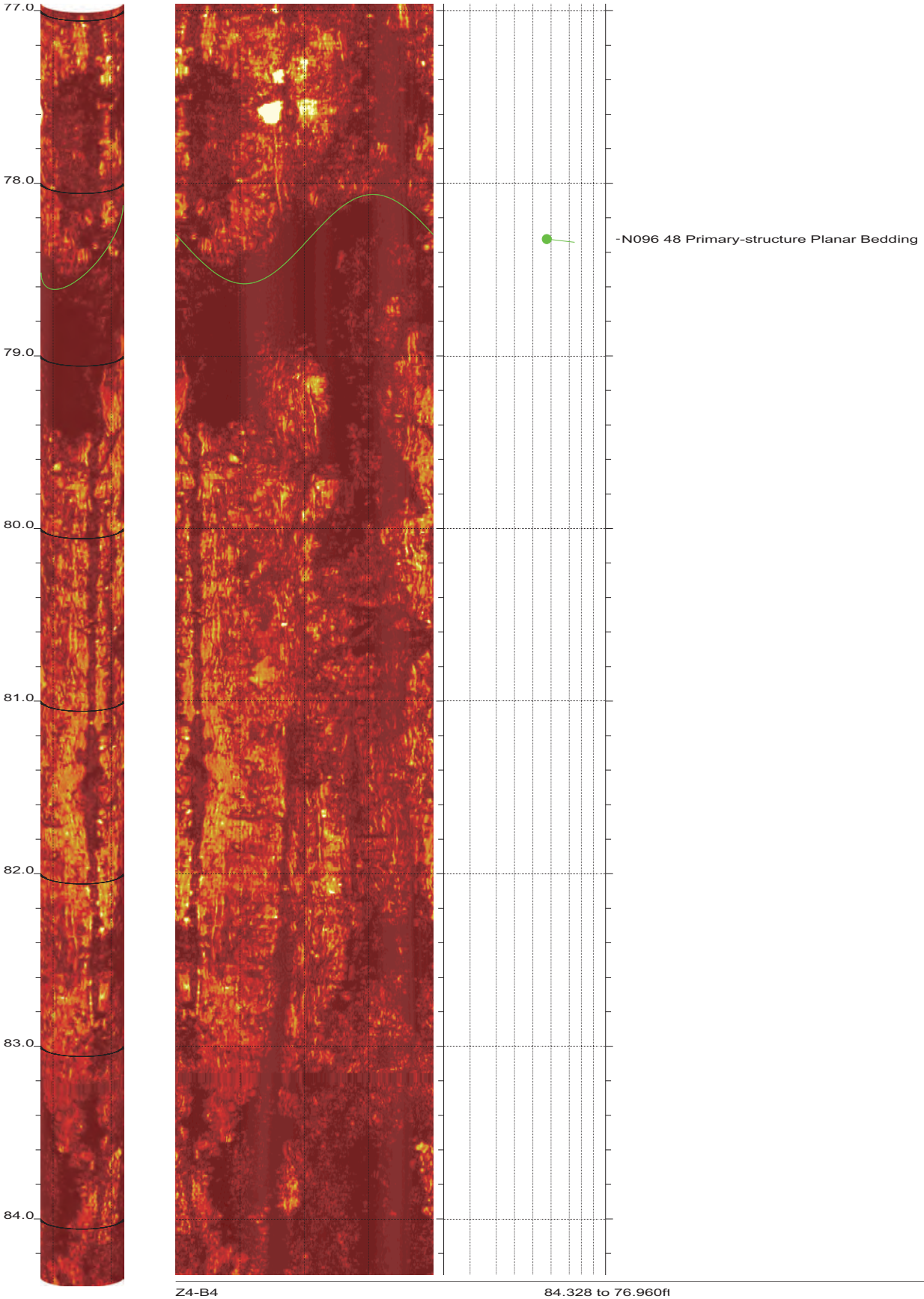
77.0
78.0
79.0
80.0
81.0
82.0
83.0
84.0
N096 48 Primary-structure Planar Bedding
Z4-B4
84.328 to 76.960fl
11

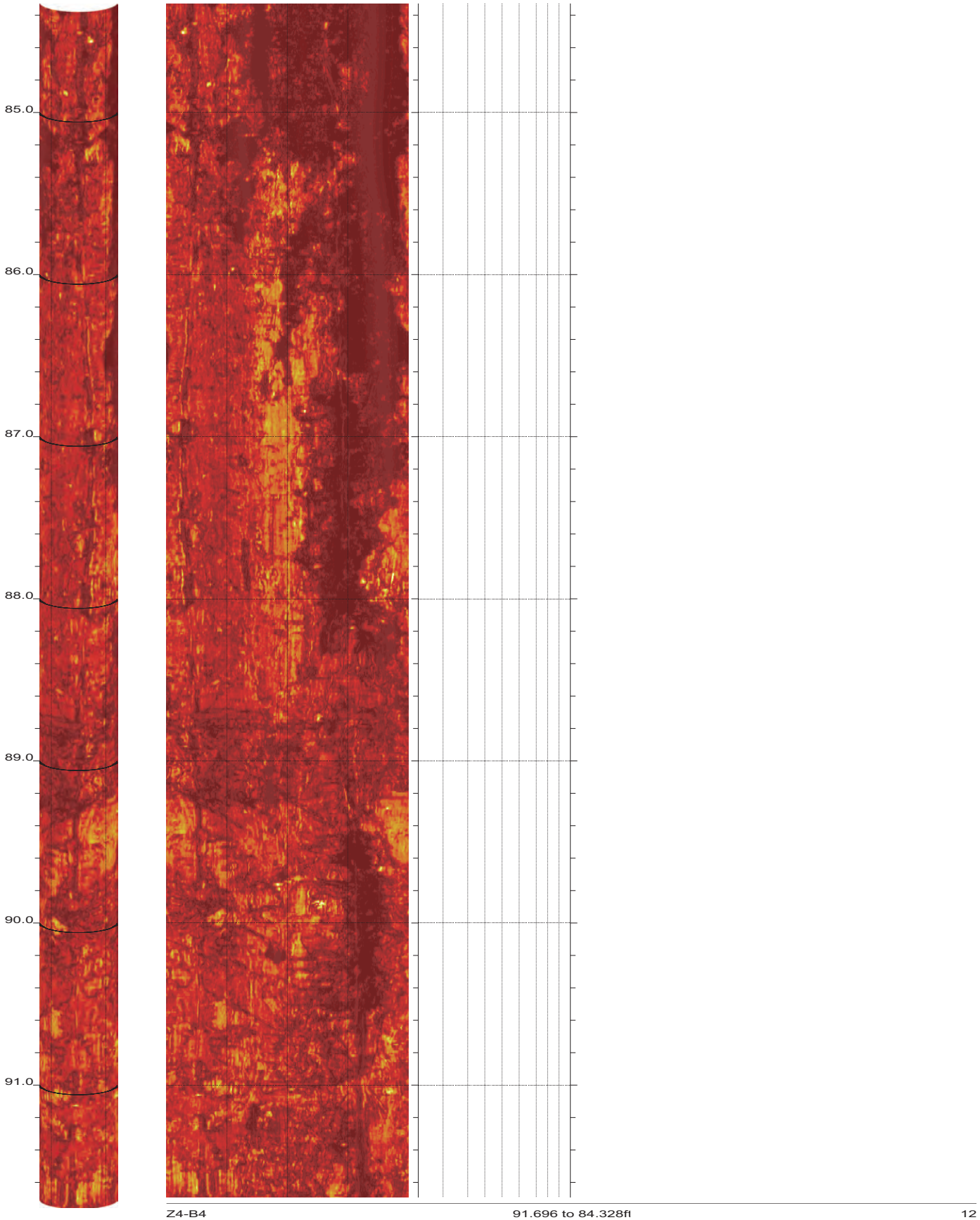

SR-710 Boring Z4-B4 Acoustic Televiewer Dips rev 1 Sheet 12 of 37

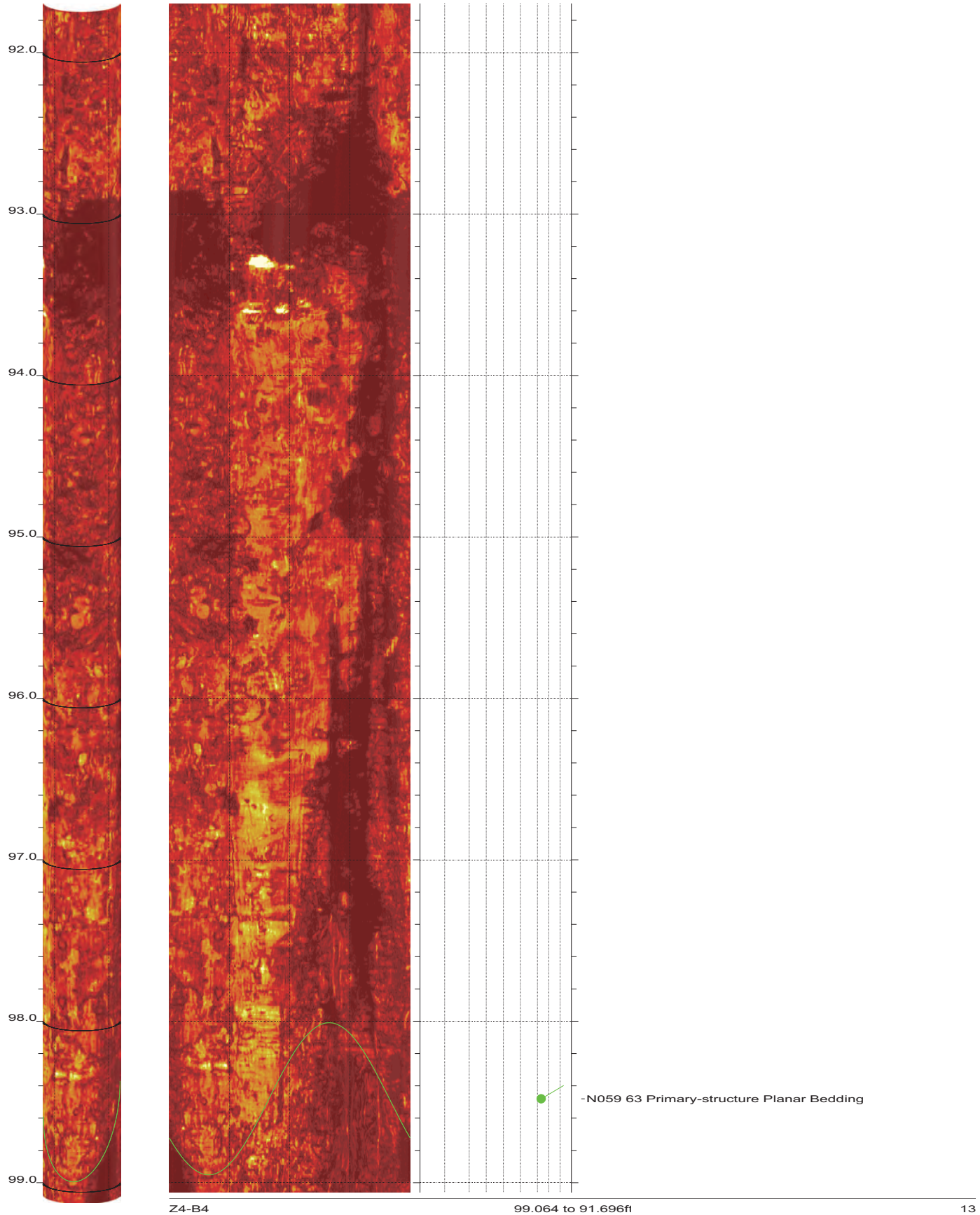

SR-710 Boring Z4-B4 Acoustic Televiewer Dips rev 1 Sheet 13 of 37

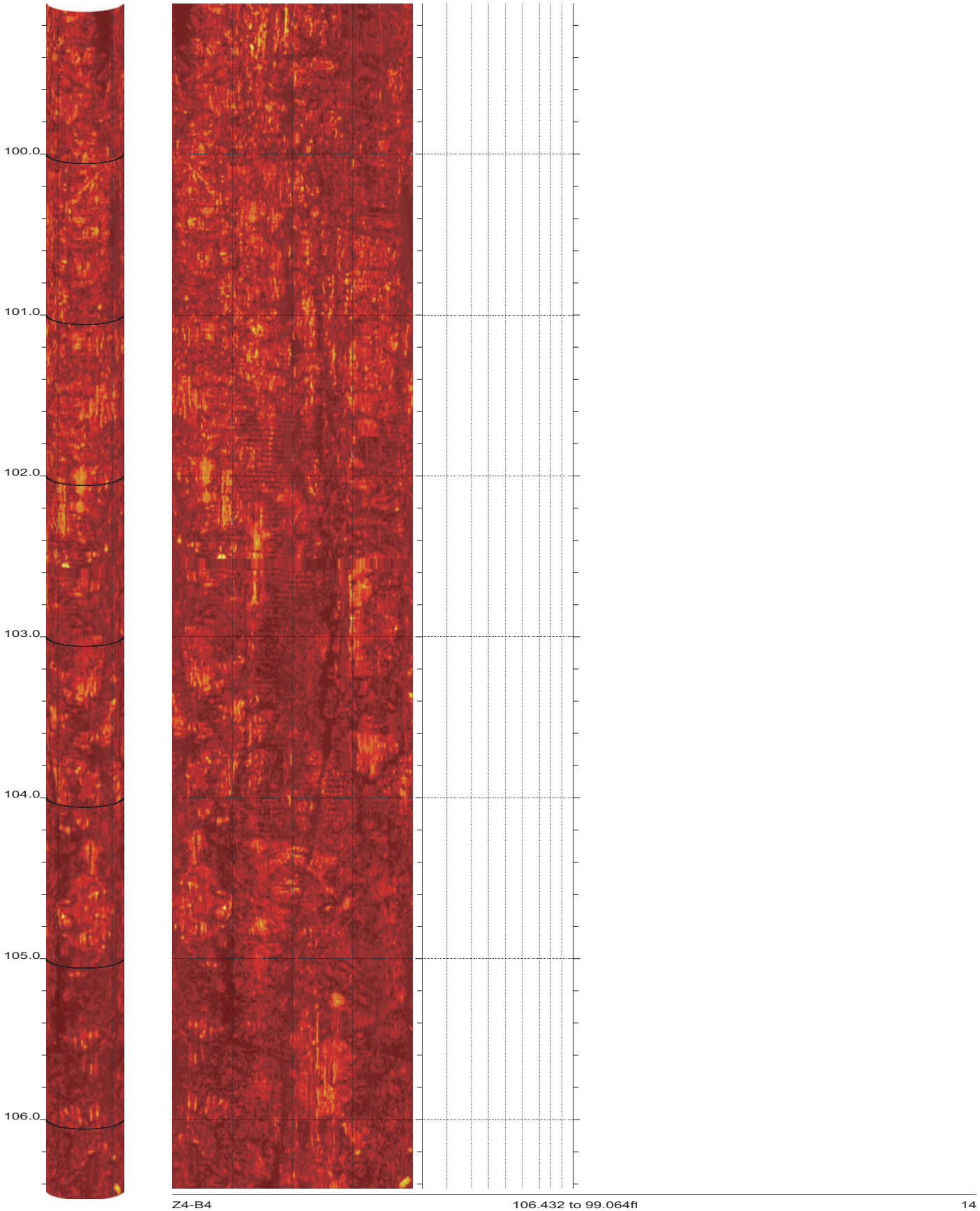
100.0
101.0
102.0
103.0
104.0
105.0
106.0
Z4-B4
106.432 to 99.064ft
14

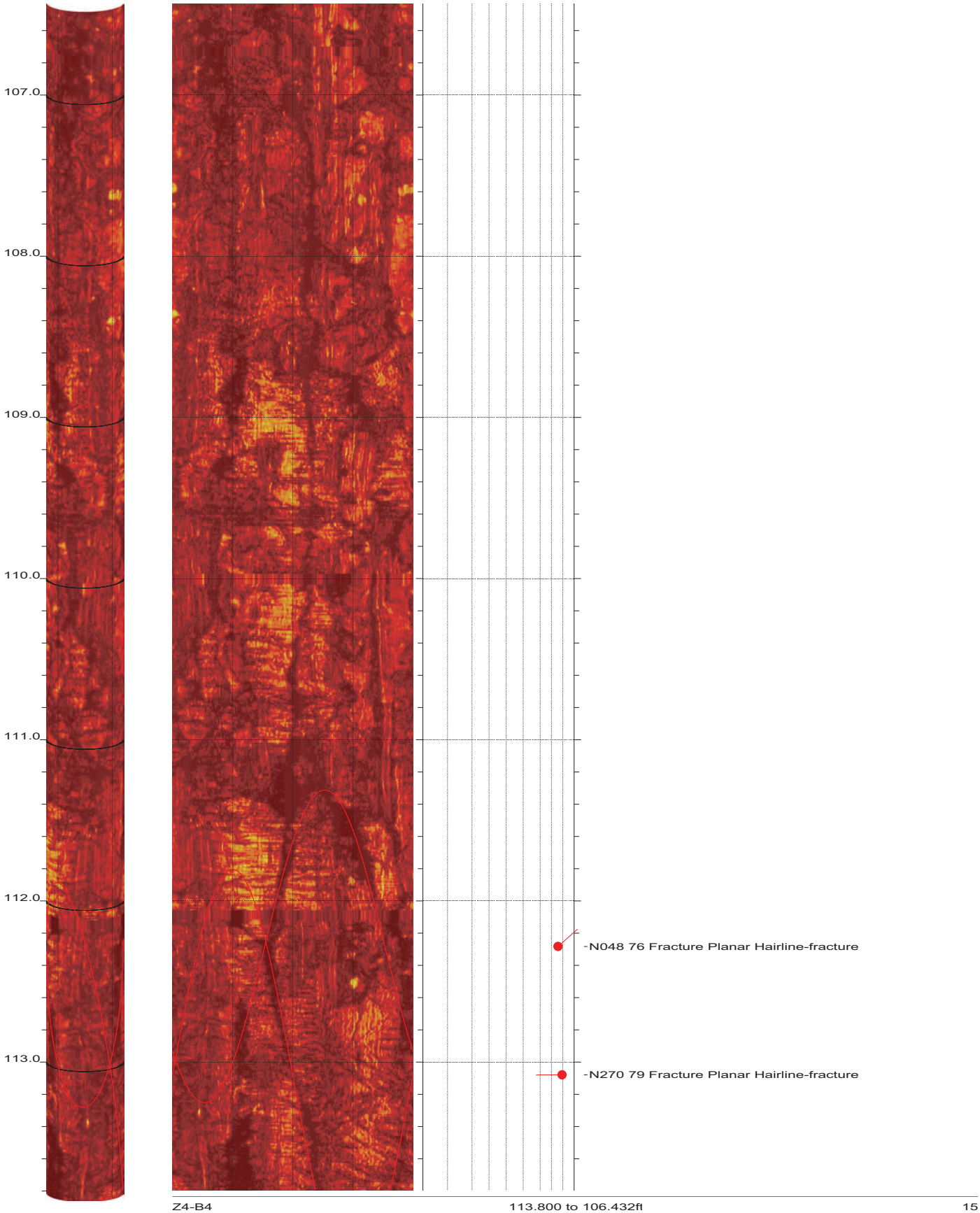

SR-710 Boring Z4-B4 Acoustic Televiewer Dips rev 1 Sheet 15 of 37

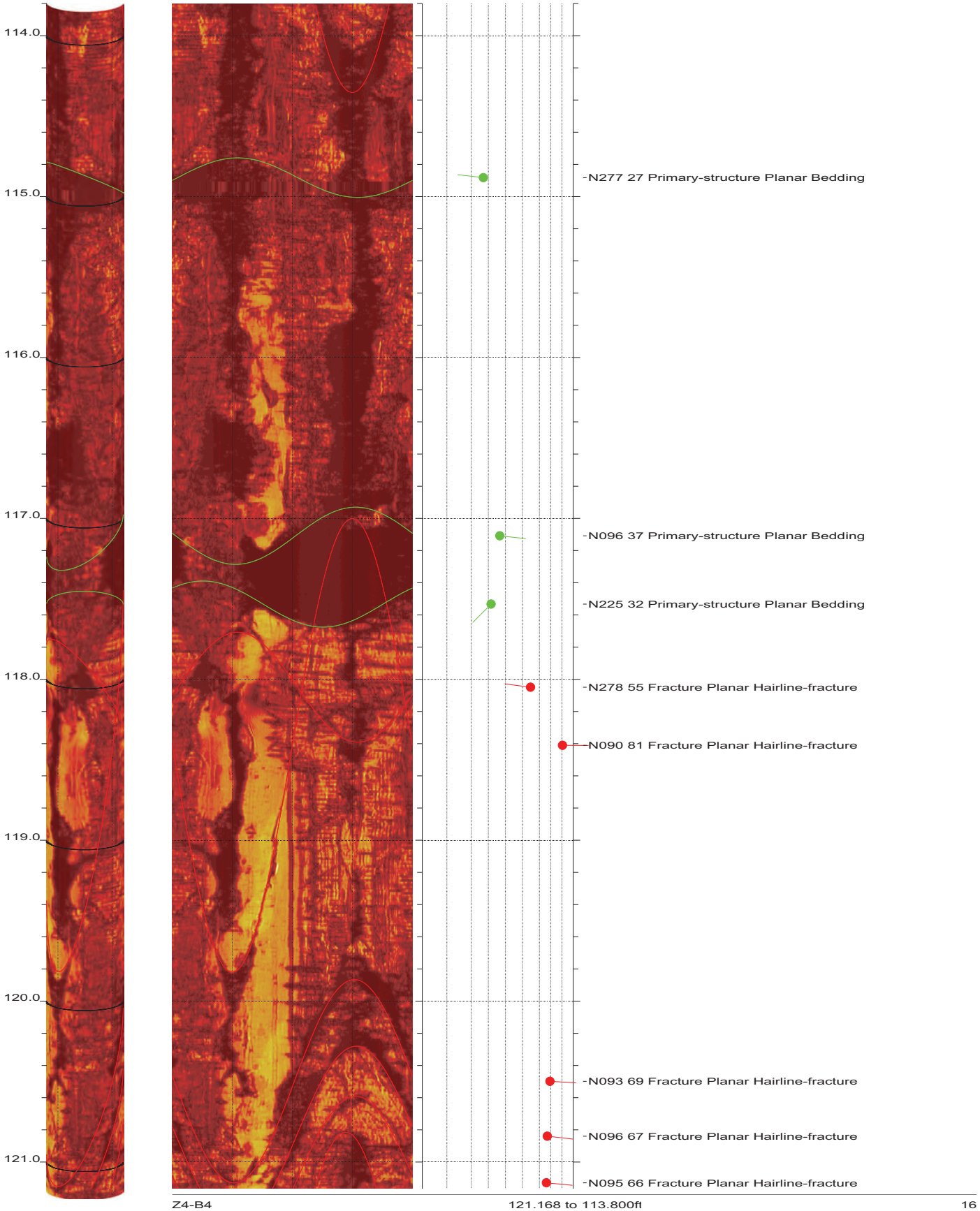

SR-710 Boring Z4-B4 Acoustic Televiewer Dips rev 1 Sheet 16 of 37

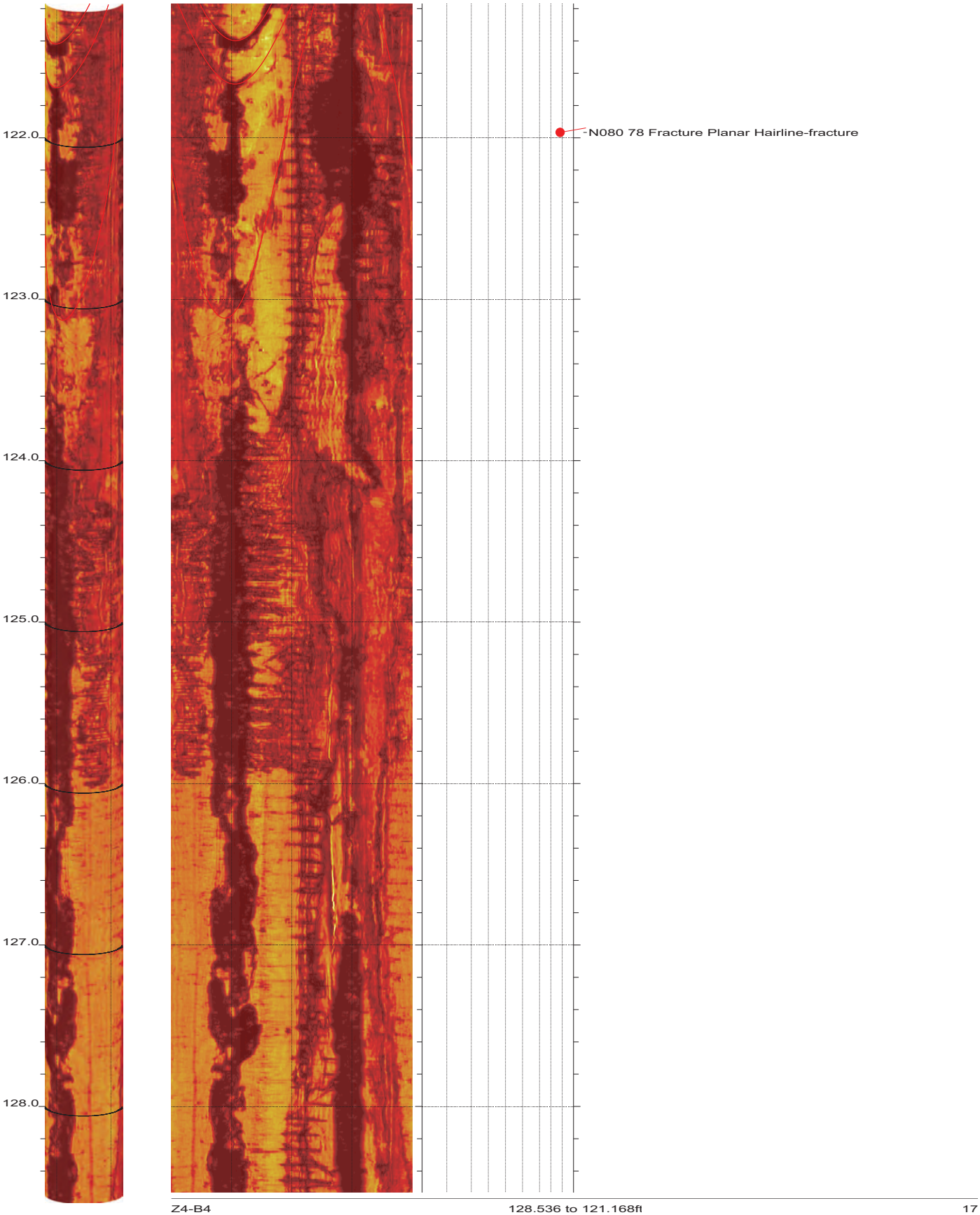
122.0
123.0
124.0
125.0
126.0
127.0
128.0
N080 78 Fracture Planar Hairline-fracture
Z4-B4
128.536 to 121.168ft
17

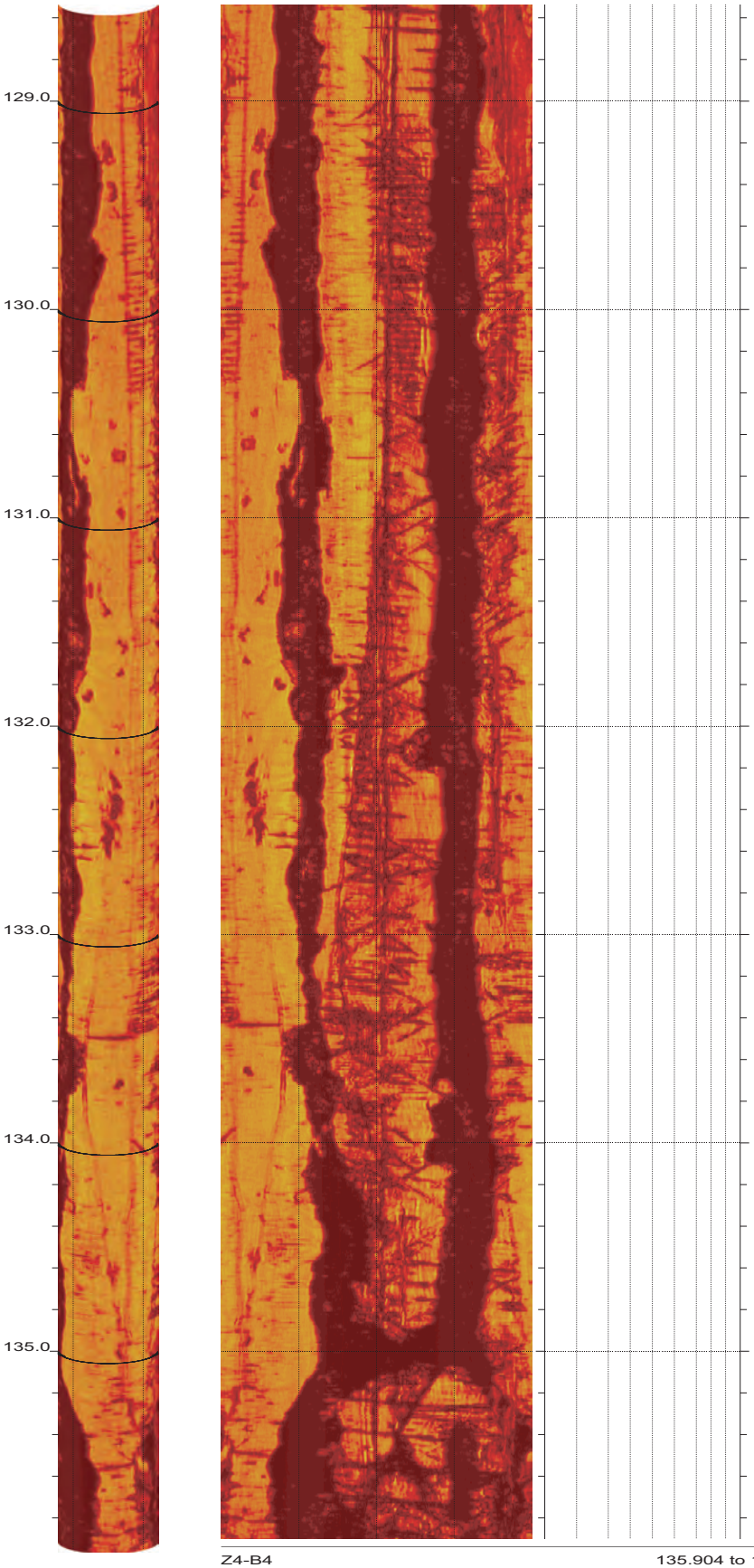

Z4-B4 135.904 to 128.536ft 18

SR-710 Boring Z4-B4 Acoustic Televiewer Dips rev 1 Sheet 18 of 37

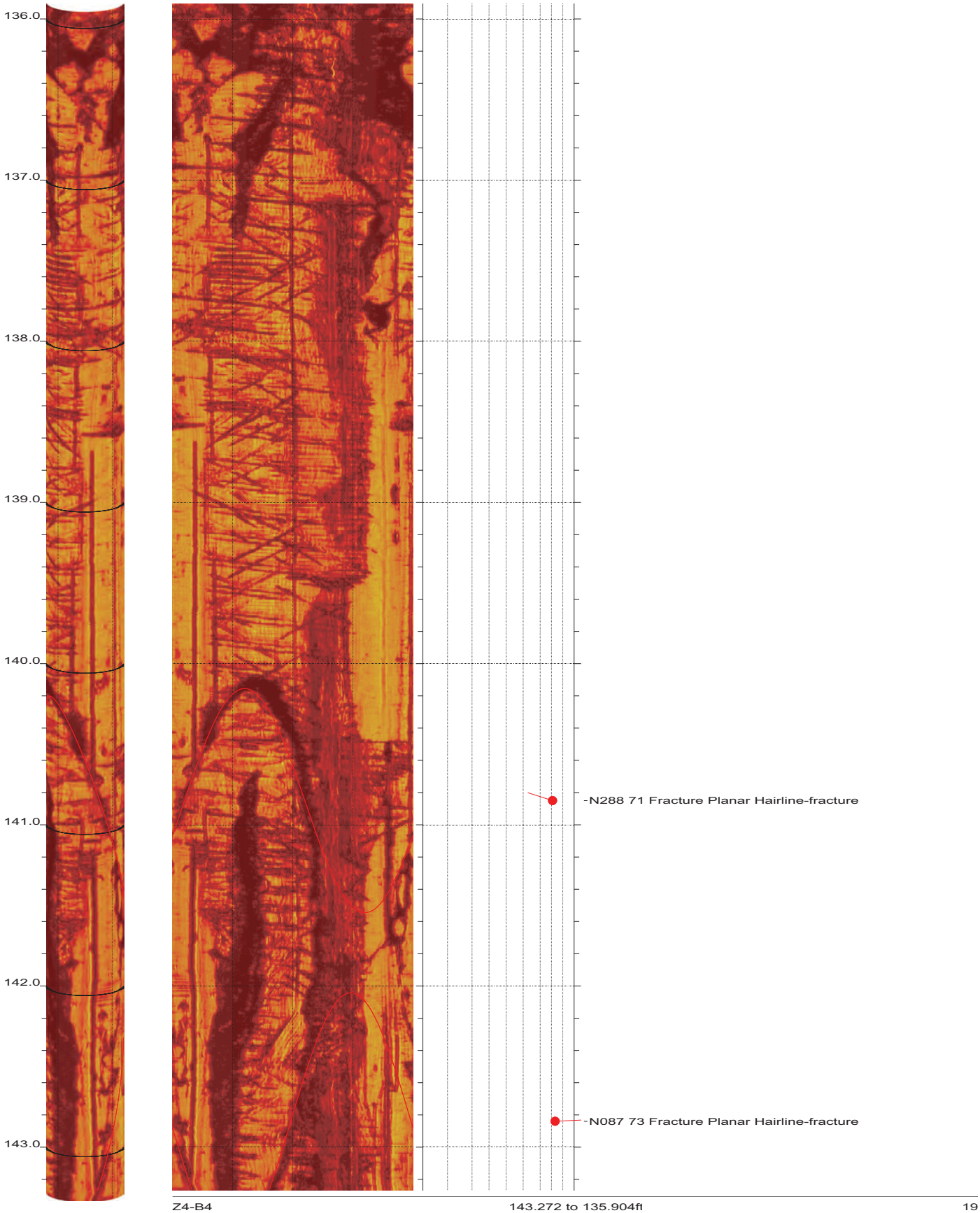

SR-710 Boring Z4-B4 Acoustic Televiewer Dips rev 1 Sheet 19 of 37

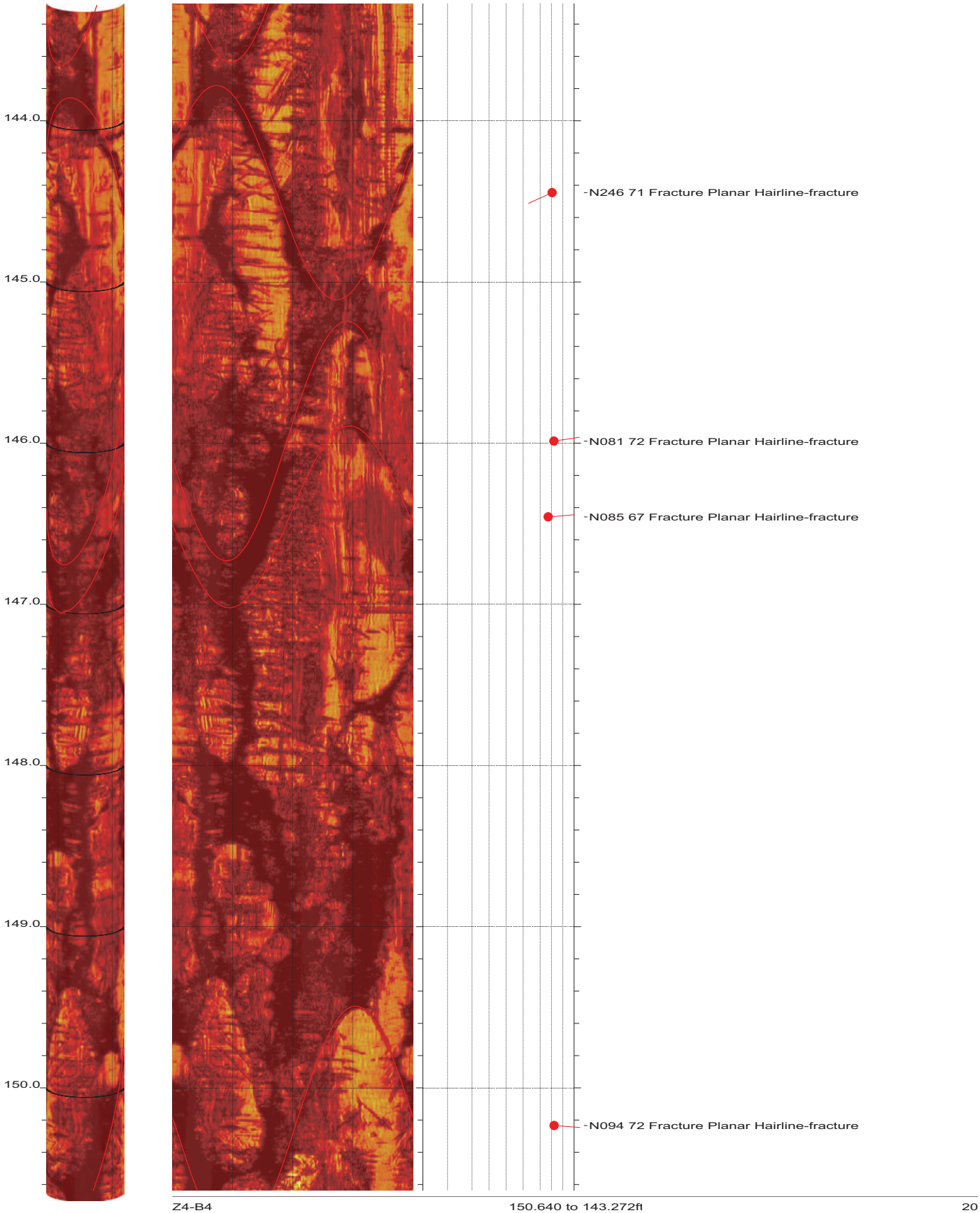

SR-710 Boring Z4-B4 Acoustic Televiewer Dips rev 1 Sheet 20 of 37

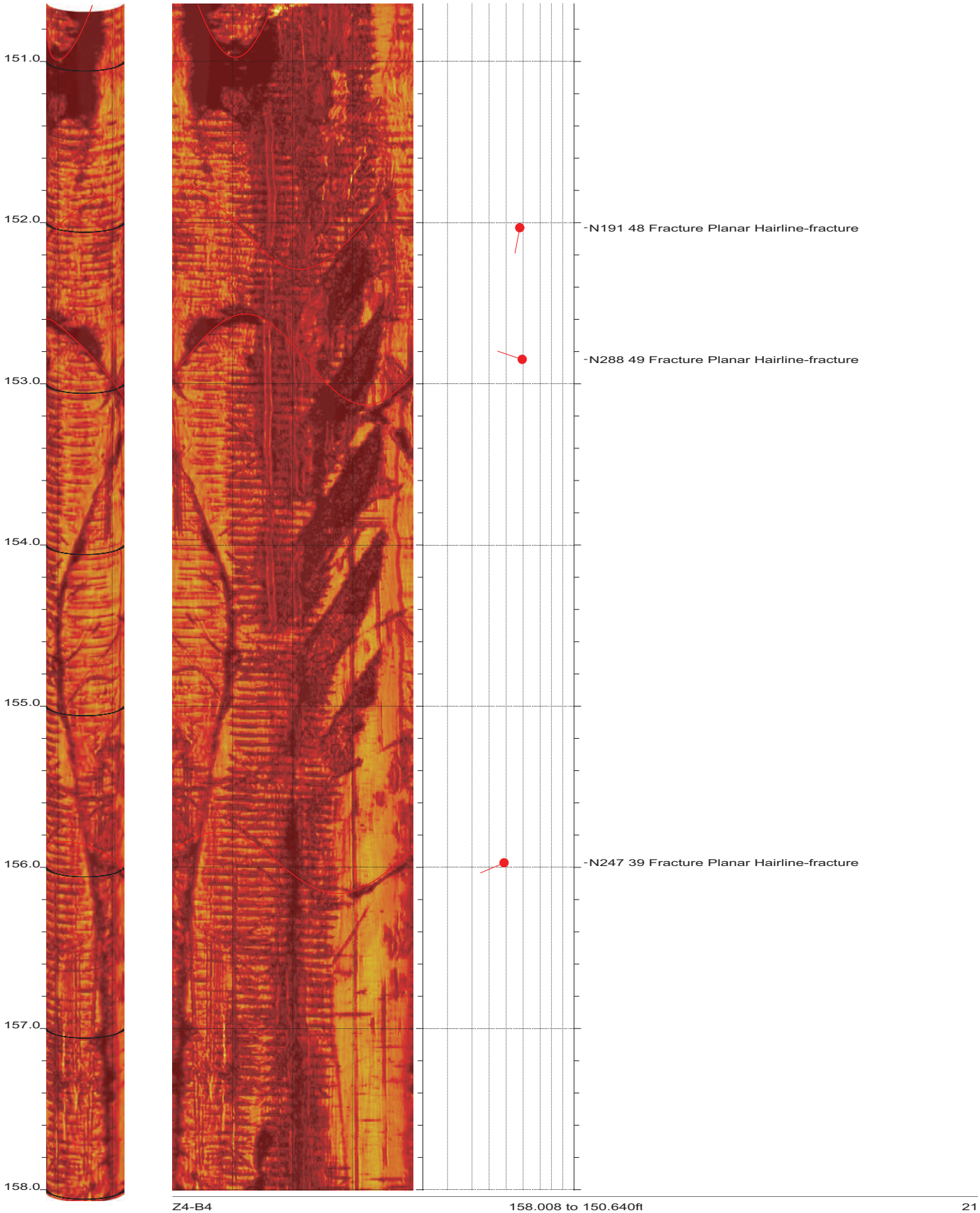

SR-710 Boring Z4-B4 Acoustic Televiewer Dips rev 1 Sheet 21 of 37

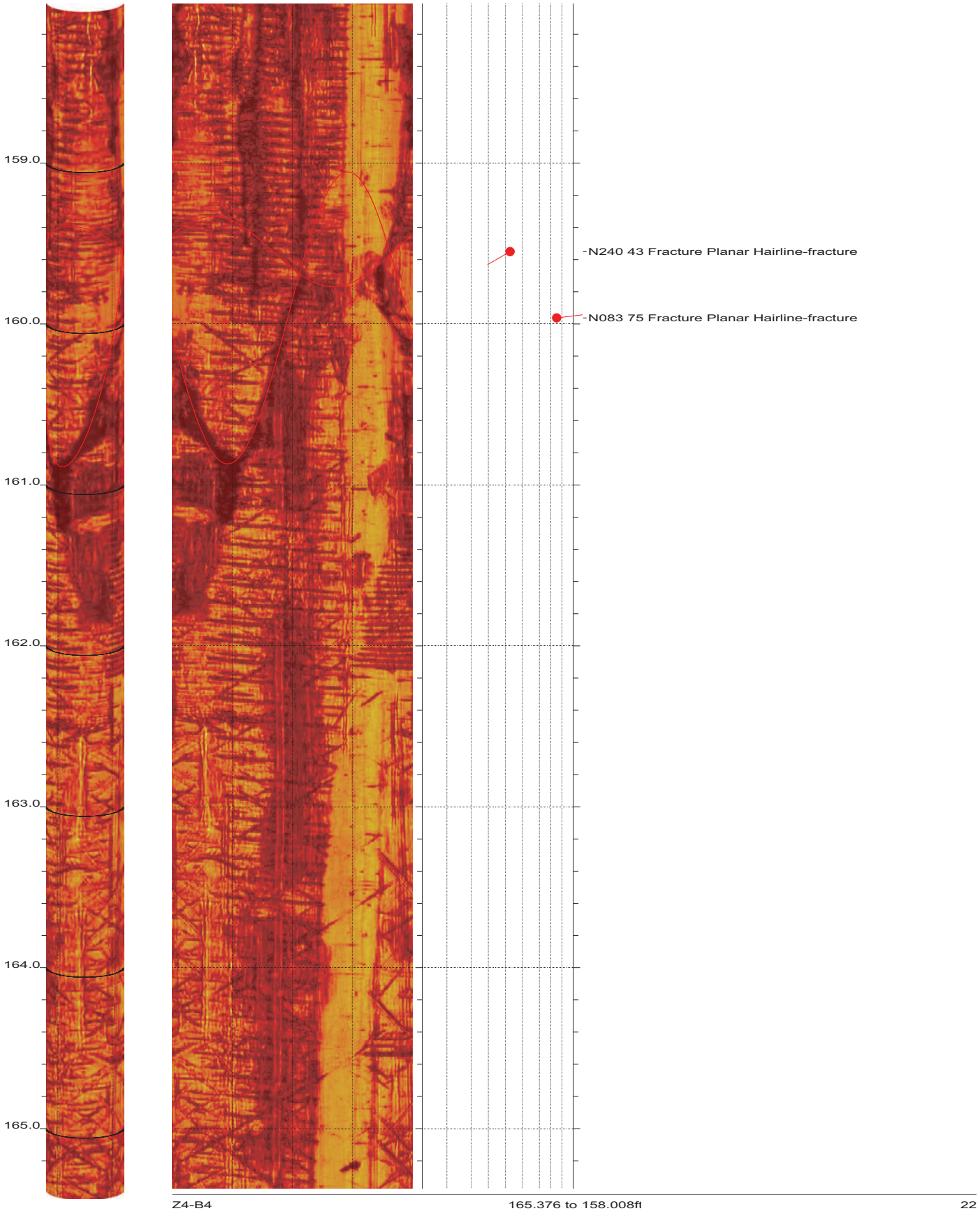

SR-710 Boring Z4-B4 Acoustic Televiewer Dips rev 1 Sheet 22 of 37

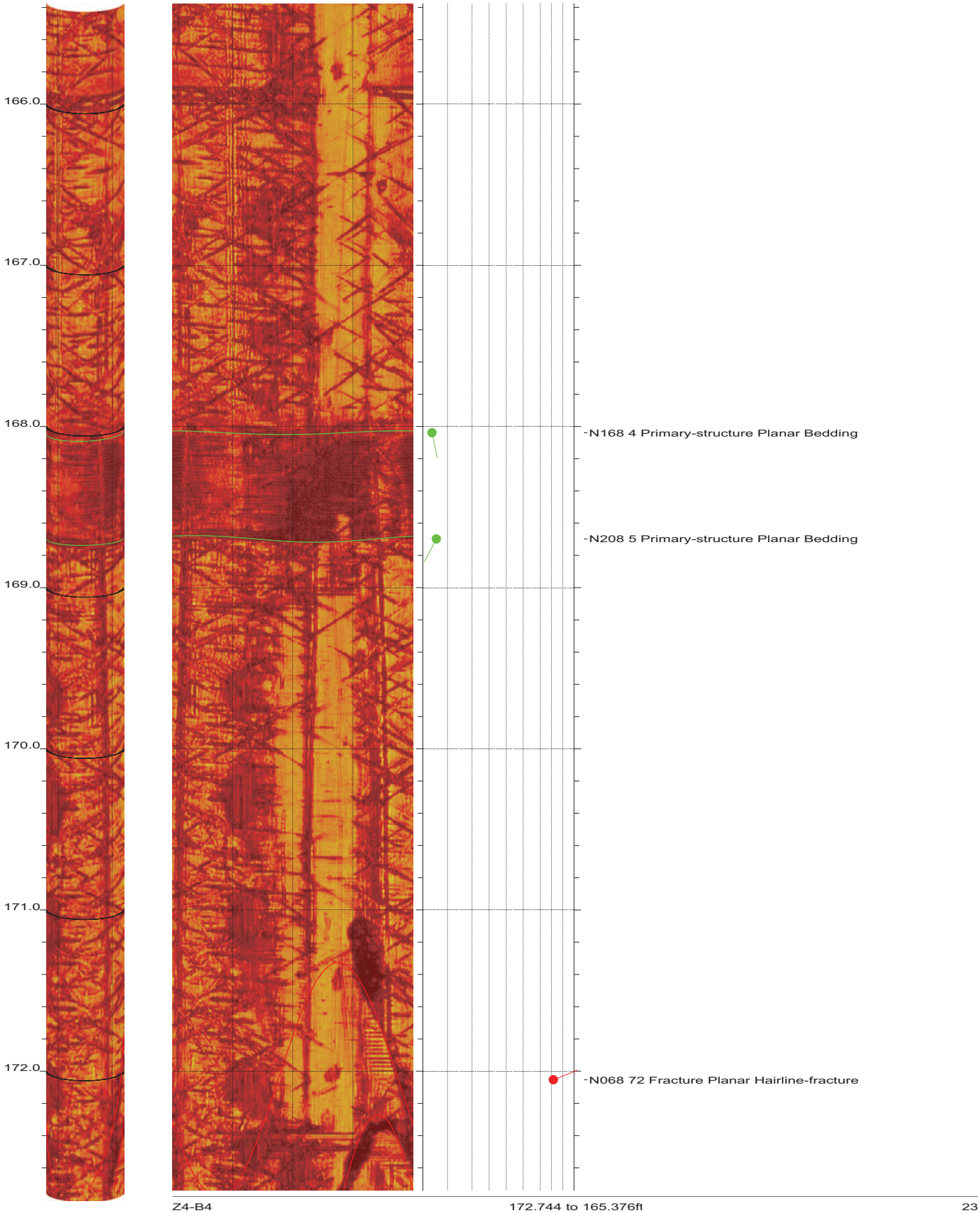

SR-710 Boring Z4-B4 Acoustic Televiewer Dips rev 1 Sheet 23 of 37

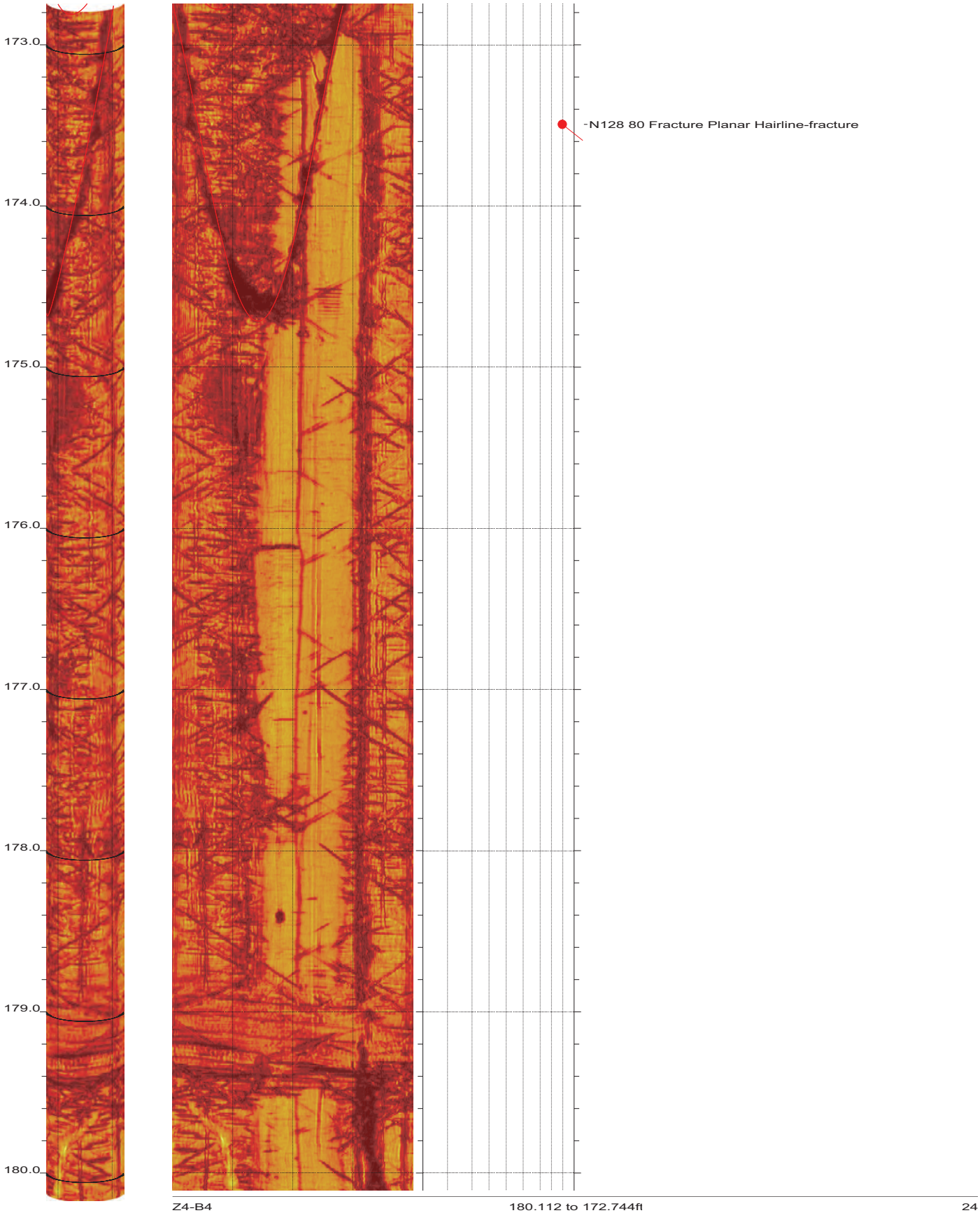
173.0
174.0
175.0
176.0
177.0
178.0
179.0
180.0
N128 80 Fracture Planar Hairline-fracture
Z4-B4
180.112 to 172.744ft
24

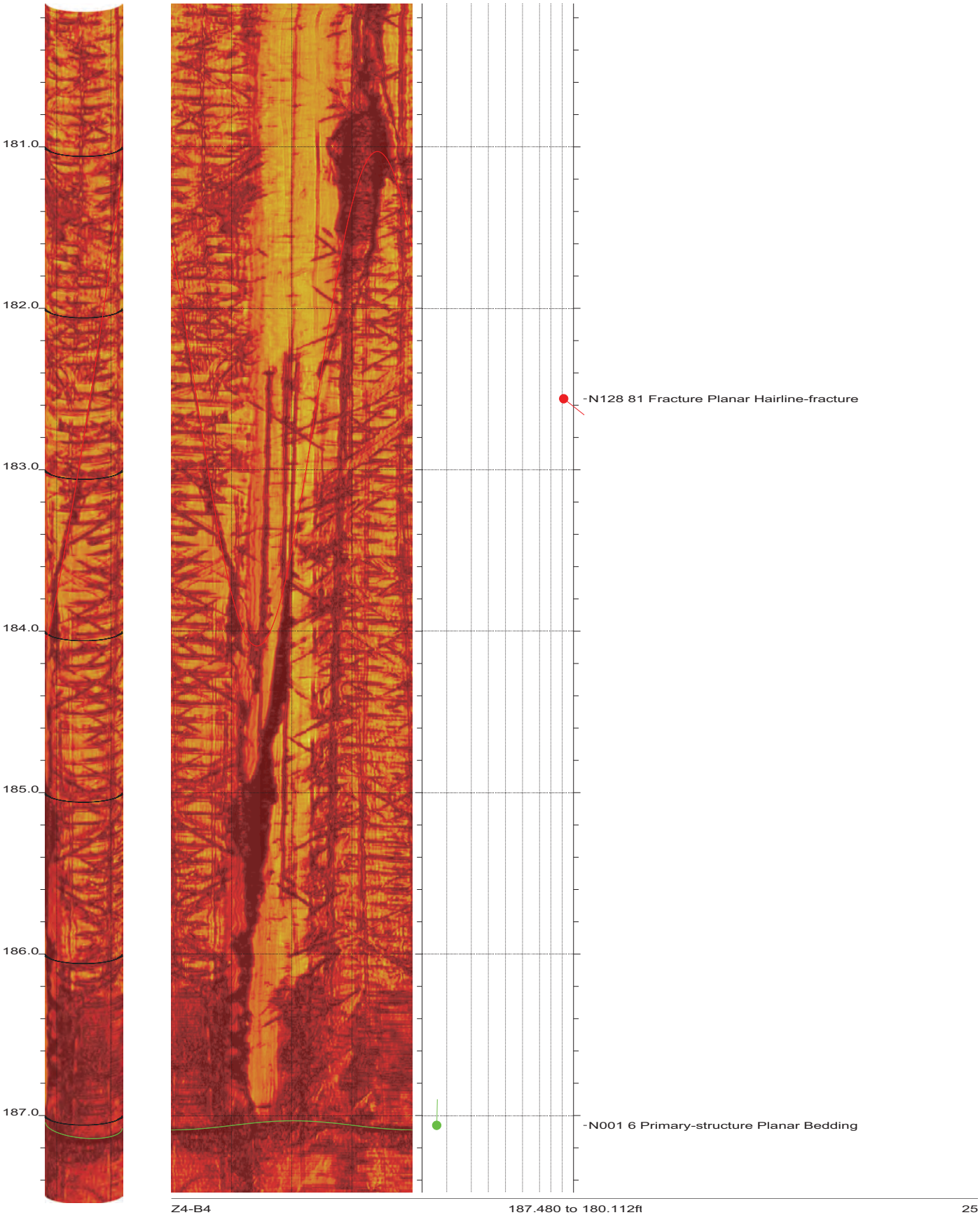
181.0
182.0
183.0
184.0
185.0
186.0
187.0
N128 81 Fracture Planar Hairline-fracture
N001 6 Primary-structure Planar Bedding
Z4-B4
187.480 to 180.112ft
25

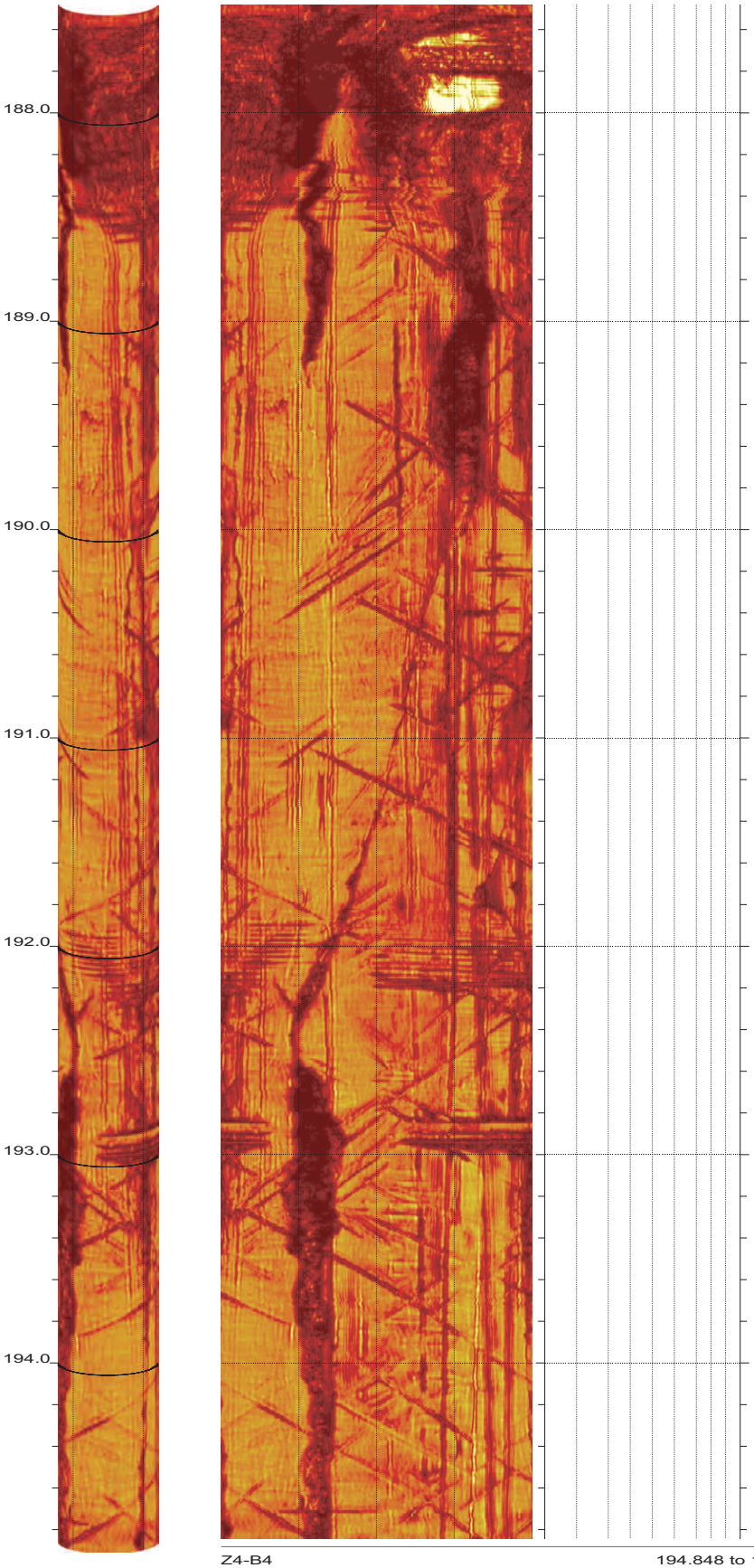

Z4-B4 194.848 to 187.480ft 26

SR-710 Boring Z4-B4 Acoustic Televiewer Dips rev 1 Sheet 26 of 37

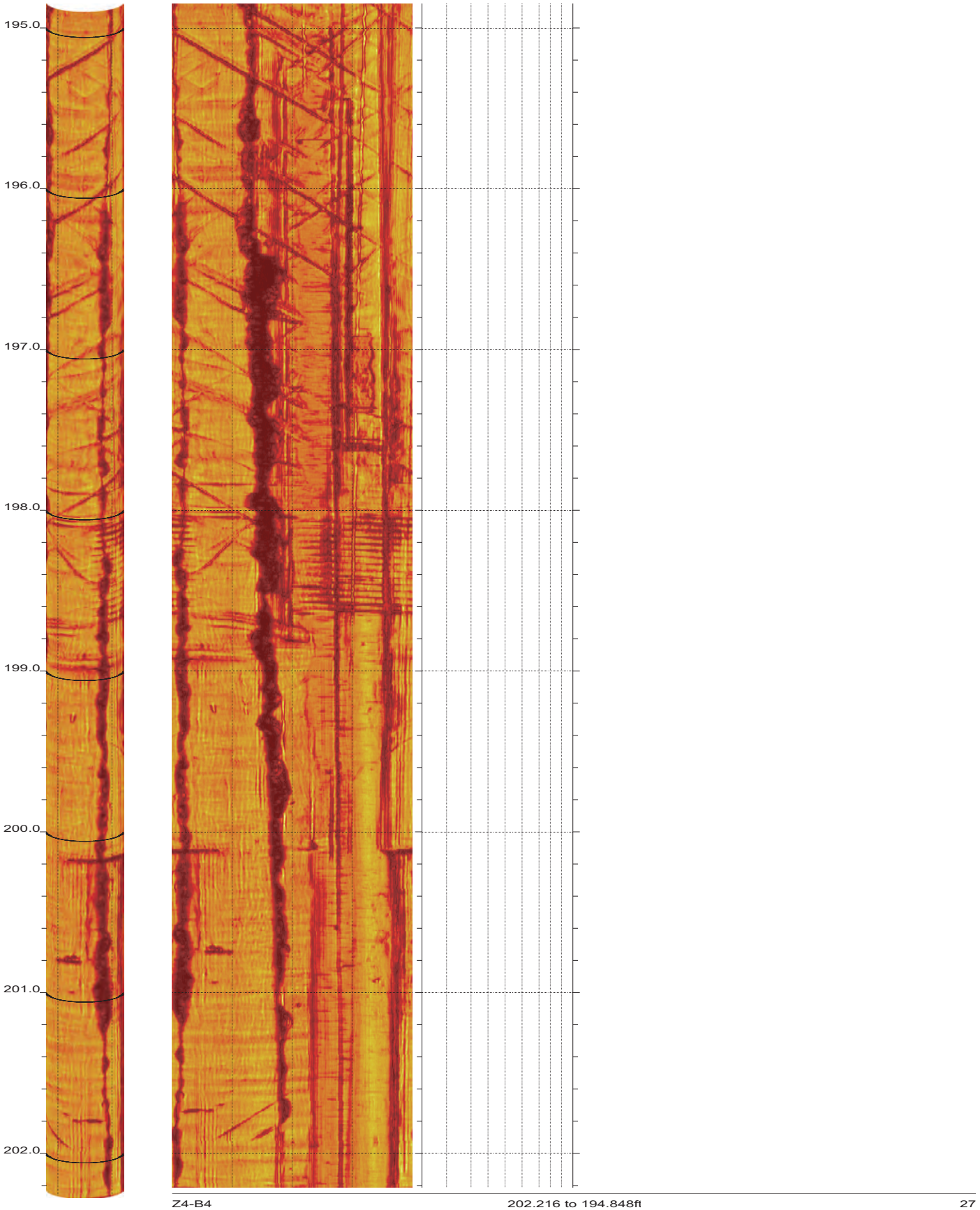

SR-710 Boring Z4-B4 Acoustic Televiewer Dips rev 1 Sheet 27 of 37

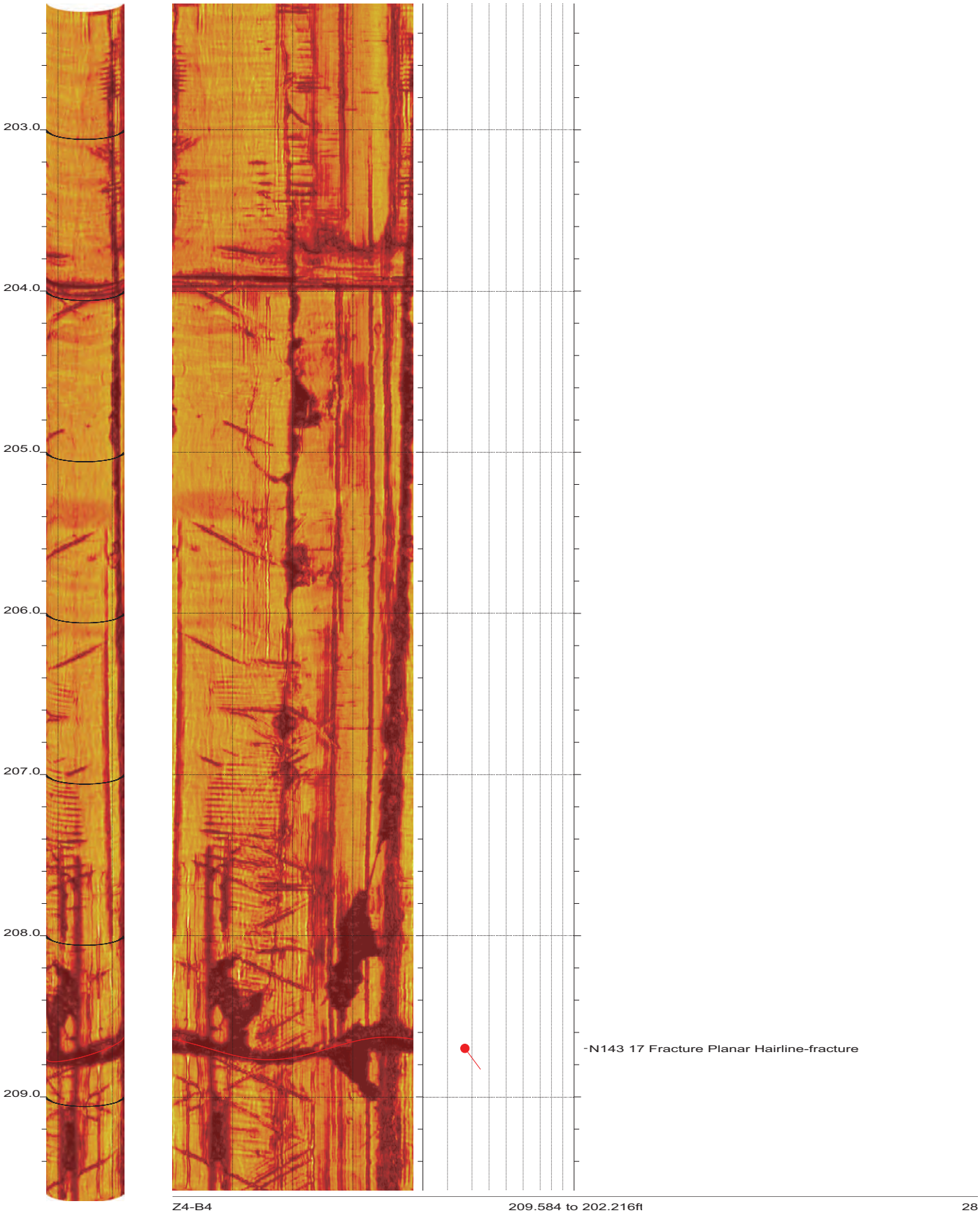

SR-710 Boring Z4-B4 Acoustic Televiewer Dips rev 1 Sheet 28 of 37

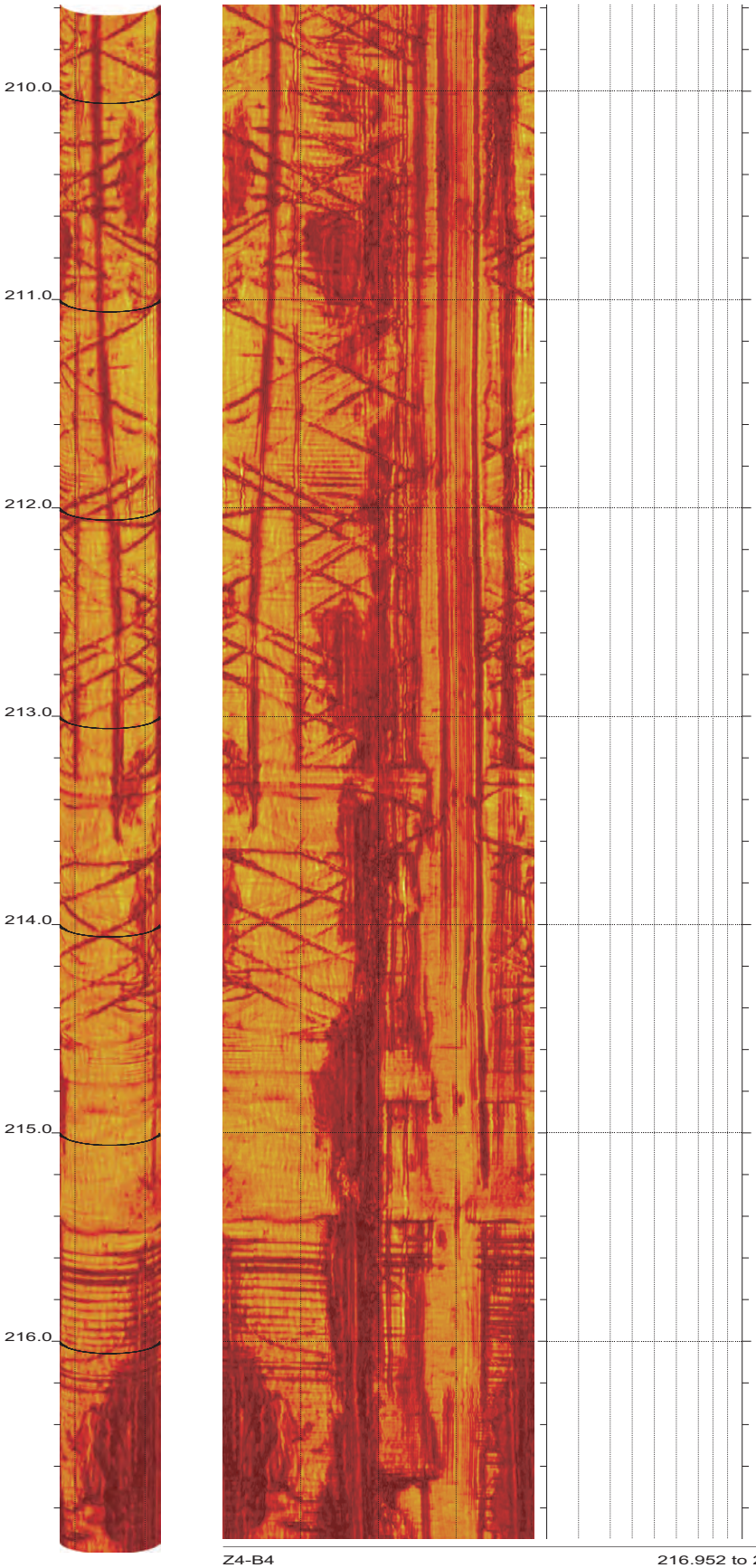

Z4-B4 216.952 to 209.584ft 29

SR-710 Boring Z4-B4 Acoustic Televiewer Dips rev 1 Sheet 29 of 37

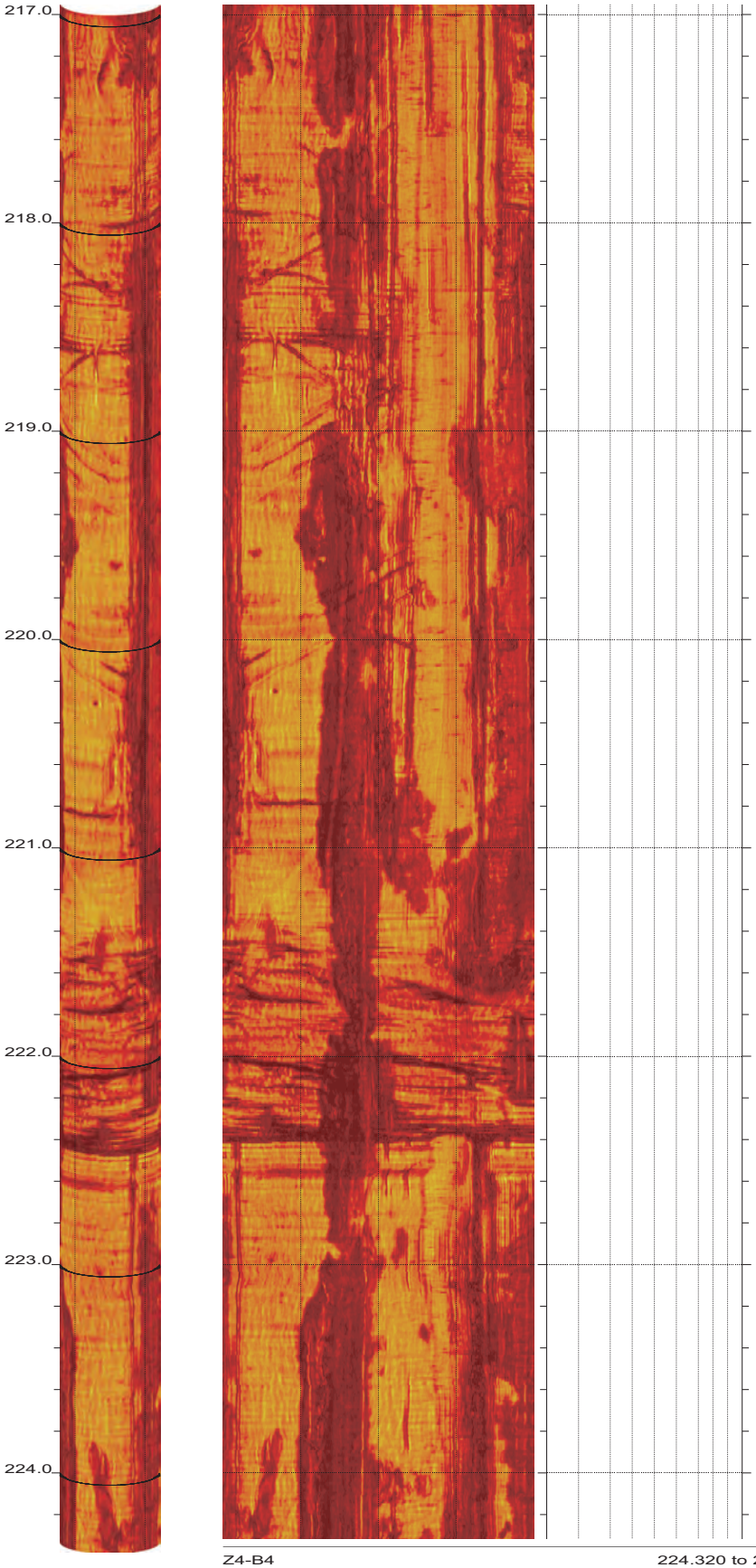

Z4-B4 224.320 to 216.952ft 30

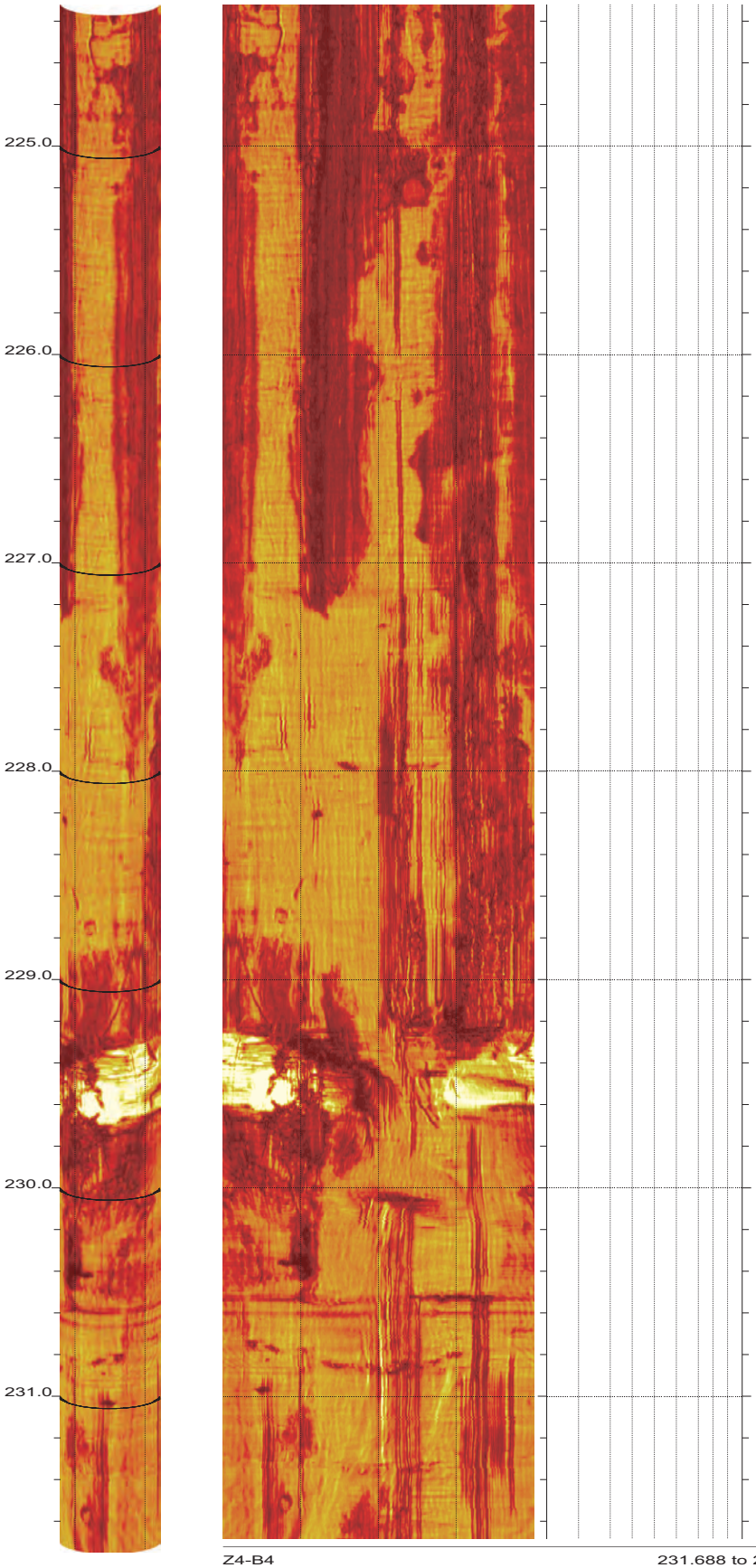

Z4-B4 231.688 to 224.320ft 31

SR-710 Boring Z4-B4 Acoustic Televiewer Dips rev 1 Sheet 31 of 37

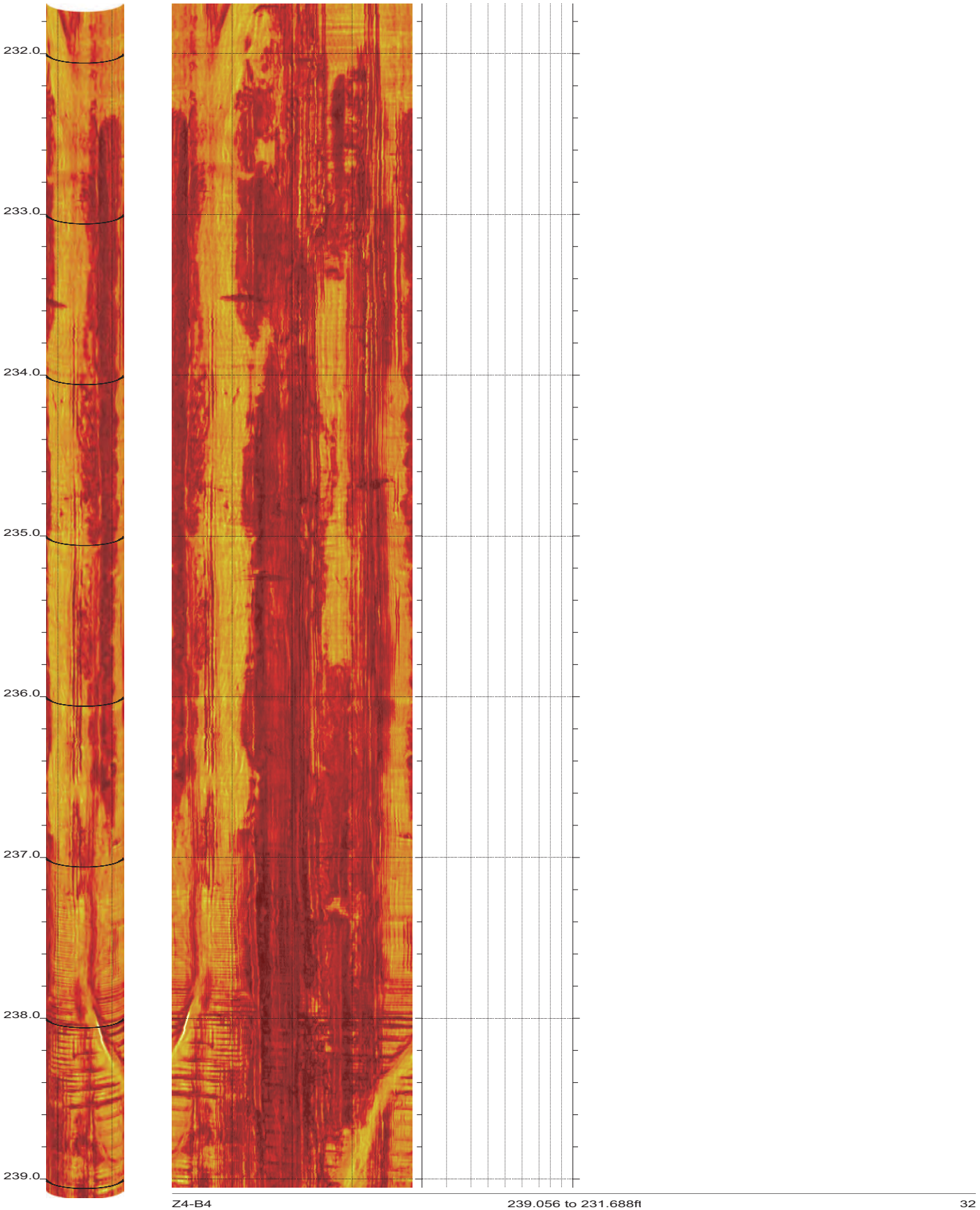
232.0
233.0
234.0
235.0
236.0
237.0
238.0
239.0
Z4-B4
239.056 to 231.688ft
32

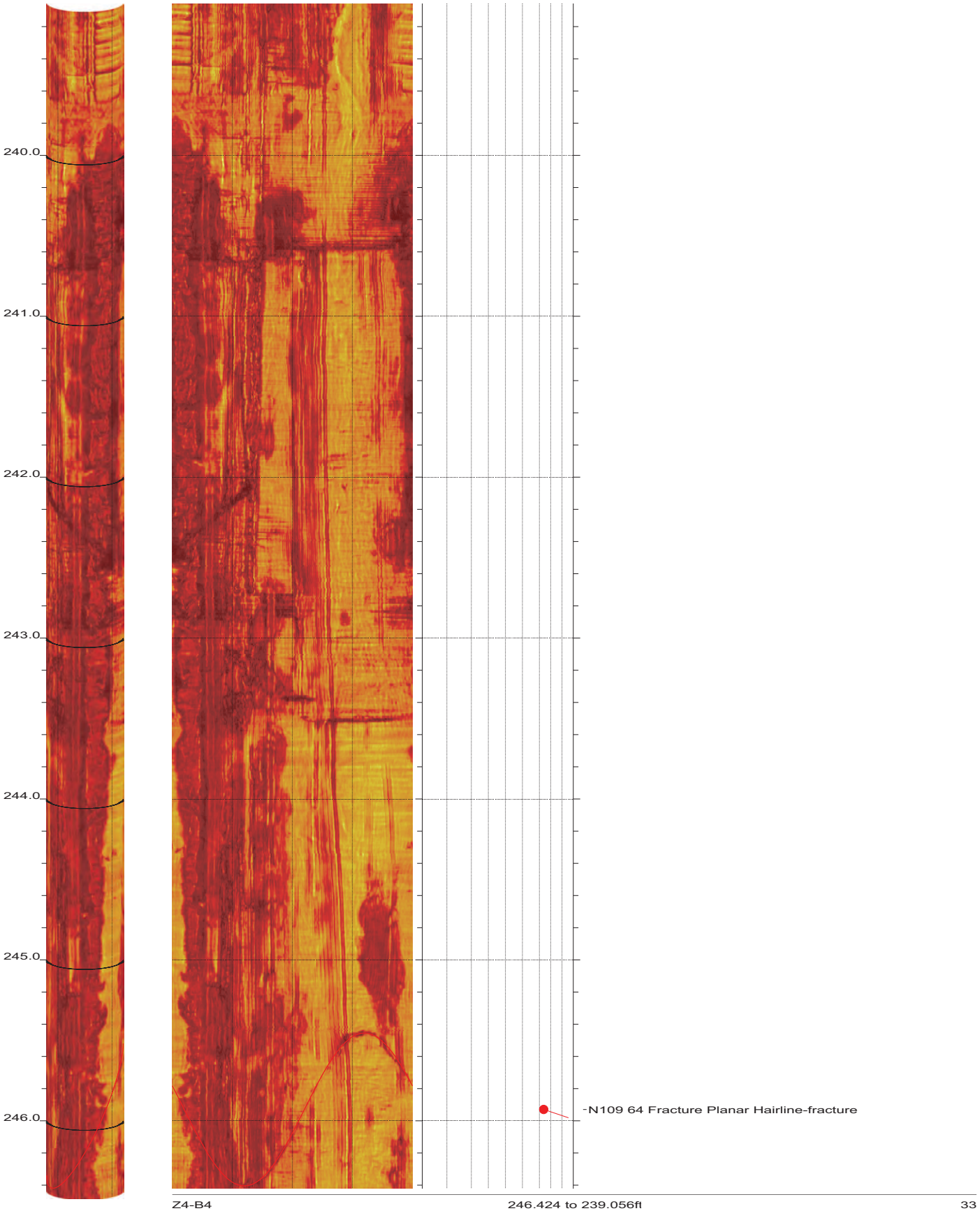

SR-710 Boring Z4-B4 Acoustic Televiewer Dips rev 1 Sheet 33 of 37

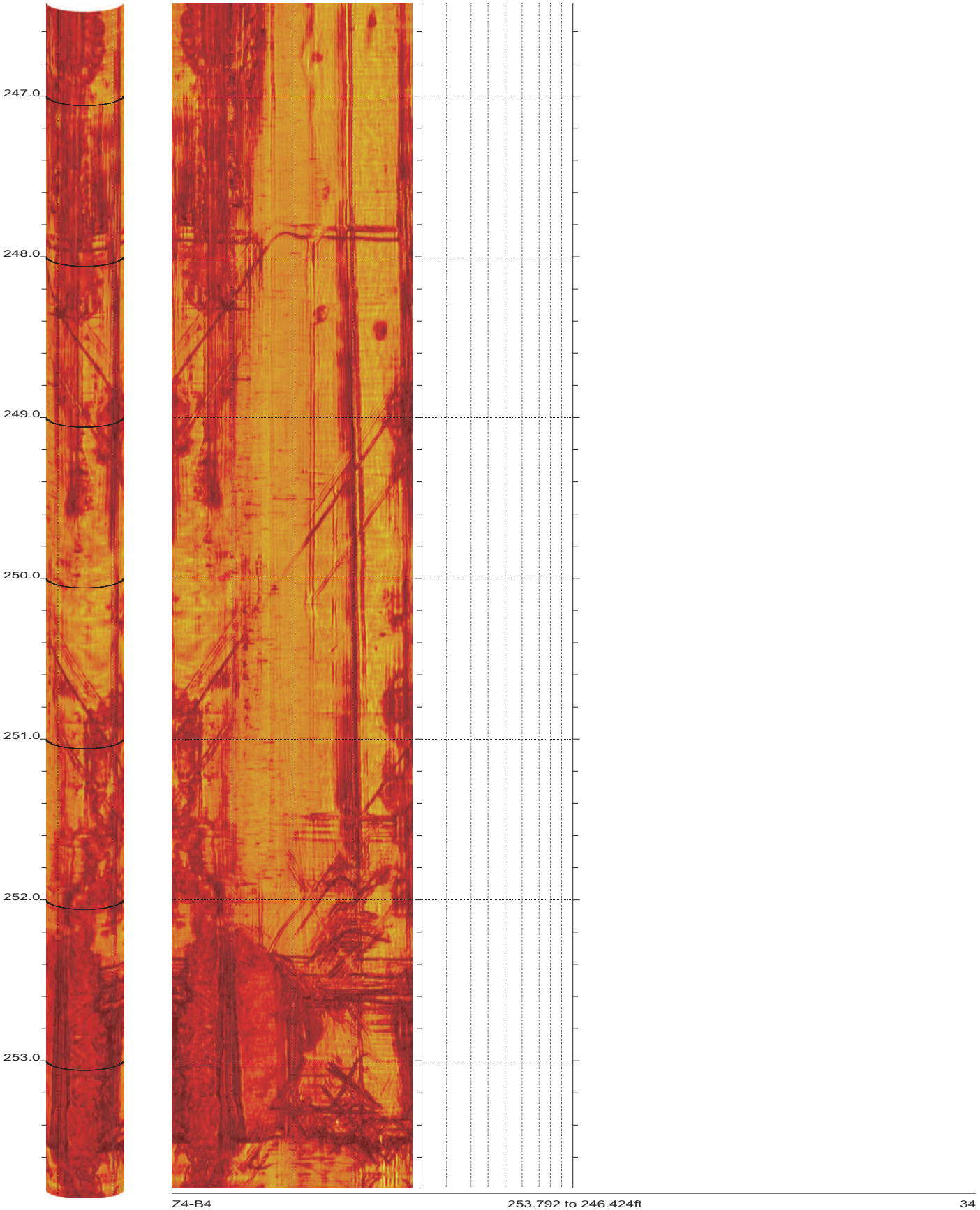
247.0
248.0
249.0
250.0
251.0
252.0
253.0
Z4-B4
253.792 to 246.424ft
34

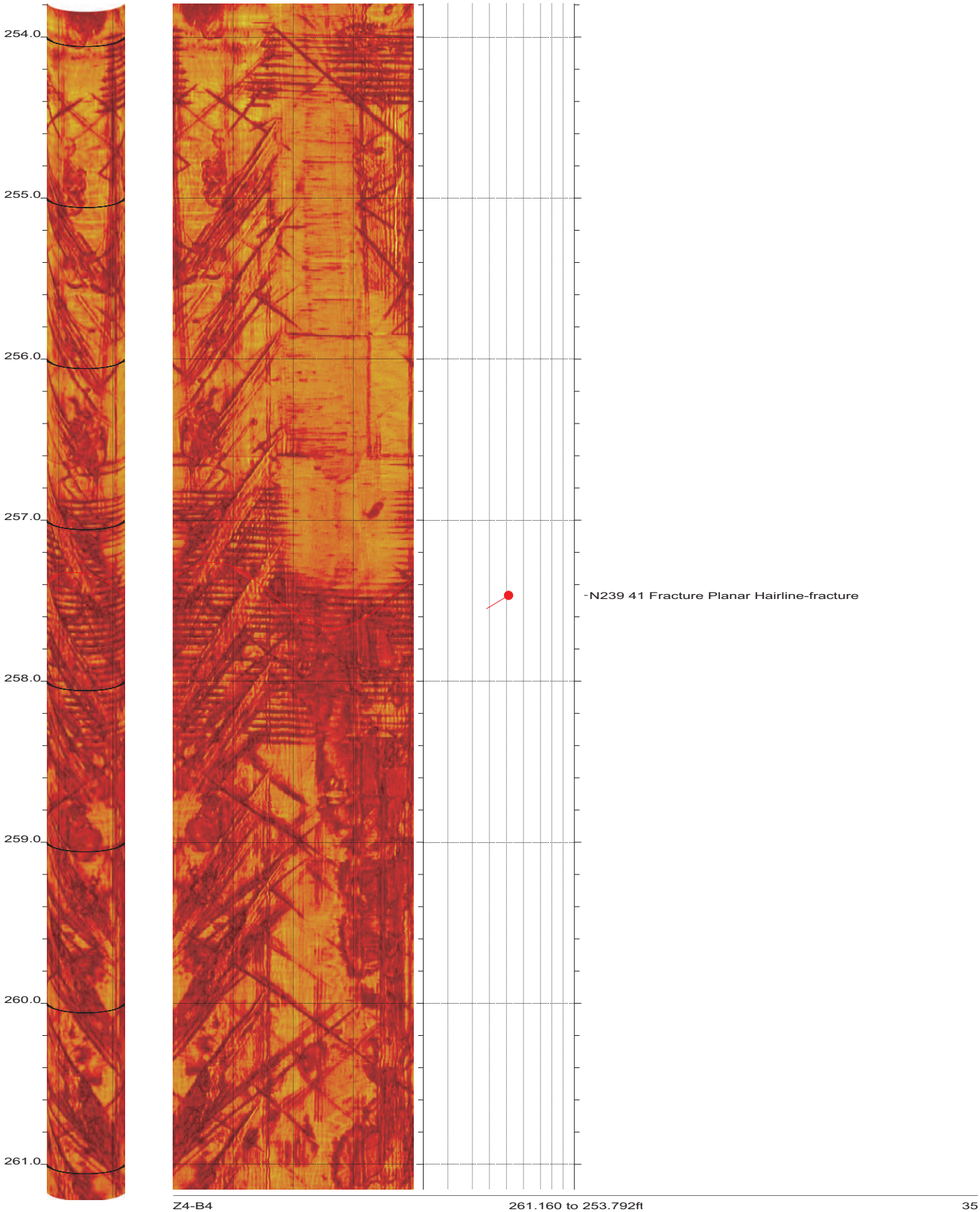

SR-710 Boring Z4-B4 Acoustic Televiewer Dips rev 1 Sheet 35 of 37

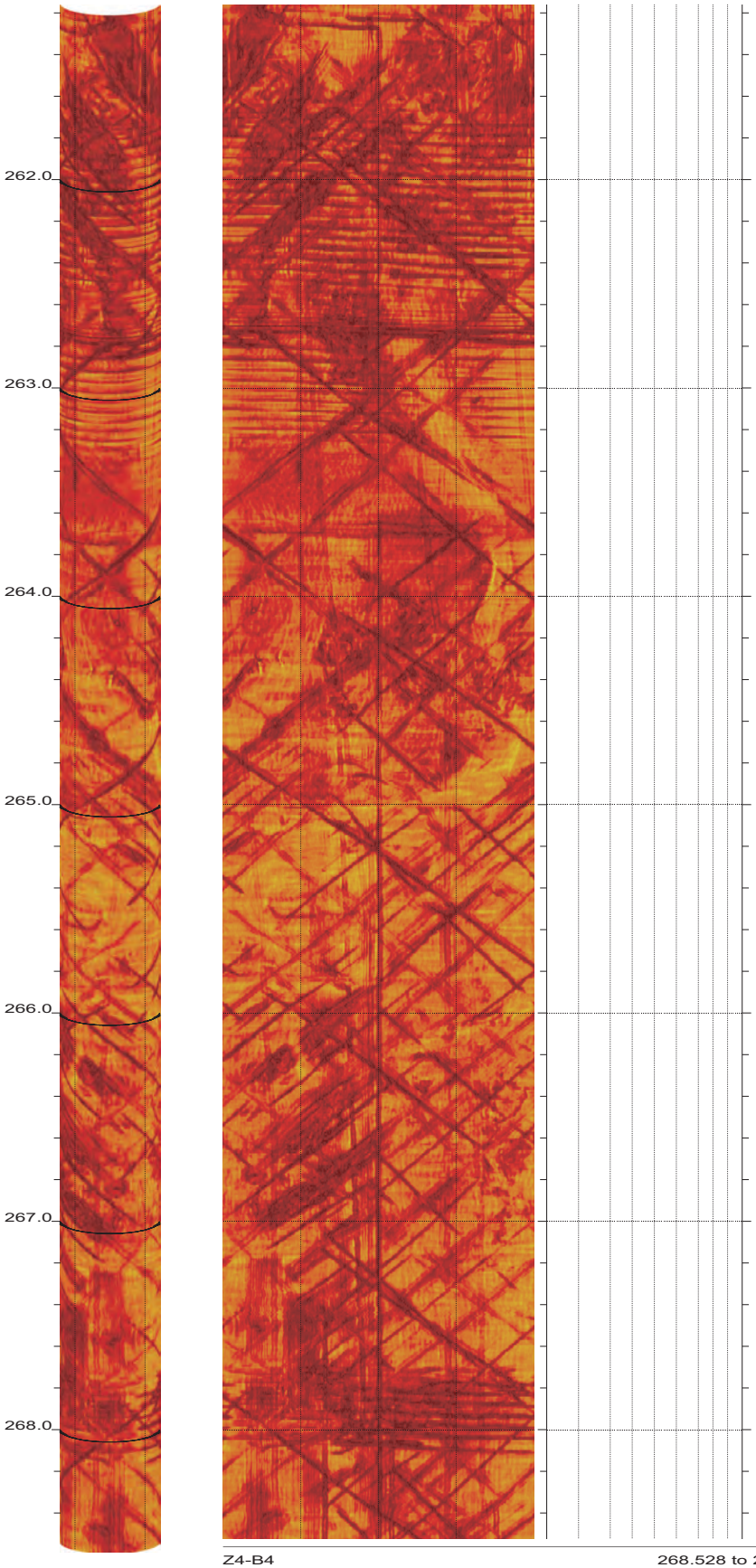

Z4-B4 268.528 to 261.160ft 36

SR-710 Boring Z4-B4 Acoustic Televiewer Dips rev 1 Sheet 36 of 37

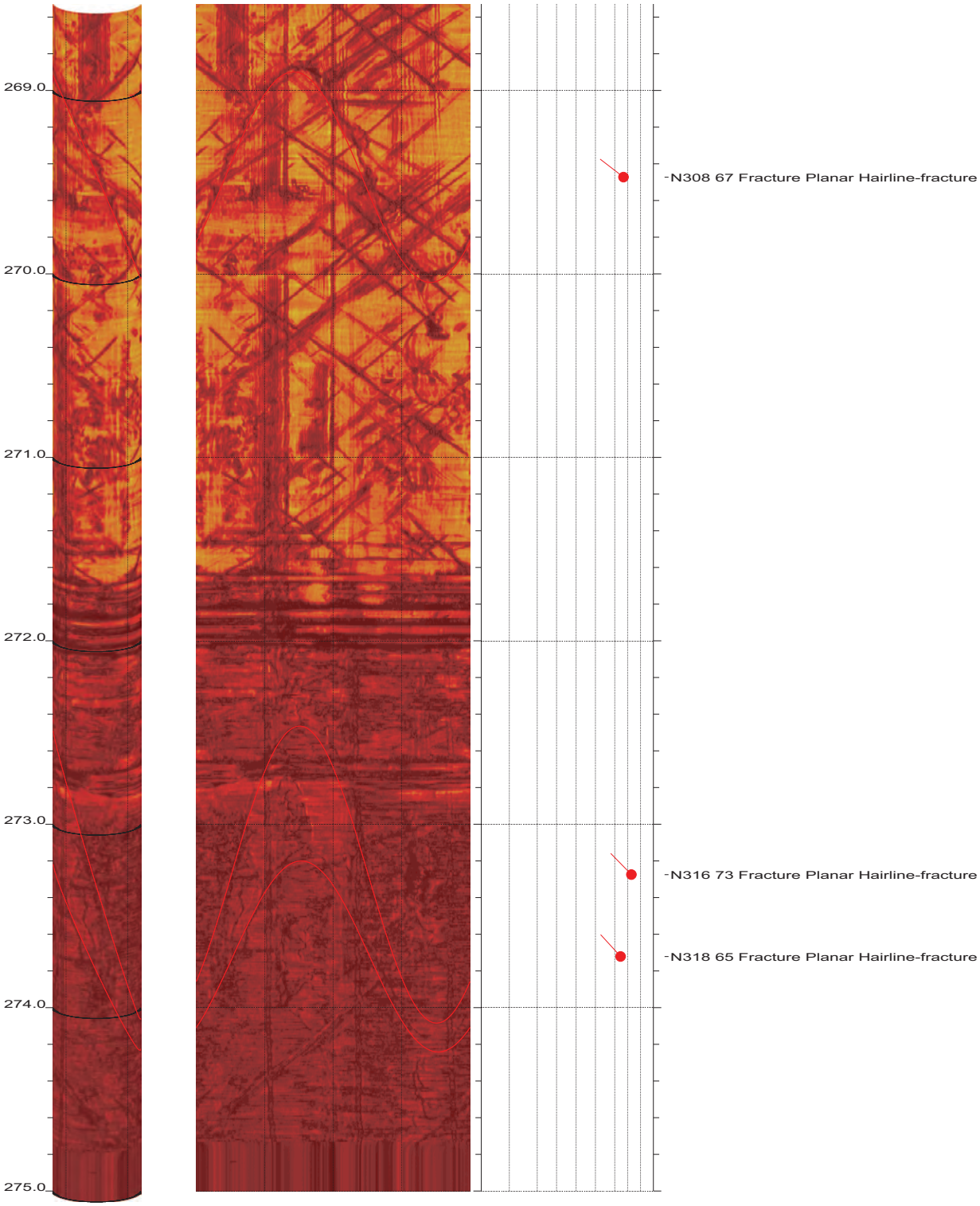
269.0
270.0
271.0
272.0
273.0
274.0
275.0
N308 67 Fracture Planar Hairline-fracture
N316 73 Fracture Planar Hairline-fracture
N318 65 Fracture Planar Hairline-fracture

APPENDIX D

GEOPHYSICAL LOGGING SYSTEMS – NIST TRACEABLE CALIBRATION PROCEDURES AND CALIBRATION RECORDS

CALIBRATION PROCEDURE FOR

GEOVision SEISMIC RECORDER/LOGGER

Reviewed 4/6/06

Objective

The timing/sampling accuracy of seismic recorders or data loggers is required for several GEOVision field procedures including Seismic Refraction, Downhole Seismic Velocity Logging, and P-S Suspension Logging. This procedure describes the method for measuring the timing accuracy of a seismic data logger, such as the OYO Model 170, OYO/Robertson Model 3403, Geometrics Strataview or Geometrics Geode. The objective of this procedure is to verify that the timing accuracy of the recorder is accurate to within 1%.

Frequency of Calibration

The calibration of each GEOVision seismic data logger is twelve (12) months. In the case of rented seismic data loggers, calibration must be performed prior to use.

Test Equipment Required

The following equipment is required. Item #2 must have current NIST traceable calibration.

1. Function generator, Krohn Hite 5400B or equivalent
2. Frequency counter, HP 5315A or equivalent
3. Test cables, from item 1 to item 2, and from item 1 to subject data logger.

Procedure

This procedure is designed to be performed using the accompanying Seismograph Calibration Data Sheet with the same revision number. All data must be entered and the procedure signed by the technician performing the test.

1. Record all identification data on the form provided.
2. Connect function generator to data logger (such as OYO Model 170) using test cable
3. Connect the function generator to the frequency counter using test cable.

4. Set up generator to produce a 100.0 Hz, 0.25 volt (amplitude is approximate, modify as necessary to yield less than full scale waveforms on logger display) peak square wave or sine wave. Verify frequency using the counter and initial space on the data sheet.

5. Initialize data logger and record a data record of at least 0.1 second using a 100 microsecond or less sample period.

6. Measure the recorded square wave frequency by measuring the duration of 9 cycles of data. This measurement can be made using the data logger display device, or by printing out a paper tape. If a paper tape can be printed, the resulting printout must be attached to this procedure. Record the data in the space provided.

7. Repeat steps 5 and 6 three more times using separate files.

Criteria

The duration for 9 cycles in any file must be 90.0 milliseconds plus or minus 0.9 milliseconds, corresponding to an average frequency for the nine cycles of 100.0 Hz plus or minus 1 Hz (obtained by dividing 9 cycles by the duration in milliseconds).

If the results are outside this range, the data logger must be marked with a GEOVision REJECT tag until it can be repaired and retested.

If results are acceptable affix label indicating the initials of the person performing the calibration, the date of calibration, and the due date for the next calibration (12 months).

Procedure Approval

Approved by:

John G. Diehl	President
Name	Title
Signature	April 6, 2006
	Date

Client Approval (if required):

Name	Title
Signature	Date

GEOVision SUSPENSION PS SEISMIC LOGGER/RECORDER

CALIBRATION PROCEDURE

Reviewed 7/21/08

Objective

The timing/sampling accuracy of seismic recorders or data loggers is required for several GEOVision field procedures including Seismic Refraction, Downhole P-S Seismic Velocity Logging, and Suspension P-S Seismic Velocity Logging. This procedure describes the method for measuring the timing accuracy of a seismic data logger, such as the OYO Model 170 or OYO/Robertson Model 3403. The objective of this procedure is to verify that the timing accuracy of the recorder is accurate to within 1%.

Frequency of Calibration

The calibration of each GEOVision seismic data logger is twelve (12) months. In the case of rented seismic logger/recorders, calibration must be performed prior to use.

Test Equipment Required

The following equipment is required. Item #2 must have current NIST traceable calibration.

1. Function generator, Krohn Hite 5400B or equivalent
2. Frequency counter, HP 5315A or equivalent
3. Test cables, from item 1 to item 2, and from item 1 to subject data logger.

Procedure

This procedure is designed to be performed using the accompanying Suspension P-S Seismic Logger/Recorder Calibration Data Form with the same revision number. All data must be entered and the procedure signed by the technician performing the test.

1. Record all identification data on the form provided.
2. Connect function generator to data logger (such as OYO Model 170) using test cable
3. Connect the function generator to the frequency counter using test cable.
4. Set signal generator to target frequency specified on data form, 0.25 volt (amplitude is approximate, modify as necessary to yield less than full scale waveforms on

logger display) peak sine wave. Verify frequency using the counter and note actual frequency on the data form.

5. Set data logger to file length specified on data form and record a data file to disk. Note file name on data form.

6. Measure the duration of 9 complete sine wave cycles on the data file. This measurement must be made using the analysis program PSLOG.EXE version 1.00, and saved as a .sps pick file. Note the duration in milliseconds in the spaces provided on the data form. Calculate average recorded sine wave frequency for each channel pair (Hn, Hr, V) by dividing the duration by 9. Note the average frequency of each channel pair on the data form.

7. Repeat steps 4 through 6 until all target frequencies have been recorded, producing 6 separate data and pick files.

Criteria

The average frequency for the nine cycles (obtained by dividing 9 cycles by the duration in seconds) must be within plus or minus 1% of the actual frequency for each of the 6 records.

If the results are outside this range, the data logger must be marked with a GEOVision REJECT tag until it can be repaired and retested.

If results are acceptable affix label indicating the initials of the person performing the calibration, the date of calibration, and the due date for the next calibration (12 months).

Procedure Approval

Approved by:

John G. Diehl	President
Name	Title
Signature	July 21, 2008
	Date

Calibration Laboratory Approval (if required):

Name	Title
Signature	Date

EDISON ESI℠

A SOUTHERN CALIFORNIA EDISON® Company

Metrology
7300 Fenwick Lane
Westminster, CA 92683
Phone: 866-723-2257

Calibration Report

NVLAP Accredited
Calibration

GEOVision Geophysical Services
1124 Olympic Drive
Corona, CA 92881-3390

TEST NUMBER
558549

NVLAP®
Lab Code:105014-0

Manufacturer:	Oyo
Model Number:	3403
Description:	Unit, Suspension Telemetry,
Asset Number:	160024
Serial Number:	160024
PO Number:	8200-080122-01

Condition As Found:	In Tolerance
Condition As Left:	In Tolerance
Calibration Date:	08/01/2008
Calibration Due Date:	08/01/2009
Calibration Interval:	12 Months

Remarks:

This unit was calibrated with the customer's old procedure and specifications which have been reviewed by Metrology Engineering and documented in SCE Document M013684. The data can be found on page 2 of this report with the original observation data on page 3. The unit was then calibrated with the customer's new procedure and specification's which have been reviewed by Metrology Engineering and documented in SCE Document M013987. The data can be found on pages 4 and 5 of this report with the original observation data on page 6 of this report. Corrected Copy: This record created to add missing maximum error calculations on page 6 of 6. CAB 8-5-08

Standards Utilized

I.D. No.	Mfg.	Model No.	Description	Cal. Date	Due Date
S1-01252	Hewlett Packard	5335A OPT 010,203040	Counter, Universal,	07/17/2008	01/17/2009
S1-01347	Hewlett Packard	3325A	Generator, Function, Synthesizer	04/24/2008	10/24/2008
S1-03686	Fluke	910	Standard, Frequency, Controlled, Gps	01/22/2008	01/22/2009

Procedure: Customer
Temperature: 23° C
Humidity: 52% RH
Test No.: 558549

Calibration Performed By:			Quality Reviewer:	
Branson, Craig A CAB	Metrologist	714-895-0714		8-5-08
Name	Title	Phone	Name	Date

This report may not be reproduced, except in full, without written permission of this laboratory. This report must not be used by the client to claim product certification, approval, or endorsement by NVLAP, NIST, or any agency of the Federal Government. The results stated in this report relate only to the items tested or calibrated. Measurements reported herein are traceable to SI units via national standards maintained by NIST. This calibration is in compliance with NVLAP laboratory accreditation criteria established by NIST/NVLAP under the specific scope of accreditation for lab code 105014-0.

Test No. 558549
Asset No. 160024

Custom Specification Report

Oyo 3403 Unit, Suspension Telemetry,

STEP NUM	FUNCTION TESTED	NOMINAL VALUE	AS FOUND	AS LEFT	Out of Tol	CALIBRATION TOLERANCE
	CH HN Frequency Square Wave	100.0 Hz	100.0	Same		99.0 to 101.0 Hz [EMU 0.000500 Hz]
	"	100.0 Hz	100.0	Same		99.0 to 101.0 Hz [EMU 0.000500 Hz]
	Sine Wave	100.0 Hz	100.0	Same		99.0 to 101.0 Hz [EMU 0.000500 Hz]
	"	100.0 Hz	100.0	Same		99.0 to 101.0 Hz [EMU 0.000500 Hz]
	CH HR Frequency Square Wave	100.0 Hz	100.0	Same		99.0 to 101.0 Hz [EMU 0.000500 Hz]
	"	100.0 Hz	100.0	Same		99.0 to 101.0 Hz [EMU 0.000500 Hz]
	Sine Wave	100.0 Hz	100.0	Same		99.0 to 101.0 Hz [EMU 0.000500 Hz]
	"	100.0 Hz	100.0	Same		99.0 to 101.0 Hz [EMU 0.000500 Hz]
	CH V Frequency Square Wave	100.0 Hz	100.0	Same		99.0 to 101.0 Hz [EMU 0.000500 Hz]
	"	100.0 Hz	100.0	Same		99.0 to 101.0 Hz [EMU 0.000500 Hz]
	Sine Wave	100.0 Hz	100.0	Same		99.0 to 101.0 Hz [EMU 0.000500 Hz]
	"	100.0 Hz	100.0	Same		99.0 to 101.0 Hz [EMU 0.000500 Hz]

Remarks:

MudCats CPM: Version 2.2.2 (Professional)
Src DUI: {4A70366A-164D-4E33-8F79-34E3FDFFA198} (c)
Doc DUI: {293A3A00-D536-43A0-A1E5-945133CD4CF7} (o)

ATTACHMENT 1
Page 1 of 1

Customer

SEISMOGRAPH CALIBRATION DATA SHEET REV 4/6/06

INSTRUMENT DATA

SYSTEM MFR:	OYO	MODEL NO.:	3403
SERIAL NO.:	160024	CALIBRATION DATE:	8/1/2008
BY:	CRAIG BRANSON	DUE DATE:	8/1/2009
COUNTER MFR:	HEWLETT PACKARD	MODEL NO.:	5335A
SERIAL NO.:	2626A09881	CALIBRATION DATE:	7/17/2008
BY:	SCE #S1-01252	DUE DATE:	1/17/2009
FCTN GEN MFR:	HEWLETT PACKARD	MODEL NO.:	3325A
SERIAL NO.:	2652A25647	CALIBRATION DATE:	4/24/2008
BY:	SCE #S1-01347	DUE DATE:	10/24/2008

SYSTEM SETTINGS:

GAIN:	2
FILTER:	10 KHZ
RANGE:	100 MILLISEC
DELAY:	0
STACK: 1 (STD)	1
PULSE:	1.6
DISPLAY:	NA
SYSTEM: DATE = CORRECT DATE & TIME	8/1/2008 715

PROCEDURE:

SET FREQUENCY TO 100.0HZ SQUAREWAVE WITH AMPLITUDE APPROXIMATELY 0.25 VOLT PEAK. RECORD BOTH ON DISK AND PAPER TAPE, IF AVAILABLE. ANALYZE AND PRINT WAVEFORMS FROM ANALYSIS UTILITY. ATTACH PAPER COPIES OF PRINTOUT AND PAPER TAPES, IF AVAILABLE, TO THIS FORM. AVERAGE FREQUENCY MUST BE BETWEEN 99.0 AND 101.0 HZ.

AS FOUND 100.0 HZ AS LEFT 100.0 HZ

WAVEFORM	FILE NO	FREQUENCY	TIME FOR 9 CYCLES Hn	TIME FOR 9 CYCLES Hr	TIME FOR 9 CYCLES V	AVERAGE FREQ.
SQUARE	501	100.0	90.00 MS	90.00 MS	90.00 MS	100.0 HZ
SQUARE	502	100.0	90.00 MS	90.00 MS	90.00 MS	100.0 HZ
SINE	503	100.0	90.00 MS	90.00 MS	90.00 MS	100.0 HZ
SINE	504	100.0	90.00 MS	90.00 MS	90.00 MS	100.0 HZ

CALIBRATED BY: CRAIG BRANSON (NAME) 8/1/2008 (DATE) Craig Branson (SIGNATURE)

Seismic recorder/Logger Calibration Data Sheet Rev 1.30 4-6-06

Test No. 558549
Asset No. 160024

Custom Specification Report

Oyo 3403 Logger/Recorder, Seismic, PS Suspension

STEP NUM	FUNCTION TESTED	NOMINAL VALUE	AS FOUND	AS LEFT	Out of Tol	CALIBRATION TOLERANCE
	CH HN Frequency Sine Wave	50.00 Hz	50.00	Same		49.50 to 50.50 Hz [EMU 0.000250]
	"	100.0 Hz	100.0	Same		99.0 to 101.0 Hz [EMU 0.000500]
	"	200.0 Hz	200.0	Same		198.0 to 202.0 Hz [EMU 0.001000]
	"	500.0 Hz	500.0	Same		495.0 to 505.0 Hz [EMU 0.002500]
	"	1000 Hz	1000	Same		990 to 1010 Hz [EMU 0.005000]
	"	2000 Hz	2000	Same		1980 to 2020 Hz [EMU 0.010000]
	CH HR Frequency Sine Wave	50.00 Hz	49.95	Same		49.50 to 50.50 Hz [EMU 0.000250]
	"	100.0 Hz	100.0	Same		99.0 to 101.0 Hz [EMU 0.000500]
	"	200.0 Hz	200.2	Same		198.0 to 202.0 Hz [EMU 0.001000]
	"	500.0 Hz	500.0	Same		495.0 to 505.0 Hz [EMU 0.002500]
	"	1000 Hz	1001	Same		990 to 1010 Hz [EMU 0.005000]
	"	2000 Hz	2000	Same		1980 to 2020 Hz [EMU 0.010000]
	CH V Frequency Sine Wave	50.00 Hz	50.00	Same		49.50 to 50.50 Hz [EMU 0.000250]
	"	100.0 Hz	100.0	Same		99.0 to 101.0 Hz [EMU 0.000500]
	"	200.0 Hz	199.8	Same		198.0 to 202.0 Hz [EMU 0.001000]
	"	500.0 Hz	500.0	Same		495.0 to 505.0 Hz [EMU 0.002500]

Remarks:

MudCats CPM: Version 2.2.2 (Professional)
Src DUI: {9548AF3D-C74D-4C9F-AEEF-21EF560BC451} (c)
Doc DUI: {AAAE8731-399D-47BC-98B7-62728C8250BE} (o)

ATTACHMENT 2
Page 1 of 2

Customer

Test No. 558549
Asset No. 160024

Custom Specification Report

Oyo 3403 Logger/Recorder, Seismic, PS Suspension

STEP NUM	FUNCTION TESTED	NOMINAL VALUE	AS FOUND	AS LEFT	Out of Tol	CALIBRATION TOLERANCE
	CH V Frequency Sine Wave	1000 Hz	1000	Same		990 to 1010 Hz [EMU 0.005000]
	|	2000 Hz	1998	Same		1980 to 2020 Hz [EMU 0.010000]

Remarks:

GEOVision geophysical services PAGE 6 OF 6

SUSPENSION PS SEISMIC LOGGER/RECORDER CALIBRATION DATA FORM

INSTRUMENT DATA

System mfg.:	Oyo	Model no.:	3403
Serial no.:	160024	Calibration date:	8/1/2008
By:	Craig Branson	Due date:	8/1/2009
Counter mfg.:	Hewlett-Packard	Model no.:	5335A
Serial no.:	2626A09881	Calibration date:	7/17/2008
By:	SCE #S1-01252	Due date:	1/17/2009
Signal generator mfg.:	Hewlett-Packard	Model no.:	3325A
Serial no.:	2652A25647	Calibration date:	4/24/2008
By:	SCE #S1-01347	Due date:	10/24/2008

SYSTEM SETTINGS:

Gain:	2
Filter	10KHz
Range:	See sample period in table below
Delay:	0
Stack (1 std)	1
System date = correct date and time	8/1/2008 728

PROCEDURE:

Set sine wave frequency to target frequency with amplitude of approximately 0.25 volt peak
Note actual frequency on data form.
Set sample period and record data file to disk. Note file name on data form.
Pick duration of 9 cycles using PSLOG.EXE program, note duration on data form, and save as .sps file. Calculate average frequency for each channel pair and note on data form.

Average frequency must be within +/- 1% of actual frequency at all data points.

Maximum error ((AVG-ACT)/ACT*100)% As found 0.10% As left 0.10%

Target Frequency (Hz)	Actual Frequency (Hz)	Sample Period (microS)	File Name	Time for 9 cycles Hn (msec)	Average Frequency Hn (Hz)	Time for 9 cycles Hr (msec)	Average Frequency Hr (Hz)	Time for 9 cycles V (msec)	Average Frequency V (Hz)
50.00	50.00	200	505	180.0	50.00	180.2	49.95	180.0	50.00
100.0	100.0	100	506	90.00	100.0	90.00	100.0	90.00	100.0
200.0	200.0	50	507	45.00	200.0	44.95	200.2	45.05	199.8
500.0	500.0	20	508	18.00	500.0	18.00	500.0	18.00	500.0
1000	1000	10	509	9.000	1000	8.990	1001	9.000	1000
2000	2000	5	510	4.500	2000	4.500	2000	4.505	1998

Calibrated by: Craig Branson (Name) 8/1/2008 (Date) Craig Branson (Signature)

Witnessed by: Robert Steller (Name) 8/1/2008 (Date) (Signature)

Suspension PS Seismic Recorder/Logger Calibration Data Form Rev 2.0 July 21, 2008

GEOVision Borehole Geophysics depth wheel verification

Performed by Robert Steller

	Depth reading in #1	Depth reading out	Depth reading in #2
Depth wheel S/N 101 500 pulse/revolution (gear 1:5, encoder 100 ppr) Circumference = 983mm (3225.07 millifeet)	100.1 feet (30.51 m) September 23, 2006	99.95 feet (30.46 m) September 23, 2006	100.05 feet (30.50 m) September 23, 2006
Depth wheel S/N 103 500 pulse/revolution (gear 1:5, encoder 100 ppr) Circumference = 994mm (3261.15 millifeet)	100.00 feet (30.48) m September 23, 2006	100.00 feet (30.48 m) September 23, 2006	100.00 feet (30.48) m September 23, 2006
Aries winch 200 pulse/revolution (gear 1:1, encoder 200 ppr) Circumference = 305.9mm (1003.51 millifeet)	100.05 feet (30.50 m) September 23, 2006	100.05 feet (30.50 m) September 23, 2006	100.00 feet (30.48 m) September 23, 2006
Robertson Depth wheel For MiniWinch 1000 pulse/revolution (gear 1:1, encoder 1000 ppr) Circumference = 400mm (1312 millifeet)	99.92 feet (30.46 m) Re-verified June 7, 2007	100.10 feet (30.51 m) Re-verified June 7, 2007	99.90 feet (30.45 m) Re-verified June 7, 2007
Robertson Smartwinch 200 S/N 5802 5000 pulse/revolution (gear 1:4, encoder 1250 ppr) Circumference = 404mm (1326 millifeet)	99.99 feet (30.48 m) June 6, 2007	99.97 feet (30.47 m) June 6, 2007	100.00 feet (30.48 m) June 6, 2007
Comprobe winch 500 pulse/revolution (gear 1:1, encoder 500 ppr) Circumference = 1000mm (3.281 feet)	100.1 feet (30.5 m) Re-verified June 7, 2007	100.1 feet (30.5 m) Re-verified June 7, 2007	100.1 feet (30.5 m) Re-verified June 7, 2007

All measurements taken with a Stanley 100-foot flexible stainless steel tape model number 34-130, and a Keeson 300-foot fiberglass tape, both marked in feet, inches and 1/8ths of inches. Enough cable was spooled off of the winch to allow the cable and tape measures to be laid flat on the parking lot surface side-by-side. A permanent marker was used to mark a 100.0-foot interval on the cable, and the marks were also tagged with electrical tape for visibility. The cable was then spooled back onto the winch. When the first mark was at the top of the measuring wheel, a matching permanent mark was placed, and the recording system (Robertson Micrologger) was set to 0.0 feet depth. The cable was spooled in to the second mark, and the distance was recorded. The recording system was set to 0.0 feet again, and the cable spooled out to the first mark again, and the distance was recorded. The process was repeated one more time to spool the cable back onto the winch, and the distance was recorded.

Estimated accuracy is of these measurements is +/- 0.1 foot or +/- 0.03m.

GEOVision Suspension PS probe Receiver 1–Receiver 2 (R1-R2) spacing verification

Performed by Robert Steller on September 23, 2006

	R2 center to R1 center hanging dry	R2 center to R1 center hanging submerged	R1 bottom to source center hanging submerged with 1m isolation tube S/N 280068	R1 center to source center hanging submerged with 1m isolation tube S/N 280068
Receiver S/N 30086	40.2in 1.02m	40.0in 1.02m	76.0in 1.93m	83.5in 2.12m
Receiver S/N 20042	39.8in 1.01m	39.6in 1.01m	75.7in 1.92m	83.2in 2.11m
Receiver S/N 12008	40.2in 1.02m	40.0in 1.02m	76.0in 1.93m	83.5in 2.12m

All measurements taken with a Lufkin 3.7m flexible steel tape model number HV1034DM, marked in mm and 100th of feet. Probe suspended in 3-inch diameter clear PVC pipe, using chain clamp placed between bottom and center of Receiver 2 hard section (See Figure). Probe "bounced" to establish unrestricted hanging length before measurement. Probe allowed to relax for 5 minutes prior to each measurement. Water level set to submerge bottom of Receiver 2 hard section.. Estimated accuracy due to hysterisis in rubber section approximately +/- 0.01' or +/- 0.003m.

APPENDIX E

BORING GEOPHYSICAL LOGGING FIELD MEASUREMENT PROCEDURES

PROCEDURE FOR

OYO P-S SUSPENSION SEISMIC VELOCITY LOGGING

Background

This procedure describes a method for measuring shear and compressional wave velocities in soil and rock. The OYO P-S Suspension Method is applied by generating shear and compressional waves in a borehole using the OYO P-S Suspension Logger borehole tool and measuring the travel time between two receiver geophones or hydrophones located in the same tool.

Objective

The outcome of this procedure is a plot and table of P and S_H wave velocity versus depth for each borehole. Standard analysis is performed on receiver to receiver data. Data is presented in report format, with digital data files transmitted in Excel, Word or ASCII format.

Instrumentation

1. OYO Model 170 Digital Logging Recorder or equivalent
2. OYO P-S Suspension Logger probe or equivalent, including two sets horizontal and vertical geophones, seismic source, and power supply for the source and receivers
3. Winch and winch controller, with logging cable
4. Batteries to operate P-S Logger and winch

The Suspension P-S Logger system, manufactured by OYO Corporation, or the Robertson Digital P-S Suspension Probe with the Robertson Micrologger2 are currently the only commercially available suspension logging systems. As shown in Figure 1, these systems consists of a borehole probe suspended by a cable and a recording/control electronics package on the surface.

The suspension system probe consists of a combined reversible polarity solenoid horizontal shear-wave generator (S_H) and compressional-wave generator (P), joined to

two biaxial geophones by a flexible isolation cylinder. The separation of the two geophones is one meter, allowing average wave velocity in the region between the geophones to be determined by inversion of the wave travel time between the two geophones. The total length of the probe is approximately 7 meters; the center point of the geophones is approximately 4 meters above the bottom end of the probe.

The probe receives control signals from, and sends the amplified geophone signals to, the instrumentation package on the surface via an armored 4 or 7 conductor cable. The cable is wound onto the drum of a winch and is used to support the probe. Cable travel is measured by a rotary encoder to provide probe depth data.

The entire probe is suspended by the cable and may be centered in the borehole by nylon "whiskers." Therefore, source motion is not coupled directly to the borehole walls; rather, the source motion creates a horizontally propagating pressure wave in the fluid filling the borehole and surrounding the source. This pressure wave produces a horizontal displacement of the soil forming the wall of the borehole. This displacement propagates up and down the borehole wall, in turn causing a pressure wave to be generated in the fluid surrounding the geophones as the soil displacement wave passes their location.

Environmental Conditions

The OYO P-S Suspension Logging Method can be used in either cased or uncased boreholes. For best results, the uncased borehole must be between 10 and 20 cm in diameter, or 4 to 8 inches. A cased borehole may be as small as 3 inches, if properly grouted (see below) and the grout annulus does not exceed 1 inch.

Uncased boreholes are preferred because the effects of the casing and grouting are removed. It is recommended that the borehole be drilled using the rotary mud method. This method does little damage to the borehole wall, and the drilling fluid coats and seals the borehole wall reducing fluid loss and wall collapse. The borehole fluid is required for the logging, and must be well circulated prior to logging.

If the borehole must be cased, the casing must be PVC and properly installed and grouted. Any voids in the grout will cause problems with the data. Likewise, large grout bulbs used to fill cavities will also cause problems. The grout must be set before testing. This means the grouting must take place at least 48 hours before testing.

For borehole casing, applicable preparation procedures are presented in ASTM Standard D4428/D4428M-91 Section 4.1 (see ASTM website for copy).

Calibration

Calibration of the digital recorder is required. Calibration is limited to the timing accuracy of the recorder. GEOVision's Seismograph Calibration Procedure or equivalent should be used. Calibration must be performed on an annual basis.

Measurement Procedure

The entire probe is lowered into the borehole to a specific measurement depth by the winch. A measurement sequence is then initiated by the operator from the instrumentation package control panel. No further operator intervention is then needed to complete the measurement sequence described below.

The system electronics activates the SH-wave source in one direction and records the output of the two horizontally oriented geophone axes which are situated parallel to the axis of motion of the source. The source is then activated in the opposite direction, and the horizontal output signals are again recorded, producing a SH-wave record of polarity opposite to the previous record. The source is finally actuated in the first direction again, and the responses of the vertical geophone axes to the resultant P-wave are recorded during this sampling.

The data from each geophone during each source activation is recorded as a different channel on the recording system. The seismograph has at least six channels (two simultaneous recording channels), each with at least a 12 bit 1024 sample record. Newer seismographs may have longer record lengths. The recorded data is displayed on a CRT or LCD display and possibly on paper tape output as six channels with a common time scale. Data is stored on digital media for further processing. Up to 8 sampling sequences can be stacked (averaged) to improve the signal to noise ratio of the signals.

Review of the data on the display or paper tape allows the operator to set the gains, filters, delay time, pulse length (energy), sample rate, and stacking number in order to optimize the quality of the data before recording. In the case of the Model 170, printed data is verified by the operator prior to moving the probe. In the case of the Robertson Micrologger2, storage on the hard disk should be verified from time-to-time, certainly before exiting the borehole.

Typical depth spacing for measurements is 1.0 meters, or 3.3 feet. Alternative spacing is 0.5 meter, or 1.6 feet.

Required Field Records

1) Field log for each borehole showing

   a) Borehole identification

   b) Date of test

   c) Tester or data recorder

d) Description of measurement

e) Any deviations from test plan and action taken as a result

f) QA Review

2) Paper output records are no longer required, since the Micrologger2 cannot generate them. However, data must be stored in at least 2 places prior to leaving the site

3) List of record ID numbers (for data on digital media) and corresponding depth

4) Diskettes, CDRom, or USB flash drives with backup copies of data on hard disk, labeled with borehole designation, record ID numbers, date, and tester name.

An example Field Log is attached to this procedure.

Analysis

Following completion of field work, the recorded digital records are processed by computer using the OYO Corporation software program PSLOG and interactively analyzed by an experienced geophysicist to produce plots and tables of P and S_H wave velocity versus depth.

The digital time series records from each depth are transferred to a personal computer for analysis. Figure 2 shows a sample of the data from a single depth. These digital records are analyzed to locate the first minima on the vertical axis records, indicating the arrival of P-wave energy. The difference in travel time between these arrivals is used to calculate the P-wave velocity for that 1-meter interval. When observable, P-wave arrivals on the horizontal axis records are used to verify the velocities determined from the vertical axis data. In addition, the soil velocity calculated from the travel time from source to first receiver is compared to the velocity derived from the travel time between receivers.

The digital records are studied to establish the presence of clear SH-wave pulses, as indicated by the presence of opposite polarity pulses on each pair of horizontal records. Ideally, the SH-wave signals from the ‘normal’ and ‘reverse’ source pulses are very nearly inverted images of each other. Digital FFT – IFFT lowpass filtering are used to remove the higher frequency P-wave signal from the SH-wave signal.

The first maxima are picked for the ‘normal’ signals and the first minima are picked for the 'reverse' signals. The absolute arrival time of the ‘normal’ and ‘reverse’ signals may vary by +/- 0.2 milliseconds, due to differences in actuation time of the solenoid source caused by constant mechanical bias in the source or by borehole inclination. This variation does not affect the velocity determinations, as the differential time is measured between arrivals of waves created by the same source actuation. The final velocity

value is the average of the values obtained from the 'normal' and 'reverse' source actuations.

In Figure 2, the time difference over the 1-meter interval of 1.70 millisecond is equivalent to a SH-wave velocity of 588 m/sec. Whenever possible, time differences are determined from several phase points on the S_H -wave pulse trains to verify the data obtained from the first arrival of the S_H -wave pulse. In addition, the soil velocity calculated from the travel time from source to first receiver is compared to the velocity derived from the travel time between receivers.

Figure 3 is a sample composite plot of the far normal horizontal geophone records for a range of depths. This plot shows the waveforms at each depth, clearly showing the S-wave arrivals. This display format is used during analysis to observe trends in velocity with changing depth.

Once the proper picks are entered in PSLOG, the picks are transferred to an Excel spreadsheet where Vs and Vp are calculated. The spreadsheet allows output for presentation in charts and tables.

Standard analysis is performed on receiver 1 to receiver 2 data, with separate analysis performed on source to receiver data as a quality assurance procedure.

Registered Geophysicist Antony Martin Date 9/11/06

QA Review 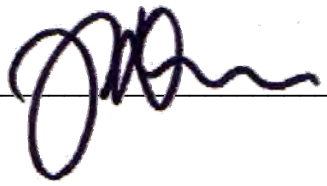 Date 9/11/06

References:

1. "In Situ P and S Wave Velocity Measurement", Ohya, S. 1986. Proceedings of In-Situ '86, *Use of In-Situ Tests In Geotechnical Engineering*, an ASCE Specialty Conference sponsored by the Geotechnical Engineering Division of ASCE and co-sponsored by the Civil Engineering Dept of Virginia Tech.

2. Guidelines for Determining Design Basis Ground Motions, Report TR-102293, Electric Power Research Institute, Palo Alto, California, November 1993, Sections 7 and 8.

3. "Standard test Methods for Crosshole Seismic Testing", ASTM Standard D4428/D4428M-91, July 1991, Philadelphia, PA

OYO SUSPENSION P-S VELOCITY LOGGING SETUP

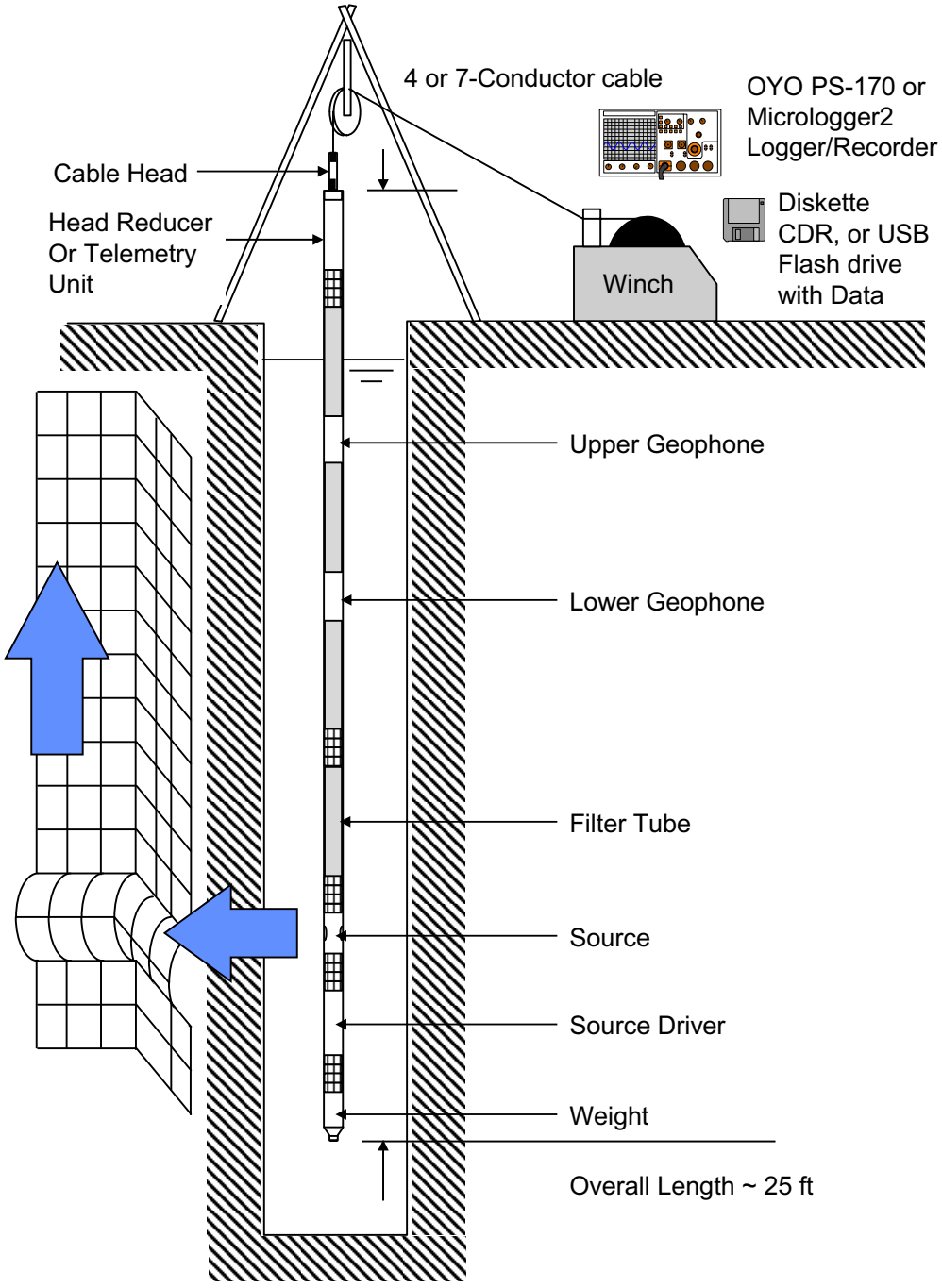

Figure 1. Suspension PS logging method setup

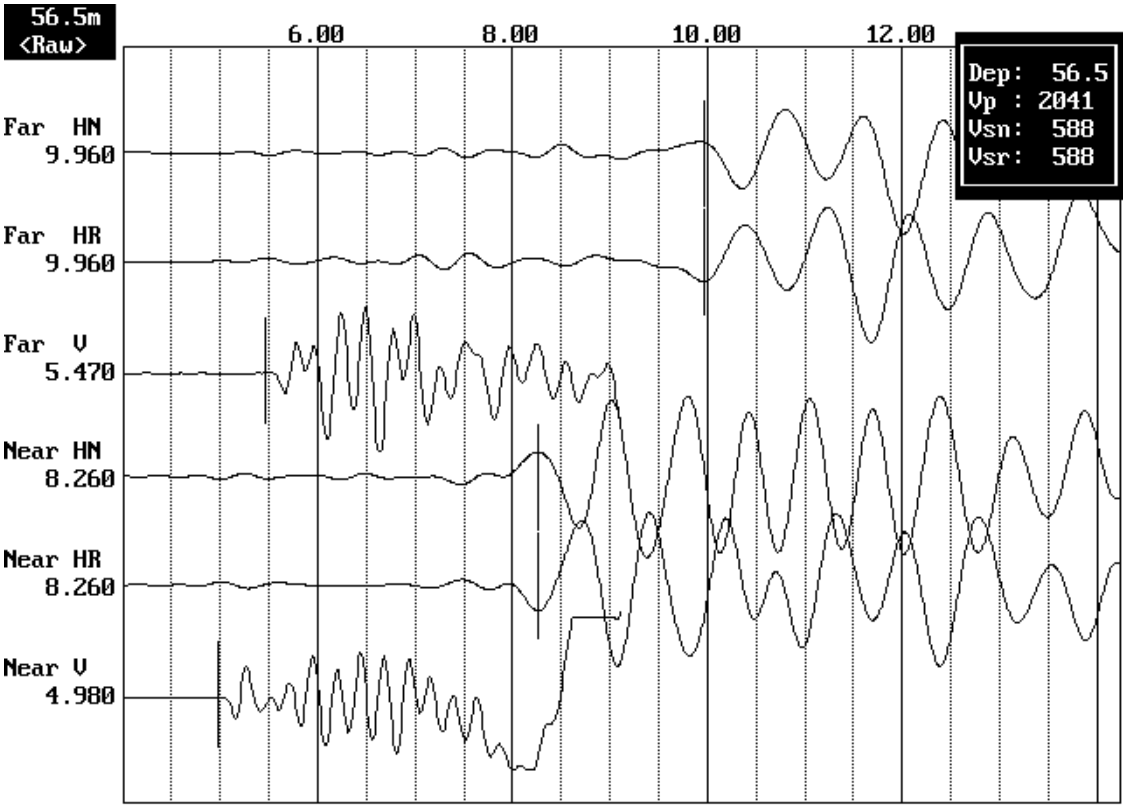

Figure 2. Sample suspension method waveform data showing horizontal normal and reversed (HR and HN), and vertical (V) waveforms received at the near (bottom 3 channels) and far (top 3 channels) geophones. The arrivals in milliseconds for each pick are shown on the left. The box in the upper right corner shows the depth in the borehole and the velocities calculated based on the picks.

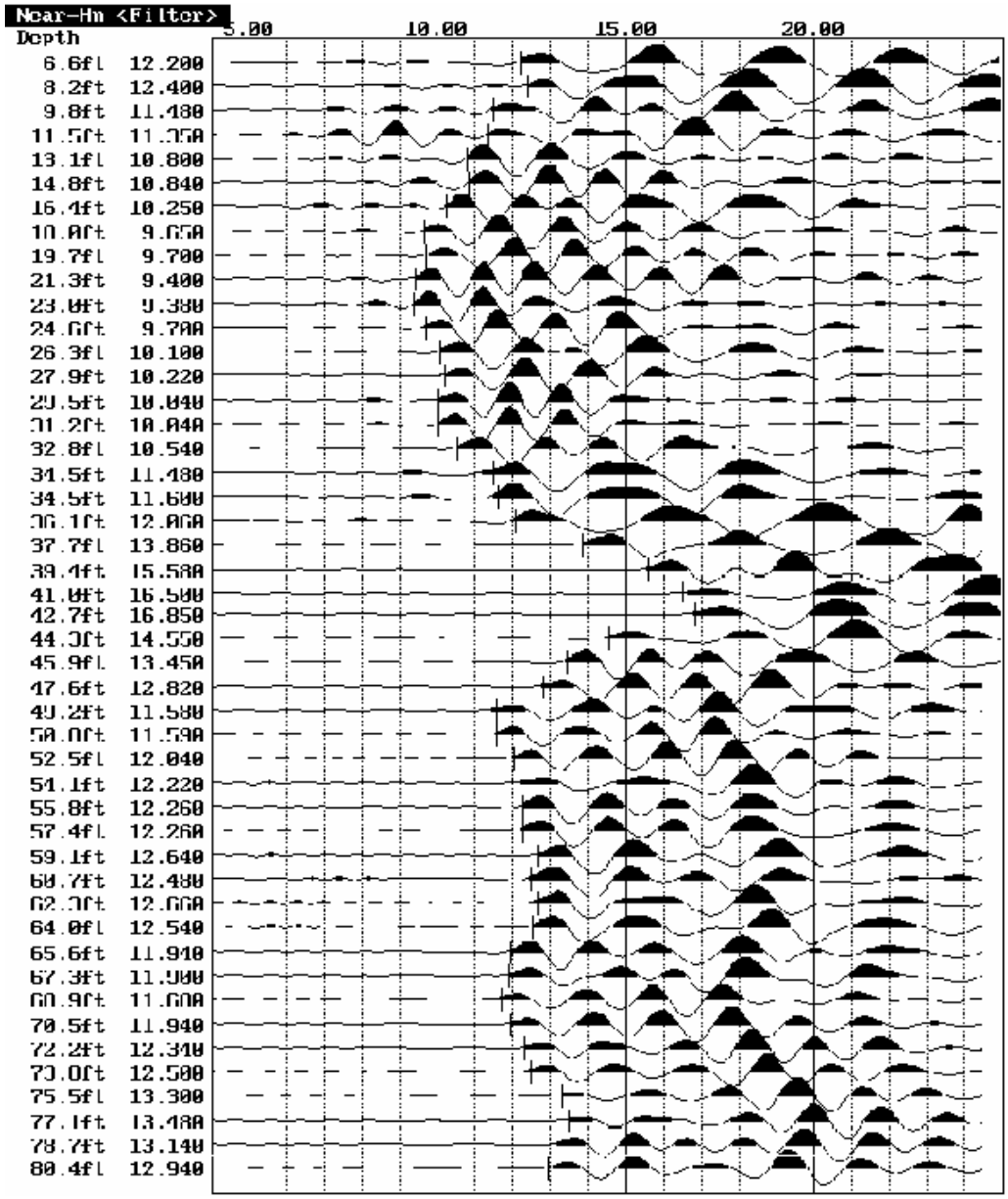

Figure 3. Sample composite waveform plot for normal shear waves received at the near geophone in a single borehole

GEOVision
geophysical services

P-S SUSPENSION VELOCITY FIELD LOG

SITE:_____ DATE:_____
CLIENT:_____ JOB:_____
AUTHOR:_____ PAGE 1 OF _____

CONTACT:_____ _OFFICE__ PHONE:_____
_____ PHONE:_____
CONTACT:_____ _OFFICE__ PHONE:_____
_____ PHONE:_____
CONTACT:_____ _____ PHONE:_____
_____ PHONE:_____
CONTACT:_____ _____ PHONE:_____
_____ PHONE:_____
DRILLER:_____ _____ PHONE:_____
COMPANY:_____ _____ PHONE:_____

DIRECTIONS TO SITE:_____
_____
_____
_____
_____

GENERAL SITE CONDITIONS/LOCATION:_____
_____

EA#:_____
BOREHOLE DESIGNATION:_____LOCATION:_____
_____
COUNTY:_____RANGE:_____TOWNSHIP:_____SECTION:_____
BOREHOLE CONSTRUCTION: CASED_____ UNCASED_____
DIAMETERS AND DEPTH RANGES: _____ 0 TO _____ ; _____, _____ TO _____
BOREHOLE TOTAL DEPTH AS DRILLED:_____
CONDUCTOR CASING?: YES____ DEPTH TO BOTTOM OF CASING_____; NO____
DEPTH TO BEDROCK:_____ DEPTH TO WATER TABLE:_____
BOREHOLE FLUID: WATER_____; FRESH WATER MUD_____; SALT WATER MUD _____;
OTHER:_____
DEPTH TO BOREHOLE FLUID:_____ TIME SINCE LAST CIRCULATION:_____

GEOVision Geophysical Services 1151 Pomona Road, Suite P, Corona, CA 92882 Ph (951) 549-1234 Fx (951) 549-1236

GEOVision
geophysical services

SITE:_____ DATE:_____
CLIENT:_____ JOB:_____
AUTHOR:_____ PAGE 2 OF _____

LOGGING CREW:_____
VEHICLE(S) USED AND MILEAGE: _____
MOBILIZED FROM:_____ DEPARTURE TIME:_____
ARRIVED ON SITE:_____
STANDBY TIME:_____ CAUSE:_____
LOGGING STARTED:_____ LOGGING COMPLETED:_____
STANDBY TIME:_____ CAUSE:_____
LOGGING STARTED:_____ LOGGING COMPLETED:_____
DEMOBILIZED TO:_____ ARRIVAL TIME:_____
ADDITIONAL DEMOB TIME:_____ REASON:_____

BATTERIES CHANGED BEFORE LOGGING: YES_____; NO_____; STORED WITH NEW_____

WINCH	COMPROBE ☐		GREY ☐	OYO ☐	RG ☐	OTH ☐			
INSTRUMENT	OYO	12004 ☐	15014 ☐	19029 ☐		RG	160023 ☐	160024 ☐	
RECEIVER S/N		12008 ☐	20042 ☐	26066 ☐	11001 ☐		23053 ☐		

MAINTENANCE PERFORMED ON SITE:_____
_____
_____
_____
EQUIPMENT PROBLEMS OR FAILURES:_____
_____
_____

SUGGESTIONS, ADDITIONS, CHANGES:_____
_____
_____

COMMENTS:_____
_____
_____
_____
_____
_____

GEOVision Geophysical Services 1151 Pomona Road, Suite P, Corona, CA 92882 Ph (951) 549-1234 Fx (951) 549-1236

GEOVISION SUSPENSION LOGGING FIELD NOTES

SITE: _____ DATE: _____

CLIENT: _____ JOB: _____

AUTHOR: _____ PAGE _____ OF _____

DEPTH METERS	DEPTH FEET	UNFILTERED FILE NO.	FILTERED FILE NO.	COMMENTS CASING, WATER, ROCK, ETC
0.5	1.64			
1.0	3.28			
1.5	4.92			
2.0	6.56			
2.5	8.20			
3.0	9.84			
3.5	11.48			
4.0	13.12			
4.5	14.76			
5.0	16.40			
5.5	18.04			
6.0	19.69			
6.5	21.33			
7.0	22.97			
7.5	24.61			
8.0	26.25			
8.5	27.89			
9.0	29.53			
9.5	31.17			
10.0	32.81			
10.5	34.45			
11.0	36.09			
11.5	37.73			
12.0	39.37			
12.5	41.01			
13.0	42.65			
13.5	44.29			
14.0	45.93			
14.5	47.57			
15.0	49.21			
15.5	50.85			
16.0	52.49			
16.5	54.13			
17.0	55.77			
17.5	57.41			
18.0	59.06			

GEOVISION SUSPENSION LOGGING FIELD NOTES

SITE: _____ DATE: _____

CLIENT: _____ JOB: _____

AUTHOR: _____ PAGE _____ OF

DEPTH METERS	DEPTH FEET	UNFILTERED FILE NO.	FILTERED FILE NO.	COMMENTS CASING, WATER, ROCK, ETC
18.5	60.70			
19.0	62.34			
19.5	63.98			
20.0	65.62			
20.5	67.26			
21.0	68.90			
21.5	70.54			
22.0	72.18			
22.5	73.82			
23.0	75.46			
23.5	77.10			
24.0	78.74			
24.5	80.38			
25.0	82.02			
25.5	83.66			
26.0	85.30			
26.5	86.94			
27.0	88.58			
27.5	90.22			
28.0	91.86			
28.5	93.50			
29.0	95.14			
29.5	96.78			
30.0	98.43			
30.5	100.07			
31.0	101.71			
31.5	103.35			
32.0	104.99			
32.5	106.63			
33.0	108.27			
33.5	109.91			
34.0	111.55			
34.5	113.19			
35.0	114.83			
35.5	116.47			
36.0	118.11			

PROCEDURE FOR USING THE ROBERTSON GEOLOGGING HI-RESOLUTION ACOUSTIC TELEVIEWER (HiRAT)

Reviewed 2/13/06

Background

The acoustic televiewer is a device for producing a qualitative image of the wall of a borehole. Because it uses ultrasound rather than visible light it is able to work in dirty or opaque borehole fluids, although heavy drilling mud will cause excessive dispersion of the acoustic beam. The picture below shows the sonde's lower nylon section, and one of the bowspring attachments which are used to centralize the sonde in the borehole.

Pulses of ultrasound (0.5 - 1.5MHz) are generated by a piezo-electric resonator. The pulses are transmitted through the oil in which the resonator is immersed, through the wall of the acoustic housing, then propagate through the borehole fluid and are reflected from the wall of the borehole. The reflected energy is picked up by the same transducer, from which is recorded both the ***amplitude*** of the returned pulse and the ***travel-time*** which have elapsed. Blanking must be applied to prevent the transducer from registering reflections from the inside surface of the acoustic housing. The material of the housing is chosen so that its acoustic properties are similar to the oil which fills it. The housing is not designed to withstand borehole fluid pressures, but has a piston device to allow equalization between inside and outside pressure.

The ***amplitude*** of the returned pulse is a function of the acoustic reflectivity of the borehole wall. If the beam strikes a hard borehole wall normally to the surface the energy will be returned to the transducer and a strong return will be recorded. If the formation is softer, then less energy will be reflected. Also, if the surface of the borehole is rough, or effectively missing because of the presence of a fracture or other structure, then energy will be dispersed and a poor return will be recorded.

The ***travel-time*** is a simple function of the diameter of the borehole and the velocity of sound in the borehole fluid (typically 1.5Km/sec). An A/D converter monitors the output from the transducer once the blanking period has expired and a comparator is used to detect the peak amplitude during the sampling window.

The coaxially-mounted transducer has a planar radiating surface, but the vibration characteristics are such that the acoustic pulse is emitted as a 'pencil' beam. The emitted beam is deflected by a planar mirror so that it leaves the acoustic housing at right angles to the sonde axis. The mirror is rotated to scan the borehole wall. The ultrasound pulses are synchronized with rotation of the mirror so that up to 360 pulses are emitted in every revolution. Because of the time which must elapse for the two-way transit of the borehole fluid, there is an upper limit upon the number of radial samples that may be acquired from a borehole of a particular radius. In larger boreholes, therefore, it may be necessary to reduce the number of radial samples. The sonde is able to operate at 90, 180 or 360 samples per revolution.

An image of the borehole wall is produced by moving the sonde along the borehole axis while it is scanning radially. By the same logic as shown above, it can be seen that any horizontal point will be imaged by more than one sweep of the acoustic beam so long as the axial movement of the sonde during one complete sweep is no greater than the beam diameter. An upper limit is therefore imposed upon the logging speed which will be a function of the rotational speed of the transducer, the radial sampling interval and borehole diameter.

Objective

The objective of this procedure is to provide a pseudo “core” of the borehole, and map the orientation and angles of cracks and voids in rock boreholes.

Instrumentation

This procedure is written specifically for the Robertson Geologging High-Resolution Acoustic Televiewer (HiRAT). The required equipment includes:

1. The Robertson High-Resolution Acoustic Televiewer (HiRAT) sonde with centralizers
2. A 4-conductor wire-line winch with cable at least 30m (100ft) longer than the depth of the borehole (RG Smart Winch or equivalent. GEOVision has adapted all our 4-conductor winches)
3. A sheave with depth encoder with minimum 500 pulse/revolution
4. A Robertson Geologging Micrologger II
5. A laptop with Winlogger installed and the following minimum system requirements:
    - Windows 98SE or above
    - 64M System memory
    - 800x600x24 SVGA Display with DirectX 8.0
    - 500Mhz CPU
    - USB 2.0 connection
6. Battery power supply with cables

Environmental Conditions

This tool is designed for fluid-filled boreholes between 67 and 150mm (3-6in) in rock. Since fine cracks are usually not visible in the walls of soil borings, the televiewers add very little information from a soil boring than a simple video. Now if the boring has soil AND rock, televiewer visuals in the soil may still be useful.

Calibration

The acoustic televiewer uses the variability in reflectance and the travel time to make an image of the borehole wall, mostly resulting from relative differences of materials and the physical characteristics of the wall. Since these are relative measurements, no field calibration of the sonde is required. However, it is important that the same location in the borehole be checked at the start and finish of the logging to make sure that the response or functionality haven't changed during the measurement.

A test fixture may be used to check function of the acoustic televiewer prior to use. This test fixture should comprise a plastic pipe, with a known internal diameter between 3 and 6 inches. This should be filled with water and the sonde stood upright in the fixture. A target made of metal or metal foil is glued on the inside of the container, or optionally on a seal and shaft so that it can be moved in and out on a line radial to the center-line of the pipe. A representation of this is shown in the figure below.

The purpose of this test fixture is to check the ability of the sonde to differentiate between materials of different acoustic reflectances, and different travel times, and to check the calibration of the caliper function of the sensor using the measured diameter of the pipe. However, if calibrated caliper measurements are required, it is recommended that a mechanical 3-arm caliper tool be used for this purpose because it can be calibrated in the field prior to use. The HiRAT will give very accurate results but this procedure does not cover calibration.

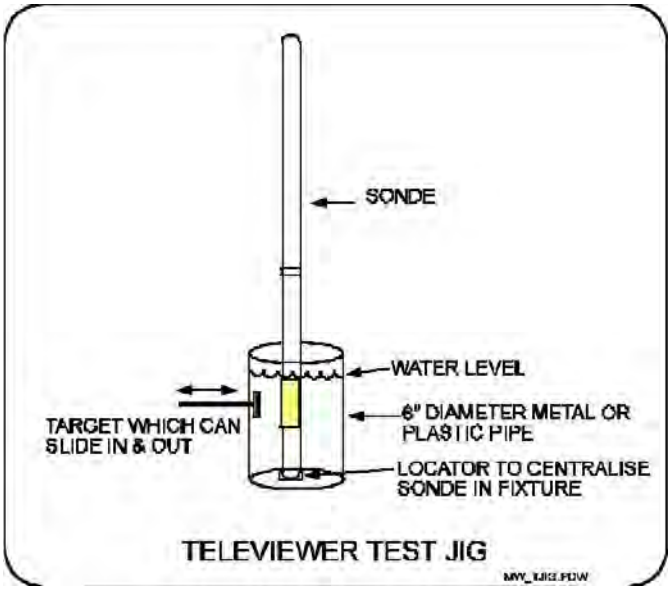

Hi-RAT Field Procedure

Because the logging software is a standalone module, there are a number of settings which must be initialized independently of the WinLogger software. These include the depth measurement subsystem and sonde operating modes. Click on 'System' on the menu bar to show the following dialog boxes:

1.0 Log Mode

The sonde can operate in three distinct modes:

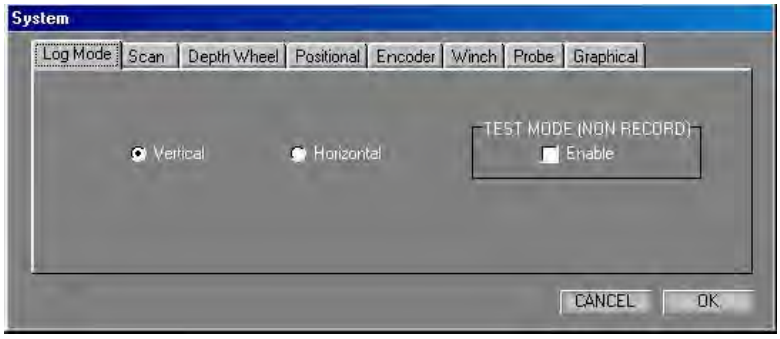

- Vertical mode is used for boreholes which are drilled from the surface and are deviated at less than 70 degrees from the vertical. Most exploration boreholes will fall into this class. In this mode the image is orientated according to compass directions (magnetic co-ordinates).

- Horizontal mode is used for boreholes which are sub-horizontal so their inclination will probably exceed 70 degrees from the vertical. Boreholes in this class would normally be drilled as part of ground investigations for tunneling and mining, drilling ahead of a drive to determine the nature and extent of fracturing. In this mode the image is orientated according to gravitational coordinates (up/down) since there is no unique point of the image circle which can be orientated to North with any precision.

- Test mode is used to exercise all sonde functions without creating a log. The image will scroll on the screen in the normal fashion, and orientation readouts will be refreshed continuously.

2.0 Scan Parameters

The scan parameters control the radial sampling of the borehole. The values will be retained between logging sessions, so the sonde will be initialized correctly at power-on. There are three parameters in the dialog:

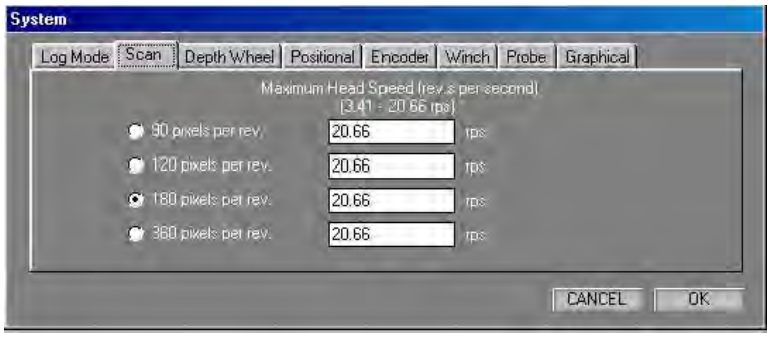

- The radial sampling rate can be set to one of 90, 120, 180, 360 samples per revolution. There is a relationship between the logging speed and the radial sampling rate, since the time taken to send the dataset to the surface depends upon its length. The size of the log file is also determined by the radial sampling rate. The probe will always try to use the maximum head speed entered. If limited by a low Baud rate or a large 'window' setting then the probe will reduce its head speed automatically to compensate - see sonde operation section.

3.0 Depth Wheel Configuration

The depth measurement system is dependent upon the combination of depth measurement wheel with its calibrated groove, and the shaft encoder which translates rotation into pulses which are counted by the logging system controller. Two parameters are therefore required: depth wheel circumference and encoder pulse rate. The encoder parameters are covered in a subsequent topic.

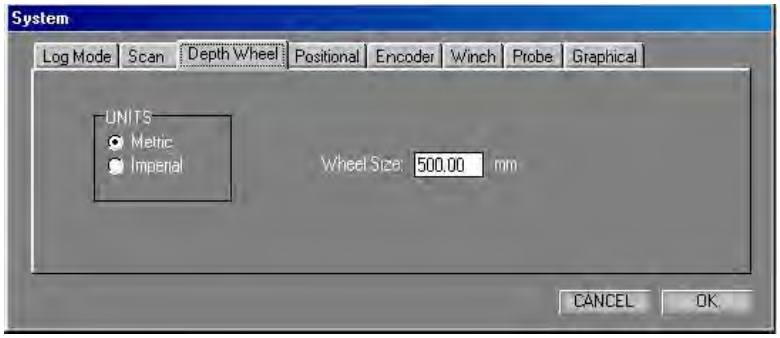

- Select Metric or Imperial depth measurement units from the left-hand pane.

- Type the circumference of the depth measurement wheel into the 'wheel size' box. The standard sizes of GEOVision wheels are 1000mm. If you are measuring in Imperial units (or changing back to metric units), the standard wheel size can be converted automatically by clicking the left mouse button and choosing the appropriate conversion. The size is always specified in units of 1/1000 of the depth unit i.e. millimetres (mm) or millifeet (mft).

4.0 Encoder Configuration

The depth measurement system is dependent upon the combination of depth measurement wheel with its calibrated groove, and the shaft encoder which translates rotation into pulses which are counted by the logging system controller. The depth wheel circumference is covered in a previous topic. In order to accommodate a variety of encoders, their operational characteristics can be configured in the software.

- Select supply voltage from the radio buttons in the left-hand pane. The options are 5 Volt and 12 Volt. GEOVision encoders are always specified for 5 Volt operation.

- Type the number of pulses emitted per revolution into the central box. The standard values for all GEOVision winches are 500 pulses/rev.

- The logical direction of movement can be reversed if required to accommodate the directional characteristics (phase lead or lag) of the different encoder types.

5.0 Winch and Cable Configuration

Support for remote control of the RG Smart Winch is provided, and can be enabled by checking the ***Enable*** control in the left-hand Smart Winch pane. If the Smart Winch control is enabled, it is also necessary to select the measure units in force - select ***Metric*** or ***Imperial*** from the radio buttons on offer.

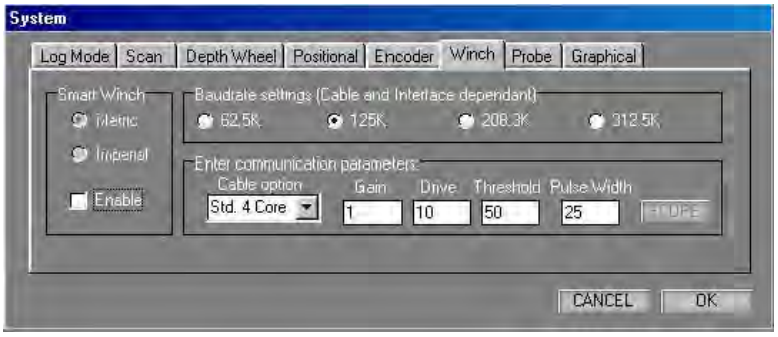

The Baud settings can be chosen to match the *quality* of the communication channel. The channel will be effected by cable type and length. Typically a Baudrate of 312.5K is used. The remaining controls in the dialog relate to the communications parameters. The operation is entirely compatible with the WinLogger software operation and the values would be expected to be the same as those in force for logging six-channel type sondes with that software. (Certain probe types may be fitted with a digital interface that does not require set-up and in this case the parameter edit boxes will not appear.)

- ***Cable Option*** is used to select the logging cable type which is available on the winch. The options are *Not Connected*, *Std. 4 Core*, *Differential* and *Monocable*. The only cable types used in GEOVision systems is Std. 4 Core. Select the appropriate type from the drop-down menu box. Note this value can only be changed when the probe power is turned off.

- ***Gain*** is related to cable length and uphole signal attenuation. Gain values range from 0-3 and control the amplification applied to the incoming signal. Use the *Scope* dialog to visualize the incoming signals. Gain should be set so that the signal reaches between 70% and 100% of the height of the display, generally obtained with a setting of 0 for GEOVision winches. If the peak height exceeds this level, clipping will result in artifacts which will be detected erroneously. Click *Apply* to set the parameters before proceeding to the *Scope* dialog.

- ***Threshold*** is the level at which the incoming signals are detected. Gain and Threshold are related, and can be visualized using the *Scope* dialog. Set the gain so that the signal reaches between 70% and 100% of the height of the display. Then adjust the threshold so that it is between 50% and 70% of the height of the pulses displayed and clear of any region of 'overshoot' of the positive and negative pulses. This will ensure that peaks are detected and noise is ignored. Generally a setting of 25 is used for GEOVision winches. When the scope dialog is displayed, the position of the mouse is reported as a threshold value to make it simpler to infer the correct setting. The scope option is greyed out when the probe power is turned off.

- ***Drive*** sets the strength of the downhole signal. It is not possible to visualize the downhole signal, but the effect of insufficient drive is to disable downhole communication, which will result in the commands being ignored by the sonde. Values range from 0 -127, and for GEOVision winches will be around 10. Increase the drive for longer cables.

- ***Pulse Width*** This is the width of the transmitted communication pulses in 100nS steps. The default is 25 equivalent to 2.5uS. The range is from 8 to 64. The pulse width can be reduced to prevent signal overshoot on short cables. The default value is used in most cases. Note any changes only come into effect during a log. (Note setting too large a pulse width when using the highest Baud rates will automatically be prevented within the probe and the pulse width reduced.)

IMPORTANT Please note the effects of changing 'Baud' will not appear until the first new log is made. The setting for 'threshold' may be effected by an increase in the 'Baud' rate please recheck 'threshold' if 'Baud' is altered using the 'Scope' function after making a short test log.

The parameters which are entered will be applied automatically if you close the dialog with ***OK***. The above parameters once set correctly will be remembered by the system and should never need to be altered.

6.0 Probe Configuration

The probe is normally energized at 90 Volts from the surface. However, it may be necessary to compensate for voltage drop on longer cables due to the higher power draw of this sonde. The voltage at

the surface may be increased in order to deliver 90 Volts at the sonde. Simply type the value into the text box provided. The voltage should be set at 90V for all GEOVision winches. Values outside the indicated range will be rejected.

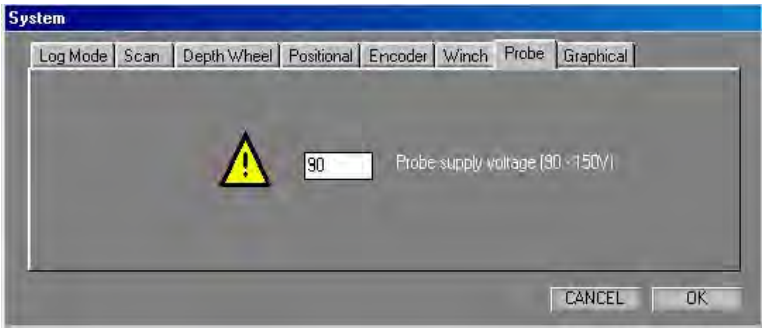

7.0 Positional Configuration

The probe includes a 3-axis orientation package, and is capable of producing a borehole image aligned to geographic North. This is achieved by determining and applying two image rotation parameters:

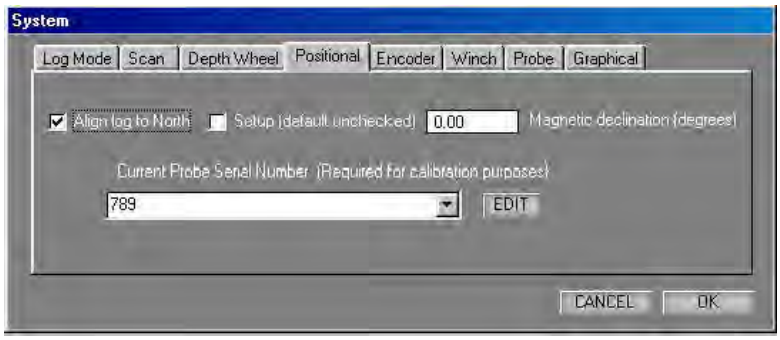

- ***Magnetic Declination*** is used to correct for the difference between Magnetic North and True North. The value varies from place to place, so the local value must be inserted here if you wish to perform this correction during data collection. This correction may also be made during processing. If the value is zero, the log will be referred to Magnetic North.
- ***Align to North*** is a check-box used to select image rotation to start at Magnetic North. If in addition a value is set for Magnetic Declination (see above) the image will be rotated to start at True North. If the box is not checked, the image will not be oriented to geographic co-ordinates, but will use the local co-ordinate frame of the sonde (X, Y, Z axis of the orientation module). This mode may be used to inspect the inside of magnetic casing, where an orientated image would be subjected to random effects caused by the metalwork.
- Set-up mode is selected by checking the ***Setup*** box, and is used to determine the required image rotation offset to correct for the angle between the axis of the orientation package and the index mark of the rotating transducer section. In set-up mode the normal sonde azimuth display is modified, and will instead show the 'relative bearing' which is measured between the high side of the borehole and the orientation sensor index. Check ***Setup***, then OK to close the dialog. The icon adjacent to the sonde azimuth readout at the top of the screen is modified with the legend CAL when the system is in set-up mode. The sonde must now be placed in a stand or jig so that it

is inclined at about 20 degrees to the vertical, and adjacent to a target fixed to the jig so that it is directly above the transducer in the vertical plane. Lower the sonde with its attachment into a large bucket of water so that the transducer and target are fully immersed. Start the radial amplitude display, when it will be possible to see the strong signal returning from the target. Rotate the sonde so that the image of the target moves to the top of the display. When the two are coincident, the 'relative bearing' reads out the image rotation offset. This value is fixed for the sonde unless it is disassembled and rebuilt, at which point the procedure MUST be repeated. Please see the additional topic on the Radial Amplitude Display for further details.

- The ***Serial Number*** list box is used to select the sonde which is in use. When the appropriate sonde is selected, the image rotation offset determined by the above procedure is selected. To edit the image offset click the '***Edit***' and enter the new offset. Several serial numbers and associated offsets can be stored and selected as required.

8.0 Graphical

The palette can be changed between a colored and grey scale setting. The changes affect the log screen palette display and are also applied when replaying a log. Selecting Full range in the 'AGC Palette' will cause the software to spread the palette over the full 16bit signal. 'Mid range' will spread the palette over the first quarter of the 16bit range and 'Low range' will spread the palette over the first eighth of the 16 bit range. In most cases the 'Low range' selection is used. Note these settings do not affect the stored log data in any way. The 'Filter Width' is applied to the Natural Gamma trace data and is a simply running average filter. The range of the filter width is from 1 to 50 (x 10 millidepth units ie. mm or mft).

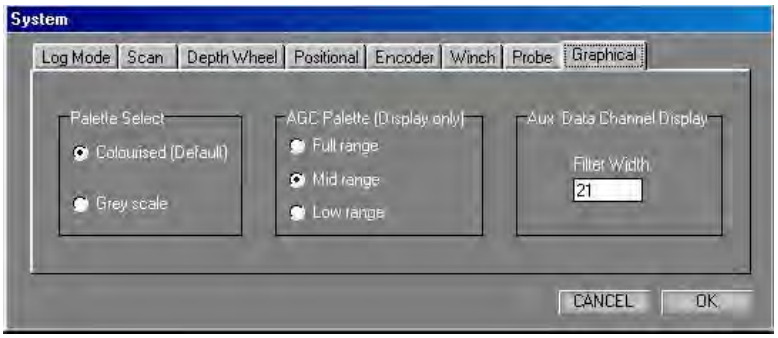

9.0 Sonde Operation

When the operations specified above have been reviewed and the correct settings have been selected, the system is ready for use. The main screen area is divided into 3 horizontal elements. At the top is the depth and orientation readout, together with the scale headings for the scrolling display of unwrapped borehole image.

On the left side of the depth track is the travel time display, with text boxes for sonde inclination, azimuth and head temperature.

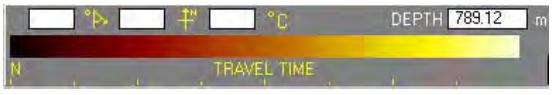

On the right side is the display of amplitude and indication of current operating mode. Located in the center above the depth track are the text boxes for depth and cable speed (computed at the surface). The ranges for the 'Natural Gamma' channel overlay (optional) are shown above the Amplitude.

The central area is utilized for the scrolling display of unwrapped borehole data. The display is orientated with the left edge corresponding to North point of the aligned image data (if orientation is selected) according to the outputs of the sonde's orientation package.

The lower area has controls for the winch (applicable to RG Smart Winch only), depth initialization and sonde control.

The winch control area is only displayed when RG SmartWinch operation is enabled - see section 5 - and has four controls. Set Target Speed by typing the required speed into the window and pressing Enter.

Cable movement is initiated by clicking on either the UP or DOWN arrow control.

Cable movement is halted by clicking on the square STOP control.

Depth is initialized by typing the required value into the entry box and pressing Enter. The entry box is not available at times when the system is in logging mode and the depth should not be changed by user entry.

Sonde power is applied by clicking on the green-colored 1 button. Power is turned off by clicking on the red-colored 0 button. There is no indicator for the state of the power supply on the desktop, so the external indicators should be observed for this purpose.

To make a log ensure that the Test Mode is disabled - see section 1, Log Mode setting. Click File|New Log and select a filename. Old logs may be overwritten if necessary -TAKE CARE. The header editor will be started automatically. A previous set of header data may be loaded by clicking LOAD and choosing a template.

To start logging, click on the red Record (circle) control. The log data will start to scroll down the screen after a brief pause for synchronization. The messages "DSP2: Detecting data stream" and "Updating probe settings" will be observed at the bottom of the screen during this process. Note that the screen scrolling direction is not affected by the actual direction of movement of the sonde. To cease logging, click on the black STOP control (square). The data should be immediately backed up to a USB drive, CD, or other data storage prior to beginning another log.

If the data display from a probe which is properly connected appears to occupy only half of the track area,

with the remainder filled with random colors such as green which are not part of the regular palette, then it is most likely that the downhole data communication is not functioning properly. This symptom is due to the fact that the probe settings cannot be communicated properly, and it is operating in its default power-up mode. If this is the case, the Drive setting of the System|Winch dialog should be increased or decreased accordingly. See section 5 for full details.

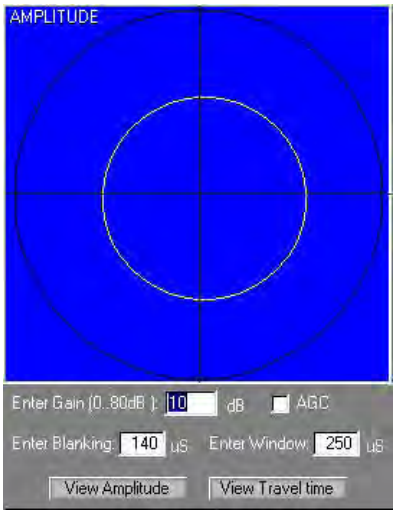

To adjust the sonde gain it is necessary to use the Radial Amplitude plot, which is enabled by clicking on the circle with cross-hairs symbol. When the dialog is active a new window will open on top of the unwrapped data display. In this display, the data is presented as a 'polar' plot. Press the 'View Amplitude' button to display the amplitude plot. This plot shows amplitude increasing towards the outside of the circle and the compass direction following the sweep of the transducer. The line indicating the data is drawn in the regular palette, so that high amplitudes are drawn in white and low amplitudes in black/brown. The picture here shows the image of the inside of a cylinder.

If the data is concentrated in a small circle at the center, the gain is too low and should be increased. If the data is obviously clipped at the outside of the circle, then the gain should be reduced. Type the new gain value into the entry box and press Enter. The ideal would be to set a gain value which allows the peak values to be displayed without clipping, with the majority of the data around the half-way level. It may also be necessary to adjust the blanking to ensure that internal reflections from the acoustic housing are not detected at the new gain value. This will be apparent in the unwrapped data display as pronounced patterning unrelated to the true target. The AGC option causes the probe to set gain automatically thus preventing signal saturation in most cases. (The gain is varied in 6dB steps

Blanking Period and window length can be set independently. Blanking is set to avoid reflections from the housing of the acoustic transducer or random reflections from a rugose borehole, and window length is set to accommodate the range of borehole radius that might be expected. An error will be indicated if the sum of the blanking period and window length would be greater than 409 microseconds, which is the maximum range of the timer. The default value for the blanking period is 145 microseconds, which is the minimum required for the two-way transit from the transceiver to the outer surface of the acoustic housing. It is not advisable to reduce this value beyond the default setting, although it may be increased for larger boreholes at the rate of 1.5mm of one-way travel per microsecond.

Window Length (sample time) defines the period during which the arrival gate remains open to detect the returned acoustic pulse. The acoustic pulse will travel in water at a speed of approximately 1.5mm per microsecond. The default window length is 150 microseconds, which is equivalent to 225 mm of (two-way) travel in the borehole fluid, or approximately 110mm of borehole diameter. If this is added to the default blanking period, which is equivalent to the outside diameter of the acoustic housing, it can be seen that the default set-up will be correct for boreholes up to 150mm. An error will be indicated if the sum of the blanking period and window length would be greater than 409 microseconds, which is the maximum range of the timer. Choose your window setting to best match the borehole diameter.

Pressing the ‘View Travel time’ button changes the display to that shown below:

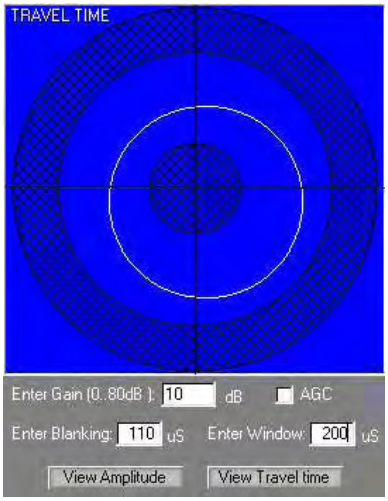

The unhatched ring between the two cross hatched zones represents the sample window. The width of this ring will vary with window length value. The profile of a cylinder is represented here appearing as a circle in the sample window.

Pressing this button displays the following dialog box:

This box allows you to enable the Natural Gamma option by checking the ‘Enable Overlay’ check box. The Overlay appears as a trace upon the Amplitude plot. The trace range and color can also be set by this dialog. The level of filtering can also be altered (see section 8) (note that any displayed trace data is automatically aligned with the acoustic scan data but only when logging up. The Natural Gamma sensor occupies a higher position in the probe so sufficient data has to be prebuffered so that the acoustic data can depth aligned with gamma. The prebuffering results in a delay at the start of a log before correct gamma data appears this is normal.)

Data Analysis and Interpretation

RG-DIP, the manufacturer’s image interpretation package, offers manual and automatic feature recognition options. Feature orientations (dip/strike and azimuth) are automatically calculated. Display options include stereographic projections of zone axes, orientation frequency plots and 'synthetic cores' for comparison with real core data. The last option is invaluable for orientating core samples, particularly in the case of incomplete recovery.

Reporting

The final report will include the objective and scope of the survey, location of the boreholes, discussion of instrumentation and procedures in the field and lab. For each borehole there will be a plot showing the dip/strike and azimuth of features. The next page shows an example.

Assumptions and limitations of the results will be discussed. Supporting references will be listed as necessary

Required Field Records

Field log for each borehole showing

a) Location and description of the borehole

b) Date of test

c) Field personnel

d) Instrumentation

e) Any deviations from test plan and action taken as a result

This procedure has been reviewed and approved by the undersigned:

Professional Geophysicist Anthony Martin Date Feb 13. 2006

QA Review 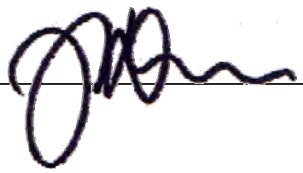 Date Feb 13. 2006

B-XXX	Company	Geovision Geophysical Services
	Location	Somewhere Dam

BH	B-XXX Acoustic Televiewer		
Date	7/8/05	BH Fluid	Air/Water
Casing	4" Steel to 15 ft		
File Name	BXXXdown1		
Depth Drilled	300 feet		
Depth Logged	299.3 feet		
Logged by	Rob Steller		
Client	Best Customer Inc.		

Notes:

1) All orientations referenced to True North

2) Tadpole tails indicate dip direction with True North as up.

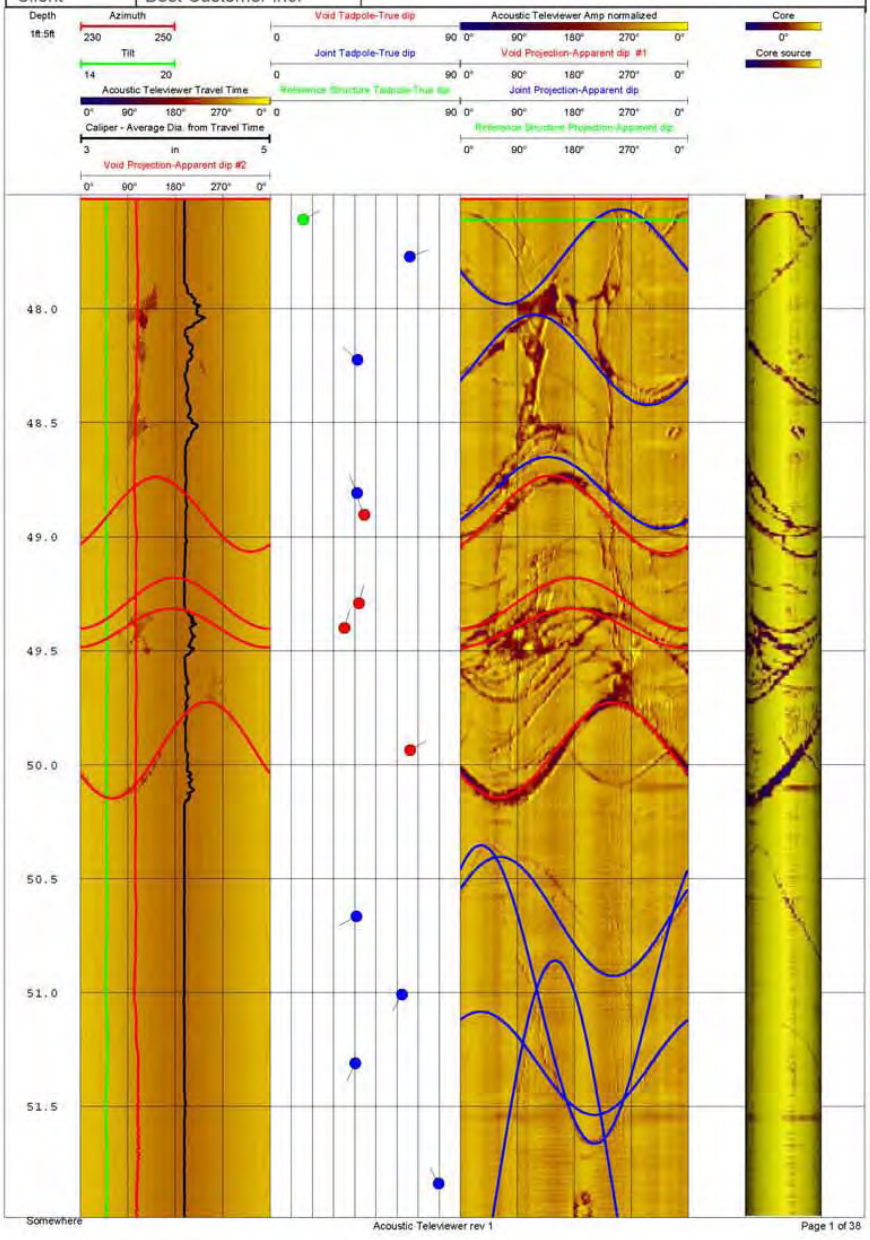

The following downhole data was prepared by Caltrans Drilling Services (See CH2M HILL, 2010)

LA 710 Tunnel boring Z1 B8

COMPANY	: CALTRANS			OTHER SERVICES:	
WELL	: Z1 B8			IND-CAL	
LOCATION/FIELD	: LA 710 TUNNEL			AC TEL	
COUNTY	: LA			PSLOG	
LOCATION	: CA				
SECTION	: None	TOWNSHIP	: None	RANGE	: None
DATE	: 1/08/09	PERMANENT DATUM	: None		
DEPTH DRILLER	: 200 FT			KB	: NA
LOG BOTTOM	: 201.5	LOG MEASURED FROM:	GL	DF	: NA
LOG TOP	: -0.2	DRL MEASURED FROM:	GL	GL	: NA
CASING DIAMETER	: 3.9	LOGGING UNIT	: 7311		
CASING TYPE	: none	FIELD OFFICE	: 7311		
CASING THICKNESS:	0	RECORDED BY	: DH/DL		
BIT SIZE	: 3.95 IN	BOREHOLE FLUID	: 0	FILE	: PROCESSE
MAGNETIC DECL.	: 12.85	RM	: 0	TYPE	: 9065A
MATRIX DENSITY	: 2.71	RM TEMPERATURE	: 0	LGDATE	: 1/08/09.
NEUTRON MATRIX	: DOLOMITE	MATRIX DELTA T	: 140		
				THRESH:	2500

THIS LOG MEASURED IN FEET, CALIPER MEASURED IN INCHES
EA: 07-187900. GL ELEVATION ESTIMATED FROM HANDHELD GPS 377 FT

ALL SERVICES PROVIDED SUBJECT TO STANDARD TERMS AND CONDITIONS

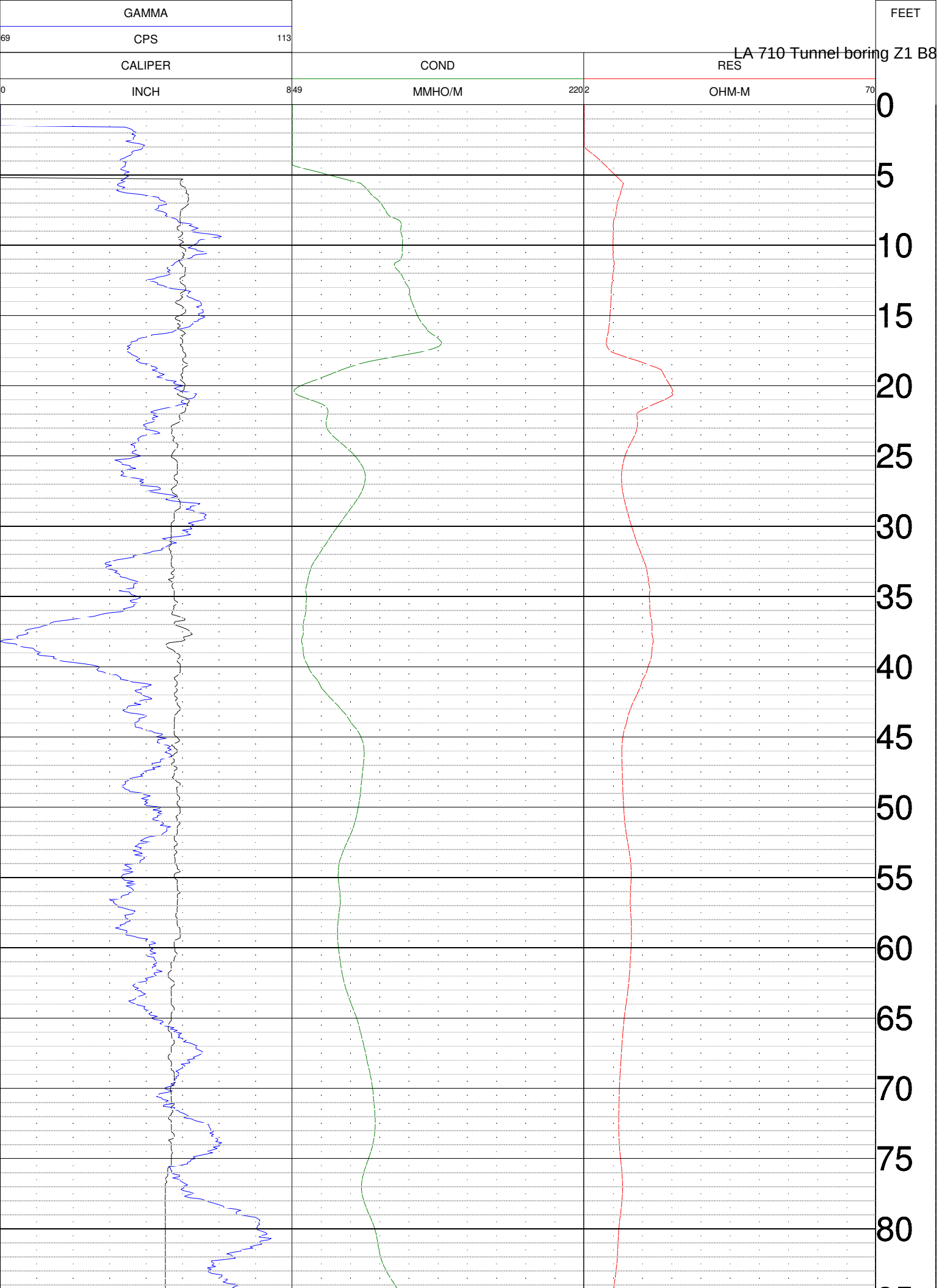
GAMMA
69
CPS
113
CALIPER
0
INCH
8
COND
49
MMHO/M
220
RES
2
OHM-M
70
FEET
LA 710 Tunnel boring Z1 B8
0
5
10
15
20
25
30
35
40
45
50
55
60
65
70
75
80

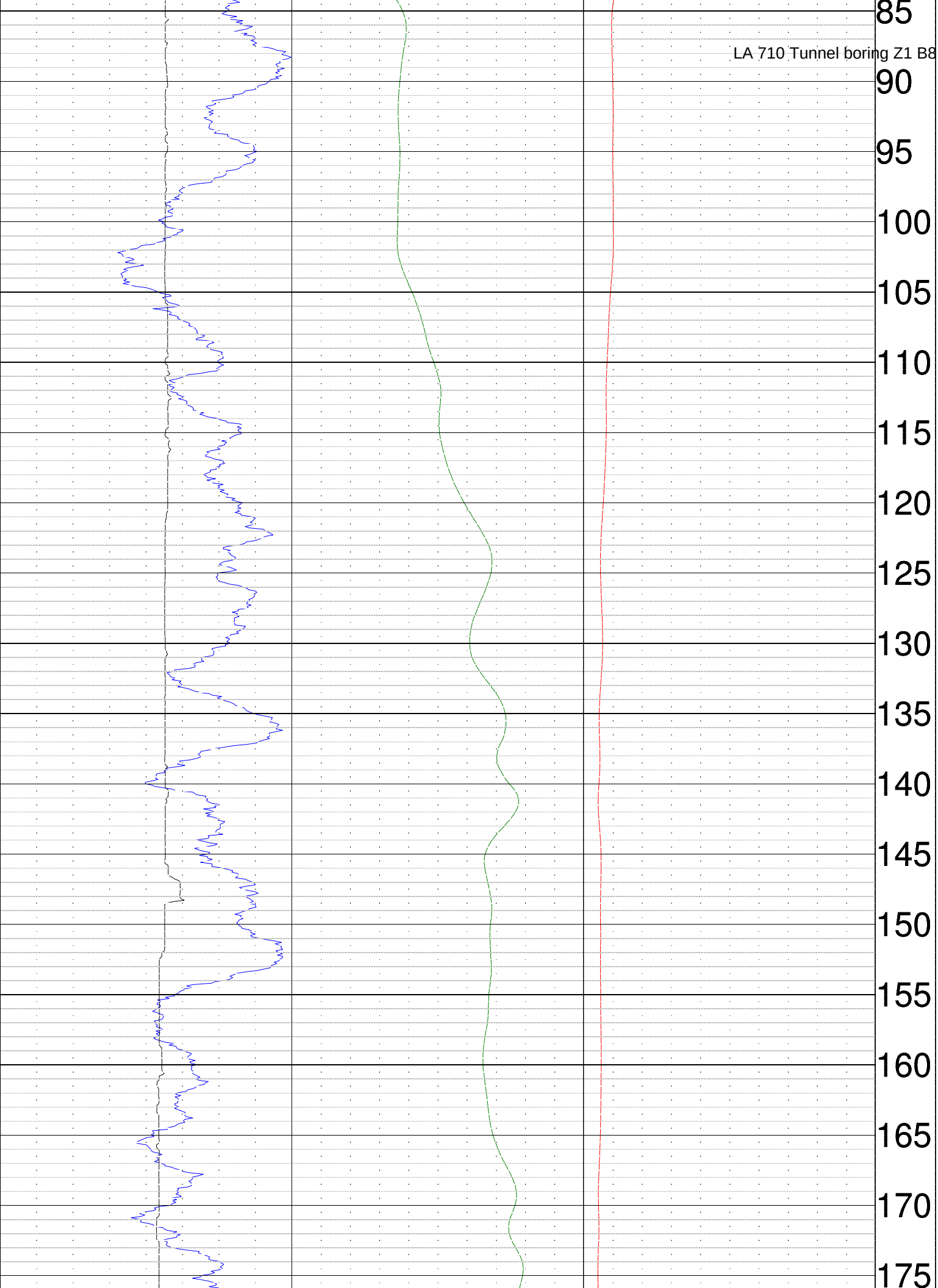
LA 710 Tunnel boring Z1 B8
85
90
95
100
105
110
115
120
125
130
135
140
145
150
155
160
165
170
175

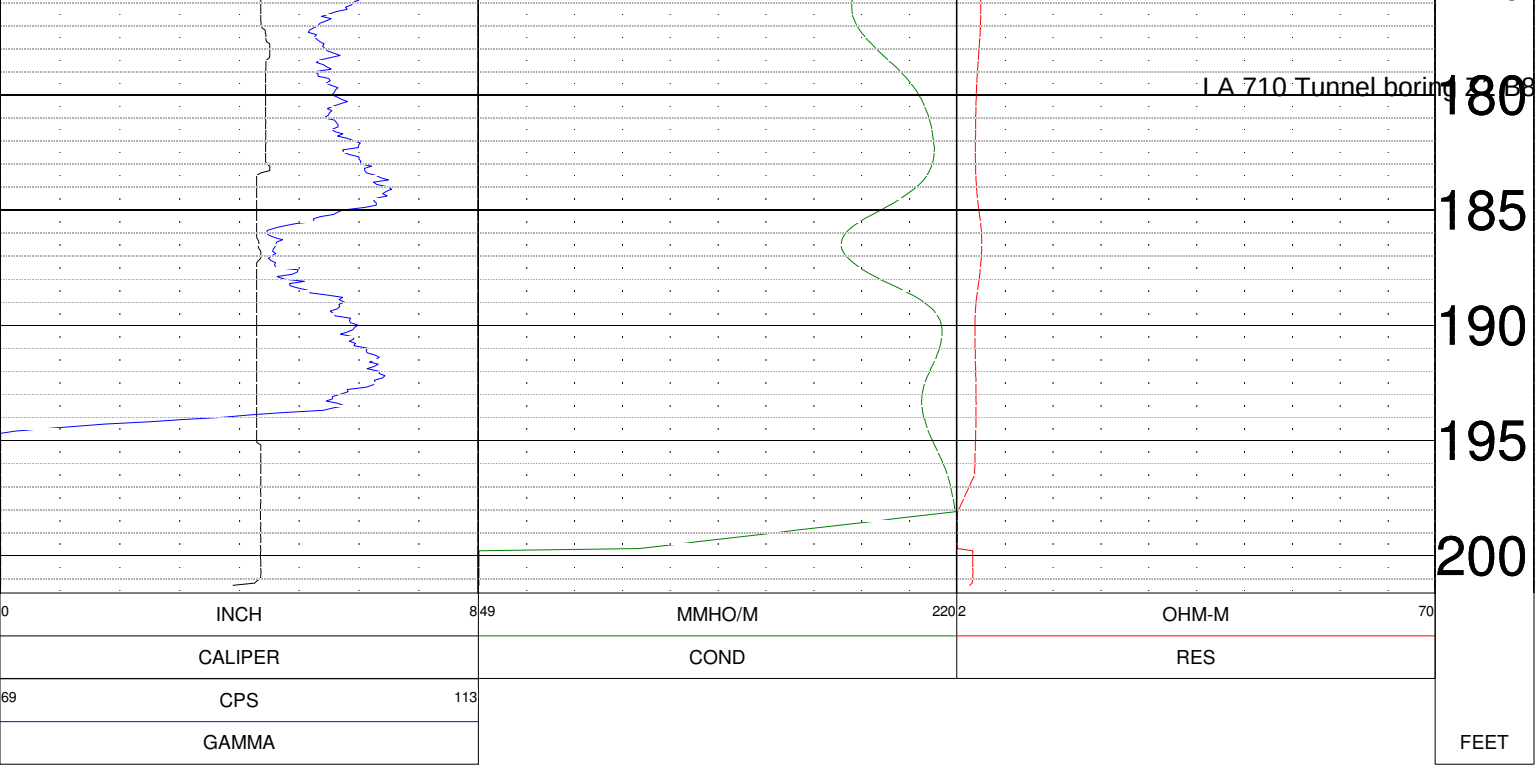
I A 710 Tunnel boring 2 of 8
180
185
190
195
200
0
INCH
8
49
MMHO/M
220
2
OHM-M
70
CALIPER
COND
RES
69
CPS
113
GAMMA
FEET

Table 2. LA 710 Tunnel
Boring Z1 B8
PS Suspension Log Data Summary

Top of Hole Elevation (m)	Depth (m)	Depth (ft)	Vs (m/s)	Vs (ft/s)	Vp (m/s)	Vp (ft/s)	γ	ρ(Vp) (g/cc)	ρ(Vp) (lb/ft^3)	G (GPa)	E (GPa)	K (GPa)	G ($10^3 lb/ft^2$)	E ($10^3 lb/ft^2$)	K ($10^3 lb/ft^2$)
Not Provided	1	3.3	214	702		NA	NA	NA	NA	NA	NA	NA	NA	NA	NA
	1.5	4.9	203	666		NA	NA	NA	NA	NA	NA	NA	NA	NA	NA
	2	6.6	215	706		NA	NA	NA	NA	NA	NA	NA	NA	NA	NA
	2.5	8.2	242	795		NA	NA	NA	NA	NA	NA	NA	NA	NA	NA
	3	9.8	255	836		NA	NA	NA	NA	NA	NA	NA	NA	NA	NA
	3.5	11.5	258	847		NA	NA	NA	NA	NA	NA	NA	NA	NA	NA
	4	13.1	233	763		NA	NA	NA	NA	NA	NA	NA	NA	NA	NA
	4.5	14.8	198	650		NA	NA	NA	NA	NA	NA	NA	NA	NA	NA
	5	16.4	196	643		NA	NA	NA	NA	NA	NA	NA	NA	NA	NA
	5.5	18.0	242	795		NA	NA	NA	NA	NA	NA	NA	NA	NA	NA
	6	19.7	299	979		NA	NA	NA	NA	NA	NA	NA	NA	NA	NA
	6.5	21.3	241	791	515	1691	NA	NA	NA	NA	NA	NA	NA	NA	NA
	7	23.0	194	637	382	1252	NA	NA	NA	NA	NA	NA	NA	NA	NA
	7.5	24.6	187	613	495	1624	NA	NA	NA	NA	NA	NA	NA	NA	NA
	8	26.2	198	650	833	2734	NA	NA	NA	NA	NA	NA	NA	NA	NA
	8.5	27.9	219	717	1163	3815	NA	NA	NA	NA	NA	NA	NA	NA	NA
	9	29.5	237	777	1613	5292	0.49	1.94	121.09	0.109	0.324	4.901	2269	6758	102358
	9.5	31.2	242	795	1786	5859	0.49	2.06	128.62	0.121	0.361	6.408	2529	7539	133836
	10	32.8	261	858	2000	6562	0.49	2.18	136.25	0.149	0.445	8.531	3116	9292	178175
	10.5	34.4	253	831	1613	5292	0.49	1.94	121.09	0.124	0.370	4.880	2596	7723	101922
	11	36.1	267	875	1471	4825	NA	NA	NA	NA	NA	NA	NA	NA	NA
	11.5	37.7	290	951	1563	5126	NA	NA	NA	NA	NA	NA	NA	NA	NA
	12	39.4	328	1076	1667	5468	0.48	1.98	123.58	0.213	0.630	5.215	4445	13155	108922
	12.5	41.0	286	937	1613	5292	0.48	1.94	121.09	0.158	0.470	4.835	3307	9814	100975
	13	42.7	274	899	1613	5292	0.49	1.94	121.09	0.146	0.432	4.852	3041	9032	101330
	13.5	44.3	317	1042	1613	5292	0.48	1.94	121.09	0.195	0.579	4.785	4083	12083	99940
	14	45.9	339	1112	1667	5468	0.48	1.98	123.58	0.227	0.673	5.196	4751	14048	108513
	14.5	47.6	333	1094	1667	5468	0.48	1.98	123.58	0.220	0.651	5.206	4594	13590	108723
	14.9	48.9	342	1122	1667	5468	0.48	1.98	123.58	0.231	0.684	5.190	4833	14285	108405
	14.9	48.9	308	1009	1724	5657	0.48	2.02	126.09	0.191	0.567	5.749	3994	11850	120076
	15.4	50.5	348	1141	1667	5468	0.48	1.98	123.58	0.240	0.708	5.180	5002	14778	108179
	15.5	50.9	360	1182	1724	5657	0.48	2.02	126.09	0.262	0.775	5.655	5478	16184	118097
	15.9	52.2	354	1161	1667	5468	0.48	1.98	123.58	0.248	0.732	5.168	5181	15297	107940
	16	52.5	370	1215	1724	5657	0.48	2.02	126.09	0.277	0.818	5.635	5787	17080	117685
	16.4	53.8	345	1131	1613	5292	0.48	1.94	121.09	0.231	0.681	4.738	4817	14220	98961
	16.5	54.1	400	1312	1667	5468	0.47	1.98	123.58	0.317	0.931	5.077	6615	19441	106028
	16.9	55.4	412	1353	1667	5468	0.47	1.98	123.58	0.337	0.988	5.050	7031	20634	105474

γ = Poisson's Ratio ρ(Vp) = Vp-derived density G = Shear Modulus E = Young's Modulus K = Bulk Modulus
Shaded cells denote questionable data.

Table 2. LA 710 Tunnel
Boring Z1 B8
PS Suspension Log Data Summary

Top of Hole Elevation (m)	Depth (m)	Depth (ft)	Vs (m/s)	Vs (ft/s)	Vp (m/s)	Vp (ft/s)	γ	ρ(Vp) (g/cc)	ρ(Vp) (lb/ft^3)	G (GPa)	E (GPa)	K (GPa)	G ($10^3 lb/ft^2$)	E ($10^3 lb/ft^2$)	K ($10^3 lb/ft^2$)
	17	55.8	354	1161	1563	5126	NA	NA	NA	NA	NA	NA	NA	NA	NA
	17.4	57.1	333	1094	1613	5292	0.48	1.94	121.09	0.216	0.637	4.758	4501	13302	99383
	17.5	57.4	348	1141	1667	5468	0.48	1.98	123.58	0.240	0.708	5.180	5002	14778	108179
	17.9	58.7	348	1141	1724	5657	0.48	2.02	126.09	0.244	0.723	5.678	5104	15094	118596
	18	59.1	377	1238	1724	5657	0.47	2.02	126.09	0.288	0.848	5.621	6007	17719	117392
	18.5	60.7	357	1172	1724	5657	0.48	2.02	126.09	0.258	0.761	5.661	5381	15901	118227
	18.5	60.7	374	1226	1724	5657	0.48	2.02	126.09	0.282	0.833	5.628	5895	17395	117540
	19	62.3	400	1312	1786	5859	0.47	2.06	128.62	0.330	0.971	6.130	6885	20290	128029
	19	62.3	364	1193	1786	5859	0.48	2.06	128.62	0.272	0.805	6.206	5690	16823	129621
	19.5	64.0	364	1193	1667	5468	0.48	1.98	123.58	0.262	0.772	5.150	5467	16128	107558
	19.5	64.0	348	1141	1724	5657	0.48	2.02	126.09	0.244	0.723	5.678	5104	15094	118596
	20	65.6	354	1161	1667	5468	0.48	1.98	123.58	0.248	0.732	5.168	5181	15297	107940
	20	65.6	364	1193	1724	5657	0.48	2.02	126.09	0.267	0.789	5.648	5578	16475	117964
	20.5	67.3	339	1112	1667	5468	0.48	1.98	123.58	0.227	0.673	5.196	4751	14048	108513
	21	68.9	315	1033	1667	5468	0.48	1.98	123.58	0.196	0.582	5.237	4101	12153	109379
	21.5	70.5	331	1085	1667	5468	0.48	1.98	123.58	0.216	0.640	5.211	4518	13370	108824
	22	72.2	357	1172	1667	5468	0.48	1.98	123.58	0.253	0.745	5.162	5274	15567	107816
	22.5	73.8	345	1131	1667	5468	0.48	1.98	123.58	0.235	0.696	5.185	4916	14529	108293
	23	75.5	364	1193	1667	5468	0.48	1.98	123.58	0.262	0.772	5.150	5467	16128	107558
	23.5	77.1	385	1262	1724	5657	0.47	2.02	126.09	0.299	0.881	5.606	6240	18394	117081
	24	78.7	385	1262	1563	5126	NA	NA	NA	NA	NA	NA	NA	NA	NA
	24	78.7	377	1238	1667	5468	0.47	1.98	123.58	0.282	0.830	5.123	5888	17344	106998
	24.5	80.4	388	1274	1724	5657	0.47	2.02	126.09	0.305	0.898	5.598	6362	18746	116918
	25	82.0	400	1312	1724	5657	0.47	2.02	126.09	0.323	0.951	5.573	6750	19865	116402
	25.5	83.7	392	1287	1724	5657	0.47	2.02	126.09	0.311	0.915	5.590	6487	19109	116751
	26	85.3	370	1215	1667	5468	0.47	1.98	123.58	0.272	0.801	5.137	5671	16720	107286
	26.5	86.9	392	1287	1667	5468	0.47	1.98	123.58	0.304	0.895	5.093	6358	18702	106370
	27	88.6	440	1442	1724	5657	0.47	2.02	126.09	0.390	1.144	5.484	8151	23885	114534
	27.5	90.2	455	1491	1724	5657	0.46	2.02	126.09	0.417	1.221	5.448	8716	25497	113780
	28	91.9	460	1508	1724	5657	0.46	2.02	126.09	0.427	1.248	5.435	8917	26070	113511
	28.5	93.5	440	1442	1724	5657	0.47	2.02	126.09	0.390	1.144	5.484	8151	23885	114534
	29	95.1	455	1491	1724	5657	0.46	2.02	126.09	0.417	1.221	5.448	8716	25497	113780
	29.5	96.8	471	1544	1724	5657	0.46	2.02	126.09	0.447	1.306	5.408	9342	27274	112945
	30	98.4	488	1600	1786	5859	0.46	2.06	128.62	0.490	1.431	5.916	10239	29891	123556
	30.5	100.1	506	1661	1786	5859	0.46	2.06	128.62	0.528	1.538	5.865	11031	32129	122500
	31	101.7	513	1682	1852	6076	0.46	2.10	131.15	0.552	1.612	6.468	11539	33658	135081
	31.5	103.3	533	1750	1786	5859	0.45	2.06	128.62	0.586	1.701	5.788	12239	35519	120889

γ = Poisson's Ratio ρ(Vp) = Vp-derived density G = Shear Modulus E = Young's Modulus K = Bulk Modulus
Shaded cells denote questionable data.

Table 2. LA 710 Tunnel
Boring Z1 B8
PS Suspension Log Data Summary

Top of Hole Elevation (m)	Depth (m)	Depth (ft)	Vs (m/s)	Vs (ft/s)	Vp (m/s)	Vp (ft/s)	γ	ρ(Vp) (g/cc)	ρ(Vp) (lb/ft^3)	G (GPa)	E (GPa)	K (GPa)	G ($10^3 lb/ft^2$)	E ($10^3 lb/ft^2$)	K ($10^3 lb/ft^2$)
	32	105.0	526	1727	1786	5859	0.45	2.06	128.62	0.571	1.658	5.809	11919	34624	121316
	32.5	106.6	656	2151	1786	5859	0.42	2.06	128.62	0.886	2.520	5.388	18502	52622	112539
	33	108.3	588	1930	1667	5468	0.43	1.98	123.58	0.685	1.958	4.586	14306	40883	95773
	33.5	109.9	465	1526	1667	5468	0.46	1.98	123.58	0.428	1.249	4.928	8944	26078	102922
	34	111.5	367	1204	1613	5292	0.47	1.94	121.09	0.261	0.769	4.698	5455	16068	98110
	34.5	113.2	317	1042	1667	5468	0.48	1.98	123.58	0.200	0.591	5.233	4167	12344	109292
	35	114.8	276	905	1724	5657	0.49	2.02	126.09	0.154	0.457	5.799	3210	9546	121121
	35.5	116.5	345	1131	1786	5859	0.48	2.06	128.62	0.245	0.725	6.243	5116	15151	130386
	36	118.1	460	1508	1852	6076	0.47	2.10	131.15	0.444	1.303	6.612	9275	27215	138099
	36.5	119.8	449	1475	1852	6076	0.47	2.10	131.15	0.424	1.246	6.639	8863	26033	138649
	37	121.4	430	1411	1724	5657	0.47	2.02	126.09	0.374	1.096	5.506	7804	22894	114996
	37.5	123.0	417	1367	1667	5468	0.47	1.98	123.58	0.344	1.008	5.041	7178	21056	105277
	38.5	126.3	465	1526	1724	5657	0.46	2.02	126.09	0.437	1.277	5.422	9126	26662	113233
	39	128.0	460	1508	1667	5468	0.46	1.98	123.58	0.418	1.221	4.941	8740	25500	103195
	39.5	129.6	455	1491	1724	5657	0.46	2.02	126.09	0.417	1.221	5.448	8716	25497	113780
	40	131.2	460	1508	1724	5657	0.46	2.02	126.09	0.427	1.248	5.435	8917	26070	113511
	40.5	132.9	426	1396	1667	5468	0.47	1.98	123.58	0.358	1.050	5.021	7487	21938	104866
	41	134.5	421	1381	1613	5292	0.46	1.94	121.09	0.344	1.006	4.587	7182	21020	95808
	41.5	136.2	488	1600	1724	5657	0.46	2.02	126.09	0.481	1.400	5.363	10038	29241	112017
	42	137.8	635	2083	1786	5859	0.43	2.06	128.62	0.831	2.371	5.462	17346	49527	114080
	42.5	139.4	667	2187	1667	5468	0.40	1.98	123.58	0.880	2.472	4.326	18376	51627	90347
	43	141.1	513	1682	1724	5657	0.45	2.02	126.09	0.531	1.542	5.296	11094	32205	110609
	43.5	142.7	494	1620	1724	5657	0.46	2.02	126.09	0.493	1.434	5.348	10287	29943	111685
	44	144.4	513	1682	1724	5657	0.45	2.02	126.09	0.531	1.542	5.296	11094	32205	110609
	44.5	146.0	526	1727	1786	5859	0.45	2.06	128.62	0.571	1.658	5.809	11919	34624	121316
	45	147.6	541	1773	1786	5859	0.45	2.06	128.62	0.602	1.745	5.767	12572	36449	120445
	45.5	149.3	541	1773	1786	5859	0.45	2.06	128.62	0.602	1.745	5.767	12572	36449	120445
	46	150.9	533	1750	1786	5859	0.45	2.06	128.62	0.586	1.701	5.788	12239	35519	120889
	46.5	152.6	541	1773	1786	5859	0.45	2.06	128.62	0.602	1.745	5.767	12572	36449	120445
	47	154.2	548	1798	1786	5859	0.45	2.06	128.62	0.619	1.791	5.745	12919	37414	119983
	47	154.2	541	1773	1786	5859	0.45	2.06	128.62	0.602	1.745	5.767	12572	36449	120445
	47.5	155.8	556	1823	1786	5859	0.45	2.06	128.62	0.636	1.839	5.722	13280	38418	119501
	48	157.5	506	1661	1786	5859	0.46	2.06	128.62	0.528	1.538	5.865	11031	32129	122500
	48.5	159.1	513	1682	1786	5859	0.46	2.06	128.62	0.542	1.577	5.847	11316	32930	122120
	49	160.8	548	1798	1786	5859	0.45	2.06	128.62	0.619	1.791	5.745	12919	37414	119982
	49.5	162.4	635	2083	1786	5859	0.43	2.06	128.62	0.831	2.371	5.462	17346	49527	114080
	50	164.0	851	2792	1786	5859	0.35	2.06	128.62	1.492	4.038	4.580	31166	84338	95653

γ = Poisson's Ratio ρ(Vp) = Vp-derived density G = Shear Modulus E = Young's Modulus K = Bulk Modulus
Shaded cells denote questionable data.

Table 2. LA 710 Tunnel
Boring Z1 B8
PS Suspension Log Data Summary

Top of Hole Elevation (m)	Depth (m)	Depth (ft)	Vs (m/s)	Vs (ft/s)	Vp (m/s)	Vp (ft/s)	γ	ρ(Vp) (g/cc)	ρ(Vp) (lb/ft^3)	G (GPa)	E (GPa)	K (GPa)	G ($10^3 lb/ft^2$)	E ($10^3 lb/ft^2$)	K ($10^3 lb/ft^2$)
	50.5	165.7	513	1682	1724	5657	0.45	2.02	126.09	0.531	1.542	5.296	11094	32205	110609
	51	167.3	348	1141	1724	5657	0.48	2.02	126.09	0.244	0.723	5.678	5104	15094	118596
	51.5	169.0	404	1326	1724	5657	0.47	2.02	126.09	0.330	0.970	5.565	6887	20260	116219
	52	170.6	460	1508	1724	5657	0.46	2.02	126.09	0.427	1.248	5.435	8917	26070	113511
	52.5	172.2	488	1600	1786	5859	0.46	2.06	128.62	0.490	1.431	5.916	10239	29891	123556
	53	173.9	494	1620	1786	5859	0.46	2.06	128.62	0.502	1.466	5.900	10493	30610	123217
	53.5	175.5	526	1727	1786	5859	0.45	2.06	128.62	0.571	1.658	5.809	11919	34624	121315
	54	177.2	556	1823	1852	6076	0.45	2.10	131.15	0.648	1.881	6.340	13542	39286	132410
	54.5	178.8	548	1798	1639	5378	0.44	1.96	122.33	0.588	1.691	4.482	12288	35319	93605
	55	180.4	506	1661	1724	5657	0.45	2.02	126.09	0.518	1.505	5.314	10815	31424	110981
	55.5	182.1	513	1682	1724	5657	0.45	2.02	126.09	0.531	1.542	5.296	11094	32205	110609
	56	183.7	417	1367	1724	5657	0.47	2.02	126.09	0.351	1.030	5.537	7324	21517	115636
	56.5	185.4	500	1640	1923	6309	0.46	2.14	133.69	0.535	1.567	7.206	11182	32735	150502
	56.5	185.4	513	1682	1923	6309	0.46	2.14	133.69	0.563	1.646	7.169	11763	34387	149728
	57	187.0	526	1727	2000	6562	0.46	2.18	136.25	0.605	1.769	7.924	12627	36941	165494
	57	187.0	513	1682	1923	6309	0.46	2.14	133.69	0.563	1.646	7.169	11763	34387	149728
	57.5	188.6	552	1813	1786	5859	0.45	2.06	128.62	0.629	1.820	5.731	13134	38012	119696

γ = Poisson's Ratio ρ(Vp) = Vp-derived density G = Shear Modulus E = Young's Modulus K = Bulk Modulus
Shaded cells denote questionable data.

Figure 1. LA 710 Tunnel
Boring Z1 B8
Downhole Interval Velocities

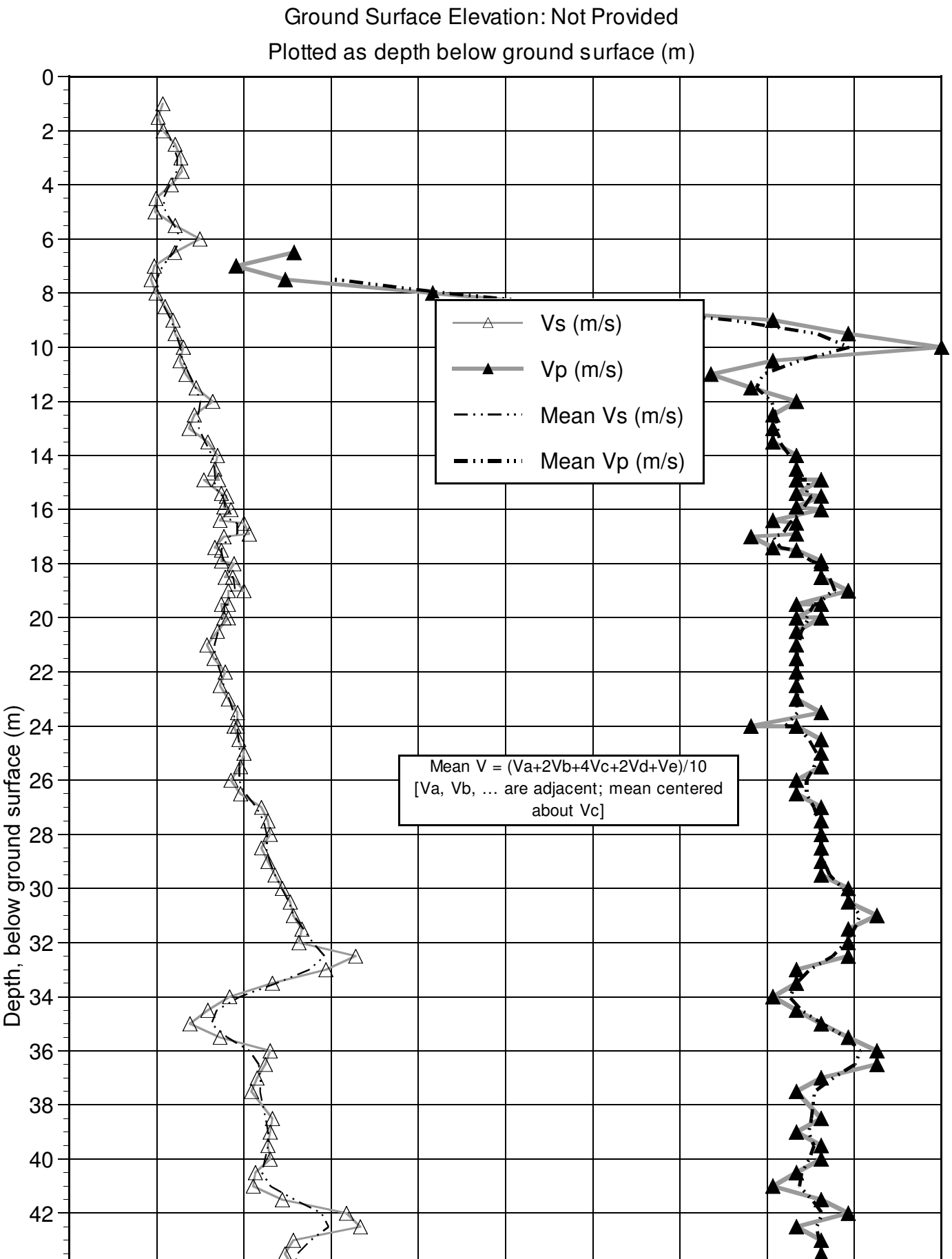

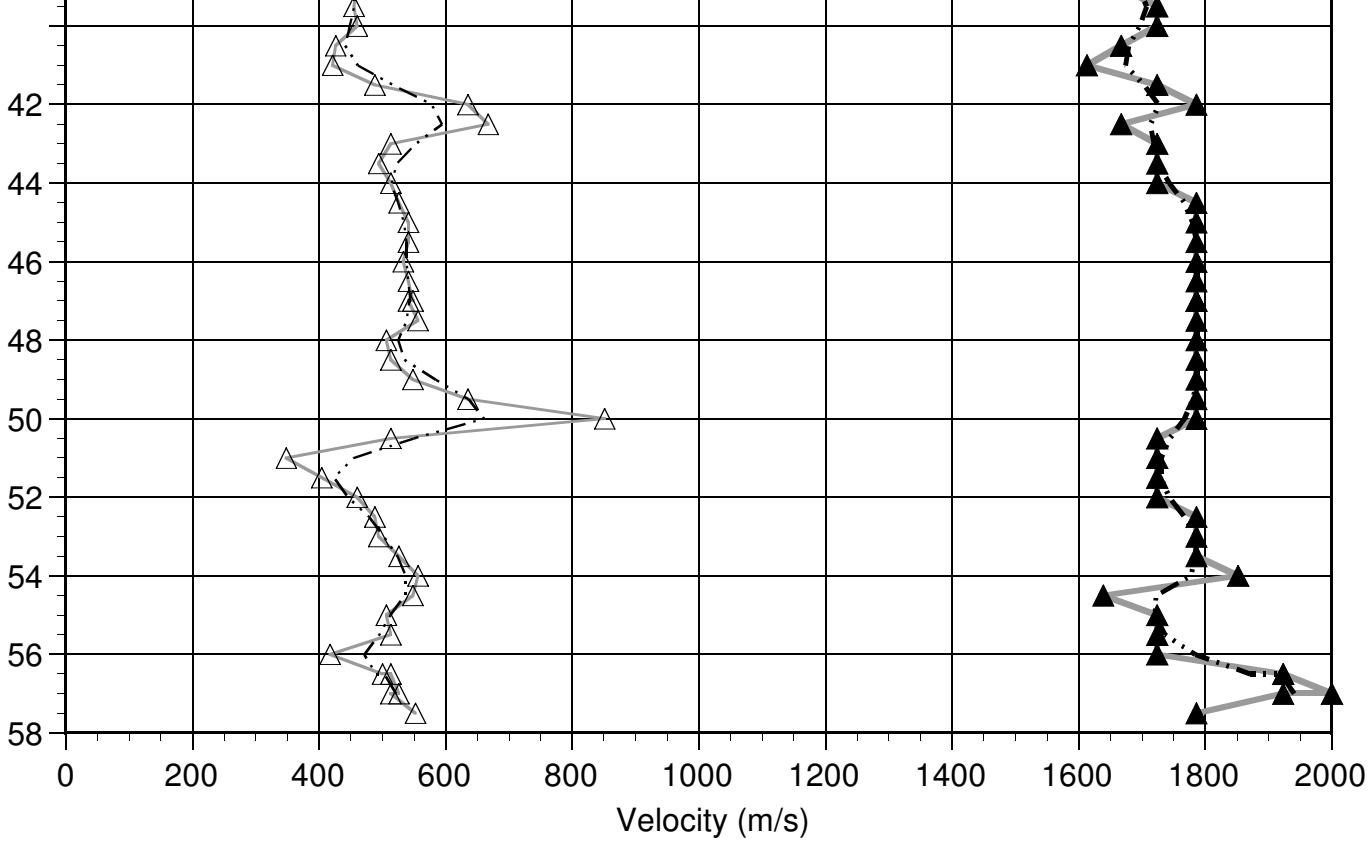
42
44
46
48
50
52
54
56
58
0
200
400
600
800
1000
1200
1400
1600
1800
2000
Velocity (m/s)

LA 710 Tunnel boring Z2 B5

COMPANY	: CALTRANS				
WELL	: Z2 B5				
LOCATION/FIELD	: LA 710 TUNNEL				
COUNTY	: LA				
LOCATION	: CA				
SECTION	: None	TOWNSHIP	: NONE	RANGE	: None
DATE	: 4/14/09	PERMANENT DATUM	: None		
DEPTH DRILLER	: 91.44			KB	: NA
LOG BOTTOM	: 90.6	LOG MEASURED FROM:	GL	DF	: NA
LOG TOP	: 1.2	DRL MEASURED FROM:	GL	GL	: NA
CASING DIAMETER	: n/a	LOGGING UNIT	: 7311		
CASING TYPE	: N/A	FIELD OFFICE	: 7311		
CASING THICKNESS:	N/A	RECORDED BY	: DH/DL		
BIT SIZE	: 10.8CM	BOREHOLE FLUID	: 0	FILE	: PROCESSE
MAGNETIC DECL.	: 12.85	RM	: 0	TYPE	: 9065A
MATRIX DENSITY	: 2.71	RM TEMPERATURE	: 0	LGDATE	: 4/14/09.
NEUTRON MATRIX	: DOLOMITE	MATRIX DELTA T	: 140		
				THRESH:	2500

OTHER SERVICES:
IND-CAL
AC TEL
PS LOG

CALIPER LOG IS APPROXIMATE, AND STARTS AT ~82M DEPTH
EA: 07-187900. GL ELEVATION ESTIMATED FROM HANDHELD GPS 143.9M

ALL SERVICES PROVIDED SUBJECT TO STANDARD TERMS AND CONDITIONS

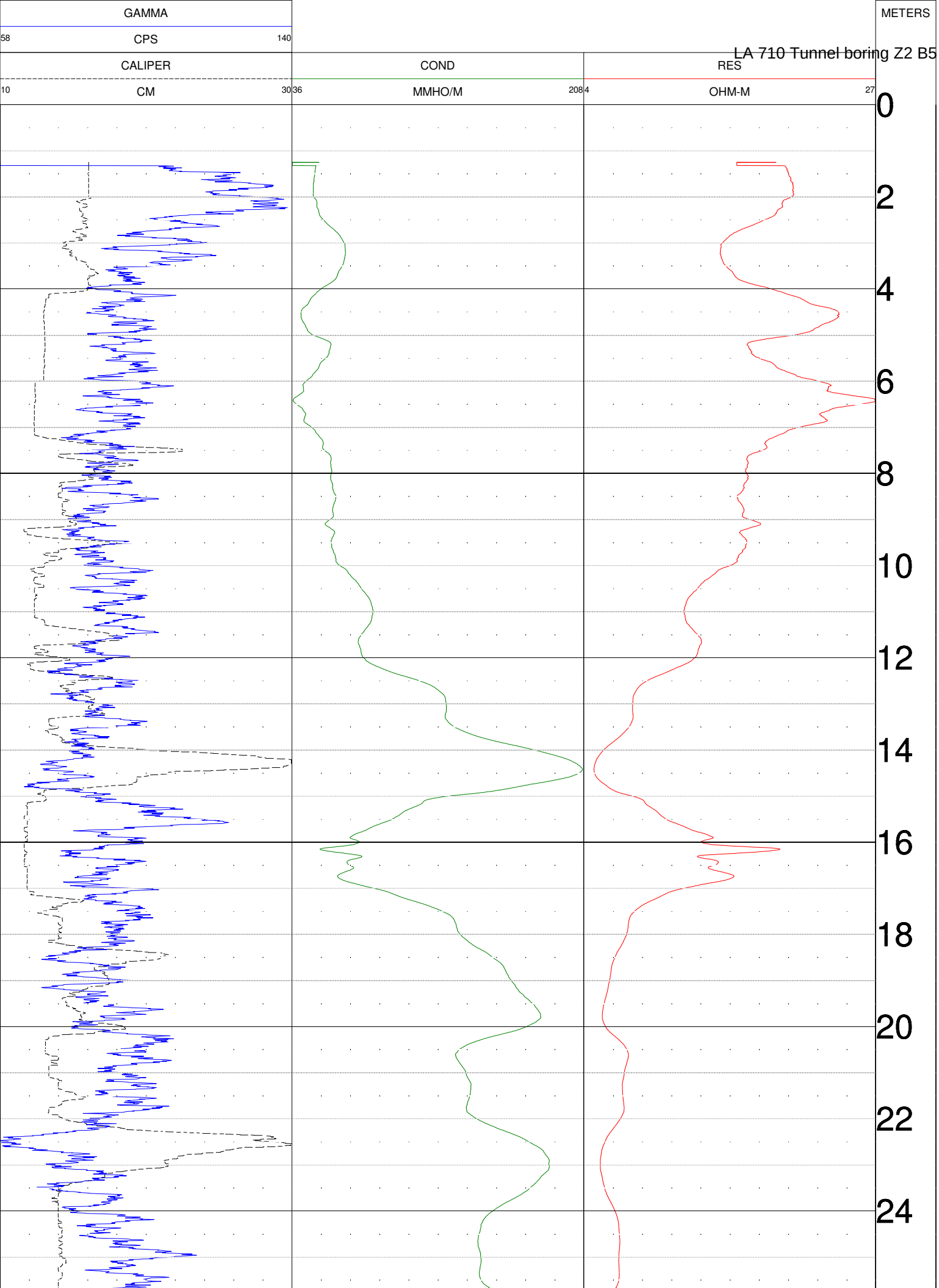
GAMMA
58
CPS
140
CALIPER
10
CM
30
COND
36
MMHO/M
208
RES
4
OHM-M
27
METERS
LA 710 Tunnel boring Z2 B5
0
2
4
6
8
10
12
14
16
18
20
22
24

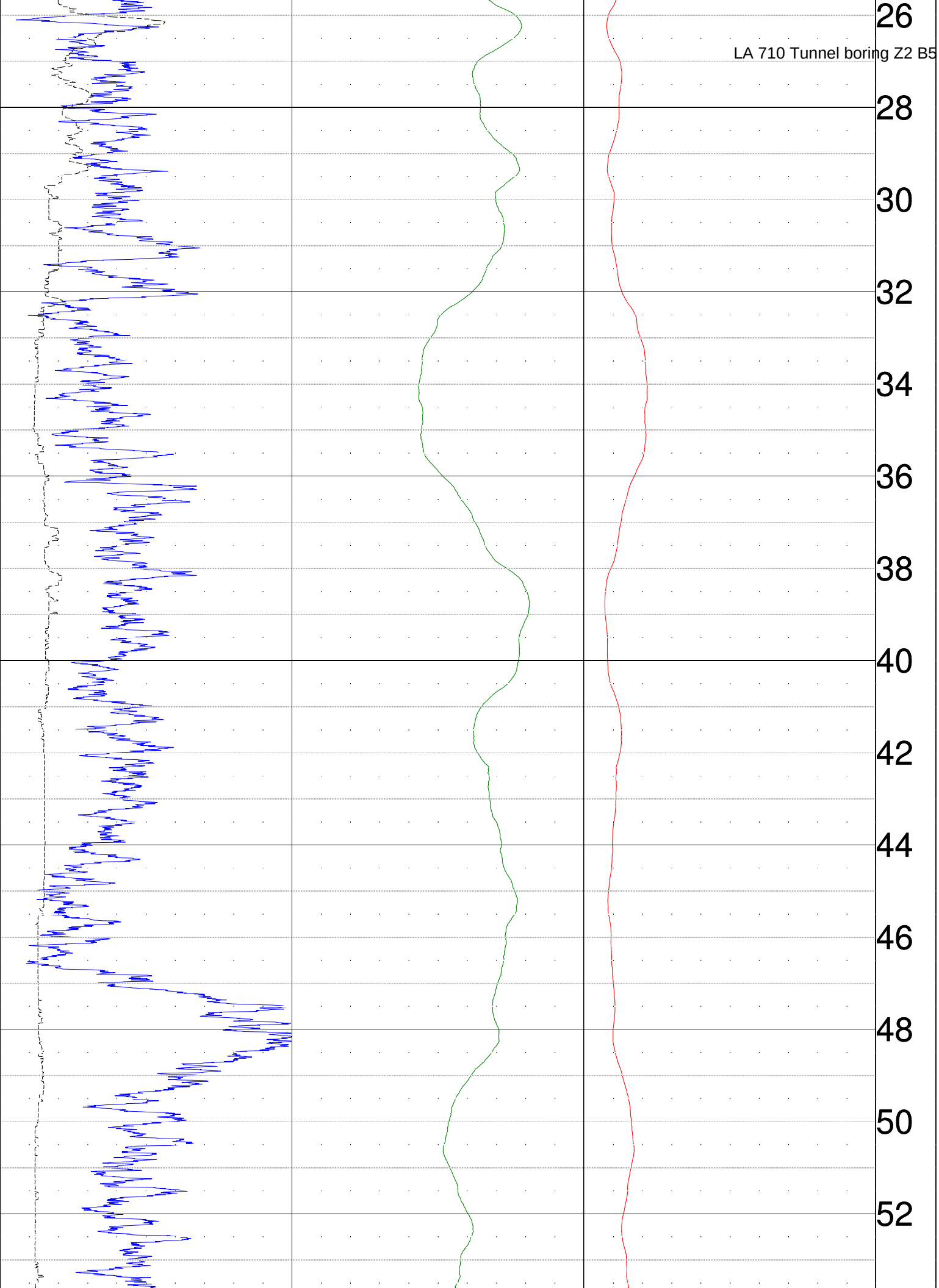
LA 710 Tunnel boring Z2 B5
26
28
30
32
34
36
38
40
42
44
46
48
50
52

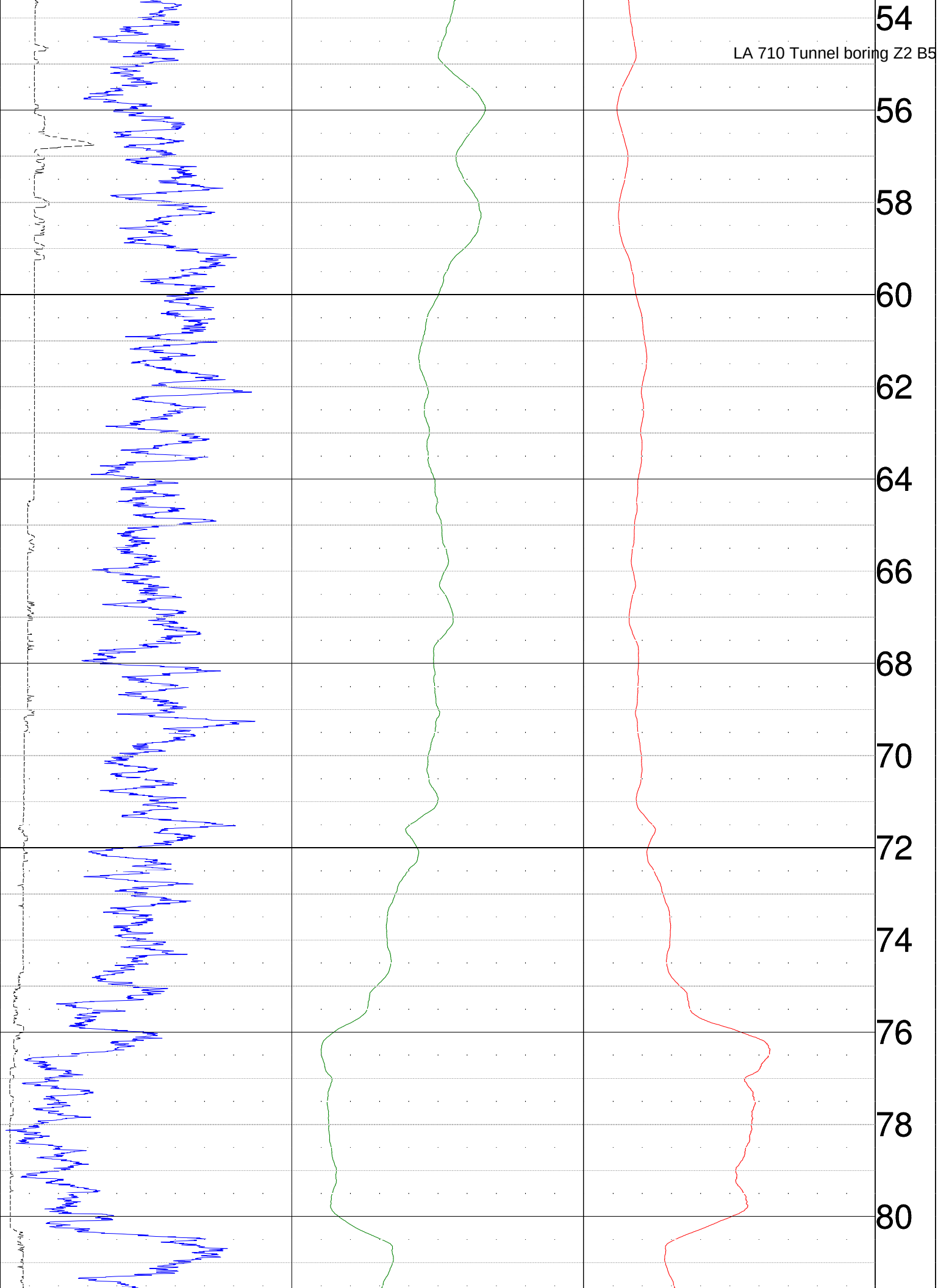
LA 710 Tunnel boring Z2 B5
54
56
58
60
62
64
66
68
70
72
74
76
78
80

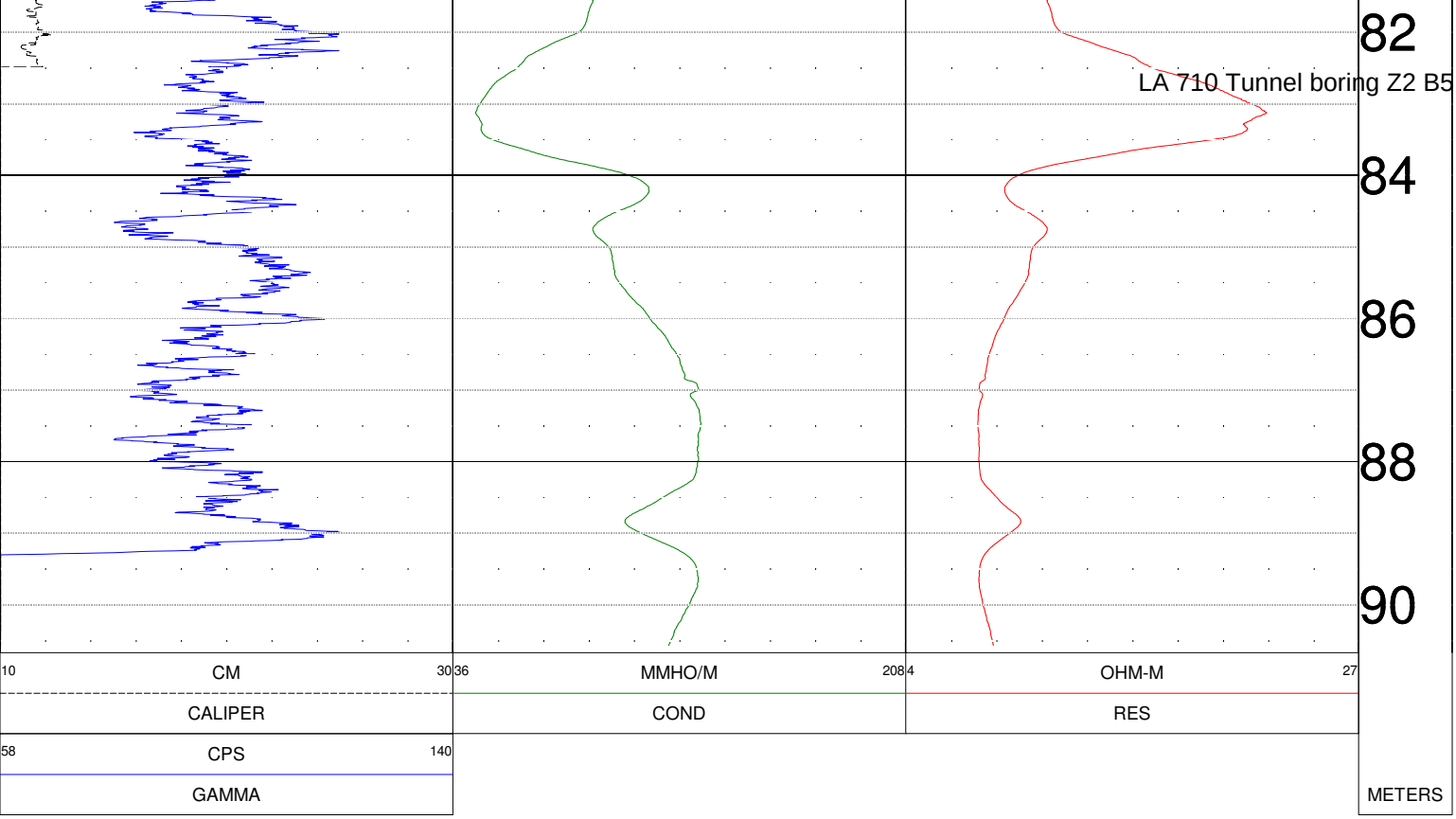
LA 710 Tunnel boring Z2 B5
82
84
86
88
90
10
CM
30
CALIPER
36
MMHO/M
208
COND
4
OHM-M
27
RES
58
CPS
140
GAMMA
METERS

Table 2. LA 710 tunnel
Boring Z2 B5
PS Suspension Log Data Summary

Top of Hole Elevation (m)	Depth (m)	Depth (ft)	Vs (m/s)	Vs (ft/s)	Vp (m/s)	Vp (ft/s)	γ	ρ(Vp) (g/cc)	ρ(Vp) (lb/ft^3)	G (GPa)	E (GPa)	K (GPa)	G ($10^3 lb/ft^2$)	E ($10^3 lb/ft^2$)	K ($10^3 lb/ft^2$)
Not Provided	2	6.6	323	1058		NA	NA	NA	NA	NA	NA	NA	NA	NA	NA
	2.5	8.2	336	1101		NA	NA	NA	NA	NA	NA	NA	NA	NA	NA
	3	9.8	279	916		NA	NA	NA	NA	NA	NA	NA	NA	NA	NA
	3.5	11.5	239	785		NA	NA	NA	NA	NA	NA	NA	NA	NA	NA
	4	13.1	336	1101		NA	NA	NA	NA	NA	NA	NA	NA	NA	NA
	4.5	14.8	357	1172	625	2051	NA	NA	NA	NA	NA	NA	NA	NA	NA
	5	16.4	321	1052	641	2103	NA	NA	NA	NA	NA	NA	NA	NA	NA
	5.5	18.0	314	1032	806	2646	NA	NA	NA	NA	NA	NA	NA	NA	NA
	6	19.7	365	1197	735	2412	NA	NA	NA	NA	NA	NA	NA	NA	NA
	6.5	21.3	357	1172	714	2343	NA	NA	NA	NA	NA	NA	NA	NA	NA
	7	23.0	342	1124	685	2247	NA	NA	NA	NA	NA	NA	NA	NA	NA
	7.5	24.6	279	916	943	3095	NA	NA	NA	NA	NA	NA	NA	NA	NA
	8	26.2	282	927	1515	4971	NA	NA	NA	NA	NA	NA	NA	NA	NA
	8.5	27.9	282	924	1724	5657	0.49	2.02	126.09	0.160	0.476	5.791	3347	9950	120938
	9	29.5	313	1025	1613	5292	0.48	1.94	121.09	0.189	0.561	4.793	3956	11714	100109
	9.5	31.2	281	922	1613	5292	0.48	1.94	121.09	0.153	0.454	4.842	3196	9489	101122
	10	32.8	248	812	1493	4897	NA	NA	NA	NA	NA	NA	NA	NA	NA
	10.5	34.4	331	1086	1449	4755	NA	NA	NA	NA	NA	NA	NA	NA	NA
	11	36.1	379	1243	1563	5126	NA	NA	NA	NA	NA	NA	NA	NA	NA
	11.5	37.7	360	1180	1563	5126	NA	NA	NA	NA	NA	NA	NA	NA	NA
	12	39.4	347	1139	1613	5292	0.48	1.94	121.09	0.234	0.690	4.734	4884	14415	98872
	12.5	41.0	287	943	1613	5292	0.48	1.94	121.09	0.160	0.475	4.832	3345	9925	100924
	13	42.7	230	756	1695	5561	0.49	2.00	124.84	0.106	0.317	5.603	2217	6610	117023
	13.5	44.3	286	937	1818	5965	0.49	2.08	129.88	0.170	0.505	6.651	3547	10551	138913
	14	45.9	301	988	1724	5657	0.48	2.02	126.09	0.183	0.544	5.760	3827	11361	120298
	14.5	47.6	227	746	1613	5292	0.49	1.94	121.09	0.100	0.299	4.912	2092	6235	102594
	15	49.2	244	800	1695	5561	0.49	2.00	124.84	0.119	0.354	5.586	2485	7401	116666
	15.5	50.9	394	1292	1818	5965	0.48	2.08	129.88	0.322	0.952	6.448	6735	19874	134662
	16	52.5	424	1390	1818	5965	0.47	2.08	129.88	0.374	1.099	6.380	7802	22957	133240
	16.5	54.1	417	1367	1786	5859	0.47	2.06	128.62	0.358	1.052	6.093	7470	21981	127248
	17	55.8	345	1131	1667	5468	0.48	1.98	123.58	0.235	0.696	5.185	4916	14529	108293
	17.5	57.4	266	873	1613	5292	0.49	1.94	121.09	0.137	0.408	4.863	2865	8516	101563
	18	59.1	262	859	1724	5657	0.49	2.02	126.09	0.138	0.412	5.820	2891	8604	121547
	18.5	60.7	292	959	1818	5965	0.49	2.08	129.88	0.178	0.529	6.640	3715	11046	138688
	19	62.3	314	1032	1754	5756	0.48	2.04	127.35	0.202	0.599	6.010	4213	12500	125518
	19	62.3	292	959	1754	5756	0.49	2.04	127.35	0.174	0.518	6.046	3643	10824	126279
	19.5	64.0	294	965	1754	5756	0.49	2.04	127.35	0.176	0.524	6.044	3686	10950	126222

γ = Poisson's Ratio ρ(Vp) = Vp-derived density G = Shear Modulus E = Young's Modulus K = Bulk Modulus
Shaded cells denote questionable data.

Table 2. LA 710 tunnel
Boring Z2 B5
PS Suspension Log Data Summary

Top of Hole Elevation (m)	Depth (m)	Depth (ft)	Vs (m/s)	Vs (ft/s)	Vp (m/s)	Vp (ft/s)	γ	ρ(Vp) (g/cc)	ρ(Vp) (lb/ft^3)	G (GPa)	E (GPa)	K (GPa)	G ($10^3 lb/ft^2$)	E ($10^3 lb/ft^2$)	K ($10^3 lb/ft^2$)
	19.5	64.0	291	954	1724	5657	0.49	2.02	126.09	0.171	0.507	5.777	3565	10590	120648
	19.5	64.0	289	948	1754	5756	0.49	2.04	127.35	0.170	0.506	6.052	3559	10578	126391
	20	65.6	287	943	1724	5657	0.49	2.02	126.09	0.167	0.496	5.782	3483	10351	120757
	20	65.6	289	948	1695	5561	0.49	2.00	124.84	0.167	0.496	5.522	3489	10361	115327
	20	65.6	282	924	1695	5561	0.49	2.00	124.84	0.159	0.472	5.533	3314	9848	115560
	20.5	67.3	313	1025	1754	5756	0.48	2.04	127.35	0.199	0.591	6.013	4161	12346	125588
	21	68.9	340	1116	1818	5965	0.48	2.08	129.88	0.241	0.713	6.557	5027	14899	136939
	21.5	70.5	345	1131	1818	5965	0.48	2.08	129.88	0.247	0.733	6.548	5167	15307	136753
	22	72.2	355	1163	1852	6076	0.48	2.10	131.15	0.264	0.782	6.852	5517	16342	143109
	22.5	73.8	336	1101	1754	5756	0.48	2.04	127.35	0.230	0.680	5.973	4798	14211	124739
	23	75.5	282	927	1695	5561	0.49	2.00	124.84	0.160	0.474	5.532	3333	9903	115535
	23.5	77.1	254	833	1724	5657	0.49	2.02	126.09	0.130	0.387	5.831	2717	8092	121778
	24	78.7	265	868	1695	5561	0.49	2.00	124.84	0.140	0.416	5.558	2923	8696	116082
	24.5	80.4	262	859	1724	5657	0.49	2.02	126.09	0.138	0.412	5.820	2891	8604	121546
	25	82.0	278	911	1724	5657	0.49	2.02	126.09	0.156	0.463	5.796	3255	9678	121061
	25.5	83.7	317	1042	1818	5965	0.48	2.08	129.88	0.210	0.622	6.598	4379	13000	137803
	26	85.3	316	1038	1786	5859	0.48	2.06	128.62	0.206	0.612	6.294	4309	12787	131463
	26.5	86.9	292	959	1724	5657	0.49	2.02	126.09	0.173	0.513	5.774	3607	10713	120592
	27	88.6	294	965	1724	5657	0.49	2.02	126.09	0.175	0.519	5.771	3649	10838	120535
	27.6	90.6	292	959	1695	5561	0.48	2.00	124.84	0.171	0.508	5.517	3571	10603	115218
	28	91.9	286	937	1695	5561	0.49	2.00	124.84	0.163	0.485	5.527	3409	10128	115433
	28.6	93.8	289	948	1695	5561	0.49	2.00	124.84	0.167	0.496	5.522	3489	10361	115327
	29.1	95.5	275	901	1724	5657	0.49	2.02	126.09	0.152	0.453	5.801	3184	9469	121156
	29.6	97.1	267	877	1667	5468	0.49	1.98	123.58	0.142	0.421	5.310	2956	8789	110907
	30.1	98.8	279	916	1724	5657	0.49	2.02	126.09	0.158	0.469	5.794	3291	9786	121012
	30.6	100.4	296	971	1724	5657	0.48	2.02	126.09	0.177	0.525	5.769	3693	10966	120478
	31.1	102.0	321	1052	1724	5657	0.48	2.02	126.09	0.207	0.615	5.728	4334	12846	119623
	31.6	103.7	345	1131	1754	5756	0.48	2.04	127.35	0.243	0.718	5.955	5066	14995	124381
	32.1	105.3	342	1124	1754	5756	0.48	2.04	127.35	0.239	0.708	5.960	4997	14793	124474
	33.1	108.6	331	1086	1724	5657	0.48	2.02	126.09	0.221	0.656	5.709	4625	13699	119234
	33.1	108.6	338	1108	1724	5657	0.48	2.02	126.09	0.231	0.682	5.697	4815	14252	118981
	33.6	110.2	331	1086	1724	5657	0.48	2.02	126.09	0.221	0.656	5.709	4625	13699	119234
	34.1	111.9	325	1065	1695	5561	0.48	2.00	124.84	0.211	0.624	5.464	4403	13040	114109
	34.6	113.5	321	1052	1724	5657	0.48	2.02	126.09	0.207	0.615	5.728	4334	12846	119623
	35	114.8	311	1019	1724	5657	0.48	2.02	126.09	0.195	0.578	5.745	4069	12069	119976
	35.6	116.8	316	1038	1754	5756	0.48	2.04	127.35	0.204	0.606	6.006	4267	12657	125447
	36.1	118.4	311	1019	1754	5756	0.48	2.04	127.35	0.197	0.584	6.017	4109	12195	125658

γ = Poisson's Ratio ρ(Vp) = Vp-derived density G = Shear Modulus E = Young's Modulus K = Bulk Modulus
Shaded cells denote questionable data.

Table 2. LA 710 tunnel
Boring Z2 B5
PS Suspension Log Data Summary

Top of Hole Elevation (m)	Depth (m)	Depth (ft)	Vs (m/s)	Vs (ft/s)	Vp (m/s)	Vp (ft/s)	γ	ρ(Vp) (g/cc)	ρ(Vp) (lb/ft^3)	G (GPa)	E (GPa)	K (GPa)	G ($10^3 lb/ft^2$)	E ($10^3 lb/ft^2$)	K ($10^3 lb/ft^2$)
	36.6	120.1	303	994	1754	5756	0.48	2.04	127.35	0.187	0.556	6.029	3912	11617	125920
	37.1	121.7	299	982	1754	5756	0.49	2.04	127.35	0.183	0.543	6.035	3819	11343	126044
	37.6	123.4	294	965	1724	5657	0.49	2.02	126.09	0.175	0.519	5.771	3649	10838	120535
	38.1	125.0	291	954	1724	5657	0.49	2.02	126.09	0.171	0.507	5.777	3565	10590	120648
	38.6	126.6	299	982	1667	5468	0.48	1.98	123.58	0.177	0.526	5.262	3706	10995	109906
	39.6	129.9	379	1243	1667	5468	0.47	1.98	123.58	0.284	0.837	5.120	5932	17474	106938
	40.1	131.6	373	1224	1639	5378	0.47	1.96	122.33	0.273	0.804	4.903	5698	16783	102391
	40.6	133.2	397	1302	1667	5468	0.47	1.98	123.58	0.312	0.916	5.083	6511	19141	106167
	41.1	134.8	424	1390	1695	5561	0.47	2.00	124.84	0.359	1.053	5.266	7499	21996	109981
	41.6	136.5	424	1390	1695	5561	0.47	2.00	124.84	0.359	1.053	5.266	7499	21996	109981
	42.1	138.1	424	1390	1695	5561	0.47	2.00	124.84	0.359	1.053	5.266	7499	21996	109981
	43.1	141.4	417	1367	1695	5561	0.47	2.00	124.84	0.347	1.019	5.282	7251	21286	110311
	43.1	141.4	424	1390	1667	5468	0.47	1.98	123.58	0.355	1.042	5.025	7423	21757	104950
	43.6	143.0	410	1345	1639	5378	0.47	1.96	122.33	0.329	0.965	4.827	6874	20165	100823
	44.1	144.7	385	1262	1613	5292	0.47	1.94	121.09	0.287	0.843	4.663	5993	17616	97394
	44.6	146.3	376	1233	1587	5208	0.47	1.92	119.84	0.271	0.798	4.475	5666	16662	93460
	45	147.6	382	1252	1613	5292	0.47	1.94	121.09	0.283	0.831	4.669	5901	17354	97515
	45.1	148.0	391	1282	1587	5208	0.47	1.92	119.84	0.293	0.860	4.446	6118	17959	92859
	45.5	149.3	395	1297	1639	5378	0.47	1.96	122.33	0.306	0.900	4.858	6394	18787	101464
	45.6	149.6	413	1356	1613	5292	0.46	1.94	121.09	0.331	0.970	4.604	6917	20265	96161
	46	150.9	400	1312	1639	5378	0.47	1.96	122.33	0.314	0.921	4.848	6548	19230	101258
	46.1	151.2	435	1426	1639	5378	0.46	1.96	122.33	0.370	1.083	4.772	7737	22625	99673
	46.5	152.6	424	1390	1639	5378	0.46	1.96	122.33	0.352	1.030	4.797	7348	21519	100191
	47	154.2	495	1624	1695	5561	0.45	2.00	124.84	0.490	1.425	5.091	10235	29752	106332
	47.1	154.5	467	1533	1667	5468	0.46	1.98	123.58	0.432	1.260	4.923	9028	26314	102811
	47.1	154.5	526	1727	1695	5561	0.45	2.00	124.84	0.554	1.603	5.006	11569	33473	104553
	47.5	155.8	500	1640	1695	5561	0.45	2.00	124.84	0.500	1.452	5.078	10441	30328	106057
	47.6	156.2	575	1886	1695	5561	0.44	2.00	124.84	0.660	1.896	4.864	13795	39592	101586
	48	157.5	490	1608	1639	5378	0.45	1.96	122.33	0.471	1.366	4.638	9834	28538	96876
	48	157.5	521	1709	1695	5561	0.45	2.00	124.84	0.542	1.571	5.021	11329	32807	104873
	48.5	159.1	633	2076	1667	5468	0.42	1.98	123.58	0.793	2.245	4.442	16562	46895	92766
	48.5	159.1	459	1505	1667	5468	0.46	1.98	123.58	0.417	1.216	4.944	8700	25387	103248
	49	160.8	510	1674	1695	5561	0.45	2.00	124.84	0.521	1.510	5.051	10872	31532	105483
	49	160.8	433	1420	1613	5292	0.46	1.94	121.09	0.363	1.062	4.561	7592	22185	95261
	49.5	162.4	402	1318	1754	5756	0.47	2.04	127.35	0.329	0.969	5.840	6872	20236	121974
	49.5	162.4	435	1426	1667	5468	0.46	1.98	123.58	0.374	1.095	5.000	7816	22877	104427
	50	164.0	481	1577	1695	5561	0.46	2.00	124.84	0.462	1.346	5.128	9653	28116	107108

γ = Poisson's Ratio ρ(Vp) = Vp-derived density G = Shear Modulus E = Young's Modulus K = Bulk Modulus
Shaded cells denote questionable data.

Table 2. LA 710 tunnel
Boring Z2 B5
PS Suspension Log Data Summary

Top of Hole Elevation (m)	Depth (m)	Depth (ft)	Vs (m/s)	Vs (ft/s)	Vp (m/s)	Vp (ft/s)	γ	ρ(Vp) (g/cc)	ρ(Vp) (lb/ft^3)	G (GPa)	E (GPa)	K (GPa)	G ($10^3 lb/ft^2$)	E ($10^3 lb/ft^2$)	K ($10^3 lb/ft^2$)
	50.5	165.7	472	1548	1961	6433	0.47	2.16	134.97	0.481	1.414	7.671	10047	29523	160208
	50.5	165.7	398	1307	1786	5859	0.47	2.06	128.62	0.327	0.964	6.134	6830	20132	128102
	50.5	165.7	543	1783	1754	5756	0.45	2.04	127.35	0.603	1.744	5.475	12585	36418	114357
	51	167.3	521	1709	1786	5859	0.45	2.06	128.62	0.559	1.625	5.824	11672	33931	121645
	51	167.3	476	1562	1786	5859	0.46	2.06	128.62	0.467	1.366	5.947	9757	28524	124199
	51.5	169.0	521	1709	1754	5756	0.45	2.04	127.35	0.553	1.607	5.541	11558	33556	115726
	51.5	169.0	476	1562	1613	5292	0.45	1.94	121.09	0.440	1.277	4.459	9186	26680	93136
	52	170.6	476	1562	1724	5657	0.46	2.02	126.09	0.458	1.336	5.394	9566	27907	112647
	52	170.6	481	1577	1754	5756	0.46	2.04	127.35	0.472	1.376	5.650	9848	28744	118006
	52.5	172.2	472	1548	1754	5756	0.46	2.04	127.35	0.454	1.326	5.674	9480	27701	118497
	53	173.9	467	1533	1786	5859	0.46	2.06	128.62	0.450	1.317	5.970	9396	27496	124680
	53	173.9	467	1533	1754	5756	0.46	2.04	127.35	0.445	1.302	5.685	9303	27200	118732
	53	173.9	472	1548	1754	5756	0.46	2.04	127.35	0.454	1.326	5.674	9480	27701	118496
	53.5	175.5	476	1562	1563	5126	NA	NA	NA	NA	NA	NA	NA	NA	NA
	53.5	175.5	505	1657	1786	5859	0.46	2.06	128.62	0.526	1.531	5.869	10976	31972	122574
	54	177.2	455	1491	1724	5657	0.46	2.02	126.09	0.417	1.221	5.448	8716	25497	113780
	54	177.2	510	1674	1786	5859	0.46	2.06	128.62	0.536	1.561	5.855	11201	32606	122274
	54.5	178.8	532	1745	1754	5756	0.45	2.04	127.35	0.577	1.673	5.509	12055	34944	115064
	54.5	178.8	500	1640	1818	5965	0.46	2.08	129.88	0.520	1.518	6.184	10863	31700	129158
	55	180.4	541	1773	1786	5859	0.45	2.06	128.62	0.602	1.745	5.767	12572	36449	120445
	55	180.4	532	1745	1887	6190	0.46	2.12	132.42	0.600	1.749	6.751	12534	36521	140998
	55.5	182.1	575	1886	1786	5859	0.44	2.06	128.62	0.680	1.963	5.662	14212	40994	118258
	55.5	182.1	556	1823	1818	5965	0.45	2.08	129.88	0.642	1.860	6.021	13411	38852	125761
	56	183.7	515	1691	1852	6076	0.46	2.10	131.15	0.558	1.628	6.460	11658	33995	134922
	56	183.7	556	1823	1818	5965	0.45	2.08	129.88	0.642	1.860	6.021	13411	38852	125760
	56.5	185.4	510	1674	1852	6076	0.46	2.10	131.15	0.547	1.596	6.475	11421	33326	135237
	56.5	185.4	495	1624	1887	6190	0.46	2.12	132.42	0.520	1.521	6.858	10857	31768	143235
	57	187.0	474	1555	1887	6190	0.47	2.12	132.42	0.476	1.397	6.916	9951	29182	144444
	57	187.0	526	1727	2174	7132	0.47	2.26	141.40	0.627	1.843	9.867	13104	38496	206085
	57.5	188.6	556	1823	1786	5859	0.45	2.06	128.62	0.636	1.839	5.722	13280	38418	119501
	57.5	188.6	578	1896	1923	6309	0.45	2.14	133.69	0.716	2.076	6.966	14944	43349	145485
	58	190.3	562	1843	1852	6076	0.45	2.10	131.15	0.663	1.922	6.320	13848	40140	132002
	58	190.3	532	1745	1724	5657	0.45	2.02	126.09	0.571	1.654	5.242	11936	34551	109487
	58.5	191.9	524	1718	1818	5965	0.45	2.08	129.88	0.570	1.659	6.117	11911	34655	127761
	58.5	191.9	503	1649	1786	5859	0.46	2.06	128.62	0.520	1.516	5.876	10866	31662	122721
	59	193.6	500	1640	1852	6076	0.46	2.10	131.15	0.525	1.534	6.504	10969	32044	135841
	59	193.6	508	1665	1818	5965	0.46	2.08	129.88	0.536	1.563	6.163	11196	32642	128713

γ = Poisson's Ratio ρ(Vp) = Vp-derived density G = Shear Modulus E = Young's Modulus K = Bulk Modulus
Shaded cells denote questionable data.

Table 2. LA 710 tunnel
Boring Z2 B5
PS Suspension Log Data Summary

Top of Hole Elevation (m)	Depth (m)	Depth (ft)	Vs (m/s)	Vs (ft/s)	Vp (m/s)	Vp (ft/s)	γ	ρ(Vp) (g/cc)	ρ(Vp) (lb/ft^3)	G (GPa)	E (GPa)	K (GPa)	G ($10^3 lb/ft^2$)	E ($10^3 lb/ft^2$)	K ($10^3 lb/ft^2$)
	59.5	195.2	602	1976	1852	6076	0.44	2.10	131.15	0.762	2.197	6.188	15922	45883	129236
	59.5	195.2	571	1875	1852	6076	0.45	2.10	131.15	0.686	1.986	6.290	14327	41473	131363
	60	196.9	532	1745	1852	6076	0.46	2.10	131.15	0.594	1.730	6.412	12414	36126	133914
	60	196.9	521	1709	1786	5859	0.45	2.06	128.62	0.559	1.625	5.824	11672	33931	121645
	60	196.9	500	1640	1818	5965	0.46	2.08	129.88	0.520	1.518	6.184	10863	31700	129158
	60.5	198.5	549	1803	1818	5965	0.45	2.08	129.88	0.628	1.821	6.040	13118	38035	126151
	60.5	198.5	538	1764	1786	5859	0.45	2.06	128.62	0.596	1.727	5.776	12437	36072	120625
	61	200.1	521	1709	1852	6076	0.46	2.10	131.15	0.570	1.661	6.445	11902	34684	134596
	61	200.1	515	1691	1852	6076	0.46	2.10	131.15	0.558	1.628	6.460	11658	33995	134922
	61	200.1	521	1709	1852	6076	0.46	2.10	131.15	0.570	1.661	6.445	11902	34684	134596
	61.5	201.8	495	1624	1818	5965	0.46	2.08	129.88	0.510	1.489	6.198	10649	31094	129443
	61.5	201.8	549	1803	1852	6076	0.45	2.10	131.15	0.634	1.841	6.359	13246	38459	132805
	62	203.4	667	2187	1786	5859	0.42	2.06	128.62	0.916	2.599	5.349	19124	54274	111710
	62	203.4	532	1745	1818	5965	0.45	2.08	129.88	0.589	1.711	6.093	12294	35731	127250
	62.5	205.1	556	1823	1852	6076	0.45	2.10	131.15	0.648	1.881	6.340	13542	39286	132410
	62.5	205.1	588	1930	1786	5859	0.44	2.06	128.62	0.713	2.052	5.619	14889	42854	117356
	63	206.7	602	1976	1852	6076	0.44	2.10	131.15	0.762	2.197	6.188	15922	45883	129236
	63	206.7	641	2103	1818	5965	0.43	2.08	129.88	0.855	2.443	5.738	17855	51030	119835
	63.5	208.3	610	2001	1786	5859	0.43	2.06	128.62	0.766	2.197	5.548	15998	45883	115877
	63.5	208.3	587	1924	1818	5965	0.44	2.08	129.88	0.716	2.064	5.923	14947	43105	123712
	64	210.0	602	1976	1667	5468	0.42	1.98	123.58	0.718	2.047	4.541	15004	42758	94843
	64.5	211.6	585	1919	1818	5965	0.44	2.08	129.88	0.711	2.052	5.929	14860	42865	123829
	64.5	211.6	602	1976	1786	5859	0.44	2.06	128.62	0.748	2.147	5.573	15615	44840	116388
	65	213.3	543	1783	1667	5468	0.44	1.98	123.58	0.585	1.685	4.719	12212	35183	98565
	65	213.3	541	1773	1667	5468	0.44	1.98	123.58	0.578	1.667	4.728	12080	34821	98741
	65	213.3	575	1886	1818	5965	0.44	2.08	129.88	0.687	1.985	5.961	14352	41462	124506
	65.5	214.9	543	1783	1818	5965	0.45	2.08	129.88	0.615	1.783	6.058	12834	37244	126529
	66	216.5	513	1682	1754	5756	0.45	2.04	127.35	0.536	1.559	5.564	11205	32568	116196
	66.5	218.2	493	1616	1818	5965	0.46	2.08	129.88	0.505	1.475	6.204	10544	30797	129583
	67	219.8	518	1700	1786	5859	0.45	2.06	128.62	0.553	1.608	5.832	11552	33593	121806
	67.5	221.5	571	1875	1754	5756	0.44	2.04	127.35	0.666	1.919	5.391	13912	40086	112586
	68	223.1	625	2051	1786	5859	0.43	2.06	128.62	0.805	2.302	5.497	16808	48078	114797
	68.5	224.7	625	2051	1818	5965	0.43	2.08	129.88	0.813	2.329	5.794	16973	48645	121011
	68.5	224.7	641	2103	1852	6076	0.43	2.10	131.15	0.863	2.472	6.053	18029	51633	126427
	69.5	228.0	617	2025	1818	5965	0.43	2.08	129.88	0.793	2.275	5.821	16557	47513	121566
	70	229.7	637	2090	1887	6190	0.44	2.12	132.42	0.861	2.471	6.404	17973	51607	133747
	70.5	231.3	667	2187	1852	6076	0.43	2.10	131.15	0.934	2.662	5.959	19500	55598	124465

γ = Poisson's Ratio ρ(Vp) = Vp-derived density G = Shear Modulus E = Young's Modulus K = Bulk Modulus
Shaded cells denote questionable data.

Table 2. LA 710 tunnel
Boring Z2 B5
PS Suspension Log Data Summary

Top of Hole Elevation (m)	Depth (m)	Depth (ft)	Vs (m/s)	Vs (ft/s)	Vp (m/s)	Vp (ft/s)	γ	ρ(Vp) (g/cc)	ρ(Vp) (lb/ft^3)	G (GPa)	E (GPa)	K (GPa)	G ($10^3 lb/ft^2$)	E ($10^3 lb/ft^2$)	K ($10^3 lb/ft^2$)
	71	232.9	610	2001	1786	5859	0.43	2.06	128.62	0.766	2.197	5.548	15998	45883	115877
	71.5	234.6	535	1754	1754	5756	0.45	2.04	127.35	0.583	1.690	5.501	12184	35304	114891
	71.5	234.6	565	1854	1852	6076	0.45	2.10	131.15	0.671	1.943	6.310	14005	40577	131793
	72.5	237.9	538	1764	1818	5965	0.45	2.08	129.88	0.601	1.746	6.076	12560	36476	126895
	72.5	237.9	621	2038	1852	6076	0.44	2.10	131.15	0.810	2.329	6.124	16927	48635	127896
	73	239.5	588	1930	1852	6076	0.44	2.10	131.15	0.727	2.099	6.235	15182	43842	130223
	74	242.8	617	2025	1852	6076	0.44	2.10	131.15	0.800	2.301	6.137	16718	48065	128175
	74	242.8	592	1941	1852	6076	0.44	2.10	131.15	0.736	2.123	6.224	15362	44340	129983
	74.5	244.4	671	2202	1887	6190	0.43	2.12	132.42	0.955	2.728	6.277	19955	56973	131105
	75.5	247.7	714	2343	1852	6076	0.41	2.10	131.15	1.072	3.028	5.775	22386	63244	120618
	75.5	247.7	690	2263	1887	6190	0.42	2.12	132.42	1.009	2.871	6.206	21071	59963	129617
	76	249.3	671	2202	1961	6433	0.43	2.16	134.97	0.974	2.792	7.014	20339	58317	146485
	77	252.6	578	1896	1923	6309	0.45	2.14	133.69	0.716	2.076	6.966	14944	43349	145485
	77.5	254.3	658	2158	1786	5859	0.42	2.06	128.62	0.892	2.535	5.381	18624	52947	112376
	77.5	254.3	613	2013	1786	5859	0.43	2.06	128.62	0.775	2.222	5.536	16195	46418	115615
	77.5	254.3	658	2158	1786	5859	0.42	2.06	128.62	0.892	2.535	5.381	18624	52947	112376
	78	255.9	627	2057	1754	5756	0.43	2.04	127.35	0.802	2.288	5.210	16748	47791	108806
	78.5	257.5	485	1593	1724	5657	0.46	2.02	126.09	0.476	1.387	5.370	9941	28967	112147
	79	259.2	538	1764	1786	5859	0.45	2.06	128.62	0.596	1.727	5.776	12437	36072	120625
	79.5	260.8	575	1886	1786	5859	0.44	2.06	128.62	0.680	1.963	5.662	14212	40994	118259
	80	262.5	457	1498	1818	5965	0.47	2.08	129.88	0.434	1.272	6.299	9060	26569	131562
	80.5	264.1	490	1608	1887	6190	0.46	2.12	132.42	0.510	1.492	6.872	10645	31165	143517
	81	265.7	662	2173	1923	6309	0.43	2.14	133.69	0.939	2.691	6.668	19616	56210	139256
	81.5	267.4	505	1657	1887	6190	0.46	2.12	132.42	0.541	1.581	6.830	11300	33028	142644
	82	269.0	654	2144	2083	6835	0.45	2.22	138.82	0.950	2.746	8.385	19839	57352	175117
	82.5	270.7	658	2158	2500	8202	0.46	2.39	149.21	1.035	3.027	13.559	21606	63210	283181
	83	272.3	873	2865	2778	9113	0.45	2.47	154.48	1.887	5.455	16.577	39420	113936	346210
	83.5	274.0	885	2903	2632	8634	0.44	2.43	151.84	1.905	5.471	14.304	39782	114273	298739
	84	275.6	595	1953	1961	6433	0.45	2.16	134.97	0.766	2.220	7.291	15999	46372	152272
	84.5	277.2	658	2158	2000	6562	0.44	2.18	136.25	0.945	2.719	7.471	19729	56794	156024
	85	278.9	826	2711	2000	6562	0.40	2.18	136.25	1.491	4.165	6.742	31133	86989	140818
	85.5	280.5	741	2430	1923	6309	0.41	2.14	133.69	1.175	3.320	6.353	24542	69349	132689
	86	282.2	709	2327	1852	6076	0.41	2.10	131.15	1.057	2.988	5.795	22069	62414	121040
	86.5	283.8	597	1959	1818	5965	0.44	2.08	129.88	0.742	2.135	5.889	15487	44590	122992
	87	285.4	629	2063	1786	5859	0.43	2.06	128.62	0.815	2.329	5.483	17020	48650	114515
	87	285.4	623	2044	1818	5965	0.43	2.08	129.88	0.808	2.315	5.801	16868	48359	121152
	87.4	286.7	592	1941	1786	5859	0.44	2.06	128.62	0.721	2.075	5.608	15065	43338	117121

γ = Poisson's Ratio ρ(Vp) = Vp-derived density G = Shear Modulus E = Young's Modulus K = Bulk Modulus
Shaded cells denote questionable data.

Figure 1. LA 710 Tunnel
Boring Z2 B5
Downhole Interval Velocities

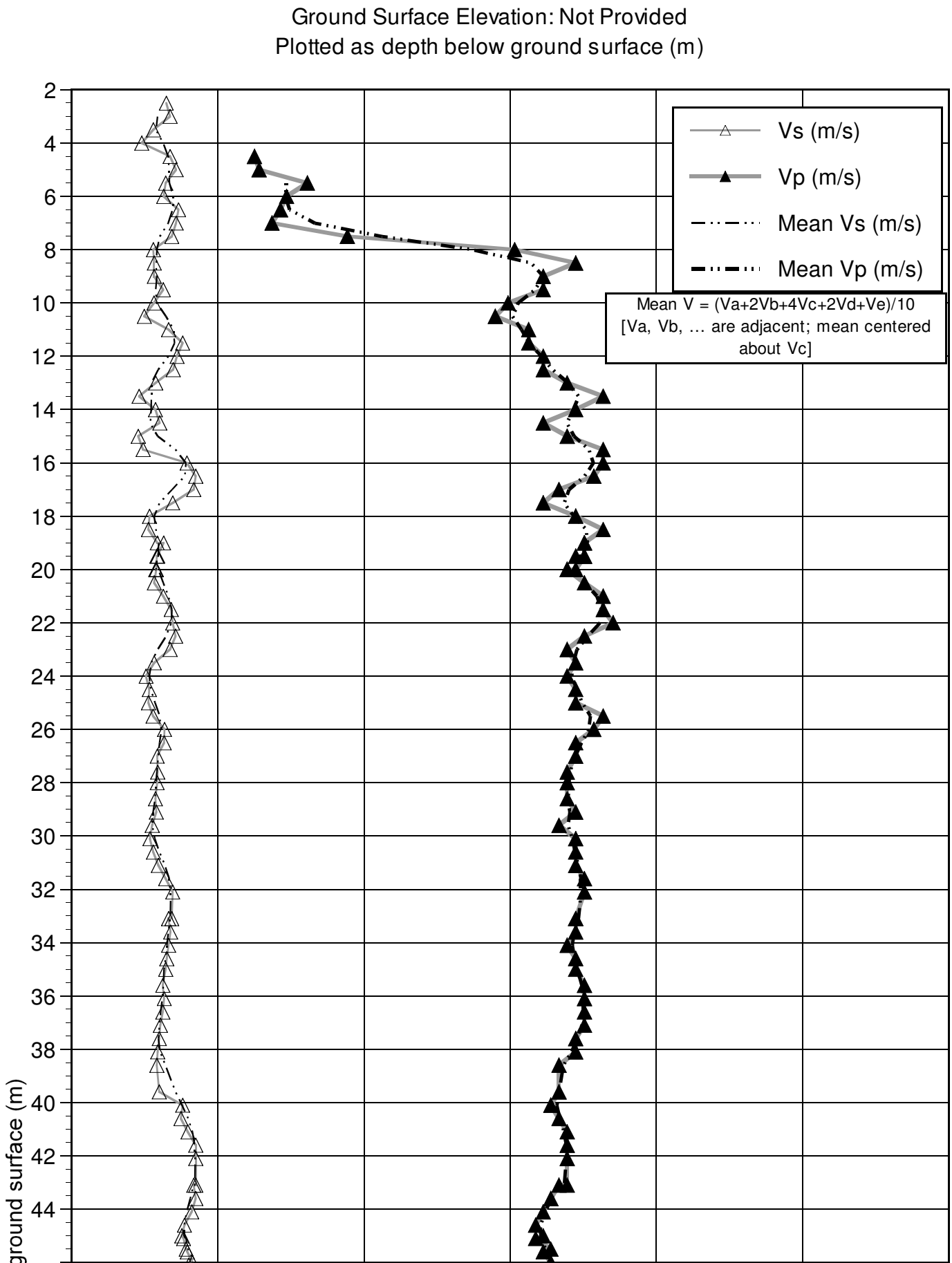

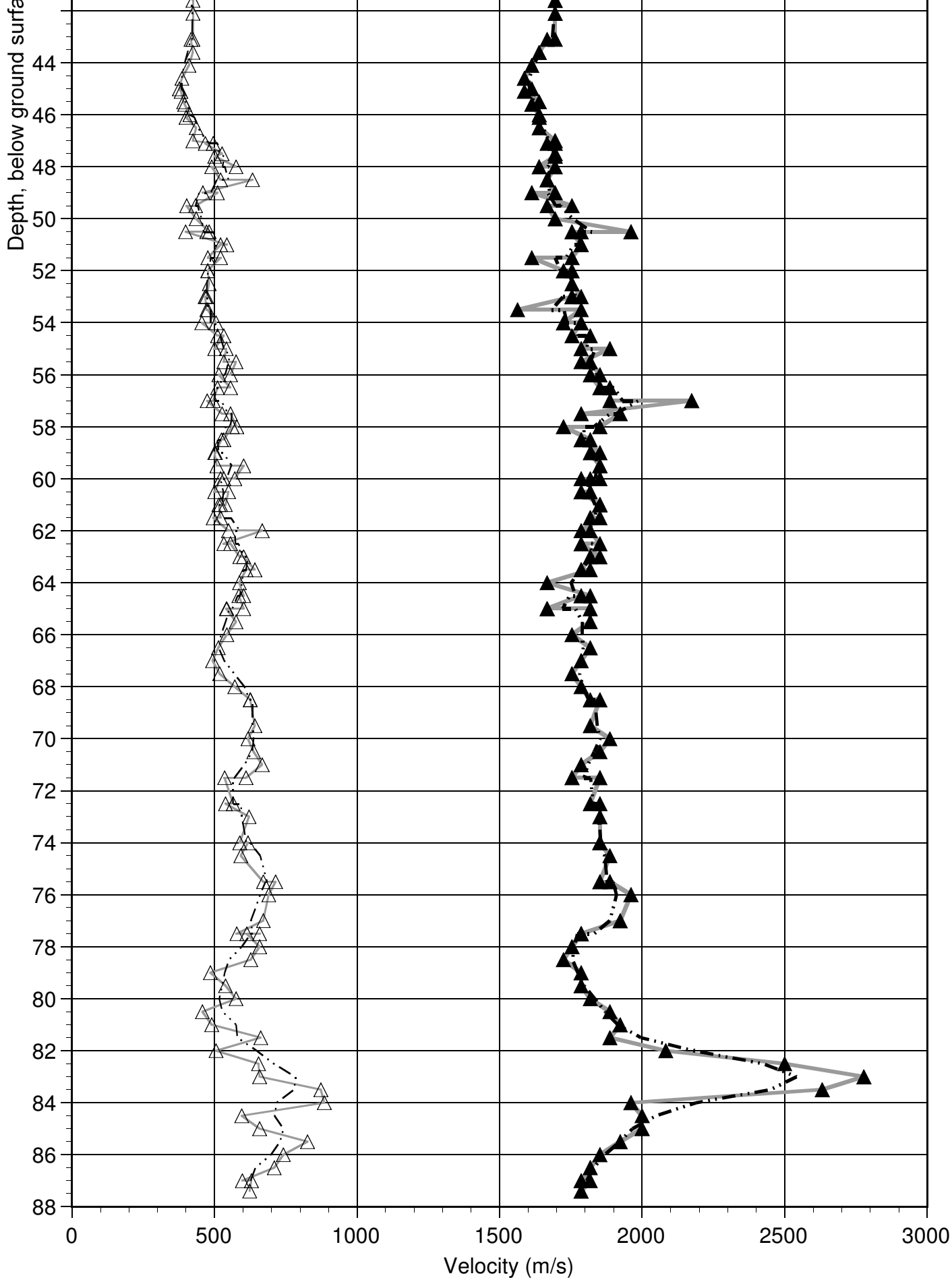
Depth, below ground surfa
44
46
48
50
52
54
56
58
60
62
64
66
68
70
72
74
76
78
80
82
84
86
88
0
500
1000
1500
2000
2500
3000
Velocity (m/s)

California Department of Transportation
Geophysical Services

Z2 B5

COMPANY	: CALTRANS	OTHER SERVICES:	
WELL	: Z2 B5		IND-CAL.
FIELD	: LA-710 Tunnel.		AC TEL.
COUNTY	: LA		PSLOG.
STATE	: CA		
LOCATION	:		
SECTION	: None		
TOWNSHIP	: NONE		
RANGE	: None		
API NO.	:		
UNIQUE WELL ID.	:		
PERMANENT DATUM	: None	ELEVATION KB	: NA
LOG MEASURED FROM	: GL	ELEVATION DF	: NA
DRL MEASURED FROM	: GL	ELEVATION GL	: 143.86
DATE	: 04/14/09	RIG NUMBER	:
DEPTH DRILLER	: 91.44m	LOGGER TD	:
BIT SIZE	: 10.8cm.	ARRIVAL TIME	:
LOG TOP	: 5.00	DEPARTURE TIME	:
LOG BOTTOM	: 90.00	CIRC STOPPED	: 4/14 AM
CASING OD	:		
CASING BOTTOM	: n/a		
CASING TYPE	: n/a		
BOREHOLE FLUID	: 0		
RM TEMPERATURE	: 0		
MUD RES	: 0		
MUD WEIGHT	:		
WITNESSED BY	:		
RECORDED BY	: DH/DL		
REMARKS 1	: POORLY INDUR., SOIL-LIKE MATERIAL, POOR QUAL. ATV LOG.		
REMARKS 2	: BH COLLAPSE NEAR BOTTOM, NO MECH. CAL. AVAIL BELOW -82.6 M		

ALL SERVICES PROVIDED SUBJECT TO STANDARD TERMS AND CONDITIONS

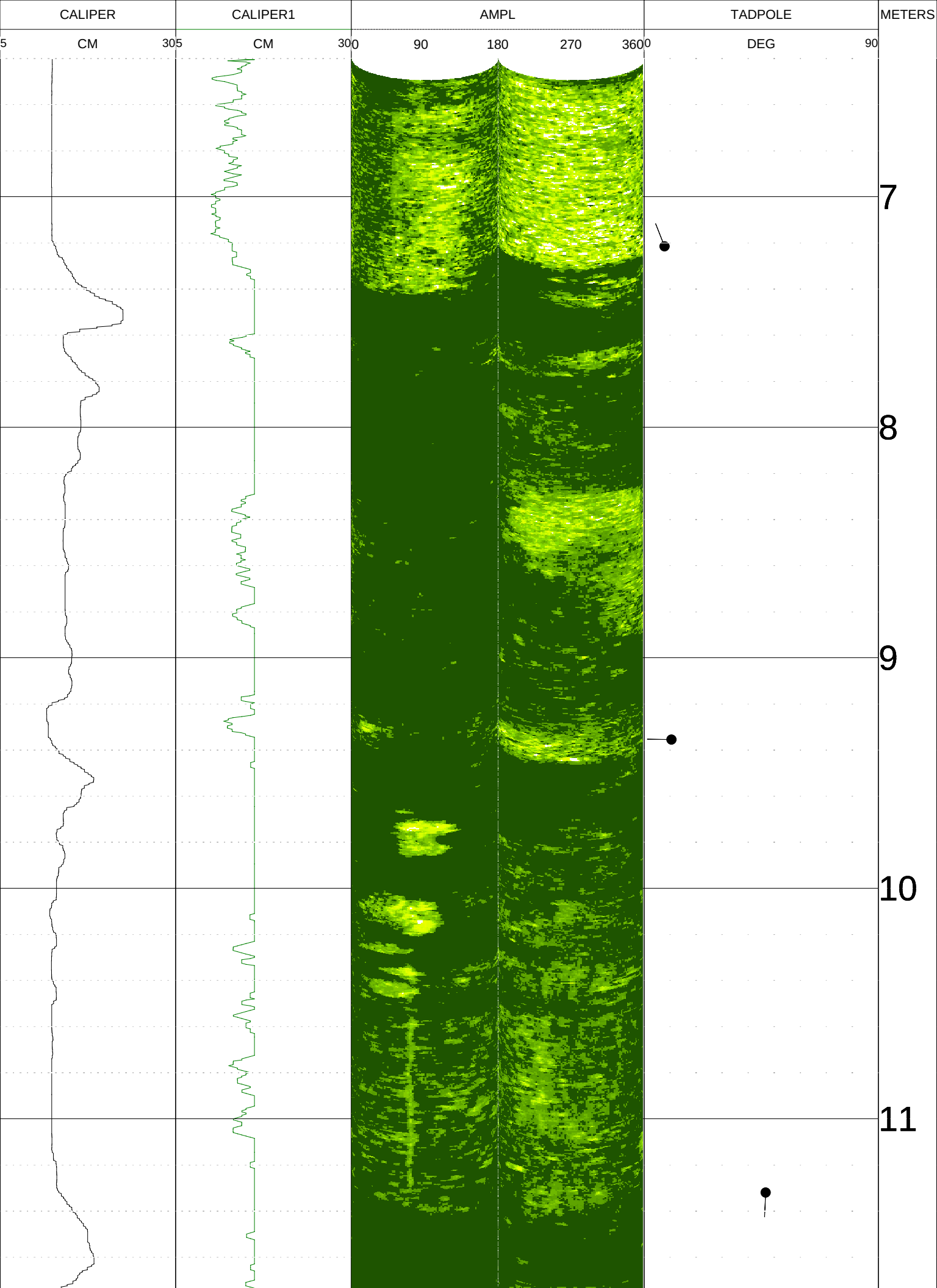
CALIPER
5
CM
30
CALIPER1
5
CM
30
AMPL
0
90
180
270
360
TADPOLE
0
DEG
90
METERS
7
8
9
10
11

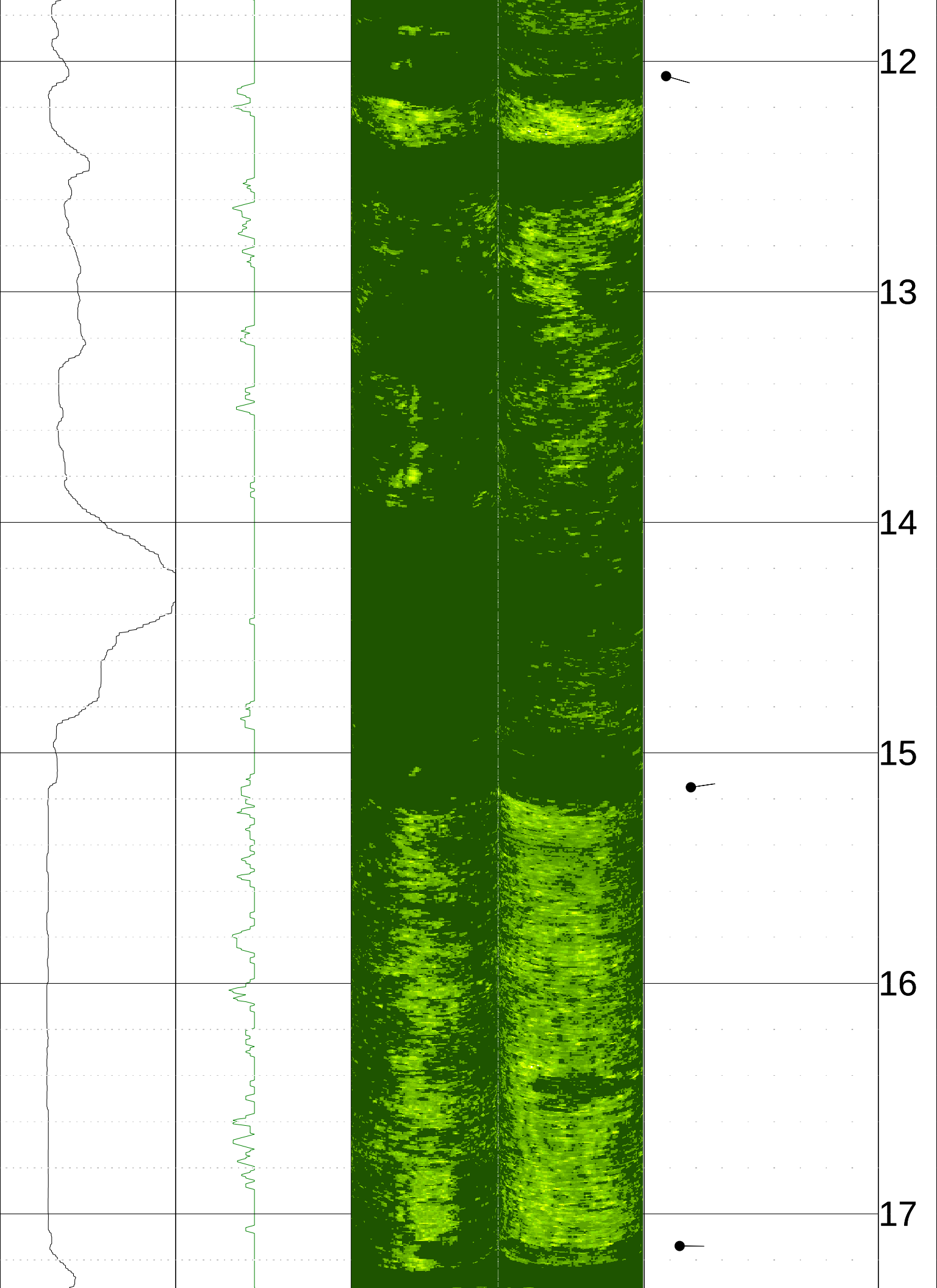
12
13
14
15
16
17

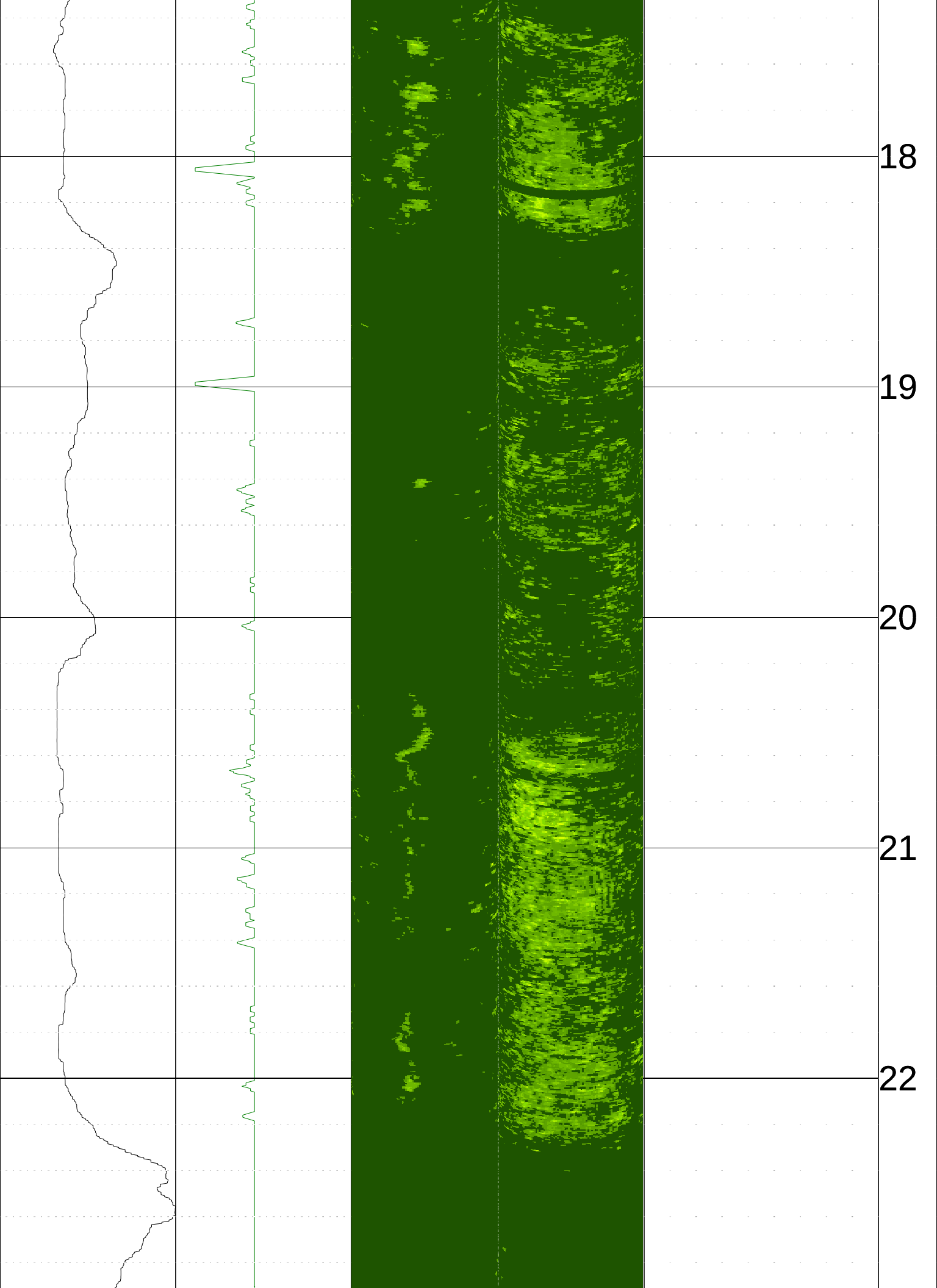
18
19
20
21
22

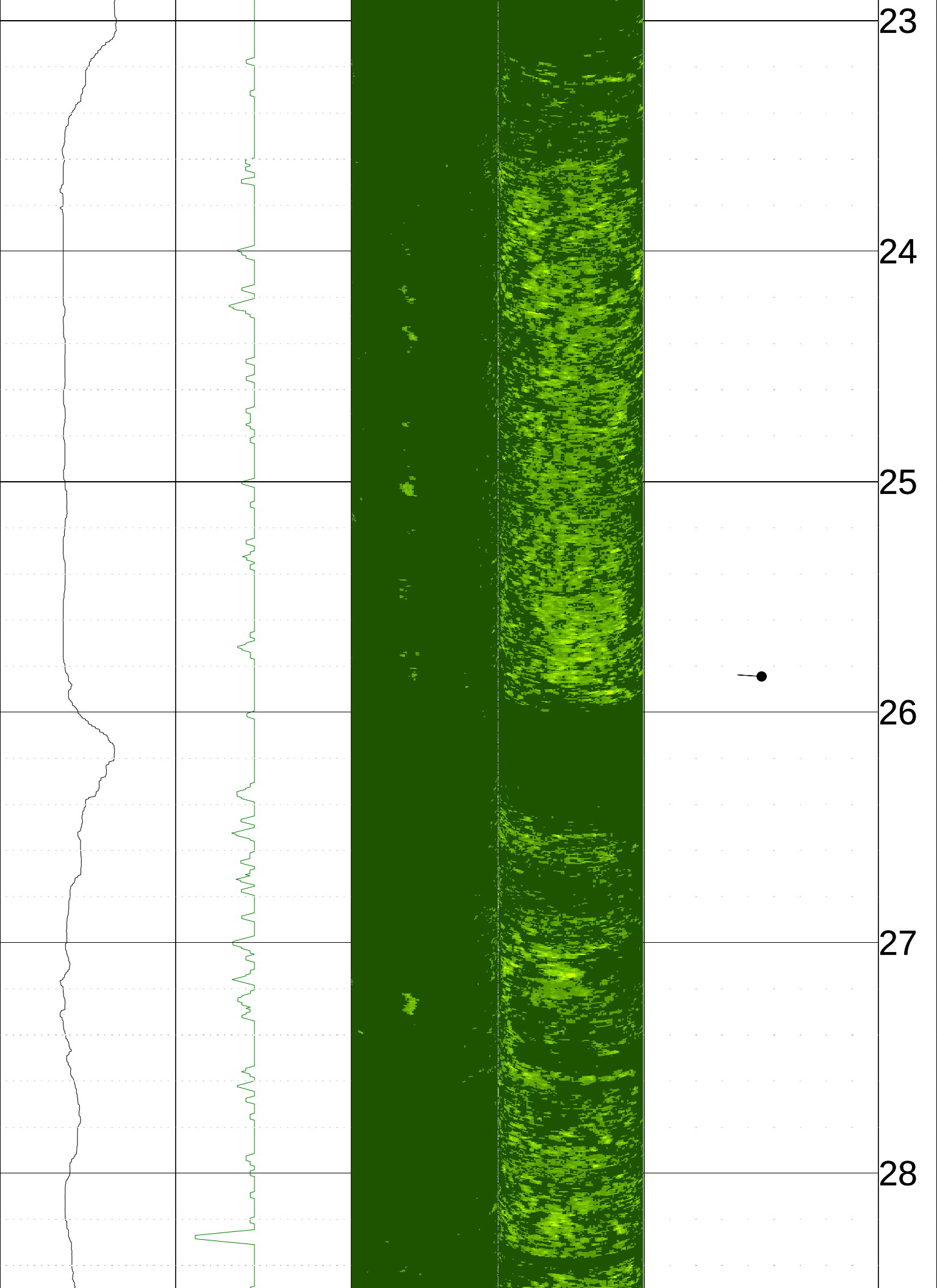
23
24
25
26
27
28

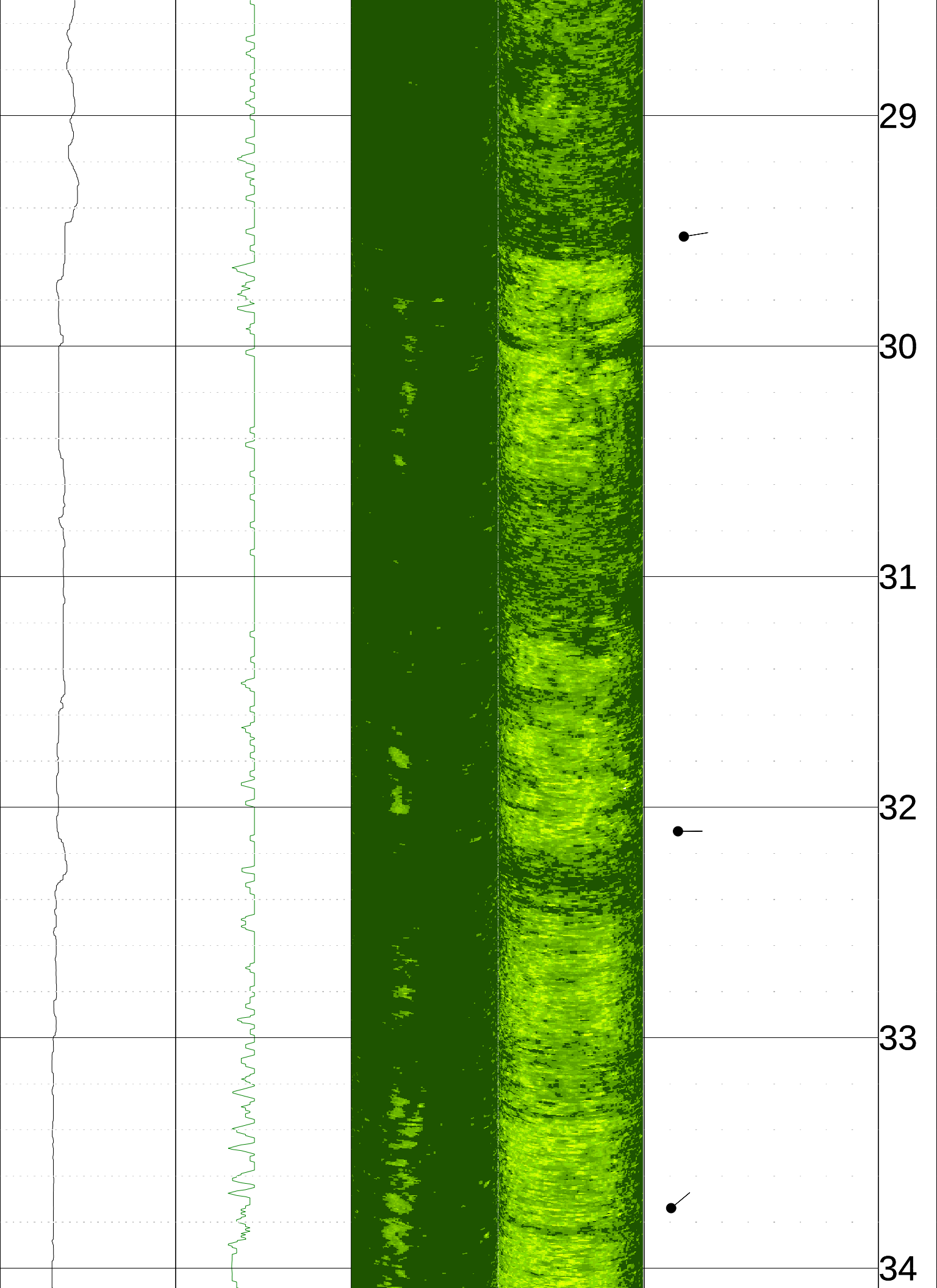
29
30
31
32
33
34

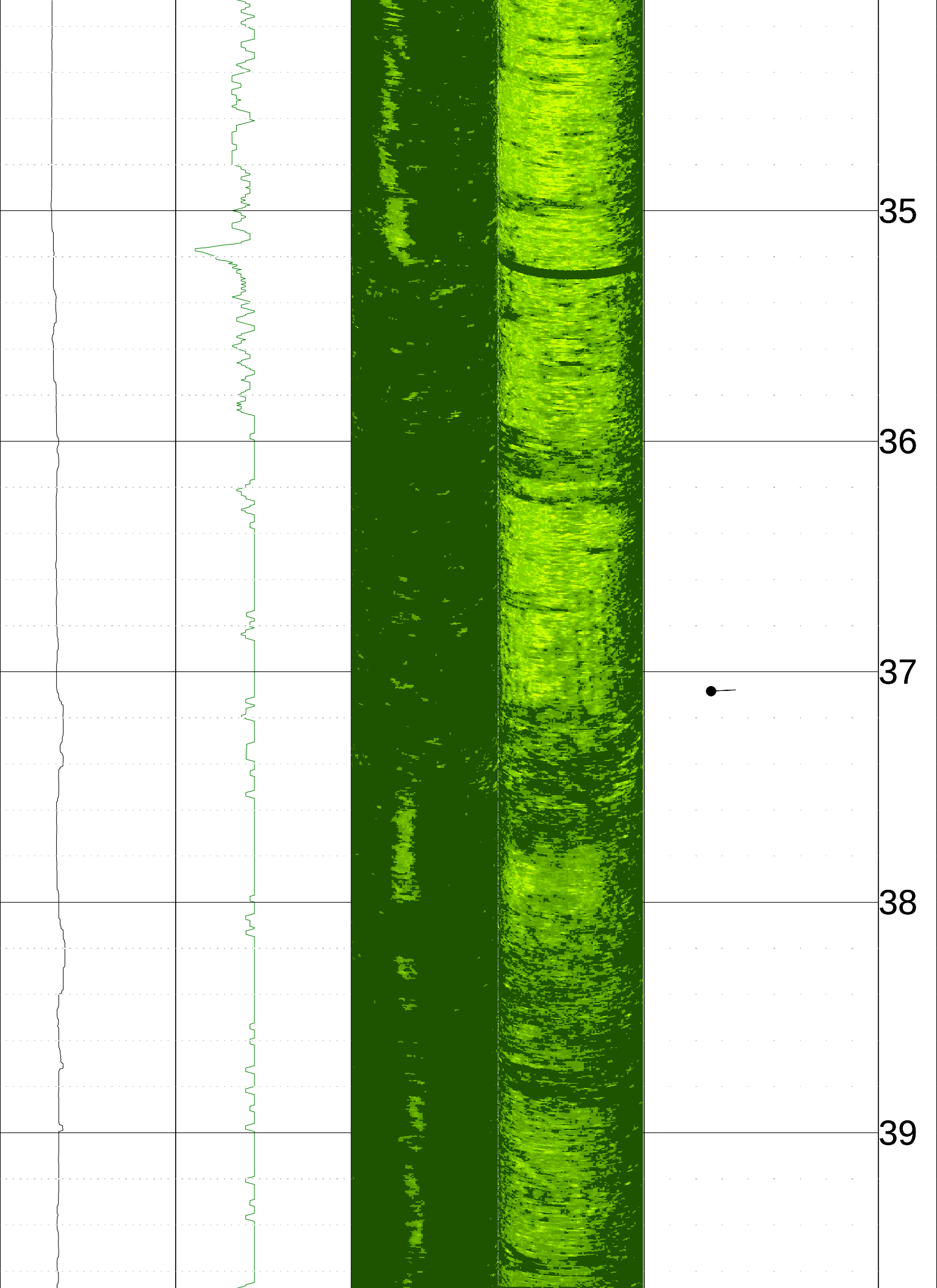
35
36
37
38
39

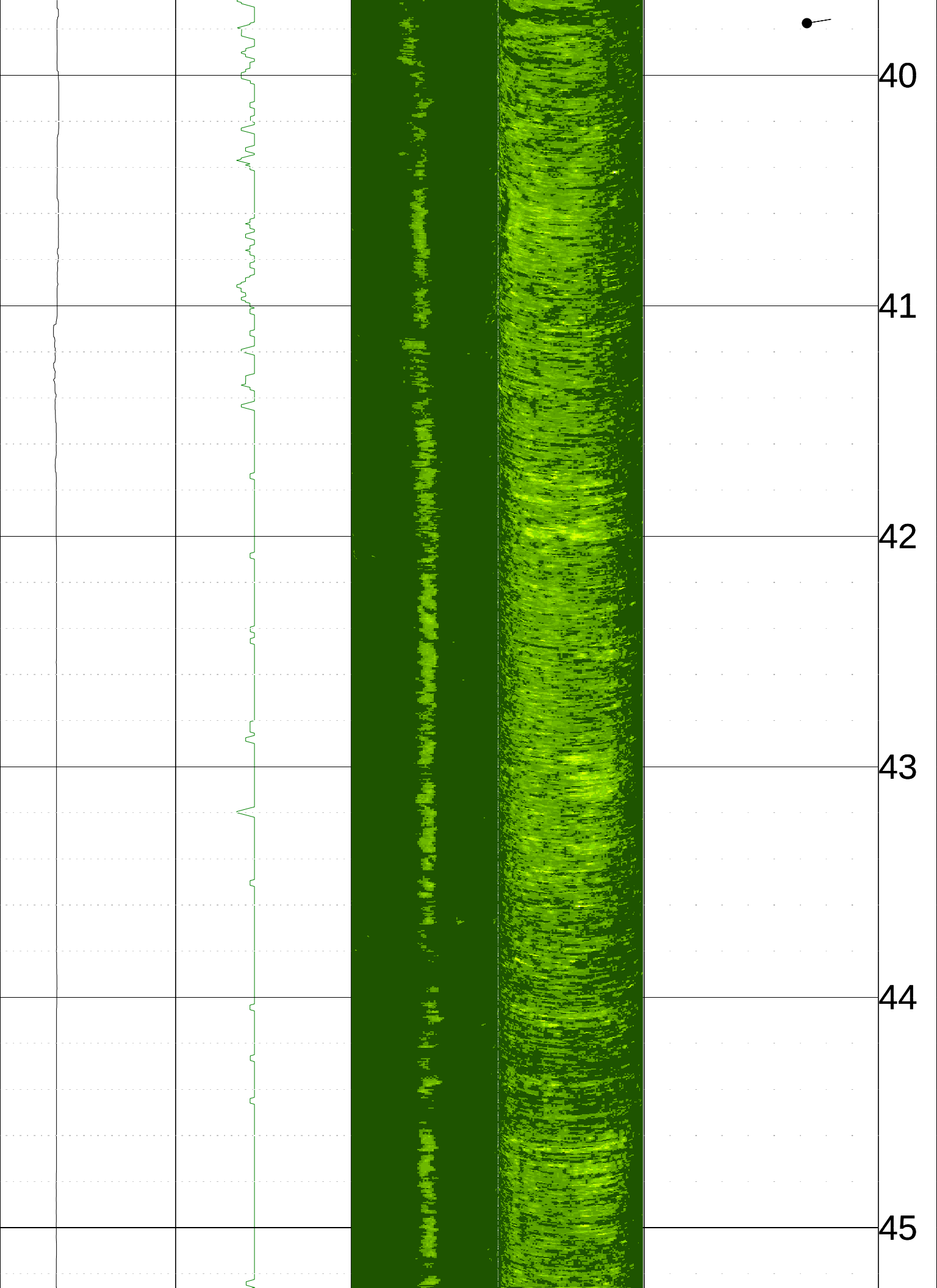
40
41
42
43
44
45

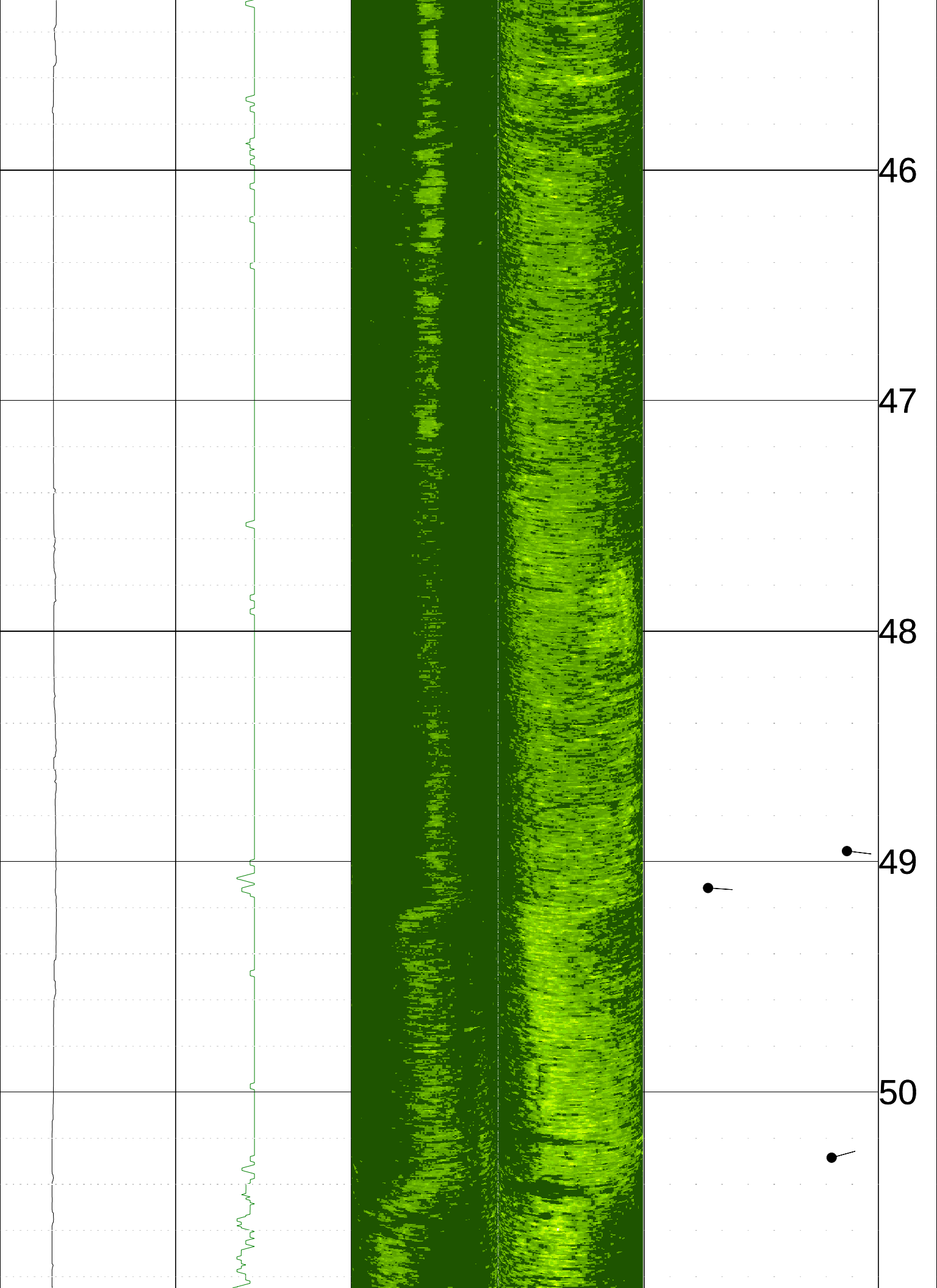
46
47
48
49
50

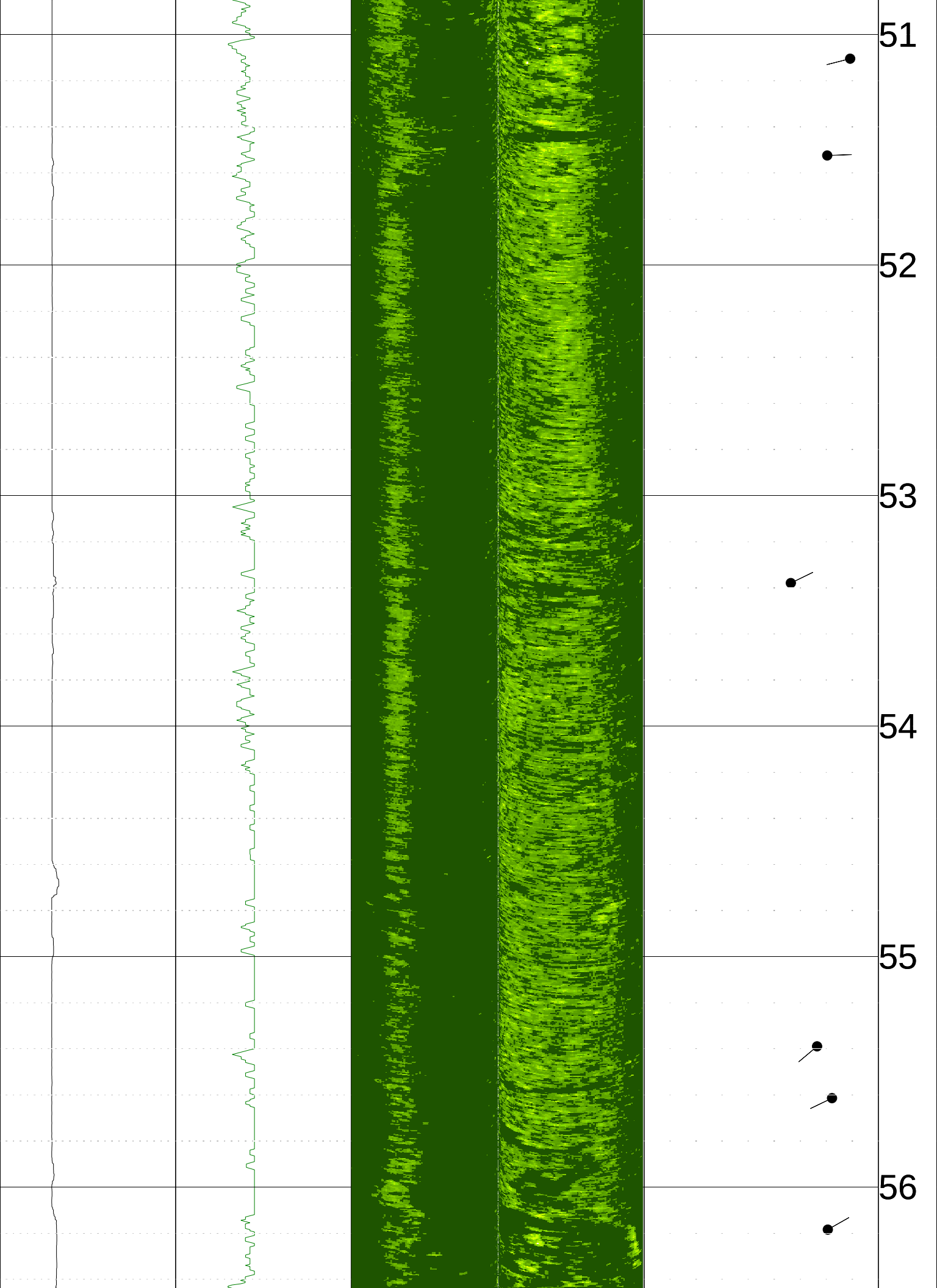
51
52
53
54
55
56

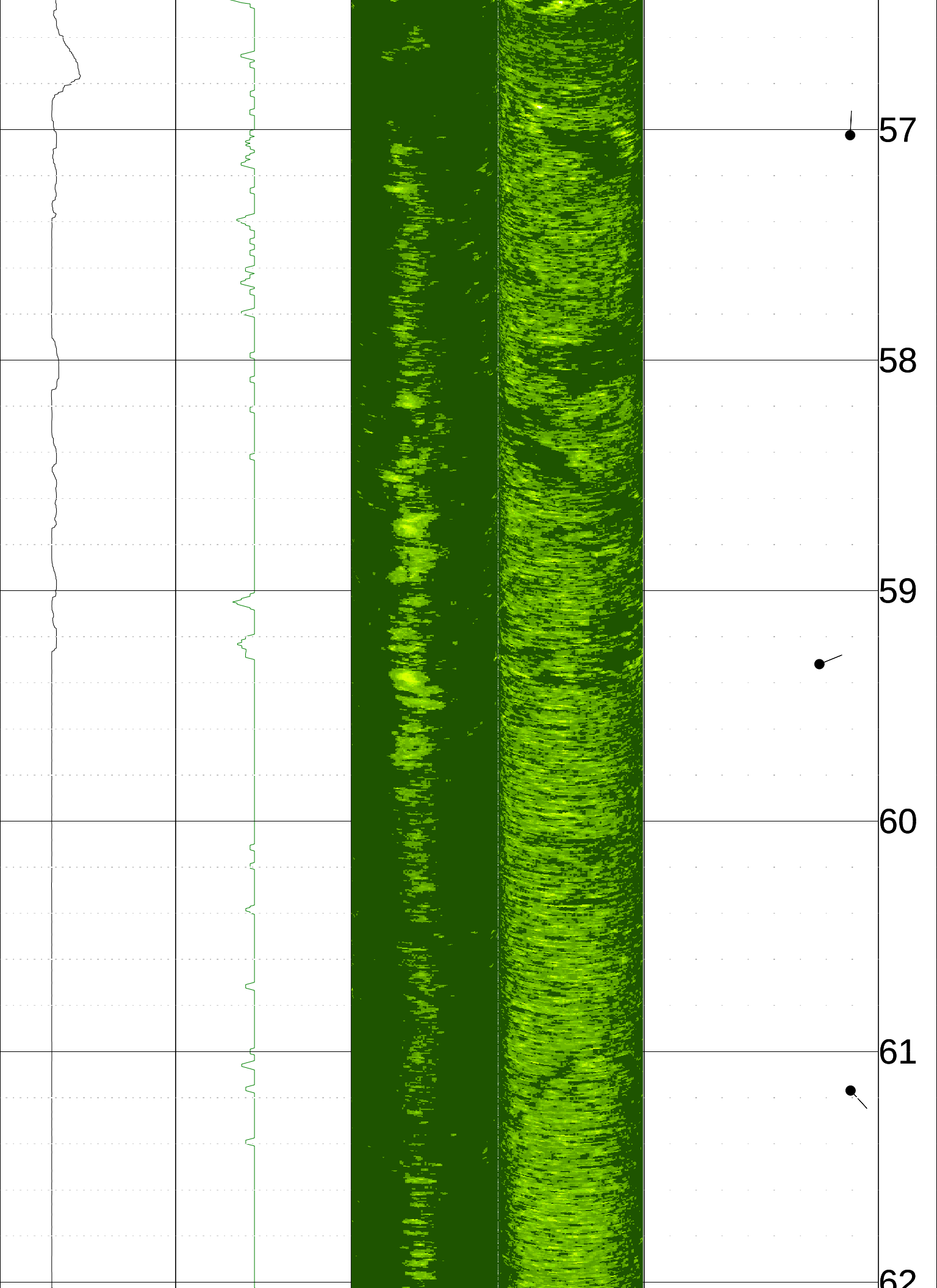
57
58
59
60
61
62

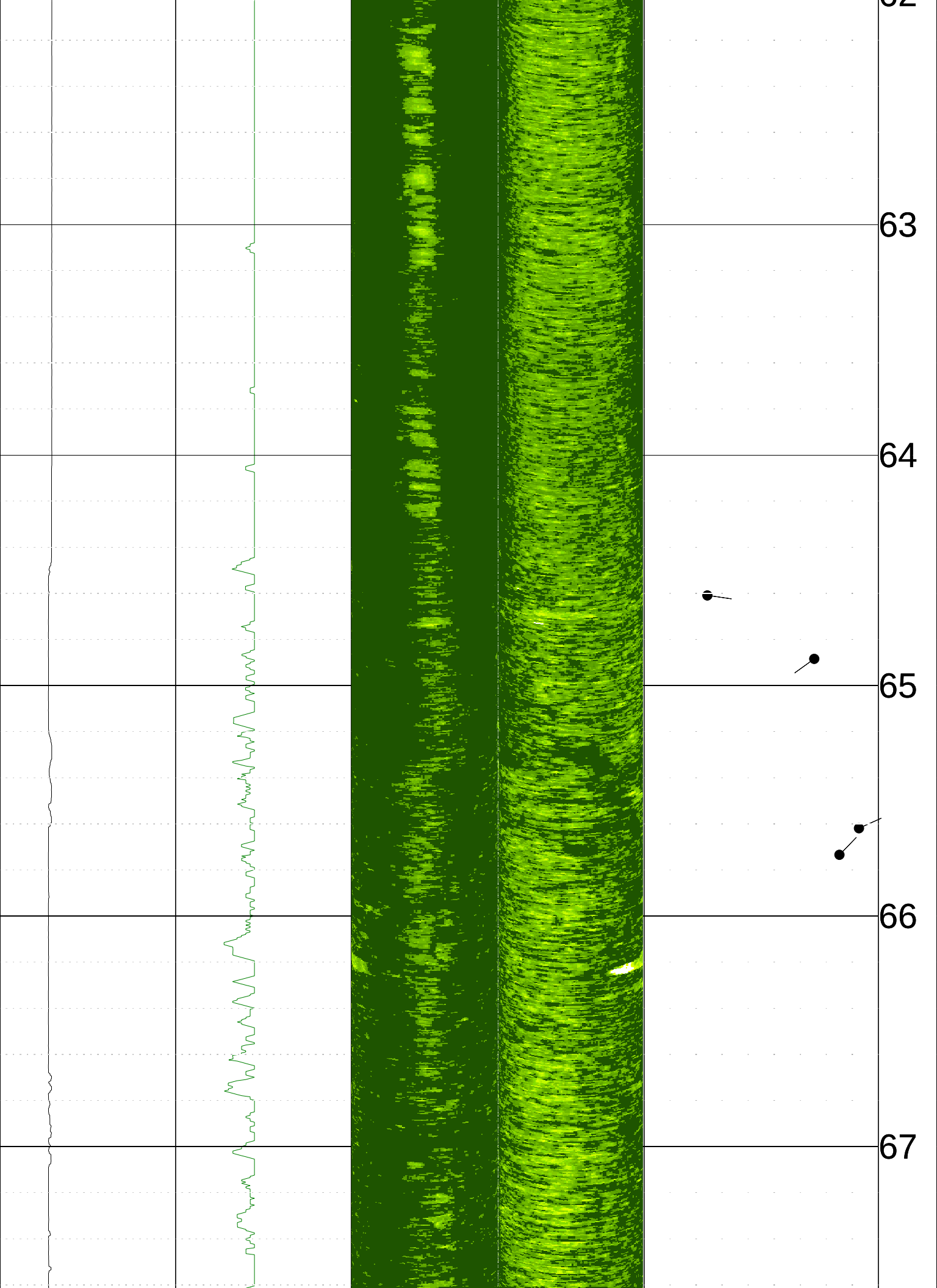
63
64
65
66
67

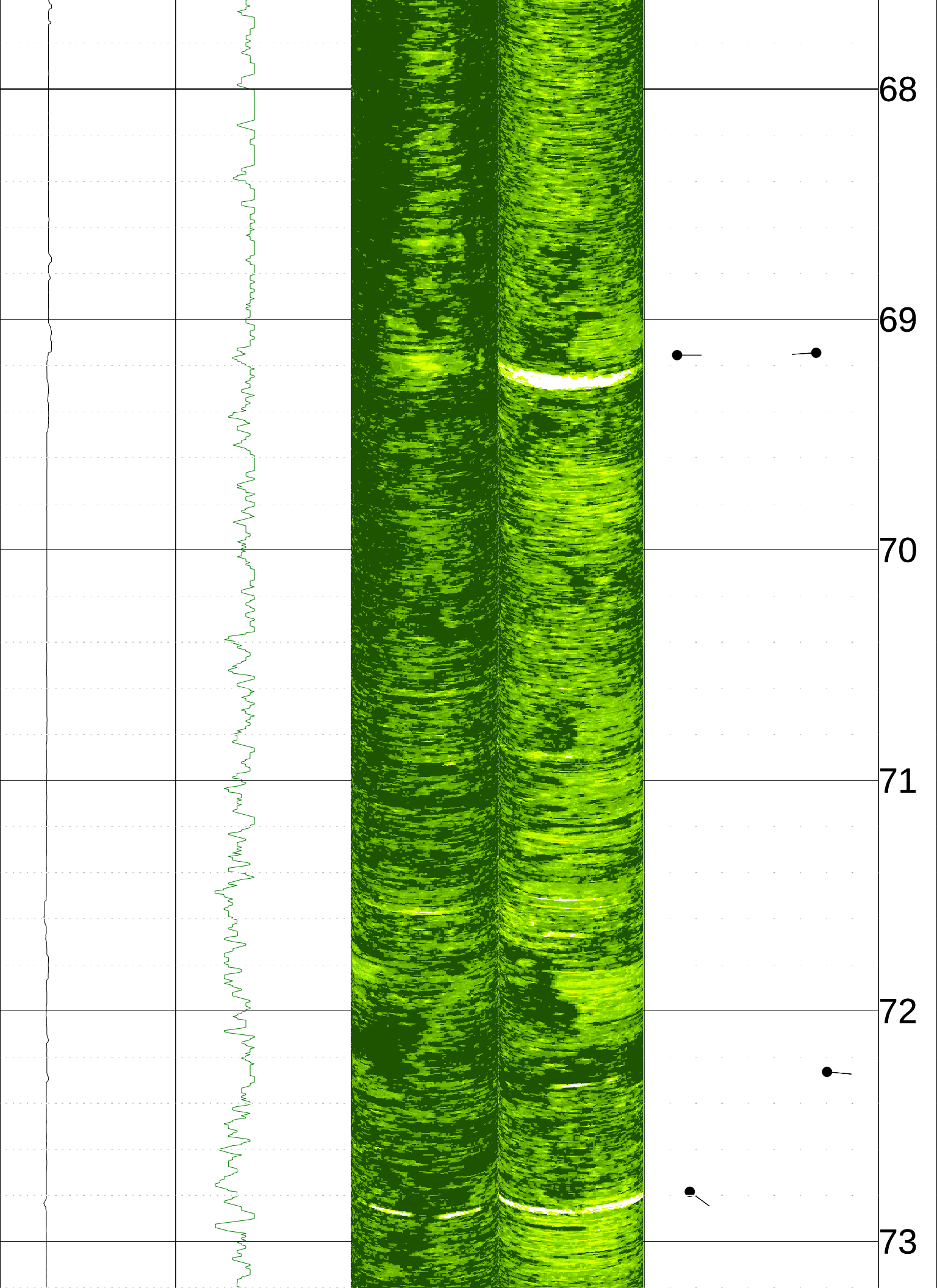
68
69
70
71
72
73

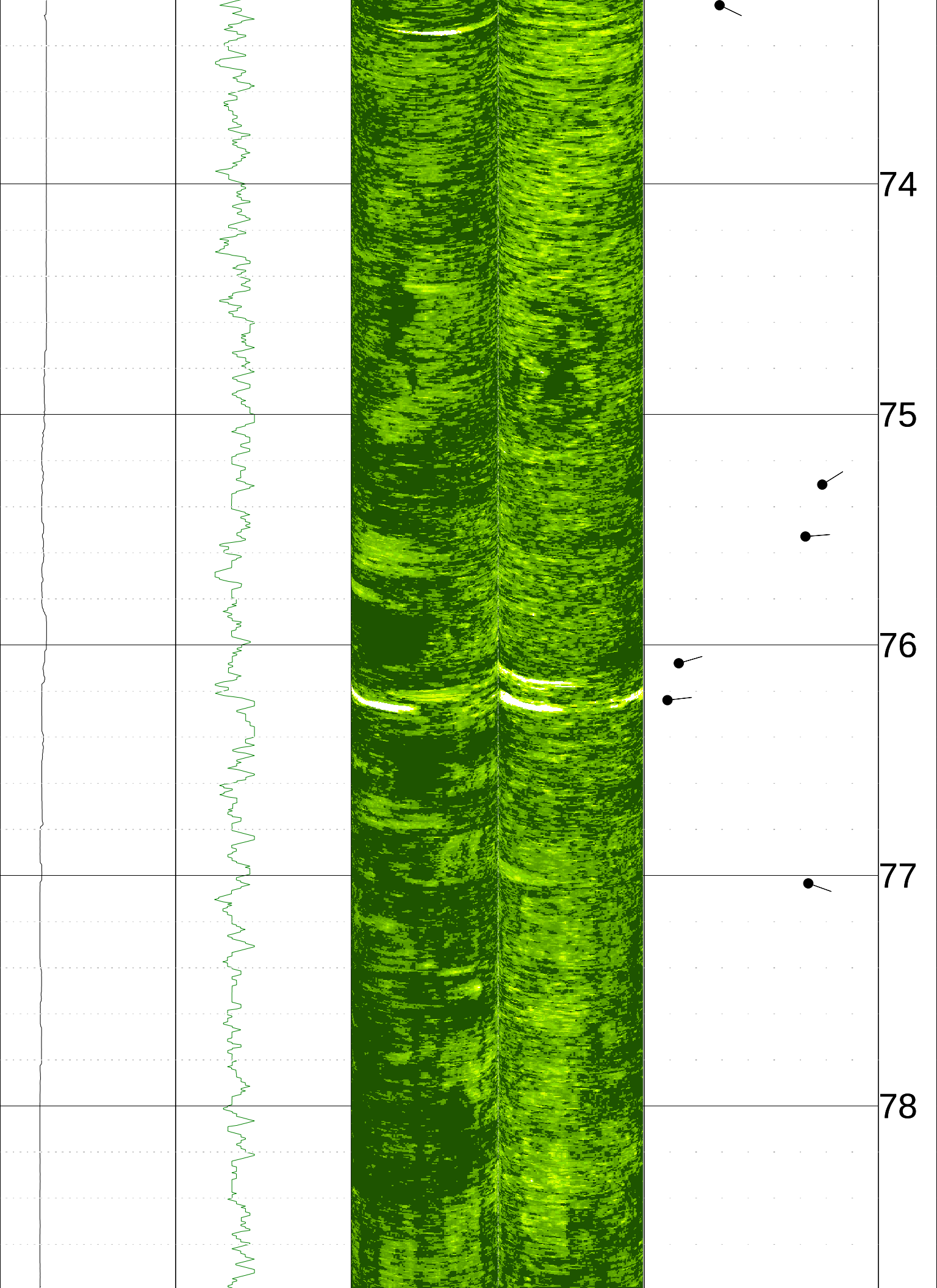
74
75
76
77
78

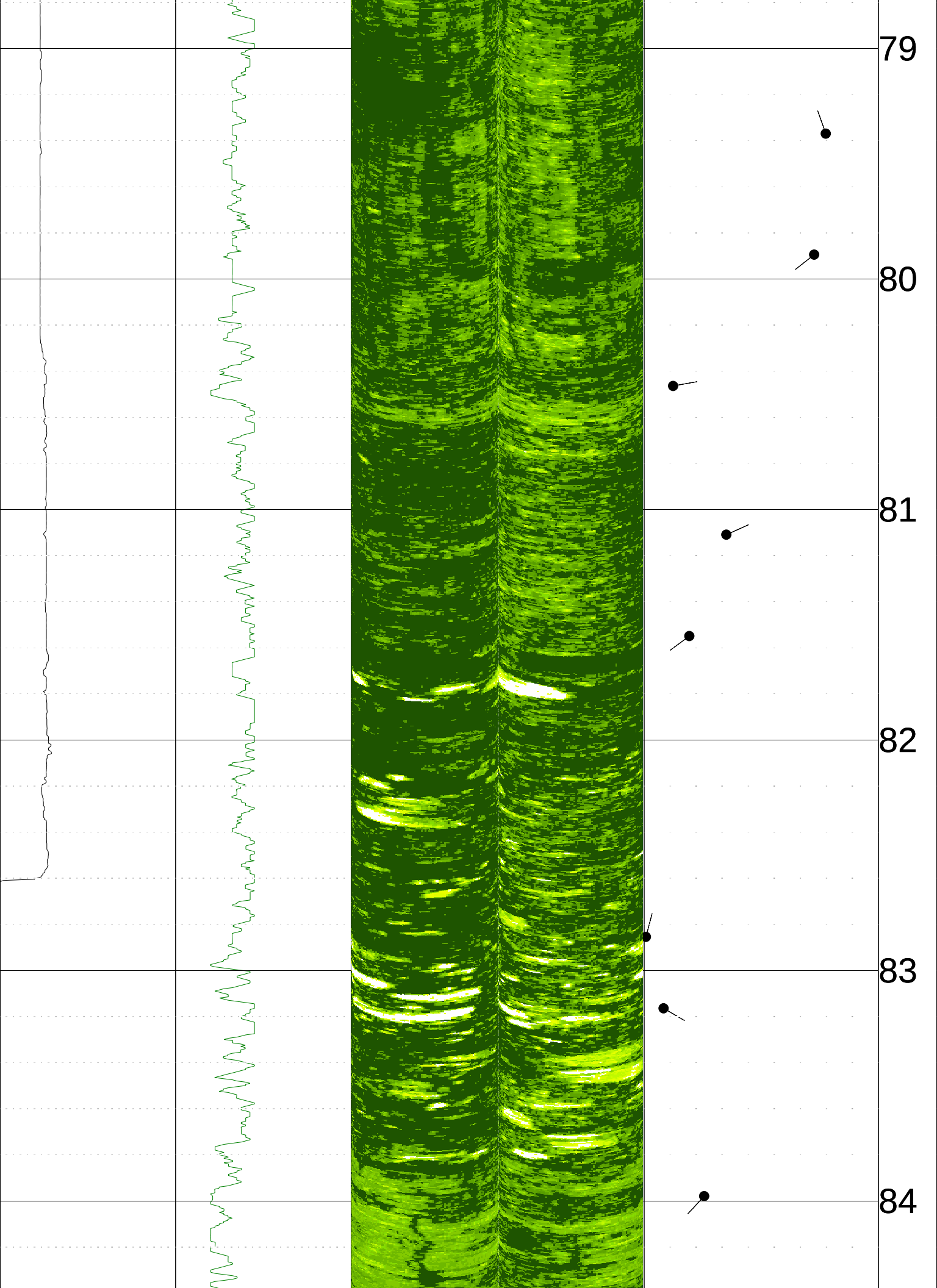
79
80
81
82
83
84

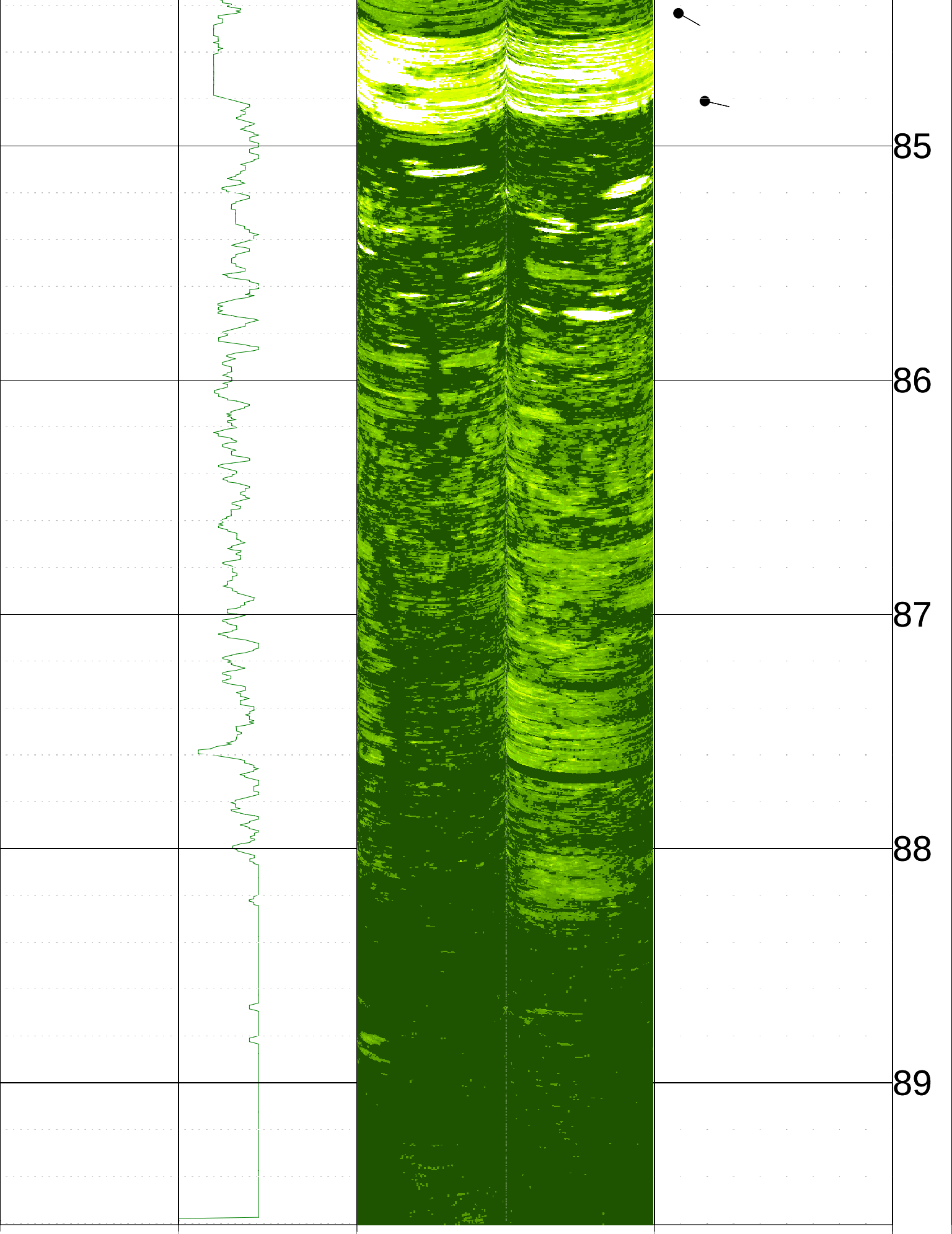
85
86
87
88
89
5
CM
30
5
CM
30
0
90
180
270
360
0
DEG
90
CALIPER
CALIPER1
AMPL
TADPOLE
METERS

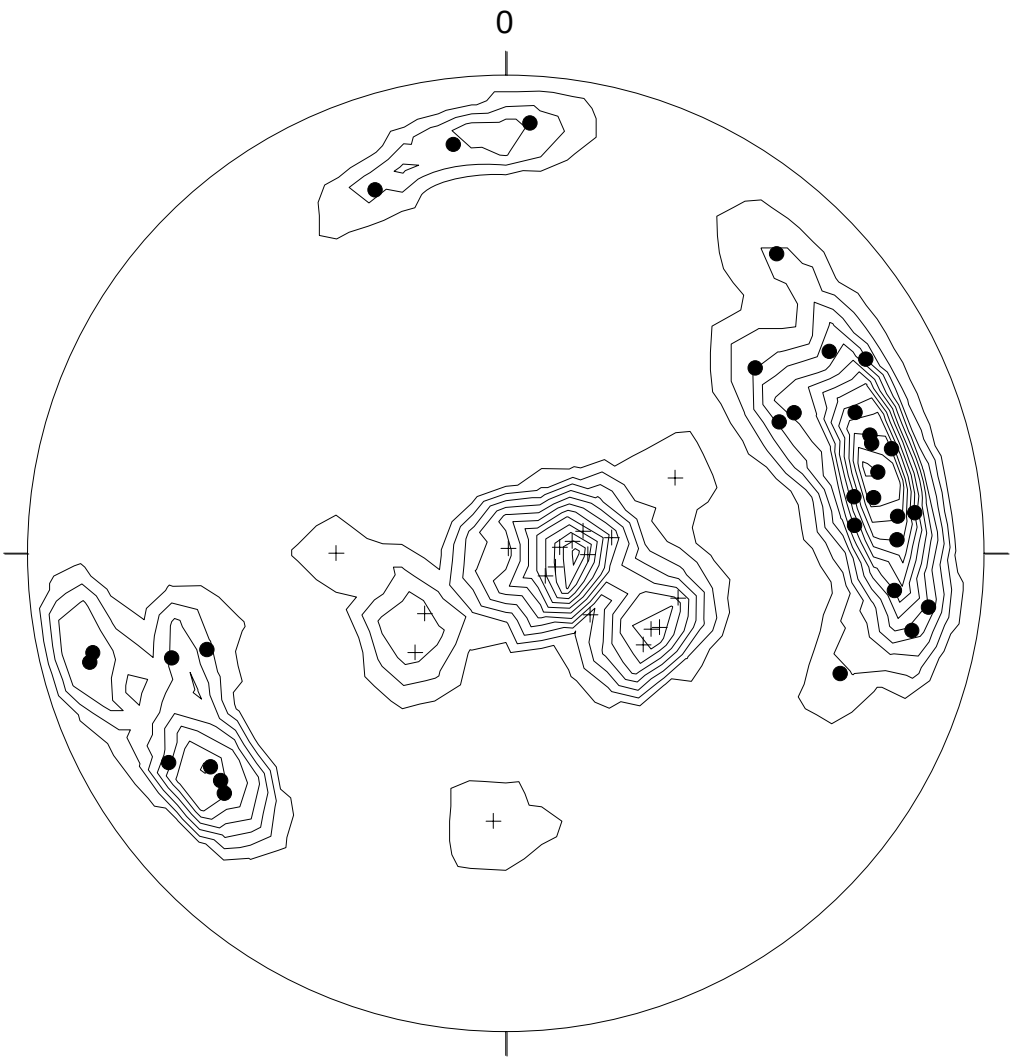

LA 710 Tunnel, boring Z2 B5

+ n=18 (P)
• n=32 (P)

Stereonet contour plot of poles to planes,
Both bedding and fractures

n=50
max. dens.=13.26 (at 76/ 24)
min. dens.=0.00
Contours at every integer between
1 and 13, inclusive:
(Multiples of random distribution)

Apparent bedding denoted as cross
Apparent fractures denoted as solid circle
Plotted on upper hemisphere

LA 710 Tunnel boring Z3 B2

COMPANY	: CALTRANS				
WELL	: Z3 B2				
LOCATION/FIELD	: LA 710 TUNNEL				
COUNTY	: LA				
LOCATION	: CA				
SECTION	: None	TOWNSHIP	: None	RANGE	: None
DATE	: 1/20/09	PERMANENT DATUM	: None		
DEPTH DRILLER	: 83.8M			KB	: NA
LOG BOTTOM	: 83.8	LOG MEASURED FROM:	GL	DF	: NA
LOG TOP	: 1.8	DRL MEASURED FROM:	GL	GL	: NA
CASING DIAMETER	: N/A	LOGGING UNIT	: 7311		
CASING TYPE	: none	FIELD OFFICE	: 7311		
CASING THICKNESS:	0	RECORDED BY	: DH/DL		
BIT SIZE	: 9.4CM	BOREHOLE FLUID	: 0	FILE	: PROCESSE
MAGNETIC DECL.	: 12.85	RM	: 0	TYPE	: 9065A
MATRIX DENSITY	: 2.71	RM TEMPERATURE	: 0	LGDATE	: 1/20/09.
NEUTRON MATRIX	: DOLOMITE	MATRIX DELTA T	: 140		
				THRESH:	2500

OTHER SERVICES:
CAL-IND
AC TEL
PSLOG

CALIPER MEASUREMENT UNITS ARE CM DIAMETER
CALIPER MEASUREMENTS REPORTED AS "UNKNOWN", "UNDER" UNITS ARE CM DIA
GL ELEVATION NOT REPORTED, MEASURED AS 24.2M BY HANDHELD GPS

ALL SERVICES PROVIDED SUBJECT TO STANDARD TERMS AND CONDITIONS

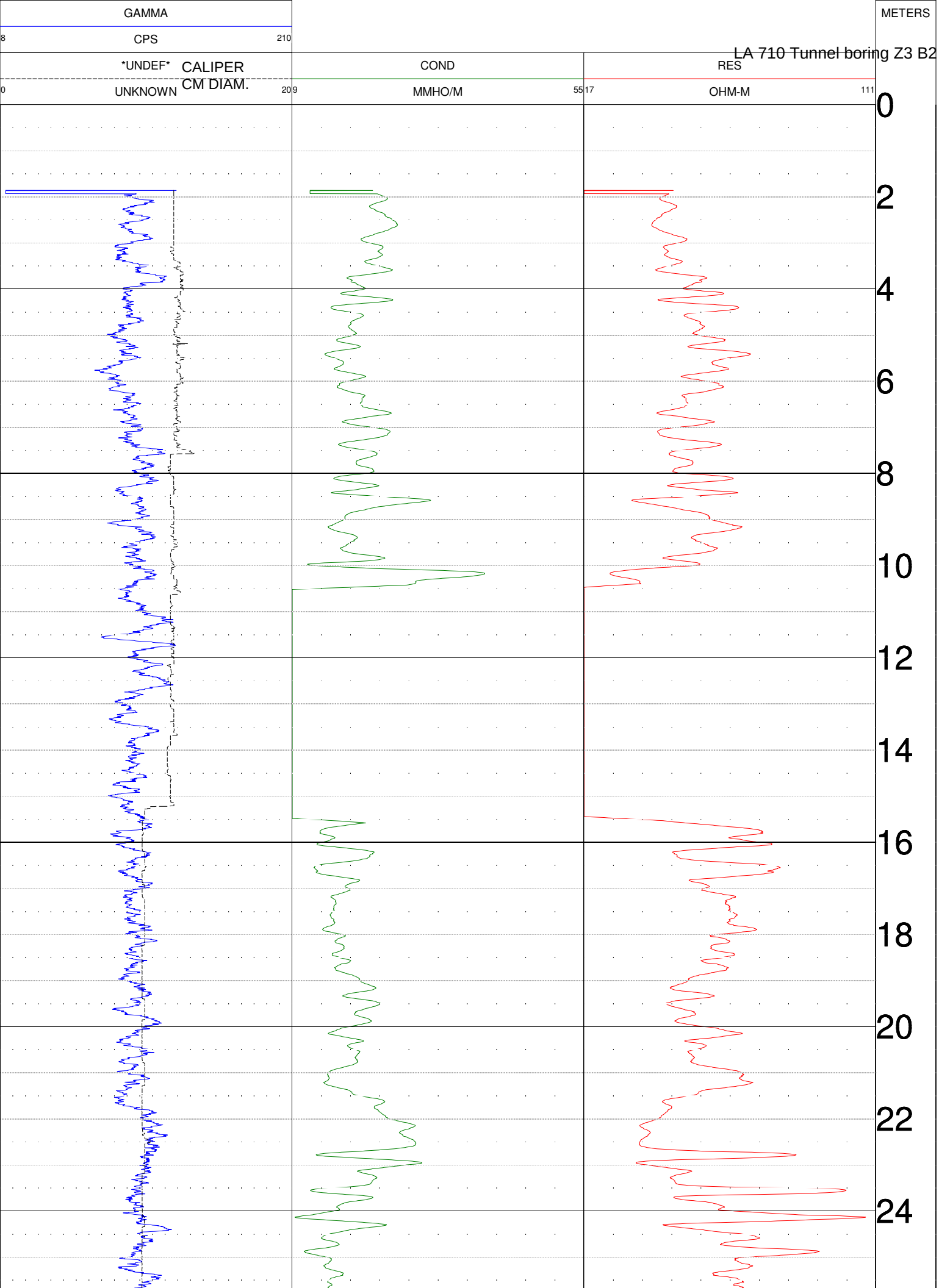
GAMMA
8
CPS
210
UNDEF
CALIPER
CM DIAM.
0
UNKNOWN
20
9
COND
MMHO/M
55
17
RES
OHM-M
111
METERS
LA 710 Tunnel boring Z3 B2
0
2
4
6
8
10
12
14
16
18
20
22
24

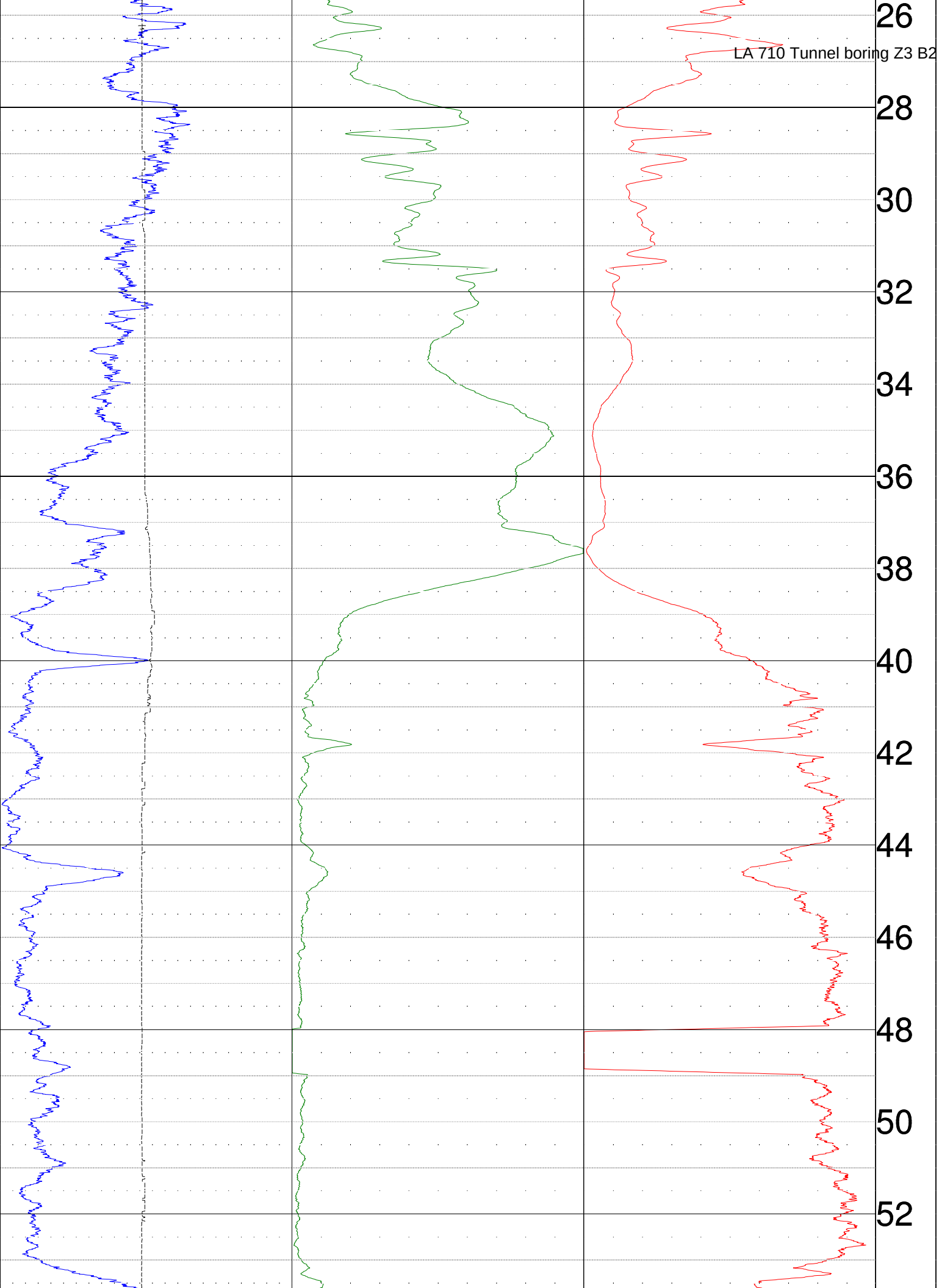
LA 710 Tunnel boring Z3 B2
26
28
30
32
34
36
38
40
42
44
46
48
50
52

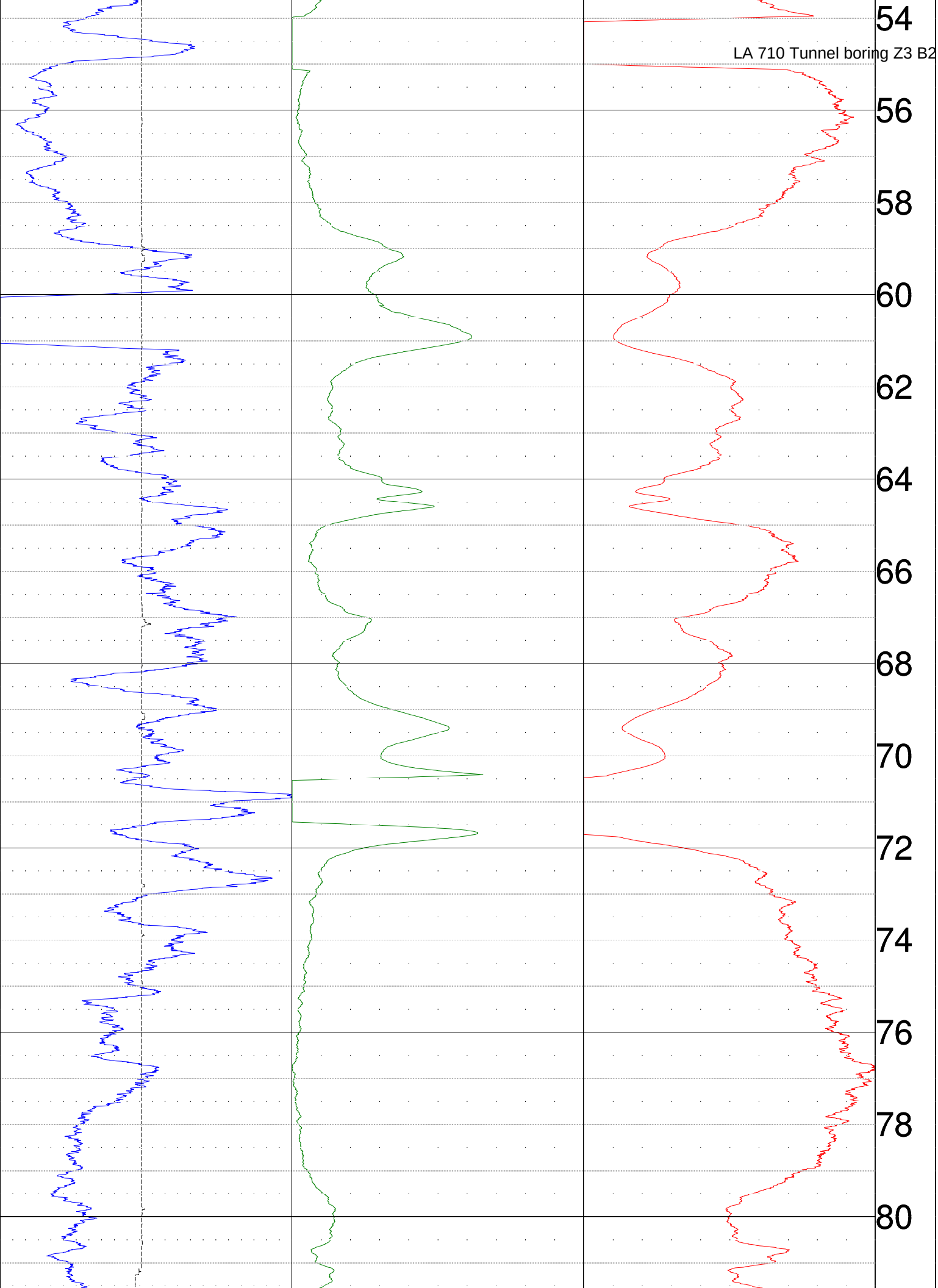
LA 710 Tunnel boring Z3 B2
54
56
58
60
62
64
66
68
70
72
74
76
78
80

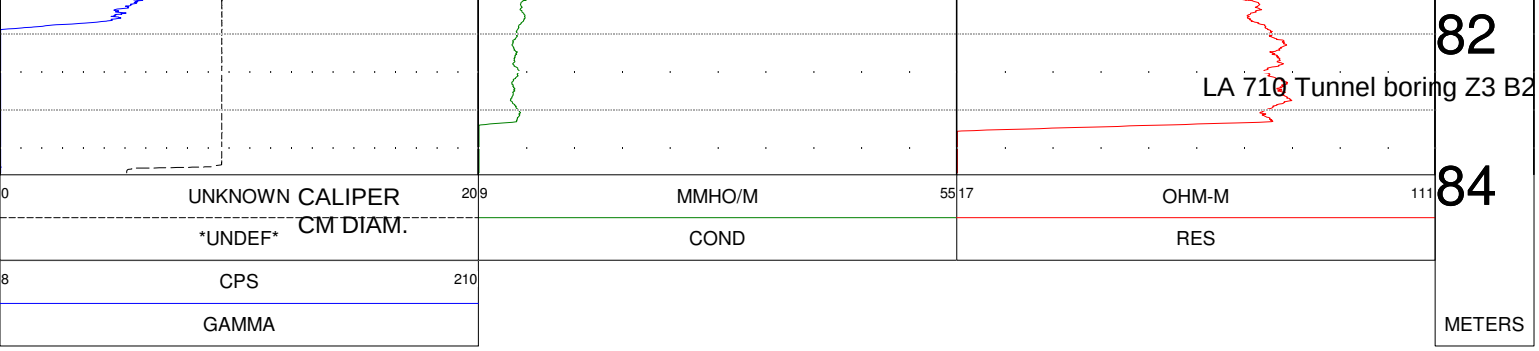
82
LA 710 Tunnel boring Z3 B2
84
0
UNKNOWN
CALIPER
CM DIAM.
20
9
MMHO/M
55
17
OHM-M
111
UNDEF
COND
RES
8
CPS
210
GAMMA
METERS

Table 2. LA 710 Tunnel
Boring Z3 B2
PS Suspension Log Data Summary

Top of Hole Elevation (m)	Depth (m)	Depth (ft)	Vs (m/s)	Vs (ft/s)	Vp (m/s)	Vp (ft/s)	γ	ρ(Vp) (g/cc)	ρ(Vp) (lb/ft^3)	G (GPa)	E (GPa)	K (GPa)	G ($10^3 lb/ft^2$)	E ($10^3 lb/ft^2$)	K ($10^3 lb/ft^2$)
Not Provided	1.5	4.9	353	1159		NA	NA	NA	NA	NA	NA	NA	NA	NA	NA
	2	6.6	402	1318		NA	NA	NA	NA	NA	NA	NA	NA	NA	NA
	2.5	8.2	350	1147		NA	NA	NA	NA	NA	NA	NA	NA	NA	NA
	3	9.8	372	1220		NA	NA	NA	NA	NA	NA	NA	NA	NA	NA
	3.5	11.5	369	1211		NA	NA	NA	NA	NA	NA	NA	NA	NA	NA
	4	13.1	356	1168		NA	NA	NA	NA	NA	NA	NA	NA	NA	NA
	4.5	14.8	385	1262		NA	NA	NA	NA	NA	NA	NA	NA	NA	NA
	5	16.4	433	1420		NA	NA	NA	NA	NA	NA	NA	NA	NA	NA
	5.5	18.0	426	1396		NA	NA	NA	NA	NA	NA	NA	NA	NA	NA
	6	19.7	556	1823		NA	NA	NA	NA	NA	NA	NA	NA	NA	NA
	6.5	21.3	375	1229	699	2294	NA	NA	NA	NA	NA	NA	NA	NA	NA
	7	23.0	350	1147	610	2001	NA	NA	NA	NA	NA	NA	NA	NA	NA
	7.5	24.6	353	1159	769	2524	NA	NA	NA	NA	NA	NA	NA	NA	NA
	8	26.2	379	1243		NA	NA	NA	NA	NA	NA	NA	NA	NA	NA
	8.5	27.9	412	1350	709	2327	NA	NA	NA	NA	NA	NA	NA	NA	NA
	9	29.5	433	1420	758	2485	NA	NA	NA	NA	NA	NA	NA	NA	NA
	9.5	31.2	439	1439		NA	NA	NA	NA	NA	NA	NA	NA	NA	NA
	10	32.8	418	1373	699	2294	NA	NA	NA	NA	NA	NA	NA	NA	NA
	10.5	34.4	397	1302	775	2543	NA	NA	NA	NA	NA	NA	NA	NA	NA
	11	36.1	429	1408		NA	NA	NA	NA	NA	NA	NA	NA	NA	NA
	11.5	37.7	418	1373	877	2878	NA	NA	NA	NA	NA	NA	NA	NA	NA
	12	39.4	386	1267	699	2294	NA	NA	NA	NA	NA	NA	NA	NA	NA
	12.5	41.0	495	1624	775	2543	NA	NA	NA	NA	NA	NA	NA	NA	NA
	13	42.7	513	1682	775	2543	NA	NA	NA	NA	NA	NA	NA	NA	NA
	13.5	44.3	505	1657	746	2448	NA	NA	NA	NA	NA	NA	NA	NA	NA
	14	45.9	495	1624	746	2448	NA	NA	NA	NA	NA	NA	NA	NA	NA
	14.5	47.6	532	1745	781	2563	NA	NA	NA	NA	NA	NA	NA	NA	NA
	15	49.2	541	1773	787	2583	NA	NA	NA	NA	NA	NA	NA	NA	NA
	15.5	50.9	518	1700	746	2448	NA	NA	NA	NA	NA	NA	NA	NA	NA
	16.5	54.1	521	1709	752	2467	NA	NA	NA	NA	NA	NA	NA	NA	NA
	17	55.8	532	1745	820	2689	NA	NA	NA	NA	NA	NA	NA	NA	NA
	17.5	57.4	552	1813	806	2646	NA	NA	NA	NA	NA	NA	NA	NA	NA
	18	59.1	562	1843	813	2667	NA	NA	NA	NA	NA	NA	NA	NA	NA
	18.5	60.7	599	1965	971	3185	NA	NA	NA	NA	NA	NA	NA	NA	NA
	19	62.3	595	1953	1000	3281	NA	NA	NA	NA	NA	NA	NA	NA	NA
	19.5	64.0	538	1764	952	3125	NA	NA	NA	NA	NA	NA	NA	NA	NA
	20	65.6	552	1813	952	3125	NA	NA	NA	NA	NA	NA	NA	NA	NA

γ = Poisson's Ratio ρ(Vp) = Vp-derived density G = Shear Modulus E = Young's Modulus K = Bulk Modulus
Shaded cells denote questionable data.

Table 2. LA 710 Tunnel
Boring Z3 B2
PS Suspension Log Data Summary

Top of Hole Elevation (m)	Depth (m)	Depth (ft)	Vs (m/s)	Vs (ft/s)	Vp (m/s)	Vp (ft/s)	γ	ρ(Vp) (g/cc)	ρ(Vp) (lb/ft^3)	G (GPa)	E (GPa)	K (GPa)	G ($10^3 lb/ft^2$)	E ($10^3 lb/ft^2$)	K ($10^3 lb/ft^2$)
	20.5	67.3	538	1764	971	3185	NA	NA	NA	NA	NA	NA	NA	NA	NA
	21	68.9	483	1585	926	3038	NA	NA	NA	NA	NA	NA	NA	NA	NA
	21.5	70.5	513	1682	1235	4050	NA	NA	NA	NA	NA	NA	NA	NA	NA
	22	72.2	610	2001	2083	6835	0.45	2.22	138.82	0.827	2.403	8.549	17267	50184	178546
	22.5	73.8	559	1833	1020	3348	NA	NA	NA	NA	NA	NA	NA	NA	NA
	23	75.5	488	1600	909	2983	NA	NA	NA	NA	NA	NA	NA	NA	NA
	23.5	77.1	505	1657	926	3038	NA	NA	NA	NA	NA	NA	NA	NA	NA
	24	78.7	495	1624	893	2929	NA	NA	NA	NA	NA	NA	NA	NA	NA
	24.5	80.4	476	1562	806	2646	NA	NA	NA	NA	NA	NA	NA	NA	NA
	25	82.0	490	1608	909	2983	NA	NA	NA	NA	NA	NA	NA	NA	NA
	25.5	83.7	500	1640	909	2983	NA	NA	NA	NA	NA	NA	NA	NA	NA
	26	85.3	488	1600	855	2804	NA	NA	NA	NA	NA	NA	NA	NA	NA
	26.4	86.6	457	1498	840	2757	NA	NA	NA	NA	NA	NA	NA	NA	NA
	26.8	87.9	513	1682	885	2903	NA	NA	NA	NA	NA	NA	NA	NA	NA
	27.5	90.2	515	1691	926	3038	NA	NA	NA	NA	NA	NA	NA	NA	NA
	28	91.9	498	1632	885	2903	NA	NA	NA	NA	NA	NA	NA	NA	NA
	28.5	93.5	510	1674	901	2956	NA	NA	NA	NA	NA	NA	NA	NA	NA
	29	95.1	578	1896	1053	3454	NA	NA	NA	NA	NA	NA	NA	NA	NA
	29.5	96.8	606	1988	1449	4755	NA	NA	NA	NA	NA	NA	NA	NA	NA
	30	98.4	568	1864	1010	3314	NA	NA	NA	NA	NA	NA	NA	NA	NA
	30	98.4	562	1843	1053	3454	NA	NA	NA	NA	NA	NA	NA	NA	NA
	30.5	100.1	541	1773	917	3010	NA	NA	NA	NA	NA	NA	NA	NA	NA
	31	101.7	588	1930	719	2360	NA	NA	NA	NA	NA	NA	NA	NA	NA
	31.5	103.3	595	1953	769	2524	NA	NA	NA	NA	NA	NA	NA	NA	NA
	32	105.0	513	1682	1124	3686	NA	NA	NA	NA	NA	NA	NA	NA	NA
	32.4	106.3	500	1640	1031	3382	NA	NA	NA	NA	NA	NA	NA	NA	NA
	32.9	107.9	546	1793	1449	4755	NA	NA	NA	NA	NA	NA	NA	NA	NA
	33.4	109.6	613	2013	1852	6076	0.44	2.10	131.15	0.791	2.275	6.150	16514	47506	128447
	33.9	111.2	602	1976	1961	6433	0.45	2.16	134.97	0.785	2.272	7.266	16386	47451	151755
	34.4	112.9	562	1843	2041	6696	0.46	2.20	137.53	0.695	2.029	8.248	14522	42375	172272
	34.9	114.5	508	1665	2083	6835	0.47	2.22	138.82	0.573	1.683	8.887	11967	35145	185614
	35.5	116.5	461	1512	2041	6696	0.47	2.20	137.53	0.468	1.378	8.552	9771	28788	178607
	36	118.1	481	1577	1852	6076	0.46	2.10	131.15	0.486	1.422	6.557	10141	29691	136944
	36.5	119.8	510	1674	1818	5965	0.46	2.08	129.88	0.542	1.578	6.156	11311	32966	128561
	36.9	121.1	599	1965	1724	5657	0.43	2.02	126.09	0.724	2.073	5.039	15126	43303	105233
	37.5	123.0	592	1941	2041	6696	0.45	2.20	137.53	0.771	2.243	8.147	16110	46851	170154
	38	124.7	662	2173	2222	7291	0.45	2.29	142.69	1.002	2.910	9.951	20937	60770	207827

γ = Poisson's Ratio ρ(Vp) = Vp-derived density G = Shear Modulus E = Young's Modulus K = Bulk Modulus
Shaded cells denote questionable data.

Table 2. LA 710 Tunnel
Boring Z3 B2
PS Suspension Log Data Summary

Top of Hole Elevation (m)	Depth (m)	Depth (ft)	Vs (m/s)	Vs (ft/s)	Vp (m/s)	Vp (ft/s)	γ	ρ(Vp) (g/cc)	ρ(Vp) (lb/ft^3)	G (GPa)	E (GPa)	K (GPa)	G ($10^3 lb/ft^2$)	E ($10^3 lb/ft^2$)	K ($10^3 lb/ft^2$)
	38.5	126.3	641	2103	1923	6309	0.44	2.14	133.69	0.880	2.530	6.747	18379	52840	140906
	39	128.0	595	1953	1563	5126	NA	NA	NA	NA	NA	NA	NA	NA	NA
	39.5	129.6	629	2063	1408	4621	NA	NA	NA	NA	NA	NA	NA	NA	NA
	39.9	130.9	658	2158	1429	4687	NA	NA	NA	NA	NA	NA	NA	NA	NA
	40.4	132.5	662	2173	1111	3645	NA	NA	NA	NA	NA	NA	NA	NA	NA
	40.9	134.2	671	2202	1163	3815	NA	NA	NA	NA	NA	NA	NA	NA	NA
	41.5	136.2	746	2448	1429	4687	NA	NA	NA	NA	NA	NA	NA	NA	NA
	42	137.8	862	2828	1695	5561	0.33	2.00	124.84	1.486	3.940	3.763	31038	82282	78595
	42.5	139.4	893	2929	1471	4825	NA	NA	NA	NA	NA	NA	NA	NA	NA
	43	141.1	952	3125	1389	4557	NA	NA	NA	NA	NA	NA	NA	NA	NA
	43.5	142.7	962	3155	1429	4687	NA	NA	NA	NA	NA	NA	NA	NA	NA
	44	144.4	935	3066	1818	5965	0.32	2.08	129.88	1.817	4.799	4.455	37952	100228	93039
	44.6	146.3	1000	3281	2000	6562	0.33	2.18	136.25	2.183	5.820	5.820	45582	121553	121553
	45	147.6	847	2780	2381	7812	0.43	2.35	146.59	1.686	4.815	11.063	35222	100556	231059
	45.6	149.6	1010	3314	2703	8867	0.42	2.45	153.16	2.503	7.103	14.583	52279	148349	304572
	46.1	151.2	1087	3566	2857	9374	0.42	2.50	155.80	2.949	8.347	16.442	61583	174327	343390
	46.6	152.9	885	2903	2778	9113	0.44	2.47	154.48	1.938	5.595	16.509	40474	116849	344805
	46.6	152.9	893	2929	2857	9374	0.45	2.50	155.80	1.990	5.753	17.720	41553	120161	370097
	46.6	152.9	943	3095	2778	9113	0.43	2.47	154.48	2.202	6.320	16.157	45996	131990	337444
	47.1	154.5	980	3217	3030	9942	0.44	2.54	158.46	2.440	7.034	20.056	50955	146907	418867
	47.6	156.2	1010	3314	2941	9650	0.43	2.52	157.13	2.568	7.361	18.349	53635	153734	383227
	48.1	157.8	917	3010	2778	9113	0.44	2.47	154.48	2.083	5.993	16.316	43499	125170	340773
	48.1	157.8	930	3052	2778	9113	0.44	2.47	154.48	2.141	6.153	16.238	44721	128514	339142
	48.1	157.8	909	2983	2778	9113	0.44	2.47	154.48	2.045	5.890	16.367	42711	123010	341821
	48.6	159.4	833	2734	2941	9650	0.46	2.52	157.13	1.748	5.091	19.443	36505	106330	406065
	49.1	161.1	714	2343	2778	9113	0.46	2.47	154.48	1.262	3.698	17.410	26368	77236	363613
	50.1	164.4	488	1600	2632	8634	0.48	2.43	151.84	0.579	1.716	16.072	12087	35832	335665
	50.6	166.0	571	1875	2778	9113	0.48	2.47	154.48	0.808	2.388	18.016	16875	49880	376269
	51.1	167.7	645	2117	2778	9113	0.47	2.47	154.48	1.030	3.031	17.720	21511	63307	370088
	51.6	169.3	870	2853	2778	9113	0.45	2.47	154.48	1.871	5.410	16.599	39078	112988	346666
	52.1	170.9	909	2983	2778	9113	0.44	2.47	154.48	2.045	5.890	16.367	42711	123010	341821
	52.5	172.2	870	2853	2778	9113	0.45	2.47	154.48	1.871	5.410	16.599	39078	112988	346666
	53.1	174.2	1250	4101	3125	10253	0.40	2.56	159.79	3.999	11.237	19.664	83530	234680	410690
	53.6	175.9	1333	4374	3571	11717	0.42	2.65	165.16	4.703	13.348	27.474	98230	278782	573803
	54.1	177.5	1600	5249	3333	10936	0.35	2.60	162.47	6.663	17.993	20.034	139149	375788	418411
	54.6	179.1	1290	4233	2941	9650	0.38	2.52	157.13	4.191	11.573	16.186	87522	241706	338043
	55.1	180.8	1176	3860	2381	7812	0.34	2.35	146.59	3.250	8.700	8.978	67880	181712	187515

γ = Poisson's Ratio ρ(Vp) = Vp-derived density G = Shear Modulus E = Young's Modulus K = Bulk Modulus
Shaded cells denote questionable data.

Table 2. LA 710 Tunnel
Boring Z3 B2
PS Suspension Log Data Summary

Top of Hole Elevation (m)	Depth (m)	Depth (ft)	Vs (m/s)	Vs (ft/s)	Vp (m/s)	Vp (ft/s)	γ	ρ(Vp) (g/cc)	ρ(Vp) (lb/ft^3)	G (GPa)	E (GPa)	K (GPa)	G ($10^3 lb/ft^2$)	E ($10^3 lb/ft^2$)	K ($10^3 lb/ft^2$)
	55.6	182.4	870	2853	2941	9650	0.45	2.52	157.13	1.903	5.527	19.236	39749	115439	401741
	56.1	184.1	952	3125	2941	9650	0.44	2.52	157.13	2.283	6.582	18.729	47681	137457	391165
	56.6	185.7	1176	3860	3333	10936	0.43	2.60	162.47	3.602	10.294	24.114	75232	214990	503634
	57.1	187.3	1333	4374	3125	10253	0.39	2.56	159.79	4.551	12.639	18.929	95039	263965	395345
	57.6	189.0	1333	4374	3333	10936	0.40	2.60	162.47	4.627	12.999	22.748	96631	271487	475101
	58.1	190.6	1333	4374	3333	10936	0.40	2.60	162.47	4.627	12.999	22.748	96631	271487	475103
	58.6	192.3	1333	4374	3333	10936	0.40	2.60	162.47	4.627	12.999	22.748	96631	271487	475101
	59.1	193.9	1111	3645	2941	9650	0.42	2.52	157.13	3.107	8.805	17.630	64899	183892	368208
	59.6	195.5	667	2187	2632	8634	0.47	2.43	151.84	1.081	3.169	15.402	22577	66182	321680
	60	196.9	769	2524	2564	8412	0.45	2.41	150.52	1.427	4.139	13.950	29797	86445	291351
	60.5	198.5	893	2929	2778	9113	0.44	2.47	154.48	1.973	5.691	16.463	41199	118851	343838
	60.6	198.8	769	2524	2500	8202	0.45	2.39	149.21	1.414	4.095	13.052	29537	85523	272605
	60.6	198.8	606	1988	2500	8202	0.47	2.39	149.21	0.878	2.579	13.768	18335	53861	287541
	61	200.1	1163	3815	3030	9942	0.41	2.54	158.46	3.432	9.703	18.733	71678	202658	391235
	61.1	200.5	588	1930	2632	8634	0.47	2.43	151.84	0.842	2.481	15.721	17577	51806	328346
	61.5	201.8	1250	4101	2941	9650	0.39	2.52	157.13	3.933	10.931	16.529	82137	228306	345223
	61.6	202.1	1176	3860	2778	9113	0.39	2.47	154.48	3.425	9.526	14.527	71530	198955	303396
	62	203.4	1250	4101	3125	10253	0.40	2.56	159.79	3.999	11.237	19.664	83530	234680	410690
	62	203.4	1282	4206	3125	10253	0.40	2.56	159.79	4.207	11.770	19.387	87869	245825	404907
	62.5	205.1	1282	4206	3226	10583	0.41	2.58	161.13	4.242	11.931	21.202	88604	249191	442805
	62.5	205.1	1299	4261	3030	9942	0.39	2.54	158.46	4.281	11.880	17.600	89413	248122	367588
	62.5	205.1	1250	4101	3333	10936	0.42	2.60	162.47	4.066	11.534	23.495	84930	240891	490703
	63	206.7	1250	4101	3030	9942	0.40	2.54	158.46	3.966	11.085	18.020	82833	231515	376362
	63	206.7	1250	4101	3125	10253	0.40	2.56	159.79	3.999	11.237	19.664	83530	234680	410692
	63.5	208.3	1190	3906	2941	9650	0.40	2.52	157.13	3.567	10.003	17.017	74501	208906	355405
	63.5	208.3	833	2734	2857	9374	0.45	2.50	155.80	1.733	5.038	18.062	36197	105226	377238
	64	210.0	1075	3528	2857	9374	0.42	2.50	155.80	2.886	8.181	16.526	60266	170853	345146
	64	210.0	1087	3566	3030	9942	0.43	2.54	158.46	2.999	8.554	19.310	62634	178652	403295
	64.5	211.6	926	3038	2857	9374	0.44	2.50	155.80	2.140	6.168	17.520	44688	128819	365915
	64.5	211.6	1351	4434	3333	10936	0.40	2.60	162.47	4.753	13.323	22.580	99260	278259	471595
	65	213.3	1471	4825	3704	12151	0.41	2.67	166.51	5.768	16.225	28.897	120471	338866	603514
	65.1	213.6	1613	5292	2941	9650	0.28	2.52	157.13	6.548	16.827	13.043	136753	351447	272402
	65.5	214.9	1282	4206	3571	11717	0.43	2.65	165.16	4.348	12.402	27.947	90820	259024	583684
	65.6	215.2	1389	4557	3333	10936	0.39	2.60	162.47	5.020	14.006	22.223	104851	292526	464143
	66	216.5	1389	4557	3704	12151	0.42	2.67	166.51	5.145	14.593	29.727	107457	304788	620866
	66	216.5	1190	3906	3226	10583	0.42	2.58	161.13	3.658	10.397	21.981	76398	217149	459077
	66.5	218.2	1389	4557	4000	13123	0.43	2.71	169.22	5.229	14.970	36.398	109205	312644	760184

γ = Poisson's Ratio ρ(Vp) = Vp-derived density G = Shear Modulus E = Young's Modulus K = Bulk Modulus
Shaded cells denote questionable data.

Table 2. LA 710 Tunnel
Boring Z3 B2
PS Suspension Log Data Summary

Top of Hole Elevation (m)	Depth (m)	Depth (ft)	Vs (m/s)	Vs (ft/s)	Vp (m/s)	Vp (ft/s)	γ	ρ(Vp) (g/cc)	ρ(Vp) (lb/ft^3)	G (GPa)	E (GPa)	K (GPa)	G ($10^3 lb/ft^2$)	E ($10^3 lb/ft^2$)	K ($10^3 lb/ft^2$)
	66.5	218.2	980	3217	2941	9650	0.44	2.52	157.13	2.419	6.955	18.548	50527	145264	387372
	67	219.8	794	2604	3571	11717	0.47	2.65	165.16	1.666	4.913	31.523	34804	102604	658372
	67	219.8	1064	3490	3333	10936	0.44	2.60	162.47	2.945	8.502	24.990	61515	177570	521922
	67.5	221.5	962	3155	3030	9942	0.44	2.54	158.46	2.347	6.778	20.179	49014	141554	421453
	67.5	221.5	962	3155	3448	11313	0.46	2.62	163.81	2.426	7.074	27.967	50670	147737	584096
	68	223.1	893	2929	2778	9113	0.44	2.47	154.48	1.973	5.691	16.463	41199	118851	343837
	68	223.1	847	2780	3226	10583	0.46	2.58	161.13	1.854	5.424	24.387	38715	113275	509323
	68.5	224.7	1190	3906	2941	9650	0.40	2.52	157.13	3.567	10.003	17.017	74501	208906	355406
	68.5	224.7	893	2929	2941	9650	0.45	2.52	157.13	2.007	5.816	19.098	41907	121466	398864
	69	226.4	943	3095	2703	8867	0.43	2.45	153.16	2.183	6.247	15.009	45602	130479	313474
	69.5	228.0	943	3095	2941	9650	0.44	2.52	157.13	2.240	6.463	18.786	46785	134990	392360
	70	229.7	1220	4001	3226	10583	0.42	2.58	161.13	3.839	10.876	21.740	80170	227143	454049
	70.1	230.0	1087	3566	3448	11313	0.44	2.62	163.81	3.100	8.959	27.068	64750	187106	565323
	70.5	231.3	1282	4206	3333	10936	0.41	2.60	162.47	4.278	12.090	23.214	89341	252512	484824
	71	232.9	1190	3906	3448	11313	0.43	2.62	163.81	3.719	10.653	26.243	77670	222501	548095
	71.5	234.6	1429	4687	4000	13123	0.43	2.71	169.22	5.532	15.787	35.994	115534	329712	751744
	72.1	236.5	1250	4101	3448	11313	0.42	2.62	163.81	4.100	11.680	25.735	85632	243940	537480
	72.6	238.2	1667	5468	3571	11717	0.36	2.65	165.16	7.349	20.001	23.947	153485	417723	500130
	73.1	239.8	1471	4825	3448	11313	0.39	2.62	163.81	5.675	15.763	23.635	118521	329215	493627
	73.5	241.1	1429	4687	3704	12151	0.41	2.67	166.51	5.443	15.379	29.330	113686	321187	612562
	74	242.8	1429	4687	4167	13670	0.43	2.73	170.58	5.576	15.986	40.002	116462	333873	835455
	74.5	244.4	1471	4825	3704	12151	0.41	2.67	166.51	5.768	16.225	28.897	120471	338866	603514
	75	246.1	1429	4687	3571	11717	0.40	2.65	165.16	5.399	15.169	26.546	112765	316815	554427
	75.4	247.4	1316	4317	3571	11717	0.42	2.65	165.16	4.580	13.022	27.638	95662	271963	577229
	75.9	249.0	1370	4494	3571	11717	0.41	2.65	165.16	4.965	14.037	27.126	103687	293174	566531
	76.4	250.7	1471	4825	3704	12151	0.41	2.67	166.51	5.768	16.225	28.897	120472	338867	603514
	77	252.6	1538	5047	4348	14265	0.43	2.75	171.94	6.519	18.623	43.372	136147	388954	905843
	77.5	254.3	1563	5126	3704	12151	0.39	2.67	166.51	6.512	18.126	27.905	136001	378557	582808
	78	255.9	1190	3906	3333	10936	0.43	2.60	162.47	3.688	10.526	23.999	77034	219838	501231
	78.5	257.5	1429	4687	3333	10936	0.39	2.60	162.47	5.311	14.739	21.835	110928	307826	456038
	79	259.2	1429	4687	4167	13670	0.43	2.73	170.58	5.576	15.986	40.002	116462	333872	835452
	79.5	260.8	1163	3815	3846	12619	0.45	2.69	167.86	3.636	10.541	34.929	75931	220154	729503
	80	262.5	1429	4687	3125	10253	0.37	2.56	159.79	5.224	14.291	18.032	109101	298479	376596
	80	262.5	1333	4374	3333	10936	0.40	2.60	162.47	4.627	12.999	22.748	96631	271487	475101

γ = Poisson's Ratio ρ(Vp) = Vp-derived density G = Shear Modulus E = Young's Modulus K = Bulk Modulus
Shaded cells denote questionable data.

Figure 1. LA 710 Tunnel
Boring Z3 B2
Downhole Interval Velocities

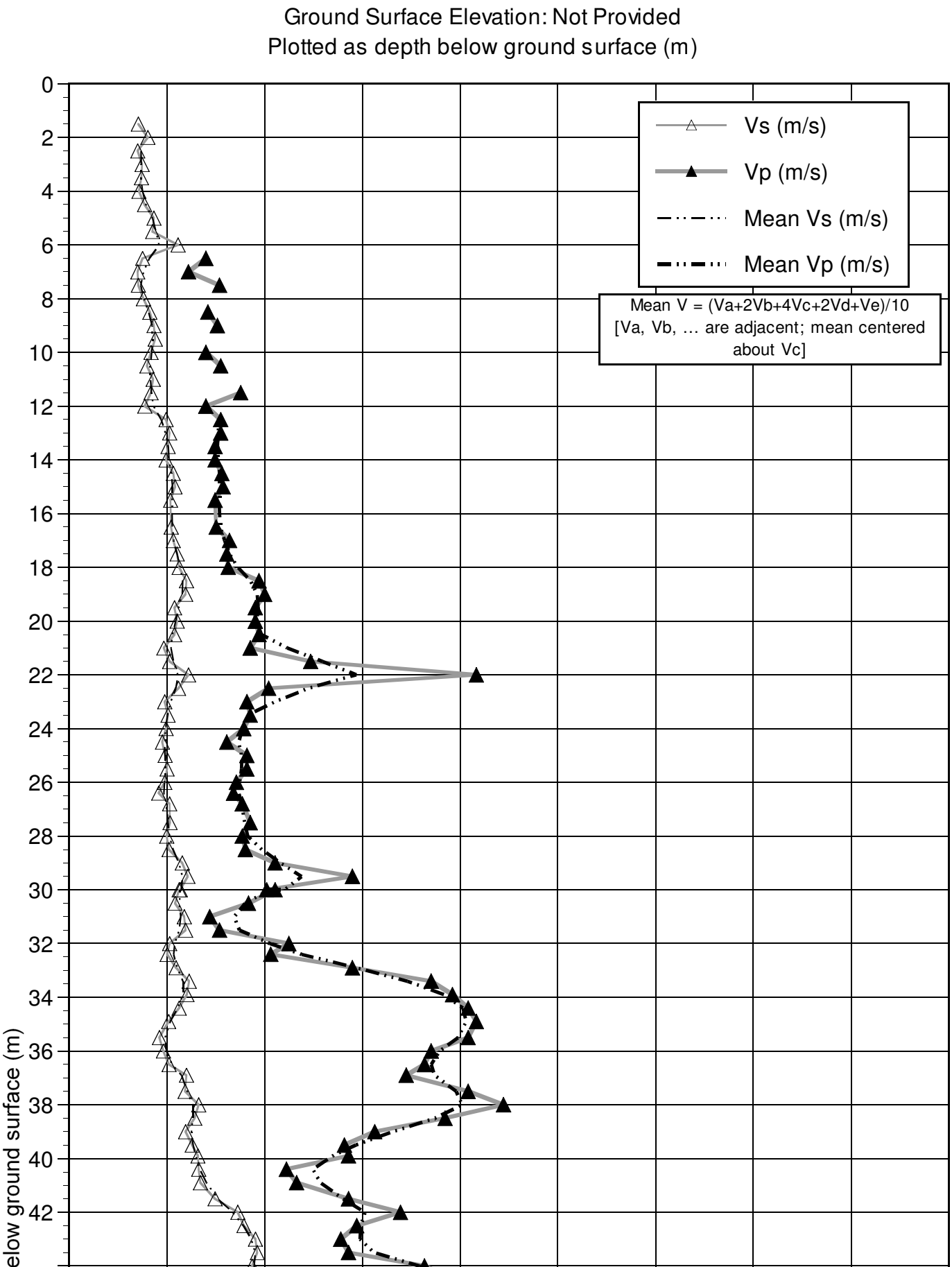

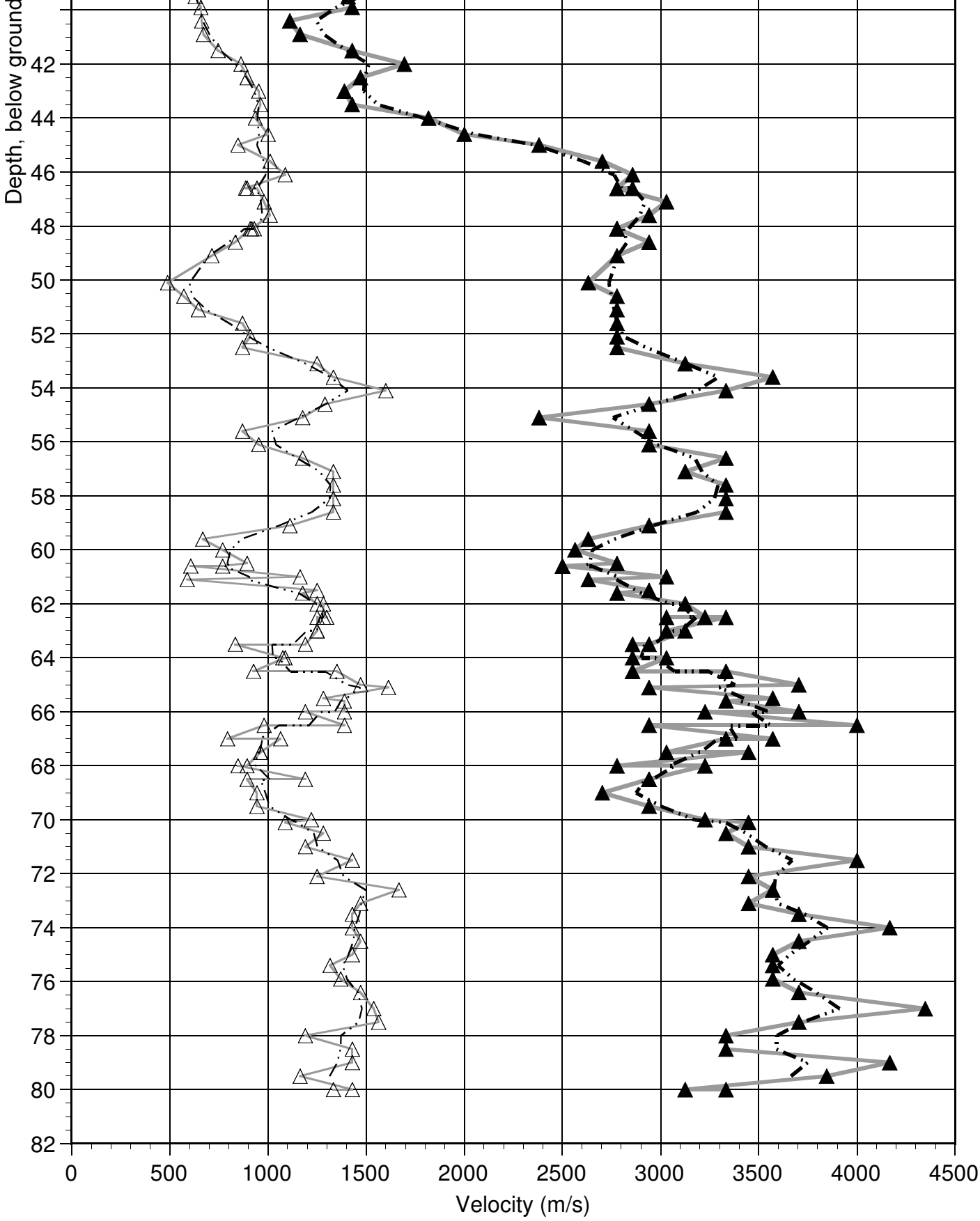
Depth, below ground
42
44
46
48
50
52
54
56
58
60
62
64
66
68
70
72
74
76
78
80
82
0
500
1000
1500
2000
2500
3000
3500
4000
4500
Velocity (m/s)

Z3 B2.

COMPANY	: CALTRANS.	OTHER SERVICES:	
WELL	: Z3 B2.		
FIELD	: LA 710 TUNNEL.		
COUNTY	: LA		
STATE	: CA		
LOCATION	:		
SECTION	: None		
TOWNSHIP	: None		
RANGE	: None		
API NO.	:		
UNIQUE WELL ID.	:		
PERMANENT DATUM	: None	ELEVATION KB	: NA
LOG MEASURED FROM	: GL	ELEVATION DF	: NA
DRL MEASURED FROM	: GL	ELEVATION GL	: 795ft.
DATE	: 1/20/09.	RIG NUMBER	:
DEPTH DRILLER	: 275	LOGGER TD	:
BIT SIZE	: 9.4	ARRIVAL TIME	:
LOG TOP	: 3.05	DEPARTURE TIME	:
LOG BOTTOM	: 83.85	CIRC STOPPED	: 0930
CASING OD	:		
CASING BOTTOM	: NA		
CASING TYPE	: none		
BOREHOLE FLUID	: 0		
RM TEMPERATURE	: 0		
MUD RES	: 0		
MUD WEIGHT	:		
WITNESSED BY	:		
RECORDED BY	: DH/DL		
REMARKS 1	: IND, Acoustic Tel, PSLog, CAL		
REMARKS 2	: EA: 07-187900		

ALL SERVICES PROVIDED SUBJECT TO STANDARD TERMS AND CONDITIONS

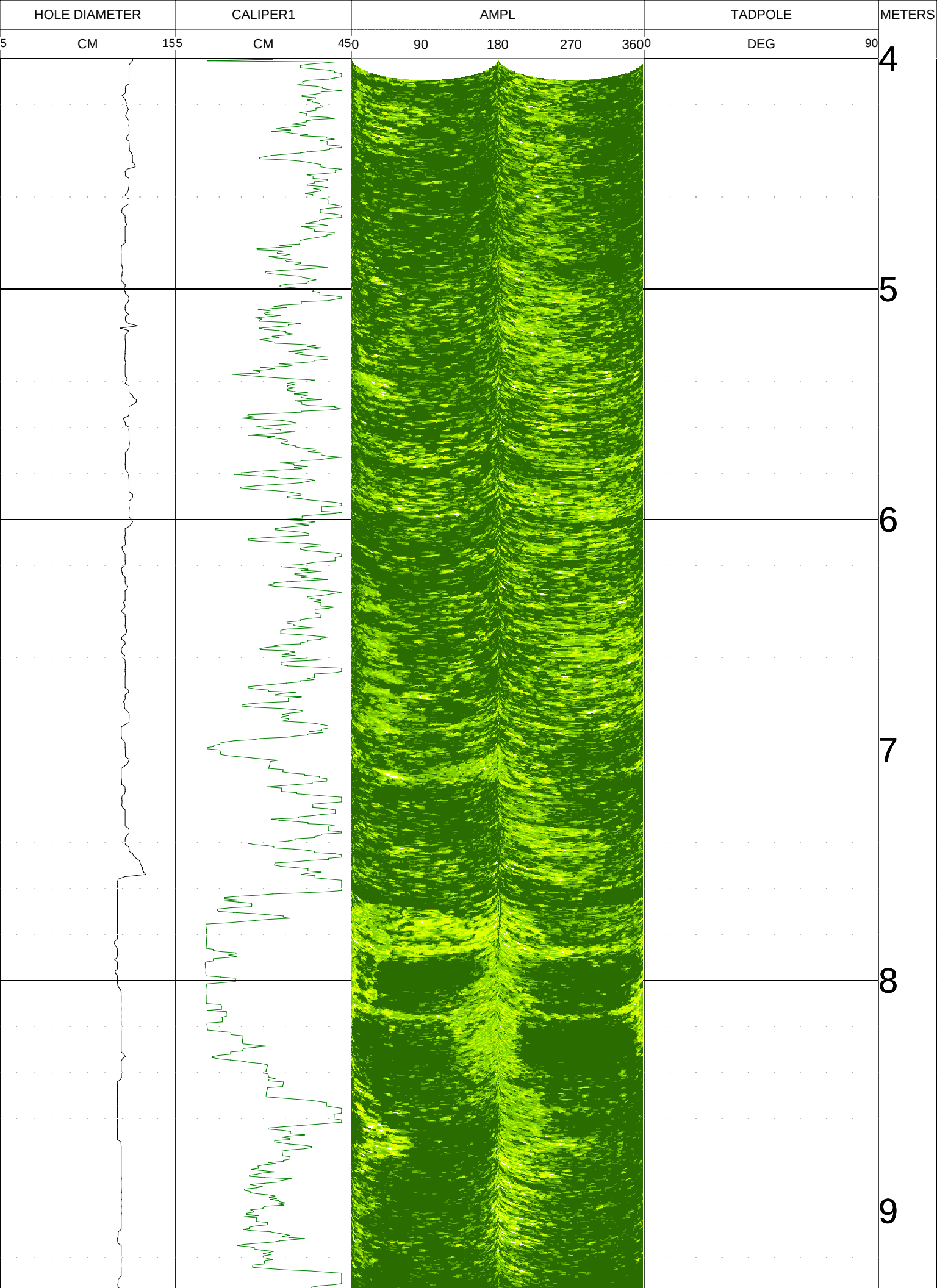
HOLE DIAMETER
5
CM
15
CALIPER1
5
CM
45
AMPL
0
90
180
270
360
TADPOLE
0
DEG
90
METERS
4
5
6
7
8
9

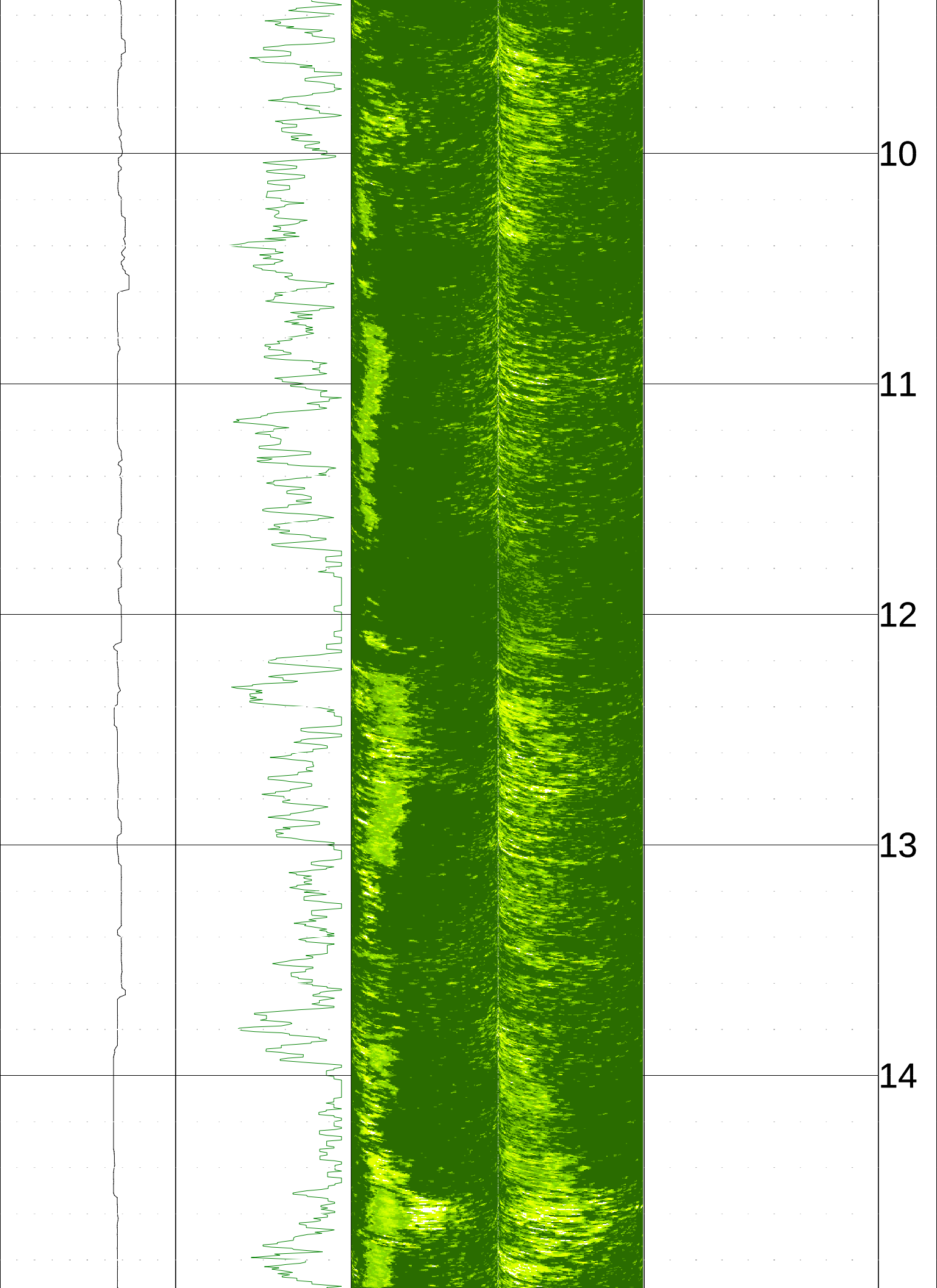
10
11
12
13
14

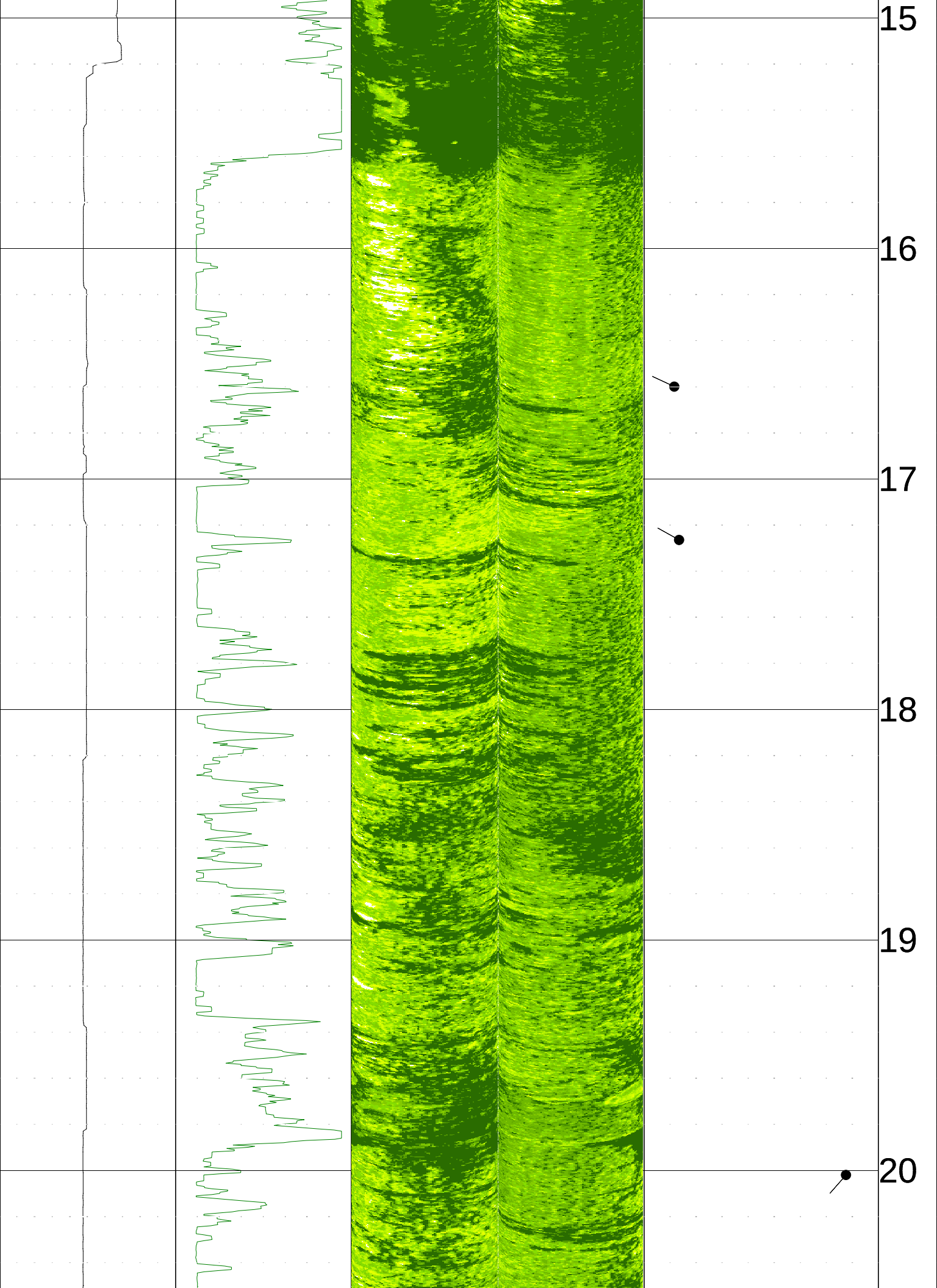
15
16
17
18
19
20

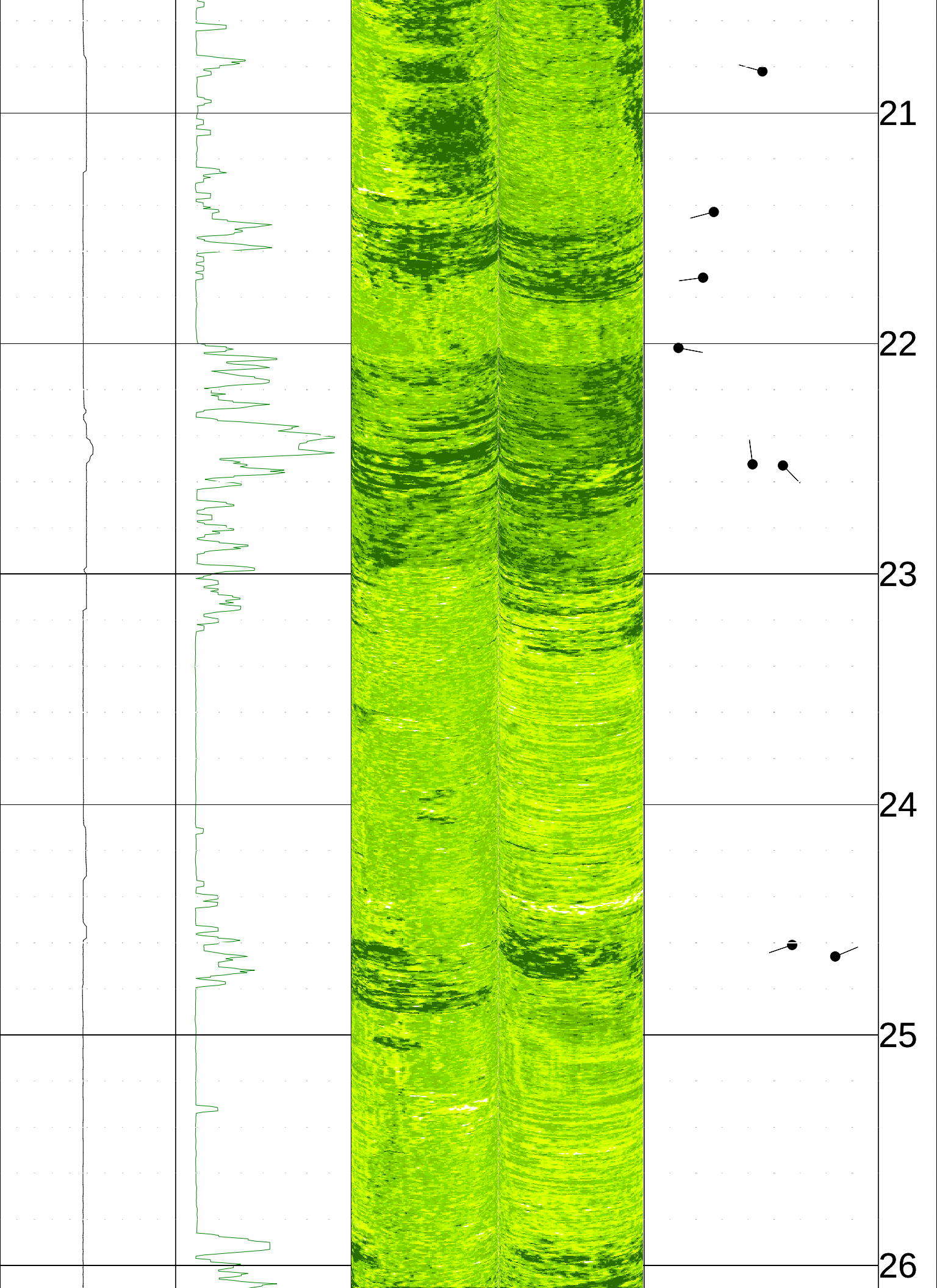
21
22
23
24
25
26

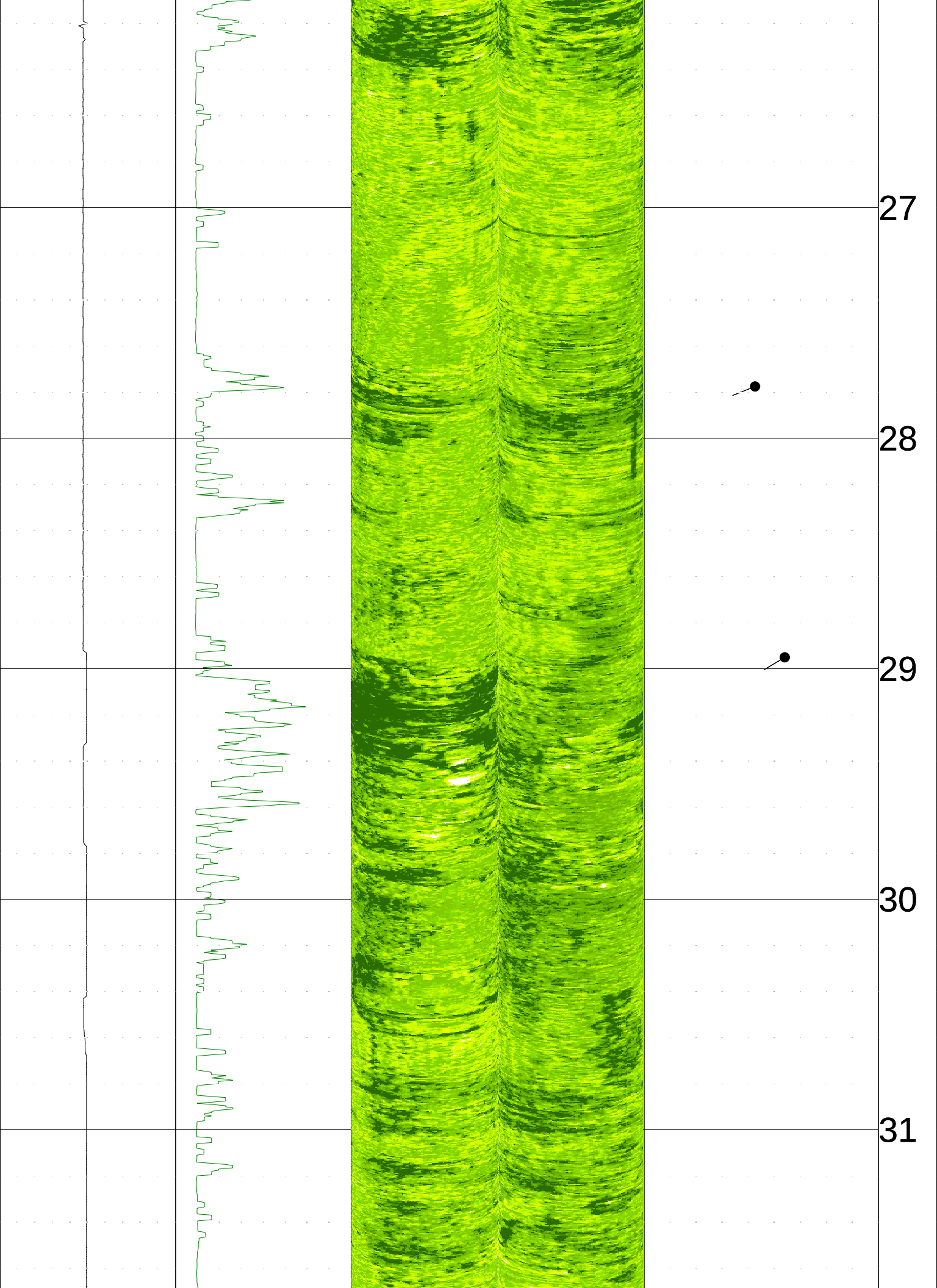
27
28
29
30
31

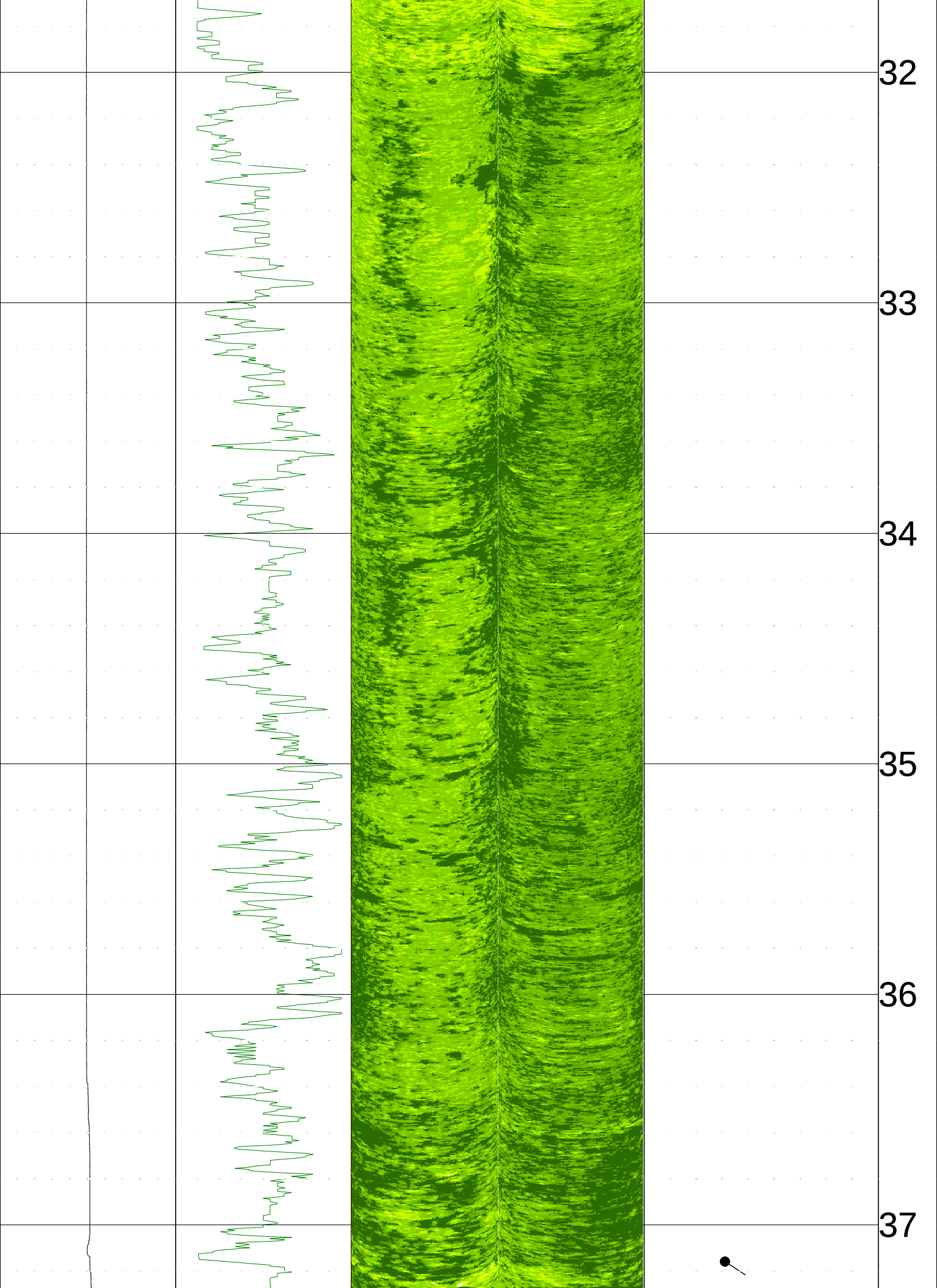
32
33
34
35
36
37

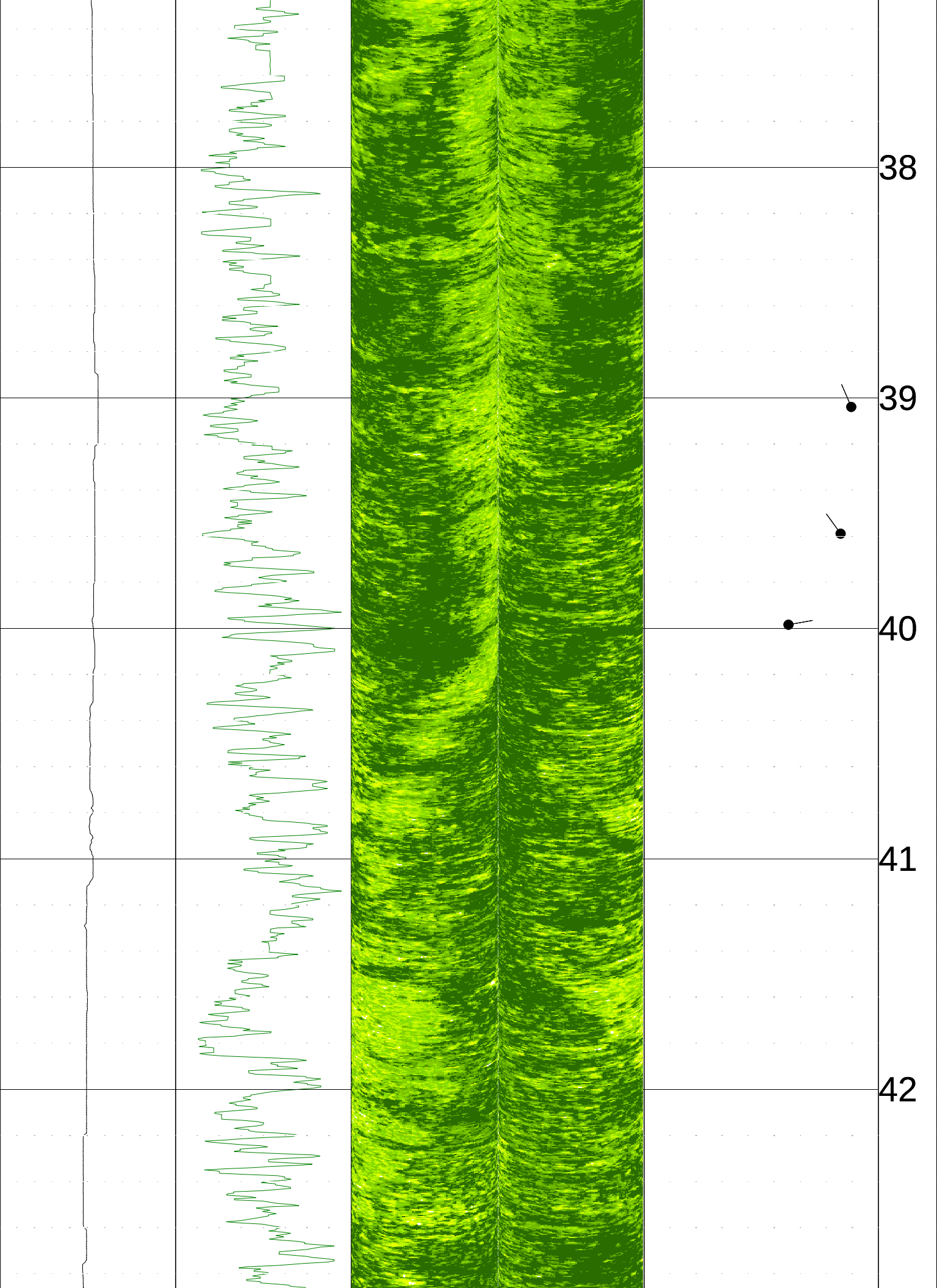
38
39
40
41
42

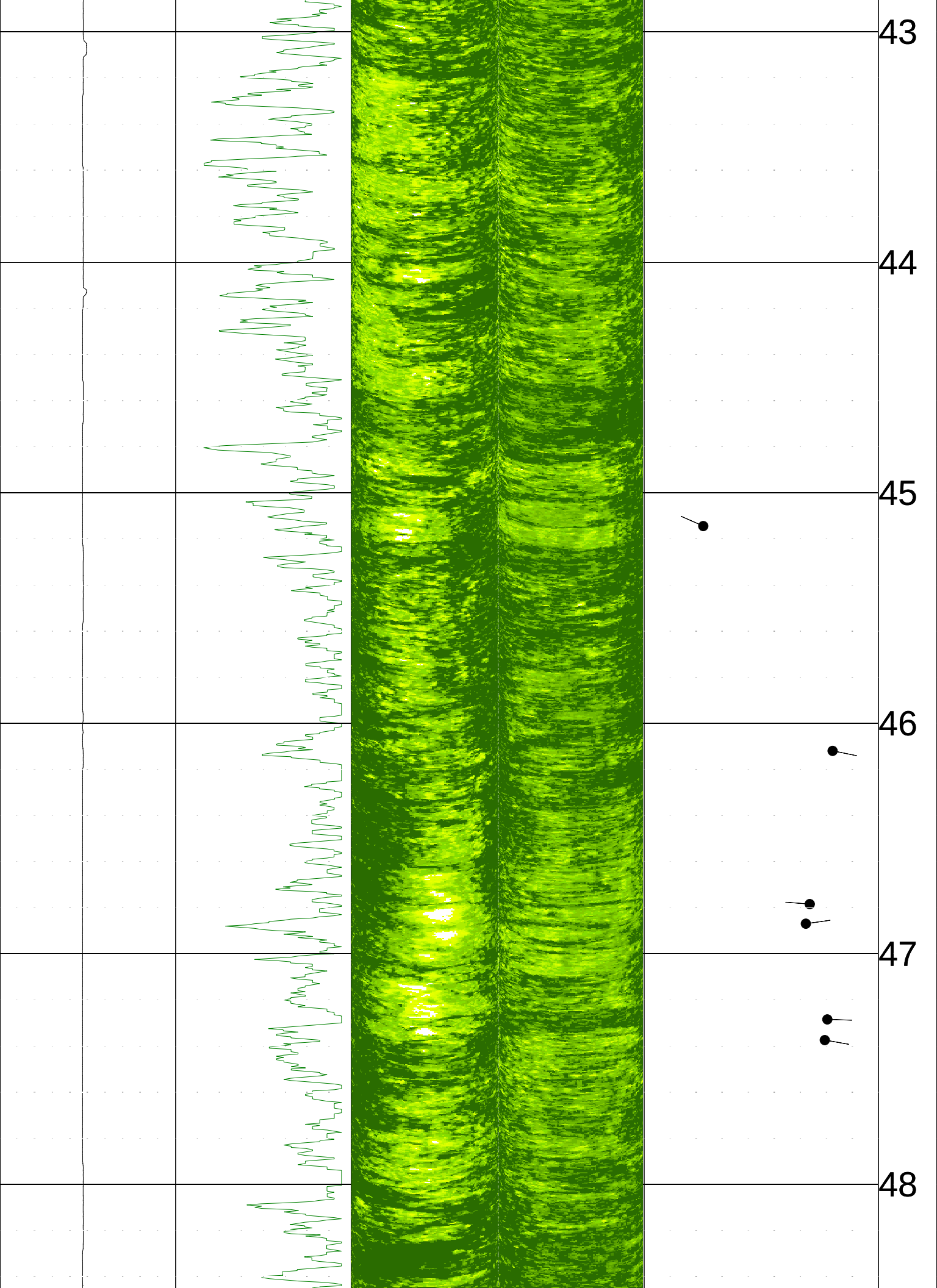
43
44
45
46
47
48

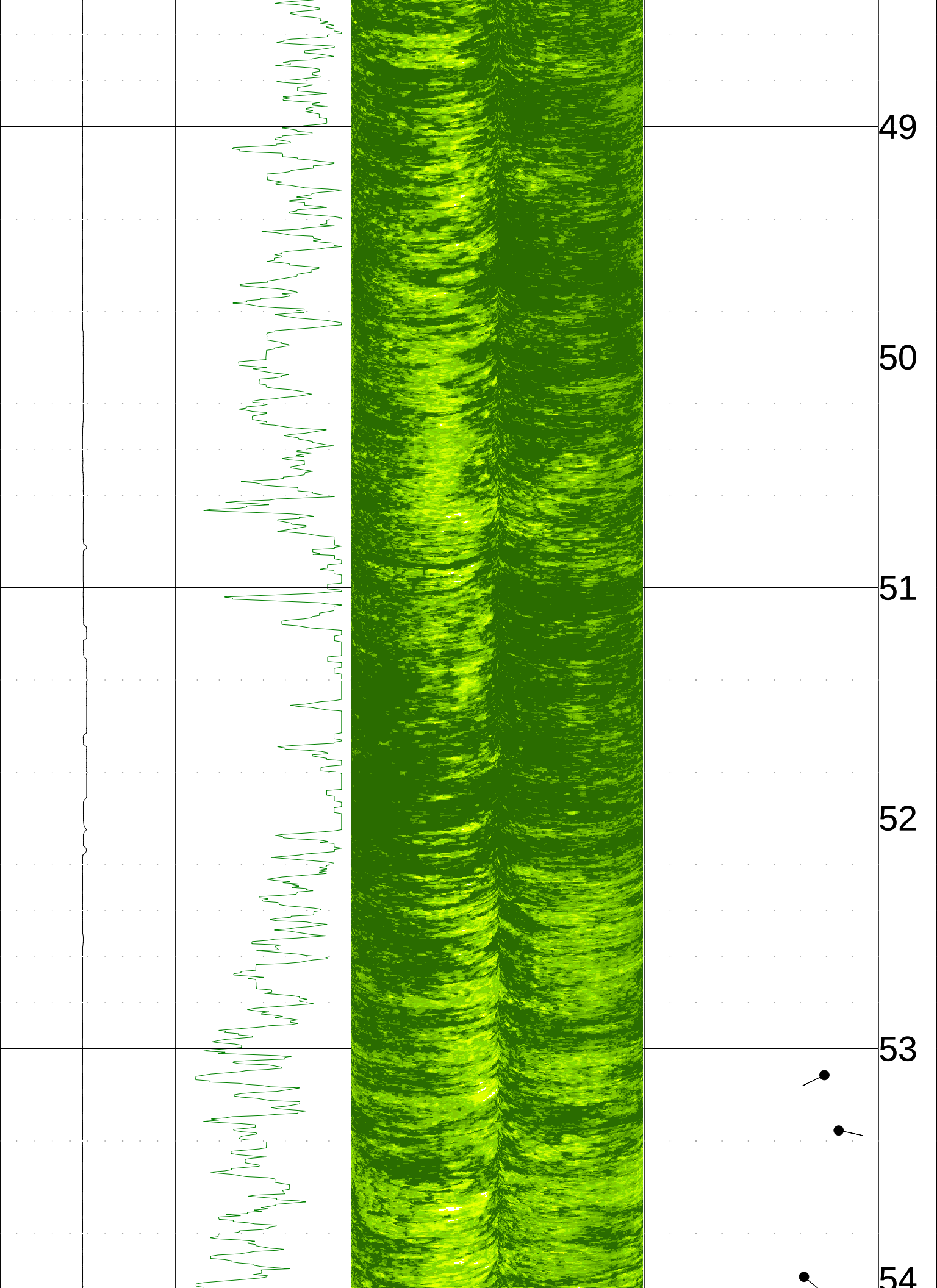
49
50
51
52
53
54

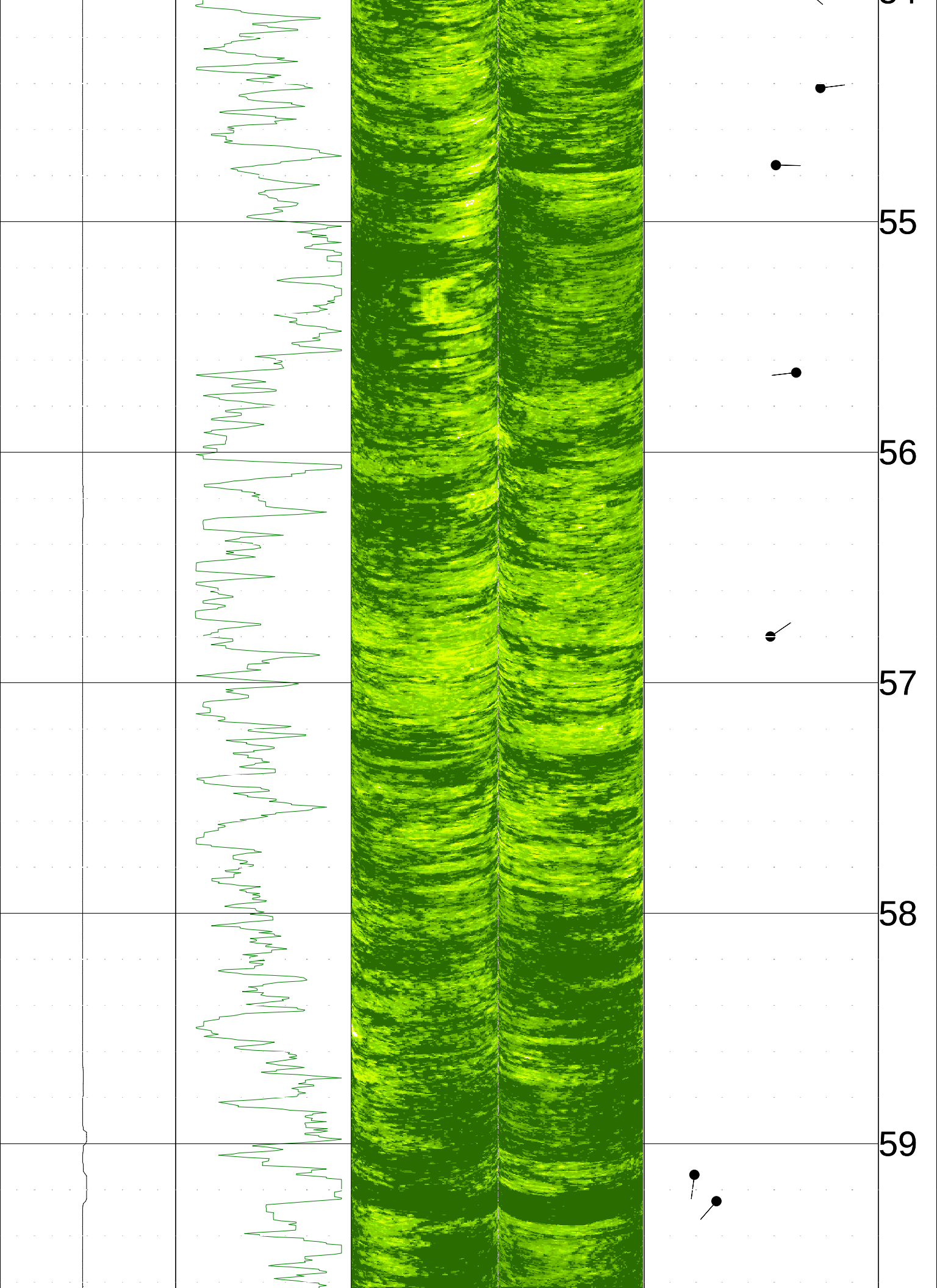
55
56
57
58
59

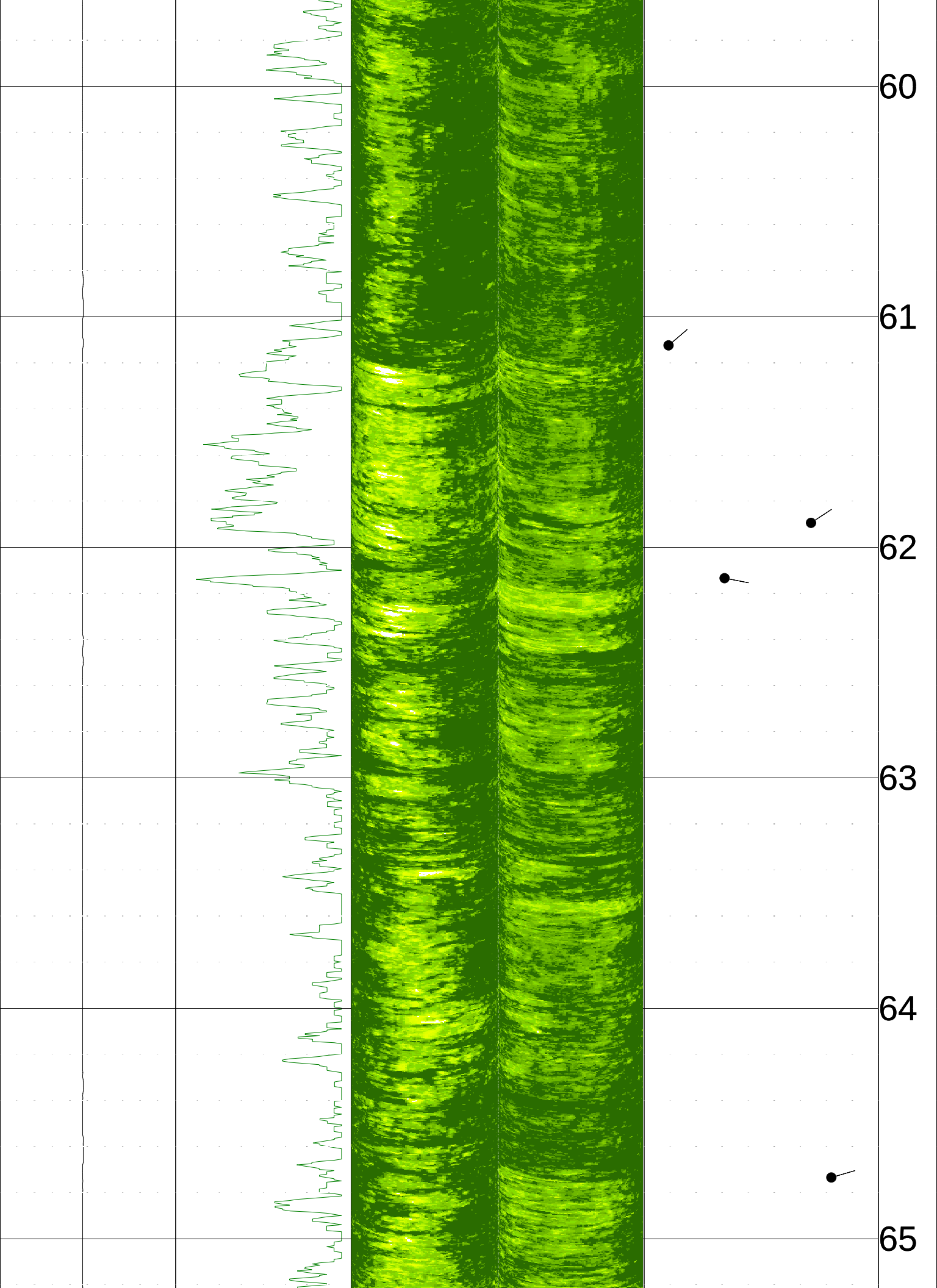
60
61
62
63
64
65

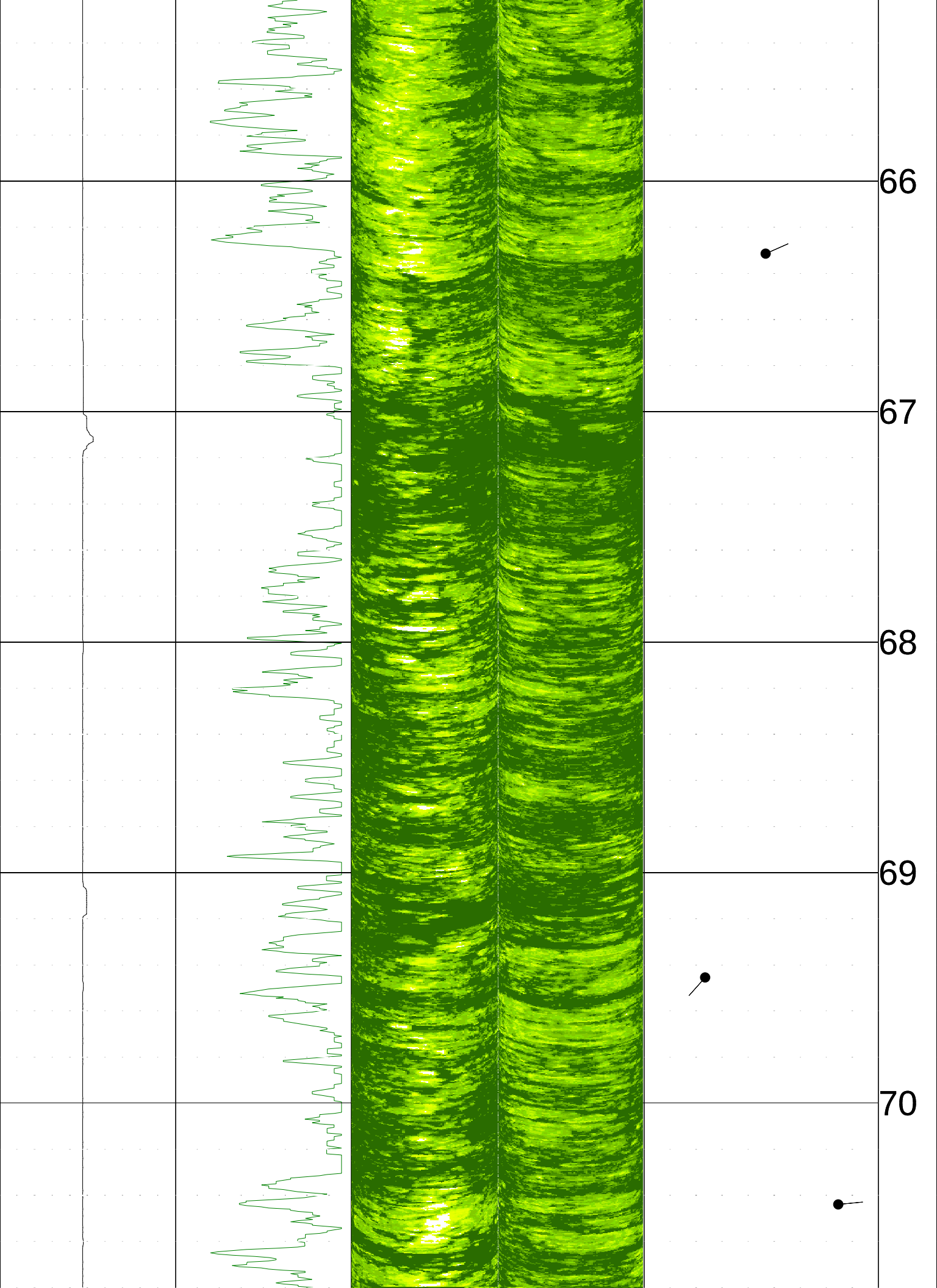
66
67
68
69
70

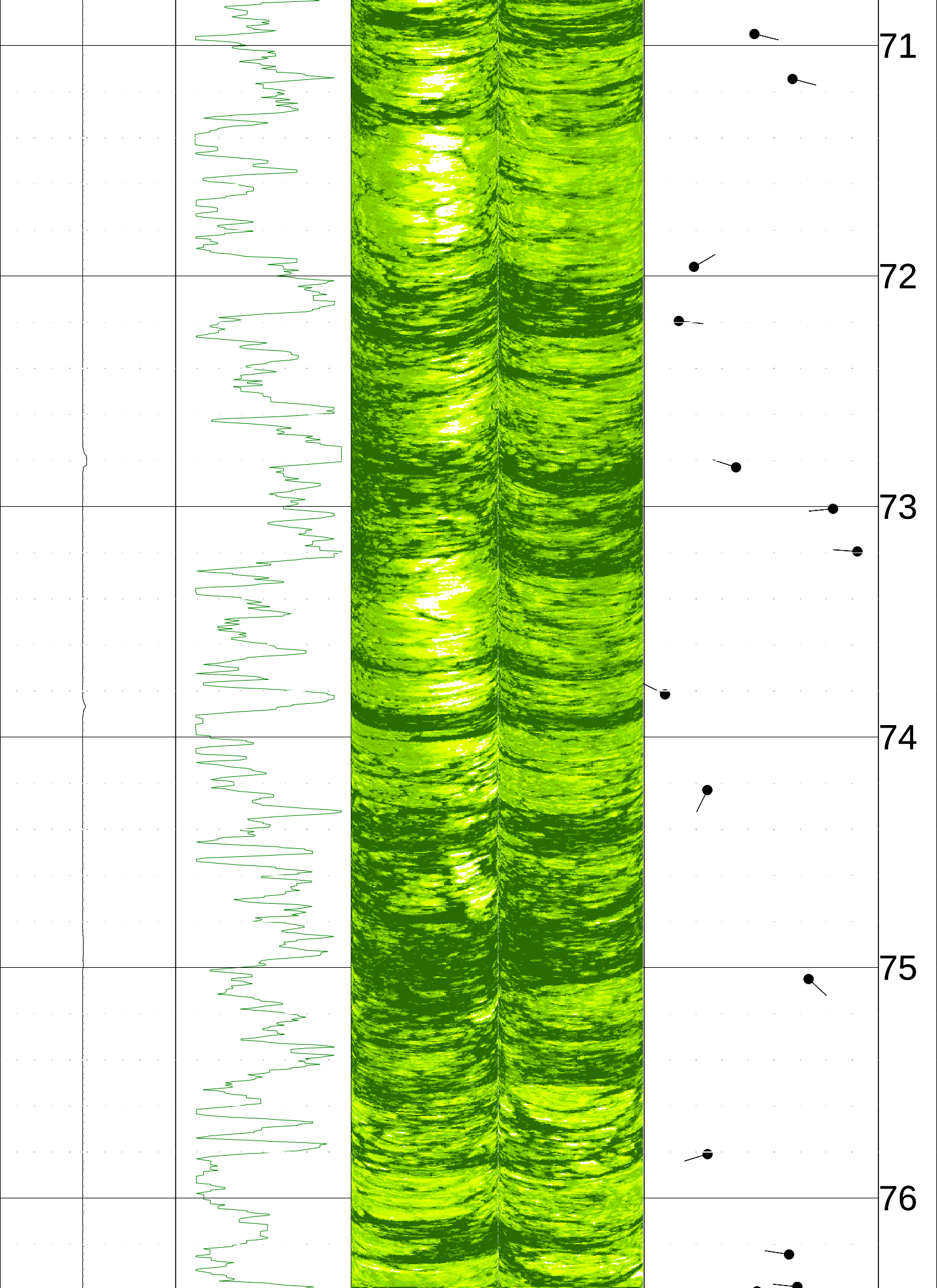
71
72
73
74
75
76

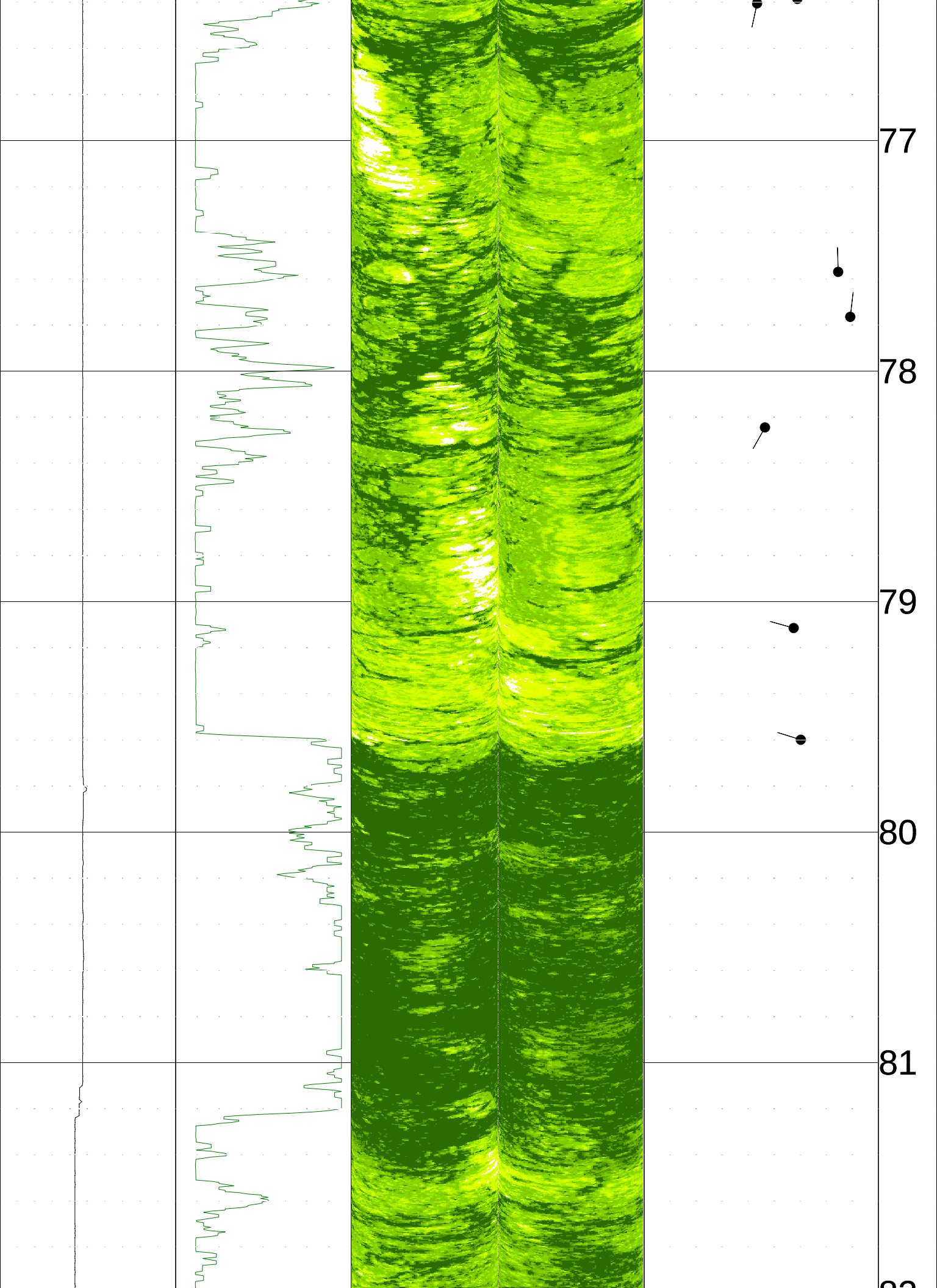
77
78
79
80
81

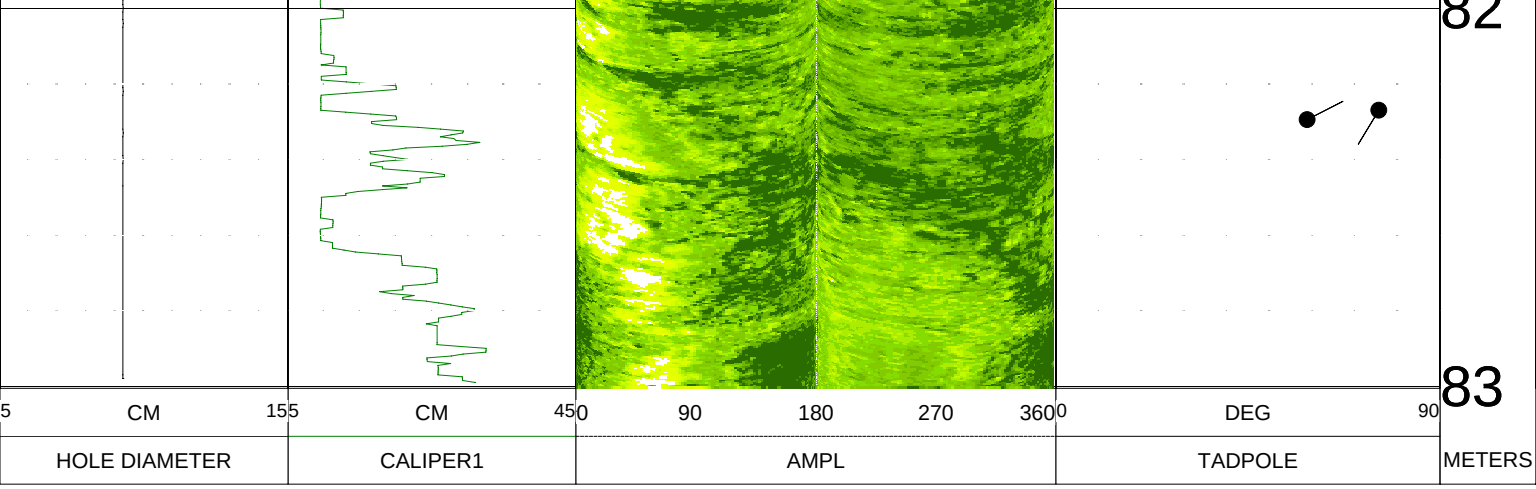
82
83
5
CM
155
CM
450
90
180
270
360
0
DEG
90
HOLE DIAMETER
CALIPER1
AMPL
TADPOLE
METERS

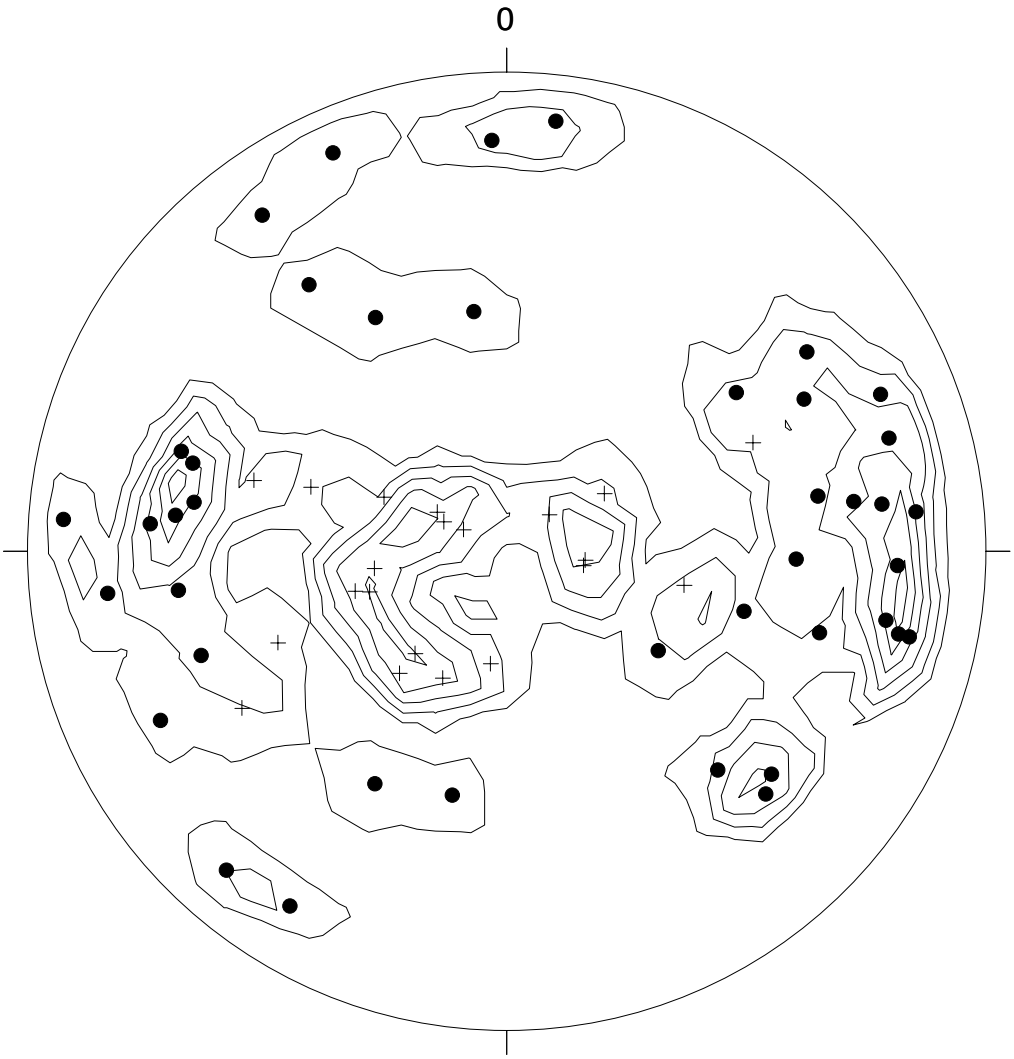

LA 710 Tunnel, boring Z3 B2

+ n=21 (P)
• n=41 (P)

Stereonet contour plot of poles to planes,
Both bedding and fractures

n=62
max. dens.= 6.72 (at 282/ 30)
min. dens.=0.00
Contours at every integer between
1 and 6, inclusive:
(Multiples of random distribution)

Apparent bedding denoted as cross
Apparent fractures denoted as solid circle
Plotted on upper hemisphere

LA 710 Tunnel boring Z3 B8

COMPANY	: CALTRANS			OTHER SERVICES:	
WELL	: Z3 B8			INDUCT	
LOCATION/FIELD	: LA 710 TUNNEL			AC TEL	
COUNTY	: LA			PS LOG	
LOCATION	: CA				
SECTION	: None	TOWNSHIP	: None	RANGE	: None
DATE	: 3/18/09	PERMANENT DATUM	: None		
DEPTH DRILLER	: 83.82M			KB	: NA
LOG BOTTOM	: 83.4	LOG MEASURED FROM:	GL	DF	: NA
LOG TOP	: 1.3	DRL MEASURED FROM:	GL	GL	: NA
CASING DIAMETER	: N/A	LOGGING UNIT	: 7311		
CASING TYPE	: N/A	FIELD OFFICE	: 7311		
CASING THICKNESS:	N/A	RECORDED BY	: DH/DG		
BIT SIZE	: 10.5CM	BOREHOLE FLUID	: 0	FILE	: ORIGINA
MAGNETIC DECL.	: 12.85	RM	: 0	TYPE	: 9511C
MATRIX DENSITY	: 2.71	RM TEMPERATURE	: 0	LGDATE	: 3/18/09.
NEUTRON MATRIX	: DOLOMITE	MATRIX DELTA T	: 140		
				THRESH:	2500

CALIPER TOOL FAILED AT SITE, NO CALTRANS CALIPER LOG
EA: 07-187900. GL ELEVATION ESTIMATED FROM HANDHELD GPS 172.8M

ALL SERVICES PROVIDED SUBJECT TO STANDARD TERMS AND CONDITIONS

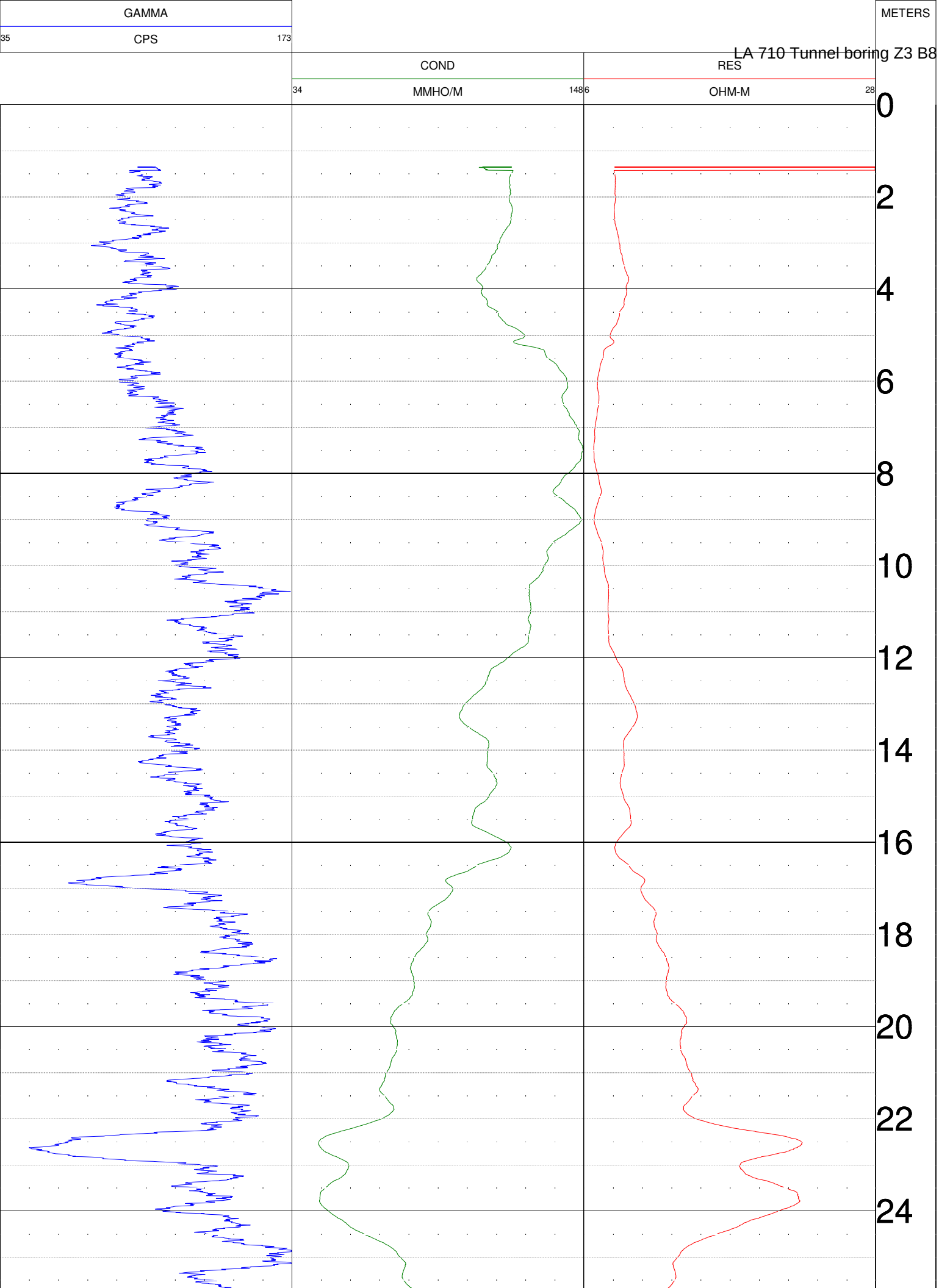
GAMMA
35
CPS
173
LA 710 Tunnel boring Z3 B8
COND
34
MMHO/M
148
RES
6
OHM-M
28
METERS
0
2
4
6
8
10
12
14
16
18
20
22
24

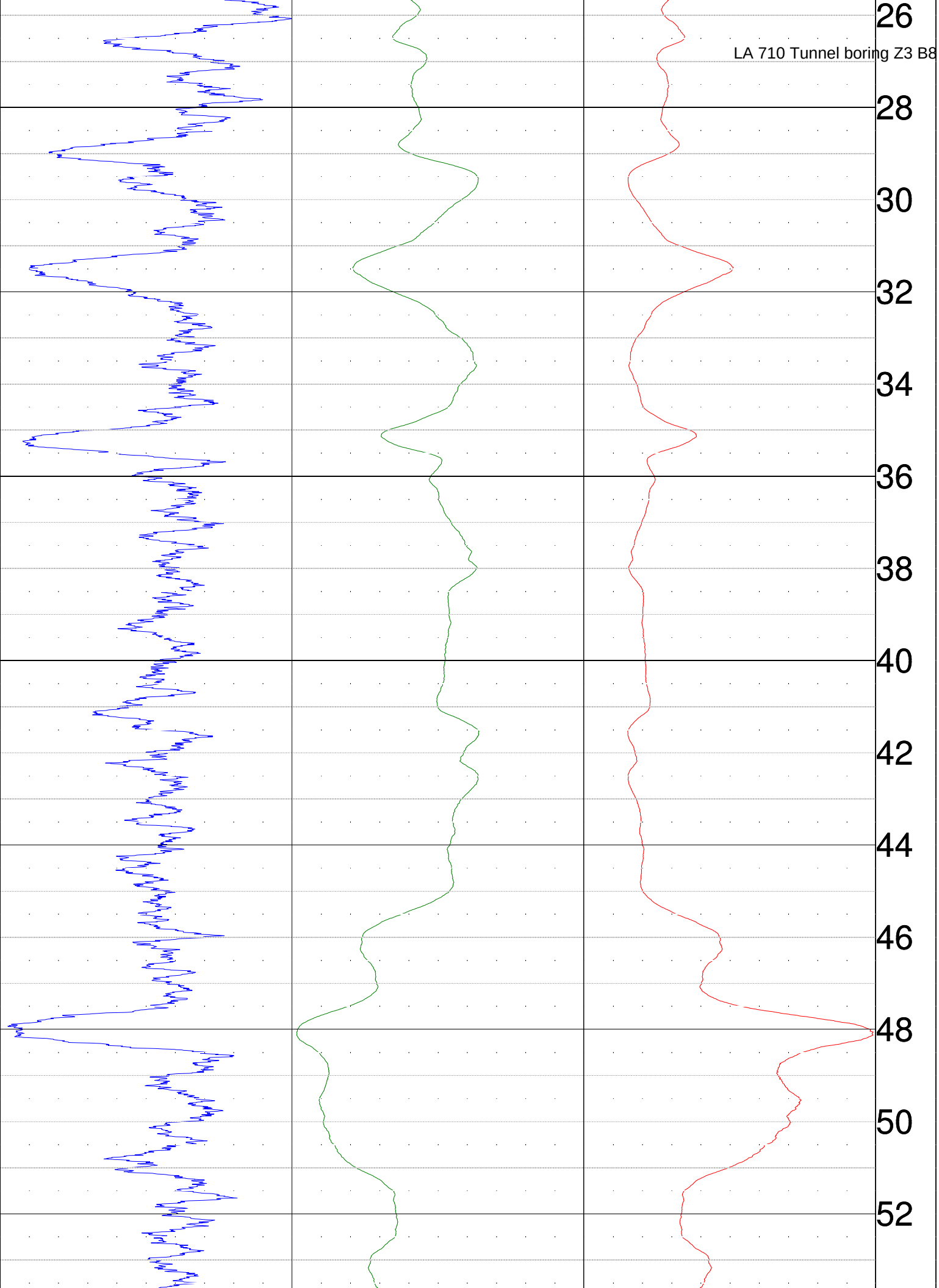
LA 710 Tunnel boring Z3 B8
26
28
30
32
34
36
38
40
42
44
46
48
50
52

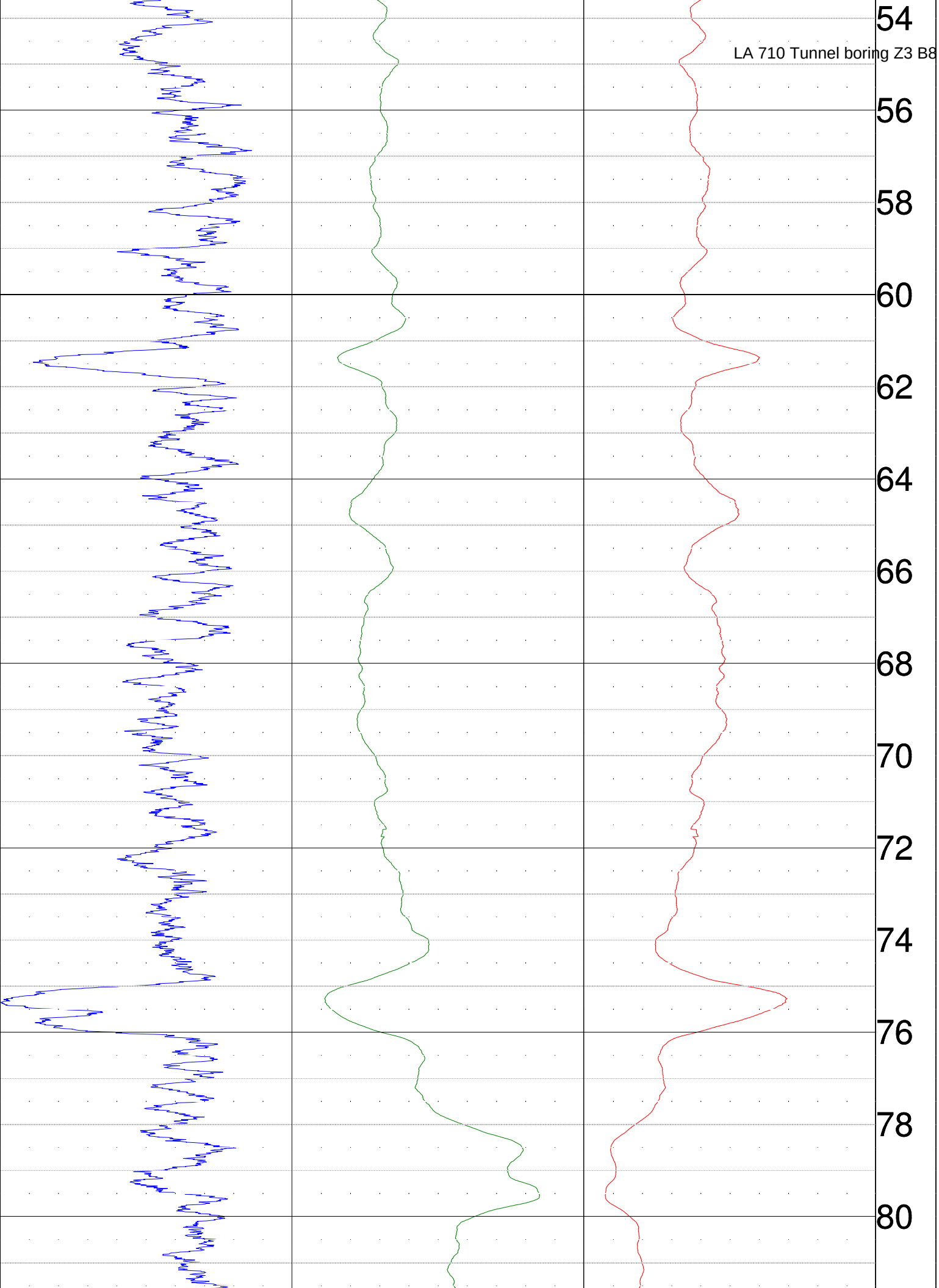
LA 710 Tunnel boring Z3 B8
54
56
58
60
62
64
66
68
70
72
74
76
78
80

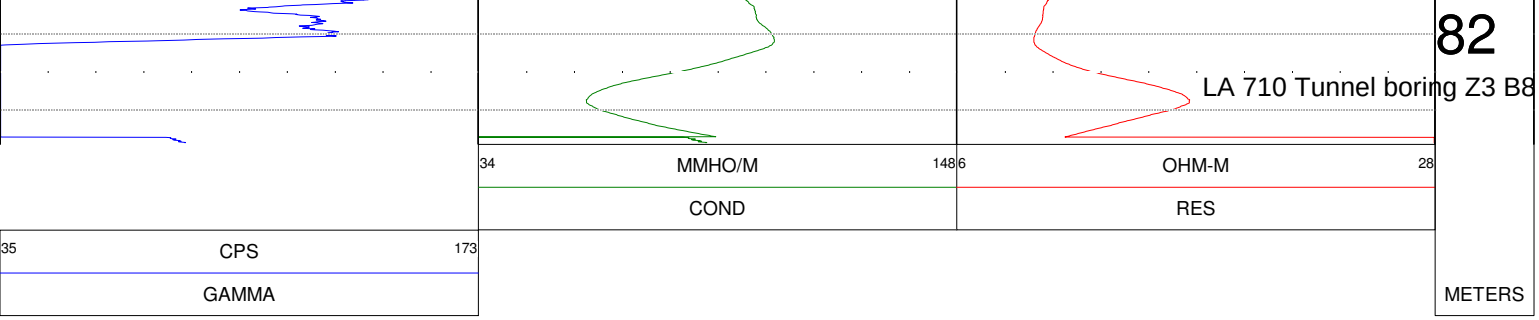
82
LA 710 Tunnel boring Z3 B8
34
MMHO/M
148
COND
6
OHM-M
28
RES
35
CPS
173
GAMMA
METERS

Table 2. LA 710 Tunnel
Boring Z3 B8
PS Suspension Log Data Summary

Top of Hole Elevation (m)	Depth (m)	Depth (ft)	Vs (m/s)	Vs (ft/s)	Vp (m/s)	Vp (ft/s)	γ	ρ(Vp) (g/cc)	ρ(Vp) (lb/ft^3)	G (GPa)	E (GPa)	K (GPa)	G ($10^3 lb/ft^2$)	E ($10^3 lb/ft^2$)	K ($10^3 lb/ft^2$)
Not Provided	1.5	4.9	189	619		NA	NA	NA	NA	NA	NA	NA	NA	NA	NA
	2	6.6	168	551		NA	NA	NA	NA	NA	NA	NA	NA	NA	NA
	2.4	7.9	165	542		NA	NA	NA	NA	NA	NA	NA	NA	NA	NA
	2.4	7.9	164	538		NA	NA	NA	NA	NA	NA	NA	NA	NA	NA
	2.4	7.9	167	549		NA	NA	NA	NA	NA	NA	NA	NA	NA	NA
	3	9.8	166	543		NA	NA	NA	NA	NA	NA	NA	NA	NA	NA
	3.5	11.5	195	641		NA	NA	NA	NA	NA	NA	NA	NA	NA	NA
	4.1	13.5	235	770		NA	NA	NA	NA	NA	NA	NA	NA	NA	NA
	4.6	15.1	244	800		NA	NA	NA	NA	NA	NA	NA	NA	NA	NA
	5.1	16.7	255	837		NA	NA	NA	NA	NA	NA	NA	NA	NA	NA
	5.1	16.7	251	824		NA	NA	NA	NA	NA	NA	NA	NA	NA	NA
	5.6	18.4	250	820	515	1691	NA	NA	NA	NA	NA	NA	NA	NA	NA
	6.1	20.0	282	927	649	2130	NA	NA	NA	NA	NA	NA	NA	NA	NA
	6.6	21.7	331	1086	1136	3728	NA	NA	NA	NA	NA	NA	NA	NA	NA
	7.1	23.3	355	1163	1316	4317	NA	NA	NA	NA	NA	NA	NA	NA	NA
	7.6	24.9	417	1367	1316	4317	NA	NA	NA	NA	NA	NA	NA	NA	NA
	8.1	26.6	476	1562	1515	4971	NA	NA	NA	NA	NA	NA	NA	NA	NA
	8.5	27.9	296	971	1250	4101	NA	NA	NA	NA	NA	NA	NA	NA	NA
	9	29.5	239	785	1220	4001	NA	NA	NA	NA	NA	NA	NA	NA	NA
	9.6	31.5	352	1155	1515	4971	NA	NA	NA	NA	NA	NA	NA	NA	NA
	10.1	33.1	385	1262	1786	5859	0.48	2.06	128.62	0.305	0.899	6.163	6365	18786	128721
	11	36.1	373	1224	1667	5468	0.47	1.98	123.58	0.276	0.812	5.131	5756	16966	107173
	11.5	37.7	357	1172	1667	5468	0.48	1.98	123.58	0.253	0.745	5.162	5274	15567	107817
	12.5	41.0	431	1414	1786	5859	0.47	2.06	128.62	0.383	1.125	6.059	7994	23488	126549
	13	42.7	455	1491	1786	5859	0.47	2.06	128.62	0.426	1.248	6.002	8890	26055	125354
	13.5	44.3	455	1491	1786	5859	0.47	2.06	128.62	0.426	1.248	6.002	8890	26055	125354
	14	45.9	455	1491	1786	5859	0.47	2.06	128.62	0.426	1.248	6.002	8890	26055	125354
	14.5	47.6	450	1478	1786	5859	0.47	2.06	128.62	0.418	1.226	6.012	8731	25599	125567
	15	49.2	450	1478	1852	6076	0.47	2.10	131.15	0.426	1.252	6.636	8903	26148	138596
	15.5	50.9	450	1478	1786	5859	0.47	2.06	128.62	0.418	1.226	6.012	8731	25599	125567
	16	52.5	439	1439	1786	5859	0.47	2.06	128.62	0.396	1.164	6.041	8277	24300	126172
	16.5	54.1	521	1709	2083	6835	0.47	2.22	138.82	0.603	1.769	8.847	12598	36954	184772
	17	55.8	641	2103	2174	7132	0.45	2.26	141.40	0.931	2.703	9.463	19438	56463	197640
	17.5	57.4	658	2158	2083	6835	0.44	2.22	138.82	0.962	2.781	8.368	20101	58077	174768
	17.5	57.4	658	2158	2083	6835	0.44	2.22	138.82	0.962	2.781	8.368	20101	58077	174768
	18	59.1	685	2247	2083	6835	0.44	2.22	138.82	1.043	3.003	8.260	21787	62721	172520
	18.5	60.7	714	2343	2174	7132	0.44	2.26	141.40	1.156	3.327	9.163	24135	69484	191377

γ = Poisson's Ratio ρ(Vp) = Vp-derived density G = Shear Modulus E = Young's Modulus K = Bulk Modulus
Shaded cells denote questionable data.

Table 2. LA 710 Tunnel
Boring Z3 B8
PS Suspension Log Data Summary

Top of Hole Elevation (m)	Depth (m)	Depth (ft)	Vs (m/s)	Vs (ft/s)	Vp (m/s)	Vp (ft/s)	γ	ρ(Vp) (g/cc)	ρ(Vp) (lb/ft^3)	G (GPa)	E (GPa)	K (GPa)	G ($10^3 lb/ft^2$)	E ($10^3 lb/ft^2$)	K ($10^3 lb/ft^2$)
	19	62.3	735	2412	2083	6835	0.43	2.22	138.82	1.202	3.436	8.048	25109	71754	168091
	19.5	64.0	735	2412	2174	7132	0.44	2.26	141.40	1.225	3.516	9.071	25576	73423	189456
	20	65.6	781	2563	2273	7456	0.43	2.31	143.99	1.408	4.035	10.037	29402	84266	209620
	20	65.6	676	2217	2174	7132	0.45	2.26	141.40	1.034	2.992	9.325	21596	62480	194763
	20	65.6	735	2412	2174	7132	0.44	2.26	141.40	1.225	3.516	9.071	25576	73423	189457
	20	65.6	746	2448	2174	7132	0.43	2.26	141.40	1.261	3.616	9.022	26345	75515	188431
	20	65.6	746	2448	2174	7132	0.43	2.26	141.40	1.261	3.616	9.022	26345	75515	188431
	20.5	67.3	746	2448	2174	7132	0.43	2.26	141.40	1.261	3.616	9.022	26345	75515	188431
	21	68.9	704	2310	2174	7132	0.44	2.26	141.40	1.123	3.238	9.206	23460	67629	192277
	21.5	70.5	735	2412	2273	7456	0.44	2.31	143.99	1.247	3.595	10.251	26044	75089	214096
	22	72.2	806	2646	2632	8634	0.45	2.43	151.84	1.582	4.582	14.734	33037	95686	307733
	22.4	73.5	746	2448	2941	9650	0.47	2.52	157.13	1.402	4.109	19.904	29276	85814	415705
	23	75.5	704	2310	2273	7456	0.45	2.31	143.99	1.143	3.308	10.390	23875	69090	216988
	23.5	77.1	685	2247	2273	7456	0.45	2.31	143.99	1.082	3.139	10.471	22603	65552	218684
	24	78.7	676	2217	2500	8202	0.46	2.39	149.21	1.091	3.188	13.483	22790	66573	281602
	24.5	80.4	893	2929	2381	7812	0.42	2.35	146.59	1.872	5.310	10.816	39097	110893	225892
	25	82.0	769	2524	2273	7456	0.44	2.31	143.99	1.365	3.918	10.094	28504	81824	210816
	25.5	83.7	806	2646	2273	7456	0.43	2.31	143.99	1.500	4.284	9.914	31329	89475	207050
	25.9	85.0	725	2377	2381	7812	0.45	2.35	146.59	1.233	3.573	11.668	25752	74629	243685
	26.4	86.6	704	2310	2273	7456	0.45	2.31	143.99	1.144	3.310	10.389	23890	69133	216968
	26.9	88.3	641	2103	2174	7132	0.45	2.26	141.40	0.931	2.704	9.463	19438	56463	197640
	27.4	89.9	667	2187	2174	7132	0.45	2.26	141.40	1.007	2.915	9.362	21024	60890	195525
	28	91.9	685	2247	2083	6835	0.44	2.22	138.82	1.043	3.003	8.260	21787	62721	172520
	28.5	93.5	735	2412	2083	6835	0.43	2.22	138.82	1.202	3.436	8.048	25109	71754	168091
	29	95.1	735	2412	2273	7456	0.44	2.31	143.99	1.247	3.595	10.251	26044	75089	214096
	29.5	96.8	541	1773	2000	6562	0.46	2.18	136.25	0.638	1.863	7.880	13318	38906	164572
	30	98.4	513	1682	2000	6562	0.46	2.18	136.25	0.574	1.682	7.965	11987	35119	166346
	30	98.4	532	1745	2083	6835	0.47	2.22	138.82	0.629	1.844	8.812	13140	38503	184049
	30	98.4	549	1803	2000	6562	0.46	2.18	136.25	0.659	1.923	7.852	13761	40160	163981
	30.5	100.1	549	1803	2083	6835	0.46	2.22	138.82	0.671	1.964	8.756	14021	41013	182875
	31	101.7	833	2734	2381	7812	0.43	2.35	146.59	1.631	4.664	11.138	34058	97418	232611
	31.5	103.3	893	2929	2941	9650	0.45	2.52	157.13	2.007	5.816	19.098	41907	121467	398865
	32	105.0	833	2734	2381	7812	0.43	2.35	146.59	1.631	4.664	11.138	34058	97418	232611
	32.5	106.6	826	2711	2222	7291	0.42	2.29	142.69	1.561	4.433	9.206	32606	92583	192268
	32.5	106.6	893	2929	2273	7456	0.41	2.31	143.99	1.839	5.181	9.462	38402	108198	197619
	32.9	107.9	752	2467	2222	7291	0.44	2.29	142.69	1.292	3.709	9.565	26987	77473	199759
	33.5	109.9	633	2076	2128	6981	0.45	2.24	140.11	0.899	2.610	8.961	18776	54505	187155

γ = Poisson's Ratio ρ(Vp) = Vp-derived density G = Shear Modulus E = Young's Modulus K = Bulk Modulus
Shaded cells denote questionable data.

Table 2. LA 710 Tunnel
Boring Z3 B8
PS Suspension Log Data Summary

Top of Hole Elevation (m)	Depth (m)	Depth (ft)	Vs (m/s)	Vs (ft/s)	Vp (m/s)	Vp (ft/s)	γ	ρ(Vp) (g/cc)	ρ(Vp) (lb/ft^3)	G (GPa)	E (GPa)	K (GPa)	G ($10^3 lb/ft^2$)	E ($10^3 lb/ft^2$)	K ($10^3 lb/ft^2$)
	34	111.5	676	2217	2174	7132	0.45	2.26	141.40	1.034	2.992	9.325	21596	62480	194762
	34.5	113.2	813	2667	2439	8002	0.44	2.37	147.90	1.566	4.502	12.006	32705	94028	250742
	35	114.8	885	2903	2857	9374	0.45	2.50	155.80	1.955	5.656	17.767	40821	118130	371073
	35.5	116.5	840	2757	2632	8634	0.44	2.43	151.84	1.718	4.958	14.554	35871	103541	303955
	36	118.1	769	2524	2326	7630	0.44	2.33	145.29	1.377	3.962	10.751	28762	82751	224534
	36.5	119.8	813	2667	2222	7291	0.42	2.29	142.69	1.511	4.299	9.273	31554	89785	193671
	37	121.4	741	2430	2000	6562	0.42	2.18	136.25	1.198	3.402	7.133	25011	71056	148981
	37.5	123.0	680	2232	2128	6981	0.44	2.24	140.11	1.039	2.998	8.775	21691	62604	183268
	38	124.7	662	2173	2128	6981	0.45	2.24	140.11	0.984	2.847	8.847	20557	59467	184780
	38.5	126.3	730	2395	2222	7291	0.44	2.29	142.69	1.218	3.506	9.664	25434	73227	201830
	39	128.0	781	2563	2174	7132	0.43	2.26	141.40	1.382	3.942	8.861	28873	82336	185061
	39.5	129.6	775	2543	2174	7132	0.43	2.26	141.40	1.361	3.885	8.889	28427	81139	185656
	39.9	130.9	763	2504	2222	7291	0.43	2.29	142.69	1.332	3.818	9.512	27818	79731	198652
	40.4	132.5	800	2625	2273	7456	0.43	2.31	143.99	1.476	4.220	9.946	30830	88130	207715
	40.9	134.2	826	2711	2326	7630	0.43	2.33	145.29	1.590	4.539	10.467	33199	94799	218616
	41.4	135.8	781	2563	2222	7291	0.43	2.29	142.69	1.395	3.989	9.427	29137	83301	196893
	42	137.8	763	2504	2273	7456	0.44	2.31	143.99	1.344	3.861	10.122	28071	80642	211394
	42.5	139.4	794	2604	2273	7456	0.43	2.31	143.99	1.453	4.157	9.977	30343	86814	208365
	43	141.1	826	2711	2273	7456	0.42	2.31	143.99	1.575	4.486	9.813	32902	93692	204952
	43.5	142.7	877	2878	2381	7812	0.42	2.35	146.59	1.807	5.137	10.903	37737	107284	227705
	44	144.4	813	2667	2273	7456	0.43	2.31	143.99	1.525	4.350	9.881	31841	90850	206367
	44.5	146.0	820	2689	2222	7291	0.42	2.29	142.69	1.536	4.365	9.240	32073	91169	192978
	45	147.6	813	2667	2273	7456	0.43	2.31	143.99	1.525	4.350	9.881	31841	90850	206367
	45.5	149.3	962	3155	2439	8002	0.41	2.37	147.90	2.190	6.168	11.173	45747	128823	233353
	46	150.9	1099	3605	2500	8202	0.38	2.39	149.21	2.886	7.968	11.090	60280	166405	231615
	46.5	152.6	1220	4001	2500	8202	0.34	2.39	149.21	3.555	9.554	10.199	74239	199535	213003
	47	154.2	935	3066	2778	9113	0.44	2.47	154.48	2.161	6.208	16.212	45140	129658	338583
	47.4	155.5	1053	3454	3030	9942	0.43	2.54	158.46	2.813	8.052	19.559	58740	168160	408486
	48.1	157.8	1053	3454	2857	9374	0.42	2.50	155.80	2.765	7.862	16.686	57755	164194	348494
	48.5	159.1	962	3155	2439	8002	0.41	2.37	147.90	2.190	6.168	11.173	45747	128823	233352
	49	160.8	962	3155	2500	8202	0.41	2.39	149.21	2.210	6.246	11.992	46152	130444	250453
	49.4	162.1	926	3038	2564	8412	0.43	2.41	150.52	2.067	5.891	13.096	43173	123046	273516
	50	164.0	952	3125	2564	8412	0.42	2.41	150.52	2.187	6.211	12.936	45676	129717	270180
	50	164.0	926	3038	2564	8412	0.43	2.41	150.52	2.067	5.891	13.096	43173	123046	273515
	50	164.0	917	3010	2564	8412	0.43	2.41	150.52	2.029	5.790	13.146	42385	120931	274567
	50.5	165.7	1042	3418	2703	8867	0.41	2.45	153.16	2.662	7.522	14.371	55597	157092	300146
	50.6	166.0	1020	3348	2703	8867	0.42	2.45	153.16	2.554	7.239	14.515	53351	151184	303142

γ = Poisson's Ratio ρ(Vp) = Vp-derived density G = Shear Modulus E = Young's Modulus K = Bulk Modulus
Shaded cells denote questionable data.

Table 2. LA 710 Tunnel
Boring Z3 B8
PS Suspension Log Data Summary

Top of Hole Elevation (m)	Depth (m)	Depth (ft)	Vs (m/s)	Vs (ft/s)	Vp (m/s)	Vp (ft/s)	γ	ρ(Vp) (g/cc)	ρ(Vp) (lb/ft^3)	G (GPa)	E (GPa)	K (GPa)	G ($10^3 lb/ft^2$)	E ($10^3 lb/ft^2$)	K ($10^3 lb/ft^2$)
	51	167.3	980	3217	2326	7630	0.39	2.33	145.29	2.237	6.227	9.604	46719	130061	200590
	51.1	167.7	1042	3418	2703	8867	0.41	2.45	153.16	2.662	7.522	14.371	55597	157092	300147
	51.5	169.0	917	3010	2381	7812	0.41	2.35	146.59	1.976	5.585	10.677	41278	116638	222983
	51.6	169.3	943	3095	2326	7630	0.40	2.33	145.29	2.071	5.806	9.825	43260	121259	205202
	52	170.6	901	2956	2439	8002	0.42	2.37	147.90	1.923	5.465	11.530	40159	114133	240804
	52.1	170.9	893	2929	2326	7630	0.41	2.33	145.29	1.855	5.245	10.113	38749	109548	211217
	52.5	172.2	862	2828	2273	7456	0.42	2.31	143.99	1.714	4.854	9.628	35800	101382	201089
	52.5	172.2	990	3248	2500	8202	0.41	2.39	149.21	2.343	6.593	11.814	48935	137701	246742
	53	173.9	1010	3314	2500	8202	0.40	2.39	149.21	2.439	6.840	11.687	50932	142858	244080
	53.1	174.2	1000	3281	2439	8002	0.40	2.37	147.90	2.369	6.629	10.935	49480	138442	228375
	53.5	175.5	943	3095	2439	8002	0.41	2.37	147.90	2.109	5.955	11.282	44037	124364	235633
	53.6	175.9	980	3217	2381	7812	0.40	2.35	146.59	2.257	6.310	10.302	47139	131792	215170
	54	177.2	893	2929	2381	7812	0.42	2.35	146.59	1.872	5.310	10.816	39097	110893	225893
	54.1	177.5	893	2929	2439	8002	0.42	2.37	147.90	1.889	5.374	11.575	39445	112232	241755
	54.3	178.1	855	2804	2381	7812	0.43	2.35	146.59	1.715	4.892	11.025	35827	102180	230253
	54.6	179.1	862	2828	2326	7630	0.42	2.33	145.29	1.730	4.913	10.281	36123	102614	214719
	55	180.4	893	2929	2326	7630	0.41	2.33	145.29	1.855	5.245	10.113	38749	109548	211217
	55.1	180.8	847	2780	2174	7132	0.41	2.26	141.40	1.627	4.589	8.535	33974	95833	178259
	55.4	181.8	917	3010	2381	7812	0.41	2.35	146.59	1.976	5.585	10.677	41278	116638	222983
	55.6	182.4	893	2929	2326	7630	0.41	2.33	145.29	1.855	5.245	10.113	38749	109548	211216
	55.9	183.4	909	2983	2273	7456	0.40	2.31	143.99	1.906	5.355	9.372	39811	111851	195740
	56	183.7	980	3217	2326	7630	0.39	2.33	145.29	2.237	6.227	9.604	46719	130061	200590
	56.4	185.0	885	2903	2222	7291	0.41	2.29	142.69	1.790	5.033	8.901	37386	105111	185894
	56.6	185.7	833	2734	2222	7291	0.42	2.29	142.69	1.587	4.502	9.171	33151	94029	191541
	56.9	186.7	794	2604	2273	7456	0.43	2.31	143.99	1.453	4.157	9.977	30343	86814	208365
	57.1	187.3	735	2412	2273	7456	0.44	2.31	143.99	1.247	3.595	10.251	26044	75089	214096
	57.4	188.3	855	2804	2326	7630	0.42	2.33	145.29	1.700	4.835	10.320	35508	100979	215538
	57.6	189.0	820	2689	2326	7630	0.43	2.33	145.29	1.564	4.469	10.502	32657	93339	219339
	58	190.3	962	3155	2381	7812	0.40	2.35	146.59	2.171	6.090	10.417	45343	127193	217564
	58	190.3	909	2983	2500	8202	0.42	2.39	149.21	1.975	5.625	12.304	41255	117478	256983
	58.5	191.9	980	3217	2439	8002	0.40	2.37	147.90	2.277	6.393	11.057	47559	133511	230937
	58.5	191.9	1010	3314	2381	7812	0.39	2.35	146.59	2.396	6.662	10.117	50039	139133	211303
	59	193.6	1020	3348	2500	8202	0.40	2.39	149.21	2.489	6.968	11.620	51976	145539	242687
	59	193.6	1031	3382	2500	8202	0.40	2.39	149.21	2.540	7.100	11.551	53054	148291	241250
	59.4	194.9	1042	3418	2439	8002	0.39	2.37	147.90	2.571	7.139	10.666	53689	149090	222763
	59.4	194.9	1053	3454	2439	8002	0.39	2.37	147.90	2.625	7.274	10.593	54825	151927	221248
	59.9	196.5	1031	3382	2381	7812	0.38	2.35	146.59	2.496	6.911	9.984	52123	144343	208524

γ = Poisson's Ratio ρ(Vp) = Vp-derived density G = Shear Modulus E = Young's Modulus K = Bulk Modulus
Shaded cells denote questionable data.

Table 2. LA 710 Tunnel
Boring Z3 B8
PS Suspension Log Data Summary

Top of Hole Elevation (m)	Depth (m)	Depth (ft)	Vs (m/s)	Vs (ft/s)	Vp (m/s)	Vp (ft/s)	γ	ρ(Vp) (g/cc)	ρ(Vp) (lb/ft^3)	G (GPa)	E (GPa)	K (GPa)	G ($10^3 lb/ft^2$)	E ($10^3 lb/ft^2$)	K ($10^3 lb/ft^2$)
	59.9	196.5	1020	3348	2381	7812	0.39	2.35	146.59	2.445	6.785	10.052	51065	141706	209935
	60.1	197.2	1031	3382	2439	8002	0.39	2.37	147.90	2.518	7.006	10.736	52588	146325	224231
	60.4	198.2	990	3248	2381	7812	0.40	2.35	146.59	2.302	6.425	10.243	48077	134178	213919
	60.6	198.8	980	3217	2381	7812	0.40	2.35	146.59	2.257	6.310	10.302	47139	131792	215170
	61	200.1	862	2828	2632	8634	0.44	2.43	151.84	1.808	5.205	14.433	37751	108714	301448
	61	200.1	952	3125	2703	8867	0.43	2.45	153.16	2.225	6.360	14.954	46475	132835	312311
	61.5	201.8	1010	3314	2778	9113	0.42	2.47	154.48	2.525	7.189	15.727	52730	150155	328463
	61.5	201.8	909	2983	2857	9374	0.44	2.50	155.80	2.063	5.955	17.623	43077	124380	368062
	62	203.4	1087	3566	2564	8412	0.39	2.41	150.52	2.849	7.922	12.054	59496	165454	251752
	62.1	203.7	1064	3490	2632	8634	0.40	2.43	151.84	2.753	7.720	13.173	57489	161237	275130
	62.5	205.1	1000	3281	2381	7812	0.39	2.35	146.59	2.348	6.542	10.181	49043	136625	212631
	62.6	205.4	1000	3281	2439	8002	0.40	2.37	147.90	2.369	6.629	10.935	49480	138442	228375
	63	206.7	935	3066	2326	7630	0.40	2.33	145.29	2.033	5.707	9.877	42455	119188	206275
	63.1	207.0	926	3038	2381	7812	0.41	2.35	146.59	2.013	5.681	10.628	42046	118647	221959
	63.5	208.3	917	3010	2326	7630	0.41	2.33	145.29	1.959	5.516	9.975	40911	115194	208334
	63.6	208.7	909	2983	2381	7812	0.41	2.35	146.59	1.941	5.491	10.724	40531	114677	223979
	64	210.0	820	2689	2326	7630	0.43	2.33	145.29	1.564	4.469	10.502	32657	93339	219339
	64.1	210.3	833	2734	2222	7291	0.42	2.29	142.69	1.587	4.502	9.171	33151	94029	191541
	64.5	211.6	885	2903	2439	8002	0.42	2.37	147.90	1.855	5.285	11.620	38750	110376	242682
	64.6	211.9	926	3038	2381	7812	0.41	2.35	146.59	2.013	5.681	10.628	42046	118647	221959
	65	213.3	1075	3528	2564	8412	0.39	2.41	150.52	2.788	7.768	12.135	58223	162246	253448
	65.1	213.6	1111	3645	2632	8634	0.39	2.43	151.84	3.003	8.357	12.840	62713	174533	268166
	65.1	213.6	1087	3566	2632	8634	0.40	2.43	151.84	2.874	8.030	13.012	60016	167702	271761
	65.1	213.6	1087	3566	2632	8634	0.40	2.43	151.84	2.874	8.030	13.012	60016	167702	271762
	65.1	213.6	1087	3566	2632	8634	0.40	2.43	151.84	2.874	8.030	13.012	60016	167702	271761
	65.5	214.9	1111	3645	2632	8634	0.39	2.43	151.84	3.003	8.357	12.840	62713	174533	268165
	66.1	216.9	1020	3348	2632	8634	0.41	2.43	151.84	2.532	7.149	13.467	52892	149316	281259
	66.5	218.2	1000	3281	2564	8412	0.41	2.41	150.52	2.411	6.801	12.637	50357	142038	263937
	67	219.8	1020	3348	2941	9650	0.43	2.52	157.13	2.621	7.504	18.279	54735	156716	381759
	67.5	221.5	1111	3645	2439	8002	0.37	2.37	147.90	2.925	8.009	10.194	61087	167262	212900
	68	223.1	1205	3953	2564	8412	0.36	2.41	150.52	3.500	9.508	11.186	73098	198582	233616
	68.5	224.7	1235	4050	2703	8867	0.37	2.45	153.16	3.739	10.232	12.935	78096	213695	270150
	69	226.4	1299	4261	2326	7630	0.27	2.33	145.29	3.925	9.997	7.353	81982	208792	153574
	69.5	228.0	1351	4434	2703	8867	0.33	2.45	153.16	4.480	11.947	11.947	93569	249518	249518
	70	229.7	1282	4206	2703	8867	0.35	2.45	153.16	4.032	10.926	12.544	84218	228203	261986
	70.5	231.3	1220	4001	2703	8867	0.37	2.45	153.16	3.649	10.013	13.056	76202	209126	272674
	71	232.9	1250	4101	2632	8634	0.35	2.43	151.84	3.800	10.294	11.776	79371	214987	245954

γ = Poisson's Ratio ρ(Vp) = Vp-derived density G = Shear Modulus E = Young's Modulus K = Bulk Modulus
Shaded cells denote questionable data.

Table 2. LA 710 Tunnel
Boring Z3 B8
PS Suspension Log Data Summary

Top of Hole Elevation (m)	Depth (m)	Depth (ft)	Vs (m/s)	Vs (ft/s)	Vp (m/s)	Vp (ft/s)	γ	ρ(Vp) (g/cc)	ρ(Vp) (lb/ft^3)	G (GPa)	E (GPa)	K (GPa)	G ($10^3 lb/ft^2$)	E ($10^3 lb/ft^2$)	K ($10^3 lb/ft^2$)
	71.5	234.6	1282	4206	2703	8867	0.35	2.45	153.16	4.032	10.926	12.544	84218	228202	261986
	72	236.2	1266	4153	2703	8867	0.36	2.45	153.16	3.931	10.688	12.679	82100	223230	264811
	72.5	237.9	1190	3906	2778	9113	0.39	2.47	154.48	3.507	9.732	14.417	73244	203251	301112
	73	239.5	1205	3953	2703	8867	0.38	2.45	153.16	3.561	9.800	13.172	74377	204686	275107
	73.4	240.8	1220	4001	2778	9113	0.38	2.47	154.48	3.680	10.162	14.187	76860	212229	296291
	74	242.8	1136	3728	2703	8867	0.39	2.45	153.16	3.168	8.824	13.697	66165	184288	286056
	74.5	244.4	1250	4101	2778	9113	0.37	2.47	154.48	3.866	10.617	13.938	80751	221749	291103
	75	246.1	1449	4755	3704	12151	0.41	2.67	166.51	5.602	15.794	29.118	117005	329859	608136
	75.5	247.7	1639	5378	5000	16404	0.44	2.82	176.04	7.578	21.822	60.394	158277	455768	1261342
	76	249.3	1389	4557	3125	10253	0.38	2.56	159.79	4.938	13.597	18.413	103124	283987	384565
	76.5	251.0	1190	3906	2703	8867	0.38	2.45	153.16	3.477	9.594	13.285	72617	200370	277454
	76.5	251.0	1205	3953	2703	8867	0.38	2.45	153.16	3.561	9.800	13.172	74377	204686	275107
	77	252.6	1190	3906	2857	9374	0.39	2.50	155.80	3.537	9.868	15.657	73872	206095	327005
	77.5	254.3	1282	4206	2632	8634	0.34	2.43	151.84	3.998	10.749	11.513	83493	224496	240459
	78	255.9	1087	3566	2500	8202	0.38	2.39	149.21	2.824	7.813	11.173	58977	163183	233353
	78	255.9	1235	4050	2778	9113	0.38	2.47	154.48	3.772	10.386	14.065	78769	216919	293745
	78.5	257.5	1190	3906	2632	8634	0.37	2.43	151.84	3.447	9.454	12.248	71992	197451	255793
	79	259.2	1020	3348	2381	7812	0.39	2.35	146.59	2.445	6.785	10.052	51065	141706	209934
	79.5	260.8		NA	2273	7456	NA	NA	NA	NA	NA	NA	NA	NA	NA

γ = Poisson's Ratio ρ(Vp) = Vp-derived density G = Shear Modulus E = Young's Modulus K = Bulk Modulus
Shaded cells denote questionable data.

Figure 1. LA 710 Tunnel
Boring Z3 B8
Downhole Interval Velocities

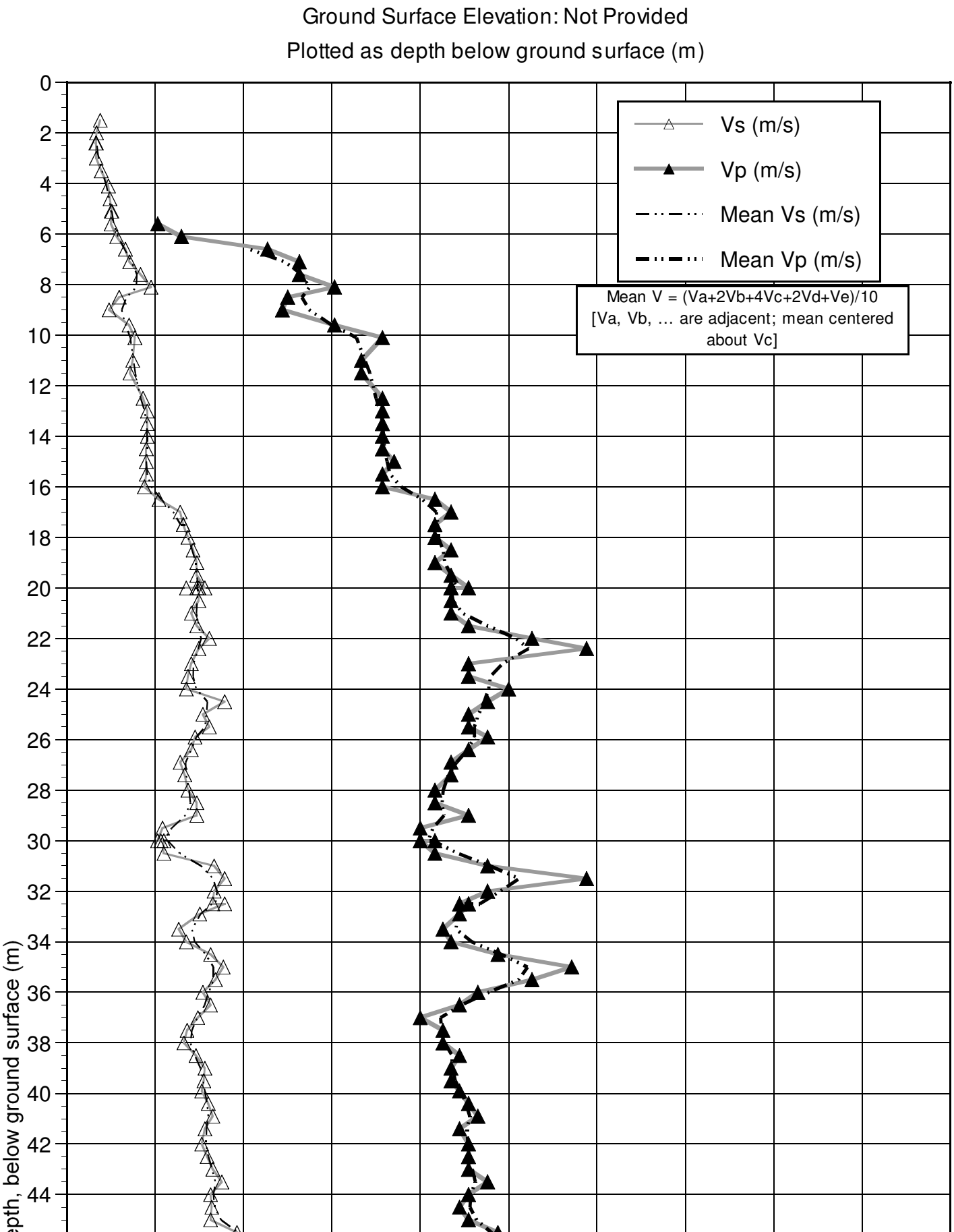

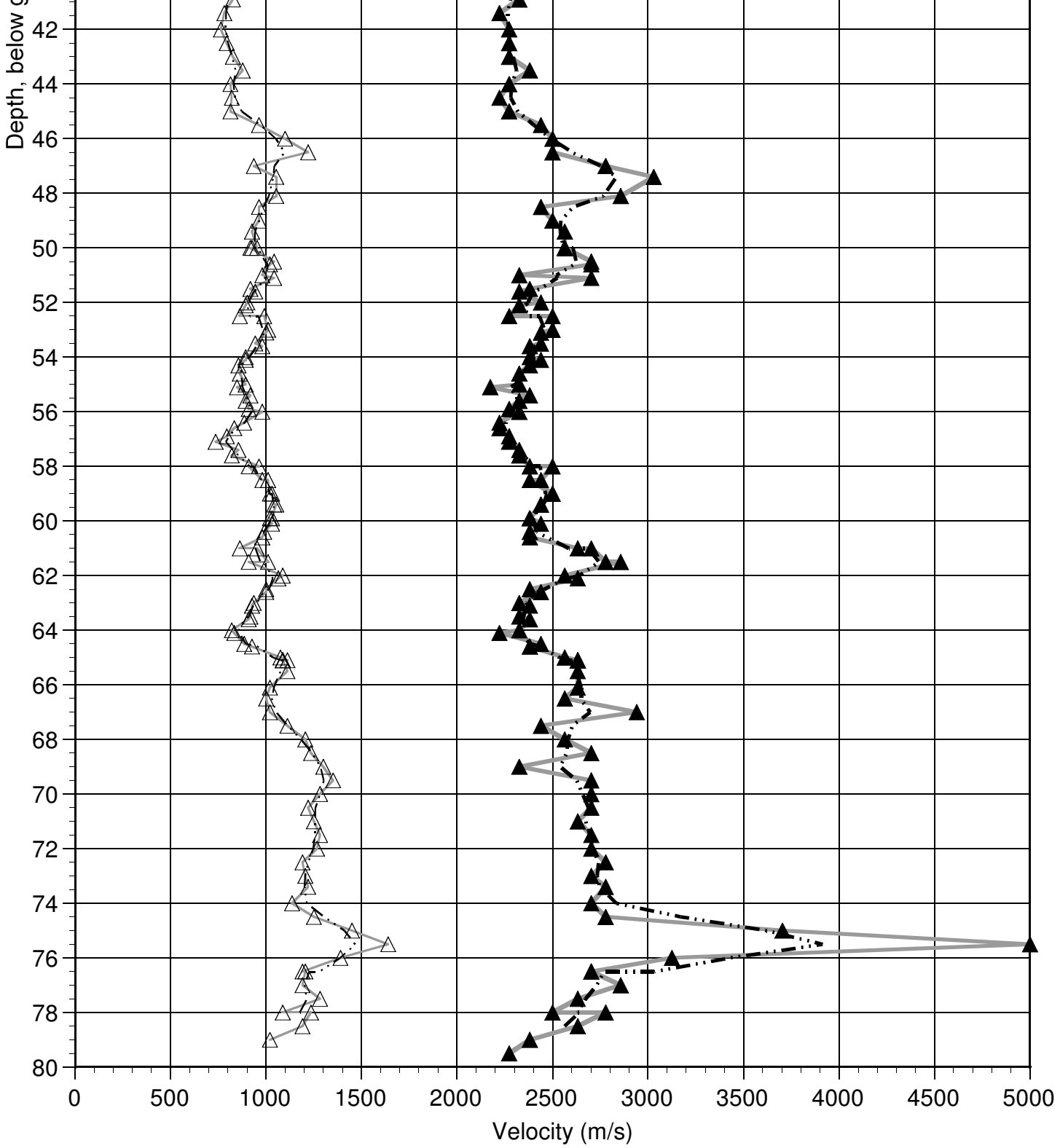
Depth, below g
42
44
46
48
50
52
54
56
58
60
62
64
66
68
70
72
74
76
78
80
0
500
1000
1500
2000
2500
3000
3500
4000
4500
5000
Velocity (m/s)

California Department of Transportation
Geophysical Services

07-187900 Z3 B8..

COMPANY	: Caltrans	OTHER SERVICES:	
WELL	: 07-187900 Z3 B8..		
FIELD	: LA Co.		
COUNTY	: LA		
STATE	: CA		
LOCATION	:		
SECTION	: None		
TOWNSHIP	: None		
RANGE	: None		
API NO.	:		
UNIQUE WELL ID.	:		
PERMANENT DATUM	: None	ELEVATION KB	: NA
LOG MEASURED FROM	: GL	ELEVATION DF	: NA
DRL MEASURED FROM	: GL	ELEVATION GL	: 172.8m.
DATE	: 03/19/09	RIG NUMBER	:
DEPTH DRILLER	: 83.82m.	LOGGER TD	:
BIT SIZE	: 10.5cm.	ARRIVAL TIME	:
LOG TOP	: 3.11	DEPARTURE TIME	:
LOG BOTTOM	: 83.80	CIRC STOPPED	: 3/18 PM
CASING OD	:		
CASING BOTTOM	: N/A		
CASING TYPE	: N/A		
BOREHOLE FLUID	: 0		
RM TEMPERATURE	: 0		
MUD RES	: 0		
MUD WEIGHT	:		
WITNESSED BY	:		
RECORDED BY	: DH/DG		
REMARKS 1	: IND, Acoustic Tel, PSLog, CAL		
REMARKS 2	: EA: 07-187900		

ALL SERVICES PROVIDED SUBJECT TO STANDARD TERMS AND CONDITIONSS

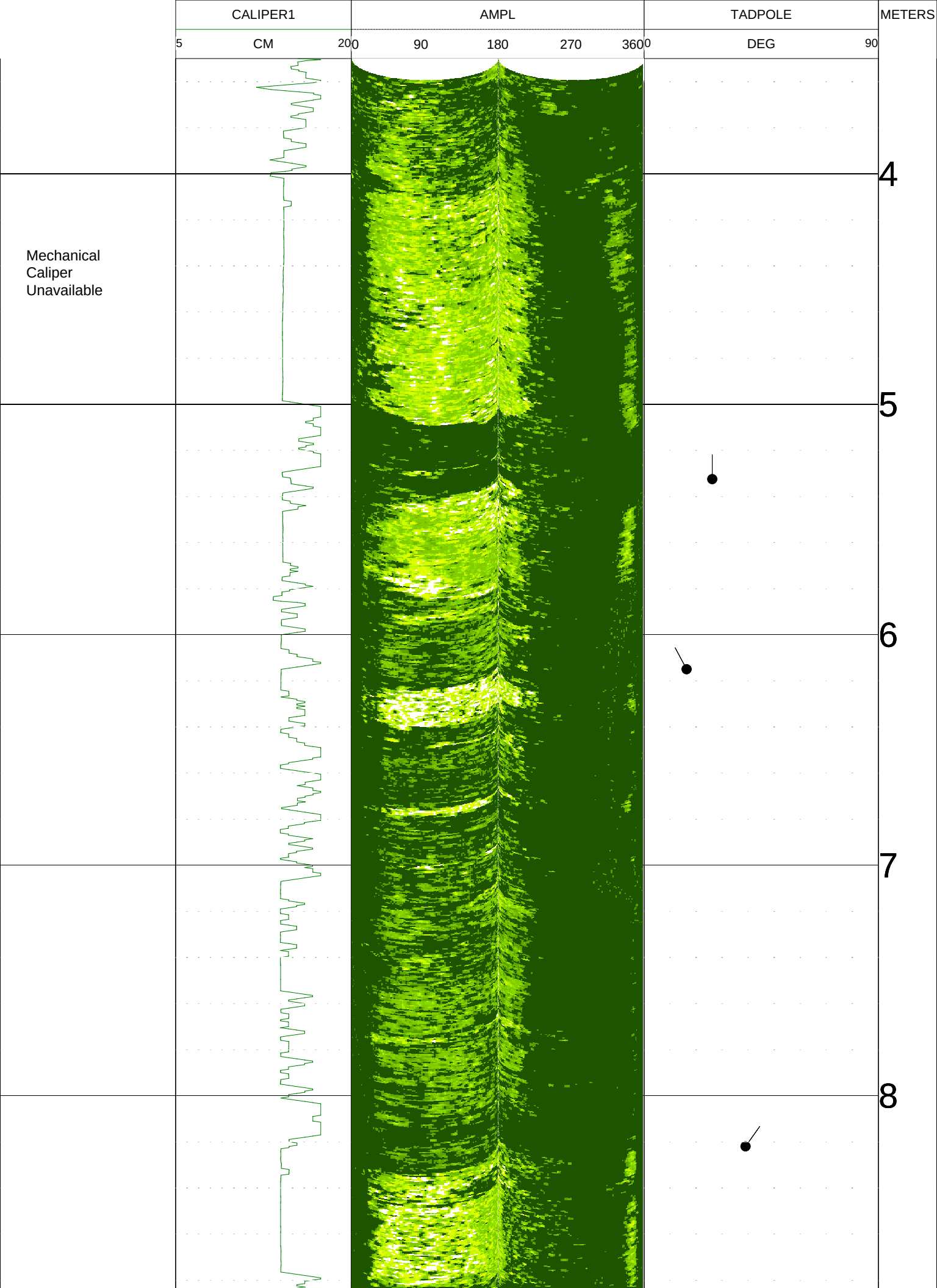
CALIPER1
AMPL
TADPOLE
METERS
5
CM
20
0
90
180
270
360
0
DEG
90
Mechanical
Caliper
Unavailable
4
5
6
7
8

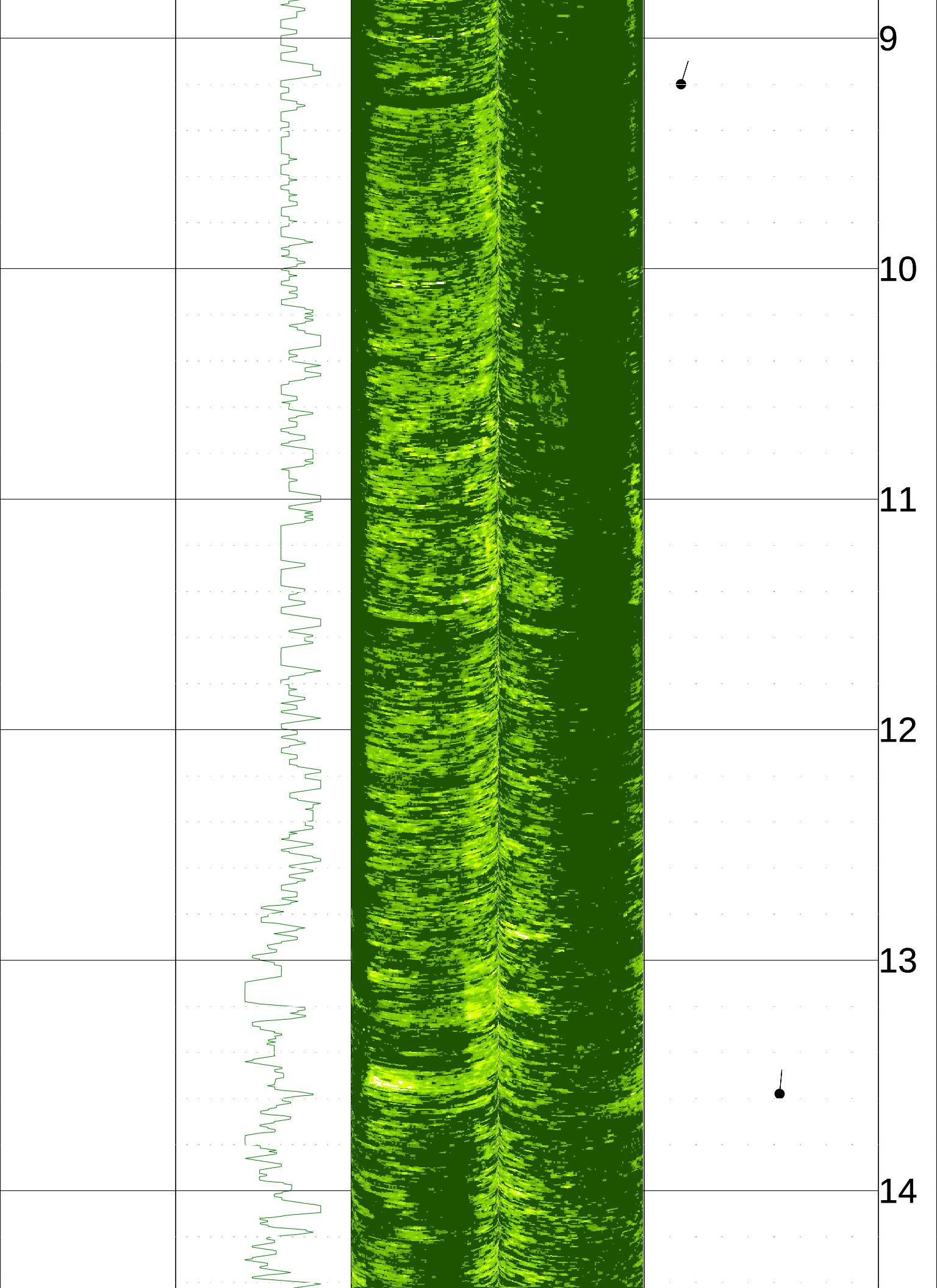
9
10
11
12
13
14

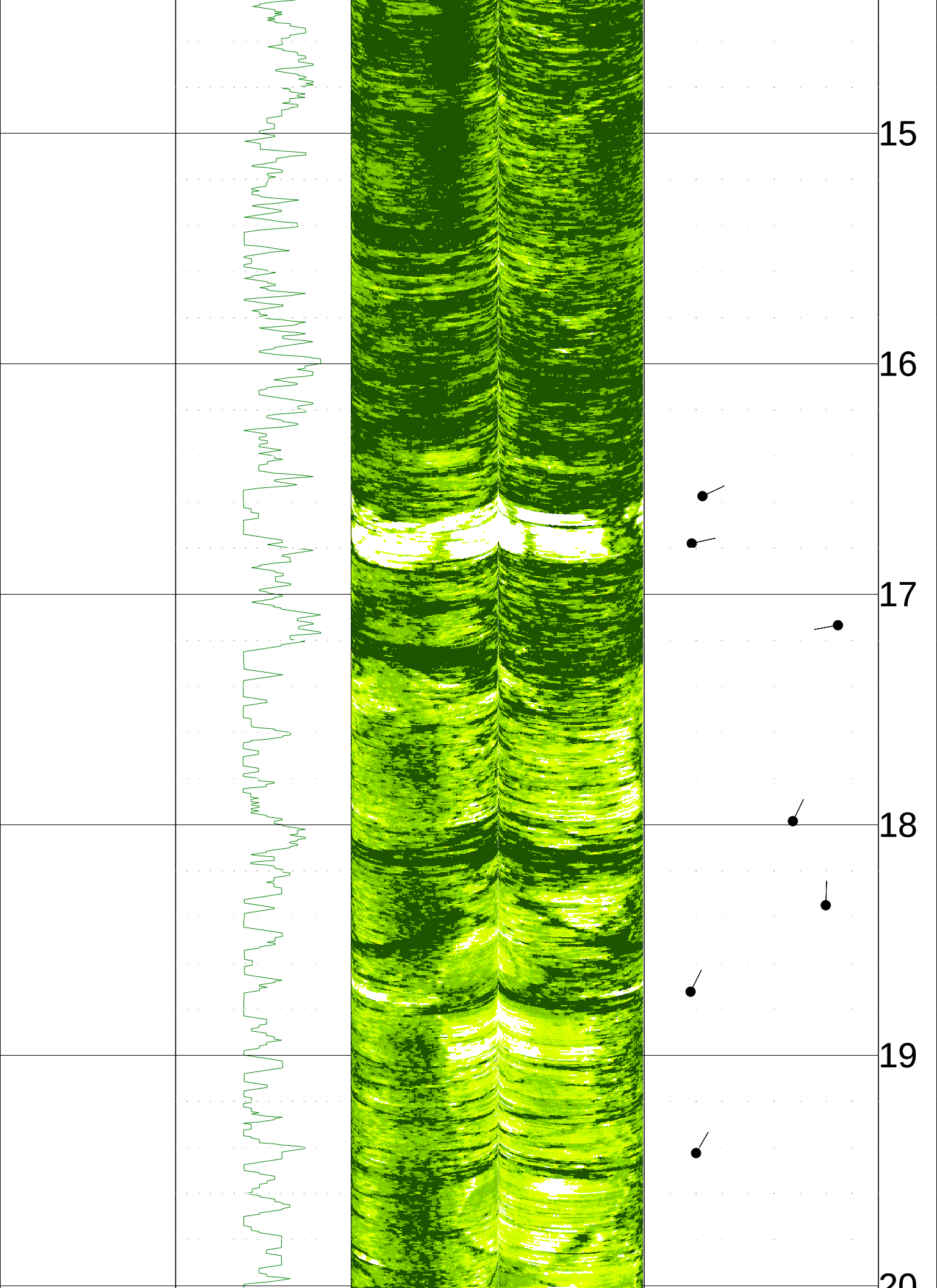
15
16
17
18
19
20

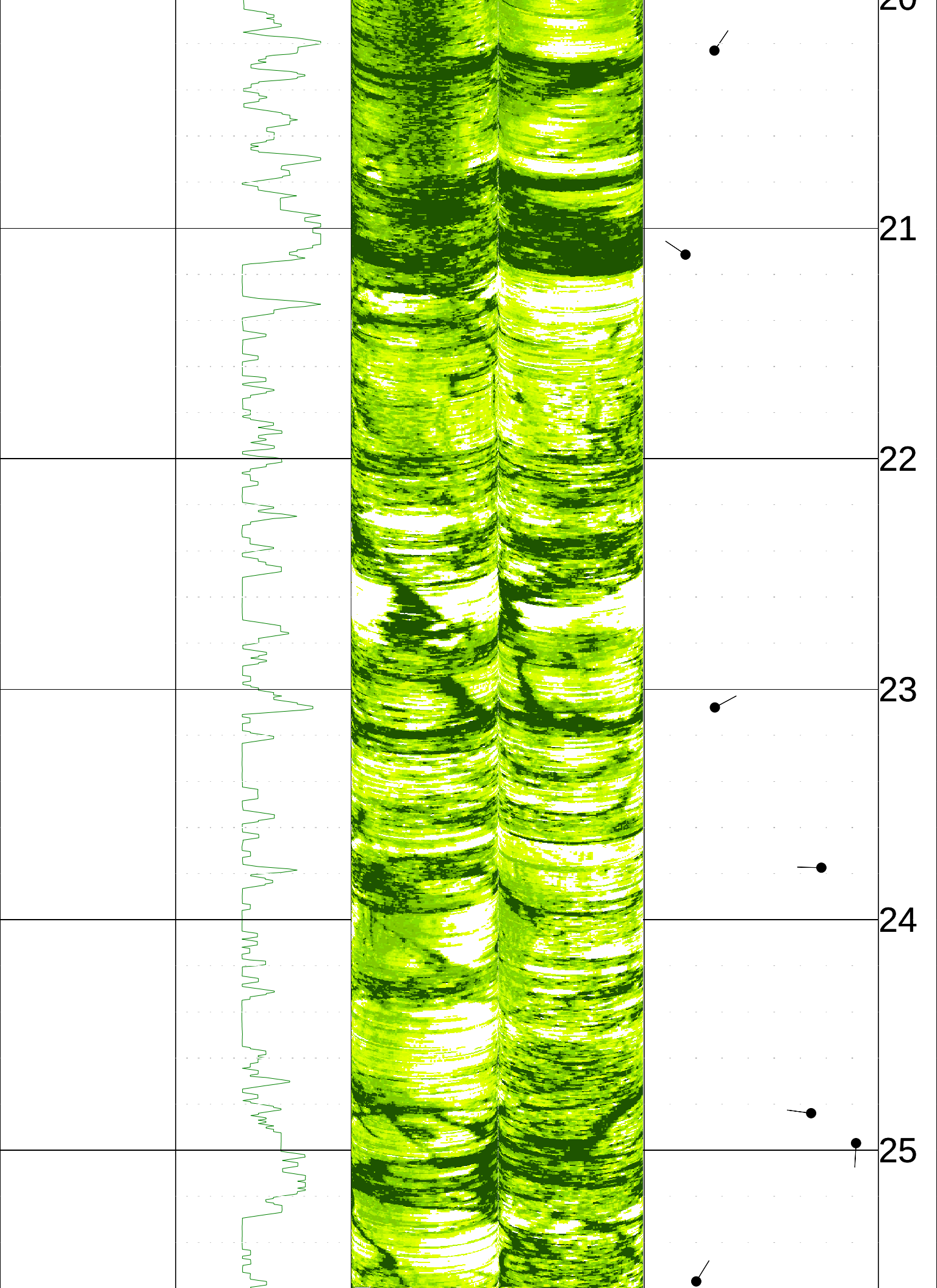
20
21
22
23
24
25

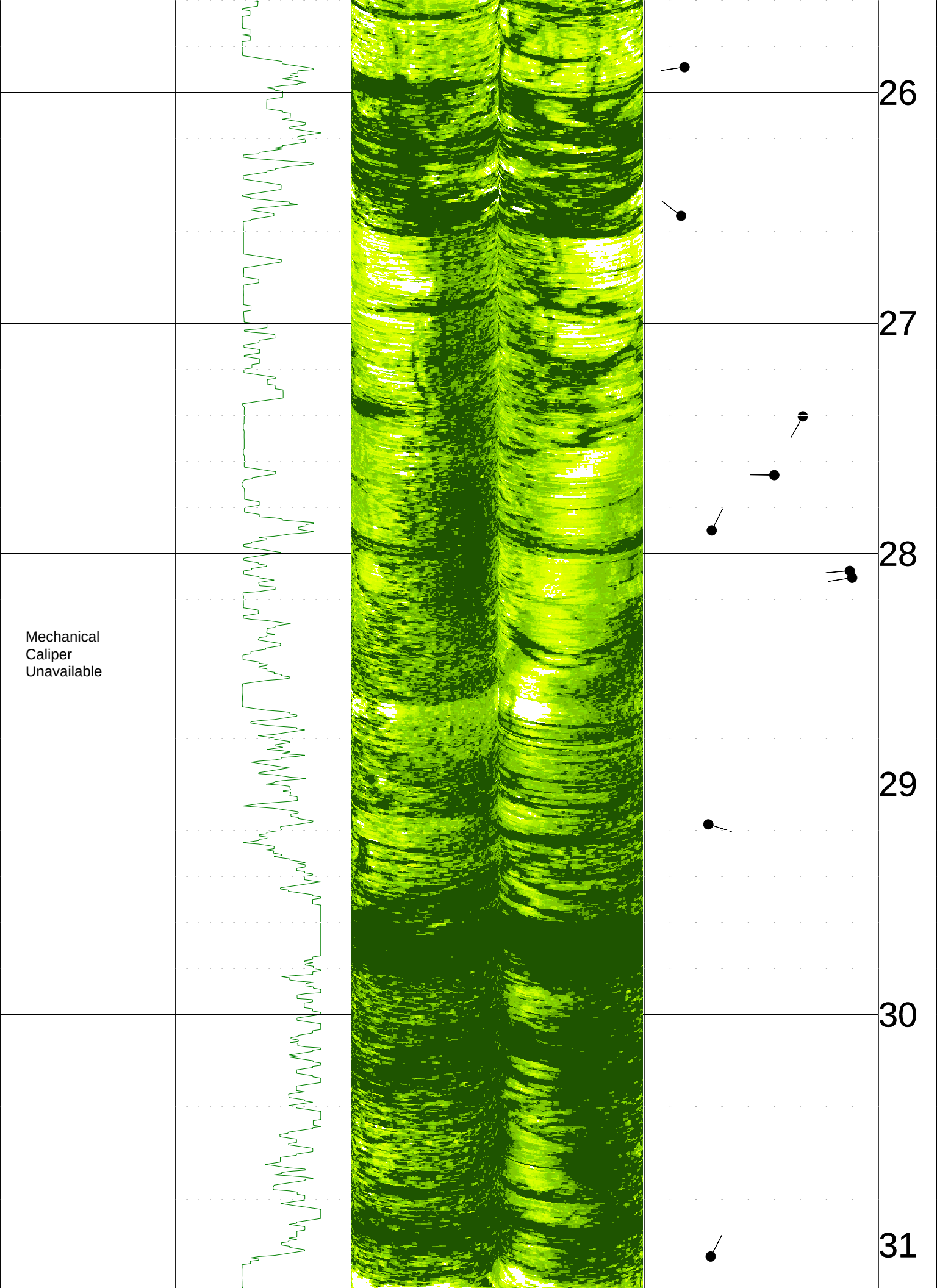
26
27
28
29
30
31
Mechanical
Caliper
Unavailable

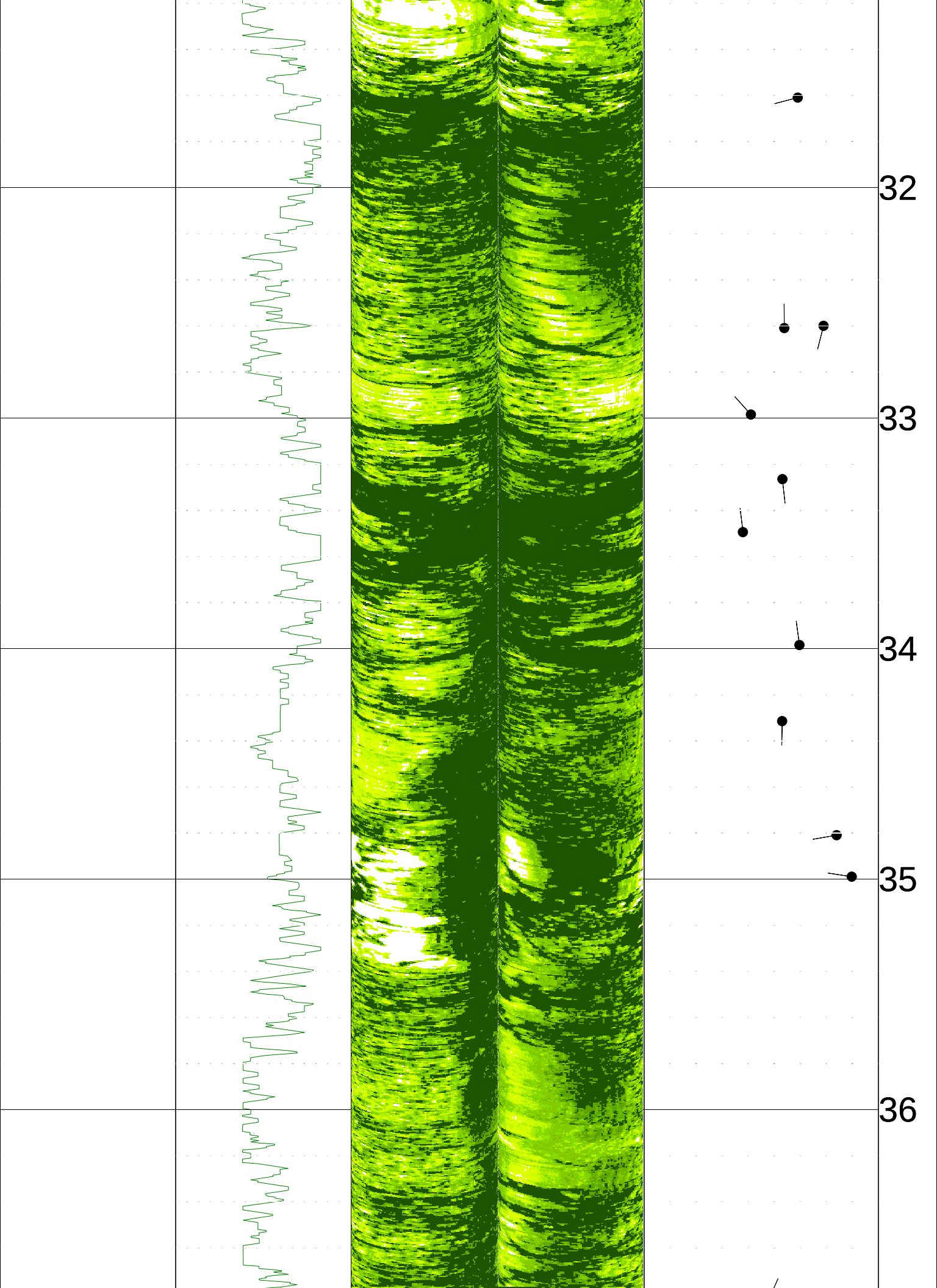
32
33
34
35
36

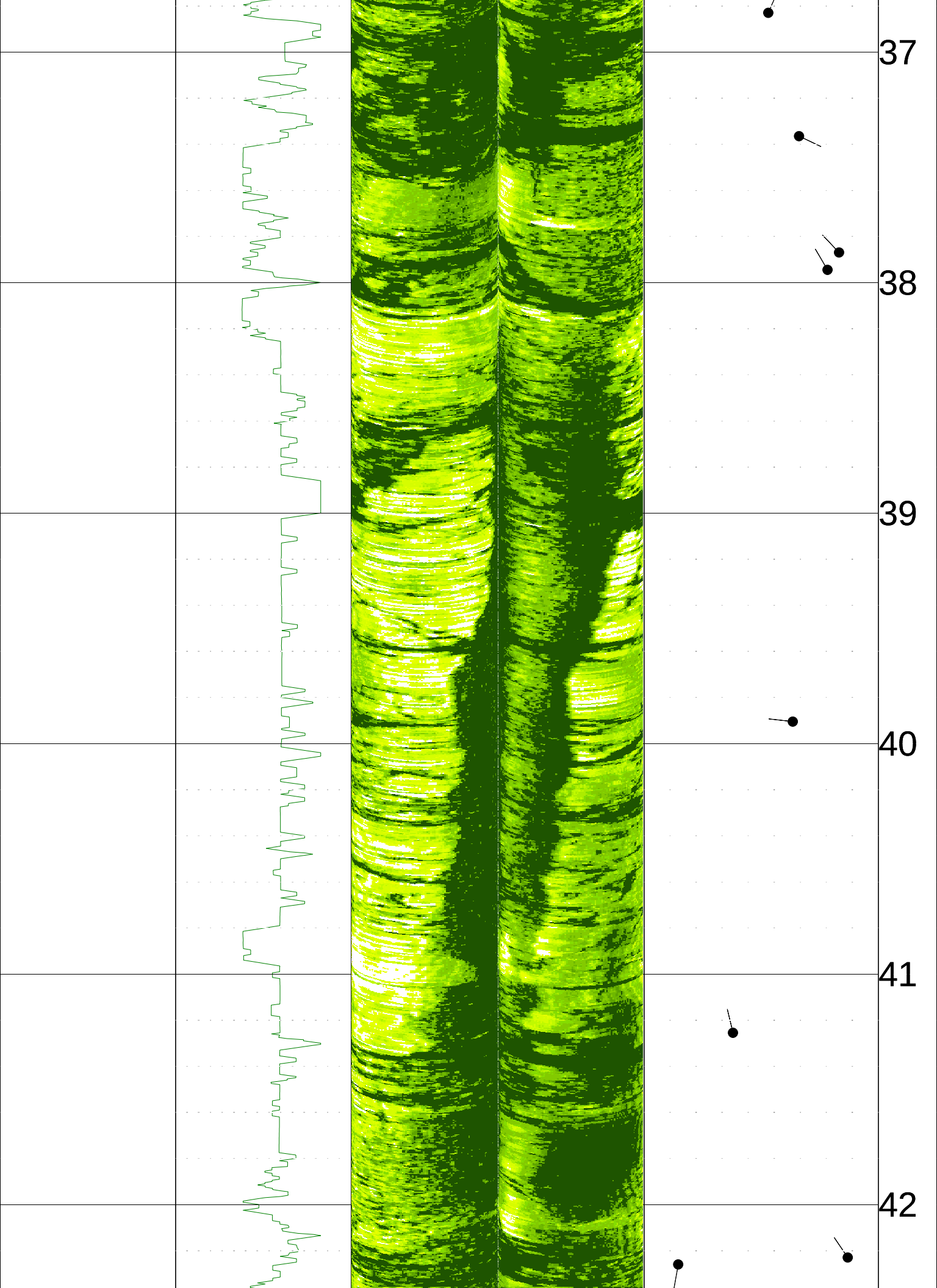
37
38
39
40
41
42

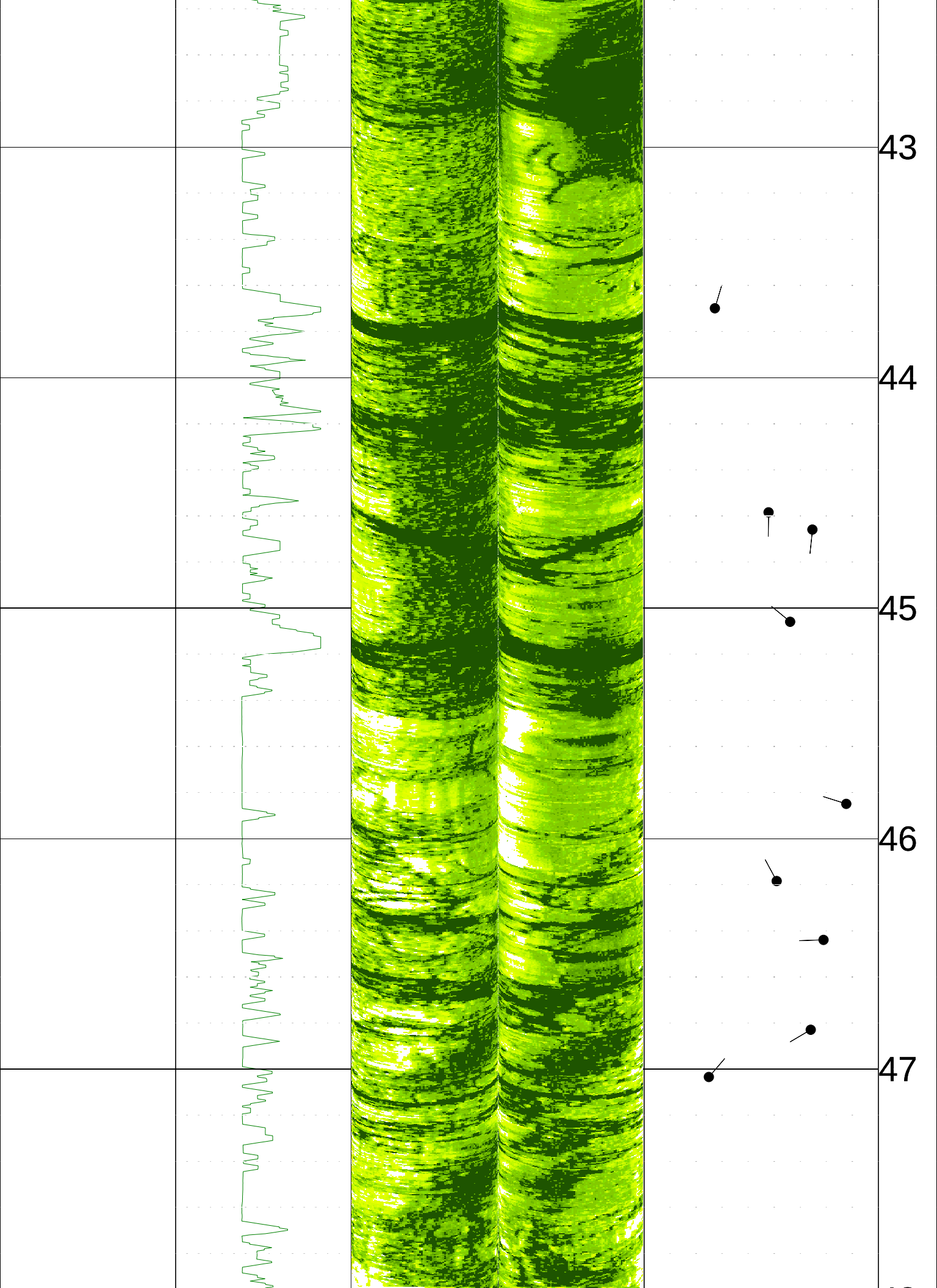
43
44
45
46
47

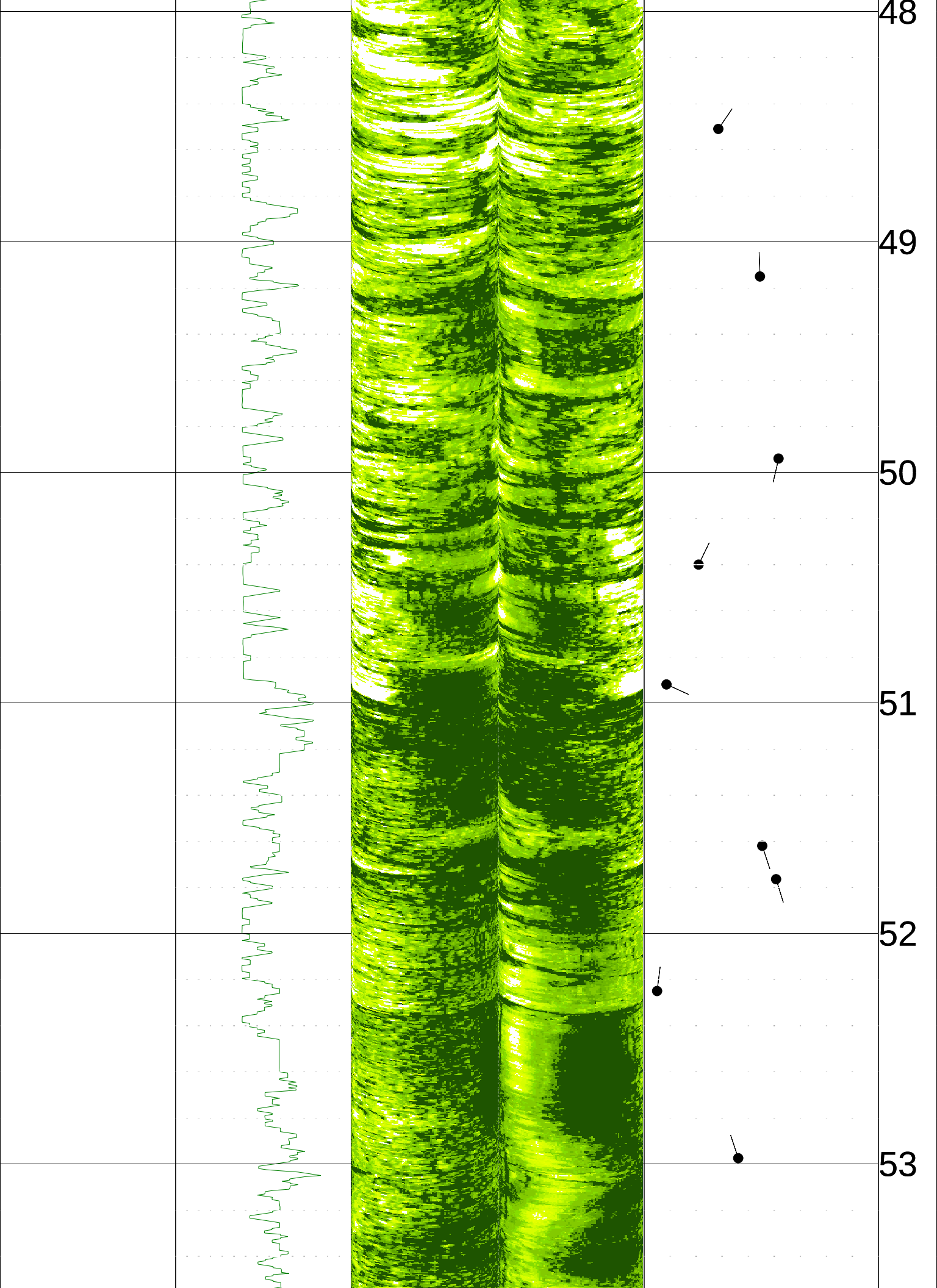
48
49
50
51
52
53

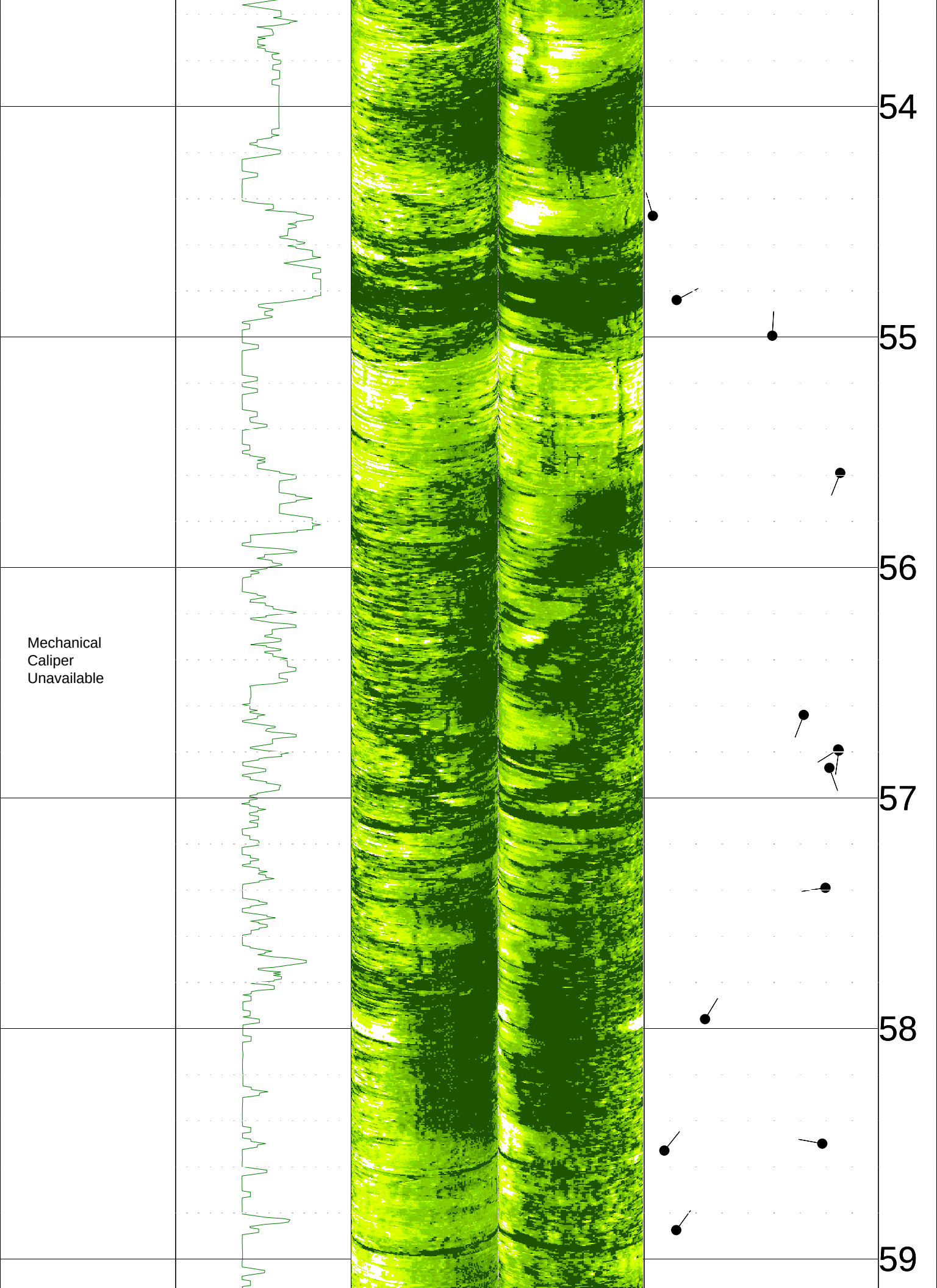
Mechanical
Caliper
Unavailable
54
55
56
57
58
59

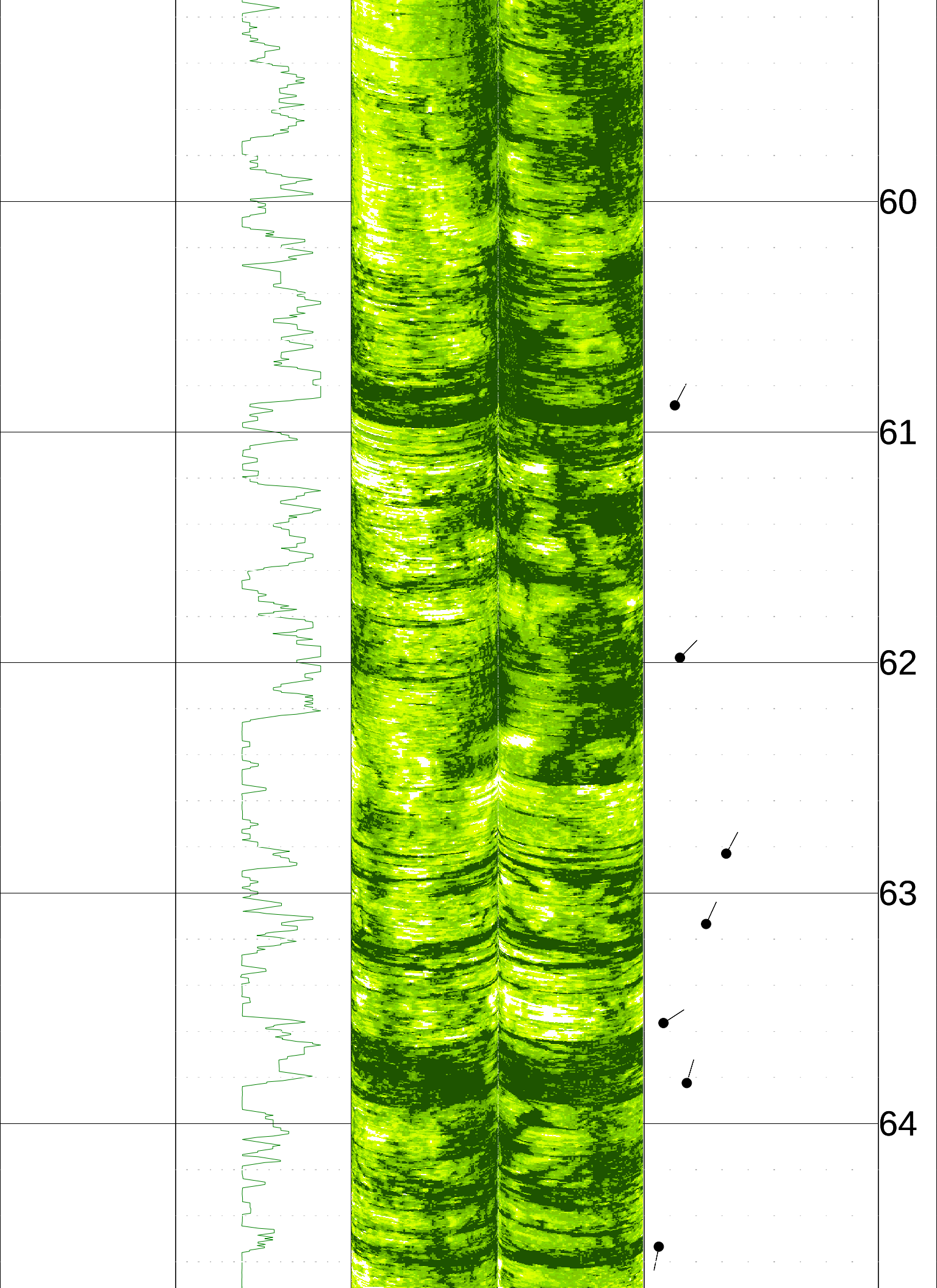
60
61
62
63
64

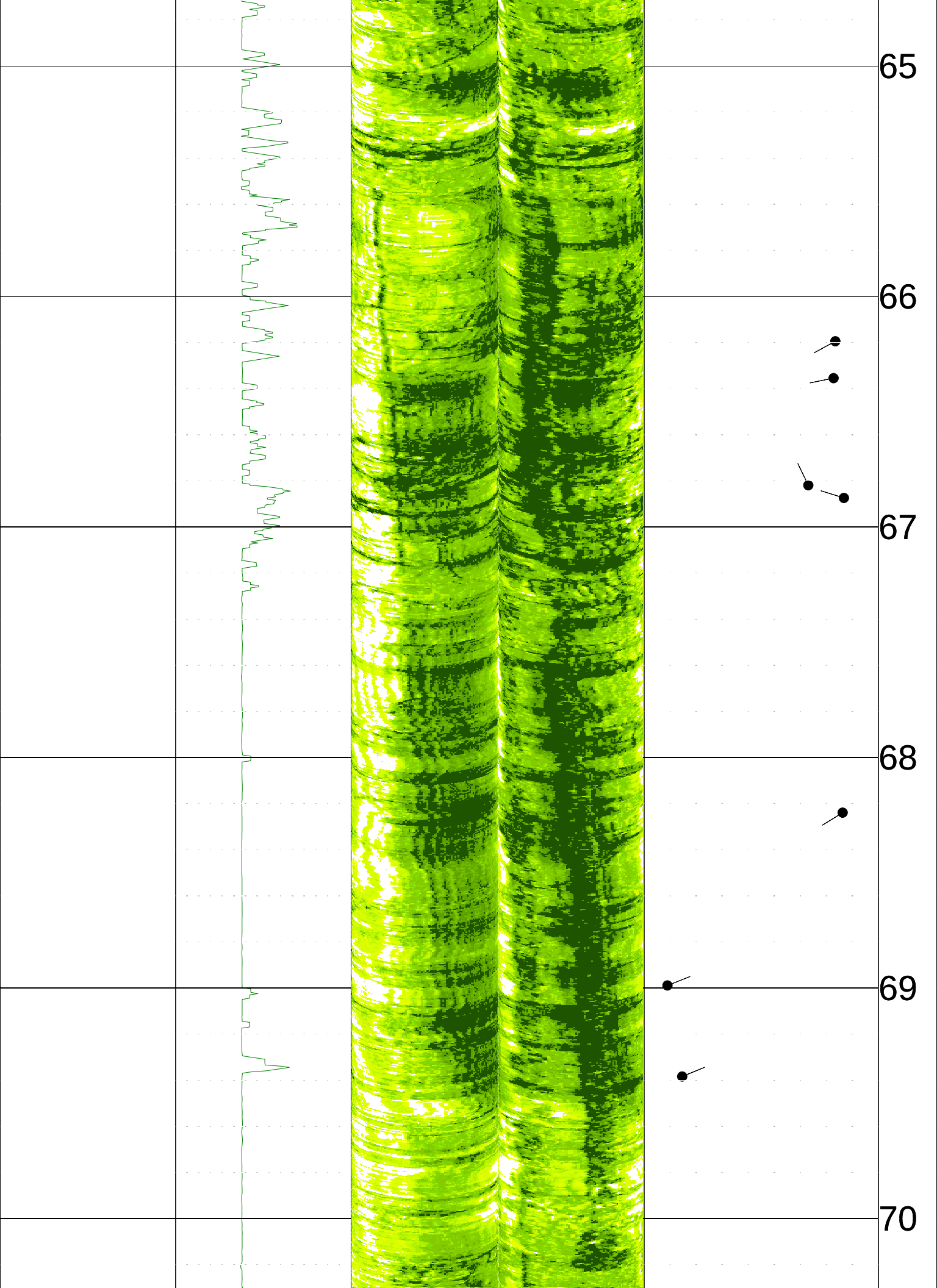
65
66
67
68
69
70

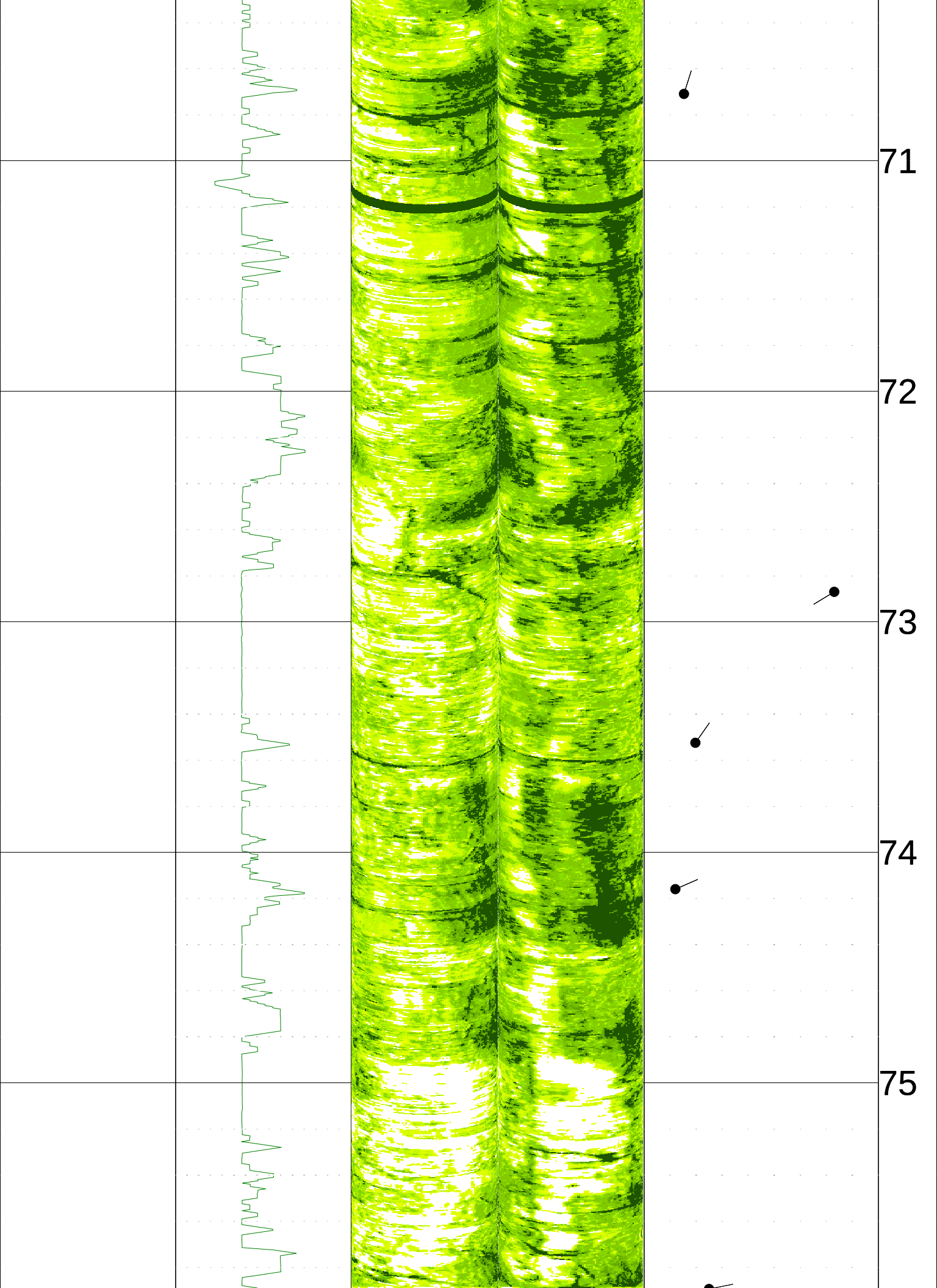
71
72
73
74
75

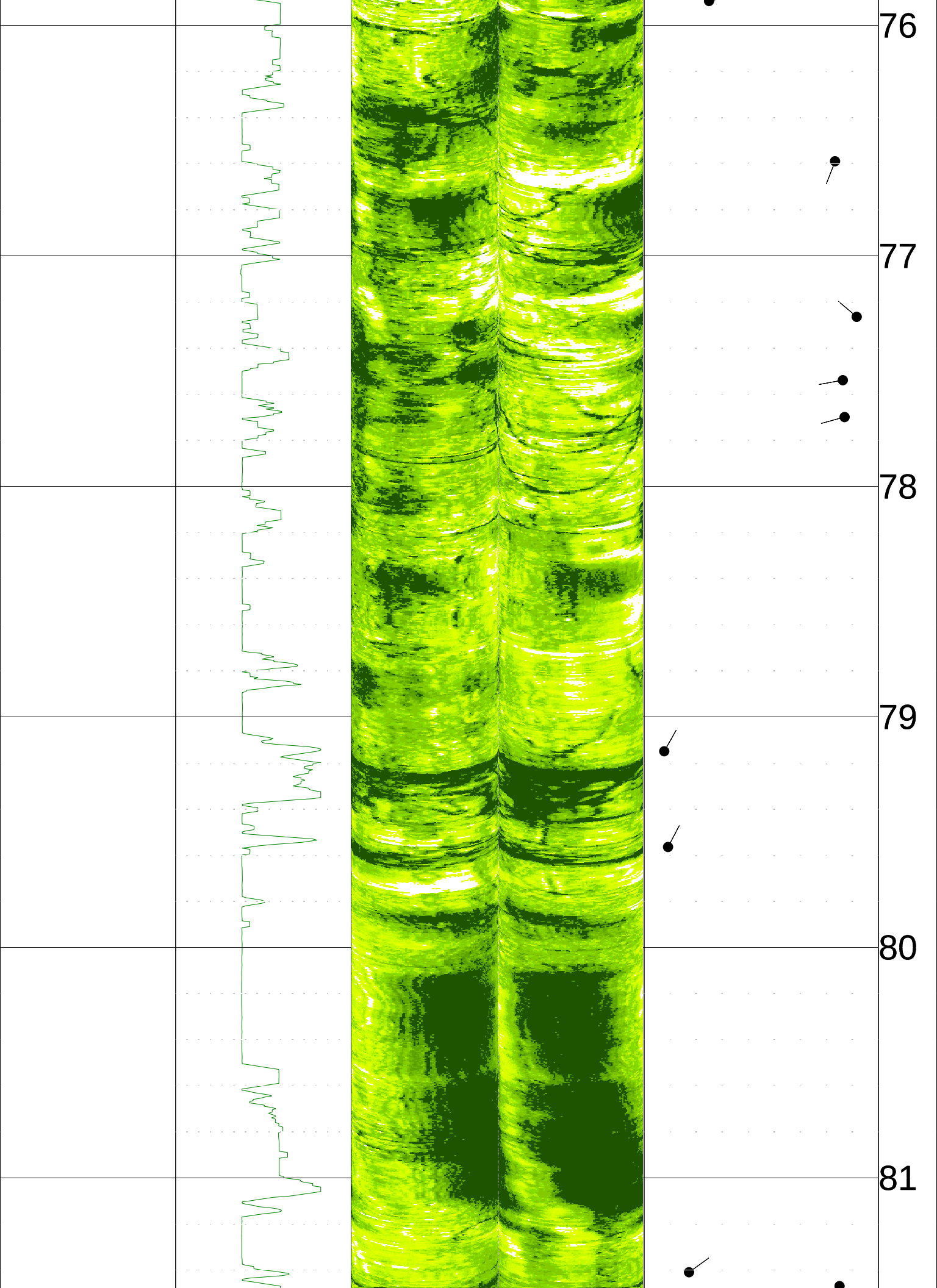
76
77
78
79
80
81

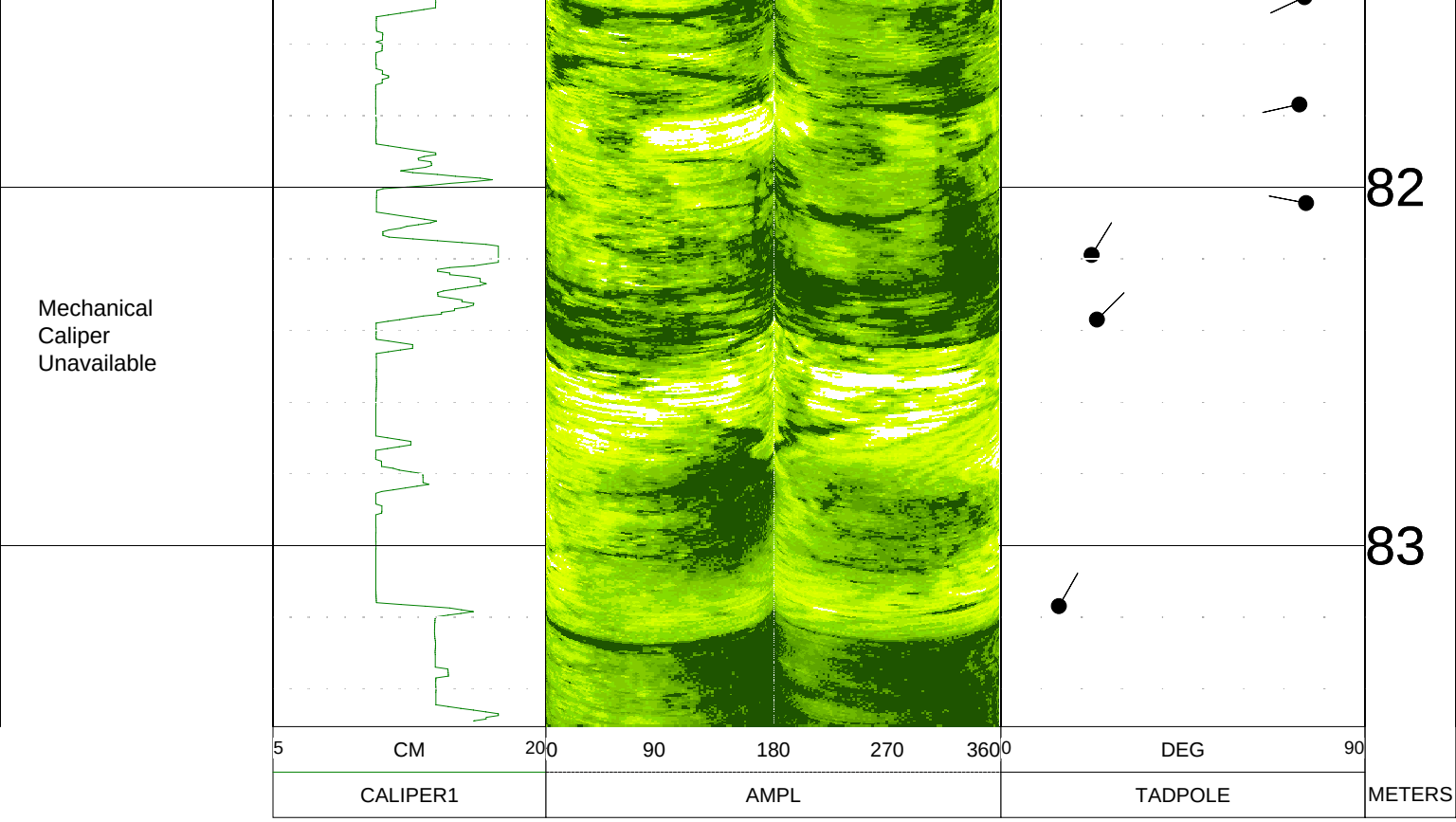
Mechanical
Caliper
Unavailable
82
83
5
CM
20
0
90
180
270
360
0
DEG
90
CALIPER1
AMPL
TADPOLE
METERS

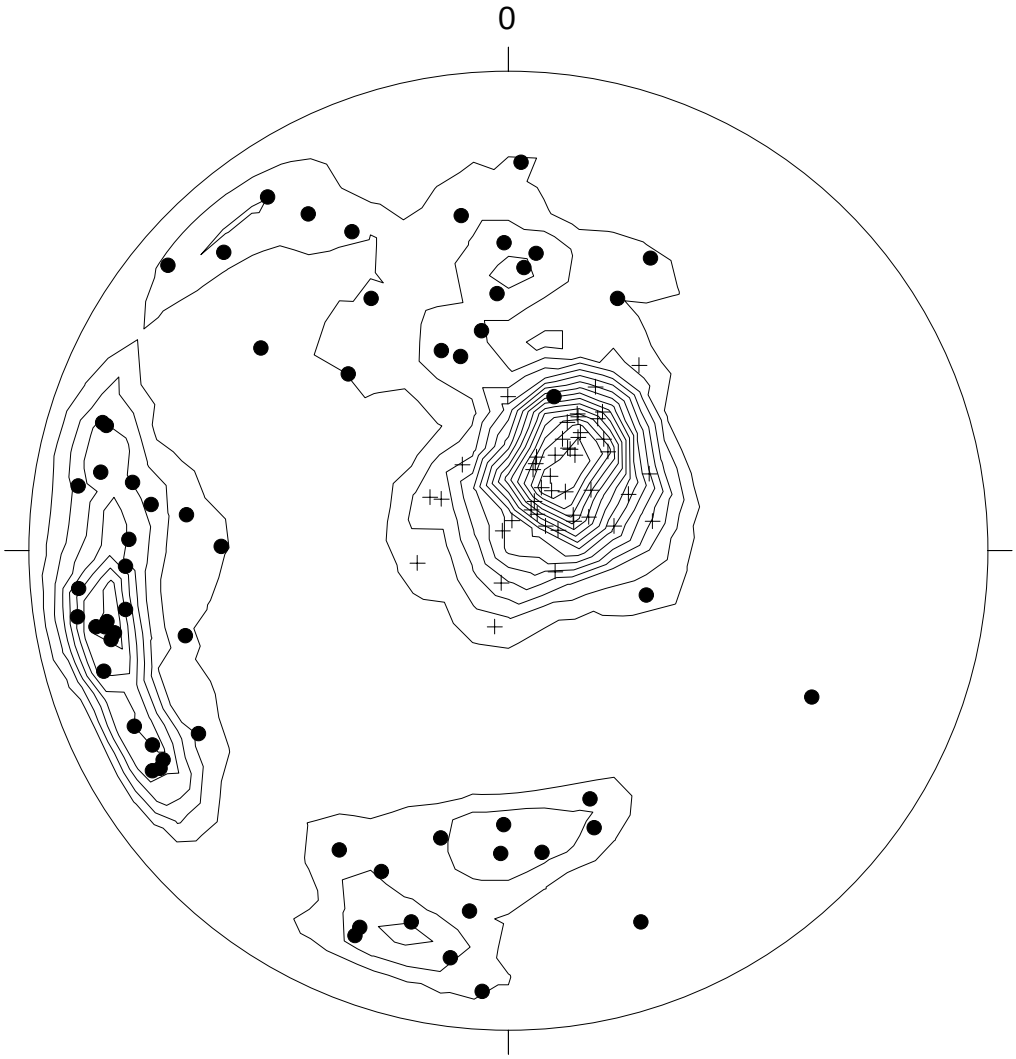

+ n=46 (P)
• n=63 (P)

LA 710 Tunnel, boring Z3 B8

Stereonet contour plot of poles to planes,
Both bedding and fractures

n=109
max. dens.= 16.05 (at 40/ 72)
min. dens.=0.00
Contours at every integer between
1 and 15, inclusive:
(Multiples of random distribution)

Apparent bedding denoted as cross
Apparent fractures denoted as solid circle
Plotted on upper hemisphere

LA 710 Tunnel boring Z3 B11

COMPANY	: CALTRANS				
WELL	: Z3 B11				
LOCATION/FIELD	: LA 710 TUNNEL				
COUNTY	: LA				
LOCATION	: CA				
SECTION	: None	TOWNSHIP	: None	RANGE	: None
DATE	: 1/21/09	PERMANENT DATUM	: None		
DEPTH DRILLER	: 83.82M			KB	: NA
LOG BOTTOM	: 83.7	LOG MEASURED FROM:	GL	DF	: NA
LOG TOP	: 1.5	DRL MEASURED FROM:	GL	GL	: NA
CASING DIAMETER	: N/A	LOGGING UNIT	: 7311		
CASING TYPE	: none	FIELD OFFICE	: 7311		
CASING THICKNESS:	0	RECORDED BY	: DH/DL		
BIT SIZE	: 9.8CM	BOREHOLE FLUID	: 0	FILE	: PROCESSE
MAGNETIC DECL.	: 12.85	RM	: 0	TYPE	: 9065A
MATRIX DENSITY	: 2.71	RM TEMPERATURE	: 0	LGDATE	: 1/21/09.
NEUTRON MATRIX	: Dolomite	MATRIX DELTA T	: 140		
				THRESH:	2500

OTHER SERVICES:
IND-CAL
AC TEL
PS LOG

NAT. GAMMA MEASURED AS API UNITS, NOT CPS
EA: 07-187900. GROUND LEVEL ELEVATION NOT ESTIMATE

ALL SERVICES PROVIDED SUBJECT TO STANDARD TERMS AND CONDITIONS

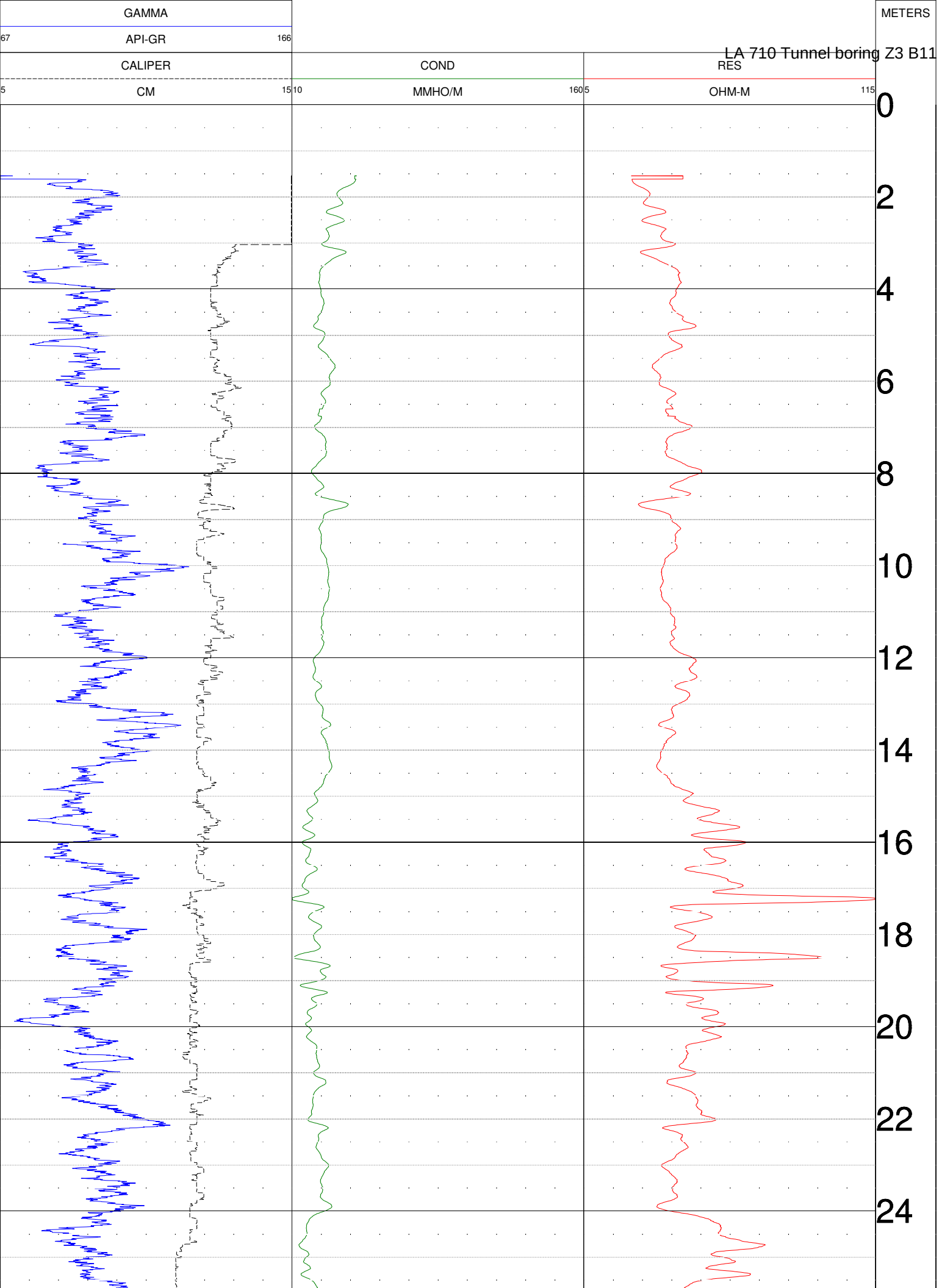
GAMMA
67
API-GR
166
CALIPER
5
CM
15
COND
10
MMHO/M
160
RES
5
OHM-M
115
METERS
LA 710 Tunnel boring Z3 B11
0
2
4
6
8
10
12
14
16
18
20
22
24

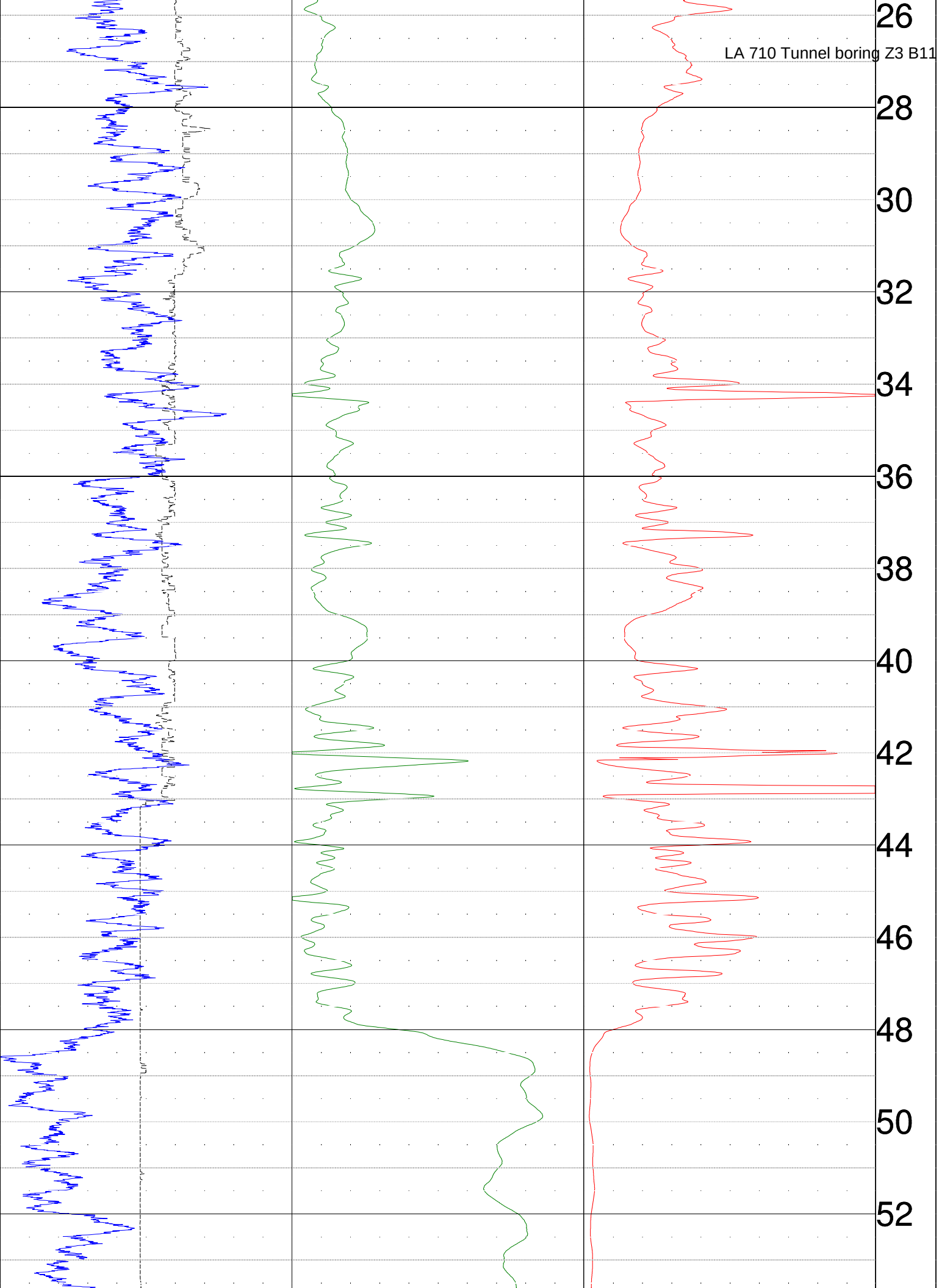
LA 710 Tunnel boring Z3 B11
26
28
30
32
34
36
38
40
42
44
46
48
50
52

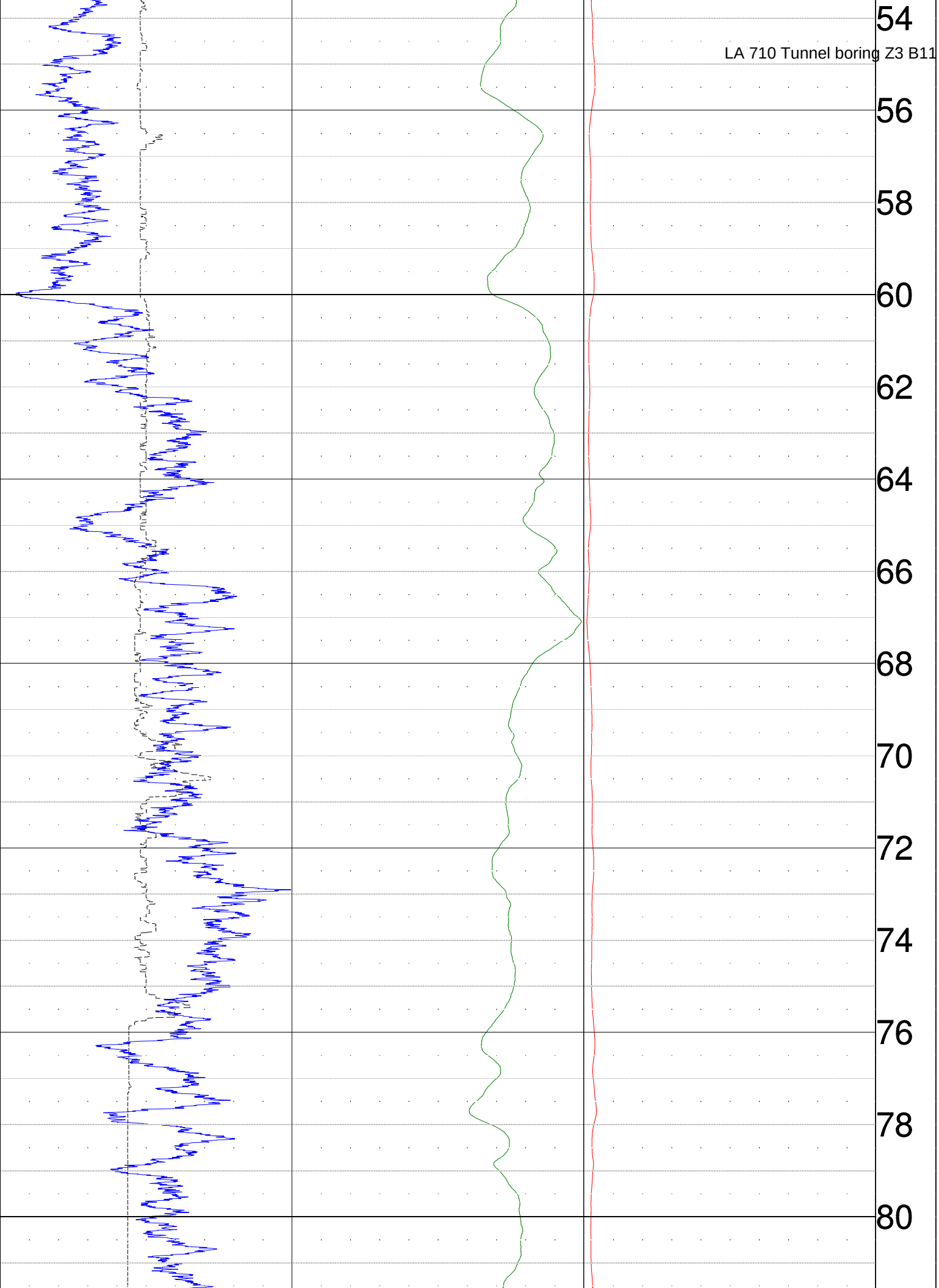
LA 710 Tunnel boring Z3 B11
54
56
58
60
62
64
66
68
70
72
74
76
78
80

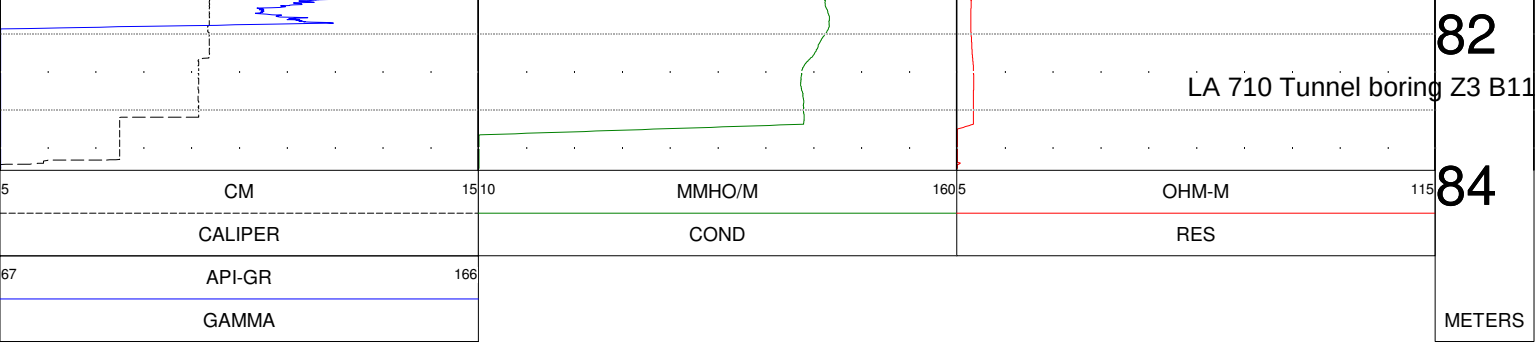
LA 710 Tunnel boring Z3 B11
82
84
5
CM
15
10
MMHO/M
160
5
OHM-M
115
CALIPER
COND
RES
67
API-GR
166
GAMMA
METERS

Table 2. LA 710 Tunnel
Boring Z3 B11
PS Suspension Log Data Summary

Top of Hole Elevation (m)	Depth (m)	Depth (ft)	Vs (m/s)	Vs (ft/s)	Vp (m/s)	Vp (ft/s)	γ	ρ(Vp) (g/cc)	ρ(Vp) (lb/ft^3)	G (GPa)	E (GPa)	K (GPa)	G ($10^3 lb/ft^2$)	E ($10^3 lb/ft^2$)	K ($10^3 lb/ft^2$)
Not Provided	3.5	11.5		NA	481	1577	NA	NA	NA	NA	NA	NA	NA	NA	NA
	4	13.1	253	828	556	1823	NA	NA	NA	NA	NA	NA	NA	NA	NA
	4.5	14.8	301	988	649	2130	NA	NA	NA	NA	NA	NA	NA	NA	NA
	5	16.4	340	1116	704	2310	NA	NA	NA	NA	NA	NA	NA	NA	NA
	5.5	18.0	379	1243	694	2278	NA	NA	NA	NA	NA	NA	NA	NA	NA
	5.9	19.4	376	1233	633	2076	NA	NA	NA	NA	NA	NA	NA	NA	NA
	6.4	21.0	360	1180	556	1823	NA	NA	NA	NA	NA	NA	NA	NA	NA
	7	23.0	316	1038	556	1823	NA	NA	NA	NA	NA	NA	NA	NA	NA
	7.5	24.6	316	1038	571	1875	NA	NA	NA	NA	NA	NA	NA	NA	NA
	8	26.2	307	1006	524	1718	NA	NA	NA	NA	NA	NA	NA	NA	NA
	8.5	27.9	316	1038	585	1919	NA	NA	NA	NA	NA	NA	NA	NA	NA
	9	29.5	382	1252	730	2395	NA	NA	NA	NA	NA	NA	NA	NA	NA
	9.5	31.2	410	1345	685	2247	NA	NA	NA	NA	NA	NA	NA	NA	NA
	9.9	32.5	397	1302	676	2217	NA	NA	NA	NA	NA	NA	NA	NA	NA
	10	32.8	382	1252	641	2103	NA	NA	NA	NA	NA	NA	NA	NA	NA
	10.4	34.1	376	1233	625	2051	NA	NA	NA	NA	NA	NA	NA	NA	NA
	10.5	34.4	362	1189	602	1976	NA	NA	NA	NA	NA	NA	NA	NA	NA
	11	36.1	368	1206	595	1953	NA	NA	NA	NA	NA	NA	NA	NA	NA
	11	36.1	355	1163	617	2025	NA	NA	NA	NA	NA	NA	NA	NA	NA
	11.5	37.7	336	1101	581	1907	NA	NA	NA	NA	NA	NA	NA	NA	NA
	11.5	37.7	355	1163	641	2103	NA	NA	NA	NA	NA	NA	NA	NA	NA
	12	39.4	329	1079	568	1864	NA	NA	NA	NA	NA	NA	NA	NA	NA
	12	39.4	340	1116	606	1988	NA	NA	NA	NA	NA	NA	NA	NA	NA
	12.5	41.0	355	1163	641	2103	NA	NA	NA	NA	NA	NA	NA	NA	NA
	12.5	41.0	329	1079	575	1886	NA	NA	NA	NA	NA	NA	NA	NA	NA
	12.9	42.3	350	1147	599	1965	NA	NA	NA	NA	NA	NA	NA	NA	NA
	13	42.7	397	1302	725	2377	NA	NA	NA	NA	NA	NA	NA	NA	NA
	13.4	44.0	397	1302	704	2310	NA	NA	NA	NA	NA	NA	NA	NA	NA
	13.5	44.3	413	1356	794	2604	NA	NA	NA	NA	NA	NA	NA	NA	NA
	13.9	45.6	410	1345	763	2504	NA	NA	NA	NA	NA	NA	NA	NA	NA
	14	45.9	424	1390	833	2734	NA	NA	NA	NA	NA	NA	NA	NA	NA
	14.4	47.2	417	1367	781	2563	NA	NA	NA	NA	NA	NA	NA	NA	NA
	14.4	47.2	424	1390	885	2903	NA	NA	NA	NA	NA	NA	NA	NA	NA
	14.4	47.2	420	1379	877	2878	NA	NA	NA	NA	NA	NA	NA	NA	NA
	14.9	48.9	427	1402	781	2563	NA	NA	NA	NA	NA	NA	NA	NA	NA
	15	49.2	397	1302	746	2448	NA	NA	NA	NA	NA	NA	NA	NA	NA
	15.5	50.9	394	1292	735	2412	NA	NA	NA	NA	NA	NA	NA	NA	NA

γ = Poisson's Ratio ρ(Vp) = Vp-derived density G = Shear Modulus E = Young's Modulus K = Bulk Modulus
Shaded cells denote questionable data.

Table 2. LA 710 Tunnel
Boring Z3 B11
PS Suspension Log Data Summary

Top of Hole Elevation (m)	Depth (m)	Depth (ft)	Vs (m/s)	Vs (ft/s)	Vp (m/s)	Vp (ft/s)	γ	ρ(Vp) (g/cc)	ρ(Vp) (lb/ft^3)	G (GPa)	E (GPa)	K (GPa)	G ($10^3 lb/ft^2$)	E ($10^3 lb/ft^2$)	K ($10^3 lb/ft^2$)
	15.5	50.9	397	1302	680	2232	NA	NA	NA	NA	NA	NA	NA	NA	NA
	16	52.5	376	1233	781	2563	NA	NA	NA	NA	NA	NA	NA	NA	NA
	16	52.5	417	1367	794	2604	NA	NA	NA	NA	NA	NA	NA	NA	NA
	16.5	54.1	391	1282	781	2563	NA	NA	NA	NA	NA	NA	NA	NA	NA
	16.5	54.1	417	1367	725	2377	NA	NA	NA	NA	NA	NA	NA	NA	NA
	17	55.8	407	1334	735	2412	NA	NA	NA	NA	NA	NA	NA	NA	NA
	17	55.8	413	1356	775	2543	NA	NA	NA	NA	NA	NA	NA	NA	NA
	17.5	57.4	400	1312	746	2448	NA	NA	NA	NA	NA	NA	NA	NA	NA
	17.5	57.4	397	1302	690	2263	NA	NA	NA	NA	NA	NA	NA	NA	NA
	17.5	57.4	392	1287	685	2247	NA	NA	NA	NA	NA	NA	NA	NA	NA
	18	59.1	420	1379	758	2485	NA	NA	NA	NA	NA	NA	NA	NA	NA
	18	59.1	388	1272	704	2310	NA	NA	NA	NA	NA	NA	NA	NA	NA
	18.5	60.7	435	1426	847	2780	NA	NA	NA	NA	NA	NA	NA	NA	NA
	18.5	60.7	417	1367	671	2202	NA	NA	NA	NA	NA	NA	NA	NA	NA
	18.9	62.0	424	1390	806	2646	NA	NA	NA	NA	NA	NA	NA	NA	NA
	18.9	62.0	439	1439	840	2757	NA	NA	NA	NA	NA	NA	NA	NA	NA
	19.4	63.6	424	1390	787	2583	NA	NA	NA	NA	NA	NA	NA	NA	NA
	19.5	64.0	439	1439	781	2563	NA	NA	NA	NA	NA	NA	NA	NA	NA
	19.9	65.3	413	1356	735	2412	NA	NA	NA	NA	NA	NA	NA	NA	NA
	20	65.6	446	1465	769	2524	NA	NA	NA	NA	NA	NA	NA	NA	NA
	20.5	67.3	435	1426	758	2485	NA	NA	NA	NA	NA	NA	NA	NA	NA
	20.8	68.2	521	1709	962	3155	NA	NA	NA	NA	NA	NA	NA	NA	NA
	21	68.9	495	1624	901	2956	NA	NA	NA	NA	NA	NA	NA	NA	NA
	21.5	70.5	568	1864	1020	3348	NA	NA	NA	NA	NA	NA	NA	NA	NA
	22	72.2	581	1907	990	3248	NA	NA	NA	NA	NA	NA	NA	NA	NA
	22.5	73.8	526	1727	917	3010	NA	NA	NA	NA	NA	NA	NA	NA	NA
	23	75.5	500	1640	893	2929	NA	NA	NA	NA	NA	NA	NA	NA	NA
	24	78.7	472	1548	847	2780	NA	NA	NA	NA	NA	NA	NA	NA	NA
	24.5	80.4	490	1608	893	2929	NA	NA	NA	NA	NA	NA	NA	NA	NA
	25	82.0	476	1562	758	2485	NA	NA	NA	NA	NA	NA	NA	NA	NA
	25.5	83.7	459	1505	855	2804	NA	NA	NA	NA	NA	NA	NA	NA	NA
	26	85.3	472	1548	990	3248	NA	NA	NA	NA	NA	NA	NA	NA	NA
	26.5	86.9	515	1691	926	3038	NA	NA	NA	NA	NA	NA	NA	NA	NA
	27	88.6	543	1783	926	3038	NA	NA	NA	NA	NA	NA	NA	NA	NA
	27.5	90.2	521	1709	901	2956	NA	NA	NA	NA	NA	NA	NA	NA	NA
	28	91.9	505	1657	847	2780	NA	NA	NA	NA	NA	NA	NA	NA	NA
	28.5	93.5	476	1562	855	2804	NA	NA	NA	NA	NA	NA	NA	NA	NA

γ = Poisson's Ratio ρ(Vp) = Vp-derived density G = Shear Modulus E = Young's Modulus K = Bulk Modulus
Shaded cells denote questionable data.

Table 2. LA 710 Tunnel
Boring Z3 B11
PS Suspension Log Data Summary

Top of Hole Elevation (m)	Depth (m)	Depth (ft)	Vs (m/s)	Vs (ft/s)	Vp (m/s)	Vp (ft/s)	γ	ρ(Vp) (g/cc)	ρ(Vp) (lb/ft^3)	G (GPa)	E (GPa)	K (GPa)	G ($10^3 lb/ft^2$)	E ($10^3 lb/ft^2$)	K ($10^3 lb/ft^2$)
	29	95.1	485	1593	741	2430	NA	NA	NA	NA	NA	NA	NA	NA	NA
	29.5	96.8	500	1640	840	2757	NA	NA	NA	NA	NA	NA	NA	NA	NA
	30	98.4	510	1674	833	2734	NA	NA	NA	NA	NA	NA	NA	NA	NA
	30.5	100.1	485	1593	806	2646	NA	NA	NA	NA	NA	NA	NA	NA	NA
	31	101.7	463	1519	1020	3348	NA	NA	NA	NA	NA	NA	NA	NA	NA
	31.5	103.3	485	1593	781	2563	NA	NA	NA	NA	NA	NA	NA	NA	NA
	32	105.0	581	1907	980	3217	NA	NA	NA	NA	NA	NA	NA	NA	NA
	32.5	106.6	625	2051	1053	3454	NA	NA	NA	NA	NA	NA	NA	NA	NA
	33	108.3	595	1953	1042	3418	NA	NA	NA	NA	NA	NA	NA	NA	NA
	33.4	109.6	581	1907	1075	3528	NA	NA	NA	NA	NA	NA	NA	NA	NA
	34	111.5	562	1843	1099	3605	NA	NA	NA	NA	NA	NA	NA	NA	NA
	34.4	112.9	617	2025	1149	3771	NA	NA	NA	NA	NA	NA	NA	NA	NA
	35	114.8	694	2278	1220	4001	NA	NA	NA	NA	NA	NA	NA	NA	NA
	35.5	116.5	667	2187	1190	3906	NA	NA	NA	NA	NA	NA	NA	NA	NA
	36	118.1	658	2158	1149	3771	NA	NA	NA	NA	NA	NA	NA	NA	NA
	36.5	119.8	667	2187	1190	3906	NA	NA	NA	NA	NA	NA	NA	NA	NA
	37	121.4	633	2076	1064	3490	NA	NA	NA	NA	NA	NA	NA	NA	NA
	37.5	123.0	625	2051	1042	3418	NA	NA	NA	NA	NA	NA	NA	NA	NA
	38	124.7	658	2158	1136	3728	NA	NA	NA	NA	NA	NA	NA	NA	NA
	38.5	126.3	658	2158	1149	3771	NA	NA	NA	NA	NA	NA	NA	NA	NA
	39	128.0	704	2310	1190	3906	NA	NA	NA	NA	NA	NA	NA	NA	NA
	39.5	129.6	735	2412	1316	4317	NA	NA	NA	NA	NA	NA	NA	NA	NA
	40	131.2	610	2001	1064	3490	NA	NA	NA	NA	NA	NA	NA	NA	NA
	40.5	132.9	532	1745	962	3155	NA	NA	NA	NA	NA	NA	NA	NA	NA
	41	134.5	526	1727	917	3010	NA	NA	NA	NA	NA	NA	NA	NA	NA
	41.5	136.2	495	1624	893	2929	NA	NA	NA	NA	NA	NA	NA	NA	NA
	42	137.8	490	1608	1099	3605	NA	NA	NA	NA	NA	NA	NA	NA	NA
	42.5	139.4	543	1783	1220	4001	NA	NA	NA	NA	NA	NA	NA	NA	NA
	43	141.1	581	1907	1149	3771	NA	NA	NA	NA	NA	NA	NA	NA	NA
	43.5	142.7	575	1886	1053	3454	NA	NA	NA	NA	NA	NA	NA	NA	NA
	44	144.4	575	1886	1000	3281	NA	NA	NA	NA	NA	NA	NA	NA	NA
	44.5	146.0	617	2025	1176	3860	NA	NA	NA	NA	NA	NA	NA	NA	NA
	45	147.6	602	1976	1220	4001	NA	NA	NA	NA	NA	NA	NA	NA	NA
	45.5	149.3	625	2051	1250	4101	NA	NA	NA	NA	NA	NA	NA	NA	NA
	46	150.9	625	2051	1205	3953	NA	NA	NA	NA	NA	NA	NA	NA	NA
	46.5	152.6	595	1953	1149	3771	NA	NA	NA	NA	NA	NA	NA	NA	NA
	47	154.2	562	1843	1111	3645	NA	NA	NA	NA	NA	NA	NA	NA	NA

γ = Poisson's Ratio ρ(Vp) = Vp-derived density G = Shear Modulus E = Young's Modulus K = Bulk Modulus
Shaded cells denote questionable data.

Table 2. LA 710 Tunnel
Boring Z3 B11
PS Suspension Log Data Summary

Top of Hole Elevation (m)	Depth (m)	Depth (ft)	Vs (m/s)	Vs (ft/s)	Vp (m/s)	Vp (ft/s)	γ	ρ(Vp) (g/cc)	ρ(Vp) (lb/ft^3)	G (GPa)	E (GPa)	K (GPa)	G ($10^3 lb/ft^2$)	E ($10^3 lb/ft^2$)	K ($10^3 lb/ft^2$)
	47.5	155.8	581	1907	1220	4001	NA	NA	NA	NA	NA	NA	NA	NA	NA
	48	157.5	538	1764	1099	3605	NA	NA	NA	NA	NA	NA	NA	NA	NA
	48.4	158.8	581	1907	1020	3348	NA	NA	NA	NA	NA	NA	NA	NA	NA
	48.9	160.4	595	1953	1136	3728	NA	NA	NA	NA	NA	NA	NA	NA	NA
	49.5	162.4	610	2001	1099	3605	NA	NA	NA	NA	NA	NA	NA	NA	NA
	50	164.0	595	1953	1163	3815	NA	NA	NA	NA	NA	NA	NA	NA	NA
	50.5	165.7	610	2001	1333	4374	NA	NA	NA	NA	NA	NA	NA	NA	NA
	51	167.3	463	1519	1613	5292	0.46	1.94	121.09	0.416	1.210	4.492	8683	25268	93807
	51.5	169.0	407	1334	1754	5756	0.47	2.04	127.35	0.337	0.992	5.829	7040	20722	121749
	52.1	170.9	476	1562	1786	5859	0.46	2.06	128.62	0.467	1.366	5.947	9757	28524	124199
	52.5	172.2	476	1562	1754	5756	0.46	2.04	127.35	0.463	1.351	5.662	9661	28215	118254
	53	173.9	442	1452	1786	5859	0.47	2.06	128.62	0.403	1.184	6.032	8424	24722	125975
	53.5	175.5	420	1379	1786	5859	0.47	2.06	128.62	0.364	1.070	6.085	7596	22344	127080
	53.9	176.8	413	1356	1724	5657	0.47	2.02	126.09	0.345	1.014	5.544	7203	21171	115797
	54.5	178.8	435	1426	1695	5561	0.46	2.00	124.84	0.378	1.107	5.241	7895	23129	109452
	55	180.4	435	1426	1786	5859	0.47	2.06	128.62	0.389	1.144	6.050	8134	23889	126363
	55.5	182.1	442	1452	1852	6076	0.47	2.10	131.15	0.411	1.209	6.656	8590	25251	139012
	56	183.7	467	1533	1852	6076	0.47	2.10	131.15	0.459	1.345	6.593	9581	28091	137692
	56.5	185.4	427	1402	1852	6076	0.47	2.10	131.15	0.384	1.129	6.693	8013	23588	139782
	57	187.0	521	1709	1887	6190	0.46	2.12	132.42	0.575	1.679	6.784	12017	35061	141688
	57.4	188.3	526	1727	1887	6190	0.46	2.12	132.42	0.588	1.713	6.768	12272	35780	141349
	58	190.3	526	1727	1961	6433	0.46	2.16	134.97	0.599	1.750	7.514	12508	36553	156926
	58.5	191.9	526	1727	1887	6190	0.46	2.12	132.42	0.588	1.713	6.768	12272	35780	141348
	59	193.6	463	1519	1852	6076	0.47	2.10	131.15	0.450	1.321	6.604	9404	27585	137927
	60	196.9	500	1640	1818	5965	0.46	2.08	129.88	0.520	1.518	6.184	10863	31700	129158
	60.5	198.5	549	1803	1923	6309	0.46	2.14	133.69	0.647	1.882	7.058	13503	39309	147407
	61.5	201.8	463	1519	1818	5965	0.47	2.08	129.88	0.446	1.307	6.283	9313	27294	131224
	62	203.4	485	1593	1923	6309	0.47	2.14	133.69	0.505	1.480	7.247	10540	30902	151358
	62	203.4	485	1593	1923	6309	0.47	2.14	133.69	0.505	1.480	7.247	10540	30902	151358
	62.5	205.1	459	1505	1923	6309	0.47	2.14	133.69	0.451	1.325	7.319	9412	27667	152862
	63	206.7	385	1262	1786	5859	0.48	2.06	128.62	0.305	0.899	6.163	6365	18786	128721
	63.5	208.3	455	1491	1786	5859	0.47	2.06	128.62	0.426	1.248	6.002	8890	26055	125354
	64	210.0	459	1505	1961	6433	0.47	2.16	134.97	0.455	1.338	7.706	9501	27954	160935
	64.5	211.6	532	1745	1923	6309	0.46	2.14	133.69	0.606	1.768	7.112	12655	36916	148538
	65	213.3	455	1491	1818	5965	0.47	2.08	129.88	0.430	1.261	6.305	8978	26334	131671
	65.5	214.9	446	1465	1786	5859	0.47	2.06	128.62	0.411	1.204	6.022	8576	25155	125774
	66	216.5	431	1414	1818	5965	0.47	2.08	129.88	0.387	1.137	6.362	8073	23738	132878

γ = Poisson's Ratio ρ(Vp) = Vp-derived density G = Shear Modulus E = Young's Modulus K = Bulk Modulus
Shaded cells denote questionable data.

Table 2. LA 710 Tunnel
Boring Z3 B11
PS Suspension Log Data Summary

Top of Hole Elevation (m)	Depth (m)	Depth (ft)	Vs (m/s)	Vs (ft/s)	Vp (m/s)	Vp (ft/s)	γ	ρ(Vp) (g/cc)	ρ(Vp) (lb/ft^3)	G (GPa)	E (GPa)	K (GPa)	G ($10^3 lb/ft^2$)	E ($10^3 lb/ft^2$)	K ($10^3 lb/ft^2$)
	66.4	217.8	431	1414	1818	5965	0.47	2.08	129.88	0.387	1.137	6.362	8073	23738	132878
	66.9	219.5	427	1402	1961	6433	0.48	2.16	134.97	0.395	1.165	7.786	8246	24328	162608
	67.5	221.5	420	1379	2000	6562	0.48	2.18	136.25	0.385	1.138	8.216	8047	23770	171600
	68	223.1	459	1505	1887	6190	0.47	2.12	132.42	0.446	1.311	6.956	9322	27380	145282
	68.5	224.7	467	1533	1961	6433	0.47	2.16	134.97	0.472	1.388	7.683	9860	28986	160457
	69	226.4	510	1674	1923	6309	0.46	2.14	133.69	0.557	1.630	7.177	11643	34047	149887
	69.5	228.0	526	1727	1961	6433	0.46	2.16	134.97	0.599	1.750	7.514	12508	36553	156926
	70	229.7	549	1803	1961	6433	0.46	2.16	134.97	0.653	1.902	7.442	13632	39734	155427
	70.5	231.3	568	1864	1852	6076	0.45	2.10	131.15	0.678	1.964	6.300	14164	41021	131580
	71	232.9	581	1907	2222	7291	0.46	2.29	142.69	0.773	2.261	10.257	16136	47223	214227
	71.5	234.6	490	1608	2000	6562	0.47	2.18	136.25	0.524	1.540	8.031	10953	32159	167725
	72	236.2	538	1764	2128	6981	0.47	2.24	140.11	0.649	1.902	9.295	13549	39722	194125
	72.5	237.9	562	1843	2083	6835	0.46	2.22	138.82	0.702	2.050	8.715	14658	42824	182026
	73	239.5	481	1577	2273	7456	0.48	2.31	143.99	0.533	1.574	11.203	11134	32882	233976
	73.5	241.1	505	1657	2083	6835	0.47	2.22	138.82	0.567	1.666	8.895	11846	34799	185774
	74	242.8	562	1843	2273	7456	0.47	2.31	143.99	0.728	2.137	10.943	15204	44622	228550
	74.5	244.4	610	2001	2273	7456	0.46	2.31	143.99	0.858	2.506	10.770	17910	52342	224941
	75	246.1	562	1843	2174	7132	0.46	2.26	141.40	0.715	2.093	9.751	14930	43722	203650
	75.5	247.7	562	1843	2128	6981	0.46	2.24	140.11	0.708	2.072	9.215	14794	43273	192464
	76	249.3	549	1803	2128	6981	0.46	2.24	140.11	0.678	1.984	9.256	14151	41441	193321
	76.5	251.0	538	1764	2041	6696	0.46	2.20	137.53	0.637	1.863	8.327	13300	38907	173902
	77	252.6	455	1491	2222	7291	0.48	2.29	142.69	0.472	1.396	10.658	9863	29159	222591
	77.4	253.9	481	1577	2083	6835	0.47	2.22	138.82	0.514	1.513	8.966	10734	31599	187257
	78	255.9	562	1843	2128	6981	0.46	2.24	140.11	0.708	2.072	9.215	14794	43273	192465
	78.4	257.2	575	1886	2222	7291	0.46	2.29	142.69	0.755	2.211	10.281	15768	46172	214719
	79	259.2		NA	2083	6835	NA	NA	NA	NA	NA	NA	NA	NA	NA
	79.5	260.8	556	1823	2128	6981	0.46	2.24	140.11	0.693	2.027	9.236	14467	42342	192901
	80	262.5	746	2448	2381	7812	0.45	2.35	146.59	1.308	3.781	11.568	27313	78963	241604
	80.5	264.1	758	2485	2222	7291	0.43	2.29	142.69	1.312	3.763	9.538	27398	78590	199212
	81.2	266.4	658	2158	2174	7132	0.45	2.26	141.40	0.980	2.842	9.397	20475	59360	196258
	81.7	268.0	633	2076	2083	6835	0.45	2.22	138.82	0.891	2.582	8.464	18603	53919	176765
	82.3	270.0	641	2103	2174	7132	0.45	2.26	141.40	0.931	2.703	9.463	19438	56463	197640

γ = Poisson's Ratio ρ(Vp) = Vp-derived density G = Shear Modulus E = Young's Modulus K = Bulk Modulus
Shaded cells denote questionable data.

Figure 1. LA 710 Tunnel
Boring Z3 B11
Downhole Interval Velocities

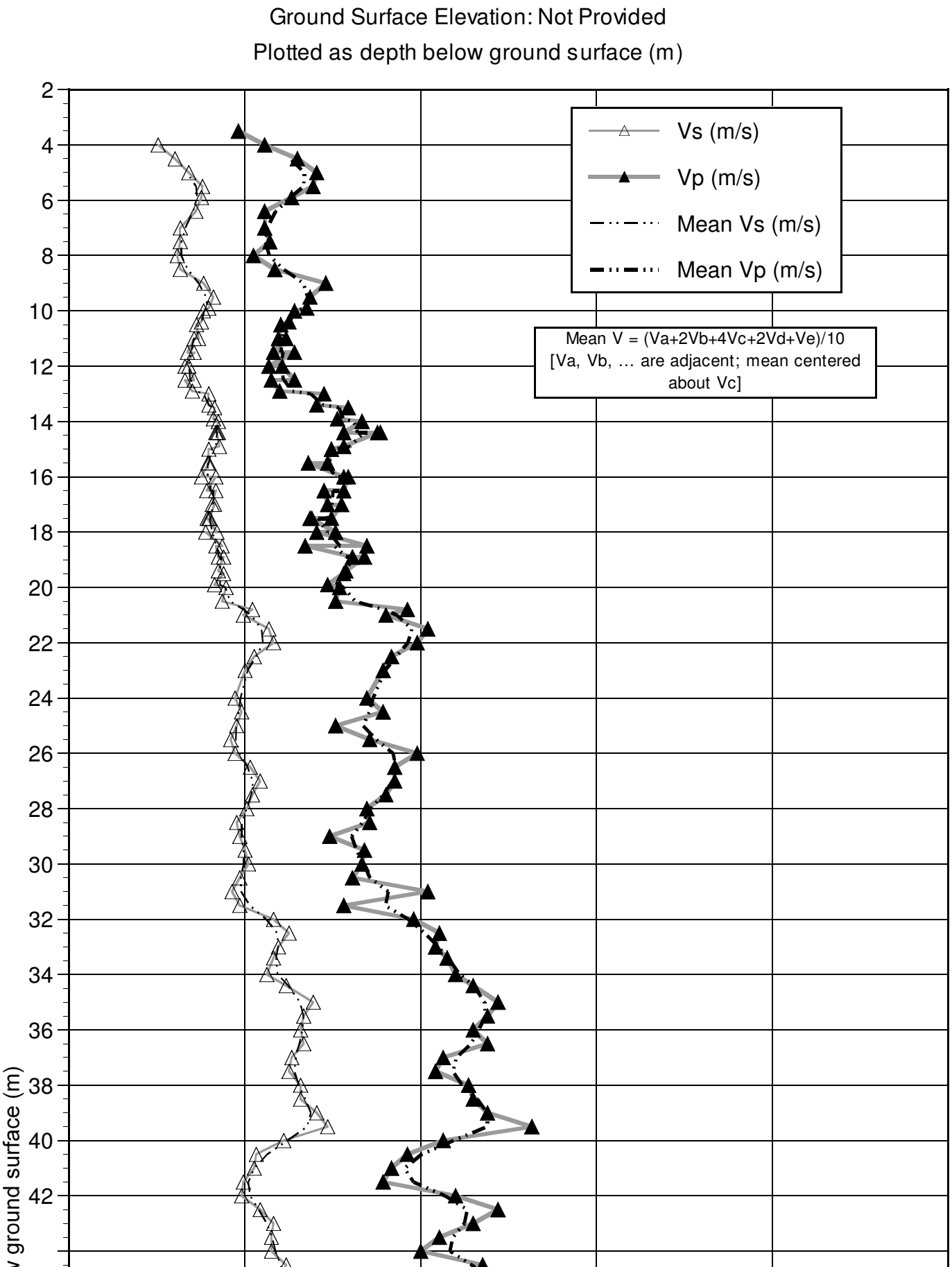

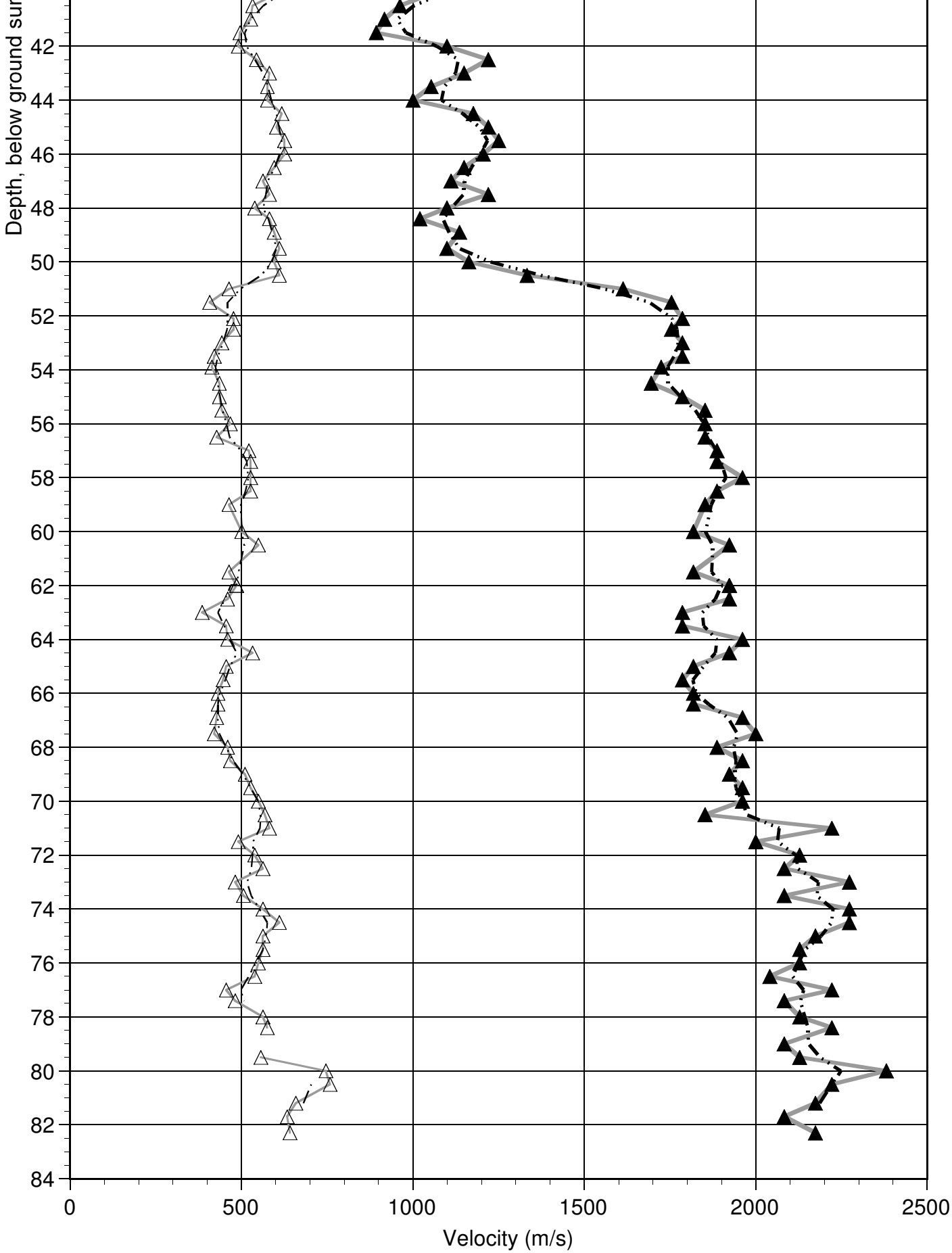
Depth, below ground surface
42
44
46
48
50
52
54
56
58
60
62
64
66
68
70
72
74
76
78
80
82
84
0
500
1000
1500
2000
2500
Velocity (m/s)

California Department of Transportation
Geophysical Services

Z3B11

COMPANY	: CALTRANS.	OTHER SERVICES:	
WELL	: Z3B11		IND-CAL.
FIELD	: LA 710 TUNNEL.		AC TEL.
COUNTY	: LA		PSLOG
STATE	: CA		
LOCATION	:		
SECTION	: None		
TOWNSHIP	: None		
RANGE	: None		
API NO.	:		
UNIQUE WELL ID.	:		
PERMANENT DATUM	: None	ELEVATION KB	: NA
LOG MEASURED FROM	: GL	ELEVATION DF	: NA
DRL MEASURED FROM	: GL	ELEVATION GL	: 0
DATE	: 1/21/09	RIG NUMBER	:
DEPTH DRILLER	: 275	LOGGER TD	:
BIT SIZE	: 98	ARRIVAL TIME	:
LOG TOP	: 4.50	DEPARTURE TIME	:
LOG BOTTOM	: 83.50	CIRC STOPPED	: 0930
CASING OD	:		
CASING BOTTOM	: NA		
CASING TYPE	: none		
BOREHOLE FLUID	: 0		
RM TEMPERATURE	: 0		
MUD RES	: 0		
MUD WEIGHT	:		
WITNESSED BY	:		
RECORDED BY	: DH/DL		
REMARKS 1	:		
REMARKS 2	: EA: 07-187900		

ALL SERVICES PROVIDED SUBJECT TO STANDARD TERMS AND CONDITIONS

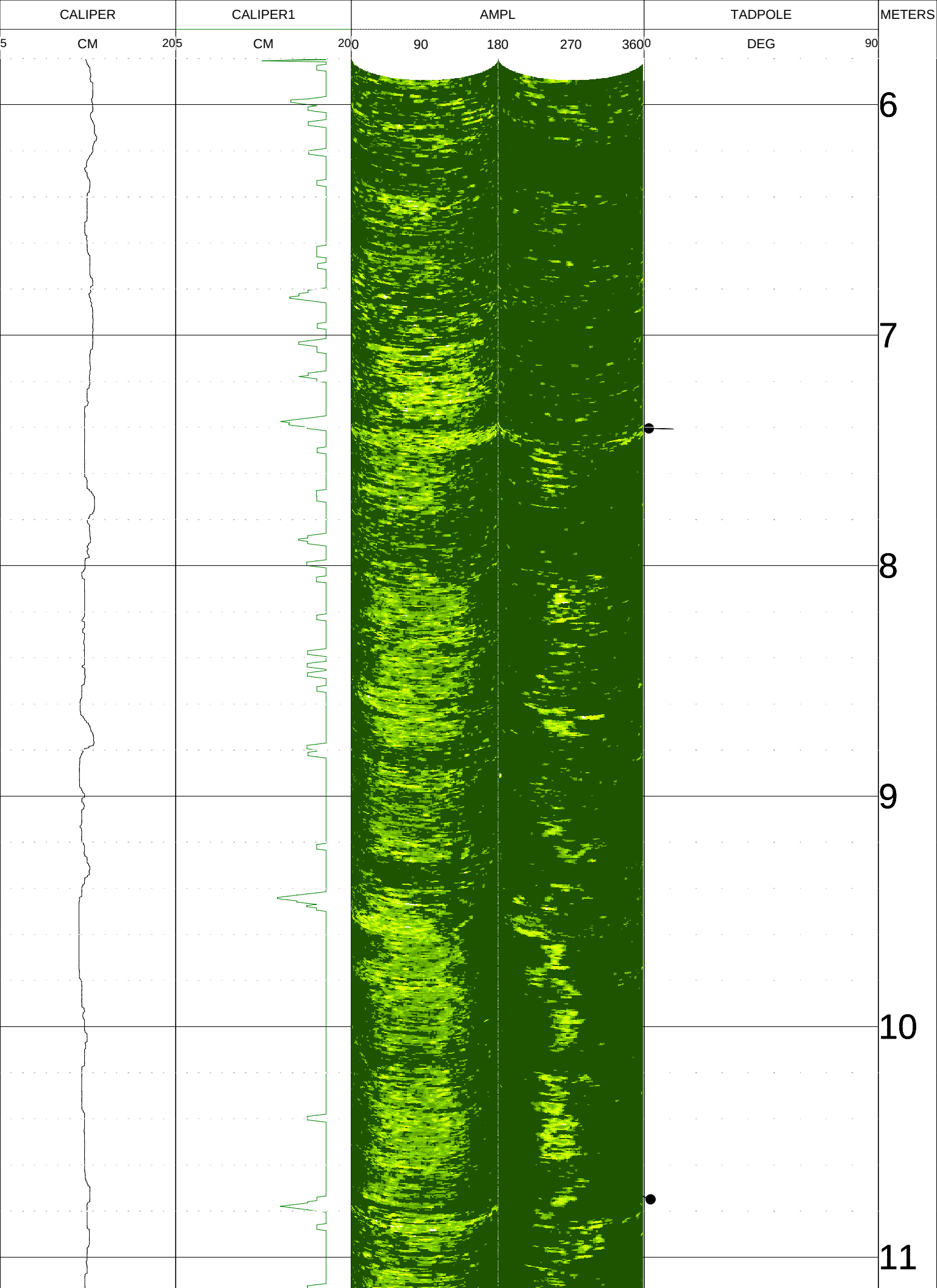
CALIPER
CALIPER1
AMPL
TADPOLE
METERS
5
CM
20
5
CM
20
0
90
180
270
360
0
DEG
90
6
7
8
9
10
11

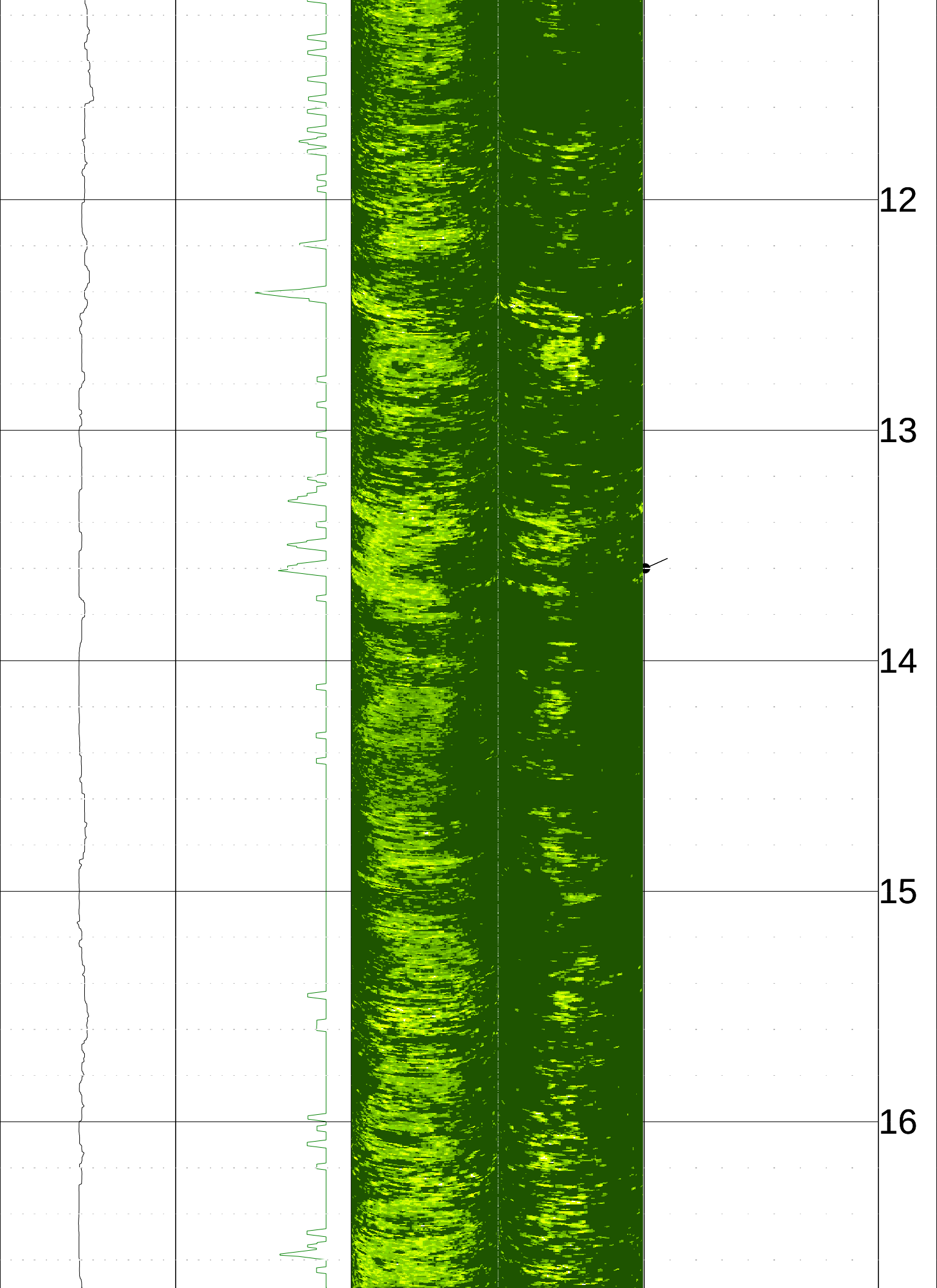
12
13
14
15
16

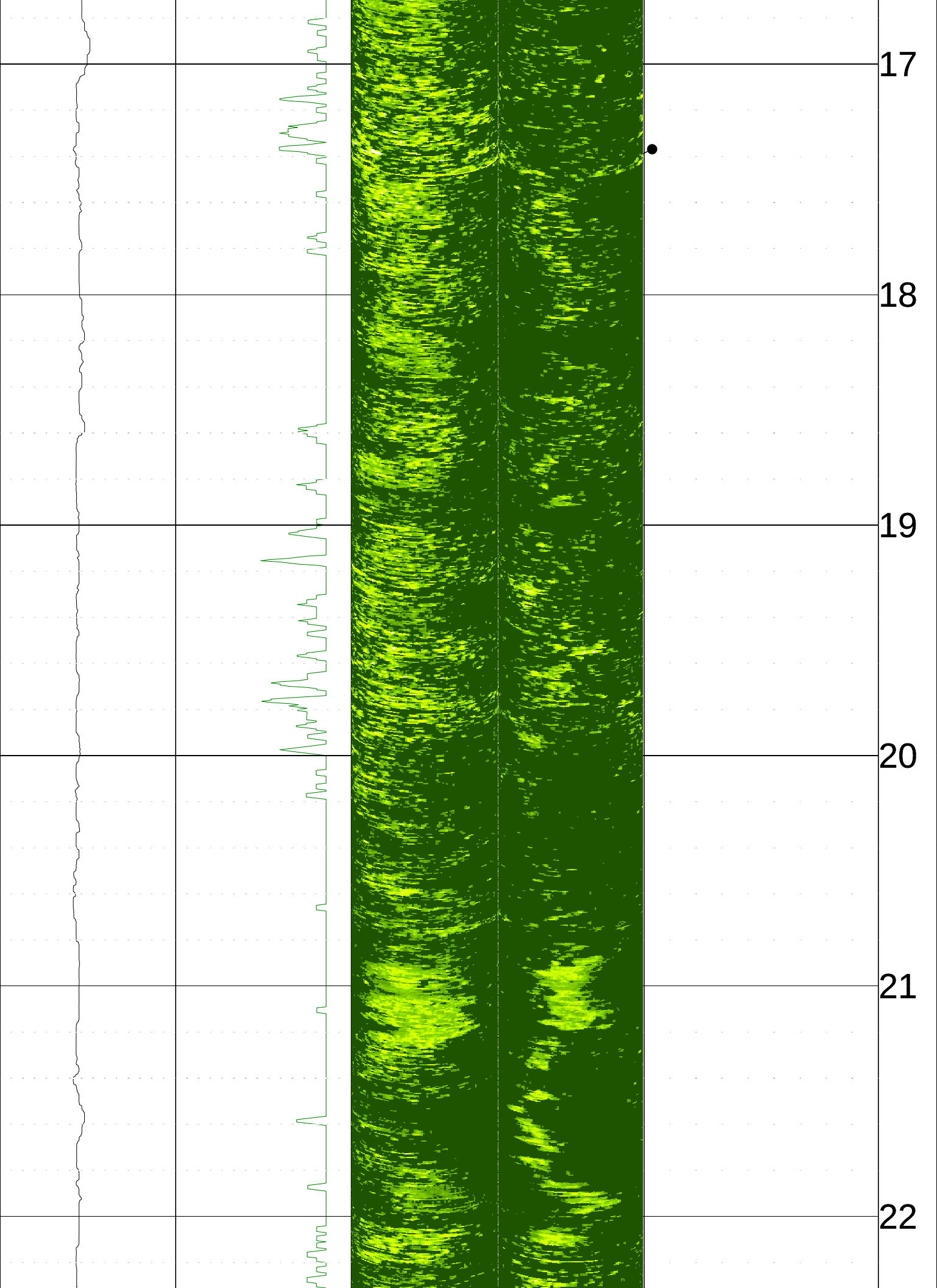
17
18
19
20
21
22

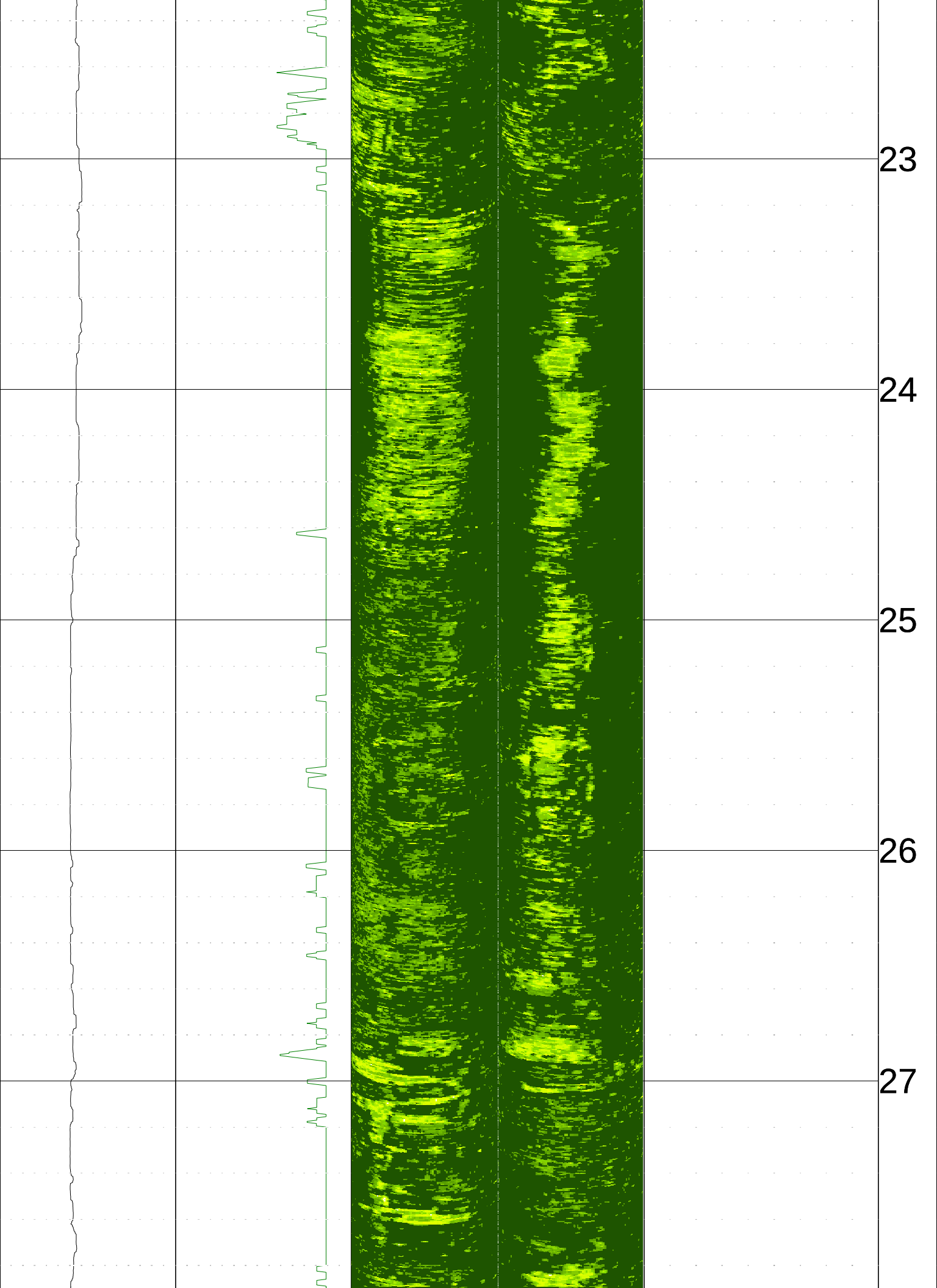
23
24
25
26
27

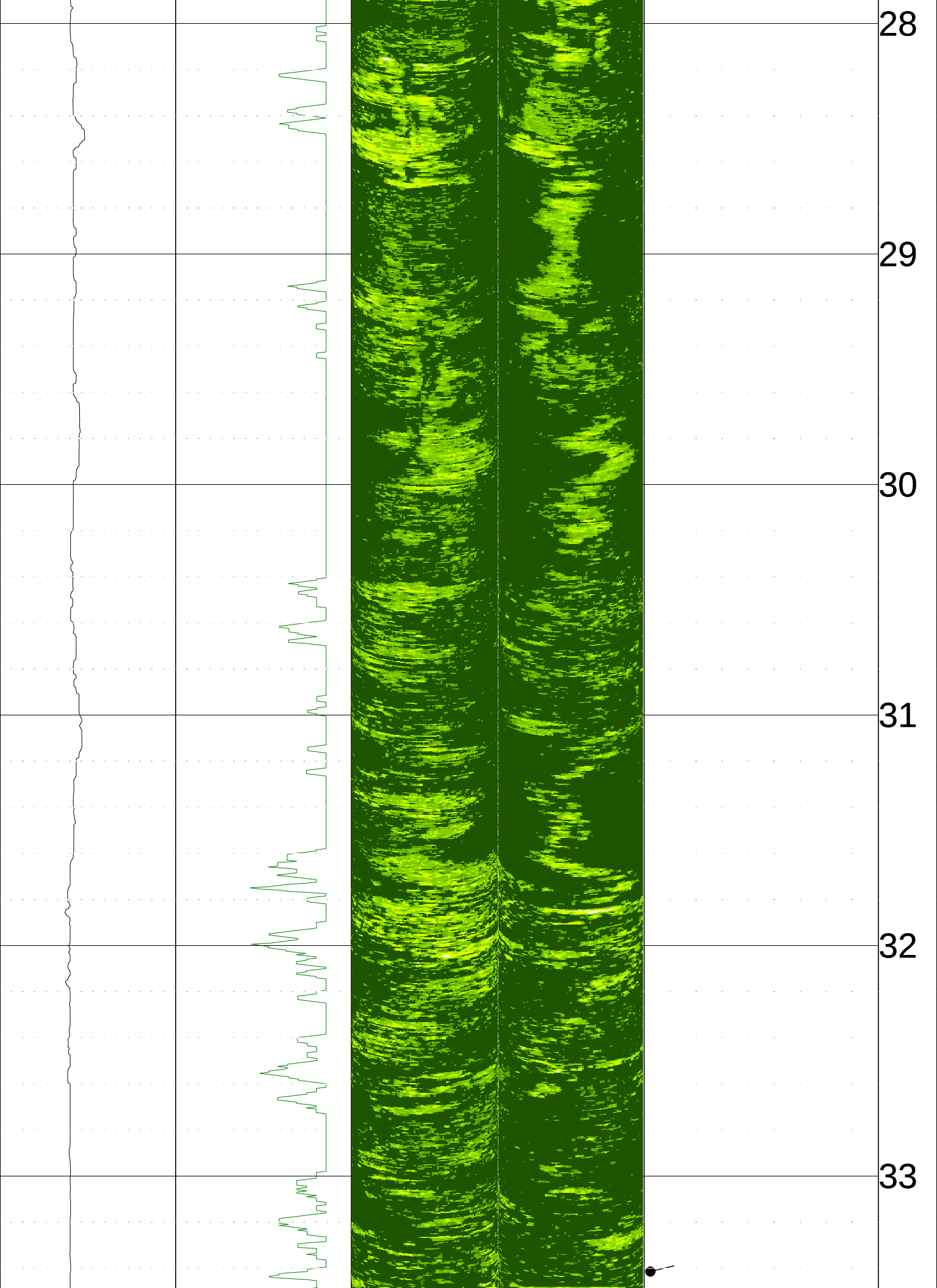
28
29
30
31
32
33

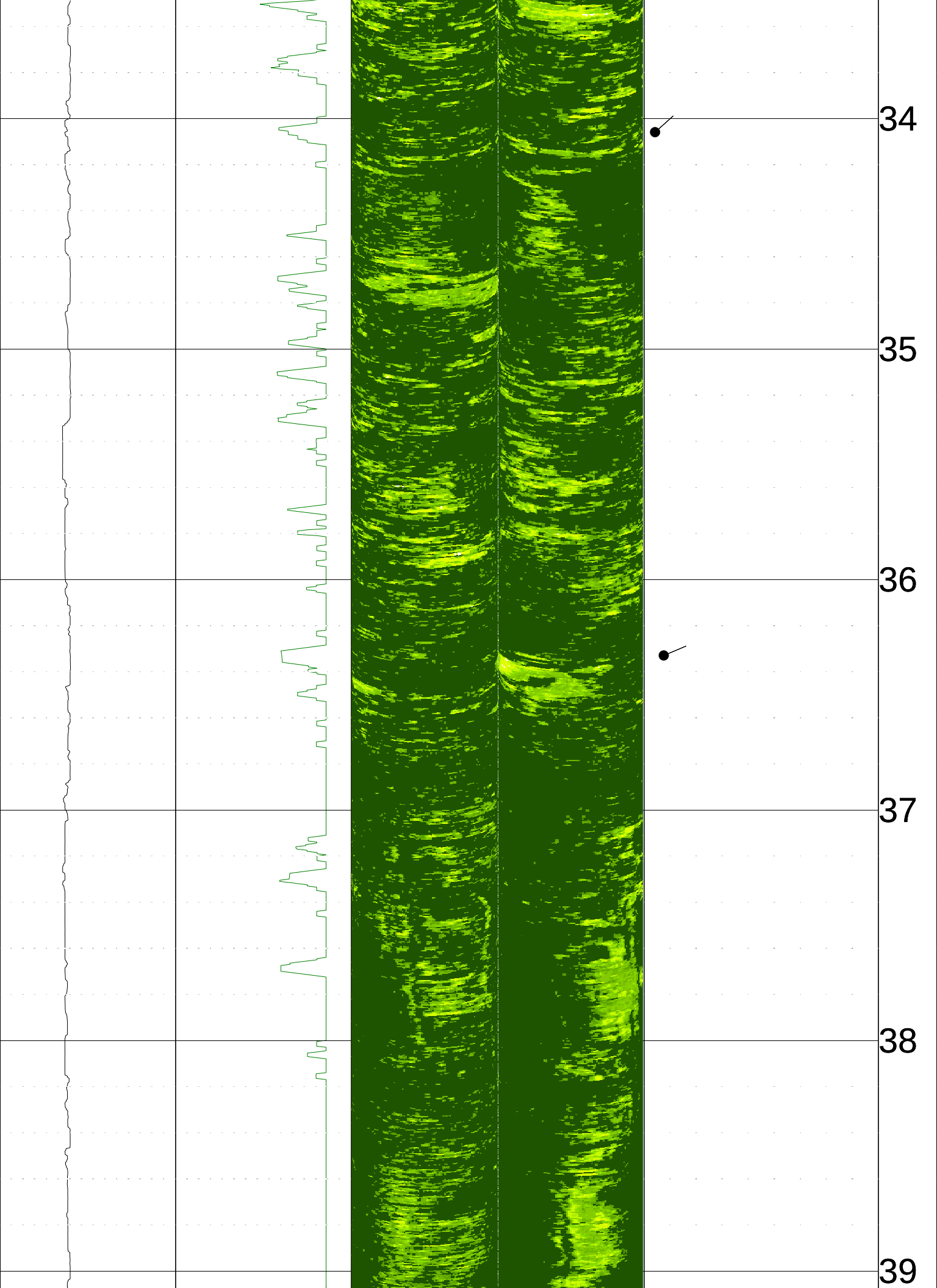
34
35
36
37
38
39

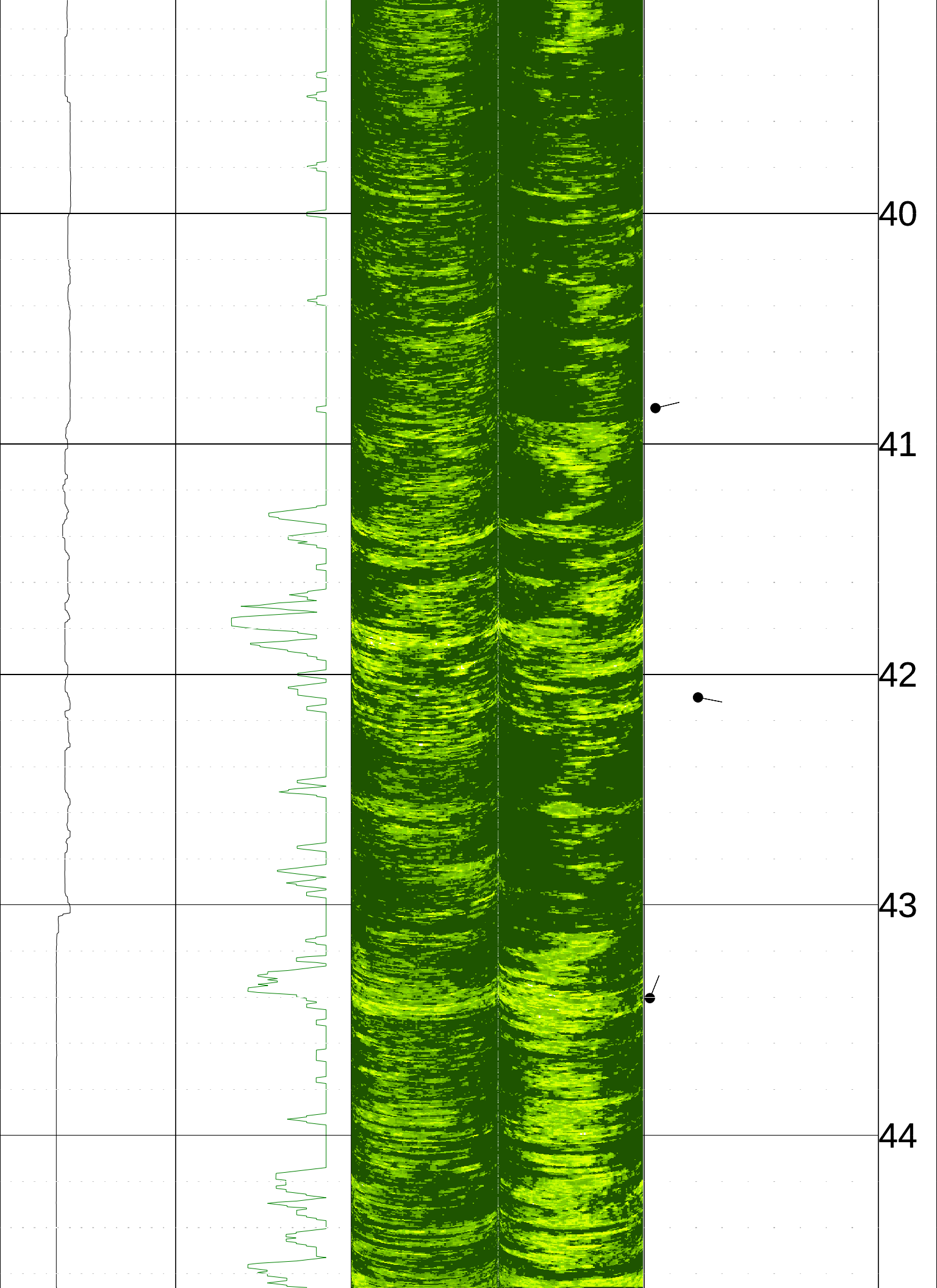
40
41
42
43
44

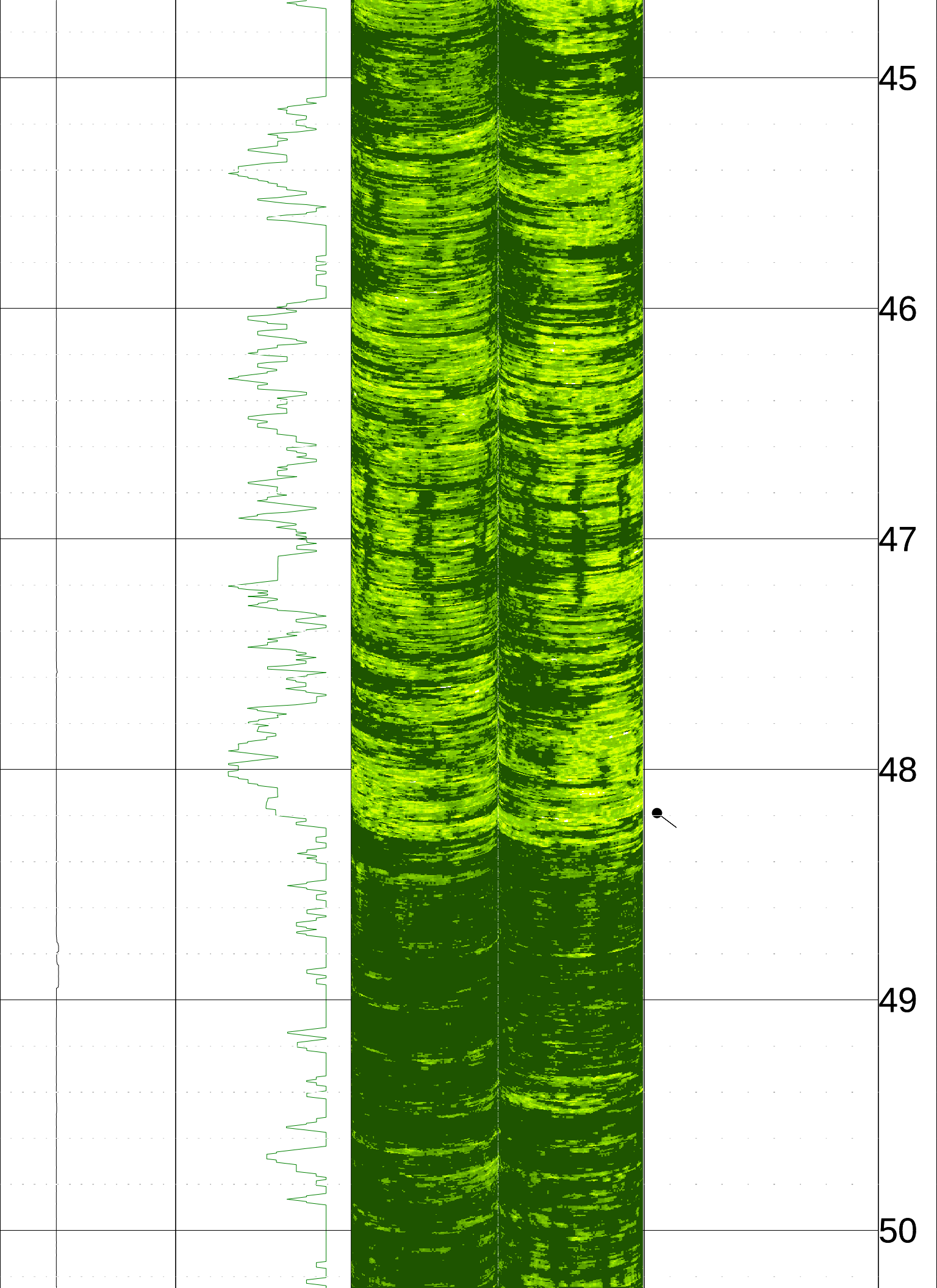
45
46
47
48
49
50

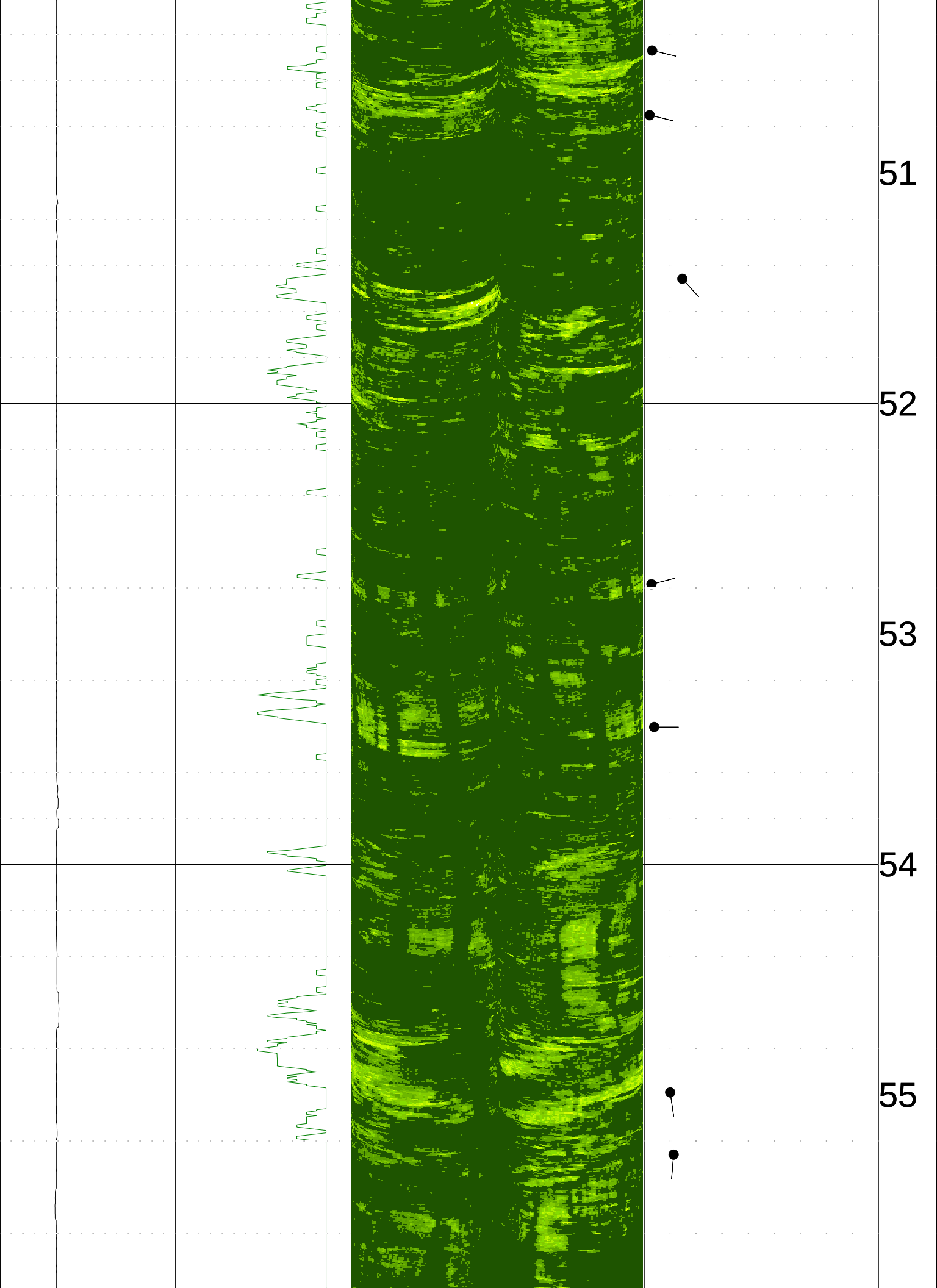
51
52
53
54
55

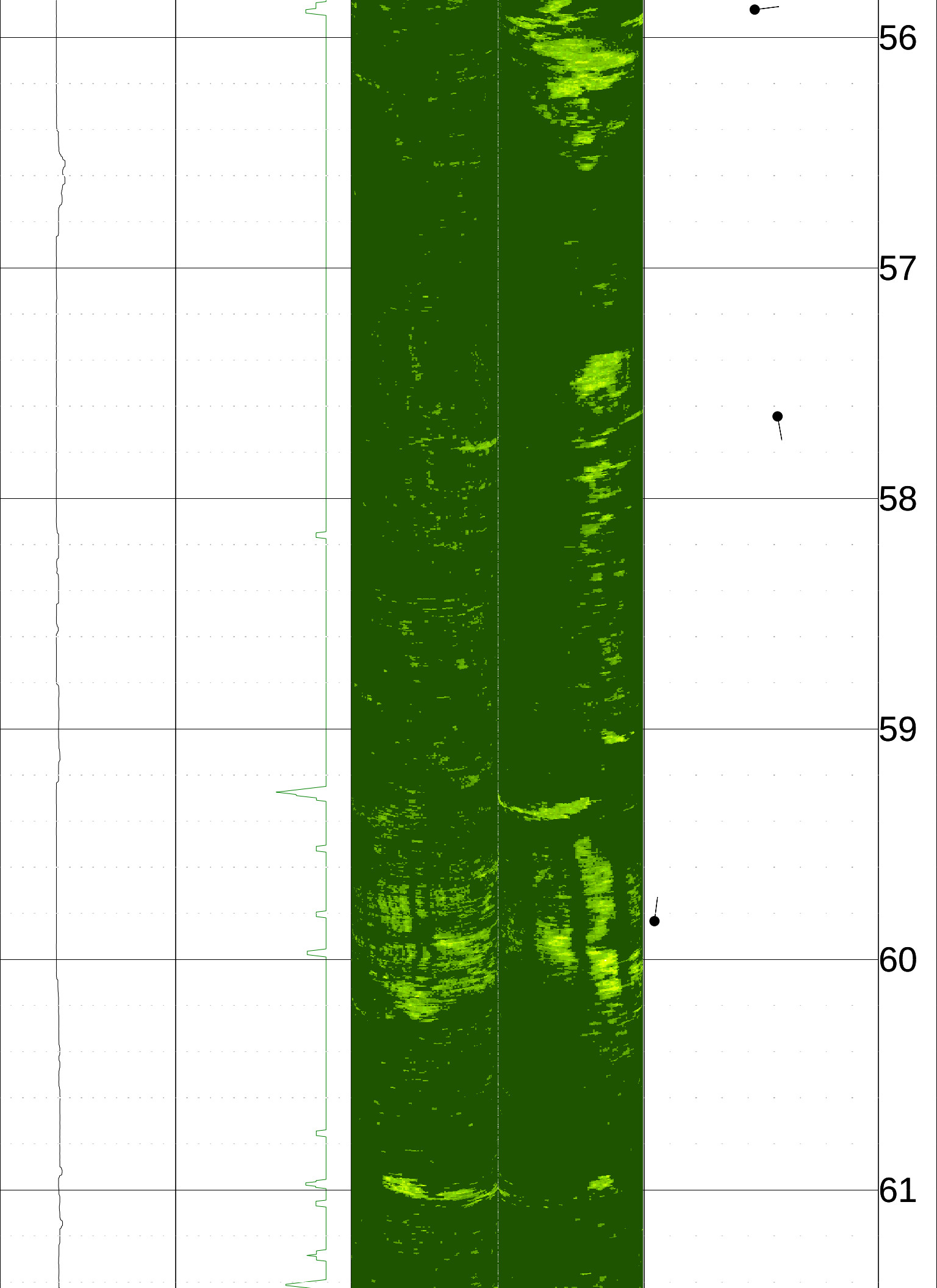
56
57
58
59
60
61

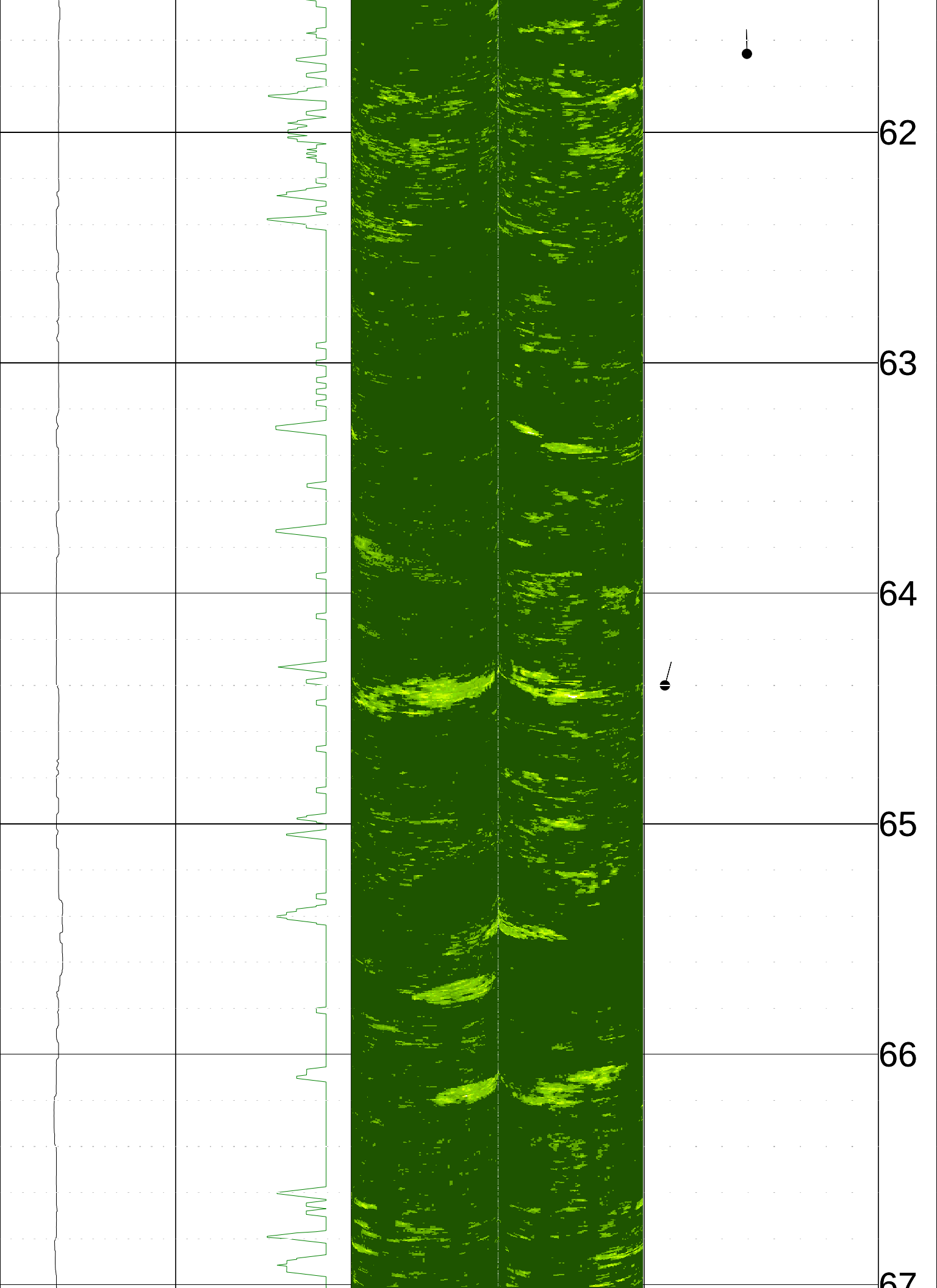
62
63
64
65
66
67

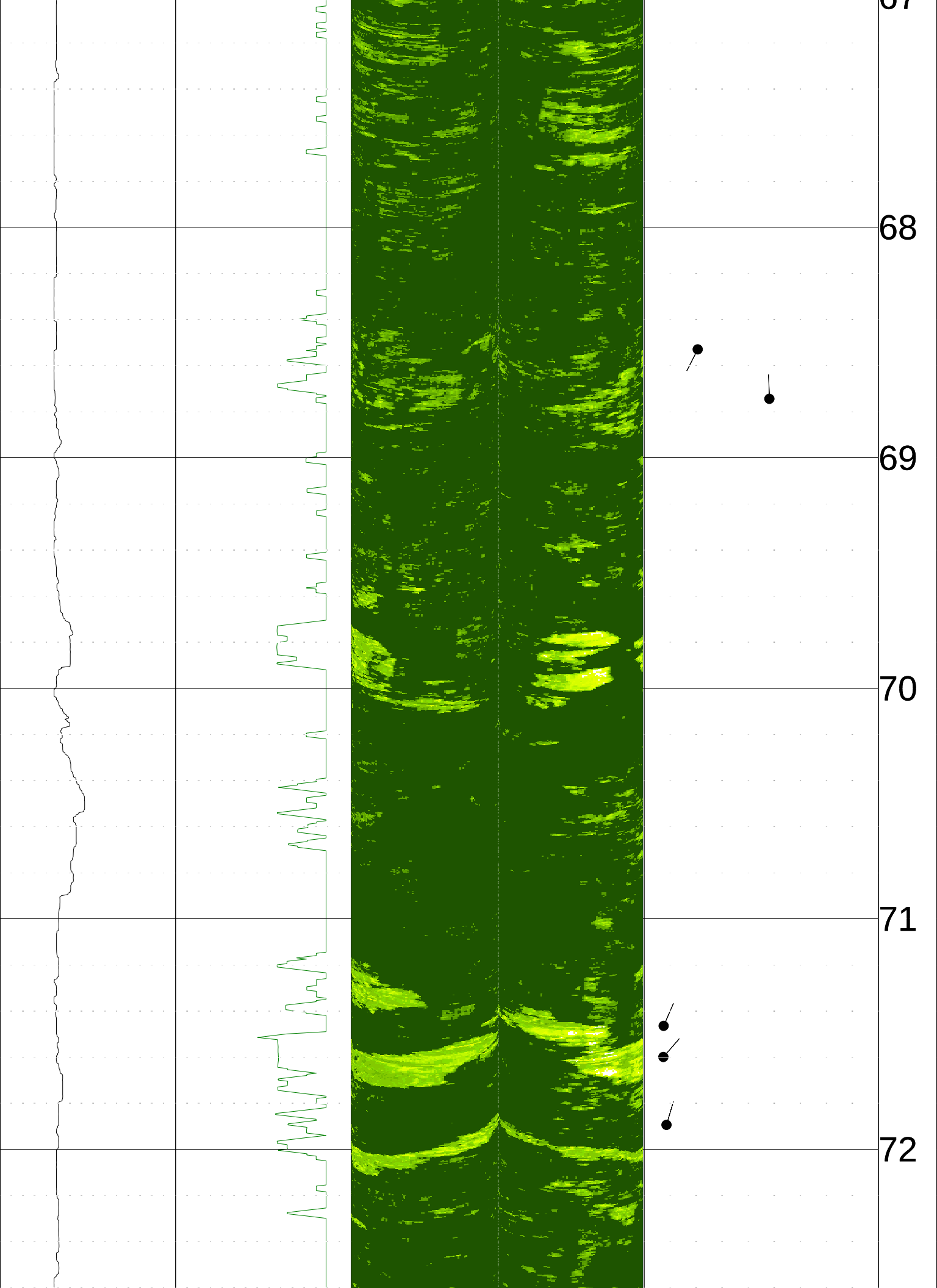
67
68
69
70
71
72

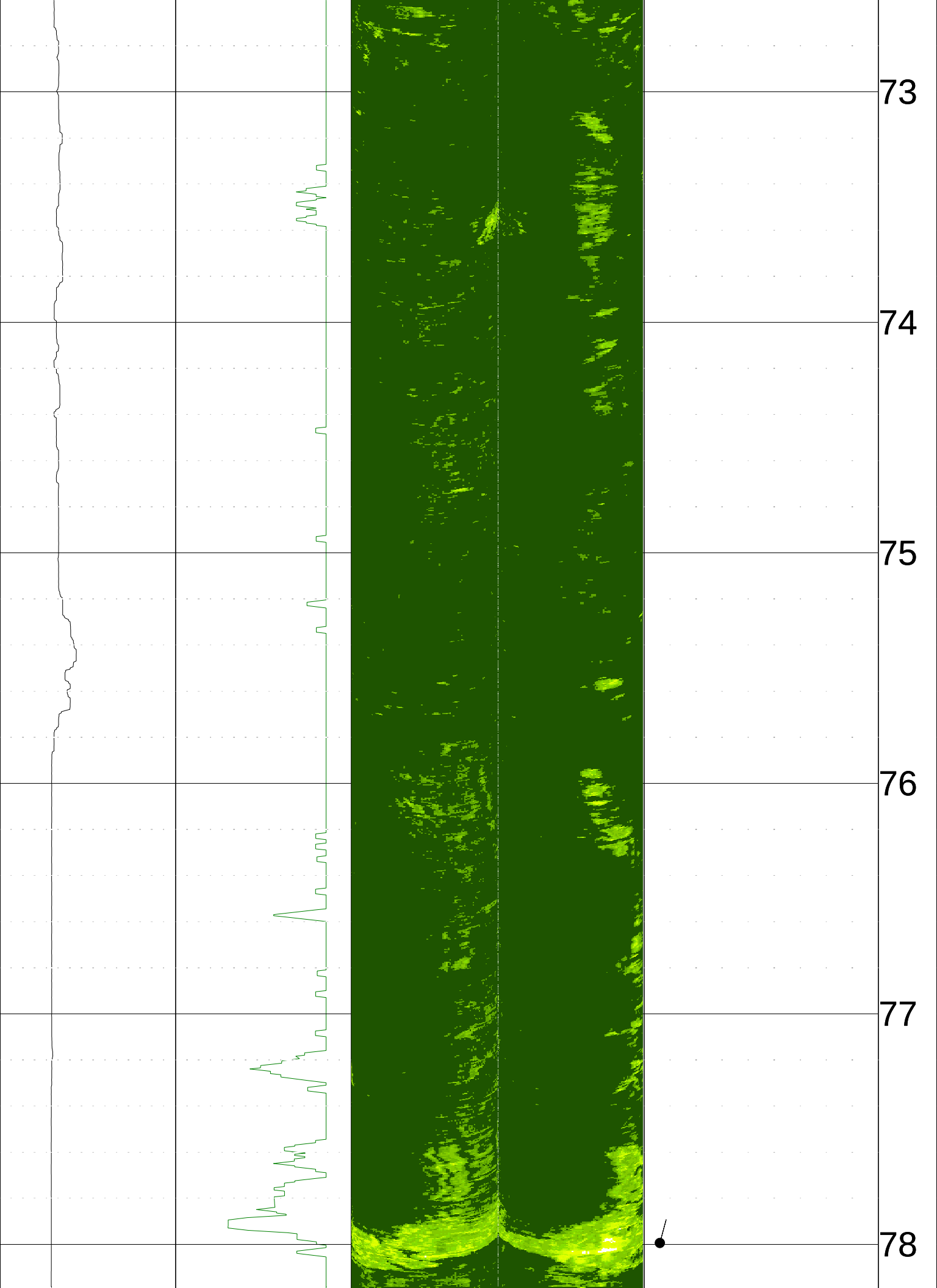
73
74
75
76
77
78

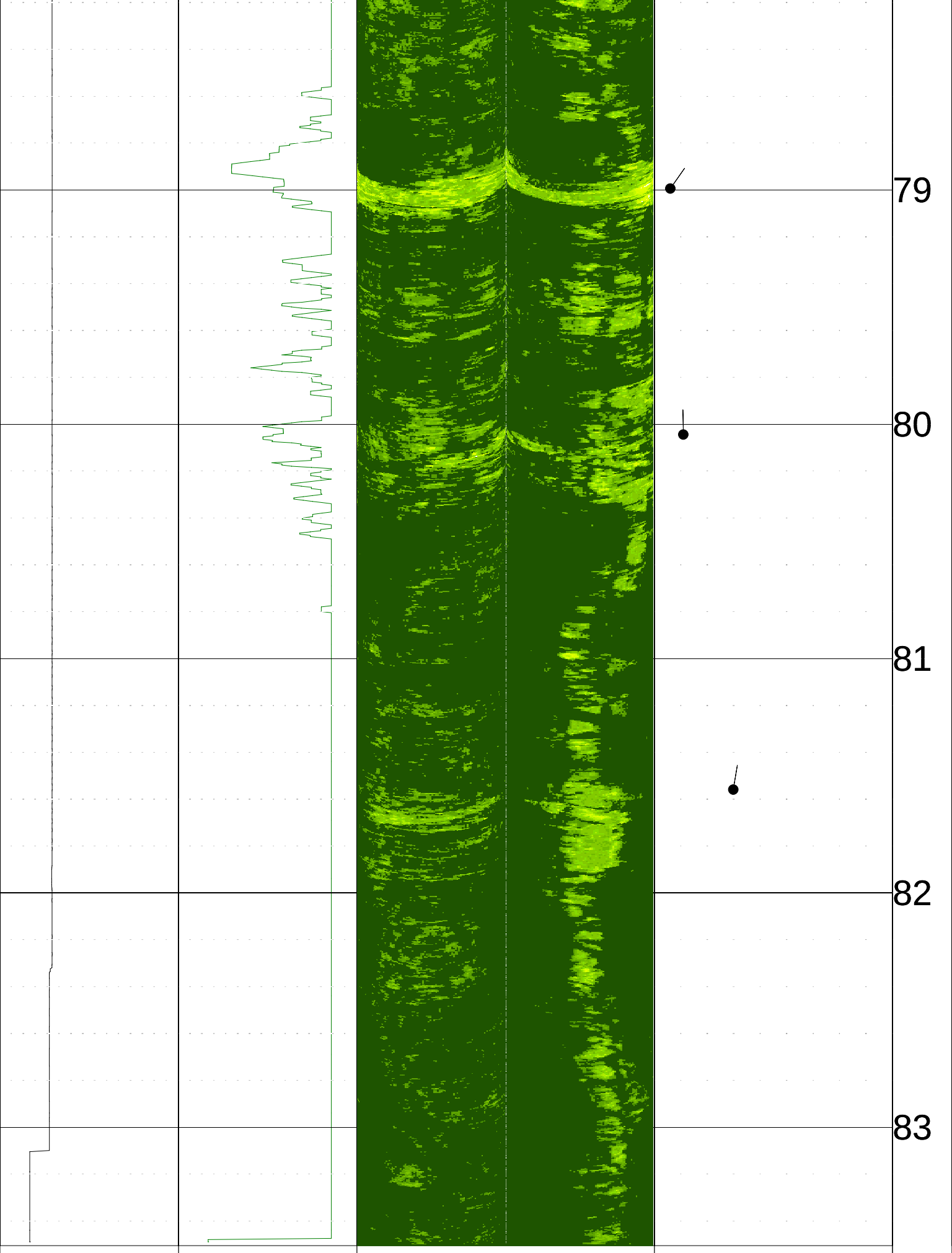
79
80
81
82
83
5
CM
20
5
CM
20
0
90
180
270
360
0
DEG
90
CALIPER
CALIPER1
AMPL
TADPOLE
METERS

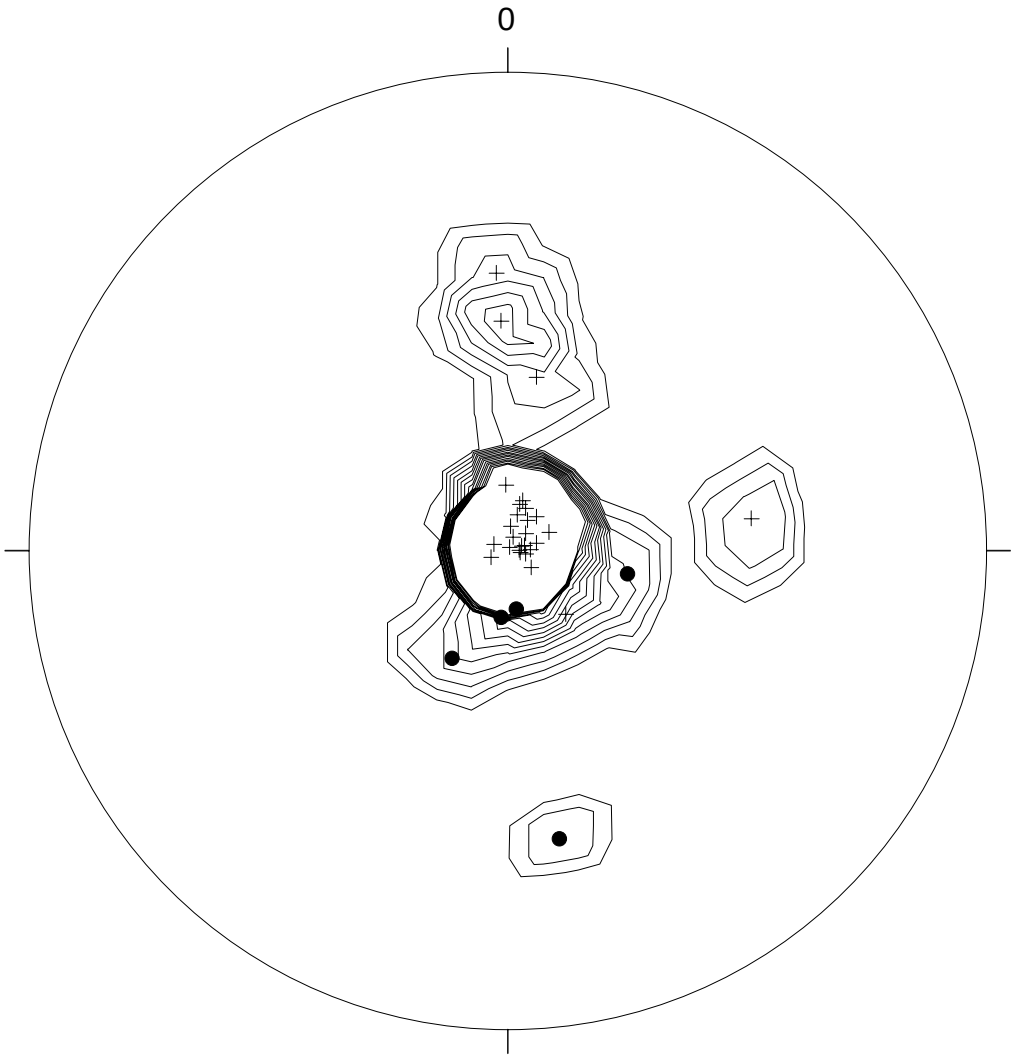

+ n=27 (P)
• n=5 (P)

LA 710 Tunnel, boring Z3 B11

Stereonet contour plot of poles to planes,
Both bedding and fractures

n=32
max. dens.= 77.95 (at 180/ 90)
min. dens.=0.00
Contours at every integer between
1 and 15, inclusive:
(Multiples of random distribution)

Apparent bedding denoted as cross
Apparent fractures denoted as solid circle
Plotted on upper hemisphere

APPENDIX B.1.2

Seismic Reflection and Surface Wave Data

Appendix B.1.2
Seismic Reflection and Surface Wave Data

The following data reports were prepared for the SR 710 Tunnel Technical Study Final Geotechnical Summary Report (CH2M HILL, 2010). However, only data relevant to the SR 710 North Study are provided herein as summarized in Tables B-1 and B-2. The full version of the following appendix is presented in the Technical Study (CH2M HILL, 2010).

TABLE B-1
Summary of Seismic Reflection Testing

Seismic Reflection Line	Approximate Location	City	Purpose/Feature Evaluated
Z3-G1	South Raymond Avenue (N/O E. Glenarm Street)	Pasadena	San Rafael Fault
Z3-G6	Winchester Avenue (N/O Concord Avenue)	Alhambra	Highland Park Fault
Z3-G7	Westmont Drive (S/O, Valley Boulevard)	Alhambra	Unnamed Fault
Z4-G2	Huntington Drive (SW/O N. Granada Avenue)	Alhambra	Alhambra Wash Fault
Z5-G2	East Shorb Street (E/O S. Hildalgo St.)	Alhambra	Alhambra Wash Fault
Z5-G3	Edgewood Drive (S/O W. Valley Blvd.)	Alhambra	Highland Park Fault

Source: CH2M HILL, 2010 (EA-07-187900)

TABLE B-2
Summary of Multichannel Analyses of Surface Waves and ReMi Testing

Number	MASW Line	Approximate Location	City
1	Z1-S20	Highbury Avenue (S/O Valley Boulevard)	Los Angeles
2	Z3-S2	Palmetto Drive (E/O S. Pasadena Avenue)	Pasadena
3	Z3-S3	S. Raymond Avenue, Along Seismic Line Z3-G1	Pasadena
4	Z3-S4	S. Raymond Avenue, Along Seismic Line Z3-G1	Pasadena
5	Z3-S5	Arlington Drive (W/O S. Pasadena Avenue)	Pasadena
6	Z3-S11	Meridian Avenue at Buena Vista Street	South Pasadena
7	Z3-S12	Brent Avenue at Hope Street	South Pasadena
8	Z3-S15	Meridian Avenue (N/O Monterey Road)	South Pasadena
9	Z3-S16	Marengo Avenue at Spruce Street	South Pasadena
10	Z3-S19	Berkshire Avenue (N/O Kendall Avenue)	South Pasadena
11	Z3-S20	Westmont Drive at Keats Street	Alhambra
12	Z3-S21	Winchester Avenue, Along Seismic Line Z3-G6	Alhambra
13	Z3-S22	Winchester Avenue, Along Seismic Line Z3-G6	Alhambra
14	Z3-S23	Westmont Drive, Along Seismic Line Z3-G7	Alhambra
15	Z3-S24	Westmont Drive, Along Seismic Line Z3-G7	Alhambra
16	Z4-S6	E. Huntington Drive, Along Seismic Line Z4-G2	Alhambra
17	Z4-S7	E. Huntington Drive, Along Seismic Line Z4-G2	Alhambra
18	Z4-S8	W. McLean Street (NE/O N. Garfield Avenue)	Alhambra
19	Z4-S9	N. Bushnell Avenue (N/O Larch Street)	Alhambra
20	Z4-S10	S. Date Avenue (S/O W. Commonwealth Avenue)	Alhambra
21	Z5-S10	W. Adams Avenue at S. 2nd Street	Alhambra
22	Z5-S11	Benito Avenue (N/O W. Shorb Street)	Alhambra
23	Z5-S12	Edgewood Drive, Along Seismic Line Z5-G3	Alhambra
24	Z5-S13	Edgewood Drive, Along Seismic Line Z5-G3	Alhambra

Source: CH2M HILL, 2010 (EA-07-187900)

GEOVision
geophysical services

REPORT

HIGH RESOLUTION SEISMIC REFLECTION SURVEY

SR-710 Tunnel Technical Study
Los Angeles County, California

Prepared for

CH2M HILL
6 Hutton Centre Drive, # 700
Santa Ana, CA 92707

Prepared by

GEOVision Geophysical Services
1124 Olympic Drive
Corona, California 92881
(951) 549-1234

Report 9001-02

October 5, 2009

TABLE OF CONTENTS

1 INTRODUCTION 1

2 SEISMIC REFLECTION BACKGROUND 2

3 PROCEDURES 4

3.1 SEISMIC EQUIPMENT 4
3.2 SITE PREPARATION 4
3.3 PARAMETER TESTING 5
3.4 DATA ACQUISITION PARAMETERS 5
3.5 DATA ACQUISITION PROCEDURES 5

4 DATA PROCESSING 7

5 INTERPRETATION 8

5.1 OVERVIEW AND DEPTH CONTROL 8
5.2 ZONE 1 10
5.2.1 Line Z1-G3 10
5.2.2 Line Z1-G4 10
5.2.3 Line Z1-G5 11
5.3 ZONE 2 11
5.3.1 Line Z2-G1 11
5.3.2 Line Z2-G2 12
5.3.3 Line Z2-G3 12
5.4 ZONE 3 13
5.4.1 Line Z3-G1 13
5.4.2 Line Z3-G2 14
5.4.3 Line Z3-G3 14
5.4.4 Line Z3-G4 15
5.4.5 Line Z3-G5 15
5.4.6 Line Z3-G6 16
5.4.7 Line Z3-G7 16
5.5 ZONE 4 17
5.5.1 Line Z4-G1 17
5.5.2 Line Z4-G2 18
5.6 ZONE 5 18
5.6.1 Line Z5-G2 18
5.6.2 Line Z5-G3 19

6 REFERENCES 20

7 CERTIFICATION 21

LIST OF TABLES

Table 1 Seismic Line Locations
Table 2 Generalized Data Acquisition Parameters
Table 3 Data Acquisition and Vibrator Parameters
Table 4 Generalized Processing Sequence
Table 5 Seismic Reflection Depth Control

LIST OF FIGURES

Figure 1 Site Map
Figure 2 Seismic Raypath Geometry
Figure 3 Photographs of Typical Seismic Reflection Field Setup
Figure 4 V_s-V_p Plot for Saturated Sediments/Rock
Figure 5 Line Z1-G3 Seismic Section Without Interpretation
Figure 6 Line Z1-G3 Seismic Section With Interpretation
Figure 7 Line Z1-G4 Seismic Section Without Interpretation
Figure 8 Line Z1-G4 Seismic Section With Interpretation
Figure 9 Line Z1-G5 Seismic Section Without Interpretation
Figure 10 Line Z1-G5 Seismic Section With Interpretation
Figure 11 Line Z2-G1 Seismic Section Without Interpretation
Figure 12 Line Z2-G1 Seismic Section With Interpretation
Figure 13 Line Z2-G2 Seismic Section Without Interpretation
Figure 14 Line Z2-G2 Seismic Section With Interpretation
Figure 15 Line Z2-G3 Seismic Section Without Interpretation
Figure 16 Line Z2-G3 Seismic Section With Interpretation
Figure 17 Line Z3-G1 Seismic Section Without Interpretation
Figure 18 Line Z3-G1 Seismic Section With Interpretation
Figure 19 Line Z3-G2 Seismic Section Without Interpretation
Figure 20 Line Z3-G2 Seismic Section With Interpretation
Figure 21 Line Z3-G3 Seismic Section Without Interpretation
Figure 22 Line Z3-G3 Seismic Section With Interpretation
Figure 23 Line Z3-G4 Seismic Section Without Interpretation
Figure 24 Line Z3-G4 Seismic Section With Interpretation
Figure 25 Line Z3-G5 Seismic Section Without Interpretation
Figure 26 Line Z3-G5 Seismic Section With Interpretation
Figure 27 Line Z3-G6 Seismic Section Without Interpretation
Figure 28 Line Z3-G6 Seismic Section With Interpretation
Figure 29 Line Z3-G7 Seismic Section Without Interpretation
Figure 30 Line Z3-G7 Seismic Section With Interpretation
Figure 31 Line Z4-G1 Seismic Section Without Interpretation
Figure 32 Line Z4-G1 Seismic Section With Interpretation
Figure 33 Line Z4-G2 Seismic Section Without Interpretation
Figure 34 Line Z4-G2 Seismic Section With Interpretation
Figure 35 Line Z5-G2 Seismic Section Without Interpretation
Figure 36 Line Z5-G2 Seismic Section With Interpretation
Figure 37 Line Z5-G3 Seismic Section Without Interpretation
Figure 38 Line Z5-G3 Seismic Section With Interpretation

1 INTRODUCTION

A high-resolution, compressional (P) wave seismic reflection survey was conducted at various sites within the SR-710 Tunnel Study Area, located in Los Angeles County, California. The surveys were conducted from January 13, 2009 to March 24, 2009. The purpose of the seismic reflection survey was to locate geologic structures potentially associated with faulting at each site.

Seventeen (17) seismic reflection lines were located strategically throughout five (5) tunnel study zones, labeled Zones 1 to 5 (Figure 1). The seismic investigation consisted of three (3) seismic lines in Zone 1 (Z1-G3 to Z1-G5), 3 seismic lines in Zone 2 (Z1-G1 to Z2-G3), 7 seismic lines in Zone 3 (Z3-G1 to Z3-G7), 2 seismic lines in Zone 4 (Z4-G1 and Z4-G2), and 2 seismic lines in Zone 5 (Z5-G2 and Z5-G3). The length of the seismic reflection lines ranged from 1,195 to 3,832 feet.

This report contains the results of the seismic reflection investigation conducted at the site. An overview of the seismic reflection method is given in Section 2. Equipment and field procedures are discussed in Section 3. Data processing is discussed in Section 4. Interpretation is presented in Section 5. References and our professional certification are presented in Sections 6 and 7, respectively.

2 SEISMIC REFLECTION BACKGROUND

Seismic reflection profiling is a standard subsurface mapping technique employed by the oil and gas exploration industry. The use of this reflection technique in shallow engineering projects has been a relatively recent development, as the formerly high production costs and serious computing requirements were prohibitive. Advances in microelectronics have led to engineering seismographs and PC-based processing that now permit the cost-effective use of reflection seismic methods in a wide variety of applications (Steeples & Miller, 1988).

Details of the general seismic reflection technique can be found in many comprehensive texts, such as Sheriff and Geldart (1995); and, therefore, only a brief synopsis of the technique is included in this report. The seismic reflection method involves projecting a wave down from the surface, and then recording the returning wave back at the surface as it reflects off formations at depth. Seismic energy will also be reflected, refracted, and diffracted at boundaries in the subsurface, in accordance with Snell's Law (Figure 2). The main design consideration for a successful seismic reflection survey is the ability to separate the reflected energy from other arrivals in processing.

Seismic reflection occurs when an acoustic wave front encounters an impedance boundary in the subsurface. Seismic impedance depends on both the velocity and density of the rock, and impedance boundaries occur where these rock properties change abruptly, usually due to changes in lithology. The reflection coefficient, R, across an interface, is expressed by a function relating the acoustic impedance of adjacent layers. R determines the relative amplitude of the reflected wavelet.

$$\mathbf{R} = \frac{\boldsymbol{\sigma}_2 \mathbf{V}_2 - \boldsymbol{\sigma}_1 \mathbf{V}_1}{\boldsymbol{\sigma}_2 \mathbf{V}_2 + \boldsymbol{\sigma}_1 \mathbf{V}_1}$$

where, R = reflection coefficient,

σ_1, σ_2 = mass density of the material on each side of the interface, and

V_1, V_2 = shear wave velocity on each side of the interface.

The sign of the reflection coefficient determines the polarity of the reflected wave. The magnitude of the reflection coefficient is critical to obtaining usable data. The seismic reflection technique will not work if the acoustic contrast is not sufficient to produce a clear reflection, regardless of the survey parameters or processing techniques employed. The ability of the seismic reflection method to detect an individual sedimentary bed is not only a function of the acoustic impedance at the top and bottom of the bed, but also depends on the layer thickness. The minimum resolvable bed thickness is often quoted as 1/4 to 1/8 of the wavelength at the target depth. Wavelength is inversely proportional to frequency.

When a reflecting boundary exists, it is important to optimize the field procedure and acquisition parameters to maximize the quality of the final processed data. Choosing the best field parameters involves determining the relative importance of several competing objectives, such as site constraints, equipment capabilities, and processing needs.

In all geophysical surveys, the objective is to extract the usable data (i.e., in this case, reflections from various lithologic boundaries) from the unwanted background information (source generated and ambient noise). In reflection seismology, it is desirable to record high frequency, high signal-to-noise ratio reflection events from the boundary of interest. The frequency of a reflection event is largely determined by the source input frequency and the filtering effect of the ground. Often, the target reflector frequency is similar to that commonly recorded for coherent noise (in particular, the noise from ground roll), making it difficult or impossible to selectively filter out the noise. Isolation of the reflection events requires careful design of field acquisition parameters, such as the source/receiver geometry, choice of source and receiver types, as well as recording parameters, such as sampling rate and filter settings.

The seismic reflection technique can be divided into two categories based on the type of source used. Compressional (P) waves, propagate through the earth as a change in pressure, and are the same as the sound waves we hear. Particle motion for P-waves is parallel with the direction of propagation of the wave. Shear (S) waves propagate through the earth by shearing adjacent particles. Particle motion in S-waves is perpendicular to the direction of wave propagation.

The frequency content of seismic reflection data is a function of both the energy source and the earth through which the energy travels. Vibratory sources have control of the frequency input to the ground, unlike impulsive sources such as a hammer or explosive. With a vibratory source the frequency input into the ground is a function of the beginning and ending frequencies of the sweep, the length of the sweep and ground coupling. The second factor is the transmission and attenuation of various frequency components in the subsurface, often termed the “earth response”. In general, there are two primary objectives in designing a sweep for high-resolution reflection surveys:

1. To record useful seismic signals at the geophones with as high a frequency as possible.
2. To start the low end of the sweep such that the appropriate depth of penetration is achieved without generating intolerable ground roll.

3 PROCEDURES

3.1 Seismic Equipment

Key equipment used to collect the high resolution seismic reflection data as shown in Figure 3 included:

- Oyo DAS-1 Seismograph (144 channel system) coupled to a computer with SEISNET acquisition software
- Input/Output Inc. RLS240M roll box
- IVI EnviroVibe energy source
- Oyo Geospace 28 Hz vertical geophones
- Seismic cables and jumper cables

The Oyo DAS-1 Seismograph (DAS) is a 24-bit, 48-channel seismic acquisition system. During this investigation the DAS was coupled to two 48-channel expansion modules to obtain 144-channel recording capability. Coupling the DAS to a computer with the SEISNET seismic acquisition software allows for real-time correlation of the seismic records, filtering, display and printing of shot records and writing of data to CD-ROM.

For this project, an IVI EnviroVibe (Figure 3) was used as the P-wave energy source. Vibratory sources function by oscillating a mass through a user-defined range of frequencies, which are transmitted into the ground. This is known as a "sweep." At the instant the vibrator begins its sweep, the seismograph begins recording the signals received from the geophones. Simultaneously, the sweep being produced by the vibrator is recorded on an auxiliary channel within the seismograph. The seismic record is obtained by cross correlating the recorded signals from the geophones with the known sweep generated by the vibrator.

3.2 Site Preparation

The end points, bends and nominal 300 ft intervals of each seismic line were marked using a Nikon total station system. The appropriate group interval (station/geophone spacing) was then marked using a fiberglass tape measure and surveyors paint with typically every 10^{th} station labeled for reference during data acquisition. The first station was labeled as station 101 with proceeding stations sequentially numbered along the profile. Group intervals of 5 to 8 ft were used for the P-wave reflection data acquisition. The endpoints and inflection points of each line were surveyed using a Trimble ProXRS GPS system with OmniStar submeter differential corrections. The locations of the seismic lines are summarized in Table 1. Relative elevation profiles for each line were surveyed using a Nikon total station system and converted to elevation using the GPS control (accurate to about 2 meters) at the ends of the line. Geophones were hot glued to the asphalt/concrete surface at the appropriate group interval and cabled into the seismograph. Seismic equipment was then set up for parameter testing and data acquisition as discussed in following sections.

3.3 Parameter Testing

Source parameter testing was carried out prior to the respective data acquisition. The receiver interval and geophone array (single geophone) had been determined before the start of the survey. Sweeps of varying frequency bandwidths were recorded into a full (144 trace) off-end or split spread configuration in an effort to bracket the usable frequencies returning to the geophones from the subsurface. The initial testing, aided by frequency filtering in the recording instruments, determined that a sweep range of 20-240 Hz or 20-200 Hz achieved the objectives of broad bandwidth, good depth of penetration and minimal ground roll generation for the P-wave reflection surveys.

With the frequency range selected, the duration and number of sweeps necessary to produce good signal-to-noise content on the shot records remained to be determined. After testing various combinations, it was determined that four, 8 second sweeps provided sufficient energy to overcome ambient noise levels, if at all possible, at the site and satisfy the data acquisition schedule. Longer sweep lengths and additional stacking did not appear to improve signal content on the shot records.

3.4 Data Acquisition Parameters

Generalized data acquisition parameters are summarized in Table 2. Specific data acquisition parameters for each seismic line including shot spacing, group interval (geophone spacing), minimum and maximum shot offset, spread geometry, sweep frequency and length and listen time are listed in Table 3.

3.5 Data Acquisition Procedures

At the start of data acquisition, the source was positioned between the appropriate receiver stations. The IVI EnviroVib communicated with the seismograph by radio link. When the operator pushed the trigger button in the recording truck, a signal was sent to the vibrator to start the sweep sequence, and the OYO DAS-1 seismograph began recording. During the sweep, a synthetic pilot trace was generated by the vibrator and sent to the seismograph. This pilot sweep is recorded on auxiliary channel 1 for correlation with the recorded data from the geophones. Data was transmitted from the seismograph to a computer where seismic acquisition software was used to correlate data, display data, print selected records, and write data to DVD.

At the beginning of the line an uncorrelated sweep was viewed either on the computer screen or on hardcopy. This provided a check to ensure that the vibrator was operating properly, and that the seismograph was being triggered correctly. Array parameters were checked (i.e., source location, sweep configuration, receiver spacing, etc.) as were all connections. The noise monitor on the seismograph was checked to identify any ambient noise problems and to isolate and correct any noisy or dead receiver channels. The noise monitor was also used to confirm the correct setting on the roll box by lightly tapping the first and last active phone.

P-wave seismic reflection data were acquired using a 5 to 8 ft geophone (group) spacing depending on spatial limitations. Seismic lines were oriented as shown in Figure 1. Conventionally, the first geophone was assigned a station number of 101 (0 ft position). Station numbers are converted to distance along the line by subtracting 101 from the station number and multiplying by the group interval (geophone spacing). Seismic lines were started with the source

located at station 100.5 (half a station/geophone spacing behind the first geophone on the line) and, therefore, the first shot had 0 channels live behind and 144 channels live in front of the vibrator. The vibrator was then "walked" into the line at 1-station increments recording the first 144 stations until there was the desired number of channels behind and in front of the source. Spread geometry for each line is summarized in Table 3. As an example, an asymmetric 48/96 split spread has 48 channels (geophones) behind and 96 channels in front of the source. Once the vibrator was located in the appropriate position, the survey was run in a symmetric or asymmetric split spread configuration. With a split spread, the live channels and vibrator were moved forward at 1-station increments, keeping the vibrator at the center of the active spread until the last live channel was reached. Once the last live channel of the line was reached, the vibrator was "walked" off the spread, in the reverse process to the start of the line. Typically, the last source location had all 144 channels behind the vibrator.

4 DATA PROCESSING

The seismic reflection data were processed by Sterling Seismic Services of Denver, Colorado. The processing flow for the data is based on a standard common mid point (CMP) reflection processing sequence with modifications for specific conditions at the survey site. Table 4 shows generalized processing sequence steps leading to the final stacks used for interpretation for the P-wave reflection data.

The seismic section resulting from processing sequences 1 to 16 in Table 4 is referred to as the Final Stack. Additional post processing steps consisting of application of a frequency wavenumber (FX) predictive enhancement filter and spectral balancing over the 40 to 240 Hz frequency range were applied to the seismic sections. These seismic sections were used for interpretation after automatic gain control and application of a 10-20-125-175 Hz band pass filter was completed.

5 INTERPRETATION

5.1 Overview and Depth Control

The processed P-wave seismic sections without and with interpretation for the seventeen (17) seismic reflection profiles (Z1-G3 to Z1-G5, Z2-G1 to Z2-G3, Z3-G1 to Z3-G7, Z4-G1 to Z4-G2 and Z5-G2 to Z5-G3) acquired during this investigation are presented in Figures 5 to 38. These figures represent the P-wave seismic reflection data in a trace amplitude format with a band pass filter applied. The trace amplitude format displays the relative signal strength as energy is reflected from various subsurface features using either a color or gray scale display. The seismic sections included herein are displayed using a gray scale color bar with the white and black representing the highest amplitude negative and positive polarity reflections, respectively. The figures are presented with time in seconds on the vertical axis and distance in feet on the horizontal axis. Generally, the seismic images are presented at a scale with only minor estimated vertical exaggeration. A ground surface reference is added to the figures and corresponds to the top of the seismic image, except for Line Z1-G3 where a floating elevation datum was used during processing because of a large bend in the line.

A seismic workstation equipped with either the Seismic Microtechnology, Inc. 2-D interpretation package or SeiSee SEG-Y file viewing package was used for final display of the data. Typical applications of the seismic interpretation packages include: filtering, color display of seismic data, attribute calculation, digital picking (logging) of seismic event travel times, GIS mapping of seismic data, fault tracking and gain functions.

Because the primary purpose of this investigation was to locate potential faults, conversion of the seismic sections from time to depth was not required. However, a rudimentary depth scale was desired to permit identification of potential reflectors (i.e. water table versus top of bedrock). With the exception of seismic lines Z3-G1 and Z3-G3, borehole velocity data were not available to convert the time-sections to approximate depth. Even with borehole control, only rudimentary and approximate depth conversion would be possible in this geologic environment because geologic units are steeply dipping in many areas and, therefore, significant lateral velocity variation may be common. Additionally, a variable water table depth beneath a seismic line would also have a significant impact on depth.

Without borehole control, estimates of depth to groundwater and the P-wave velocity of unsaturated and saturated sediments is necessary to place a rudimentary depth scale on the seismic images. The only available geophysical data to estimate P-wave velocity structure consisted of the seismic reflection shot records and multichannel analysis of surface waves (MASW) soundings located near the ends of the seismic lines. Approximate depth to groundwater was estimated by simple, two or three layer seismic refraction analysis of surface wave seismic records and/or seismic reflection records. The surface wave sounding profiles were generally long enough to estimate depth to groundwater if shallower than 13 m (43 ft). The seismic reflection shot records were long enough to estimate depth to groundwater if shallower than 70 m (230 ft). Ground water depths estimated using this approach are probably only accurate to about 25% of depth because interpretation of unsaturated sediment P-wave velocity was complicated by high velocity asphalt first arrival data. Estimated groundwater depths for each seismic line are summarized in Table 5. Surface wave soundings were conducted near the

ends of the seismic lines to develop S-wave velocity models to depths of 200 ft (60m), or more. To use these S-wave velocity models to develop approximate depth scales on the P-wave seismic sections it was necessary to determine an approximate relationship between P- and S-wave velocities. In the unsaturated zone, P-wave velocity was assumed to be twice the S-wave velocity (Poisson's ratio of 0.33), a reasonable assumption. Borehole velocity logs from 23 boreholes collected as part of this investigation and reported separately were used to develop an approximate relationship between S-wave velocity (Vs) and P-wave velocity (Vp) of the saturated sediments and rock. Figure 4 is a plot of over 3,500 Vs-Vp measurements made in saturated sediments and rock as part of the borehole geophysical logging program. A linear trend was fit to these measurements and used to relate S-wave velocity of saturated sediments derived from surface wave modeling to P-wave velocity. Depths on the seismic sections will be overestimated if the depth to the saturated zone is underestimated or if the saturated zone identified in the refraction survey is a perched water-bearing zone with lower-velocity, unsaturated sediments below. If the water table depth is underestimated by 10 ft (3 m) then the depth to underlying geologic structures could be overestimated by depths of 30 ft (10m), or more.

Geophysical data used for depth control are summarized in Table 5. Seismic lines Z3-G1 and Z3-G3 used borehole velocity logs from Z3-B4 and Z3-B7, respectively, for depth control. The remaining seismic lines used the S-wave velocity models derived from surface wave soundings, modeled approximate groundwater depth, and the Vs-Vp function for saturated sediments and rock derived from all available borehole velocity logs to estimate depth control. Estimated depths were extrapolated to 600 ft assuming a constant P-wave velocity below the maximum depth of the surface wave model or borehole velocity log. Table 3 also contains the bedrock formation expected to be encountered in the vicinity of each seismic line.

Surface wave soundings conducted near the ends of each seismic line, and reported separately, were used to determine if a significant lateral velocity variation occurred along each seismic line. Surface wave soundings, however, were not able to determine if the water table depth was highly variable beneath the line.

As is typical with seismic reflection data, data quality decreases on the edges of the section due to a decrease in data redundancy (fold).

Potential faulting is most easily observed by looking for disruptions in continuous reflectors, diffractions, offset bedding, abrupt changes in apparent dip of bedding, and other potential geologic structures indicative of faulting. Without good reflectively in the seismic section (i.e. multiple parallel reflectors from geologic strata), fault interpretation is limited to identification of diffractions and other discontinuities and may be highly subjective. Depending upon the amount of reflectivity in the seismic section, alternate interpretations of the seismic data will be possible. As an example, multiple offset reflectors are necessary to estimate the orientation of a possible fault and to make conclusive interpretation of the presence of a fault. If only a single strong reflector is present in a seismic section, then apparent small offsets or disruptions in the reflector are not conclusive evidence of faulting and accurate identification of fault orientation is not possible.

5.2 Zone 1

Three 1,912 ft (583 m) seismic reflection profiles, Z1-G3 to Z1-G5, were conducted in Zone 1 as shown on Figure 1.

5.2.1 Line Z1-G3

The processed P-wave seismic sections for Line Z1-G3 without and with interpretation are presented in Figures 5 and 6, respectively. An approximate depth scale has been added to Figure 6 using the S-wave velocity model for Z1-S6, estimated groundwater depth of 66 ft (20 m), and approach previously discussed. As shown in Figure 1, surface wave soundings Z1-S5 and Z1-S6 were conducted in the southwestern and northeastern portions of seismic line Z1-G3, respectively. The S-wave velocity models for these soundings are very similar (**GEO***Vision*, 2009) indicating that there may not be significant lateral velocity variation in the immediate vicinity of the seismic line. However, groundwater depth, which impacts P-wave velocity variation, may be highly variable beneath this line because there is over 100 ft (30 m) of elevation change. Therefore, the depth scale shown on Figure 6 may only be applicable to the northeast end of the line and accuracy will be highly dependent on the modeled water table accuracy.

A subhorizontal seismic horizon possibly associated with the top of bedrock or base of a weathering zone within bedrock is interpreted near 0.1 s (~ 50 ft) on the seismic section for line Z1-G3 (Figure 6). This horizon is not a strong continuous reflector and is interpreted as apparent truncation of underlying southwesterly dipping discontinuous reflectors. Bedrock outcrops in the vicinity of the seismic line confirm the apparent southwest dip of seismic reflectors identified in Figure 6. Interpretation of faulting in this seismic image is complicated by the combination of dipping bedding and a significant bend in the seismic line. There are two anomalous zones identified near 850 and 1,150 ft on the seismic line where there are disruptions in bedrock reflectors that could be associated with faulting. However, it is possible that at least one of these anomalies is related to the bend in the seismic line and associated change in apparent (along line) dip of geologic units.

5.2.2 Line Z1-G4

The processed P-wave seismic sections for Line Z1-G4 without and with interpretation are presented in Figures 7 and 8, respectively. An approximate depth scale has been added to Figure 8 using the S-wave velocity model for Z1-S15, estimated groundwater depth of 10 ft (3 m), and procedure discussed in the previous section. As shown in Figure 1, surface wave soundings Z1-S14 and Z1-S15 were conducted in the southwestern and northeastern portions of seismic line Z1-G4, respectively. The S-wave velocity models for these soundings are different (**GEO***Vision*, 2009) indicating that there may be significant lateral velocity variation in the immediate vicinity of the seismic line. Additionally, there may be slight variation in groundwater depth beneath this line associated with the 25 ft (8 m) of elevation change. Therefore, the depth scale shown on Figure 8 is only applicable to the northeast end of the line.

A weak, subhorizontal, discontinuous reflector possibly associated with the top of bedrock is interpreted between 0.05 and 0.08 s (~ 40 to 90 ft) on the seismic section for line Z1-G4 (Figure 8). There is poor reflectivity (absence of seismic reflectors) below the interpreted top of bedrock indicating that geologic units are either too steeply dipping for the seismic reflection method to image or that the geologic units are massive rather than interbedded. There is not enough

reflectivity on this seismic line to make an accurate fault interpretation. Possible discontinuities that could be associated with minor faulting are identified in the vicinity of 280, 720 and 1,250 ft on the seismic line; however, there is insufficient reflectivity to make a conclusive interpretation.

5.2.3 Line Z1-G5

The processed P-wave seismic sections for Line Z1-G5 without and with interpretation are presented in Figures 9 and 10, respectively. An approximate depth scale has been added to Figure 10 using the S-wave velocity model for Z1-S16, estimated groundwater depth of 10 ft (3 m), and procedure discussed in the previous section. As shown in Figure 1, surface wave soundings Z1-S16 and Z1-S17 were conducted in the northern and southern portions of seismic line Z1-G5, respectively. It was not possible to develop a model for the surface wave data collected at Z1-S17 and, therefore, data on the potential lateral velocity variation along the seismic line is not available.

There is excellent reflectivity on this seismic line with multiple parallel seismic reflectors with which to interpret offset layers or discontinuities potentially associated with faulting. A subhorizontal seismic horizon possibly associated with the top of bedrock or base of a weathering zone within bedrock is interpreted in the 0.07 to 0.085 s range (~ 70 to 120 ft) on the seismic section for line Z1-G5 (Figure 10). This horizon is interpreted by both a discontinuous reflection event and apparent truncation of underlying dipping reflectors. Seismic reflectors associated with subsurface geologic structures appear to have an apparent northerly dip in the southern portion of the line and are subhorizontal/slightly dipping in the northern portion on the line. There is a significant change in dip of reflectors between 700 and 800 ft on the seismic line, which could be associated with faulting. The change in dip of bedding to the north may just be related to a syncline with the axis of the syncline located between a position of about 1,300 and 1,600 ft. The disrupted reflectors in the 700 to 800 ft range, however, may still be related to faulting rather than only folding.

5.3 Zone 2

Three seismic reflection profiles, Z2-G1 to Z2-G3, were conducted in Zone 2 as shown on Figure 1. Lines Z2-G1 and Z2-G3 have lengths of 1,792.5 ft and Line Z2-G3 has a length of 1,434 ft.

5.3.1 Line Z2-G1

The processed P-wave seismic sections for Line Z2-G1 without and with interpretation are presented in Figures 11 and 12, respectively. An approximate depth scale has been added to Figure 12 using the S-wave velocity model for Z2-S2, estimated groundwater depth of 10 ft (3 m), and approach previously discussed. As shown in Figure 1, surface wave soundings Z2-S2 and Z2-S3 were conducted in the northern and southern portions of seismic line Z2-G1, respectively. The S-wave velocity models for these soundings are very similar (**GEO***Vision*, 2009) indicating that there may not be significant lateral velocity variation in the immediate vicinity of the seismic line. There is only about 25 ft (8 m) of elevation change along the seismic line and groundwater depth may not be highly variable. Therefore, the approximate depth scale shown on Figure 12 may be applicable to the entire line providing that velocity assumptions and the groundwater depth estimate represent actual site conditions.

A subhorizontal, continuous seismic reflector possibly associated with the top of bedrock is interpreted between 0.055 and 0.07 s (~ 60 to 100 ft) on the line Z2-G1 seismic section (Figure 12). There is only minor reflectivity below the interpreted bedrock surface possibly due to bedrock consisting of massive rather than interbedded geologic units or steeply dipping geologic units. The absence of significant reflectivity within the bedrock unit makes accurate and conclusive fault interpretation difficult. There are two anomalous zones identified between 600 and 650 ft and 1,140 and 1,180 ft on the seismic line that could be associated with potential faulting. Both of these anomalous zones were identified based on disruptions of limited bedrock reflectors.

5.3.2 Line Z2-G2

The processed P-wave seismic sections for Line Z2-G2 without and with interpretation are presented in Figures 13 and 14, respectively. An approximate depth scale has been added to Figure 14 using the S-wave velocity model for Z2-S8, estimated groundwater depth of 23 ft (7 m), and approach previously discussed. As shown in Figure 1, surface wave soundings Z2-S7 and Z2-S8 were conducted in the southwestern and northeastern portions of seismic line Z2-G2, respectively. The S-wave velocity models for these soundings are very similar above a depth of 130 ft (40 m) but somewhat different and greater depths (**GEO***Vision*, 2009) indicating that there may be some lateral velocity variation in the immediate vicinity of the seismic line. There is only about 20 ft (6 m) of elevation change along the seismic line and groundwater depth may not be highly variable. The approximate depth scale shown on Figure 12 may primarily apply to the northeastern side of the seismic line providing that velocity assumptions and the groundwater depth estimate represent actual site conditions.

A subhorizontal, continuous seismic reflector possibly associated with the top of bedrock is interpreted between 0.1 and 0.12 s (~ 175 to 225 ft) on the line Z2-G2 seismic section (Figure 12). The surface wave soundings along this seismic line indicate that bedrock may be shallower, possibly in the 125 to 150 ft depth range. An incorrect groundwater depth estimate, the presence of a perched water table and/or lower P-wave velocities in unsaturated and saturates sediments could easily account for this depth discrepancy. There is only minor reflectivity below the interpreted bedrock surface possibly due to bedrock consisting of massive rather than interbedded geologic units or steeply dipping geologic units. The absence of significant reflectivity within the bedrock unit makes accurate and conclusive fault interpretation difficult. There are two anomalous zones identified between 750 and 775 ft and 1,475 and 1,525 ft on the seismic line that could be associated with potential faulting. Both of these anomalous zones were identified based on disruptions of limited bedrock reflectors.

5.3.3 Line Z2-G3

The processed P-wave seismic sections for Line Z2-G3 without and with interpretation are presented in Figures 15 and 16, respectively. An approximate depth scale has been added to Figure 16 using the S-wave velocity model for Z2-S10, estimated groundwater depth of 30 ft (9 m), and previously discussed approach. As shown in Figure 1, surface wave soundings Z2-S10 and Z2-S11 were conducted in the northwestern and southeastern portions of seismic line Z2-G3, respectively. The S-wave velocity models for these soundings are very similar (**GEO***Vision*, 2009) indicating that there may not be significant lateral velocity variation in the immediate vicinity of the seismic line. There is, however, about 70 ft (21 m) of elevation change along the

seismic line increasing the possibility of significant variation in groundwater depth, which would cause variation in depth along the seismic line.

A subhorizontal, continuous seismic reflector possibly associated with the top of bedrock is interpreted between 0.06 and 0.075 s (~ 60 to 125 ft) on the line Z2-G3 seismic section (Figure 12). There is some reflectivity below the interpreted bedrock surface indicating that sedimentary units may have a slight apparent dip to the southeast along the seismic line. There are no apparent large offsets in bedrock reflectors indicative of conclusive faulting. There is, however, a minor discontinuity in the upper bedrock reflectors near 650 ft on the seismic line, which could potentially be associated with minor faulting.

5.4 Zone 3

Seven seismic reflection profiles, Z3-G1 to Z3-G7, were conducted in Zone 3 as shown on Figure 1. Lines Z3-G1 and Z3-G3 have lengths of 1,912 ft. Line Z3-G2 has a length of 1,195 ft. Line Z3-G4 has a length of 1,434 ft. Lines Z3-G5 and Z3-G7 have lengths of 1,578 ft and Line Z3-G6 has a length of 1,506 ft.

5.4.1 Line Z3-G1

The processed P-wave seismic sections for Line Z3-G1 without and with interpretation are presented in Figures 17 and 18, respectively. An approximate depth scale has been added to Figure 18 using the P-wave velocity log from borehole Z3-B4. As shown in Figure 1, surface wave soundings Z3-S3 and Z3-S4 were conducted in the northern and southern portions of seismic line Z3-G1, respectively. The S-wave velocity models for these soundings are very similar (**GEO***Vision*, 2009) indicating that there may not be significant lateral velocity variation in the immediate vicinity of the seismic line. There is only about 15 ft (4.5 m) of elevation change along the seismic line and groundwater depth may not be highly variable. Therefore, the approximate depth scale shown on Figure 12 may be applicable to the entire line providing that velocity assumptions and the groundwater depth estimate represent actual site conditions.

A subhorizontal, continuous seismic reflector possibly associated with the top of bedrock or weathering contact within bedrock is interpreted between 0.14 and 0.16 s (~ 175 to 270 ft) on the line Z3-G1 seismic section (Figure 18). This reflector appears too deep for groundwater or the bedrock surface, which were encountered in borehole Z3-B4 at about 148 ft (45 m) and 185 ft (56 m), respectively. Assuming some lateral velocity variation in P-wave velocity across the site, the reflector may be associated with the top of crystalline bedrock but could also be associated with an abrupt contact between highly weathered and slightly weathered bedrock.

There is no reflectivity below the interpreted bedrock reflector because bedrock consists of crystalline rock, which has no bedding. The absence of significant reflectivity within the bedrock unit makes conclusive fault interpretation impossible. There are multiple discontinuities in the bedrock reflector, approximately located near 200, 550, 840, 1,100, 1,340 and 1,440 ft. Many of these bedrock discontinuities may be associated with topographic variation of the bedrock surface or bedrock weathering contacts. It is also possible that some of the discontinuities are related to bedrock offsets caused by faulting rather than erosion.

5.4.2 Line Z3-G2

The processed P-wave seismic sections for Line Z3-G2 without and with interpretation are presented in Figures 19 and 20, respectively. An approximate depth scale has been added to Figure 20 using the S-wave velocity model for Z3-S6, estimated groundwater depth of 16 ft (5 m), and previously discussed methodology. As shown in Figure 1, surface wave soundings Z3-S6 and Z3-S7 were conducted near the north and south ends of seismic line Z3-G2, respectively. The S-wave velocity models for these soundings differ by more than 10 % (**GEO***Vision*, 2009) indicating that there may be some lateral velocity variation in the immediate vicinity of the seismic line. There is only about 3 ft (1 m) of elevation change along the seismic line and groundwater depth may not be highly variable. The approximate depth scale shown on Figure 12 may vary by 10% or more across the seismic line.

Subhorizontal, continuous seismic reflectors possibly associated with top of bedrock and/or a weathering zone within bedrock are interpreted between 0.03 and 0.04 s (~ 40 to 60 ft) and 0.05 and 0.07 s (~ 100 to 175 ft) on the line Z3-G2 seismic section (Figure 20). The surface wave soundings along this seismic line indicate that bedrock may be associated with the upper reflector with the lower reflector associated with a change in weathering within bedrock or other bedrock structure. There is only minor reflectivity below the interpreted bedrock surface possibly due to bedrock consisting of massive rather than interbedded geologic units or steeply dipping geologic units. The absence of significant reflectivity within the bedrock unit makes accurate and conclusive fault interpretation difficult. There are two anomalous zones identified near 420 and 700 ft on the seismic line that could be associated with potential faulting. Both of these anomalous zones were identified based on disruptions of limited bedrock reflectors.

5.4.3 Line Z3-G3

The processed P-wave seismic sections for Line Z3-G3 without and with interpretation are presented in Figures 21 and 22, respectively. An approximate depth scale has been added to Figure 22 using the P-wave velocity log from borehole Z3-B7. As shown in Figure 1, surface wave soundings Z3-S9 and Z3-S10 were conducted near the southwest and northeast ends of seismic line Z3-G3, respectively. The S-wave velocity models for these soundings are significantly different (**GEO***Vision*, 2009) indicating that there may be some lateral velocity variation in the immediate vicinity of the seismic line. There is also about 26 ft (8 m) of elevation change along the seismic line, which may contribute to variable water table depth and associated lateral velocity variation and groundwater depth may not be highly variable. The approximate depth scale shown on Figure 22 is most applicable in the central portion of the seismic line near the borehole.

Subhorizontal, discontinuous seismic reflectors possibly associated with groundwater, top of bedrock and/or a weathering zone within bedrock are interpreted between 0.04 and 0.055 s (~ 60 to 100 ft) and 0.06 and 0.09 s (~ 120 to 270 ft) on the line Z3-G3 seismic section (Figure 22). The surface wave soundings and borehole along this seismic line indicate that bedrock may be associated with the upper reflector, although there may not be an abrupt change in velocity between weathered bedrock and overlying sediments in the vicinity of the seismic line. The lower reflector may be associated with a change in weathering within bedrock or other bedrock structure. There is only minor reflectivity below the interpreted bedrock surface possibly due to bedrock consisting of massive rather than interbedded geologic units or steeply dipping geologic units. The bedrock reflectors identified on the seismic section (Figure 22) occur at depths below

600 ft. The seismic reflection survey was not designed to image to these depths and there is a possibility that the reflection events are associated with coherent noise. The absence of significant reflectivity within the bedrock unit makes accurate and conclusive fault interpretation difficult. There are two anomalous zones identified between 450 and 500 ft and 1,000 and 1,050 ft that could be associated with potential faulting. Both of these anomalous zones were identified based on disruptions of limited bedrock reflectors.

5.4.4 Line Z3-G4

The processed P-wave seismic sections for Line Z3-G4 without and with interpretation are presented in Figures 23 and 24, respectively. An approximate depth scale has been added to Figure 24 using the S-wave velocity model for Z3-S13, estimated groundwater depth of 56 ft (17 m), and previously discussed methodology. As shown in Figure 1, surface wave soundings Z3-S13 and Z3-S14 were conducted near the northeast and southwest ends of seismic line Z3-G4, respectively. There is also a borehole (Z3-B9) located near this seismic line, which indicates that crystalline basement rock is present beneath the line. The S-wave velocity models for the surface wave soundings are very similar (**GEO***Vision*, 2009) indicating that there may be only minor lateral velocity variation in the immediate vicinity of the seismic line. There is only about 20 ft (6 m) of elevation change along the seismic line and groundwater depth may not be highly variable.

Subhorizontal, continuous seismic reflectors possibly associated with groundwater and top of crystalline bedrock are interpreted between 0.05 and 0.06 s (~ 30 to 45 ft) and 0.085 and 0.115 s (~ 80 to 200 ft) on the line Z3-G4 seismic section (Figure 24). Nearby borehole Z3-B9 indicates that the lower reflector may be associated with the top of crystalline basement. The upper reflector may be associated with the water table or sediment layer above the water table.

There is no reflectivity below the interpreted bedrock reflector because bedrock consists of crystalline rock, which has no bedding. The absence of significant reflectivity within the bedrock unit makes conclusive fault interpretation impossible. There is a significant drop in the interpreted bedrock surface between 220 and 320 ft, which may be erosional or potentially related to faulting. There are also other disruptions in the possible bedrock reflector near 750, 1,030 and 1,210 ft.

5.4.5 Line Z3-G5

The processed P-wave seismic sections for Line Z3-G5 without and with interpretation are presented in Figures 25 and 26, respectively. An approximate depth scale has been added to Figure 26 using the S-wave velocity model for Z3-S17, estimated groundwater depth of 26 ft (8 m), and previously discussed methodology. As shown in Figure 1, surface wave soundings Z3-S17 and Z3-S18 were conducted in the north central and south central portions of seismic line Z3-G5, respectively. The S-wave velocity models for these soundings are generally similar although there is apparent variation in bedrock depth (**GEO***Vision*, 2009) indicating that there may be some lateral velocity variation in the immediate vicinity of the seismic line. There is also about 62 ft (19 m) of elevation change along the seismic line, which may contribute to variable water table depth and associated lateral velocity variation. The approximate depth scale shown on Figure 26 may only apply to the central portion of the seismic line.

A high amplitude, subhorizontal, continuous seismic reflector possibly associated with top of bedrock is interpreted between 0.04 and 0.1 s (~ 140 ft) on the line Z3-G5 seismic section

(Figure 26). The surface wave soundings along this seismic line indicate that bedrock may be located in the 70 to 85 ft (21 to 26 m) depth range. If groundwater were about 15 to 20 ft (4.5 to 6 m) deeper than that used for depth control then the high amplitude reflector would be in the appropriate depth range. The possible bedrock reflector is continuous except for minor discontinuities at 230 and 450 ft, which could be associated with faulting. A more diffuse reflector that may be associated with a possible weathering zone within bedrock is interpreted between 0.14 and 0.17 s (~ 375 to 500 ft). Below the lower reflector, geologic units appear to have apparent dip in a northerly direction. Many of these reflectors are very deep relative to the data acquisition geometry and, therefore, could be related to coherent noise rather than geologic structure. Additionally, several small diffractions appear to line up in the vicinity of 800 ft on the profile beneath the lower reflector. Although unlikely, the possibility that these diffractions are associated with minor faulting cannot be discounted.

5.4.6 Line Z3-G6

The processed P-wave seismic sections for Line Z3-G6 without and with interpretation are presented in Figures 27 and 28, respectively. An approximate depth scale has been added to Figure 28 using the S-wave velocity model for Z3-S21, estimated groundwater depth of 52 ft (16 m), and previously discussed methodology. As shown in Figure 1, surface wave soundings Z3-S21 and Z3-S22 were conducted in the northern and southern portions of seismic line Z3-G6, respectively. The S-wave velocity models for these soundings are generally similar (**GEO***Vision*, 2009) indicating that there may not be significant lateral velocity variation in the immediate vicinity of the seismic line. There is about 45 ft (14 m) of elevation change along the seismic line, which may contribute to variable water table depth and associated lateral velocity variation. The approximate depth scale shown on Figure 28 may apply to much of the seismic line.

A subhorizontal, continuous seismic reflector possibly associated with top of bedrock is interpreted between 0.085 and 0.1 s (~ 100 to 115 ft) on the line Z3-G6 seismic section (Figure 28). The surface wave soundings along this seismic line indicate that bedrock may be located in the 92 to 102 ft (28 to 31 m) depth range, which confirms that the reflector may be associated with the top of bedrock. There is excellent reflectively below the interpreted bedrock surface with multiple parallel seismic reflectors with which to interpret offset layers or discontinuities potentially associated with faulting. There is a significant disruption and possible offset of reflectors in the 910 to 950 ft range, which may be associated with faulting. There is also a minor disruption in reflectors between 375 and 440 ft, which could be associated with faulting.

5.4.7 Line Z3-G7

The processed P-wave seismic sections for Line Z3-G7 without and with interpretation are presented in Figures 29 and 30, respectively. An approximate depth scale has been added to Figure 30 using the S-wave velocity model for Z3-S23, estimated groundwater depth of 39 ft (12 m), and previously discussed methodology. As shown in Figure 1, surface wave soundings Z3-S23 and Z3-S24 were conducted in the northern and southern portions of seismic line Z3-G7, respectively. The S-wave velocity models for these soundings are different (**GEO***Vision*, 2009) indicating that there may be significant lateral velocity variation in the immediate vicinity of the seismic line. There is about 25 ft (8 m) of elevation change along the seismic line, which may contribute to variable water table depth and associated lateral velocity variation. The

approximate depth scale shown on Figure 28 may only apply to the northern portion of the seismic line.

A subhorizontal, discontinuous seismic reflector possibly associated with top of bedrock is interpreted between 0.06 and 0.085 s (~ 40 to 100 ft) on the line Z3-G7 seismic section (Figure 30). A borehole located in the vicinity of the seismic line (Z1-B8) indicates that the uppermost bedrock zone may be highly weathered and not easily distinguished from overlying sediments based on S-wave velocity. Therefore, the surface wave soundings along this seismic line were only able to indicate that bedrock may be located in the 23 to 118 ft (7 to 36 m) depth range, which is consistent with the interpretation of the bedrock reflector. There is good reflectively below the interpreted bedrock surface in the southern half of the seismic line with multiple parallel seismic reflectors with which to interpret offset layers or discontinuities potentially associated with faulting. There is a significant change in reflectivity in the northern portion of the line associated with a possible fault interpreted between 880 and 920 ft. Additionally, there is also a minor disruption in reflectors around 250 ft on the line, which could also be associated with faulting.

5.5 Zone 4

Two seismic reflection profiles, Z4-G1 and Z4-G2, were conducted in Zone 4 as shown on Figure 1. Lines Z4-G1 and Z4-G2 have lengths of 3,832 and 1,912 ft, respectively.

5.5.1 Line Z4-G1

The processed P-wave seismic sections for Line Z4-G1 without and with interpretation are presented in Figures 31 and 32, respectively. An approximate depth scale has been added to Figure 32 using the S-wave velocity model for Z4-S2, estimated groundwater depth of 210 ft (64 m), and approach previously discussed. As shown in Figure 1, surface wave soundings Z4-S2, Z4-S3 and Z4-S4 were conducted in the northern, central and southern portions of seismic line Z4-G1, respectively. The S-wave velocity models for these soundings are very different (**GEO***Vision*, 2009) indicating that there may be significant lateral velocity variation in the immediate vicinity of the seismic line. There is also over 120 ft (37 m) of elevation change along the seismic line, which may contribute to variable groundwater depth and associated lateral velocity variation. Additionally, groundwater depths are not accurately resolved on this seismic line, which may contribute to significant depth errors. The approximate depth scale shown on Figure 32 may only be applicable to the northern portion of the seismic line and may have errors in excess of 25%.

Seismic line Z4-G1 crosses the Raymond Fault Zone. A scarp associated with the fault is located between about 1,200 and 2,000 ft on the seismic line. Bedrock may be located at depths in excess of 500 ft beneath this seismic line and there is no clear seismic reflection associated with the top of bedrock. There is not much reflectively in the seismic section, possibly because the old alluvium overlying bedrock does not have laterally extensive continuous bedding, and/or energy attenuation through the thick unsaturated zone. The absence of significant reflectively makes accurate fault interpretation difficult. There is, however, a significant change in reflectively on the seismic line between 800 and 2,000 ft revealed by abrupt termination change in apparent dip of reflectors at the southern end and change in dip of reflectors and possible large diffractions at the northern end of the zone. Potential faults are identified in the vicinity of 900,

1,500 and 2,000 ft on the seismic line although, given the minimal reflectivity, alternative interpretations are possible.

5.5.2 Line Z4-G2

The processed P-wave seismic sections for Line Z4-G2 without and with interpretation are presented in Figures 33 and 34, respectively. An approximate depth scale has been added to Figure 34 using the S-wave velocity model for Z4-S6, estimated groundwater depth of 215 ft (65 m), and approach previously discussed. As shown in Figure 1, surface wave soundings Z4-S6 and Z4-S7 were conducted in the northeastern and southwestern portions of seismic line Z4-G2, respectively. The S-wave velocity models for these soundings are very similar (**GEO***Vision*, 2009) indicating that there may not be significant lateral velocity variation in the immediate vicinity of the seismic line. There is also only 5 ft (1.5 m) of elevation change along the seismic line. Groundwater depths are not accurately resolved beneath this seismic line, however, there is no reason to believe that there is significant depth variation of the water table beneath the line. The approximate depth scale shown on Figure 34 may be applicable to the entire seismic line, providing the assumptions made to estimate depths are reasonably valid.

A high amplitude, subhorizontal, continuous seismic reflector possibly associated with the water table is interpreted between 0.15 and 0.175 s (~ 170 to 220 ft) on the line Z4-G2 seismic section (Figure 34). Another continuous reflector is identified between 0.28 and 0.3 s (~ 525 to 600 ft). The location of this reflector is such that the possibility that it is a multiple reflection from the possible water table cannot be discounted. Other than the two reflectors identified above there is not sufficient reflectivity in the seismic section for detailed fault interpretation. Two possible fault-like anomalies are identified in the seismic section near 1,220 and 1,520 ft. These structures are primarily identified by changes in apparent dip and disruptions of the water table reflector, which may occur if a fault acts as a groundwater barrier. These features cannot be accurately mapped on the seismic section due to absence of reflectivity and, therefore, cannot be confirmed as faults.

5.6 Zone 5

Two seismic reflection profiles, Z5-G2 and Z5-G3, were conducted in Zone 5 as shown on Figure 1. Both lines Z5-G2 and Z5-G3 have a length of 1,912 ft.

5.6.1 Line Z5-G2

The processed P-wave seismic sections for Line Z5-G2 without and with interpretation are presented in Figures 33 and 34, respectively. An approximate depth scale has been added to Figure 34 using the S-wave velocity model for Z5-S8, estimated groundwater depth of 184 ft (56 m), and approach previously discussed. As shown in Figure 1, surface wave soundings Z5-S8, and Z5-S9 were conducted in the eastern and western portions of seismic line Z5-G2, respectively. The S-wave velocity models for these soundings are very similar (**GEO***Vision*, 2009) indicating that there may not be significant lateral velocity variation in the immediate vicinity of the seismic line. There is about 36 ft (11 m) of elevation change along the seismic line, which may contribute to variable groundwater depth and some associated lateral velocity variation. Groundwater depth is not well constrained along this seismic line. The approximate depth scale shown on Figure 36 may be applicable to much of the seismic line providing the groundwater depth estimate is reasonably accurate.

The seismic section has good reflectivity with multiple discontinuous reflectors to approximate depths of over 600 ft. Reflectors associated with the water table or bedrock surface were not identified to a high degree of confidence. Bedrock is expected to be very deep in the vicinity of this seismic line. A possible fault-like anomaly was identified in the seismic section at about 740 ft and was identified by disruptions in several reflectors, particularly those in the 600 ft depth range. A more subtle anomalous zone that could be associated with faulting was identified between 1,600 and 1,650 ft.

5.6.2 Line Z5-G3

The processed P-wave seismic sections for Line Z5-G3 without and with interpretation are presented in Figures 37 and 38, respectively. An approximate depth scale has been added to Figure 38 using the S-wave velocity model for Z5-S12, estimated groundwater depth of 52 ft (16 m), and approach previously discussed. As shown in Figure 1, surface wave soundings Z5-S12, and Z5-S13 were conducted in the northern and southern portions of seismic line Z5-G3, respectively. The S-wave velocity models for these soundings are very similar (**GEO***Vision*, 2009) indicating that there may not be significant lateral velocity variation in the immediate vicinity of the seismic line. There is only about 16 ft (5 m) of elevation change along the seismic line. The approximate depth scale shown on Figure 38 may be applicable to the entire seismic line providing the groundwater depth estimate is accurate.

A high amplitude, subhorizontal, continuous seismic reflector possibly associated with the top of bedrock is interpreted between 0.14 and 0.16 s (~ 280 to 330 ft) on the line Z5-G3 seismic section (Figure 38). This reflector appears to be much too deep to be associated with the water table, although the reflector could be associated with a continuous geologic layer within alluvial sediments rather than bedrock. There is not significant reflectivity below the interpreted bedrock reflector until depths below 600 ft where possible northward dipping geologic units are identified. Several possible, but not conclusive, fault-like anomalies are identified in the seismic section at 300 and 920 ft and 1,350 to 1,450 ft. These structures were identified by disruption of the potential top of bedrock reflector and underlying reflectors at depth. Reduction of fold (data redundancy) at the ends of the seismic line may contribute to possible incorrect interpretation of the structures at 300 ft and 1,400 ft.

6 REFERENCES

Claerbout, J. F., 1985, Imaging the Earth's Interior, Blackwell Scientific Publications.

Geldart, L.P., Telford, W.M., Sheriff, R.E., 1995, Applied Geophysics, Second Edition, Cambridge University Press.

GEO*Vision* Inc., 2009, Draft Report, Surface Wave Measurements, SR-710 Potential Tunnel Corridors, Los Angeles County, California, prepared for CH2M Hill, July 31, 2009.

Steeples, Don W., and Miller, Richard D., 1988, Seismic Reflection Methods Applied To Engineering, Environmental, and Ground Water Problems, Proc. of SAGEEP, March, Golden, CO, p. 409-460.

Sheriff, R.E., Geldart, L.P., 1985, History, Theory and Data Acquisition, Exploration Seismology, Volume 1, Cambridge University Press.

7 CERTIFICATION

All geophysical data, analysis, interpretations, conclusions, and recommendations in this document have been prepared under the supervision of and reviewed by a **GEO*Vision*** California Professional Geophysicist.

October 5, 2009

Antony J. Martin — Date
California Professional Geophysicist GP989
GEO*Vision* Geophysical Services

* This geophysical investigation was conducted under the supervision of a California Professional Geophysicist using industry standard methods and equipment. A high degree of professionalism was maintained during all aspects of the project from the field investigation and data acquisition, through data processing interpretation and reporting. All original field data files, field notes and observations, and other pertinent information are maintained in the project files and are available for the client to review for a period of at least one year.

  A professional geophysicist's certification of interpreted geophysical conditions comprises a declaration of his/her professional judgment. It does not constitute a warranty or guarantee, expressed or implied, nor does it relieve any other party of its responsibility to abide by contract documents, applicable codes, standards, regulations or ordinances.

TABLES

Table 1. Seismic Line Locations

Line	Station	Position (ft)	Northing (US ft)	Easting (US ft)	Elevation (ft MSL)
Z1-G3	101	0	1853598	6487832	579
Z1-G3	251	1200	1854484	6488636	525
Z1-G3	238	1096	1854396	6488580	536
Z1-G3	340	1912	1855142	6488901	477
Z1-G4	101	0	1851571	6503615	427
Z1-G4	340	1912	1853095	6504768	450
Z1-G5	101	0	1851287	6507737	449
Z1-G5	340	1912	1853200	6507732	459
Z2-G1	101	0	1866438	6496103	519
Z2-G1	175	555	1866977	6496229	492
Z2-G1	181	600	1867019	6496244	493
Z2-G1	340	1792.5	1868182	6496515	517
Z2-G2	101	0	1860667	6500501	503
Z2-G2	340	1792.5	1861576	6502044	519
Z2-G3	101	0	1854399	6508688	482
Z2-G3	333	1392	1855642	6508062	541
Z2-G3	340	1434	1855692	6508069	556
Z3-G1	101	0	1868860	6516666	739
Z3-G1	340	1912	1870771	6516652	755
Z3-G2	101	0	1867383	6512290	685
Z3-G2	340	1195	1868579	6512310	687
Z3-G3	101	0	1865627	6509704	584
Z3-G3	340	1912	1866908	6511124	608
Z3-G4	101	0	1863281	6510441	612
Z3-G4	340	1434	1864450	6511274	631
Z3-G5	101	0	1858529	6510383	579
Z3-G5	125	144	1858674	6510377	588
Z3-G5	158	342	1858864	6510328	598
Z3-G5	209	648	1859164	6510324	614
Z3-G5	258	942	1859462	6510322	626
Z3-G5	302	1206	1859727	6510318	633
Z3-G5	336	1410	1859921	6510377	636
Z3-G5	364	1578	1860066	6510461	643
Z3-G6	101	0	1851978	6513112	425
Z3-G6	364	1578	1853555	6513105	471
Z3-G7	101	0	1848225	6513201	423
Z3-G7	170	414	1848639	6513200	432
Z3-G7	244	858	1849084	6513199	415
Z3-G7	300	1194	1849419	6513201	418
Z3-G7	340	1434	1849659	6513201	418
Z3-G7	364	1578	1849803	6513202	415

California State Plane coordinate system, North American Datum 1983, Zone V (0405), US Survey Feet.
Horizontal accuracy is approximately 1m, vertical accuracy is approximately 2m.

Table 1 (continued) Seismic Line Locations

Line	Station	Position (ft)	Northing (US ft)	Easting (US ft)	Elevation (ft MSL)
Z4-G1	101	0	1866934	6528963	569
Z4-G1	180	632	1867563	6528843	580
Z4-G1	209	864	1867761	6528740	584
Z4-G1	580	3832	1869568	6528421	677
Z4-G2	101	0	1861662	6521381	556
Z4-G2	340	1912	1862851	6522877	550
Z4-G3	101	0	1851789	6526290	398
Z4-G3	340	1912	1851899	6528198	362
Z5-G3	101	0	1848497	6516641	420
Z5-G3	340	1912	1850408	6516625	435

California State Plane coordinate system, North American Datum 1983, Zone V (0405), US Survey Feet.
Horizontal accuracy is approximately 1m, vertical accuracy is approximately 2m.

Table 2. Generalized Data Acquisition Parameters

Shot Spacing	6 – 8 ft , centered on half stations
Geophone Group Interval	5 – 8 ft
Maximum CDP Fold	72
Maximum Offset	429 to 956 ft
Minimum Offset	2.5 – 4 ft
Spread Geometry	Walk on to asymmetric split spread/symmetric split spread, walk off
Seismograph	OYO DAS-1 Recorder
Number of Channels	144
Sample Rate	0.5 ms
Record Length	8 second sweep, 0.5 – 1 seconds after correlation
Field Filters	3 Hz lo-cut
Seismic Source	IVI Envirovibe
Geophones	OYO Geospace 28 Hz vertical

Table 3. Data Acquisition and Vibrator Parameters

Line	Line Length (feet)	Shot Spacing (feet)	Group Interval (feet)	Minimum Offset (feet)	Nominal Maximum Offset (feet)	Normal Spread Geometry	Sweep Frequency (Hz)	Sweep Length (sec)	Listen Time (sec)
Z1-G3	1912	8	8	4	860	asymmetric 36/108 split	20 - 240	8	1
Z1-G4	1912	8	8	4	764	asymmetric 48/96 split	20 - 240	8	1
Z1-G5	1912	8	8	4	764	asymmetric 48/96 split	20 - 240	8	1
Z2-G1	1792.5	7.5	7.5	3.75	716.25	asymmetric 48/96 split	20 - 200	8	1
Z2-G2	1792.5	7.5	7.5	3.75	716.25	asymmetric 48/96 split	20 - 240	8	1
Z2-G3	1434	6	6	3	645	asymmetric 36/108 split	20 - 240	8	1
Z3-G1	1912	8	8	4	764	asymmetric 48/96 split	20 - 240	8	1
Z3-G2	1195	5	5	2.5	597.5	asymmetric 24/120 split	20 -240	8	0.5
Z3-G3	1912	8	8	4	764	asymmetric 48/96 split	20 - 240	8	1
Z3-G4	1434	6	6	3	573	asymmetric 48/96 split	20 - 240	8	1
Z3-G5	1578	6	6	3	573	asymmetric 48/96 split	20 - 240	8	1
Z3-G6	1506	6	6	3	429	symmetric 72/72 split	20 - 240	8	0.5
Z3-G7	1578	6	6	3	429	symmetric 72/72 split	20 - 240	8	0.5
Z4-G1	3832	8	8	4	764	asymmetric 48/96 split	20 - 200	8	1
Z4-G2	1912	8	8	4	764	asymmetric 48/96 split	20 - 240	8	1
Z5-G2	1912	8	8	4	956	asymmetric 24/120 split	20 - 240	8	1
Z5-G3	1912	8	8	4	860	asymmetric 36/108 split	20 - 240	8	1

Table 4. Generalized Processing Sequence

Sequence #	Description
1	SEG2 TO INTERNAL FORMAT CONVERSION
2	VIBROSEIS CORRELATION
3	GEOMETRY, SURVEY IMPORT AND TRACE EDITING
4	TRUE AMPLITUDE GAIN RECOVERY
5	TRACE TO TRACE EDITING
6	ELEVATION / DATUM STATICS APPLICATION:
	DATUM: INTERMEDIATE FLOATING/NMO DATUM
	VC: 6000 FEET/SEC
7	SURFACE CONSISTENT AMPLITUDE ANALYSIS AND COMPENSATION
8	MINIMUM PHASE CORRECTION FILTER FOR VIBROSEIS DATA
9	SURFACE CONSISTENT DECONVOLUTION:
	TYPE: SPIKING OPERATOR LENGTH: 160 MSEC NOISE: 0.1%
10	SPECTRAL WHITENING: 20-240 HZ
11	COMMON DEPTH POINT GATHERS:
	CDP BIN SIZE: 2.5 – 4 FEET
	PASS 1: VELOCITY AND MUTE ANALYSIS
	PASS 1: NORMAL MOVEOUT CORRECTION AND MUTE APPLICATION
	PASS 1: SURFACE CONSISTENT AUTOMATIC STATICS APPLICATION
	PASS 2: VELOCITY AND MUTE ANALYSIS
	PASS 2: NORMAL MOVEOUT CORRECTION AND MUTE APPLICATION
	PASS 2: SURFACE CONSISTENT AUTOMATIC STATICS APPLICATION
12	SURFACE/SOURCE WAVE / LINEAR NOISE ATTENUATION
13	TIME-VARIANT AMPLITUDE EQUALIZATION
	PASS 3: VELOCITY AND MUTE ANALYSIS
	PASS 3: NORMAL MOVEOUT CORRECTIONS AND MUTE APPLICATION
	PASS 3: SURFACE CONSISTENT AUTOMATIC STATICS APPLICATION
14	CDP CONSISTENT TRIM STATICS: 4 MSEC MAXIMUM SHIFT
15	COMMON DEPTH POINT STACK
16	FINAL DATUM CORRECTION:
	DATUM: FIXED FOR EACH LINE
	VC: 6000 FEET/SEC
17	FX PREDICTIVE ENHANCEMENT FILTER
18	SPECTRAL BALANCING: 40-240 HZ

Table 5. Seismic Reflection Depth Control

Line	Depth Control Source	Estimated Groundwater Depth		Groundwater Depth Source[1]	Expected Bedrock Type
		m	ft		
Z1-G3	Z1-S6	20	66	SR	Puente Fm
Z1-G4	Z1-S15	3	10	SW	Puente Fm
Z1-G5	Z1-S16	3	10	SW	Puente Fm
Z2-G1	Z2-S2	3	10	SW	Topanga Fm
Z2-G2	Z2-S8	7	23	SW	Puente Fm/Topanga Fm
Z2-G3	Z2-S10	9	30	SW	Puente Fm
Z3-G1	Z3-S3 & Z3-B4	45	148	B	Crystalline Basement
Z3-G2	Z3-S6	5	16	SW	Topanga Fm
Z3-G3	Z3-S10 & Z3-B7	3	10	B/SW	Topanga Fm
Z3-G4	Z3-S13	17	56	SR	Topanga Fm/Crystalline Basement
Z3-G5	Z3-S17	8	26	SW	Topanga Fm
Z3-G6	Z3-S21	16	52	SR	Puente Fm
Z3-G7	Z3-S23	12	39	SW	Puente Fm
Z4-G1	Z4-S2	64	210	SR	Puente Fm
Z4-G2	Z4-S6	65	213	SR	Puente Fm
Z5-G2	Z5-S8	56	184	SR	Puente Fm
Z5-G3	Z5-S12	16	52	SW	Puente Fm

1) SR - Seismic Reflection Data, SW - Surface Wave Data, B - Borehole Data

FIGURES

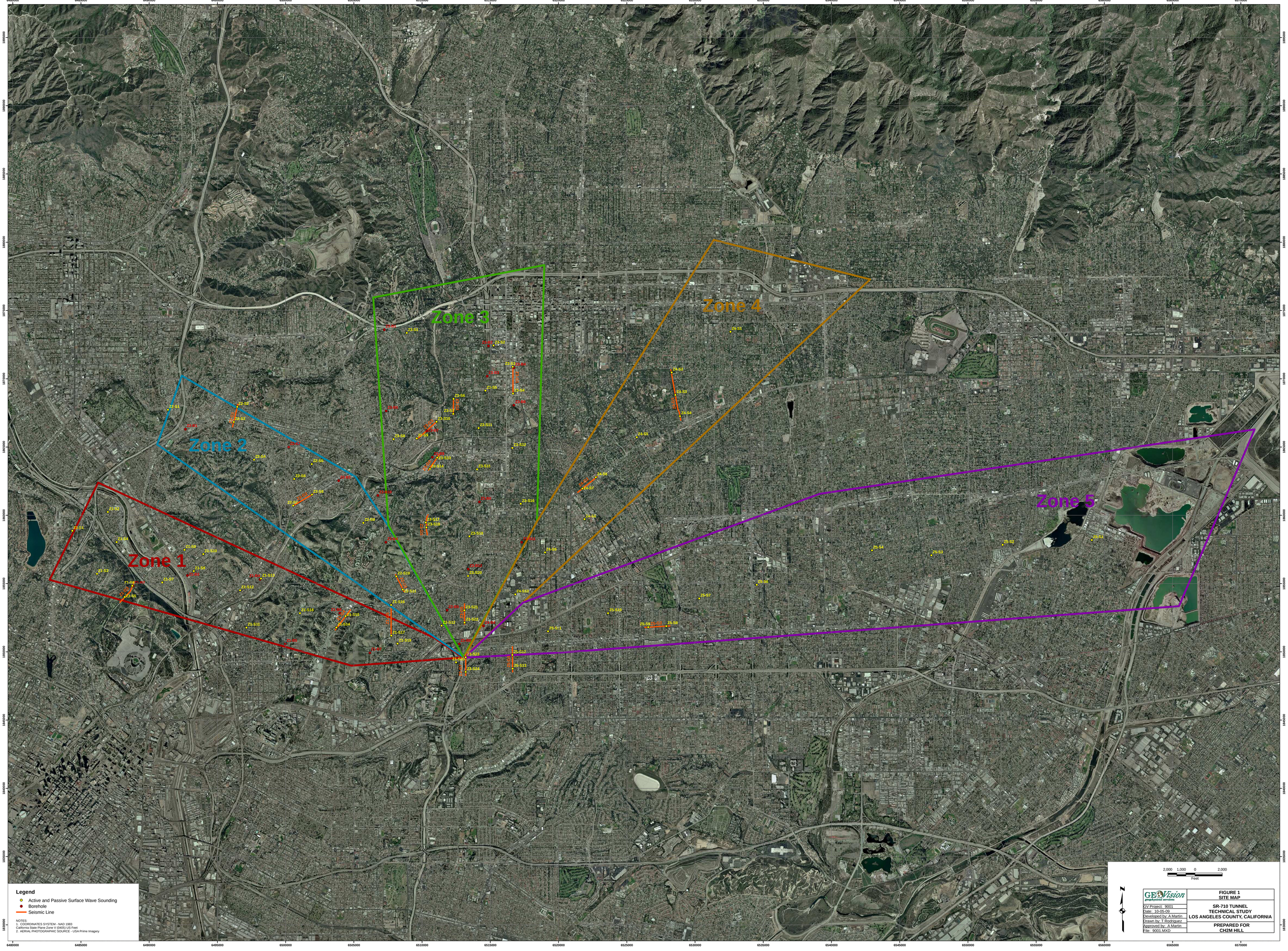
Zone 1
Zone 2
Zone 3
Zone 4
Zone 5
Legend
Active and Passive Surface Wave Sounding
Borehole
Seismic Line
NOTES:
1. COORDINATES SYSTEM - NAD 1983
California State Plane Zone V (0405) US Feet
2. AERIAL PHOTOGRAPHIC SOURCE - USA Prime Imagery
2,000 1,000 0 2,000
Feet
N
GEOVision geophysical services
FIGURE 1
SITE MAP
GV Project: 9001
Date: 10-05-09
Developed by: A Martin
Drawn by: T Rodriguez
Approved by: A Martin
File: 9001.MXD
SR-710 TUNNEL
TECHNICAL STUDY
LOS ANGELES COUNTY, CALIFORNIA
PREPARED FOR
CH2M HILL

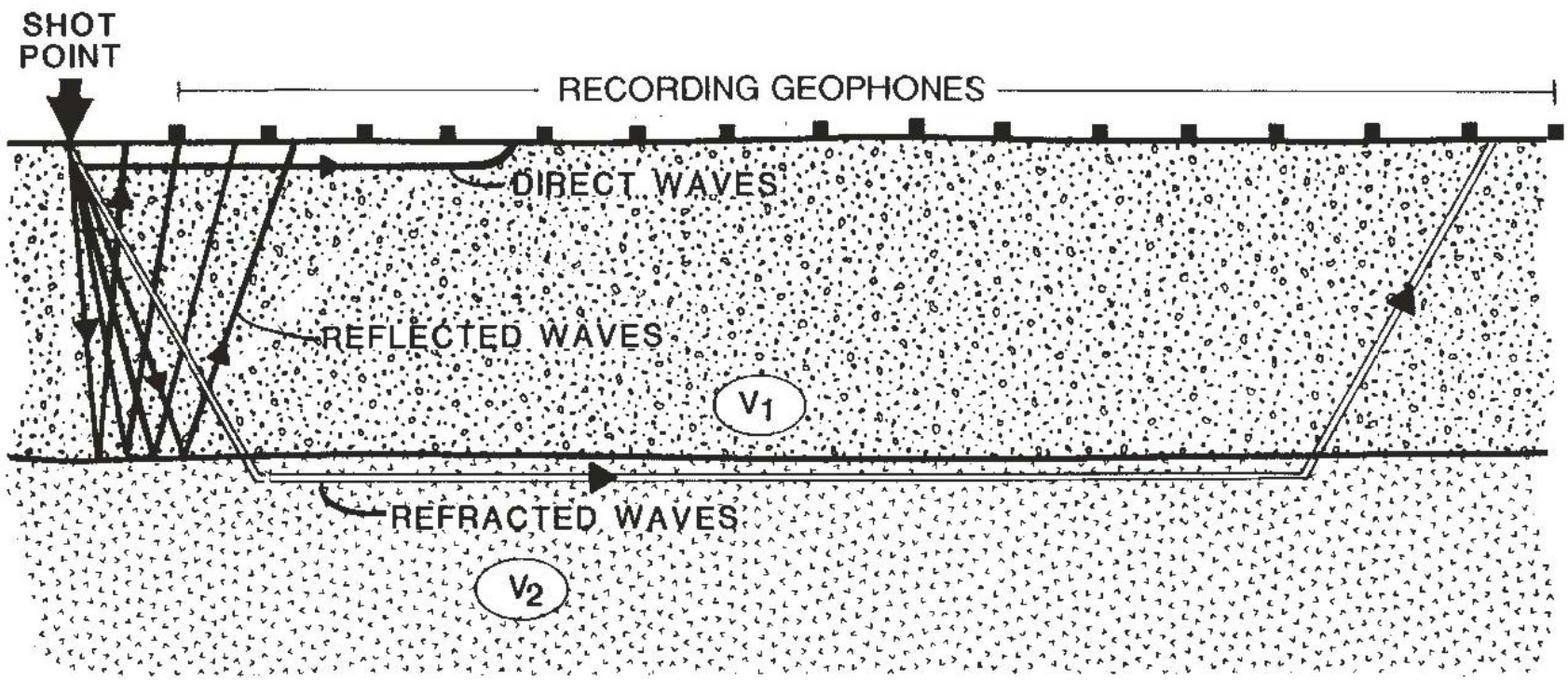

GEOVision geophysical services	FIGURE 2 SEISMIC RAYPATH GEOMETRY
Project # 9001 Date: AUG 4, 2009 Drawn By: A MARTIN Approved By:	SR-710 TUNNEL TECHNICAL STUDY LOS ANGELES COUNTY, CALIFORNIA
File R:\...Project Files\2009\9001ch2mhill\REFLReport\FIGURES\Figure2.cdr	PREPARED FOR CH2M HILL

TYPICAL SEISMIC LINE

SEISMIC RECORDING SYSTEM

IVI ENVIROVIBE

GEOVision geophysical services	FIGURE 3 PHOTOGRAPHS OF TYPICAL SEISMIC REFLECTION FIELD SETUP
Project # 9001 Date: AUG 4, 2009 Drawn By: A MARTIN Approved By:	SR-710 TUNNEL TECHNICAL STUDY LOS ANGELES COUNTY, CALIFORNIA
File R:\...Project Files\2009\9001ch2mhill\REFLReport\FIGURES\Figure3.cdr	PREPARED FOR CH2M HILL

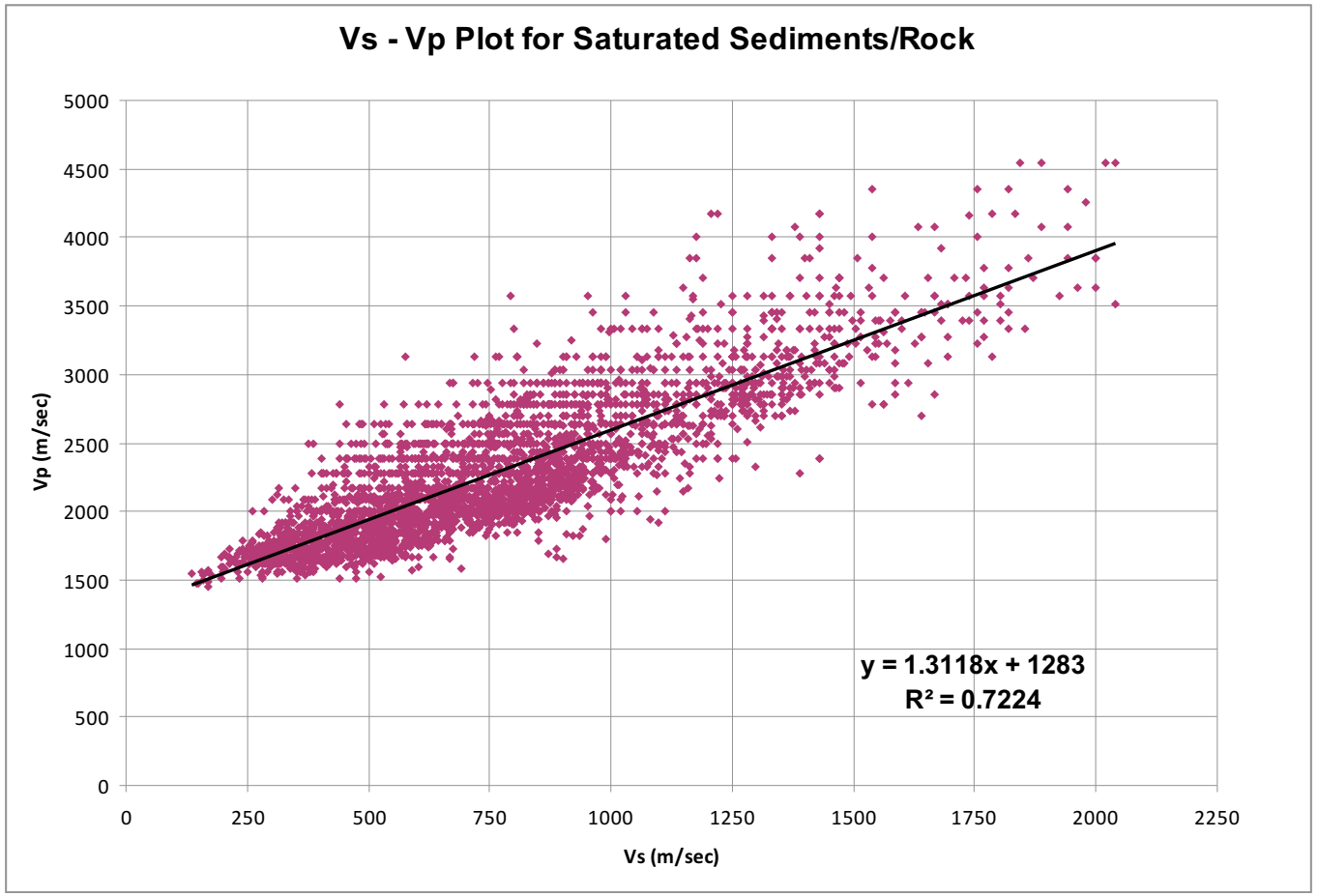

GEOVision geophysical services

Project # 9001	FIGURE 4 V_S - V_P PLOT FOR SATURATED SEDIMENTS/ROCK
Date: AUG 4, 2009	SR-710 TUNNEL TECHNICAL STUDY LOS ANGELES COUNTY, CALIFORNIA
Drawn By: A MARTIN	
Approved By: Anthony J Martin	PREPARED FOR CH2M HILL

File R:\...Project Files\2009\9001ch2mhill\REFLReport\FIGURES\Figure4.cdr

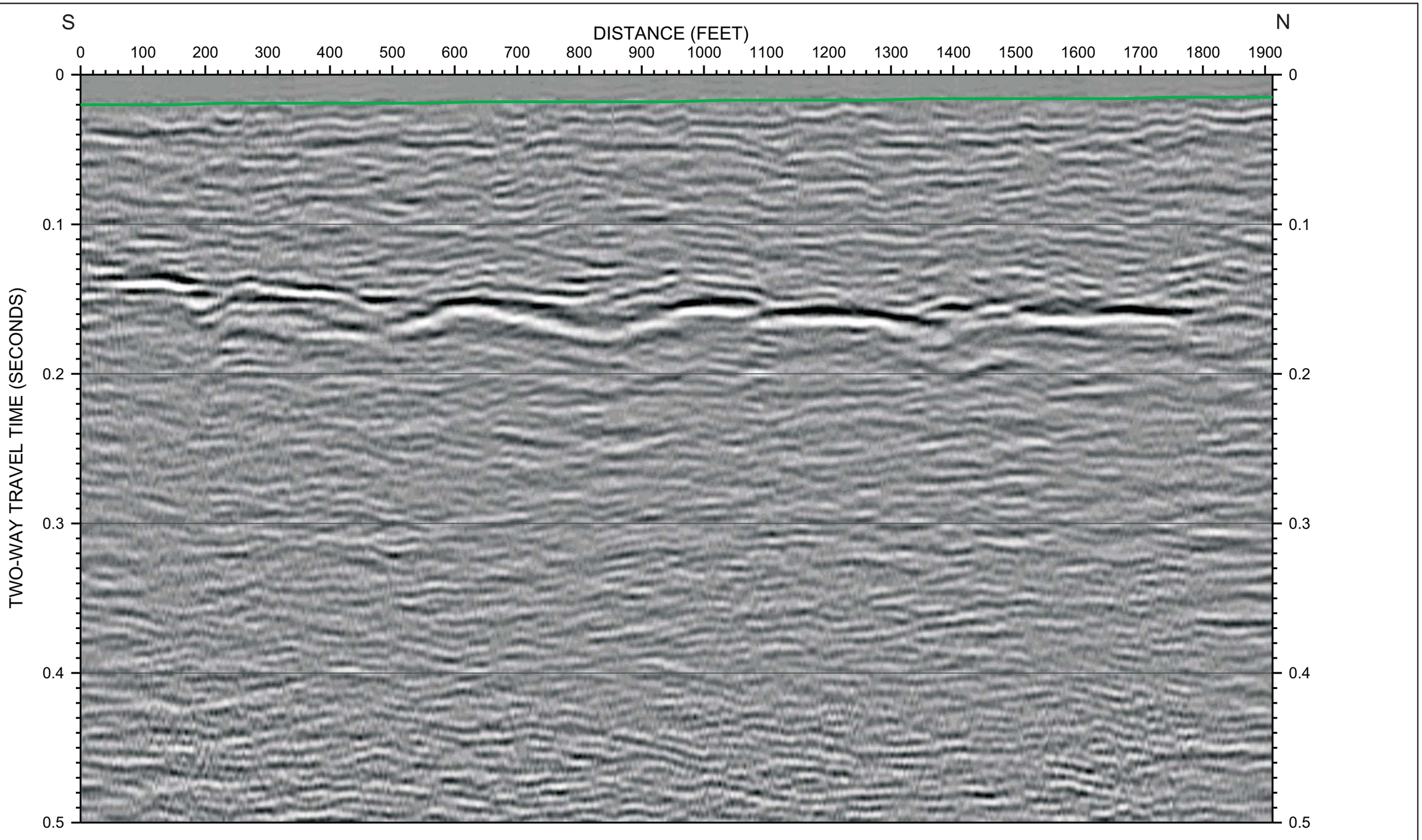

LINE Z3-G1

LEGEND

Ground Surface Reference

GEOVision geophysical services

Project #	9001
Date:	AUG 5, 2009
Drawn By:	A MARTIN
Approved By:	

File R:\...Project Files\2009\9001ch2mhill\REFLReport\FIGURES\Figure17.cdr

FIGURE 17
LINE Z3-G1 SEISMIC SECTION
WITHOUT INTERPRETATION

SR-710 TUNNEL TECHNICAL STUDY
LOS ANGELES COUNTY, CALIFORNIA

PREPARED FOR
CH2M HILL

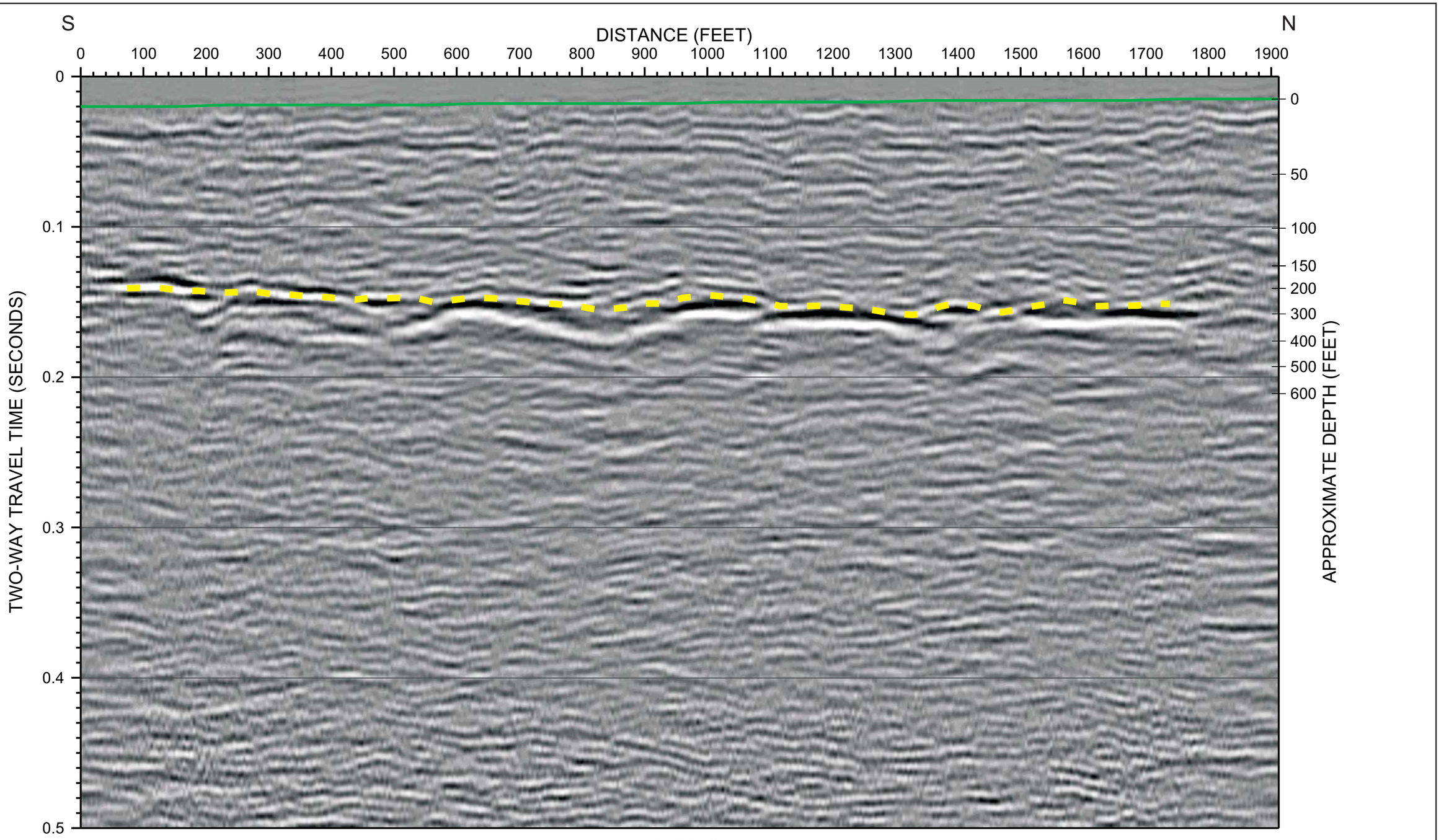

LINE Z3-G1

LEGEND

- Ground Surface Reference
- Interpreted Water Table or Top of Bedrock
- Interpreted Top of Bedrock or Weathering Contact within Bedrock
- Example Seismic Reflector
- Possible Fault, dotted where uncertain

GEOVision geophysical services

Project #	9001
Date:	AUG 5, 2009
Drawn By:	A MARTIN
Approved By:	

File R:\...Project Files\2009\9001ch2mhill\REFLReport\FIGURES\Figure18.cdr

FIGURE 18
LINE Z3-G1 SEISMIC SECTION
WITH INTERPRETATION

SR-710 TUNNEL TECHNICAL STUDY
LOS ANGELES COUNTY, CALIFORNIA

PREPARED FOR
CH2M HILL

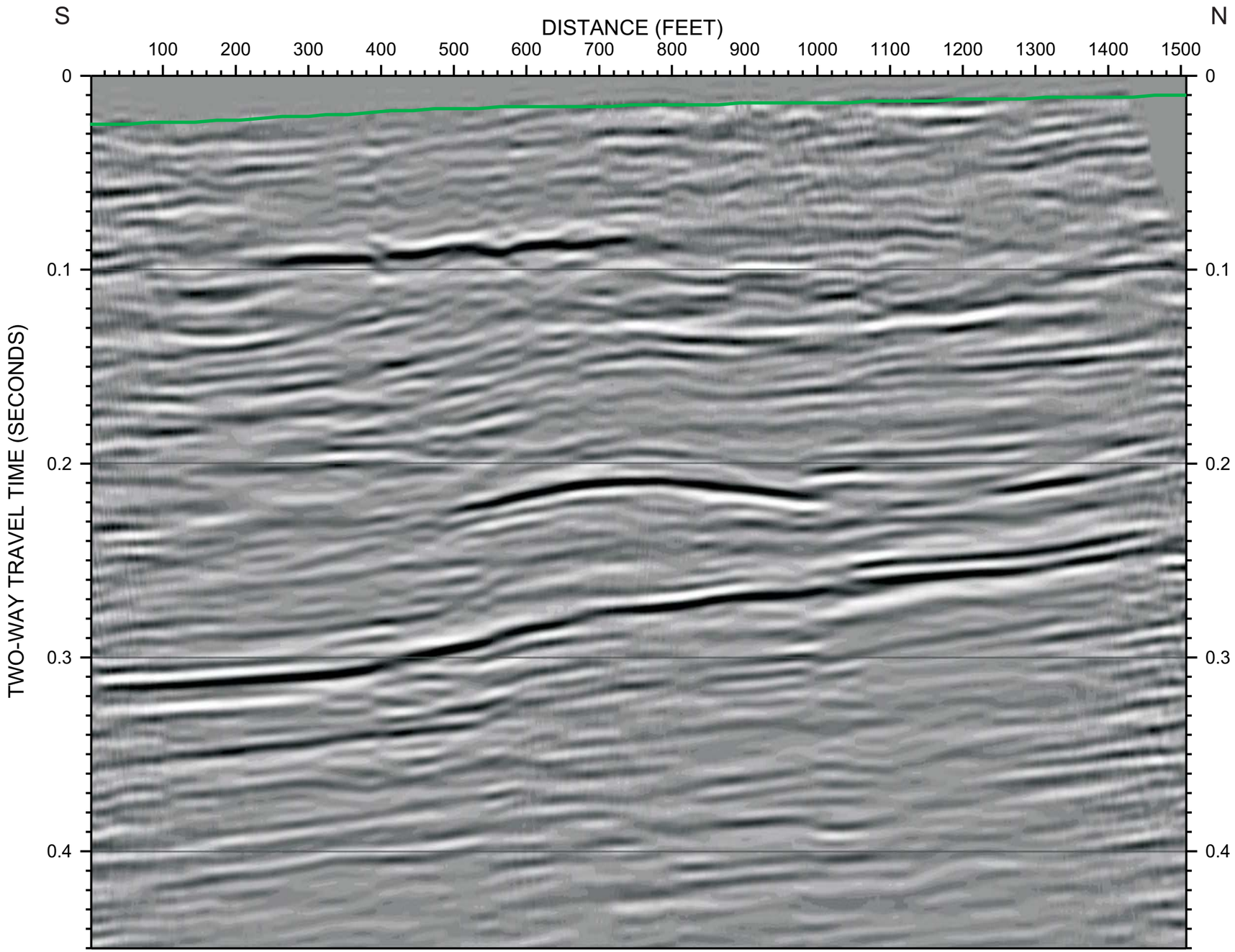

LINE Z3-G6

LEGEND

Ground Surface Reference

GEOVision geophysical services

Project #	9001
Date:	AUG 5, 2009
Drawn By:	A MARTIN
Approved By:	

File R:\...Project Files\2009\9001ch2mhill\REFLReport\FIGURES\Figure27.cdr

FIGURE 27
LINE Z3-G6 SEISMIC SECTION
WITHOUT INTERPRETATION

SR-710 TUNNEL TECHNICAL STUDY
LOS ANGELES COUNTY, CALIFORNIA

PREPARED FOR
CH2M HILL

S

N

DISTANCE (FEET)

100 200 300 400 500 600 700 800 900 1000 1100 1200 1300 1400 1500

TWO-WAY TRAVEL TIME (SECONDS)

0 0.1 0.2 0.3 0.4

APPROXIMATE DEPTH (FEET)

0 50 100 150 200 300 400 500 600

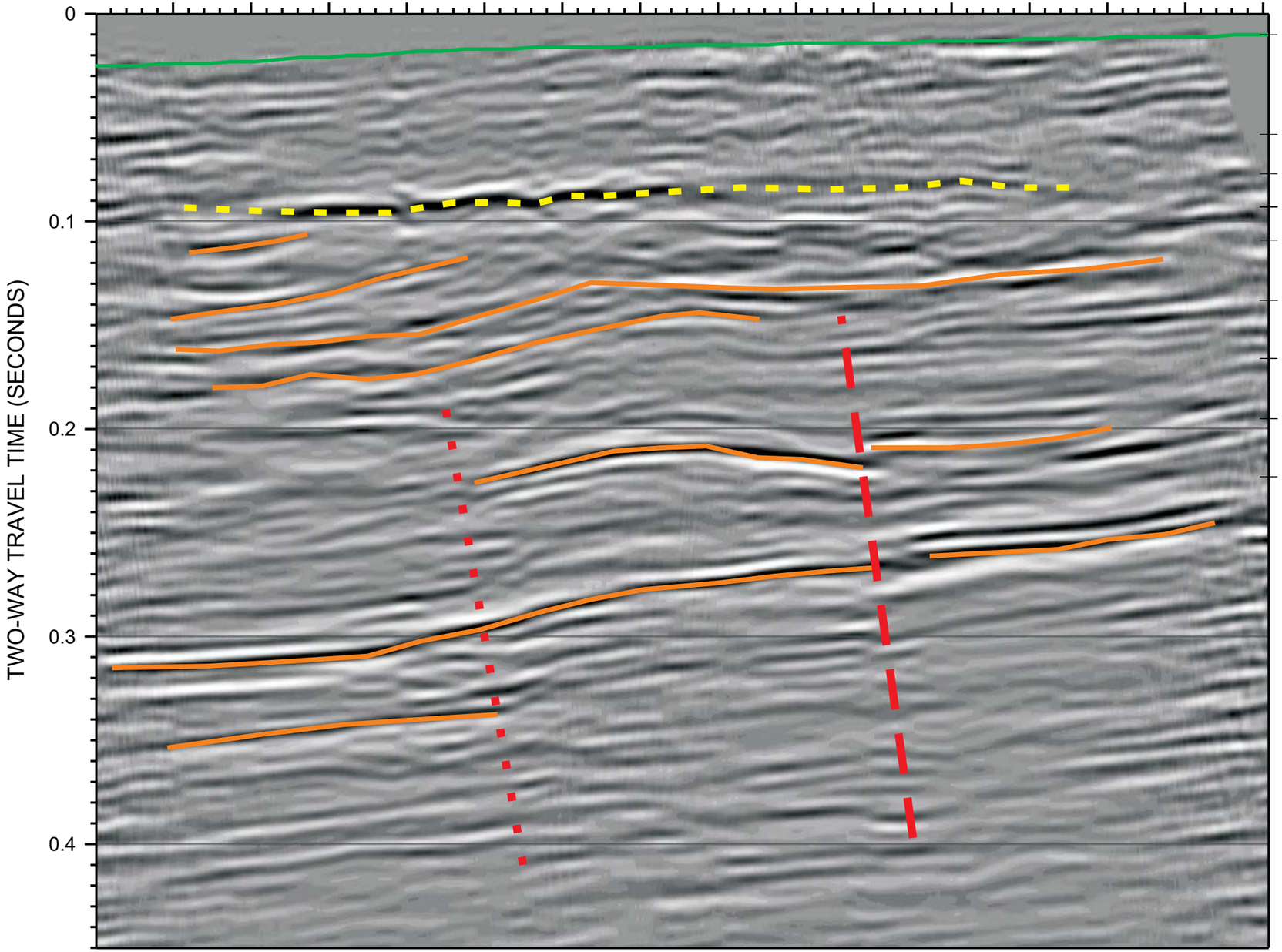

LINE Z3-G6

LEGEND

- Ground Surface Reference
- Interpreted Water Table or Top of Bedrock
- Interpreted Top of Bedrock or Weathering Contact within Bedrock
- Example Seismic Reflector
- Possible Fault, dotted where uncertain

GEOVision geophysical services

Project #	9001
Date:	AUG 5, 2009
Drawn By:	A MARTIN
Approved By:	

File R:\...Project Files\2009\9001ch2mhill\REFLReport\FIGURES\Figure28.cdr

FIGURE 28
LINE Z3-G6 SEISMIC SECTION
WITH INTERPRETATION

SR-710 TUNNEL TECHNICAL STUDY
LOS ANGELES COUNTY, CALIFORNIA

PREPARED FOR
CH2M HILL

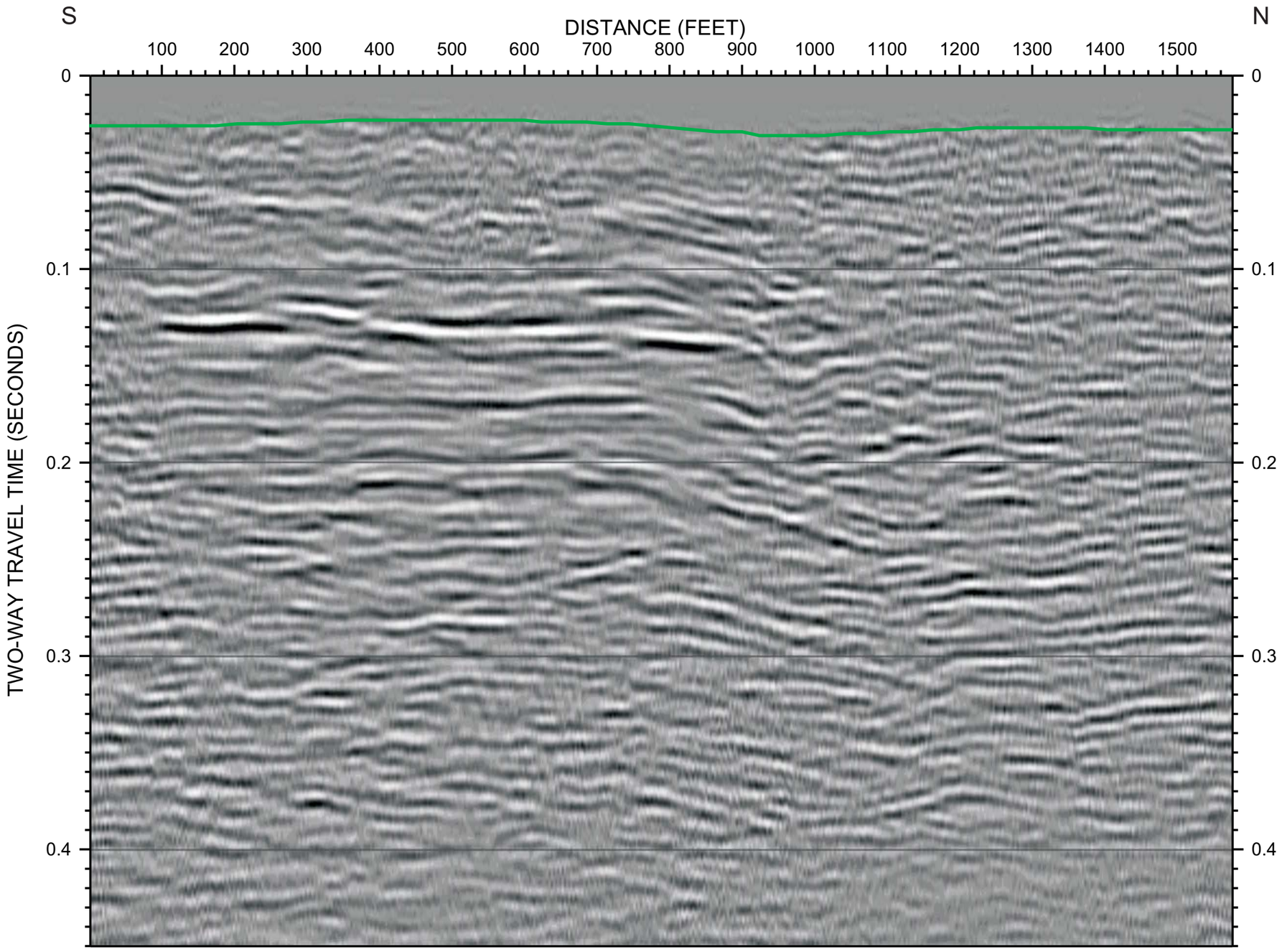

LINE Z3-G7

LEGEND

Ground Surface Reference

GEOVision geophysical services

Project #	9001
Date:	AUG 5, 2009
Drawn By:	A MARTIN
Approved By:	

File R:\...Project Files\2009\9001ch2mhill\REFLReport\FIGURES\Figure29.cdr

FIGURE 29
LINE Z3-G7 SEISMIC SECTION
WITHOUT INTERPRETATION

SR-710 TUNNEL TECHNICAL STUDY
LOS ANGELES COUNTY, CALIFORNIA

PREPARED FOR
CH2M HILL

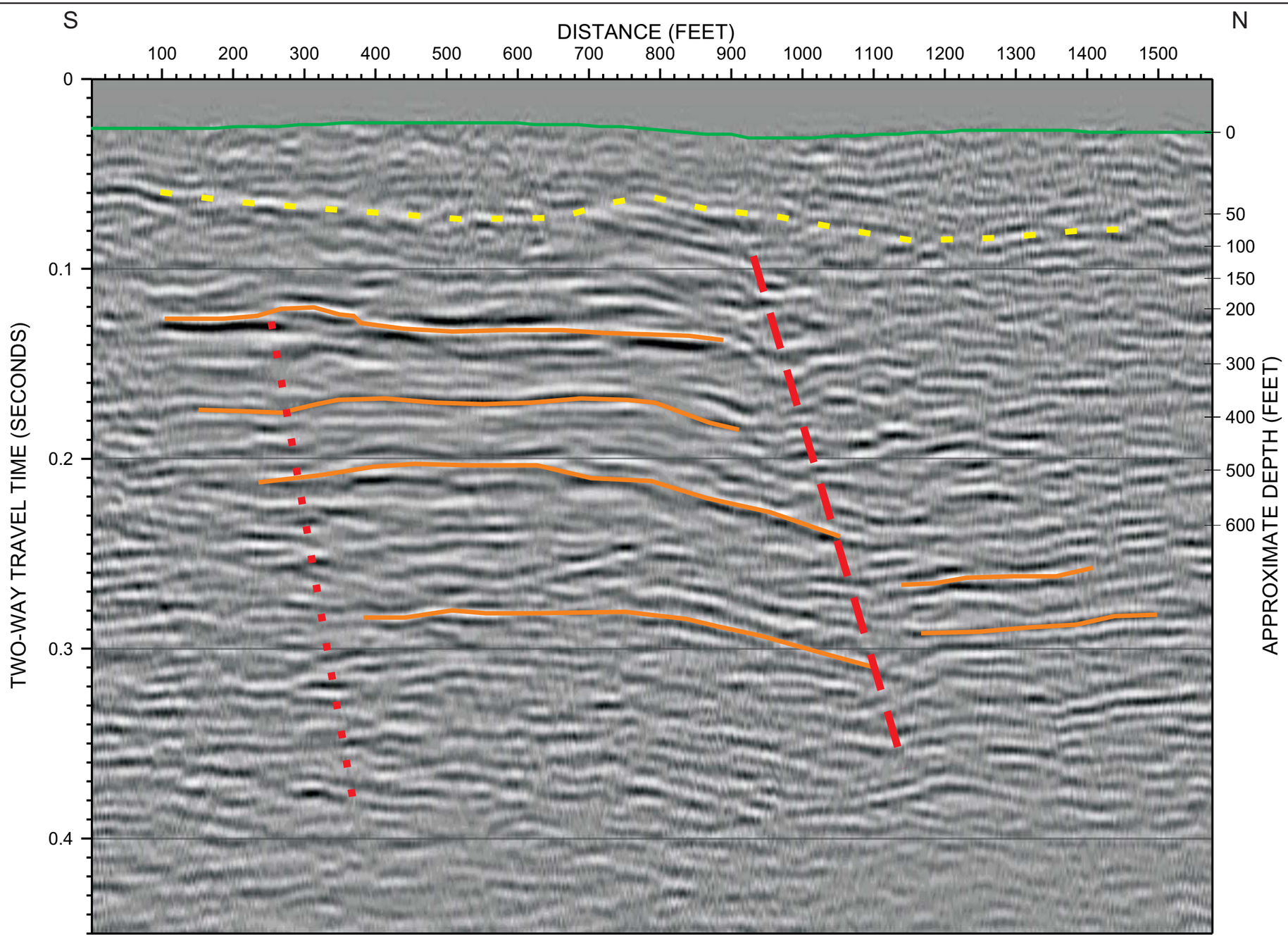

LINE Z3-G7

LEGEND

- Ground Surface Reference
- Interpreted Water Table or Top of Bedrock
- Interpreted Top of Bedrock or Weathering Contact within Bedrock
- Example Seismic Reflector
- Possible Fault, dotted where uncertain

GEOVision geophysical services

Project #	9001
Date:	AUG 5, 2009
Drawn By:	A MARTIN
Approved By:	

File R:\...Project Files\2009\9001ch2mhill\REFLReport\FIGURES\Figure30.cdr

FIGURE 30
LINE Z3-G7 SEISMIC SECTION
WITH INTERPRETATION

SR-710 TUNNEL TECHNICAL STUDY
LOS ANGELES COUNTY, CALIFORNIA

PREPARED FOR
CH2M HILL

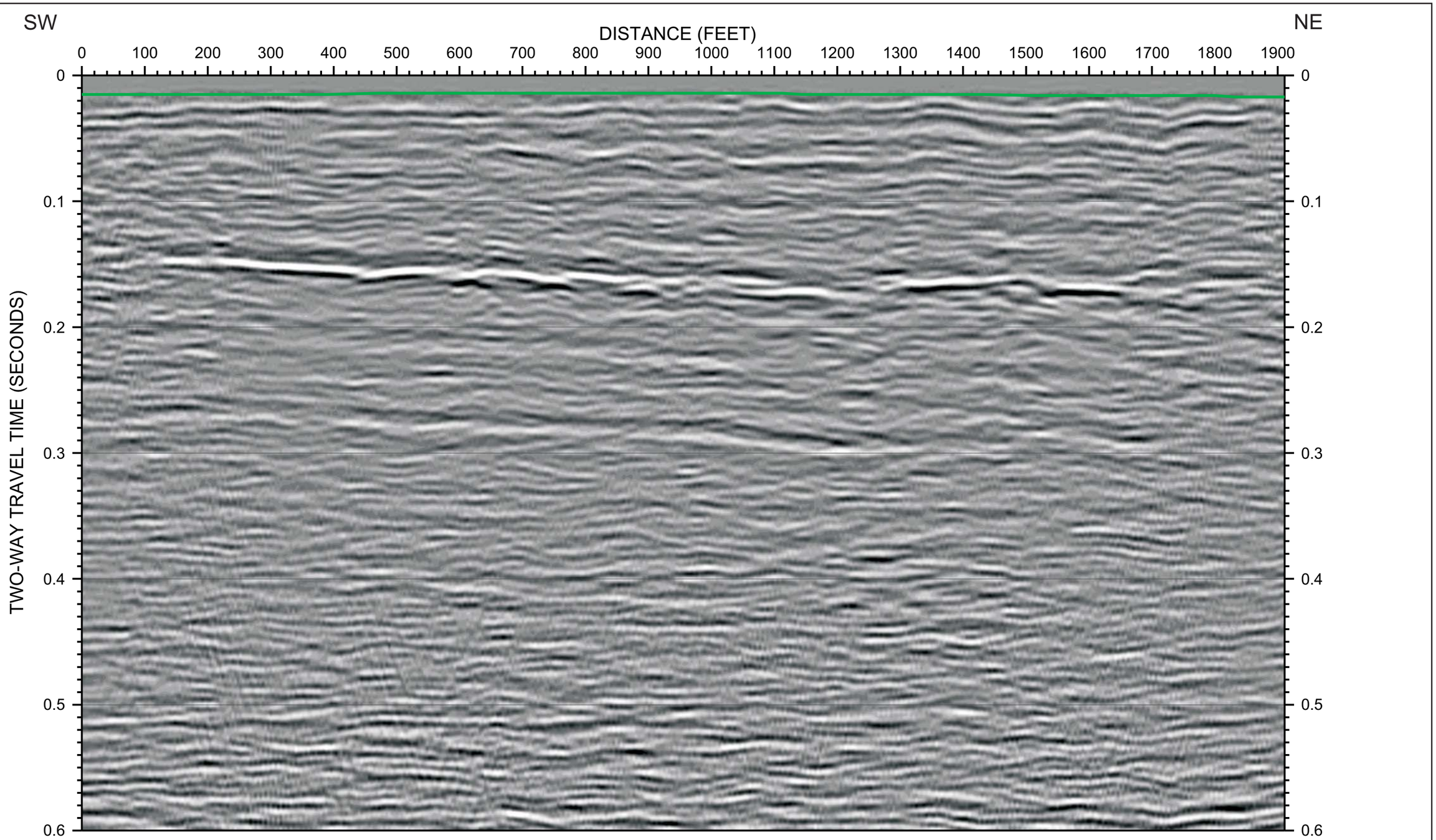

LINE Z4-G2

LEGEND

Ground Surface Reference

GEOVision geophysical services

Project #	9001
Date:	AUG 5, 2009
Drawn By:	A MARTIN
Approved By:	

File R:\...Project Files\2009\9001ch2mhill\REFLReport\FIGURES\Figure33.cdr

FIGURE 33
LINE Z4-G2 SEISMIC SECTION
WITHOUT INTERPRETATION

SR-710 TUNNEL TECHNICAL STUDY
LOS ANGELES COUNTY, CALIFORNIA

PREPARED FOR
CH2M HILL

SW

NE

DISTANCE (FEET)

0 100 200 300 400 500 600 700 800 900 1000 1100 1200 1300 1400 1500 1600 1700 1800 1900

TWO-WAY TRAVEL TIME (SECONDS)

0 0.1 0.2 0.3 0.4 0.5 0.6

APPROXIMATE DEPTH (FEET)

0 50 100 150 200 300 400 500 600

LINE Z4-G2

LEGEND

- Ground Surface Reference
- Interpreted Water Table or Top of Bedrock
- Interpreted Top of Bedrock or Weathering Contact within Bedrock
- Example Seismic Reflector
- Possible Fault, dotted where uncertain

GEOVision geophysical services

Project #	9001
Date:	AUG 5, 2009
Drawn By:	A MARTIN
Approved By:	

File R:\...Project Files\2009\9001ch2mhill\REFLReport\FIGURES\Figure34.cdr

FIGURE 34
LINE Z4-G2 SEISMIC SECTION
WITH INTERPRETATION

SR-710 TUNNEL TECHNICAL STUDY
LOS ANGELES COUNTY, CALIFORNIA

PREPARED FOR
CH2M HILL

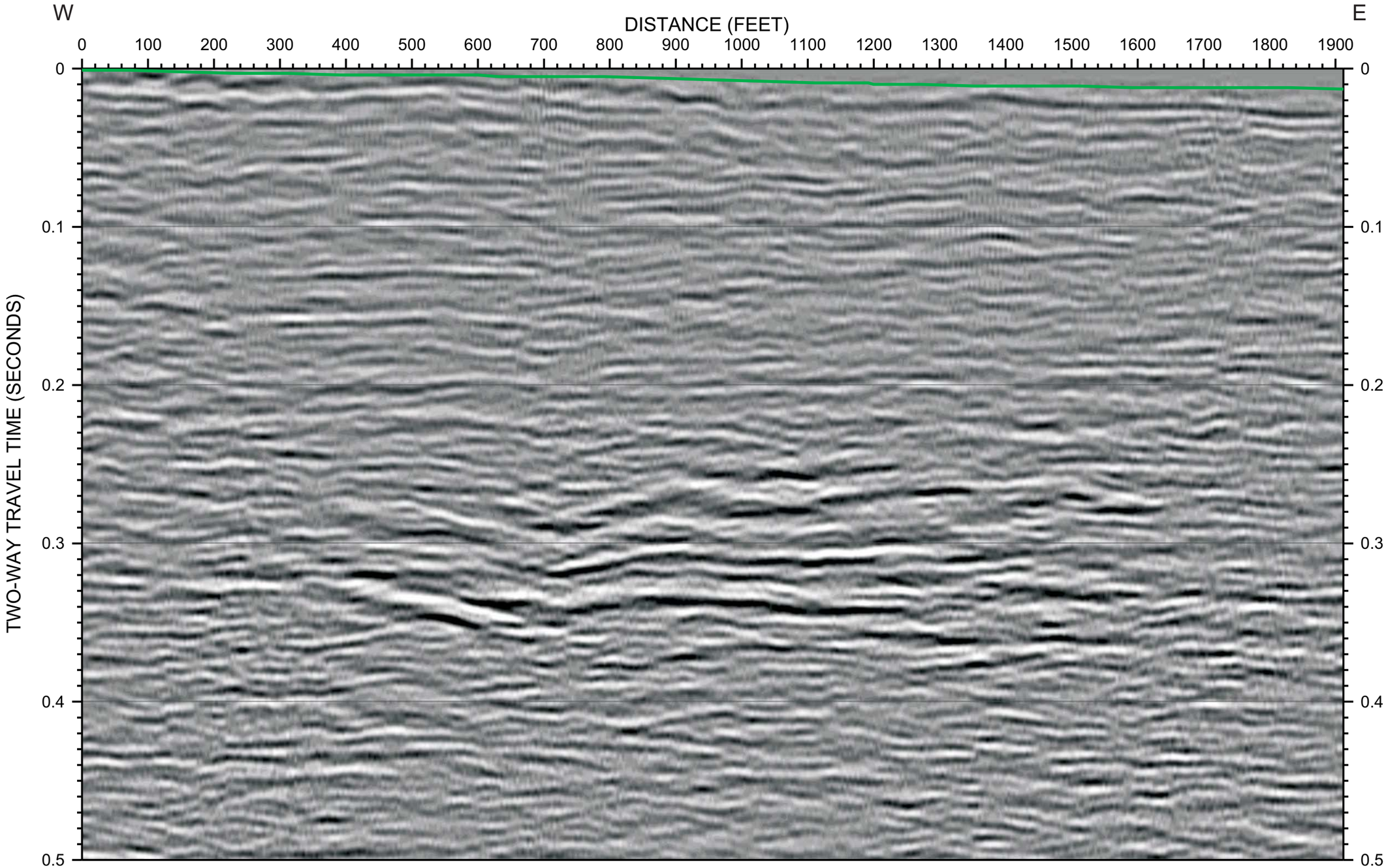

LINE Z5-G2

LEGEND

Ground Surface Reference

GEOVision geophysical services

Project #	9001
Date:	AUG 5, 2009
Drawn By:	A MARTIN
Approved By:	

File R:\...Project Files\2009\9001ch2mhill\REFLReport\FIGURES\Figure35.cdr

FIGURE 35
LINE Z5-G2 SEISMIC SECTION
WITHOUT INTERPRETATION

SR-710 TUNNEL TECHNICAL STUDY
LOS ANGELES COUNTY, CALIFORNIA

PREPARED FOR
CH2M HILL

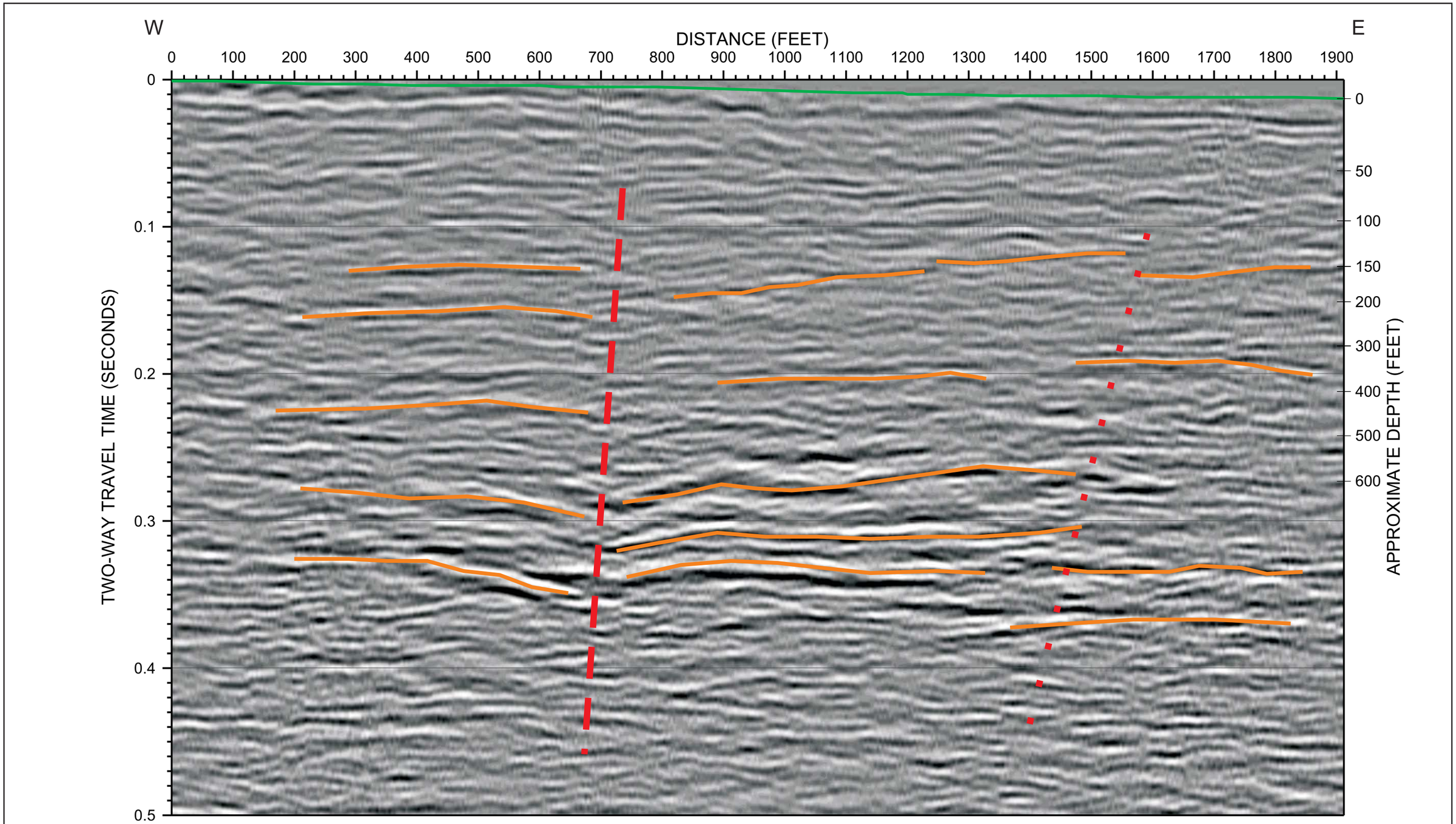

LINE Z5-G2

LEGEND

- Ground Surface Reference
- Interpreted Water Table or Top of Bedrock
- Interpreted Top of Bedrock or Weathering Contact within Bedrock
- Example Seismic Reflector
- Possible Fault, dotted where uncertain

GEOVision geophysical services

Project #	9001
Date:	AUG 5, 2009
Drawn By:	A MARTIN
Approved By:	

File R:\...Project Files\2009\9001ch2mhill\REFLReport\FIGURES\Figure36.cdr

FIGURE 36
LINE Z5-G2 SEISMIC SECTION
WITH INTERPRETATION

SR-710 TUNNEL TECHNICAL STUDY
LOS ANGELES COUNTY, CALIFORNIA

PREPARED FOR
CH2M HILL

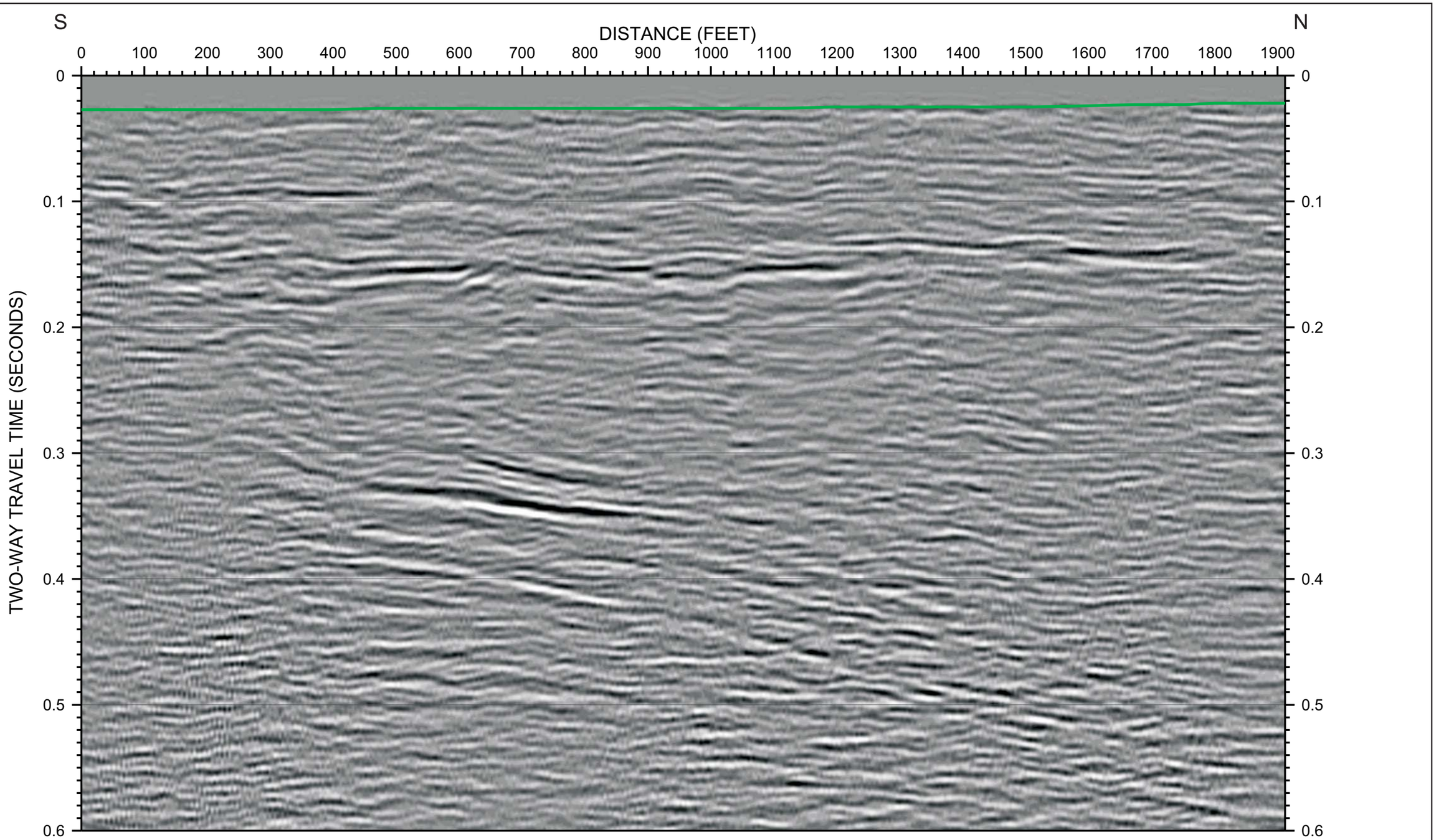

LINE Z5-G3

LEGEND

Ground Surface Reference

GEOVision geophysical services

Project #	9001
Date:	AUG 5, 2009
Drawn By:	A MARTIN
Approved By:	

File R:\...Project Files\2009\9001ch2mhill\REFLReport\FIGURES\Figure37.cdr

FIGURE 37
LINE Z5-G3 SEISMIC SECTION
WITHOUT INTERPRETATION

SR-710 TUNNEL TECHNICAL STUDY
LOS ANGELES COUNTY, CALIFORNIA

PREPARED FOR
CH2M HILL

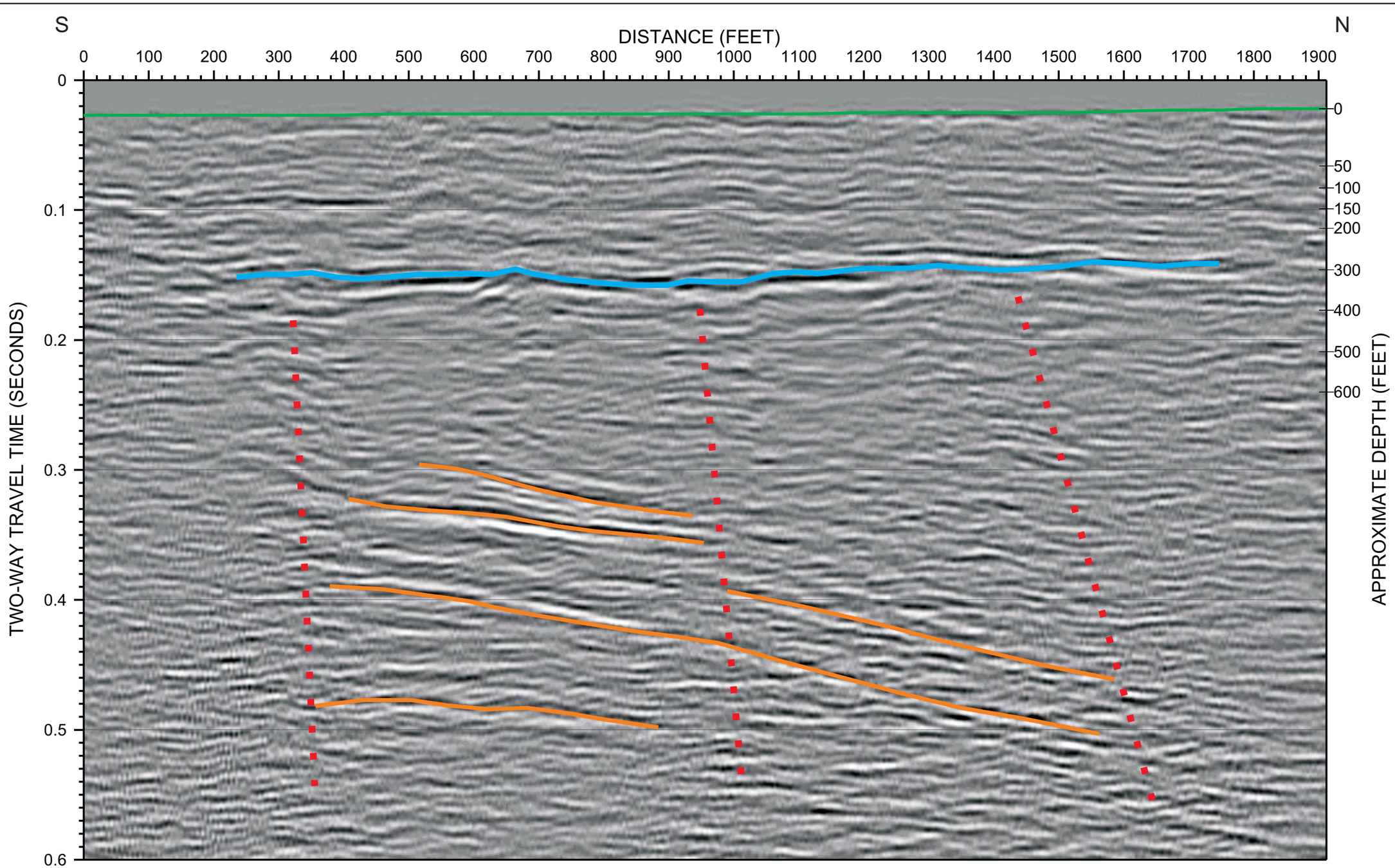

LINE Z5-G3

LEGEND

- Ground Surface Reference
- Interpreted Water Table or Top of Bedrock
- Interpreted Top of Bedrock or Weathering Contact within Bedrock
- Example Seismic Reflector
- Possible Fault, dotted where uncertain

GEOVision geophysical services

Project #	9001
Date:	AUG 5, 2009
Drawn By:	A MARTIN
Approved By:	

File R:\...Project Files\2009\9001ch2mhill\REFLReport\FIGURES\Figure38.cdr

FIGURE 38
LINE Z5-G3 SEISMIC SECTION
WITH INTERPRETATION

SR-710 TUNNEL TECHNICAL STUDY
LOS ANGELES COUNTY, CALIFORNIA

PREPARED FOR
CH2M HILL

GEOVision
geophysical services

REPORT

SURFACE WAVE MEASUREMENTS

SR-710 Tunnel Technical Study
Los Angeles County, California

Prepared for

CH2M HILL
6 Hutton Centre Drive, # 700
Santa Ana, CA 92707

Prepared by

GEOVision Geophysical Services
1124 Olympic Drive
Corona, California 92881
(951) 549-1234

Report 9001-01

October 5, 2009

TABLE OF CONTENTS

1 INTRODUCTION....1

2 OVERVIEW OF THE SURFACE WAVE METHODS....2

3 FIELD PROCEDURES....4

4 DATA REDUCTION AND MODELING....5

5 INTERPRETATION AND RESULTS....7

5.1 ZONE 1....7
5.2 ZONE 2....9
5.3 ZONE 3....10
5.4 ZONE 4....13
5.5 ZONE 5....14

6 CONCLUSIONS....16

7 REFERENCES....17

8 CERTIFICATION....18

APPENDIX A TECHNICAL NOTE – ACTIVE AND PASSIVE SURFACE WAVE TECHNIQUES

LIST OF TABLES

TABLE 1 SURFACE WAVE SOUNDING LOCATIONS
TABLE 2 ACTIVE AND PASSIVE SURFACE WAVE SOUNDING GEOMETRY
TABLE 3 VELOCITY MODEL FOR SURFACE WAVE ARRAY Z1-S1
TABLE 4 VELOCITY MODEL FOR SURFACE WAVE ARRAY Z1-S2
TABLE 5 VELOCITY MODEL FOR SURFACE WAVE ARRAY Z1-S3
TABLE 6 VELOCITY MODEL FOR SURFACE WAVE ARRAY Z1-S4
TABLE 7 VELOCITY MODEL FOR SURFACE WAVE ARRAY Z1-S5
TABLE 8 VELOCITY MODEL FOR SURFACE WAVE ARRAY Z1-S6
TABLE 9 VELOCITY MODEL FOR SURFACE WAVE ARRAY Z1-S7
TABLE 10 VELOCITY MODEL FOR SURFACE WAVE ARRAY Z1-S8
TABLE 11 VELOCITY MODEL FOR SURFACE WAVE ARRAY Z1-S9
TABLE 12 VELOCITY MODEL FOR SURFACE WAVE ARRAY Z1-S10
TABLE 13 VELOCITY MODEL FOR SURFACE WAVE ARRAY Z1-S11
TABLE 14 VELOCITY MODEL FOR SURFACE WAVE ARRAY Z1-S12
TABLE 15 VELOCITY MODEL FOR SURFACE WAVE ARRAY Z1-S13
TABLE 16 VELOCITY MODEL FOR SURFACE WAVE ARRAY Z1-S14
TABLE 17 VELOCITY MODEL FOR SURFACE WAVE ARRAY Z1-S15
TABLE 18 VELOCITY MODEL FOR SURFACE WAVE ARRAY Z1-S16
TABLE 19 VELOCITY MODEL FOR SURFACE WAVE ARRAY Z1-S18
TABLE 20 VELOCITY MODEL FOR SURFACE WAVE ARRAY Z1-S19
TABLE 21 VELOCITY MODEL FOR SURFACE WAVE ARRAY Z1-S20
TABLE 22 SUMMARY OF ZONE 1 SURFACE WAVE INVESTIGATION
TABLE 23 VELOCITY MODEL FOR SURFACE WAVE ARRAY Z2-S1
TABLE 24 VELOCITY MODEL FOR SURFACE WAVE ARRAY Z2-S2
TABLE 25 VELOCITY MODEL FOR SURFACE WAVE ARRAY Z2-S3
TABLE 26 VELOCITY MODEL FOR SURFACE WAVE ARRAY Z2-S4
TABLE 27 VELOCITY MODEL FOR SURFACE WAVE ARRAY Z2-S5
TABLE 28 VELOCITY MODEL FOR SURFACE WAVE ARRAY Z2-S6
TABLE 29 VELOCITY MODEL FOR SURFACE WAVE ARRAY Z2-S7
TABLE 30 VELOCITY MODEL FOR SURFACE WAVE ARRAY Z2-S8
TABLE 31 VELOCITY MODEL FOR SURFACE WAVE ARRAY Z2-S9
TABLE 32 VELOCITY MODEL FOR SURFACE WAVE ARRAY Z2-S10
TABLE 33 VELOCITY MODEL FOR SURFACE WAVE ARRAY Z2-S11
TABLE 34 VELOCITY MODEL FOR SURFACE WAVE ARRAY Z2-S12
TABLE 35 SUMMARY OF ZONE 2 SURFACE WAVE INVESTIGATION
TABLE 36 VELOCITY MODEL FOR SURFACE WAVE ARRAY Z3-S1
TABLE 37 VELOCITY MODEL FOR SURFACE WAVE ARRAY Z3-S2
TABLE 38 VELOCITY MODEL FOR SURFACE WAVE ARRAY Z3-S3
TABLE 39 VELOCITY MODEL FOR SURFACE WAVE ARRAY Z3-S4
TABLE 40 VELOCITY MODEL FOR SURFACE WAVE ARRAY Z3-S5
TABLE 41 VELOCITY MODEL FOR SURFACE WAVE ARRAY Z3-S6
TABLE 42 VELOCITY MODEL FOR SURFACE WAVE ARRAY Z3-S7
TABLE 43 VELOCITY MODEL FOR SURFACE WAVE ARRAY Z3-S8
TABLE 44 VELOCITY MODEL FOR SURFACE WAVE ARRAY Z3-S9
TABLE 45 VELOCITY MODEL FOR SURFACE WAVE ARRAY Z3-S10
TABLE 46 VELOCITY MODEL FOR SURFACE WAVE ARRAY Z3-S11
TABLE 47 VELOCITY MODEL FOR SURFACE WAVE ARRAY Z3-S12
TABLE 48 VELOCITY MODEL FOR SURFACE WAVE ARRAY Z3-S13
TABLE 49 VELOCITY MODEL FOR SURFACE WAVE ARRAY Z3-S14
TABLE 50 VELOCITY MODEL FOR SURFACE WAVE ARRAY Z3-S15
TABLE 51 VELOCITY MODEL FOR SURFACE WAVE ARRAY Z3-S16
TABLE 52 VELOCITY MODEL FOR SURFACE WAVE ARRAY Z3-S17
TABLE 53 VELOCITY MODEL FOR SURFACE WAVE ARRAY Z3-S18
TABLE 54 VELOCITY MODEL FOR SURFACE WAVE ARRAY Z3-S19
TABLE 55 VELOCITY MODEL FOR SURFACE WAVE ARRAY Z3-S20
TABLE 56 VELOCITY MODEL FOR SURFACE WAVE ARRAY Z3-S21
TABLE 57 VELOCITY MODEL FOR SURFACE WAVE ARRAY Z3-S22
TABLE 58 VELOCITY MODEL FOR SURFACE WAVE ARRAY Z3-S23

TABLE 59 VELOCITY MODEL FOR SURFACE WAVE ARRAY Z3-S24
TABLE 60 SUMMARY OF ZONE 3 SURFACE WAVE INVESTIGATION
TABLE 61 VELOCITY MODEL FOR SURFACE WAVE ARRAY Z4-S1
TABLE 62 VELOCITY MODEL FOR SURFACE WAVE ARRAY Z4-S2
TABLE 63 VELOCITY MODEL FOR SURFACE WAVE ARRAY Z4-S3
TABLE 64 VELOCITY MODEL FOR SURFACE WAVE ARRAY Z4-S4
TABLE 65 VELOCITY MODEL FOR SURFACE WAVE ARRAY Z4-S5
TABLE 66 VELOCITY MODEL FOR SURFACE WAVE ARRAY Z4-S6
TABLE 67 VELOCITY MODEL FOR SURFACE WAVE ARRAY Z4-S7
TABLE 68 VELOCITY MODEL FOR SURFACE WAVE ARRAY Z4-S8
TABLE 69 VELOCITY MODEL FOR SURFACE WAVE ARRAY Z4-S9
TABLE 70 VELOCITY MODEL FOR SURFACE WAVE ARRAY Z4-S10
TABLE 71 SUMMARY OF ZONE 4 SURFACE WAVE INVESTIGATION
TABLE 72 VELOCITY MODEL FOR SURFACE WAVE ARRAY Z5-S1
TABLE 73 VELOCITY MODEL FOR SURFACE WAVE ARRAY Z5-S2
TABLE 74 VELOCITY MODEL FOR SURFACE WAVE ARRAY Z5-S3
TABLE 75 VELOCITY MODEL FOR SURFACE WAVE ARRAY Z5-S4
TABLE 76 VELOCITY MODEL FOR SURFACE WAVE ARRAY Z5-S6
TABLE 77 VELOCITY MODEL FOR SURFACE WAVE ARRAY Z5-S7
TABLE 78 VELOCITY MODEL FOR SURFACE WAVE ARRAY Z5-S8
TABLE 79 VELOCITY MODEL FOR SURFACE WAVE ARRAY Z5-S9
TABLE 80 VELOCITY MODEL FOR SURFACE WAVE ARRAY Z5-S10
TABLE 81 VELOCITY MODEL FOR SURFACE WAVE ARRAY Z5-S11
TABLE 82 VELOCITY MODEL FOR SURFACE WAVE ARRAY Z5-S12
TABLE 83 VELOCITY MODEL FOR SURFACE WAVE ARRAY Z5-S13
TABLE 84 SUMMARY OF ZONE 5 SURFACE WAVE INVESTIGATION

LIST OF FIGURES

FIGURE 1 SITE MAP
FIGURE 2 PHOTOGRAPHS OF PASSIVE AND ACTIVE SURFACE ARRAY FIELD LAYOUT
FIGURE 3 TYPICAL WAVEFIELD TRANSFORMS OF ACTIVE AND PASSIVE SURFACE WAVE DATA
FIGURE 4 VELOCITY MODEL FOR ACTIVE AND PASSIVE SURFACE WAVE ARRAY Z1-S1
FIGURE 5 VELOCITY MODEL FOR ACTIVE AND PASSIVE SURFACE WAVE ARRAY Z1-S2
FIGURE 6 VELOCITY MODEL FOR ACTIVE AND PASSIVE SURFACE WAVE ARRAY Z1-S3
FIGURE 7 VELOCITY MODEL FOR ACTIVE AND PASSIVE SURFACE WAVE ARRAY Z1-S4
FIGURE 8 VELOCITY MODEL FOR ACTIVE AND PASSIVE SURFACE WAVE ARRAY Z1-S5
FIGURE 9 VELOCITY MODEL FOR ACTIVE AND PASSIVE SURFACE WAVE ARRAY Z1-S6
FIGURE 10 VELOCITY MODEL FOR ACTIVE AND PASSIVE SURFACE WAVE ARRAY Z1-S7
FIGURE 11 VELOCITY MODEL FOR ACTIVE AND PASSIVE SURFACE WAVE ARRAY Z1-S8
FIGURE 12 VELOCITY MODEL FOR ACTIVE AND PASSIVE SURFACE WAVE ARRAY Z1-S9
FIGURE 13 VELOCITY MODEL FOR ACTIVE AND PASSIVE SURFACE WAVE ARRAY Z1-S10
FIGURE 14 VELOCITY MODEL FOR ACTIVE AND PASSIVE SURFACE WAVE ARRAY Z1-S11
FIGURE 15 VELOCITY MODEL FOR ACTIVE AND PASSIVE SURFACE WAVE ARRAY Z1-S12
FIGURE 16 VELOCITY MODEL FOR ACTIVE AND PASSIVE SURFACE WAVE ARRAY Z1-S13
FIGURE 17 VELOCITY MODEL FOR ACTIVE AND PASSIVE SURFACE WAVE ARRAY Z1-S14
FIGURE 18 VELOCITY MODEL FOR ACTIVE AND PASSIVE SURFACE WAVE ARRAY Z1-S15
FIGURE 19 VELOCITY MODEL FOR ACTIVE AND PASSIVE SURFACE WAVE ARRAY Z1-S16
FIGURE 20 VELOCITY MODEL FOR ACTIVE AND PASSIVE SURFACE WAVE ARRAY Z1-S18
FIGURE 21 VELOCITY MODEL FOR ACTIVE AND PASSIVE SURFACE WAVE ARRAY Z1-S19
FIGURE 22 VELOCITY MODEL FOR ACTIVE AND PASSIVE SURFACE WAVE ARRAY Z1-S20
FIGURE 23 VELOCITY MODEL FOR ACTIVE AND PASSIVE SURFACE WAVE ARRAY Z2-S1
FIGURE 24 VELOCITY MODEL FOR ACTIVE AND PASSIVE SURFACE WAVE ARRAY Z2-S2
FIGURE 25 VELOCITY MODEL FOR ACTIVE AND PASSIVE SURFACE WAVE ARRAY Z2-S3
FIGURE 26 VELOCITY MODEL FOR ACTIVE AND PASSIVE SURFACE WAVE ARRAY Z2-S4
FIGURE 27 VELOCITY MODEL FOR ACTIVE AND PASSIVE SURFACE WAVE ARRAY Z2-S5

FIGURE 28 VELOCITY MODEL FOR ACTIVE AND PASSIVE SURFACE WAVE ARRAY Z2-S6
FIGURE 29 VELOCITY MODEL FOR ACTIVE AND PASSIVE SURFACE WAVE ARRAY Z2-S7
FIGURE 30 VELOCITY MODEL FOR ACTIVE AND PASSIVE SURFACE WAVE ARRAY Z2-S8
FIGURE 31 VELOCITY MODEL FOR ACTIVE AND PASSIVE SURFACE WAVE ARRAY Z2-S9
FIGURE 32 VELOCITY MODEL FOR ACTIVE AND PASSIVE SURFACE WAVE ARRAY Z2-S10
FIGURE 33 VELOCITY MODEL FOR ACTIVE AND PASSIVE SURFACE WAVE ARRAY Z2-S11
FIGURE 34 VELOCITY MODEL FOR ACTIVE AND PASSIVE SURFACE WAVE ARRAY Z2-S12
FIGURE 35 VELOCITY MODEL FOR ACTIVE AND PASSIVE SURFACE WAVE ARRAY Z3-S1
FIGURE 36 VELOCITY MODEL FOR ACTIVE AND PASSIVE SURFACE WAVE ARRAY Z3-S2
FIGURE 37 VELOCITY MODEL FOR ACTIVE AND PASSIVE SURFACE WAVE ARRAY Z3-S3
FIGURE 38 VELOCITY MODEL FOR ACTIVE AND PASSIVE SURFACE WAVE ARRAY Z3-S4
FIGURE 39 VELOCITY MODEL FOR ACTIVE AND PASSIVE SURFACE WAVE ARRAY Z3-S5
FIGURE 40 VELOCITY MODEL FOR ACTIVE AND PASSIVE SURFACE WAVE ARRAY Z3-S6
FIGURE 41 VELOCITY MODEL FOR ACTIVE AND PASSIVE SURFACE WAVE ARRAY Z3-S7
FIGURE 42 VELOCITY MODEL FOR ACTIVE AND PASSIVE SURFACE WAVE ARRAY Z3-S8
FIGURE 43 VELOCITY MODEL FOR ACTIVE AND PASSIVE SURFACE WAVE ARRAY Z3-S9
FIGURE 44 VELOCITY MODEL FOR ACTIVE AND PASSIVE SURFACE WAVE ARRAY Z3-S10
FIGURE 45 VELOCITY MODEL FOR ACTIVE AND PASSIVE SURFACE WAVE ARRAY Z3-S11
FIGURE 46 VELOCITY MODEL FOR ACTIVE AND PASSIVE SURFACE WAVE ARRAY Z3-S12
FIGURE 47 VELOCITY MODEL FOR ACTIVE AND PASSIVE SURFACE WAVE ARRAY Z3-S13
FIGURE 48 VELOCITY MODEL FOR ACTIVE AND PASSIVE SURFACE WAVE ARRAY Z3-S14
FIGURE 49 VELOCITY MODEL FOR ACTIVE AND PASSIVE SURFACE WAVE ARRAY Z3-S15
FIGURE 50 VELOCITY MODEL FOR ACTIVE AND PASSIVE SURFACE WAVE ARRAY Z3-S16
FIGURE 51 VELOCITY MODEL FOR ACTIVE AND PASSIVE SURFACE WAVE ARRAY Z3-S17
FIGURE 52 VELOCITY MODEL FOR ACTIVE AND PASSIVE SURFACE WAVE ARRAY Z3-S18
FIGURE 53 VELOCITY MODEL FOR ACTIVE AND PASSIVE SURFACE WAVE ARRAY Z3-S19
FIGURE 54 VELOCITY MODEL FOR ACTIVE AND PASSIVE SURFACE WAVE ARRAY Z3-S20
FIGURE 55 VELOCITY MODEL FOR ACTIVE AND PASSIVE SURFACE WAVE ARRAY Z3-S21
FIGURE 56 VELOCITY MODEL FOR ACTIVE AND PASSIVE SURFACE WAVE ARRAY Z3-S22
FIGURE 57 VELOCITY MODEL FOR ACTIVE AND PASSIVE SURFACE WAVE ARRAY Z3-S23
FIGURE 58 VELOCITY MODEL FOR ACTIVE AND PASSIVE SURFACE WAVE ARRAY Z3-S24
FIGURE 59 VELOCITY MODEL FOR ACTIVE AND PASSIVE SURFACE WAVE ARRAY Z4-S1
FIGURE 60 VELOCITY MODEL FOR ACTIVE AND PASSIVE SURFACE WAVE ARRAY Z4-S2
FIGURE 61 VELOCITY MODEL FOR ACTIVE AND PASSIVE SURFACE WAVE ARRAY Z4-S3
FIGURE 62 VELOCITY MODEL FOR ACTIVE AND PASSIVE SURFACE WAVE ARRAY Z4-S4
FIGURE 63 VELOCITY MODEL FOR ACTIVE AND PASSIVE SURFACE WAVE ARRAY Z4-S5
FIGURE 64 VELOCITY MODEL FOR ACTIVE AND PASSIVE SURFACE WAVE ARRAY Z4-S6
FIGURE 65 VELOCITY MODEL FOR ACTIVE AND PASSIVE SURFACE WAVE ARRAY Z4-S7
FIGURE 66 VELOCITY MODEL FOR ACTIVE AND PASSIVE SURFACE WAVE ARRAY Z4-S8
FIGURE 67 VELOCITY MODEL FOR ACTIVE AND PASSIVE SURFACE WAVE ARRAY Z4-S9
FIGURE 68 VELOCITY MODEL FOR ACTIVE AND PASSIVE SURFACE WAVE ARRAY Z4-S10
FIGURE 69 VELOCITY MODEL FOR ACTIVE AND PASSIVE SURFACE WAVE ARRAY Z5-S1
FIGURE 70 VELOCITY MODEL FOR ACTIVE AND PASSIVE SURFACE WAVE ARRAY Z5-S2
FIGURE 71 VELOCITY MODEL FOR ACTIVE AND PASSIVE SURFACE WAVE ARRAY Z5-S3
FIGURE 72 VELOCITY MODEL FOR ACTIVE AND PASSIVE SURFACE WAVE ARRAY Z5-S4
FIGURE 73 VELOCITY MODEL FOR ACTIVE AND PASSIVE SURFACE WAVE ARRAY Z5-S6
FIGURE 74 VELOCITY MODEL FOR ACTIVE AND PASSIVE SURFACE WAVE ARRAY Z5-S7
FIGURE 75 VELOCITY MODEL FOR ACTIVE AND PASSIVE SURFACE WAVE ARRAY Z5-S8
FIGURE 76 VELOCITY MODEL FOR ACTIVE AND PASSIVE SURFACE WAVE ARRAY Z5-S9
FIGURE 77 VELOCITY MODEL FOR ACTIVE AND PASSIVE SURFACE WAVE ARRAY Z5-S10
FIGURE 78 VELOCITY MODEL FOR ACTIVE AND PASSIVE SURFACE WAVE ARRAY Z5-S11
FIGURE 79 VELOCITY MODEL FOR ACTIVE AND PASSIVE SURFACE WAVE ARRAY Z5-S12
FIGURE 80 VELOCITY MODEL FOR ACTIVE AND PASSIVE SURFACE WAVE ARRAY Z5-S13

1 INTRODUCTION

In-situ seismic measurements using active and passive surface wave techniques were performed at various sites within the SR-710 Tunnel Study Areas, located in Los Angeles County, California. The measurements were conducted from February 24, 2009 through May 19, 2009. The purpose of this investigation was to provide shear (S) wave velocity profiles to a depth of 60 meters (200 ft) to support site characterization and screening of the five tunnel study zones. Some of the surface wave soundings were acquired near the ends of the 17 seismic reflection profiles acquired during the investigation to provide additional data for seismic interpretation.

The active surface wave technique utilized during this investigation consisted of the multi-channel analysis of surface waves (MASW) method. The passive surface wave techniques utilized consisted of the refraction microtremor and the array microtremor methods. At many sites active surface wave techniques (SASW and MASW) with the utilization of portable energy sources, such as hammers and weight drops, are sufficient to obtain a 30 m S-wave velocity sounding. Larger energy sources, such as a bulldozer, may be used to image to depths of up to 100 m, but are not typically applicable in developed urban environments. Passive surface wave techniques, such as the refraction microtremor method of Louie, 2001 or the array microtremor technique, can be used to extend depth of investigation at sites that have adequate noise levels.

S-wave velocity models developed from surface wave soundings have many potential applications related to site characterization including correlation of seismic properties between boreholes; estimating depth to bedrock (providing there is sufficient contrast in velocity between bedrock and overlying sediments), estimating N-value using emperical correlations between S-wave velocity and N-value, estimation of excavatability or rippability of rock. The S-wave velocity models can also be used to determine average S-wave velocity over depth intervals. For example, the average shear wave velocity of the upper 30 m or 100 ft (V_S30) is used in the Uniform Building Code (UBC) and International Building Code (IBC) to separate sites into classes for seismic design.

MASW and refraction microtremor data were collected at 78 locations within the five tunnel study zones, labeled Zones 1 to 5 (Figure 1). Array microtremor data, using an “L” shaped array, were collected at 69 of the locations. The 78 surface wave soundings included 20 soundings in Zone 1, 12 soundings in Zone 2, 24 soundings in Zone 3, 10 soundings in Zone 4 and 12 soundings in Zone 5 as shown on Figure 1. A total of 35 surface wave soundings were conducted on seismic reflection profiles acquired as part of this investigation and reported separately. The remaining 43 surface wave soundings were distributed throughout the tunnel study zones.

This report contains the results of the active and passive surface wave measurements conducted at 78 locations at the site. An overview of the surface wave methods is given in Section 2. Field and data reduction and modeling procedures are discussed in Sections 3 and 4, respectively. Interpretation and results are presented in Section 5. Section 6 presents our conclusions. References and our professional certification are presented in Sections 7 and 8, respectively.

2 OVERVIEW OF THE SURFACE WAVE METHODS

A discussion of active and passive surface wave methods is provided in the technical note included as Appendix A. Active surface wave techniques include the spectral analysis of surface waves (SASW) and multi-channel array surface wave (MASW) methods. Passive surface wave techniques include the refraction and array microtremor methods.

The basis of surface wave methods is the dispersive characteristic of Rayleigh waves when propagating in a layered medium. The phase velocity, V_R, depends primarily on the material properties (V_S, mass density, and Poisson's ratio or compression wave velocity) over a depth of approximately one wavelength. Waves of different wavelengths, λ, (or frequencies, f) sample different depths. As a result of the variance in the shear stiffness of the layers, waves with different wavelengths travel at different phase velocities; hence, dispersion. A surface wave dispersion curve, or dispersion curve for short, is the variation of V_R with λ or f.

The MASW method is an in-situ seismic method for determining shear wave velocity (V_S) profiles [Park et al., 1999a and 1999b, Foti, 2000]. Surface wave techniques are non-invasive and non-destructive, with all testing performed on the ground surface at strain levels in the soil in the elastic range (< 0.001%). MASW testing consists of collecting multi-channel seismic data in the field and applying a wavefield transform to obtain the dispersion curve and data modeling.

A detailed description of the MASW method is given by Park, 1999a and 1999b. Ground motions are recorded by 24 or more geophones spaced 1 to 2 m apart and aligned in a linear array and connected to a seismograph. A wavefield transform, such as the f-k or τ-p transform, is applied to the time history data to isolate the surface wave dispersion curve. PICKWIN95, software developed by Oyo Corporation is typically used to process the MASW data and obtain the dispersion curve.

The refraction microtremor technique is a passive surface wave technique developed by Dr. John Louie at University of Nevada, Reno. A detailed description of this technique can be found in Louie, 2001. The refraction microtremor method differs from the more established array microtremor technique in that it uses a linear receiver array rather than a triangular or circular array. Unlike the MASW method, which uses an active energy source (i.e. hammer), the microtremor technique records background noise emanating from ocean wave activity, wind noise, traffic, industrial activity, construction, etc. Refraction microtremor field procedures consist of laying out a linear array of 24, 4.5 to 8 Hz geophones and recording 10, or more, 15 to 60 second noise records. These noise records are reduced using the software package SeisOpt® ReMi™ v2.0 by Optim™ Software and Data Services. This package is used to generate and combine the slowness (p) – frequency (f) transform of the noise records. The surface wave dispersion curve is picked at the lower envelope of the surface wave energy identified in the p-f spectrum.

A detailed discussion of the array microtremor method can be found in Okada, 2003. This technique uses 4 to 24 receivers aligned in a 2-dimensional array. Triangle, circle, semi-circle and "L" shaped arrays are commonly used, although any 2-dimensional arrangement of receivers can be used. Receivers typically consist of 1 to 4.5 Hz geophones. The triangle array, which

consists of several embedded equilateral triangles, is often used as it provides good results with a relatively small number of geophones. With this array the outer side of the triangle should be at least equal to the desired depth of investigation. The "L" array is useful at sites located at the corner of perpendicular intersecting streets. Typically 10 to 20, 30-second noise records are acquired for analysis. The surface wave dispersion curve is estimated by calculating the spatial autocorrelation (SPAC) function for the time-history data. A first-order Bessel function is fit to the SPAC function to obtain the dispersion curve (phase velocity at each frequency). PICKWIN95, software developed by Oyo Corporation is typically used to process the array microtremor data and obtain the dispersion curve.

The active and passive surface wave techniques compliment one another as outlined below:

- SASW/MASW techniques image the shallow velocity structure which cannot be imaged by the microtremor technique and is needed for an accurate V_S30/V_S100' estimate.
- Microtremor techniques work best in noisy environments where SASW/MASW depth investigation may be limited.
- In a noisy environment the microtremor technique will usually extend the depth of an SASW/MASW sounding.
- The degree of fit in the overlapping portion of the dispersion curves from the two techniques provides a level of confidence in the results.

The dispersion curves generated from the active and passive surface wave soundings are generally combined and modeled. Typically WinSASW V1, developed at the University of Texas at Austin, or WINSASW V2 (Joh, 2002) is used to model the data, whereby through iterative forward and/or inverse modeling, a V_S profile is found whose theoretical dispersion curve is a close fit to the field data.

The final model profile is assumed to represent actual site conditions. Several options exist for forward modeling: a formulation that takes into account only fundamental-mode Rayleigh wave motion (called the 2-D solution) and one that includes all stress waves and incorporates receiver geometry (3-D solution) [Roesset et al., 1991].

The theoretical model used to interpret the dispersion assumes horizontally layered, laterally invariant, homogeneous-isotropic material. Although these conditions are seldom strictly met at a site, the results of active and/or passive surface wave testing provide a good "global" estimate of the material properties along the array. The results may be more representative of the site than a borehole "point" estimate.

Based on our experience at other sites, the shear wave velocity models determined by surface wave testing are within 20% of the velocities that would be determined by other seismic methods [Brown, 1998]. The average velocity of the upper 30 m or 100 ft, however, is much more accurate than this, often to better than 5%, because it is less sensitive to the layering in the model.

3 FIELD PROCEDURES

MASW and refraction microtremor data were collected at 78 locations within the five SR-710 tunnel study zones (Figure 1). The approximate locations of the surface wave soundings are presented in Table 1. Array microtremor data were collected at 69 of the 78 surface wave locations as shown in Table 2.

A typical MASW field layout is shown in Appendix A and Figure 2. MASW equipment used during this investigation consisted of a Geometrics Geode signal enhancement seismograph, 4.5 Hz vertical geophones, seismic cable with 1 to 3 m (3.3 to 9.8 ft) takeouts, a 3 lb hammer, a 16 lb sledge hammer, a truck-mounted accelerated weight drop (AWD) and an aluminum plate. MASW data were acquired along a linear array with 1 to 2 m (3.3 to 6.6 ft) geophone spacing as outlined in Table 2. Shot points were typically located 1, 3 and 5 m (3.3, 9.8 and 16.4 ft) from the end geophone locations. Typically, the 3 lb hammer was used for the 1 m (3.3 ft) offset source locations, a 16 lb sledge hammer was used for the 3 m (9.8 ft) offset source locations, and the 16 lb sledge hammer and/or AWD were used for the 5 m (16.4 ft) offset source locations. Only the hammer energy sources could be used for the MASW survey at some locations because of space or permitting limitations. Data from the transient impacts (hammers) were averaged 5 times to improve the signal-to-noise ratio. Surface waves were monitored by 24 Oyo Geospace 4.5 Hz geophones and recorded by a Geometrics Geode signal enhancement seismograph. Photographs of typical MASW equipment are presented in Appendix A. All field data was saved to hard disk and documented in a field notebook.

Refraction microtremor measurements were made along a linear array of 24, 4.5 Hz geophones with a 6 m (19.7 ft) geophone spacing, as possible. When a 6 m geophone spacing was not possible due to space limitations, it was adjusted to a 4 or 5.5 m (13.1 or 18 ft) spacing as outlined in Table 2. The refraction microtremor arrays were typically located along sidewalks. A typical field layout is shown in Appendix A. A Geometrics Geode, 24 bit, 24-channel seismic recording system was used to record thirty 30 second noise records using a 2 ms sample rate. Data were stored on a laptop computer for later processing and field geometry and associated files names were documented in a field notebook.

Array microtremor measurements were made along a 24-channel “L”-shaped array using 4.5Hz geophones with a geophone spacing of 6 m (19.7 ft) when possible. When a geophone spacing of 6 m was not possible because of space limitations, a 5 or 5.5 m (16.4 or 18 ft) geophone spacing was used as outlined in Table 2. The array microtremor measurements were typically made along sidewalks of intersecting streets. Occasionally, the geometry of the streets required that the intersecting legs of the array were at an angle other than 90 degrees (i.e. “V” shaped rather than “L” shaped array). A Geometrics Geode, 24 bit, 24-channel seismic recording system was used to record thirty 30 second noise records using a 2ms sample rate. Data were stored on a laptop computer for later processing and field geometry and associated files names were documented in a field notebook.

Surface wave sounding locations or seismic lines to which they were tied were surveyed with a Trimble Pro XRS GPS system with OmniStar submeter differential corrections. Estimated accuracy of the locations and elevations are nominally about 1 m (3.3 ft) and 2 m (6.6 ft), respectively.

4 DATA REDUCTION AND MODELING

The MASW data were reduced using the software PICKWIN95 developed by Oyo Corporation and the following steps:

- Input seismic record into software.
- Enter receiver spacing, geometry and wavelength restrictions, as necessary.
- Apply wavefield transform to seismic record to convert the data to phase velocity – frequency space.
- Identify and pick dispersion curve.
- Repeat for all shot records and merge dispersion curves.
- Convert dispersion curves to WinSASW format for modeling.

The refraction microtremor data were reduced using the Optim™ Software and Data Services SeisOpt® ReMi™ v4.0 data analysis package. Data reduction steps included the following:

- Conversion of SEG-2 format field files to SEG-Y format.
- Data preprocessing which includes trace-equalization gaining and DC offset removal.
- Erasing receiver geometry present in the file header.
- Computing the velocity spectrum of each record by p-f transformation.
- Combining the individual p-f transforms into one image.
- Picking and saving the velocity spectrum image.
- Conversion of the dispersion curve to WinSASW format for modeling.

The array microtremor and refraction microtremor data were reduced using the software PICKWIN95 developed by Oyo Corporation and the following steps:

- Input all seismic records into software.
- Enter receiver spacing, geometry and wavelength restrictions, as necessary.
- Calculate the SPAC function for each seismic record and average.
- For each frequency calculate the degree of fit of a first-order Bessel function to the SPAC function for a multitude of phase velocities.
- Identify and pick dispersion curve as the best fit of the Bessel function for each frequency.
- Convert dispersion curves to WinSASW format for modeling

Example wavefield transforms of the MASW and microtremor data are presented in Figure 3. The surface wave dispersion curves from the active and passive surface wave data were combined to obtain a composite surface wave dispersion curve. Due to lateral velocity variation at many of the surface wave sounding locations, most likely related to subsurface bedrock topography or the often steeply dipping bedrock units, it was not always possible to combine all of the passive surface wave data sets with the MASW data. The datasets with the best agreement were used to create the composite dispersion curve.

The location of surface wave sounding Z1-S17 was such that reliable active and passive surface wave data were not obtained. An S-wave velocity model was not generated for this sounding.

Once a composite surface wave dispersion curve was developed an iterative forward modeling process was used to generate an S-wave velocity model for the sounding. During this process an initial velocity model was generated based on general characteristics of the dispersion curve. The theoretical dispersion curve was then generated using the 2-D modeling algorithm (fundamental mode Rayleigh wave dispersion module) and compared to the field dispersion curve. Adjustments were then made to the thickness and velocities of each layer and the process repeated until an acceptable fit to the field data was obtained.

Data inputs into the modeling software included layer thickness, S-wave velocity, P-wave velocity and mass density. P-wave velocity and mass density only have a very small influence (i.e. less than 10%) on the S-wave velocity model generated from a surface wave dispersion curve. However, realistic assumptions for P-wave velocity, which is impacted significantly by the location of the water table, and mass density will slightly improve the accuracy of the S-wave velocity model.

Constant mass density values of 1.9 to 2.3 g/cc were used in the velocity profiles for subsurface soils and rock. Within the normal range encountered in geotechnical engineering, variation in mass density has a negligible effect on surface wave dispersion. During data modeling, the compression wave velocity, V_P, of unsaturated soils was estimated using a Poisson's ratio, ν, of 0.33 and the relationship:

$$V_P = V_S\,[(2(1-\nu))/(1-2\nu)]^{0.5}.$$

Several approaches were used to estimate groundwater depth in the vicinity of the surface wave soundings. These included a simple, interactive, 2 to 3 layer seismic refraction analysis of MASW shot records and/or selected seismic reflection shot records; review of borehole velocity logs, and interpolation between boreholes or seismic reflection lines. Groundwater depth was assumed for modeling purposes when reasonable estimates could not be made from available surface and borehole geophysical data.

Borehole velocity logs within each of the five tunnel study zones (Zones 1 to 5) were reviewed to correlate P-wave velocity of saturated sediments with S-wave velocity. Borehole velocity and geologic logs were also reviewed to determine if S-wave velocity could be used to differentiate bedrock from overlying sediments. Borehole velocity logs (reported separately) for 6 boreholes (Z1-B3, Z1-B4, Z1-B5, Z1-B6, Z1-B7 and Z1-B8) were available in Zone 1. Borehole velocity logs for 4 boreholes (Z2-B1, Z2-B3, Z2-B4 and Z2-B5) were available in Zone 2. Borehole velocity logs for 12 boreholes (Z3-B1 to Z3-B12) were available in Zone 3. A borehole velocity log for one borehole (Z4-B4) was available in Zone 4. Borehole velocity logs were not available for Zone 5.

5 INTERPRETATION AND RESULTS

5.1 Zone 1

Twenty (20) surface wave soundings were conducted within Zone 1 (Z1-S1 to Z1-S20) as shown in Figure 1. Six of these surface wave soundings were located near the ends of seismic reflection lines and the remaining 14 soundings were distributed throughout the zone.

The fit of the theoretical dispersion curve to the experimental data collected at each site and the modeled V_S profiles for Z1-S1 to Z1-S16 and Z1-S18 to Z1-S20 are presented in Figures 4 to 22, respectively. The resolution decreases gradually with depth because of the loss of sensitivity of the dispersion curve to changes in V_S at greater depth. The V_S depth profiles used to match the field data are provided in tabular form as Tables 3 to 21. The location of surface wave sounding Z1-S17 was such that reliable active and passive surface wave data were not obtained and, therefore, an S-wave velocity model was not generated.

The surface wave phase velocities from the microtremor measurements are generally in good agreement with those from the MASW data in the region of overlapping wavelength. Differences in the surface wave dispersion curves between the two techniques result from the passive surface wave data being averaged over much longer arrays with lateral velocity variation having differing affects on the various data sets. The estimated depths of investigation for the combined active and passive surface wave soundings are between 60 and 70 m (197 and 230 ft), as shown on Tables 3 to 21.

For the purpose of data modeling, groundwater depths for 16 of the soundings (Z1-S2, Z1-S4 and Z1-S7 to Z1-S20) were estimated from simple seismic refraction analysis of MASW shot records with groundwater modeled in the 3 to 10 m (10 to 33 ft) depth range. The other 4 soundings (Z1-S1, Z1-S3, Z1-S5 and Z1-S6) were located at higher elevations in areas with outcropping bedrock. The MASW arrays were not long enough to map approximate groundwater depth at these locations. For the purpose of data modeling, groundwater was assumed to be at a depth of 50 m (164 ft) for Z1-S1 and Z1-S3, 45 m (148 ft) for Z1-S5 and 30 m (98 ft) for Z1-S6. Seismic reflection shot records along seismic line Z1-G3 (Figure 1) indicate that groundwater may be shallower along surface wave soundings Z1-S5 and Z1-S6; however, groundwater depth is not expected to have much impact on the S-wave velocity models in this area. Based on review of six (6) Zone 1 borehole velocity logs, the inferred P-wave velocity of saturated sediments was assumed to range from 1,650 to 2,150 m/s (5,413 to 7,054 ft/s) depending upon S-wave velocity. The modeled/assumed saturated sediments can be identified in Tables 3 to 21 based on inferred P-wave velocity of 1,650 m/s (5,413 ft/s), or greater.

Review of 6 available borehole velocity logs in Zone 1 (Z1-B3, Z1-B4, Z1-B5, Z1-B6, Z1-B7 and Z1-B8), geologic maps and borehole geologic logs indicate that bedrock in Zone 1 primarily consists of siltstone, shale and sandstone units of the Puente Formation. Overlying sediments were typically observed to have S-wave velocity below 350 m/s (1,148 ft/s), although sediment velocities up to 450 m/s (1,476 ft/s) were observed. Decomposed and intensely fractured sedimentary rock was found to often have S-wave velocity in the sediment range. Highly to moderately weathered bedrock often had S-wave velocity in the 350 to 600 m/s range (1,148 to

1,969 ft/s) and slightly weathered and fresh rock were found to often have S-wave velocity greater than 700 m/s (2,297 ft/s). Therefore, S-wave velocity above 350 m/s (1,148 ft/s) in the surface wave velocity models (Figures 4 to 22 and Tables 3 to 21) are generally associated with bedrock. Lower velocities will typically be associated with sediments and occasionally decomposed rock.

The average S-wave velocity of the upper 30 and 60 m (V_S30 and V_S60) and the modeled S-wave velocity at a depth of 60 m (197 ft) for the Zone 1 surface wave soundings are summarized in Table 22. V_S30 and V_S60 range from 181 to 500 m/s (594 to 1641 ft/s) and 269 to 580 m/s (884 to 1,903 ft/s), respectively. Fifteen (15) of the surface wave soundings have V_S30 less than 360 m/s (1,181 ft/s). S-wave velocity at a depth of 60 m (197 ft) ranges from 675 to 850 m/s (2,215 to 2,789 ft/s).

S-wave velocity models were generated for surface wave soundings near each end of two of the three seismic reflection profiles acquired in Zone 1 (Z1-G3 and Z1-G4). Surface wave soundings Z1-S5 and Z1-S6 were conducted in the southwestern and northeastern portions of seismic line Z1-G3, respectively. The S-wave velocity models for these soundings are very similar indicating that there may not be significant lateral velocity variation in the immediate vicinity of the seismic line. Surface wave soundings Z1-S14 and Z1-S15 were conducted in the southwestern and northeastern portions of seismic line Z1-G4, respectively. The S-wave velocity models for these soundings are different with moderately weathered bedrock about 11 m (36 ft) shallower in the vicinity of Z1-S15 located near the northeast end of the line. It should be noted that the surface wave data acquired along Z1-S14 and Z1-S15 were difficult to model due to significant lateral velocity variation of the sediments and highly variable bedrock depths, which cannot adequately be represented by a 1-D model. MASW data and passive "L" array data were in good agreement for Z1-S14 yielding an S-wave velocity model with very low sediment velocity and the lowest Zone 1 V_S30 (181 m/s). The low V_S30 was primarily the result of the very low sediment velocities in the upper 10 m (33 ft), which were in the 125 to 160 m/s (410 to 525 ft/s) range. The passive linear array data acquired along a 138 m profile at this site were in very poor agreement with the MASW data acquired along a 34.5 m profile and "L" array data and were, therefore, not used for modeling. Explanations for the difference between the different data sets include significant variation of near surface sediment velocity and bedrock depth over the longer passive linear array or negative impact of a directional noise bias on passive linear array data. Models of the passive linear array data (not included) indicate that near surface sediment velocities may be higher and bedrock as much as 6 m (20 ft) shallower adjacent to the MASW array. Only passive "L" array data were used to model Z1-S15, which was similar to Z1-S14, because the MASW data could not be accurately reduced, possibly due to complicated shallow velocity structure, and passive linear array data were noisy, possibly due to limited azimuth of noise sources (i.e. unidirectional rather than omnidirectional noise sources).

Three boreholes are located within about 175 m (574 ft) of surface wave soundings: Z1-B3 about 172 m (565 ft) from Z1-S8, Z1-B4 about 25 m (82 ft) of Z1-S13, and Z1-B6 about 148 m (486 ft) from Z1-S15. Borehole locations are shown on Figure 1. Borehole S-wave velocity data for Z1-B3 are plotted with the surface wave S-wave velocity model for Z1-S8 in Figure 11. This plot illustrates the resolution differences between the two methods with the surface wave velocity models providing more averaged (i.e. thicker layer) velocity models. The two velocity models are in reasonable agreement given the distance between the surface wave sounding and

the borehole and resolution limitations of the surface wave methods relative to borehole PS Suspension velocity log. Borehole S-wave velocity data for Z1-B6 are plotted with the surface wave S-wave velocity model for Z1-S14, located about 330 m (1,083 ft) and the closer Z1-S15 in Figures 17 and 18, respectively. The sediment velocities are much higher in the PS Suspension velocity log, likely due to significant lateral sediment velocity variation discussed previously for these surface wave soundings. The bedrock velocities between the two methods are in good agreement considering likely variation of bedrock depth and weathering. Borehole S-wave velocity data for Z1-B4 are plotted with the surface wave S-wave velocity model for Z1-S13 in Figure 16. The two velocity models are in good agreement considering the resolution capabilities of the two methods and potential lateral velocity variation in this geologic environment. Assuming that the subsurface velocity structure is the same beneath the surface wave sounding as at the borehole location, the surface wave method does not detect a possible 5 m (16 ft) thick low velocity layer at a depth of 19 m (62.3 ft) and as a result overestimates the depth to the higher velocity underlying sedimentary rock. It is not possible to resolve a low velocity layer of this thickness and depth due to the presence of underlying high velocity rock.

5.2 Zone 2

Twelve (12) surface wave soundings were conducted within Zone 2 (Z2-S1 to Z2-S12) as shown in Figure 1. Six of these surface wave soundings were located near the ends of seismic reflection lines and the remaining 6 soundings were distributed throughout the zone.

The fit of the theoretical dispersion curve to the experimental data collected at each site and the modeled V_S profiles for Z2-S1 to Z2-S12 are presented in Figures 23 to 34, respectively. The resolution decreases gradually with depth because of the loss of sensitivity of the dispersion curve to changes in V_S at greater depth. The V_S depth profiles used to match the field data are provided in tabular form as Tables 23 to 34.

The surface wave phase velocities from the microtremor measurements are generally in good agreement with those from the MASW data in the region of overlapping wavelength. Differences in the surface wave dispersion curves between the two techniques result from the passive surface wave data being averaged over much longer arrays with lateral velocity variation having differing affects on the various data sets. The estimated depths of investigation for the combined active and passive surface wave soundings are between 60 and 70 m (197 and 230 ft), as shown on Tables 23 to 34.

For the purpose of data modeling, groundwater depths for 11 of the 12 soundings (Z2-S1 to Z2-S4 and Z2-S6 to Z2-S12) were estimated from simple seismic refraction analysis of MASW shot records with groundwater modeled in the 2 to 9 m (7 to 30 ft) depth range. The MASW array was not long enough at Z2-S5 to map approximate groundwater depth, which was estimated to be greater than 14 m (46 ft) deep. For the purpose of data modeling, groundwater was assumed to be at a depth of 15 m (49 ft) at Z2-S5. Based on review of four (4) Zone 2 borehole velocity logs, the inferred P-wave velocity of saturated sediments was assumed to range from 1,650 to 2,750 m/s (5,413 to 9,022 ft/s) depending upon S-wave velocity. The modeled/assumed saturated sediments can be identified in Tables 23 to 34 based on inferred P-wave velocity of 1,650 m/s (5,413 ft/s), or greater.

Review of 4 available borehole velocity logs in Zone 2 (Z2-B1, Z2-B3, Z2-B4 and Z2-B5) and geologic maps indicates that bedrock in Zone 1 primarily consists of siltstone, claystone, sandstone and conglomerate units of the Fernando, Puente and Topanga Formations. Overlying sediments were typically observed to have S-wave velocity below 350 m/s (1,148 ft/s). Decomposed and intensely fractured sedimentary rock was found to often have S-wave velocity in the sediment range. S-wave velocity of the sedimentary bedrock ranged from about 350 m/s (1,148 ft/s) to over 1,500 m/s (4,921 ft/s). The variable S-wave velocity in the sedimentary rock is a function of degree of weathering, fracturing and lithology. S-wave velocity above 350 m/s (1,148 ft/s) in the surface wave velocity models (Figures 23 to 34 and Tables 23 to 34) is most likely associated with bedrock. Lower velocities will typically be associated with sediments and/or decomposed/highly weathered and fractured rock.

V_S30, V_S60 and the modeled S-wave velocity at a depth of 60 m (197 ft) for the Zone 2 surface wave soundings are summarized in Table 35. V_S30 and V_S60 range from 256 to 423 m/s (838 to 1,389 ft/s) and 330 to 552 m/s (1,081 to 1,811 ft/s), respectively. Eight (8) of the 12 surface wave soundings have V_S30 less than 360 m/s (1,181 ft/s). S-wave velocity at a depth of 60 m (197 ft) ranges from 420 to 825 m/s (1,378 to 2,707 ft/s).

S-wave velocity models were generated for surface wave soundings near each end of the three seismic reflection profiles acquired in Zone 2 (Z2-G1 to Z2-G3). Surface wave soundings Z2-S3 and Z2-S2 were conducted in the southern and northern portions of seismic line Z2-G1, respectively. The S-wave velocity models for these soundings are very similar, with less than 10% velocity variation in bedrock, indicating that there may not be significant lateral velocity variation in the immediate vicinity of the seismic line. Surface wave soundings Z2-S7 and Z2-S8 were conducted in the southwestern and northeastern portions of seismic line Z2-G2, respectively. The S-wave velocity models for these soundings are similar in the upper 40 m (131 ft) and different at greater depths. The significant lateral velocity variation at depth may be related to changes in bedrock weathering, fracturing or lithology associated with dipping sedimentary units. Surface wave soundings Z2-S10 and Z2-S11 were conducted in the northwestern and southeastern portions of seismic line Z2-G3, respectively. The S-wave velocity models for these soundings are very similar, with less than 10% velocity variation in bedrock, indicating that there may not be significant lateral velocity variation in the immediate vicinity of the seismic line.

No boreholes were drilled in close proximity to any of the surface wave soundings conducted in Zone 2.

5.3 Zone 3

Twenty four (24) surface wave soundings were conducted within Zone 3 (Z3-S1 to Z3-S24) as shown in Figure 1. Fourteen (14) of these surface wave soundings were located near the ends of 7 seismic reflection lines and the remaining 10 soundings were distributed throughout the zone.

The fit of the theoretical dispersion curve to the experimental data collected at each site and the modeled V_S profiles for Z3-S1 to Z3-S24 are presented in Figures 35 to 58, respectively. The resolution decreases gradually with depth because of the loss of sensitivity of the dispersion curve to changes in V_S at greater depth. The V_S depth profiles used to match the field data are provided in tabular form as Tables 36 to 59.

The surface wave phase velocities from the microtremor measurements are generally in good agreement with those from the MASW data in the region of overlapping wavelength. Differences in the surface wave dispersion curves between the two techniques result from the passive surface wave data being averaged over much longer arrays with lateral velocity variation having differing affects on the various data sets. The estimated depths of investigation for the combined active and passive surface wave soundings are between 60 and 75 m (197 and 246 ft), as shown on Tables 36 to 59.

For the purpose of data modeling, groundwater depths for 16 of the 24 soundings (Z3-S1, Z3-S6, Z3-S7, Z3-S9 to Z3-S11, Z3-S13, Z3-S14, Z3-S16 to Z3-S18 and Z3-S20 to Z3-S24) were estimated from simple seismic refraction analysis of MASW or seismic reflection shot records with groundwater modeled in the 3 to 17 m (10 to 56 ft) depth range. Groundwater depths for 4 soundings (Z3-S2 to Z3-S5) were interpreted from nearby borehole velocity logs and interpolated as necessary. Groundwater in the vicinity of these surface wave soundings was modeled in the 30 to 45 m (98 to 148 ft) depth range. The MASW profiles were not long enough to image depth to groundwater at four of the sounding locations (Z3-S8, Z3-S12, Z3-S15 and Z3-S19). Simple seismic refraction analysis of the MASW shot records indicated that groundwater was deeper than 14 m (46 ft) at these locations and for the purpose of modeling groundwater was assumed to be at a depth of 15 m (49 ft). Based on review of 12 Zone 3 borehole velocity logs, the inferred P-wave velocity of saturated sediments was assumed to range from 1,500 to 3,500 m/s (4,921 to 11,483 ft/s) depending upon S-wave velocity. The modeled/assumed saturated sediments can be identified in Tables 36 to 59 based on inferred P-wave velocity of 1,500 m/s (4,921 ft/s), or greater.

Review of 12 available borehole velocity logs in Zone 3 (Z3-B1 to Z3-B12), geologic maps, geologic cross sections and borehole geologic logs indicates that bedrock in Zone 3 consists of siltstone, claystone, sandstone and conglomerate units of the Fernando, Puente and Topanga Formations and crystalline basement rock. Overlying sediments are typically observed to have S-wave velocity in the 175 to 600 m/s (574 to 1,969 ft/s) range. The higher sediment velocities are typically associated with older alluvial deposits encountered in boreholes Z3-B2 to Z3-B4 located north of the Eagle Rock Fault. Typically, a thinner sequence of sediments overlie bedrock south of the Eagle Rock Fault and sediment S-wave velocity rarely exceeded 400 m/s (1,312 ft/s). S-wave velocity of sedimentary rock encountered in the boreholes is in the 325 to 1,850 m/s (1,066 to 6,070 ft/s) range. S-wave velocity of 375 to 450 m/s (1,230 to 1,476 ft/s) is more typical of the lowest velocity for sedimentary rock in many of the boreholes. The variable S-wave velocity in the sedimentary rock is a function of degree of weathering, fracturing and lithology. S-wave velocity of decomposed to weathered crystalline basement rock encountered in boreholes is typically in the 650 to 1,400 m/s (2,133 to 4,593 ft/s) range, but is expected to get much higher as weathering decreases. In areas with crystalline basement north of the Eagle Rock Fault, S-wave velocity over 650 m/s (2,133 ft/s) is probably associated with bedrock with lower velocities associated with overlying sediments. South of the Eagle Rock Fault, S-wave velocity over 400 m/s (1,312 ft/s) will commonly be associated with sedimentary bedrock. Lower velocities will often be associated with sediments; however, there is quite a bit of overlap in sediment and highly weathered sedimentary rock S-wave velocity within Zone 3.

The average S-wave velocity of the upper 30 and 60 m (V_S30 and V_S60) and the modeled S-wave velocity at a depth of 60 m (197 ft) for the Zone 3 surface wave soundings are summarized

in Table 60. V_S30 and V_S60 range from 313 to 496 m/s (1,027 to 1627 ft/s) and 361 to 662 m/s (1,184 to 2,172 ft/s), respectively. Twelve (12) of the 24 surface wave soundings have V_S30 less than 360 m/s (1,181 ft/s). S-wave velocity at a depth of 60 m (197 ft) in highly variable in Zone 3, ranging from 435 to 1,250 m/s (1,427 to 4,101 ft/s).

S-wave velocity models were generated for surface wave soundings near each end of the 7 seismic reflection profiles acquired in Zone 3 (Z3-G1 to Z3-G7). Surface wave soundings Z3-S3 and Z3-S4 were conducted at the northern and southern ends of seismic line Z3-G1, respectively. The S-wave velocity models for these soundings are very similar and V_S30 is almost identical indicating that there is no significant lateral velocity variation along the seismic line. Surface wave soundings Z3-S6 and Z3-S7 were conducted at the northern and southern ends of seismic line Z3-G2, respectively. There is more than a 10% difference in the S-wave velocity models and V_S30 for these soundings indicating that there is significant lateral velocity variation along the seismic line, possibly resulting from a geologic structure bisecting the line or steeply dipping geologic units. Surface wave soundings Z3-S9 and Z3-S10 were conducted at the southwestern and northeastern ends of seismic line Z3-G3, respectively. There is a large difference in the S-wave velocity models and V_S30 for these soundings indicating that there is significant lateral velocity variation along the seismic line, possibly resulting from a geologic structure bisecting the line or steeply dipping geologic units. Surface wave soundings Z3-S13 and Z3-S14 were conducted in the northeastern and southwestern portions of seismic line Z3-G4, respectively. The S-wave velocity models for these soundings are very similar and V_S30 is almost identical indicating that there is no significant lateral velocity variation along the seismic line. Surface wave soundings Z3-S17 and Z3-S18 were conducted in the north central and south central portions of seismic line Z3-G5, respectively. The S-wave velocity models for these soundings are very similar, except for small variation in the depth of high velocity bedrock. There is about an 11% difference in V_S30 and V_S60 between the two soundings, therefore some lateral velocity variation associated with deepening bedrock or variation of the weathering profile is present. Surface wave soundings Z3-S21 and Z3-S22 were conducted in the northern and southern portions of seismic line Z3-G6, respectively. There is some variation of near surface and deep velocity structure in the S-wave velocity models for these soundings. Additionally, there is about a 6 to 8% difference in V_S30 and V_S60 between the two soundings and, therefore, some lateral velocity variation occurs along the seismic line. Surface wave soundings Z3-S23 and Z3-S24 were conducted near the northern and southern ends of seismic line Z3-G7, respectively. There is a large difference in the S-wave velocity models and V_S30 for these soundings indicating that there is significant lateral velocity variation along the seismic line, possibly resulting from a geologic structure bisecting the line, steeply dipping geologic units or variable bedrock weathering.

Four (4) boreholes are located within about 155 m (509 ft) of surface wave soundings: Z3-B2 about 114 m (375 ft) from Z3-S2, Z3-B4 about 34 m (110 ft) from Z3-S3, Z3-B9 about 110 m (360 ft) from Z3-S13 and Z3-B12 about 155 m (509 ft) from Z3-S20. Additionally, borehole Z3-B7 is located on seismic reflection line Z3-G3 between surface wave soundings Z3-S9 and Z3-S10. Borehole locations are shown on Figure 1.

Borehole S-wave velocity data for Z3-B2 are plotted with the surface wave S-wave velocity model for Z3-S2 in Figure 36. This plot illustrates the resolution differences between the two methods with the surface wave velocity models providing more averaged (i.e. thicker layer) velocity models. The surface wave velocity model generally has much lower S-wave velocity

than the velocity log, which may be the result of lateral velocity variation in the sediments overlying weathered crystalline basement rocks and variable depth to and weathering profile of the basement rock. Borehole S-wave velocity data for Z3-B4 are plotted with the surface wave S-wave velocity model for Z3-S3 in Figure 37. The two velocity models are in good agreement considering the differing resolution capabilities of the two methods. Borehole S-wave velocity data for Z3-B9 are plotted with the surface wave S-wave velocity model for Z3-S13 in Figure 47. The surface wave velocity model generally has slightly lower S-wave velocity than the velocity log, which may be the result of lateral velocity variation between the borehole and surface wave sounding locations. Borehole S-wave velocity data for Z3-B12 are plotted with the surface wave S-wave velocity model for Z3-S20 in Figure 54. The two velocity models are in good agreement considering the differing resolution capabilities of the two methods and distance between the test locations. Borehole S-wave velocity data for Z3-B7 are plotted along the surface wave S-wave velocity models for Z3-S9 and Z3-S10 on Figure 43 and 44, respectively. Both the borehole and surface wave soundings are located on seismic reflection line Z3-G3. As previously discussed, there is significant difference between the two surface wave models. As would be expected, the borehole S-wave velocities lie between the two surface wave models although they are more similar to Z3-S10 below a depth of 30 m (98 ft).

5.4 Zone 4

Ten (10) surface wave soundings were conducted within Zone 4 (Z4-S1 to Z2-S10) as shown in Figure 1. Five of these surface wave soundings were located on seismic reflection lines and the remaining 5 soundings were distributed throughout the zone.

The fit of the theoretical dispersion curve to the experimental data collected at each site and the modeled V_S profiles for Z4-S1 to Z4-S10 are presented in Figures 59 to 68, respectively. The resolution decreases gradually with depth because of the loss of sensitivity of the dispersion curve to changes in V_S at greater depth. The V_S depth profiles used to match the field data are provided in tabular form as Tables 61 to 70.

The surface wave phase velocities from the microtremor measurements are generally in good agreement with those from the MASW data in the region of overlapping wavelength. Differences in the surface wave dispersion curves between the two techniques result from the passive surface wave data being averaged over much longer arrays with lateral velocity variation having differing affects on the various data sets. The estimated depths of investigation for the combined active and passive surface wave soundings are between 60 and 70 m (197 and 230 ft), as shown on Tables 61 to 70.

For the purpose of data modeling, attempts were made to estimate groundwater depth from simple seismic refraction analysis of MASW shot records and seismic records at the ends of two seismic reflection profiles. MASW profiles were not long enough to determine approximate groundwater depth. Groundwater depth was estimated to be on the order of 65 m (213 ft) in the vicinity of seismic reflection profiles Z4-G1 and Z4-G2. Therefore, for data modeling, groundwater was assumed to be 65 m (213 ft) deep in the vicinity of surface wave soundings Z4-S1 to Z4-S7 and then, based on borehole and geophysical control in the adjacent zones, shallow to the southwest between Z4-S8 and Z4-S10. Based on review of a single Zone 4 borehole velocity log, the inferred P-wave velocity of saturated sediments was assumed to range from

1,600 to 1,750 m/s (5,249 to 5,741 ft/s) depending upon S-wave velocity. The modeled/assumed saturated sediments can be identified in Tables 61 to 70 based on inferred P-wave velocity of 1,600 m/s (5,249 ft/s), or greater.

Review of the borehole velocity log for Z4-B4, located in the southwestern corner of Zone 4 (Figure 1), geologic maps and cross sections indicates that bedrock in Zone 4 primarily consists of siltstone, claystone and sandstone units of the Puente Formation and crystalline basement rock. Bedrock is expected to deepen to the northeast and with the exception of the southwestern portion of Zone 4 may exceed 120 m (400 ft) in depth. The borehole velocity log for Z4-B4 indicates that seismic velocity alone may not be useful to distinguish sedimentary rock from overlying sediments. Sediments encountered in the upper 26 m (85 ft) in this borehole have S-wave velocity in the 275 to 550 m/s (902 to 1,804 ft/s) range, whereas decomposed rock immediately beneath the sediments has an S-wave velocity as low as 300 m/s (984 ft/s). Thick sequences of old alluvial sediments in the northeastern portion of Zone 4 may have S-wave velocity increasing with depth to over 600 m/s (1,969 ft/s), similar to the velocities observed in some units of the Puente Formation.

V_S30, V_S60 and the modeled S-wave velocity at a depth of 60 m (197 ft) for the Zone 4 surface wave soundings are summarized in Table 71. V_S30 and V_S60 range from 288 to 373 m/s (944 to 1,225 ft/s) and 349 to 484 m/s (1,144 to 1,589 ft/s), respectively. Seven (7) of the 10 surface wave soundings have V_S30 less than 360 m/s (1,181 ft/s). S-wave velocity at a depth of 60 m (197 ft) ranges from 475 to 600 m/s (1,558 to 1,969 ft/s) with the exception of Z4-S1, which has a modeled S-wave velocity of 850 m/s (2,789 ft/s) at this depth.

S-wave velocity models were generated for surface wave soundings near each end of the two seismic reflection profiles acquired in Zone 4 (Z4-G1 and Z4-G2). Surface wave soundings Z4-S2 to Z4-S4 were conducted in the northern, central and southern portions of seismic line Z4-G1, respectively. The S-wave velocity models for these soundings are quite variable, as may be expected because the Raymond Fault Zone bisects the seismic line. Surface wave soundings Z4-S6 and Z4-S7 were conducted in the northeastern and southwestern portions of seismic line Z4-G2, respectively. The S-wave velocity models for these soundings are almost identical indicating that there is not significant lateral velocity variation in the immediate vicinity of the seismic line.

No boreholes were drilled in close proximity to any of the surface wave soundings conducted in Zone 4.

5.5 Zone 5

Twelve (12) surface wave soundings were conducted within Zone 5 (Z5-S1 to Z5-S4 and Z5-S6 to S5-S13) as shown in Figure 1. Four of these surface wave soundings were located on seismic reflection lines and the remaining 8 soundings were distributed throughout the zone.

The fit of the theoretical dispersion curve to the experimental data collected at each site and the modeled V_S profiles for Z5-S1 to Z5-S4 and Z5-S6 to Z5-S13 are presented in Figures 69 to 80, respectively. The resolution decreases gradually with depth because of the loss of sensitivity of the dispersion curve to changes in V_S at greater depth. The V_S depth profiles used to match the field data are provided in tabular form as Tables 72 to 83.

The surface wave phase velocities from the microtremor measurements are generally in good agreement with those from the MASW data in the region of overlapping wavelength. Differences in the surface wave dispersion curves between the two techniques result from the passive surface wave data being averaged over much longer arrays with lateral velocity variation having differing affects on the various data sets. The estimated depths of investigation for the combined active and passive surface wave soundings are between 60 and 70 m (197 and 230 ft), as shown on Tables 72 to 83.

For the purpose of data modeling, attempts were made to estimate groundwater depth from simple seismic refraction analysis of MASW shot records and seismic records at the ends of two seismic reflection profiles. MASW profiles were not long enough to determine approximate groundwater depth. Groundwater depth was estimated to be on the order of 56 m (184 ft) and 16 m (52 ft) in the vicinity of seismic reflection profiles Z5-G2 and Z5-G3, respectively. Therefore, for data modeling, groundwater was assumed to be 50 to 56 m (164 to 184 ft) deep in the vicinity of surface wave soundings Z5-S1 to Z5-S9, 40 m (131 ft) at Z5-S10, 25 m (82 ft) at Z5-S11 and 16 m (52 ft) at Z5-S12 and Z5-S13. Subsurface geologic conditions in Zone 5 are expected to be similar to those in Zone 4 and, therefore, the inferred P-wave velocity of saturated sediments was assumed to range from 1,600 to 1,750 m/s (5,249 to 5,741 ft/s) depending upon S-wave velocity. The modeled/assumed saturated sediments can be identified in Tables 72 to 83 based on inferred P-wave velocity of 1,600 m/s (5,249 ft/s), or greater.

Boreholes were not drilled in Zone 5. Review of geologic maps and cross sections indicates that bedrock in Zone 5 primarily consists of siltstone, claystone and sandstone units of the Puente Formation and siltstone and claystone of the Fernando Formation. Bedrock is expected to deepen to the east and, with the exception of the western corner of Zone 5, may significantly exceed 120 m (400 ft) in depth. Because the geology in Zone 5 is expected to be similar to that in Zone 4, it is unlikely that S-wave velocity if useful for distinguishing bedrock from overlying sediments. Additionally, bedrock over most of Zone 5 is much deeper than the surface wave soundings can image.

V_S30, V_S60 and the modeled S-wave velocity at a depth of 60 m (197 ft) for the Zone 5 surface wave soundings are summarized in Table 84. V_S30 and V_S60 range from 303 to 392 m/s (994 to 1,287 ft/s) and 362 to 435 m/s (1,187 to 1,429 ft/s), respectively. Eight (8) of the 12 surface wave soundings have V_S30 less than 360 m/s (1,181 ft/s). S-wave velocity at a depth of 60 m (197 ft) ranges from 475 to 625 m/s (1,558 to 2,051 ft/s) and in nominally in the 500 to 550 m/s (1,640 to 1,804 ft/s) range.

S-wave velocity models were generated for surface wave soundings near each end of the two seismic reflection profiles acquired in Zone 5 (Z5-G2 and Z5-G3). Surface wave soundings Z5-S8 and Z5-S9 were conducted in the eastern and western portions of seismic line Z5-G2, respectively. The S-wave velocity models for these soundings are typically within 10% of seismic velocity and V_S30 and V_S60 are within 5% indicating that there is not significant lateral velocity variation in the immediate vicinity of the seismic line. Surface wave soundings Z5-S12 and Z5-S13 were conducted in the northern and southern portions of seismic line Z5-G3, respectively. The S-wave velocity models, V_S30 and V_S60 for these soundings are typically within 11% of seismic velocity indicating that there is not significant lateral velocity variation in the immediate vicinity of the seismic line.

6 CONCLUSIONS

Active and passive surface wave data were collected at 78 locations within the five SR-710 Tunnel Study Zones, located in Los Angeles County, California. The measurements were conducted from February 24, 2009 through May 19, 2009. The purpose of the investigation was to support site characterization and screening efforts and a seismic reflection survey conducted as part of the investigation and reported separately. Surface wave sounding locations are shown on Figure 1 along with the five tunnel study zones, borehole locations and seismic reflection lines. A total of 35 of the surface wave soundings were conducted on seismic reflection lines and the remaining 43 soundings were distributed throughout the tunnel study zones.

The S-wave velocity models derived from the surface wave soundings and summaries are presented as Figures 4 to 80 and Tables 3 to 84. The average S-wave velocity of the upper 30 and 60 m (V_S30 and V_S60) and the modeled S-wave velocity at a depth of 60 m (197 ft) for the surface wave soundings conducted in Zones 1 to 5 are summarized in Tables 22, 35, 60, 71 and 84, respectively. V_S30 and V_S60 range from 181 to 500 m/s (594 to 1641 ft/s) and 269 to 662 m/s (884 to 2,172 ft/s), respectively. Fifty (50) of the surface wave soundings have V_S30 less than 360 m/s (1,181 ft/s). Modeled S-wave velocity at a depth of 60 m (197 ft) is highly variable ranging from about 420 to 1,250 m/s (1,378 to 4,101 ft/s).

Surface wave data were acquired and modeled at least two locations on each of the 17 seismic reflection lines except for Z1-G5, where one of the surface wave soundings did not yield data that could be modeled. The surface wave soundings indicated than 9 of the seismic lines (Z1-G3, Z2-G1, Z2-G2, Z2-G3, Z3-G1, Z3-G4, Z4-G2, Z5-G2 and Z5-G3) have only minor lateral velocity variation. Therefore, potential geologic structures bisecting these lines do not have a significant impact on subsurface velocity structure. There is significant lateral velocity variation along the other 7 seismic reflection lines (Z1-G4, Z3-G2, Z3-G3, Z3-G5, Z3-G6, Z3-G7 and Z4-G1). The lateral velocity variation along these seismic lines may be the result of a geologic structure, such as a fault, bisecting the line or, alternatively, may be the result of dipping geologic units, variable bedrock depths or variable bedrock weathering profiles.

Review of borehole velocity logs from boreholes primarily located in Zones 1 to 3 indicated that S-wave velocity may be applicable for differentiating sediments from shallow sedimentary rock in Zones 1 and 2. In these zones, S-wave velocity below 350 m/s (1,148 ft/s) was typically found to be associated with sediments, whereas higher velocities were associated with sedimentary rock. However, decomposed rock was occasionally found to have S-wave velocity in the sediment range. The application of S-wave velocity to differentiate sediments from bedrock was more difficult in Zone 3 due to thick accumulations of high velocity, old alluvial sediments in the northern portion of the zone. In areas with crystalline basement north of the Eagle Rock Fault, S-wave velocity over 650 m/s (2,133 ft/s) was found to be typically associated with bedrock and lower velocities associated with overlying sediments. South of the Eagle Rock Fault, S-wave velocity over 400 m/s (1,312 ft/s) was often found to be associated with sedimentary bedrock. However, there was some overlap in S-wave velocity between sediments and weathered sedimentary rock in Zone 3. There was limited borehole control in Zones 4 and 5, and with the exception of the southwestern corner of these zones, bedrock was expected to be much deeper than the exploration limits of the surface wave method.

7 REFERENCES

Brown, L.T., 1998, "Comparison of V_S profiles from SASW and borehole measurements at strong motion sites in Southern California", Master's thesis, University of Texas at Austin.

Foti, S., 2000, "Multistation Methods for Geotechnical Characterization using Surface Waves", Ph.D. Dissertation, Politecnico di Torino, Italy.

Joh, S.H., 2002, "WinSASW Version 2.0, Data Interpretation and Analysis for SASW Measurements", Department of Civil Engineering, Chung-Ang University, Anseong, Korea.

Louie, J.N., 2001, "Faster, Better: Shear-Wave Velocity to 100 Meters Depth from Refraction Microtremor Arrays", Bulletin of the Seismological Society of America, vol. 91, no. 2, p. 347-364.

Okada, H, 2003, "The Microtremor Survey Method," Society of Exploration Geophysics Geophysical Monograph Series, Number 12, 135p.

Park, C.B., Miller, R.D. and Xia, J., 1999a, "Multimodal analysis of high frequency surface waves", *Proceedings of the Symposium on the Application of Geophysics to Engineering and Environmental Problems '99*, 115-121.

Park, C.B., Miller, R.D. and Xia, J., 1999b, "Multichannel analysis of surface waves", Geophysics, Vol 64, No. 3, 800-808.

Roesset, J.M., Chang, D.W. and Stokoe, K.H., II, 1991, "Comparison of 2-D and 3-D Models for Analysis of Surface Wave Tests," *Proceedings,* 5th *International Conference on Soil Dynamics and Earthquake Engineering*, Karlsruhe, Germany.

8 CERTIFICATION

All geophysical data, analysis, interpretations, conclusions, and recommendations in this document have been prepared under the supervision of and reviewed by a **GEO*Vision*** California Professional Geophysicist.

10/05/09

Antony J. Martin — Date
California Professional Geophysicist GP989
GEO*Vision* Geophysical Services

* This geophysical investigation was conducted under the supervision of a California Professional Geophysicist using industry standard methods and equipment. A high degree of professionalism was maintained during all aspects of the project from the field investigation and data acquisition, through data processing interpretation and reporting. All original field data files, field notes and observations, and other pertinent information are maintained in the project files and are available for the client to review for a period of at least one year.

  A professional geophysicist's certification of interpreted geophysical conditions comprises a declaration of his/her professional judgment. It does not constitute a warranty or guarantee, expressed or implied, nor does it relieve any other party of its responsibility to abide by contract documents, applicable codes, standards, regulations or ordinances.

APPENDIX A

TECHNICAL NOTE

ACTIVE AND PASSIVE SURFACE WAVE TECHNIQUES

ACTIVE AND PASSIVE SURFACE WAVE TECHNIQUES

GEOVision geophysical services

Overview

Active and passive surface wave techniques are relatively new in-situ seismic methods for determining shear wave velocity (V_S) profiles. Testing is performed on the ground surface, allowing for less costly measurements than with traditional borehole methods. The basis of surface wave techniques is the dispersive characteristic of Rayleigh waves when traveling through a layered medium. Rayleigh wave velocity is determined by the material properties (primarily shear wave velocity, but also to a lesser degree compression wave velocity and material density) of the subsurface to a depth of approximately 1 to 2 wavelengths. As shown in the adjacent diagram, longer wavelengths penetrate deeper and their velocity is affected by the material properties at greater depth. Surface wave testing consists of measuring the surface wave dispersion curve at a site and modeling it to obtain the corresponding shear wave velocity profile.

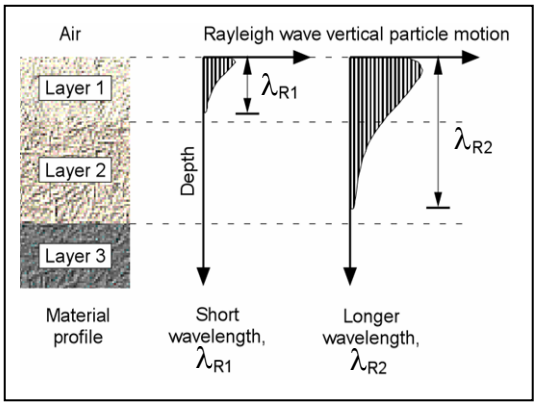

Active Surface Wave Techniques

Active surface wave techniques measure surface waves generated by dynamic sources such as hammers, weight drops, electromechanical shakers, vibroseis and bulldozers. These techniques include the spectral analysis of surface waves (SASW) and multi-channel array surface wave (MASW) methods.

Hammer Energy Sources

Accelerated Weight Drop

Electromechanical Shaker

Bulldozer Energy Source

1124 Olympic Drive, Corona, California 92881 ph. 951-549-1234 fx 951-549-1236 www.geovision.com

The SASW method is optimized for conducting V_S depth soundings. A dynamic source is used to generate surface waves of different wavelengths (or frequencies) which are monitored by two or more receivers at known offsets. An expanding receiver spread and optimized source-receiver geometry are used to minimize near field effects, body wave signal and attenuation. A dynamic signal analyzer is typically used to calculate the phase and coherence of the cross spectrum of the time history data collected at a pair of receivers. During data analysis, an interactive masking process is used to discard low quality data and to unwrap the phase spectrum, as shown in the figure below. The dispersion curve (Rayleigh wave phase velocity versus frequency or alternatively wavelength) is calculated from the unwrapped phase spectrum.

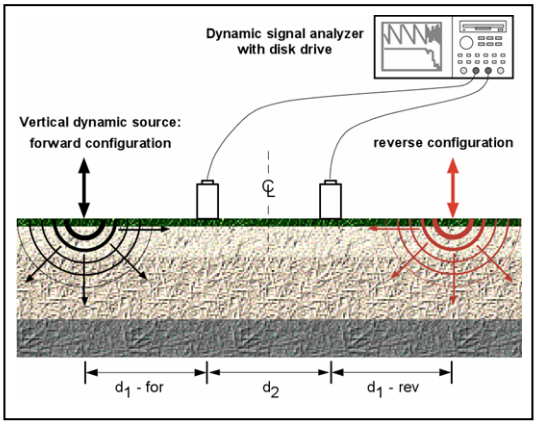

SASW Setup

HP Dynamic Signal Analyzer

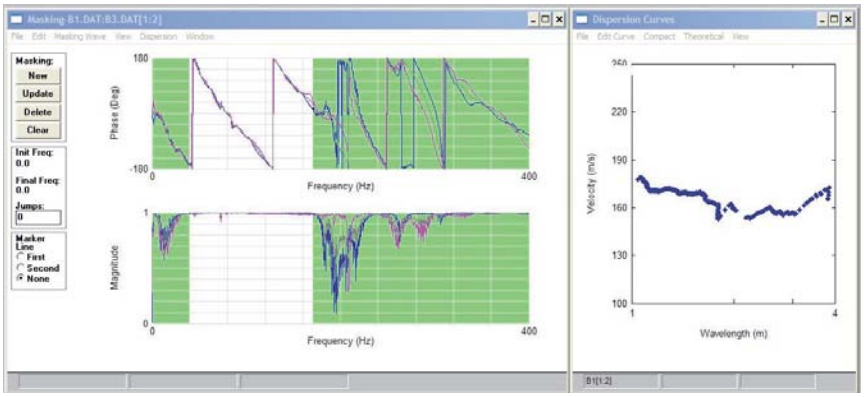

Masking of Wrapped Phase Spectrum and Resulting Dispersion Curve

The MASW field layout is similar to that of the seismic refraction technique. Twenty four, or more, geophones are laid out in a linear array with 1 to 2m spacing and connected to a multi-channel seismograph as shown below. This technique is ideally suited to 2D V_S imaging, with data collected in a roll-along manner similar to that of the seismic reflection technique. The source is offset at a predetermined distance from the near geophone usually determined by field testing. The Rayleigh wave dispersion curve is obtained by a wavefield transformation of the seismic record such as the f-k or τ-p transforms. These transforms are very effective at isolating surface wave energy from that of body waves. The dispersion curve is picked as the peak of the surface wave energy in slowness (or velocity) – frequency space as shown. One advantage of the MASW technique is that the wavefield transformation may not only identify the fundamental mode but also higher modes of surface waves. At some sites, particularly those with large velocity inversions, higher surface wave modes may contain more energy than the fundamental mode.

MASW Field Setup

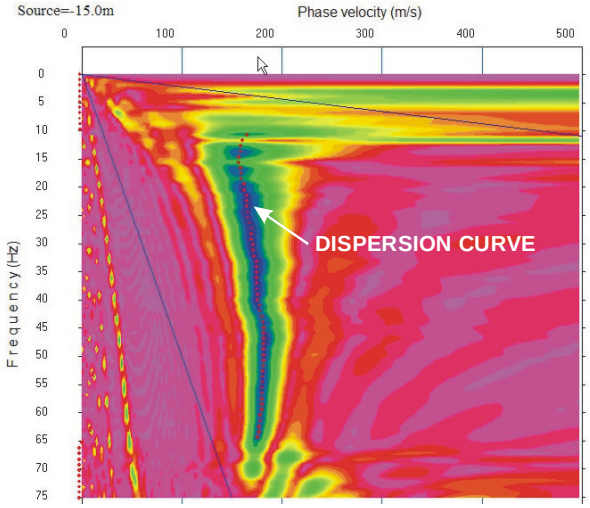

Wavefield Transform of MASW data

Passive Surface Wave Techniques

Passive surface wave techniques measure noise; surface waves from ocean wave activity, traffic, factories, etc. These techniques include the array microtremor and refraction microtremor (REMI) techniques.

The array microtremor technique typically uses 7 or more 4.5- or 1-Hz geophones arranged in a two-dimensional array. The most common arrays are the triangle, circle, semi-circle and "L" arrays. The triangle array, which consists of several embedded equilateral triangles, is often used as it provides good results with a relatively small number of geophones. With this array the outer side of the triangle should be at least as long as the desired depth of investigation. Typically, fifteen to twenty 30-second noise records are acquired for analysis. The spatial autocorrelation (SPAC) technique is one of several methods that can be used to estimate the Rayleigh wave dispersion curve. A first order Bessel function is fit to the SPAC function to determine the phase velocity for particular frequency. The image shown below shows the degree of fitness of the Bessel function to the SPAC function for a wide range of phase velocity and frequency. The dispersion curve, is the peak (best fit), as shown in the figure below.

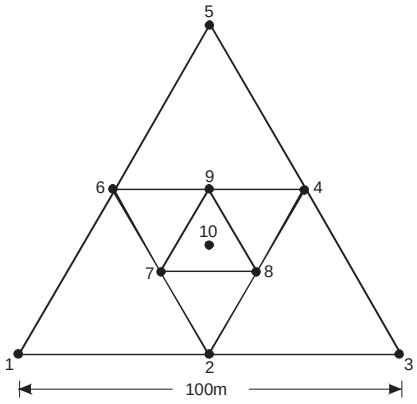

Triangle Array Geometry

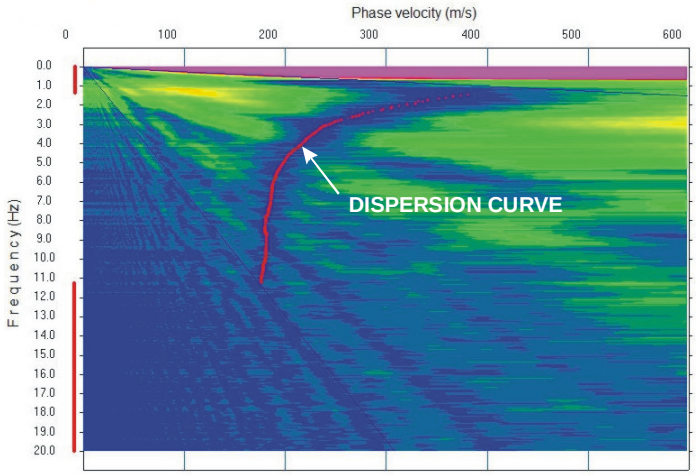

Dispersion Curve from Array Microtremor Measurements

The refraction microtremor (REMI) technique uses a field layout similar to the seismic refraction method (hence its name). Twenty-four, 4.5 Hz geophones are laid out in a linear array with a spacing of 6 to 8m and fifteen to twenty 30-second noise records are acquired. A slowness-frequency (p-f) wavefield transform is used to separate Rayleigh wave energy from that of other waves. Because the noise field can originate from any direction, the wavefield transform is conducted for multiple vectors through the geophone array, all of which are summed. The dispersion curve is defined as the lower envelope of the Rayleigh wave energy in p-f space. Because the lower envelope is picked rather than the energy peak (energy traveling along the profile is slower than that approaching from an angle), this technique may be somewhat more subjective than the others, particularly at low frequencies. The SPAC technique can also be used to extract the surface wave dispersion curve from linear array microtremor data providing there are omni-directional noise sources.

Refraction Microtremor Array Layout

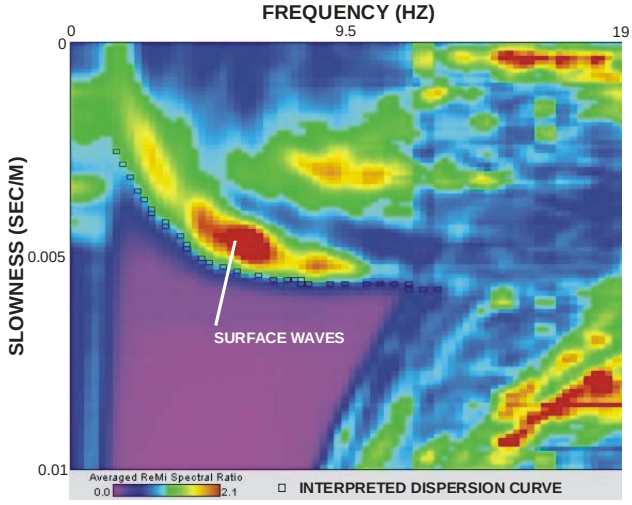

Wavefield Transform of REMI Data

Depth of Investigation

Active surface wave investigations typically use various sized sledge hammers to image the shear wave velocity structure to depths of up to 15m. Weight drops and electromechanical shakers can often be used to image to depths of 30m. Bulldozers and vibroseis trucks can be used to image to depths as great as 100m. Passive surface wave techniques can often image shear wave velocity structure to depths of over 100m, given sufficient noise sources and space for the receiver array. Large passive arrays, utilizing long-period seismometers with GPS clocks have been used to image shear wave velocity structure to depths of several kilometers.

Combined Active and Passive Surface Wave Testing

The combined use of active and passive techniques may offer significant advantages on many investigations. It can be very costly to mobilize large energy sources for 30m/100ft active surface wave soundings. In urban environments, the combined use of active and passive surface wave techniques can image to these depths without the need for large energy sources. We have found that dispersion curves from active and passive surface wave techniques are generally in good agreement, making the combined use of the two techniques viable. It is not recommended that passive surface wave techniques be applied alone for UBC/IBC site classification investigations. Microtremor techniques do not generally characterize near surface velocity, which may have a significant impact of the average shear wave velocity of the upper 30m or 100ft and so should always be used in conjunction with SASW or MASW. An SASW sounding to a depth of 30m requires at least a 60m linear array. If sufficient space is not available for this, it may be possible to use a 45m triangle array on the site or place a 100-200m long REMI array along an adjacent sidewalk or an "L" array at an adjacent street intersection.

Microtremor Measurements along Sidewalk

Modeling

There are several options for interpreting surface wave dispersion curves, depending on the accuracy required in the shear wave velocity profile. A simple empirical analysis can be done to estimate the average shear wave velocity profile. For greater accuracy, forward modeling of fundamental-mode Rayleigh wave dispersion as well as full stress wave propagation can be performed using several software packages. A formal inversion scheme may also be used. With many of the analytical approaches, background information on the site can be incorporated into the model and the resolution of the final profile may be quantified.

Applications

Active and passive surface wave testing can be used to obtain V_S profiles for:

- UBC/IBC site classification for seismic design
- Earthquake site response
- Seismic microzonation
- Liquefaction analysis
- Soil compaction control
- Mapping subsurface stratigraphy
- Locating potentially weak zones in earthen embankments and levees

Case History

The figures below show the surface wave dispersion curves and alternative shear wave velocity models for a site in Los Angeles, California. All of the previous figures illustrating SASW, MASW, array and refraction microtremor techniques were from this site. The dispersion curves from all four methods are shown on the left along with the theoretical dispersion curves for alternative S-wave velocity versus depth models on the right. Conditions at this site were very poor for active surface wave techniques because of the presence of very low velocity hydraulic fill. In fact, with active surface wave techniques it was only possible to image to a depth of about 12.5m with energy sources typically capable of imaging to 30m. There is excellent agreement in the dispersion curves generated from all of the methods over the overlapping wavelength ranges. The minor differences probably result from variable velocity of the hydraulic fill within the sampling volume of the specific methods. Two Vs versus depth models were generated to illustrate the difficulty modeling the highly variable, near surface velocity structure evident in the PS log. The two surface wave models yielded similar values for the average shear-wave velocity of the upper 30m (V_S30), 201 and 202 m/s, illustrating that Vs30 is much more tightly constrained than the actual layer thicknesses and velocities in the models. V_S30 estimated from the PS log (194 m/s) is within 4% of that estimated from the two surface wave models (201 and 202 m/s). The small differences in V_S30 between the two methods may easily result from the different sampling regimes (borehole versus large area) rather than errors in either of the methods.

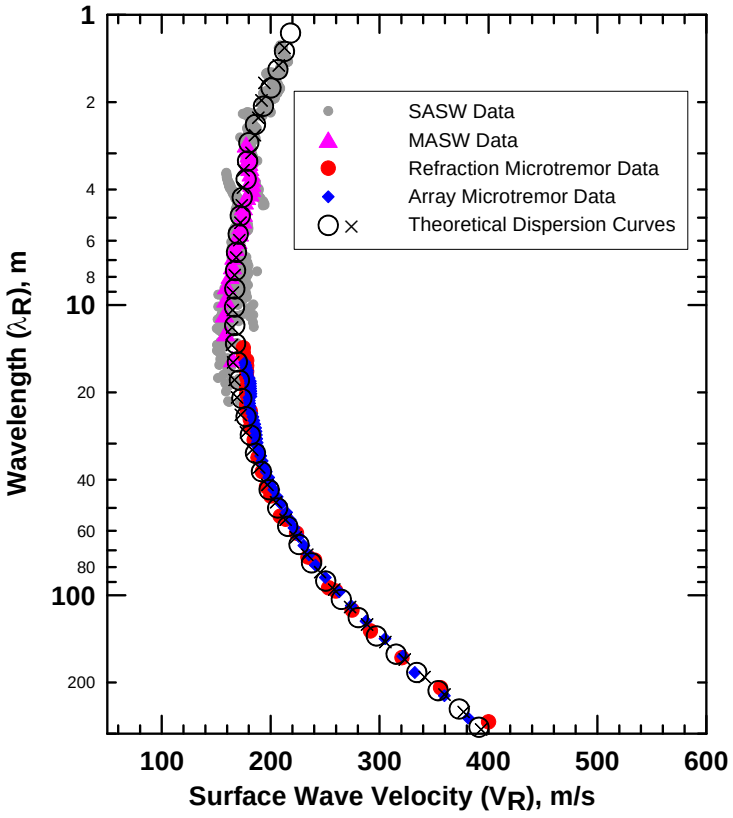

Field Data and Theoretical Dispersion Curve

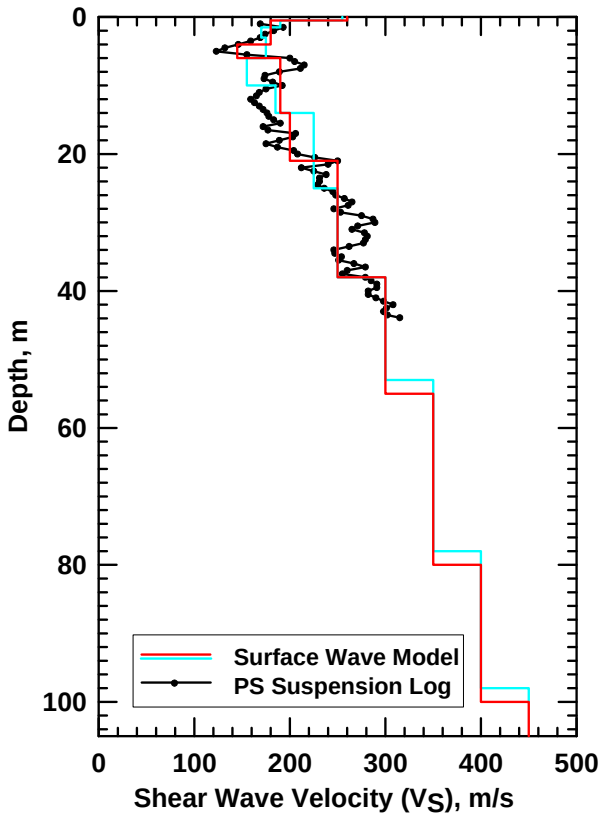

VS Model

In contrast to borehole measurements which are point estimates, surface wave testing is a global measurement, that is, a much larger volume of the subsurface is sampled. The resulting profile is representative of the subsurface properties averaged over distances of up to several hundred feet. Although surface wave techniques do not have the layer sensitivity or accuracy (velocity and layer thickness) of borehole techniques; the average velocity over a large depth interval (i.e. the average shear wave velocity of the upper 30m or 100ft) is very well constrained. Because surface wave methods are non-invasive and non-destructive, it is relatively easy to obtain the necessary permits for testing. At sites that are favorable for surface wave propagation, active and passive surface wave techniques allow appreciable cost and time savings.

TABLES

Table 1 Surface Wave Sounding Locations

Surface Wave Sounding	Northing (ft)	Easting (ft)	Elevation (ft)	Elevation (m)
Z1-S1	1858859	6484375	602	184
Z1-S2	1860241	6486978	365	111
Z1-S3	1855713	6486181	572	174
Z1-S4	1858034	6487619	354	108
Z1-S5	1854017	6488212	558	170
Z1-S6	1854836	6488769	495	151
Z1-S7	1855081	6490960	339	103
Z1-S8	1855912	6493275	343	105
Z1-S9	1857467	6492596	373	114
Z1-S10	1857156	6493973	405	124
Z1-S11	1851776	6497134	388	118
Z1-S12	1854510	6496669	375	114
Z1-S13	1855365	6498202	387	118
Z1-S14	1851778	6503719	430	131
Z1-S15	1852614	6504404	443	135
Z1-S16	1853425	6507732	458	140
Z1-S17	1851189	6507746	451	137
Z1-S18	1852828	6501056	519	158
Z1-S19	1850601	6508208	460	140
Z1-S20	1849226	6512497	410	125
Z2-S1	1867725	6491385	495	151
Z2-S2	1867940	6496459	512	156
Z2-S3	1866836	6496205	498	152
Z2-S4	1864067	6497693	589	179
Z2-S5	1863749	6501923	562	171
Z2-S6	1862660	6500632	560	171
Z2-S7	1860704	6500564	504	154
Z2-S8	1861511	6501933	518	158
Z2-S9	1859442	6505698	565	172
Z2-S10	1855524	6508114	529	161
Z2-S11	1854560	6508588	489	149
Z2-S12	1851917	6511435	435	133
Z3-S1	1873355	6508880	856	261
Z3-S2	1872437	6515241	803	245
Z3-S3	1870876	6516649	760	232
Z3-S4	1868917	6516666	740	226
Z3-S5	1869134	6514649	792	241
Z3-S6	1868529	6512309	685	209
Z3-S7	1867430	6512291	685	209

California State Plane coordinate system, North American Datum 1983, Zone V (0405), US Survey Feet
Horizontal accuracy is approximately 1m, vertical accuracy is approximately 2m.

Table 1 (continued) Surface Wave Sounding Locations

Surface Wave Sounding	Northing (ft)	Easting (ft)	Elevation (ft)	Elevation (m)
Z3-S8	1865577	6507915	629	192
Z3-S9	1865625	6509614	581	177
Z3-S10	1866852	6511062	606	185
Z3-S11	1866385	6514149	752	229
Z3-S12	1864933	6516620	662	202
Z3-S13	1864229	6511117	628	191
Z3-S14	1863395	6510579	624	190
Z3-S15	1863362	6514035	653	199
Z3-S16	1860840	6517236	576	176
Z3-S17	1859471	6510276	626	191
Z3-S18	1859110	6510324	616	188
Z3-S19	1858453	6513474	563	171
Z3-S20	1855555	6513374	527	161
Z3-S21	1853042	6513102	455	139
Z3-S22	1852143	6513121	430	131
Z3-S23	1849598	6513201	418	127
Z3-S24	1848525	6513200	430	131
Z4-S1	1873443	6532600	689	210
Z4-S2	1870461	6528291	675	206
Z4-S3	1868812	6528564	608	185
Z4-S4	1867261	6528903	572	174
Z4-S5	1865714	6525732	558	170
Z4-S6	1862787	6522740	551	168
Z4-S7	1861952	6521747	553	168
Z4-S8	1859713	6521908	536	164
Z4-S9	1857271	6519012	525	160
Z4-S10	1854206	6516832	494	150
Z5-S1	1858186	6559083	338	103
Z5-S2	1857834	6552545	319	97
Z5-S3	1857071	6547330	328	100
Z5-S4	1857431	6542974	349	106
Z5-S6	1854909	6534525	361	110
Z5-S7	1853910	6530313	371	113
Z5-S8	1851881	6527893	375	114
Z5-S9	1851805	6526574	400	122
Z5-S10	1852828	6523633	440	134
Z5-S11	1851500	6519232	458	139
Z5-S12	1849766	6516622	436	133
Z5-S13	1848767	6516641	422	129

California State Plane coordinate system, North American Datum 1983, Zone V (0405), US Survey Feet
Horizontal accuracy is approximately 1m, vertical accuracy is approximately 2m.

Table 2 Active and Passive Surface Wave Sounding Geometry

Surface Wave Sounding	MASW Receiver Spacing (m)	Passive Linear Array Receiver Spacing (m)	Passive "L" Array Receiver Spacing (m)
Z1-S1	1.5	4	NC
Z1-S2	1.5	6	6
Z1-S3	1.5	6	6
Z1-S4	1.5	6	6
Z1-S5	1.5	6	6
Z1-S6	1.5	6	NC
Z1-S7	1.5	6	6
Z1-S8	1.5	6	NC
Z1-S9	1.5	6	6
Z1-S10	1.5	6	6
Z1-S11	1.5	6	6
Z1-S12	1.5	6	6
Z1-S13	1.5	6	6
Z1-S14	1.5	6	6
Z1-S15	1.5	6	6
Z1-S16	1.5	6	6
Z1-S17	1.5	6	6
Z1-S18	1.5	6	6
Z1-S19	1.5	6	6
Z1-S20	1.5	6	6
Z2-S1	1.5	6	6
Z2-S2	1.5	6	6
Z2-S3	1.5	6	6
Z2-S4	1.5	6	6
Z2-S5	1.5	6	6
Z2-S6	1.5	6	6
Z2-S7	1.5	6	5
Z2-S8	1.5	5.5	5.5
Z2-S9	1.5	6	6
Z2-S10	1.5	6	6
Z2-S11	1.5	6	6
Z2-S12	1.5	6	6
Z3-S1	1.5	6	6
Z3-S2	1.5	6	6
Z3-S3	1.5	6	6
Z3-S4	1.5	6	6
Z3-S5	1.5	6	6
Z3-S6	1.5	6	6
Z3-S7	1.5	6	6

Surface Wave Sounding	MASW Receiver Spacing (m)	Passive Linear Array Receiver Spacing (m)	Passive "L" Array Receiver Spacing (m)
Z3-S8	1.5	6	6
Z3-S9	1.5	6	6
Z3-S10	1.5	6	NC
Z3-S11	1.5	6	6
Z3-S12	1.5	6	6
Z3-S13	1.5	6	NC
Z3-S14	1.5	6	6
Z3-S15	1.5	6	6
Z3-S16	1.5	6	6
Z3-S17	1.5	6	6
Z3-S18	1.5	6	6
Z3-S19	1.5	6	6
Z3-S20	1.5	6	6
Z3-S21	1 & 2	6	6
Z3-S22	1.5	6	6
Z3-S23	1 & 2	6	NC
Z3-S24	1.5	6	6
Z4-S1	1.5	6	6
Z4-S2	1.5	6	NC
Z4-S3	1.5	6	NC
Z4-S4	1.5	6	NC
Z4-S5	1.5	6	6
Z4-S6	1.5	6	6
Z4-S7	1.5	6	6
Z4-S8	1.5	6	6
Z4-S9	1.5	6	6
Z4-S10	1.5	6	6
Z5-S1	1.5	6	6
Z5-S2	1.5	6	6
Z5-S3	1.5	6	6
Z5-S4	1.5	6	6
Z5-S6	1.5	6	6
Z5-S7	1.5	6	6
Z5-S8	1.5	6	6
Z5-S9	1.5	6	6
Z5-S10	1.5	6	6
Z5-S11	1.5	6	6
Z5-S12	1.5	6	6
Z5-S13	1.5	6	6

Note: NC = Not Conducted

Table 20 Velocity Model for Surface Wave Array Z1-S19

Approx. Elevation of Top of Layer		Depth to Top of Layer		Layer Thickness		S-Wave Velocity		Inferred P-Wave Velocity	
m	ft	m	ft	m	ft	m/s	ft/s	m/s	ft/s
140	518.4	0	0.0	1.5	4.9	265	869	530	1739
138.5	513.5	1.5	4.9	1.5	4.9	400	1312	799.9	2624
137	508.5	3	9.8	2	6.6	550	1804	1149.9	3773
135	502.0	5	16.4	2	6.6	550	1804	1850	6070
133	495.4	7	23.0	9	29.5	475	1558	1850	6070
124	465.9	16	52.5	15	49.2	575	1886	1850	6070
109	416.7	31	101.7	15	49.2	650	2133	1850	6070
94	367.5	46	150.9	>14	>45.9	750	2461	2150	7054

Approximate depth of investigation is 60m.

Table 21 Velocity Model for Surface Wave Array Z1-S20

Approx. Elevation of Top of Layer		Depth to Top of Layer		Layer Thickness		S-Wave Velocity		Inferred P-Wave Velocity	
m	ft	m	ft	m	ft	m/s	ft/s	m/s	ft/s
125	459.3	0	0.0	1.5	4.9	195	640	390	1280
123.5	454.4	1.5	4.9	1.5	4.9	285	935	570	1870
122	449.5	3	9.8	3	9.8	285	935	1650	5413
119	439.6	6	19.7	8	26.2	300	984	1650	5413
111	413.4	14	45.9	11.5	37.7	375	1230	1850	6070
99.5	375.7	25.5	83.7	26	85.3	515	1690	1850	6070
73.5	290.4	51.5	169.0	>18.5	>60.7	775	2543	2150	7054

Approximate depth of investigation is 70m.

Table 22 Summary of Zone 1 Surface Wave Investigation

Surface Wave Array	Vs30 (m/s)	Vs30 (ft/s)	Vs60 (m/s)	Vs60 (ft/s)	Vs @ 60m (m/s)	Vs @ 60m (ft/s)
Z1-S1	362	1188	452	1481	725	2379
Z1-S2	299	982	382	1254	700	2297
Z1-S3	394	1292	512	1680	750	2461
Z1-S4	315	1033	423	1387	700	2297
Z1-S5	317	1039	430	1412	800	2625
Z1-S6	323	1059	439	1440	800	2625
Z1-S7	295	967	384	1259	700	2297
Z1-S8	280	919	368	1209	675	2215
Z1-S9	302	990	398	1307	800	2625
Z1-S10	328	1077	437	1433	800	2625
Z1-S11	359	1177	477	1565	850	2789
Z1-S12	378	1240	487	1599	775	2543
Z1-S13	354	1161	455	1492	800	2625
Z1-S14	181	594	269	884	700	2297
Z1-S15	230	754	336	1102	850	2789
Z1-S16	249	818	317	1041	550	1804
Z1-S18	273	894	364	1194	725	2379
Z1-S19	500	1641	580	1903	750	2461
Z1-S20	335	1099	422	1384	775	2543

Note: Vs30 = average S-wave velocity of upper 30 m. Vs60 = average S-wave velocity of upper 60 m.

Table 36 Velocity Model for Surface Wave Array Z3-S1

Approx. Elevation of Top of Layer		Depth to Top of Layer		Layer Thickness		S-Wave Velocity		Inferred P-Wave Velocity	
m	ft	m	ft	m	ft	m/s	ft/s	m/s	ft/s
261	856.3	0	0.0	1.5	4.9	240	787	480	1575
259.5	851.4	1.5	4.9	3.5	11.5	360	1181	720	2362
256	839.9	5	16.4	12	39.4	360	1181	1750	5741
244	800.5	17	55.8	21	68.9	525	1722	2100	6890
223	731.6	38	124.7	30	98.4	725	2379	2100	6890
193	633.2	68	223.1	>2	>6.6	900	2953	2400	7874

Approximate depth of investigation is 70m.

Table 37 Velocity Model for Surface Wave Array Z3-S2

Approx. Elevation of Top of Layer		Depth to Top of Layer		Layer Thickness		S-Wave Velocity		Inferred P-Wave Velocity	
m	ft	m	ft	m	ft	m/s	ft/s	m/s	ft/s
245	803.8	0	0.0	1.75	5.7	150	492	300	984
243.25	798.1	1.75	5.7	3.75	12.3	310	1017	620	2034
239.5	785.8	5.5	18.0	10	32.8	375	1230	750	2460
229.5	753.0	15.5	50.9	17	55.8	425	1394	850	2788
212.5	697.2	32.5	106.6	20	65.6	500	1640	1925	6316
192.5	631.6	52.5	172.2	20	65.6	650	2133	2100	6890
172.5	565.9	72.5	237.9	>2.5	>8.2	1000	3281	2800	9186

Approximate depth of investigation is 75m.

Table 38 Velocity Model for Surface Wave Array Z3-S3

Approx. Elevation of Top of Layer		Depth to Top of Layer		Layer Thickness		S-Wave Velocity		Inferred P-Wave Velocity	
m	ft	m	ft	m	ft	m/s	ft/s	m/s	ft/s
232	761.2	0	0.0	2	6.6	235	771	470	1542
230	754.6	2	6.6	3.5	11.5	260	853	520	1706
226.5	743.1	5.5	18.0	16.5	54.1	405	1329	810	2657
210	689.0	22	72.2	15	49.2	450	1476	900	2953
195	639.8	37	121.4	8	26.2	600	1969	1200	3937
187	613.5	45	147.6	12	39.4	600	1969	2100	6890
175	574.1	57	187.0	>13	>42.7	800	2625	2800	9186

Approximate depth of investigation is 70m.

Table 39 Velocity Model for Surface Wave Array Z3-S4

Approx. Elevation of Top of Layer		Depth to Top of Layer		Layer Thickness		S-Wave Velocity		Inferred P-Wave Velocity	
m	ft	m	ft	m	ft	m/s	ft/s	m/s	ft/s
226	741.5	0	0.0	7	23.0	275	902	550	1804
219	718.5	7	23.0	14	45.9	390	1280	780	2559
205	672.6	21	68.9	15	49.2	475	1558	950	3116
190	623.4	36	118.1	9	29.5	650	2133	1300	4265
181	593.8	45	147.6	11	36.1	650	2133	2100	6890
170	557.7	56	183.7	>14	>45.9	900	2953	2800	9186

Approximate depth of investigation is 70m.

Table 40 Velocity Model for Surface Wave Array Z3-S5

Approx. Elevation of Top of Layer		Depth to Top of Layer		Layer Thickness		S-Wave Velocity		Inferred P-Wave Velocity	
m	ft	m	ft	m	ft	m/s	ft/s	m/s	ft/s
241	790.7	0	0.0	1.75	5.7	245	804	490	1608
239.25	784.9	1.75	5.7	5.25	17.2	375	1230	750	2460
234	767.7	7	23.0	10	32.8	500	1640	1000	3281
224	734.9	17	55.8	10	32.8	650	2133	1300	4265
214	702.1	27	88.6	3	9.8	750	2461	1500	4921
211	692.3	30	98.4	7	23.0	750	2461	2400	7874
204	669.3	37	121.4	10	32.8	1000	3281	2800	9186
194	636.5	47	154.2	>23	>75.5	1200	3937	2800	9186

Approximate depth of investigation is 70m.

Table 41 Velocity Model for Surface Wave Array Z3-S6

Approx. Elevation of Top of Layer		Depth to Top of Layer		Layer Thickness		S-Wave Velocity		Inferred P-Wave Velocity	
m	ft	m	ft	m	ft	m/s	ft/s	m/s	ft/s
209	685.7	0	0.0	2	6.6	270	886	540	1772
207	679.1	2	6.6	3	9.8	325	1066	650	2133
204	669.3	5	16.4	2	6.6	325	1066	1750	5741
202	662.7	7	23.0	8	26.2	370	1214	1750	5741
194	636.5	15	49.2	8	26.2	465	1526	1925	6316
186	610.2	23	75.5	17	55.8	650	2133	2100	6890
169	554.5	40	131.2	20	65.6	775	2543	2400	7874
149	488.8	60	196.9	>10	>32.8	1000	3281	2800	9186

Approximate depth of investigation is 70m.

Table 45 Velocity Model for Surface Wave Array Z3-S10

Approx. Elevation of Top of Layer		Depth to Top of Layer		Layer Thickness		S-Wave Velocity		Inferred P-Wave Velocity	
m	ft	m	ft	m	ft	m/s	ft/s	m/s	ft/s
185.0	607.0	0	0.0	2.5	8.2	175	574	350	1148
182.5	598.8	2.5	8.2	0.5	1.6	310	1017	620	2034
182.0	597.1	3	9.8	2.5	8.2	310	1017	1750	5741
179.5	588.9	5.5	18.0	5	16.4	440	1444	1925	6316
174.5	572.5	10.5	34.4	20	65.6	520	1706	2100	6890
154.5	506.9	30.5	100.1	>39.5	>129.6	740	2428	2400	7874

Approximate depth of investigation is 70m.

Table 46 Velocity Model for Surface Wave Array Z3-S11

Approx. Elevation of Top of Layer		Depth to Top of Layer		Layer Thickness		S-Wave Velocity		Inferred P-Wave Velocity	
m	ft	m	ft	m	ft	m/s	ft/s	m/s	ft/s
229.0	751.3	0	0.0	2	6.6	215	705	430	1411
227.0	744.8	2	6.6	3	9.8	260	853	520	1706
224.0	734.9	5	16.4	4	13.1	280	919	560	1837
220.0	721.8	9	29.5	1.5	4.9	325	1066	650	2133
218.5	716.9	10.5	34.4	12.5	41.0	325	1066	1750	5741
206.0	675.9	23	75.5	20	65.6	415	1362	1925	6316
186.0	610.2	43	141.1	>27	>88.6	625	2051	2100	6890

Approximate depth of investigation is 70m.

Table 47 Velocity Model for Surface Wave Array Z3-S12

Approx. Elevation of Top of Layer		Depth to Top of Layer		Layer Thickness		S-Wave Velocity		Inferred P-Wave Velocity	
m	ft	m	ft	m	ft	m/s	ft/s	m/s	ft/s
202	662.7	0	0.0	1.5	4.9	200	656	400	1312
200.5	657.8	1.5	4.9	2	6.6	260	853	520	1706
198.5	651.2	3.5	11.5	3.5	11.5	235	771	470	1542
195	639.8	7	23.0	8.5	27.9	340	1115	680	2231
186.5	611.9	15.5	50.9	11.5	37.7	350	1148	1750	5741
175	574.1	27	88.6	22	72.2	400	1312	1925	6316
153	502.0	49	160.8	>35	>114.8	675	2215	2100	6890

Approximate depth of investigation is 70m.

Table 50 Velocity Model for Surface Wave Array Z3-S15

Approx. Elevation of Top of Layer		Depth to Top of Layer		Layer Thickness		S-Wave Velocity		Inferred P-Wave Velocity	
m	ft	m	ft	m	ft	m/s	ft/s	m/s	ft/s
199	652.9	0	0.0	1.5	4.9	190	623	380	1247
197.5	648.0	1.5	4.9	2.5	8.2	260	853	520	1706
195	639.8	4	13.1	2.5	8.2	300	984	600	1969
192.5	631.6	6.5	21.3	8.5	27.9	350	1148	700	2297
184	603.7	15	49.2	4	13.1	350	1148	1750	5741
180	590.6	19	62.3	16	52.5	400	1312	1925	6316
164	538.1	35	114.8	16	52.5	500	1640	2100	6890
148	485.6	51	167.3	>19	>62.3	750	2461	2100	6890

Approximate depth of investigation is 70m.

Table 51 Velocity Model for Surface Wave Array Z3-S16

Approx. Elevation of Top of Layer		Depth to Top of Layer		Layer Thickness		S-Wave Velocity		Inferred P-Wave Velocity	
m	ft	m	ft	m	ft	m/s	ft/s	m/s	ft/s
176	577.4	0	0.0	2.5	8.2	225	738	450	1476
173.5	569.2	2.5	8.2	5	16.4	380	1247	760	2493
168.5	552.8	7.5	24.6	2.5	8.2	370	1214	740	2427
166	544.6	10	32.8	12	39.4	370	1214	1750	5741
154	505.2	22	72.2	20	65.6	425	1394	1925	6316
134	439.6	42	137.8	>28	>91.9	500	1640	1925	6316

Approximate depth of investigation is 70m.

Table 52 Velocity Model for Surface Wave Array Z3-S17

Approx. Elevation of Top of Layer		Depth to Top of Layer		Layer Thickness		S-Wave Velocity		Inferred P-Wave Velocity	
m	ft	m	ft	m	ft	m/s	ft/s	m/s	ft/s
191	626.6	0	0.0	2	6.6	215	705	430	1411
189	620.1	2	6.6	6	19.7	290	951	580	1903
183	600.4	8	26.2	8	26.2	290	951	1750	5741
175	574.1	16	52.5	5.5	18.0	350	1148	1750	5741
169.5	556.1	21.5	70.5	10	32.8	700	2297	2100	6890
159.5	523.3	31.5	103.3	10	32.8	800	2625	2400	7874
149.5	490.5	41.5	136.2	>28.5	>93.5	1250	4101	2800	9186

Approximate depth of investigation is 70m.

Table 53 Velocity Model for Surface Wave Array Z3-S18

Approx. Elevation of Top of Layer		Depth to Top of Layer		Layer Thickness		S-Wave Velocity		Inferred P-Wave Velocity	
m	ft	m	ft	m	ft	m/s	ft/s	m/s	ft/s
188	616.8	0	0.0	1.5	4.9	195	640	390	1280
186.5	611.9	1.5	4.9	6.5	21.3	285	935	570	1870
180	590.6	8	26.2	11	36.1	285	935	1750	5741
169	554.5	19	62.3	7	23.0	350	1148	1750	5741
162	531.5	26	85.3	10	32.8	650	2133	2100	6890
152	498.7	36	118.1	10	32.8	800	2625	2400	7874
142	465.9	46	150.9	>24	>78.7	1250	4101	2800	9186

Approximate depth of investigation is 70m.

Table 54 Velocity Model for Surface Wave Array Z3-S19

Approx. Elevation of Top of Layer		Depth to Top of Layer		Layer Thickness		S-Wave Velocity		Inferred P-Wave Velocity	
m	ft	m	ft	m	ft	m/s	ft/s	m/s	ft/s
171	561.0	0	0.0	1.5	4.9	260	853	520	1706
169.5	556.1	1.5	4.9	2.5	8.2	400	1312	799.9	2624
167	547.9	4	13.1	5	16.4	320	1050	640	2100
162	531.5	9	29.5	6	19.7	350	1148	700	2297
156	511.8	15	49.2	4	13.1	350	1148	1750	5741
152	498.7	19	62.3	11	36.1	375	1230	1750	5741
141	462.6	30	98.4	35	114.8	550	1804	2100	6890
106	347.8	65	213.3	>5	>16.4	705	2313	2100	6890

Approximate depth of investigation is 70m.

Table 55 Velocity Model for Surface Wave Array Z3-S20

Approx. Elevation of Top of Layer		Depth to Top of Layer		Layer Thickness		S-Wave Velocity		Inferred P-Wave Velocity	
m	ft	m	ft	m	ft	m/s	ft/s	m/s	ft/s
161	528.2	0	0.0	2	6.6	255	837	510	1673
159	521.7	2	6.6	5	16.4	315	1033	630	2067
154	505.2	7	23.0	3	9.8	315	1033	1750	5741
151	495.4	10	32.8	10	32.8	350	1148	1750	5741
141	462.6	20	65.6	15	49.2	375	1230	1750	5741
126	413.4	35	114.8	30	98.4	550	1804	2100	6890
96	315.0	65	213.3	>5	>16.4	700	2297	2100	6890

Approximate depth of investigation is 70m.

Table 56 Velocity Model for Surface Wave Array Z3-S21

Approx. Elevation of Top of Layer		Depth to Top of Layer		Layer Thickness		S-Wave Velocity		Inferred P-Wave Velocity	
m	ft	m	ft	m	ft	m/s	ft/s	m/s	ft/s
139	456.0	0	0.0	2	6.6	320	1050	640	2100
137	449.5	2	6.6	8	26.2	300	984	600	1969
129	423.2	10	32.8	6	19.7	350	1148	699.9	2296
123	403.5	16	52.5	15	49.2	350	1148	1750	5741
108	354.3	31	101.7	30	98.4	450	1476	1925	6316
78	255.9	61	200.1	>9	>29.5	650	2133	2100	6890

Approximate depth of investigation is 70m.

Table 57 Velocity Model for Surface Wave Array Z3-S22

Approx. Elevation of Top of Layer		Depth to Top of Layer		Layer Thickness		S-Wave Velocity		Inferred P-Wave Velocity	
m	ft	m	ft	m	ft	m/s	ft/s	m/s	ft/s
131	429.8	0	0.0	3	9.8	275	902	550	1804
128	419.9	3	9.8	8	26.2	385	1263	769.9	2526
120	393.7	11	36.1	5	16.4	350	1148	700	2297
115	377.3	16	52.5	12	39.4	350	1148	1750	5741
103	337.9	28	91.9	25	82.0	450	1476	1925	6316
78	255.9	53	173.9	>17	>55.8	700	2297	2100	6890

Approximate depth of investigation is 70m.

Table 58 Velocity Model for Surface Wave Array Z3-S23

Approx. Elevation of Top of Layer		Depth to Top of Layer		Layer Thickness		S-Wave Velocity		Inferred P-Wave Velocity	
m	ft	m	ft	m	ft	m/s	ft/s	m/s	ft/s
127	416.7	0	0.0	1.5	4.9	175	574	350	1148
125.5	411.7	1.5	4.9	2.5	8.2	285	935	570	1870
123	403.5	4	13.1	3	9.8	335	1099	670	2198
120	393.7	7	23.0	5	16.4	375	1230	749.9	2460
115	377.3	12	39.4	24	78.7	375	1230	1750	5741
91	298.6	36	118.1	26	85.3	450	1476	1925	6316
65	213.3	62	203.4	>8	>26.2	665	2182	2100	6890

Approximate depth of investigation is 70m.

Table 59 Velocity Model for Surface Wave Array Z3-S24

Approx. Elevation of Top of Layer		Depth to Top of Layer		Layer Thickness		S-Wave Velocity		Inferred P-Wave Velocity	
m	ft	m	ft	m	ft	m/s	ft/s	m/s	ft/s
131	429.8	0	0.0	1.5	4.9	240	787	480	1575
129.5	424.9	1.5	4.9	2.5	8.2	275	902	550	1804
127	416.7	4	13.1	5	16.4	325	1066	650	2133
122	400.3	9	29.5	3	9.8	450	1476	899.9	2952
119	390.4	12	39.4	13	42.7	450	1476	1925	6316
106	347.8	25	82.0	28	91.9	525	1722	1925	6316
78	255.9	53	173.9	>17	>55.8	700	2297	2100	6890

Approximate depth of investigation is 70m.

Table 60 Summary of Zone 3 Surface Wave Investigation

Surface Wave Array	Vs30 (m/s)	Vs30 (ft/s)	Vs60 (m/s)	Vs60 (ft/s)	Vs @ 60m (m/s)	Vs @ 60m (ft/s)
Z3-S1	405	1329	501	1644	725	2379
Z3-S2	355	1165	423	1388	650	2133
Z3-S3	373	1223	451	1479	800	2625
Z3-S4	374	1227	468	1535	900	2953
Z3-S5	496	1627	662	2172	1200	3937
Z3-S6	414	1358	528	1732	1000	3281
Z3-S7	478	1568	609	1998	975	3199
Z3-S8	370	1214	424	1391	550	1804
Z3-S9	313	1027	361	1184	435	1427
Z3-S10	412	1352	528	1732	740	2428
Z3-S11	316	1037	391	1283	625	2051
Z3-S12	314	1030	377	1237	675	2215
Z3-S13	396	1299	479	1572	725	2379
Z3-S14	393	1289	482	1581	725	2379
Z3-S15	337	1106	412	1352	750	2461
Z3-S16	365	1198	410	1345	500	1640
Z3-S17	351	1152	522	1713	1250	4101
Z3-S18	315	1033	468	1535	1250	4101
Z3-S19	351	1152	428	1404	550	1804
Z3-S20	339	1112	407	1335	700	2297
Z3-S21	333	1093	381	1250	650	2133
Z3-S22	354	1161	411	1348	700	2297
Z3-S23	342	1122	382	1253	450	1476
Z3-S24	396	1298	463	1519	700	2297

Note: Vs30 = average S-wave velocity of upper 30 m. Vs60 = average S-wave velocity of upper 60 m.

Table 64 Velocity Model for Surface Wave Array Z4-S4

Approx. Elevation of Top of Layer		Depth to Top of Layer		Layer Thickness		S-Wave Velocity		Inferred P-Wave Velocity	
m	ft	m	ft	m	ft	m/s	ft/s	m/s	ft/s
174	570.9	0	0.0	3	9.8	265	869	530	1739
171	561.0	3	9.8	3	9.8	275	902	550	1804
168	551.2	6	19.7	9	29.5	285	935	570	1870
159	521.7	15	49.2	25	82.0	440	1444	880	2887
134	439.6	40	131.2	20	65.6	500	1640	1000	3281
114	374.0	60	196.9	5	16.4	600	1969	1200	3937
109	357.6	65	213.3	>5	>16.4	600	1969	1750	5741

Approximate depth of investigation is 70m.

Table 65 Velocity Model for Surface Wave Array Z4-S5

Approx. Elevation of Top of Layer		Depth to Top of Layer		Layer Thickness		S-Wave Velocity		Inferred P-Wave Velocity	
m	ft	m	ft	m	ft	m/s	ft/s	m/s	ft/s
170	557.7	0	0.0	2	6.6	245	804	490	1608
168	551.2	2	6.6	3	9.8	275	902	550	1804
165	541.3	5	16.4	4	13.1	250	820	500	1640
161	528.2	9	29.5	11	36.1	350	1148	700	2297
150	492.1	20	65.6	13	42.7	400	1312	800	2624
137	449.5	33	108.3	17	55.8	500	1640	1000	3281
120	393.7	50	164.0	15	49.2	600	1969	1200	3937
105	344.5	65	213.3	>5	>16.4	600	1969	1750	5741

Approximate depth of investigation is 70m.

Table 66 Velocity Model for Surface Wave Array Z4-S6

Approx. Elevation of Top of Layer		Depth to Top of Layer		Layer Thickness		S-Wave Velocity		Inferred P-Wave Velocity	
m	ft	m	ft	m	ft	m/s	ft/s	m/s	ft/s
168	551.2	0	0.0	2	6.6	265	869	530	1739
166	544.6	2	6.6	3	9.8	255	837	510	1673
163	534.8	5	16.4	4	13.1	300	984	600	1969
159	521.7	9	29.5	11	36.1	350	1148	700	2297
148	485.6	20	65.6	13	42.7	400	1312	800	2624
135	442.9	33	108.3	20	65.6	500	1640	1000	3281
115	377.3	53	173.9	12	39.4	550	1804	1100	3609
103	337.9	65	213.3	>5	>16.4	550	1804	1750	5741

Approximate depth of investigation is 70m.

Table 67 Velocity Model for Surface Wave Array Z4-S7

Approx. Elevation of Top of Layer		Depth to Top of Layer		Layer Thickness		S-Wave Velocity		Inferred P-Wave Velocity	
m	ft	m	ft	m	ft	m/s	ft/s	m/s	ft/s
168	551.2	0	0.0	1.5	4.9	235	771	470	1542
166.5	546.3	1.5	4.9	2.5	8.2	265	869	530	1739
164	538.1	4	13.1	5	16.4	300	984	600	1969
159	521.7	9	29.5	11	36.1	350	1148	700	2297
148	485.6	20	65.6	15	49.2	400	1312	800	2624
133	436.4	35	114.8	20	65.6	500	1640	1000	3281
113	370.7	55	180.4	10	32.8	550	1804	1100	3609
103	337.9	65	213.3	>5	>16.4	550	1804	1750	5741

Approximate depth of investigation is 70m.

Table 68 Velocity Model for Surface Wave Array Z4-S8

Approx. Elevation of Top of Layer		Depth to Top of Layer		Layer Thickness		S-Wave Velocity		Inferred P-Wave Velocity	
m	ft	m	ft	m	ft	m/s	ft/s	m/s	ft/s
164	538.1	0	0.0	1.5	4.9	190	623	380	1247
162.5	533.1	1.5	4.9	2.5	8.2	250	820	500	1640
160	524.9	4	13.1	6	19.7	300	984	600	1969
154	505.2	10	32.8	6	19.7	350	1148	700	2297
148	485.6	16	52.5	15	49.2	400	1312	800	2624
133	436.4	31	101.7	14	45.9	500	1640	1000	3281
119	390.4	45	147.6	10	32.8	600	1969	1200	3937
109	357.6	55	180.4	>15	>49.2	600	1969	1750	5741

Approximate depth of investigation is 70m.

Table 69 Velocity Model for Surface Wave Array Z4-S9

Approx. Elevation of Top of Layer		Depth to Top of Layer		Layer Thickness		S-Wave Velocity		Inferred P-Wave Velocity	
m	ft	m	ft	m	ft	m/s	ft/s	m/s	ft/s
160	524.9	0	0.0	1	3.3	210	689	420	1378
159	521.7	1	3.3	2	6.6	290	951	580	1903
157	515.1	3	9.8	4.5	14.8	275	902	550	1804
152.5	500.3	7.5	24.6	6.5	21.3	350	1148	700	2297
146	479.0	14	45.9	12	39.4	400	1312	800	2624
134	439.6	26	85.3	24	78.7	500	1640	1000	3281
110	360.9	50	164.0	>20	>65.6	500	1640	1700	5577

Approximate depth of investigation is 70m.

Table 70 Velocity Model for Surface Wave Array Z4-S10

Approx. Elevation of Top of Layer		Depth to Top of Layer		Layer Thickness		S-Wave Velocity		Inferred P-Wave Velocity	
m	ft	m	ft	m	ft	m/s	ft/s	m/s	ft/s
150.0	492.1	0	0.0	1.5	4.9	245	804	490	1608
148.5	487.2	1.5	4.9	4.5	14.8	315	1033	630	2067
144.0	472.4	6	19.7	5	16.4	350	1148	700	2297
139.0	456.0	11	36.1	17	55.8	410	1345	820	2690
122.0	400.3	28	91.9	7	23.0	475	1558	950	3116
115.0	377.3	35	114.8	30	98.4	475	1558	1700	5577
85.0	278.9	65	213.3	>5	>16.4	525	1722	1700	5577

Approximate depth of investigation is 70m.

Table 71 Velocity Summary of Zone 4 Surface Wave Investigation

Surface Wave Array	Vs30 (m/s)	Vs30 (ft/s)	Vs60 (m/s)	Vs60 (ft/s)	Vs @ 60m (m/s)	Vs @ 60m (ft/s)
Z4-S1	362	1188	484	1589	850	2789
Z4-S2	369	1210	443	1454	600	1969
Z4-S3	288	944	349	1144	500	1640
Z4-S4	341	1120	398	1307	600	1969
Z4-S5	328	1076	401	1315	600	1969
Z4-S6	337	1105	402	1318	550	1804
Z4-S7	337	1107	399	1308	550	1804
Z4-S8	333	1093	412	1353	600	1969
Z4-S9	355	1164	415	1361	500	1640
Z4-S10	373	1225	418	1372	475	1558

Note: Vs30 = average S-wave velocity of upper 30 m. Vs60 = average S-wave velocity of upper 60 m.

Table 78 Velocity Model for Surface Wave Array Z5-S8

Approx. Elevation of Top of Layer		Depth to Top of Layer		Layer Thickness		S-Wave Velocity		Inferred P-Wave Velocity	
m	ft	m	ft	m	ft	m/s	ft/s	m/s	ft/s
114	374.0	0	0.0	2.5	8.2	305	1001	610	2001
111.5	365.8	2.5	8.2	3.5	11.5	335	1099	670	2198
108	354.3	6	19.7	6	19.7	275	902	550	1804
102	334.6	12	39.4	10	32.8	400	1312	800	2624
92	301.8	22	72.2	20	65.6	475	1558	950	3116
72	236.2	42	137.8	14	45.9	550	1804	1100	3609
58	190.3	56	183.7	>14	>45.9	550	1804	1700	5577

Approximate depth of investigation is 70m.

Table 79 Velocity Model for Surface Wave Array Z5-S9

Approx. Elevation of Top of Layer		Depth to Top of Layer		Layer Thickness		S-Wave Velocity		Inferred P-Wave Velocity	
m	ft	m	ft	m	ft	m/s	ft/s	m/s	ft/s
122	400.3	0	0.0	2	6.6	210	689	420	1378
120	393.7	2	6.6	6	19.7	315	1033	630	2067
114	374.0	8	26.2	10	32.8	320	1050	640	2100
104	341.2	18	59.1	35	114.8	475	1558	950	3116
69	226.4	53	173.9	3	9.8	500	1640	1000	3281
66	216.5	56	183.7	>14	>45.9	500	1640	1700	5577

Approximate depth of investigation is 70m.

Table 80 Velocity Model for Surface Wave Array Z5-S10

Approx. Elevation of Top of Layer		Depth to Top of Layer		Layer Thickness		S-Wave Velocity		Inferred P-Wave Velocity	
m	ft	m	ft	m	ft	m/s	ft/s	m/s	ft/s
134	439.6	0	0.0	2	6.6	300	984	600	1969
132	433.1	2	6.6	9	29.5	275	902	550	1804
123	403.5	11	36.1	14	45.9	375	1230	750	2460
109	357.6	25	82.0	8	26.2	525	1722	1050	3445
101	331.4	33	108.3	7	23.0	550	1804	1100	3609
94	308.4	40	131.2	27	88.6	550	1804	1700	5577
67	219.8	67	219.8	>3	>9.8	665	2182	1750	5741

Approximate depth of investigation is 70m.

Table 81 Velocity Model for Surface Wave Array Z5-S11

Approx. Elevation of Top of Layer		Depth to Top of Layer		Layer Thickness		S-Wave Velocity		Inferred P-Wave Velocity	
m	ft	m	ft	m	ft	m/s	ft/s	m/s	ft/s
139	456.0	0	0.0	1.5	4.9	190	623	380	1247
137.5	451.1	1.5	4.9	3.5	11.5	285	935	570	1870
134	439.6	5	16.4	7	23.0	350	1148	700	2297
127	416.7	12	39.4	8	26.2	400	1312	800	2625
119	390.4	20	65.6	5	16.4	465	1526	930	3051
114	374.0	25	82.0	30	98.4	465	1526	1700	5577
84	275.6	55	180.4	>15	>49.2	525	1722	1725	5659

Approximate depth of investigation is 70m.

Table 82 Velocity Model for Surface Wave Array Z5-S12

Approx. Elevation of Top of Layer		Depth to Top of Layer		Layer Thickness		S-Wave Velocity		Inferred P-Wave Velocity	
m	ft	m	ft	m	ft	m/s	ft/s	m/s	ft/s
133	436.4	0	0.0	2.5	8.2	275	902	550	1804
130.5	428.1	2.5	8.2	2	6.6	255	837	510	1673
128.5	421.6	4.5	14.8	4.5	14.8	350	1148	700	2297
124	406.8	9	29.5	7	23.0	450	1476	900	2953
117	383.9	16	52.5	20	65.6	450	1476	1600	5249
97	318.2	36	118.1	>34	>111.5	500	1640	1700	5577

Approximate depth of investigation is 70m.

Table 83 Velocity Model for Surface Wave Array Z5-S13

Approx. Elevation of Top of Layer		Depth to Top of Layer		Layer Thickness		S-Wave Velocity		Inferred P-Wave Velocity	
m	ft	m	ft	m	ft	m/s	ft/s	m/s	ft/s
129	423.2	0	0.0	2.5	8.2	205	673	410	1345
126.5	415.0	2.5	8.2	2.5	8.2	300	984	600	1969
124	406.8	5	16.4	7	23.0	350	1148	700	2297
117	383.9	12	39.4	4	13.1	400	1312	800	2624
113	370.7	16	52.5	14	45.9	400	1312	1600	5249
99	324.8	30	98.4	29	95.1	450	1476	1700	5577
70	229.7	59	193.6	>11	>36.1	550	1804	1725	5659

Approximate depth of investigation is 70m.

Table 84 Summary of Zone 5 Surface Wave Investigation

Surface Wave Array	Vs30 (m/s)	Vs30 (ft/s)	Vs60 (m/s)	Vs60 (ft/s)	Vs @ 60m (m/s)	Vs @ 60m (ft/s)
Z5-S1	325	1065	386	1265	475	1558
Z5-S2	320	1050	367	1205	500	1640
Z5-S3	320	1049	381	1251	500	1640
Z5-S4	303	994	362	1187	500	1640
Z5-S6	329	1080	396	1299	625	2051
Z5-S7	366	1202	426	1396	525	1722
Z5-S8	364	1196	428	1403	550	1804
Z5-S9	353	1157	407	1335	500	1640
Z5-S10	348	1141	425	1396	550	1804
Z5-S11	367	1205	414	1358	525	1722
Z5-S12	392	1287	435	1429	500	1640
Z5-S13	351	1151	395	1297	550	1804

Note: Vs30 = average S-wave velocity of upper 30 m. Vs60 = average S-wave velocity of upper 60 m.

FIGURES

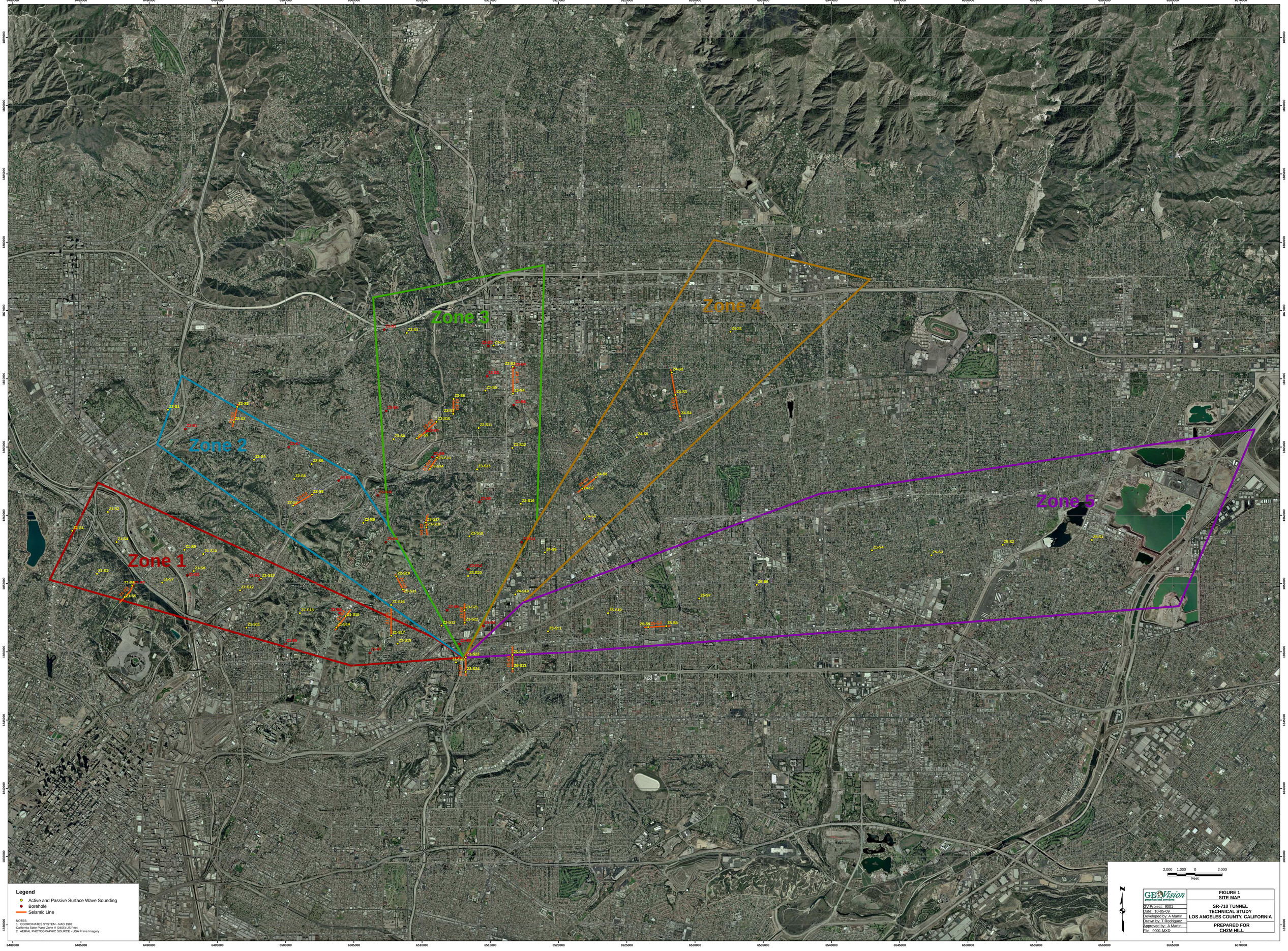
Zone 1
Zone 2
Zone 3
Zone 4
Zone 5
Legend
Active and Passive Surface Wave Sounding
Borehole
Seismic Line
NOTES:
1. COORDINATES SYSTEM - NAD 1983
California State Plane Zone V (0405) US Feet
2. AERIAL PHOTOGRAPHIC SOURCE - USA Prime Imagery
2,000 1,000 0 2,000
Feet
N
GEOVision geophysical services
FIGURE 1
SITE MAP
GV Project: 9001
Date: 10-05-09
Developed by: A Martin
Drawn by: T Rodriguez
Approved by: A Martin
File: 9001.MXD
SR-710 TUNNEL
TECHNICAL STUDY
LOS ANGELES COUNTY, CALIFORNIA
PREPARED FOR
CH2M HILL

TYPICAL PASSIVE SURFACE WAVE SETUP

SEISMIC RECORDER SYSTEM

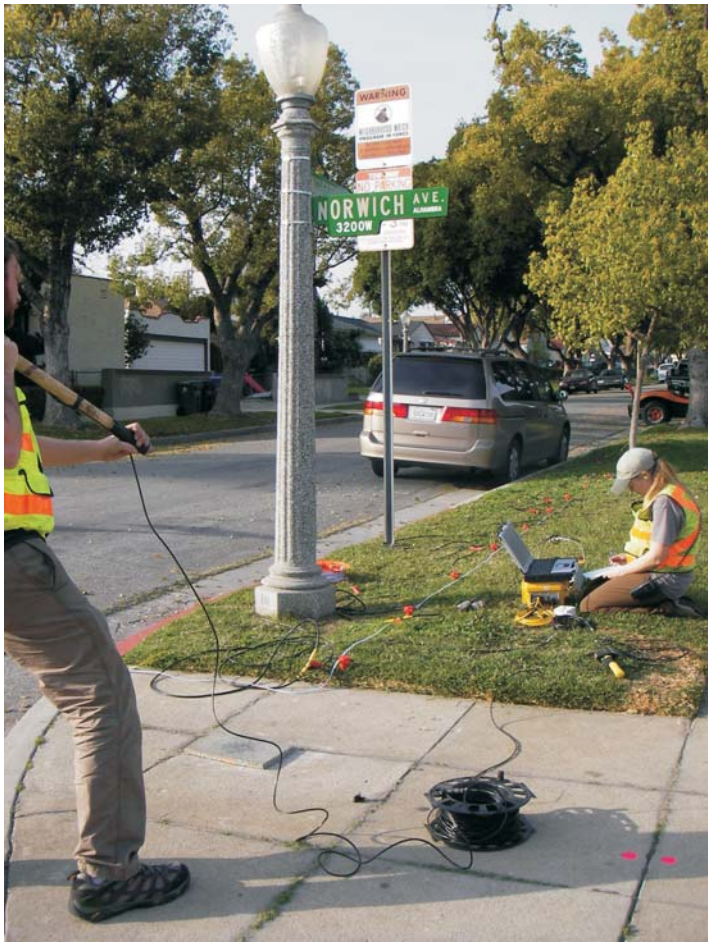

TYPICAL MASW SETUP

GEOVision geophysical services	FIGURE 2 PHOTOGRAPHS OF PASSIVE AND ACTIVE SURFACE ARRAY FIELD LAYOUT
Project # 9001	SR-710 TUNNEL TECHNICAL STUDY LOS ANGELES COUNTY, CALIFORNIA
Date: JUL 17, 2009	
Drawn By: A MARTIN	
Approved By: Antony J Martin	PREPARED FOR CH2M HILL
File R:\...Project Files\2009\9001ch2mhill\report\figures\Figure2.cdr	

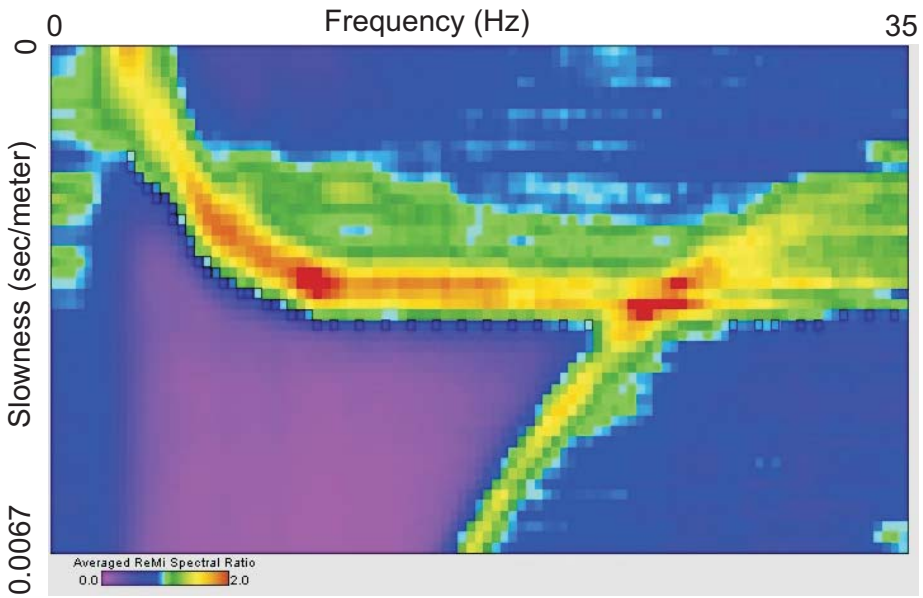

Wavefield Transform of Linear Array Passive Surface Wave Data using Optim SeisOpt ReMi Data Analysis Package (Z2-S2)

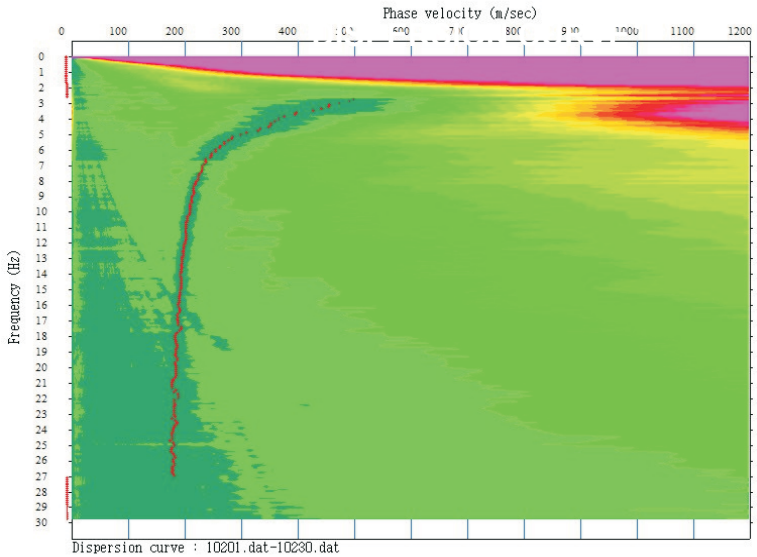

Wavefield Transform of "L" array Passive Surface Wave Data using Spatial Autocorrelation Method (Z1-S16)

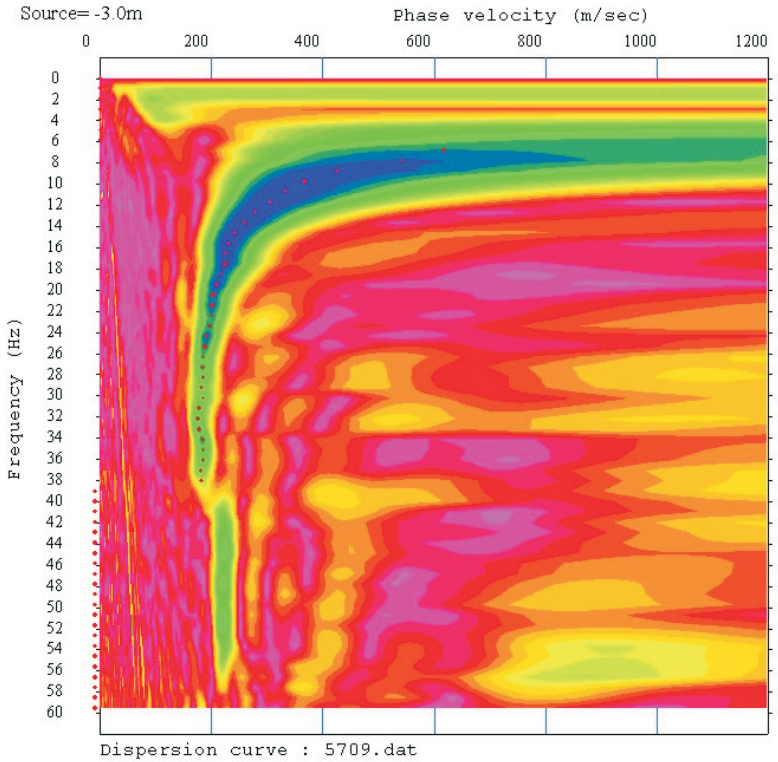

Wavefield Transform of MASW Data (Z2-S6)

GEOVision geophysical services	FIGURE 3 TYPICAL WAVEFIELD TRANSFORMS OF ACTIVE AND PASSIVE SURFACE WAVE DATA
Project # 9001	SR-710 TUNNEL TECHNICAL STUDY LOS ANGELES COUNTY, CALIFORNIA
Date: JUL 20, 2009	
Drawn By: A MARTIN	
Approved By:	PREPARED FOR CH2M HILL
File R:\...Project Files\2009\9001ch2mhill\report\figures\Figure 3.cdr	

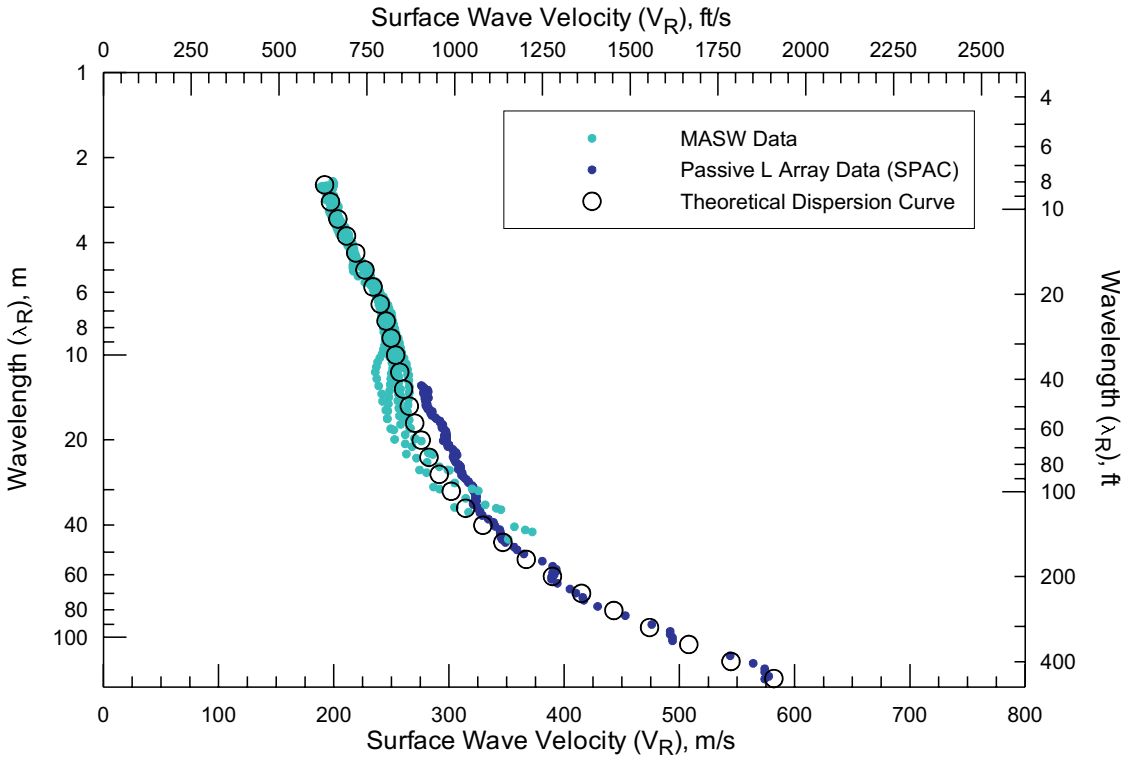

Comparison of Field Experimental Data and Theoretical Dispersion Curve from Active and Passive Surface Wave Array Z1-S20

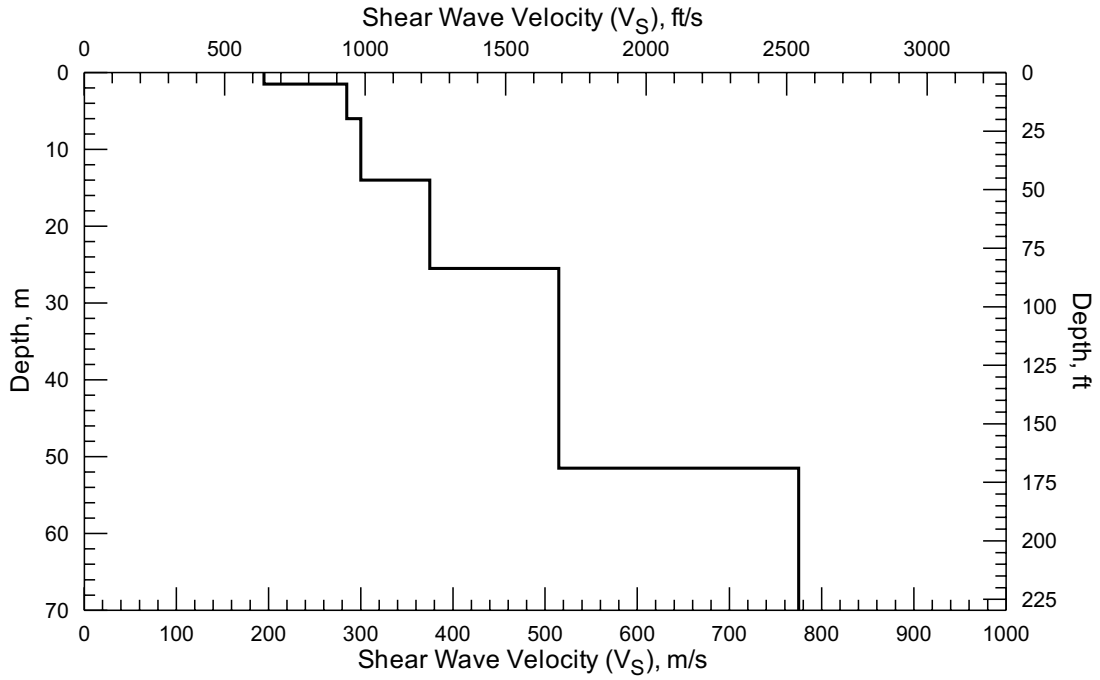

V_S Model from Active and Passive Surface Wave Array Z1-S20

GEOVision geophysical services	FIGURE 22 VELOCITY MODEL FOR ACTIVE AND PASSIVE SURFACE WAVE ARRAY Z1-S20
Project # 9001	NEAR WEST VALLEY BLVD AND HIGHBURY AVE, LOS ANGELES, CALIFORNIA
Date: JUL 17, 2008	
Drawn By: A MARTIN	PREPARED FOR CH2M HILL
Approved By: Antony J Martin	
File R:\...Project Files\2009\9001ch2mhill\report\figures\Figure22.cdr	

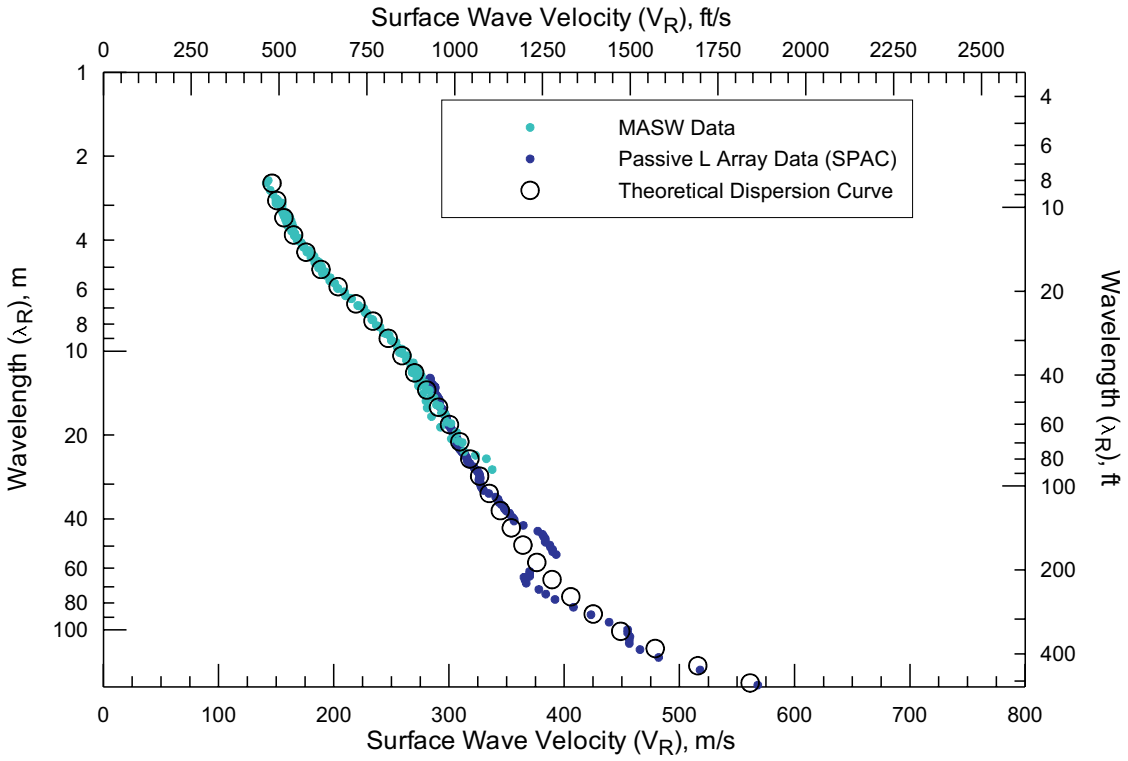

Comparison of Field Experimental Data and Theoretical Dispersion Curve from Active and Passive Surface Wave Array Z3-S2

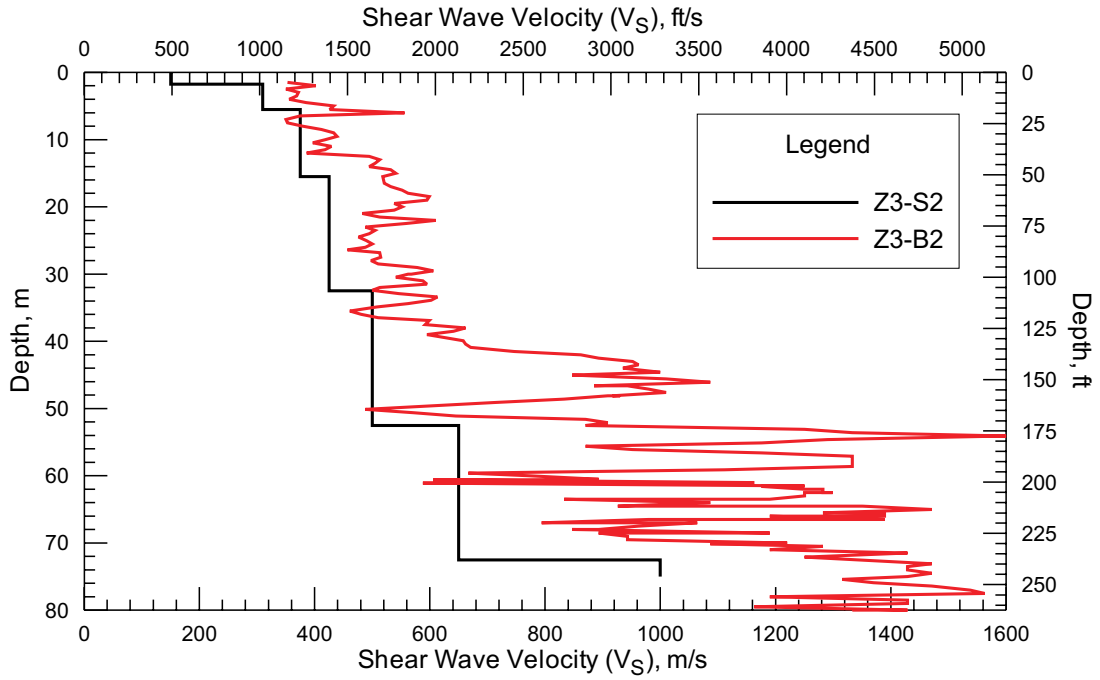

V_S Model from Active and Passive Surface Wave Array Z3-S2

GEOVision geophysical services	FIGURE 36 VELOCITY MODEL FOR ACTIVE AND PASSIVE SURFACE WAVE ARRAY Z3-S2
Project # 9001 Date: JUL 24, 2009 Drawn By: A MARTIN Approved By: Antony J Martin File R:\...Project Files\2009\9001ch2mhill\report\figures\Figure36.cdr	PASADENA AVE AND PALMETTO DR, PASADENA, CALIFORNIA
	PREPARED FOR CH2M HILL

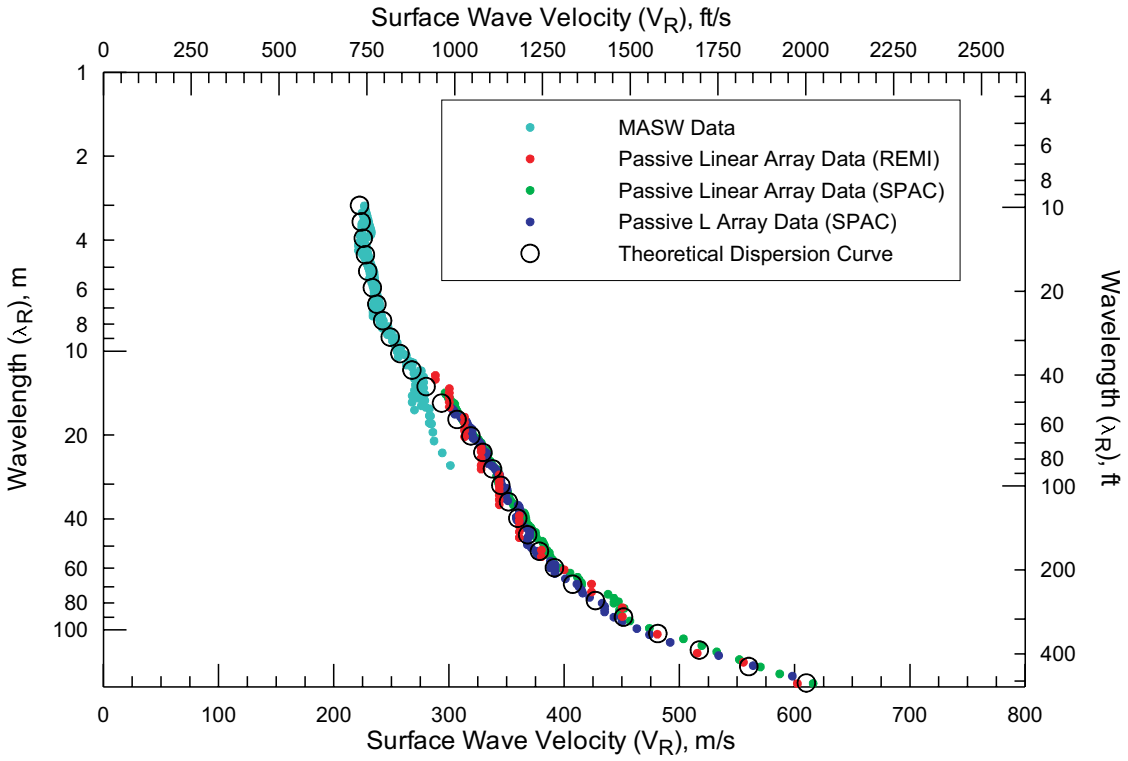

Comparison of Field Experimental Data and Theoretical Dispersion Curve from Active and Passive Surface Wave Array Z3-S3

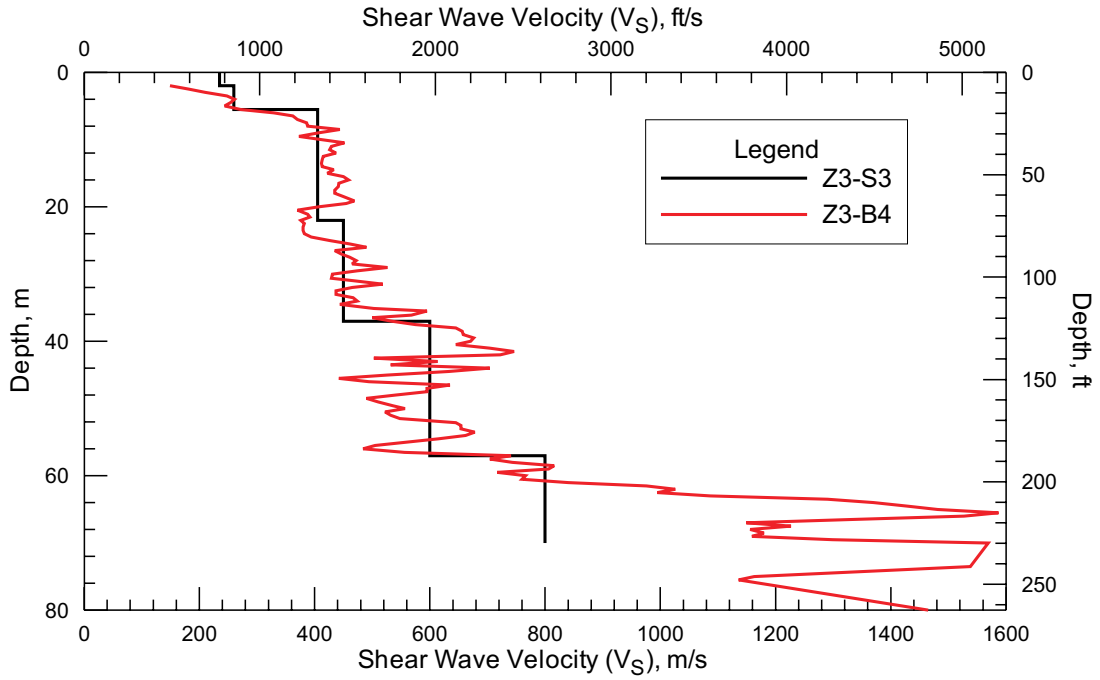

V_S Model from Active and Passive Surface Wave Array Z3-S3

GEOVision geophysical services	FIGURE 37 VELOCITY MODEL FOR ACTIVE AND PASSIVE SURFACE WAVE ARRAY Z3-S3
Project # 9001 Date: JUL 24, 2009 Drawn By: A MARTIN Approved By: Antony J. Martin File R:\...Project Files\2009\9001ch2mhill\report\figures\Figure37.cdr	RAYMOND AVE AND FILLMORE ST, PASADENA, CALIFORNIA
	PREPARED FOR CH2M HILL

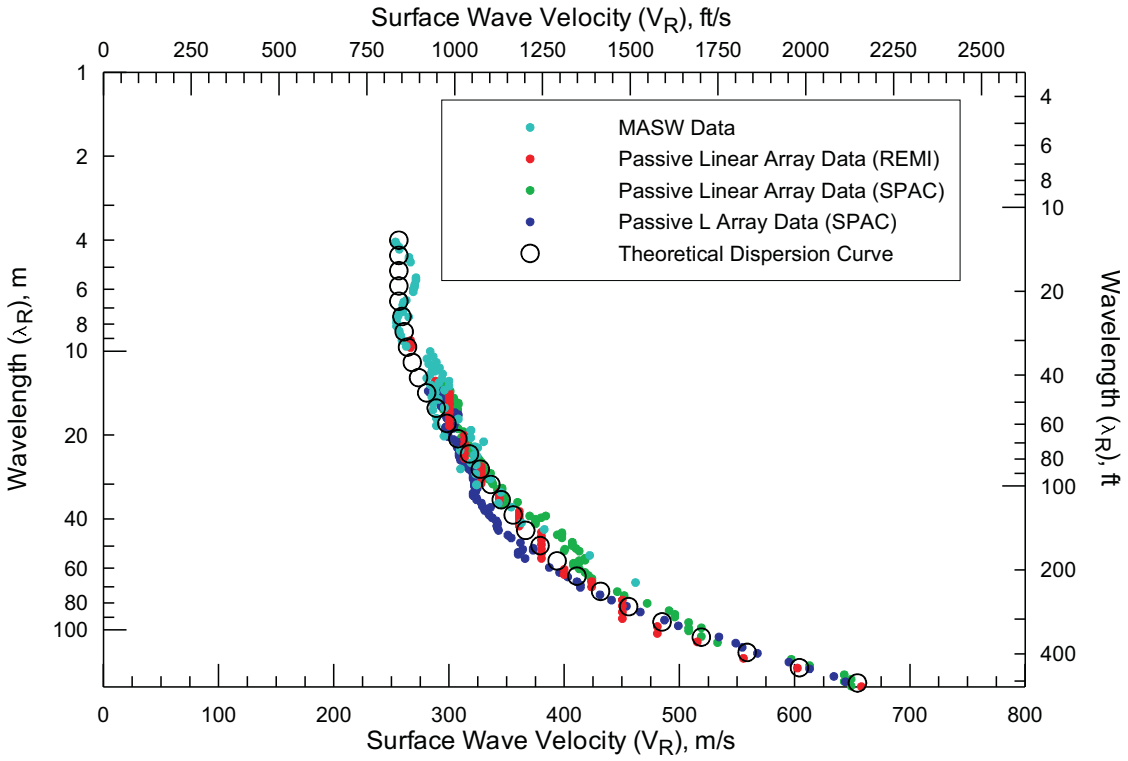

Comparison of Field Experimental Data and Theoretical Dispersion Curve from Active and Passive Surface Wave Array Z3-S4

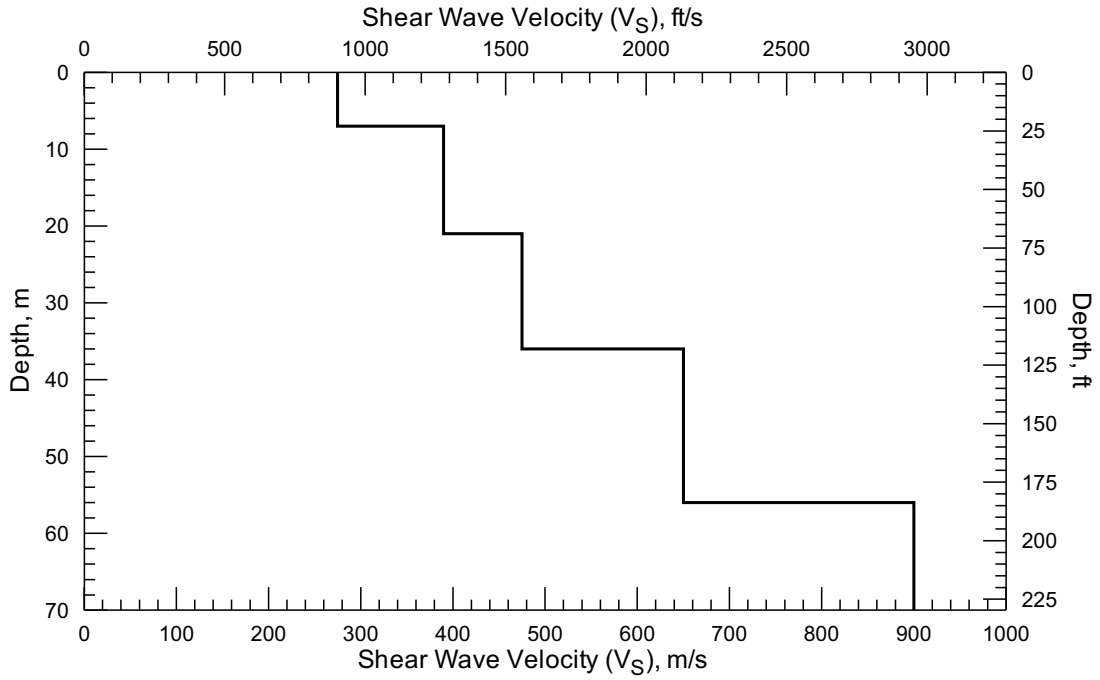

V_S Model from Active and Passive Surface Wave Array Z3-S4

GEOVision geophysical services	FIGURE 38 VELOCITY MODEL FOR ACTIVE AND PASSIVE SURFACE WAVE ARRAY Z3-S4
Project # 9001 Date: JUL 24, 2009 Drawn By: A MARTIN Approved By: Antony J Martin File R:\...Project Files\2009\9001ch2mhill\report\figures\Figure38.cdr	RAYMOND AVE AND GLENARM ST, PASADENA, CALIFORNIA
	PREPARED FOR CH2M HILL

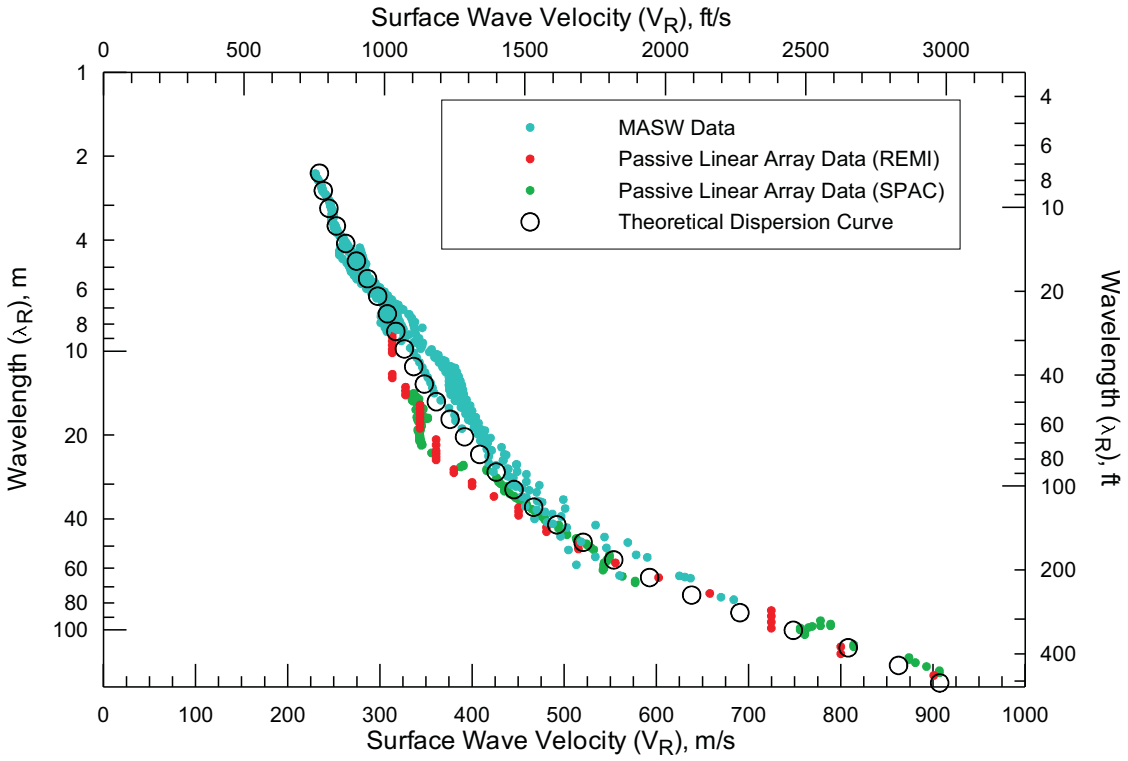

Comparison of Field Experimental Data and Theoretical Dispersion Curve from Active and Passive Surface Wave Array Z3-S5

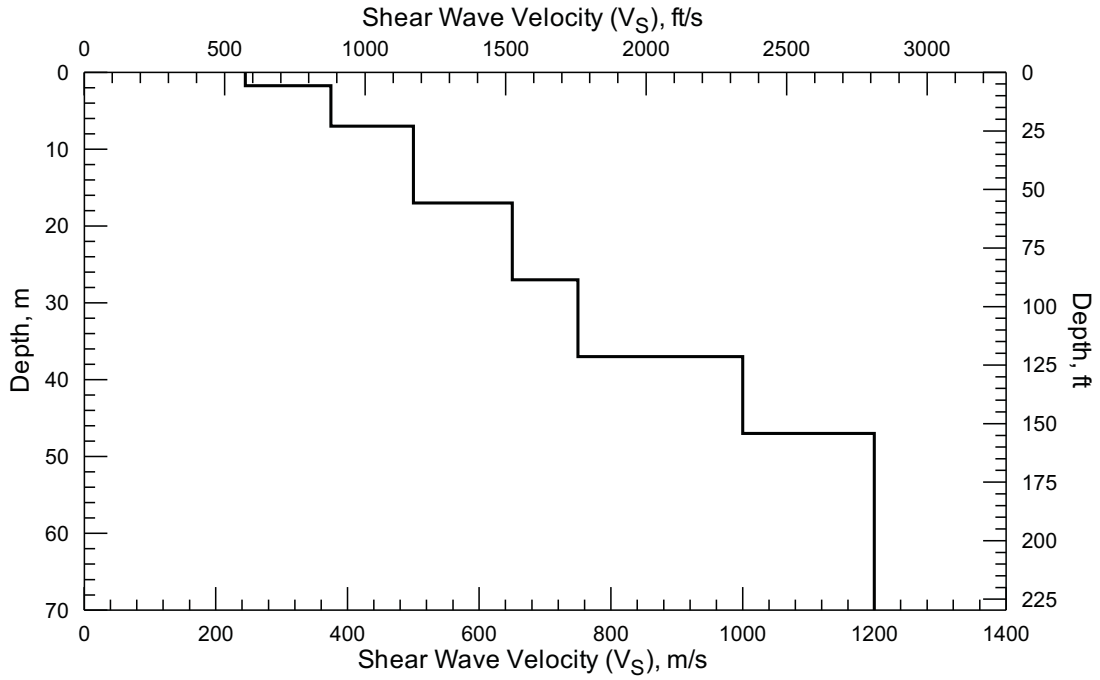

V_S Model from Active and Passive Surface Wave Array Z3-S5

GEOVision geophysical services	FIGURE 39 VELOCITY MODEL FOR ACTIVE AND PASSIVE SURFACE WAVE ARRAY Z3-S5
Project # 9001 Date: JUL 24, 2009 Drawn By: A MARTIN Approved By: Antony J Martin File R:\...Project Files\2009\9001ch2mhill\report\figures\Figure39.cdr	PASADENA AVE AND ARLINGTON DR, PASADENA, CALIFORNIA
	PREPARED FOR CH2M HILL

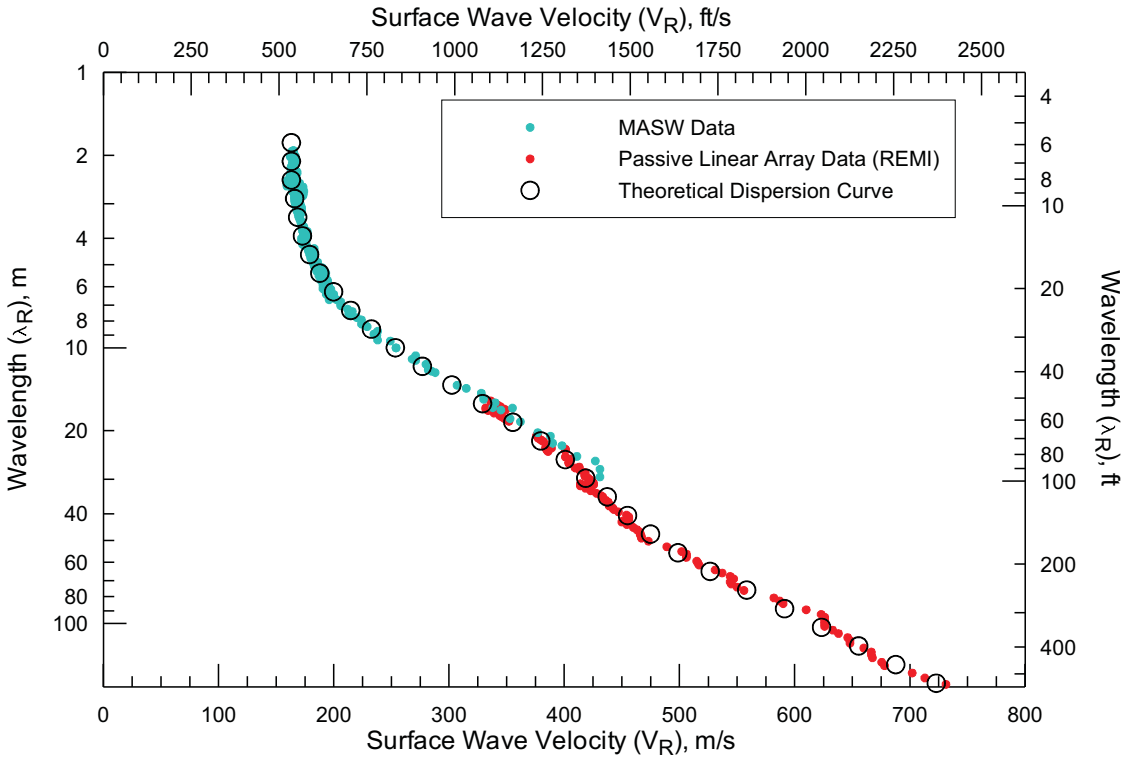

Comparison of Field Experimental Data and Theoretical Dispersion Curve from Active and Passive Surface Wave Array Z3-S11

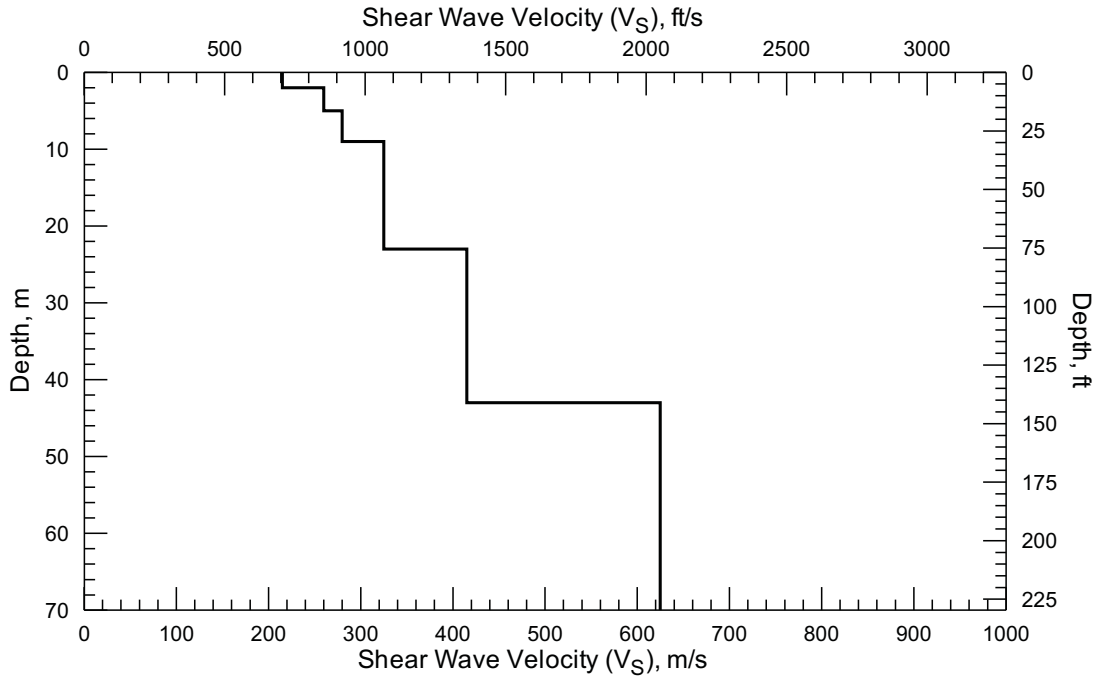

V_S Model from Active and Passive Surface Wave Array Z3-S11

GEOVision geophysical services	FIGURE 45 VELOCITY MODEL FOR ACTIVE AND PASSIVE SURFACE WAVE ARRAY Z3-S11
Project # 9001 Date: JUL 24, 2009 Drawn By: A MARTIN Approved By: Antony J Martin File R:\...Project Files\2009\9001ch2mhill\report\figures\Figure45.cdr	MERIDIAN AVE AND BUENA VISTA ST, SOUTH PASADENA, CALIFORNIA
	PREPARED FOR CH2M HILL

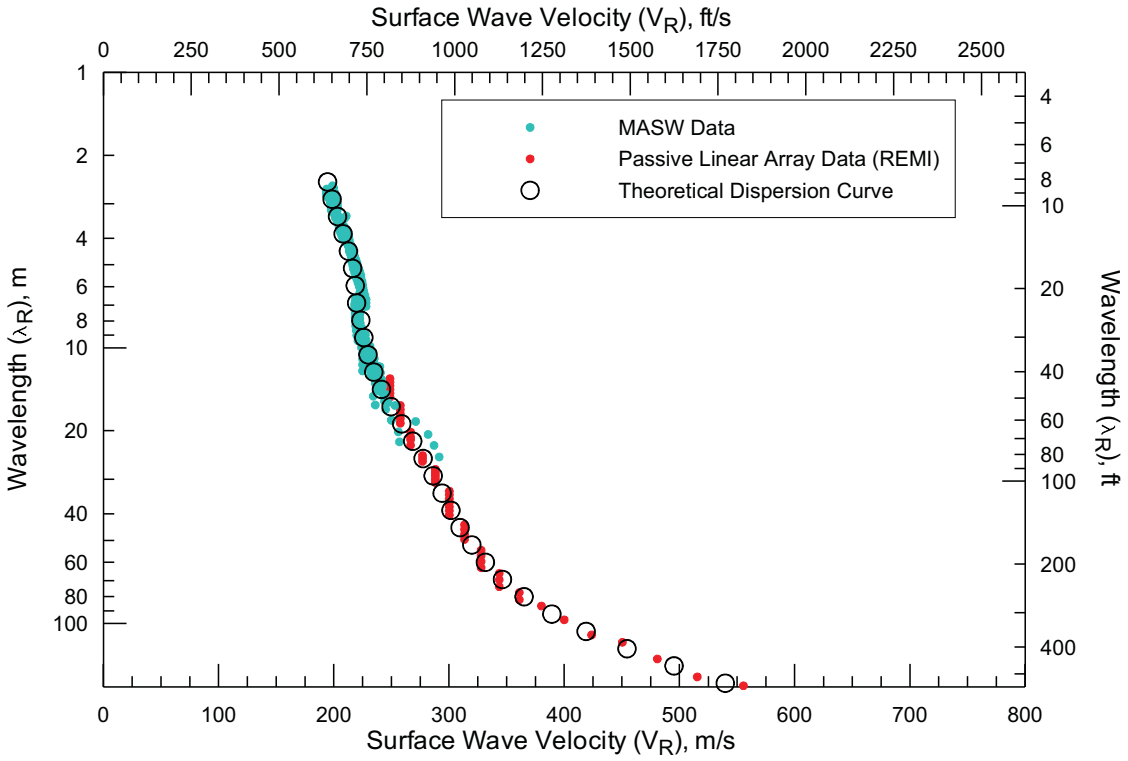

Comparison of Field Experimental Data and Theoretical Dispersion Curve from Active and Passive Surface Wave Array Z3-S12

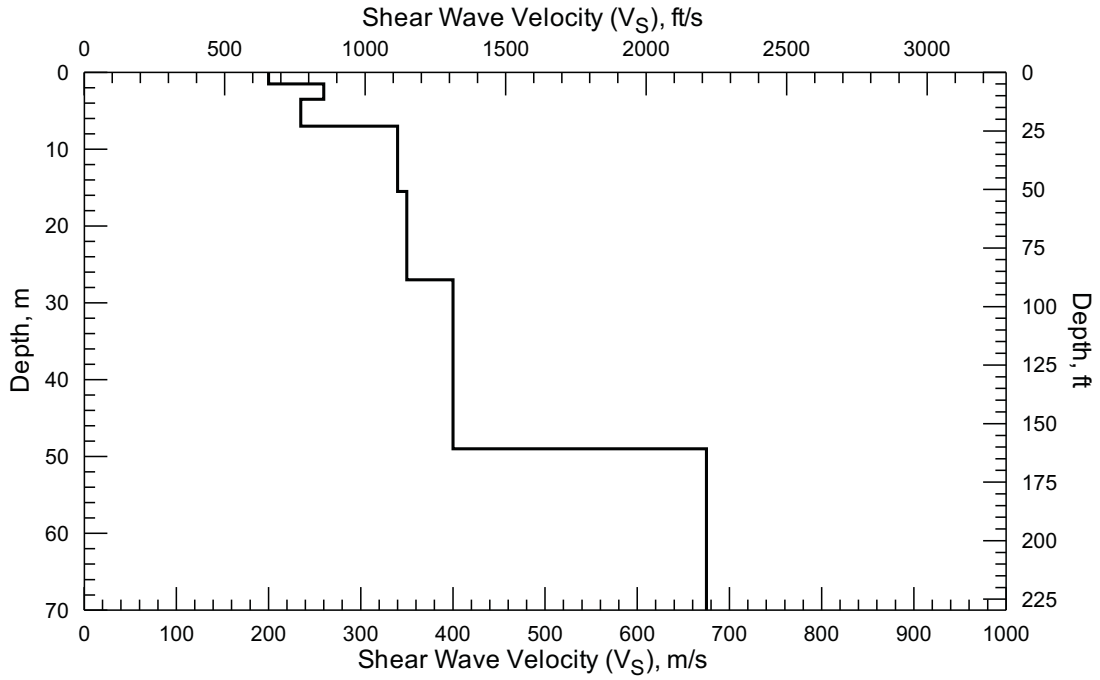

V_S Model from Active and Passive Surface Wave Array Z3-S12

GEOVision geophysical services	FIGURE 46 VELOCITY MODEL FOR ACTIVE AND PASSIVE SURFACE WAVE ARRAY Z3-S12
Project # 9001 Date: JUL 24, 2009 Drawn By: A MARTIN Approved By: Antony J Martin File R:\...Project Files\2009\9001ch2mhill\report\figures\Figure46.cdr	BRENT AVE AND HOPE ST, SOUTH PASADENA, CALIFORNIA
	PREPARED FOR CH2M HILL

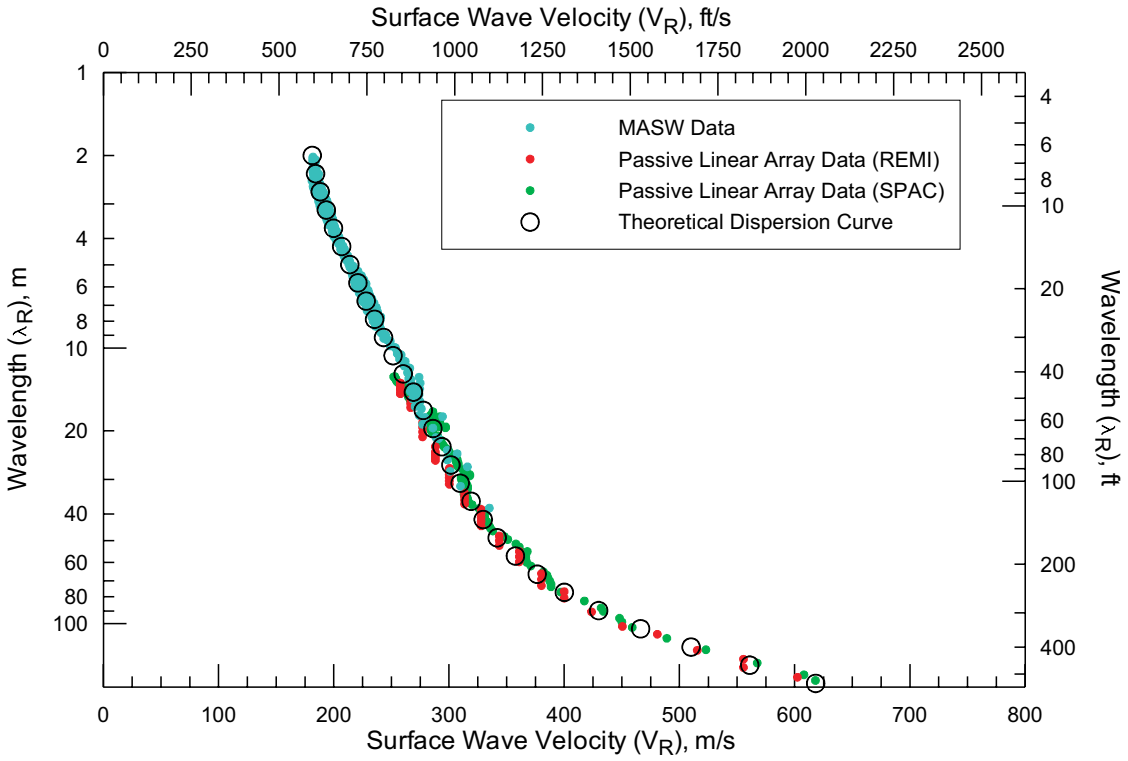

Comparison of Field Experimental Data and Theoretical Dispersion Curve from Active and Passive Surface Wave Array Z3-S15

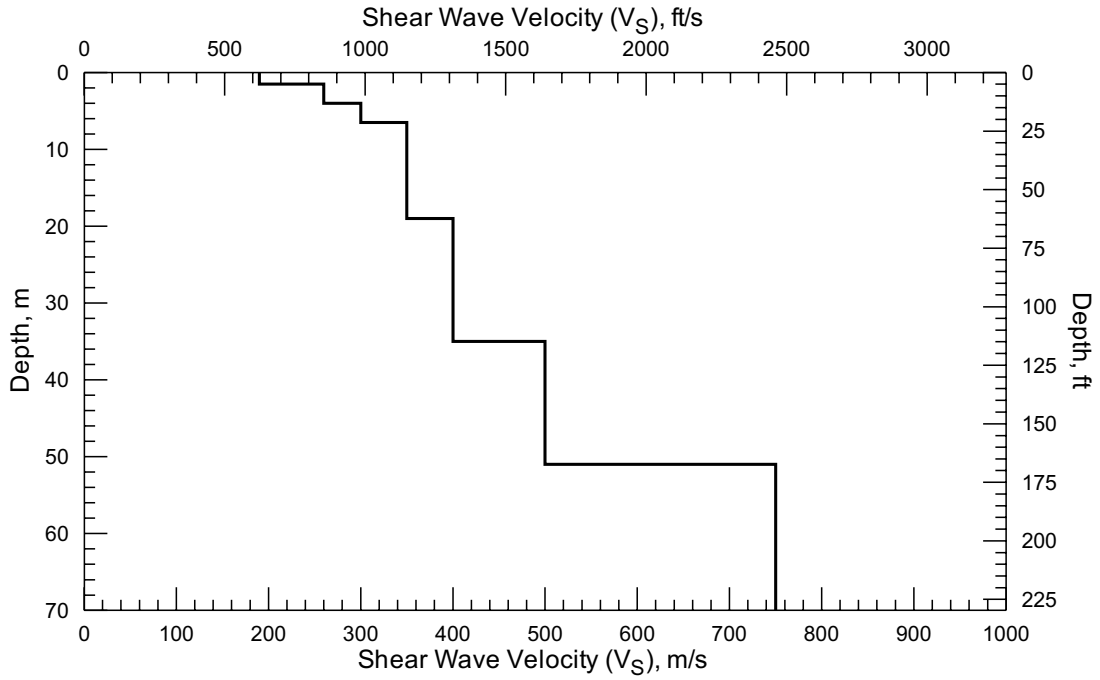

V_S Model from Active and Passive Surface Wave Array Z3-S15

GEOVision geophysical services	FIGURE 49 VELOCITY MODEL FOR ACTIVE AND PASSIVE SURFACE WAVE ARRAY Z3-S15
Project # 9001 Date: JUL 27, 2009 Drawn By: A MARTIN Approved By: Antony J Martin File R:\...Project Files\2009\9001ch2mhill\report\figures\Figure49.cdr	MONTEREY RD AND MERIDIAN AVE, SOUTH PASADENA, CALIFORNIA
	PREPARED FOR CH2M HILL

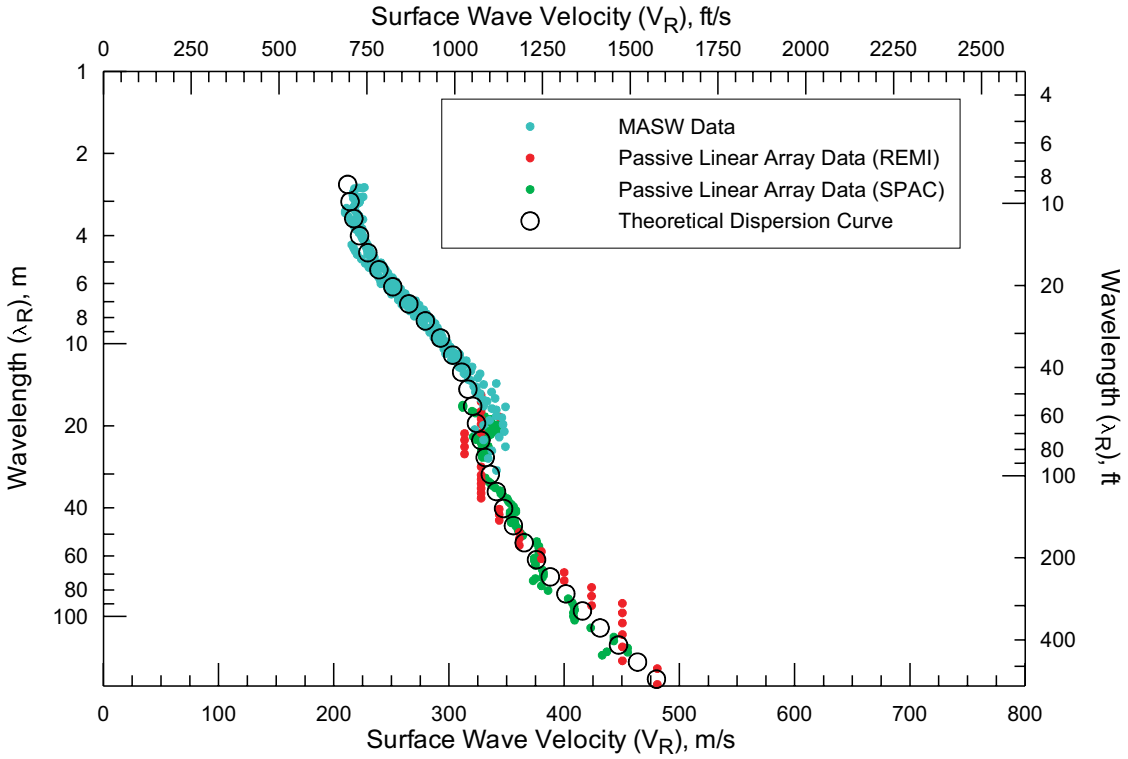

Comparison of Field Experimental Data and Theoretical Dispersion Curve from Active and Passive Surface Wave Array Z3-S16

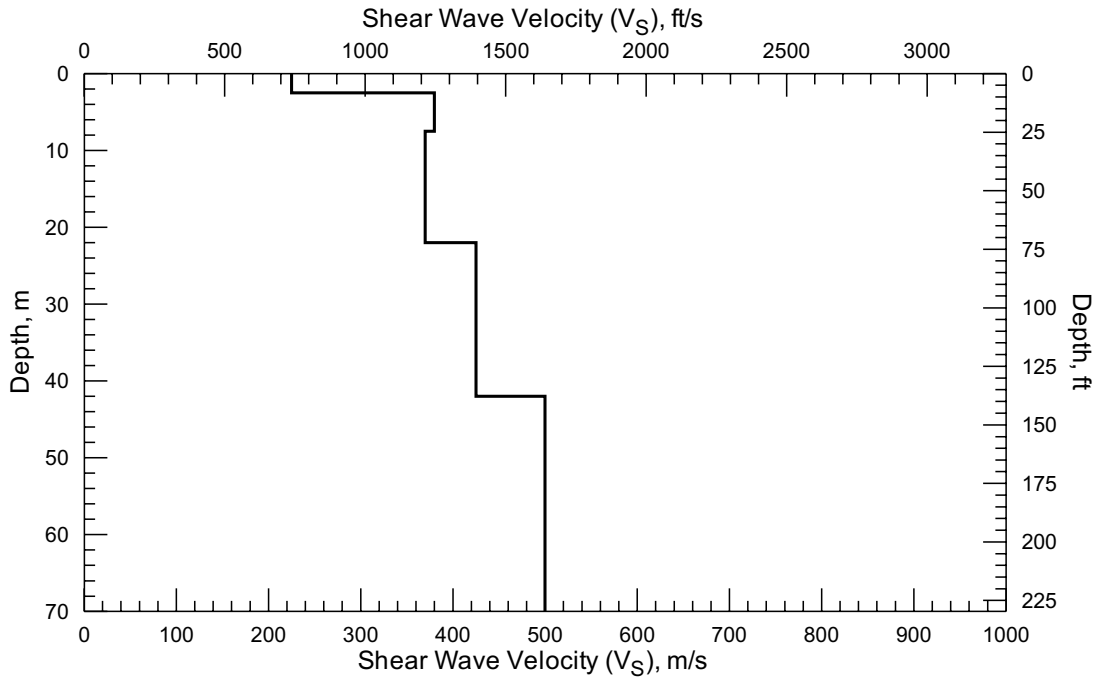

V_S Model from Active and Passive Surface Wave Array Z3-S16

GEOVision geophysical services	FIGURE 50 VELOCITY MODEL FOR ACTIVE AND PASSIVE SURFACE WAVE ARRAY Z3-S16
Project # 9001 Date: JUL 27, 2009 Drawn By: A MARTIN Approved By: Antony J Martin File R:\...Project Files\2009\9001ch2mhill\report\figures\Figure50.cdr	MARENGO AVE AND SPRUCE ST, SOUTH PASADENA, CALIFORNIA
	PREPARED FOR CH2M HILL

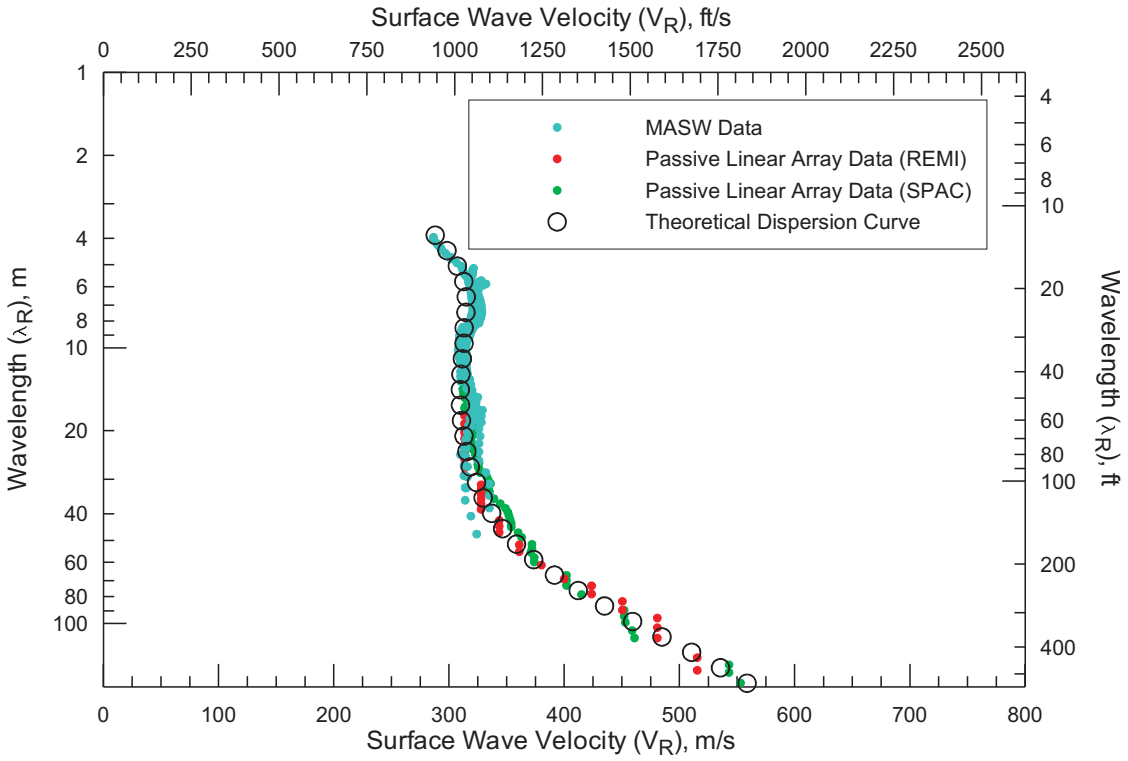

Comparison of Field Experimental Data and Theoretical Dispersion Curve from Active and Passive Surface Wave Array Z3-S19

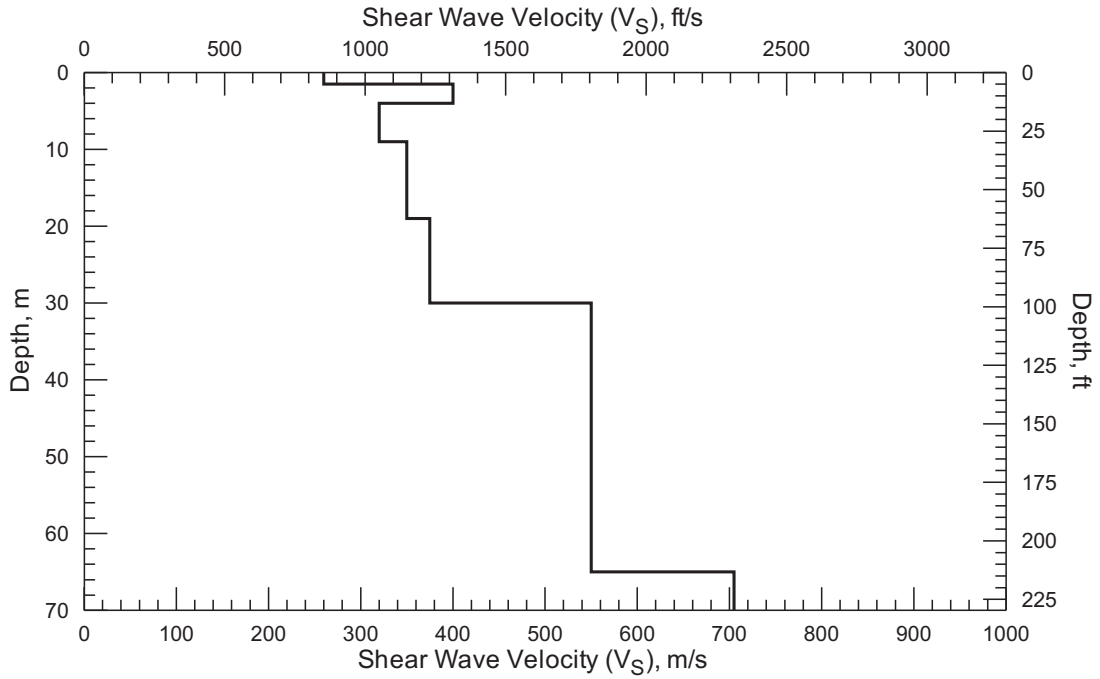

V_S Model from Active and Passive Surface Wave Array Z3-S19

GEOVision geophysical services	FIGURE 53 VELOCITY MODEL FOR ACTIVE AND PASSIVE SURFACE WAVE ARRAY Z3-S19
Project # 9001 Date: JUL 27, 2009 Drawn By: A MARTIN Approved By: Antony J Martin File R:\...Project Files\2009\9001ch2mhill\report\figures\Figure53.cdr	BERKSHIRE AVE AND KENDALL AVE, LOS ANGELES, CALIFORNIA PREPARED FOR CH2M HILL

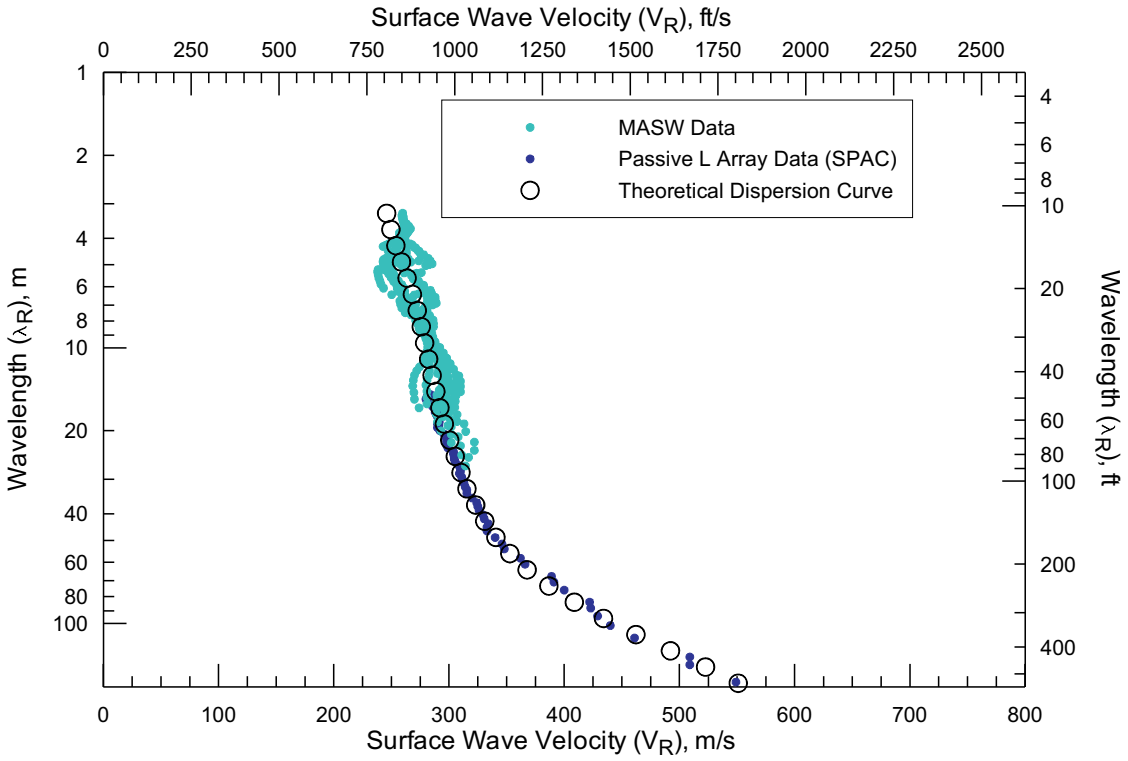

Comparison of Field Experimental Data and Theoretical Dispersion Curve from Active and Passive Surface Wave Array Z3-S20

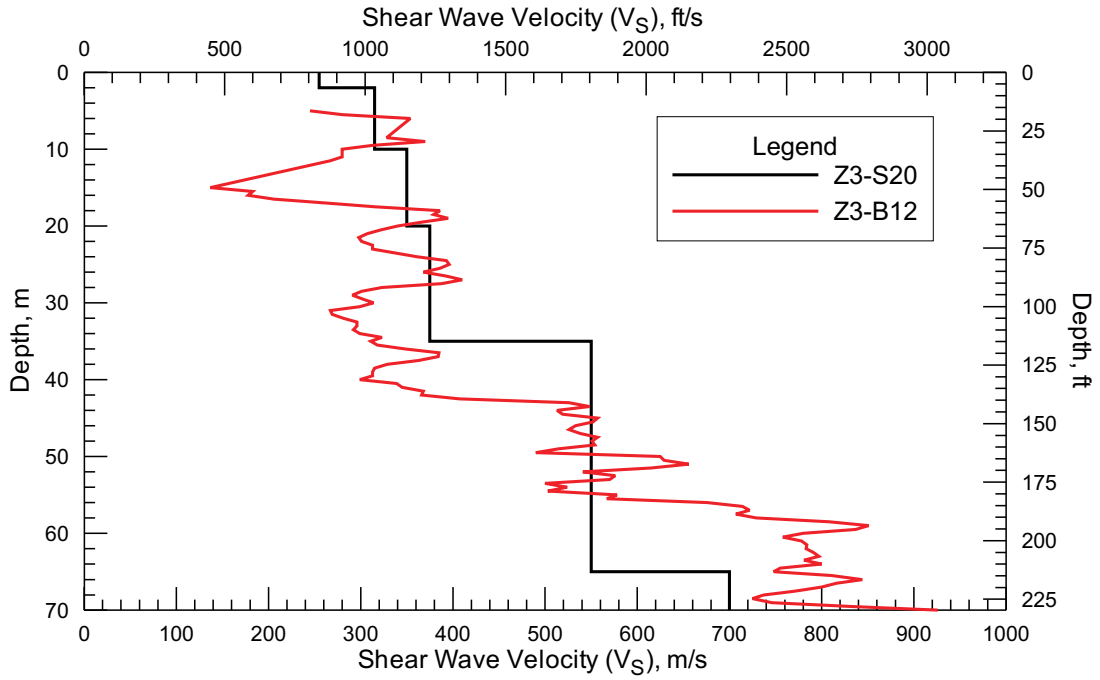

V_S Model from Active and Passive Surface Wave Array Z3-S20

GEOVision geophysical services	FIGURE 54 VELOCITY MODEL FOR ACTIVE AND PASSIVE SURFACE WAVE ARRAY Z3-S20
Project # 9001 Date: JUL 27, 2009 Drawn By: A MARTIN Approved By: Antony J Martin File R:\...Project Files\2009\9001ch2mhill\report\figures\Figure54.cdr	WESTMONT DR AND KEATS ST, ALHAMBRA, CALIFORNIA
	PREPARED FOR CH2M HILL

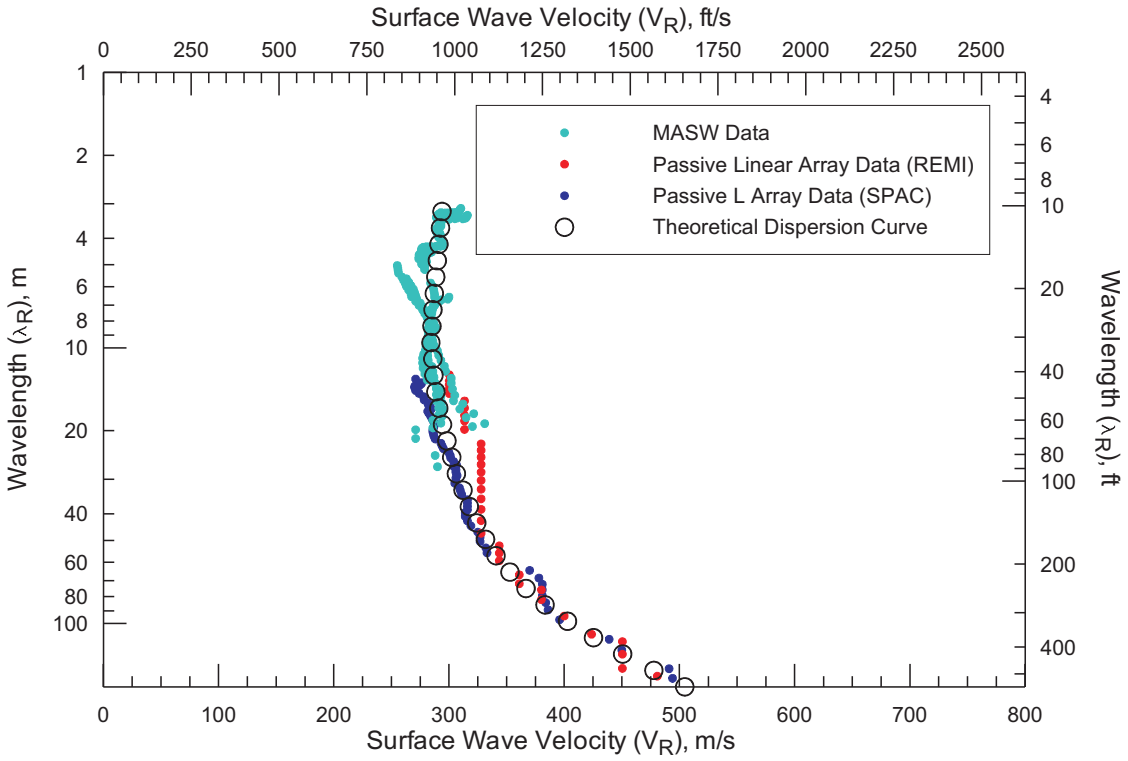

Comparison of Field Experimental Data and Theoretical Dispersion Curve from Active and Passive Surface Wave Array Z3-S21

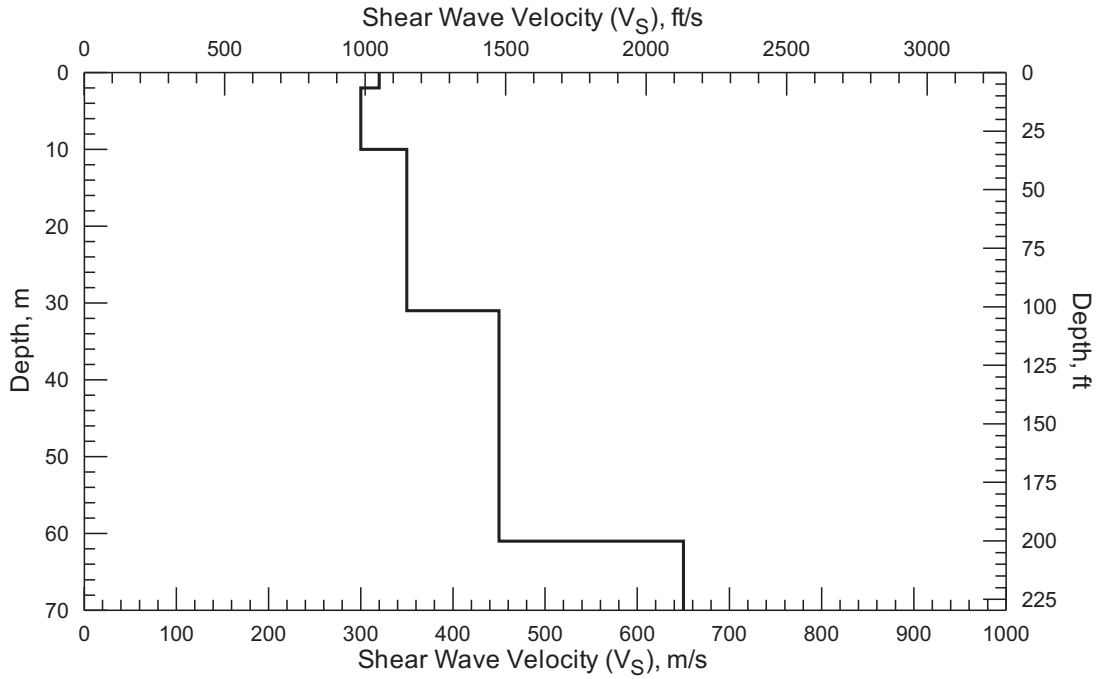

V_S Model from Active and Passive Surface Wave Array Z3-S21

GEOVision geophysical services	FIGURE 55 VELOCITY MODEL FOR ACTIVE AND PASSIVE SURFACE WAVE ARRAY Z3-S21
Project # 9001 Date: JUL 27, 2009 Drawn By: A MARTIN Approved By: Antony J Martin File R:\...Project Files\2009\9001ch2mhill\report\figures\Figure55.cdr	WINCHESTER AVE AND NORWICH AVE, ALHAMBRA, CALIFORNIA
	PREPARED FOR CH2M HILL

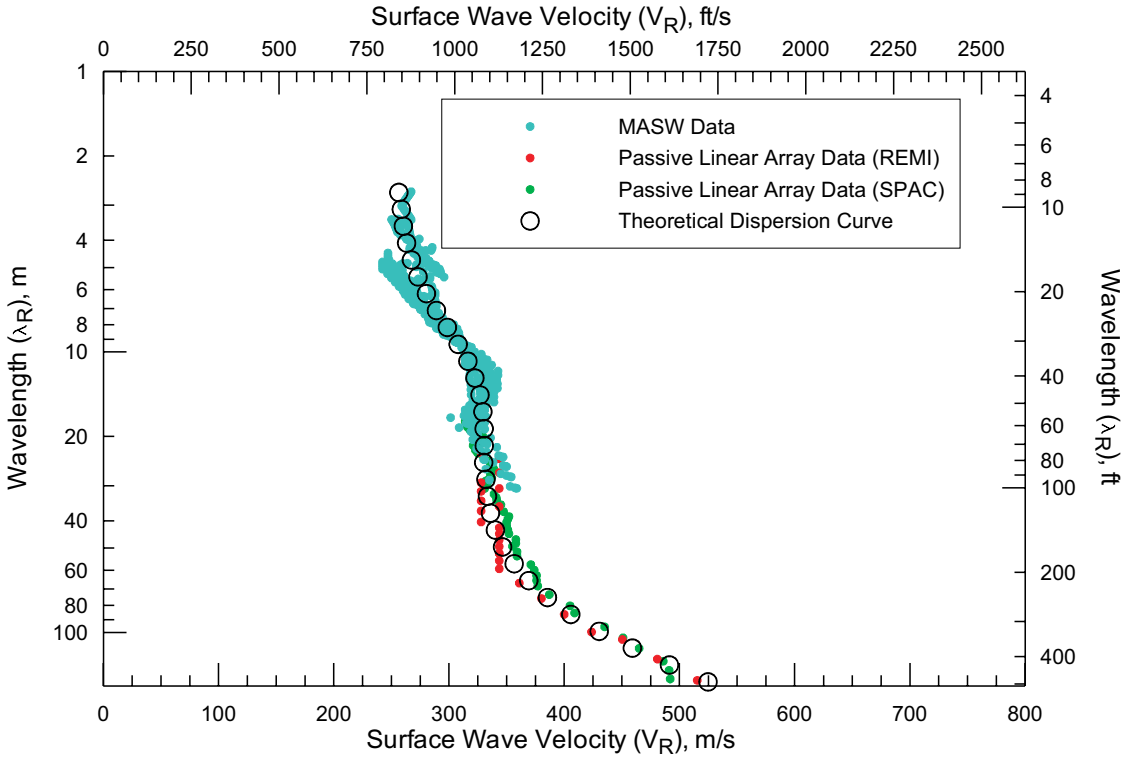

Comparison of Field Experimental Data and Theoretical Dispersion Curve from Active and Passive Surface Wave Array Z3-S22

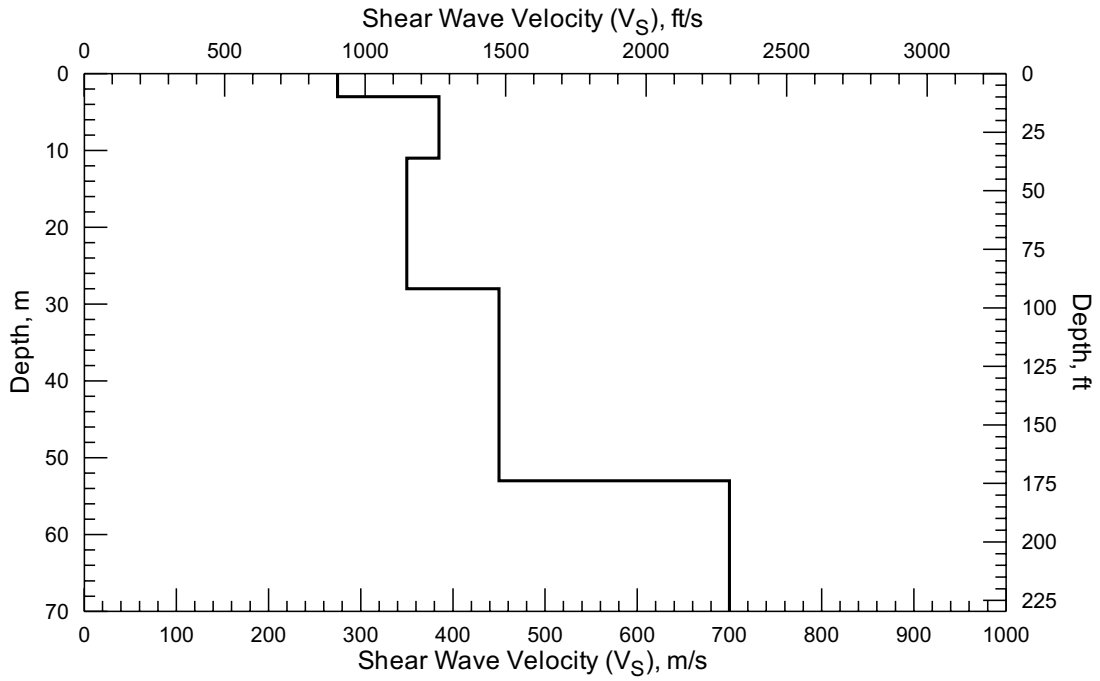

V_S Model from Active and Passive Surface Wave Array Z3-S22

GEOVision geophysical services	FIGURE 56 VELOCITY MODEL FOR ACTIVE AND PASSIVE SURFACE WAVE ARRAY Z3-S22
Project # 9001 Date: JUL 27, 2009 Drawn By: A MARTIN Approved By: Antony J. Martin File R:\...Project Files\2009\9001ch2mhill\report\figures\Figure56.cdr	WINCHESTER AVE AND CONCORD AVE, ALHAMBRA, CALIFORNIA
	PREPARED FOR CH2M HILL

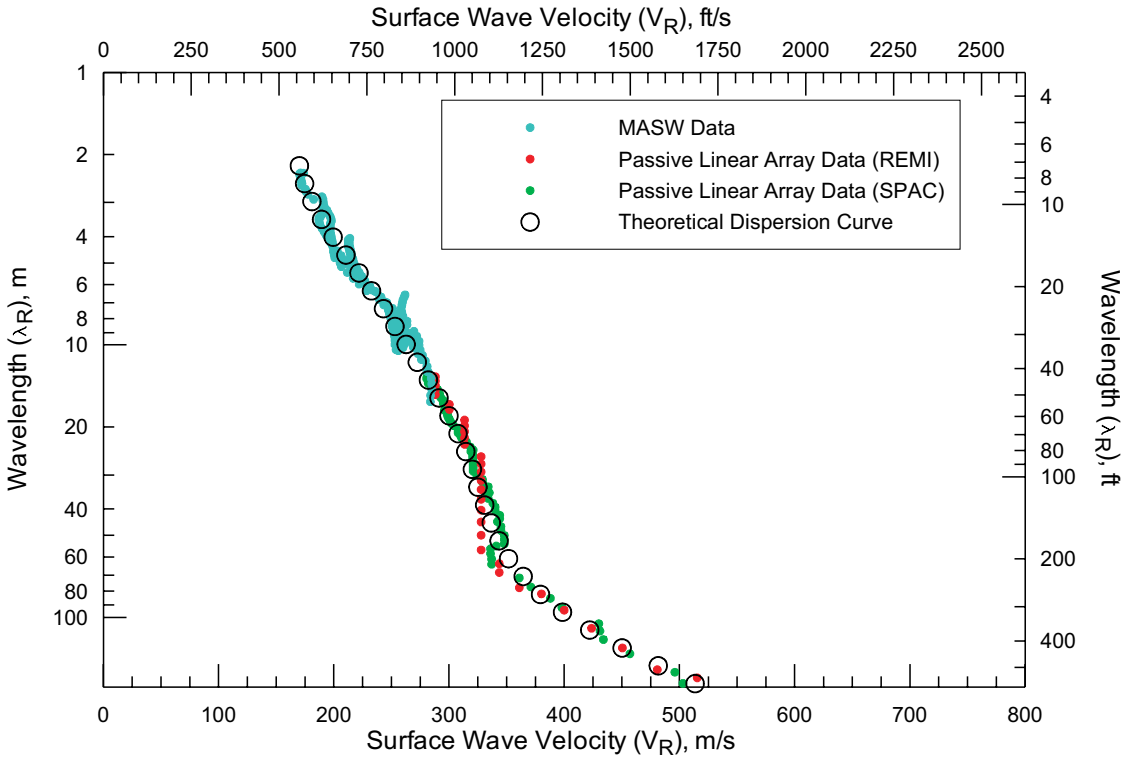

Comparison of Field Experimental Data and Theoretical Dispersion Curve from Active and Passive Surface Wave Array Z3-S23

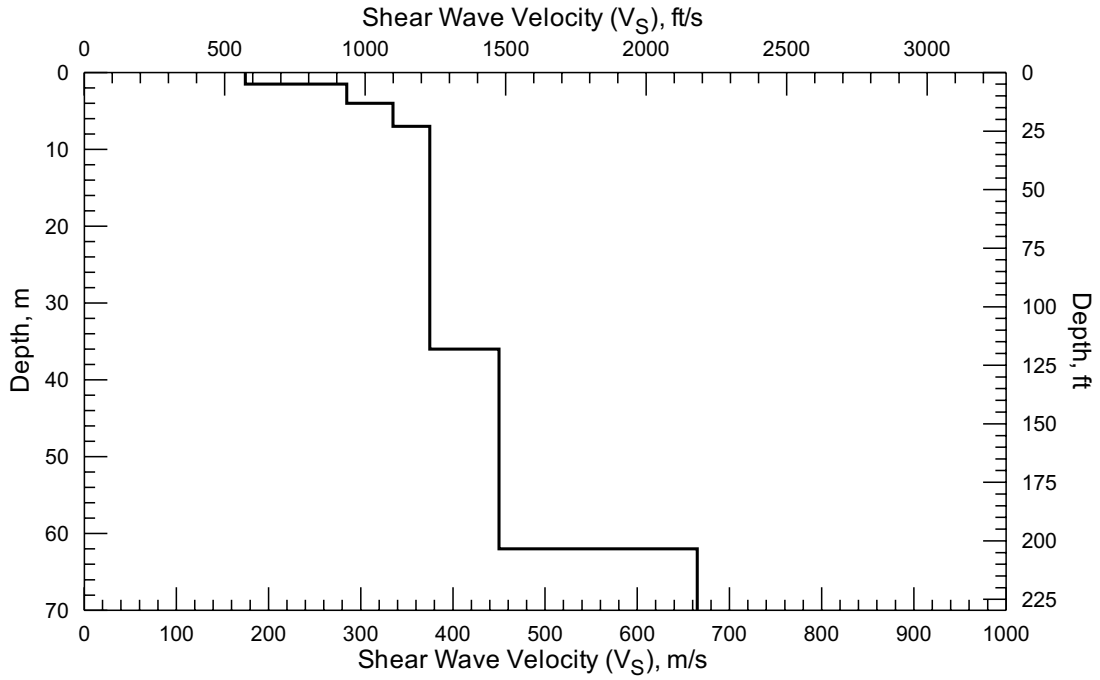

V_S Model from Active and Passive Surface Wave Array Z3-S23

GEOVision geophysical services	FIGURE 57 VELOCITY MODEL FOR ACTIVE AND PASSIVE SURFACE WAVE ARRAY Z3-S23
Project # 9001 Date: JUL 27, 2009 Drawn By: A MARTIN Approved By: Antony J. Martin File R:\...Project Files\2009\9001ch2mhill\report\figures\Figure57.cdr	WESTMONT DR AND VALLEY BLVD, ALHAMBRA, CALIFORNIA
	PREPARED FOR CH2M HILL

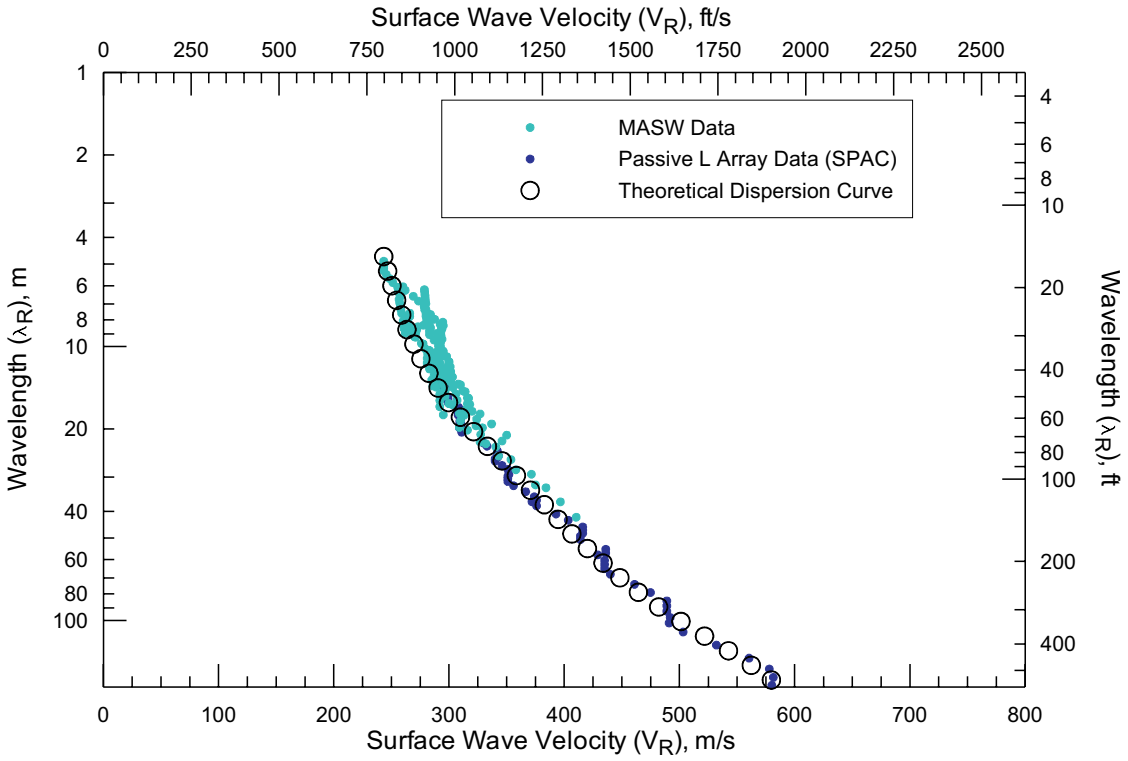

Comparison of Field Experimental Data and Theoretical Dispersion Curve from Active and Passive Surface Wave Array Z3-S24

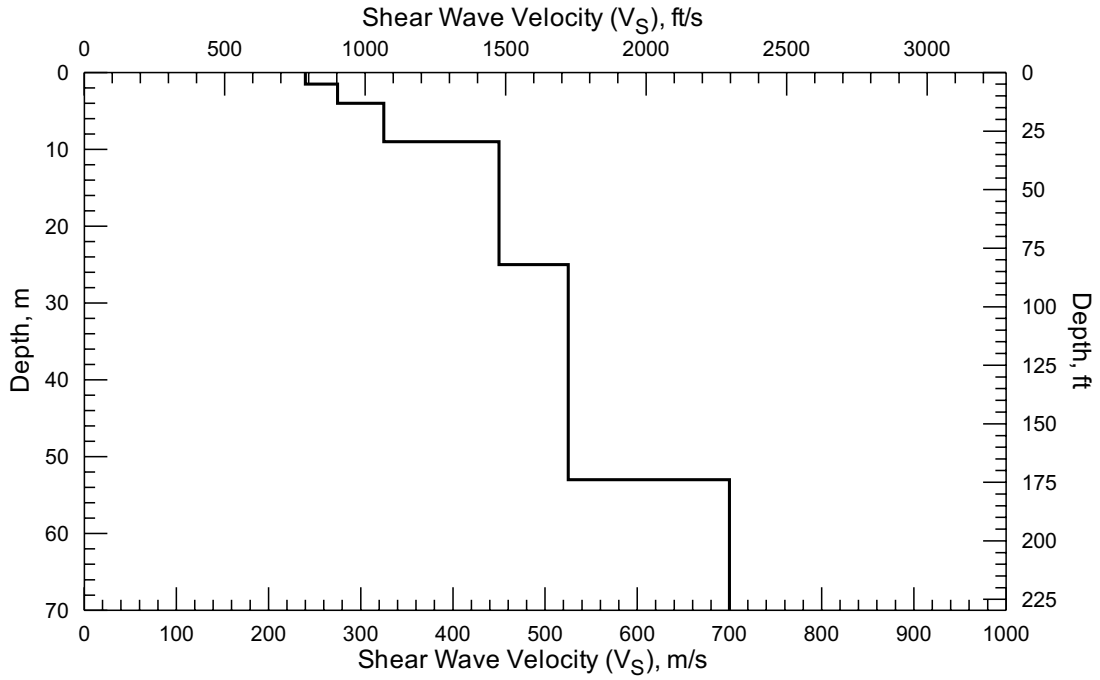

V_S Model from Active and Passive Surface Wave Array Z3-S24

GEOVision geophysical services	FIGURE 58 VELOCITY MODEL FOR ACTIVE AND PASSIVE SURFACE WAVE ARRAY Z3-S24
Project # 9001 Date: JUL 27, 2009 Drawn By: A MARTIN Approved By: Antony J. Martin File R:\...Project Files\2009\9001ch2mhill\report\figures\Figure58.cdr	WESTMONT DR AND GLENAVEN AVE, ALHAMBRA, CALIFORNIA
	PREPARED FOR CH2M HILL

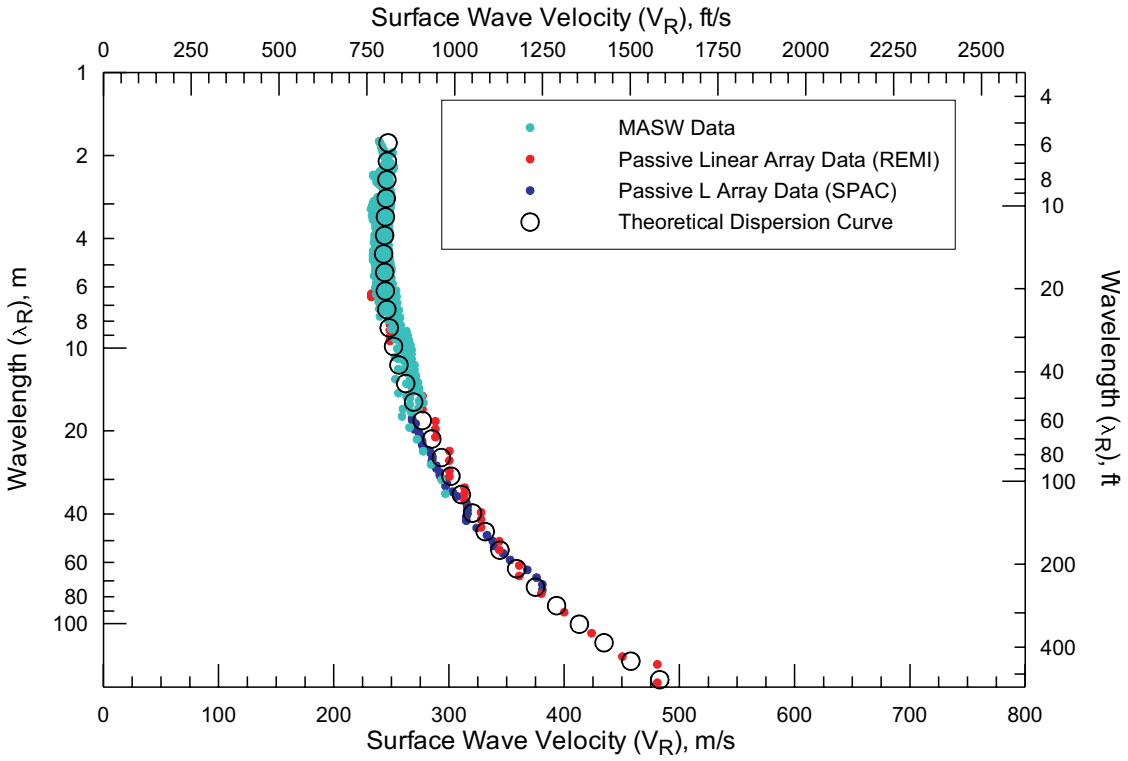

Comparison of Field Experimental Data and Theoretical Dispersion Curve from Active and Passive Surface Wave Array Z4-S6

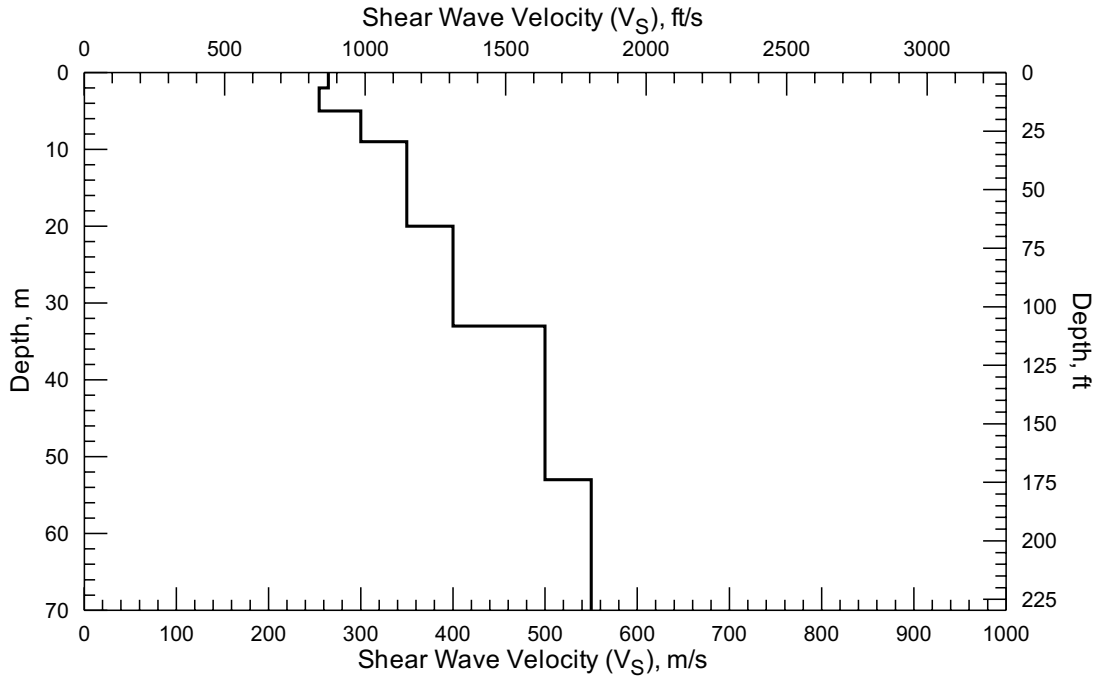

V_S Model from Active and Passive Surface Wave Array Z4-S6

GEOVision geophysical services	FIGURE 64 VELOCITY MODEL FOR ACTIVE AND PASSIVE SURFACE WAVE ARRAY Z4-S6
Project # 9001 Date: JUL 29, 2009 Drawn By: A MARTIN Approved By: Antony J Martin File R:\...Project Files\2009\9001ch2mhill\report\figures\Figure64.cdr	HUNTINGTON DR AND GRANADA AVE, SAN MARINO, CALIFORNIA
	PREPARED FOR CH2M HILL

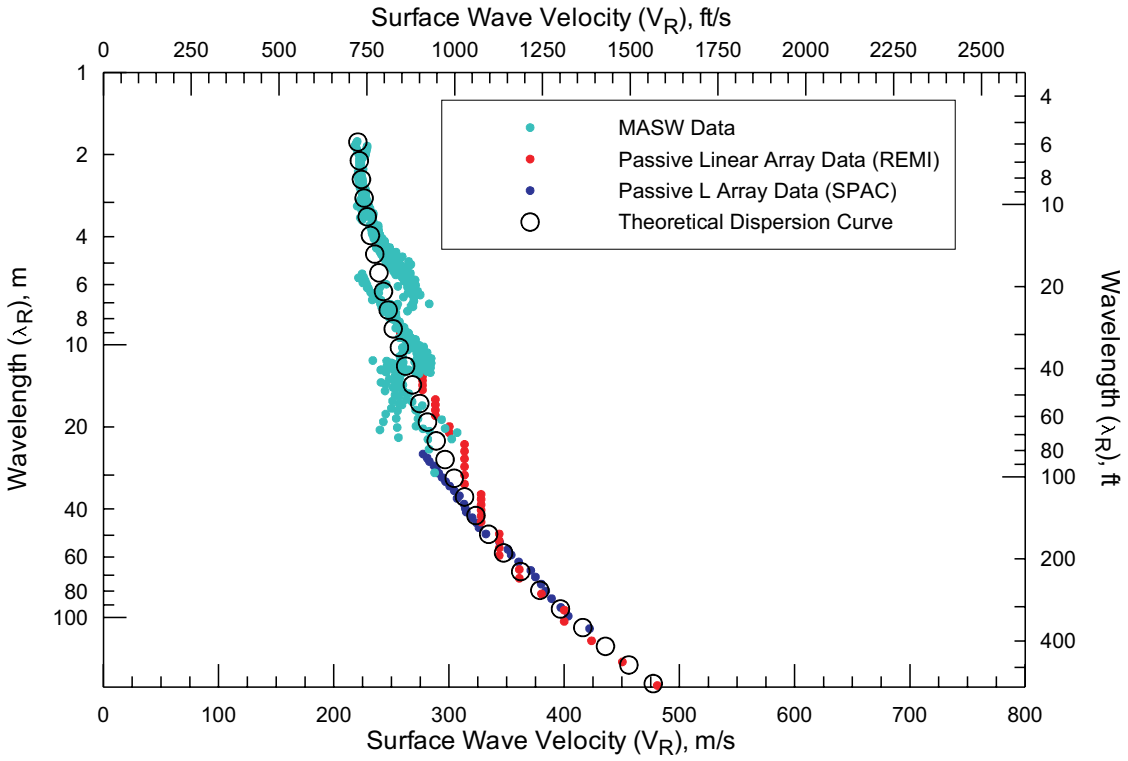

Comparison of Field Experimental Data and Theoretical Dispersion Curve from Active and Passive Surface Wave Array Z4-S7

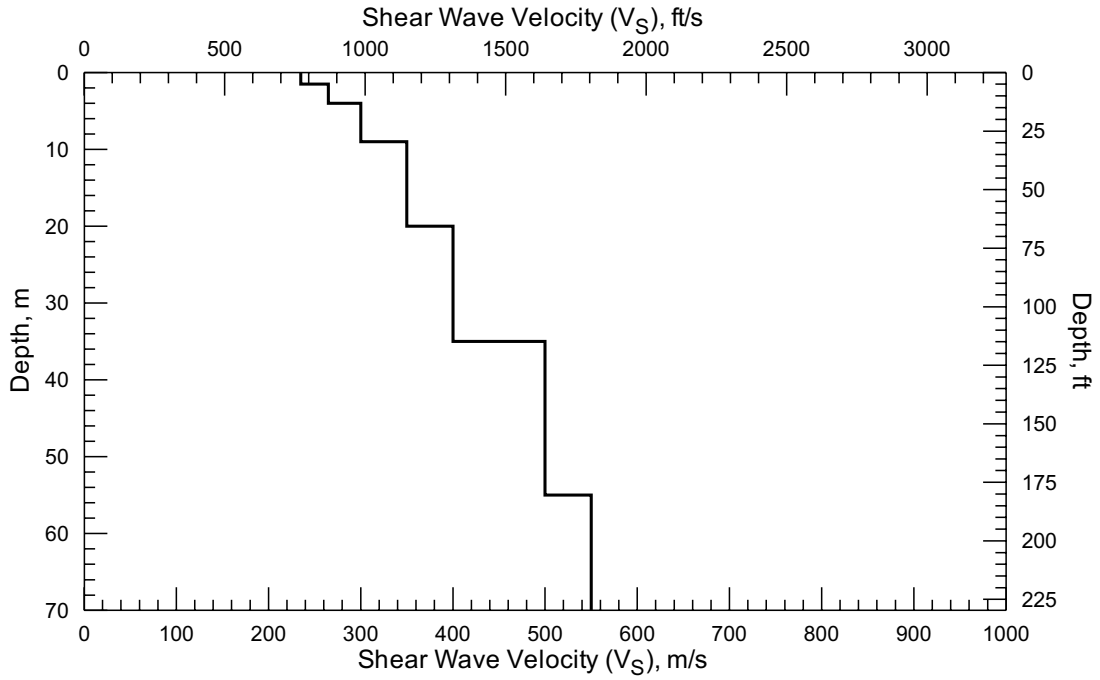

V_S Model from Active and Passive Surface Wave Array Z4-S7

GEOVision geophysical services	FIGURE 65 VELOCITY MODEL FOR ACTIVE AND PASSIVE SURFACE WAVE ARRAY Z4-S7
Project # 9001 Date: JUL 29, 2009 Drawn By: A MARTIN Approved By: Antony J Martin File R:\...Project Files\2009\9001ch2mhill\report\figures\Figure65.cdr	HUNTINGTON DR AND STORY PL, SAN MARINO, CALIFORNIA
	PREPARED FOR CH2M HILL

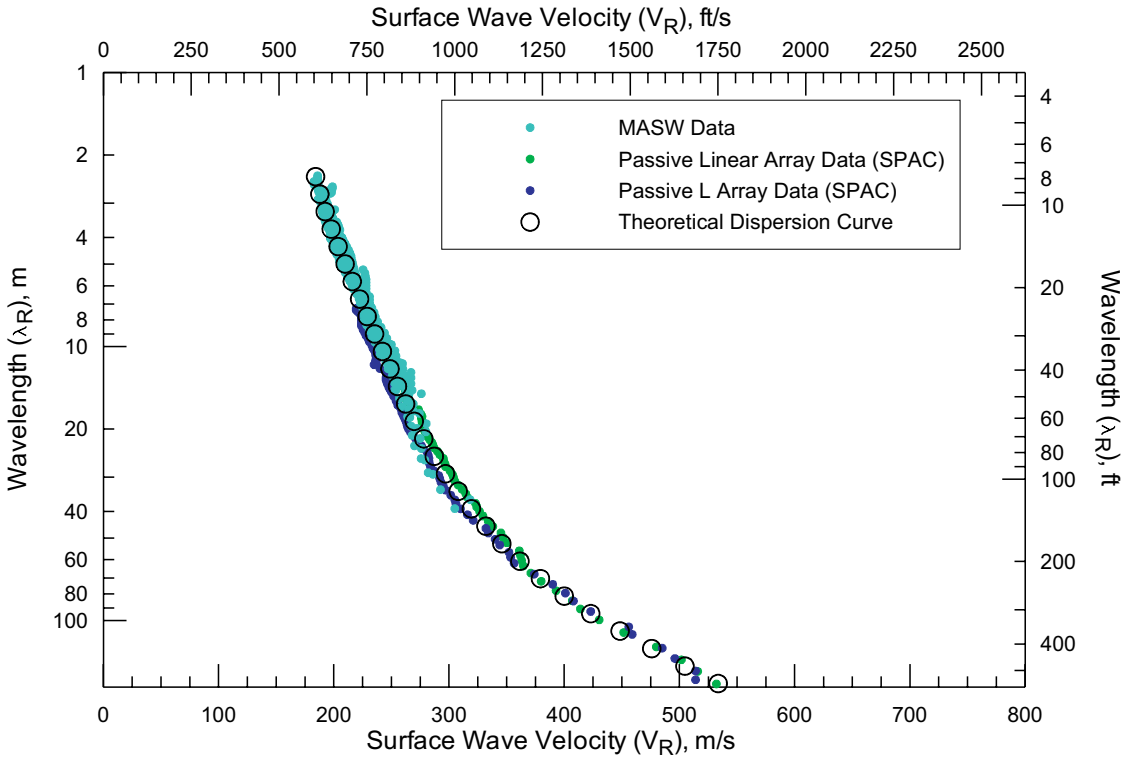

Comparison of Field Experimental Data and Theoretical Dispersion Curve from Active and Passive Surface Wave Array Z4-S8

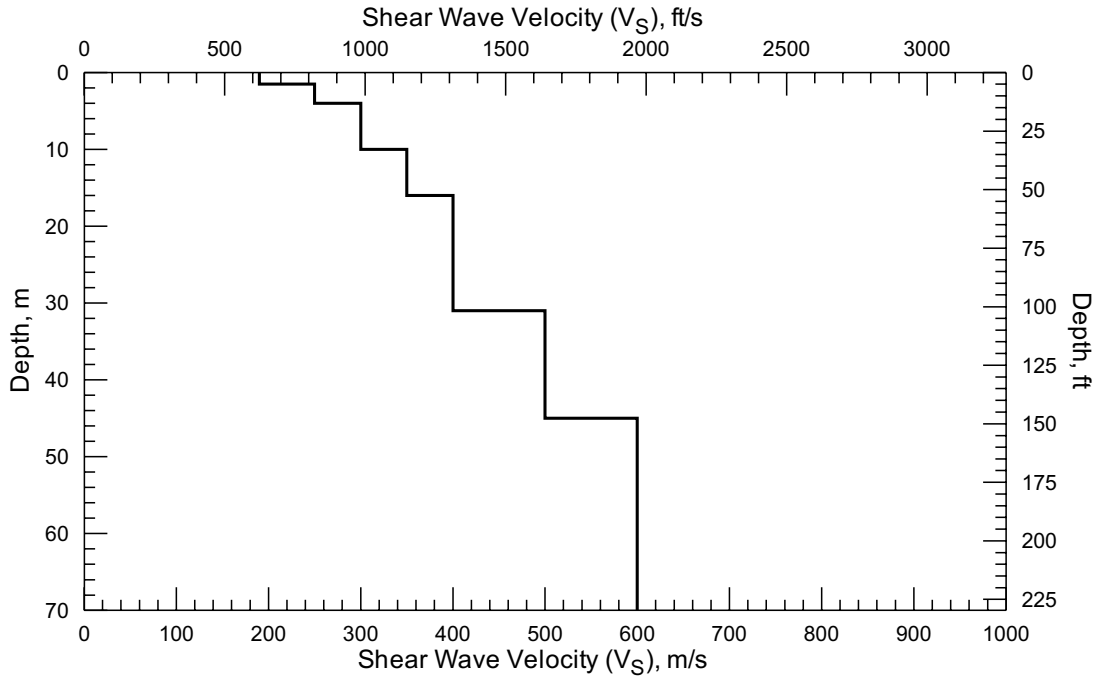

V_S Model from Active and Passive Surface Wave Array Z4-S8

GEOVision geophysical services	FIGURE 66 VELOCITY MODEL FOR ACTIVE AND PASSIVE SURFACE WAVE ARRAY Z4-S8
Project # 9001 Date: JUL 29, 2009 Drawn By: A MARTIN Approved By: Antony J Martin File R:\...Project Files\2009\9001ch2mhill\report\figures\Figure66.cdr	GARFIELD AVE AND MCLEAN ST, ALHAMBRA, CALIFORNIA
	PREPARED FOR CH2M HILL

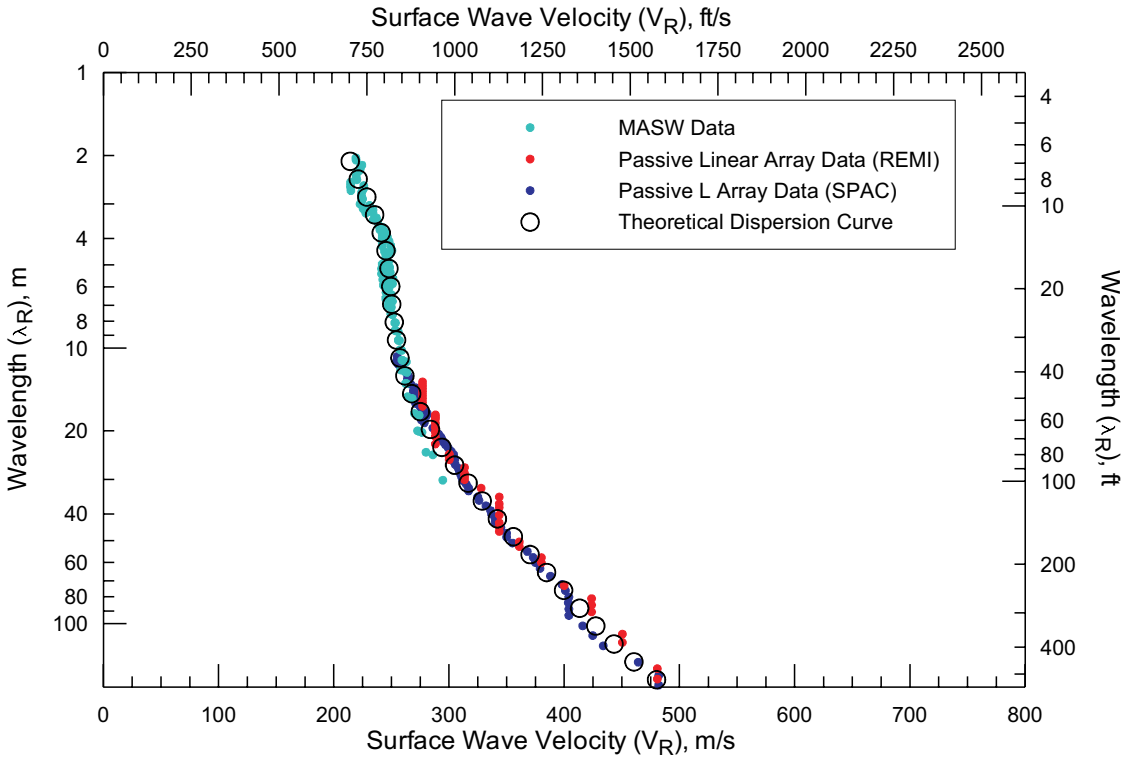

Comparison of Field Experimental Data and Theoretical Dispersion Curve from Active and Passive Surface Wave Array Z4-S9

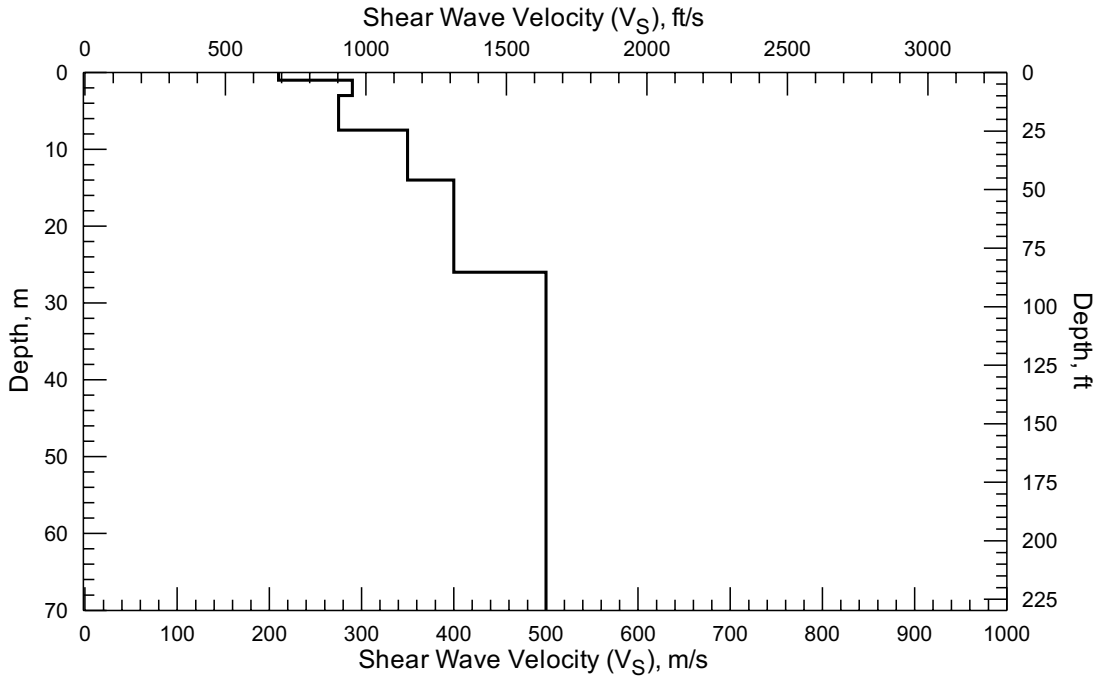

V_S Model from Active and Passive Surface Wave Array Z4-S9

GEOVision geophysical services	FIGURE 67 VELOCITY MODEL FOR ACTIVE AND PASSIVE SURFACE WAVE ARRAY Z4-S9
Project # 9001 Date: JUL 29, 2009 Drawn By: A MARTIN Approved By: Antony J. Martin File R:\...Project Files\2009\9001ch2mhill\report\figures\Figure67.cdr	BUSHNELL AVE AND LARCH ST, ALHAMBRA, CALIFORNIA
	PREPARED FOR CH2M HILL

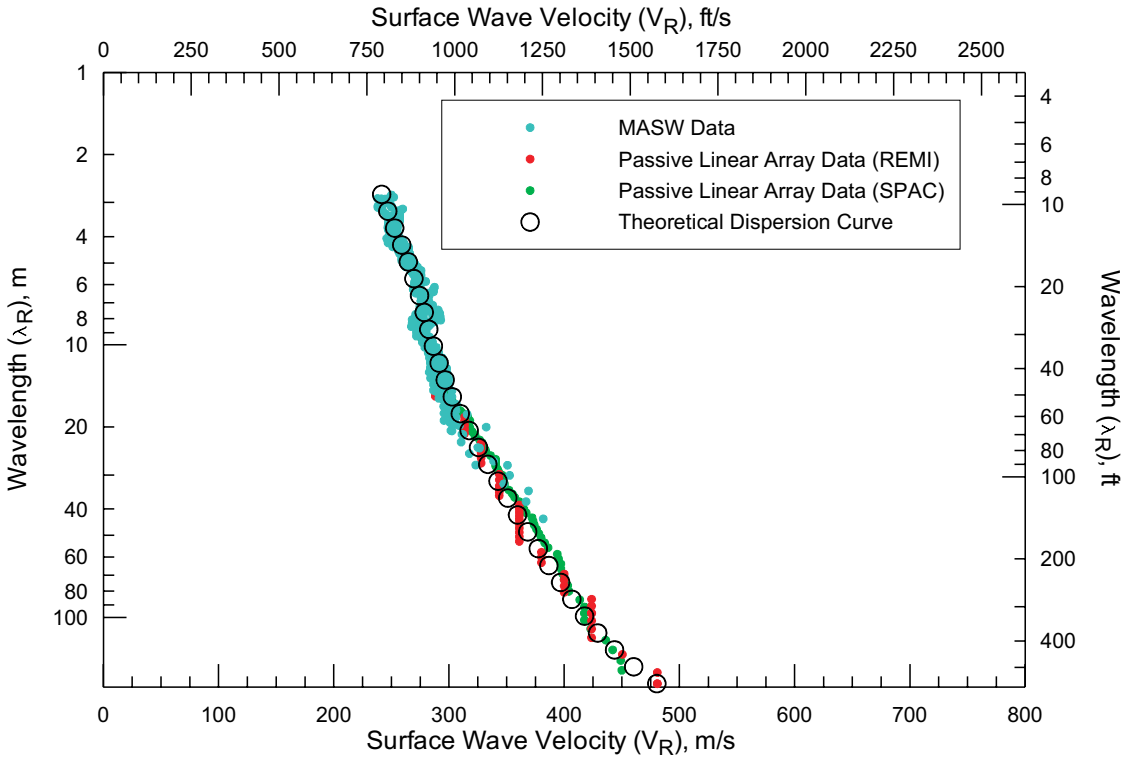

Comparison of Field Experimental Data and Theoretical Dispersion Curve from Active and Passive Surface Wave Array Z4-S10

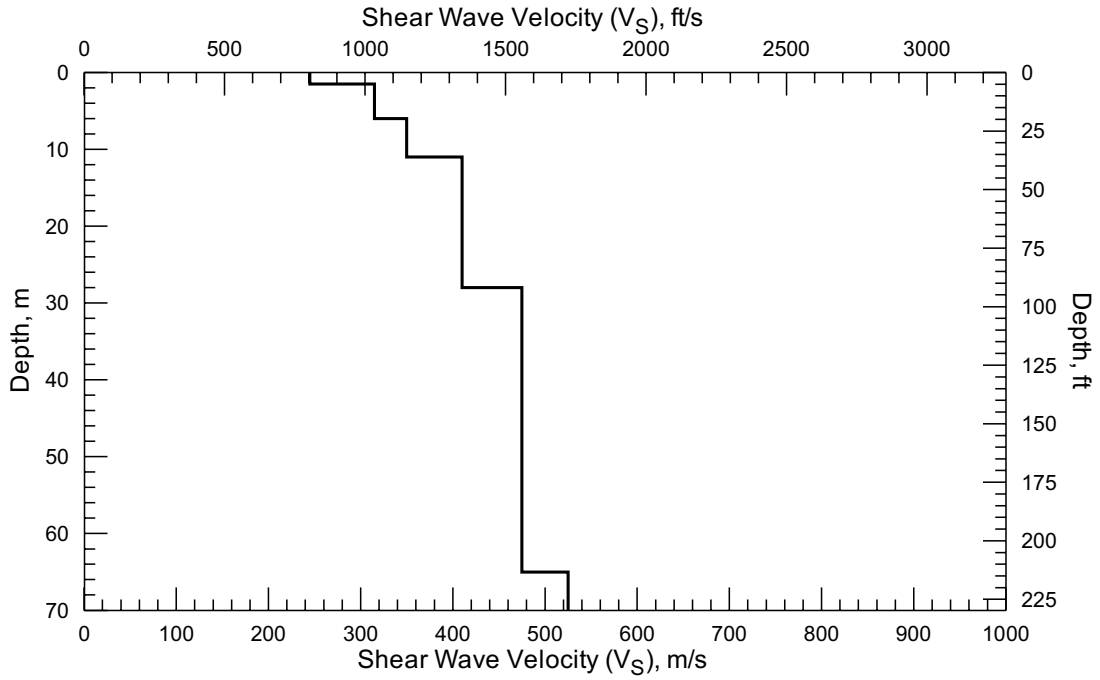

V_S Model from Active and Passive Surface Wave Array Z4-S10

GEOVision geophysical services	FIGURE 68 VELOCITY MODEL FOR ACTIVE AND PASSIVE SURFACE WAVE ARRAY Z4-S10
Project # 9001 Date: JUL 29, 2009 Drawn By: A MARTIN Approved By: Antony J. Martin File R:\...Project Files\2009\9001ch2mhill\report\figures\Figure68.cdr	COMMONWEALTH AVE AND DATE AVE, ALHAMBRA, CALIFORNIA PREPARED FOR CH2M HILL

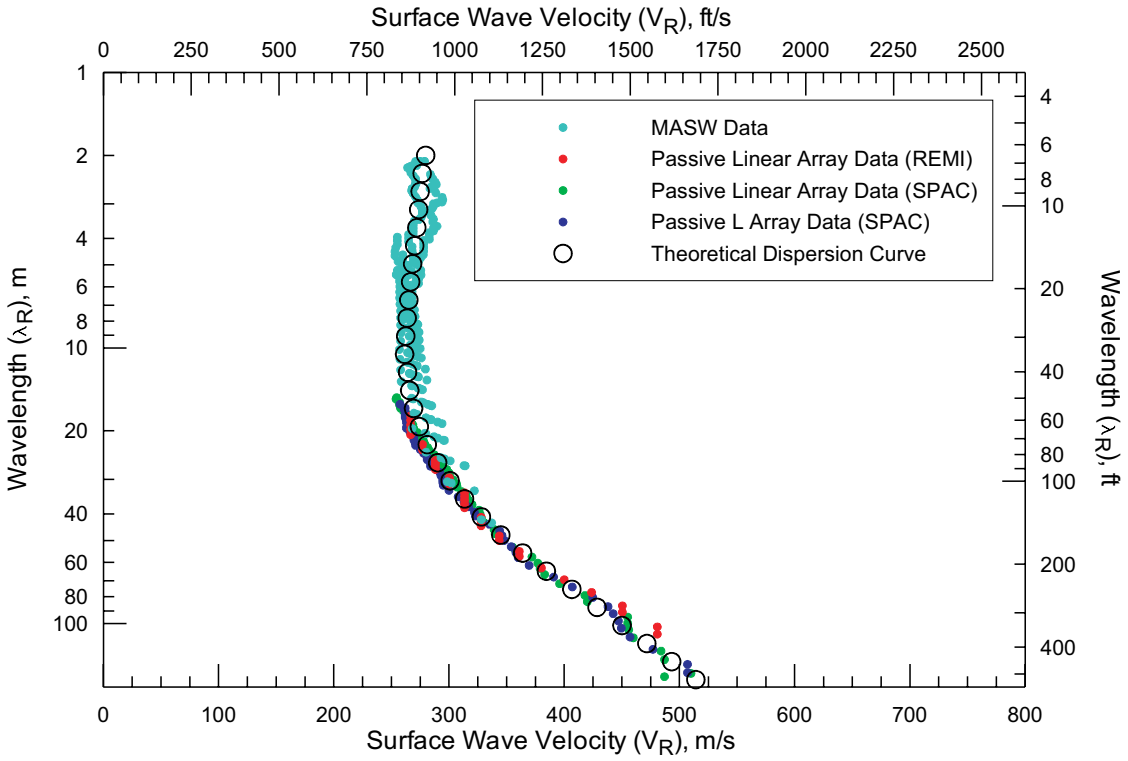

Comparison of Field Experimental Data and Theoretical Dispersion Curve from Active and Passive Surface Wave Array Z5-S10

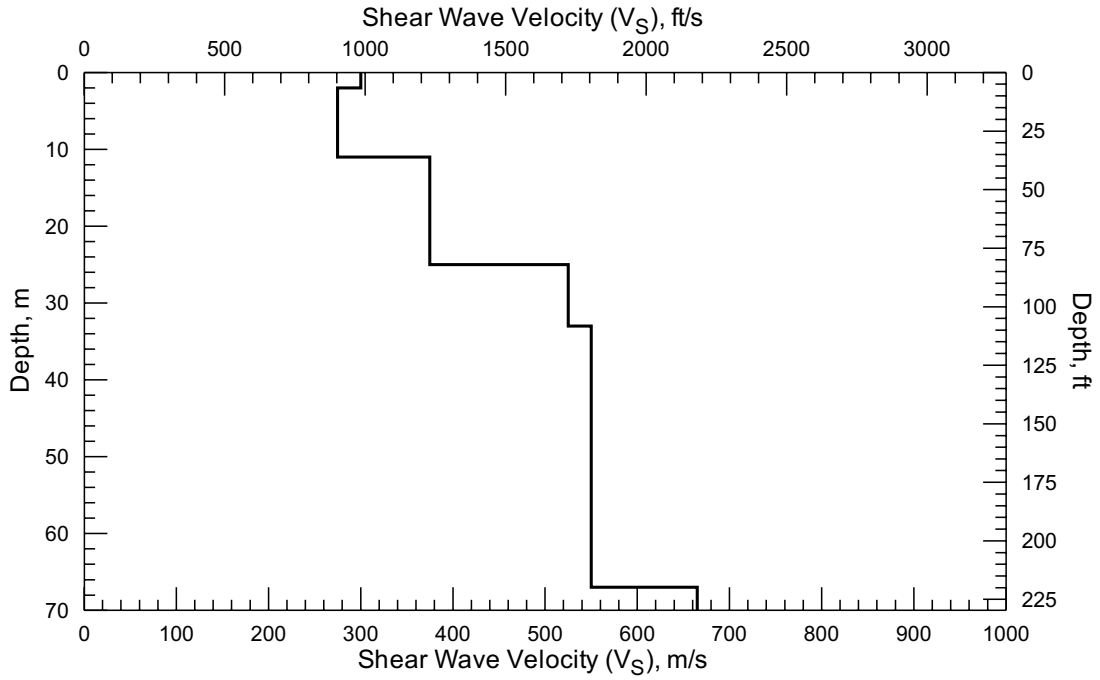

V_S Model from Active and Passive Surface Wave Array Z5-S10

GEOVision geophysical services	FIGURE 77 VELOCITY MODEL FOR ACTIVE AND PASSIVE SURFACE WAVE ARRAY Z5-S10
Project # 9001 Date: JUL 29, 2009 Drawn By: A MARTIN Approved By: Antony J Martin File R:\...Project Files\2009\9001ch2mhill\report\figures\Figure77.cdr	S 2ND ST AND W ADAMS AVE, ALHAMBRA, CALIFORNIA
	PREPARED FOR CH2M HILL

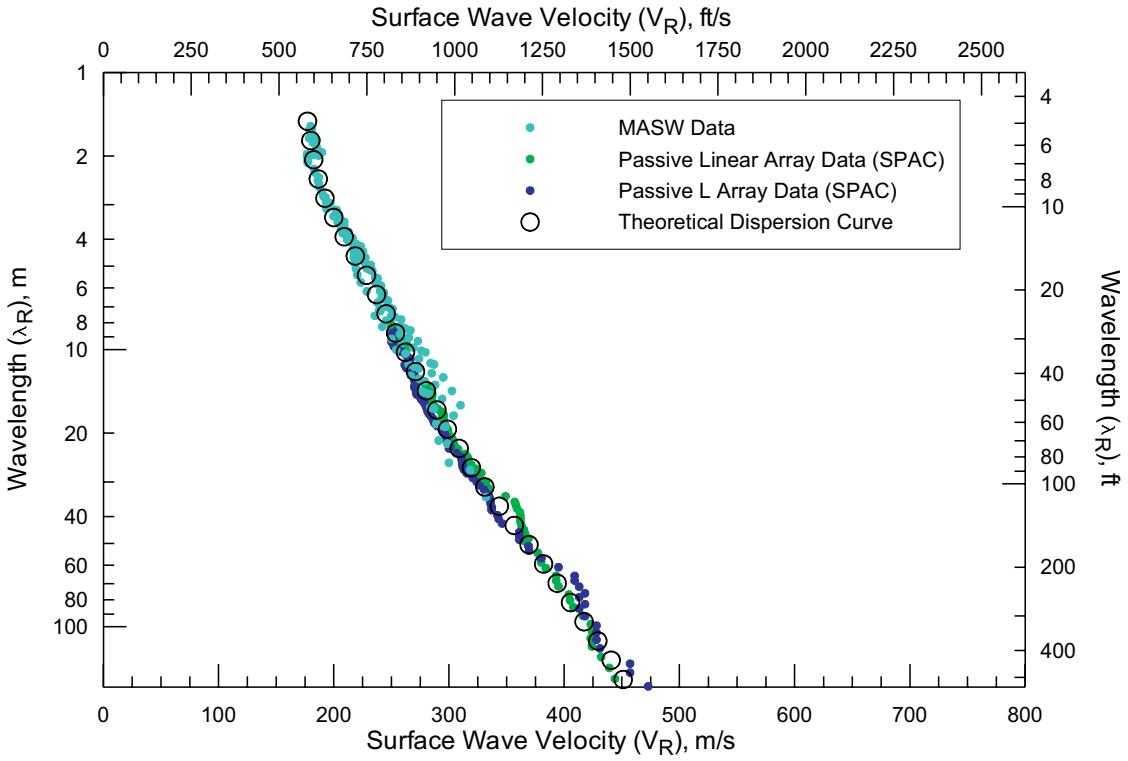

Comparison of Field Experimental Data and Theoretical Dispersion Curve from Active and Passive Surface Wave Array Z5-S11

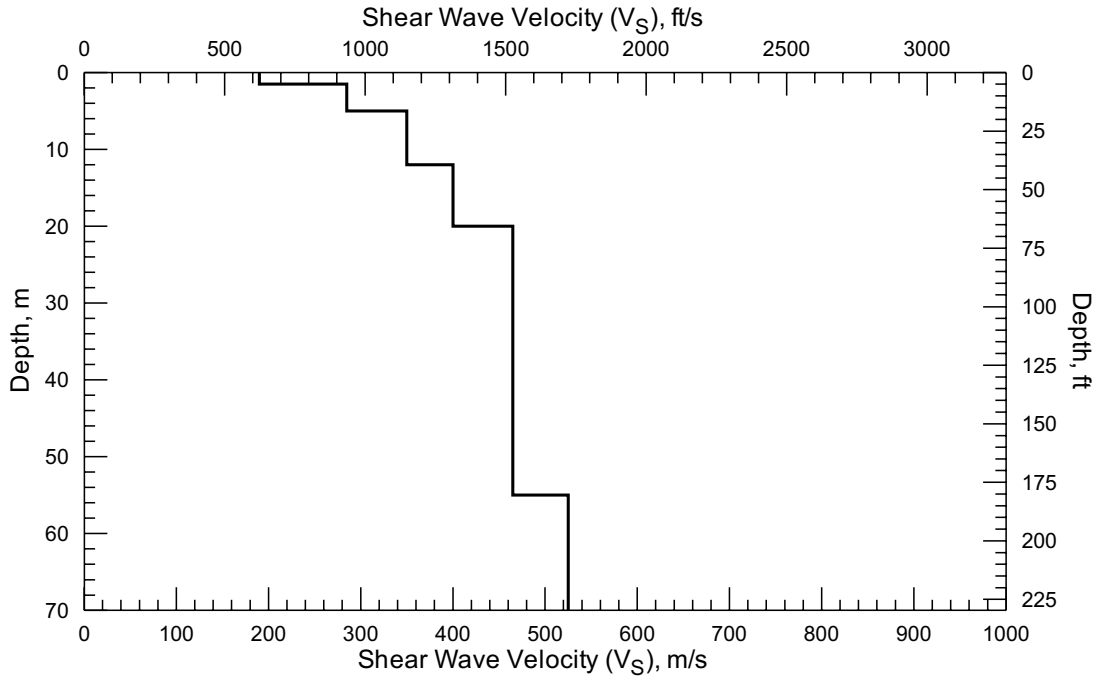

V_S Model from Active and Passive Surface Wave Array Z5-S11

GEOVision geophysical services	FIGURE 78 VELOCITY MODEL FOR ACTIVE AND PASSIVE SURFACE WAVE ARRAY Z5-S11
Project # 9001 Date: JUL 29, 2009 Drawn By: A MARTIN Approved By: Antony J Martin	SHORB ST AND BENITO AVE, ALHAMBRA, CALIFORNIA
File R:\...Project Files\2009\9001ch2mhill\report\figures\Figure78.cdr	PREPARED FOR CH2M HILL

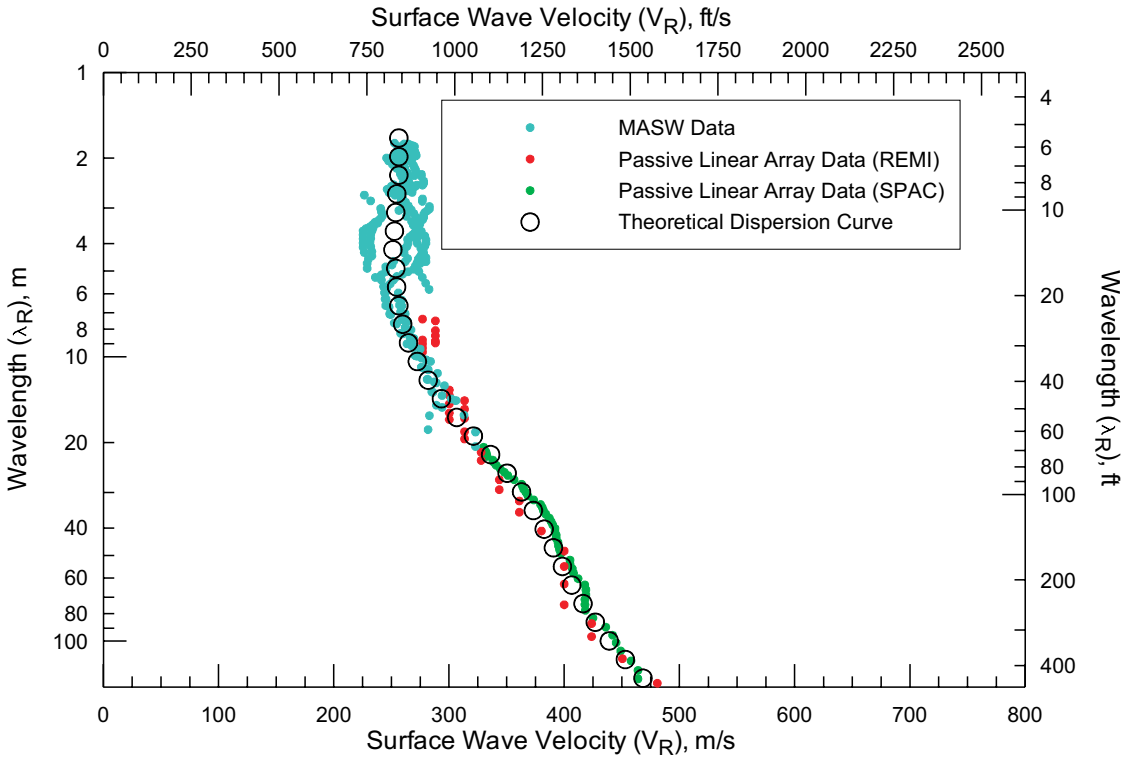

Comparison of Field Experimental Data and Theoretical Dispersion Curve from Active and Passive Surface Wave Array Z5-S12

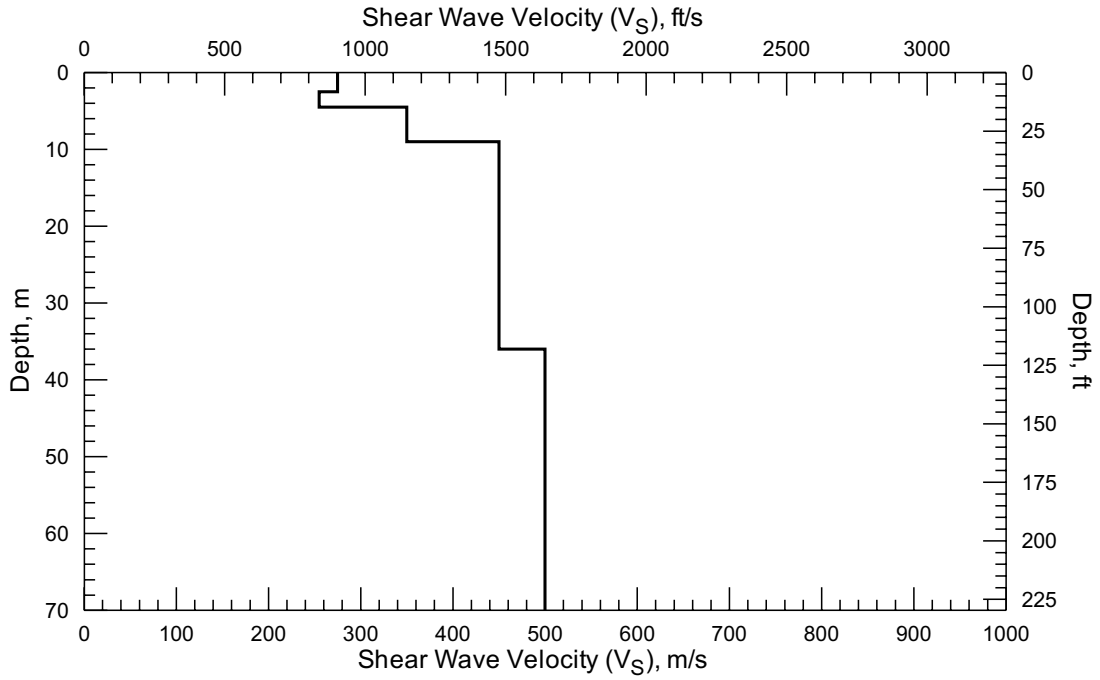

V_S Model from Active and Passive Surface Wave Array Z5-S12

GEOVision geophysical services	FIGURE 79 VELOCITY MODEL FOR ACTIVE AND PASSIVE SURFACE WAVE ARRAY Z5-S12
Project # 9001 Date: JUL 29, 2009 Drawn By: A MARTIN Approved By: Antony J Martin File R:\...Project Files\2009\9001ch2mhill\report\figures\Figure79.cdr	NORWOOD PL AND EDGEWOOD DR, ALHAMBRA, CALIFORNIA
	PREPARED FOR CH2M HILL

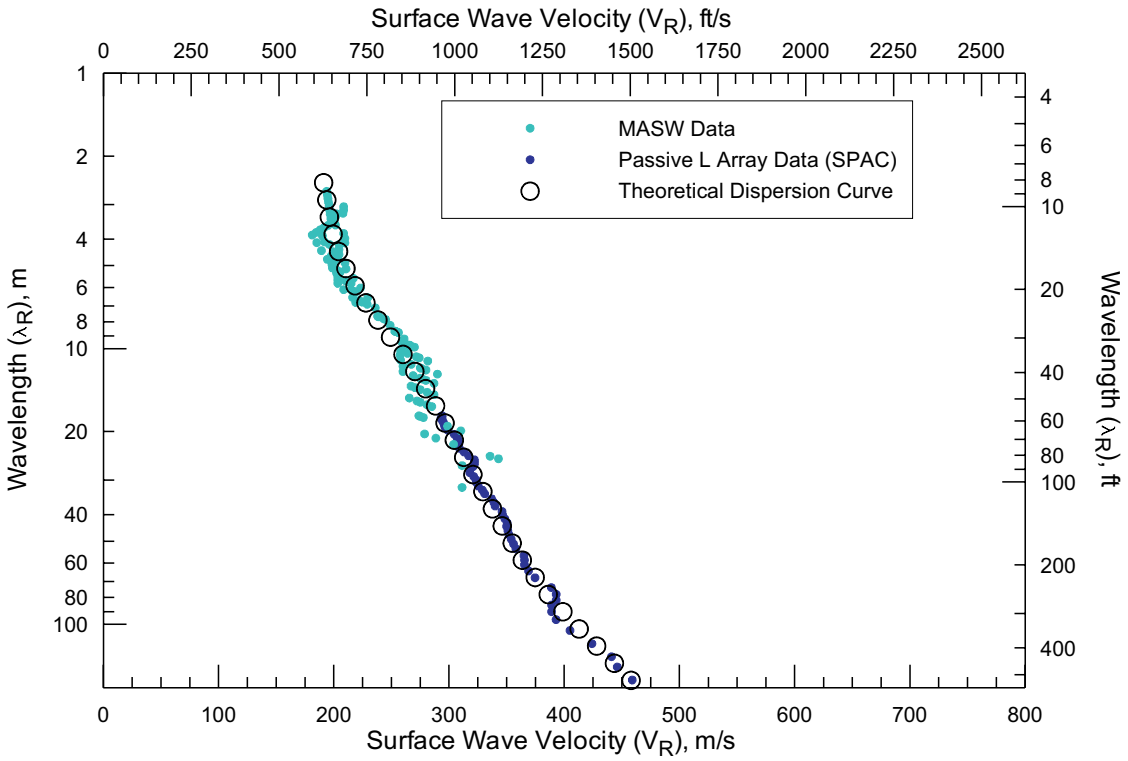

Comparison of Field Experimental Data and Theoretical Dispersion Curve from Active and Passive Surface Wave Array Z5-S13

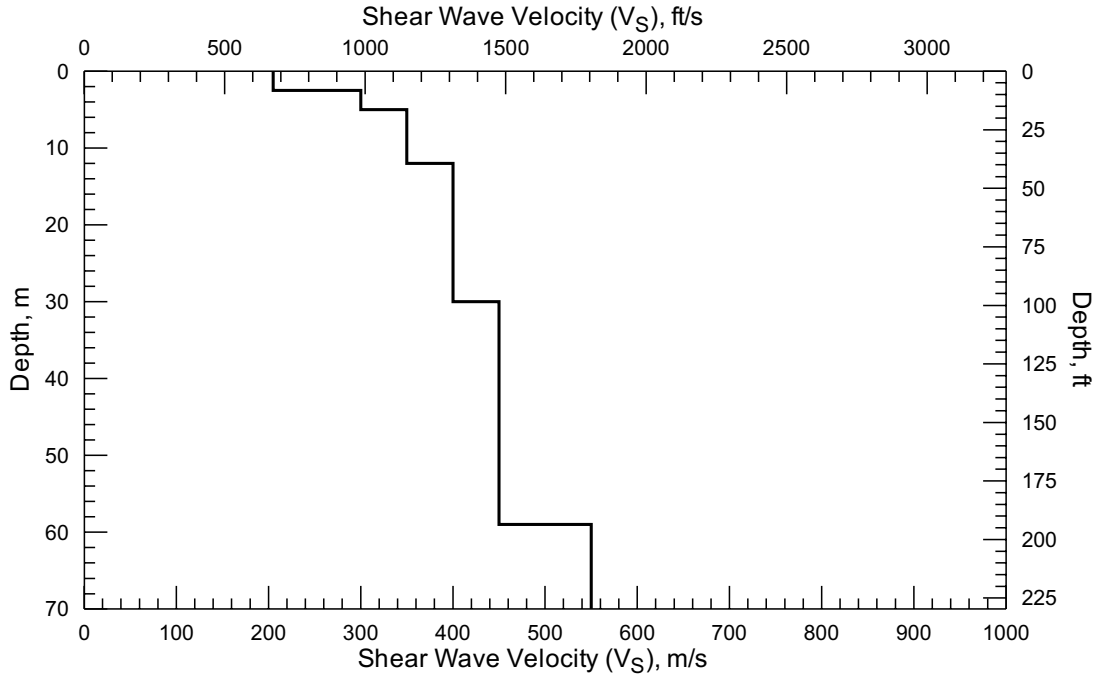

V_S Model from Active and Passive Surface Wave Array Z5-S13

GEOVision geophysical services	FIGURE 80 VELOCITY MODEL FOR ACTIVE AND PASSIVE SURFACE WAVE ARRAY Z5-S13
Project # 9001 Date: JUL 29, 2009 Drawn By: A MARTIN Approved By: Antony J Martin File R:\...Project Files\2009\9001ch2mhill\report\figures\Figure80.cdr	ROSS AVE AND EDGEWOOD DR, ALHAMBRA, CALIFORNIA PREPARED FOR CH2M HILL

APPENDIX B.2

Pressuremeter Results

Appendix B.2
Pressuremeter Results

The following data reports were prepared for the SR 710 Tunnel Technical Study Final Geotechnical Summary Report (CH2M HILL, 2010). However, only data relevant to the SR 710 North Study are provided herein as summarized in Table B-3. The full version of the following appendix is presented in the Technical Study (CH2M HILL, 2010).

TABLE B-3
Summary of Pressuremeter Tests

Boring Number	Test Number	Date Performed	Test Depth (feet)	Recovery Percent	RQD	Rock Description
R-09-Z3B2	SR710-01	1/16/2009	200.9	17	0	Wilson Quartz Diorite (Wqm)/Granitic-type and Gneissic Rock
R-09-Z3B2	SR710-02	1/16/2009	199.4	17	0	Wilson Quartz Diorite (Wqm)/Granitic-type and Gneissic Rock
R-09-Z3B2	SR710-05	1/17/2009	227	100	0	Wilson Quartz Diorite (Wqm)/Granitic-type and Gneissic Rock
R-09-Z3B2	SR710-06	1/17/2009	225	75	0	Wilson Quartz Diorite (Wqm)/Granitic-type and Gneissic Rock
R-09-Z3B2	SR710-09	1/18/2009	248	50	0	Wilson Quartz Diorite (Wqm)/Granitic-type and Gneissic Rock
R-09-Z3B2	SR710-10	1/18/2009	246.5	92	0	Wilson Quartz Diorite (Wqm)/Granitic-type and Gneissic Rock
R-09-Z3B6	SR710-43	2/20/2009	132	20	8	Topanga Formation(Ttcg)/ Conglomerate
R-09-Z3B6	SR710-47	2/23/2009	166.5	44	0	Topanga Formation(Ttcg)/ Conglomerate
R-09-Z3B6	SR710-48	2/24/2009	188.2	98	30	Topanga Formation(Ttcg)/ Conglomerate

RQD – Rock Quality Designation

Final Report of
In Situ Pressuremeter Geotechnical Testing

Conducted for:

SR-710 Tunnel Technical Study
Los Angeles County, California

Submitted to:

CH2M Hill
6 Hutton Centre Drive
Suite 700
Santa Ana, California 92707

In Situ Engineering Project Number 812
CH2M Hill Project Number 378312.04.13

August 2009

Testing conducted and report prepared by:

In Situ Engineering

6232 195th Avenue SE

Snohomish, WA 98290 360-568-2807

keith@insituengineering.com

TABLE OF CONTENTS

1.0 INTRODUCTION 2
2.0 PURPOSE 2
3.0 PRESSUREMETER 2
4.0 HOLE FORMATION 4
5.0 TEST PROCEDURE 7
6.0 QUALITY OF THE DATA 8
7.0 RANGE OF DATA 9
8.0 STANDARD METHOD OF ANALYSIS OF THE SHEAR MODULUS 10
9.0 DETERMINATION OF THE LIMIT PRESSURE 11
10.0 DETERMINATION OF THE STRENGTH PROPERTIES 15
11.0 CONCLUSIONS 20
12.0 REFERENCES 20

FIGURES

Fig. 1. Schematic details of the pressuremeter 3
Fig. 2. Test SR710-12 and Tests SR710-42 7
Fig. 3. Adjacent pressuremeter tests in same pilot hole 8
Fig. 4. Test in Sandstone (SR710-42) and Fractured Diorite (SR710-14) 9
Fig. 5. Modulus determination for Test SR710-03 11
Fig. 6. Limit Pressure determination for Test SR710-03 12
Fig. 7. Simple constant shear strength model analysis for test SR710-14 15
Fig. 8. Frictional Model for Test SR710-03 16
Fig. 9. Cohesive Models for Test SR710-15 17

TABLES

Table 1 Pressuremeter Test depth and Material Description: Tests 1-48 4
Table 2 Limit Pressure shear modulus and Shear strength (log method): Tests 1-26 13
Table 2 cont. Limit Pressure shear modulus and Shear strength (log method): Tests 27-48 14
Table 3 Material properties from Model Analysis: Tests 1-26 18
Table 3 cont. Material properties from Model Analysis: Tests 27-48 19

APPENDICES

I Pressuremeter Data and Standard Interpretation

II Pressuremeter Model Interpretation

1.0 INTRODUCTION

This report presents the results of a pressuremeter study, conducted from the 16th of January to 24th of February, 2009, in eleven boreholes within the SR-710 Tunnel Technical Study zones. The pressuremeter testing (PMT) was conducted by In Situ Engineering, Snohomish, WA under contract to CH2M Hill, Santa Ana, California. The drilling and deployment of the pressuremeter was accomplished by two groups; CalTrans, Sacramento, CA, using a CME 85 rig and Cascade Drilling, La Habra, CA using an Ingersoll Rand A-400 and a Failing Speedstar 30K drill rig. In total, 48 pressuremeter tests were attempted, of which 46 produced PMT data. The borehole name, test depths and preliminary material descriptions are presented in Table 1.

2.0 PURPOSE

The purpose of this study was to evaluate the *in-situ* modulus of the geologic formations as part of the SR-710 Tunnel Technical Study.

3.0 PRESSUREMETER

The pressuremeter used for this study was a pre-bored monocell pressuremeter. Three electronic displacement sensors, spaced 120 degrees apart are located at the center of the pressuremeter. The flexible membrane is placed over the sensors, and clamped at each end. The membrane is covered by a protective sheet of stainless steel strips. The unit is pressurized using compressed nitrogen to deform the adjacent material. The electronic signals from displacement sensors and the pressure sensor are transmitted by cable to the surface. During the test, the average expansion versus pressure is displayed on a computer screen. The pressuremeter is expanded by regulating the flow of compressed nitrogen to the PMT unit.

Fig.1 presents the essential details of the pressuremeter.

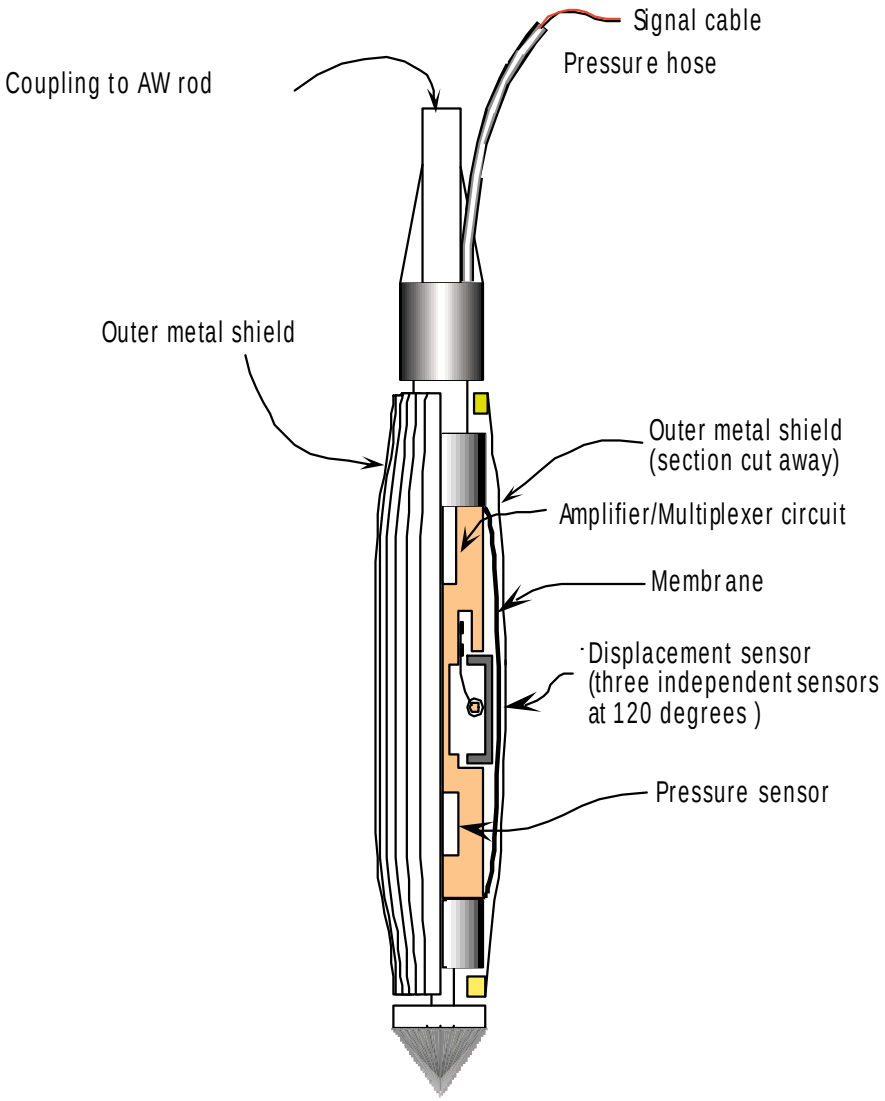

Fig. 1. Schematic details of the pressuremeter

4.0 HOLE FORMATION

The Cascade Drilling group used a PQ wireline system to advance the borehole. This allowed the hole to be continuously cased. A 5 to 6 foot test pocket for the pressuremeter was drilled using a 2 $^{15}/_{16}$ tricone bit, or NQ core barrel which was able to fit through the PQ core bit. The Caltrans system used an HQ wireline system to advance the main hole. This string had to be withdrawn from the hole and the bit changed to a casing bit to allow a 2 $^{15}/_{16}$ tricone bit, or a NQ core barrel to be used to drill the test pocket for the pressuremeter.

In general the aim is to attempt two pressuremeter tests in the one test pocket. The tests are preformed 18 inches apart. In this manner it is possible to assess the quality of the tests.

The details of the test depth and the initial sample description are given in Table 1. The RQD, percent recovery and rock description provided by CH2M Hill. It should be noted that the preliminary boring numbers shown on the plots in the appendices are different than the final boring numbers shown in the Tables of this report. The final numbers have had a prefix (R-09) added to the number and a dash removed from the final sequence. For instance the final boring number R-09-Z3B2 in Table 1 below is the same as boring number Z3-B2 in the Appendices.

Table 1 Pressuremeter Test depth and Material Description: Tests 1-48

Boring Number	Test Number	Date Performed	Test Depth (feet)	Recovery Percent	RQD	Rock Description
R-09-Z3B2	SR710-01	1/16/2009	200.9	17	0	Wilson Quartz Diorite (Wqm)/ Granitic and Gneissic Rock
R-09-Z3B2	SR710-02	1/16/2009	199.4	17	0	Wilson Quartz Diorite (Wqm)/ Granitic and Gneissic Rock
R-09-Z3B11	SR710-03	1/17/2009	192.8	100	95	Topanga Formation (Ttsl)/ Siltstone and Mudstone
R-09-Z3B11	SR710-04	1/17/2009	191.3	100	95	Topanga Formation(Ttsl)/ Siltstone and Mudstone
R-09-Z3B2	SR710-05	1/17/2009	227	100	0	Wilson Quartz Diorite (Wqm)/ Granitic and Gneissic Rock
R-09-Z3B2	SR710-06	1/17/2009	225	75	0	Wilson Quartz Diorite (Wqm)/ Granitic and Gneissic Rock
R-09-Z3B11	SR710-07	1/18/2009	208.4	100	100	Topanga Formation (Ttsl)/ Siltstone and Mudstone
R-09-Z3B11	SR710-08	1/18/2009	206.9	100	100	Topanga Formation (Ttsl)/ Siltstone and Mudstone
R-09-Z3B2	SR710-09	1/18/2009	248	50	0	Wilson Quartz Diorite (Wqm)/ Granitic and Gneissic Rock

Boring Number	Test Number	Date Performed	Test Depth (feet)	Recovery Percent	RQD	Rock Description
R-09-Z3B2	SR710-10	1/18/2009	246.5	92	0	Wilson Quartz Diorite (Wqm)/ Granitic and Gneissic Rock
R-09-Z2B1	SR710-11	1/19/2009	129	20	20	Topanga Formation (Ttsl)/ Interbedded Siltstone and Sandstone
R-09-Z2B1	SR710-12	1/19/2009	127.5	20	20	Topanga Formation (Ttsl)/ Interbedded Siltstone and Sandstone
R-09-Z2B1	SR710-13	1/20/2009	140	45	35	Topanga Formation (Ttsl)/ Interbedded Siltstone and Sandstone
R-09-Z2B1	SR710-14	1/20/2009	138.5	45	35	Topanga Formation(Ttsl)/ Interbedded Siltstone and Sandstone
R-09-Z1B7	SR710-15	1/20/2009	96.5	80	80	Puente Formation (Tpds)/ Sandy Siltstone
R-09-Z1B7	SR710-16	1/20/2009	95	80	80	Puente Formation (Tpds)/ Sandy Siltstone
R-09-Z1B7	SR710-17	1/21/2009	111.5	98	98	Puente Formation (Tpds)/ Sandy Siltstone
R-09-Z1B7	SR710-18	1/21/2009	110	98	98	Puente Formation (Tpds)/ Sandy Siltstone
R-09-Z1B7	SR710-19	1/21/2009	136	77	68	Puente Formation (Tpds)/ Sandy Siltstone
R-09-Z1B7	SR710-20	1/21/2009	134.5	77	68	Puente Formation (Tpds)/ Sandy Siltstone
R-09-Z1B3	SR710-21	1/28/2009	177.3	89	89	Puente Formation (Tpss)/ Sandstone
R-09-Z1B3	SR710-22	1/28/2009	204	83	79	Puente Formation (Tpss)/ Sandstone
R-09-Z2B2	SR710-23	1/29/2009	135.7	100	100	Fernando Formation (Tfss-cg)/ Sandstone
R-09-Z2B2	SR710-24	1/29/2009	134.2	100	100	Fernando Formation (Tfss-cg)/ Sandstone
R-09-Z2B2	SR710-25	2/4/2009	251	73	0	Fernando Formation (Tfss-cg)/ Sandstone
R-09-Z2B2	SR710-26	2/4/2009	249.5	73	0	Fernando Formation (Tfss-cg)/ Sandstone
R-09-Z1B6	SR710-27	2/4/2009	203	90	75	Puente Formation (Tpsl)/ Siltstone with interbedded Sandstone
R-09-Z1B6	SR710-28	2/5/2009	245	100	92	Puente Formation (Tpsl)/ Siltstone with interbedded Sandstone
R-09-Z3B7	ST710-29	2/6/2009	225.8	100	60	Topanga Formation (Ttss)/ Sandstone with Interbedded Siltstone

Boring Number	Test Number	Date Performed	Test Depth (feet)	Recovery Percent	RQD	Rock Description
R-09-Z3B7	SR710-30	2/6/2009	224.3	100	60	Topanga Formation (Ttss)/ Sandstone with Interbedded Siltstone
R-09-Z1B6	SR710-31	2/6/2009	332	100	100	Puente Formation (Tpsl)/ Siltstone with interbedded Sandstone
R-09-Z1B6	SR710-32	2/6/2009	330.5	100	100	Puente Formation (Tpsl)/ Siltstone with interbedded Sandstone
R-09-Z3B7	SR710-33	2/10/2009	252.5	97	50	Topanga Formation (Ttss)/ Sandstone with Interbedded Siltstone
R-09-Z3B7	SR710-34	2/10/2009	251	100	40	Topanga Formation (Ttss)/ Sandstone with Interbedded Siltstone
R-09-Z3B7	SR710-35	2/10/2009	271.6	93	0	Topanga Formation (Ttss)/ Sandstone with Interbedded Siltstone
R-09-Z3B7	SR710-36	2/10/2009	270.1	93	0	Topanga Formation (Ttss)/ Sandstone with Interbedded Siltstone
R-09-Z1B5	SR710-37	2/19/2009	278	100	100	Puente Formation (Tpss)/ Sandstone
R-09-Z1B5	SR710-38	2/19/2009	276.5	100	100	Puente Formation (Tpss)/ Sandstone
R-09-Z1B4	SR710-39	2/19/2009	332**	100	50	Puente Formation (Tpss)/ Sandstone and Siltstone
R-09-Z1B4	SR710-40	2/19/2009	330.5**	100	50	Puente Formation (Tpss)/ Sandstone and Siltstone
R-09-Z1B5	SR710-41	2/20/2009	347	20	20	Puente Formation (Tpss)/ Sandstone
R-09-Z1B5	SR710-42	2/20/2009	345.5	20	20	Puente Formation (Tpss)/ Sandstone
R-09-Z3B6	SR710-43	2/20/2009	132	20	8	Topanga Formation(Ttcg)/ Conglomerate
R-09-Z1B5	SR710-44	2/23/2009	398	100	90	Puente Formation (Tpss)/ Sandstone and Siltstone
R-09-Z1B5	SR710-45	2/23/2009	396.5	100	90	Puente Formation (Tpss)/ Sandstone and Siltstone
R-09-Z3B6	SR710-46	2/23/2009	168	44	0	Topanga Formation(Ttcg)/ Conglomerate
R-09-Z3B6	SR710-47	2/23/2009	166.5	44	0	Topanga Formation(Ttcg)/ Conglomerate
R-09-Z3B6	SR710-48	2/24/2009	188.2	98	30	Topanga Formation(Ttcg)/ Conglomerate

5.0 TEST PROCEDURE

The membrane was expanded by controlling the flow of compressed nitrogen into the pressuremeter, increasing the pressure in small steps until the membrane starts to expand against the borehole wall. Once the average strain of the borehole wall was greater than about 1.5% the pressure is reduced to no more than 40% of the maximum past pressure, then increased again.

The resulting unload-reload loop can be used to evaluate the elastic behavior of the material. In materials which behave in a linear manner, the loops will exhibit little hysteretic behavior. That is, the linear unloading path will follow the reloading path. The loops will be very tight.

The pressure is then advanced in steps until the strain is increased a further 3% before completing a second unload-reload cycle. In many tests the procedure is repeated until a third unload-reload loop is completed. If the disturbance is small, the slope of the loops will tend to be parallel. Figure 2, Test SR710-12, is a typical example.

After the strain exceeds 12%, the pressure is reduced to zero. Adjustments are made for the location of the unload-reload loops as well as the ending strain and pressure for each test based on the expertise of the field operator.

In strong materials such as that shown as SR710-42 (on the right in Fig. 2) the pressure is increased in pressure increments of about 300 to 400 psi.

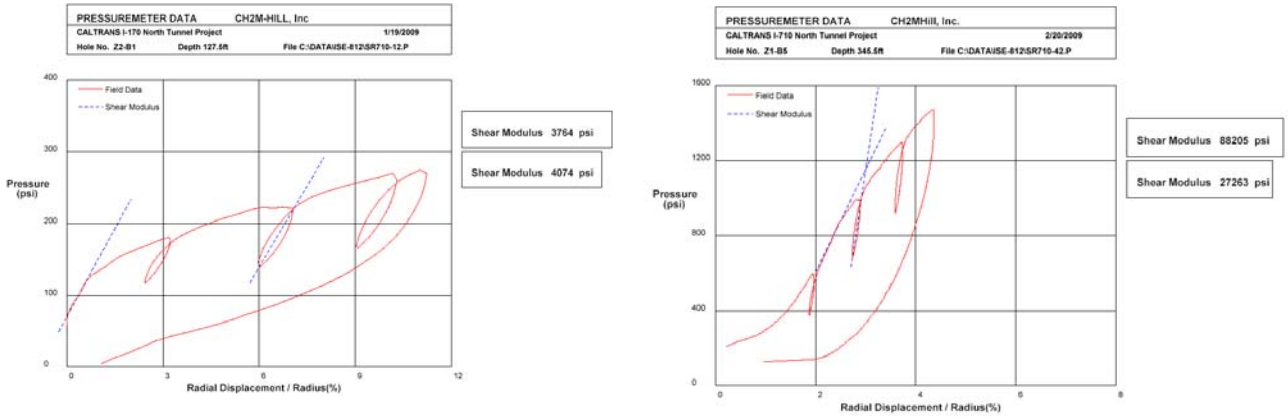

Test SR710-12 SR710-42

Fig. 2. Test SR710-12 and Tests SR710-42

(Test SR710-12 in R-09-Z2B1 at 127.5 ft and Test SR710-42 in R-09-Z1B5 at 345.5 ft)

6.0 QUALITY OF THE DATA

In general, the pressuremeter testing should reflect the material being tested. If the materials being tested are relatively uniform then adjacent tests should be similar in form. If adjacent tests are distinctly different, then either the material has changed, or some disturbance within the borehole has been encountered while performing the test.

Hence in a qualitative manner the results can be assessed as to whether the data reflects the *in-situ* material properties. In Figure 3 are two adjacent tests at 345.5 and 347 ft in Hole Z1-B5, in the same test pocket.

The maximum pressure reached in both tests is similar; in the order of 1,400 psi after a strain of about 3%. The shape of the final unloading curve, which is less influenced by the initial disturbance, is also similar in the two tests. Both these pieces of data would suggest the material at both locations is similar.

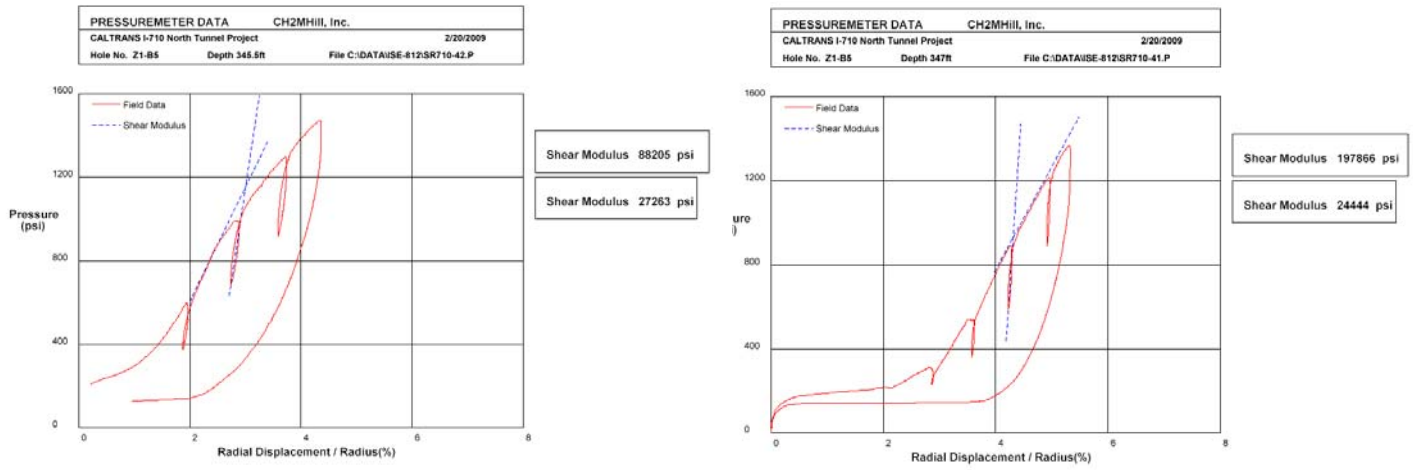

Fig. 3. Adjacent pressuremeter tests in same pilot hole

(SR710-42 at 345.5 ft and SR710-41 at 347 ft)

7.0 RANGE OF DATA

A variety of material types have been tested in this study. Typical tests examples of the strong and the weak materials are shown in Figure 4. For comparative purposes these tests have all been plotted to the same scale. The shear modulus, as represented by the slopes of the unload-reload loops (Section 9), is 90,000 psi, and 5,000 psi respectively. In terms of stiffness, these materials tested range over 18 to 1. The maximum range in this study ranges from 600,000 psi for Test 6 to 3,000 for Test 11; that is a 200 to 1 range.

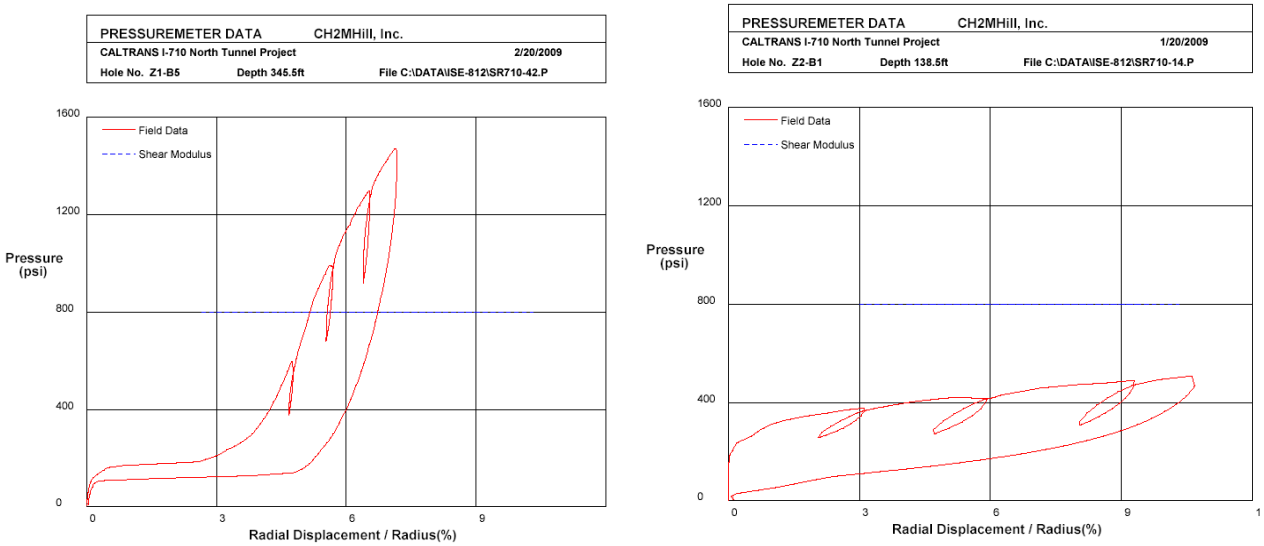

Fig. 4. Test in Sandstone (SR710-42) and Fractured Diorite (SR710-14)

8.0 STANDARD METHOD OF ANALYSIS OF THE SHEAR MODULUS

If the material surrounding the pressuremeter is assumed to extend to infinity, and assumed to behave as an idealized linear elastic, homogeneous material, which does not fail under shear or tension, then the displacement on the boundary of the pressuremeter, u_a, for a given pressure, P, is given by:

$$u_a = P(a)\,(1+\mu) / E \qquad 1)$$

where “E” is the Young’s Modulus, “a” the radius of the pressuremeter cavity, and “μ" the Poisson’s ratio. As the shear modulus, “G”, and the Young’s modulus, “E”, are related by the following relationship:

$$E=2(G)(1+\mu) \qquad 2)$$

Equation 1 reduces to:

$$u_a = 0.5P(a) / G \qquad 3)$$

Hence, the shear modulus G is given by:

$$G = 0.5 * \Delta \text{ Pressure} / \Delta(\text{radial displacement/radius}) \qquad 4)$$

The modulus for the average slope of the initial part of the pressuremeter curve (A-B in Fig.5) expressed as a Young’s modulus (assuming a Poisson's ratio of 0.33) is the same as the “pressuremeter modulus” defined in the American Society for Testing and Materials (ASTM) D4719, Section 9.5. In many tests a straight section in this part of the curve is not defined well enough to enable the modulus to be determined. However, the modulus determined from the unload-reload loops, which is often higher than the initial loading modulus, is more accurately defined and is probably more representative of the *in-situ* modulus for the material. This data is summarized in Table 2.

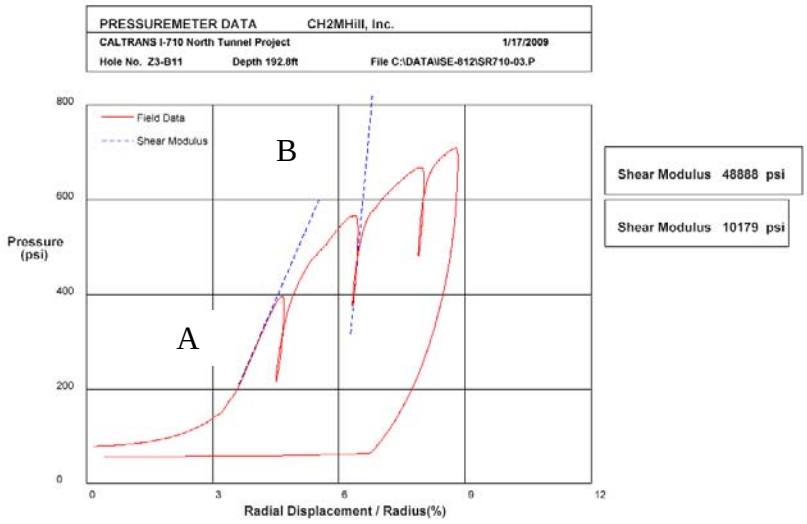

Fig. 5. Modulus determination for Test SR710-03

9.0 DETERMINATION OF THE LIMIT PRESSURE

From a visual inspection of the typical pressuremeter curve in the clay shown in Fig. 3, the pressure tends to a limit. For Test SR710-03 (Fig. 6) this limit pressure is in the range of 700 psi. To make this limit pressure a quantitative measurement, the limit pressure is defined as that pressure which occurs when the volume of the pressuremeter has doubled. However, few pressuremeter tests ever actually expand this far before reaching the limit of the strain sensing system. The pressuremeters used in this investigation will only expand to about 20% before the displacement limit is reached.

If the material being tested is assumed to behave as an elastic cohesive material, then the equation governing the pressure-displacement curve is given by:

$$P = P_L + (c)\log_e (u_a/_a) \qquad 5)$$

$$P_L = P_o + c + (c)\log_e [G/c] \qquad 6)$$

Where:

P_L" is the theoretical limit pressure at infinite expansion

"c" is the undrained cohesive strength,

"P_O" is the total *in-situ* lateral stress, and "G" is the shear modulus.

From Equation 5, a plot of pressure P against the log of u_a/a will be a straight line, provided the shear strength remains constant with strain. The slope of this line will provide a measure of the undrained shear strength, c. The Limit Pressure, as defined by the ASTM code D4719, Section 10.6, is the pressure at which the cavity has doubled in size. This doubling in size occurs when u_a/a is equal to 41%. (The origin of the strain used in the log/normal plots is the assumed origin at the *in-situ* stress state). If any disturbance is present, the above method of determining the cohesive strength usually provides an overly optimistic value. In Fig. 6, Test SR710-03 is plotted in the above manner. The above method applies to cohesive materials. However it can be used in granular materials to give an indication of the maximum or limit pressure that can be applied to the ground for the design of foundations. The shear strength determined by this method is not appropriate in granular materials.

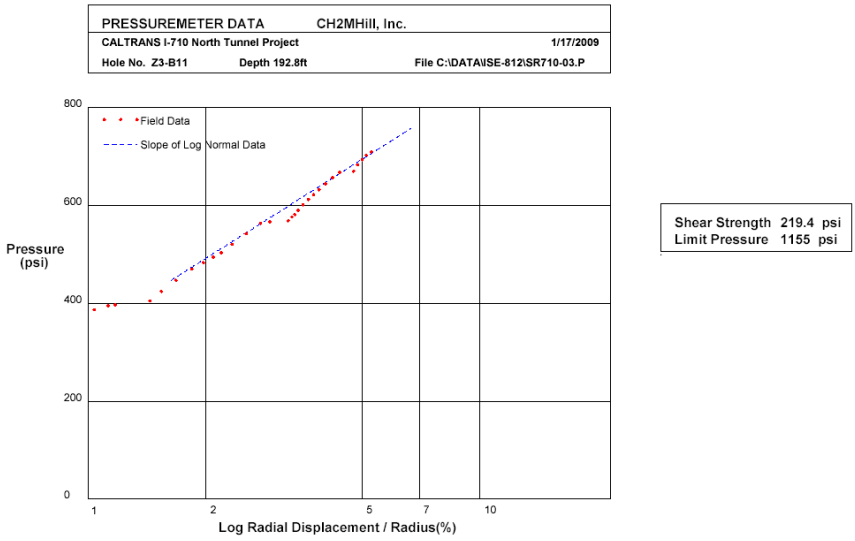

Fig. 6. Limit Pressure determination for Test SR710-03

Table 2 Limit Pressure shear modulus and Shear strength (log method): Tests 1-26

Test	Depth (ft)	Hole	Limit Pressure (psi)	Initial Shear modulus (psi)	Unload-reload Shear modulus (psi)	Shear strength (log method) (psi)
SR710-1	200.9	R-09-Z3B2	800	7,000	74,000	160
SR710-2	199.4	R-09-Z3B2	850	5,500	47,000	180
SR710-5	227	R-09-Z3B2	2,400	22,400	160,000	420
SR710-6	225	R-09-Z3B2	3,700	30,000	590,000	800
SR710-9	248	R-09-Z3B2	3,200	32,000	273,000	600
SR710-10	246.5	R-09-Z3B2	2,500	34,000	332,000	470
SR710-3	192.8	R-09-Z3B11	1,150	9,700	46,000	220
SR710-4	191.3	R-09-Z3B11	1,100	7,000	44,000	220
SR710-7	208.4	R-09-Z3B11	660	5,500	16,000	118
SR710-8	206.9	R-09-Z3B11	640	5,500	14,000	100
SR710-11	129	R-09-Z2B1	315	3,000	3,000	45
SR710-12	127.5	R-09-Z2B1	320	4,000	3,800	51
SR710-13	140	R-09-Z2B1	600	na	5,500	40
SR710-14	138.5	R-09-Z2B1	560	4,800	5,200	70
SR710-15	96.5	R-09-Z1B7	1,700	8,900	41,400	380
SR710-16	95	R-09-Z1B7	1,350	6,500	30,000	330
SR710-17	111.5	R-09-Z1B7	835	6,300	31,000	137
SR710-18	110	R-09-Z1B7	920	4,000	20,000	220
SR710-19	136	R-09-Z1B7	1,300	6,500	50,000	270
SR710-20	134.5	R-09-Z1B7	2,300	15,000	60,000	590
SR710-21	177.3	R-09-Z1B3	3,500	24,000	107,000	700
SR710-22	204	R-09-Z1B3	3,870	35,000	110,000	755
SR710-23	135.7	R-09-Z2B2	650	10,000	8,000	120
SR710-24	134.2	R-09-Z2B2	430	1,600	3,600	90
SR710-25	251	R-09-Z2B2	1,100	20,000	14,000	170
SR710-26	249.5	R-09-Z2B2	1,550	14,000	32,000	350

Table 2 cont. Limit Pressure shear modulus and Shear strength (log method): Tests 27-48

Test	Depth (ft)	Hole	Limit Pressure (psi)	Initial Shear modulus (psi)	Unload-reload Shear modulus (psi)	Shear strength (log method) (psi)
SR710-27	203	R-09-Z1B6	1,830	14,000	70,000	310
SR710-28	245	R-09-Z1B6	2,600	56,000	140,000	370
SR710-31	332	R-09-Z1B6	3,000	48,000	130,000	470
SR710-32	330.5	R-09-Z1B6	2,800	34,000	80,000	540
SR710-29	225.8	R-09-Z3B7	1,550	8,600	97,000	320
SR710-30	224.3	R-09-Z3B7	1,500	5,200	57,000	350
SR710-33	252.5	R-09-Z3B7	2,500	15,000	225,000	470
SR710-34	251	R-09-Z3B7	1,600	7,800	74,000	354
SR710-35	271.6	R-09-Z3B7	1,400	9,000	76,000	290
SR710-36	270.1	R-09-Z3B7	1,600	7,000	45,000	330
SR710-37	278	R-09-Z1B5	6,000	47,000	250,000	1,280
SR710-38	276.5	R-09-Z1B5		hole too large		
SR710-41	347	R-09-Z1B5	3,700	24,000	200,000	830
SR710-42	345.5	R-09-Z1B5	3,200	27,000	88,000	670
SR710-44	398	R-09-Z1B5	2,300	16,000	84,000	500
SR710-45	396.5	R-09-Z1B5		hole too large		
SR710-39	332	R-09-Z1B4	4,500	45,000	225,000	1,000
SR710-40	330.5	R-09-Z1B4	5,000	39,000	220,000	930
SR710-43	132	R-09-Z3B6	3,700	26,000	283,000	750
SR710-46	168	R-09-Z3B6	>2,000	69,000	450,000	>1,000
SR710-47	166.5	R-09-Z3B6	7,000	56,000	280,000	1,600
SR710-48	188.2	R-09-Z3B6	6,500	61,000	323,000	1,400

10.0 DETERMINATION OF THE STRENGTH PROPERTIES

The PMT data can sometimes be used directly to determine the *in-situ* material properties such as the cohesive strength and the friction angle. To do so, a material model and failure mechanism must be assumed. If it is assumed that the material behaves in an ideal manner, in that the material deforms at constant volume throughout the test, i.e. it does not consolidate or dilate, and the shear strength remains constant, the pressuremeter curve can be interpreted by simple analytical means. The slope of the plot of pressure against the log of the strain can be used to give a direct measure of the shear strength, as discussed in Section 8. Unfortunately, real materials do not quite behave in this manner, and the shear strength determined by this method may not be accurate, particularly in disturbed material, in materials which degrade or partial tests in an enlarged hole. The shear strength determined by plotting on a log scale is not appropriate in frictional materials. However, this method of analysis often forms a basis of rating all materials.

A more realistic method of determining the shear strength in clays is to compare the field PMT data with an ideal model pressuremeter curve based on an assumed set of material parameters. If, for instance, the material is assumed to be cohesive and fails at constant shear strength and at constant volume, then the material parameters required for this model are the shear strength, lateral stress, and shear modulus. Adjustments can be made to those three parameters until a mathematical curve can be fitted to the field data. (Fig. 7 is an example for test SR710-14) Judgment is required to adjust these three parameters to determine the best fit to the data, particularly if there is disturbance present.

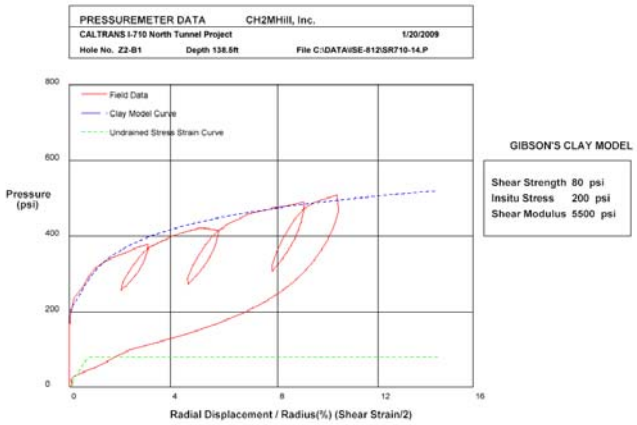

Fig. 7. Simple constant shear strength model analysis for test SR710-14

In the frictional materials, if it is assumed that it has a constant friction angle and no cohesion, then a simple model can be used to compare with the field data. Test SR710-03 which is probably a frictional material and not a cohesive material is analyzed in this manner in Fig. 8.

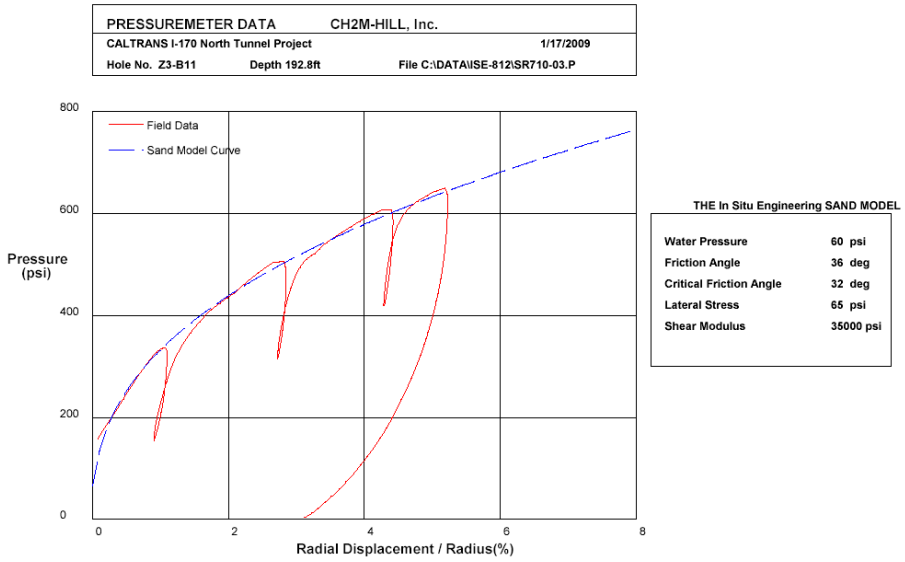

Fig. 8. Frictional Model for Test SR710-03

In rock, if it is assumed to be a cohesive material, then a possible model can be developed which uses the initial modulus, as illustrated in Fig 9a. This gives a shear strength of 420 psi. The strength determined in this manner is above that derived by the log method, which give a strength of 380 psi. In dense clays a better modulus to use is the modulus derived from the unload-reload curve. The ideal pressuremeter curve derived for this model is a poor fit to the field data (Fig 9b). However, the strength is lower; it has a minimum value of 240 psi. Hence to gain some understanding of the shear strength, the tests have been analyzed with three methods; the log method and two model methods using the initial shear modulus and the unload-reload shear modulus. Shear Strength values and friction angles are presented in Table 3.

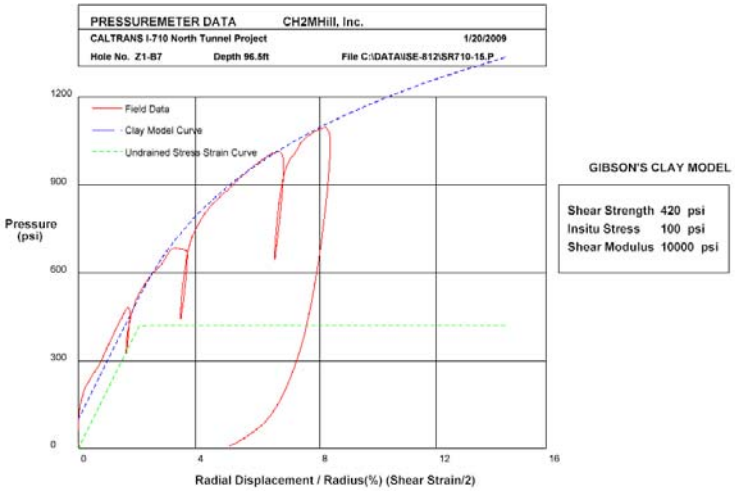

Fig 9a Initial shear modulus

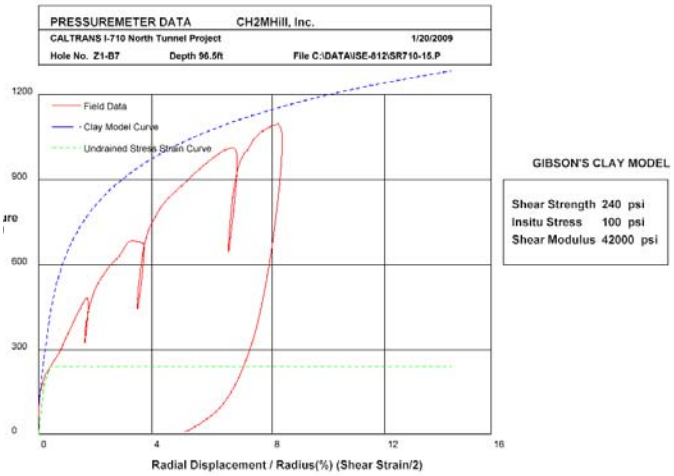

Fig 9b Unload-reload shear modulus

Fig. 9. Cohesive Models for Test SR710-15

Table 3 Material properties from Model Analysis: Tests 1-26

Test	Depth (ft)	Hole	Shear strength (model initial modulus) (psi) (Maximum)	Shear strength (model unloading modulus) (psi) (Minimum)	Shear strength log method) (psi)	Friction (model)
SR710-1	200.9	R-09-Z3B2	120	50	160	
SR710-2	199.4	R-09-Z3B2	120	50	180	
SR710-5	227	R-09-Z3B2	550	220	420	
SR710-6	225	R-09-Z3B2	900	250	800	
SR710-9	248	R-09-Z3B2	700	250	600	
SR710-10	246.5	R-09-Z3B2	400	170	470	
SR710-3	192.8	R-09-Z3B11	230	140	220	36
SR710-4	191.3	R-09-Z3B11	230	130	220	
SR710-7	208.4	R-09-Z3B11	100	50	118	
SR710-8	206.9	R-09-Z3B11	100	50	100	
SR710-11	129	R-09-Z2B1	45	na	45	
SR710-12	127.5	R-09-Z2B1	50	na	51	
SR710-13	140	R-09-Z2B1	60	na	40	
SR710-14	138.5	R-09-Z2B1	80	na	70	
SR710-15	96.5	R-09-Z1B7	420	240	380	
SR710-16	95	R-09-Z1B7	400	200	330	40
SR710-17	111.5	R-09-Z1B7	190	90	137	
SR710-18	110	R-09-Z1B7	250	110	220	
SR710-19	136	R-09-Z1B7	280	150	270	
SR710-20	134.5	R-09-Z1B7	>600	na	590	
SR710-21	177.3	R-09-Z1B3	800	400	700	
SR710-22	204	R-09-Z1B3	850	450	755	
SR710-23	135.7	R-09-Z2B2	110	na	120	
SR710-24	134.2	R-09-Z2B2	80	na	90	
SR710-25	251	R-09-Z2B2	200	na	170	
SR710-26	249.5	R-09-Z2B2	350	250	350	

Table 3 cont. Material properties from Model Analysis: Tests 27-48

Test	Depth (ft)	Hole	Shear strength (model initial modulus) (psi) (Maximum)	Shear strength (model unloading modulus) (psi) (Minimum)	Shear strength log method) (psi)	Friction (model)
SR710-27	203	R-09-Z1B6	>600	na	310	
SR710-28	245	R-09-Z1B6	400	320	370	
SR710-31	332	R-09-Z1B6	600	300	470	
SR710-32	330.5	R-09-Z1B6	525	350	540	
SR710-29	225.8	R-09-Z3B7	450	170	320	
SR710-30	224.3	R-09-Z3B7	370	150	350	
SR710-33	252.5	R-09-Z3B7	700	250	470	
SR710-34	251	R-09-Z3B7	450	150	354	
SR710-35	271.6	R-09-Z3B7			290	35
SR710-36	270.1	R-09-Z3B7			330	
SR710-37	278	R-09-Z1B5	1,200	na	1,280	
SR710-38	276.5	R-09-Z1B5				
SR710-41	347	R-09-Z1B5	1,000	na	830	
SR710-42	345.5	R-09-Z1B5	700	na	670	42
SR710-44	398	R-09-Z1B5	650	250	500	
SR710-45	396.5	R-09-Z1B5				
SR710-39	332	R-09-Z1B4	800	na	1,000	39
SR710-40	330.5	R-09-Z1B4	1,100	na	930	
SR710-43	132	R-09-Z3B6	900	400	750	
SR710-46	168	R-09-Z3B6	1,000	350	>1,000	
SR710-47	166.5	R-09-Z3B6	750	350	1,600	
SR710-48	188.2	R-09-Z3B6	750	na	1,400	

11.0 CONCLUSIONS

The objective of this study was to examine the rock properties over an extensive area of proposed routes for the North Tunnel for Interstate I-710. In this analysis the modulus has been considered for each test and some indication of the shear strength has been obtained based on a simple model. In materials that seem to be behaving in a frictional manner, a friction angle has been determined. Once the tunnel alignment has been selected, further analysis could be undertaken to obtain a more complete understanding of the material behavior for tests within range.

12.0 REFERENCES

Mair, R.J. and Wood, D.M. 1987. Pressuremeter testing: methods and interpretation. CIRIA Ground Engineering Report. Butterworths, London.

ASTM D4719. 2007. Standard tests method for pressuremeter testing in soils.

Appendix I - Pressuremeter Data and Standard Interpretation

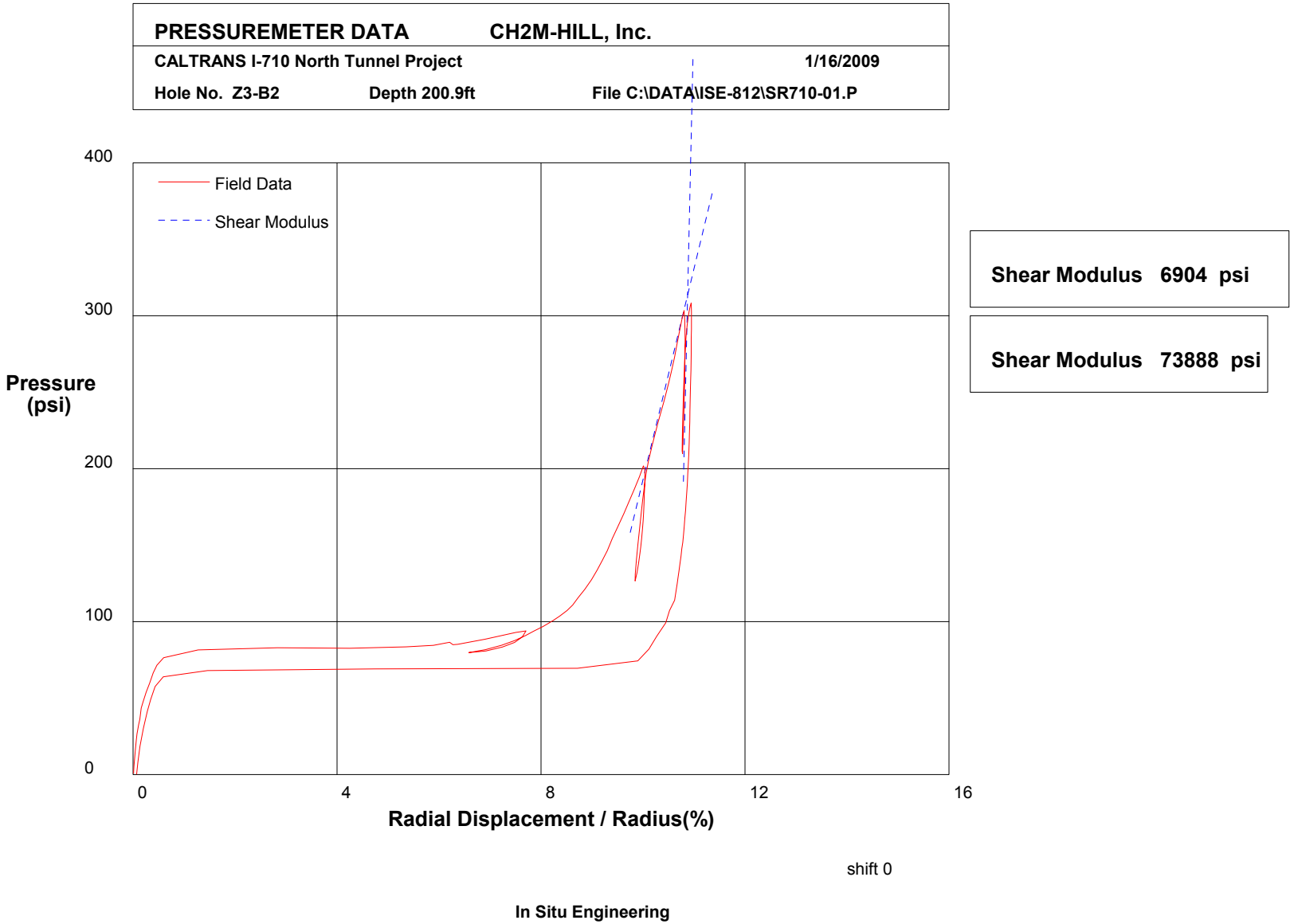

Appendix I - Pressuremeter Data and Standard Interpretation

PRESSUREMETER DATA **CH2MHill, Inc.**

CALTRANS I-710 North Tunnel Project **1/16/2009**

Hole No. Z3-B2 **Depth 200.9ft** **File C:\DATA\ISE-812\SR710-01.P**

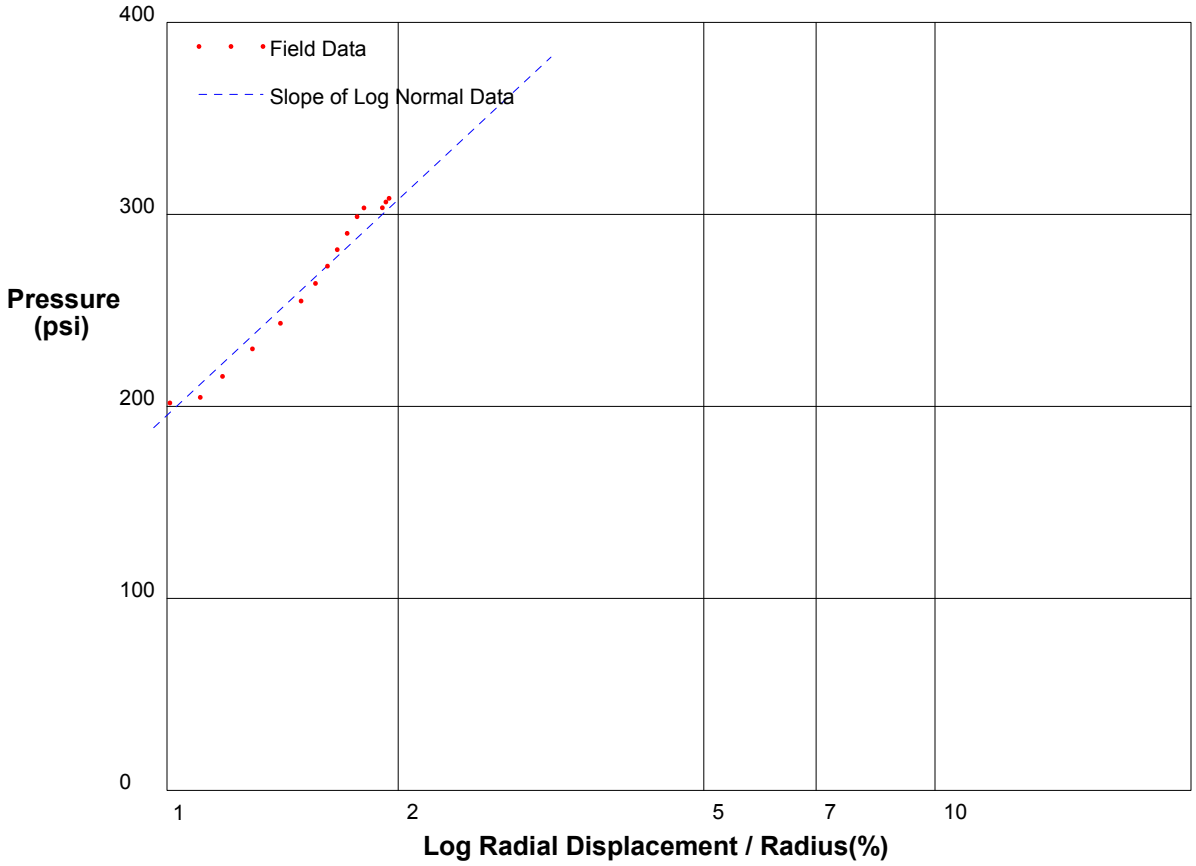

Shear Strength 162 psi
Limit Pressure 797 psi

shift 9

In Situ Engineering

Appendix I - Pressuremeter Data and Standard Interpretation

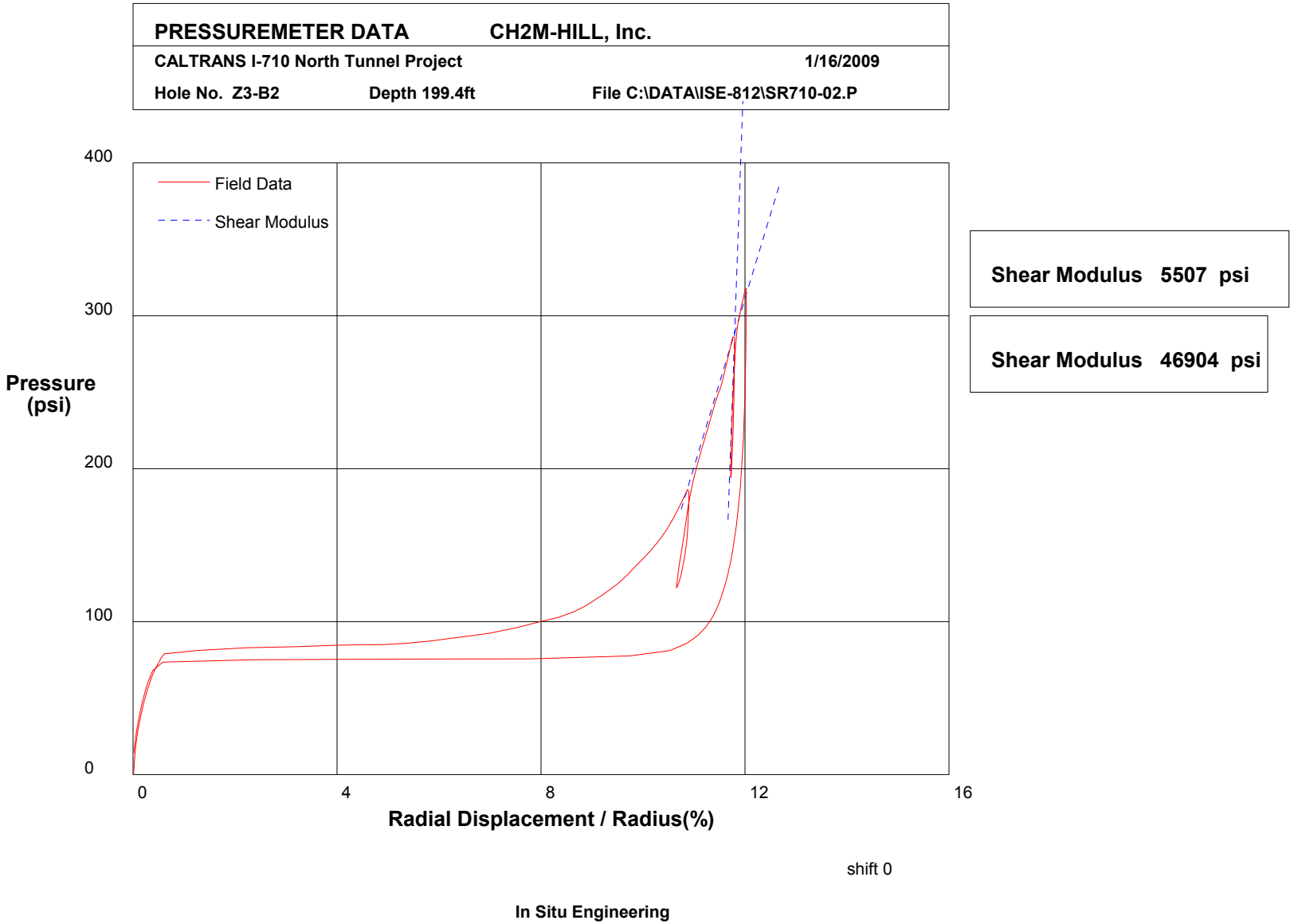

Appendix I - Pressuremeter Data and Standard Interpretation

PRESSUREMETER DATA **CH2MHill, Inc.**

CALTRANS I-710 North Tunnel Project **1/16/2009**

Hole No. Z3-B2 **Depth 199.4ft** **File C:\DATA\ISE-812\SR710-02.P**

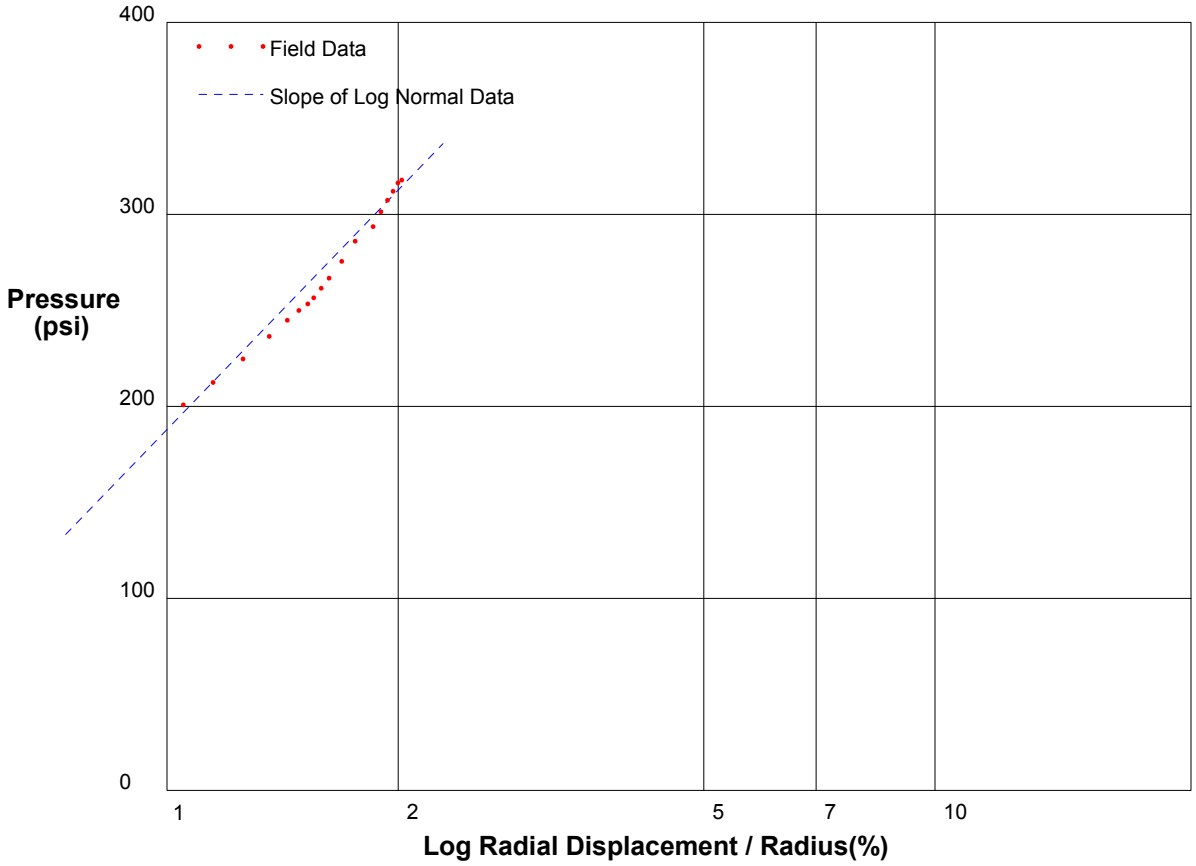

Shear Strength 179.8 psi
Limit Pressure 855 psi

shift 10

In Situ Engineering

Appendix I - Pressuremeter Data and Standard Interpretation

PRESSUREMETER DATA **CH2M-HILL, Inc.**

CALTRANS I-170 North Tunnel Project **1/17/2009**

Hole No. Z3-B11 **Depth 192.8ft** **File C:\DATA\ISE-812\SR710-03.P**

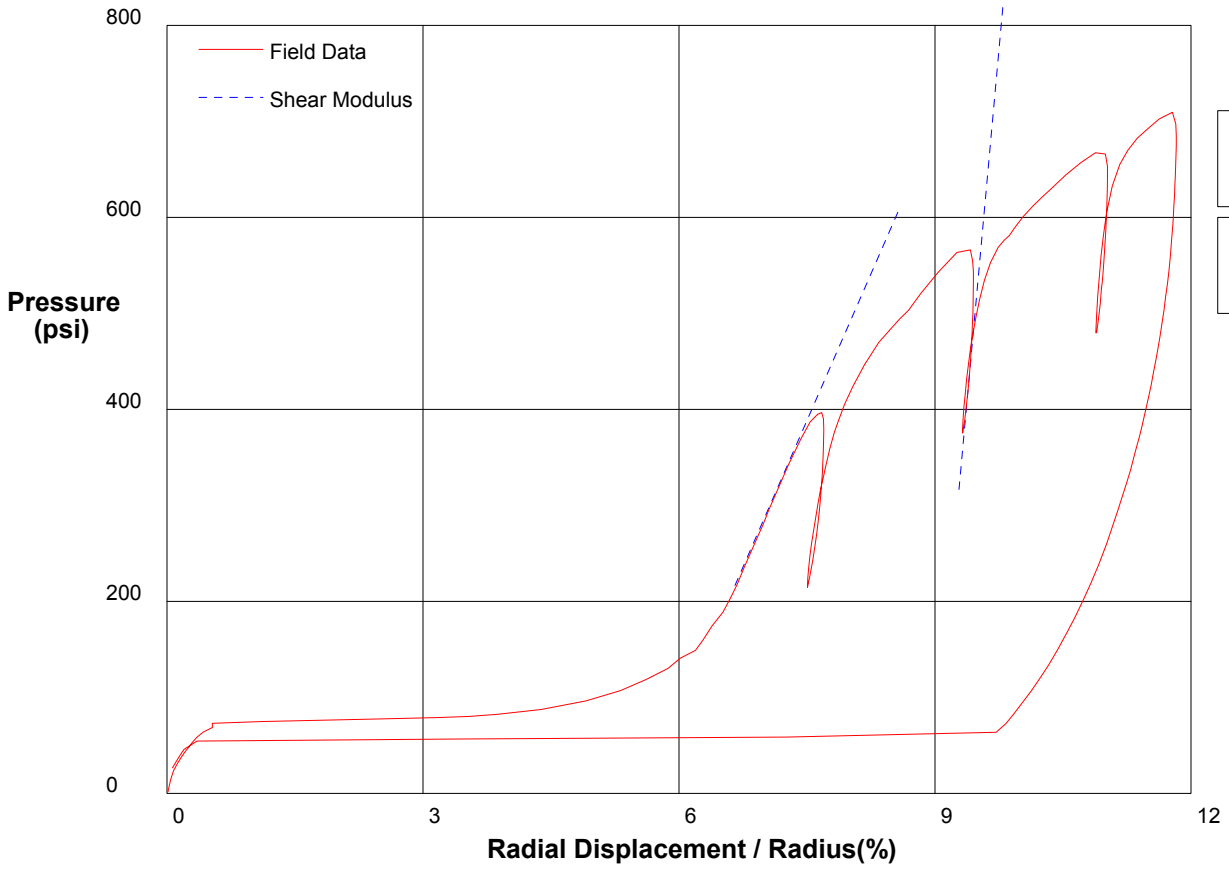

Shear Modulus 48888 psi

Shear Modulus 10179 psi

shift 0

In Situ Engineering

Appendix I - Pressuremeter Data and Standard Interpretation

PRESSUREMETER DATA **CH2MHill, Inc.**

CALTRANS I-710 North Tunnel Project **1/17/2009**

Hole No. Z3-B11 **Depth 192.8ft** **File C:\DATA\ISE-812\SR710-03.P**

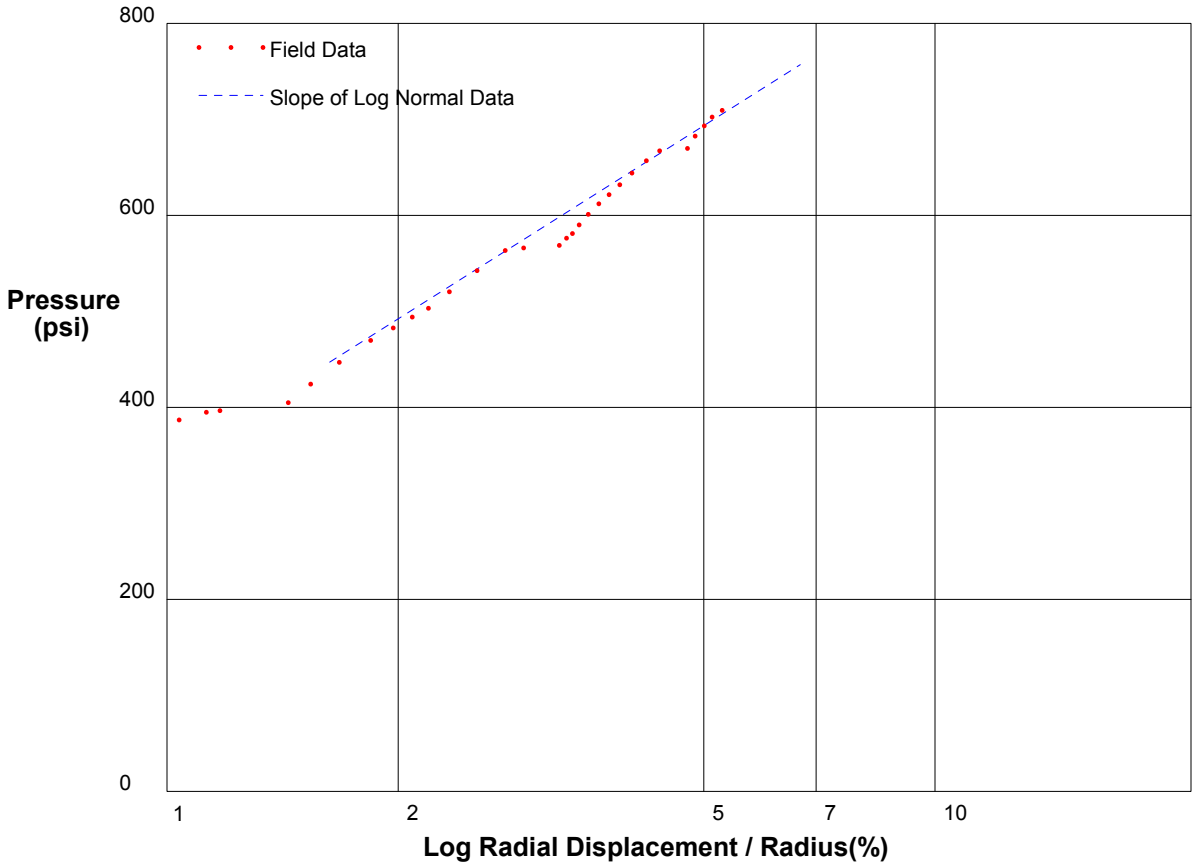

Shear Strength 219.4 psi
Limit Pressure 1155 psi

shift 6.5

In Situ Engineering

Appendix I - Pressuremeter Data and Standard Interpretation

PRESSUREMETER DATA **CH2M-HILL, Inc.**

CALTRANS I-710 North Tunnel Project **1/17/2009**

Hole No. Z3-B11 **Depth 191.3ft** **File C:\DATA\ISE-812\SR710-04.P**

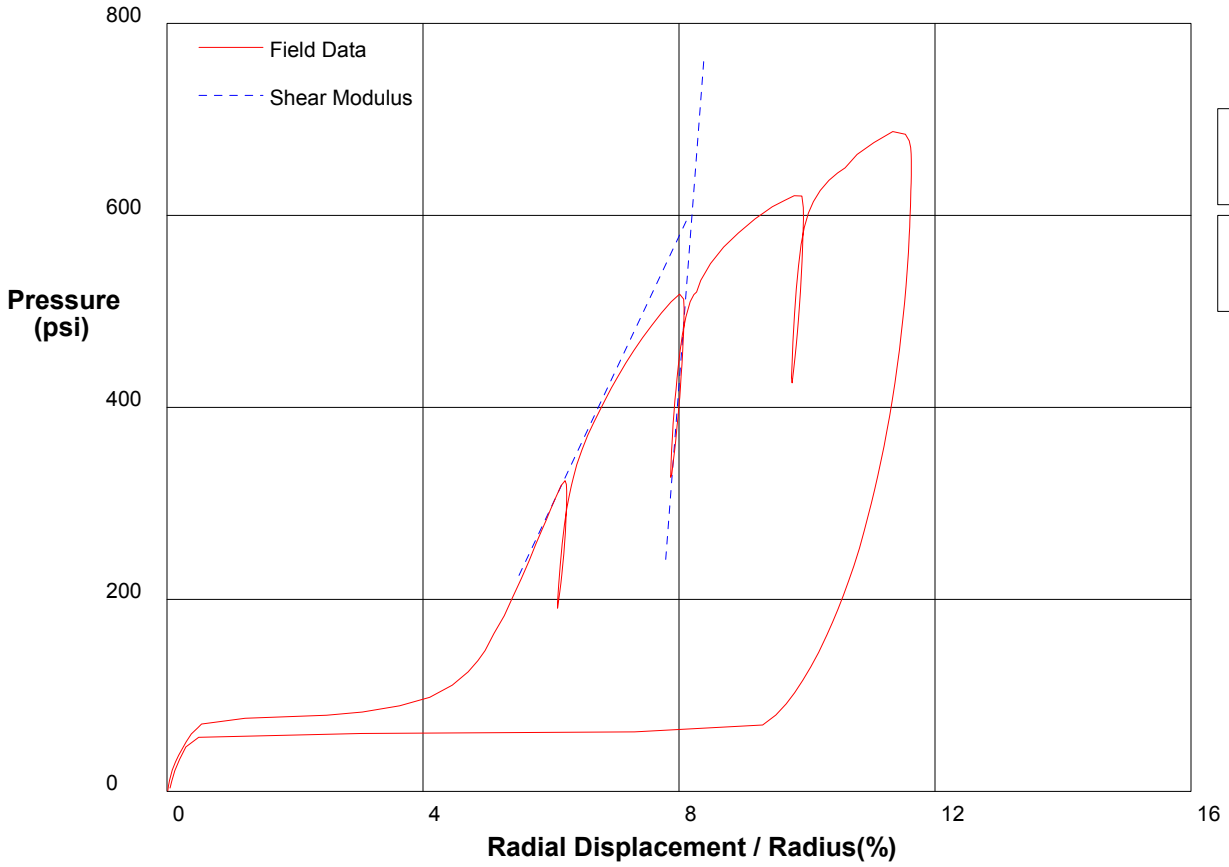

Shear Modulus 7060 psi

Shear Modulus 43563 psi

shift 0

In Situ Engineering

Appendix I - Pressuremeter Data and Standard Interpretation

PRESSUREMETER DATA **CH2MHill, Inc.**

CALTRANS I-710 North Tunnel Project **1/17/2009**

Hole No. Z3-B11 **Depth 191.3ft** **File C:\DATA\ISE-812\SR710-04.P**

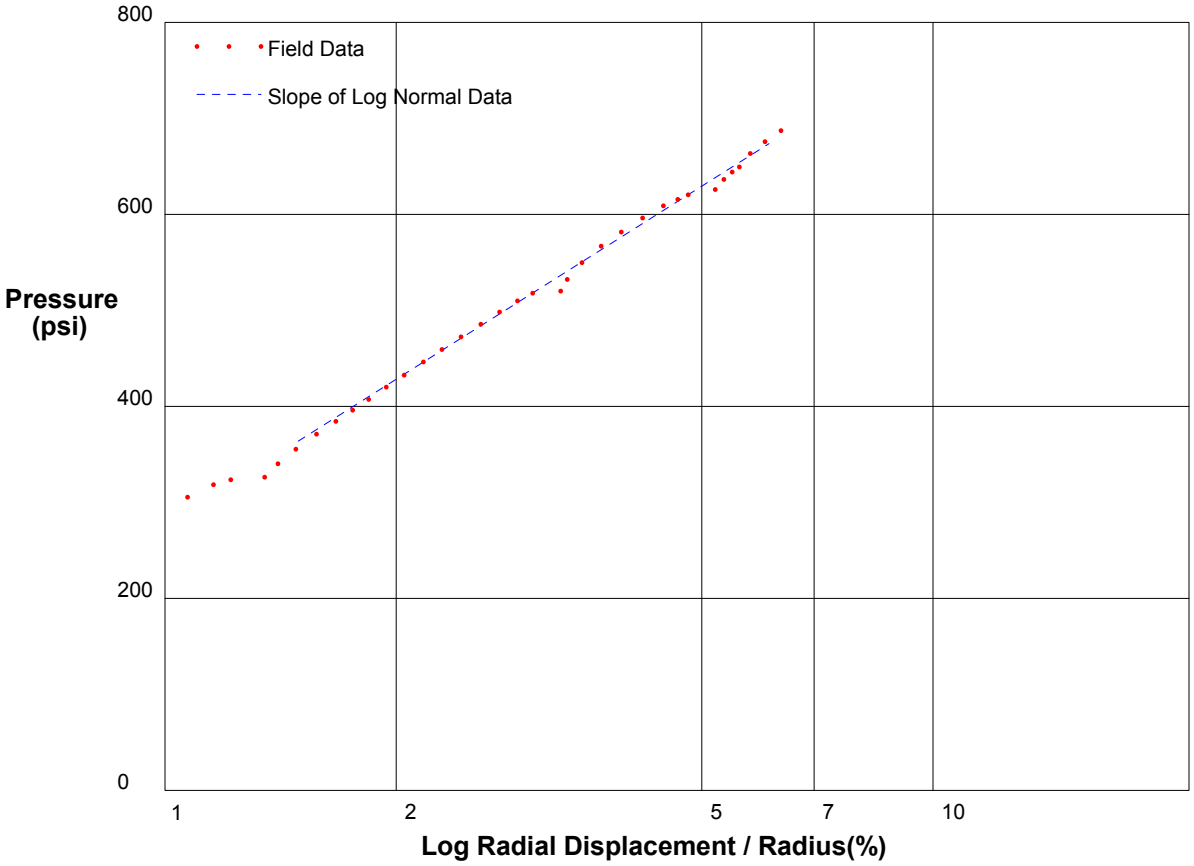

Shear Strength 219.4 psi
Limit Pressure 1091 psi

shift 5

In Situ Engineering

Appendix I - Pressuremeter Data and Standard Interpretation

PRESSUREMETER DATA **CH2M-HILL, Inc.**

CALTRANS I-710 North Tunnel Project **1/17/2009**

Hole No. Z3-B2 **Depth 227ft** **File C:\DATA\ISE-812\SR710-05.P**

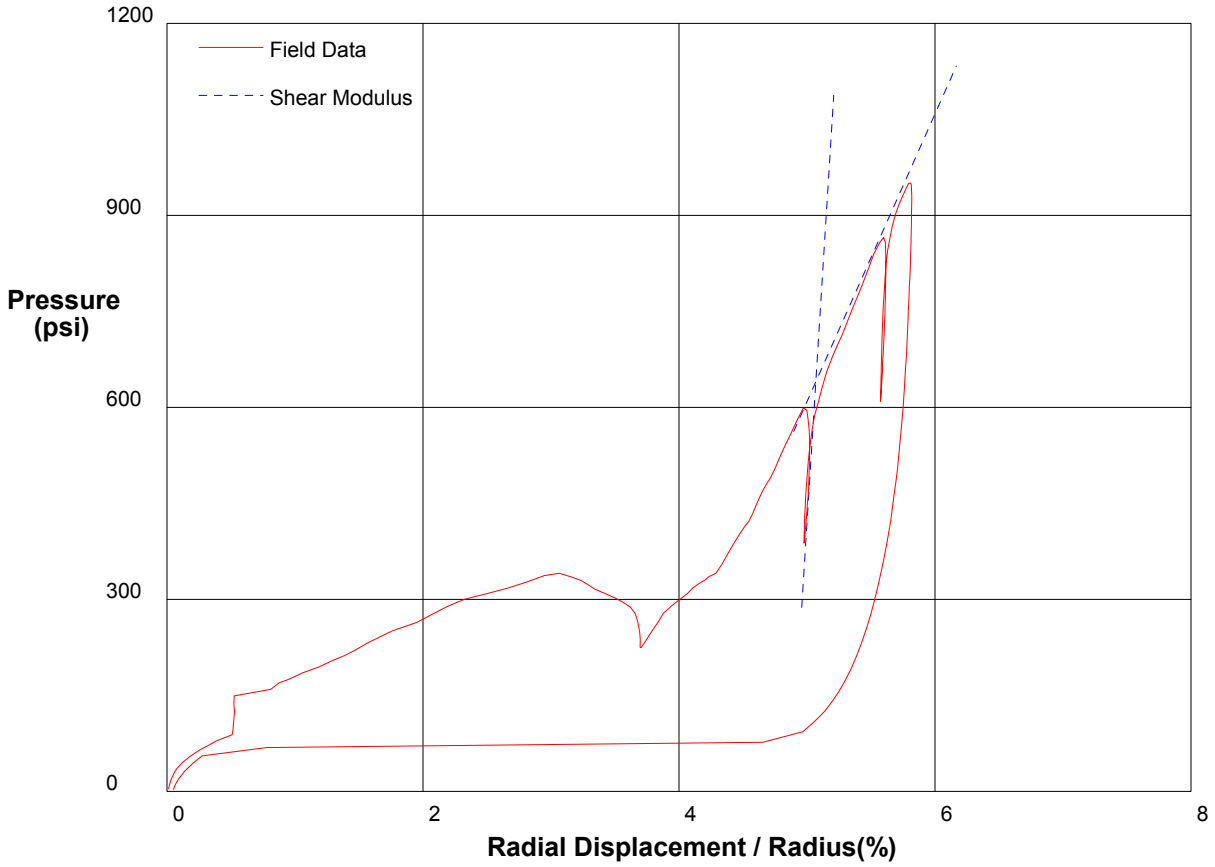

Shear Modulus 22459 psi

Shear Modulus 160000 psi

shift 0

In Situ Engineering

Appendix I - Pressuremeter Data and Standard Interpretation

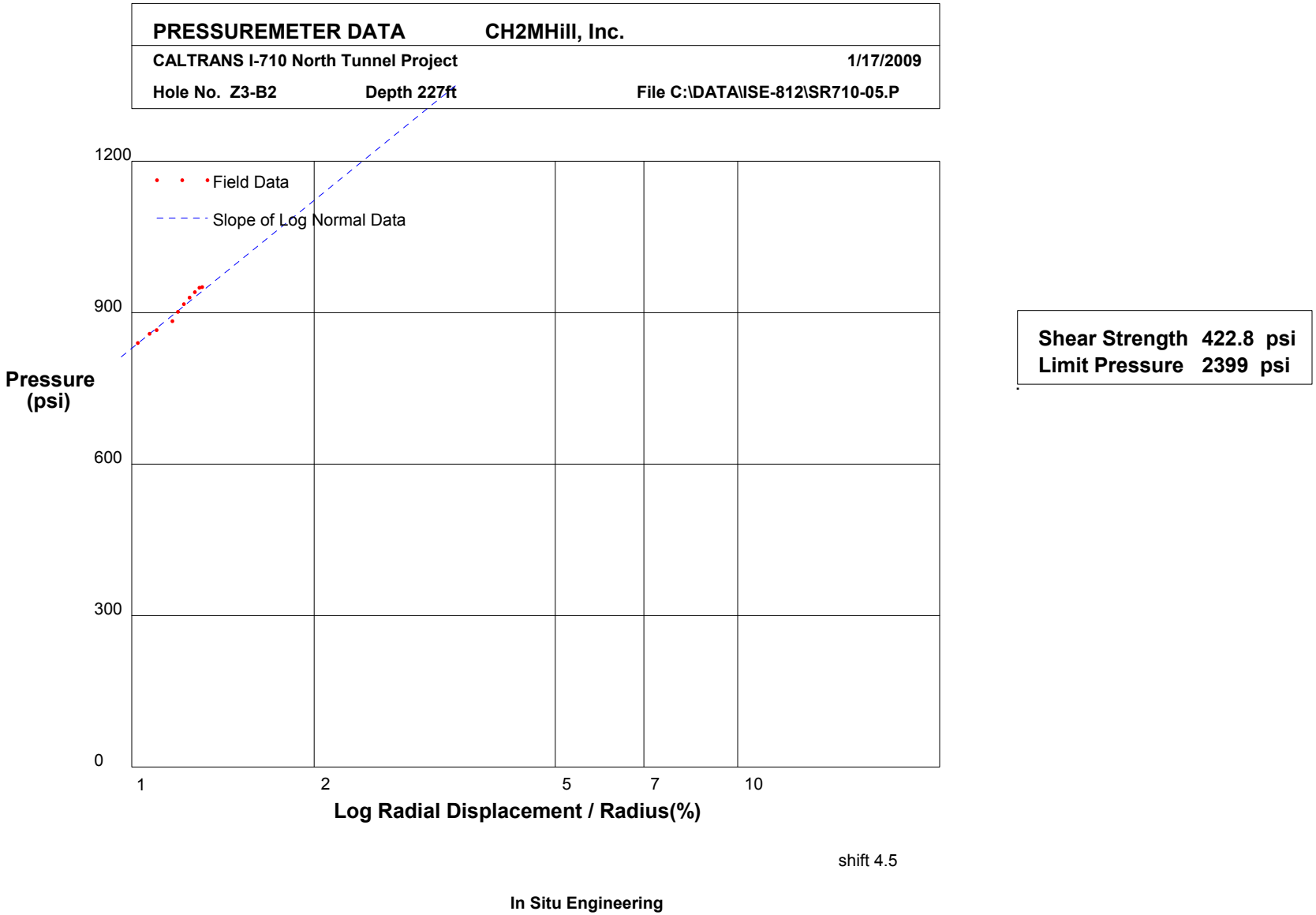

Appendix I - Pressuremeter Data and Standard Interpretation

PRESSUREMETER DATA **CH2M-HILL, Inc.**

CALTRANS I-710 North Tunnel Project **1/17/2009**

Hole No. Z3-B2 **Depth 225ft** **File C:\DATA\ISE-812\SR710-06.P**

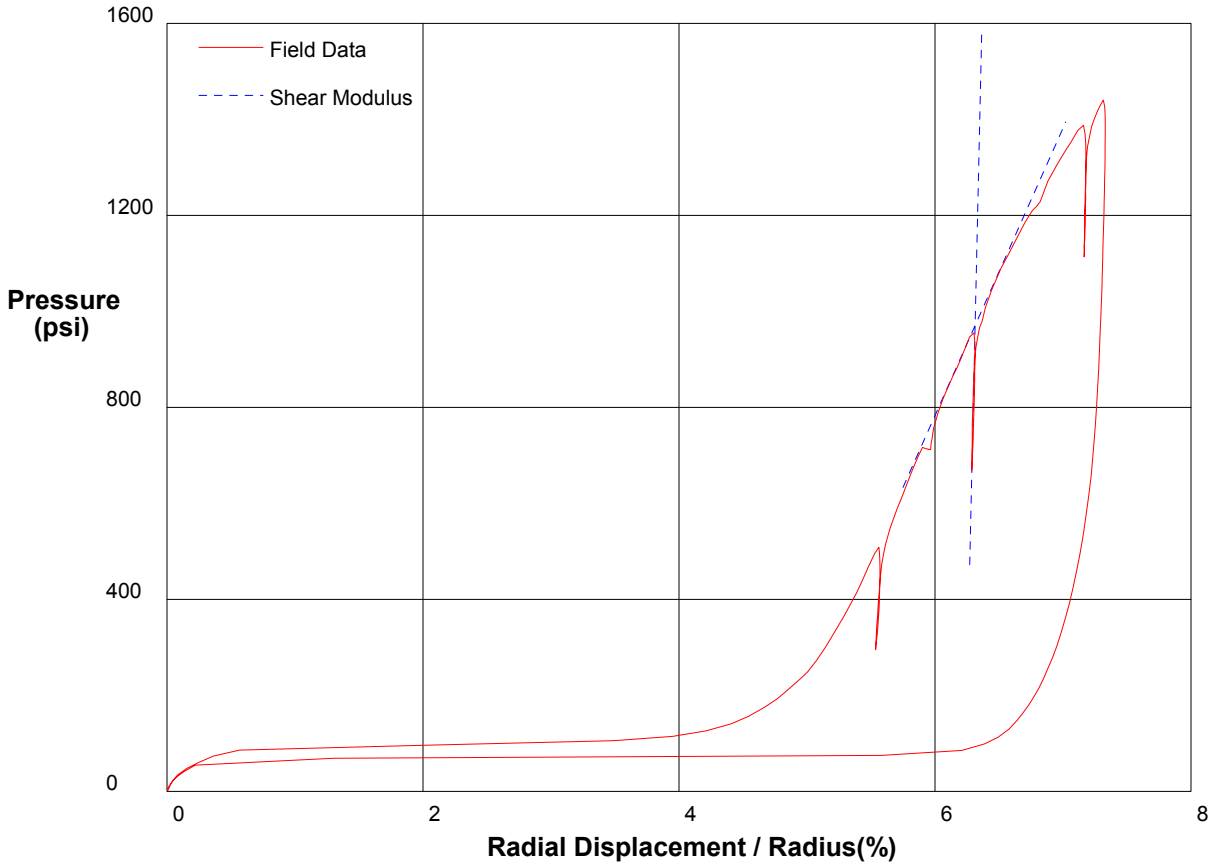

Shear Modulus 29945 psi

Shear Modulus 591111 psi

shift 0

In Situ Engineering

Appendix I - Pressuremeter Data and Standard Interpretation

PRESSUREMETER DATA **CH2MHill, Inc.**

CALTRANS I-710 North Tunnel Project **1/17/2009**

Hole No. Z3-B2 **Depth 225ft** **File C:\DATA\ISE-812\SR710-06.P**

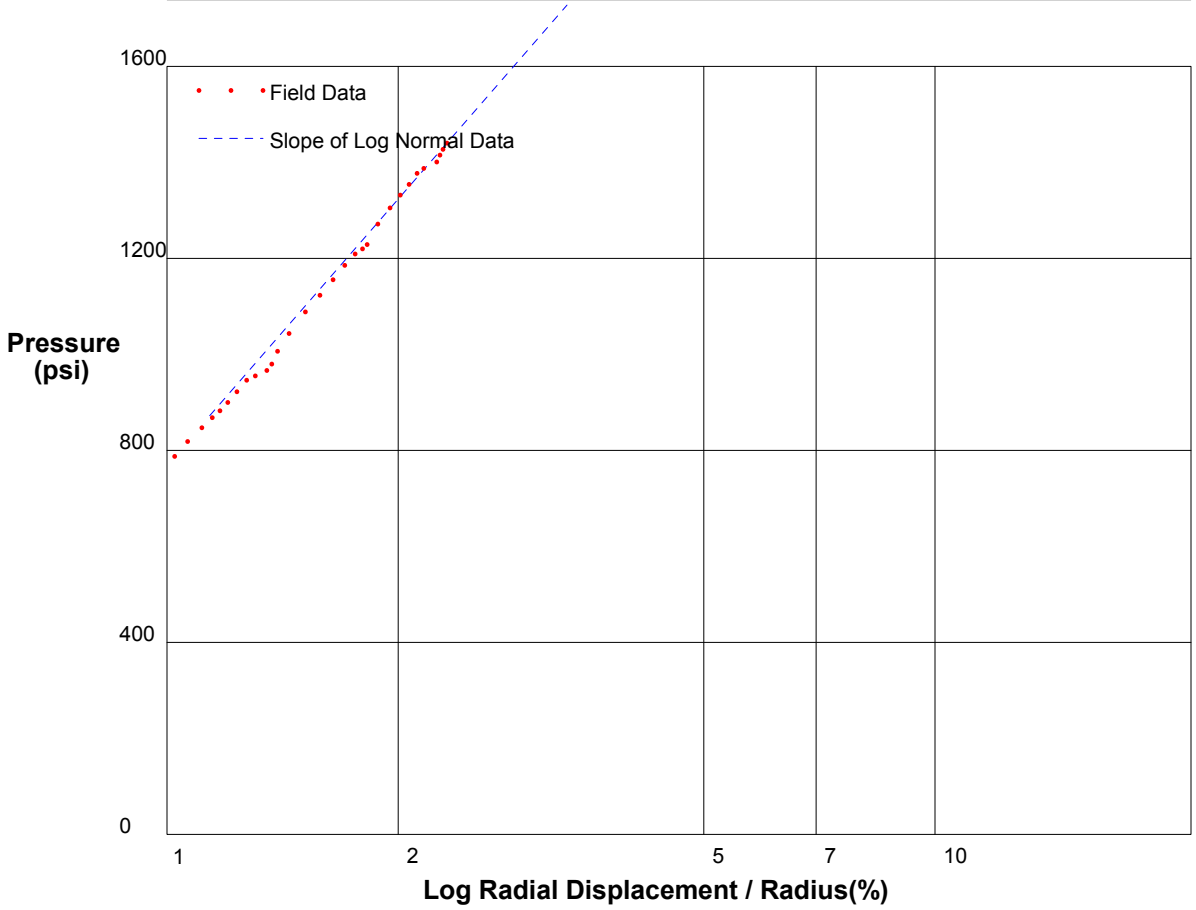

Shear Strength 798.5 psi
Limit Pressure 3735 psi

shift 5

In Situ Engineering

Appendix I - Pressuremeter Data and Standard Interpretation

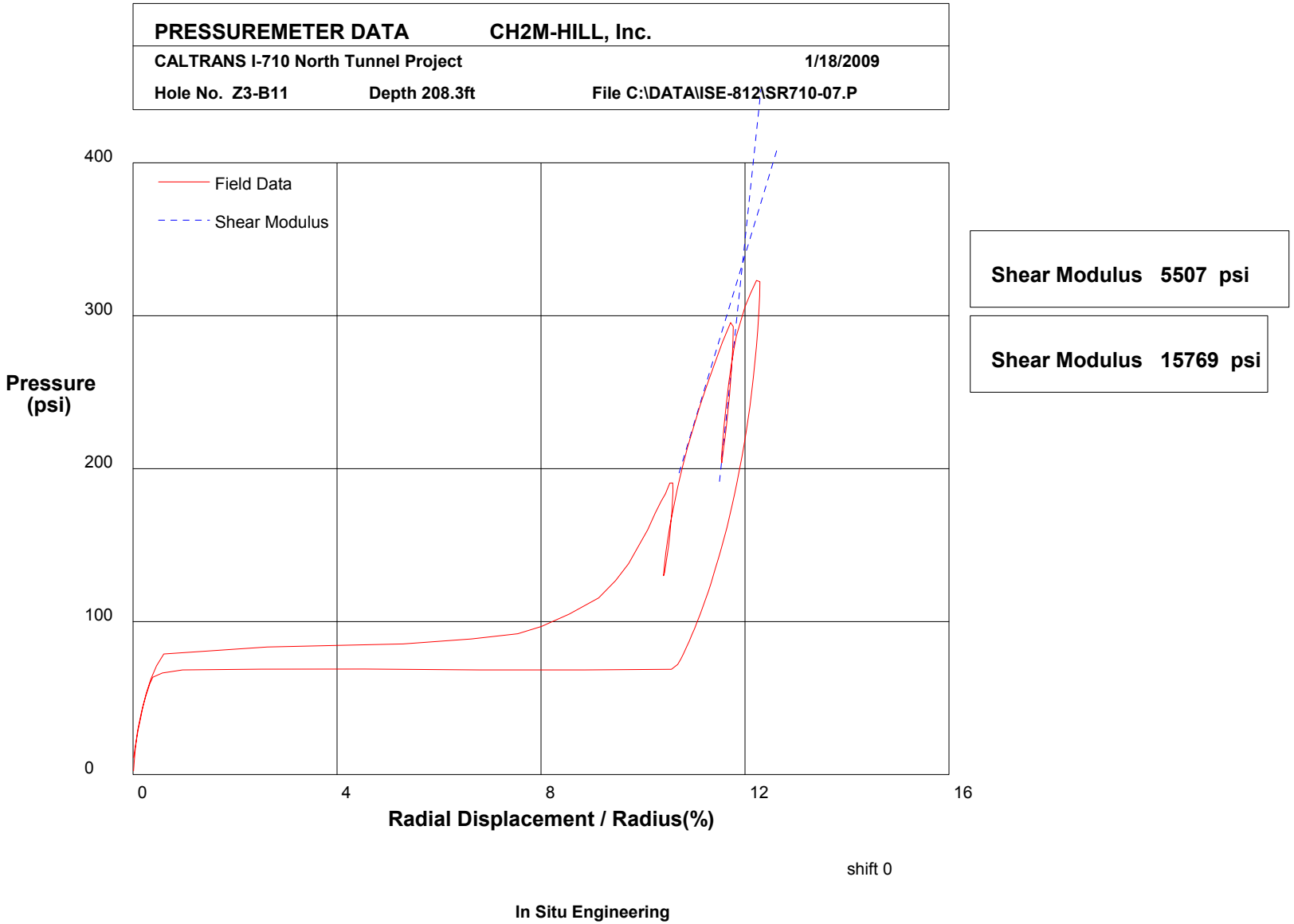

Appendix I - Pressuremeter Data and Standard Interpretation

PRESSUREMETER DATA **CH2MHill, Inc.**

CALTRANS I-710 North Tunnel Project **1/18/2009**

Hole No. Z3-B11 **Depth 208.3ft** **File C:\DATA\ISE-812\SR710-07.P**

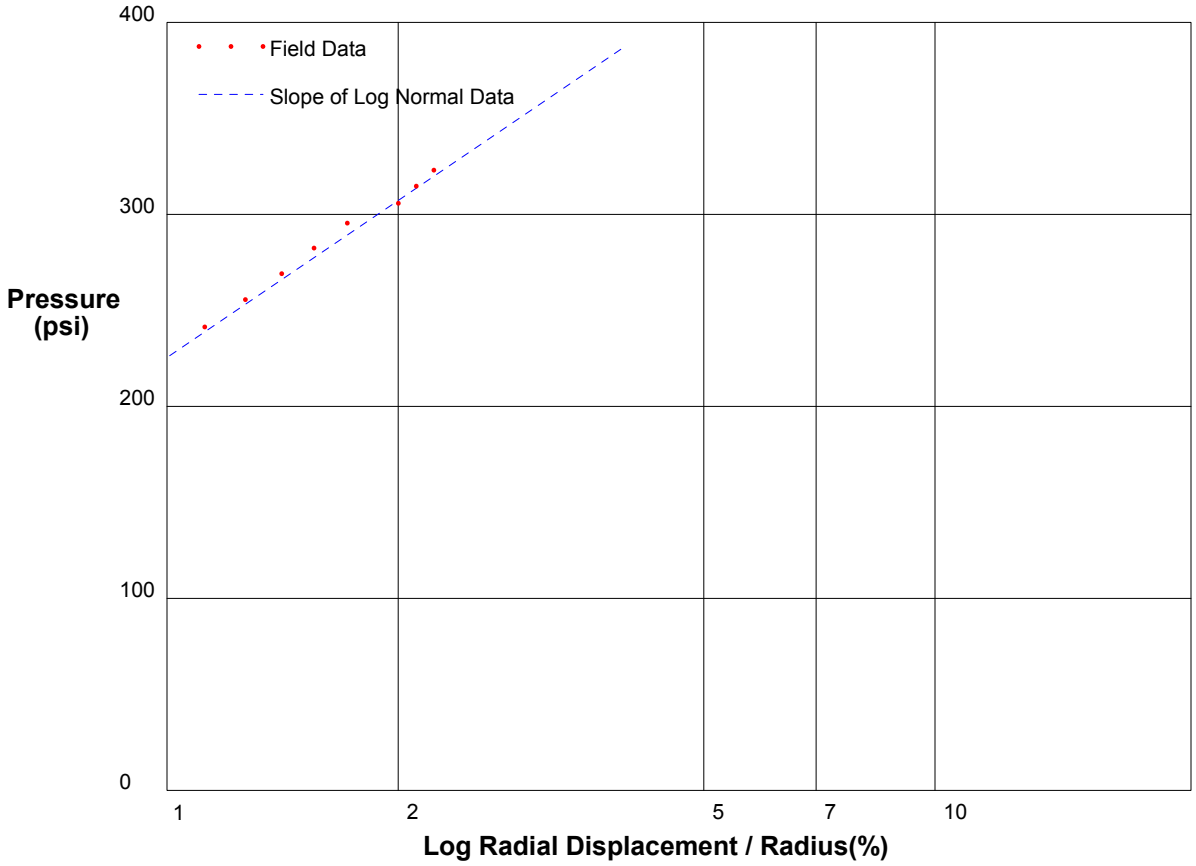

Shear Strength 118 psi
Limit Pressure 663 psi

shift 10

In Situ Engineering

Appendix I - Pressuremeter Data and Standard Interpretation

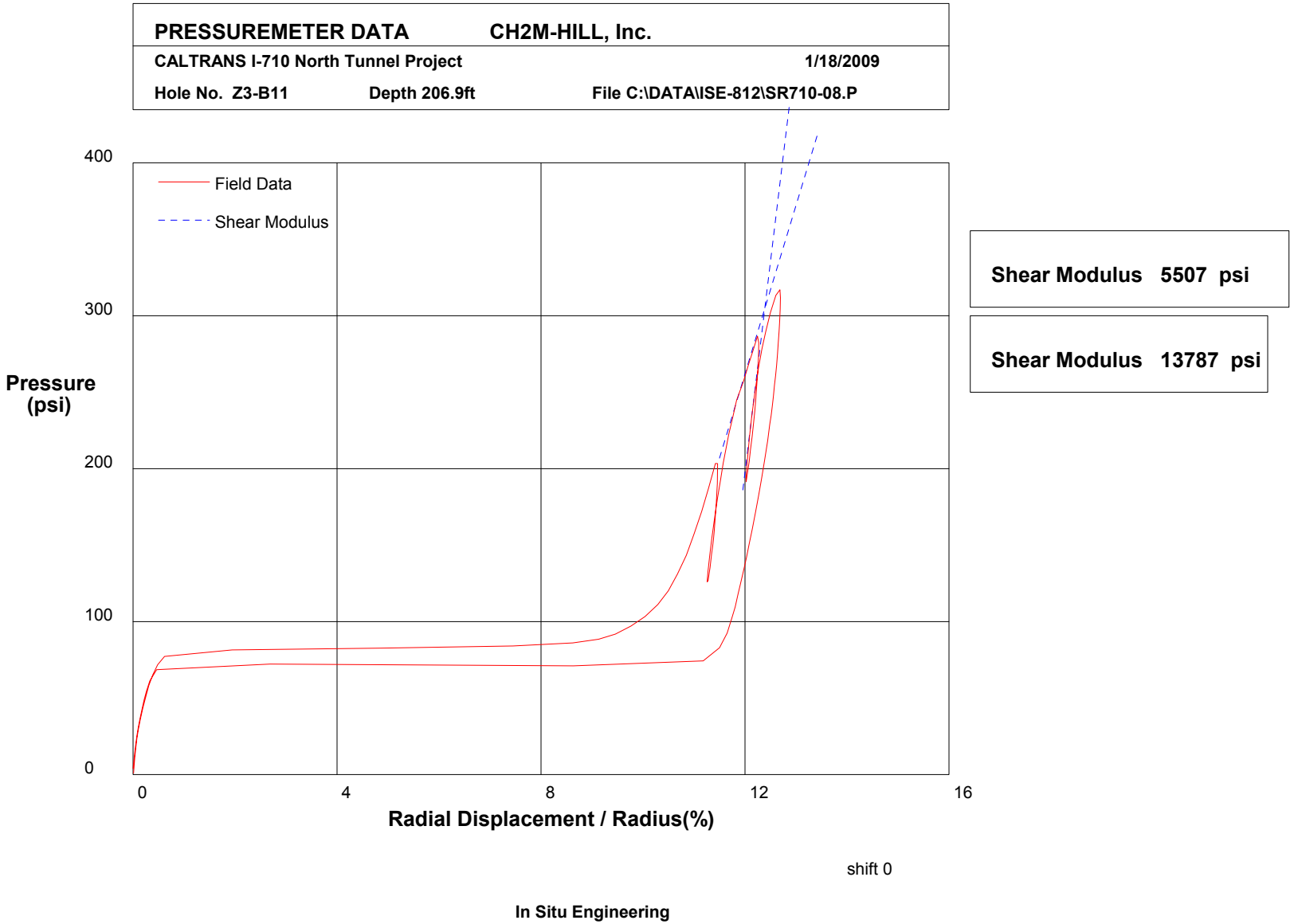

Appendix I - Pressuremeter Data and Standard Interpretation

PRESSUREMETER DATA **CH2MHill, Inc.**

CALTRANS I-710 North Tunnel Project **1/18/2009**

Hole No. Z3-B11 **Depth 206.9ft** **File C:\DATA\ISE-812\SR710-08.P**

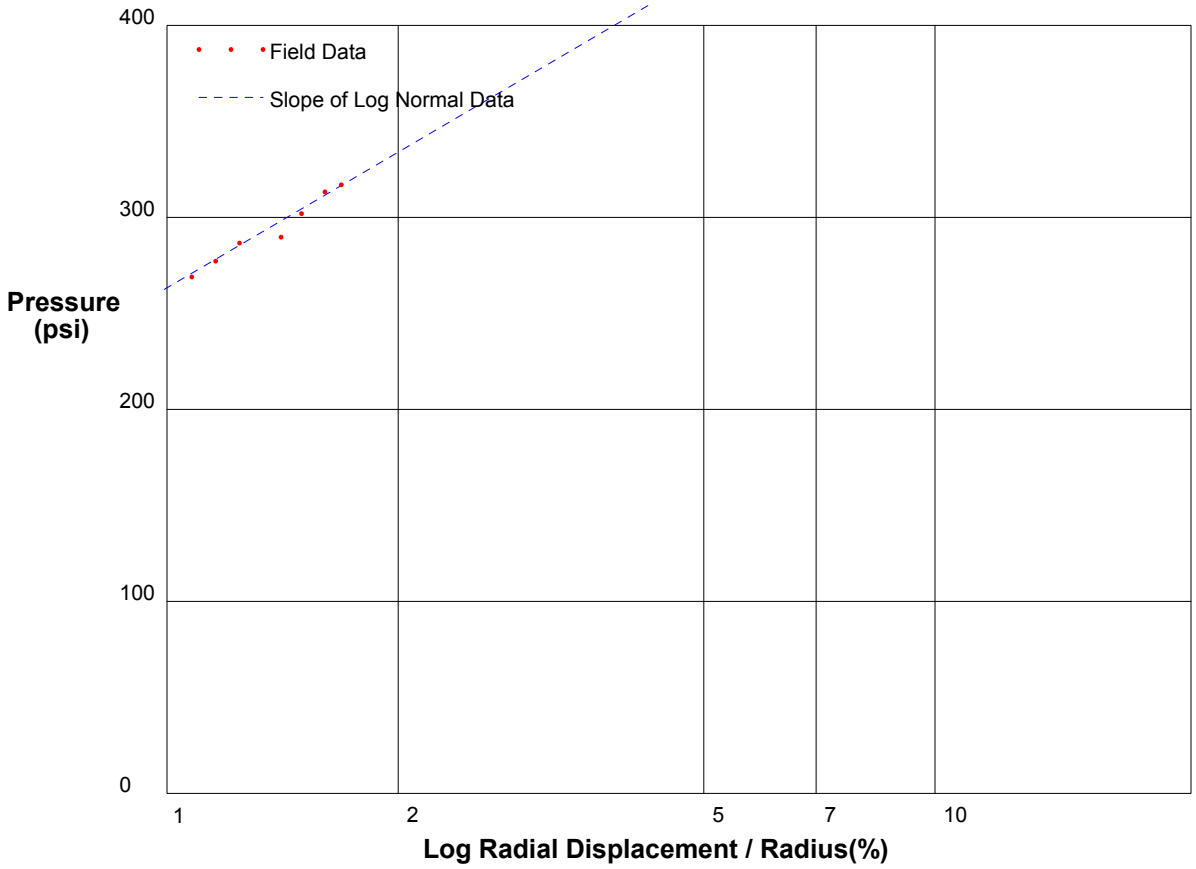

Shear Strength 101.9 psi
Limit Pressure 641 psi

shift 11

In Situ Engineering

Appendix I - Pressuremeter Data and Standard Interpretation

PRESSUREMETER DATA **CH2M-HILL, Inc.**

CALTRANS I-710 North Tunnel Project **1/18/2009**

Hole No. Z3-B2 **Depth 248ft** **File C:\DATA\ISE-812\SR710-09.P**

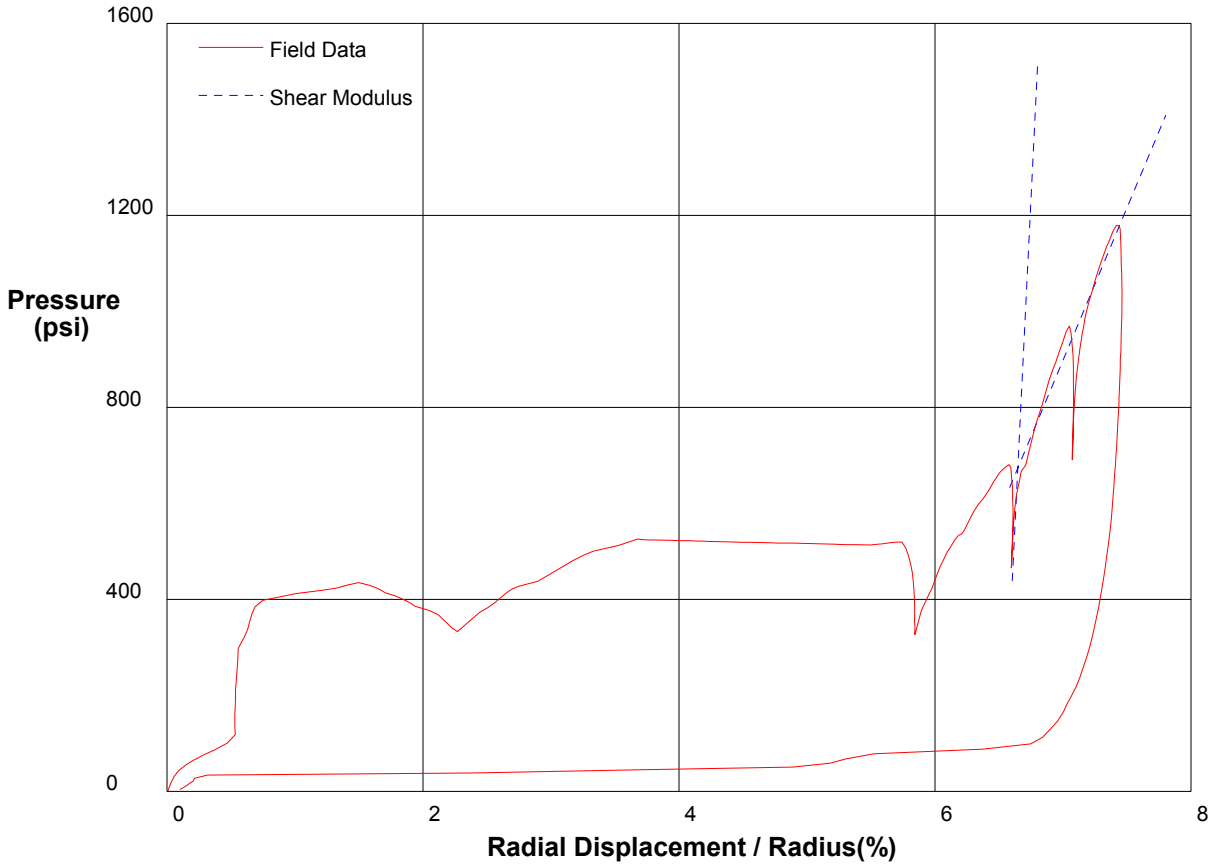

Shear Modulus 31794 psi

Shear Modulus 272982 psi

shift 0

In Situ Engineering

Appendix I - Pressuremeter Data and Standard Interpretation

PRESSUREMETER DATA **CH2MHill, Inc.**

CALTRANS I-710 North Tunnel Project **1/18/2009**

Hole No. Z3-B2 **Depth 248ft** **File C:\DATA\ISE-812\SR710-09.P**

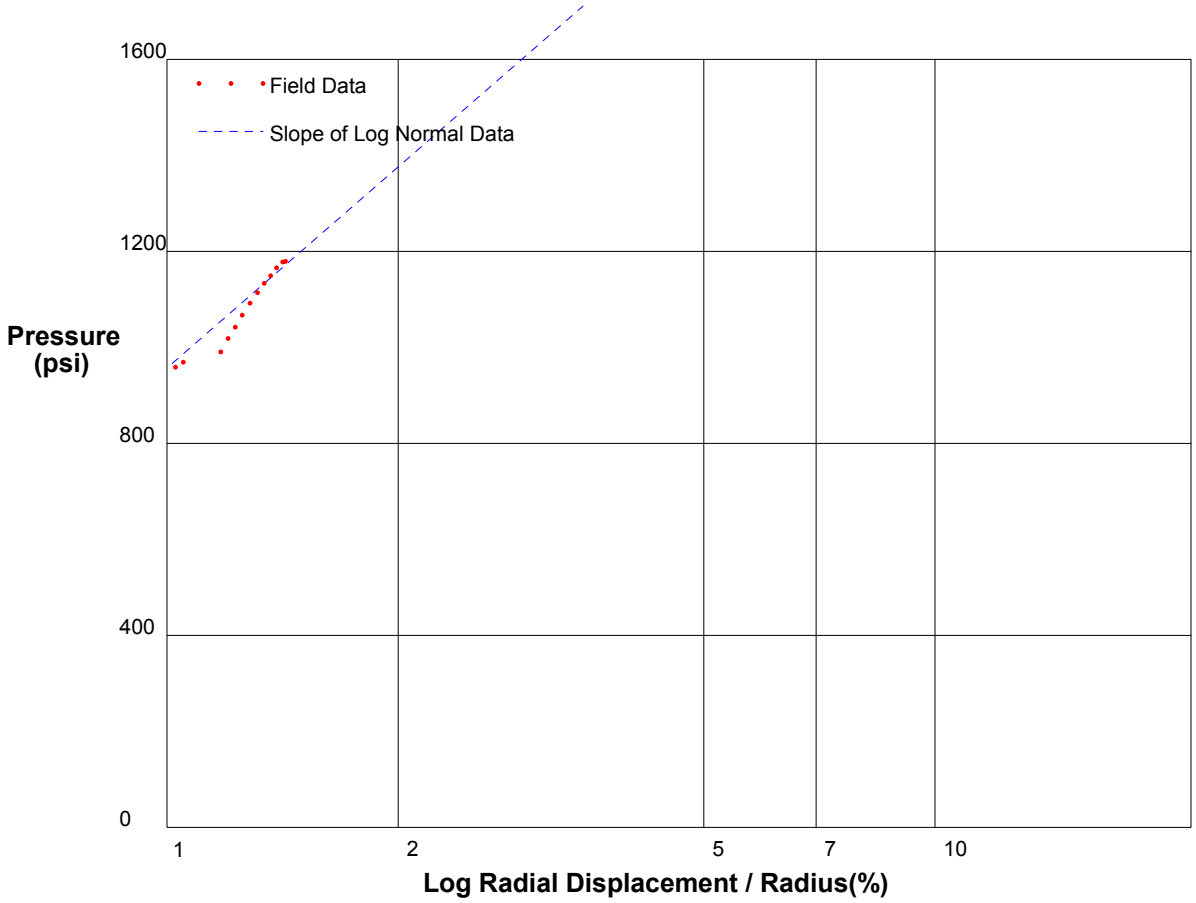

Shear Strength 604.6 psi
Limit Pressure 3202 psi

shift 6

In Situ Engineering

Appendix I - Pressuremeter Data and Standard Interpretation

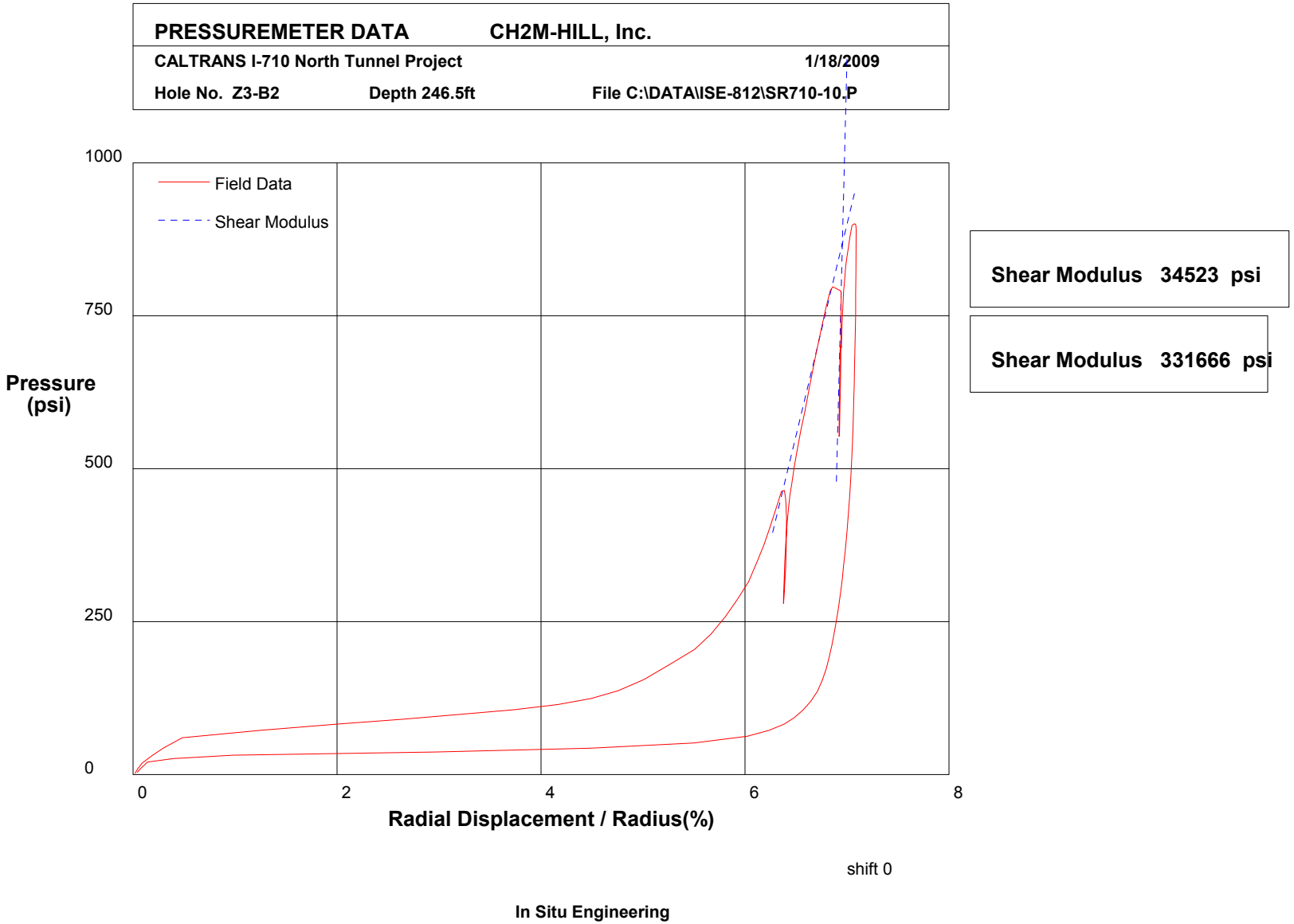

Appendix I - Pressuremeter Data and Standard Interpretation

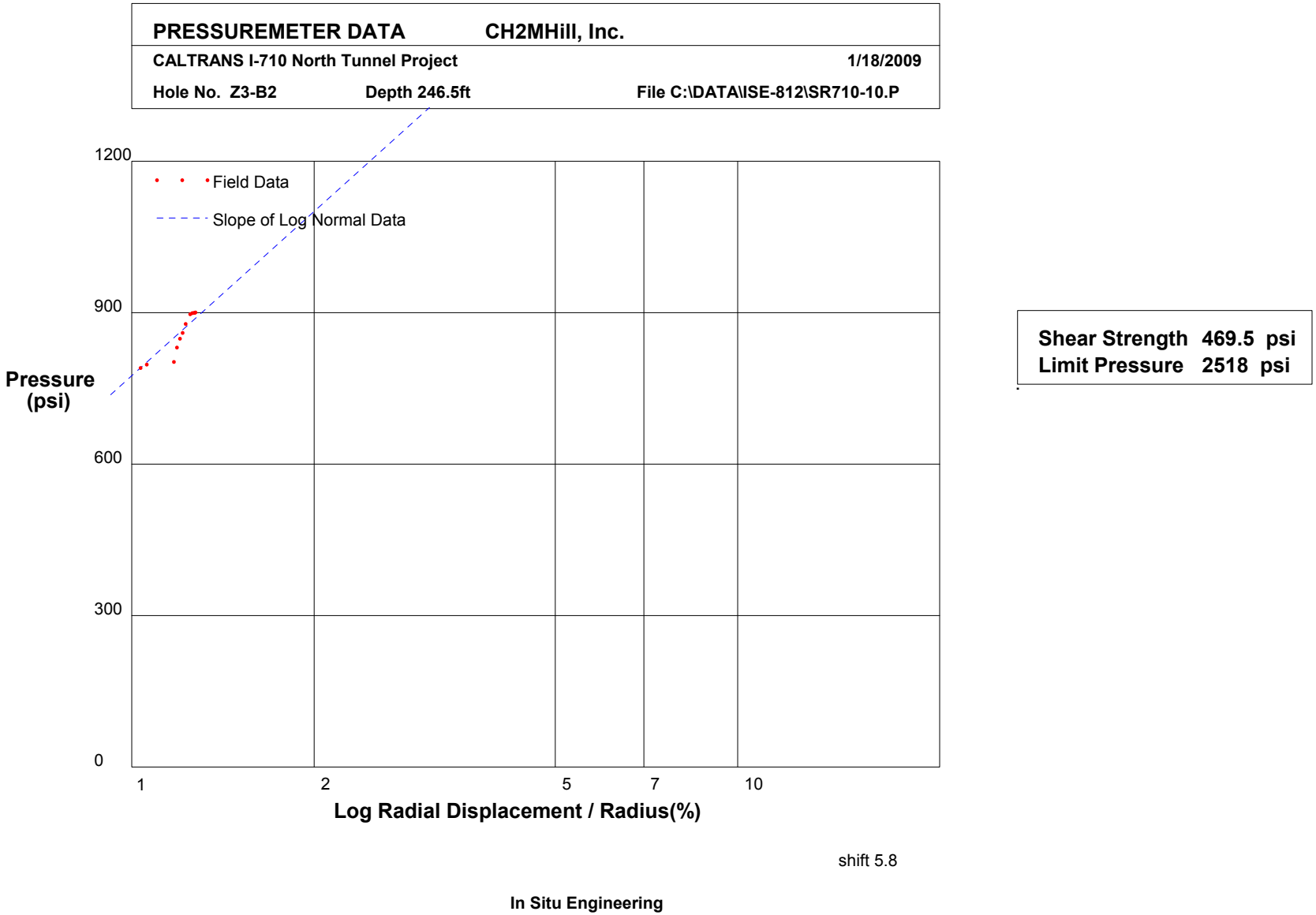

Appendix I - Pressuremeter Data and Standard Interpretation

PRESSUREMETER DATA **CH2MHill, Inc.**

CALTRANS I-710 North Tunnel Project **1/19/2009**

Hole No. Z2-B1 **Depth 129ft** **File C:\DATA\ISE-812\SR710-11.P**

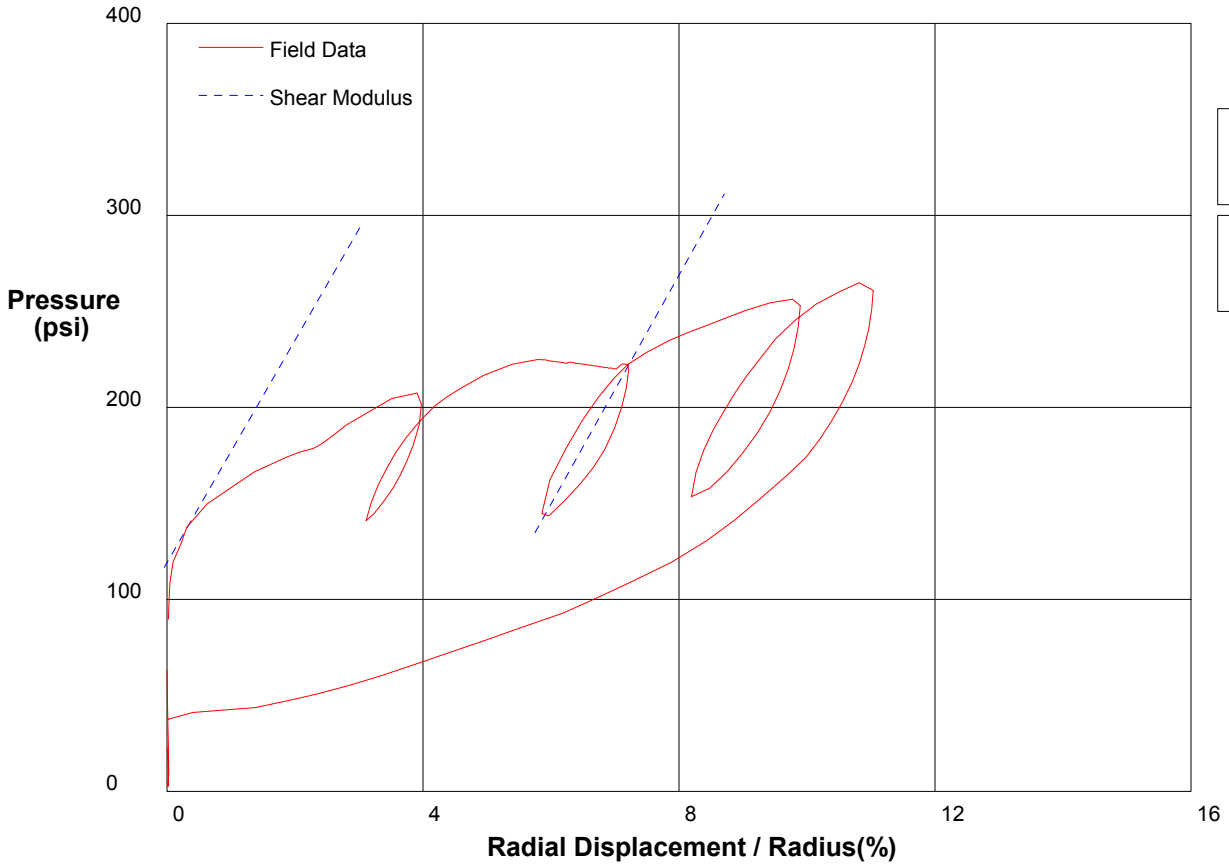

Shear Modulus 2981 psi

Shear Modulus 2897 psi

shift 0

In Situ Engineering

Appendix I - Pressuremeter Data and Standard Interpretation

PRESSUREMETER DATA **CH2M-HILL, Inc.**

CALTRANS I-710 North Tunnel Project **1/19/2009**

Hole No. Z2-B1 **Depth 129ft** **File C:\DATA\ISE-812\SR710-11.P**

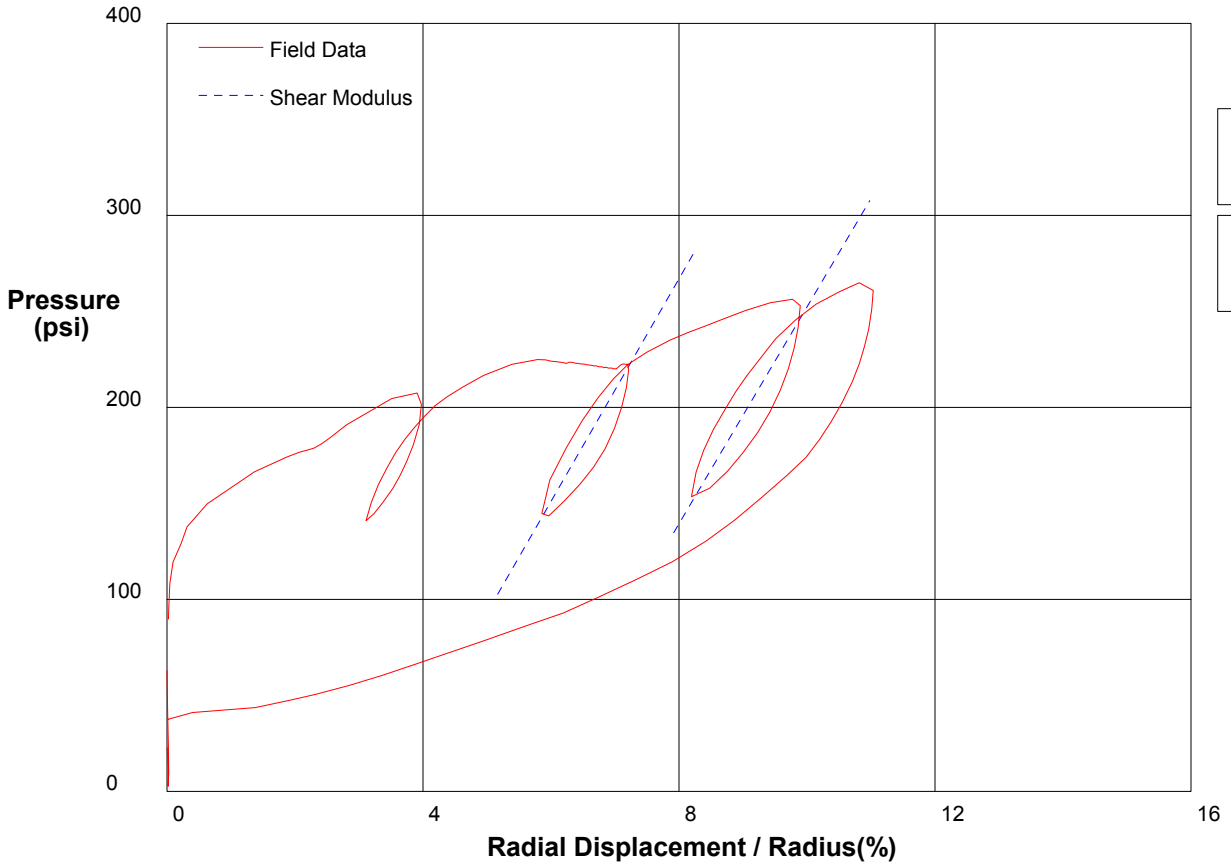

Shear Modulus 2823 psi

Shear Modulus 2897 psi

shift 0

In Situ Engineering

Appendix I - Pressuremeter Data and Standard Interpretation

PRESSUREMETER DATA **CH2MHill, Inc.**

CALTRANS I-710 North Tunnel Project **1/19/2009**

Hole No. Z2-B1 **Depth 129ft** **File C:\DATA\ISE-812\SR710-11.P**

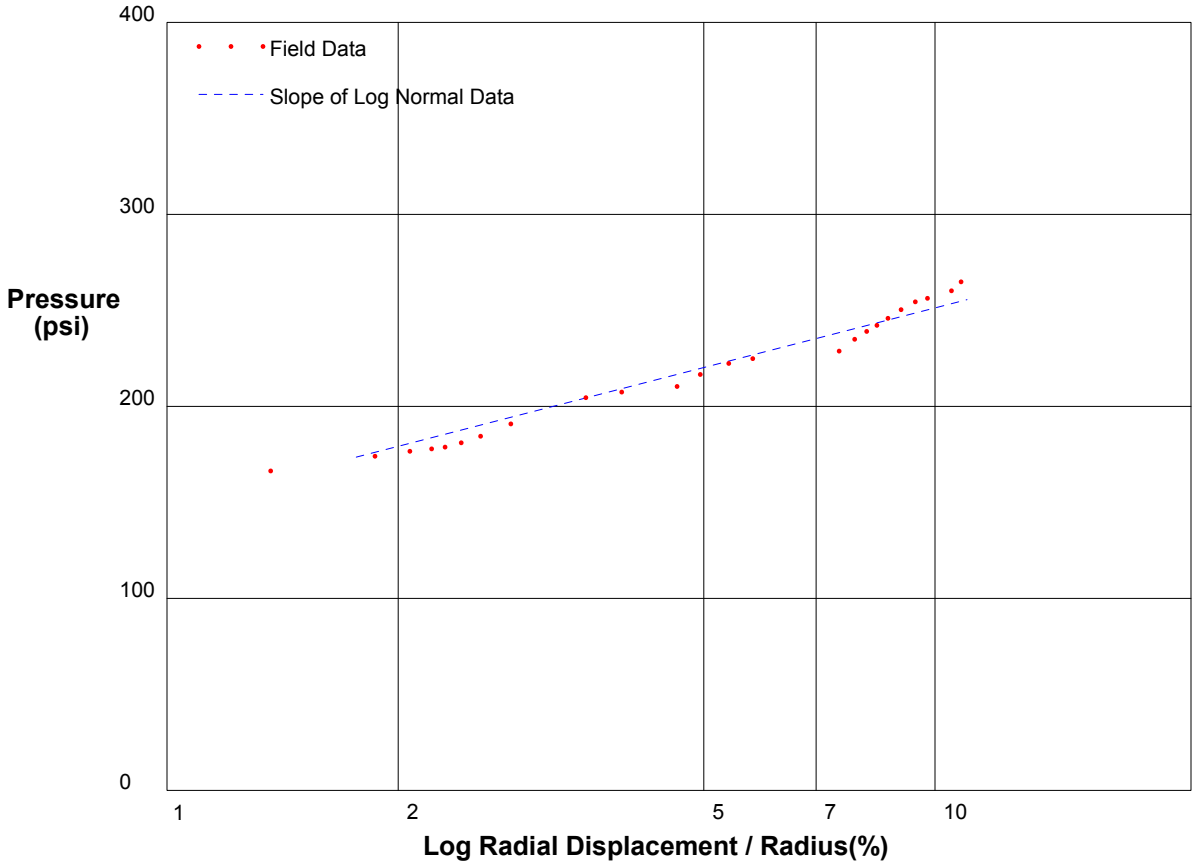

Shear Strength 44.7 psi
Limit Pressure 314 psi

shift 0

In Situ Engineering

Appendix I - Pressuremeter Data and Standard Interpretation

PRESSUREMETER DATA **CH2M-HILL, Inc**

CALTRANS I-170 North Tunnel Project **1/19/2009**

Hole No. Z2-B1 **Depth 127.5ft** **File C:\DATA\ISE-812\SR710-12.P**

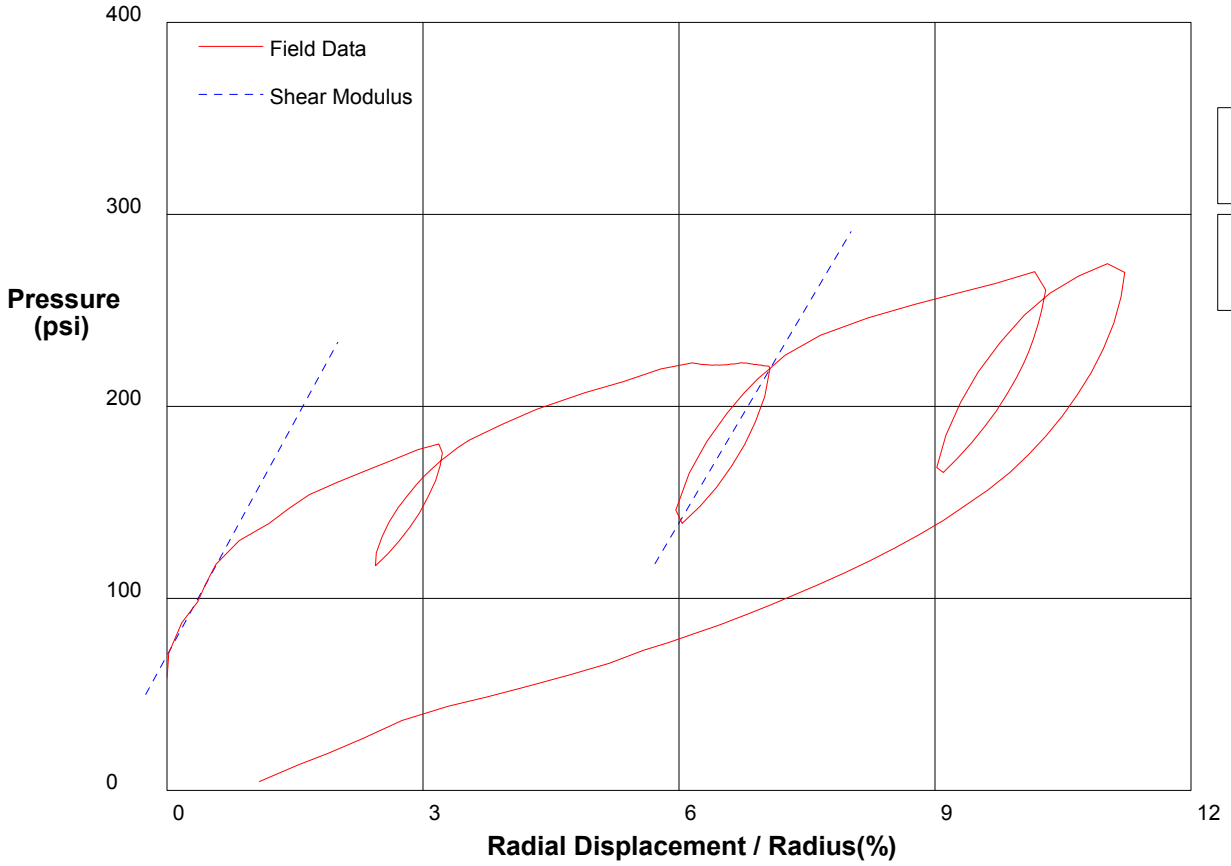

Shear Modulus 3764 psi

Shear Modulus 4074 psi

shift 0

In Situ Engineering

Appendix I - Pressuremeter Data and Standard Interpretation

PRESSUREMETER DATA **CH2MHill, Inc.**

CALTRANS I-710 North Tunnel Project **1/19/2009**

Hole No. Z2-B1 **Depth 127.5ft** **File C:\DATA\ISE-812\SR710-12.P**

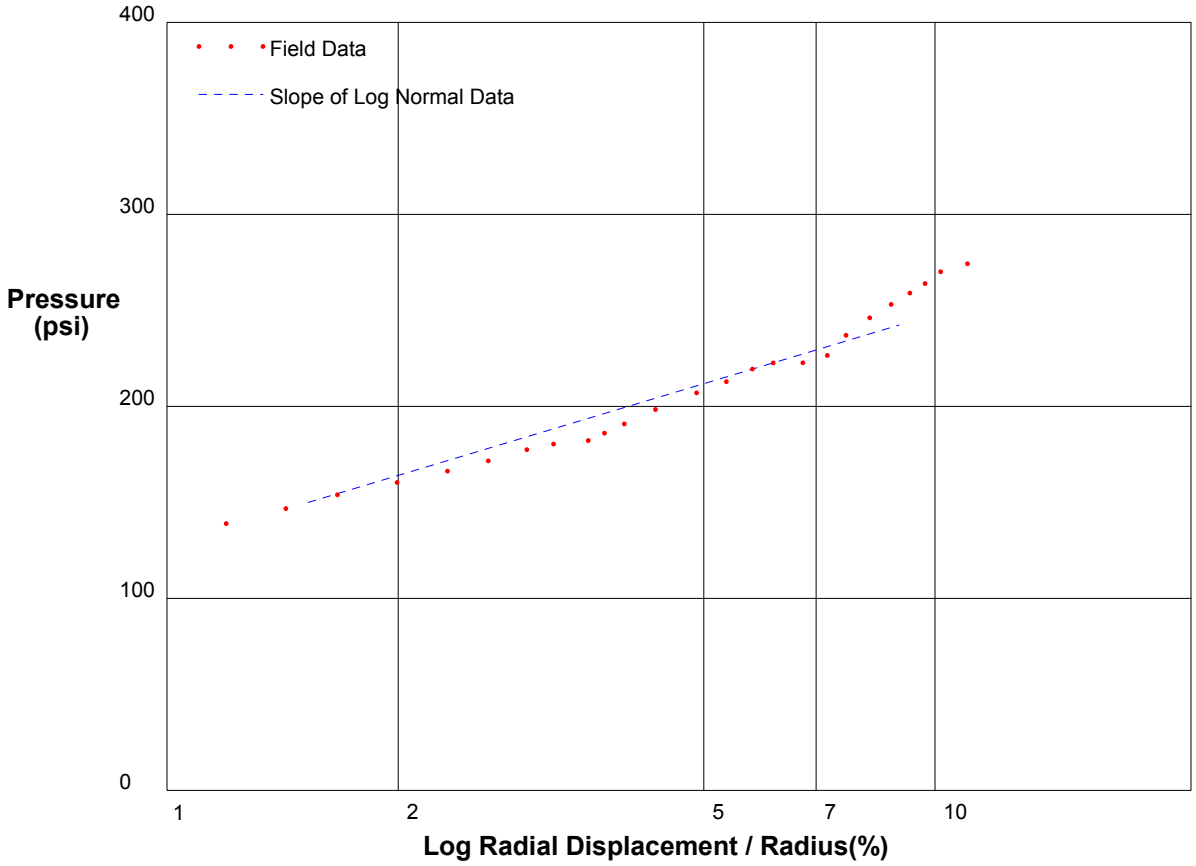

Shear Strength 52.1 psi
Limit Pressure 321 psi

shift 0

In Situ Engineering

Appendix I - Pressuremeter Data and Standard Interpretation

PRESSUREMETER DATA **CH2M-HILL, Inc.**

CALTRANS I-710 North Tunnel Project **1/20/2009**

Hole No. Z2-B1 **Depth 140ft** **File C:\DATA\ISE-812\SR710-13.P**

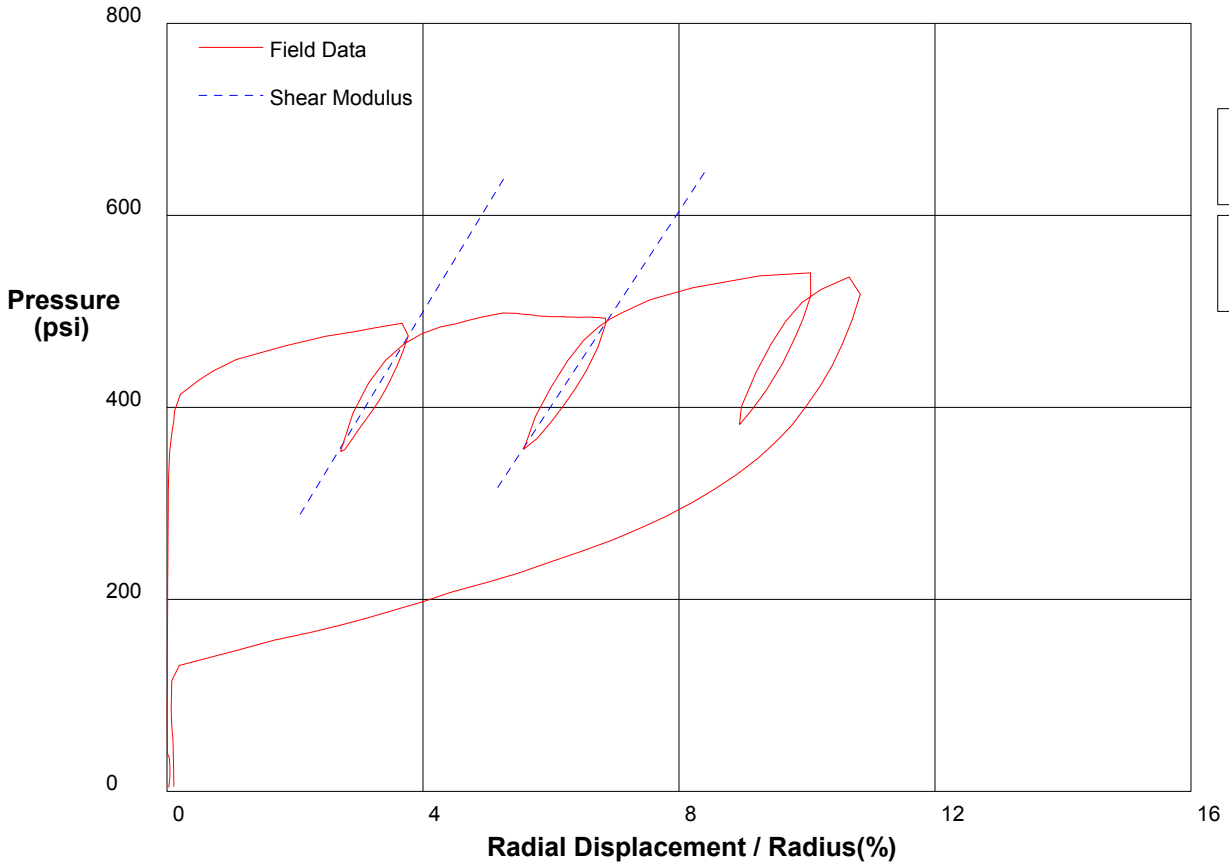

Shear Modulus 5074 psi

Shear Modulus 5497 psi

shift 0

In Situ Engineering

Appendix I - Pressuremeter Data and Standard Interpretation

PRESSUREMETER DATA **CH2MHill, Inc.**

CALTRANS I-710 North Tunnel Project **1/20/2009**

Hole No. Z2-B1 **Depth 140ft** **File C:\DATA\ISE-812\SR710-13.P**

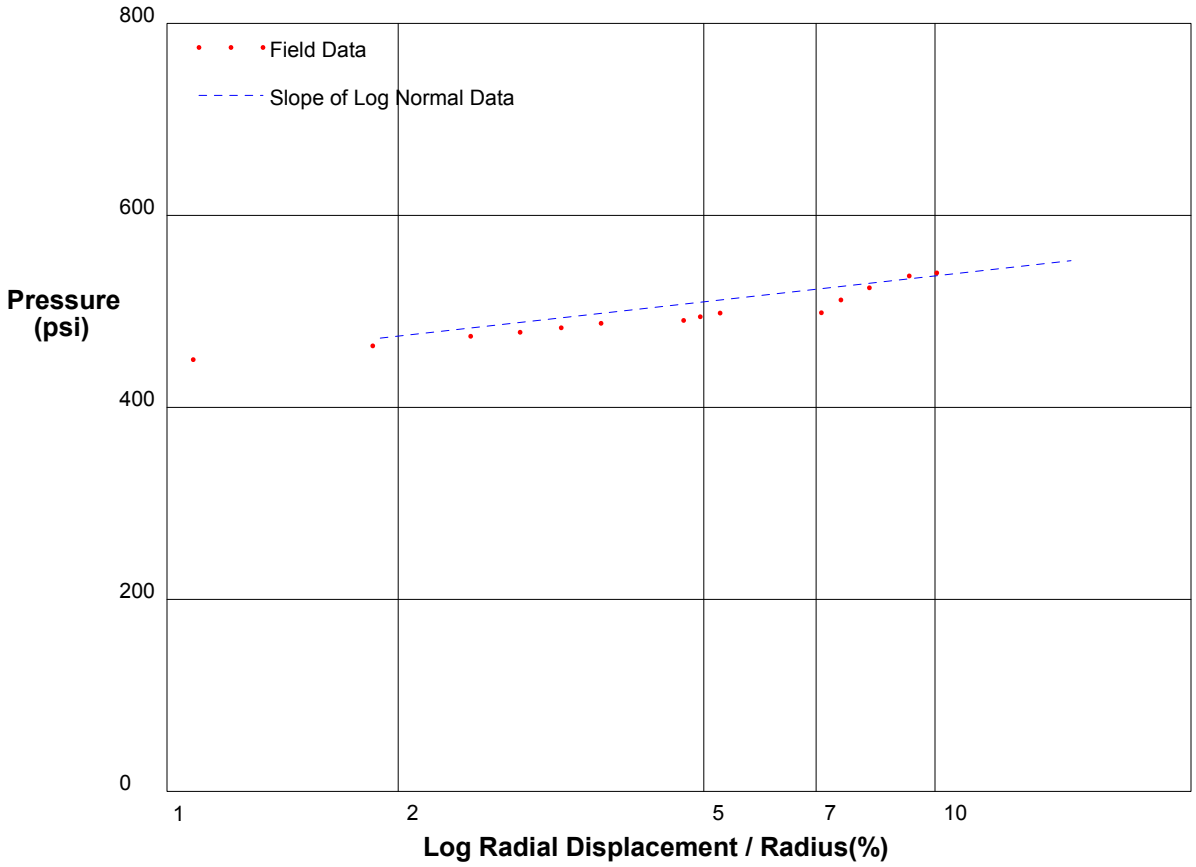

Shear Strength 38.9 psi
Limit Pressure 591 psi

shift 0

In Situ Engineering

Appendix I - Pressuremeter Data and Standard Interpretation

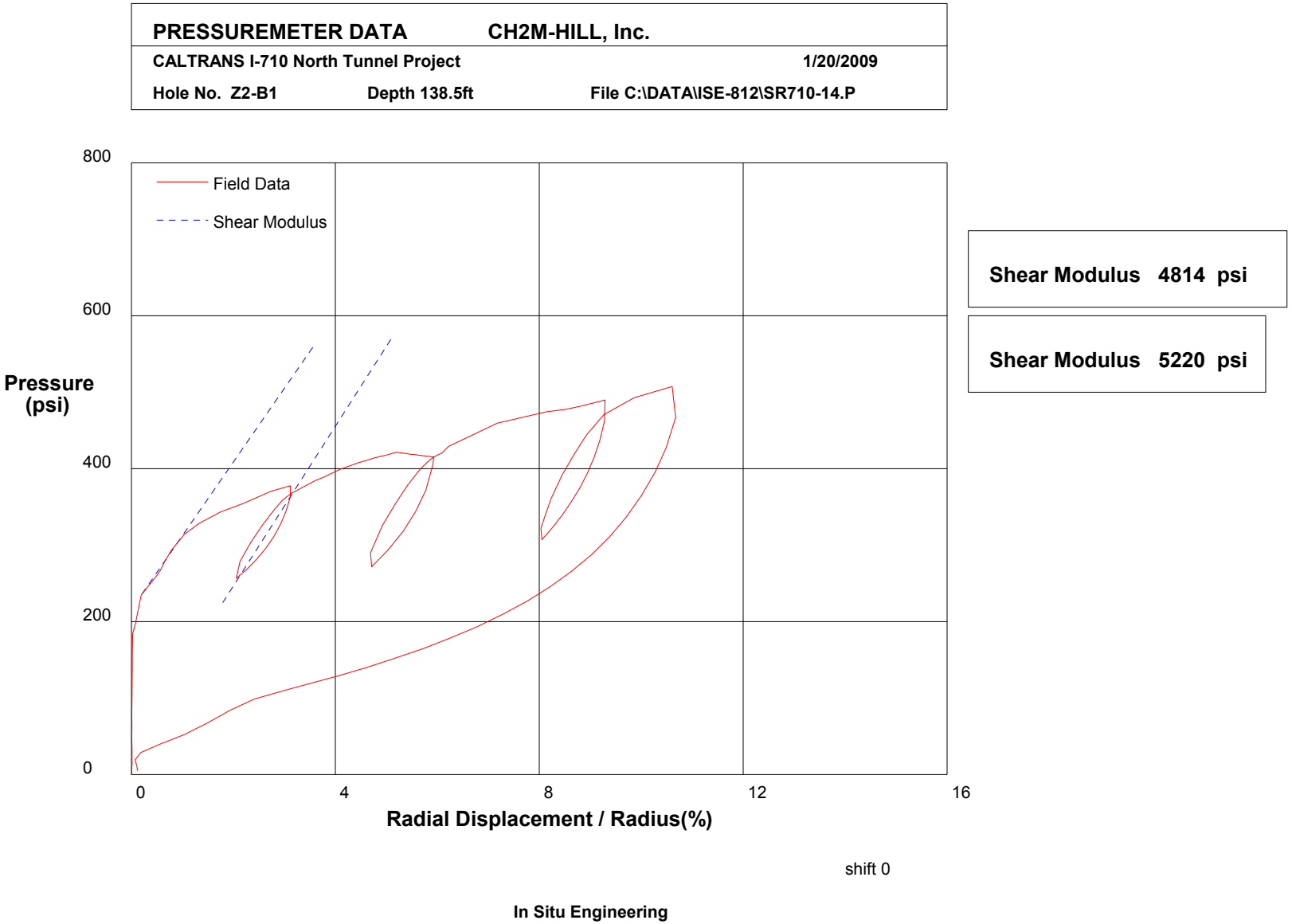

Appendix I - Pressuremeter Data and Standard Interpretation

PRESSUREMETER DATA **CH2MHill, Inc.**

CALTRANS I-710 North Tunnel Project **1/20/2009**

Hole No. Z2-B1 **Depth 138.5ft** **File C:\DATA\ISE-812\SR710-14.P**

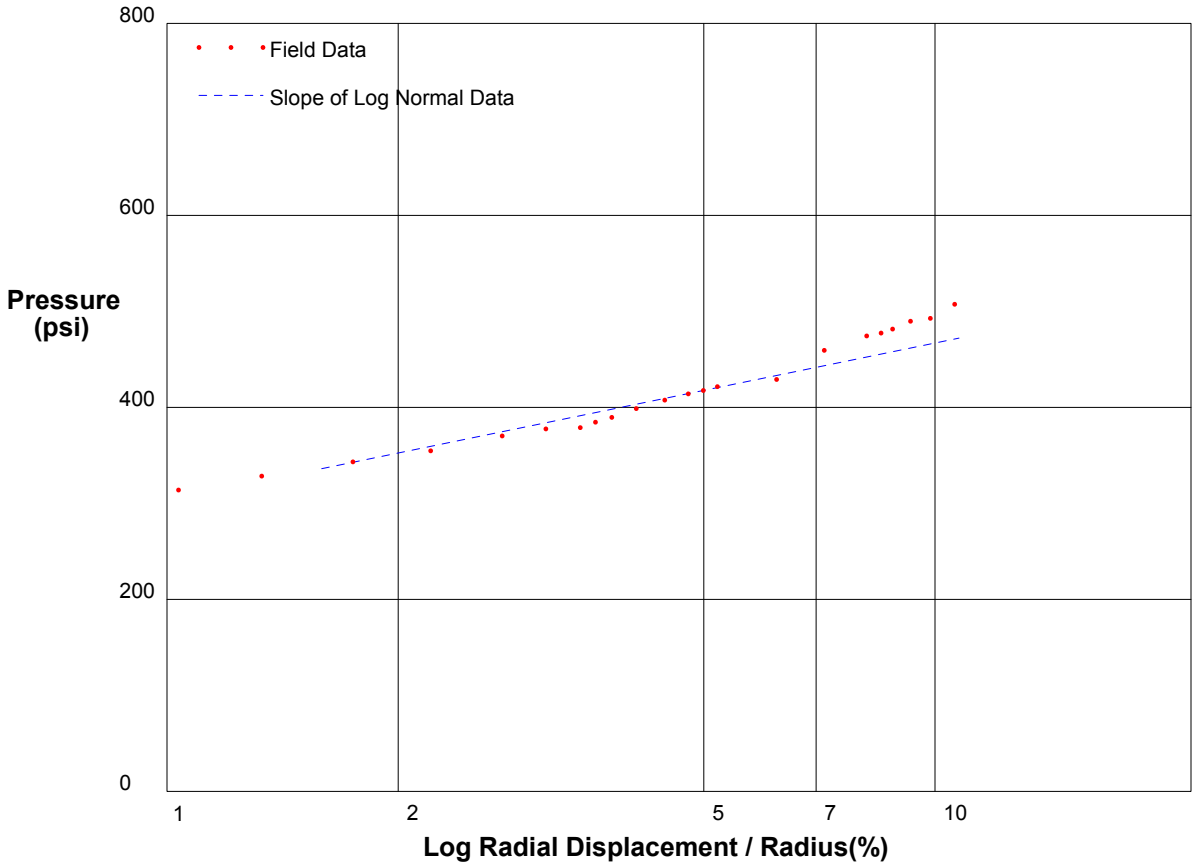

Shear Strength 71.2 psi
Limit Pressure 567 psi

shift 0

In Situ Engineering

Appendix I - Pressuremeter Data and Standard Interpretation

PRESSUREMETER DATA **CH2M-HILL, Inc.**

CALTRANS I-710 North Tunnel Project **1/20/2009**

Hole No. Z1-B7 **Depth 96.5ft** **File C:\DATA\ISE-812\SR710-15.P**

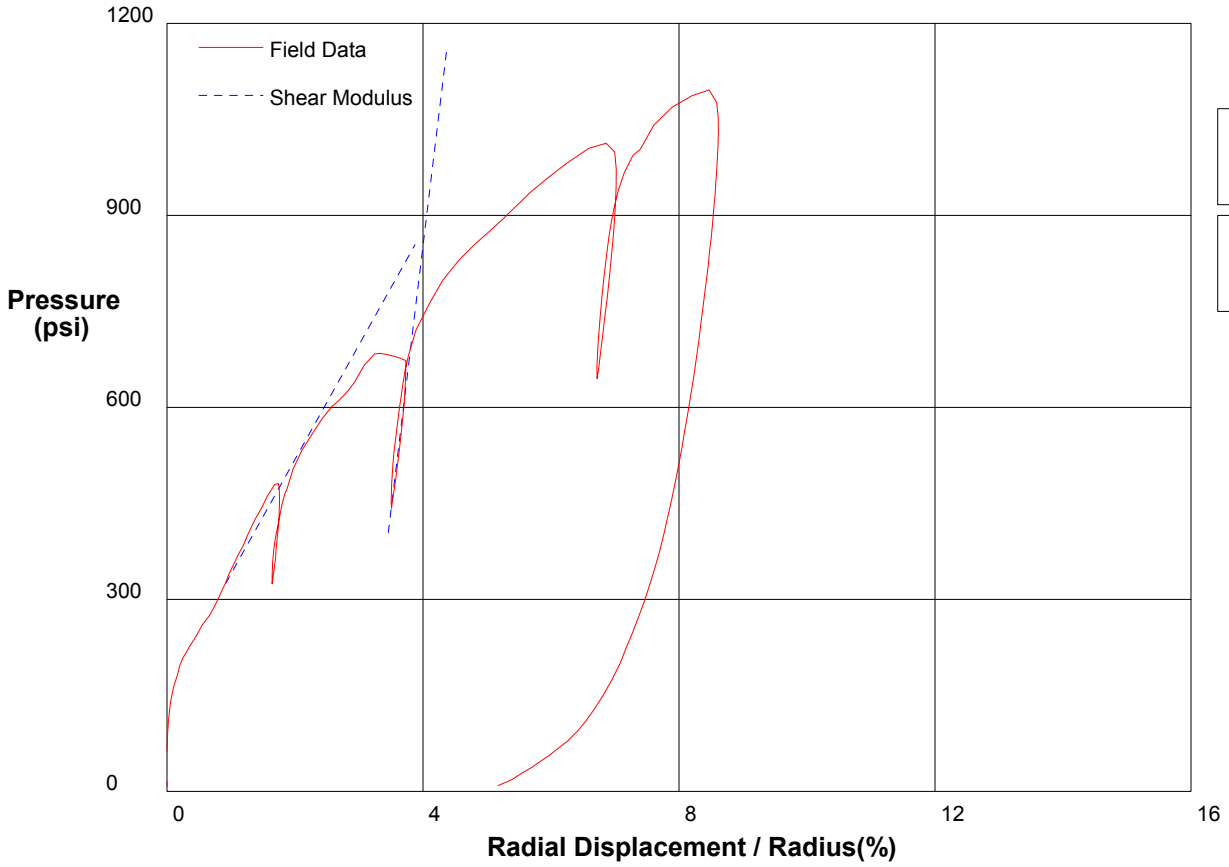

Shear Modulus 8943 psi

Shear Modulus 41363 psi

shift 0

In Situ Engineering

Appendix I - Pressuremeter Data and Standard Interpretation

PRESSUREMETER DATA **CH2MHill, Inc.**

CALTRANS I-710 North Tunnel Project **1/20/2009**

Hole No. Z1-B7 **Depth 96.5ft** **File C:\DATA\ISE-812\SR710-15.P**

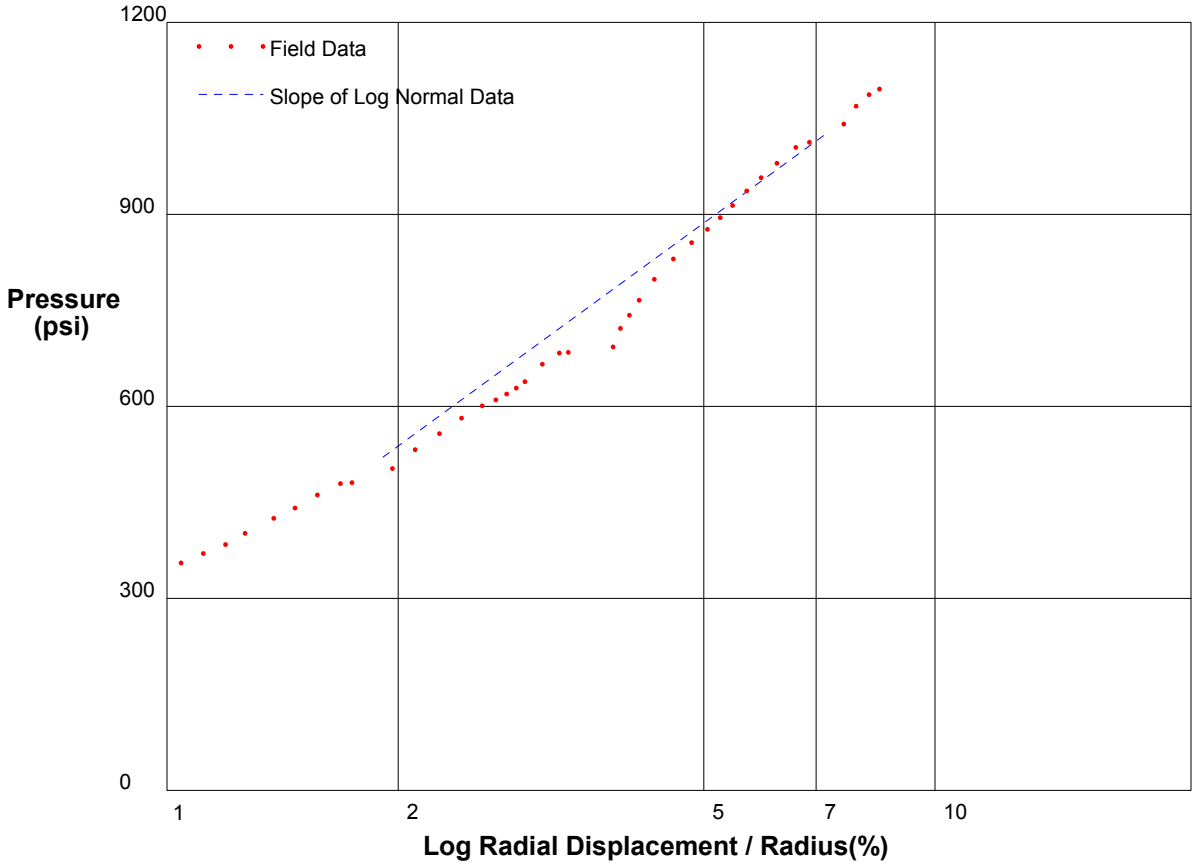

Shear Strength 380.3 psi
Limit Pressure 1686 psi

shift 0

In Situ Engineering

Appendix I - Pressuremeter Data and Standard Interpretation

PRESSUREMETER DATA **CH2M-HILL, Inc.**

CALTRANS I-710 North Tunnel Project **1/20/2009**

Hole No. Z1-B7 **Depth 95ft** **File C:\DATA\ISE-812\SR710-16.P**

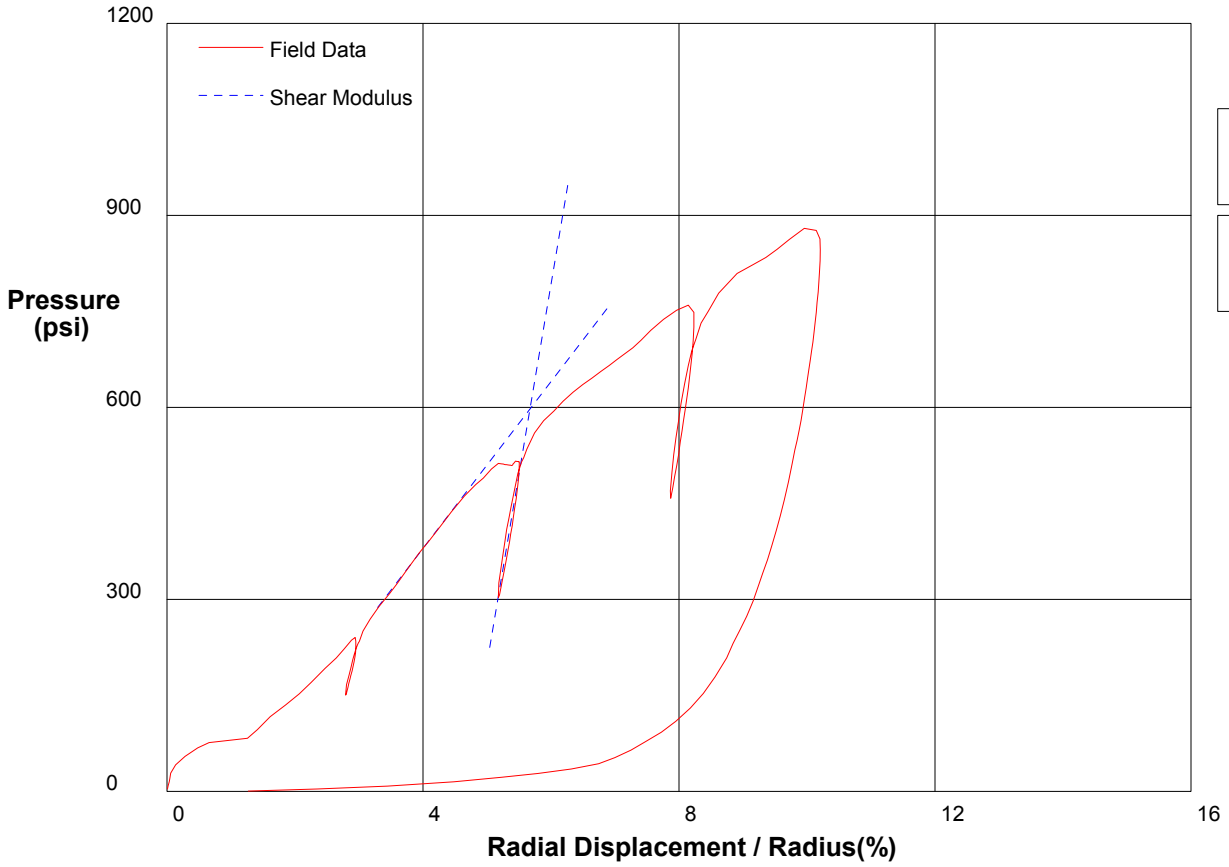

Shear Modulus 6511 psi

Shear Modulus 29576 psi

shift 0

In Situ Engineering

Appendix I - Pressuremeter Data and Standard Interpretation

PRESSUREMETER DATA **CH2MHill, Inc.**

CALTRANS I-710 North Tunnel Project **1/20/2009**

Hole No. Z1-B7 **Depth 95ft** **File C:\DATA\ISE-812\SR710-16.P**

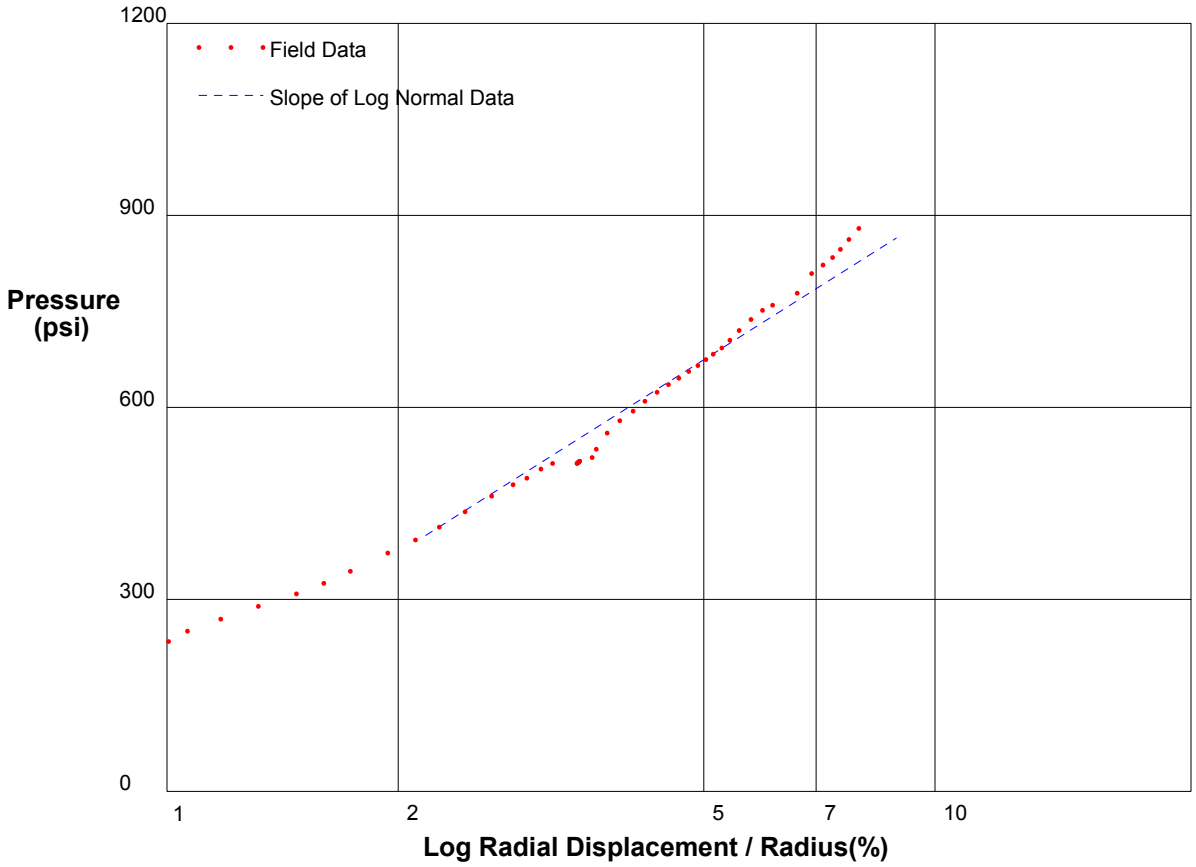

Shear Strength 329.2 psi
Limit Pressure 1367 psi

shift 2

In Situ Engineering

Appendix I - Pressuremeter Data and Standard Interpretation

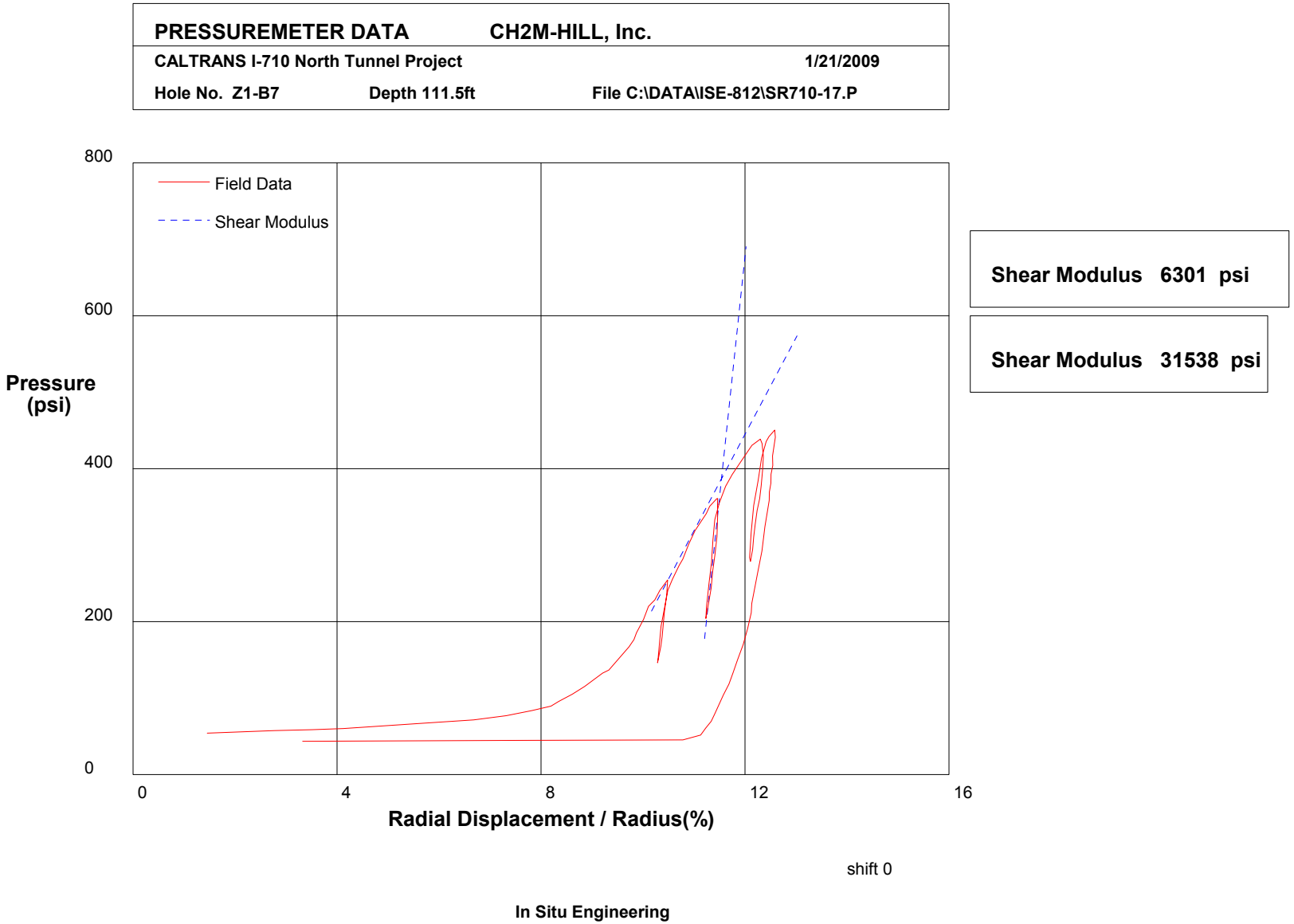

Appendix I - Pressuremeter Data and Standard Interpretation

PRESSUREMETER DATA **CH2MHill, Inc.**

CALTRANS I-710 North Tunnel Project **1/21/2009**

Hole No. Z1-B7 **Depth 111.5ft** **File C:\DATA\ISE-812\SR710-17.P**

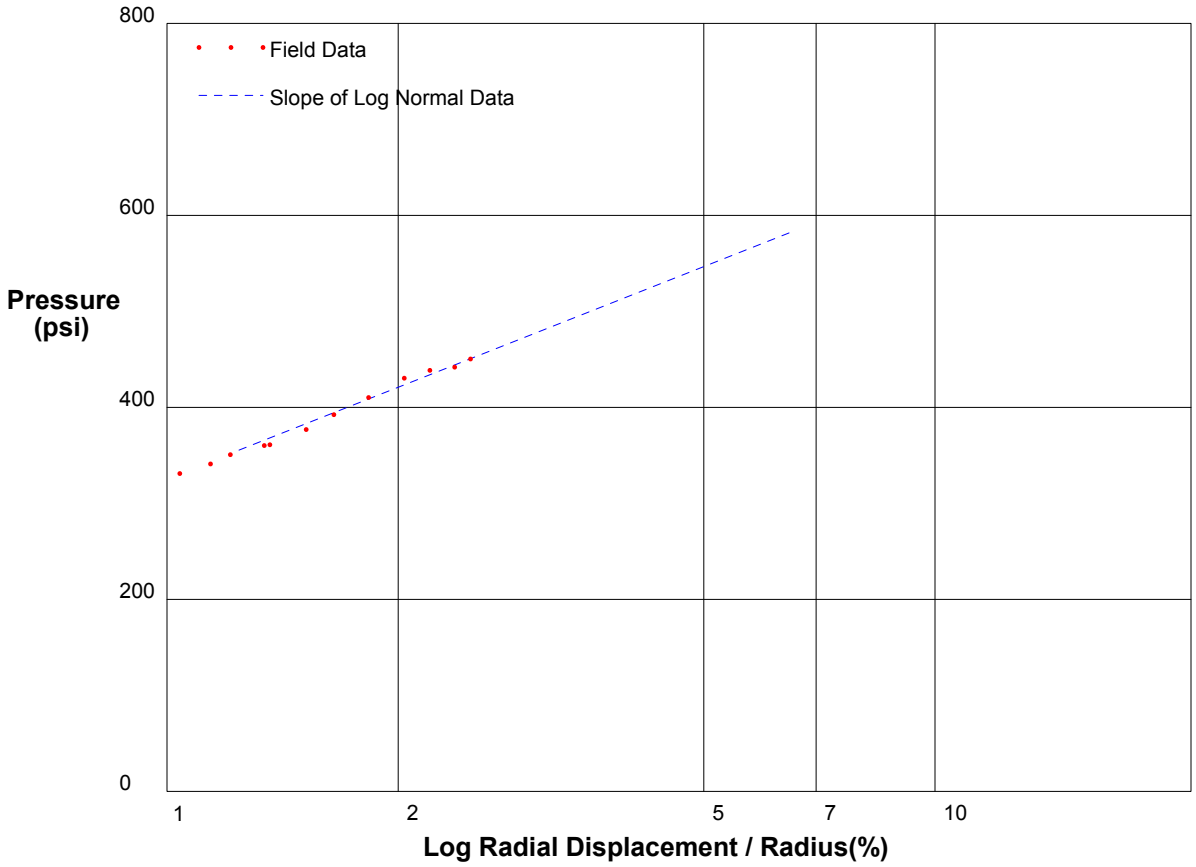

Shear Strength 137.1 psi
Limit Pressure 835 psi

shift 10.1

In Situ Engineering

Appendix I - Pressuremeter Data and Standard Interpretation

PRESSUREMETER DATA **CH2M-HILL, Inc.**

CALTRANS I-710 North Tunnel Project **1/21/2009**

Hole No. Z1-B7 **Depth 110ft** **File C:\DATA\ISE-812\SR710-18.P**

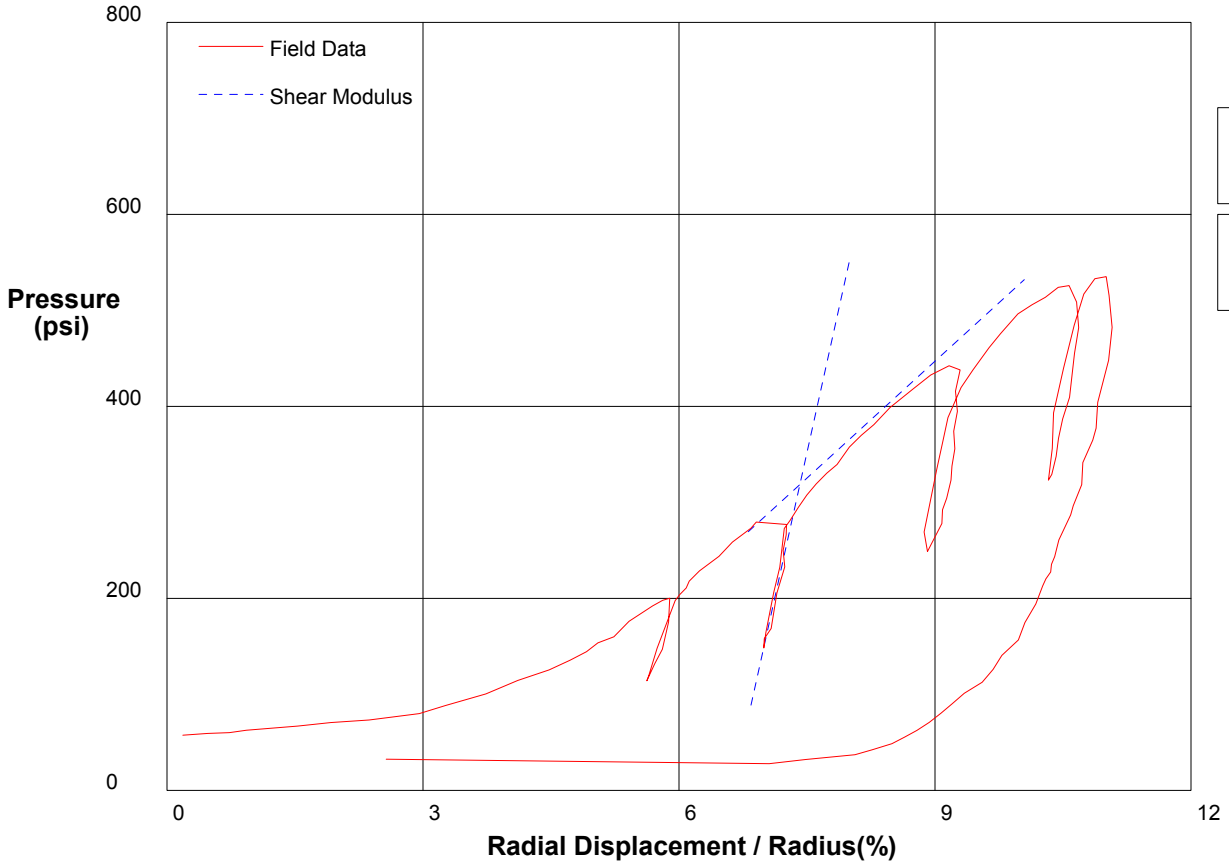

Shear Modulus 4057 psi

Shear Modulus 20060 psi

shift 0

In Situ Engineering

Appendix I - Pressuremeter Data and Standard Interpretation

PRESSUREMETER DATA **CH2MHill, Inc.**

CALTRANS I-710 North Tunnel Project **1/21/2009**

Hole No. Z1-B7 **Depth 110ft** **File C:\DATA\ISE-812\SR710-18.P**

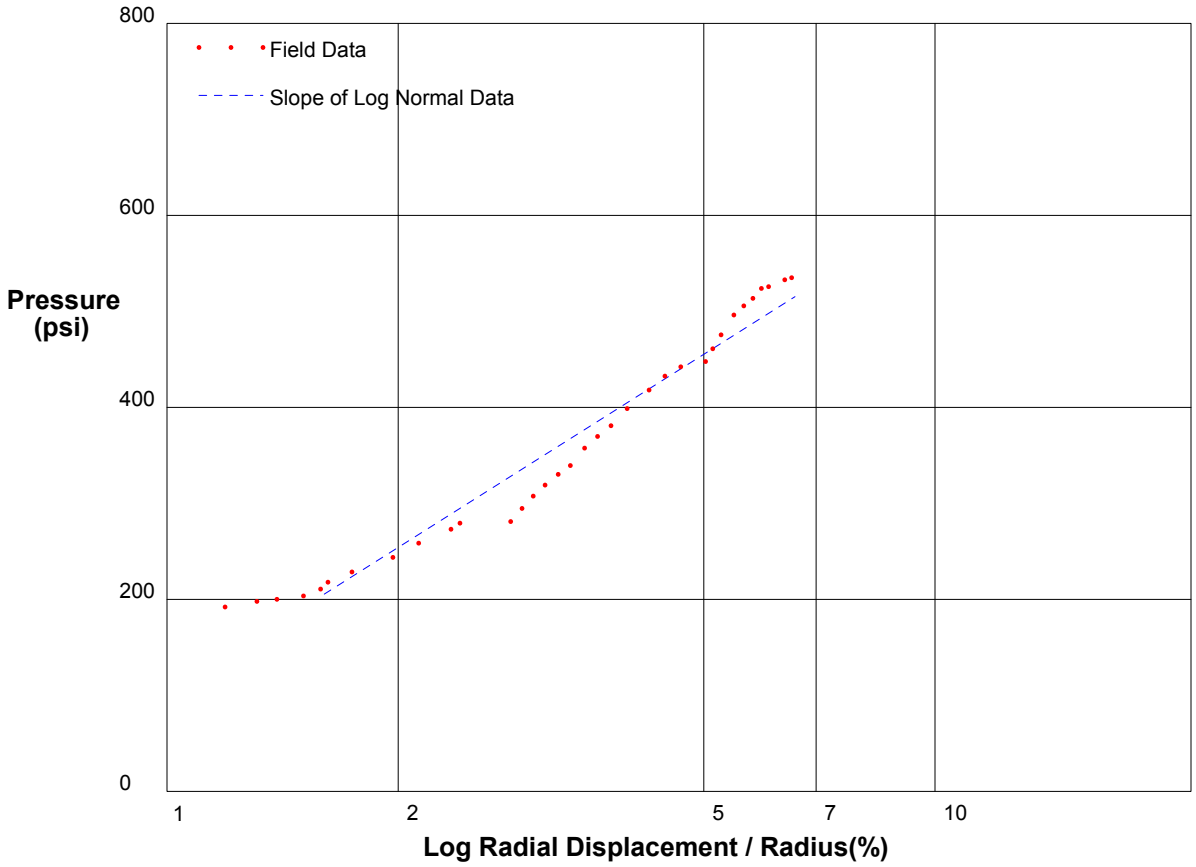

Shear Strength 219.4 psi
Limit Pressure 917 psi

shift 4.5

In Situ Engineering

Appendix I - Pressuremeter Data and Standard Interpretation

PRESSUREMETER DATA **CH2M-HILL, Inc.**

CALTRANS I-710 North Tunnel Project **1/21/2009**

Hole No. Z1-B7 **Depth 136ft** **File C:\DATA\ISE-812\SR710-19.P**

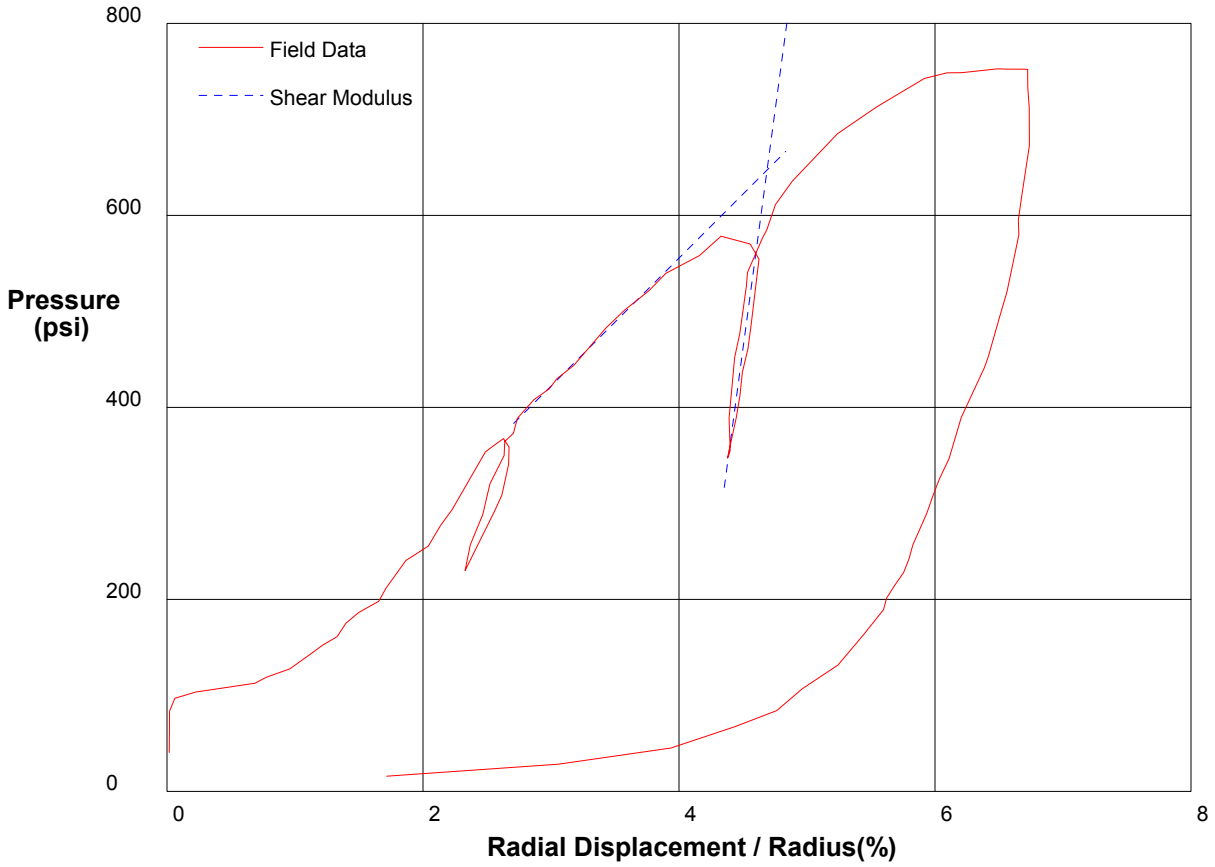

Shear Modulus 49503 psi

Shear Modulus 6666 psi

shift 0

In Situ Engineering

Appendix I - Pressuremeter Data and Standard Interpretation

PRESSUREMETER DATA **CH2MHill, Inc.**

CALTRANS I-710 North Tunnel Project **1/21/2009**

Hole No. Z1-B7 **Depth 136ft** **File C:\DATA\ISE-812\SR710-19.P**

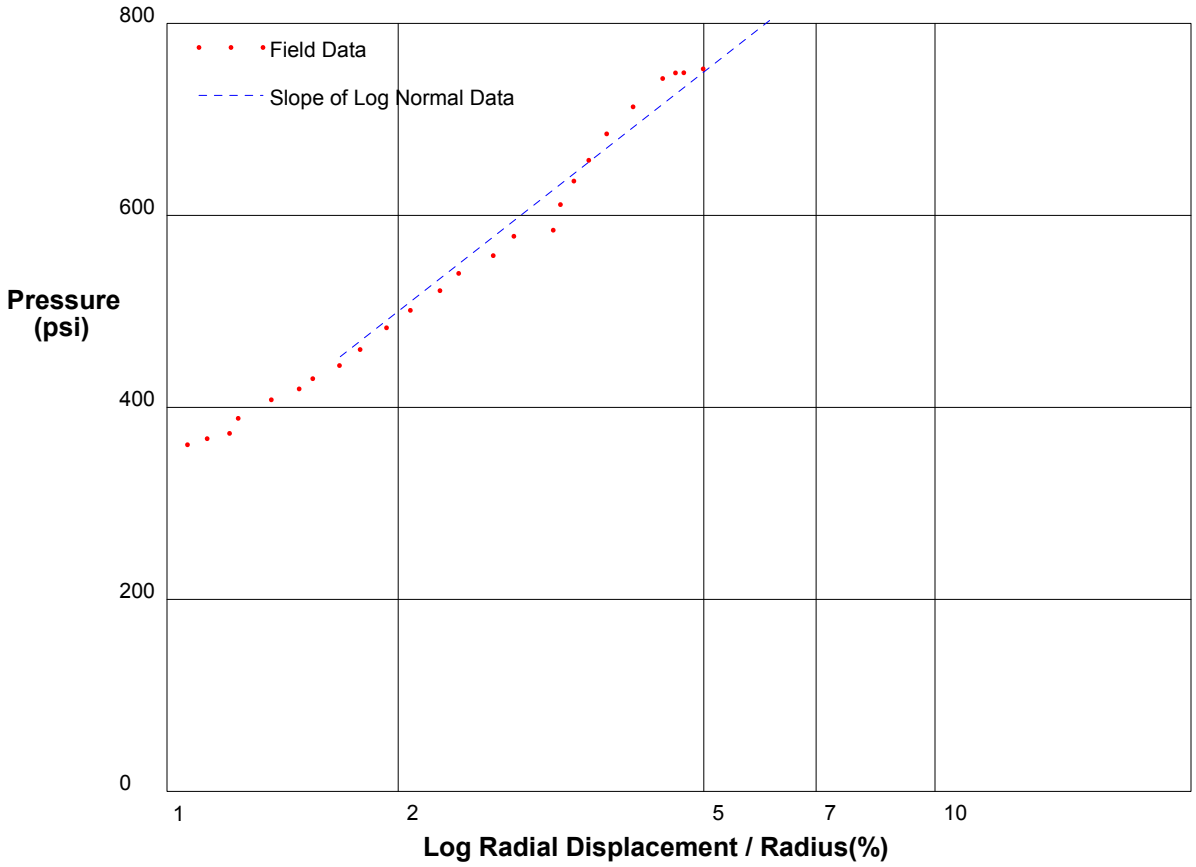

Shear Strength 272.1 psi
Limit Pressure 1321 psi

shift 1.5

In Situ Engineering

Appendix I - Pressuremeter Data and Standard Interpretation

PRESSUREMETER DATA **CH2M-HILL, Inc.**

CALTRANS I-710 North Tunnel Project **1/21/2009**

Hole No. Z1-B7 **Depth 135ft** **File C:\DATA\ISE-812\SR710-20.P**

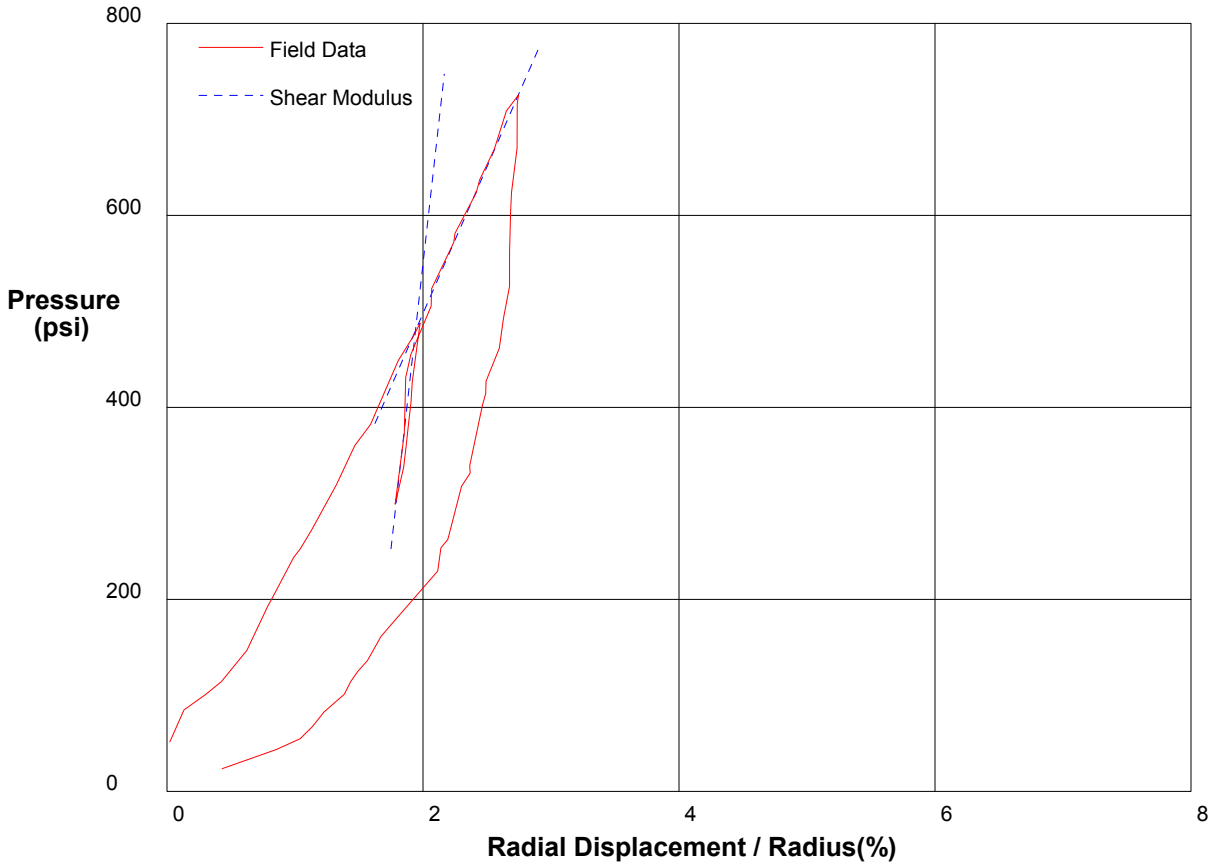

Shear Modulus 59333 psi

Shear Modulus 15268 psi

shift 0

In Situ Engineering

Appendix I - Pressuremeter Data and Standard Interpretation

PRESSUREMETER DATA **CH2MHill, Inc.**

CALTRANS I-710 North Tunnel Project **1/21/2009**

Hole No. Z1-B7 **Depth 135ft** **File C:\DATA\ISE-812\SR710-20.P**

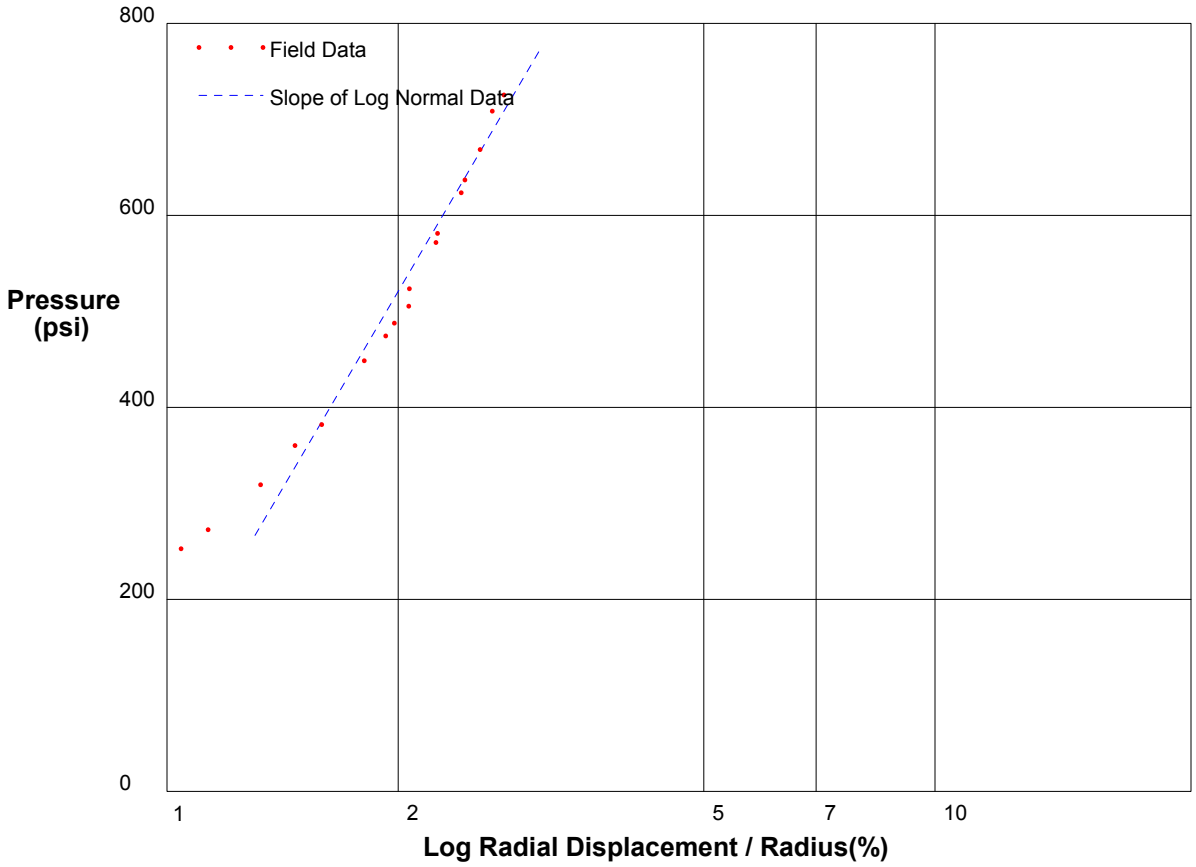

Shear Strength 592.1 psi
Limit Pressure 2309 psi

shift 0

In Situ Engineering

Appendix I - Pressuremeter Data and Standard Interpretation

PRESSUREMETER DATA **CH2MHill, Inc.**

CALTRANS I-710 North Tunnel Project **1/28/2009**

Hole No. Z1-B3 **Depth 177.3ft** **File C:\DATA\ISE-812\SR710-21.P**

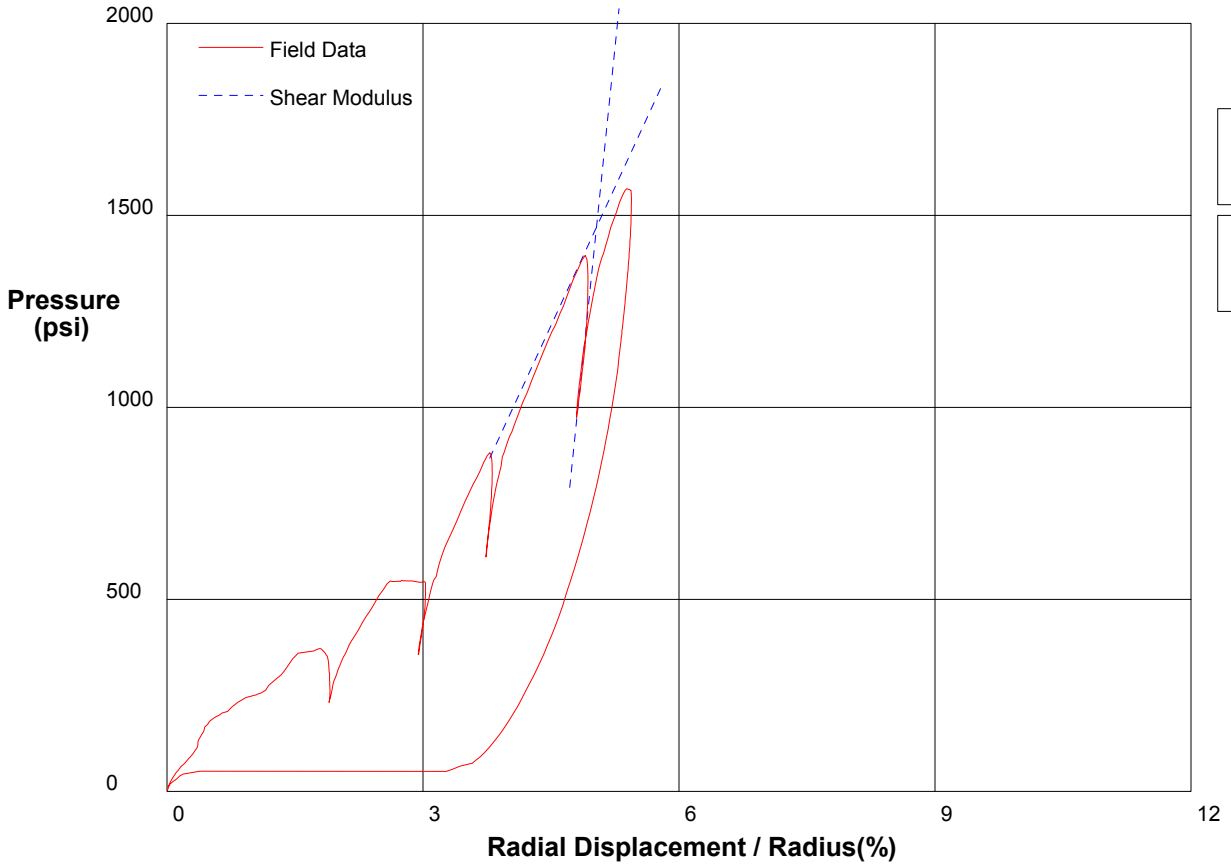

Shear Modulus 107807 psi

Shear Modulus 24031 psi

shift 0

In Situ Engineering

Appendix I - Pressuremeter Data and Standard Interpretation

PRESSUREMETER DATA **CH2M-HILL, Inc.**

CALTRANS I-710 North Tunnel Project **1/28/2009**

Hole No. Z1-B3 **Depth 177.3ft** **File C:\DATA\ISE-812\SR710-21.P**

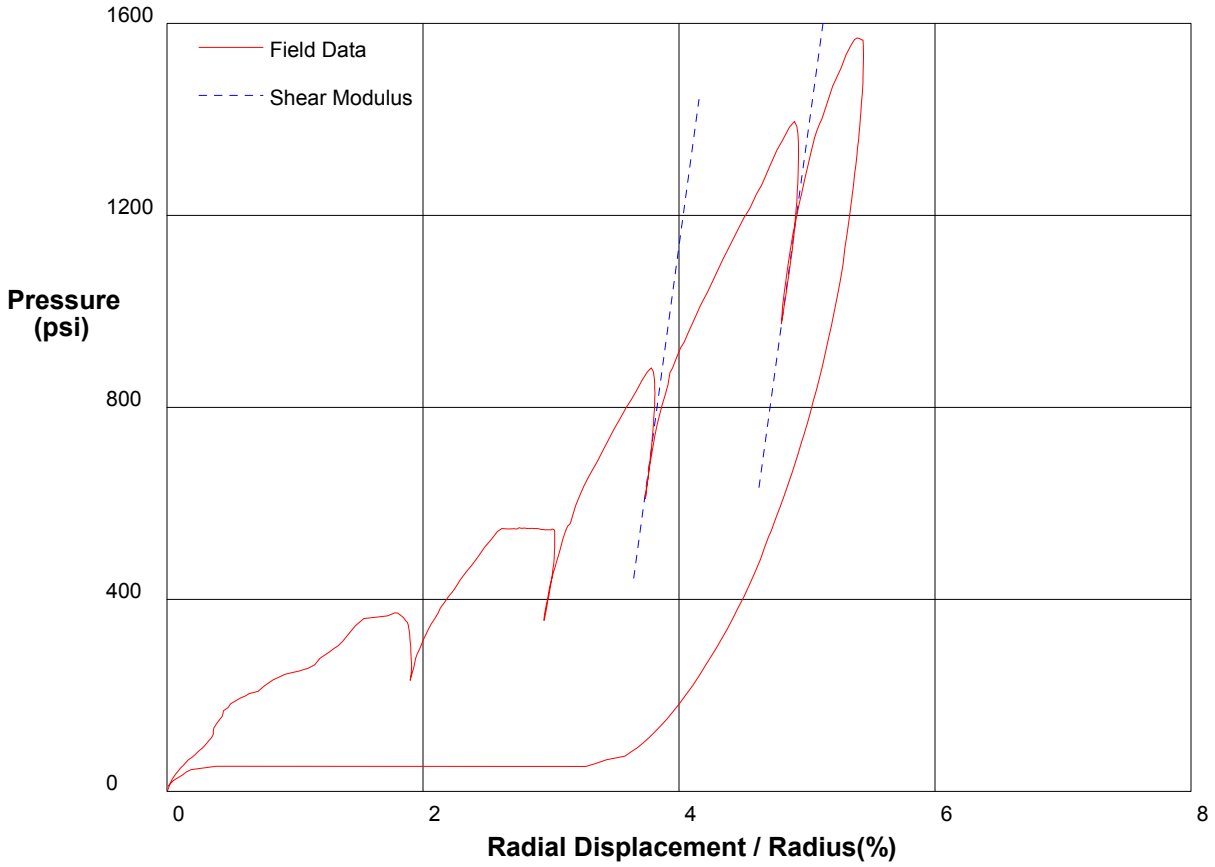

Shear Modulus 96666 psi

Shear Modulus 97687 psi

shift 0

In Situ Engineering

Appendix I - Pressuremeter Data and Standard Interpretation

PRESSUREMETER DATA **CH2MHill, Inc.**

CALTRANS I-710 North Tunnel Project **1/28/2009**

Hole No. Z1-B3 **Depth 177.3ft** **File C:\DATA\ISE-812\SR710-21.P**

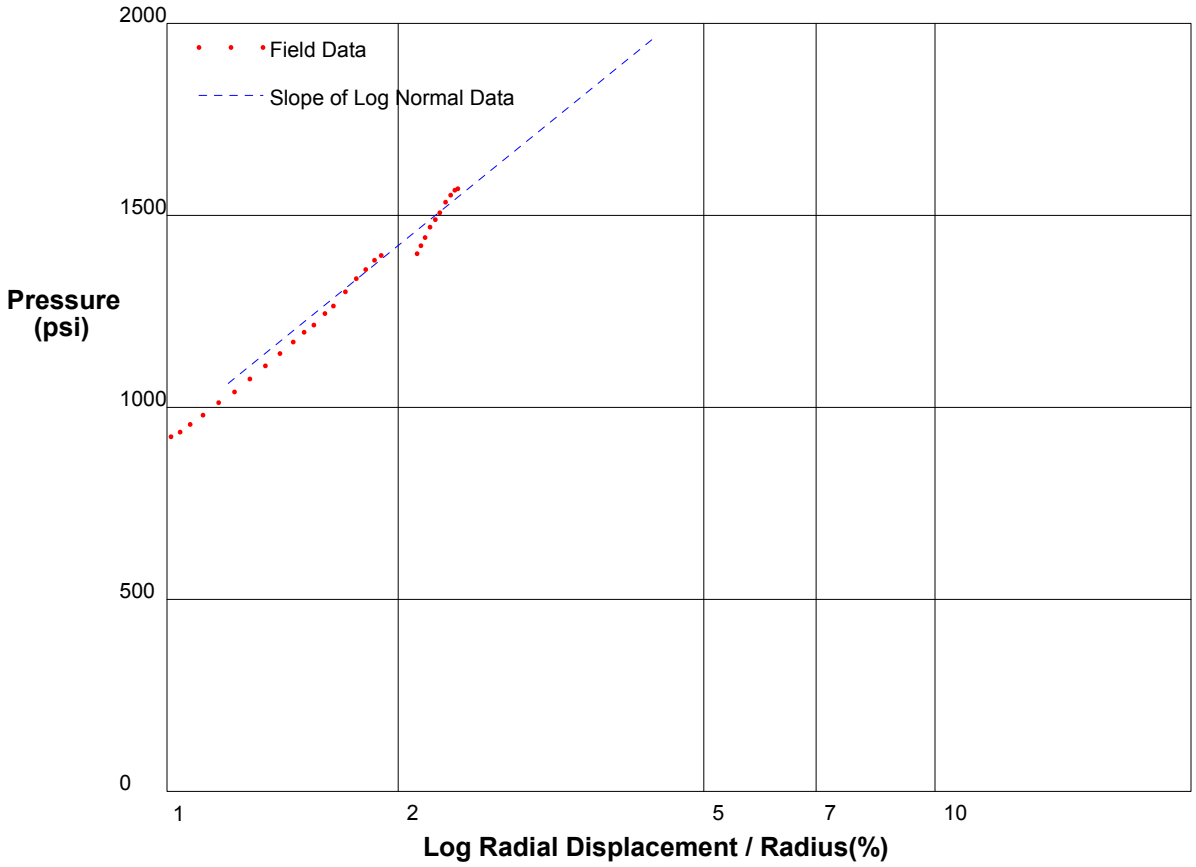

Shear Strength 704.7 psi
Limit Pressure 3549 psi

shift 3

In Situ Engineering

Appendix I - Pressuremeter Data and Standard Interpretation

PRESSUREMETER DATA **CH2MHill, Inc.**

CALTRANS I-710 North Tunnel Project **1/28/2009**

Hole No. Z1-B3 **Depth 204ft** **File C:\DATA\ISE-812\SR710-22.P**

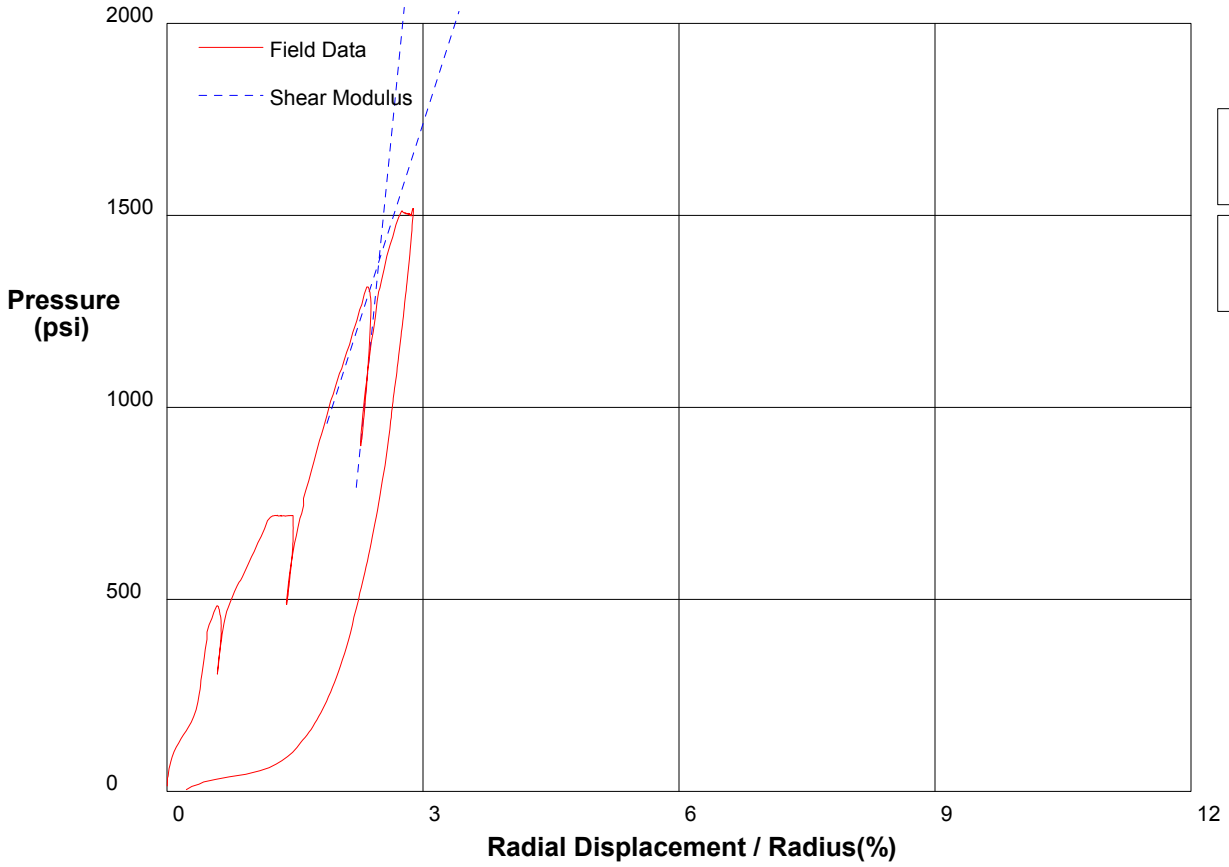

Shear Modulus 111111 psi

Shear Modulus 34680 psi

shift 0

In Situ Engineering

Appendix I - Pressuremeter Data and Standard Interpretation

PRESSUREMETER DATA **CH2M-HILL, Inc.**

CALTRANS I-710 North Tunnel Project **1/28/2009**

Hole No. Z1-B3 **Depth 204ft** **File C:\DATA\ISE-812\SR710-22.P**

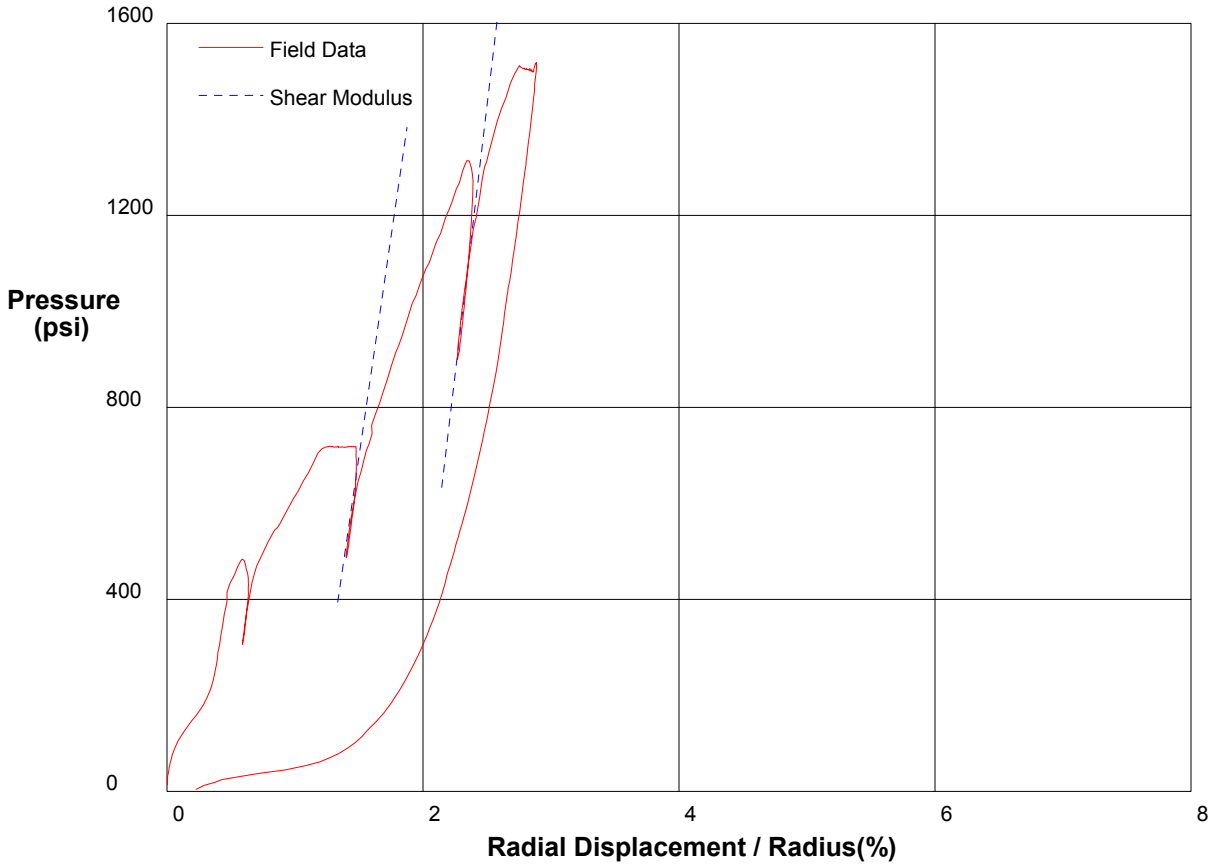

Shear Modulus 112380 psi

Shear Modulus 91282 psi

shift 0

In Situ Engineering

Appendix I - Pressuremeter Data and Standard Interpretation

PRESSUREMETER DATA **CH2MHill, Inc.**

CALTRANS I-710 North Tunnel Project **1/28/2009**

Hole No. Z1-B3 **Depth 204ft** **File C:\DATA\ISE-812\SR710-22.P**

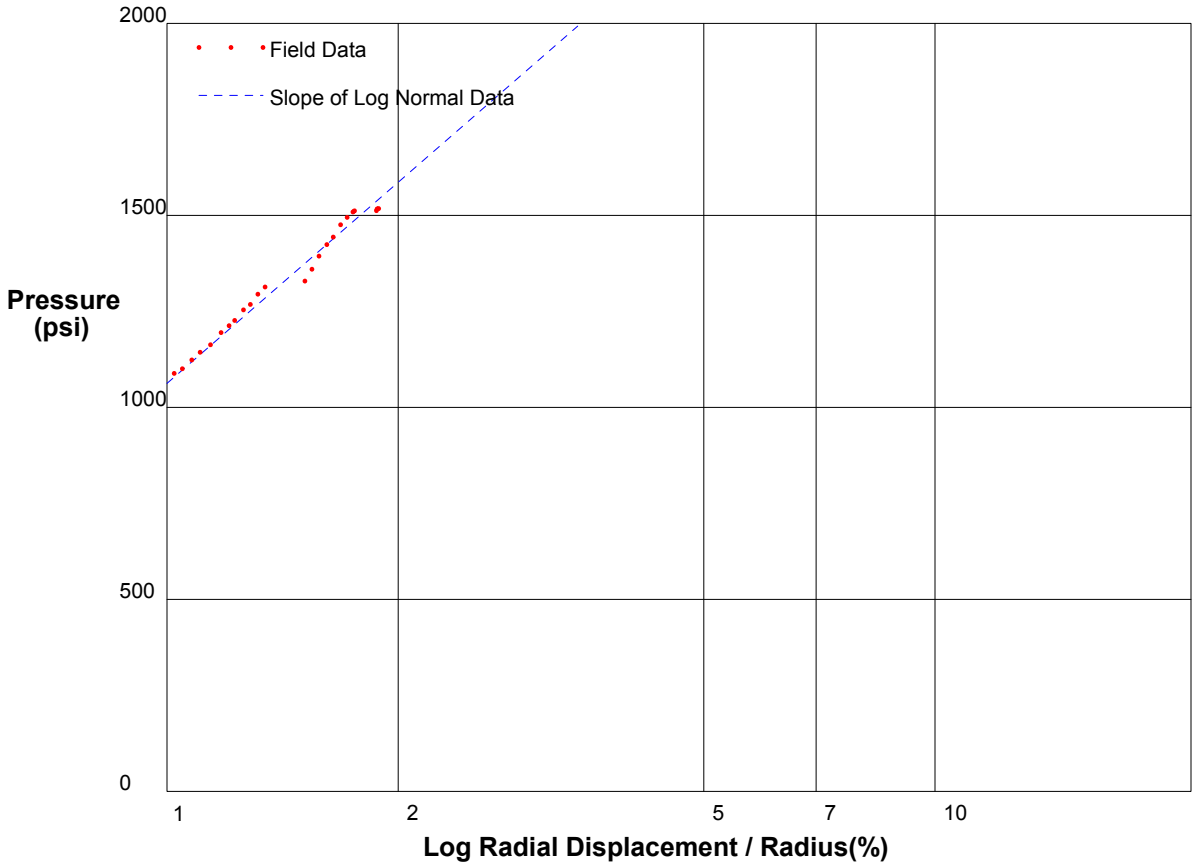

Shear Strength 755.7 psi
Limit Pressure 3869 psi

shift 1

In Situ Engineering

Appendix I - Pressuremeter Data and Standard Interpretation

PRESSUREMETER DATA **CH2MHill, Inc.**

CALTRANS I-710 North Tunnel Project **1/29/2009**

Hole No. Z2-B2 **Depth 135.7ft** **File C:\DATA\ISE-812\SR710-23.P**

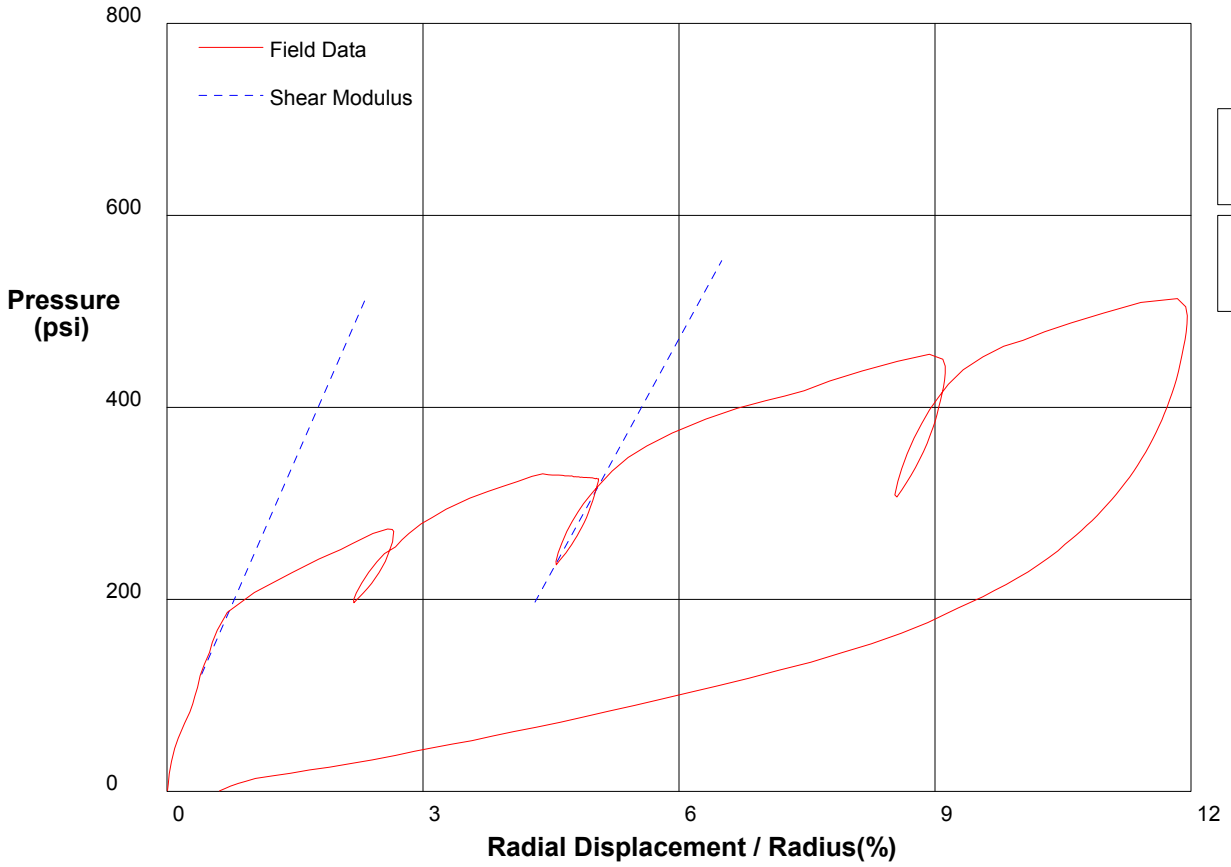

Shear Modulus 8126 psi

Shear Modulus 10179 psi

shift 0

In Situ Engineering

Appendix I - Pressuremeter Data and Standard Interpretation

PRESSUREMETER DATA **CH2M-HILL, Inc.**

CALTRANS I-710 North Tunnel Project **1/29/2009**

Hole No. Z2-B2 **Depth 135.7ft** **File C:\DATA\ISE-812\SR710-23.P**

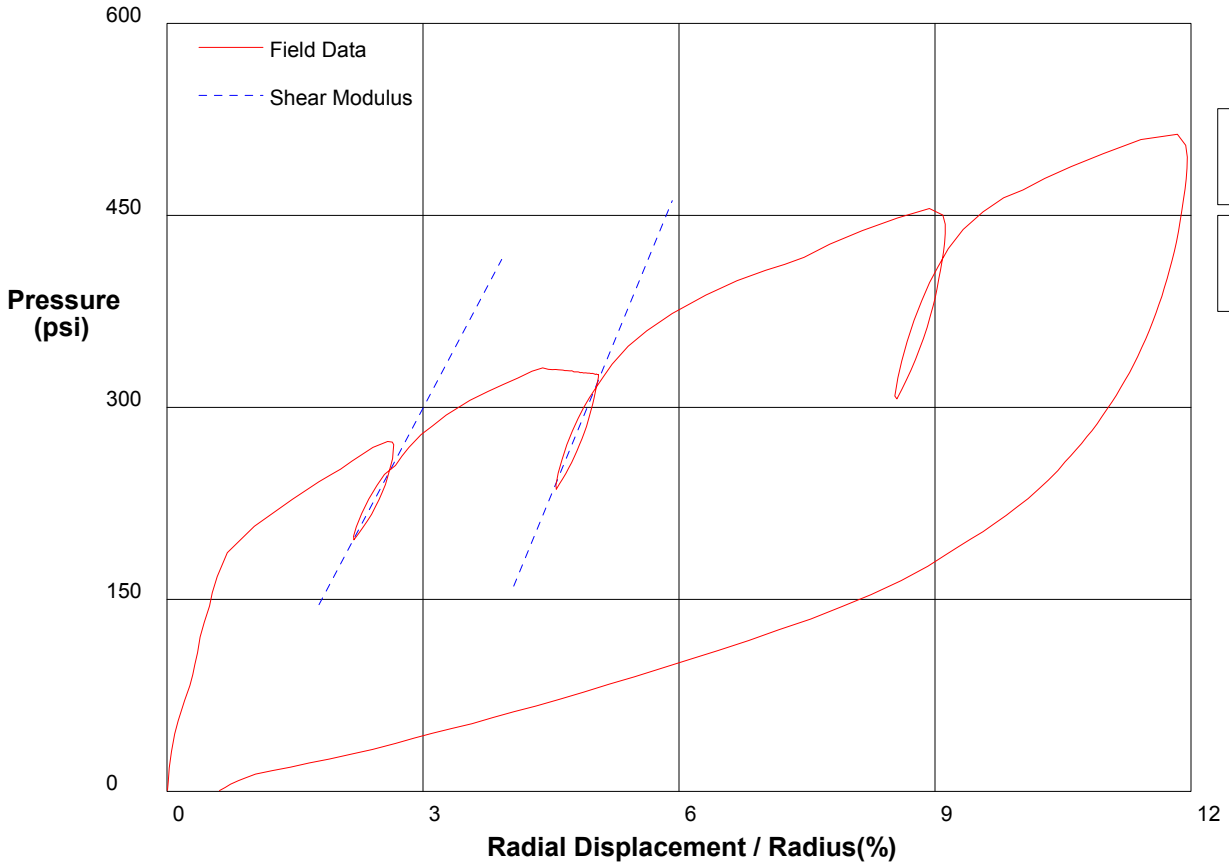

Shear Modulus 6301 psi

Shear Modulus 8095 psi

shift 0

In Situ Engineering

Appendix I - Pressuremeter Data and Standard Interpretation

PRESSUREMETER DATA **CH2M-HILL, Inc.**

CALTRANS I-710 North Tunnel Project **1/29/2009**

Hole No. Z2-B2 **Depth 135.7ft** **File C:\DATA\ISE-812\SR710-23.P**

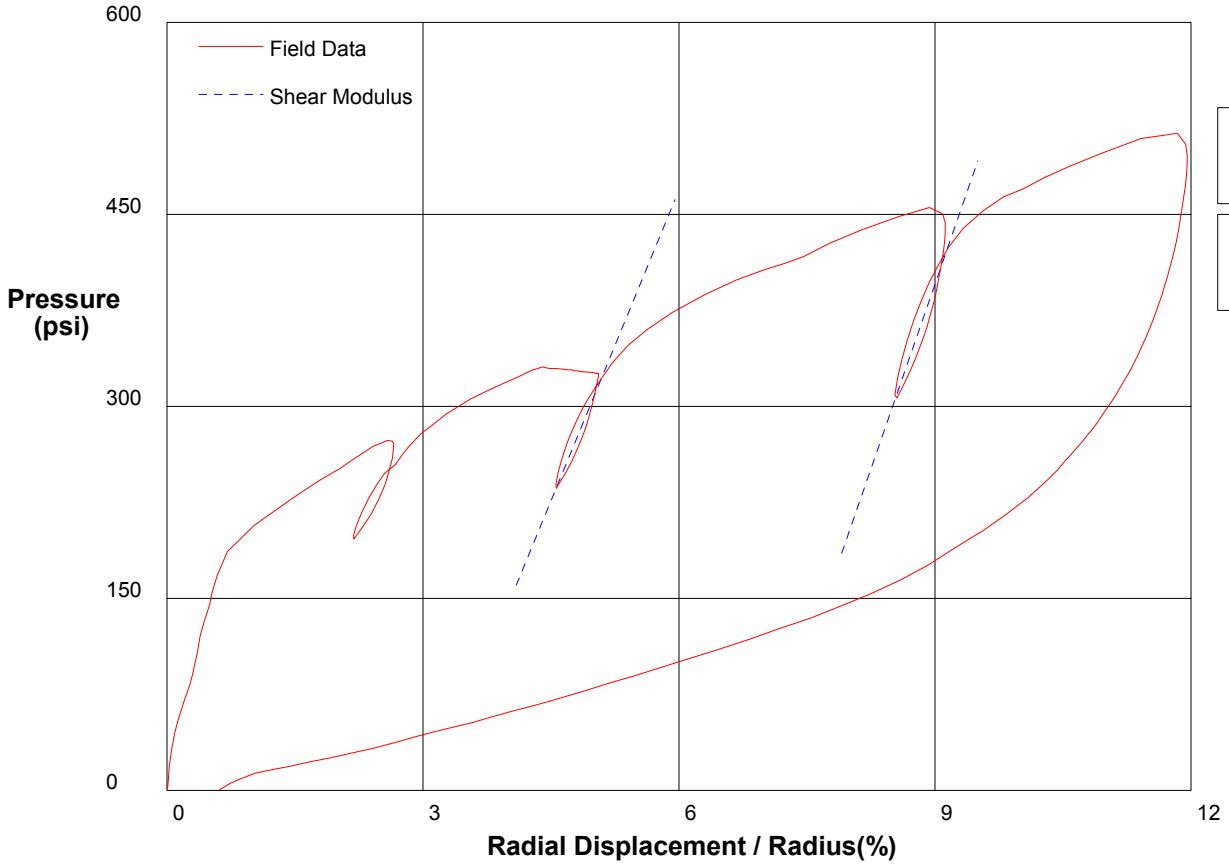

Shear Modulus 9607 psi

Shear Modulus 8095 psi

shift 0

In Situ Engineering

Appendix I - Pressuremeter Data and Standard Interpretation

PRESSUREMETER DATA **CH2MHill, Inc.**

CALTRANS I-710 North Tunnel Project **1/29/2009**

Hole No. Z2-B2 **Depth 135.7ft** **File C:\DATA\ISE-812\SR710-23.P**

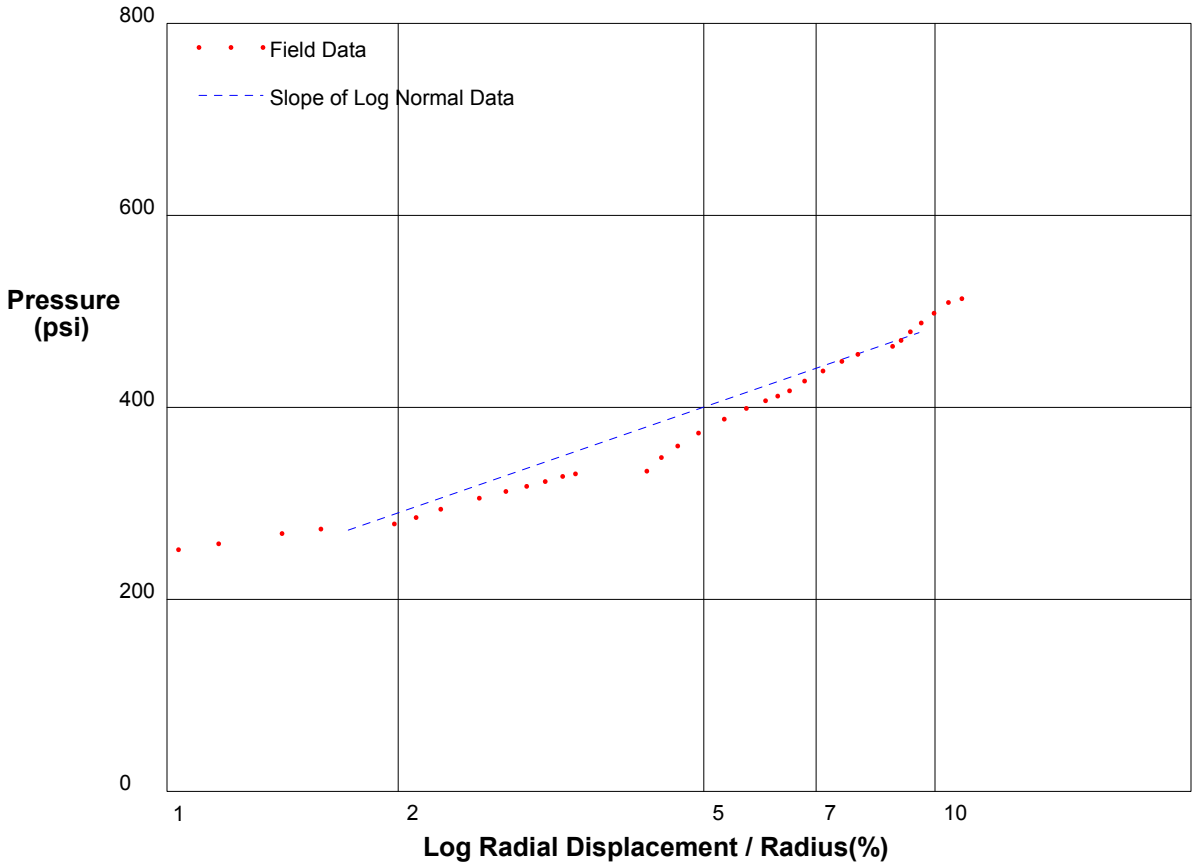

Shear Strength 120.1 psi
Limit Pressure 653 psi

shift 1

In Situ Engineering

Appendix I - Pressuremeter Data and Standard Interpretation

PRESSUREMETER DATA **CH2MHill, Inc.**

CALTRANS I-710 North Tunnel Project **1/29/2009**

Hole No. Z2-B2 **Depth 134.2ft** **File C:\DATA\ISE-812\SR710-24.P**

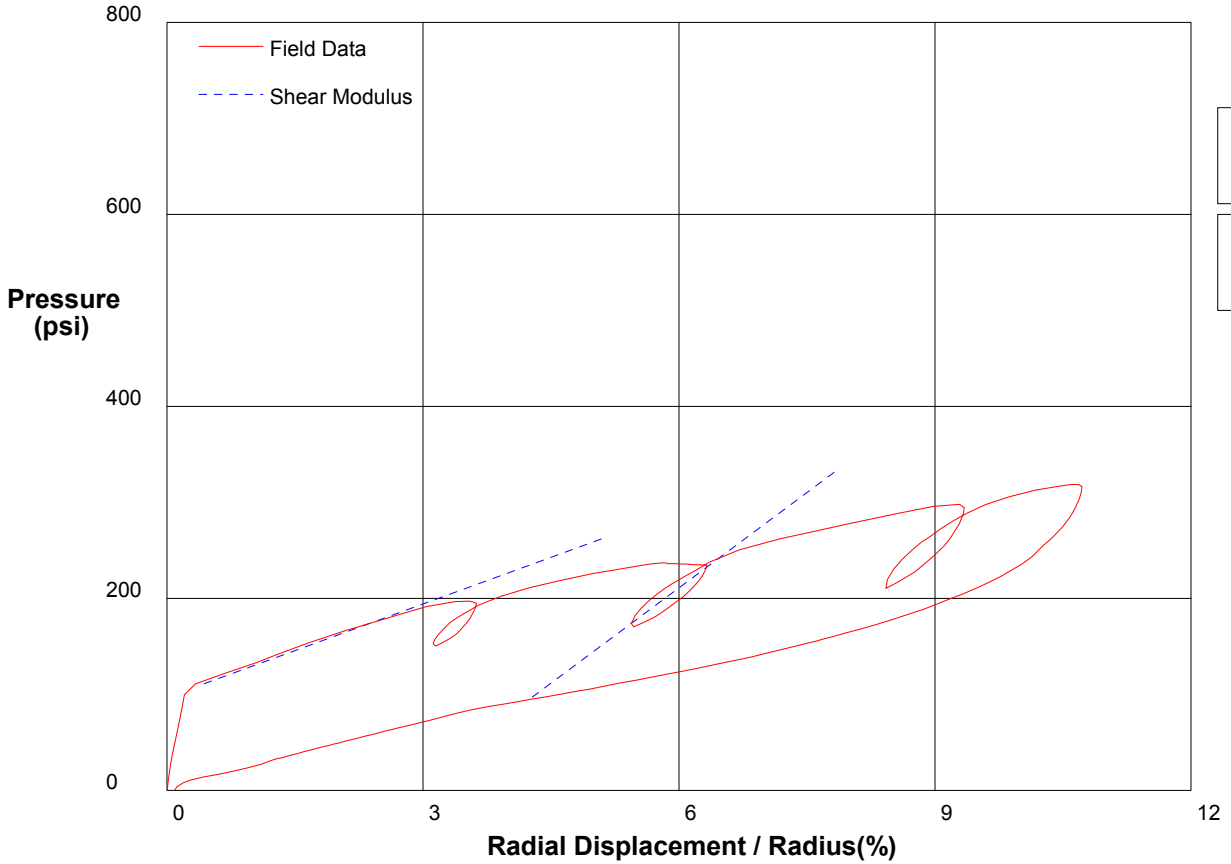

Shear Modulus 3308 psi

Shear Modulus 1620 psi

shift 0

In Situ Engineering

Appendix I - Pressuremeter Data and Standard Interpretation

PRESSUREMETER DATA **CH2M-HILL, Inc.**

CALTRANS I-710 North Tunnel Project **1/29/2009**

Hole No. Z2-B2 **Depth 134.2ft** **File C:\DATA\ISE-812\SR710-24.P**

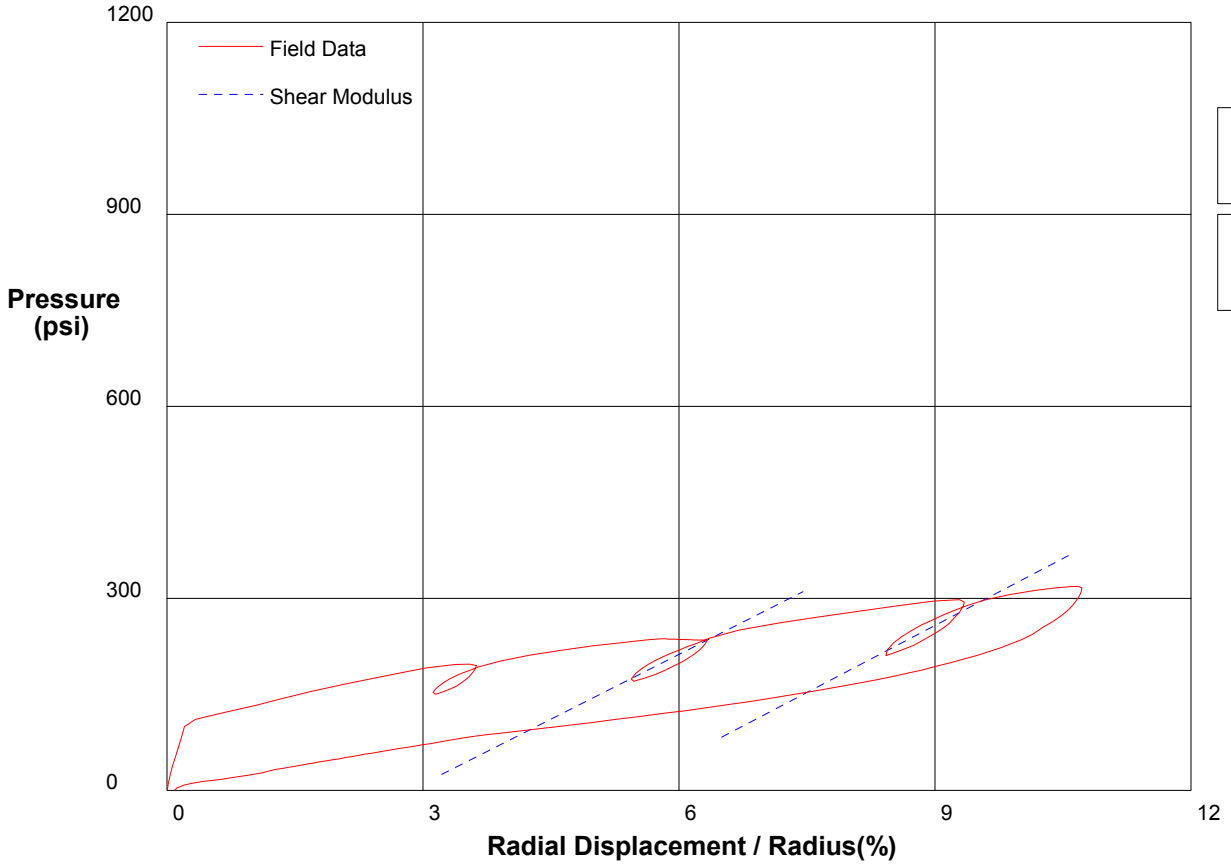

Shear Modulus 3487 psi

Shear Modulus 3370 psi

shift 0

In Situ Engineering

Appendix I - Pressuremeter Data and Standard Interpretation

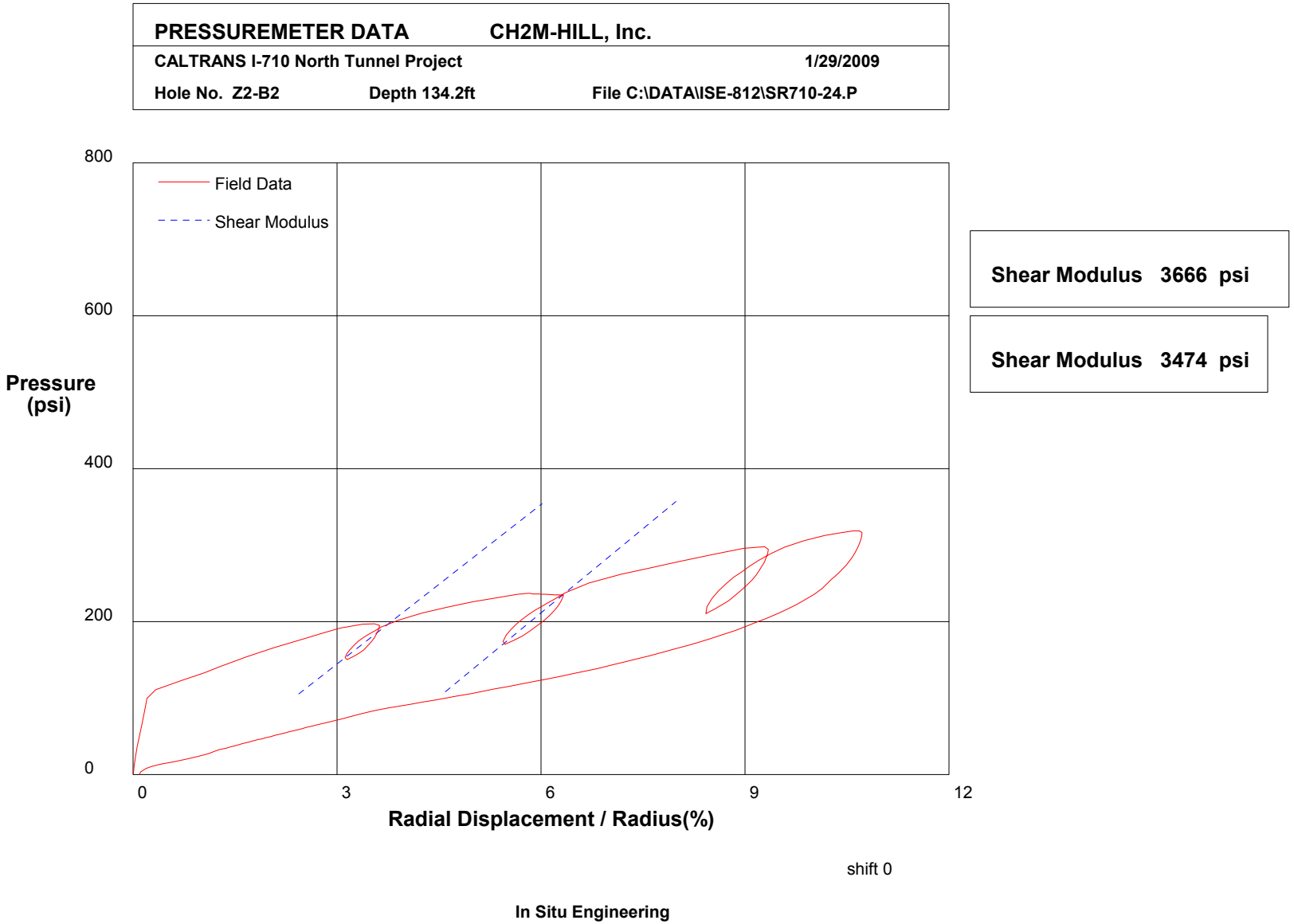

Appendix I - Pressuremeter Data and Standard Interpretation

PRESSUREMETER DATA **CH2MHill, Inc.**

CALTRANS I-710 North Tunnel Project **1/29/2009**

Hole No. Z2-B2 **Depth 134.2ft** **File C:\DATA\ISE-812\SR710-24.P**

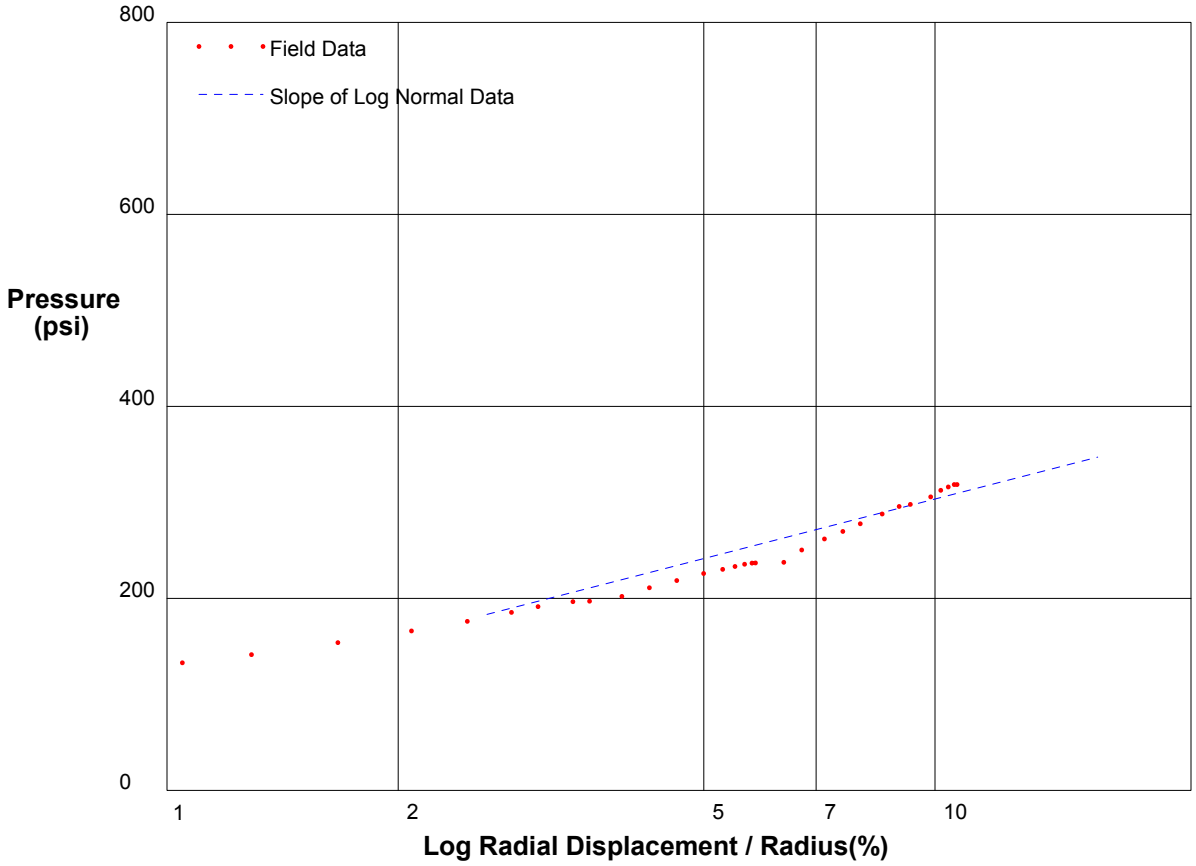

Shear Strength 89.5 psi
Limit Pressure 429 psi

shift 0

In Situ Engineering

Appendix I - Pressuremeter Data and Standard Interpretation

PRESSUREMETER DATA **CH2MHill, Inc.**

CALTRANS I-710 North Tunnel Project **2/4/2009**

Hole No. Z2-B2 **Depth 251ft** **File C:\DATA\ISE-812\SR710-25.P**

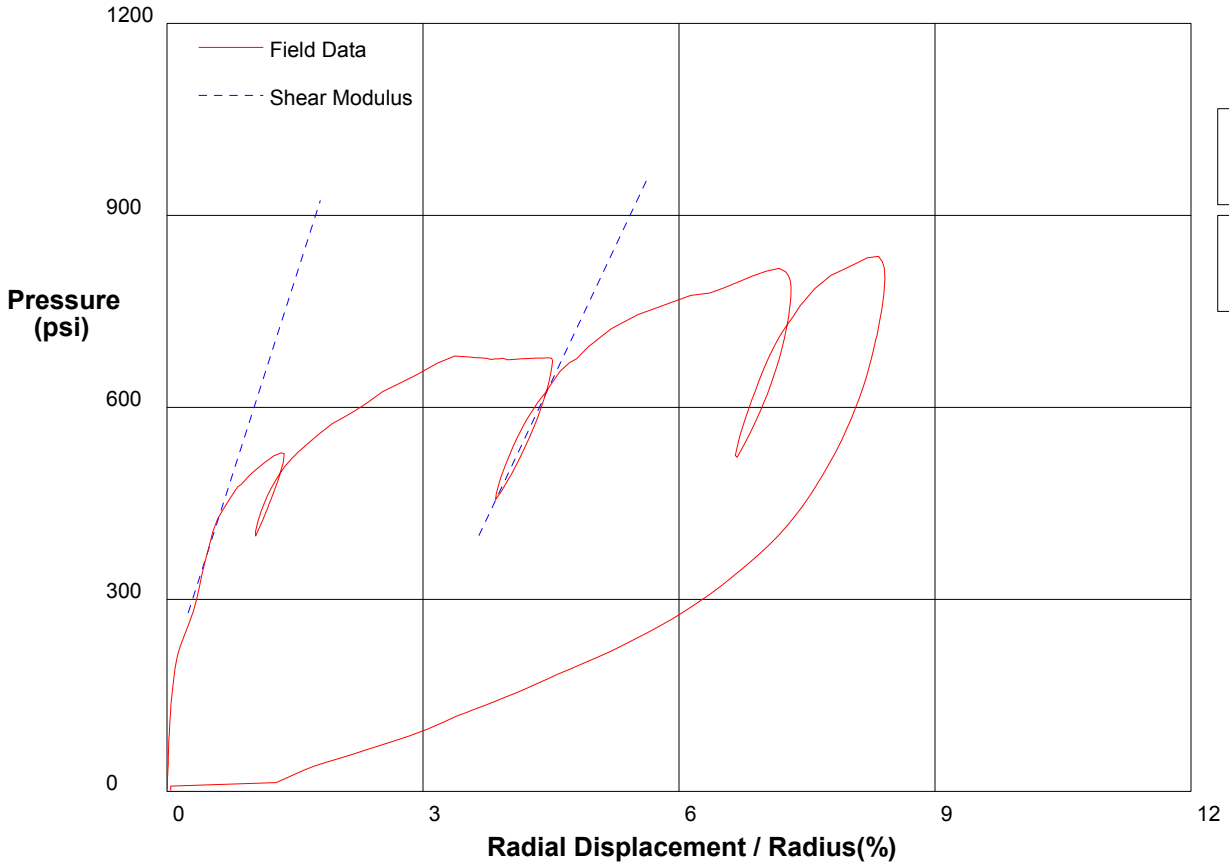

Shear Modulus 14120 psi

Shear Modulus 20808 psi

shift 0

In Situ Engineering

Appendix I - Pressuremeter Data and Standard Interpretation

PRESSUREMETER DATA **CH2M-HILL, Inc.**

CALTRANS I-710 North Tunnel Project **2/4/2009**

Hole No. Z2-B2 **Depth 251ft** **File C:\DATA\ISE-812\SR710-25.P**

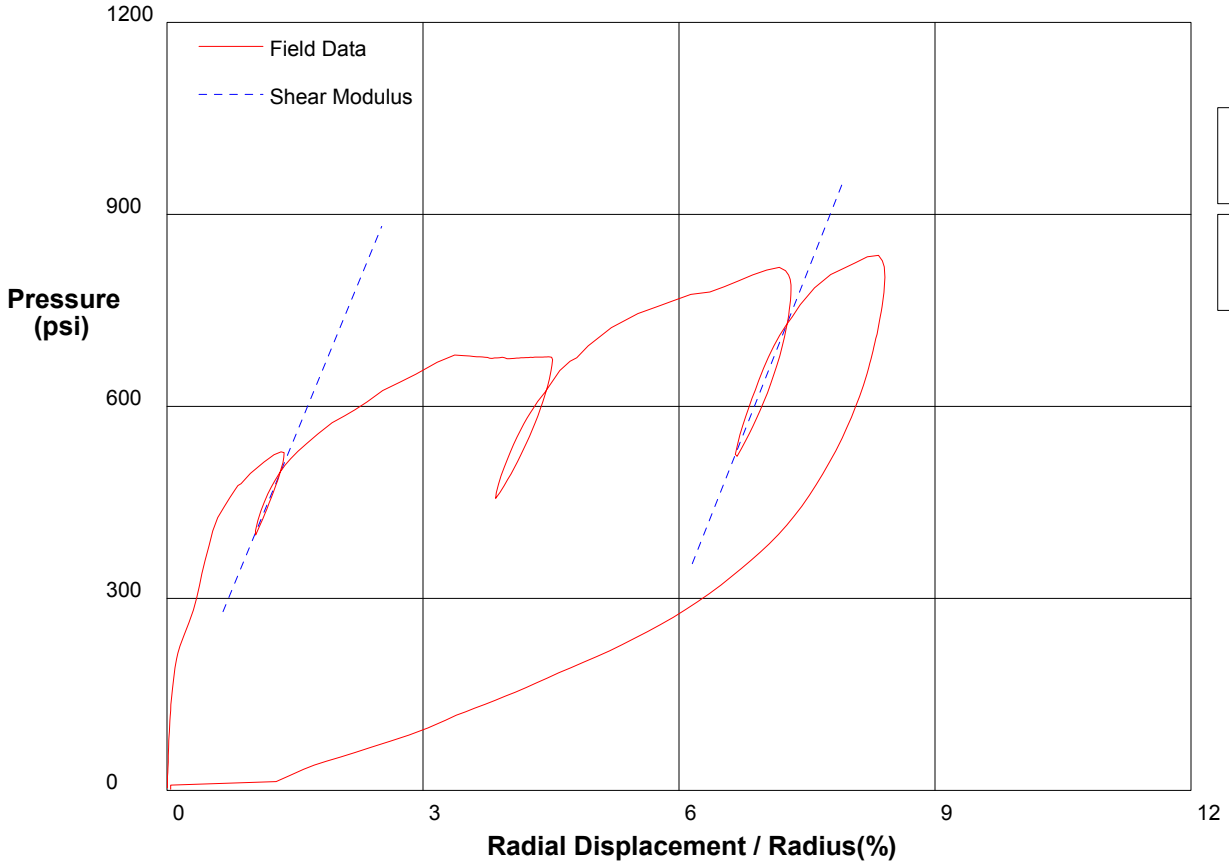

Shear Modulus 16904 psi

Shear Modulus 16190 psi

shift 0

In Situ Engineering

Appendix I - Pressuremeter Data and Standard Interpretation

PRESSUREMETER DATA **CH2M-HILL, Inc.**

CALTRANS I-710 North Tunnel Project **2/4/2009**

Hole No. Z2-B2 **Depth 251ft** **File C:\DATA\ISE-812\SR710-25.P**

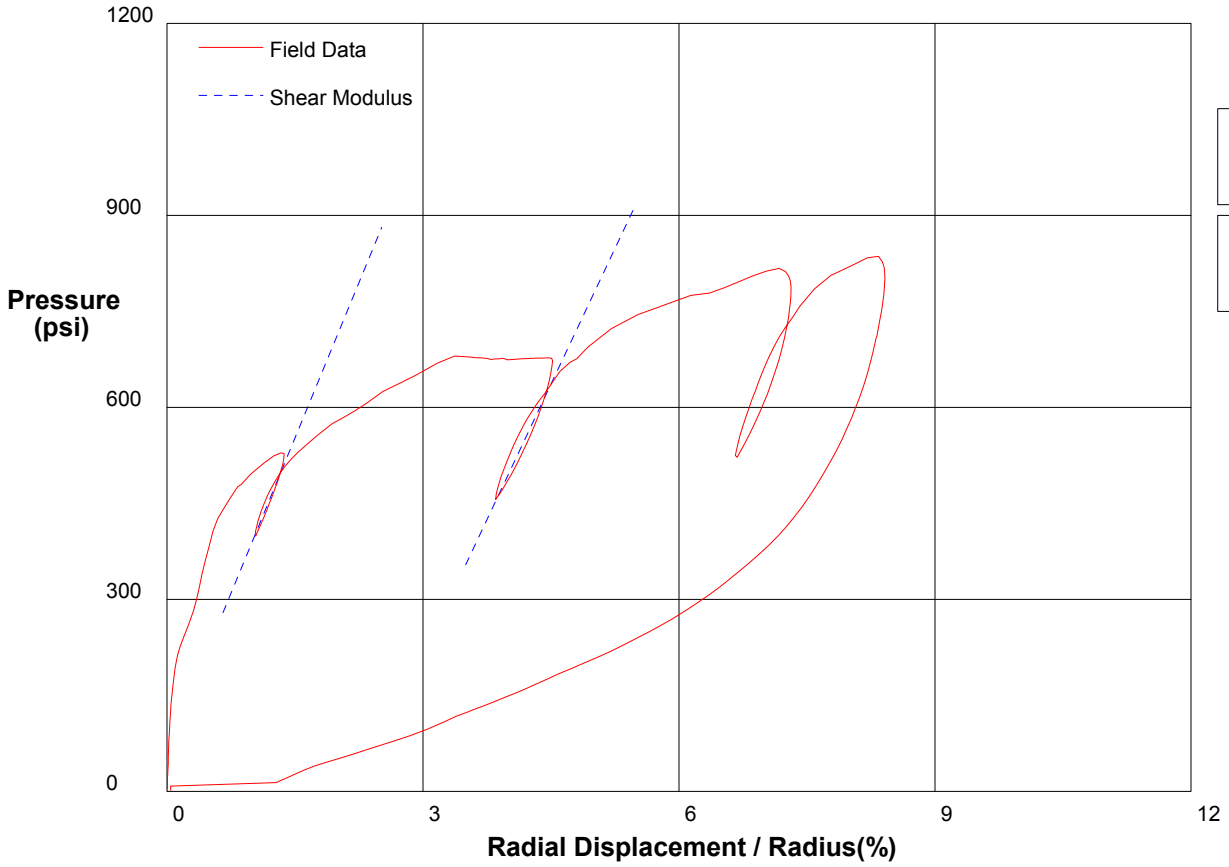

Shear Modulus 14120 psi

Shear Modulus 16190 psi

shift 0

In Situ Engineering

Appendix I - Pressuremeter Data and Standard Interpretation

PRESSUREMETER DATA **CH2MHill, Inc.**

CALTRANS I-710 North Tunnel Project **2/4/2009**

Hole No. Z2-B2 **Depth 251ft** **File C:\DATA\ISE-812\SR710-25.P**

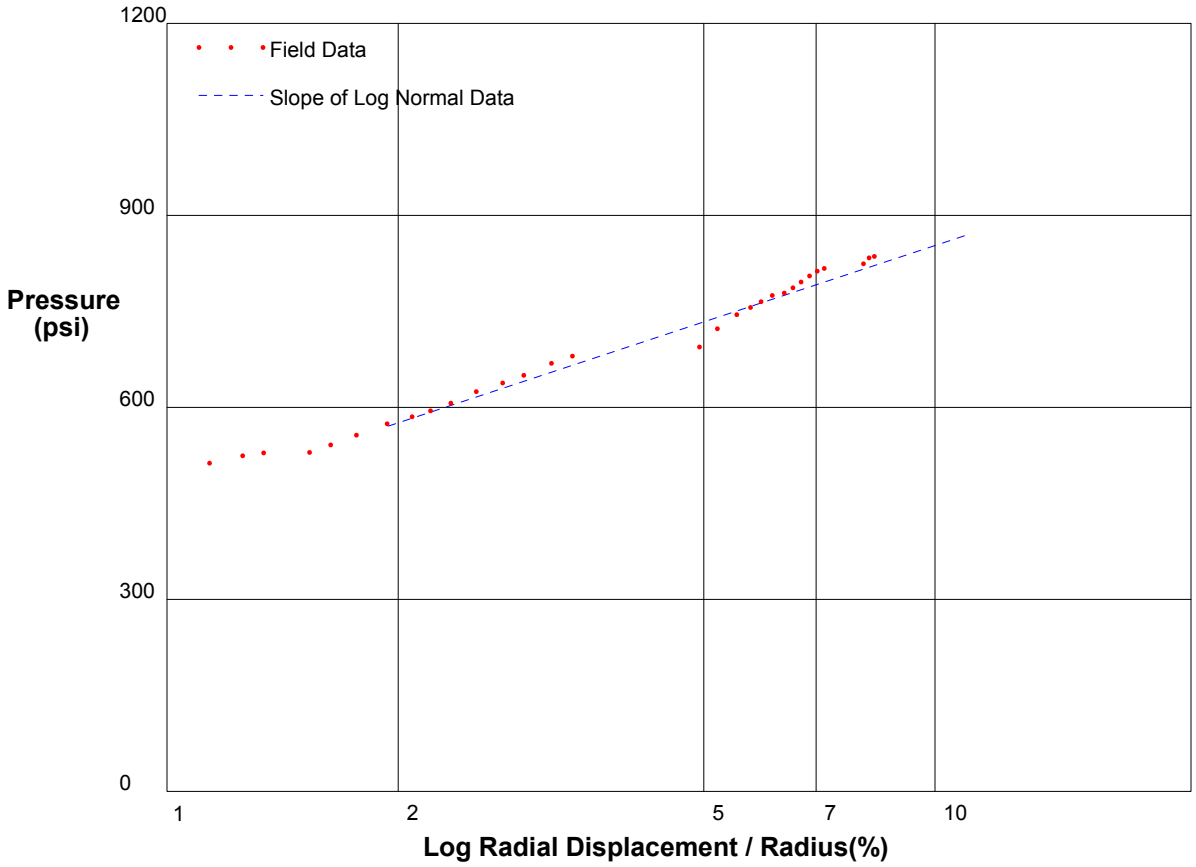

Shear Strength 172.1 psi
Limit Pressure 1095 psi

shift 0

In Situ Engineering

Appendix I - Pressuremeter Data and Standard Interpretation

PRESSUREMETER DATA **CH2MHill, Inc.**

CALTRANS I-710 North Tunnel Project **2/4/2009**

Hole No. Z2-B2 **Depth 249.5ft** **File C:\DATA\ISE-812\SR710-26.P**

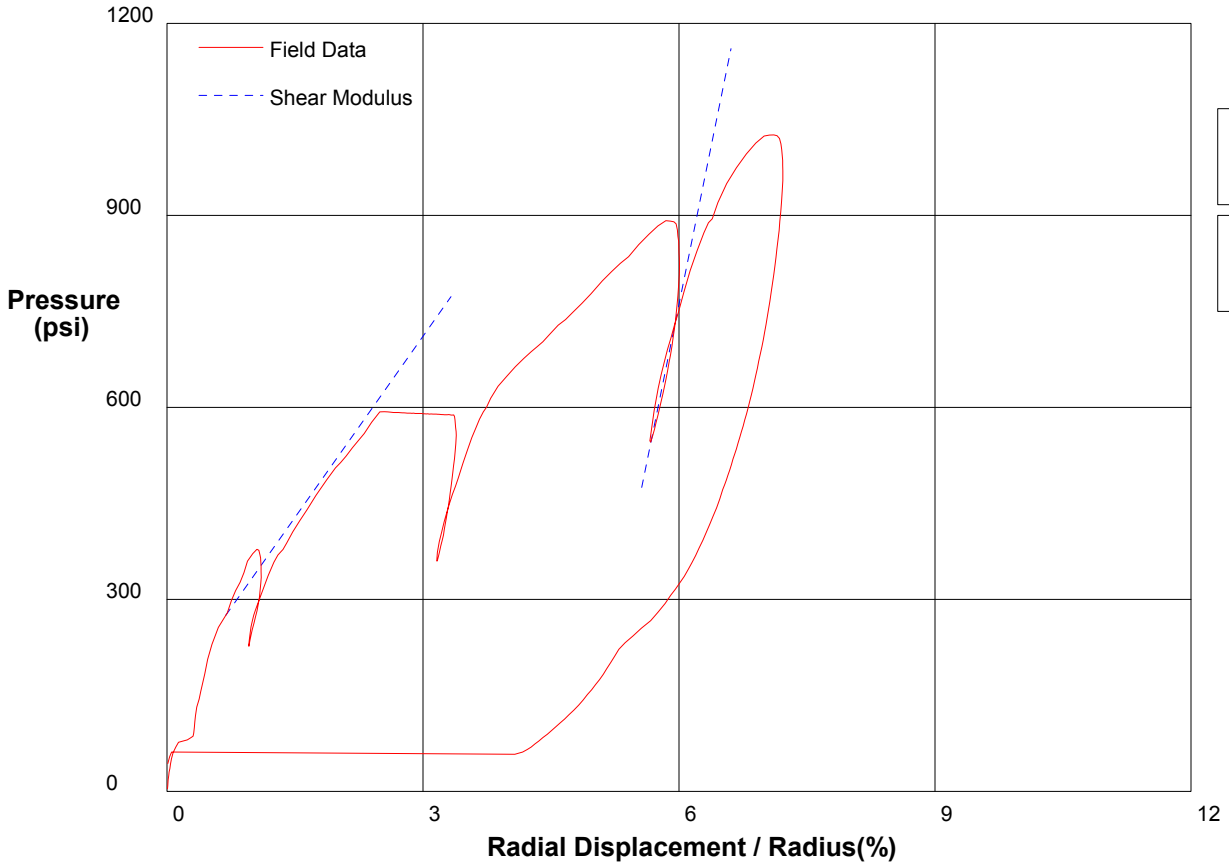

Shear Modulus 32736 psi

Shear Modulus 9428 psi

shift 0

In Situ Engineering

Appendix I - Pressuremeter Data and Standard Interpretation

PRESSUREMETER DATA **CH2M-HILL, Inc.**

CALTRANS I-710 North Tunnel Project **2/4/2009**

Hole No. Z2-B2 **Depth 249.5ft** **File C:\DATA\ISE-812\SR710-26.P**

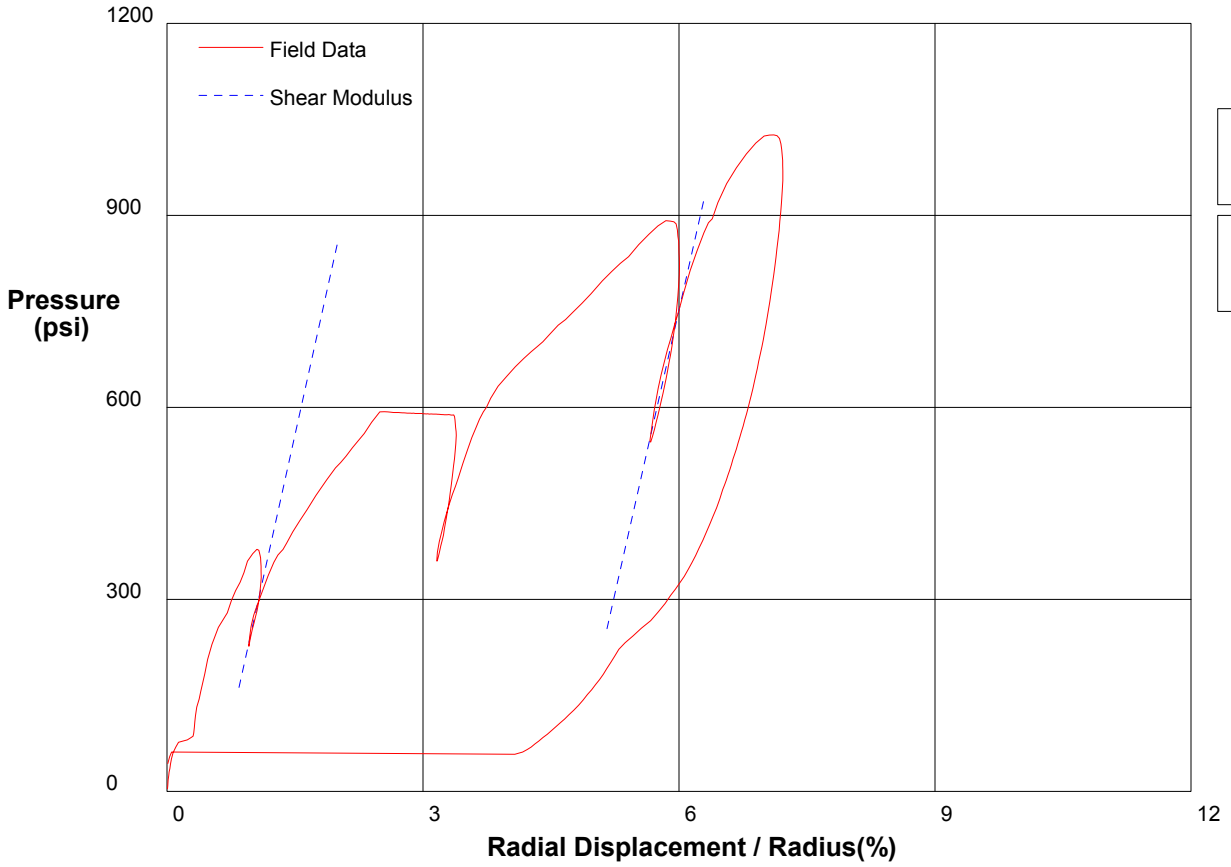

Shear Modulus 29497 psi

Shear Modulus 30090 psi

shift 0

In Situ Engineering

Appendix I - Pressuremeter Data and Standard Interpretation

PRESSUREMETER DATA **CH2M-HILL, Inc.**

CALTRANS I-710 North Tunnel Project **2/4/2009**

Hole No. Z2-B2 **Depth 249.5ft** **File C:\DATA\ISE-812\SR710-26.P**

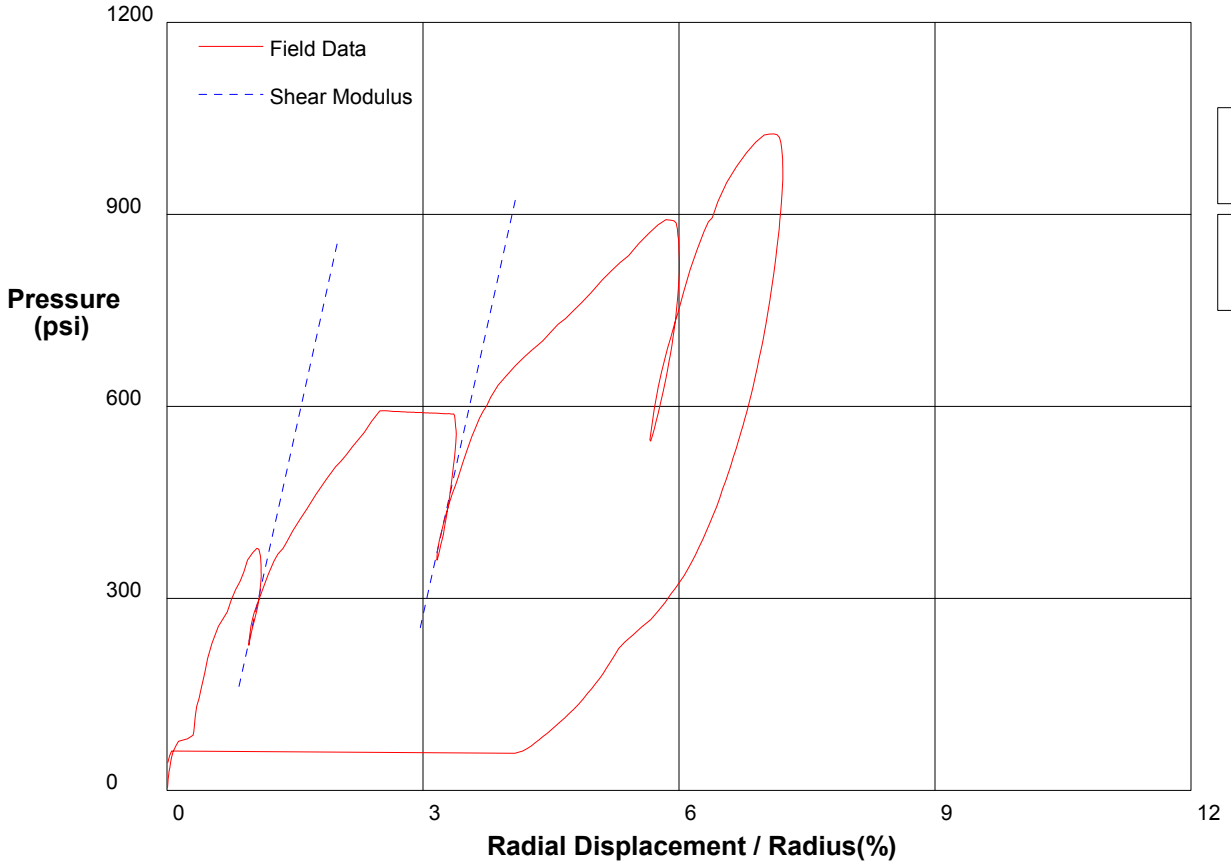

Shear Modulus 30000 psi

Shear Modulus 30090 psi

shift 0

In Situ Engineering

Appendix I - Pressuremeter Data and Standard Interpretation

PRESSUREMETER DATA **CH2MHill, Inc.**

CALTRANS I-710 North Tunnel Project **2/4/2009**

Hole No. Z2-B2 **Depth 249.5ft** **File C:\DATA\ISE-812\SR710-26.P**

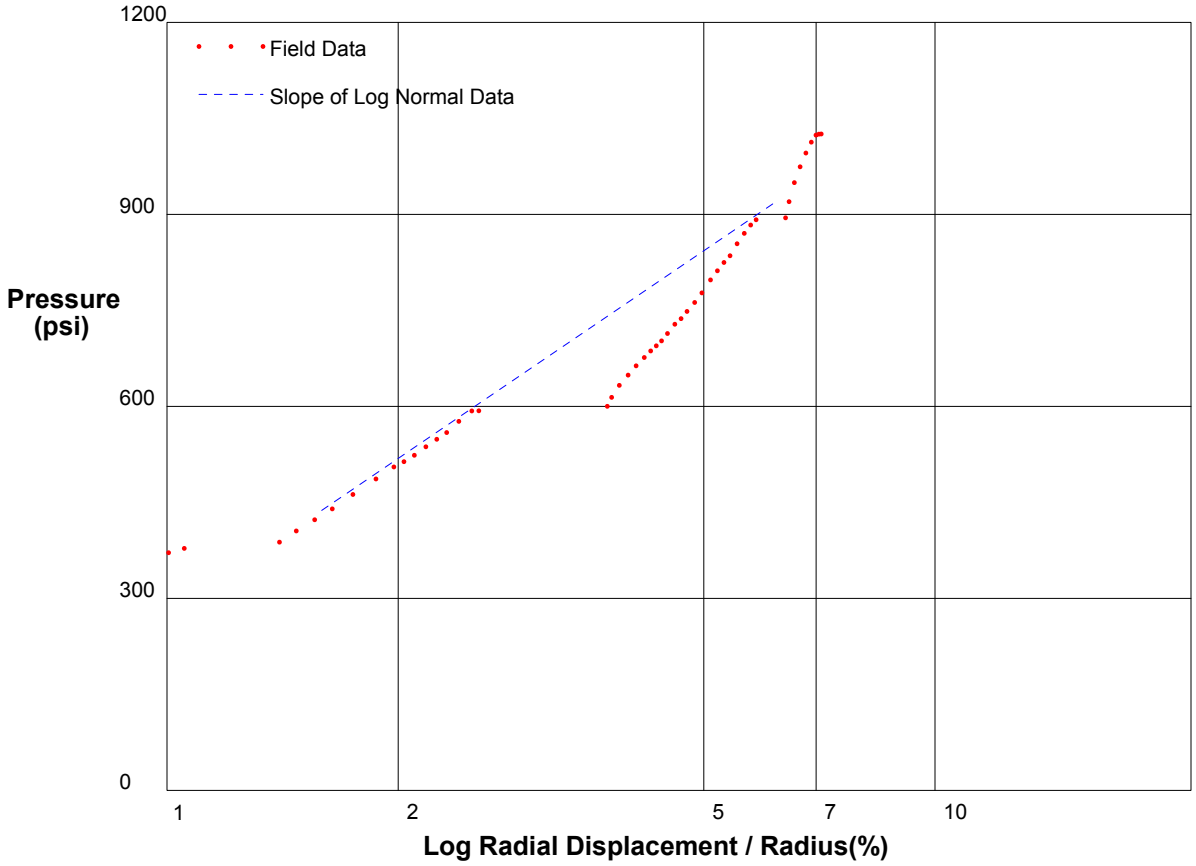

Shear Strength 354 psi
Limit Pressure 1588 psi

shift 0

In Situ Engineering

Appendix I - Pressuremeter Data and Standard Interpretation

PRESSUREMETER DATA **CH2M-HILL, Inc.**

CALTRANS I-710 North Tunnel Project **2/4/2009**

Hole No. Z1-B6 **Depth 203ft** **File C:\DATA\ISE-812\SR710-27.P**

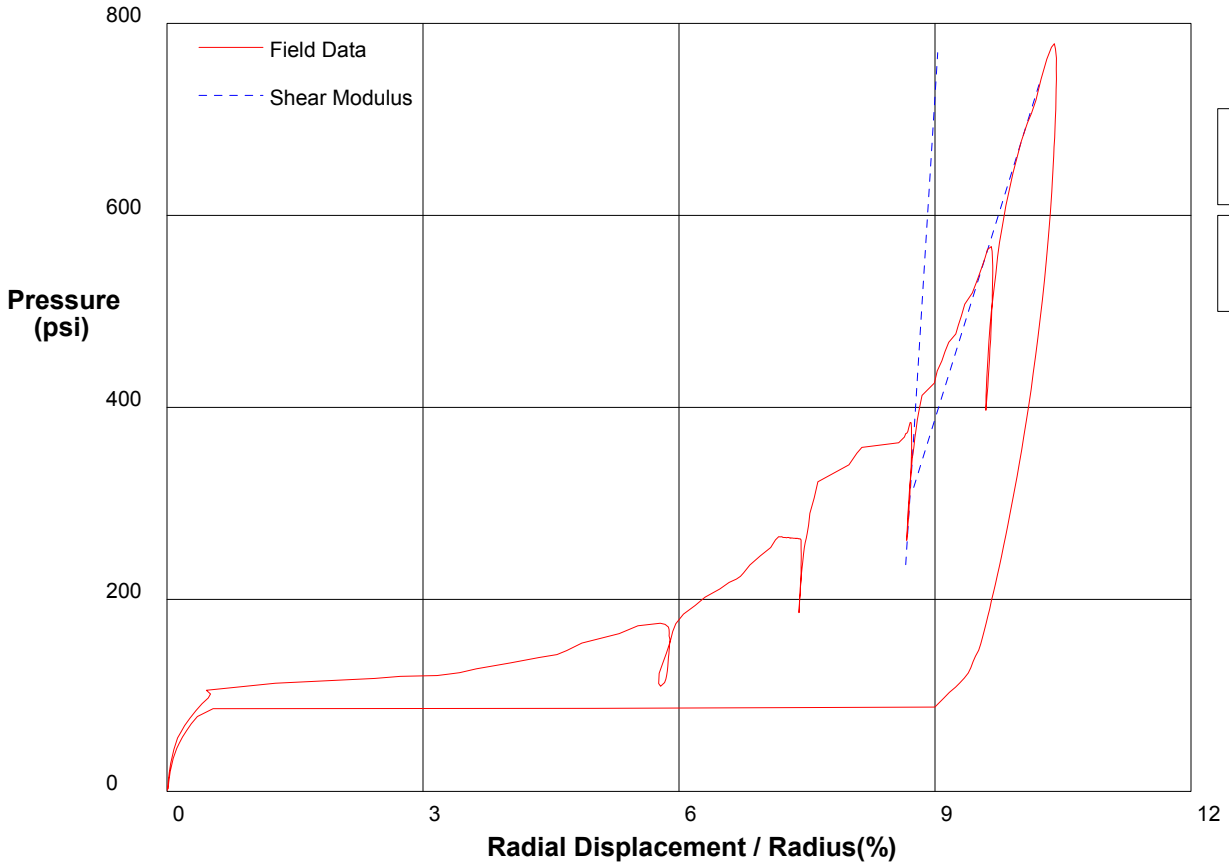

Shear Modulus 14278 psi

Shear Modulus 71111 psi

shift 0

In Situ Engineering

Appendix I - Pressuremeter Data and Standard Interpretation

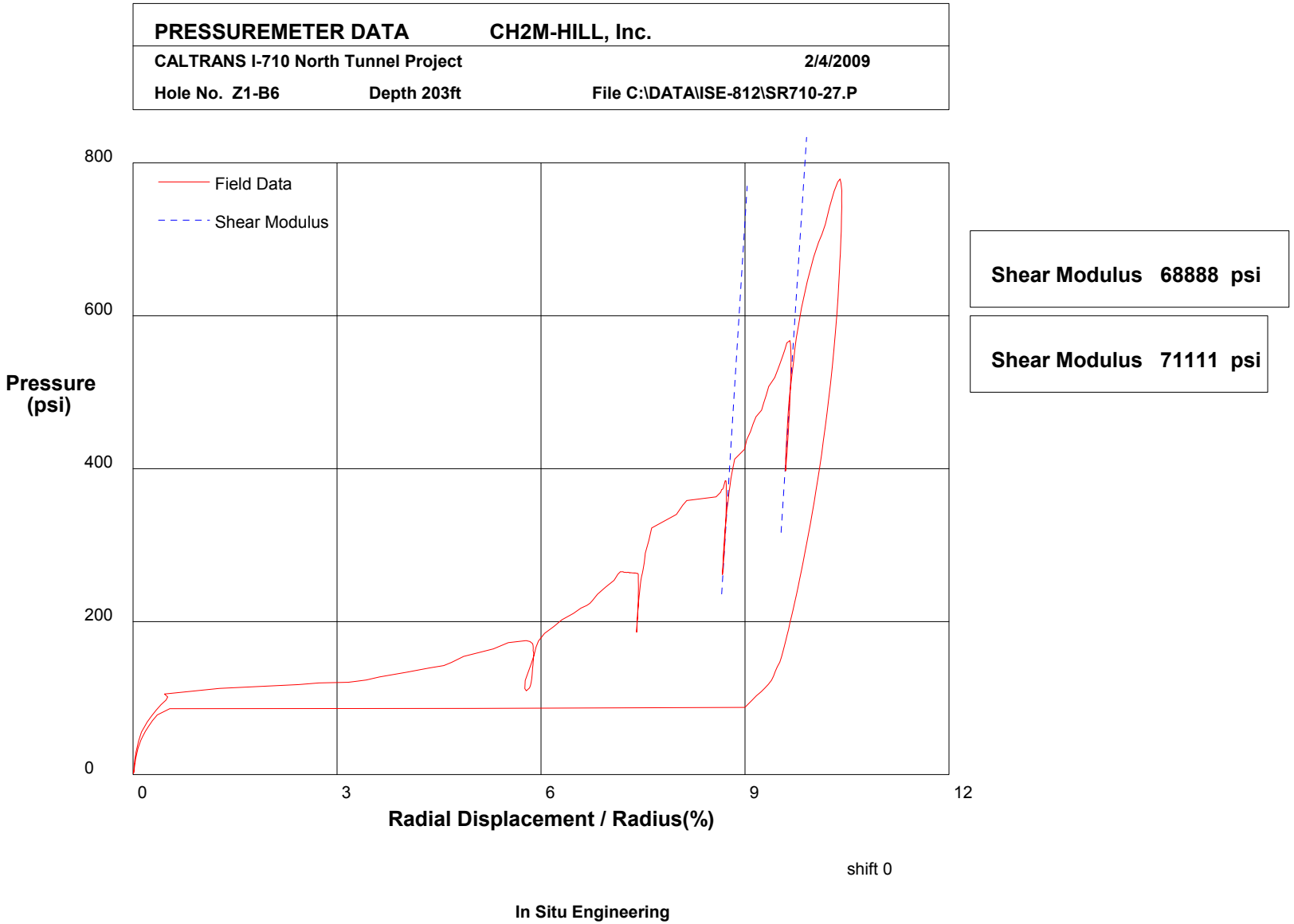

Appendix I - Pressuremeter Data and Standard Interpretation

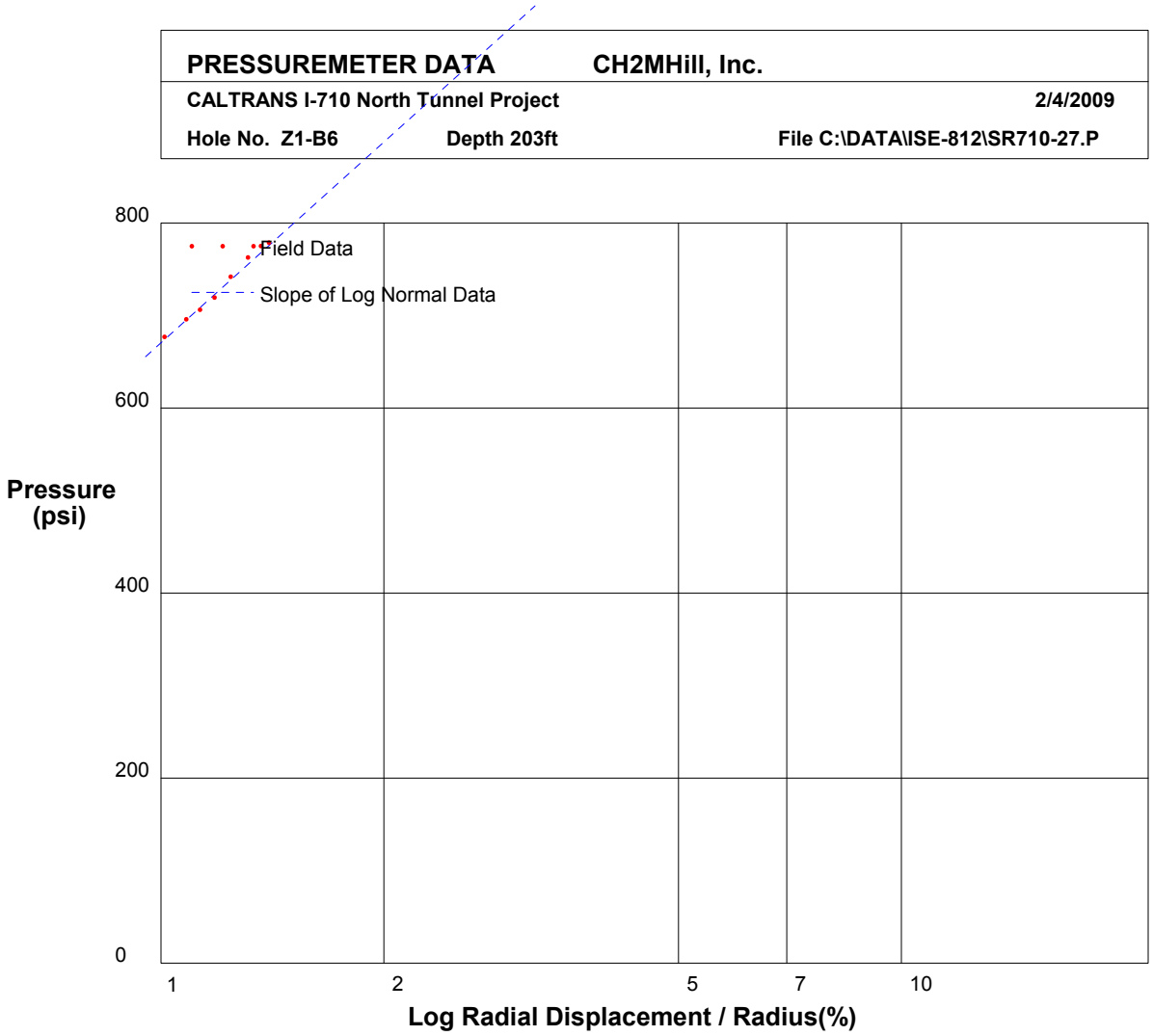

Shear Strength 313 psi
Limit Pressure 1833 psi

Appendix I - Pressuremeter Data and Standard Interpretation

PRESSUREMETER DATA **CH2MHill, Inc.**

CALTRANS I-710 North Tunnel Project **2/5/2009**

Hole No. Z1-B6 **Depth 245ft** **File C:\DATA\ISE-812\SR710-28.P**

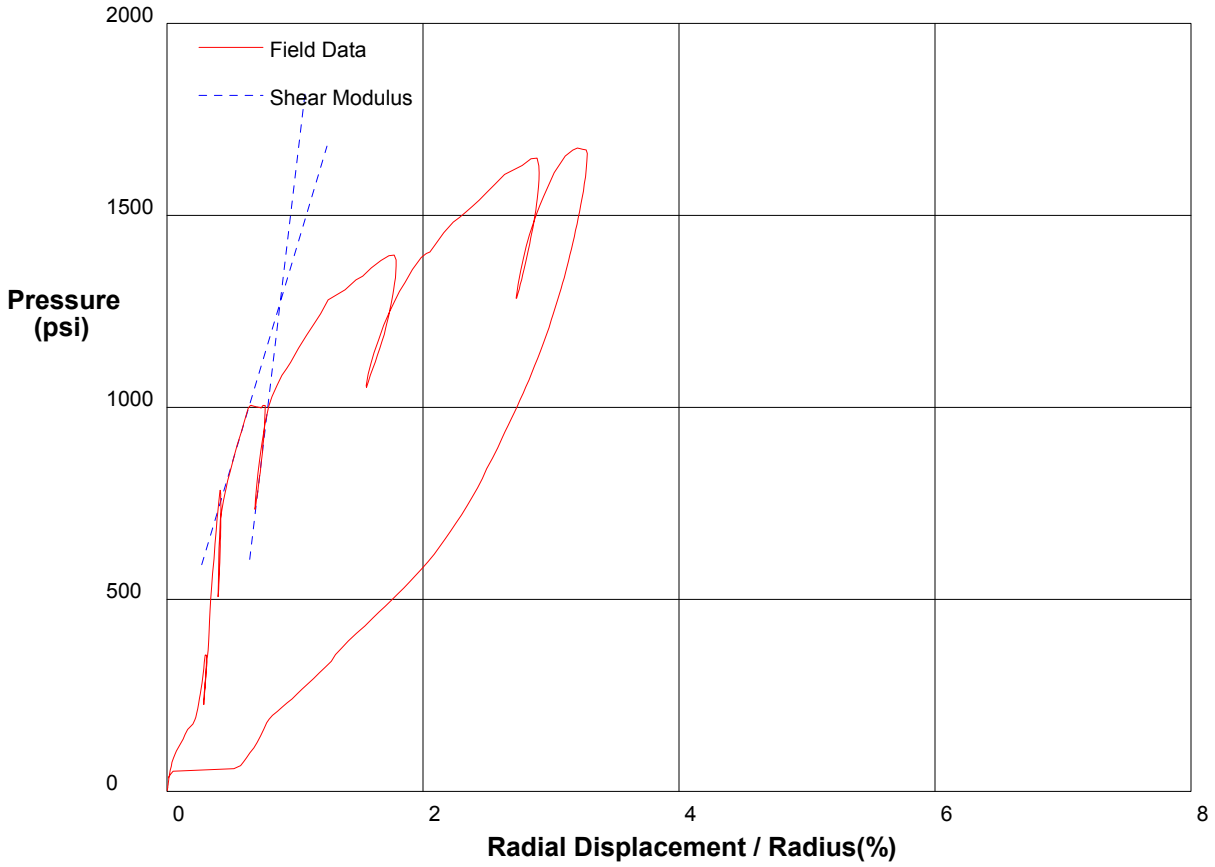

Shear Modulus 140476 psi

Shear Modulus 55673 psi

shift 0

In Situ Engineering

Appendix I - Pressuremeter Data and Standard Interpretation

PRESSUREMETER DATA **CH2M-HILL, Inc.**

CALTRANS I-710 North Tunnel Project **2/5/2009**

Hole No. Z1-B6 **Depth 245ft** **File C:\DATA\ISE-812\SR710-28.P**

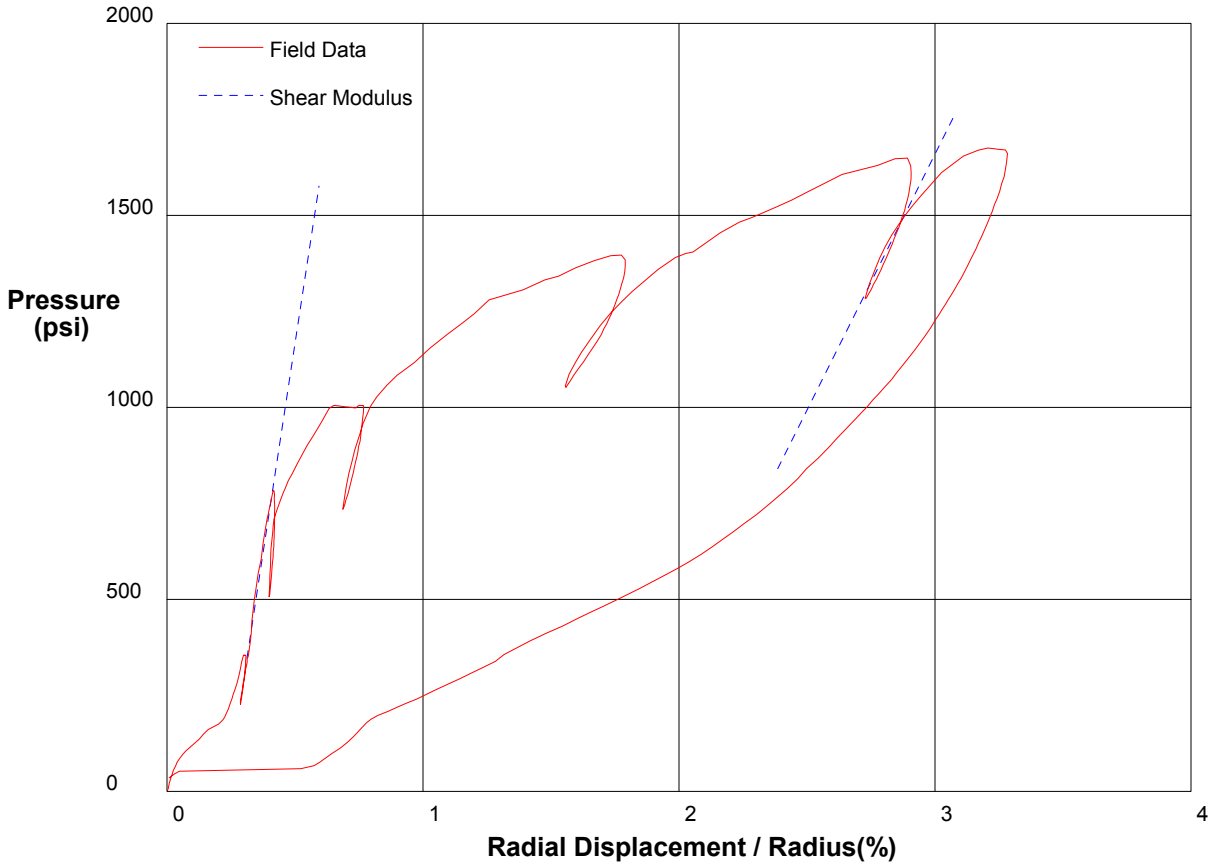

Shear Modulus 66666 psi

Shear Modulus 218518 psi

shift 0

In Situ Engineering

Appendix I - Pressuremeter Data and Standard Interpretation

PRESSUREMETER DATA **CH2M-HILL, Inc.**

CALTRANS I-710 North Tunnel Project **2/5/2009**

Hole No. Z1-B6 **Depth 245ft** **File C:\DATA\ISE-812\SR710-28.P**

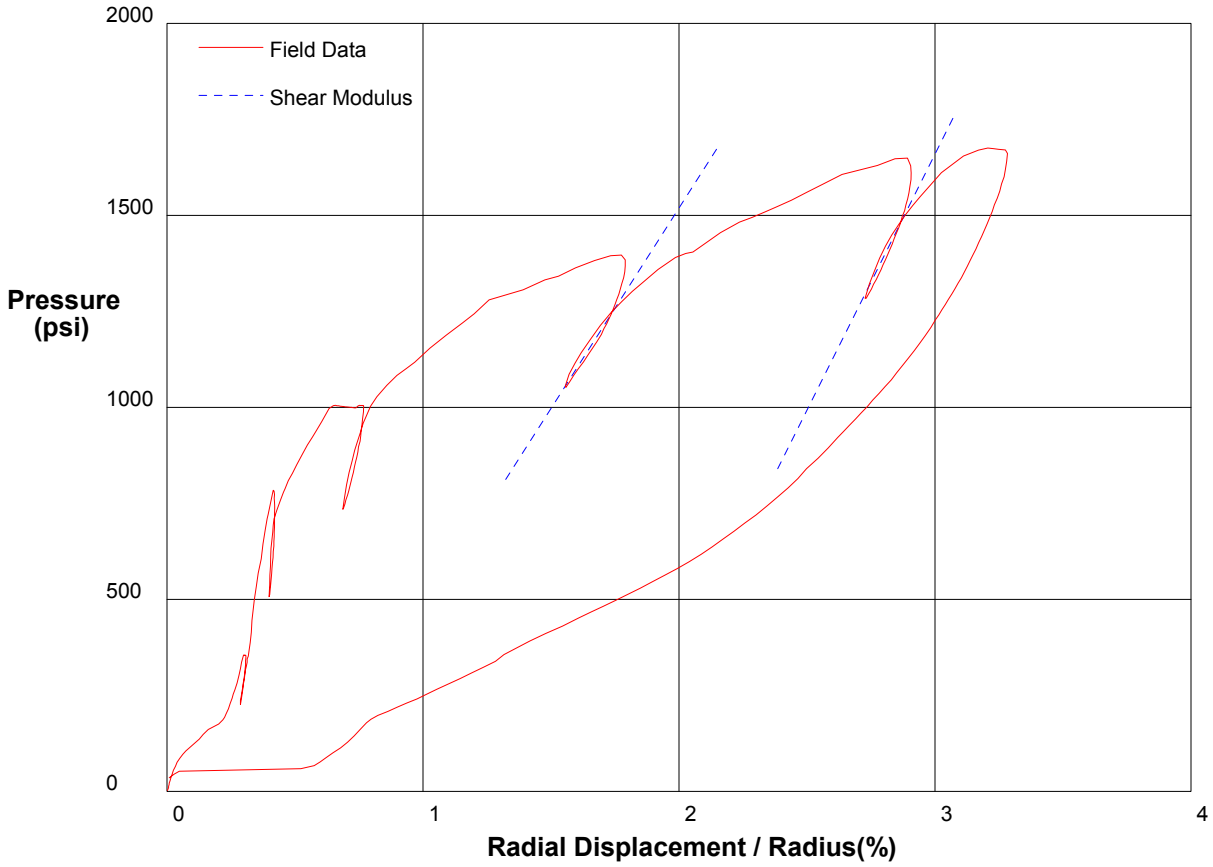

Shear Modulus 66666 psi

Shear Modulus 52201 psi

shift 0

In Situ Engineering

Appendix I - Pressuremeter Data and Standard Interpretation

PRESSUREMETER DATA **CH2M-HILL, Inc.**

CALTRANS I-710 North Tunnel Project **2/5/2009**

Hole No. Z1-B6 **Depth 245ft** **File C:\DATA\ISE-812\SR710-28.P**

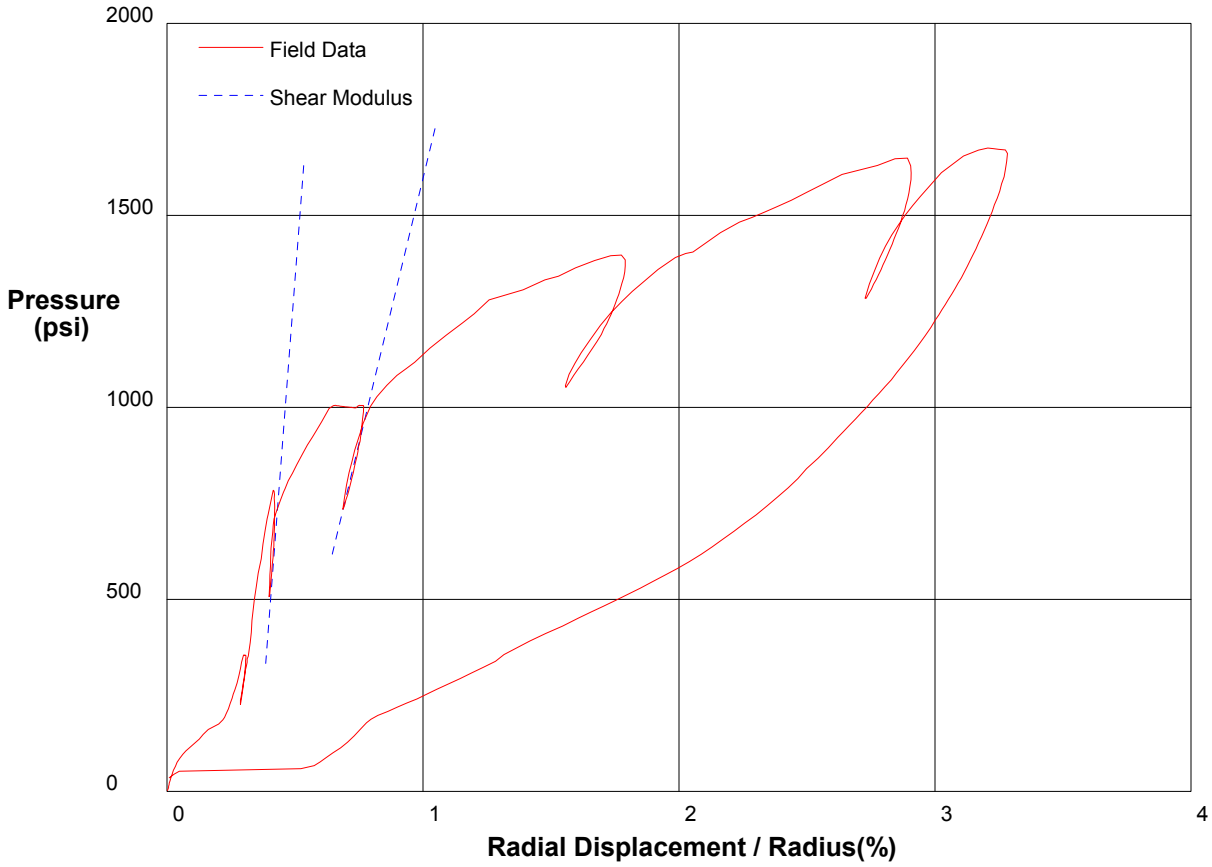

Shear Modulus 138095 psi

Shear Modulus 435632 psi

shift 0

In Situ Engineering

Appendix I - Pressuremeter Data and Standard Interpretation

PRESSUREMETER DATA **CH2MHill, Inc.**

CALTRANS I-710 North Tunnel Project **2/5/2009**

Hole No. Z1-B6 **Depth 245ft** **File C:\DATA\ISE-812\SR710-28.P**

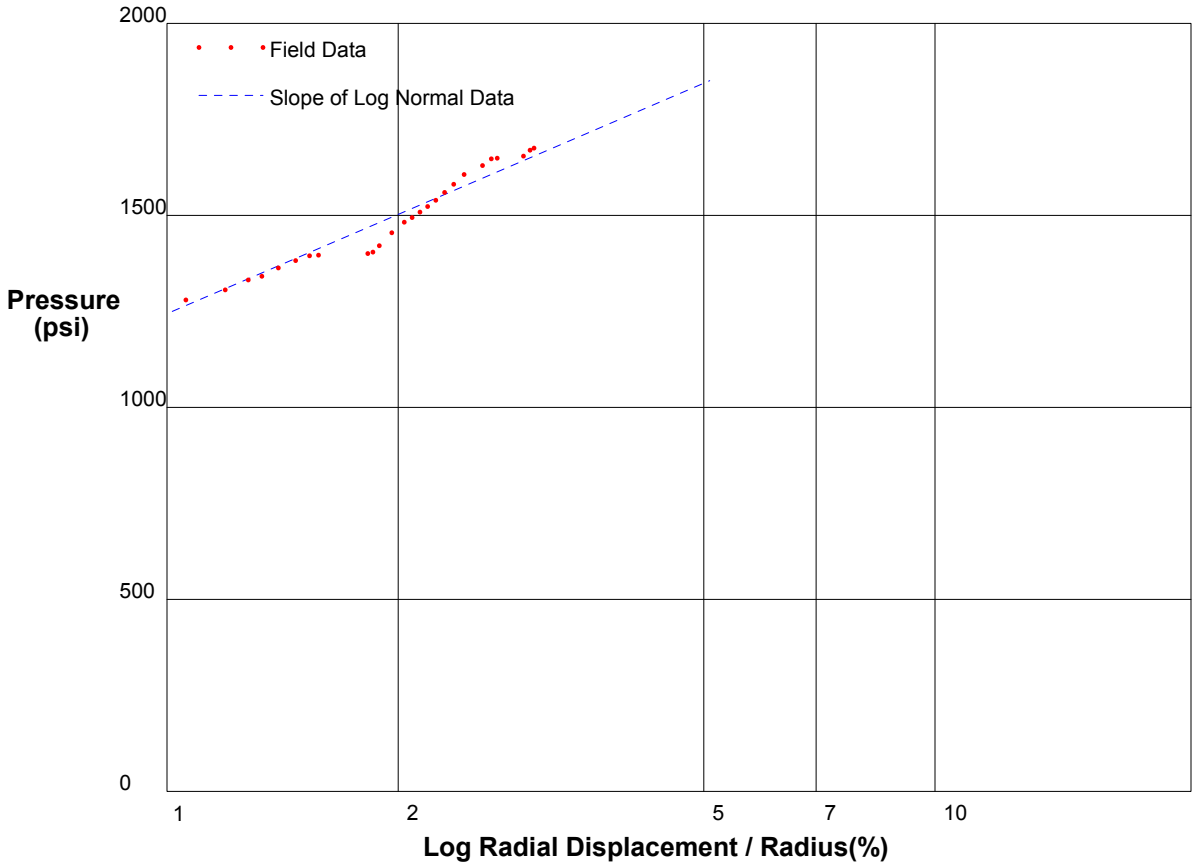

Shear Strength 372.8 psi
Limit Pressure 2628 psi

shift .2

In Situ Engineering

Appendix I - Pressuremeter Data and Standard Interpretation

PRESSUREMETER DATA **CH2MHill, Inc.**

CALTRANS I-710 North Tunnel Project **2/6/2009**

Hole No. Z3-B7 **Depth 225.8ft** **File C:\DATA\ISE-812\SR710-29.P**

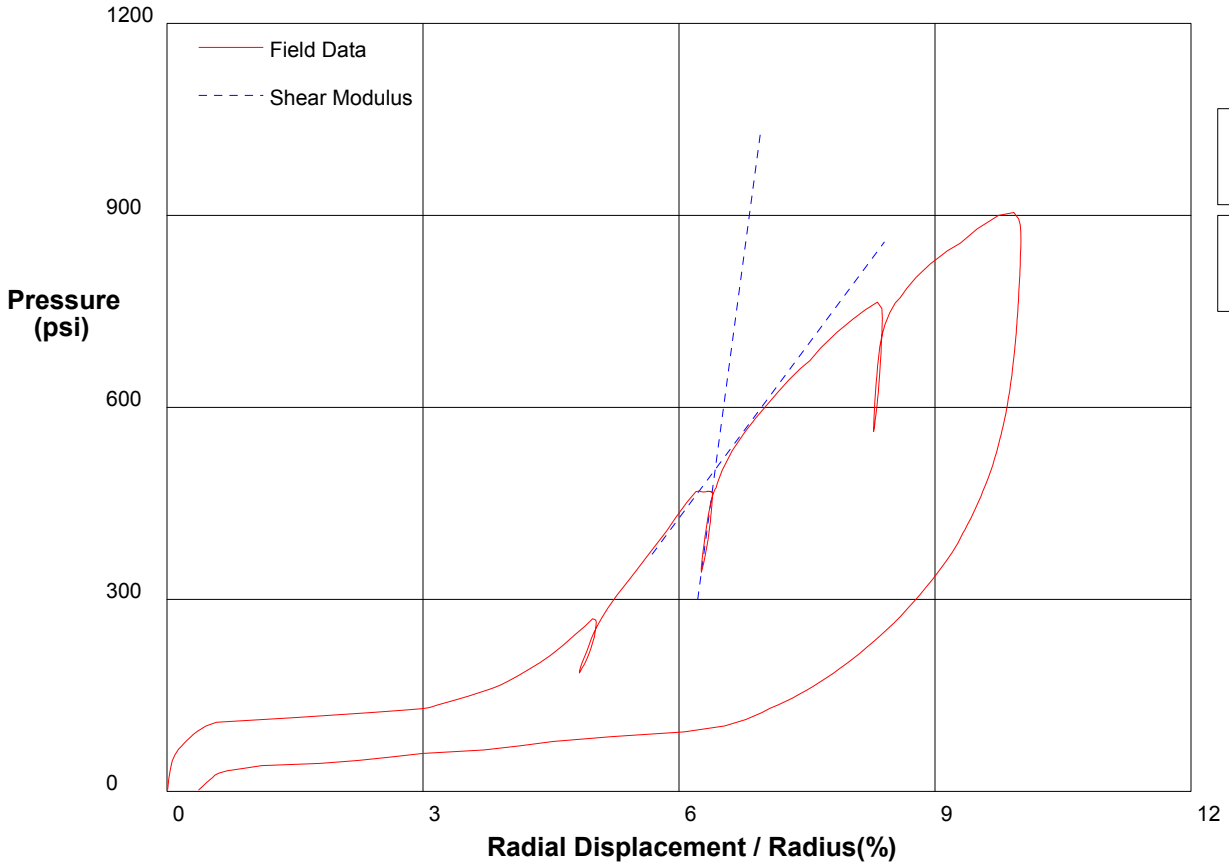

Shear Modulus 49503 psi

Shear Modulus 8965 psi

shift 0

In Situ Engineering

Appendix I - Pressuremeter Data and Standard Interpretation

PRESSUREMETER DATA **CH2MHill, Inc.**

CALTRANS I-710 North Tunnel Project **2/6/2009**

Hole No. Z3-B7 **Depth 225.8ft** **File C:\DATA\ISE-812\SR710-29.P**

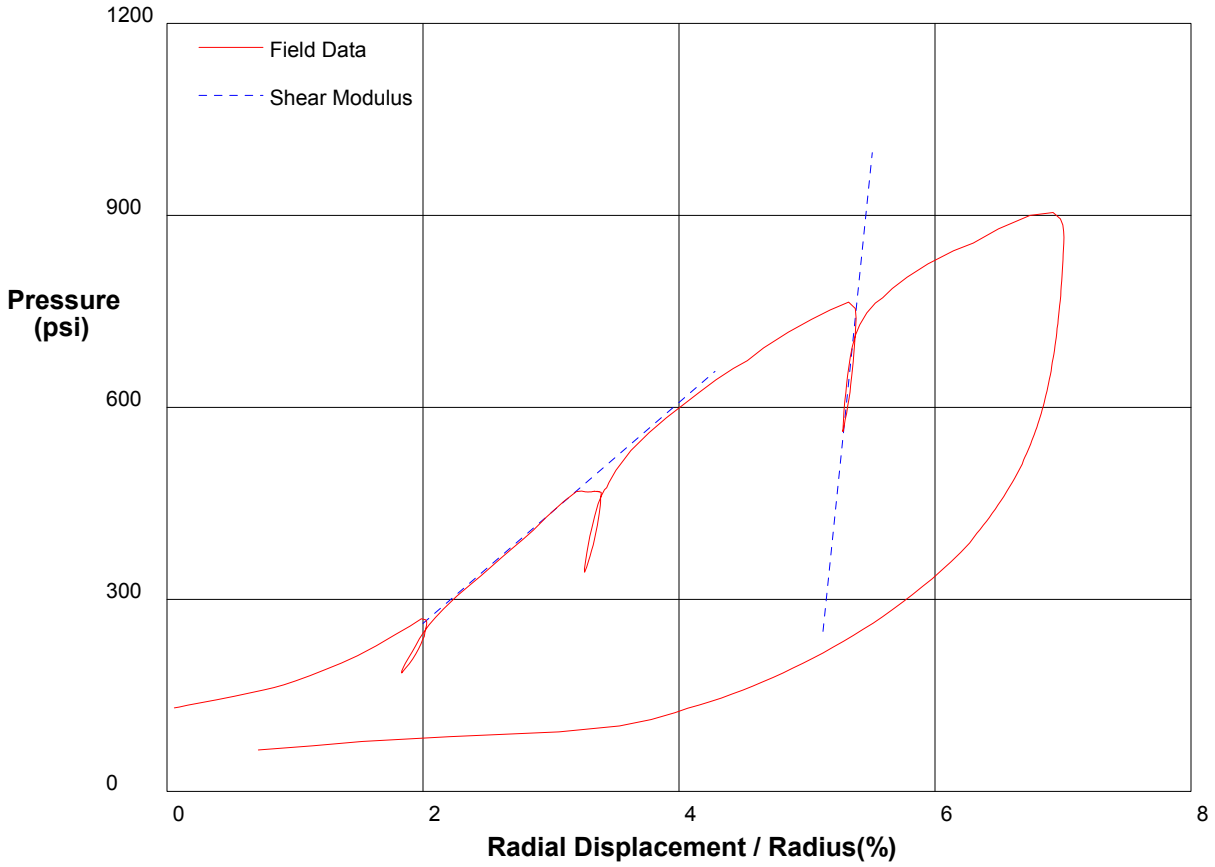

Shear Modulus 97027 psi

Shear Modulus 8630 psi

shift 3

In Situ Engineering

Appendix I - Pressuremeter Data and Standard Interpretation

PRESSUREMETER DATA **CH2MHill, Inc.**

CALTRANS I-710 North Tunnel Project **2/6/2009**

Hole No. Z3-B7 **Depth 225.8ft** **File C:\DATA\ISE-812\SR710-29.P**

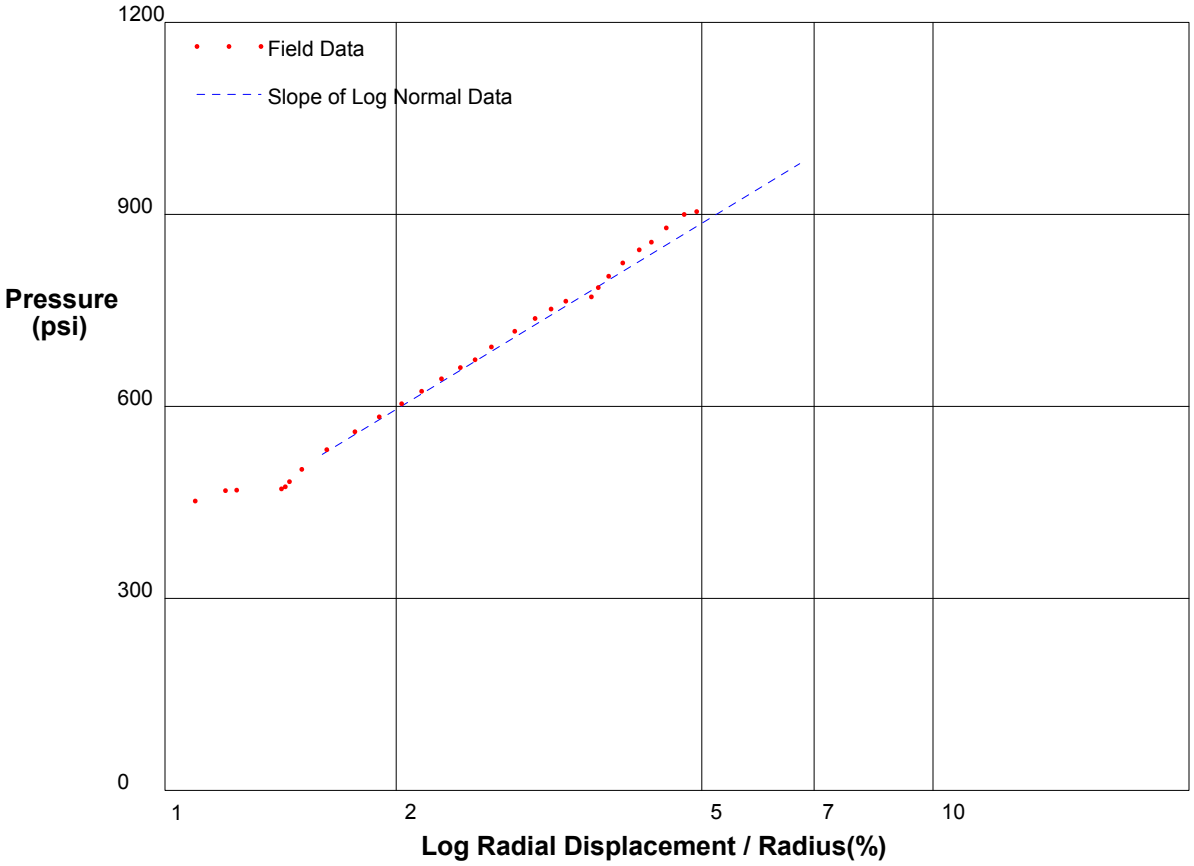

Shear Strength 317.3 psi
Limit Pressure 1553 psi

shift 5

In Situ Engineering

Appendix I - Pressuremeter Data and Standard Interpretation

PRESSUREMETER DATA **CH2MHill, Inc.**

CALTRANS I-710 North Tunnel Project **2/6/2009**

Hole No. Z3-B7 **Depth 224.3ft** **File C:\DATA\ISE-812\SR710-30.P**

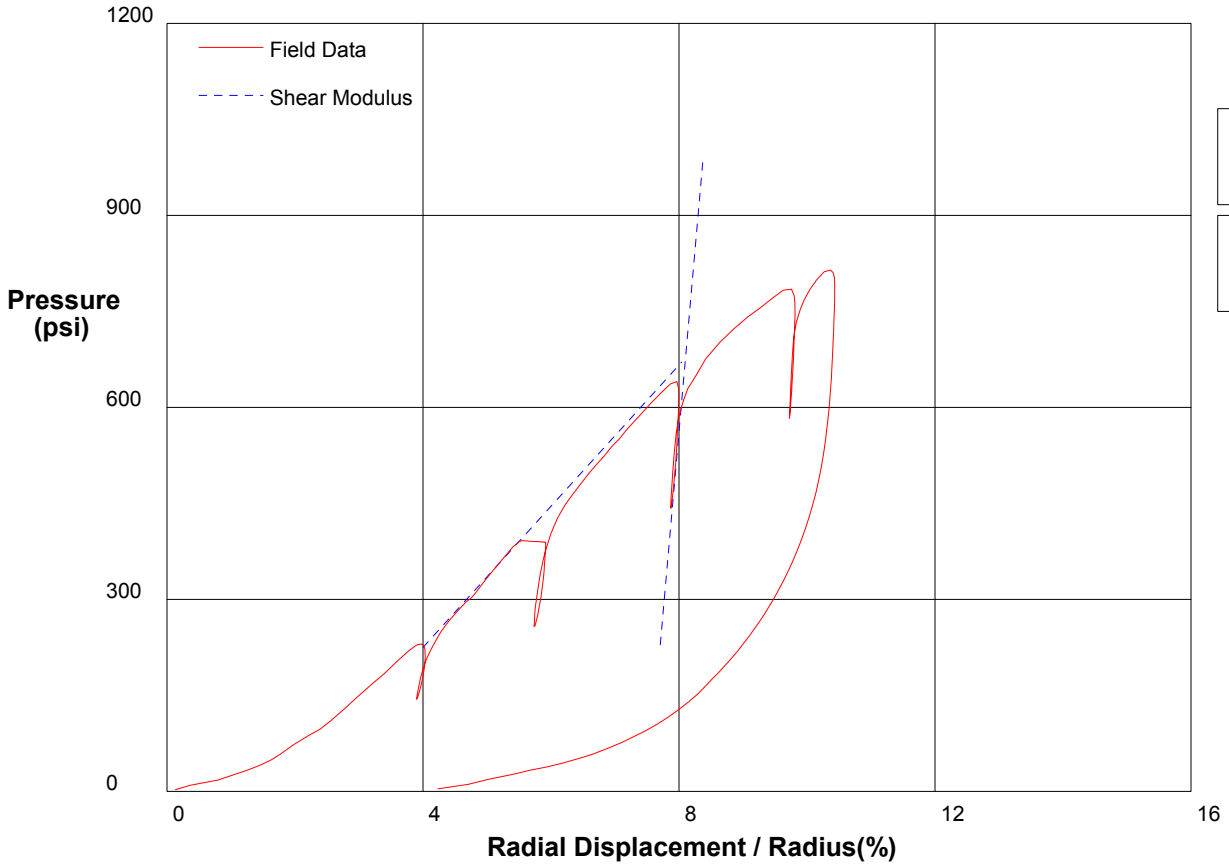

Shear Modulus 56875 psi

Shear Modulus 5515 psi

shift 0

In Situ Engineering

Appendix I - Pressuremeter Data and Standard Interpretation

PRESSUREMETER DATA **CH2MHill, Inc.**

CALTRANS I-710 North Tunnel Project **2/6/2009**

Hole No. Z3-B7 **Depth 224.3ft** **File C:\DATA\ISE-812\SR710-30.P**

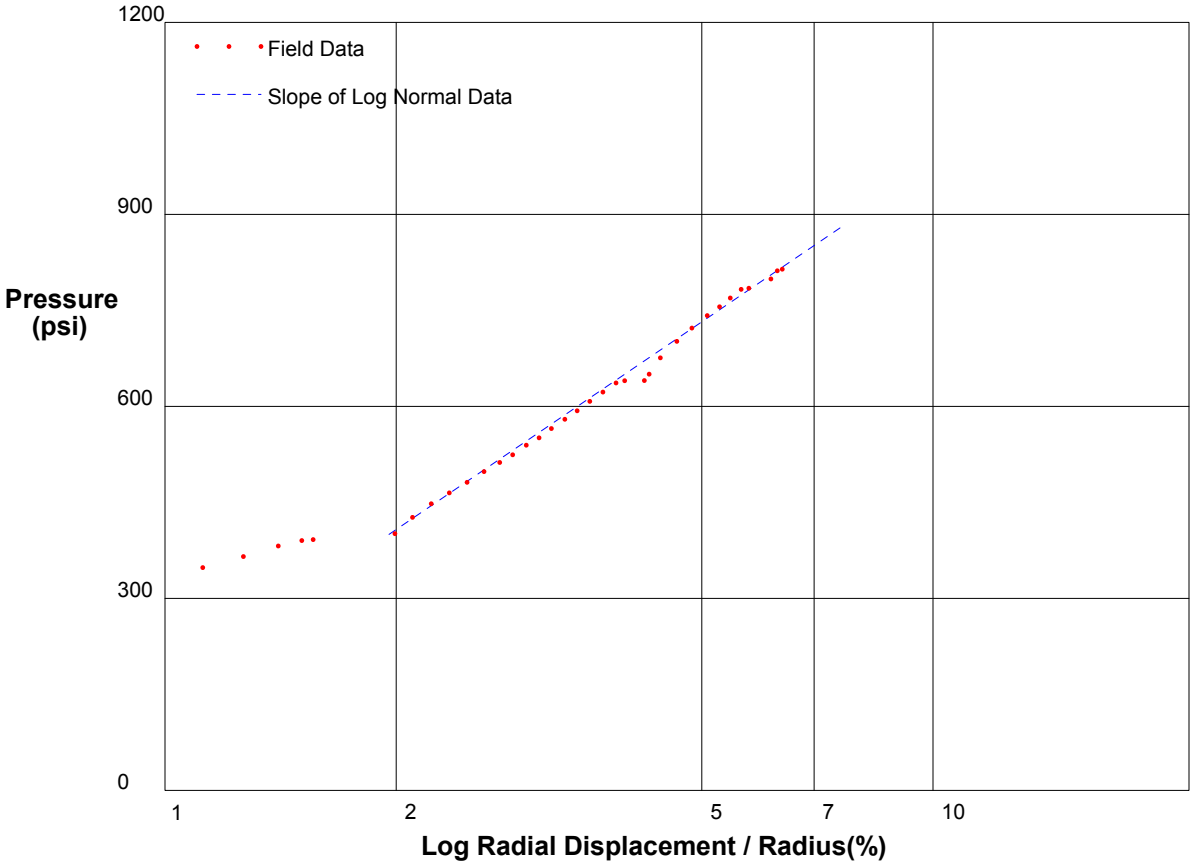

Shear Strength 354 psi
Limit Pressure 1476 psi

shift 4

In Situ Engineering

Appendix I - Pressuremeter Data and Standard Interpretation

PRESSUREMETER DATA **CH2MHill, Inc.**

CALTRANS I-710 North Tunnel Project **2/6/2009**

Hole No. Z1-B6 **Depth 332ft** **File C:\DATA\ISE-812\SR710-31.P**

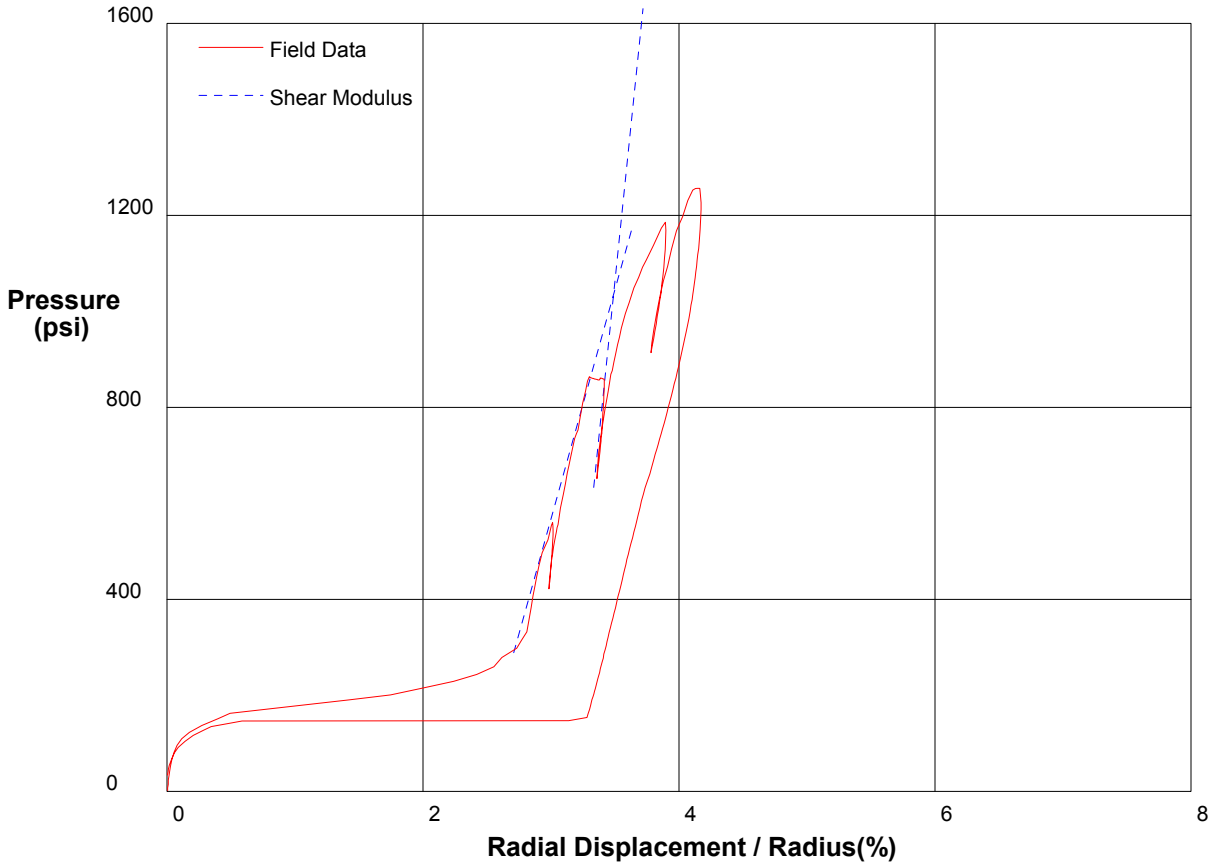

Shear Modulus 129369 psi

Shear Modulus 47790 psi

shift 0

In Situ Engineering

Appendix I - Pressuremeter Data and Standard Interpretation

PRESSUREMETER DATA **CH2MHill, Inc.**

CALTRANS I-710 North Tunnel Project **2/6/2009**

Hole No. Z1-B6 **Depth 332ft** **File C:\DATA\ISE-812\SR710-31.P**

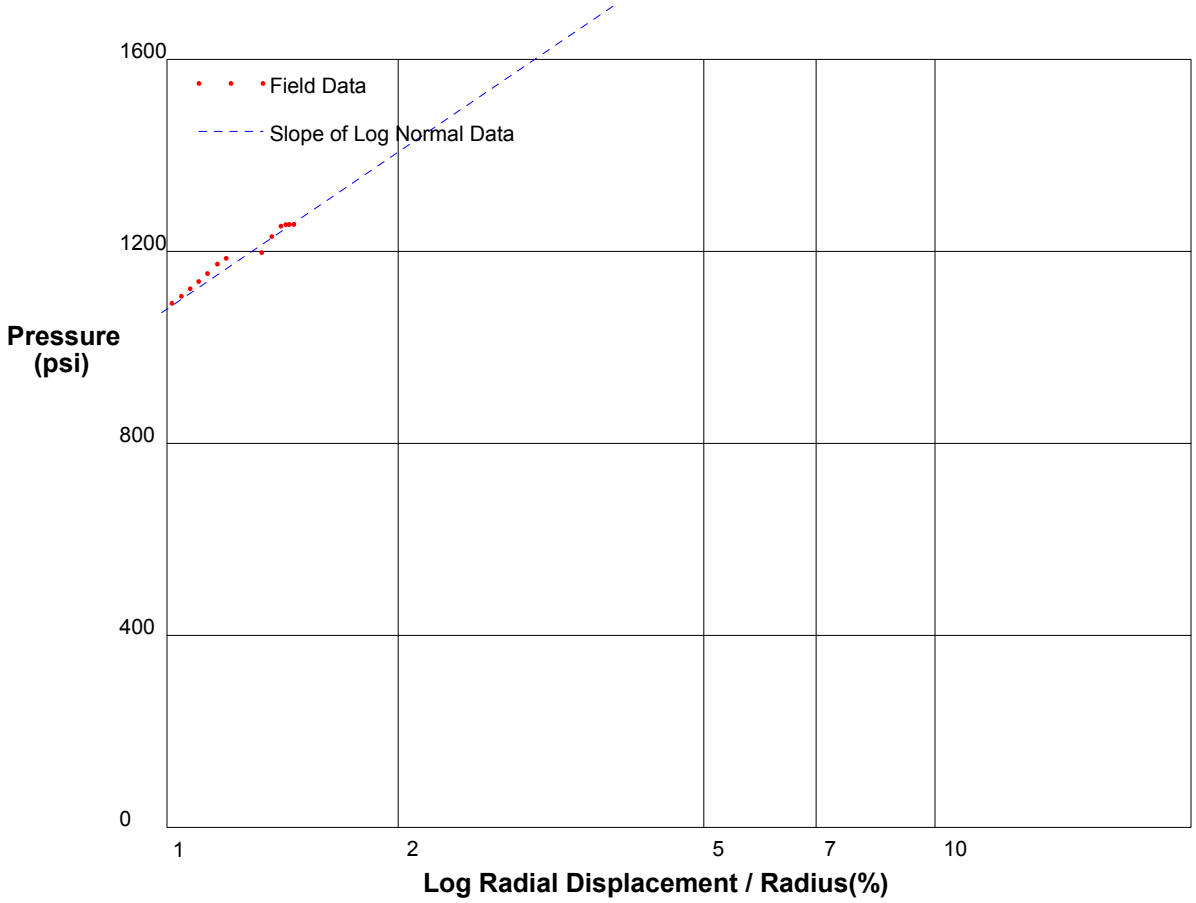

Shear Strength 472 psi
Limit Pressure 2832 psi

shift 2.7

In Situ Engineering

Appendix I - Pressuremeter Data and Standard Interpretation

PRESSUREMETER DATA **CH2MHill, Inc.**

CALTRANS I-710 North Tunnel Project **2/6/2009**

Hole No. Z1-B6 **Depth 330.5ft** **File C:\DATA\ISE-812\SR710-32.P**

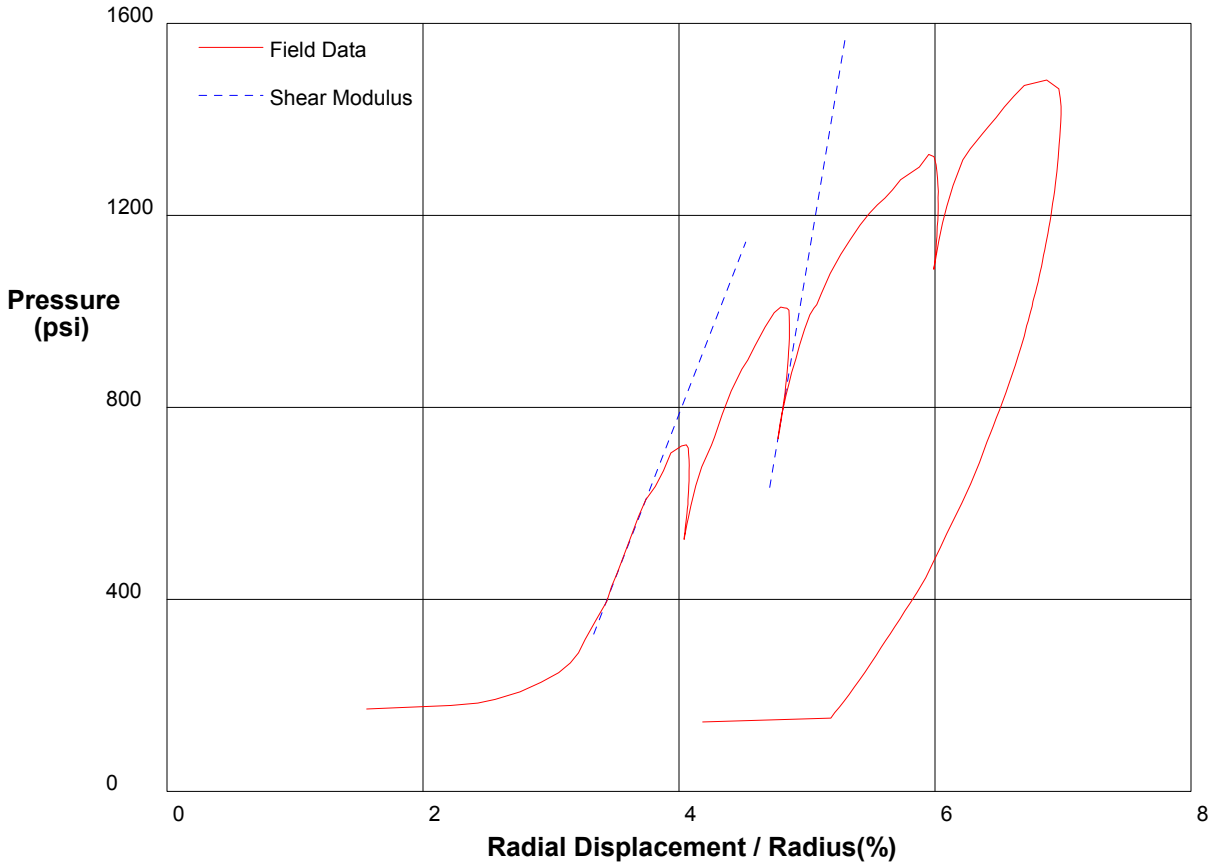

Shear Modulus 79298 psi

Shear Modulus 34385 psi

shift 4.7

In Situ Engineering

Appendix I - Pressuremeter Data and Standard Interpretation

PRESSUREMETER DATA **CH2MHill, Inc.**

CALTRANS I-710 North Tunnel Project **2/6/2009**

Hole No. Z1-B6 **Depth 330.5ft** **File C:\DATA\ISE-812\SR710-32.P**

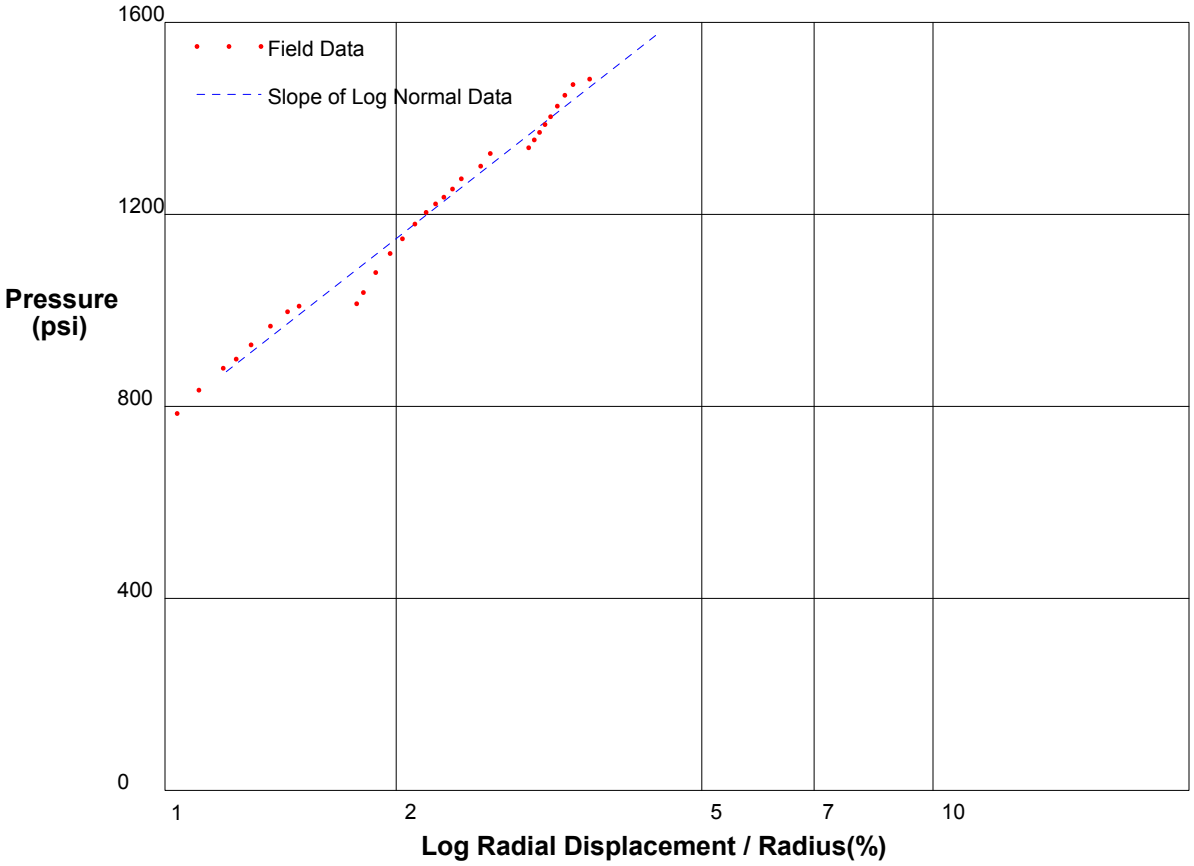

Shear Strength 544.2 psi
Limit Pressure 2793 psi

shift 8

In Situ Engineering

Appendix I - Pressuremeter Data and Standard Interpretation

PRESSUREMETER DATA **CH2MHill, Inc.**

CALTRANS I-710 North Tunnel Project **2/10/2009**

Hole No. Z3-B7 **Depth 252.5ft** **File C:\DATA\ISE-812\SR710-33.P**

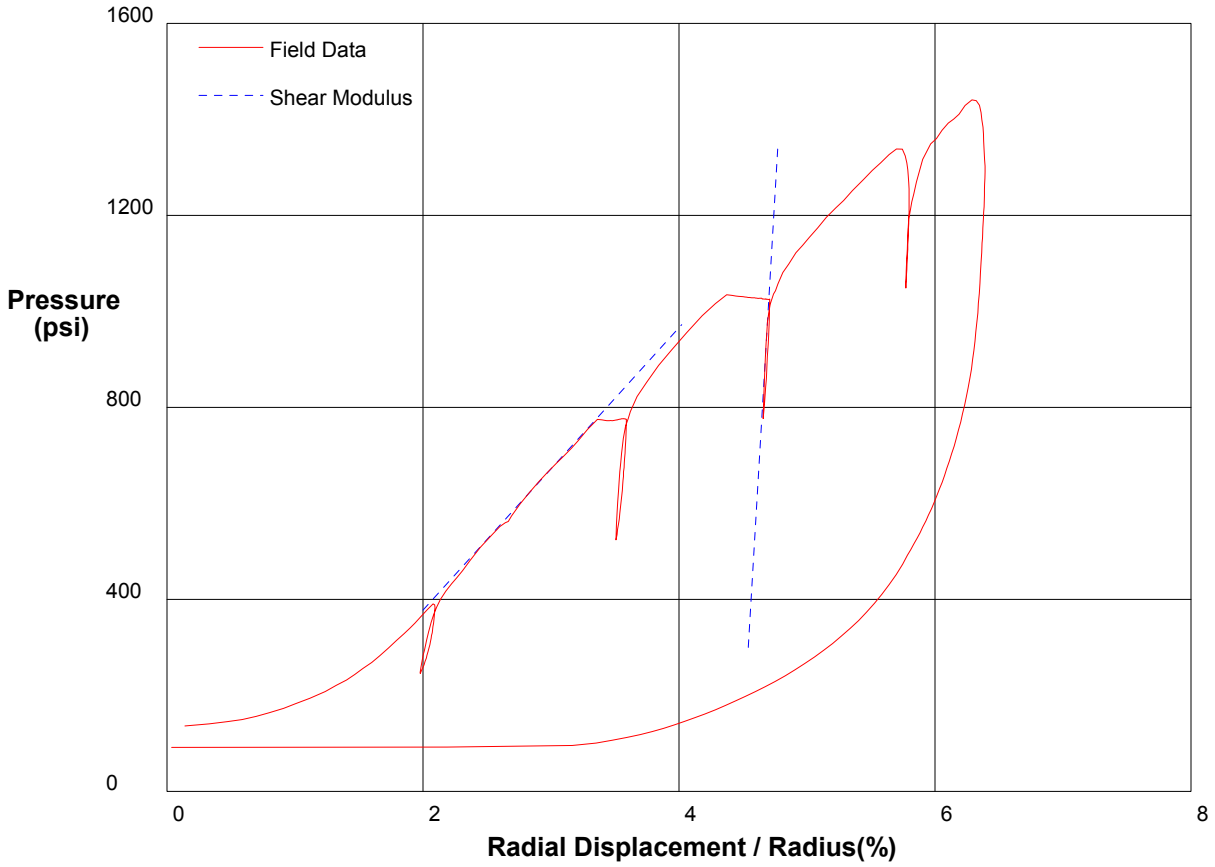

Shear Modulus 226666 psi

Shear Modulus 14707 psi

shift 4

In Situ Engineering

Appendix I - Pressuremeter Data and Standard Interpretation

PRESSUREMETER DATA **CH2MHill, Inc.**

CALTRANS I-710 North Tunnel Project **2/10/2009**

Hole No. Z3-B7 **Depth 252.5ft** **File C:\DATA\ISE-812\SR710-33.P**

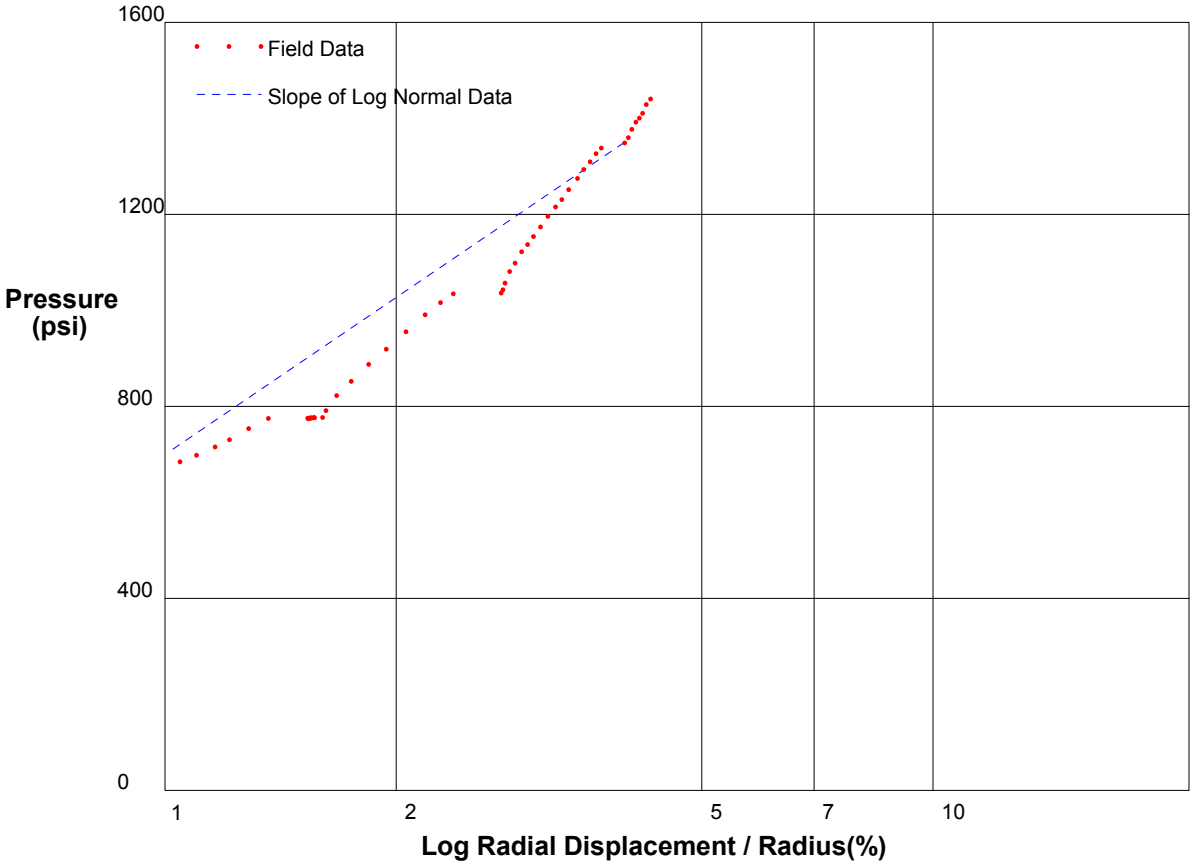

Shear Strength 472 psi
Limit Pressure 2452 psi

shift 6

In Situ Engineering

Appendix I - Pressuremeter Data and Standard Interpretation

PRESSUREMETER DATA **CH2MHill, Inc.**

CALTRANS I-710 North Tunnel Project **2/10/2009**

Hole No. Z3-B7 **Depth 251ft** **File C:\DATA\ISE-812\SR710-34.P**

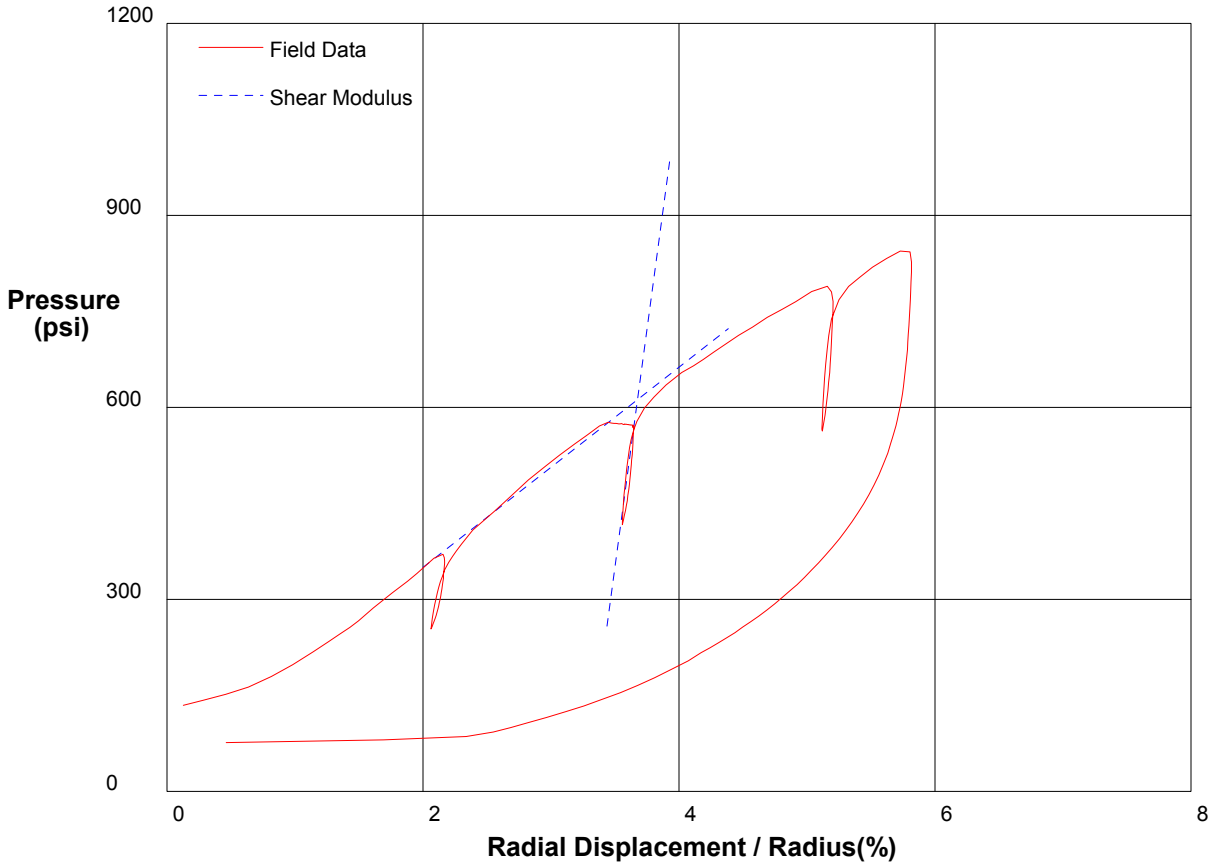

Shear Modulus 74255 psi

Shear Modulus 7816 psi

shift 5.2

In Situ Engineering

Appendix I - Pressuremeter Data and Standard Interpretation

PRESSUREMETER DATA **CH2MHill, Inc.**

CALTRANS I-710 North Tunnel Project **2/10/2009**

Hole No. Z3-B7 **Depth 251ft** **File C:\DATA\ISE-812\SR710-34.P**

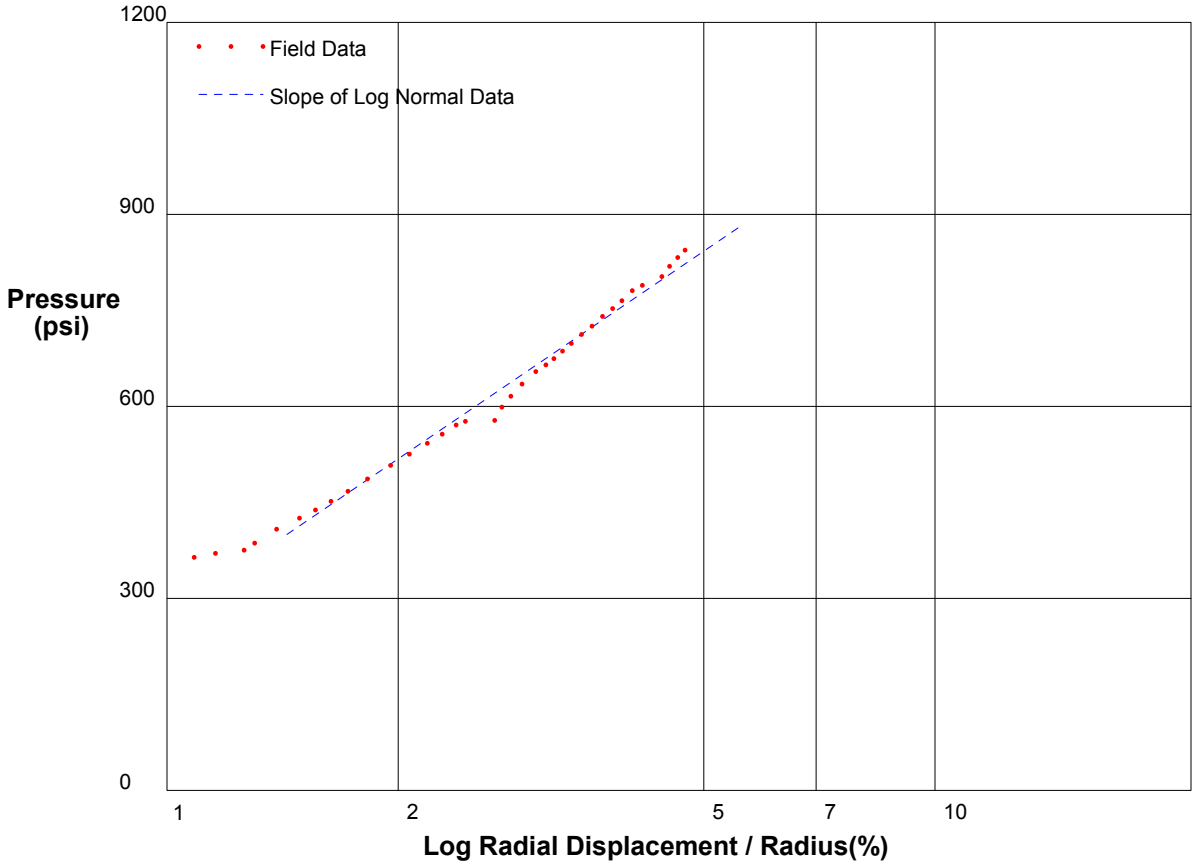

Shear Strength 354 psi
Limit Pressure 1587 psi

shift 6.2

In Situ Engineering

Appendix I - Pressuremeter Data and Standard Interpretation

PRESSUREMETER DATA **CH2MHill, Inc.**

CALTRANS I-710 North Tunnel Project **2/10/2009**

Hole No. Z3-B7 **Depth 271.6ft** **File C:\DATA\ISE-812\SR710-35.P**

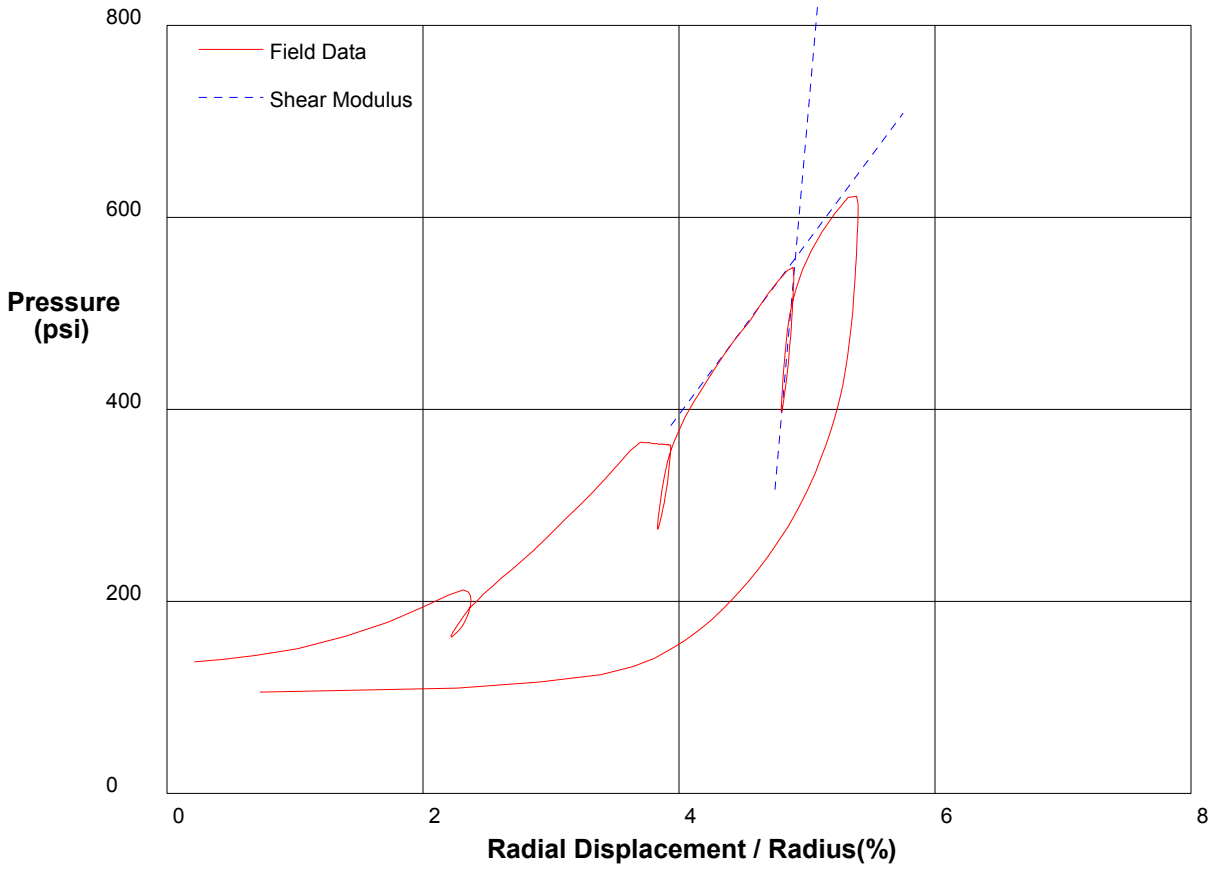

Shear Modulus 75833 psi

Shear Modulus 8965 psi

shift 7.2

In Situ Engineering

Appendix I - Pressuremeter Data and Standard Interpretation

PRESSUREMETER DATA **CH2MHill, Inc.**

CALTRANS I-710 North Tunnel Project **2/10/2009**

Hole No. Z3-B7 **Depth 271.6ft** **File C:\DATA\ISE-812\SR710-35.P**

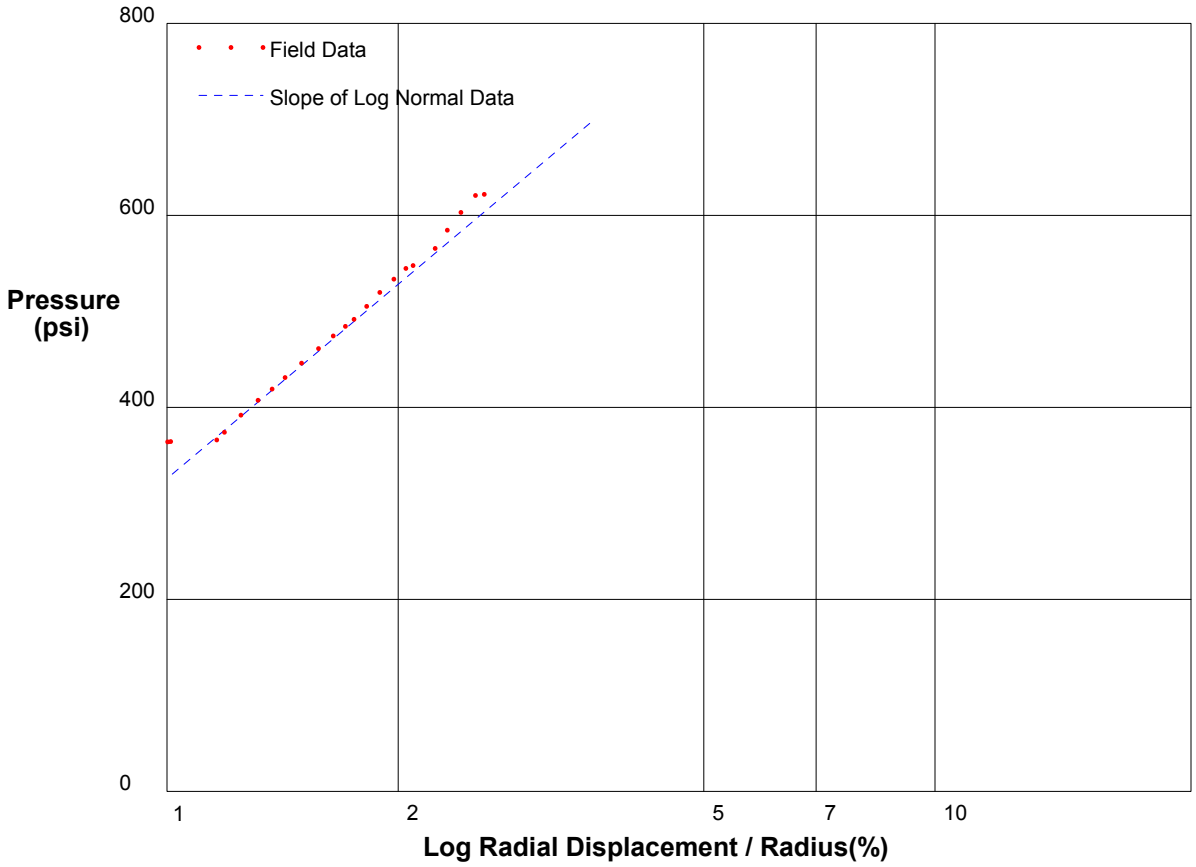

Shear Strength 291.9 psi
Limit Pressure 1410 psi

shift 10

In Situ Engineering

Appendix I - Pressuremeter Data and Standard Interpretation

PRESSUREMETER DATA **CH2MHill, Inc.**

CALTRANS I-710 North Tunnel Project **2/10/2009**

Hole No. Z3-B7 **Depth 270.1ft** **File C:\DATA\ISE-812\SR710-36.P**

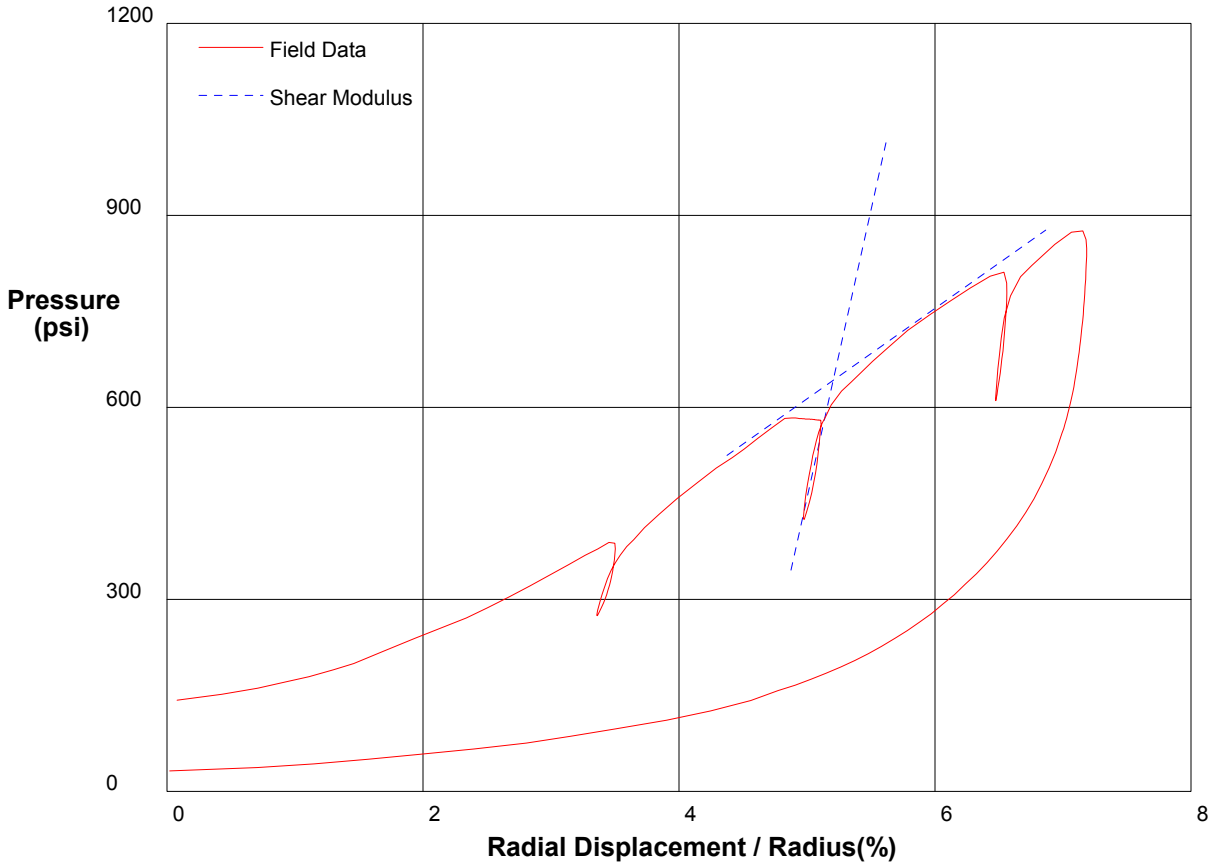

Shear Modulus 45000 psi

Shear Modulus 7071 psi

shift 4

In Situ Engineering

Appendix I - Pressuremeter Data and Standard Interpretation

PRESSUREMETER DATA **CH2MHill, Inc.**

CALTRANS I-710 North Tunnel Project **2/10/2009**

Hole No. Z3-B7 **Depth 270.1ft** **File C:\DATA\ISE-812\SR710-36.P**

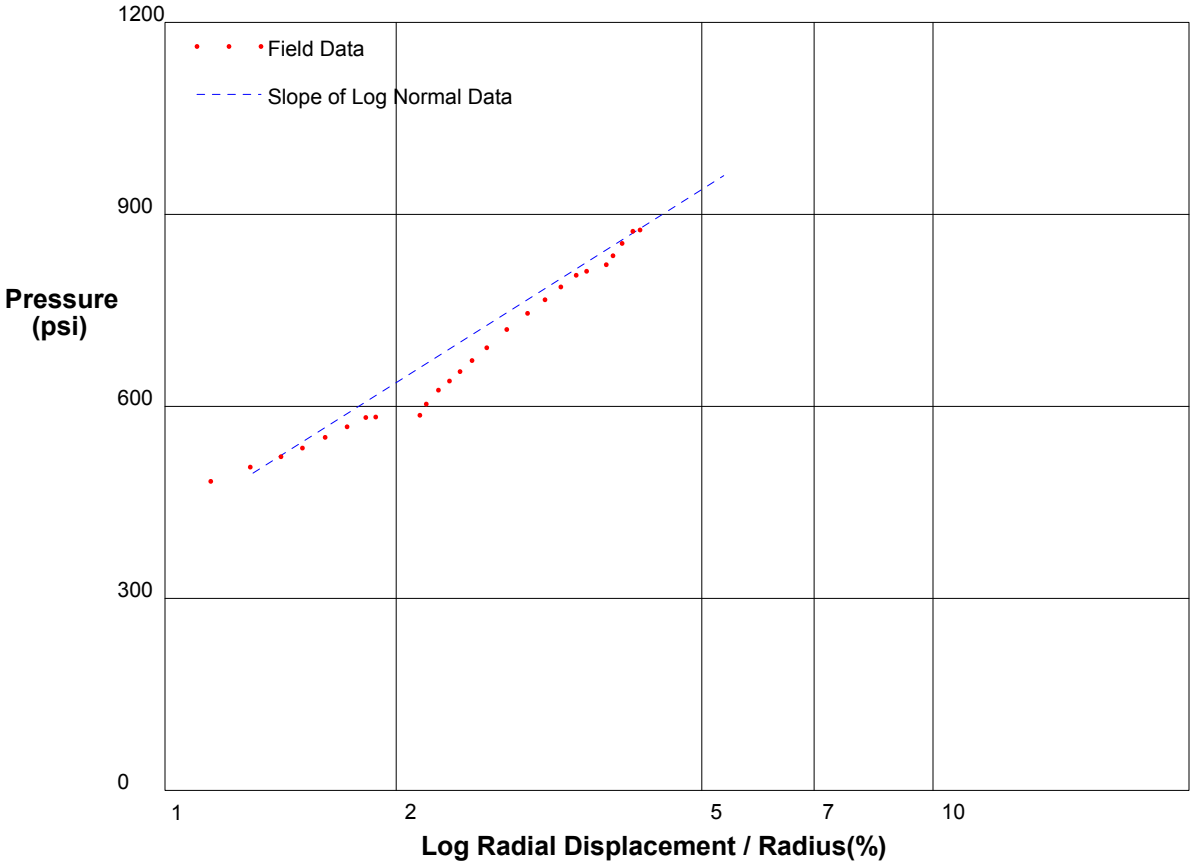

Shear Strength 329.2 psi
Limit Pressure 1631 psi

shift 7

In Situ Engineering

Appendix I - Pressuremeter Data and Standard Interpretation

PRESSUREMETER DATA **CH2MHill, Inc.**

CALTRANS I-710 North Tunnel Project **2/19/2009**

Hole No. Z1-B5 **Depth 278ft** **File C:\DATA\ISE-812\SR710-37.P**

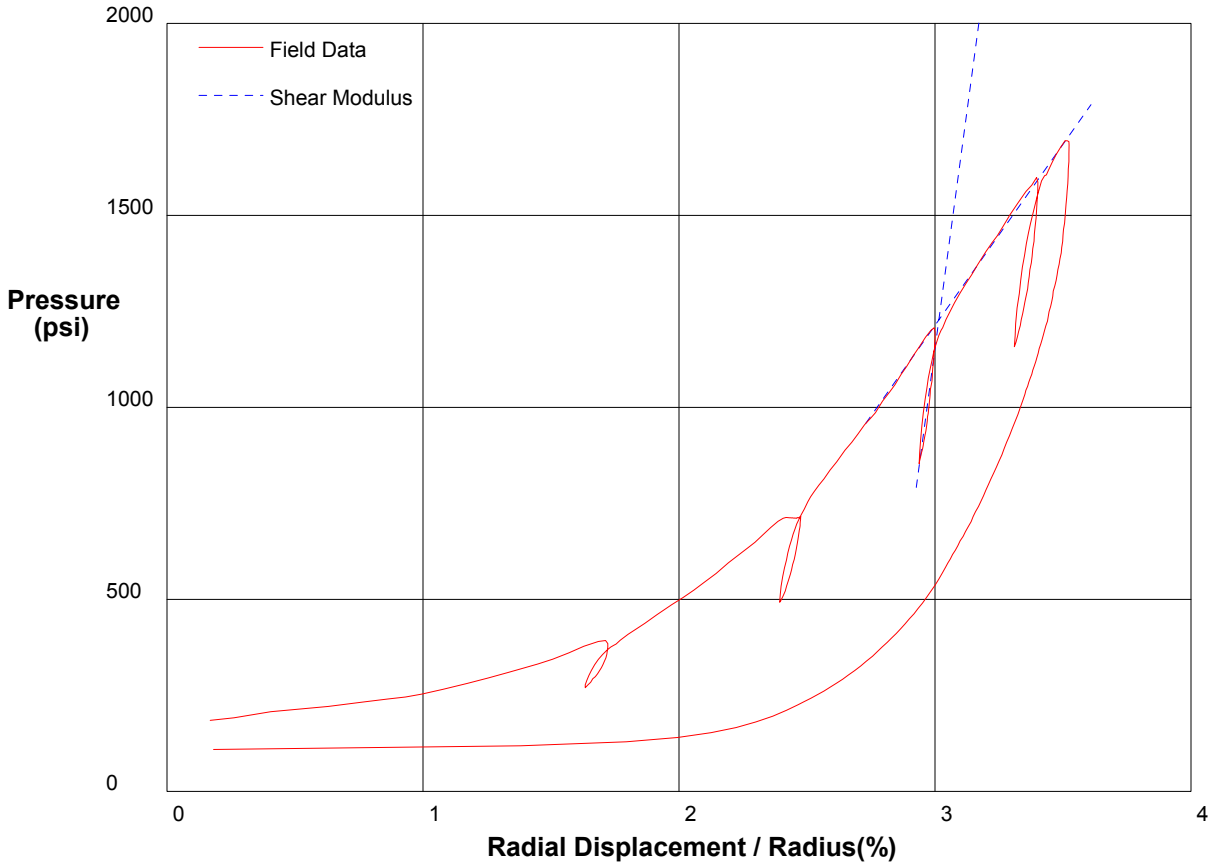

Shear Modulus 247517 psi

Shear Modulus 47140 psi

shift 2

In Situ Engineering

Appendix I - Pressuremeter Data and Standard Interpretation

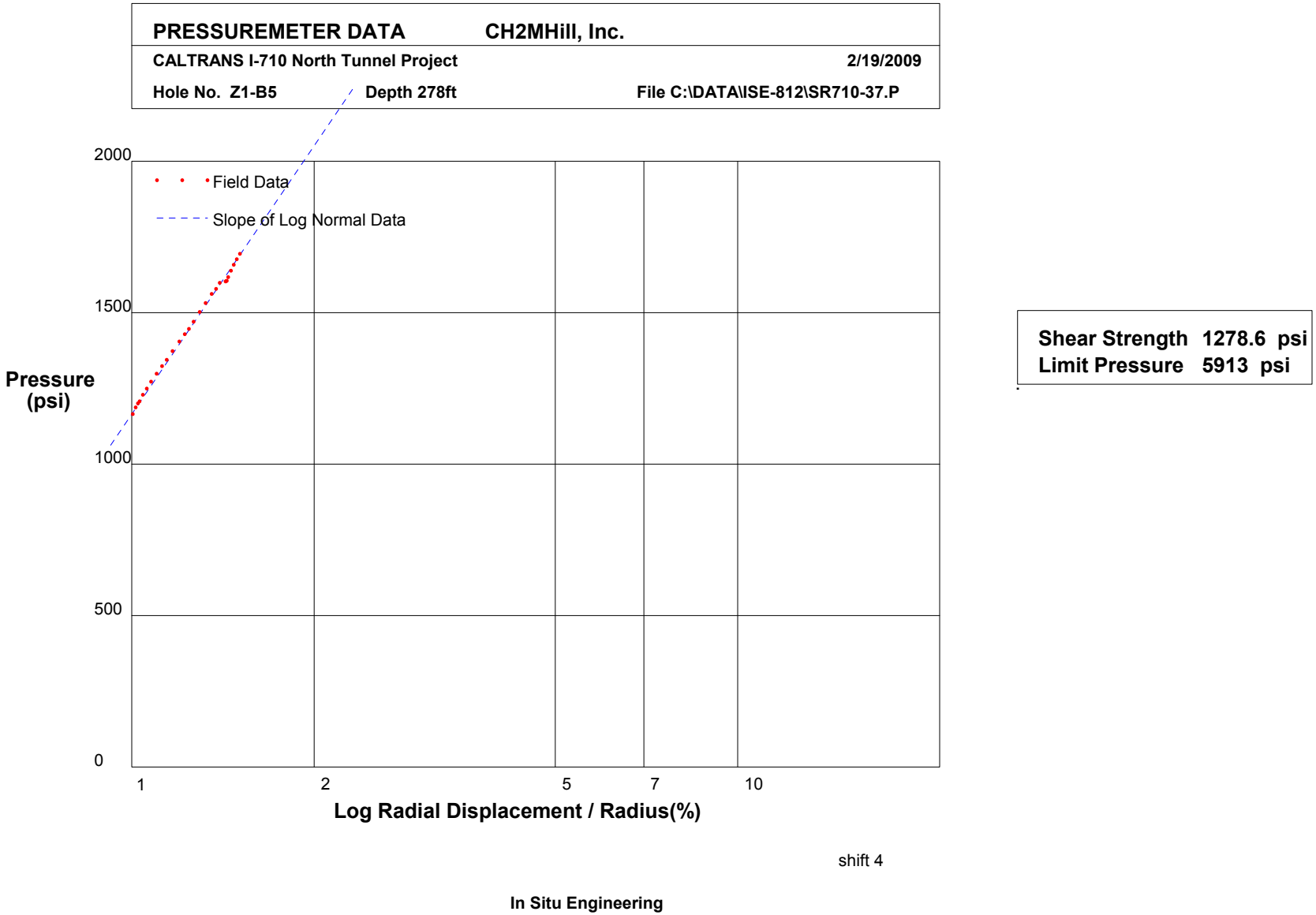

Appendix I - Pressuremeter Data and Standard Interpretation

PRESSUREMETER DATA **CH2MHill, Inc.**

CALTRANS I-710 North Tunnel Project **2/19/2009**

Hole No. Z1-B5 **Depth 276.5ft** **File C:\DATA\ISE-812\SR710-38.P**

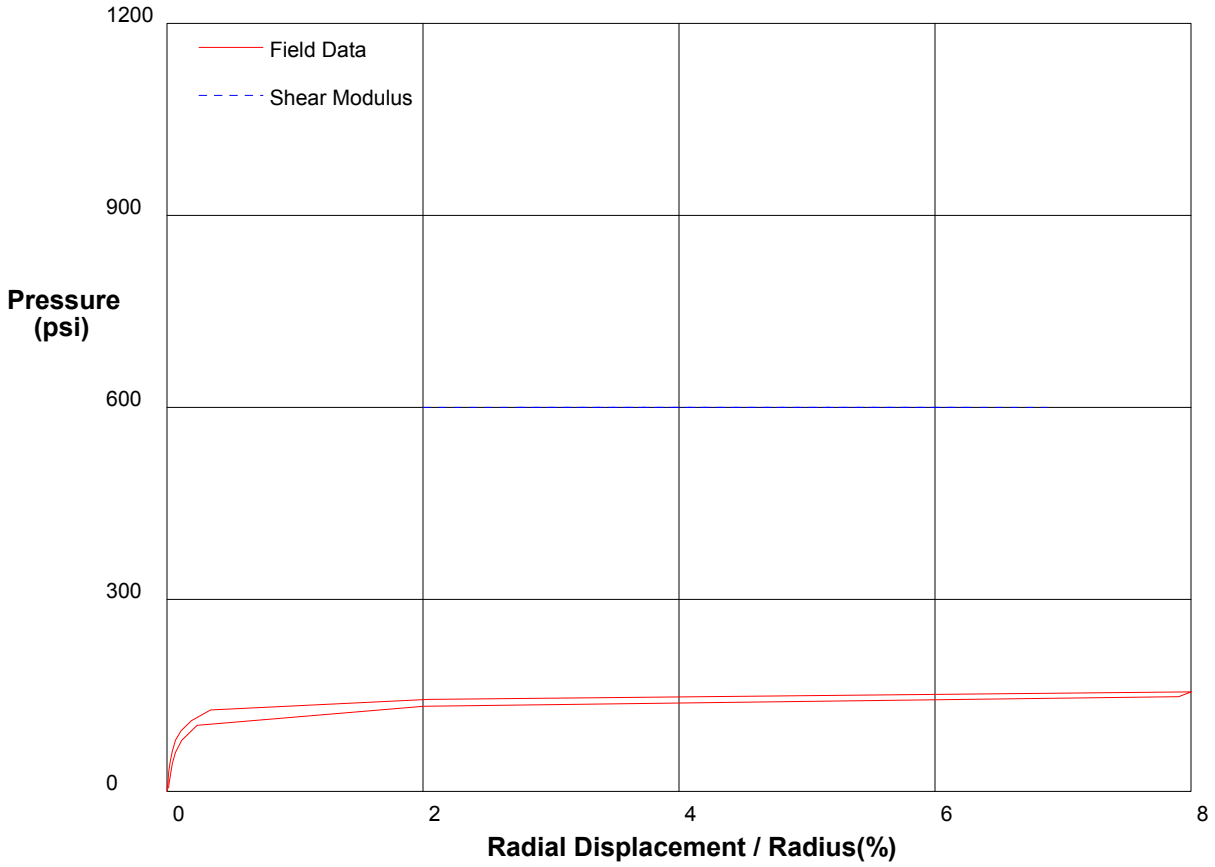

Shear Modulus 0 psi

Shear Modulus 0 psi

shift 0

In Situ Engineering

Appendix I - Pressuremeter Data and Standard Interpretation

PRESSUREMETER DATA **CH2MHill, Inc.**

CALTRANS I-710 North Tunnel Project **2/19/2009**

Hole No. Z1-B4 **Depth 332ft** **File C:\DATA\ISE-812\SR710-39.P**

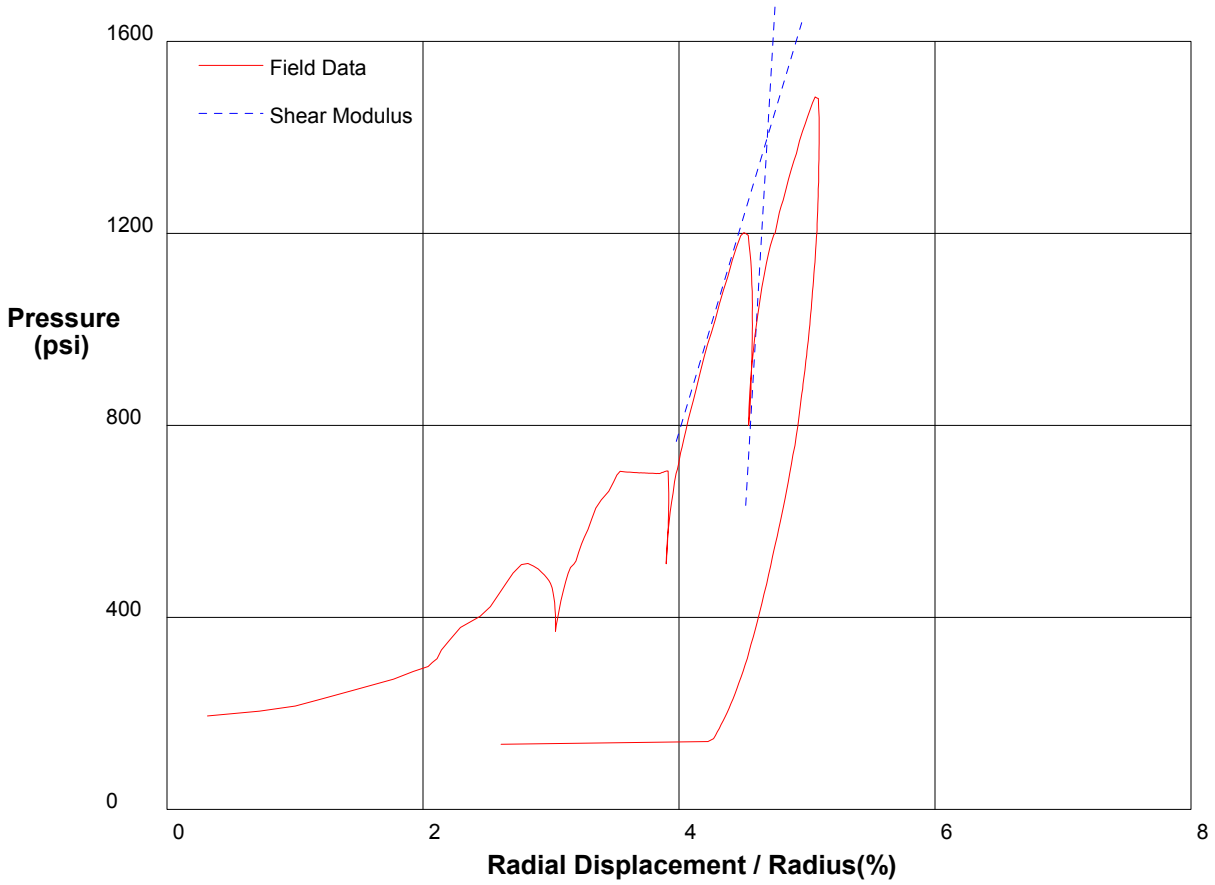

Shear Modulus 226666 psi

Shear Modulus 44539 psi

shift 2

In Situ Engineering

Appendix I - Pressuremeter Data and Standard Interpretation

PRESSUREMETER DATA **CH2MHill, Inc.**

CALTRANS I-710 North Tunnel Project **2/19/2009**

Hole No. Z1-B4 **Depth 332ft** **File C:\DATA\ISE-812\SR710-39.P**

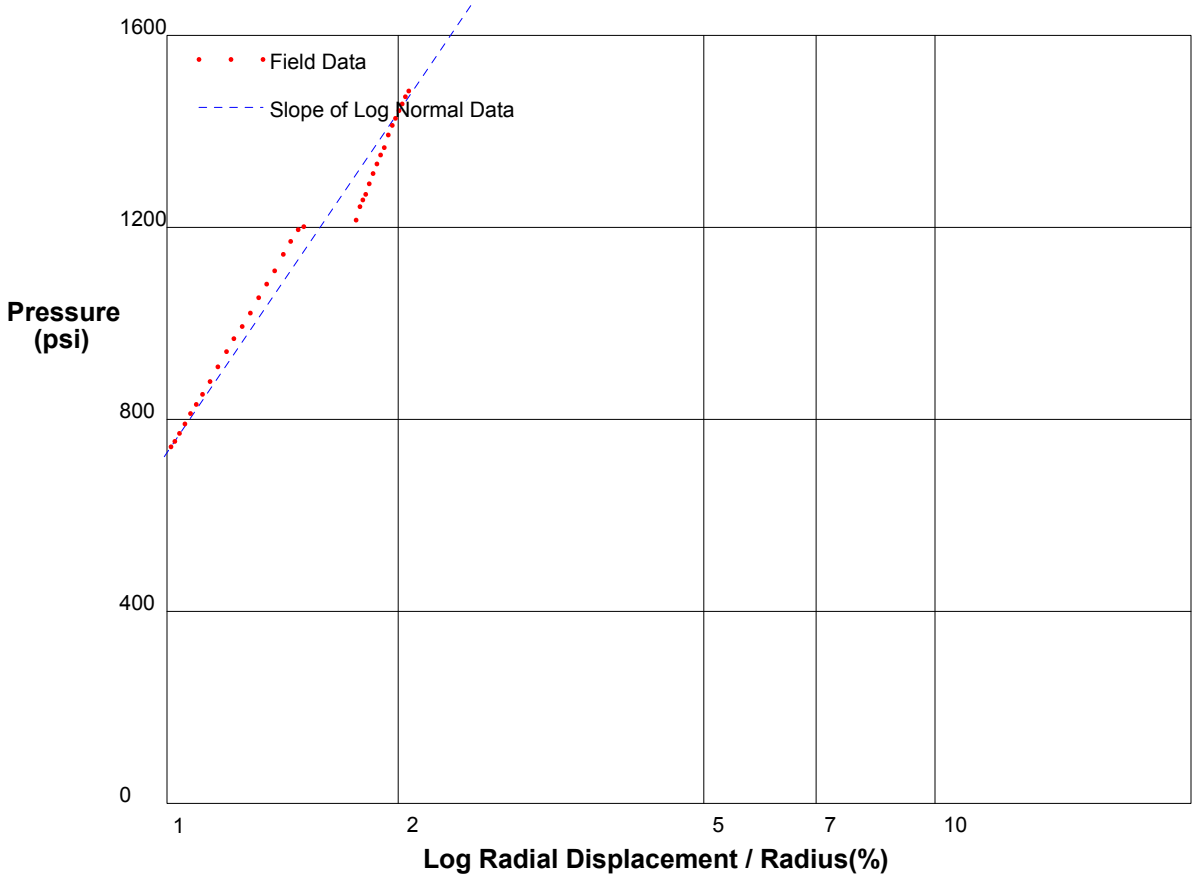

Shear Strength 1022.9 psi
Limit Pressure 4529 psi

shift 5

In Situ Engineering

Appendix I - Pressuremeter Data and Standard Interpretation

PRESSUREMETER DATA **CH2MHill, Inc.**

CALTRANS I-710 North Tunnel Project **2/19/2009**

Hole No. Z1-B4 **Depth 330.5ft** **File C:\DATA\ISE-812\SR710-40.P**

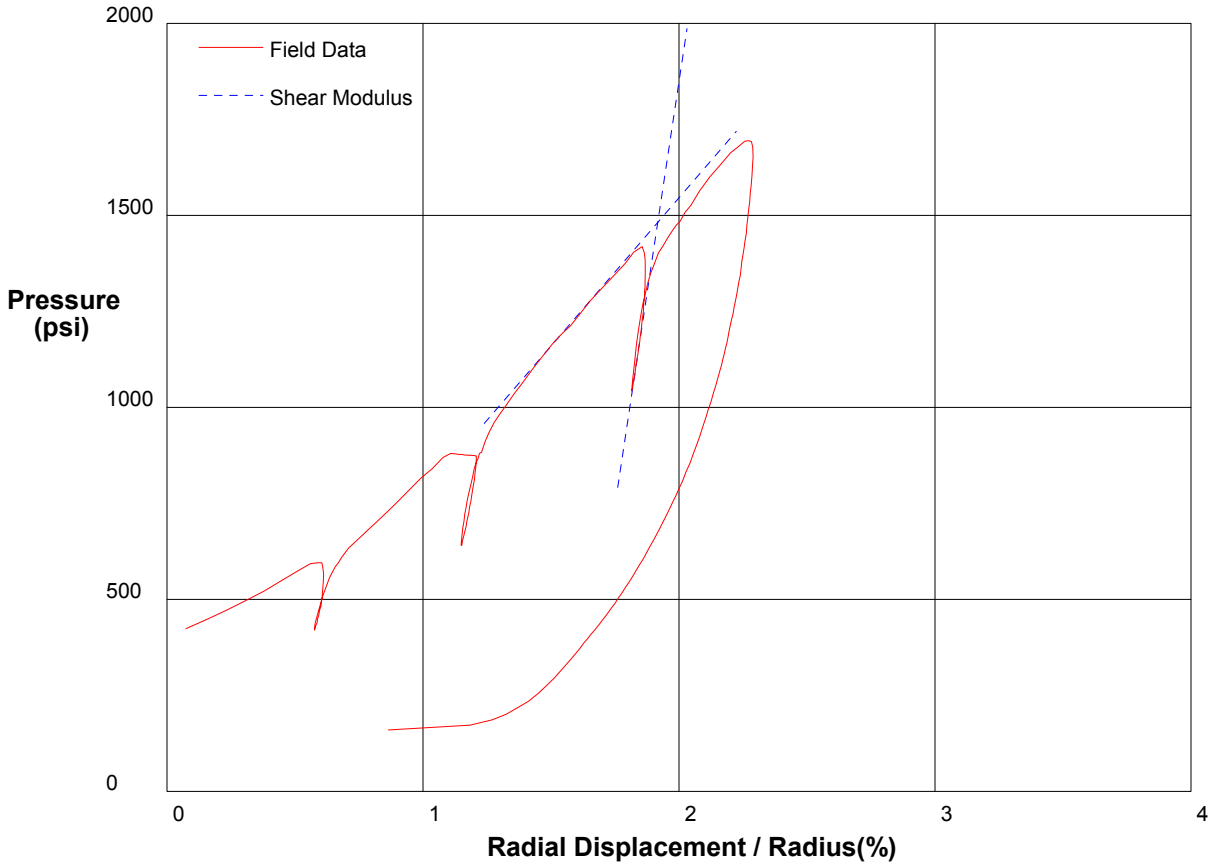

Shear Modulus 220512 psi

Shear Modulus 38624 psi

shift 4

In Situ Engineering

Appendix I - Pressuremeter Data and Standard Interpretation

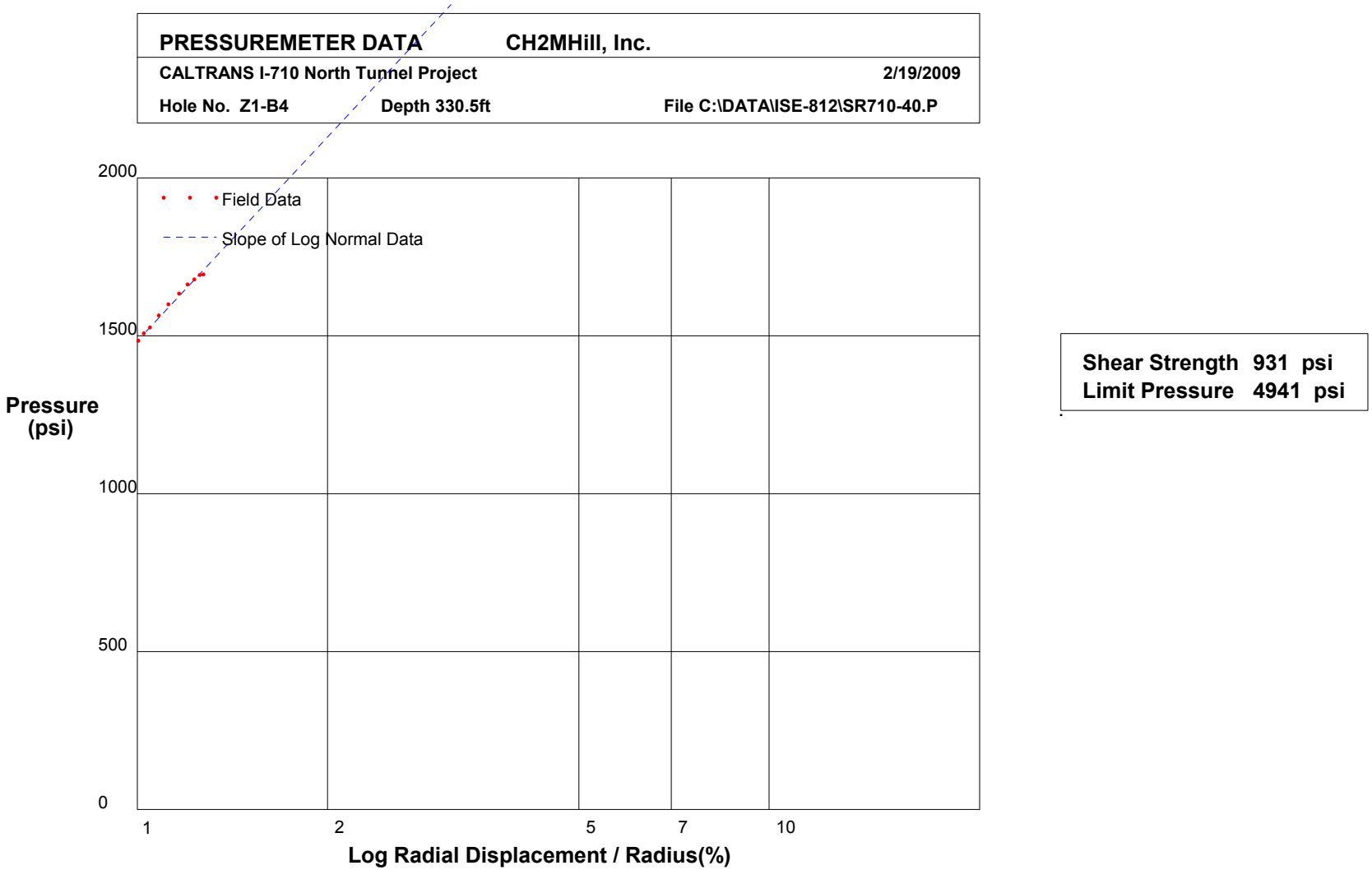

Appendix I - Pressuremeter Data and Standard Interpretation

PRESSUREMETER DATA **CH2MHill, Inc.**

CALTRANS I-710 North Tunnel Project **2/20/2009**

Hole No. Z1-B5 **Depth 347ft** **File C:\DATA\ISE-812\SR710-41.P**

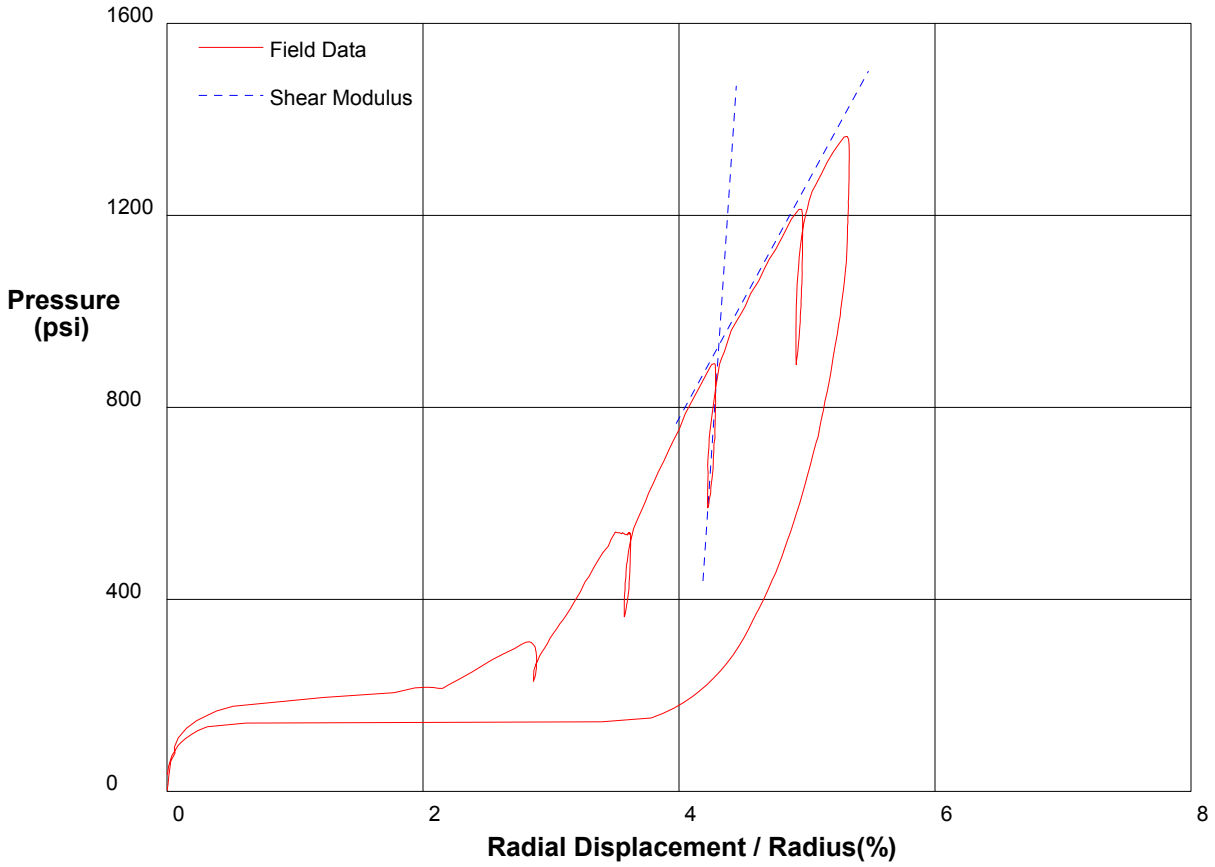

Shear Modulus 197866 psi

Shear Modulus 24444 psi

shift 0

In Situ Engineering

Appendix I - Pressuremeter Data and Standard Interpretation

PRESSUREMETER DATA **CH2MHill, Inc.**

CALTRANS I-710 North Tunnel Project **2/20/2009**

Hole No. Z1-B5 **Depth 347ft** **File C:\DATA\ISE-812\SR710-41.P**

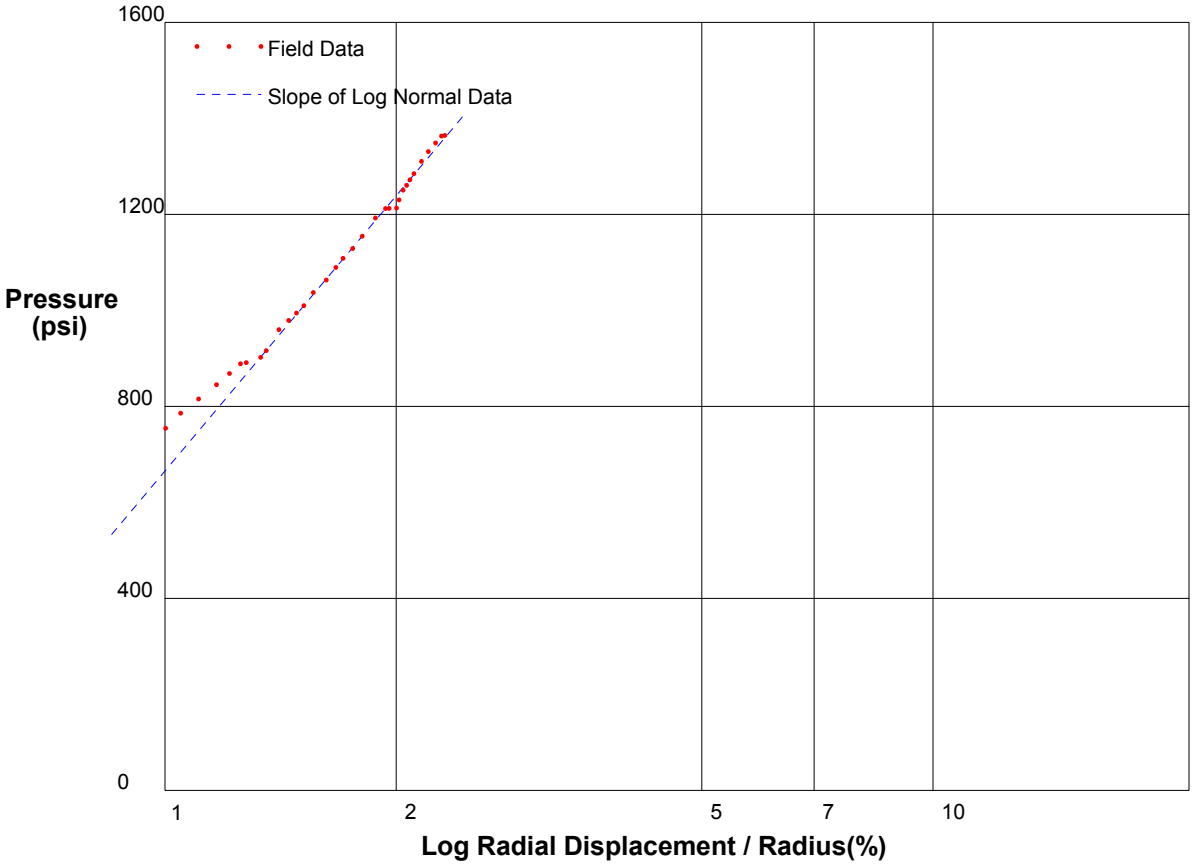

Shear Strength 826.9 psi
Limit Pressure 3736 psi

shift 3

In Situ Engineering

Appendix I - Pressuremeter Data and Standard Interpretation

PRESSUREMETER DATA **CH2MHill, Inc.**

CALTRANS I-710 North Tunnel Project **2/20/2009**

Hole No. Z1-B5 **Depth 345.5ft** **File C:\DATA\ISE-812\SR710-42.P**

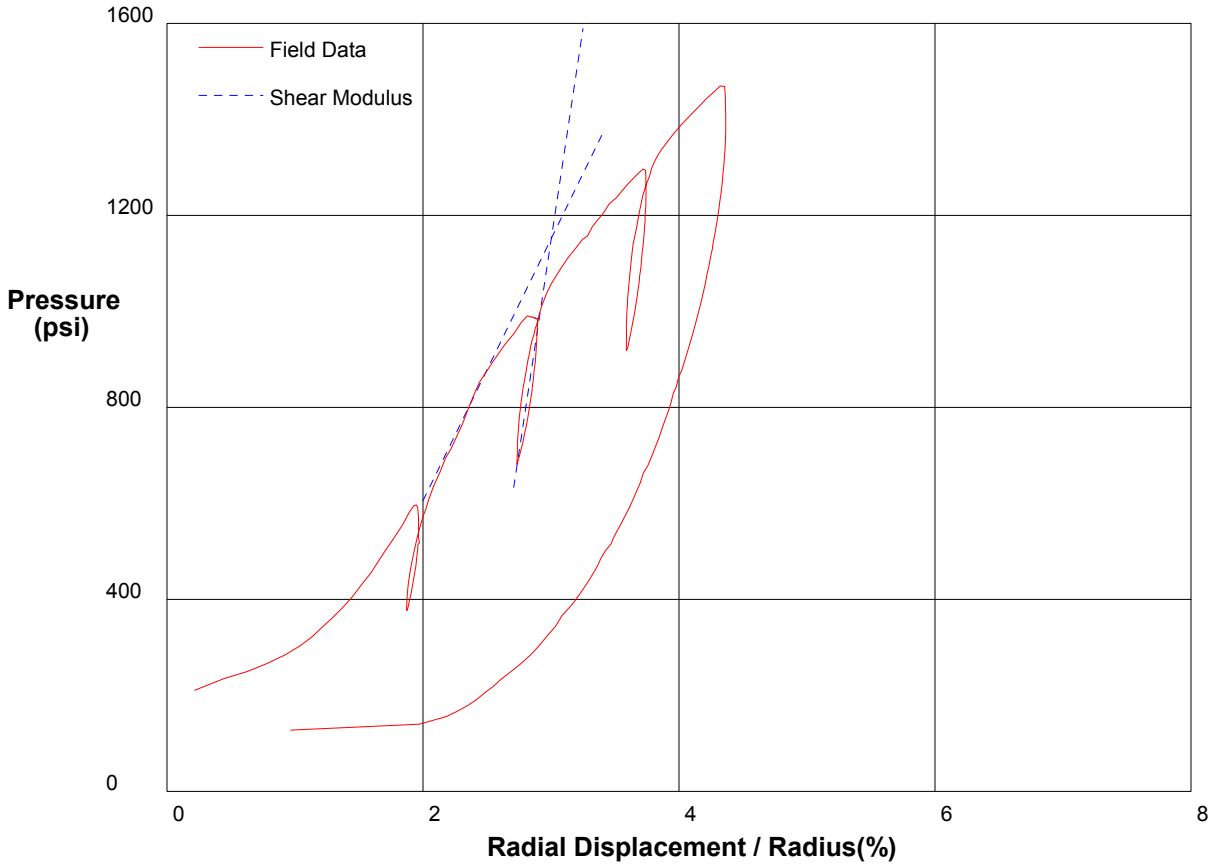

Shear Modulus 88205 psi

Shear Modulus 27263 psi

shift 2.8

In Situ Engineering

Appendix I - Pressuremeter Data and Standard Interpretation

PRESSUREMETER DATA **CH2MHill, Inc.**

CALTRANS I-710 North Tunnel Project **2/20/2009**

Hole No. Z1-B5 **Depth 345.5ft** **File C:\DATA\ISE-812\SR710-42.P**

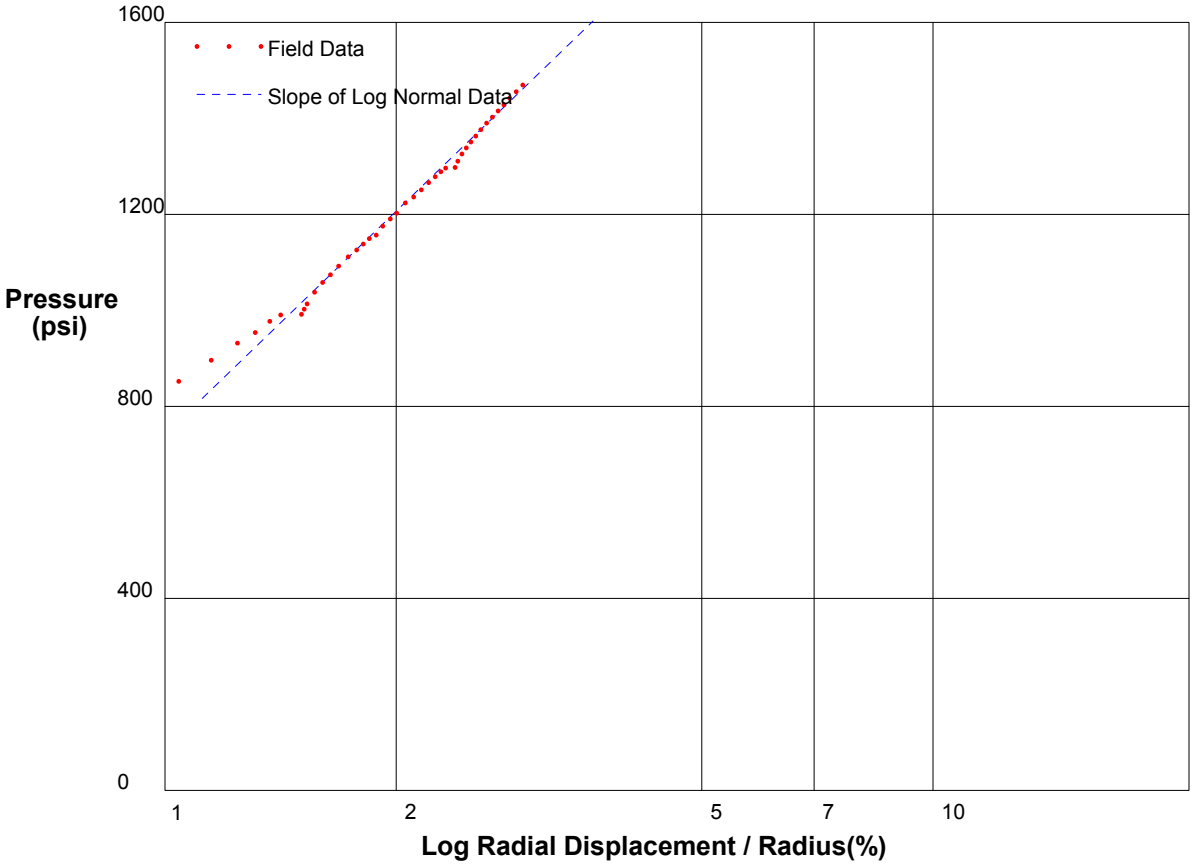

Shear Strength 671.1 psi
Limit Pressure 3233 psi

shift 4.2

In Situ Engineering

Appendix I - Pressuremeter Data and Standard Interpretation

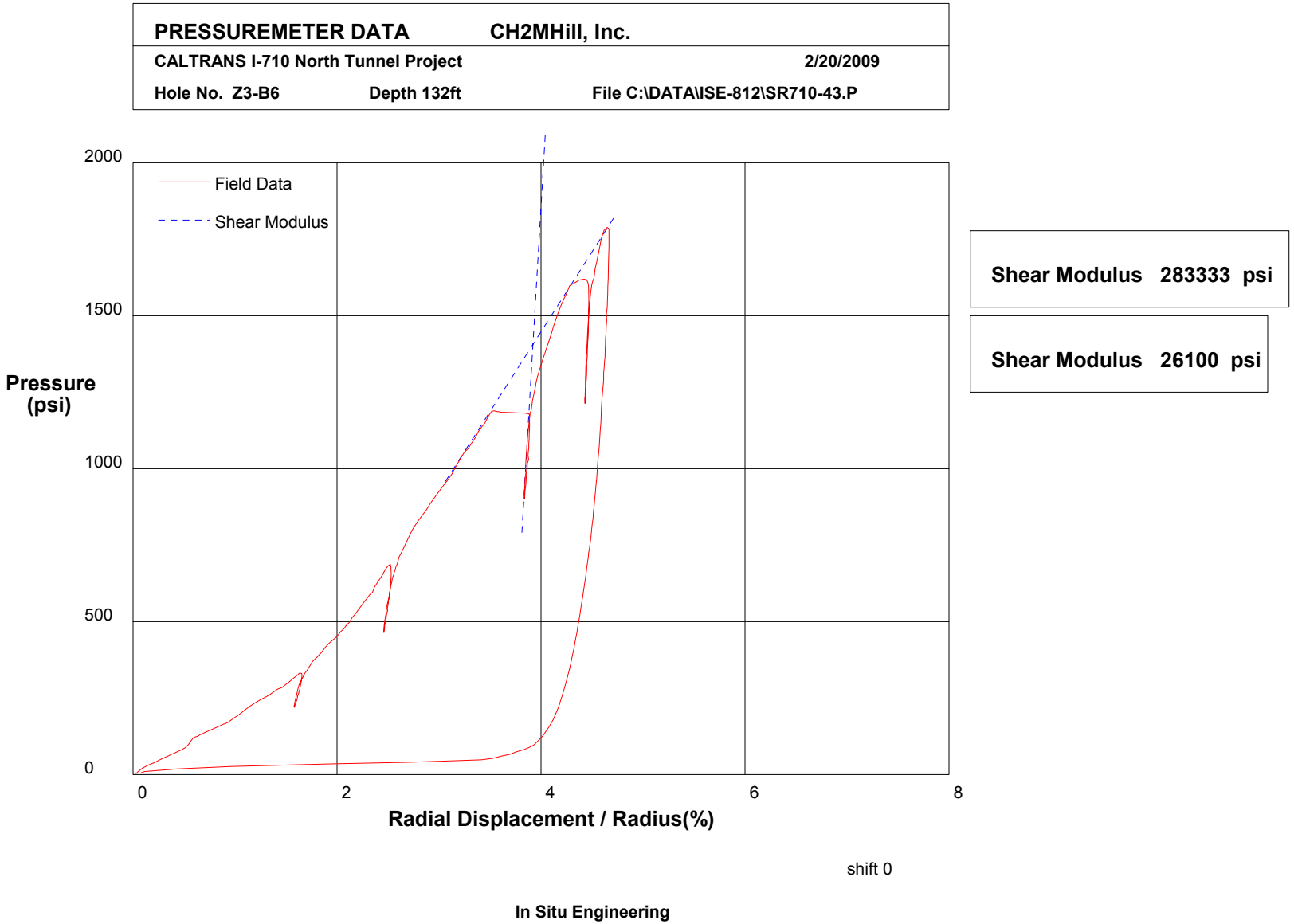

Appendix I - Pressuremeter Data and Standard Interpretation

PRESSUREMETER DATA **CH2MHill, Inc.**

CALTRANS I-710 North Tunnel Project **2/20/2009**

Hole No. Z3-B6 **Depth 132ft** **File C:\DATA\ISE-812\SR710-43.P**

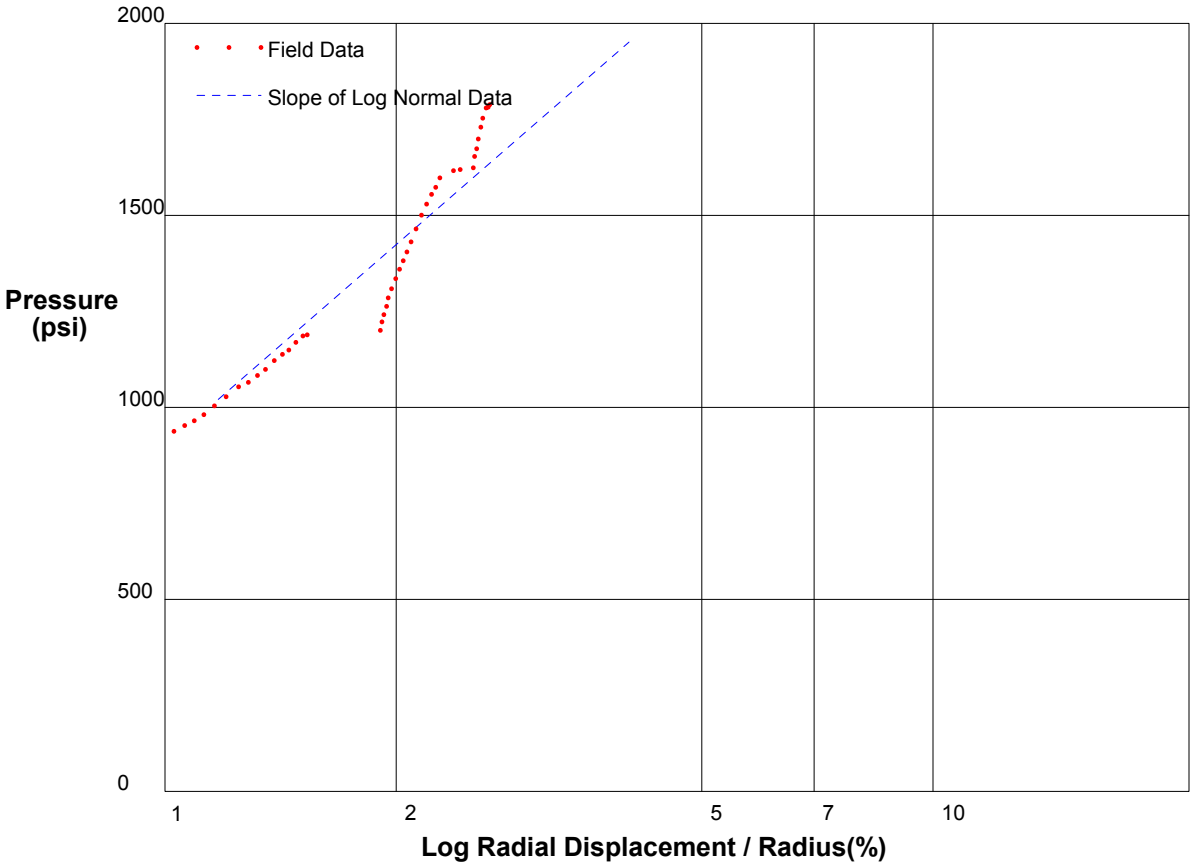

Shear Strength 755.7 psi
Limit Pressure 3706 psi

shift 2

In Situ Engineering

Appendix I - Pressuremeter Data and Standard Interpretation

PRESSUREMETER DATA **CH2MHill, Inc.**

CALTRANS I-710 North Tunnel Project **2/23/2009**

Hole No. Z1-B5 **Depth 398ft** **File C:\DATA\ISE-812\SR710-44.P**

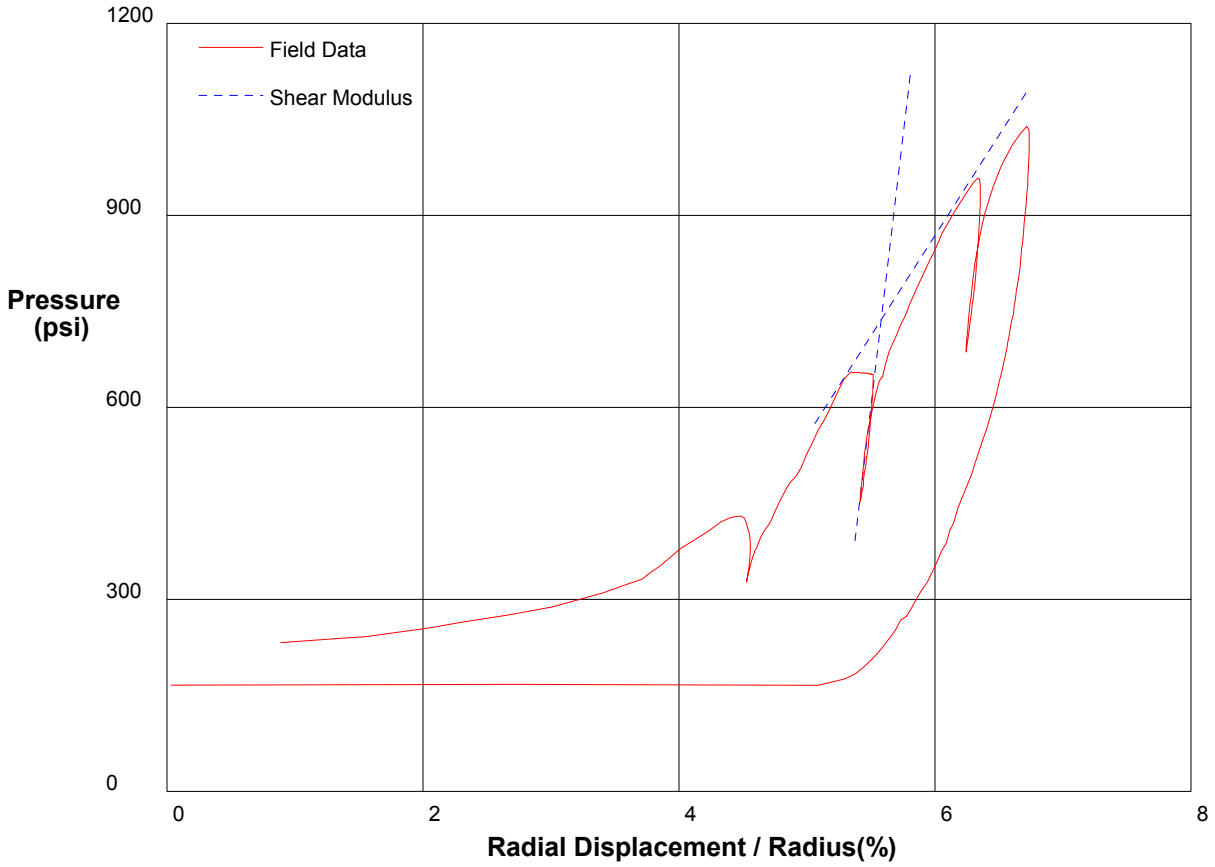

Shear Modulus 84285 psi

Shear Modulus 15660 psi

shift 1.5

In Situ Engineering

Appendix I - Pressuremeter Data and Standard Interpretation

PRESSUREMETER DATA **CH2MHill, Inc.**

CALTRANS I-710 North Tunnel Project **2/23/2009**

Hole No. Z1-B5 **Depth 398ft** **File C:\DATA\ISE-812\SR710-44.P**

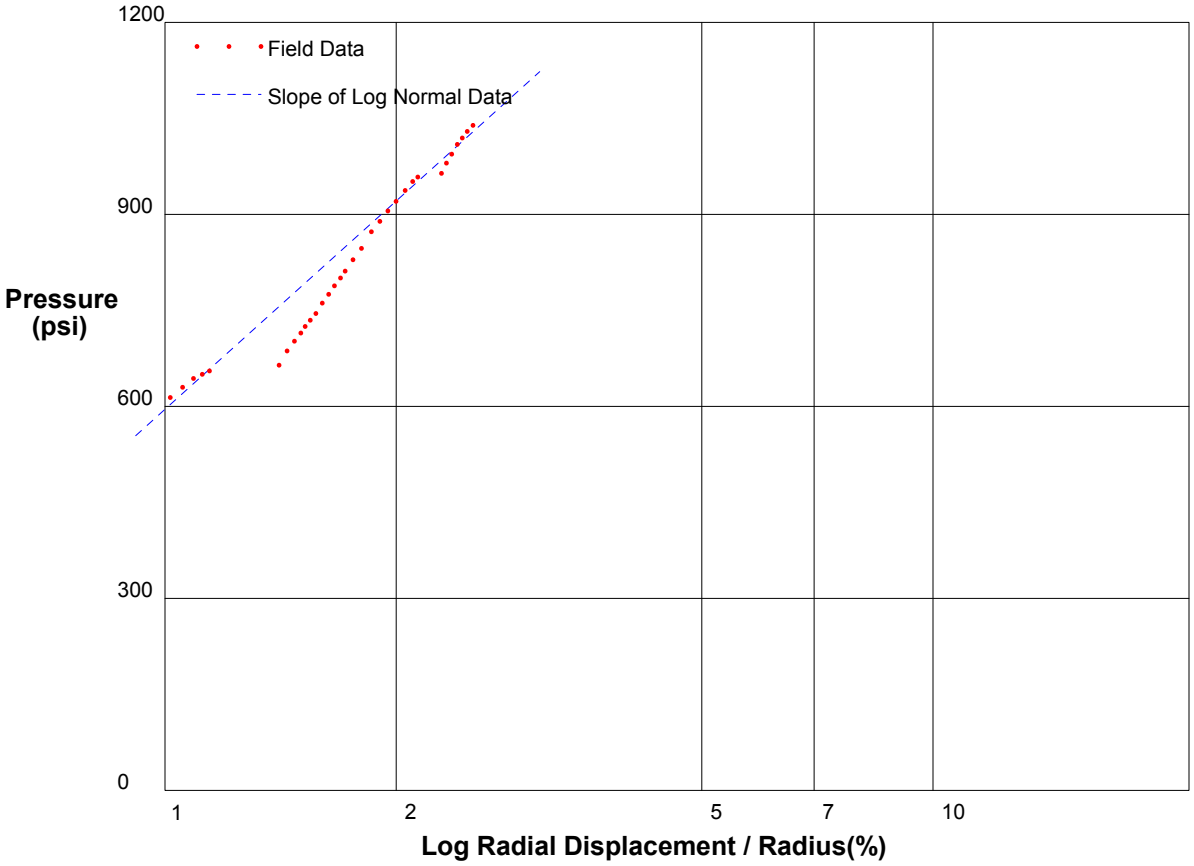

Shear Strength 469.5 psi
Limit Pressure 2339 psi

shift 5.7

In Situ Engineering

Appendix I - Pressuremeter Data and Standard Interpretation

PRESSUREMETER DATA **CH2MHill, Inc.**

CALTRANS I-710 North Tunnel Project **2/23/2009**

Hole No. Z1-B5 **Depth 396.5ft** **File C:\DATA\ISE-812\SR710-45.P**

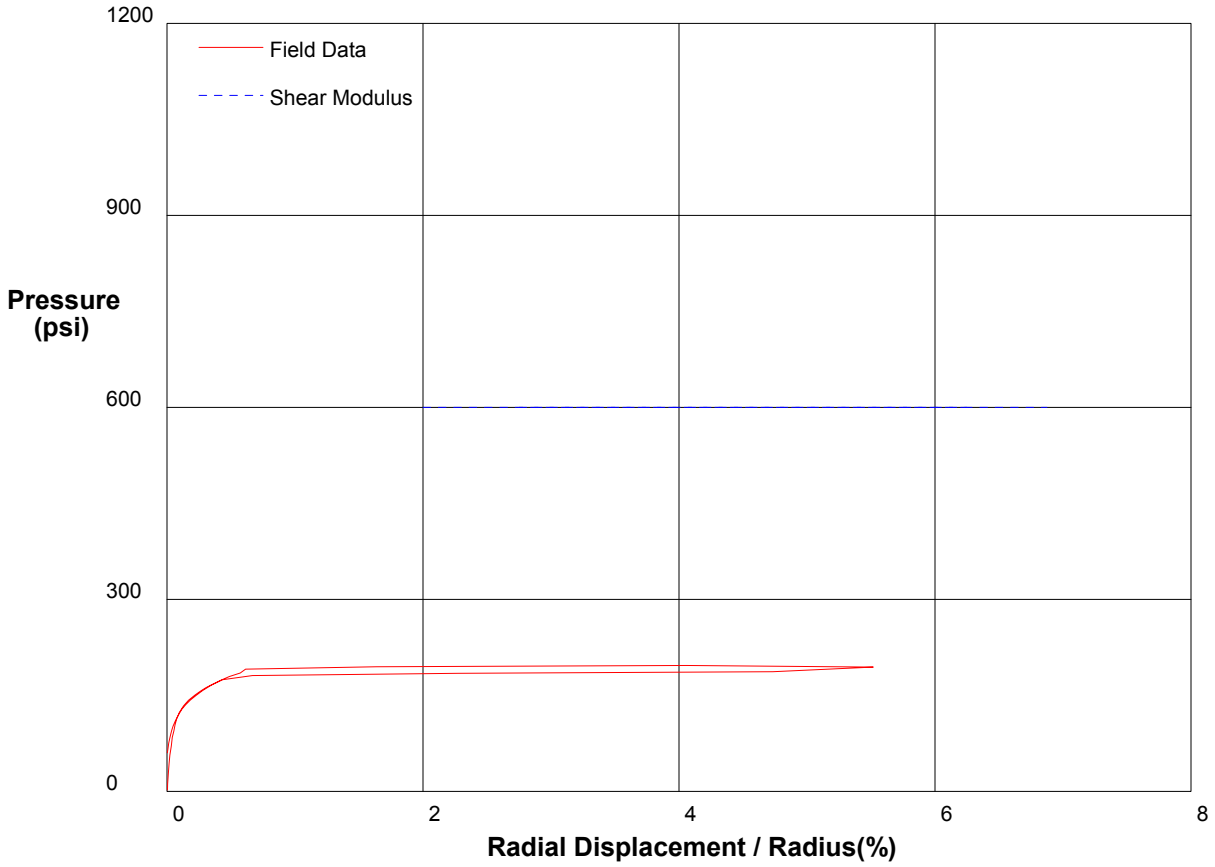

Shear Modulus 0 psi

Shear Modulus 0 psi

shift 0

In Situ Engineering

Appendix I - Pressuremeter Data and Standard Interpretation

PRESSUREMETER DATA **CH2MHill, Inc.**

CALTRANS I-710 North Tunnel Project **2/23/2009**

Hole No. Z3-B6 **Depth 168ft** **File C:\DATA\ISE-812\SR710-46.P**

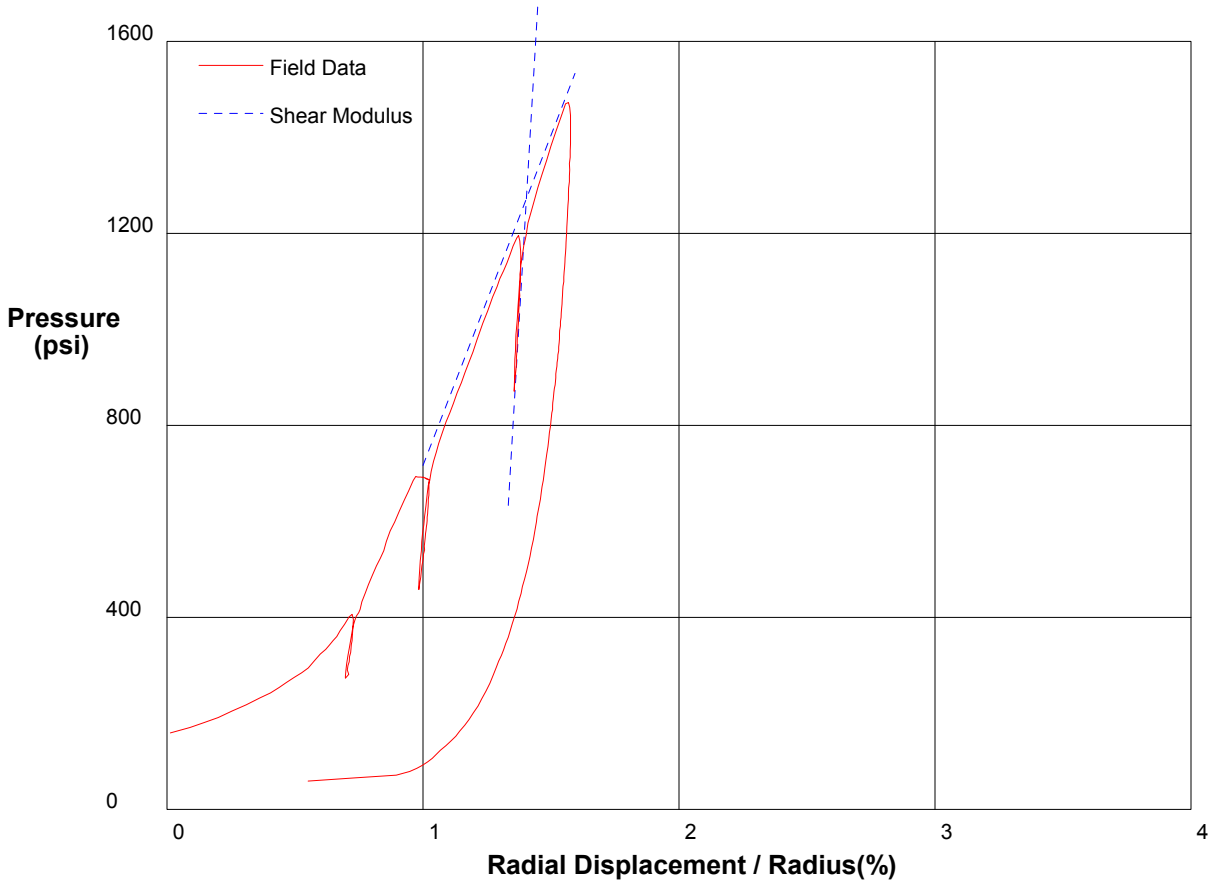

Shear Modulus 453333 psi

Shear Modulus 68771 psi

shift 2

In Situ Engineering

Appendix I - Pressuremeter Data and Standard Interpretation

PRESSUREMETER DATA **CH2MHill, Inc.**

CALTRANS I-710 North Tunnel Project **2/23/2009**

Hole No. Z3-B6 **Depth 166.5ft** **File C:\DATA\ISE-812\SR710-47.P**

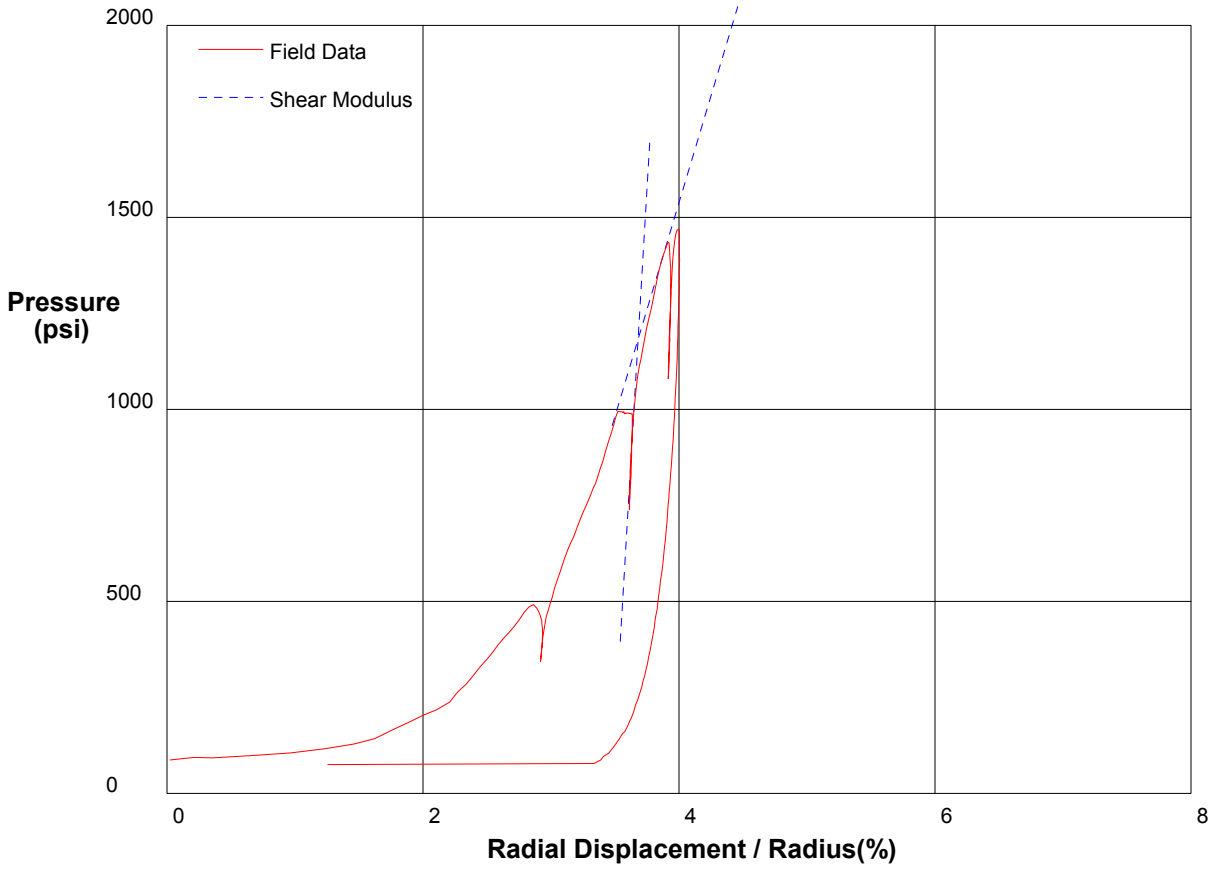

Shear Modulus 283333 psi

Shear Modulus 55673 psi

shift 3

In Situ Engineering

Appendix I - Pressuremeter Data and Standard Interpretation

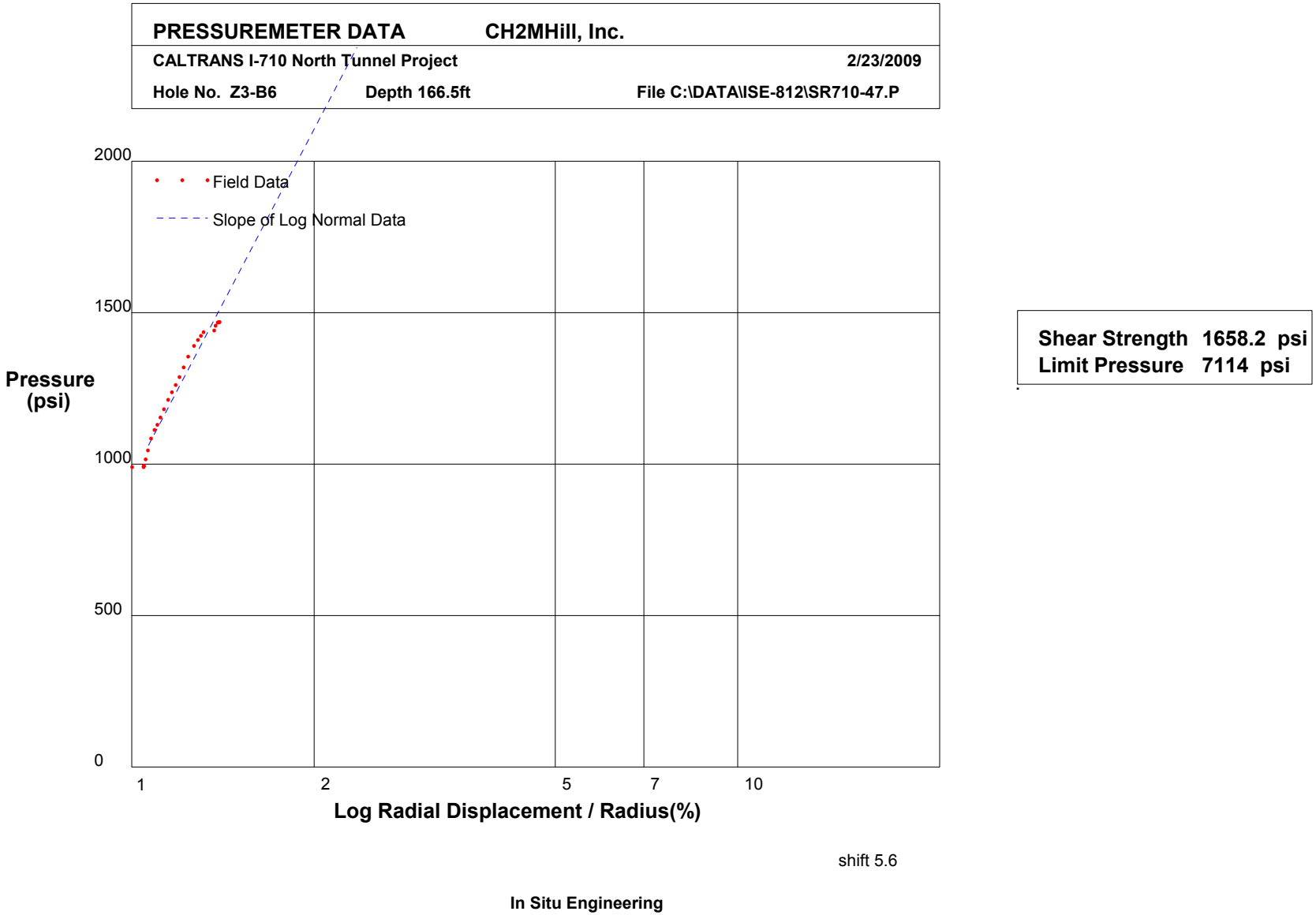

Appendix I - Pressuremeter Data and Standard Interpretation

PRESSUREMETER DATA **CH2MHill, Inc.**

CALTRANS I-710 North Tunnel Project **2/24/2009**

Hole No. Z3-B6 **Depth 188.2ft** **File C:\DATA\ISE-812\SR710-48.P**

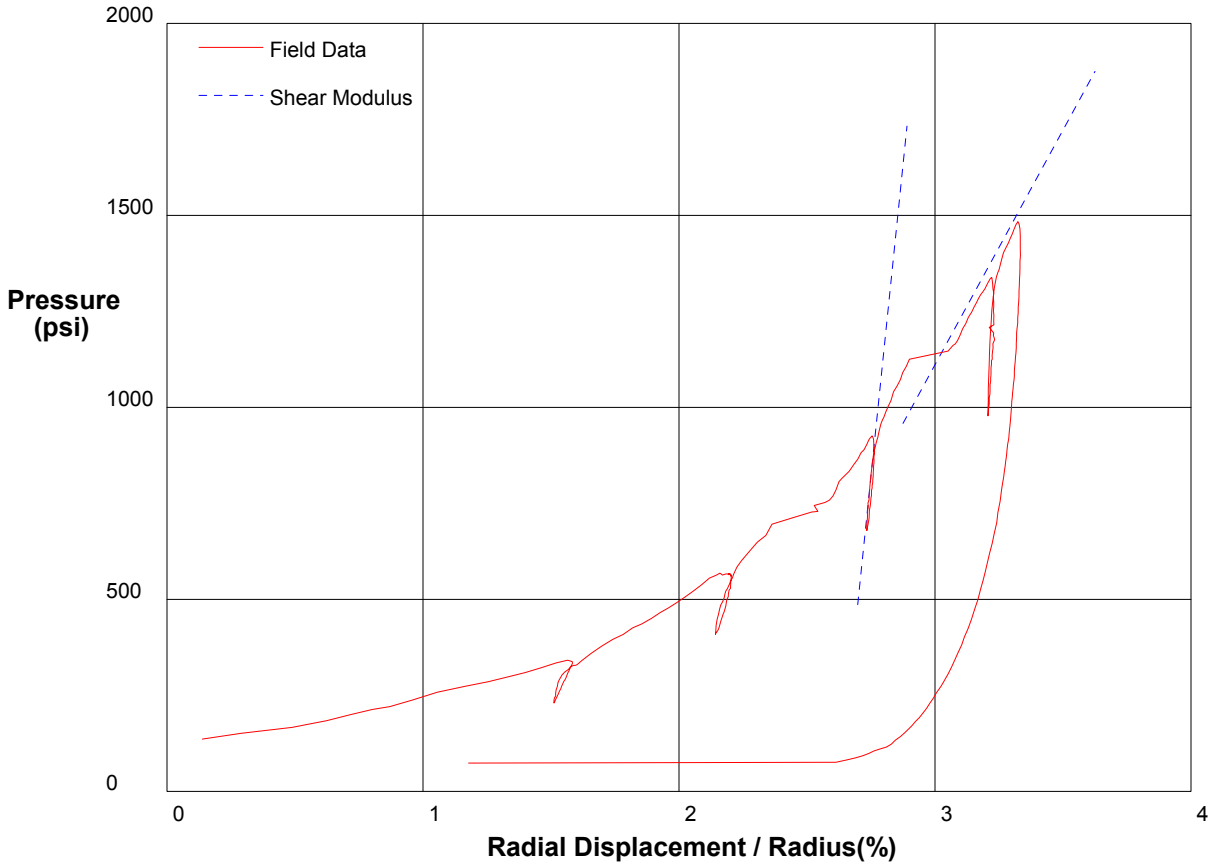

Shear Modulus 323423 psi

Shear Modulus 61111 psi

shift 1

In Situ Engineering

Appendix I - Pressuremeter Data and Standard Interpretation

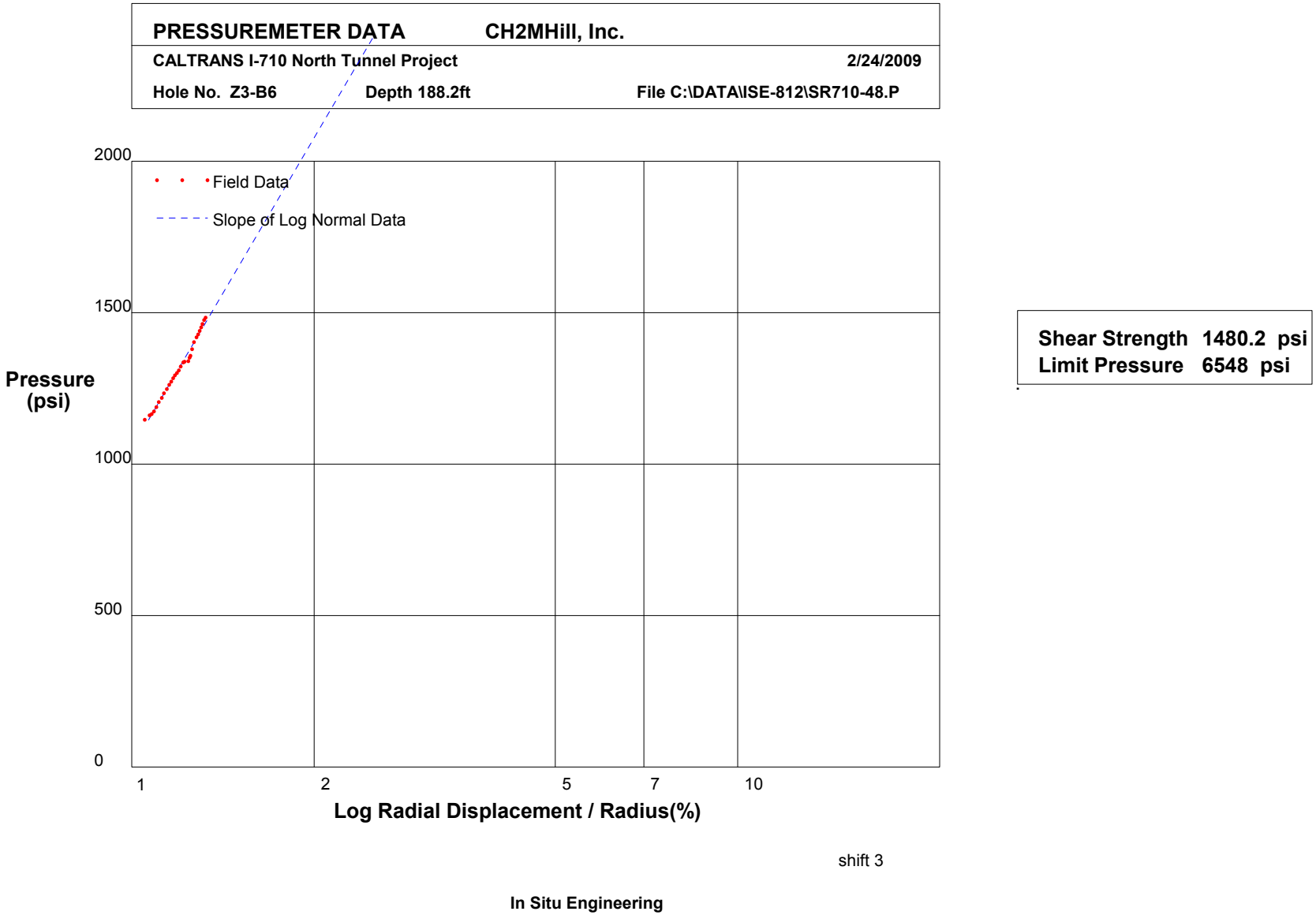

Appendix II - Pressuremeter Model Interpretation

PRESSUREMETER DATA **CH2MHill, Inc.**

CALTRANS I-710 North Tunnel Project **1/16/2009**

Hole No. Z3-B2 **Depth 200.9ft** **File C:\DATA\ISE-812\SR710-01.P**

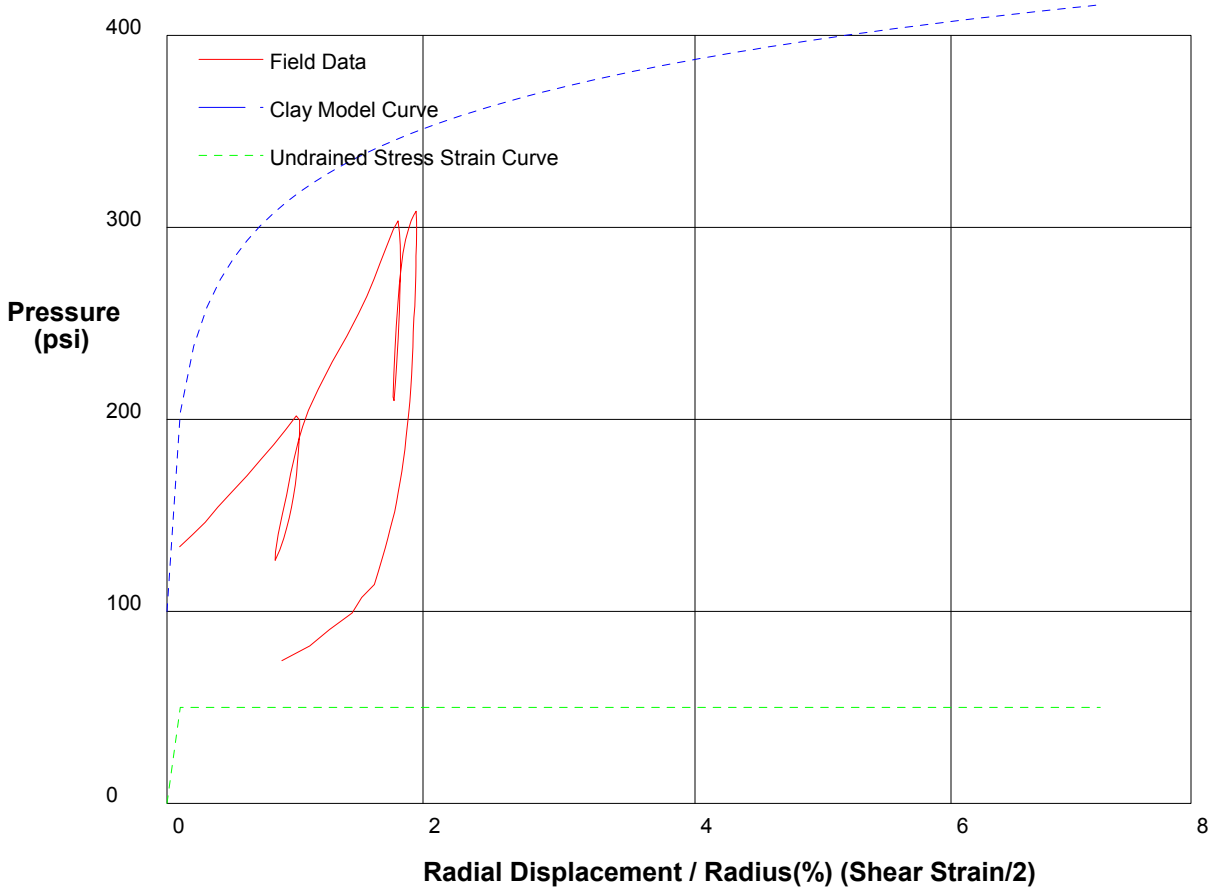

GIBSON'S CLAY MODEL

Shear Strength 50 psi
Insitu Stress 100 psi
Shear Modulus 70000 psi

shift 9

In Situ Engineering

Appendix II - Pressuremeter Model Interpretation

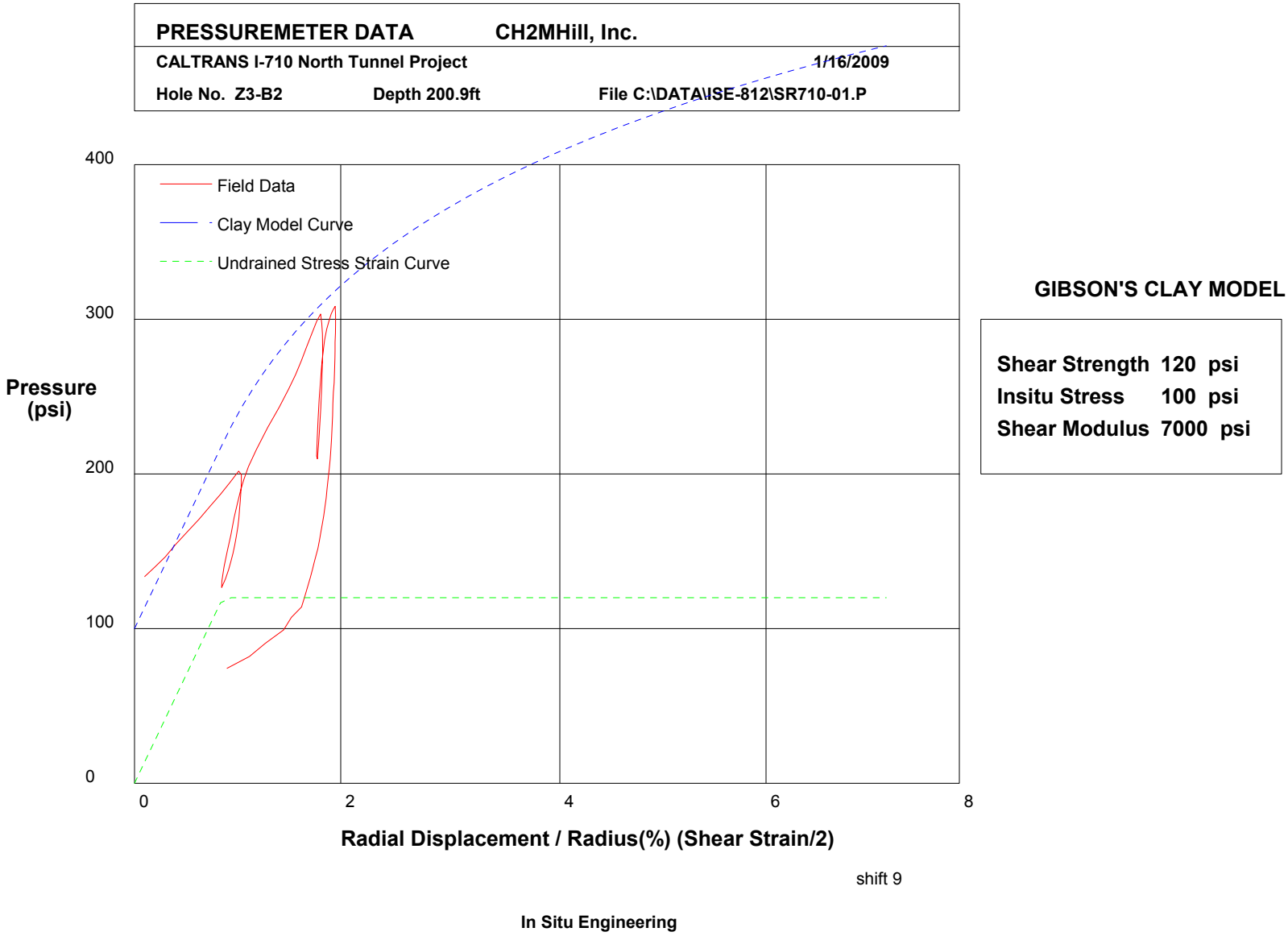

Appendix II - Pressuremeter Model Interpretation

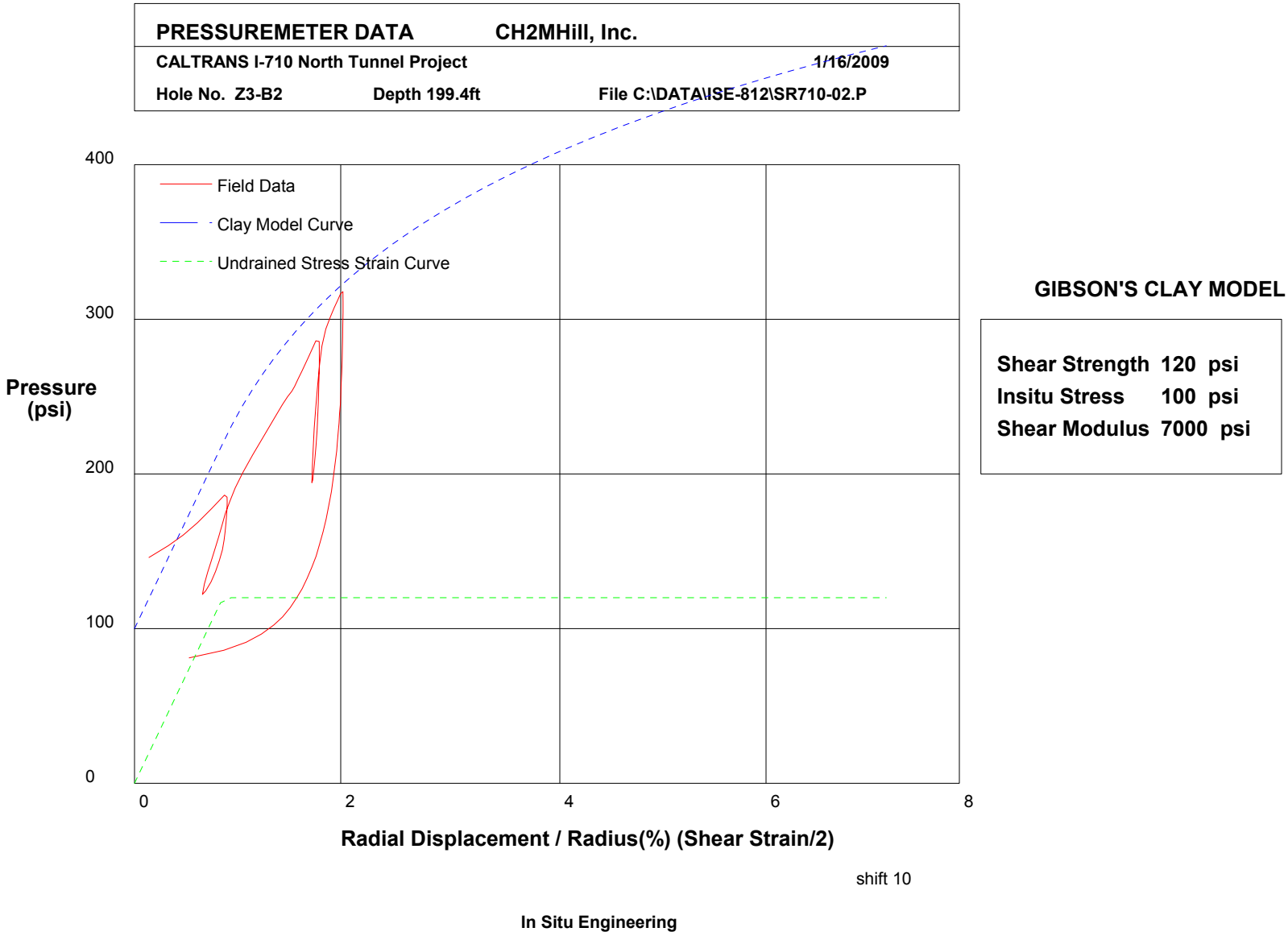

Appendix II - Pressuremeter Model Interpretation

PRESSUREMETER DATA **CH2MHill, Inc.**

CALTRANS I-710 North Tunnel Project **1/16/2009**

Hole No. Z3-B2 **Depth 199.4ft** **File C:\DATA\ISE-812\SR710-02.P**

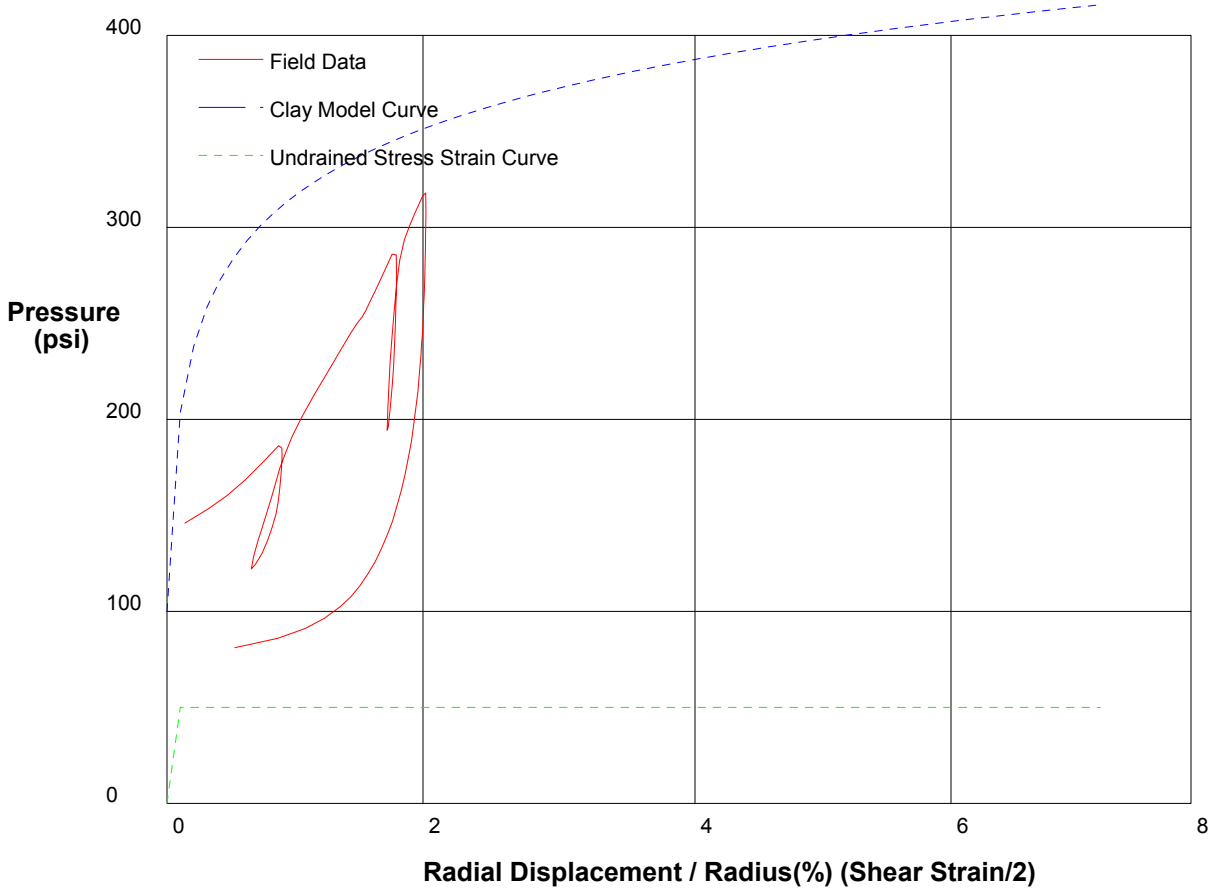

GIBSON'S CLAY MODEL

Shear Strength 50 psi
Insitu Stress 100 psi
Shear Modulus 70000 psi

shift 10

In Situ Engineering

Appendix II - Pressuremeter Model Interpretation

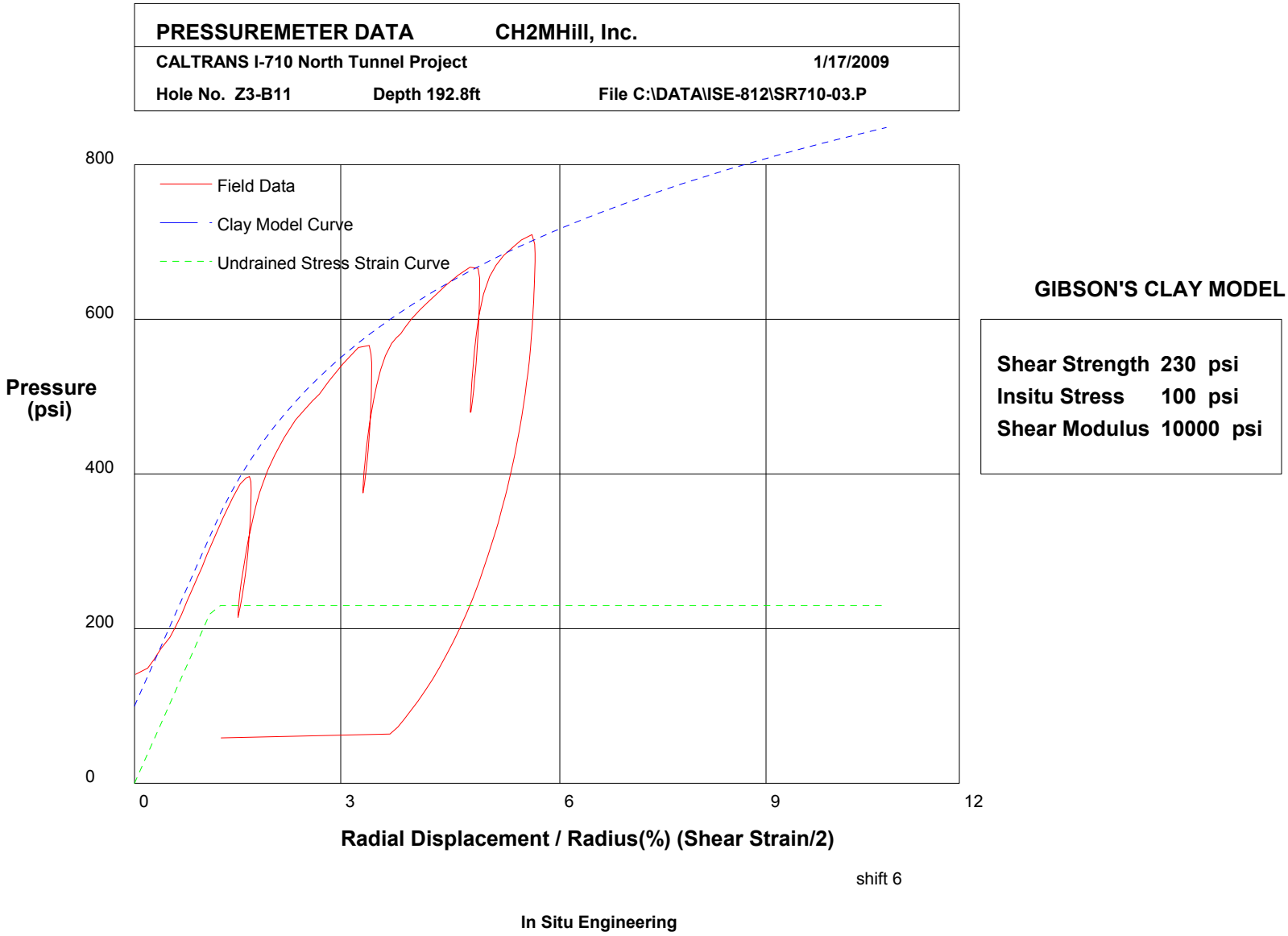

Appendix II - Pressuremeter Model Interpretation

PRESSUREMETER DATA **CH2MHill, Inc.**

CALTRANS I-710 North Tunnel Project **1/17/2009**

Hole No. Z3-B11 **Depth 192.8ft** **File C:\DATA\ISE-812\SR710-03.P**

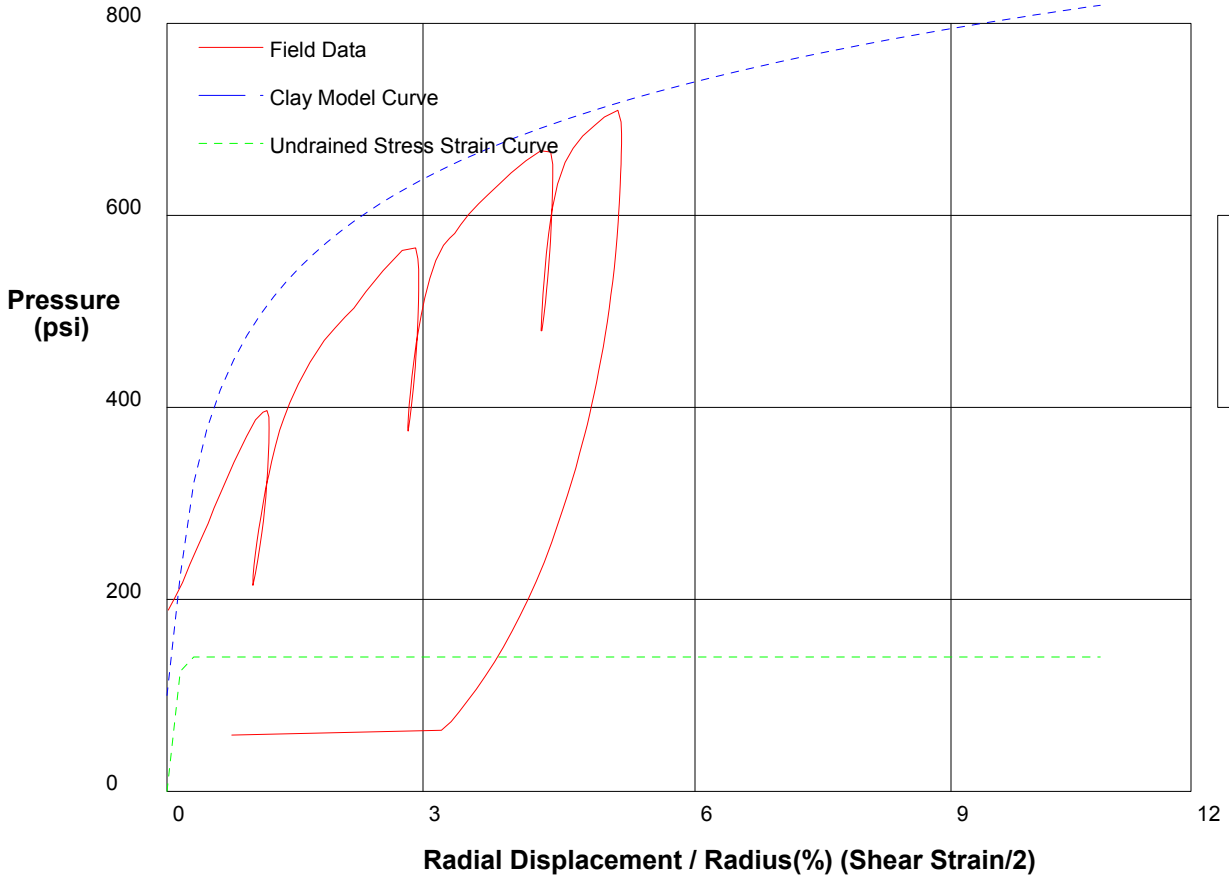

GIBSON'S CLAY MODEL

Shear Strength	**140 psi**
Insitu Stress	**100 psi**
Shear Modulus	**40000 psi**

shift 6.5

In Situ Engineering

Appendix II - Pressuremeter Model Interpretation

PRESSUREMETER DATA **CH2M-HILL, Inc.**

CALTRANS I-170 North Tunnel Project **1/17/2009**

Hole No. Z3-B11 **Depth 192.8ft** **File C:\DATA\ISE-812\SR710-03.P**

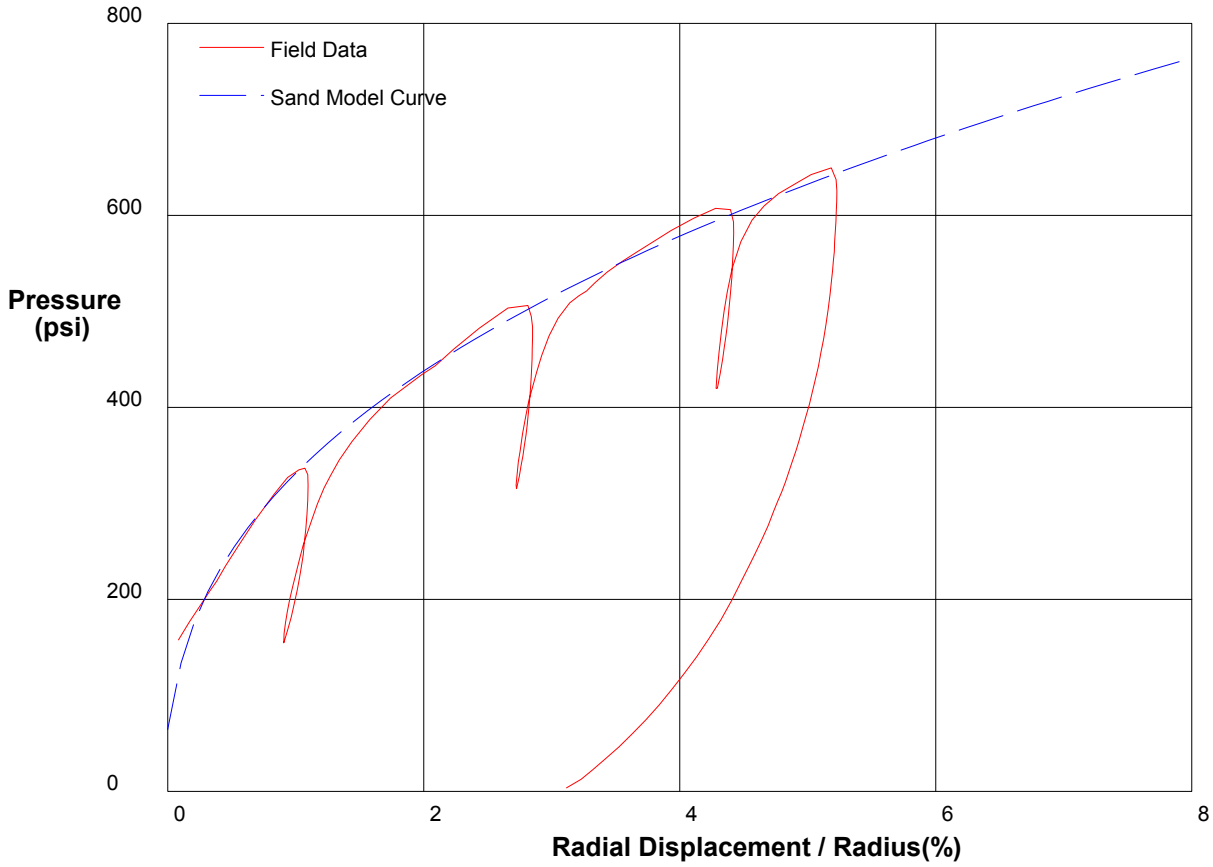

THE In Situ Engineering SAND MODEL

Water Pressure	**60 psi**
Friction Angle	**36 deg**
Critical Friction Angle	**32 deg**
Lateral Stress	**65 psi**
Shear Modulus	**35000 psi**

shift 6.6

In Situ Engineering

Appendix II - Pressuremeter Model Interpretation

PRESSUREMETER DATA **CH2MHill, Inc.**

CALTRANS I-710 North Tunnel Project **1/17/2009**

Hole No. Z3-B11 **Depth 191.3ft** **File C:\DATA\ISE-812\SR710-04.P**

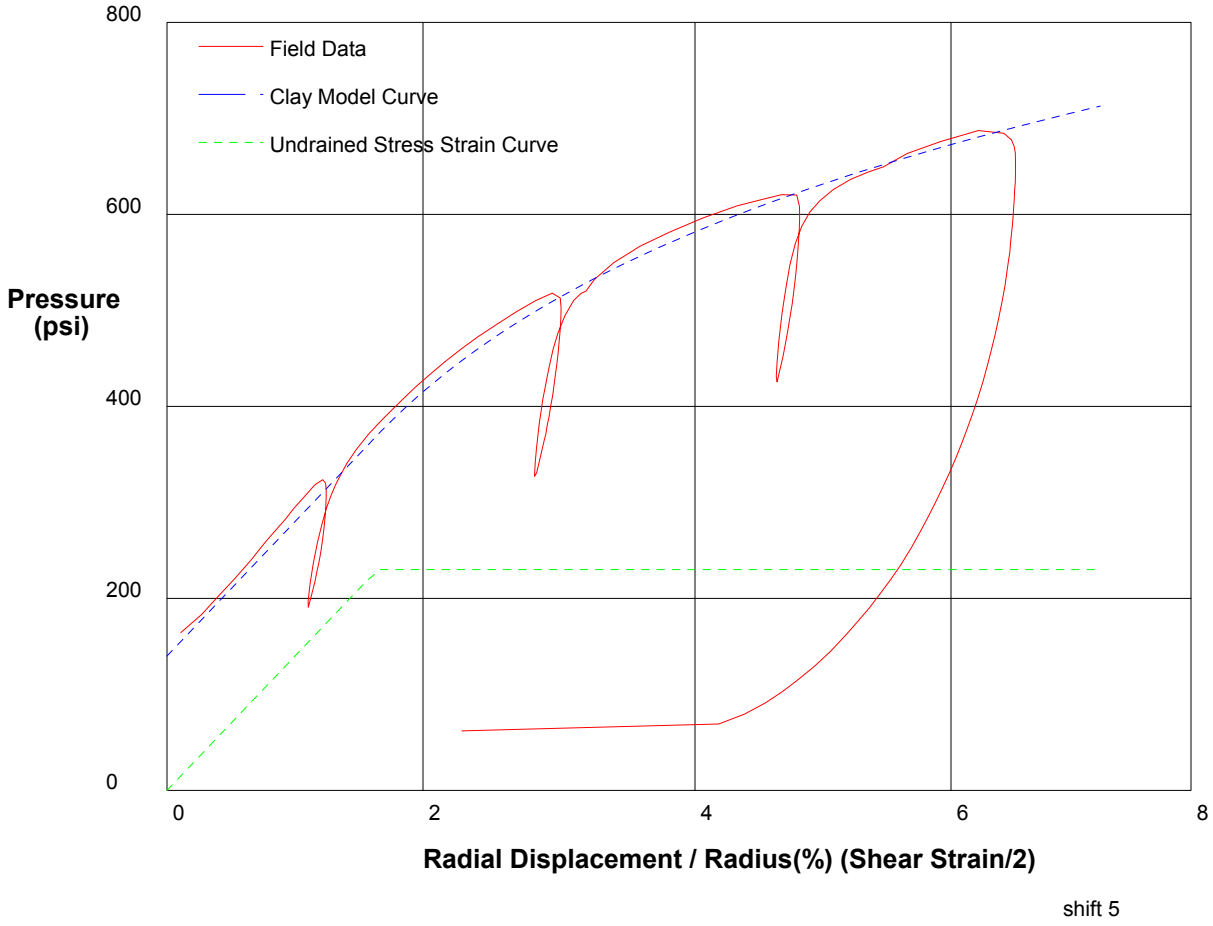

GIBSON'S CLAY MODEL

Shear Strength	**230 psi**
Insitu Stress	**140 psi**
Shear Modulus	**7000 psi**

shift 5

In Situ Engineering

Appendix II - Pressuremeter Model Interpretation

PRESSUREMETER DATA **CH2MHill, Inc.**

CALTRANS I-710 North Tunnel Project **1/17/2009**

Hole No. Z3-B11 **Depth 191.3ft** **File C:\DATA\ISE-812\SR710-04.P**

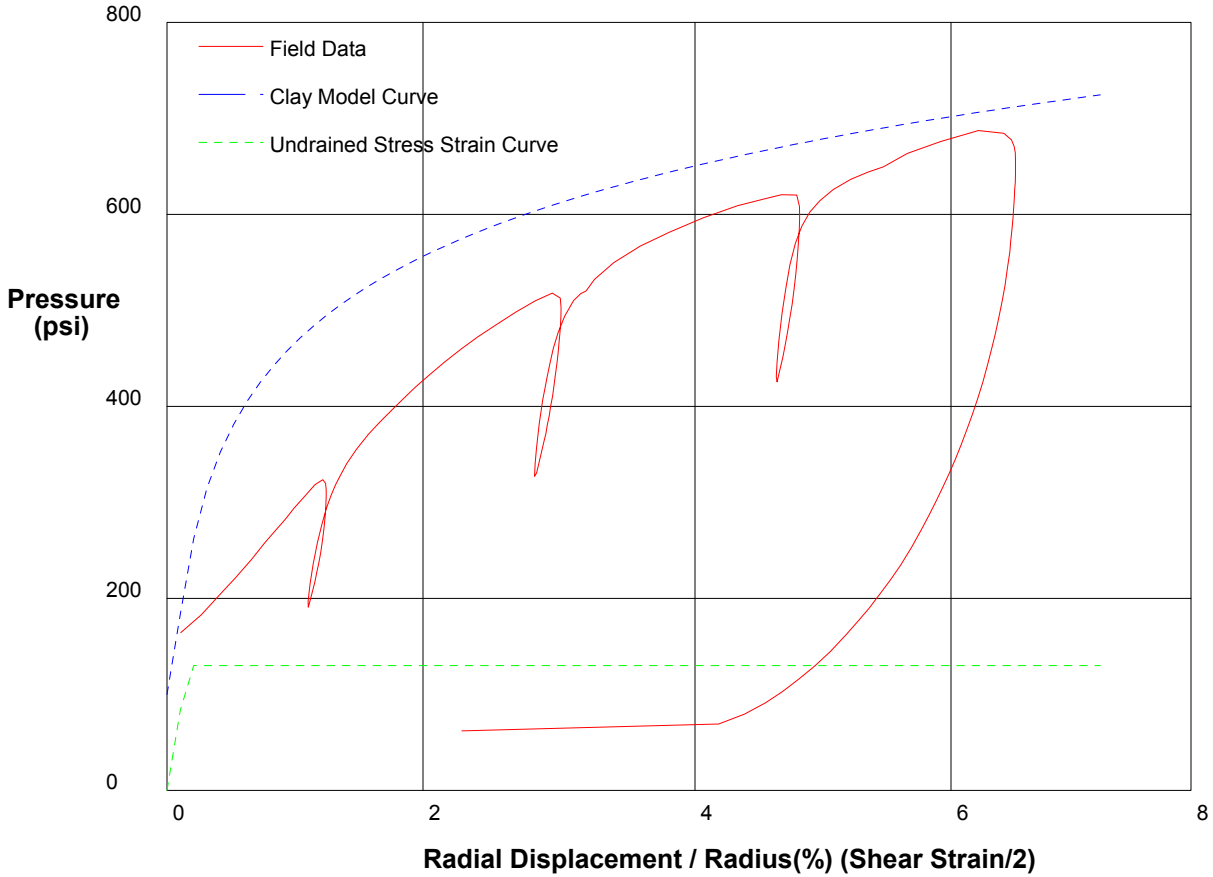

GIBSON'S CLAY MODEL

Shear Strength	**130 psi**
Insitu Stress	**100 psi**
Shear Modulus	**40000 psi**

shift 5

In Situ Engineering

Appendix II - Pressuremeter Model Interpretation

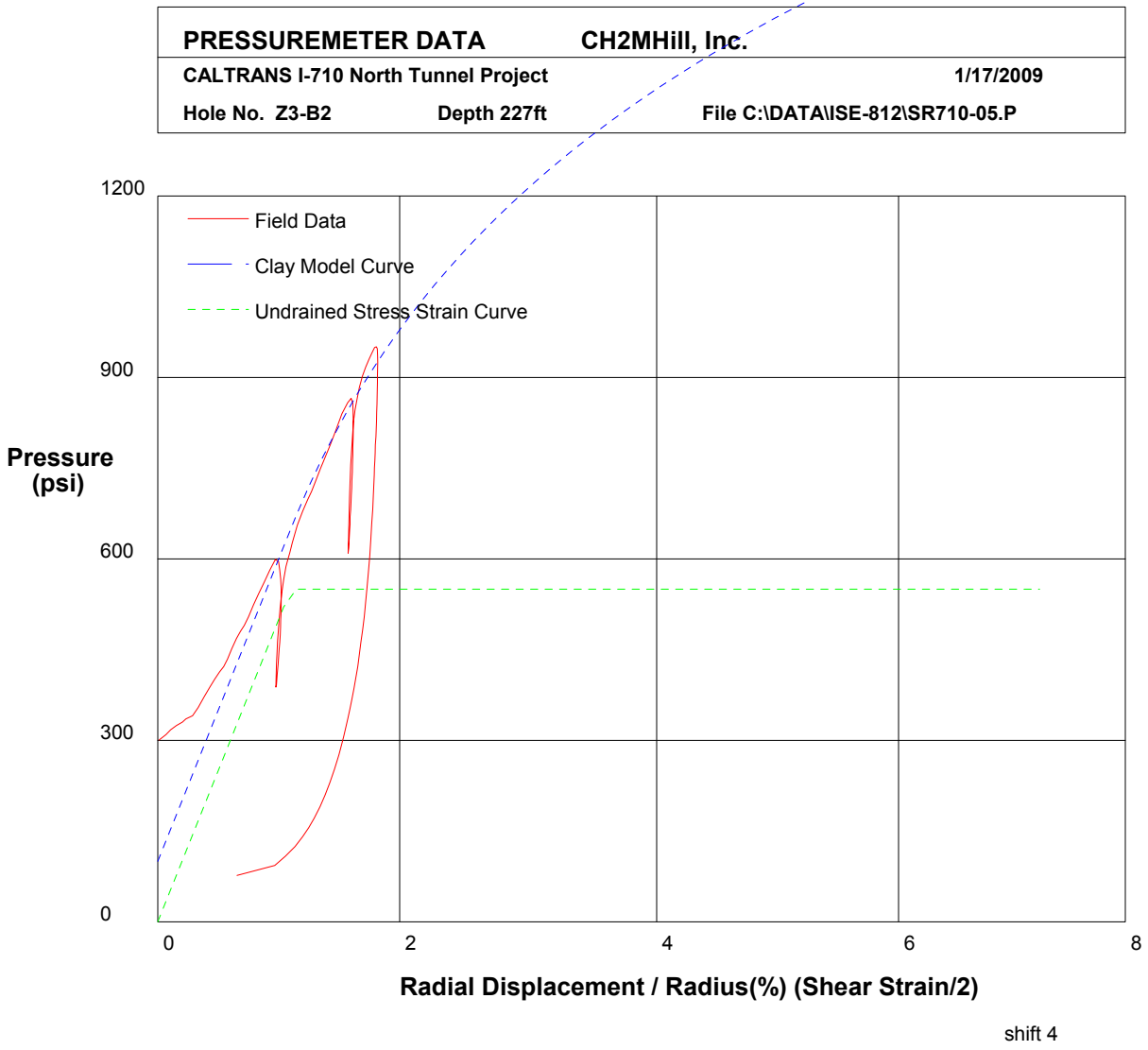

GIBSON'S CLAY MODEL

Shear Strength	**550 psi**
Insitu Stress	**100 psi**
Shear Modulus	**25000 psi**

In Situ Engineering

Appendix II - Pressuremeter Model Interpretation

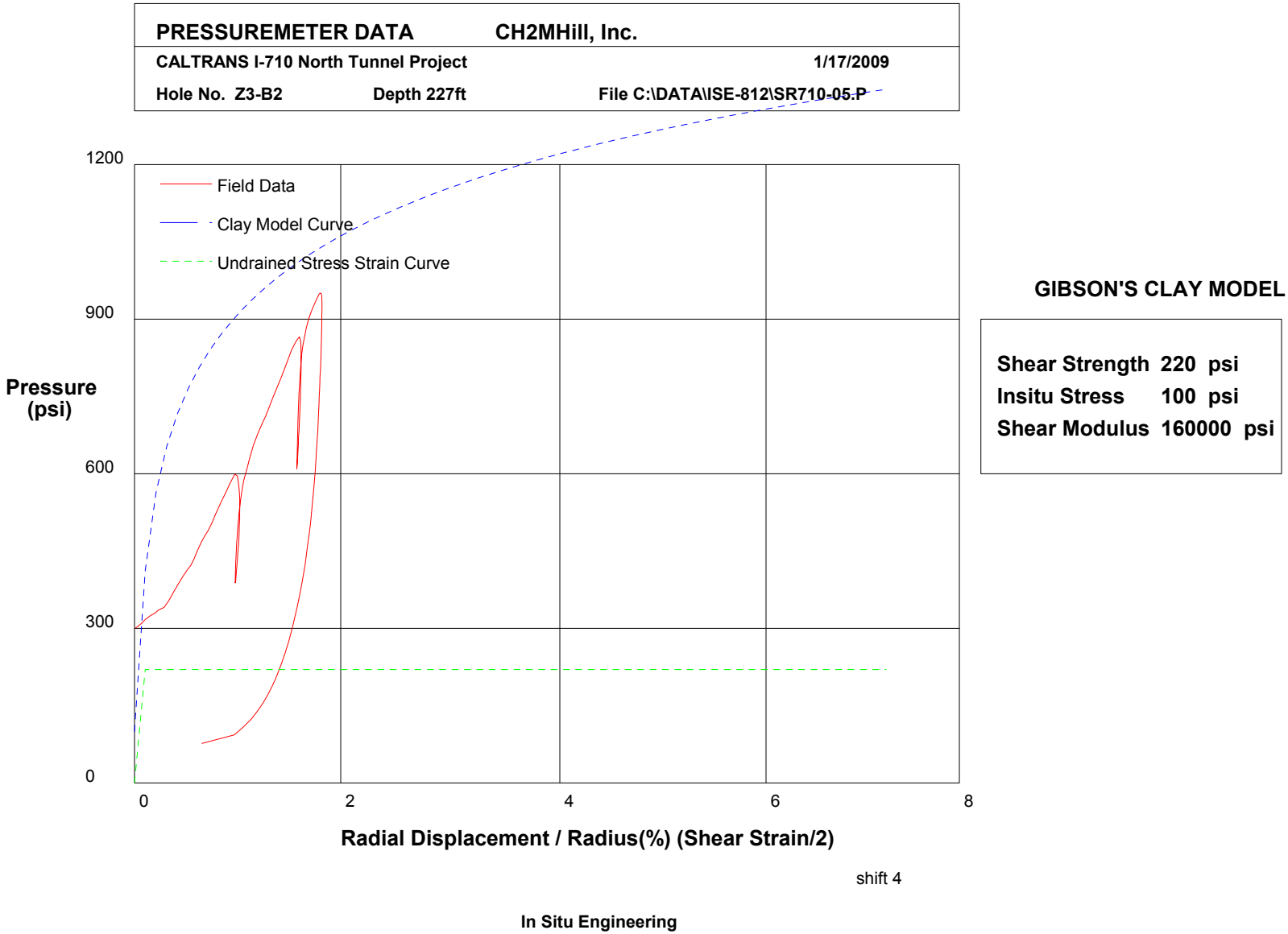

Appendix II - Pressuremeter Model Interpretation

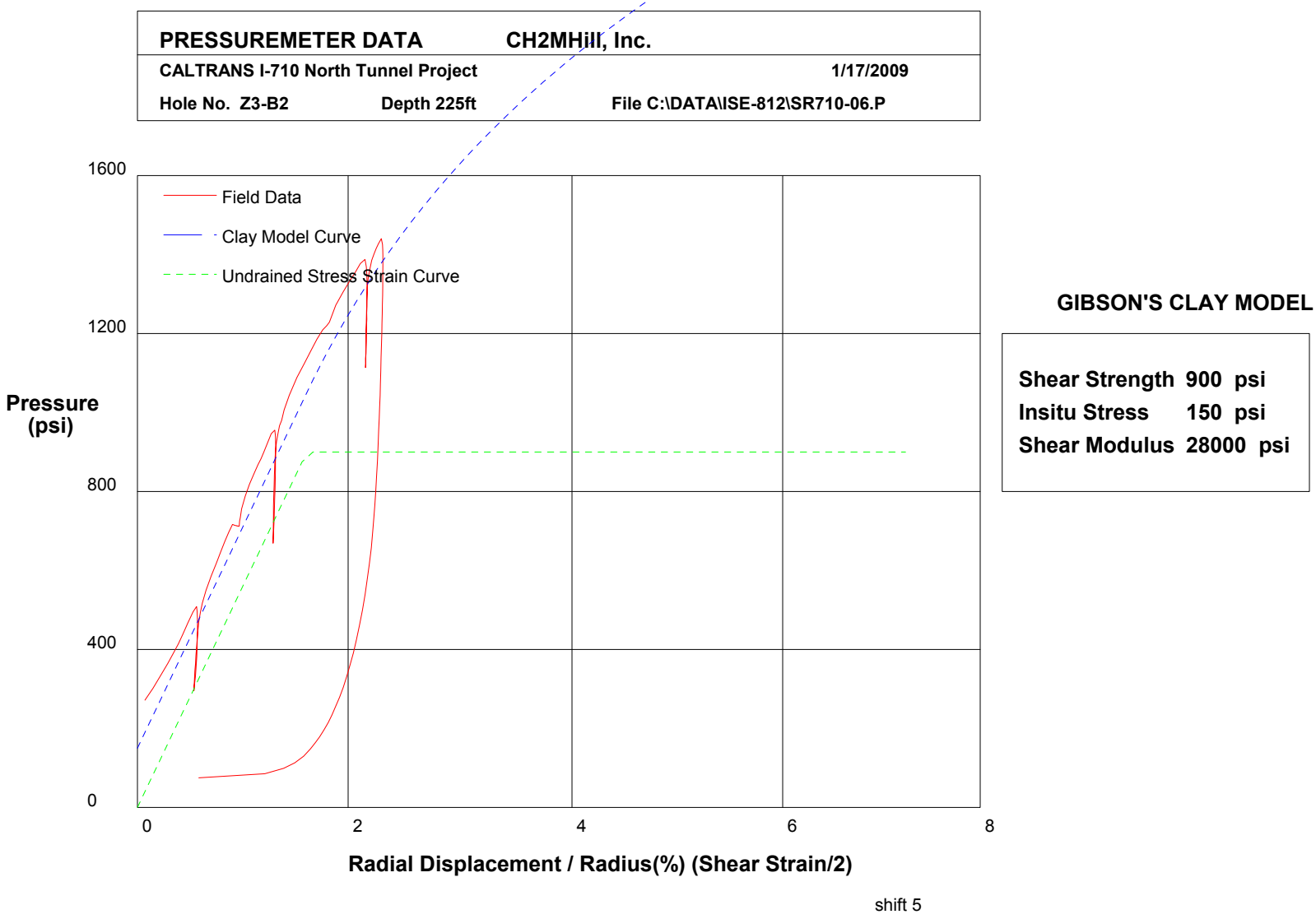

Appendix II - Pressuremeter Model Interpretation

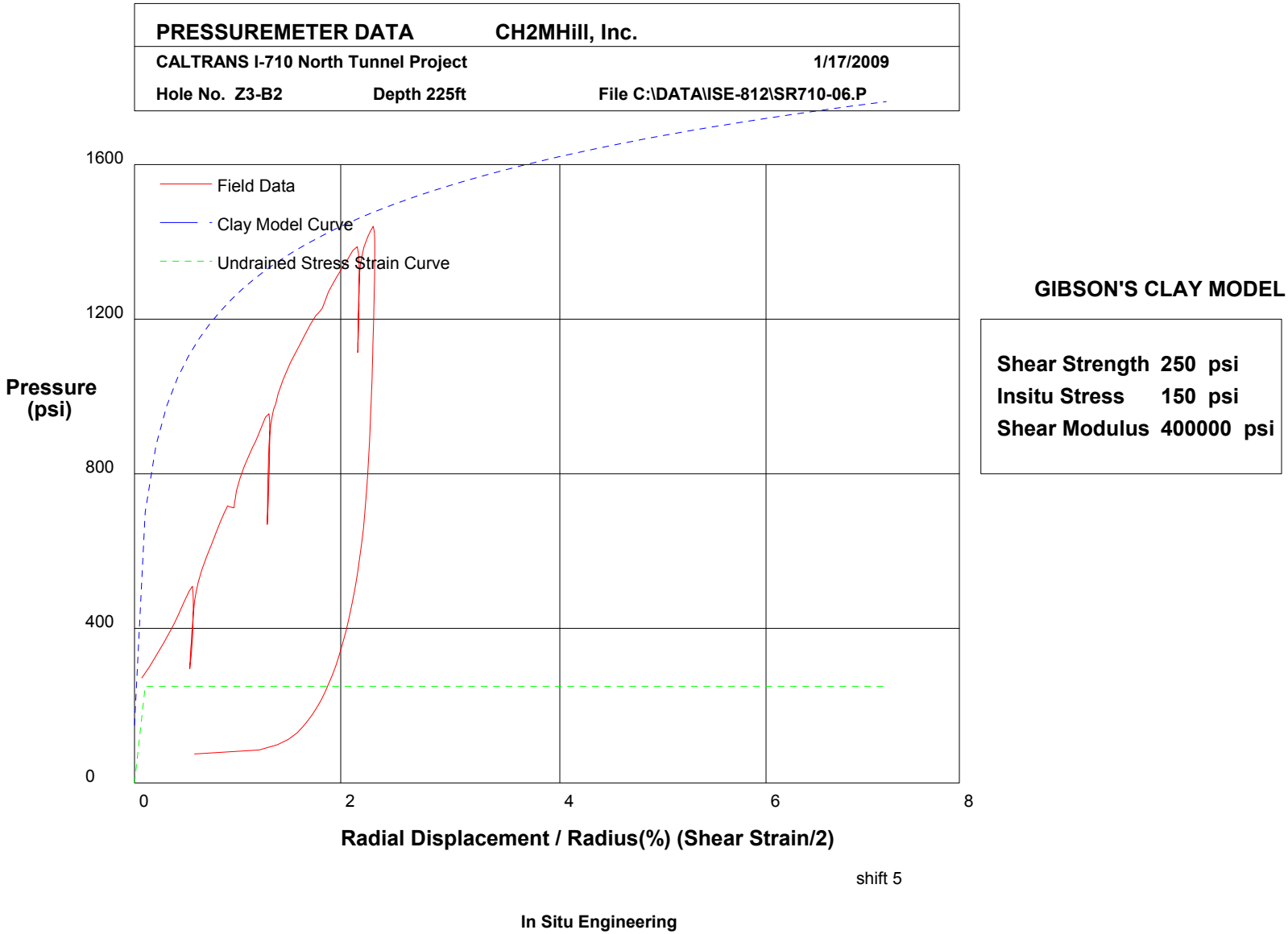

Appendix II - Pressuremeter Model Interpretation

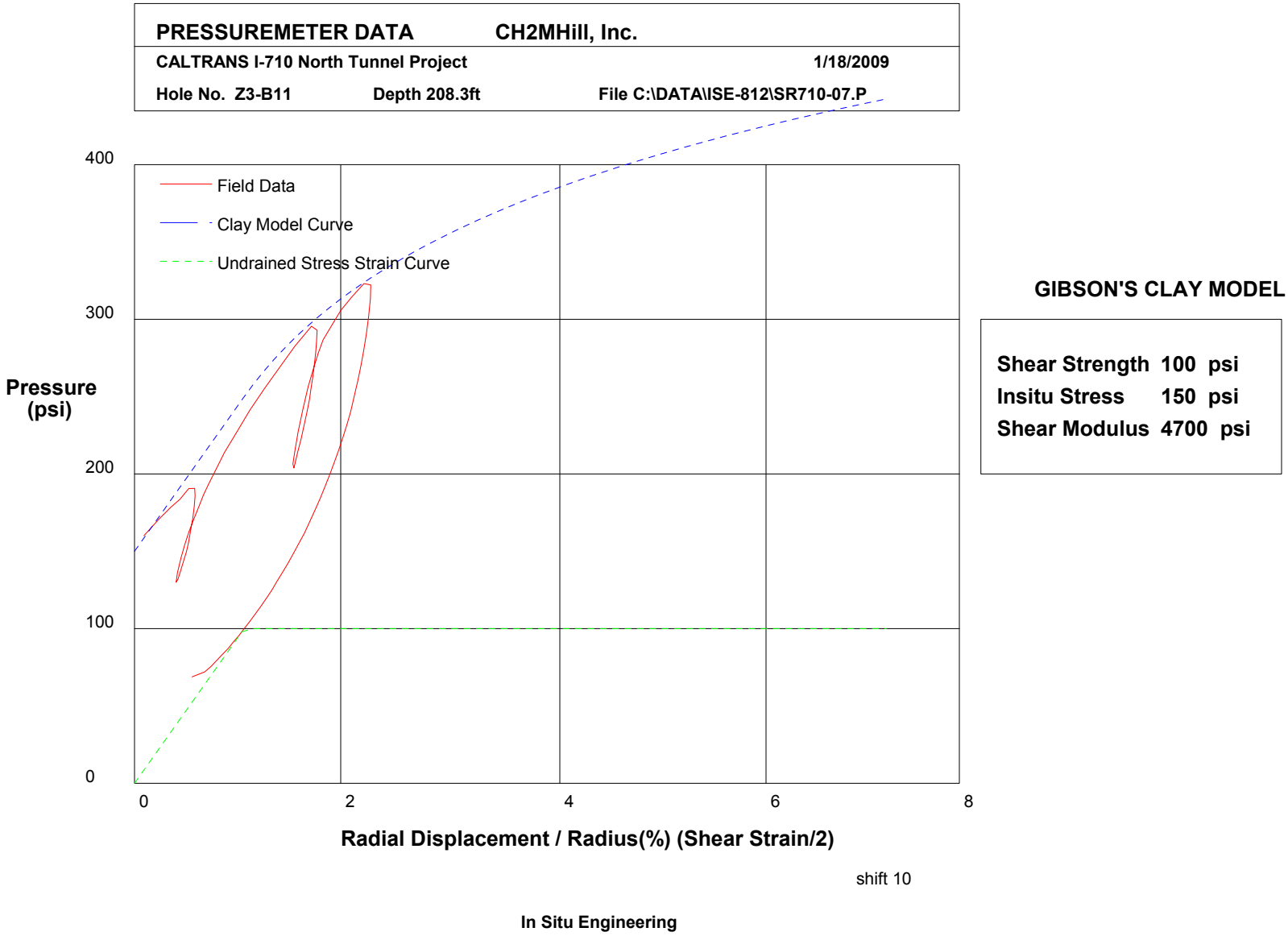

Appendix II - Pressuremeter Model Interpretation

PRESSUREMETER DATA **CH2MHill, Inc.**

CALTRANS I-710 North Tunnel Project **1/18/2009**

Hole No. Z3-B11 **Depth 208.3ft** **File C:\DATA\ISE-812\SR710-07.P**

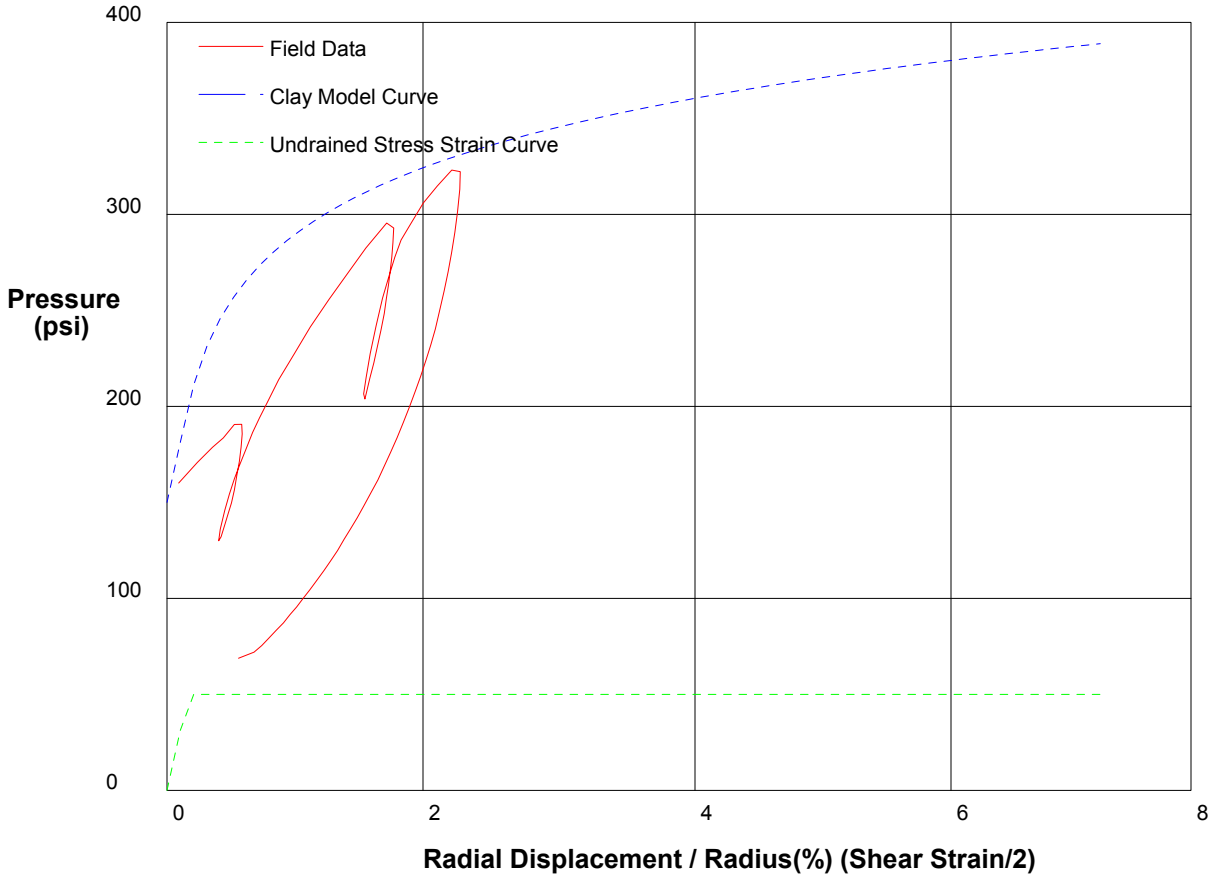

GIBSON'S CLAY MODEL

Shear Strength	**50 psi**
Insitu Stress	**150 psi**
Shear Modulus	**15000 psi**

shift 10

In Situ Engineering

Appendix II - Pressuremeter Model Interpretation

PRESSUREMETER DATA **CH2MHill, Inc.**

CALTRANS I-710 North Tunnel Project **1/18/2009**

Hole No. Z3-B11 **Depth 206.9ft** **File C:\DATA\ISE-812\SR710-08.P**

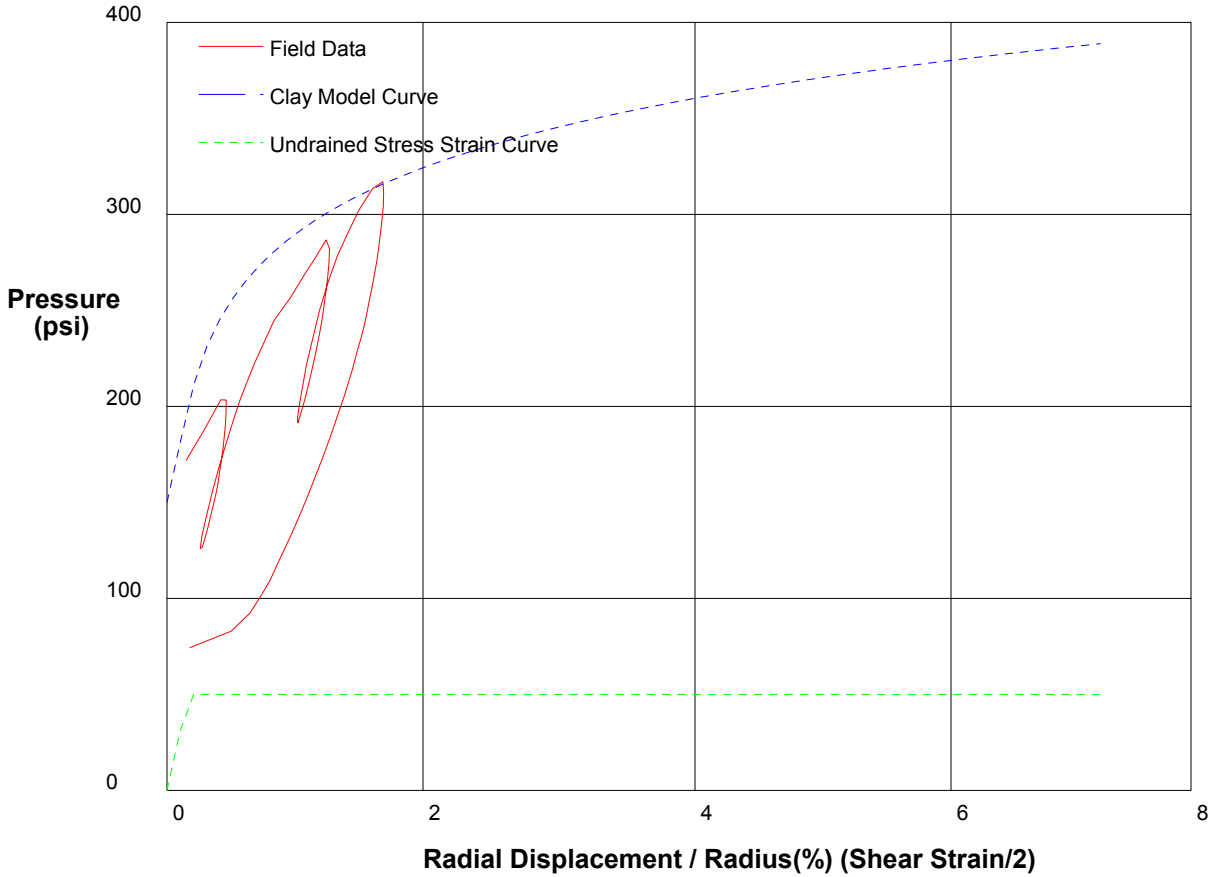

GIBSON'S CLAY MODEL

Shear Strength 50 psi
Insitu Stress 150 psi
Shear Modulus 15000 psi

shift 11

In Situ Engineering

Appendix II - Pressuremeter Model Interpretation

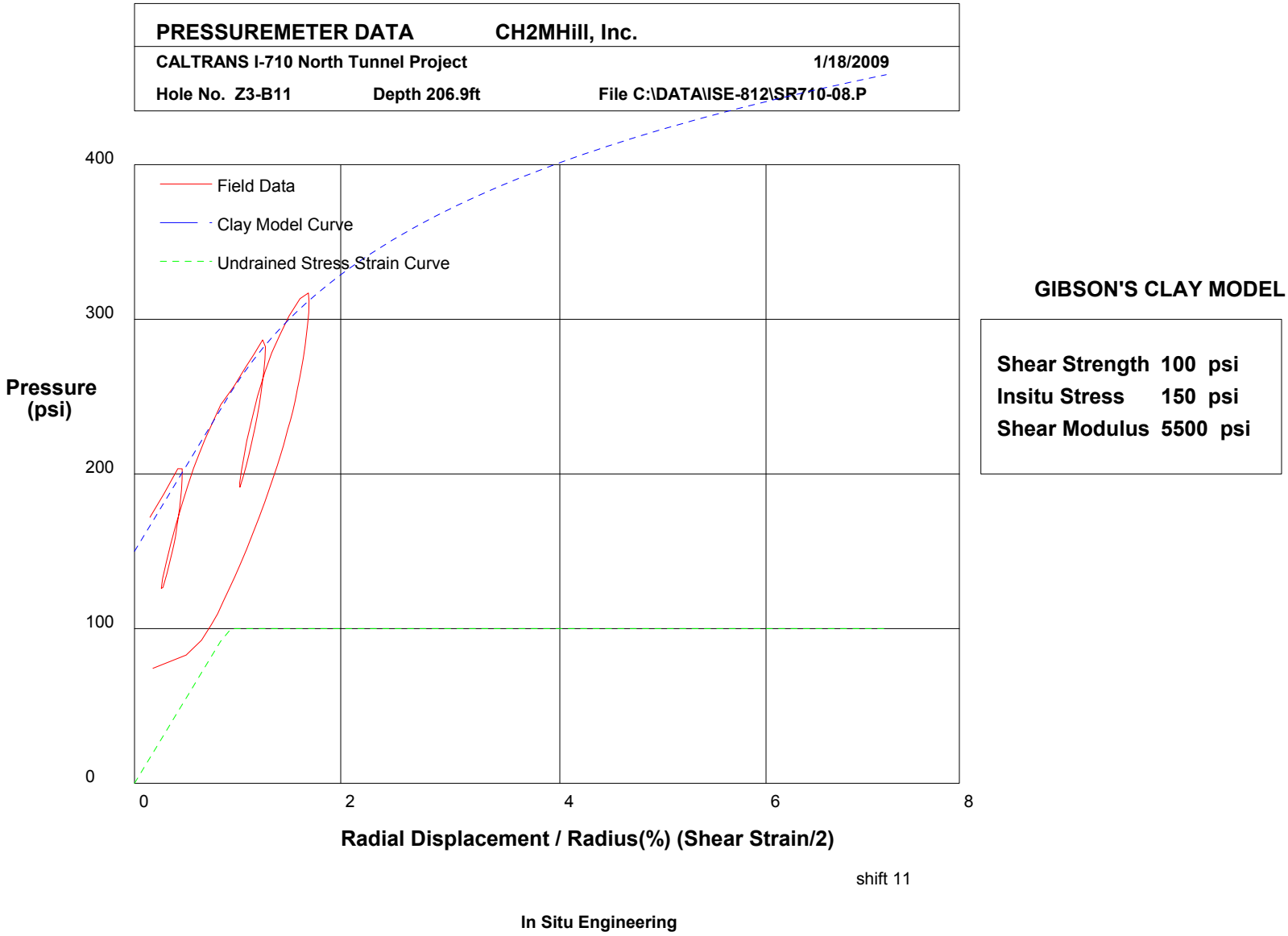

Appendix II - Pressuremeter Model Interpretation

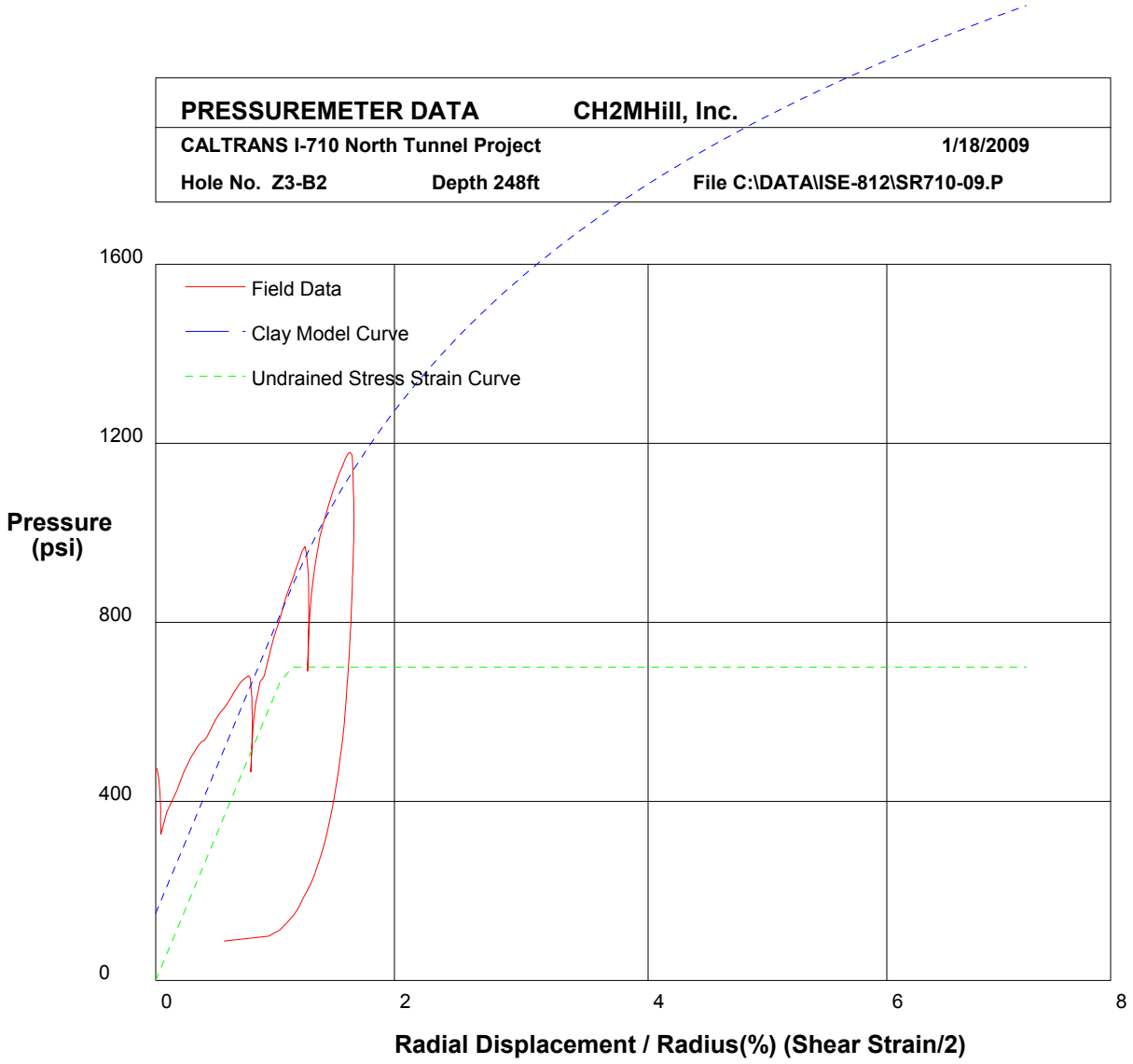

GIBSON'S CLAY MODEL

Shear Strength	**700 psi**
Insitu Stress	**150 psi**
Shear Modulus	**32000 psi**

Appendix II - Pressuremeter Model Interpretation

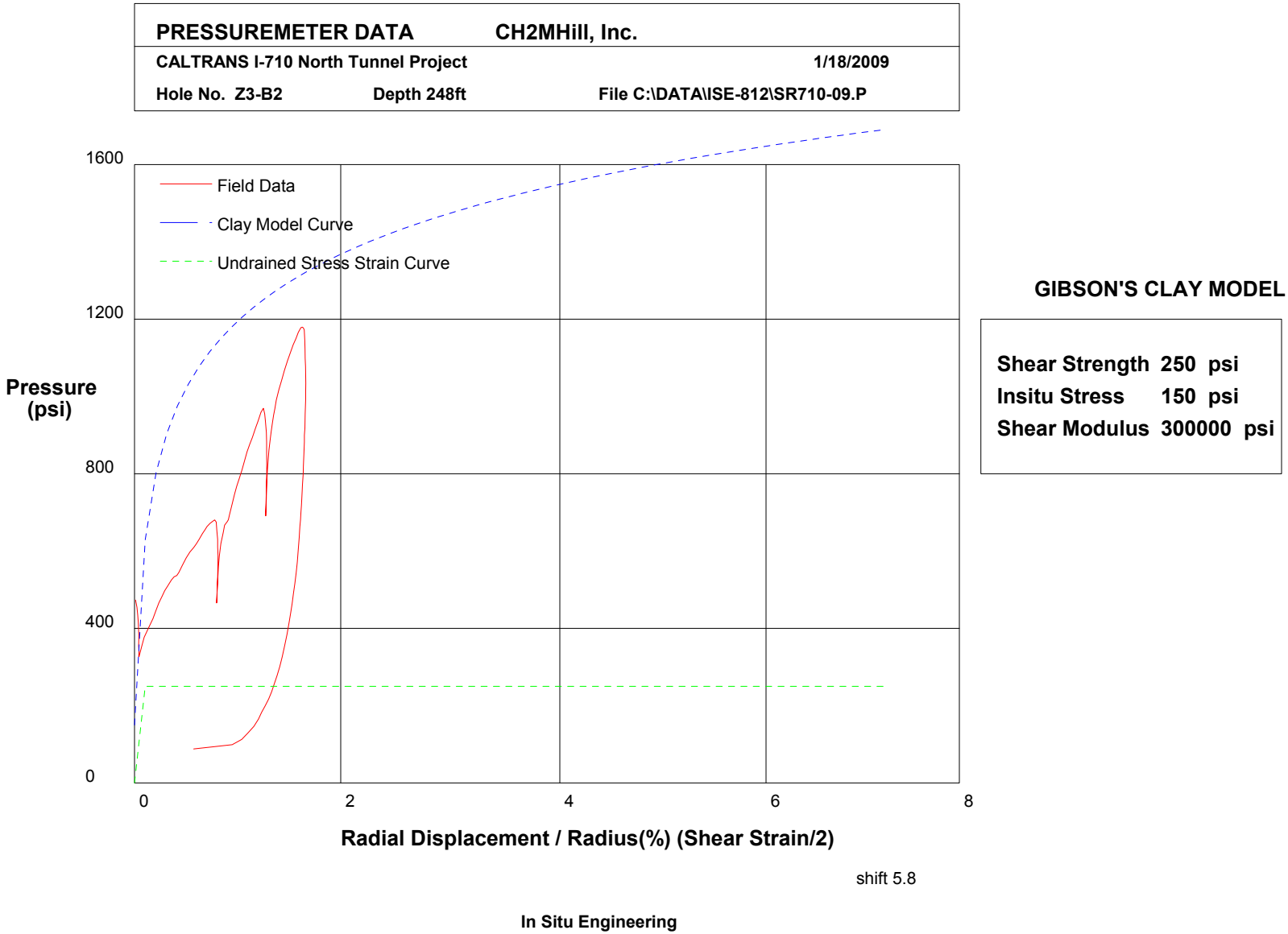

Appendix II - Pressuremeter Model Interpretation

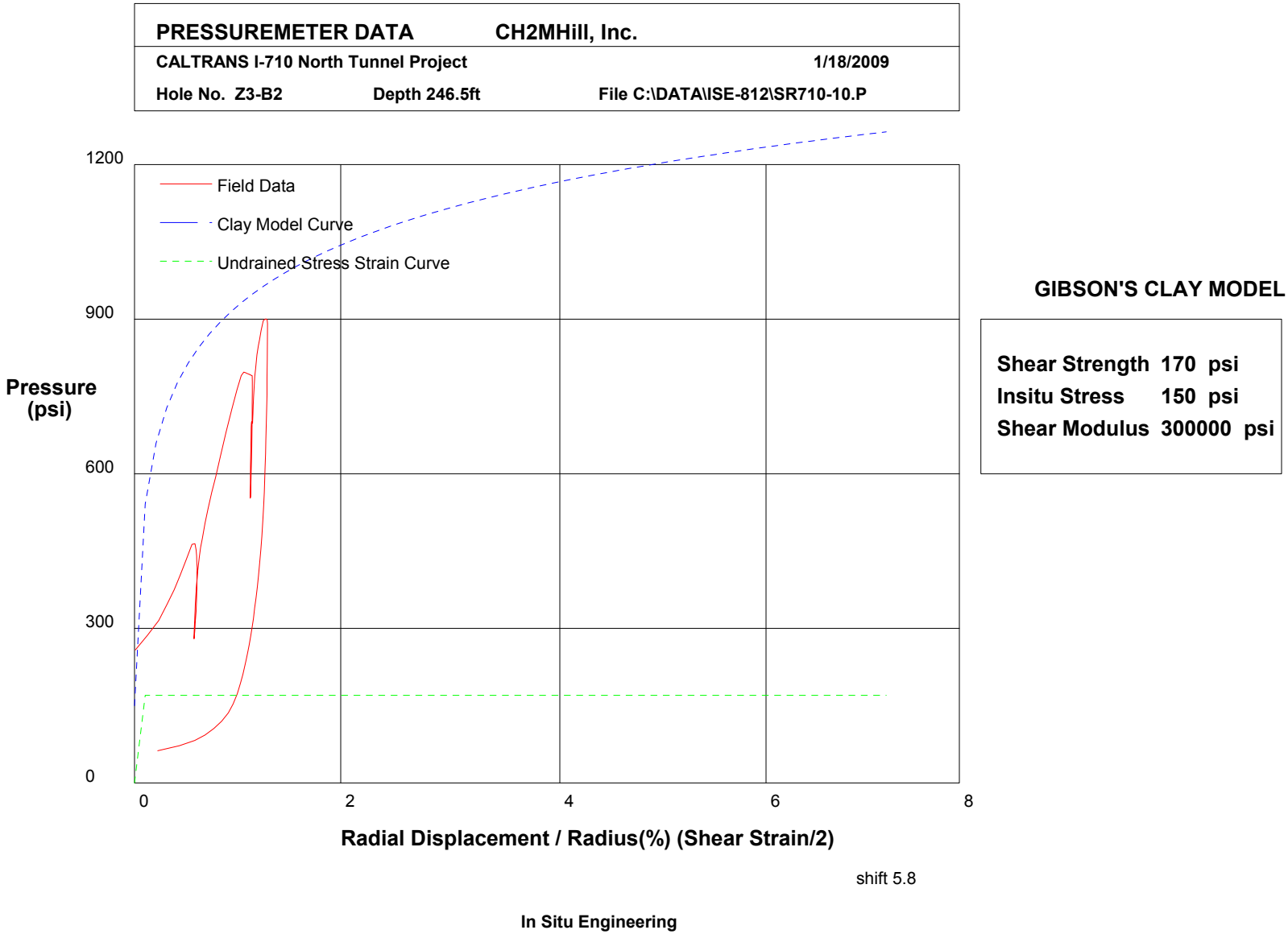

Appendix II - Pressuremeter Model Interpretation

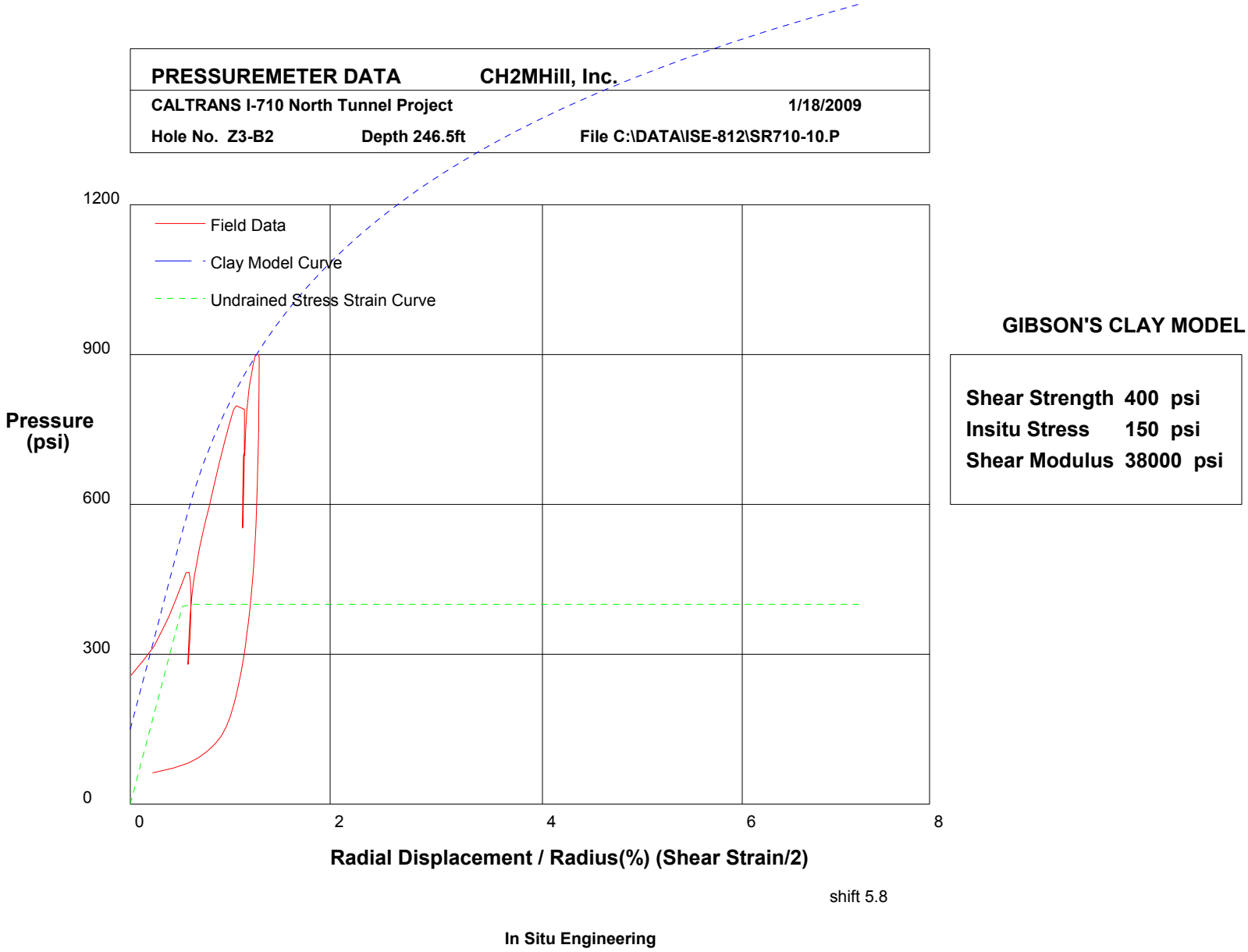

Appendix II - Pressuremeter Model Interpretation

PRESSUREMETER DATA **CH2MHill, Inc.**

CALTRANS I-710 North Tunnel Project **1/19/2009**

Hole No. Z2-B1 **Depth 129ft** **File C:\DATA\ISE-812\SR710-11.P**

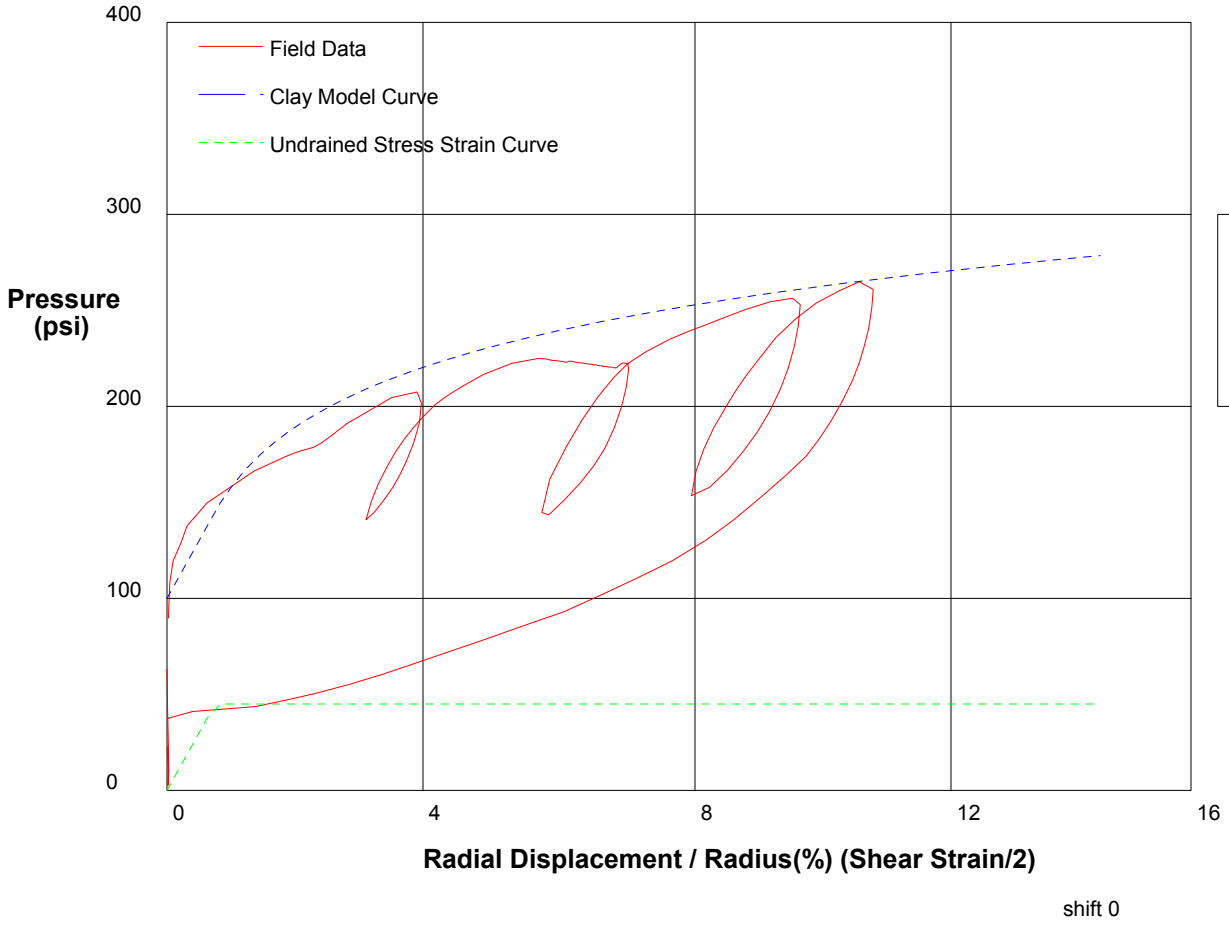

GIBSON'S CLAY MODEL

Shear Strength	**45 psi**
Insitu Stress	**100 psi**
Shear Modulus	**3000 psi**

shift 0

In Situ Engineering

Appendix II - Pressuremeter Model Interpretation

PRESSUREMETER DATA **CH2MHill, Inc.**

CALTRANS I-710 North Tunnel Project **1/19/2009**

Hole No. Z2-B1 **Depth 127.5ft** **File C:\DATA\ISE-812\SR710-12.P**

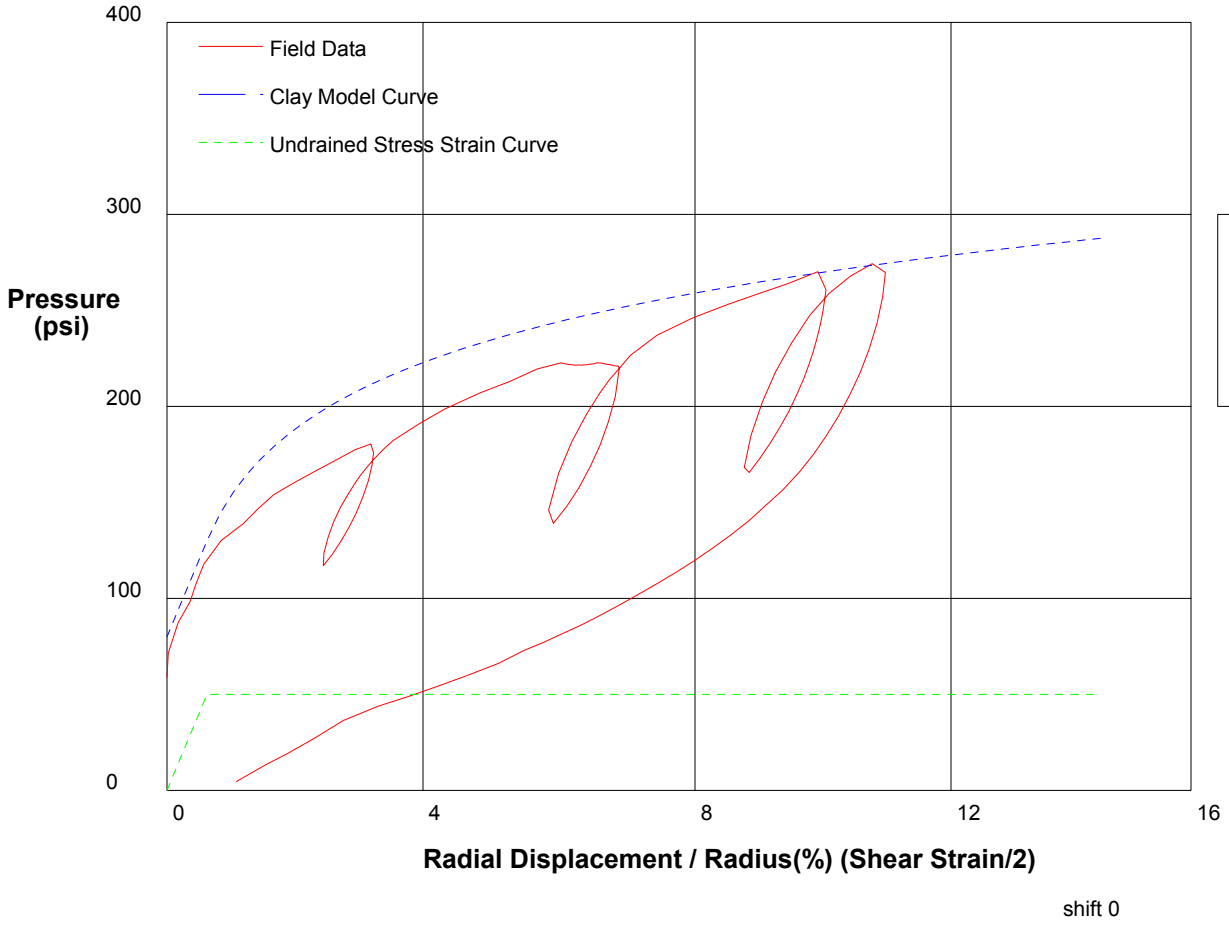

GIBSON'S CLAY MODEL

Shear Strength 50 psi
Insitu Stress 80 psi
Shear Modulus 4000 psi

shift 0

In Situ Engineering

Appendix II - Pressuremeter Model Interpretation

PRESSUREMETER DATA **CH2MHill, Inc.**

CALTRANS I-710 North Tunnel Project **1/20/2009**

Hole No. Z2-B1 **Depth 140ft** **File C:\DATA\ISE-812\SR710-13.P**

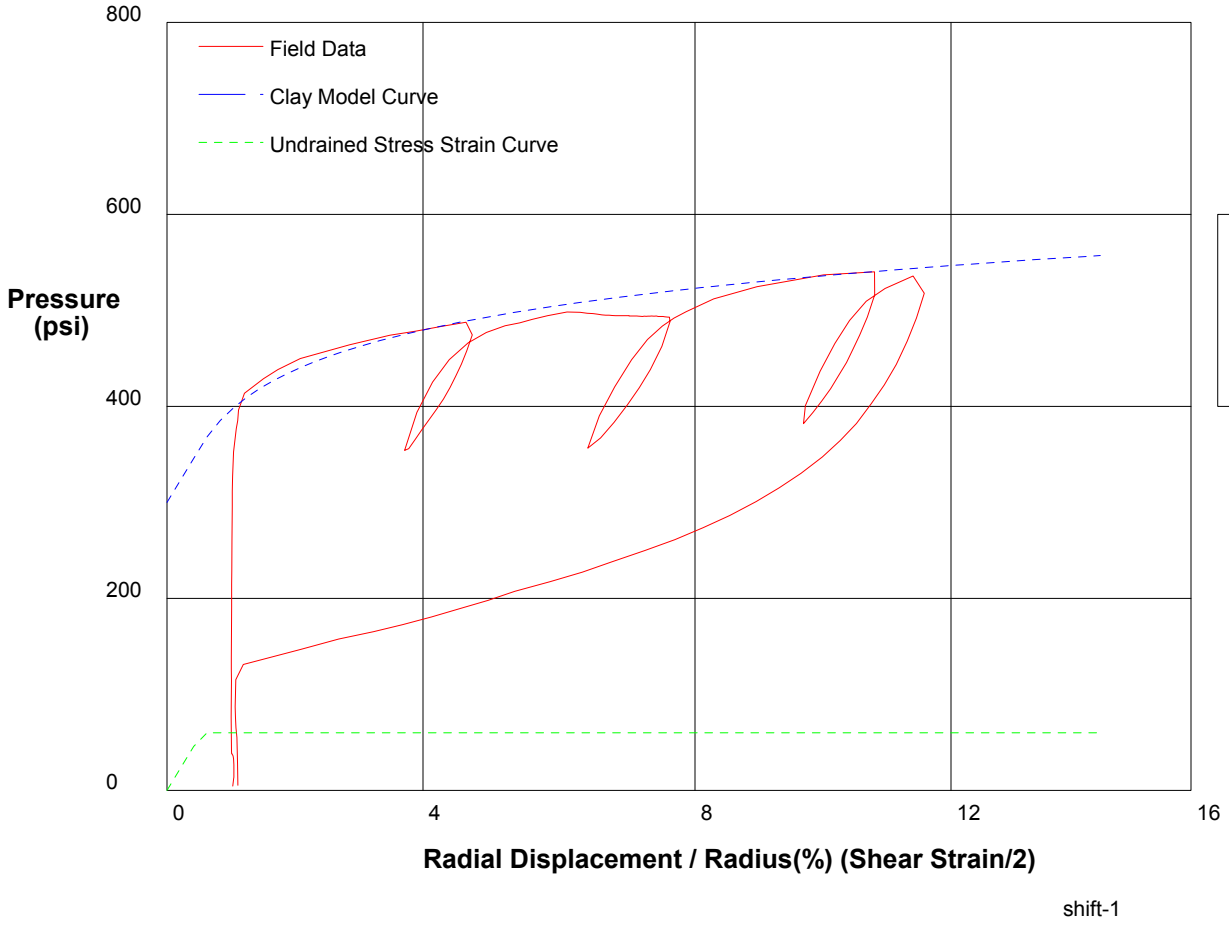

GIBSON'S CLAY MODEL

Shear Strength 60 psi
Insitu Stress 300 psi
Shear Modulus 5500 psi

shift-1

In Situ Engineering

Appendix II - Pressuremeter Model Interpretation

PRESSUREMETER DATA **CH2MHill, Inc.**

CALTRANS I-710 North Tunnel Project **1/20/2009**

Hole No. Z2-B1 **Depth 138.5ft** **File C:\DATA\ISE-812\SR710-14.P**

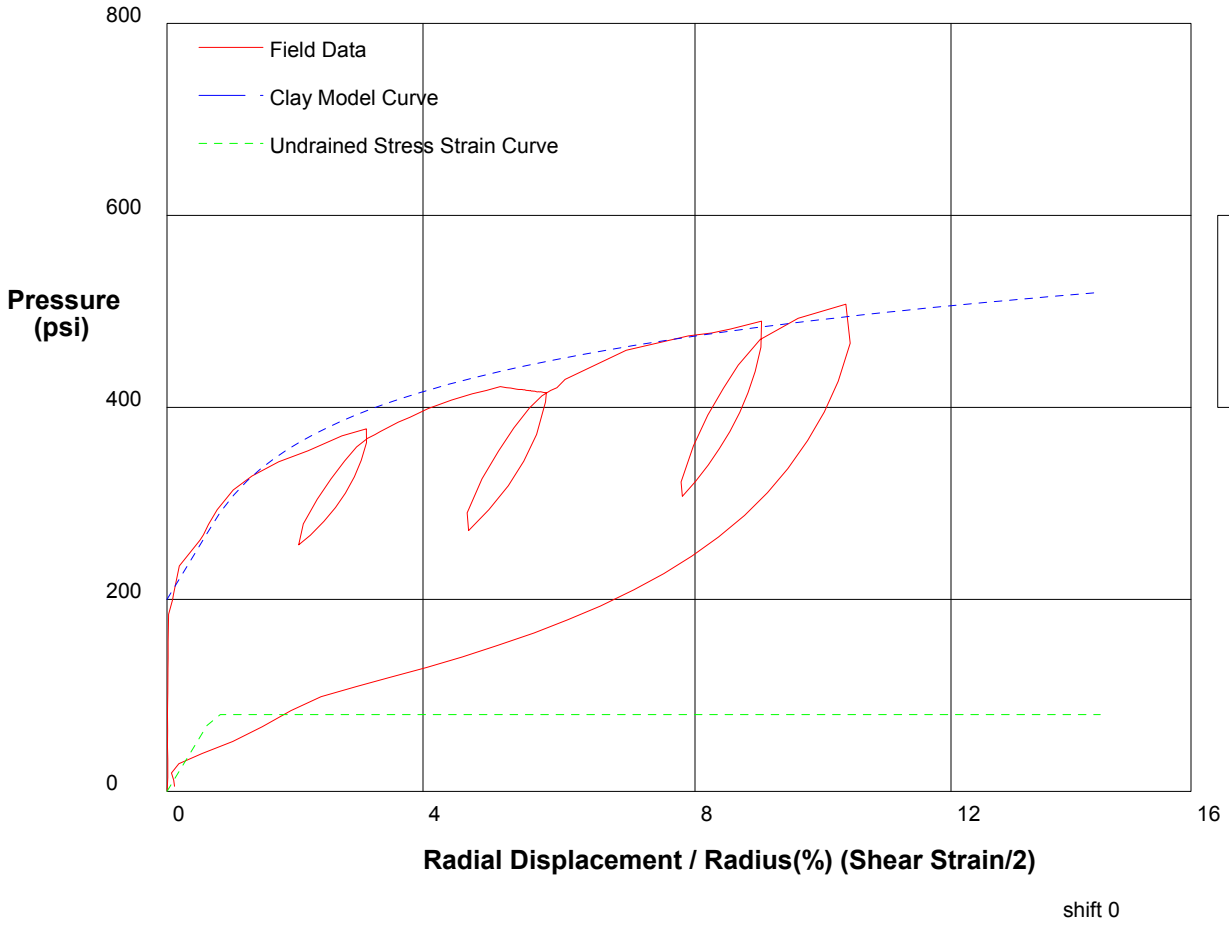

GIBSON'S CLAY MODEL

Shear Strength 80 psi
Insitu Stress 200 psi
Shear Modulus 5500 psi

shift 0

In Situ Engineering

Appendix II - Pressuremeter Model Interpretation

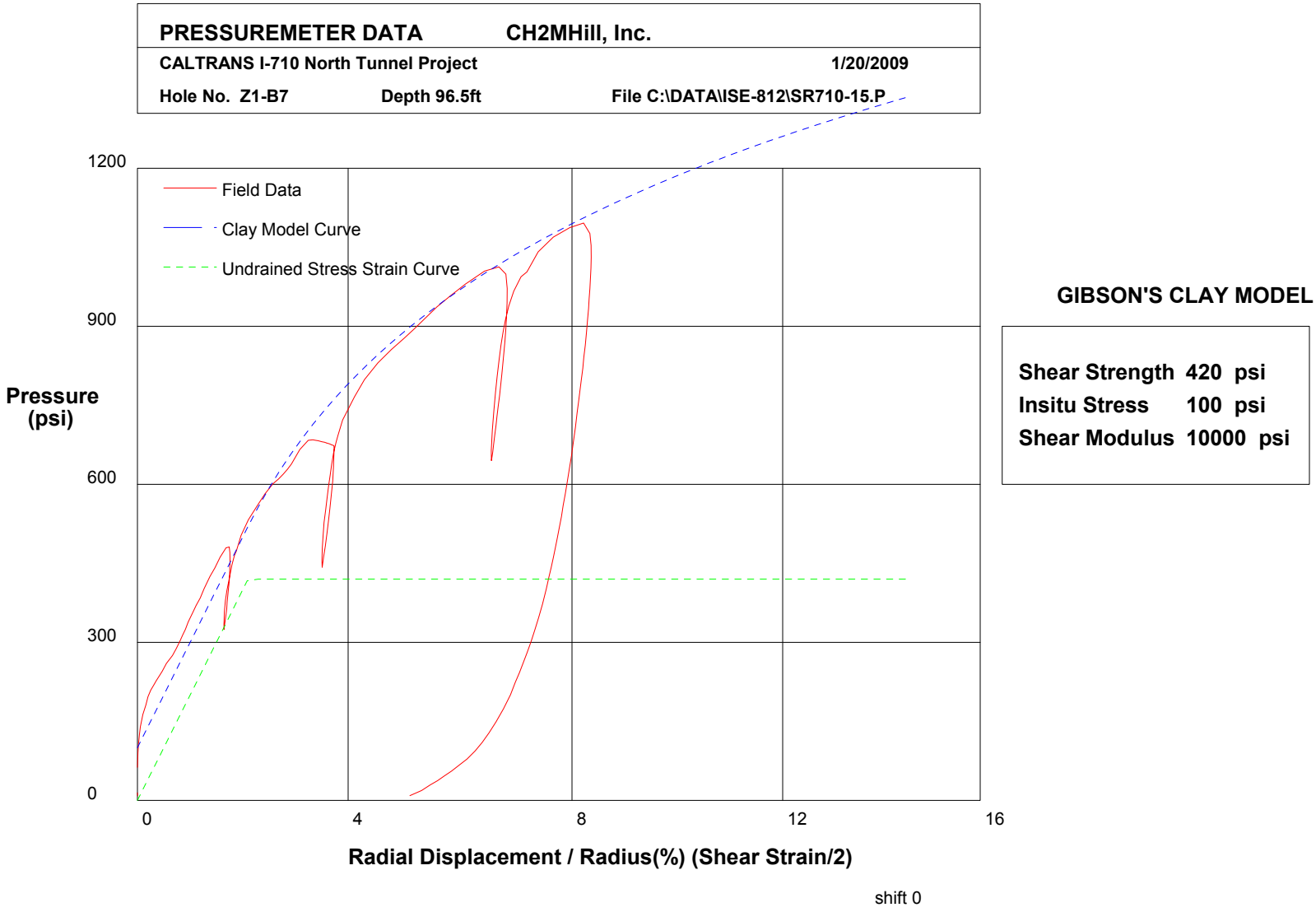

Appendix II - Pressuremeter Model Interpretation

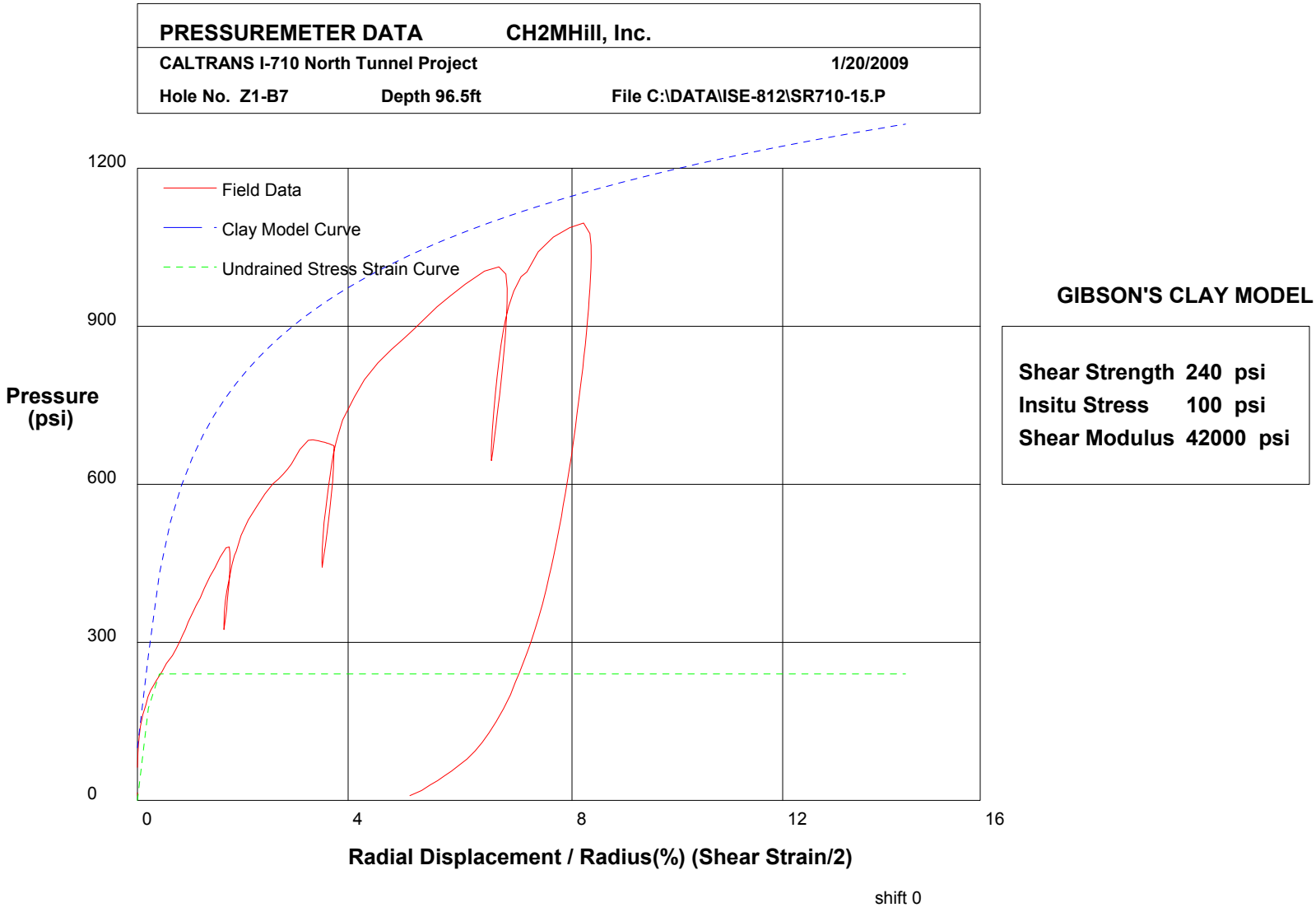

Appendix II - Pressuremeter Model Interpretation

PRESSUREMETER DATA **CH2MHill, Inc.**

CALTRANS I-710 North Tunnel Project **1/20/2009**

Hole No. Z1-B7 **Depth 95ft** **File C:\DATA\ISE-812\SR710-16.P**

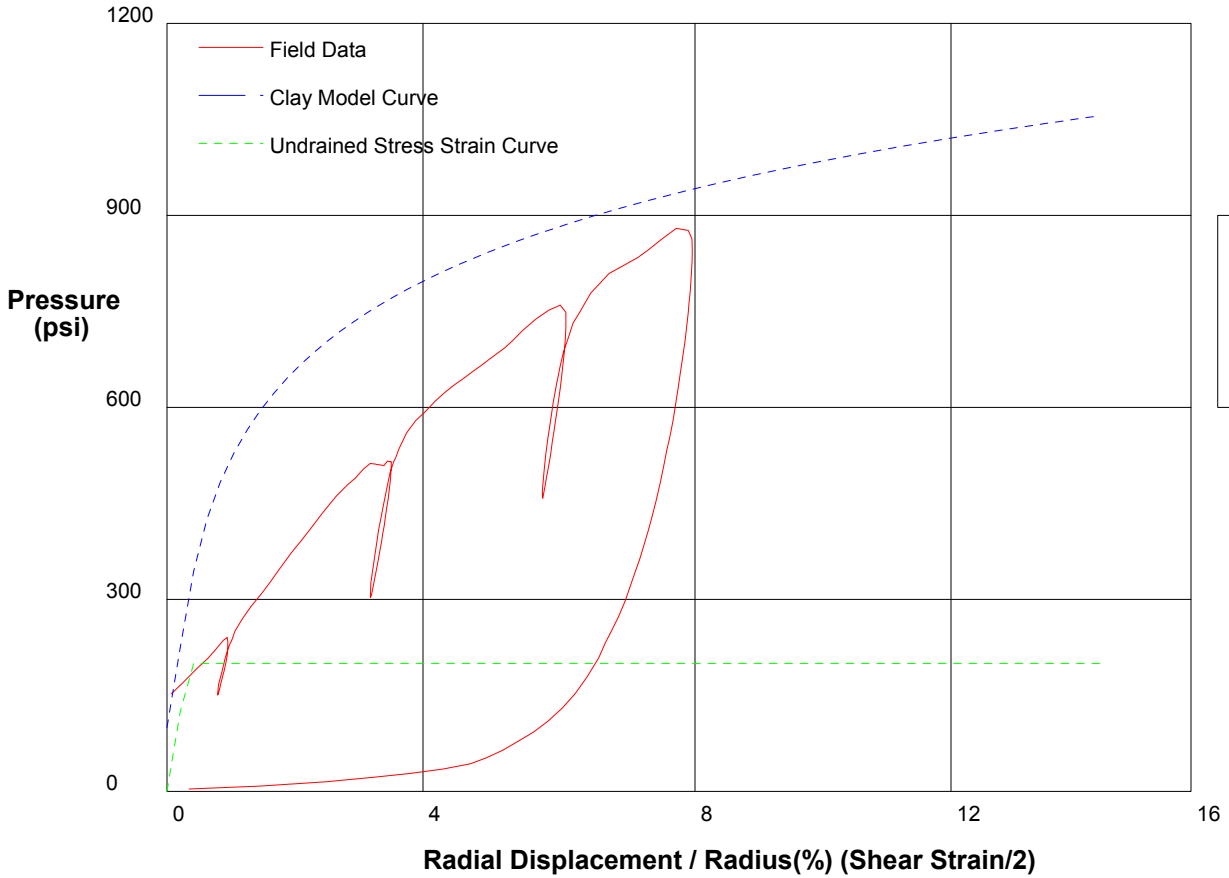

GIBSON'S CLAY MODEL

Shear Strength 200 psi
Insitu Stress 100 psi
Shear Modulus 30000 psi

shift 2

In Situ Engineering

Appendix II - Pressuremeter Model Interpretation

PRESSUREMETER DATA **CH2MHill, Inc.**

CALTRANS I-710 North Tunnel Project **1/20/2009**

Hole No. Z1-B7 **Depth 95ft** **File C:\DATA\ISE-812\SR710-16.P**

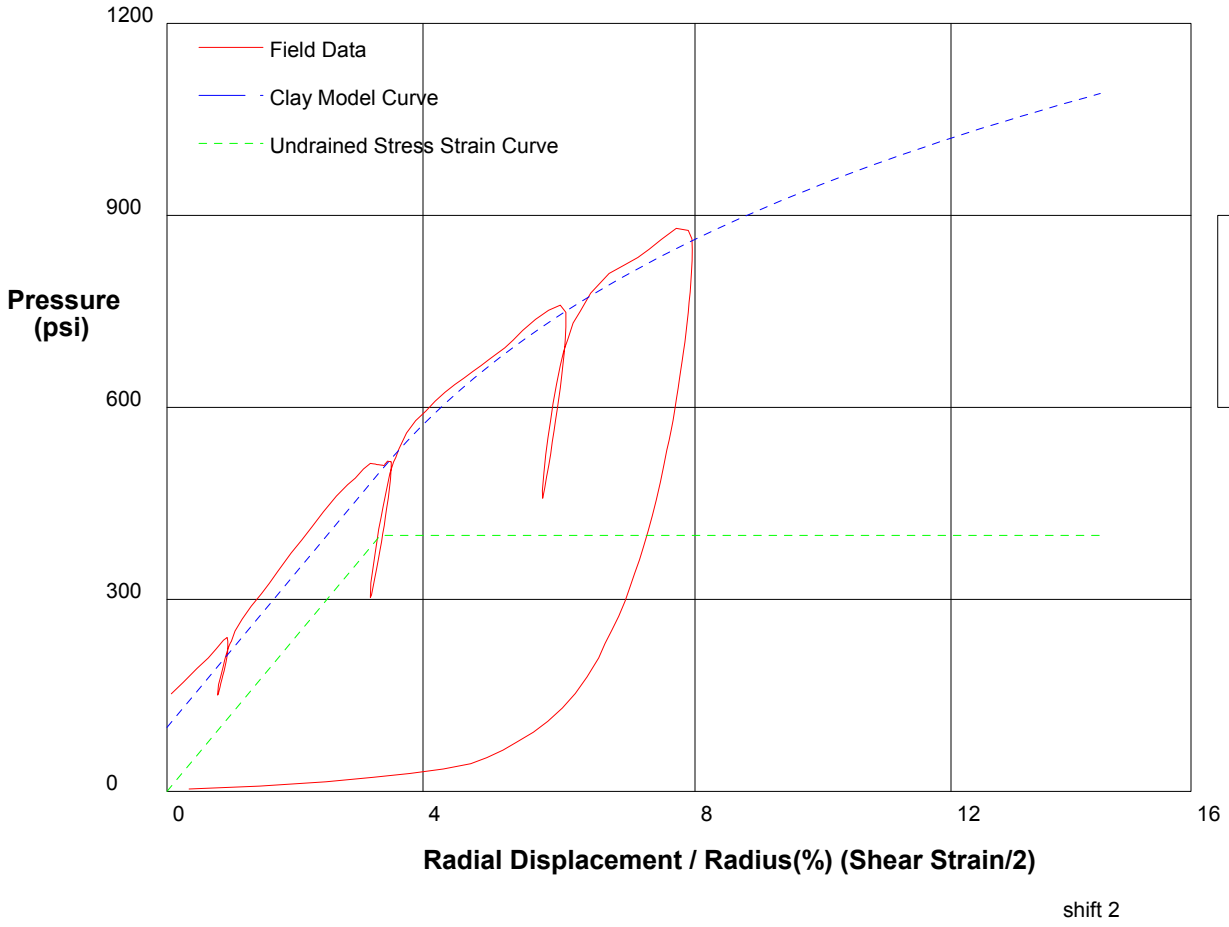

GIBSON'S CLAY MODEL

Shear Strength	**400 psi**
Insitu Stress	**100 psi**
Shear Modulus	**6000 psi**

shift 2

In Situ Engineering

Appendix II - Pressuremeter Model Interpretation

PRESSUREMETER DATA **CH2MHill, Inc.**

CALTRANS I-710 North Tunnel Project **1/20/2009**

Hole No. Z1-B7 **Depth 95ft** **File C:\DATA\ISE-812\SR710-16.P**

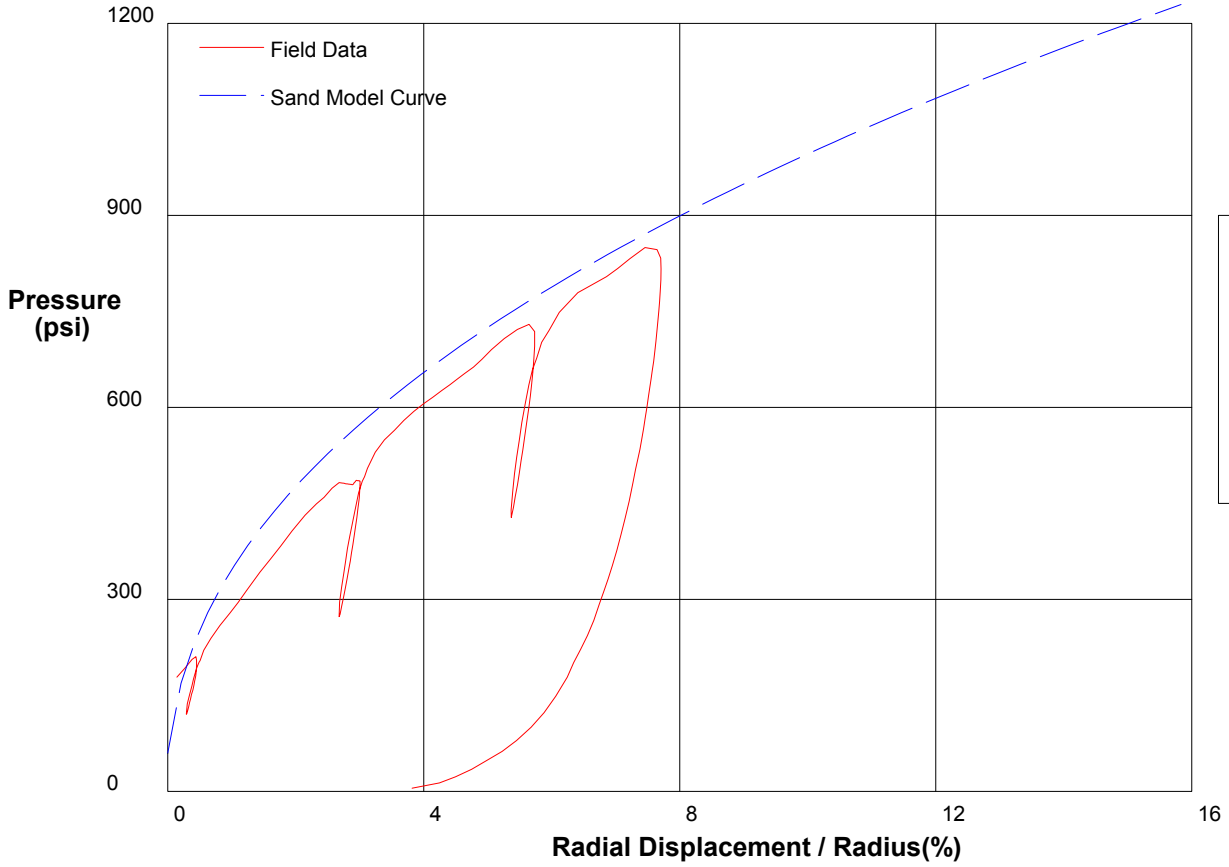

THE In Situ Engineering SAND MODEL

Water Pressure	**30 psi**
Friction Angle	**40 deg**
Critical Friction Angle	**32 deg**
Lateral Stress	**60 psi**
Shear Modulus	**30000 psi**

shift 2.5

In Situ Engineering

Appendix II - Pressuremeter Model Interpretation

PRESSUREMETER DATA **CH2MHill, Inc.**

CALTRANS I-710 North Tunnel Project **1/21/2009**

Hole No. Z1-B7 **Depth 111.5ft** **File C:\DATA\ISE-812\SR710-17.P**

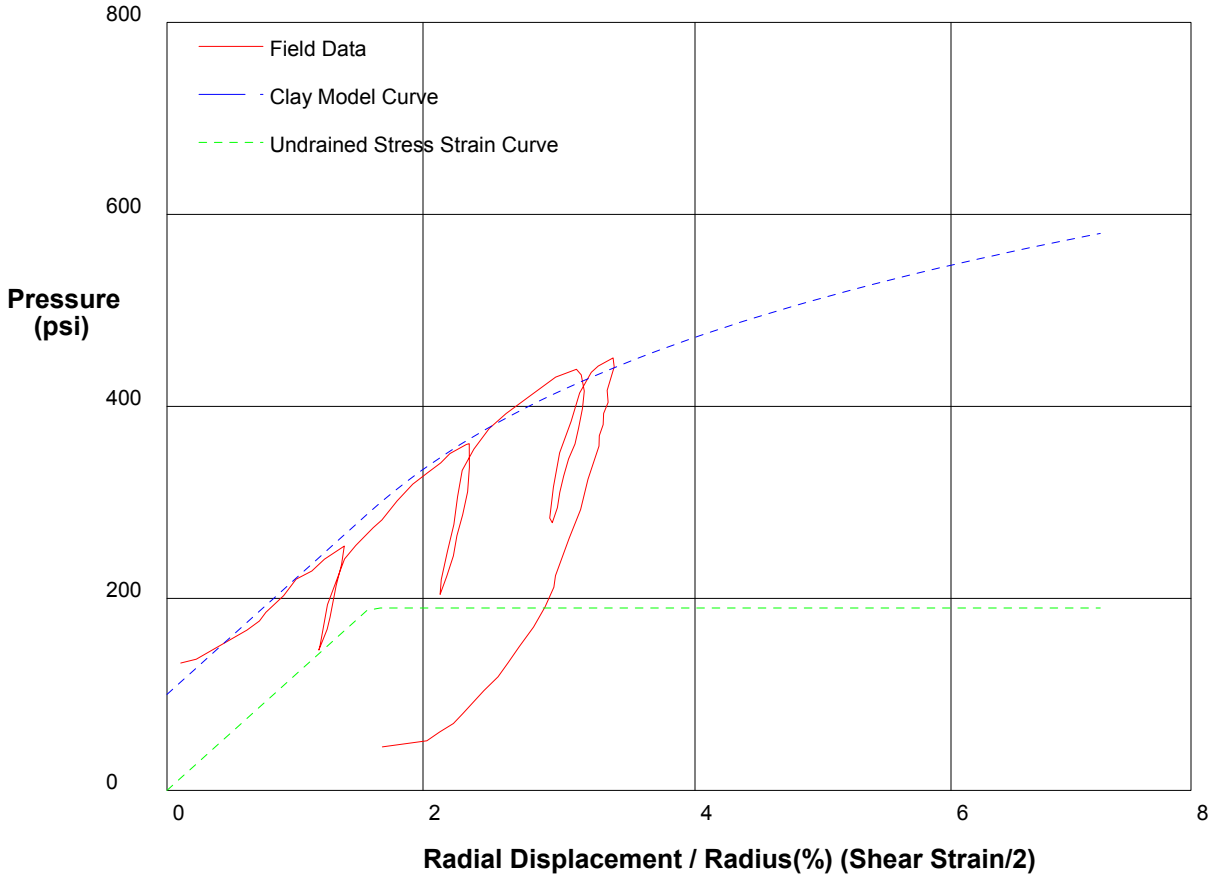

GIBSON'S CLAY MODEL

Shear Strength 190 psi
Insitu Stress 100 psi
Shear Modulus 6000 psi

shift 9.1

In Situ Engineering

Appendix II - Pressuremeter Model Interpretation

PRESSUREMETER DATA **CH2MHill, Inc.**

CALTRANS I-710 North Tunnel Project **1/21/2009**

Hole No. Z1-B7 **Depth 111.5ft** **File C:\DATA\ISE-812\SR710-17.P**

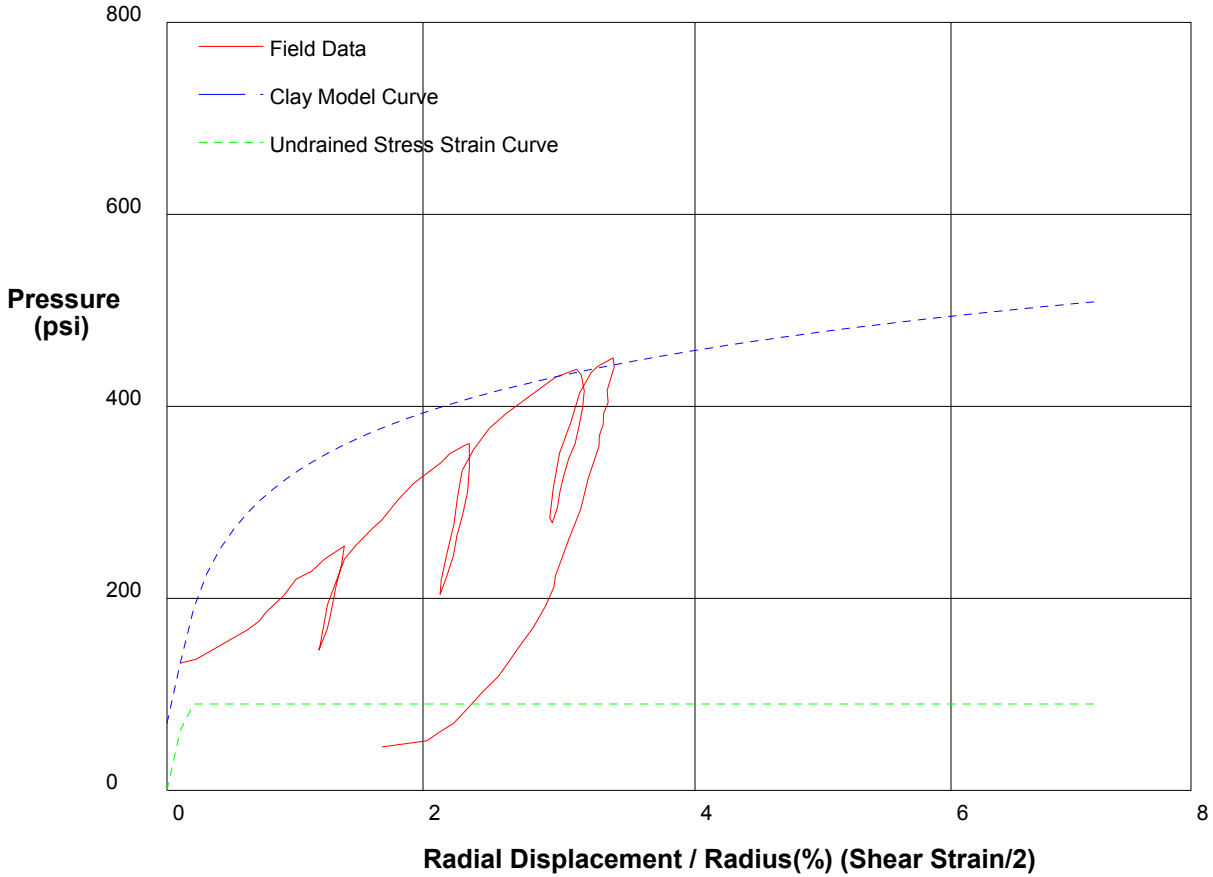

GIBSON'S CLAY MODEL

Shear Strength 90 psi
Insitu Stress 70 psi
Shear Modulus 30000 psi

shift 9.1

In Situ Engineering

Appendix II - Pressuremeter Model Interpretation

PRESSUREMETER DATA **CH2MHill, Inc.**

CALTRANS I-710 North Tunnel Project **1/21/2009**

Hole No. Z1-B7 **Depth 110ft** **File C:\DATA\ISE-812\SR710-18.P**

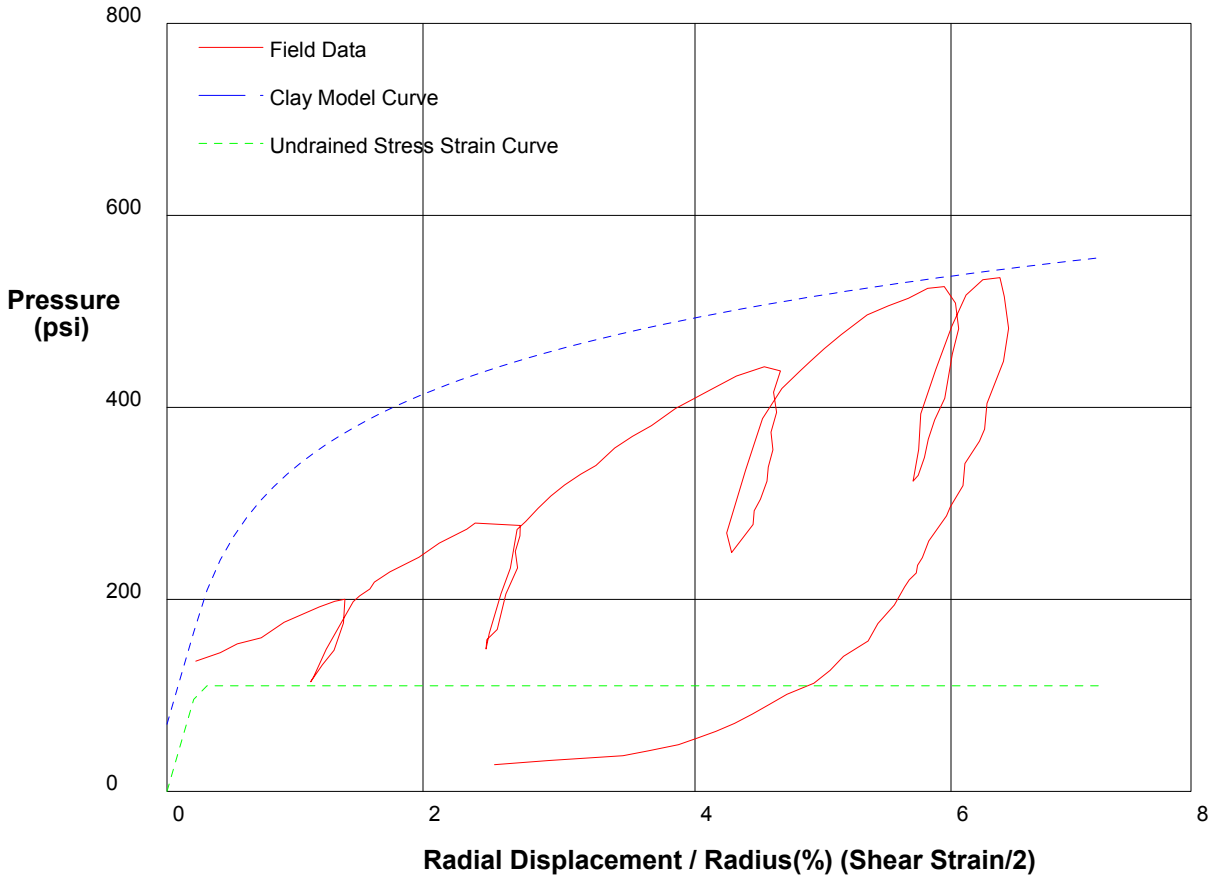

GIBSON'S CLAY MODEL

Shear Strength 110 psi
Insitu Stress 70 psi
Shear Modulus 23000 psi

shift 4.5

In Situ Engineering

Appendix II - Pressuremeter Model Interpretation

PRESSUREMETER DATA **CH2MHill, Inc.**

CALTRANS I-710 North Tunnel Project **1/21/2009**

Hole No. Z1-B7 **Depth 110ft** **File C:\DATA\ISE-812\SR710-18.P**

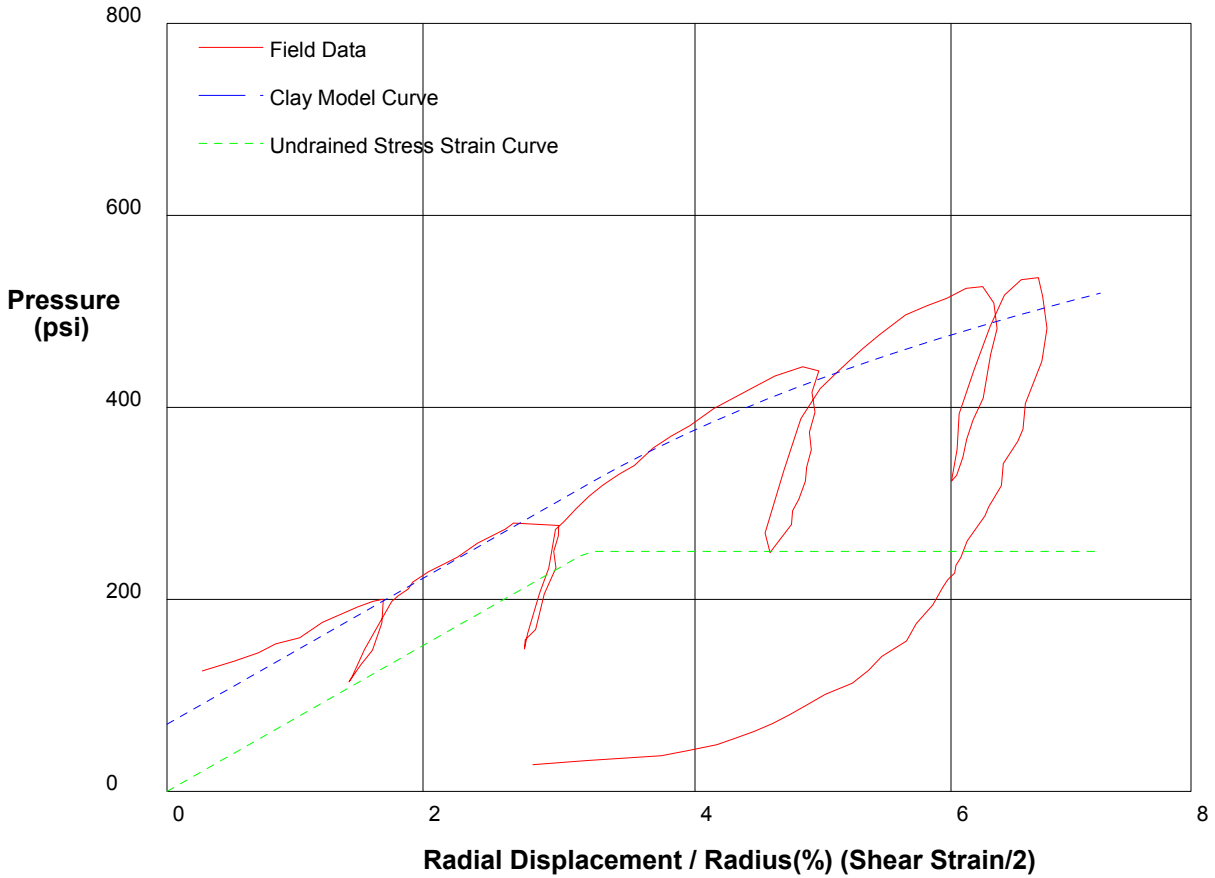

GIBSON'S CLAY MODEL

Shear Strength 250 psi
Insitu Stress 70 psi
Shear Modulus 3800 psi

shift 4.2

In Situ Engineering

Appendix II - Pressuremeter Model Interpretation

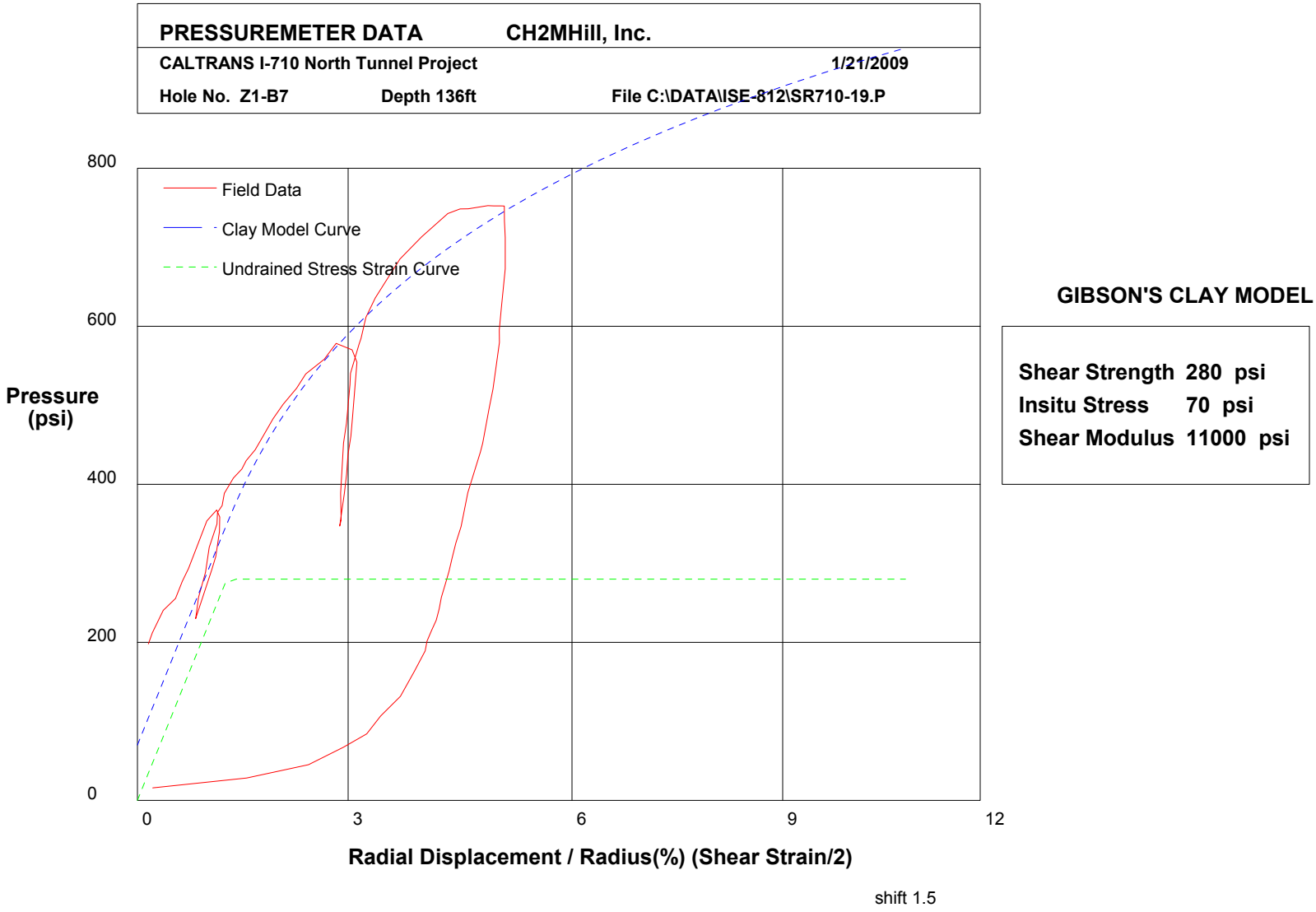

Appendix II - Pressuremeter Model Interpretation

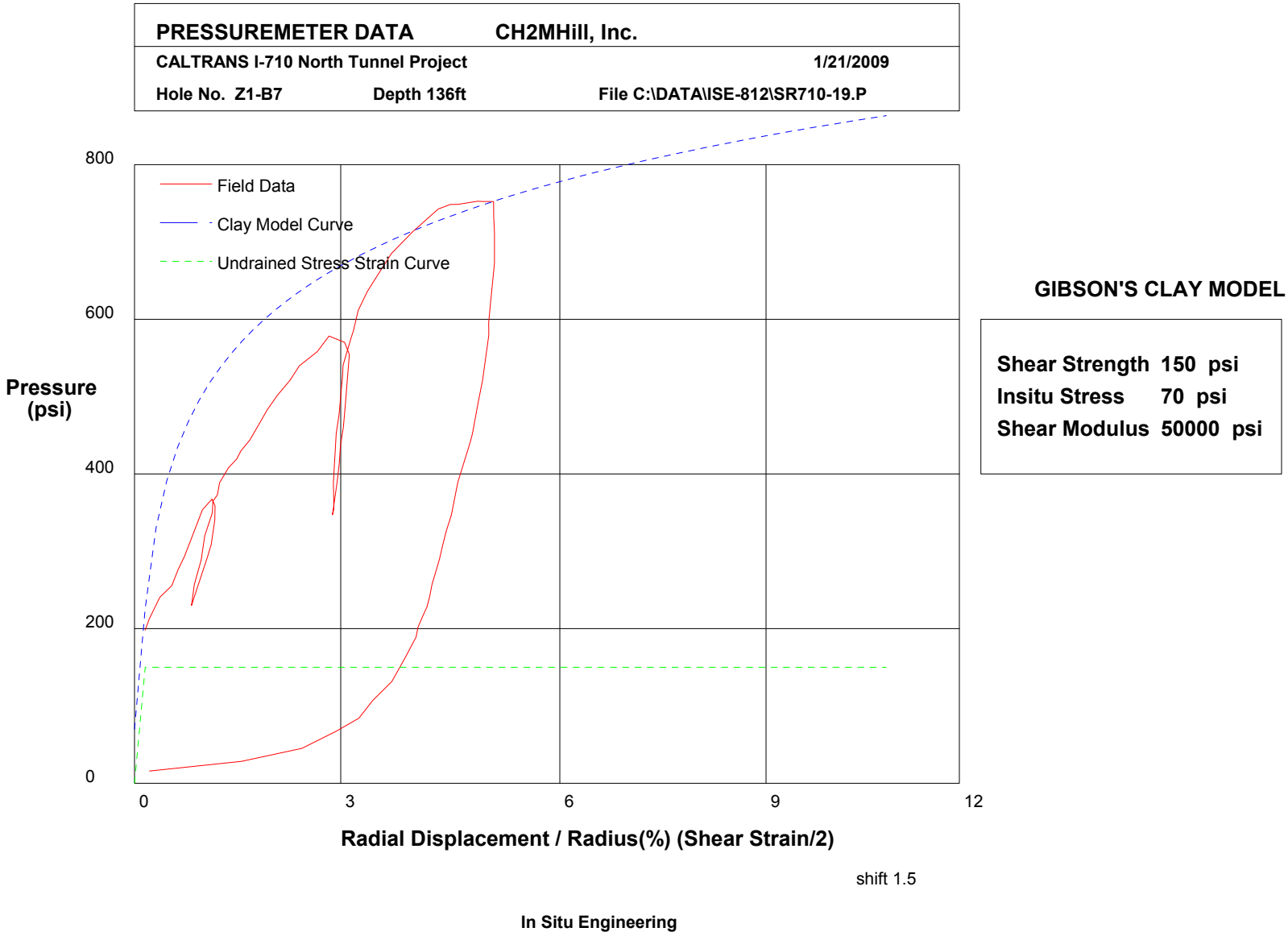

Appendix II - Pressuremeter Model Interpretation

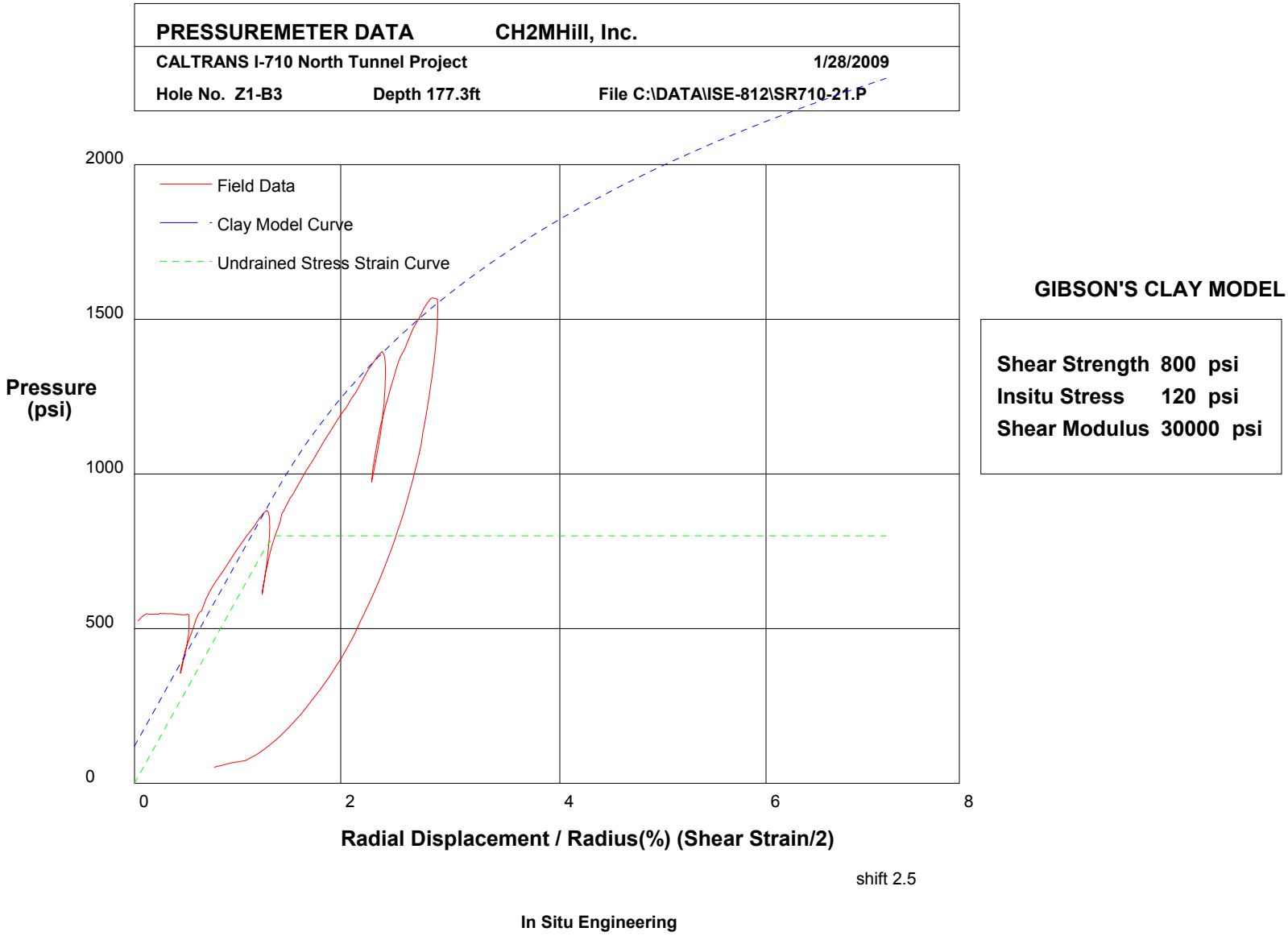

Appendix II - Pressuremeter Model Interpretation

PRESSUREMETER DATA **CH2MHill, Inc.**

CALTRANS I-710 North Tunnel Project **1/28/2009**

Hole No. Z1-B3 **Depth 177.3ft** **File C:\DATA\ISE-812\SR710-21.P**

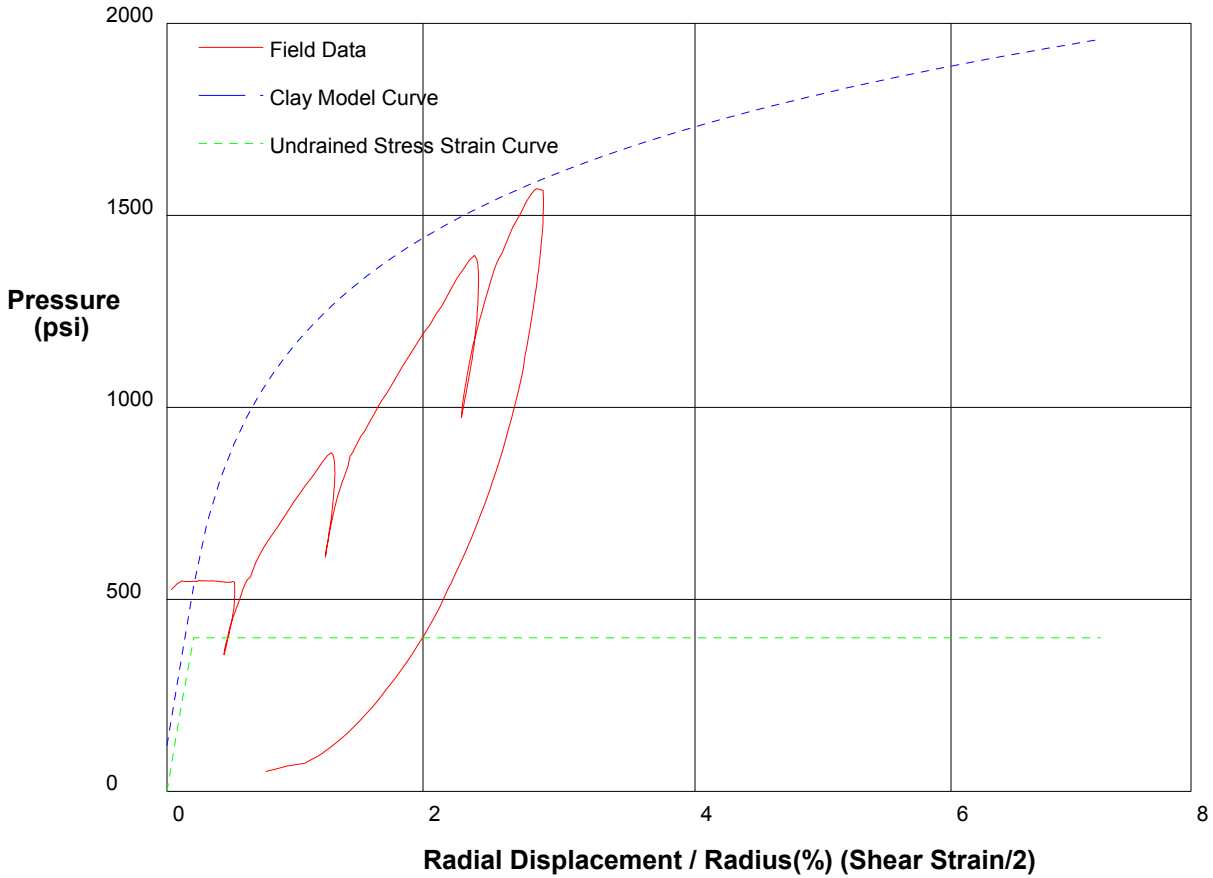

GIBSON'S CLAY MODEL

Shear Strength	**400 psi**
Insitu Stress	**120 psi**
Shear Modulus	**100000 psi**

shift 2.5

In Situ Engineering

Appendix II - Pressuremeter Model Interpretation

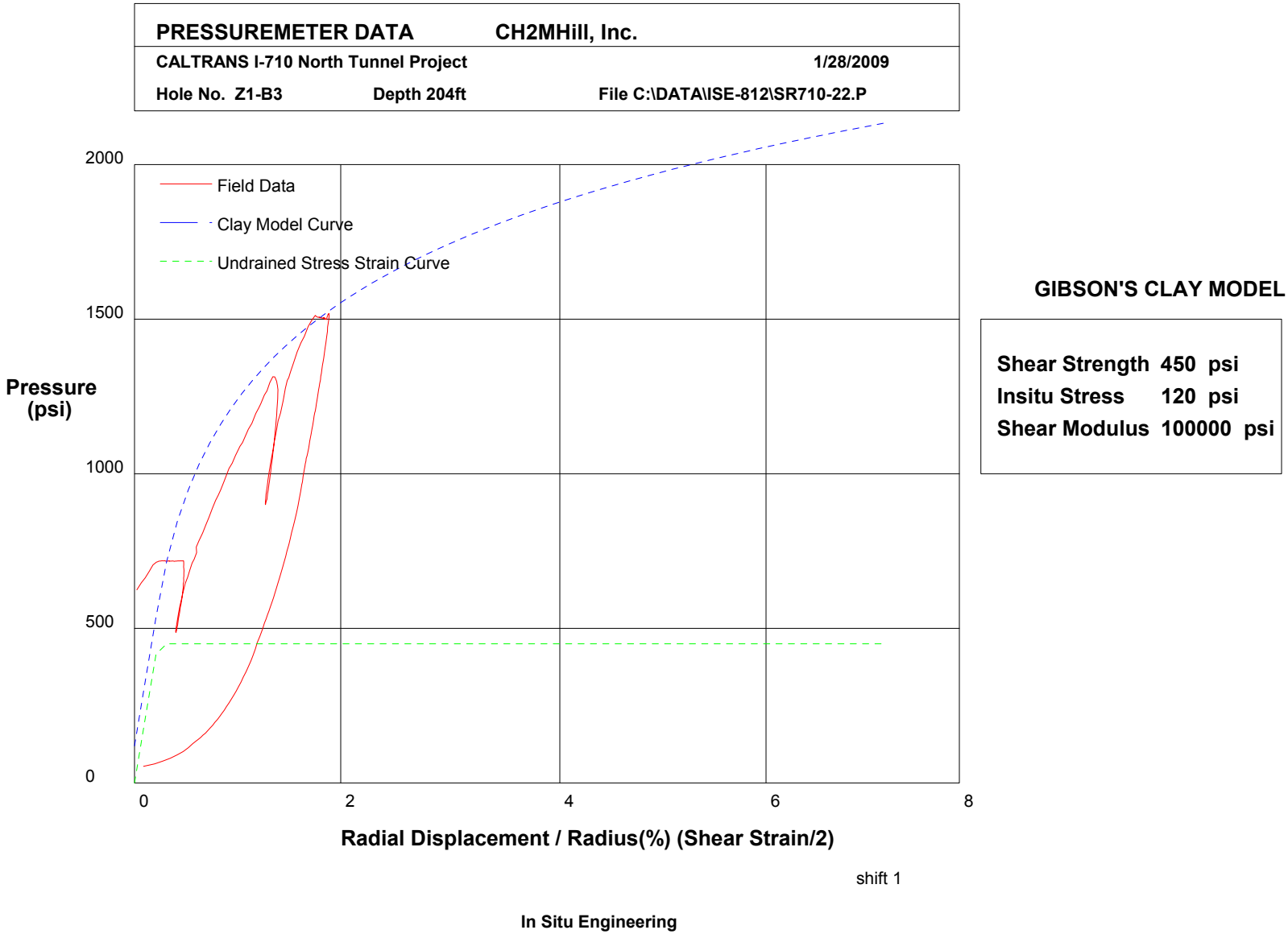

Appendix II - Pressuremeter Model Interpretation

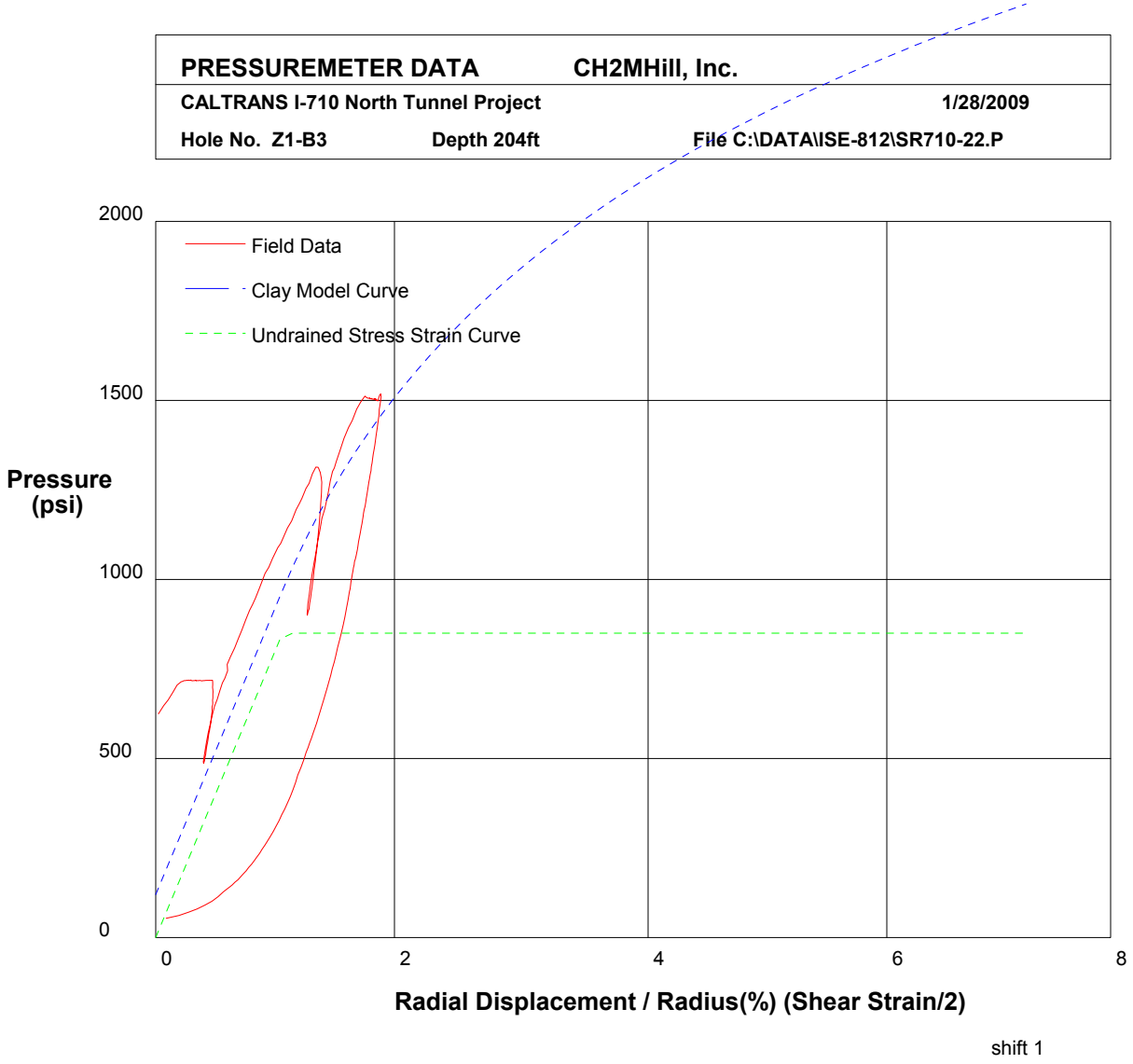

GIBSON'S CLAY MODEL

Shear Strength	**850 psi**
Insitu Stress	**120 psi**
Shear Modulus	**40000 psi**

Appendix II - Pressuremeter Model Interpretation

PRESSUREMETER DATA **CH2MHill, Inc.**

CALTRANS I-710 North Tunnel Project **1/29/2009**

Hole No. Z2-B2 **Depth 135.7ft** **File C:\DATA\ISE-812\SR710-23.P**

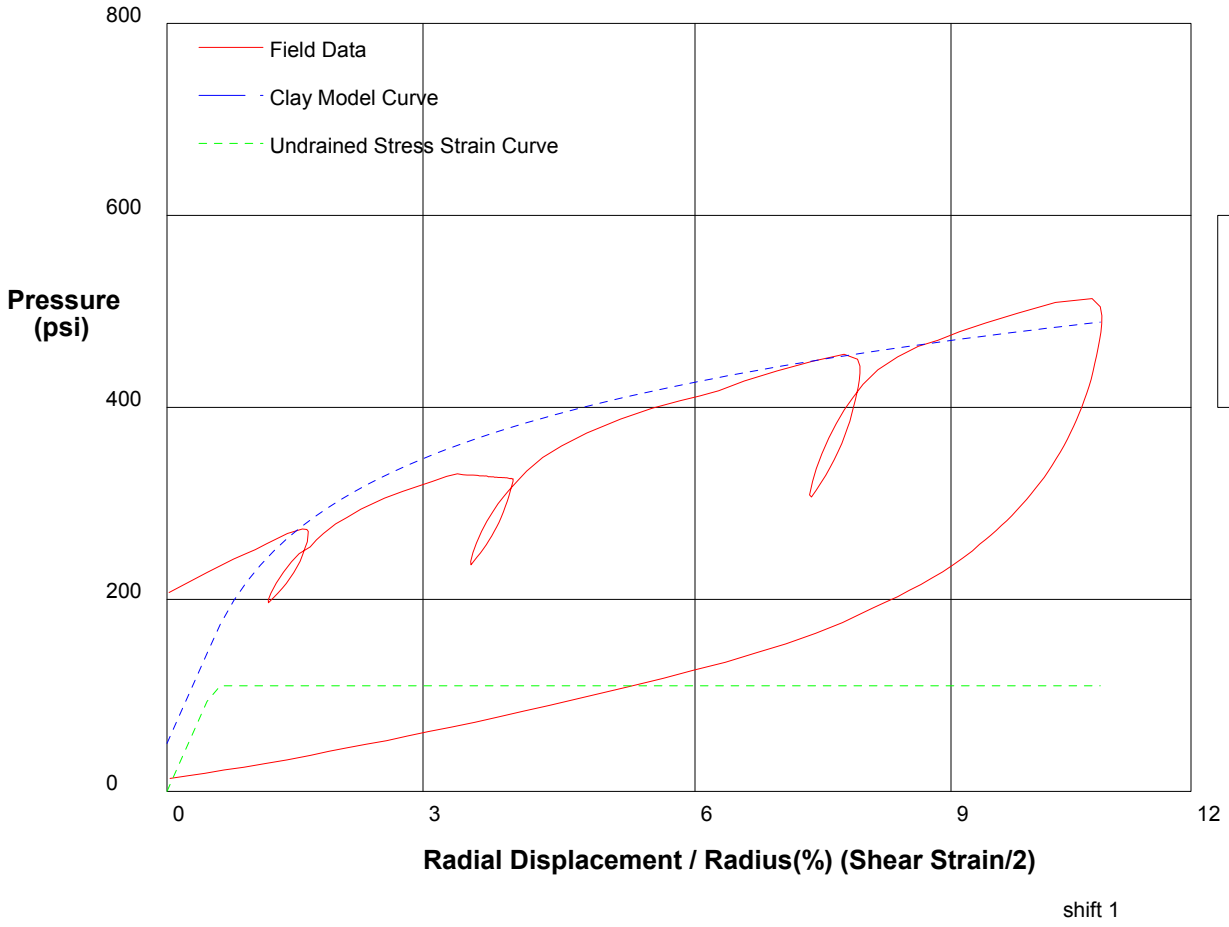

GIBSON'S CLAY MODEL

Shear Strength 110 psi
Insitu Stress 50 psi
Shear Modulus 10000 psi

shift 1

In Situ Engineering

Appendix II - Pressuremeter Model Interpretation

PRESSUREMETER DATA **CH2MHill, Inc.**

CALTRANS I-710 North Tunnel Project **1/29/2009**

Hole No. Z2-B2 **Depth 134.2ft** **File C:\DATA\ISE-812\SR710-24.P**

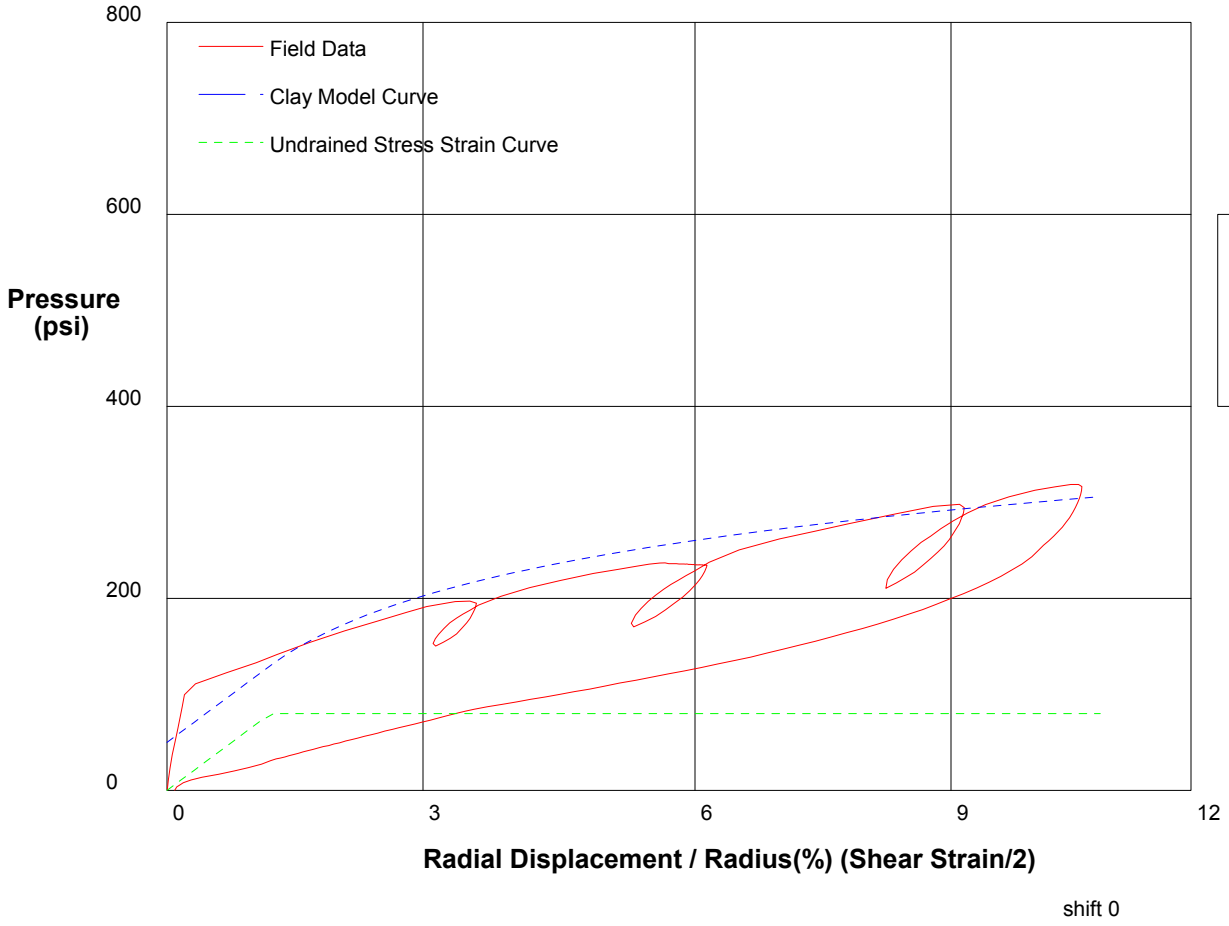

GIBSON'S CLAY MODEL

Shear Strength 80 psi
Insitu Stress 50 psi
Shear Modulus 3300 psi

shift 0

In Situ Engineering

Appendix II - Pressuremeter Model Interpretation

PRESSUREMETER DATA **CH2MHill, Inc.**

CALTRANS I-710 North Tunnel Project **2/4/2009**

Hole No. Z2-B2 **Depth 251ft** **File C:\DATA\ISE-812\SR710-25.P**

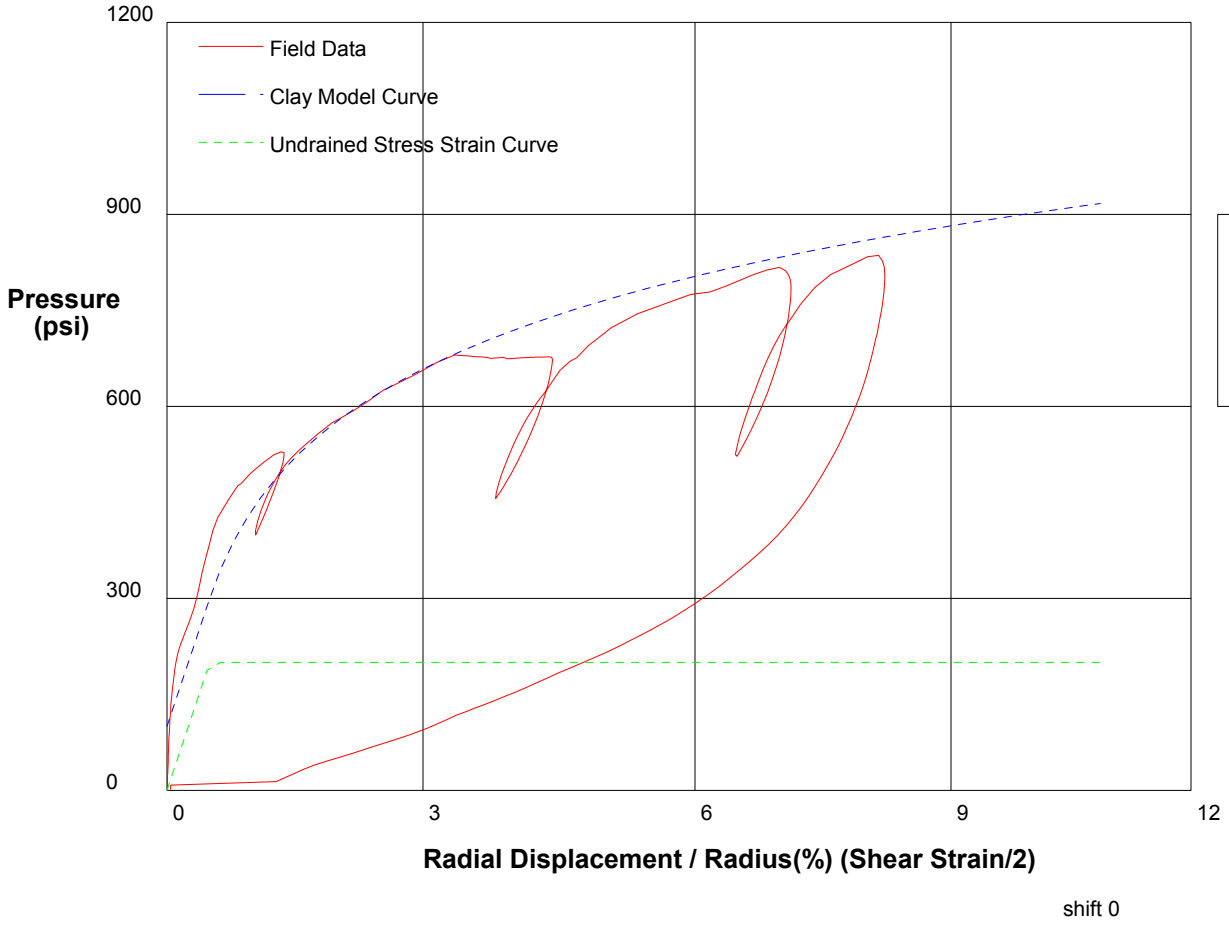

GIBSON'S CLAY MODEL

Shear Strength 200 psi
Insitu Stress 100 psi
Shear Modulus 20000 psi

shift 0

In Situ Engineering

Appendix II - Pressuremeter Model Interpretation

PRESSUREMETER DATA **CH2MHill, Inc.**

CALTRANS I-710 North Tunnel Project **2/4/2009**

Hole No. Z2-B2 **Depth 249.5ft** **File C:\DATA\ISE-812\SR710-26.P**

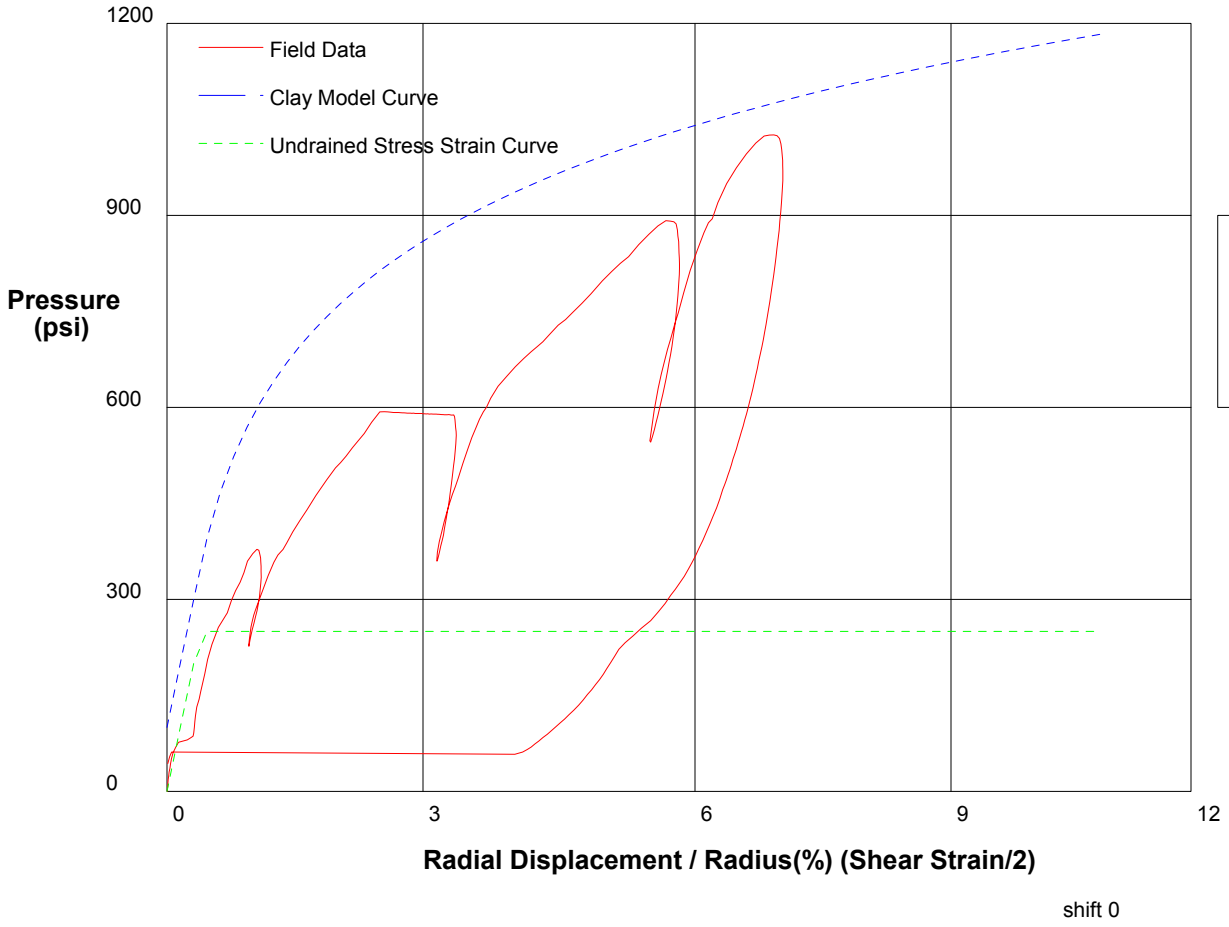

GIBSON'S CLAY MODEL

Shear Strength	**250 psi**
Insitu Stress	**100 psi**
Shear Modulus	**32000 psi**

shift 0

In Situ Engineering

Appendix II - Pressuremeter Model Interpretation

PRESSUREMETER DATA **CH2MHill, Inc.**

CALTRANS I-710 North Tunnel Project **2/4/2009**

Hole No. Z2-B2 **Depth 249.5ft** **File C:\DATA\ISE-812\SR710-26.P**

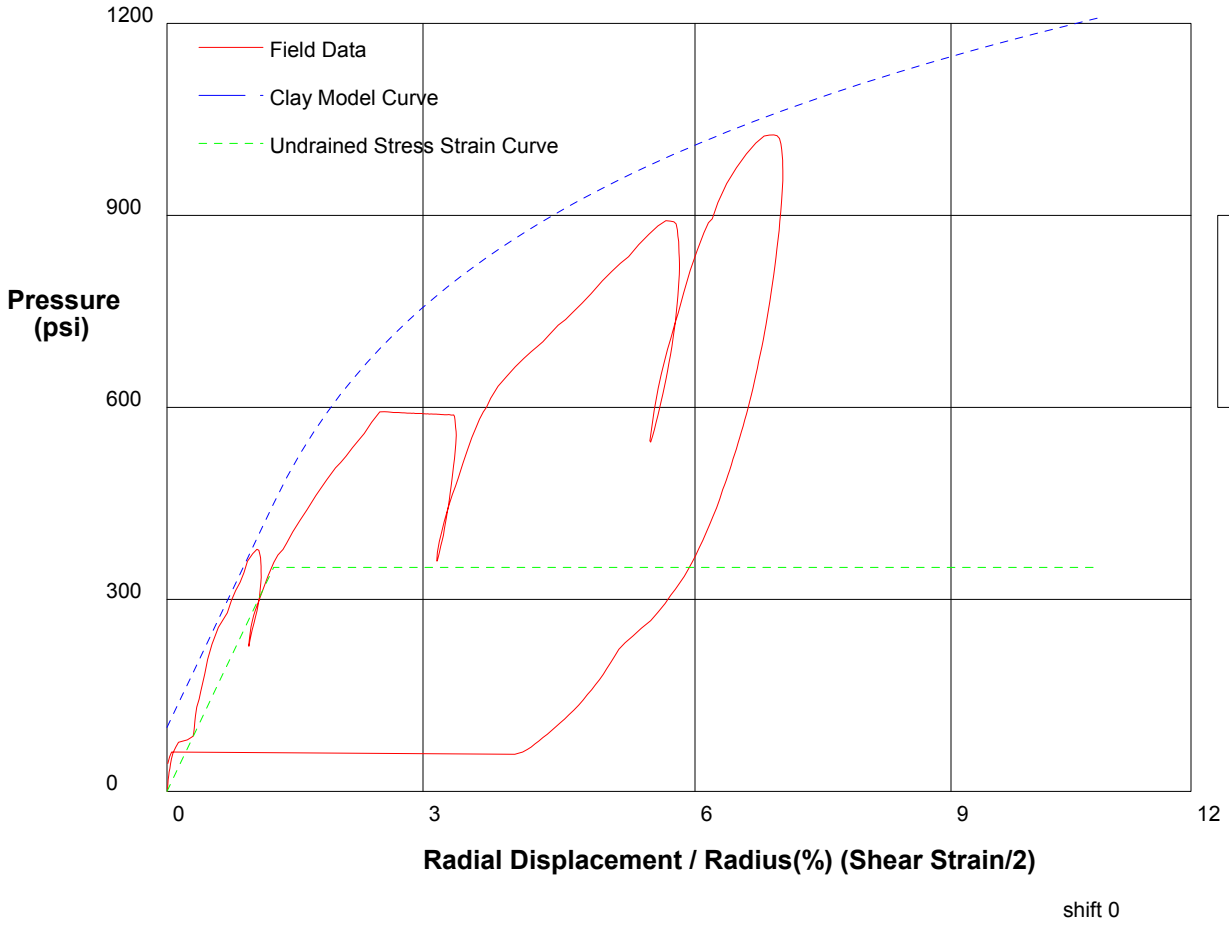

GIBSON'S CLAY MODEL

Shear Strength	**350 psi**
Insitu Stress	**100 psi**
Shear Modulus	**14000 psi**

shift 0

In Situ Engineering

Appendix II - Pressuremeter Model Interpretation

PRESSUREMETER DATA **CH2M-HILL, Inc.**

CALTRANS I-710 North Tunnel Project **2/5/2009**

Hole No. Z1-B6 **Depth 245ft** **File C:\DATA\ISE-812\SR710-28.P**

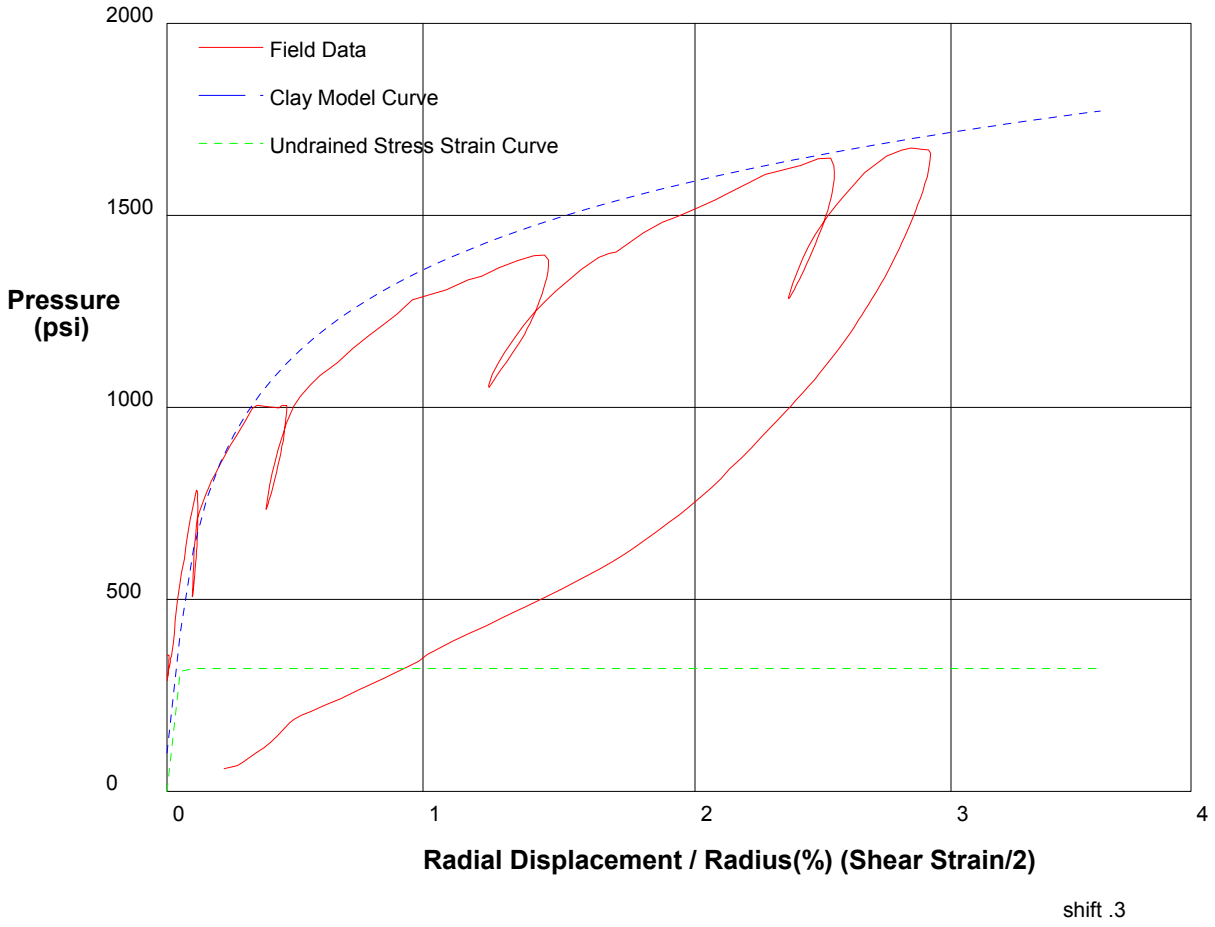

GIBSON'S CLAY MODEL

Shear Strength	**320 psi**
Insitu Stress	**100 psi**
Shear Modulus	**300000 psi**

shift .3

In Situ Engineering

Appendix II - Pressuremeter Model Interpretation

PRESSUREMETER DATA **CH2MHill, Inc.**

CALTRANS I-710 North Tunnel Project **2/5/2009**

Hole No. Z1-B6 **Depth 245ft** **File C:\DATA\ISE-812\SR710-28.P**

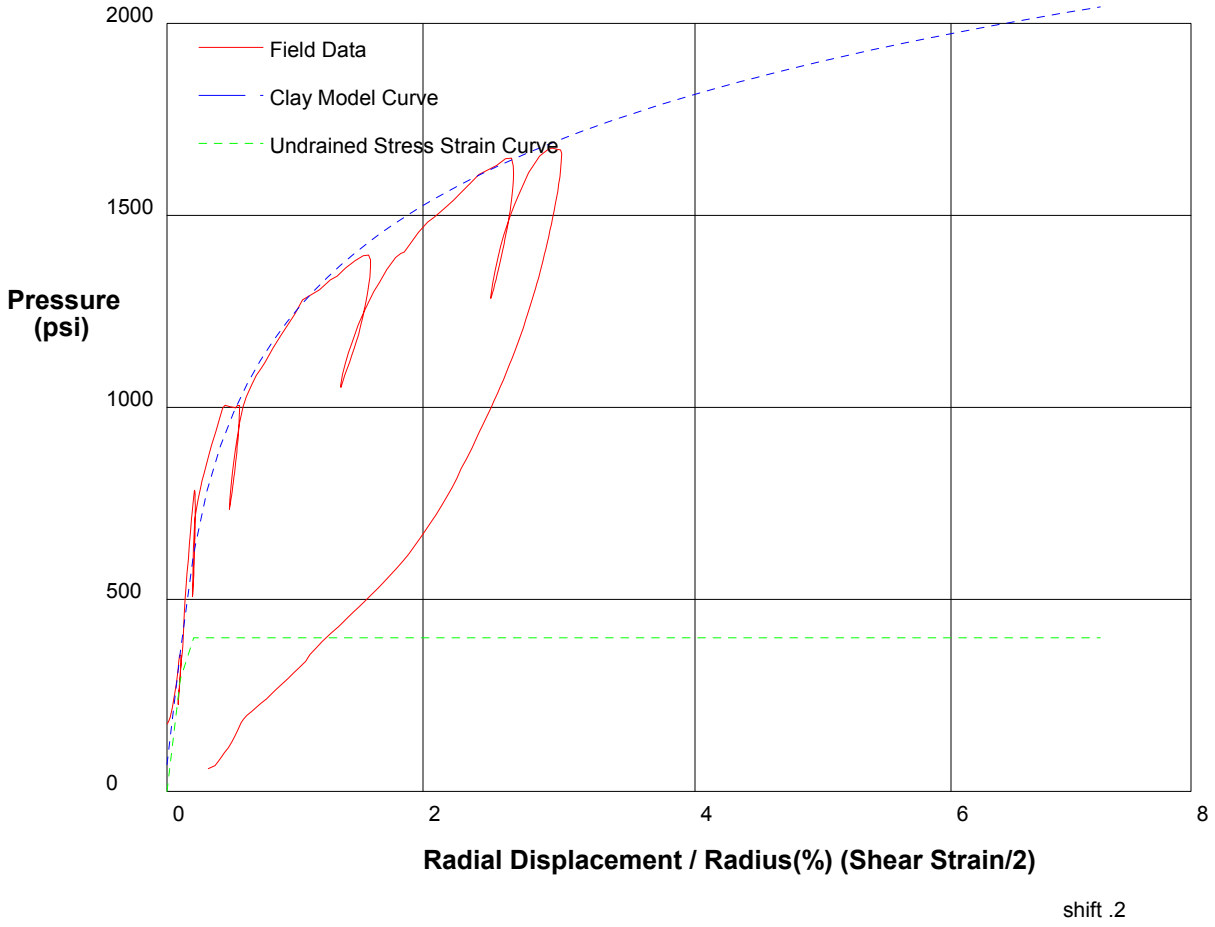

GIBSON'S CLAY MODEL

Shear Strength 400 psi
Insitu Stress 70 psi
Shear Modulus 140000 psi

shift .2

In Situ Engineering

Appendix II - Pressuremeter Model Interpretation

PRESSUREMETER DATA **CH2MHill, Inc.**

CALTRANS I-710 North Tunnel Project **2/6/2009**

Hole No. Z3-B7 **Depth 225.8ft** **File C:\DATA\ISE-812\SR710-29.P**

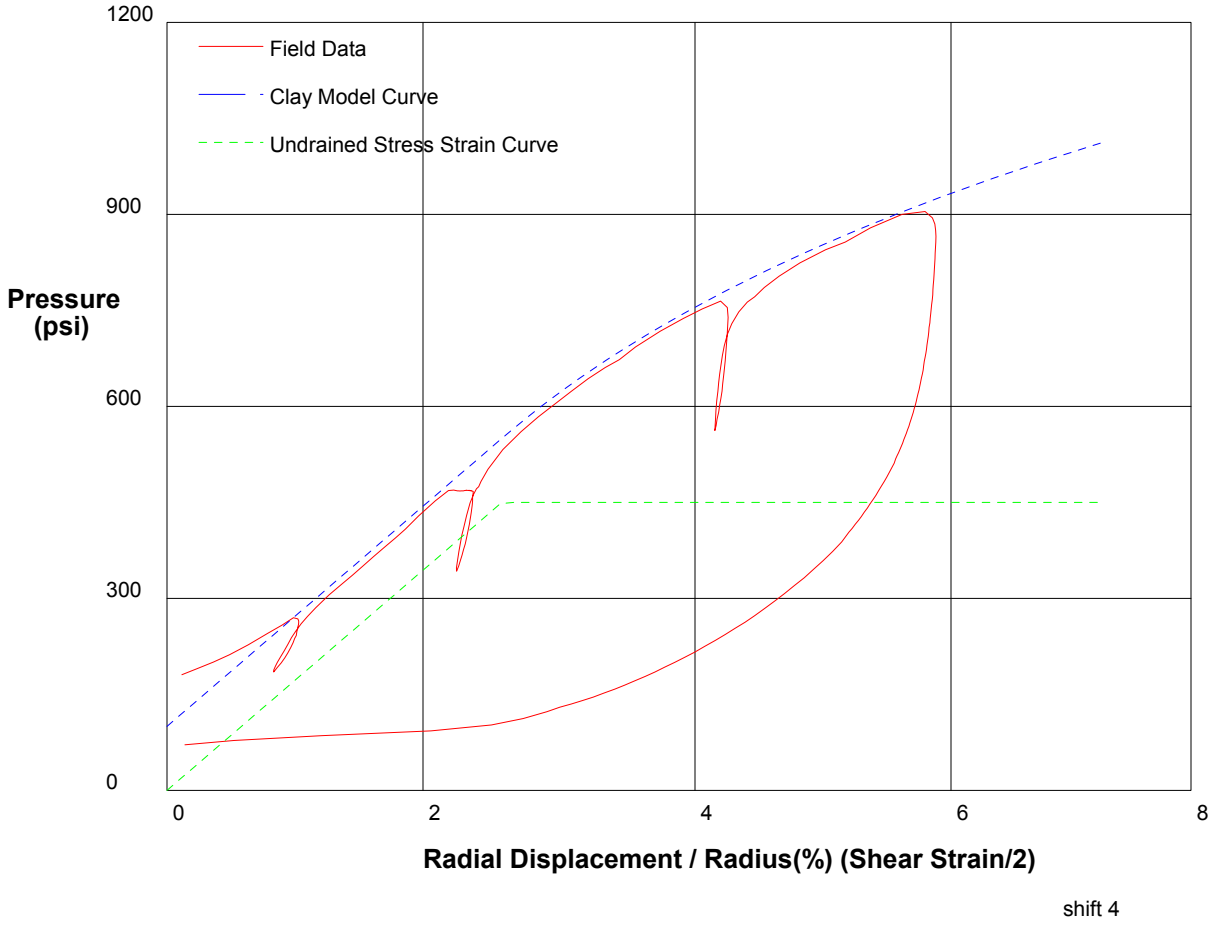

GIBSON'S CLAY MODEL

Shear Strength	**450 psi**
Insitu Stress	**100 psi**
Shear Modulus	**8600 psi**

shift 4

In Situ Engineering

Appendix II - Pressuremeter Model Interpretation

PRESSUREMETER DATA **CH2MHill, Inc.**

CALTRANS I-710 North Tunnel Project **2/6/2009**

Hole No. Z3-B7 **Depth 225.8ft** **File C:\DATA\ISE-812\SR710-29.P**

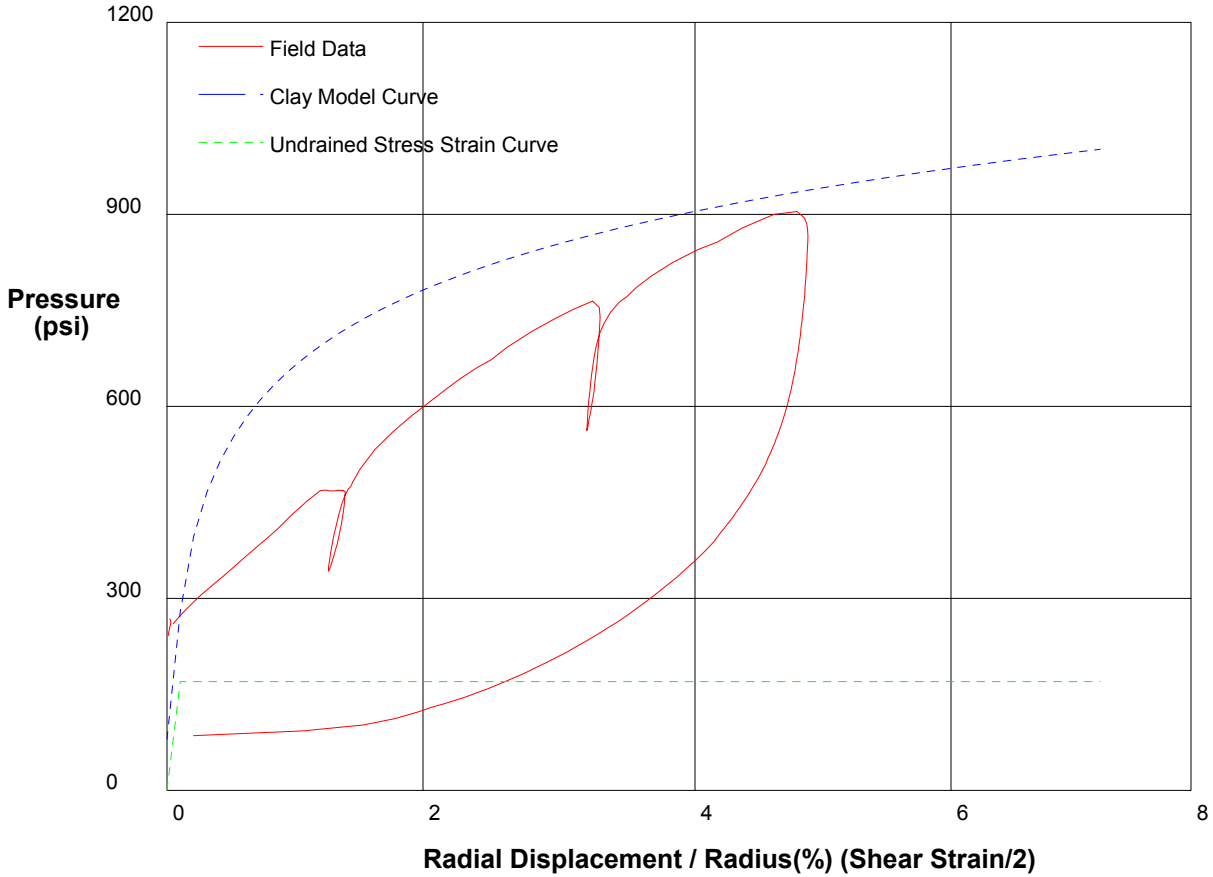

GIBSON'S CLAY MODEL

Shear Strength 170 psi
Insitu Stress 80 psi
Shear Modulus 97000 psi

shift 5

In Situ Engineering

Appendix II - Pressuremeter Model Interpretation

PRESSUREMETER DATA **CH2MHill, Inc.**

CALTRANS I-710 North Tunnel Project **2/6/2009**

Hole No. Z3-B7 **Depth 225.8ft** **File C:\DATA\ISE-812\SR710-29.P**

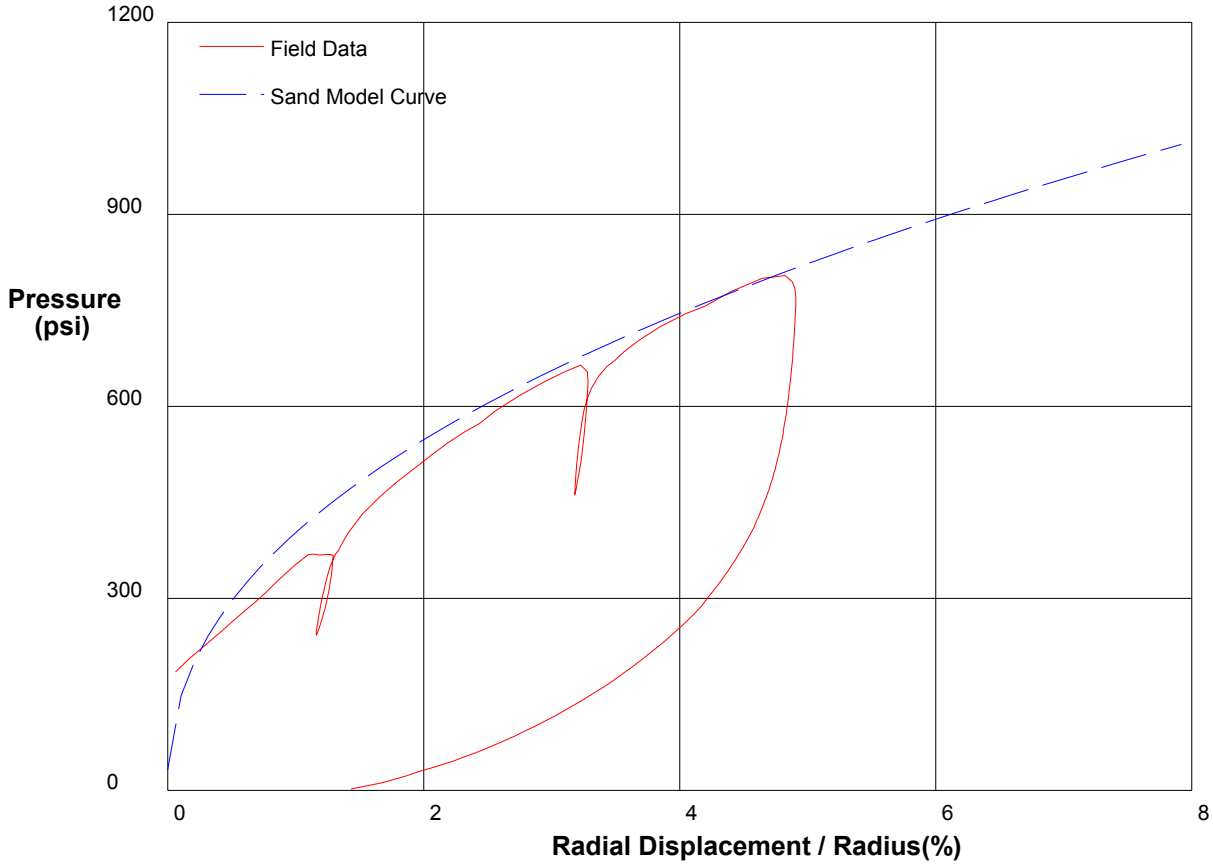

THE In Situ Engineering SAND MODEL

Water Pressure	**100 psi**
Friction Angle	**39 deg**
Critical Friction Angle	**32 deg**
Lateral Stress	**33 psi**
Shear Modulus	**97000 psi**

shift 5.1

In Situ Engineering

Appendix II - Pressuremeter Model Interpretation

PRESSUREMETER DATA **CH2MHill, Inc.**

CALTRANS I-710 North Tunnel Project **2/6/2009**

Hole No. Z3-B7 **Depth 224.3ft** **File C:\DATA\ISE-812\SR710-30.P**

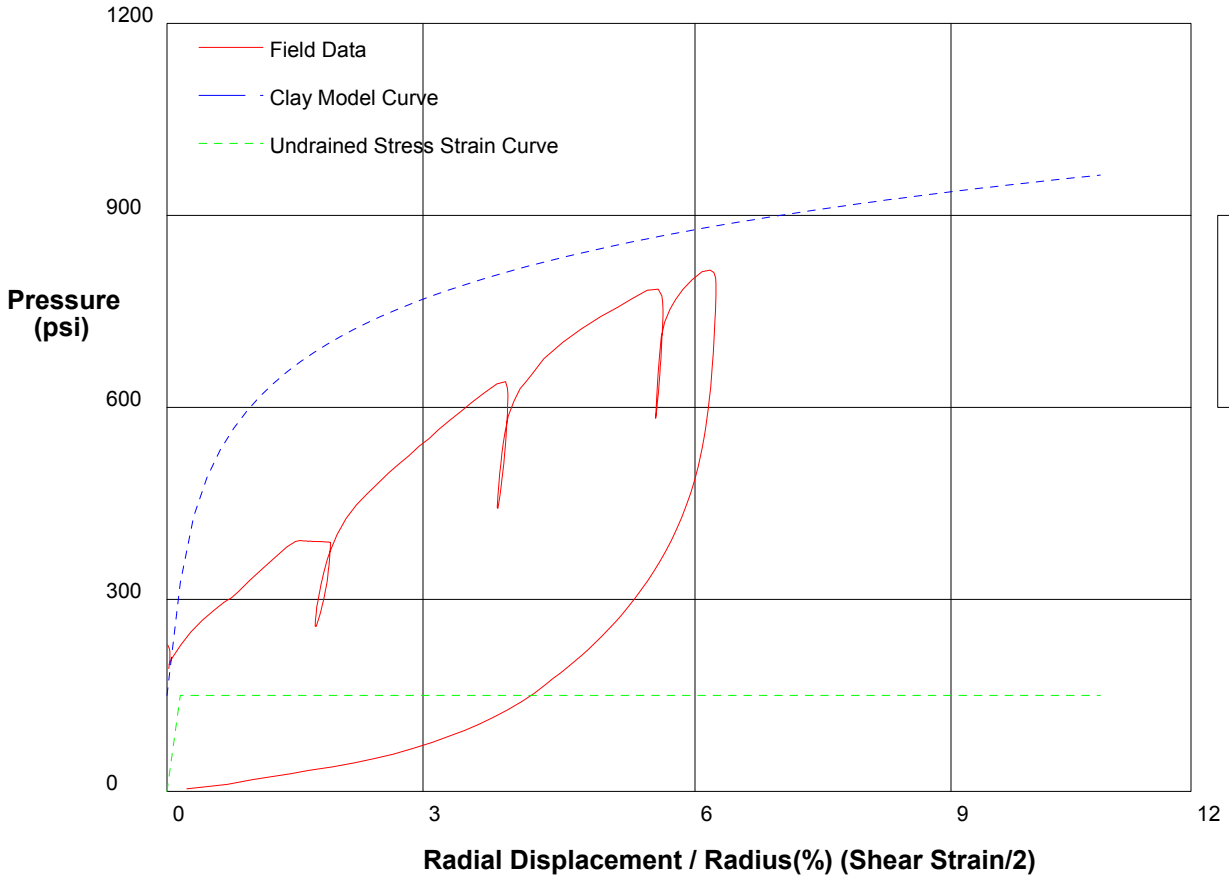

GIBSON'S CLAY MODEL

Shear Strength	**150 psi**
Insitu Stress	**150 psi**
Shear Modulus	**57000 psi**

shift 4

In Situ Engineering

Appendix II - Pressuremeter Model Interpretation

PRESSUREMETER DATA **CH2MHill, Inc.**

CALTRANS I-710 North Tunnel Project **2/6/2009**

Hole No. Z3-B7 **Depth 224.3ft** **File C:\DATA\ISE-812\SR710-30.P**

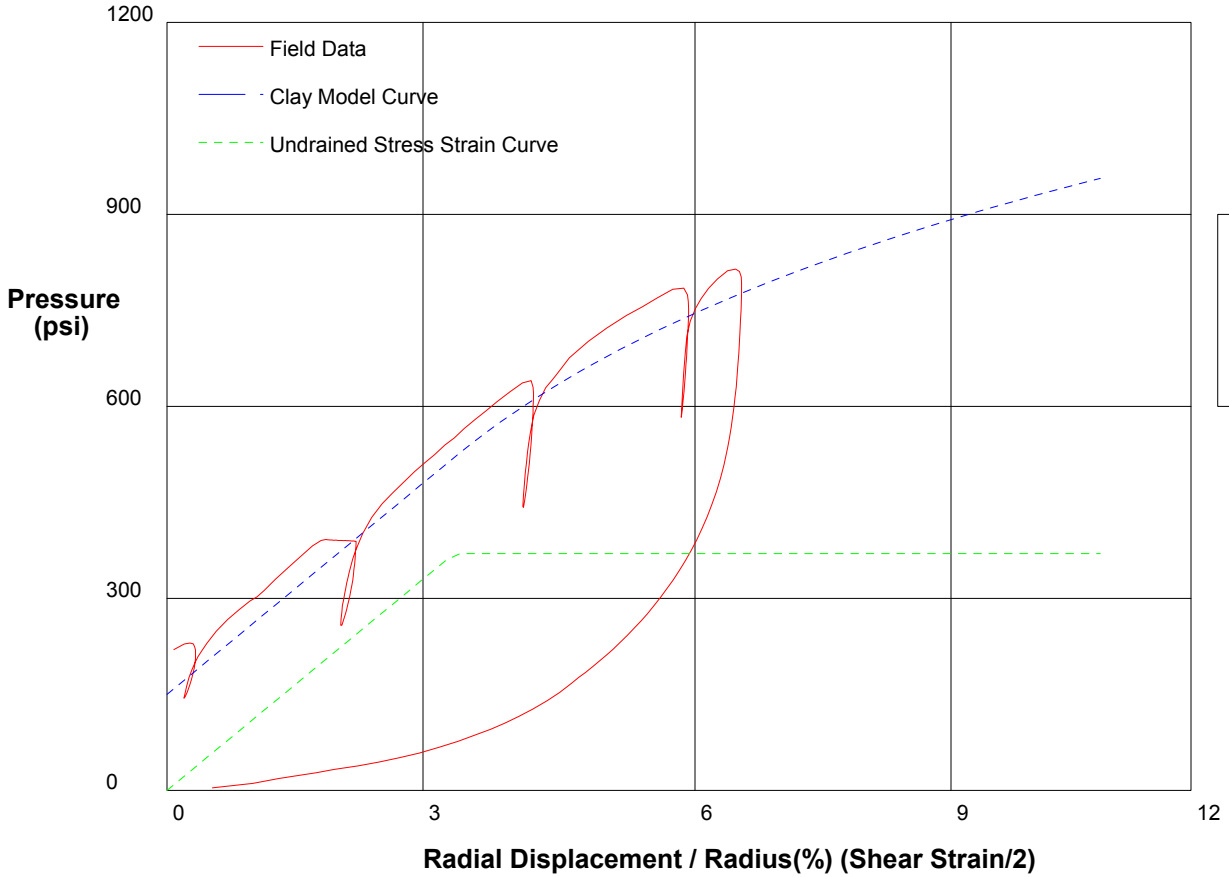

GIBSON'S CLAY MODEL

Shear Strength 370 psi
Insitu Stress 150 psi
Shear Modulus 5500 psi

shift 3.7

In Situ Engineering

Appendix II - Pressuremeter Model Interpretation

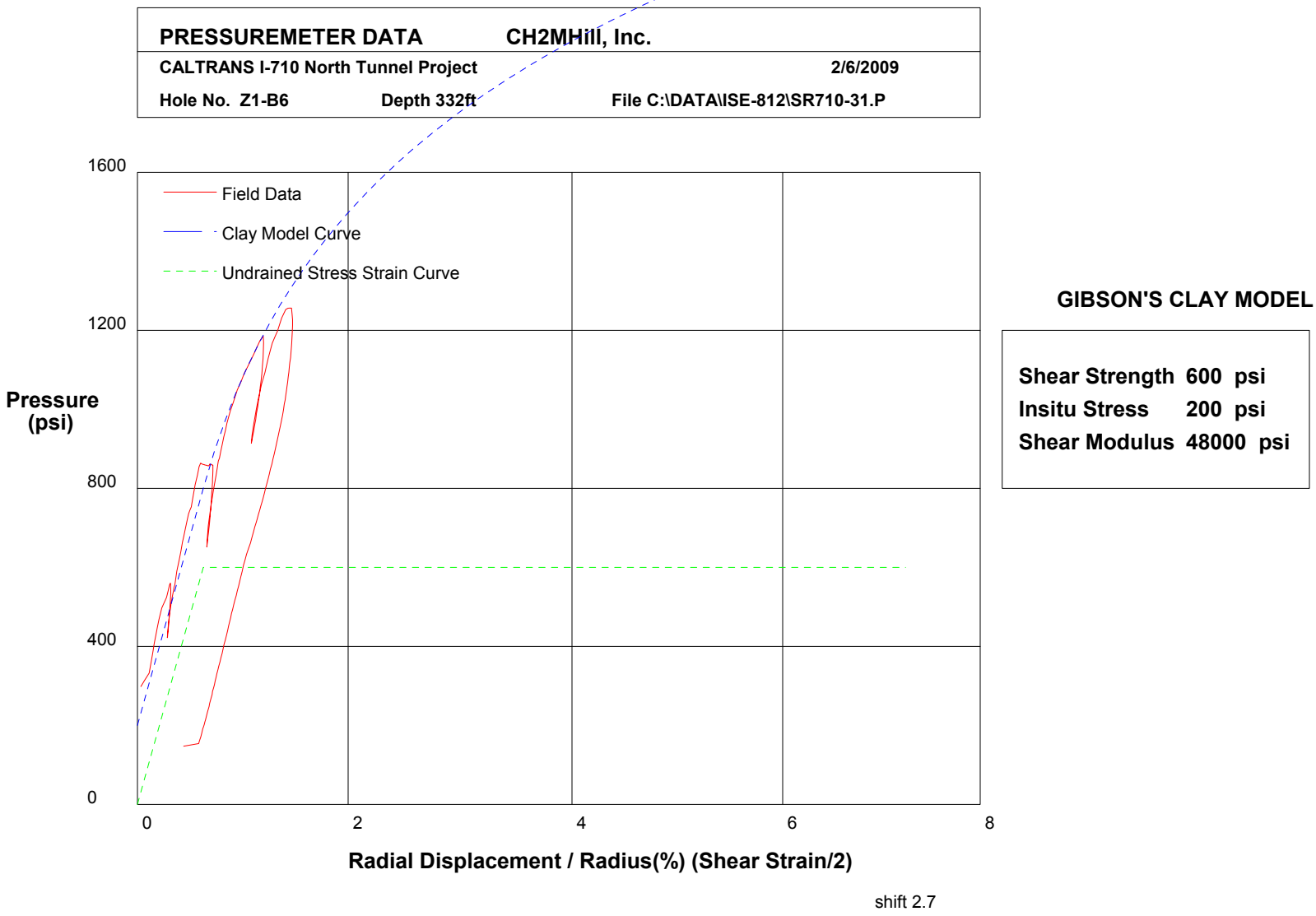

Appendix II - Pressuremeter Model Interpretation

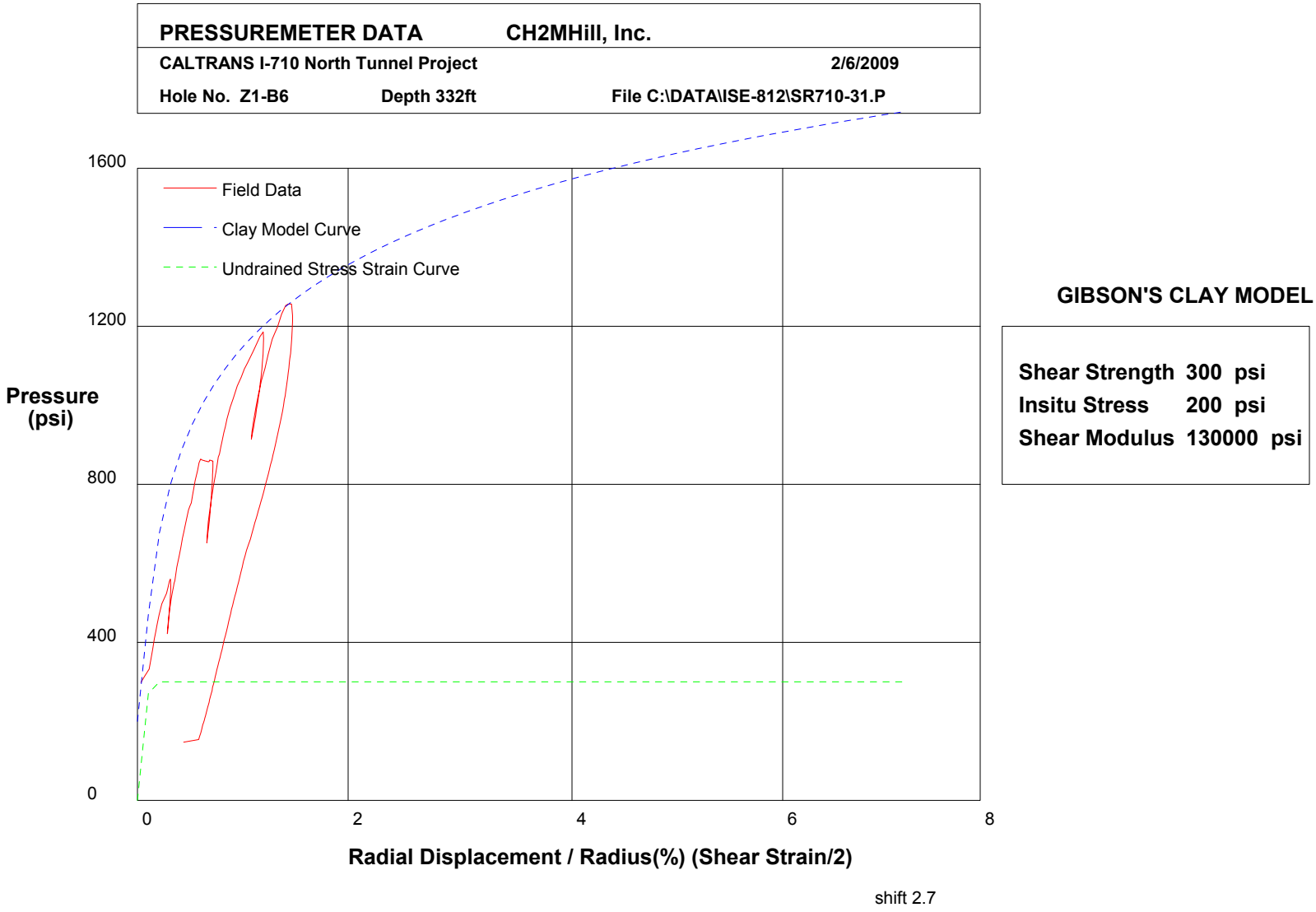

Appendix II - Pressuremeter Model Interpretation

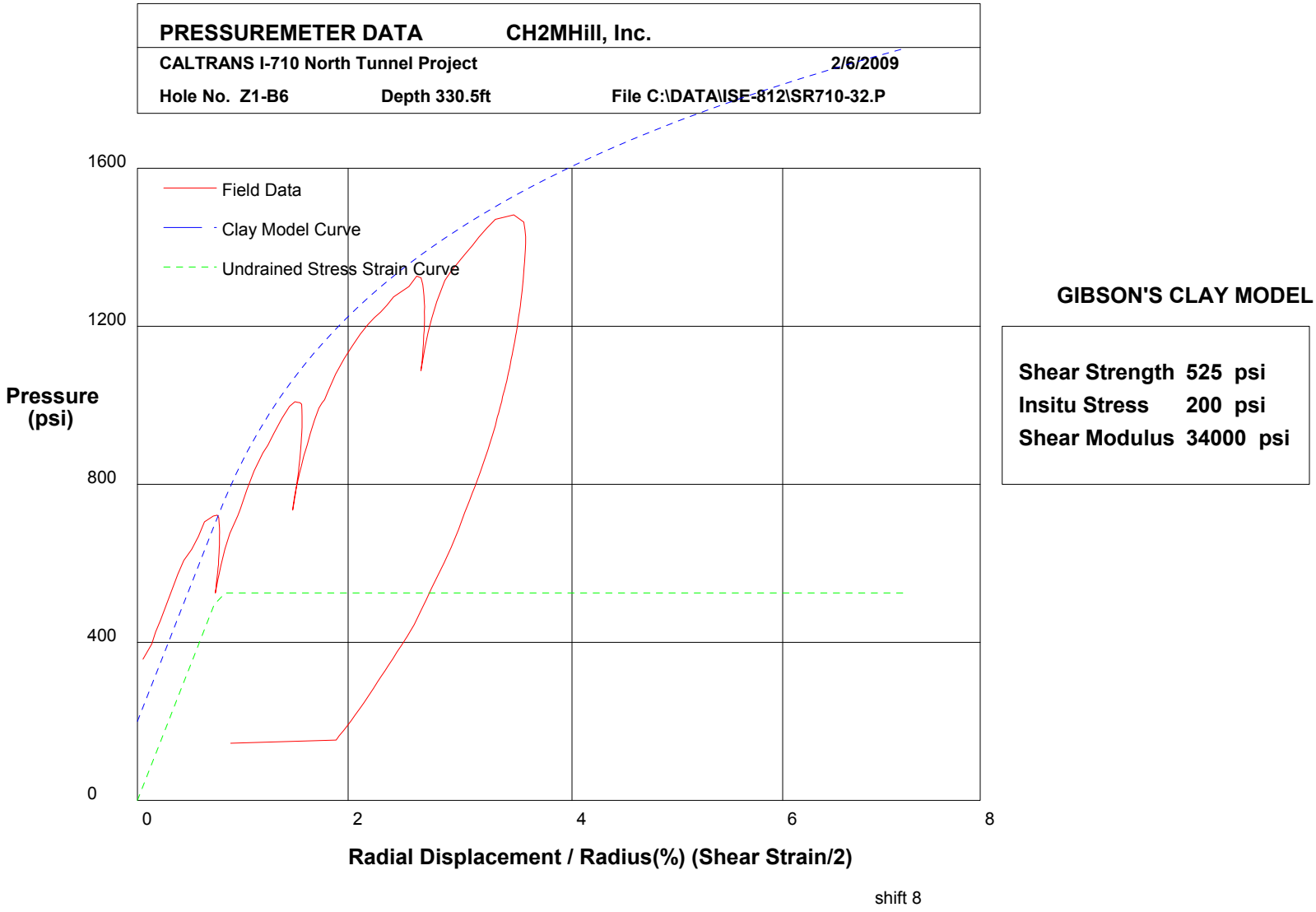

Appendix II - Pressuremeter Model Interpretation

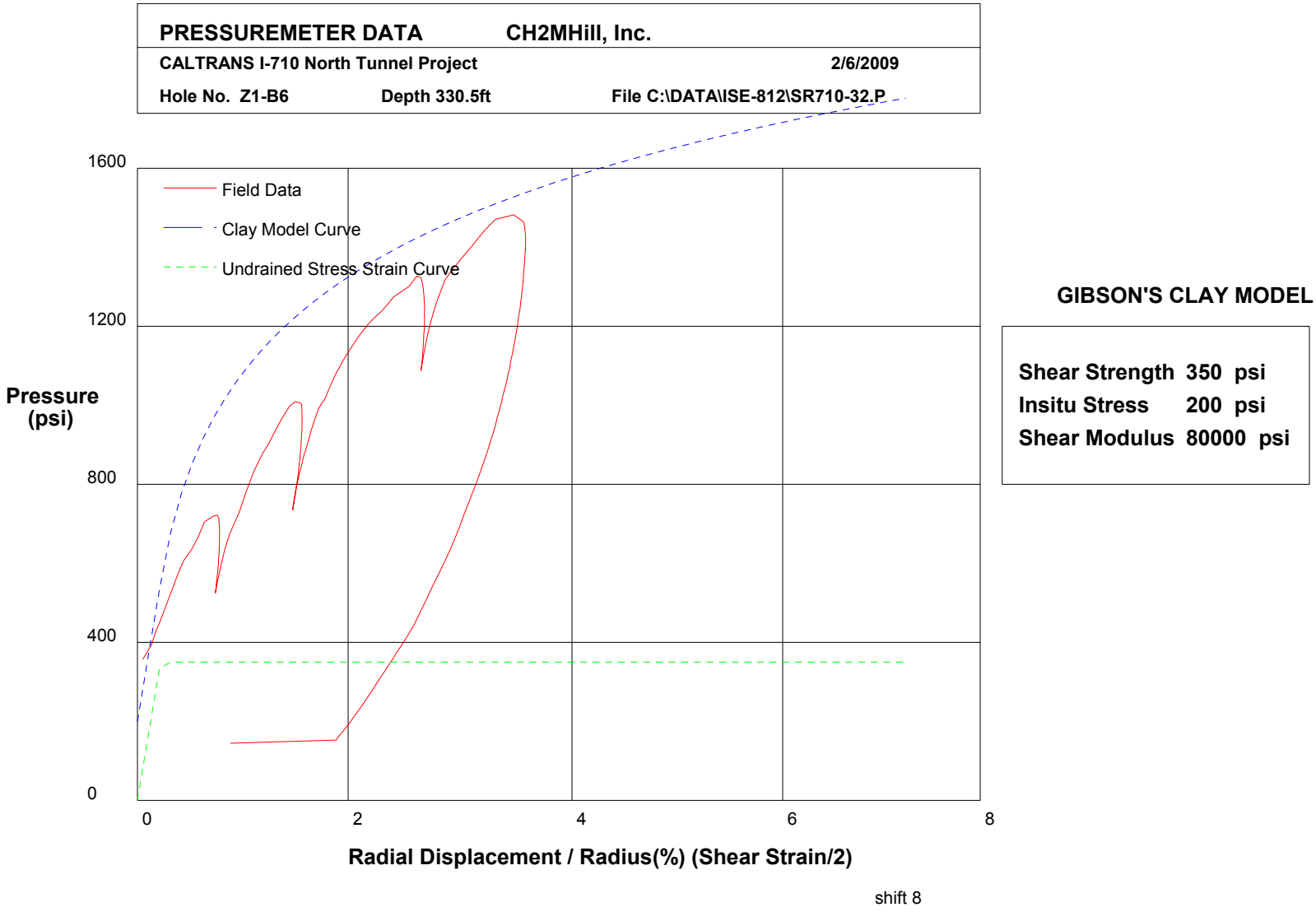

Appendix II - Pressuremeter Model Interpretation

PRESSUREMETER DATA **CH2MHill, Inc.**

CALTRANS I-710 North Tunnel Project **2/10/2009**

Hole No. Z3-B7 **Depth 252.5ft** **File C:\DATA\ISE-812\SR710-33.P**

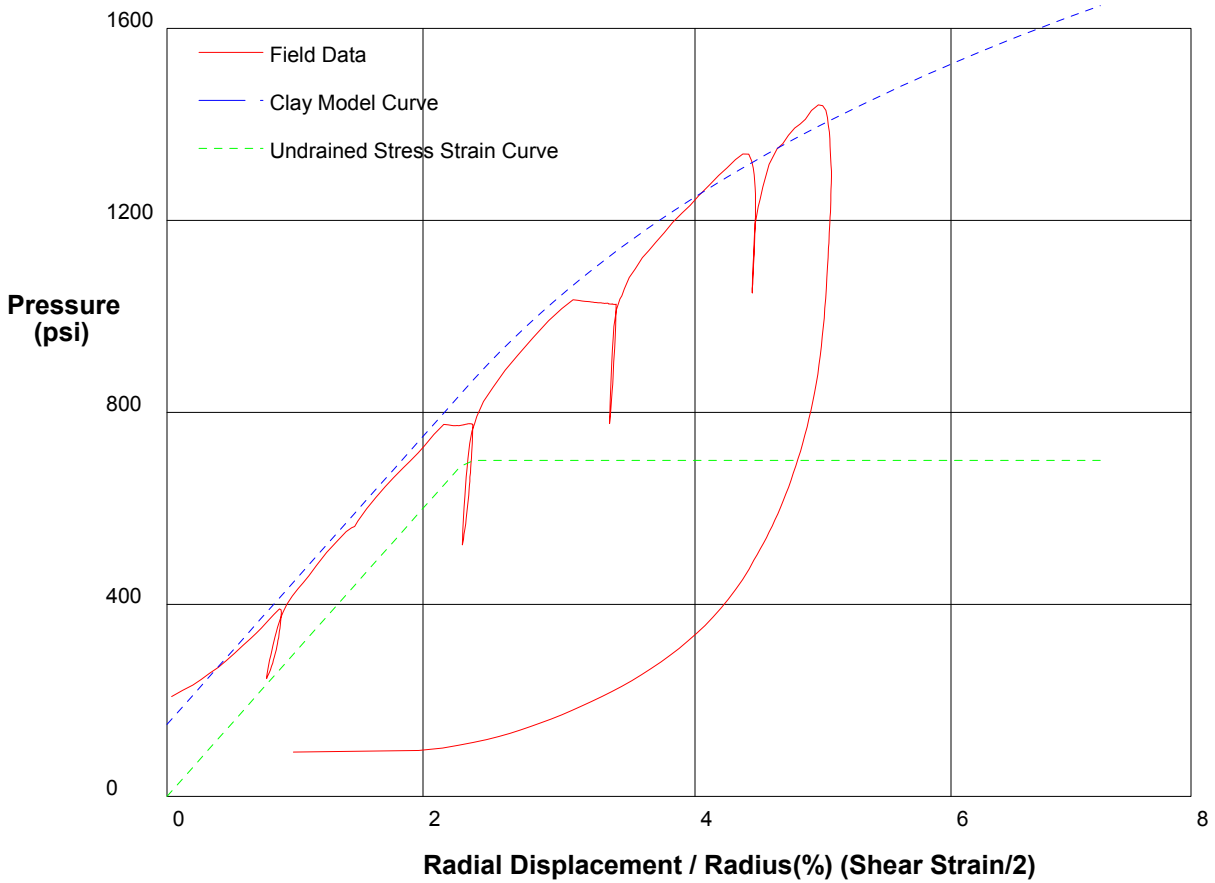

GIBSON'S CLAY MODEL

Shear Strength	**700 psi**
Insitu Stress	**150 psi**
Shear Modulus	**15000 psi**

shift 5.2

In Situ Engineering

Appendix II - Pressuremeter Model Interpretation

PRESSUREMETER DATA **CH2MHill, Inc.**

CALTRANS I-710 North Tunnel Project **2/10/2009**

Hole No. Z3-B7 **Depth 252.5ft** **File C:\DATA\ISE-812\SR710-33.P**

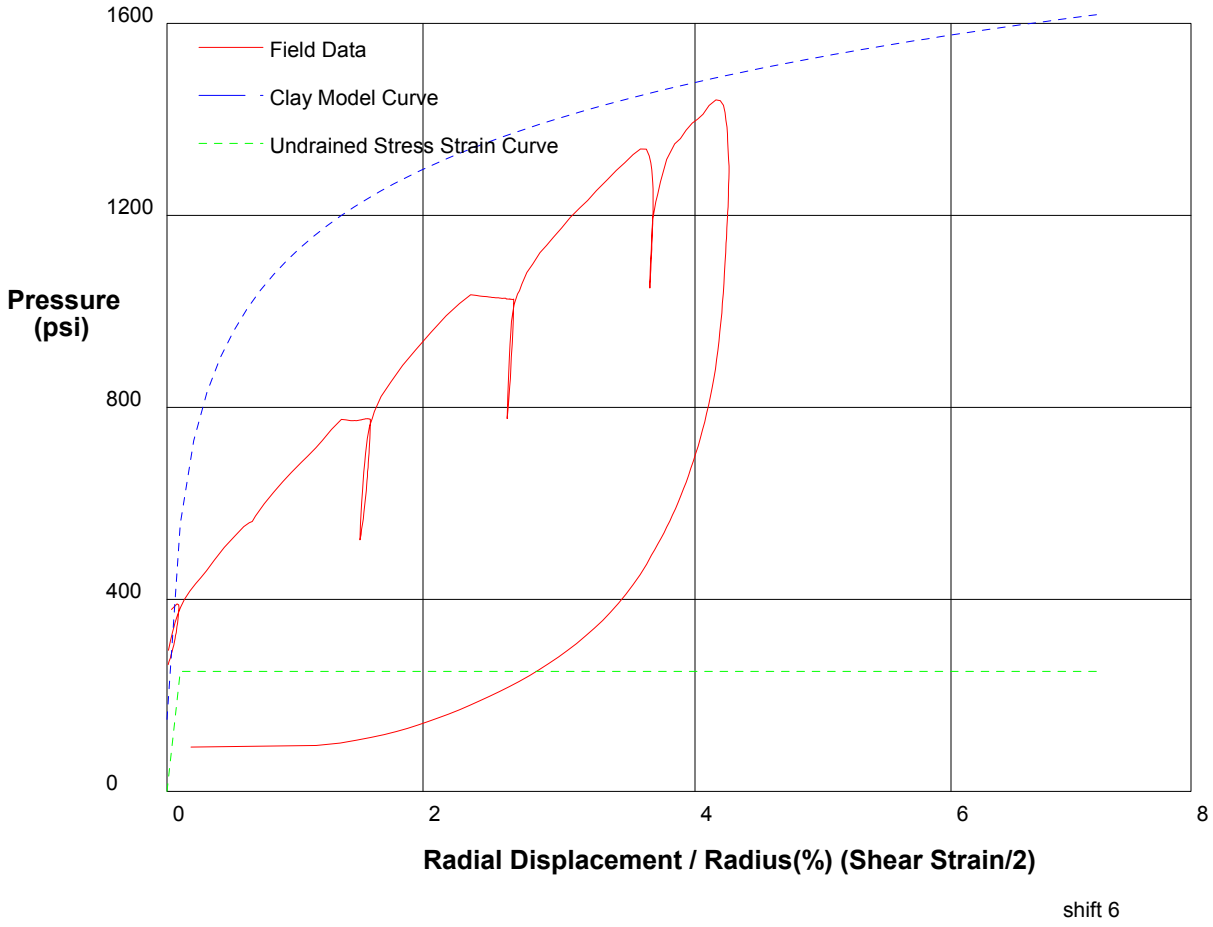

GIBSON'S CLAY MODEL

Shear Strength	**250 psi**
Insitu Stress	**150 psi**
Shear Modulus	**225000 psi**

shift 6

In Situ Engineering

Appendix II - Pressuremeter Model Interpretation

PRESSUREMETER DATA **CH2MHill, Inc.**

CALTRANS I-710 North Tunnel Project **2/10/2009**

Hole No. Z3-B7 **Depth 251ft** **File C:\DATA\ISE-812\SR710-34.P**

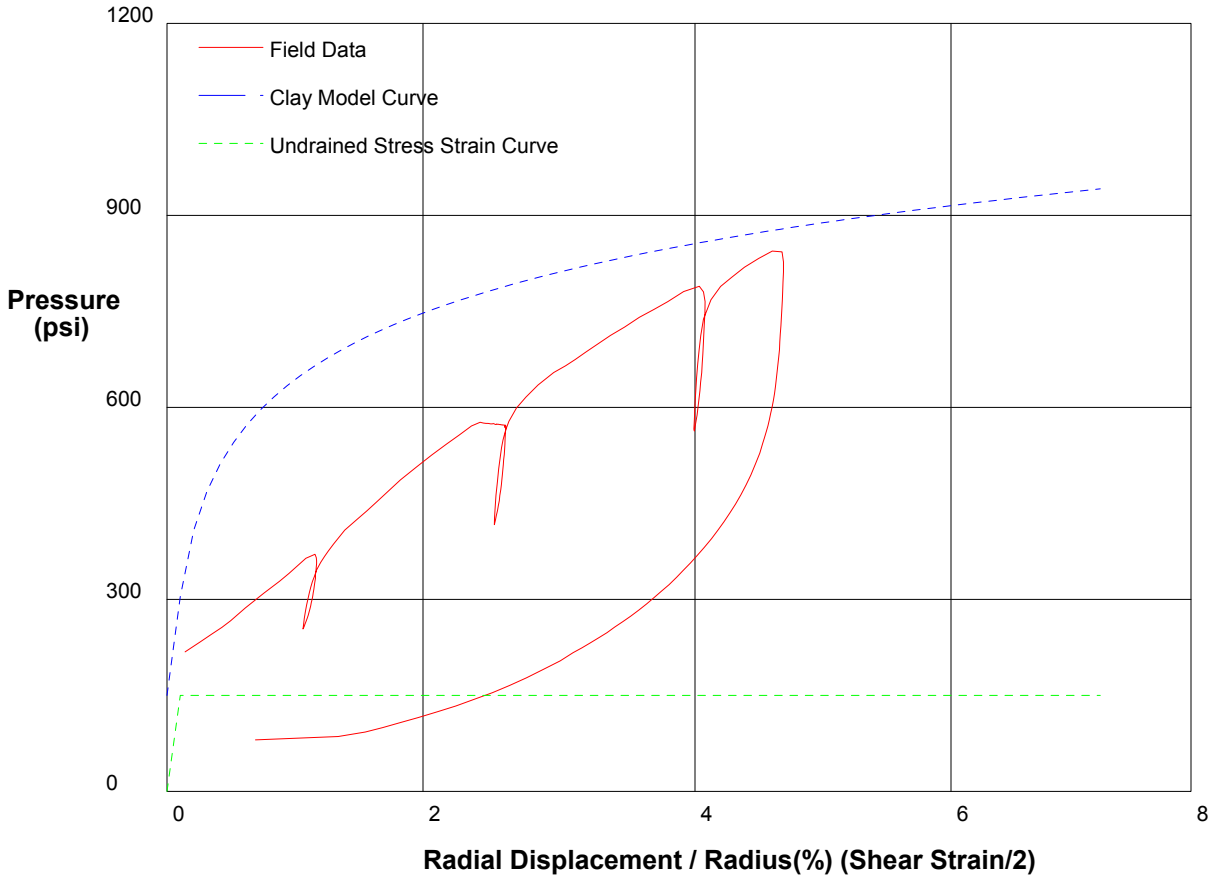

GIBSON'S CLAY MODEL

Shear Strength	**150 psi**
Insitu Stress	**150 psi**
Shear Modulus	**74000 psi**

shift 6.2

In Situ Engineering

Appendix II - Pressuremeter Model Interpretation

PRESSUREMETER DATA **CH2MHill, Inc.**

CALTRANS I-710 North Tunnel Project **2/10/2009**

Hole No. Z3-B7 **Depth 251ft** **File C:\DATA\ISE-812\SR710-34.P**

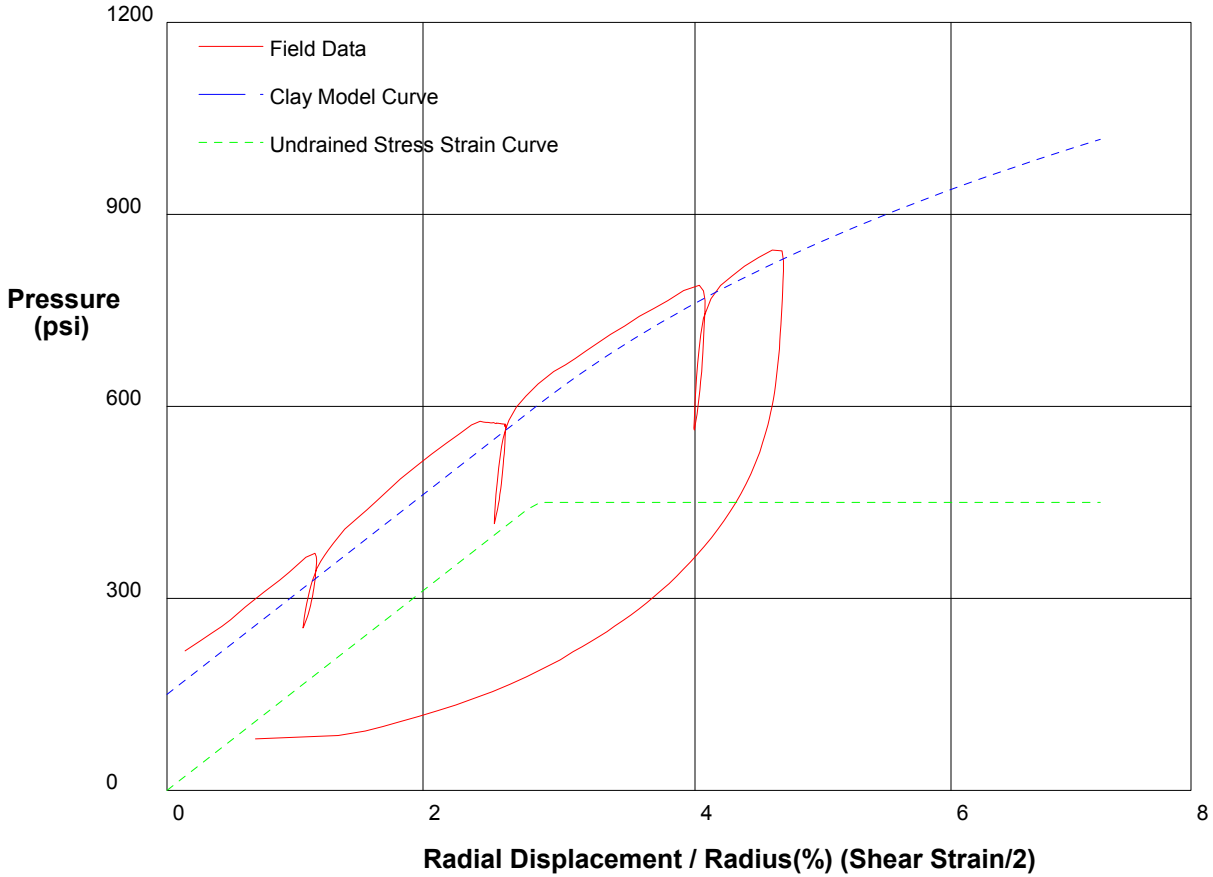

GIBSON'S CLAY MODEL

Shear Strength	**450 psi**
Insitu Stress	**150 psi**
Shear Modulus	**7800 psi**

shift 6.2

In Situ Engineering

Appendix II - Pressuremeter Model Interpretation

PRESSUREMETER DATA **CH2MHill, Inc.**

CALTRANS I-710 North Tunnel Project **2/10/2009**

Hole No. Z3-B7 **Depth 251ft** **File C:\DATA\ISE-812\SR710-34.P**

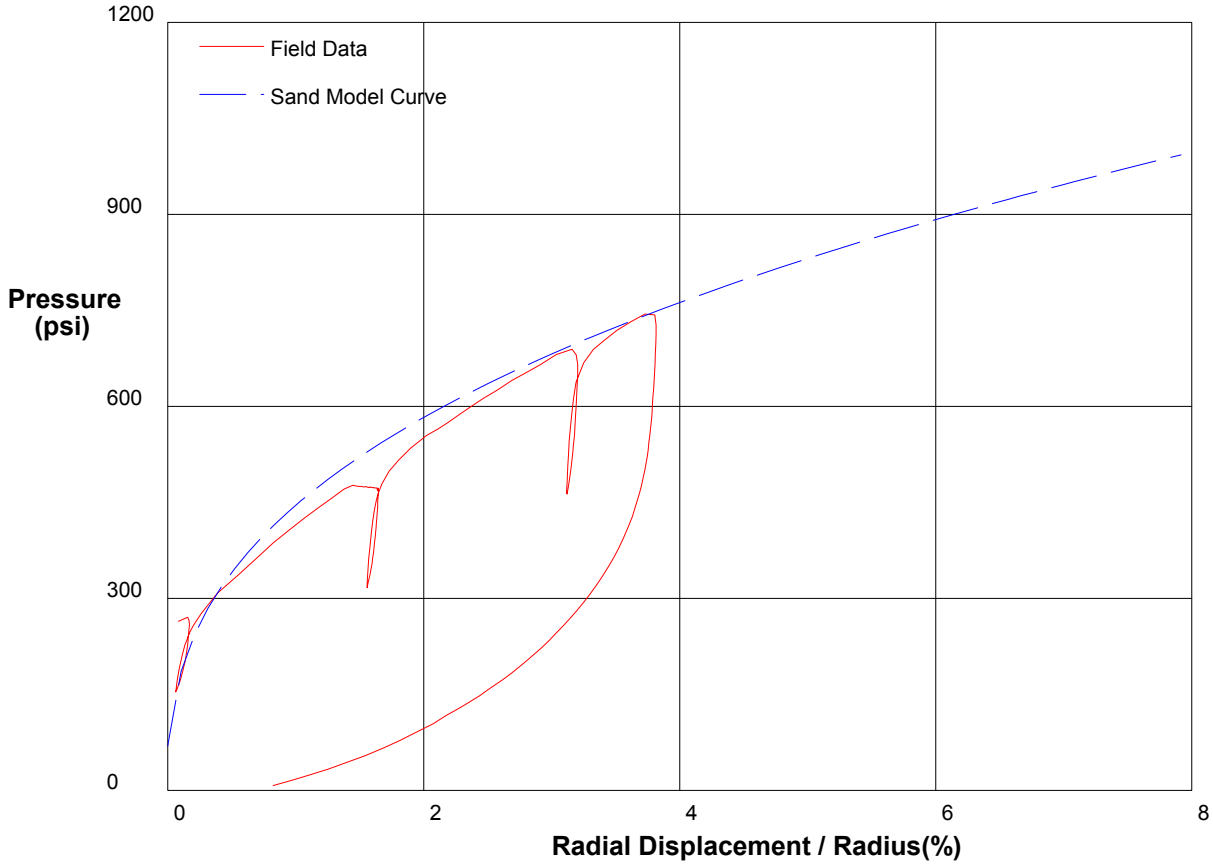

THE In Situ Engineering SAND MODEL

Water Pressure	**100 psi**
Friction Angle	**35 deg**
Critical Friction Angle	**32 deg**
Lateral Stress	**70 psi**
Shear Modulus	**74000 psi**

shift 7.2

In Situ Engineering

Appendix II - Pressuremeter Model Interpretation

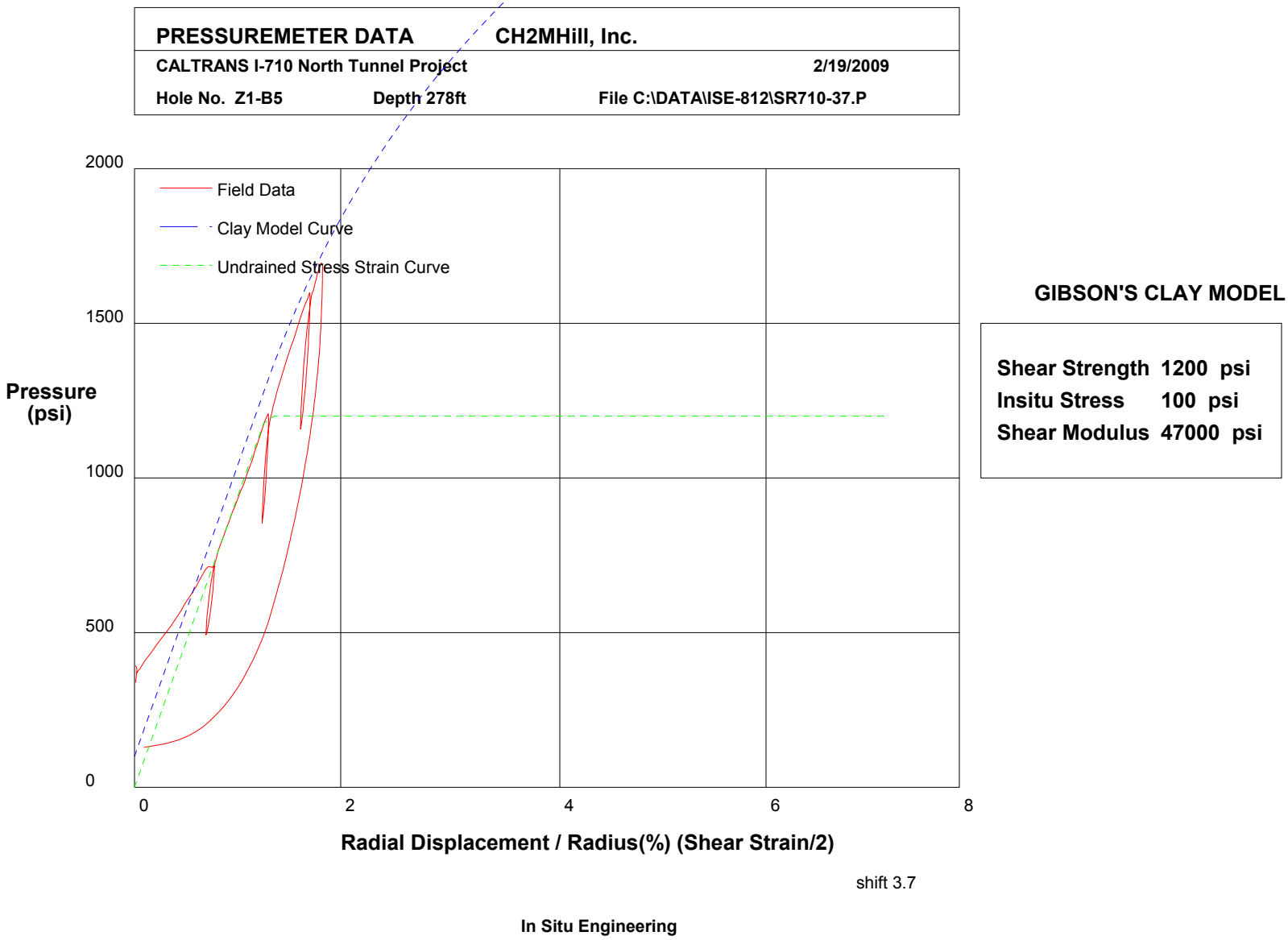

Appendix II - Pressuremeter Model Interpretation

PRESSUREMETER DATA **CH2MHill, Inc.**

CALTRANS I-710 North Tunnel Project **2/19/2009**

Hole No. Z1-B5 **Depth 278ft** **File C:\DATA\ISE-812\SR710-37.P**

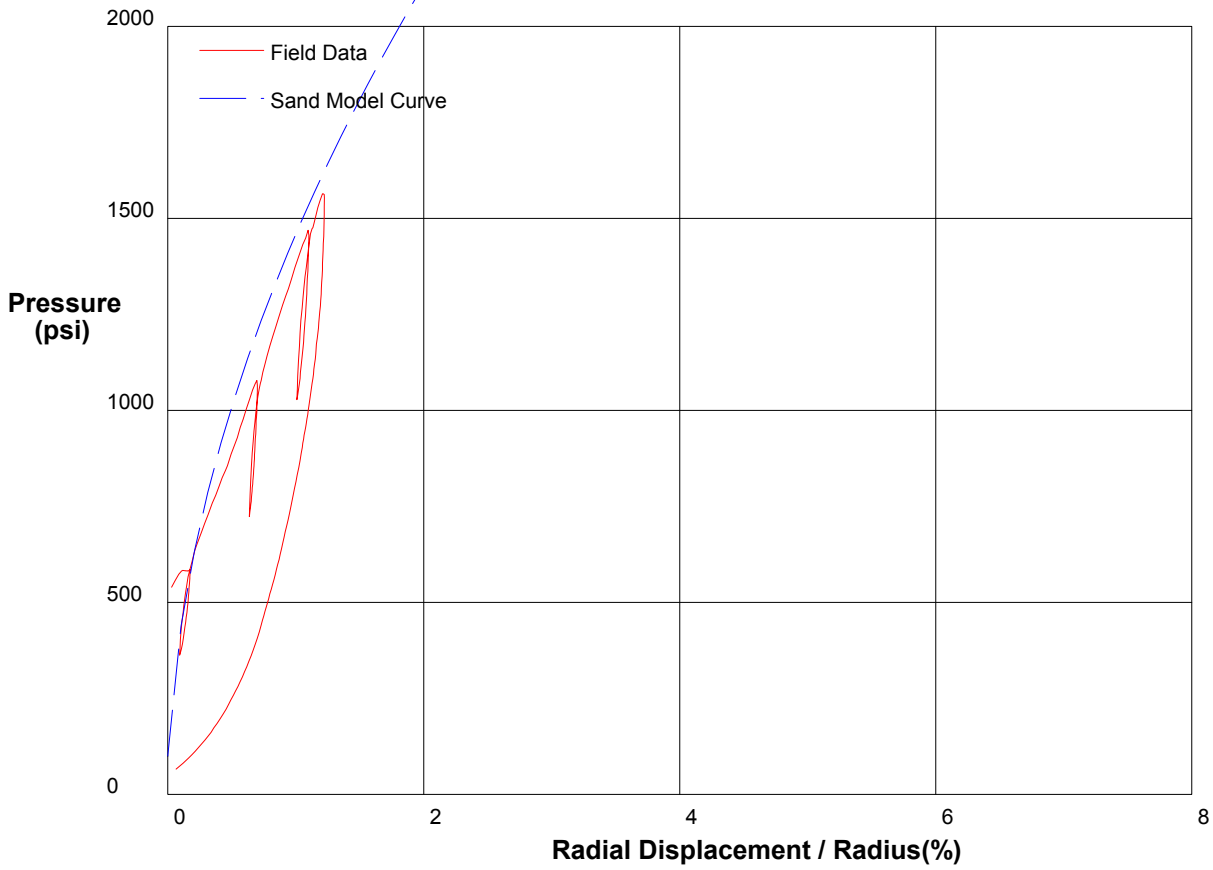

THE In Situ Engineering SAND MODEL

Water Pressure	**130 psi**
Friction Angle	**45 deg**
Critical Friction Angle	**32 deg**
Lateral Stress	**100 psi**
Shear Modulus	**200000 psi**

shift 4.3

In Situ Engineering

Appendix II - Pressuremeter Model Interpretation

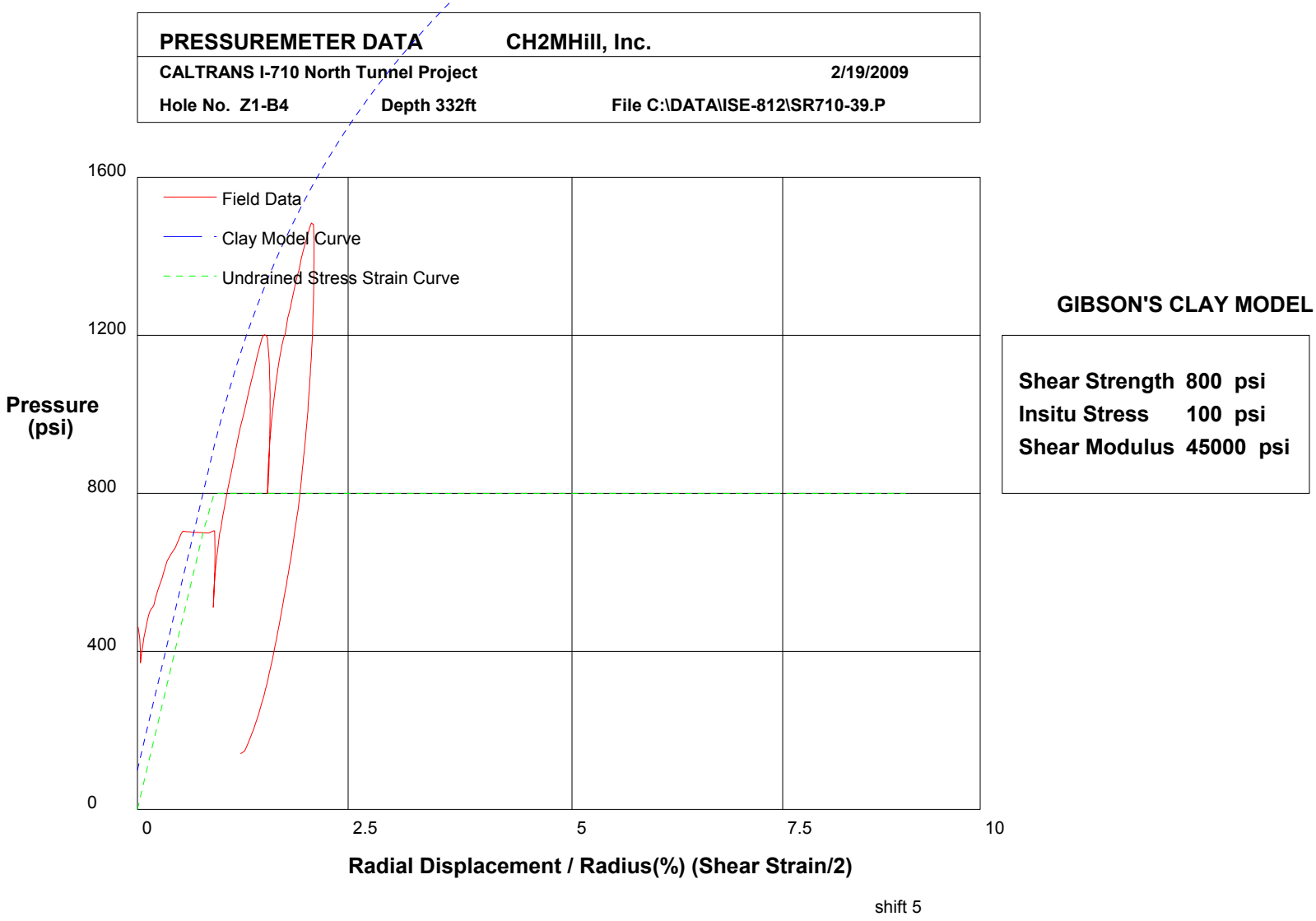

Appendix II - Pressuremeter Model Interpretation

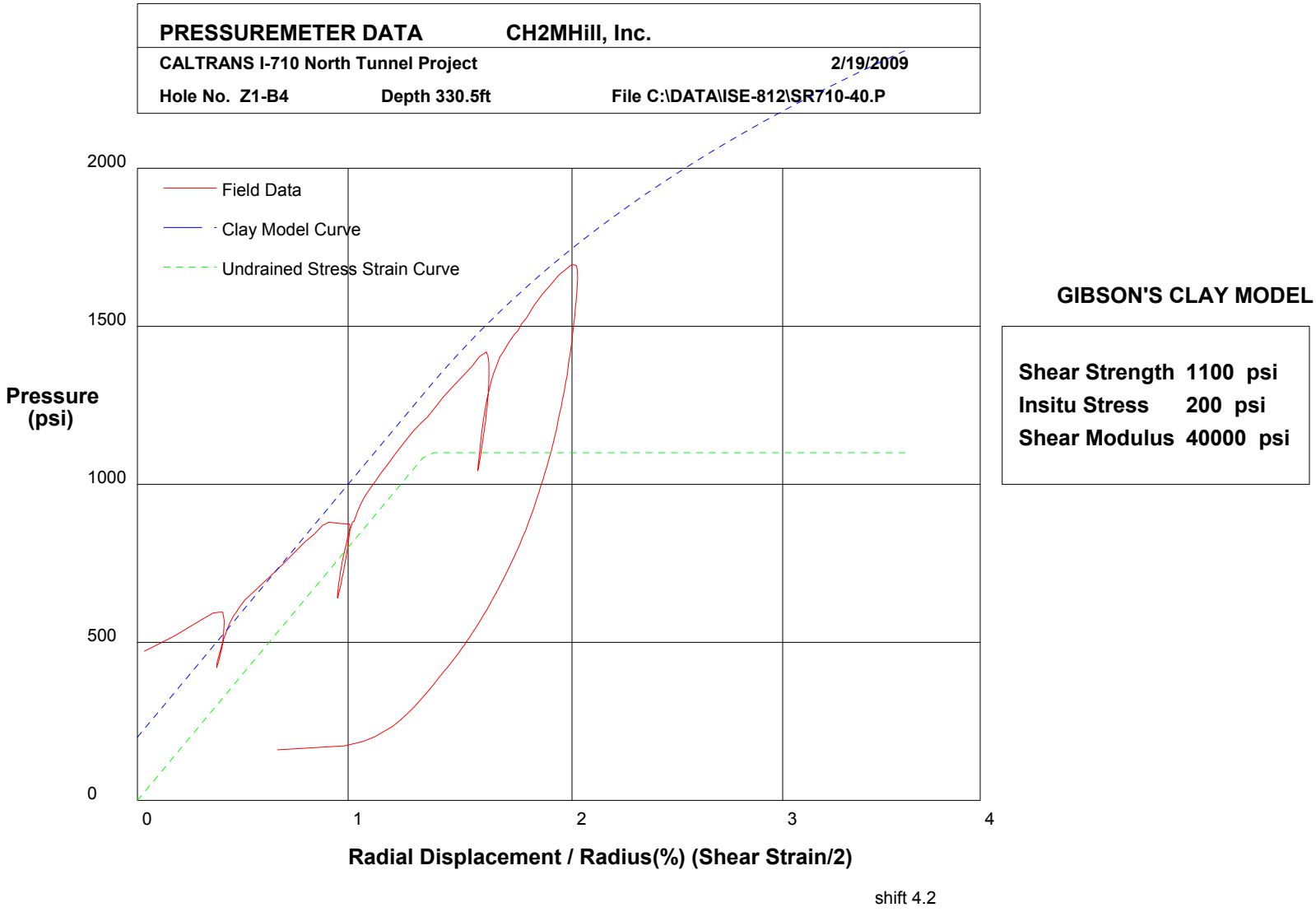

Appendix II - Pressuremeter Model Interpretation

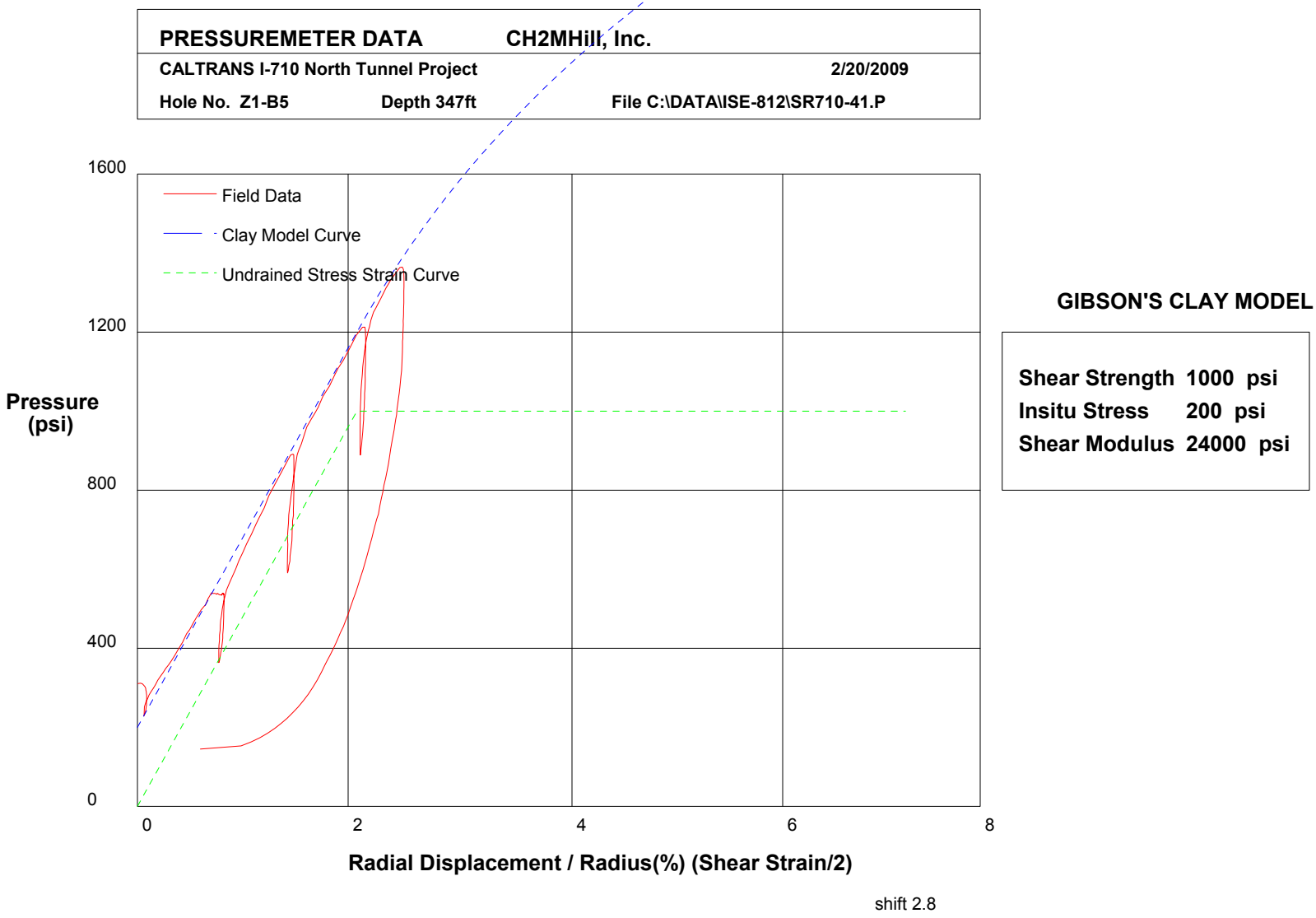

Appendix II - Pressuremeter Model Interpretation

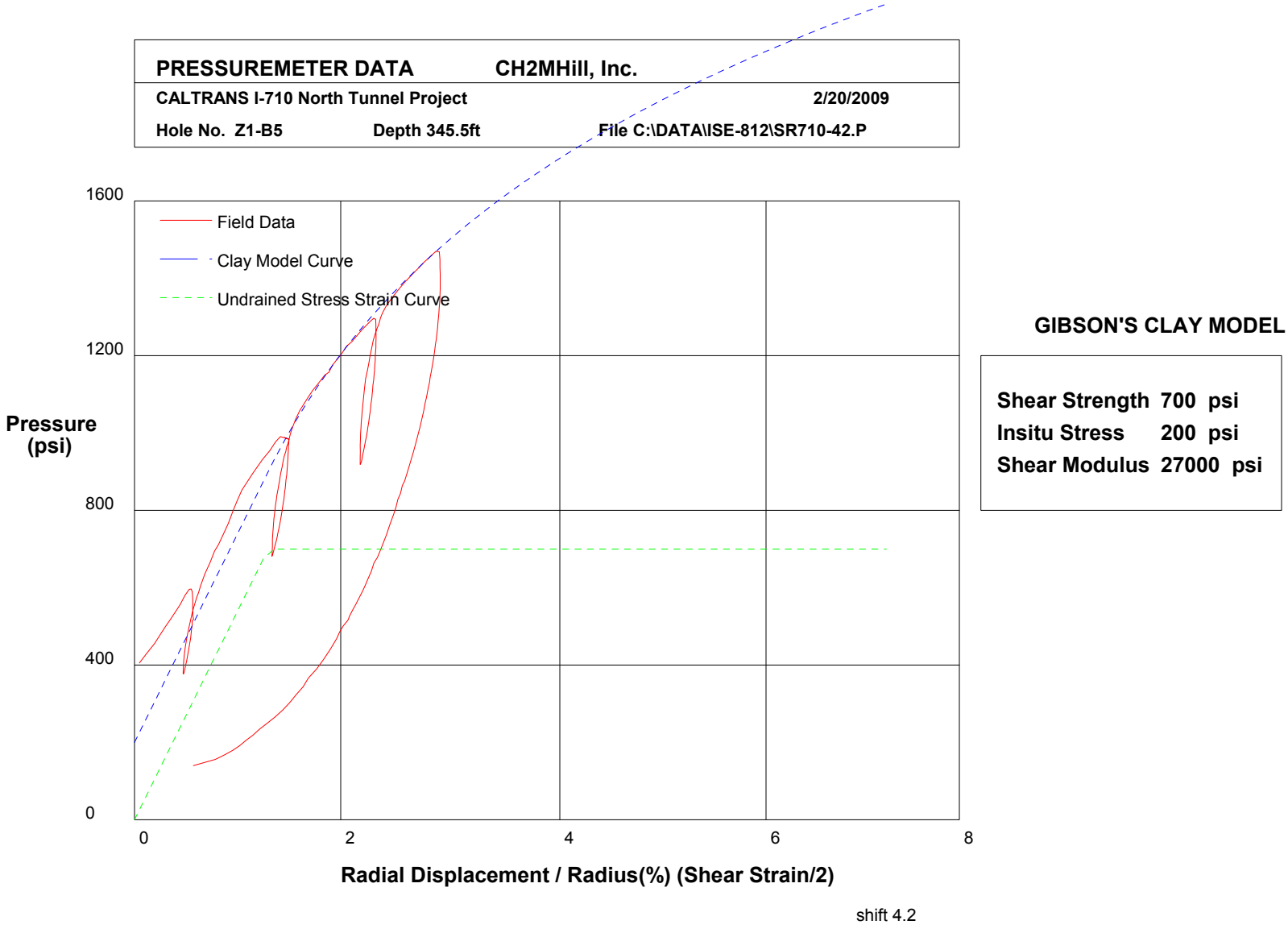

Appendix II - Pressuremeter Model Interpretation

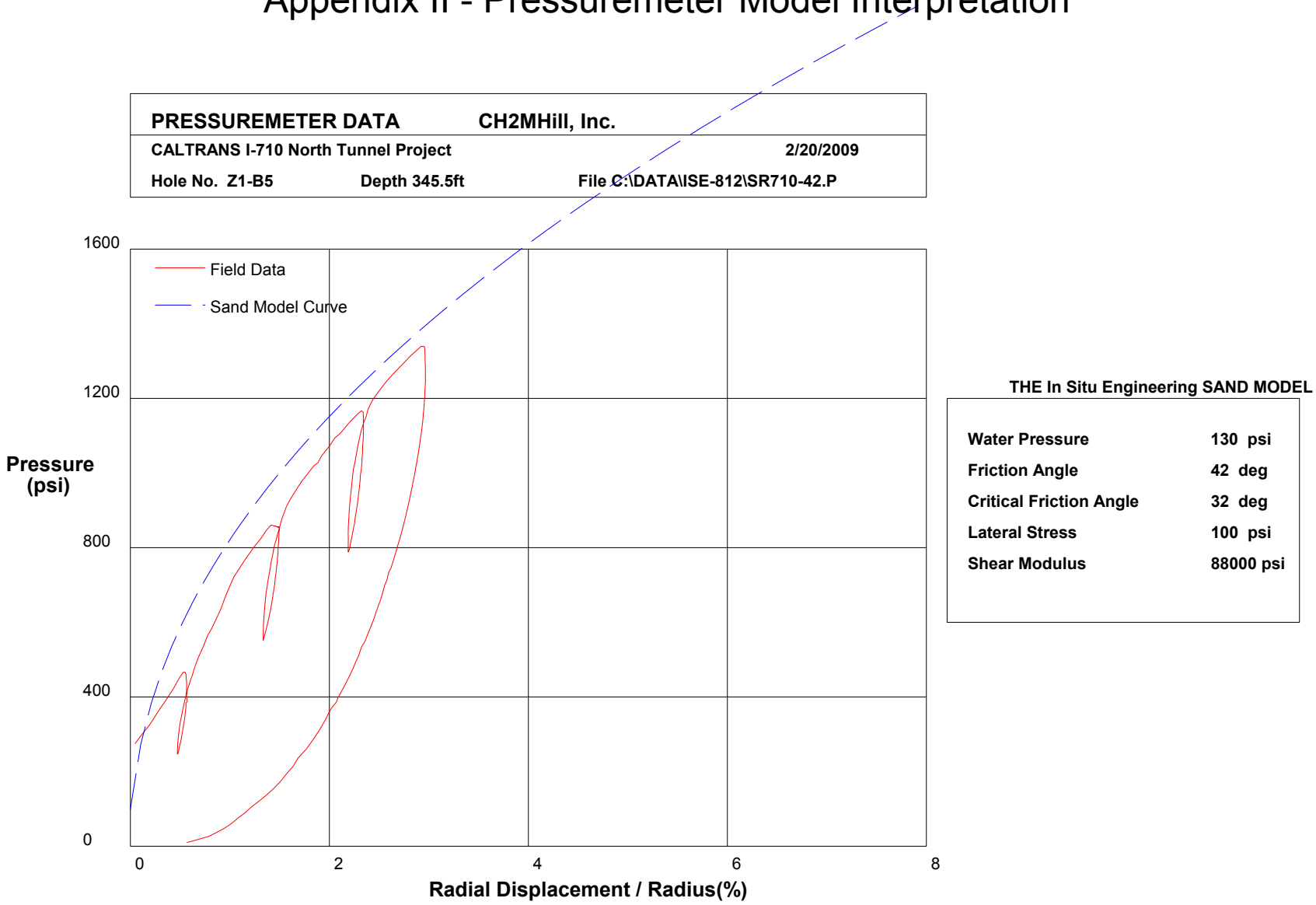

Appendix II - Pressuremeter Model Interpretation

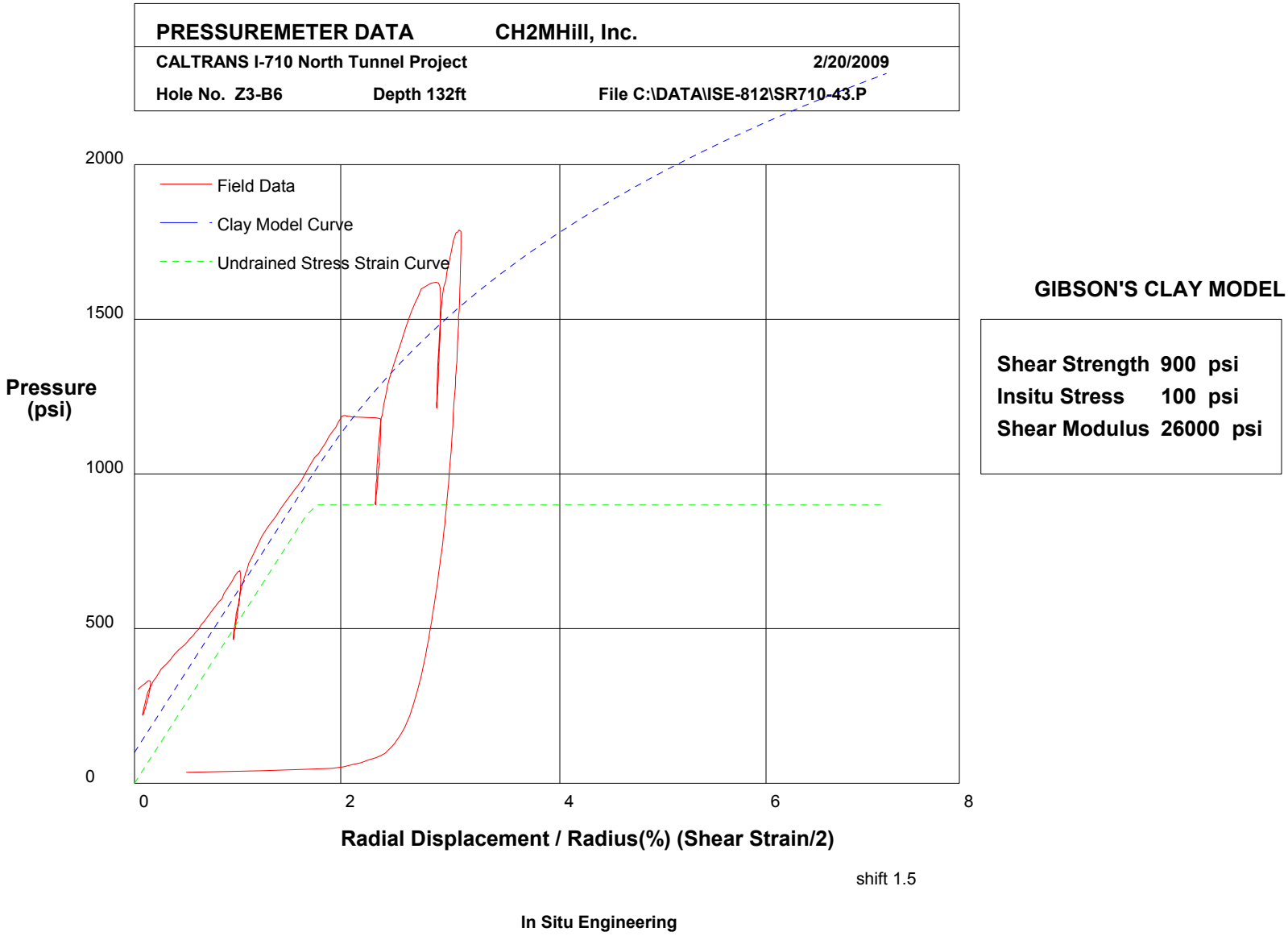

Appendix II - Pressuremeter Model Interpretation

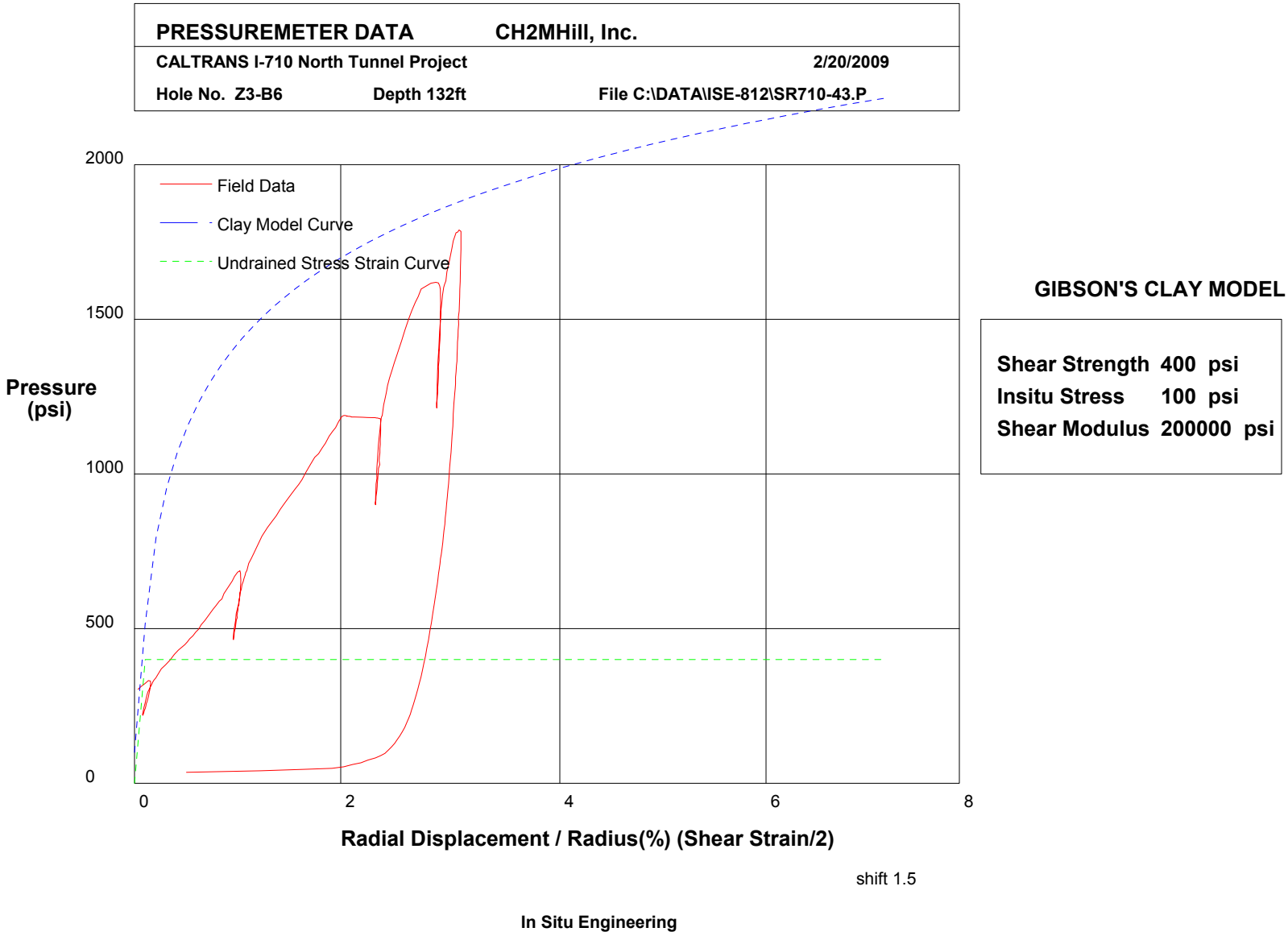

Appendix II - Pressuremeter Model Interpretation

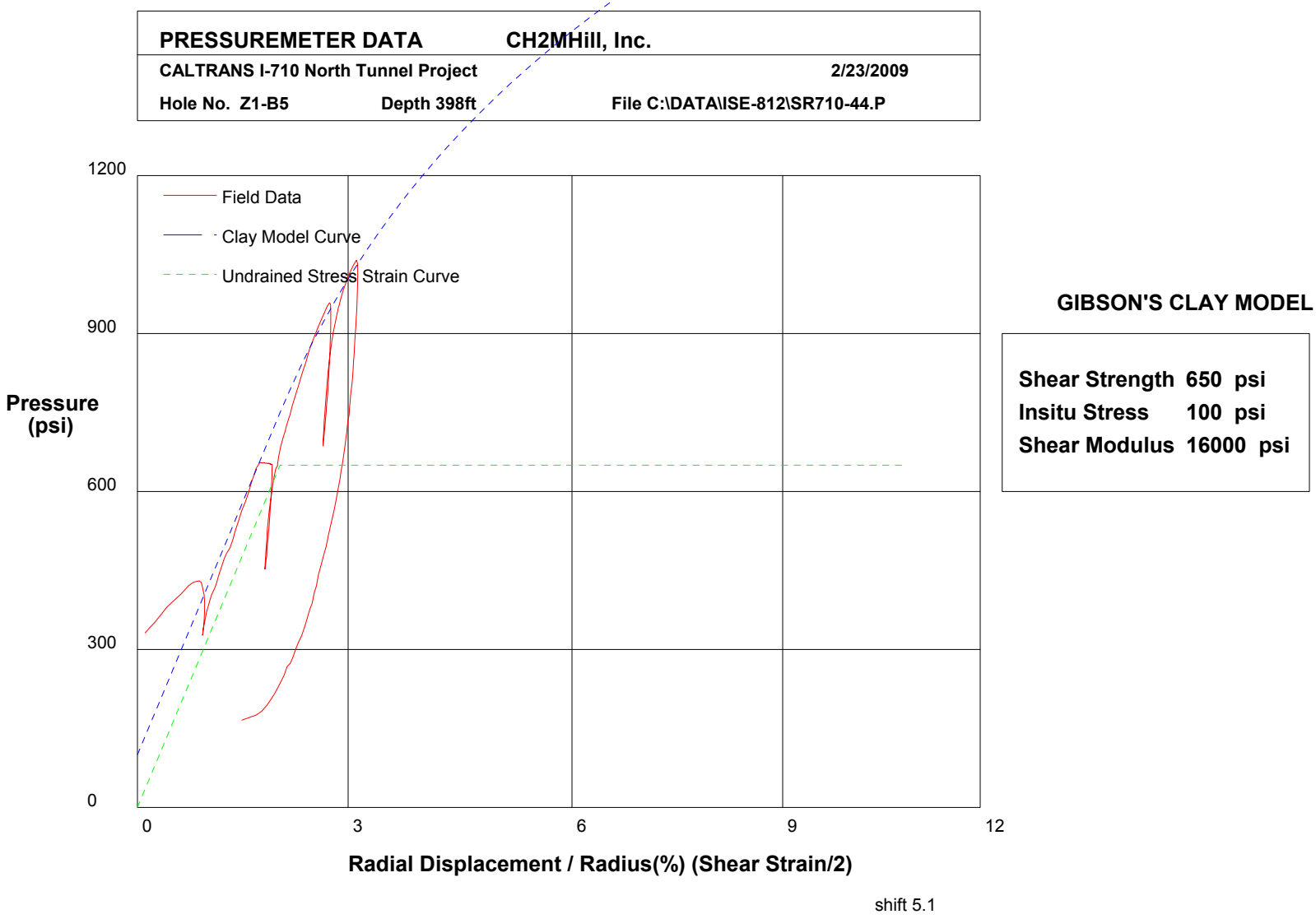

Appendix II - Pressuremeter Model Interpretation

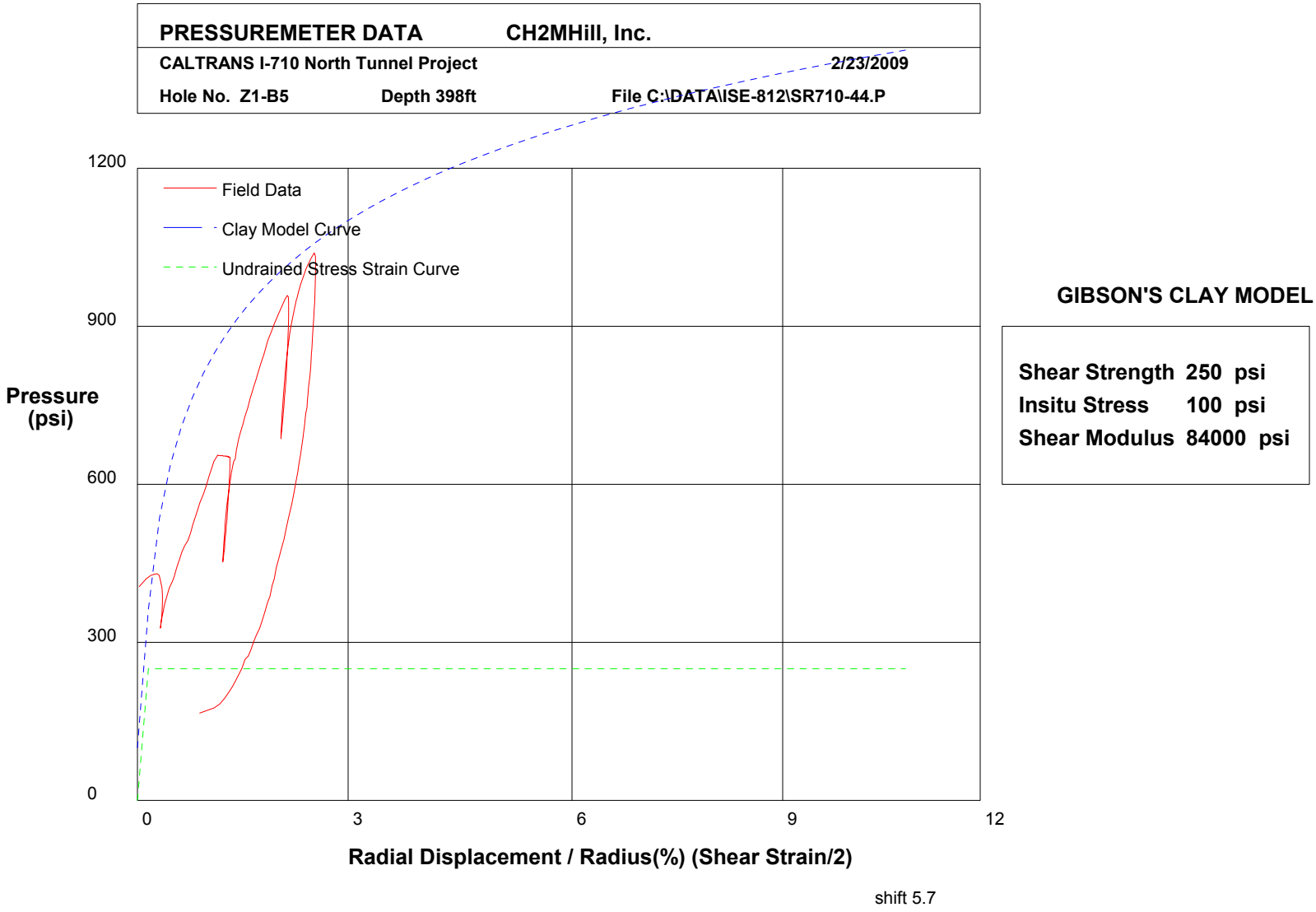

Appendix II - Pressuremeter Model Interpretation

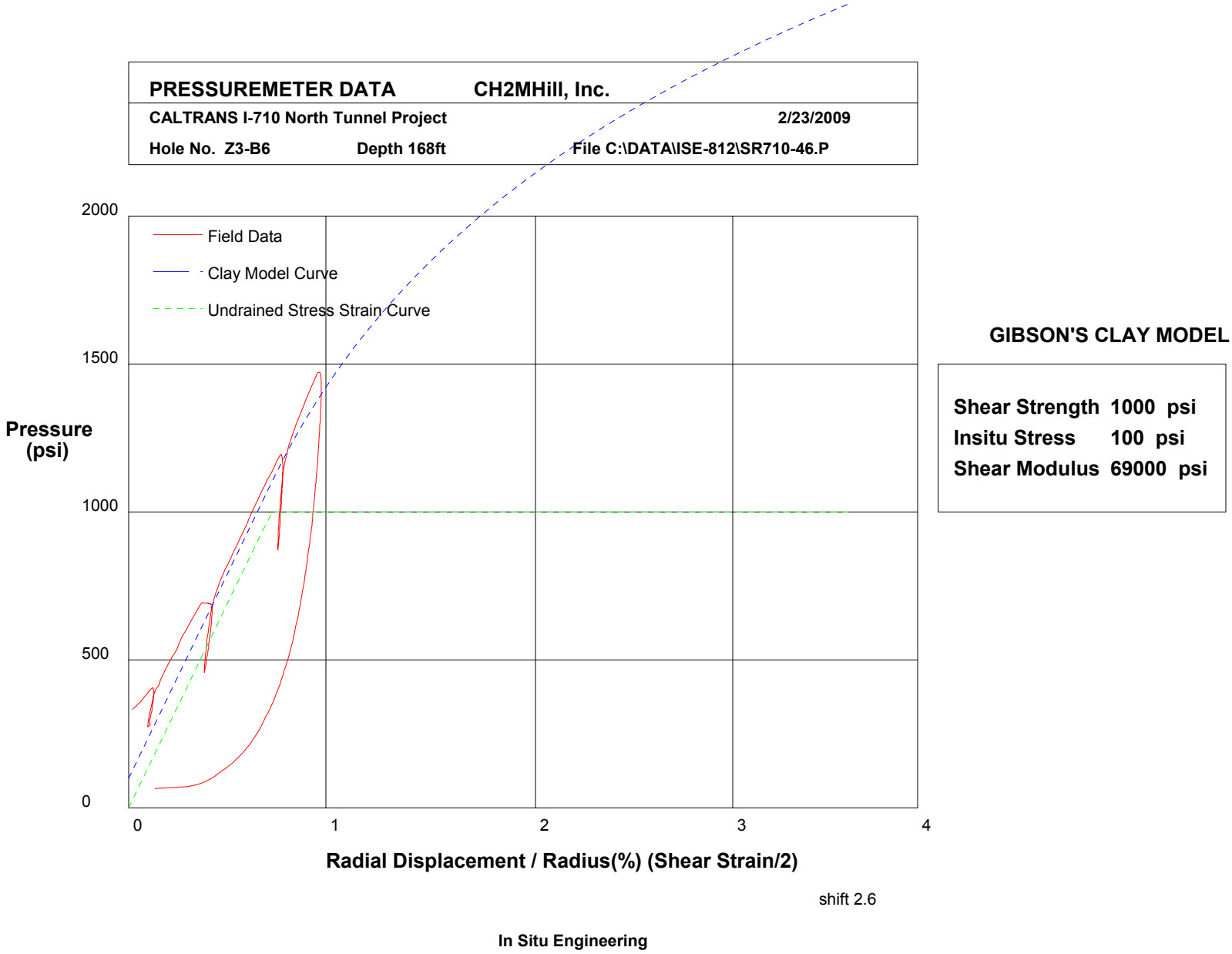

Appendix II - Pressuremeter Model Interpretation

PRESSUREMETER DATA **CH2MHill, Inc.**

CALTRANS I-710 North Tunnel Project **2/23/2009**

Hole No. Z3-B6 **Depth 168ft** **File C:\DATA\ISE-812\SR710-46.P**

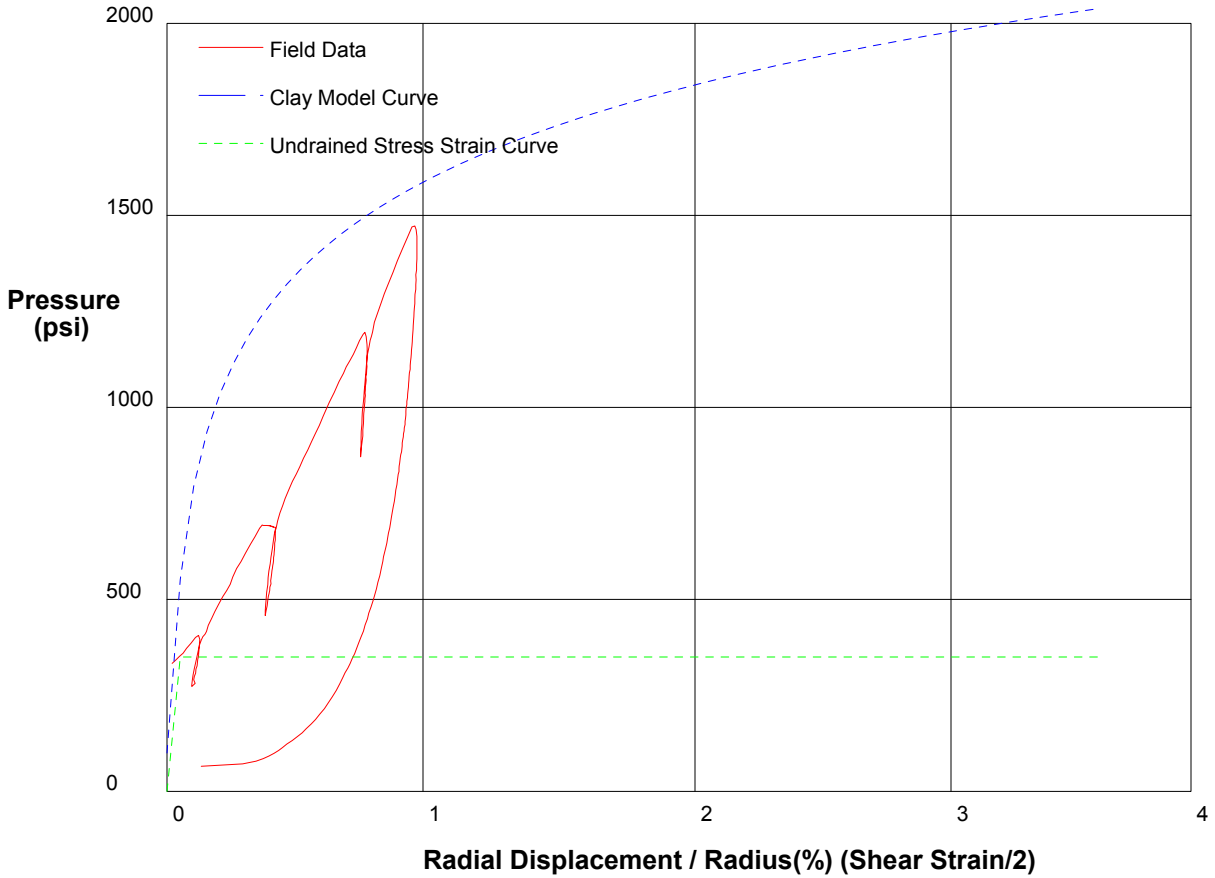

GIBSON'S CLAY MODEL

Shear Strength	**350 psi**
Insitu Stress	**100 psi**
Shear Modulus	**450000 psi**

shift 2.6

In Situ Engineering

Appendix II - Pressuremeter Model Interpretation

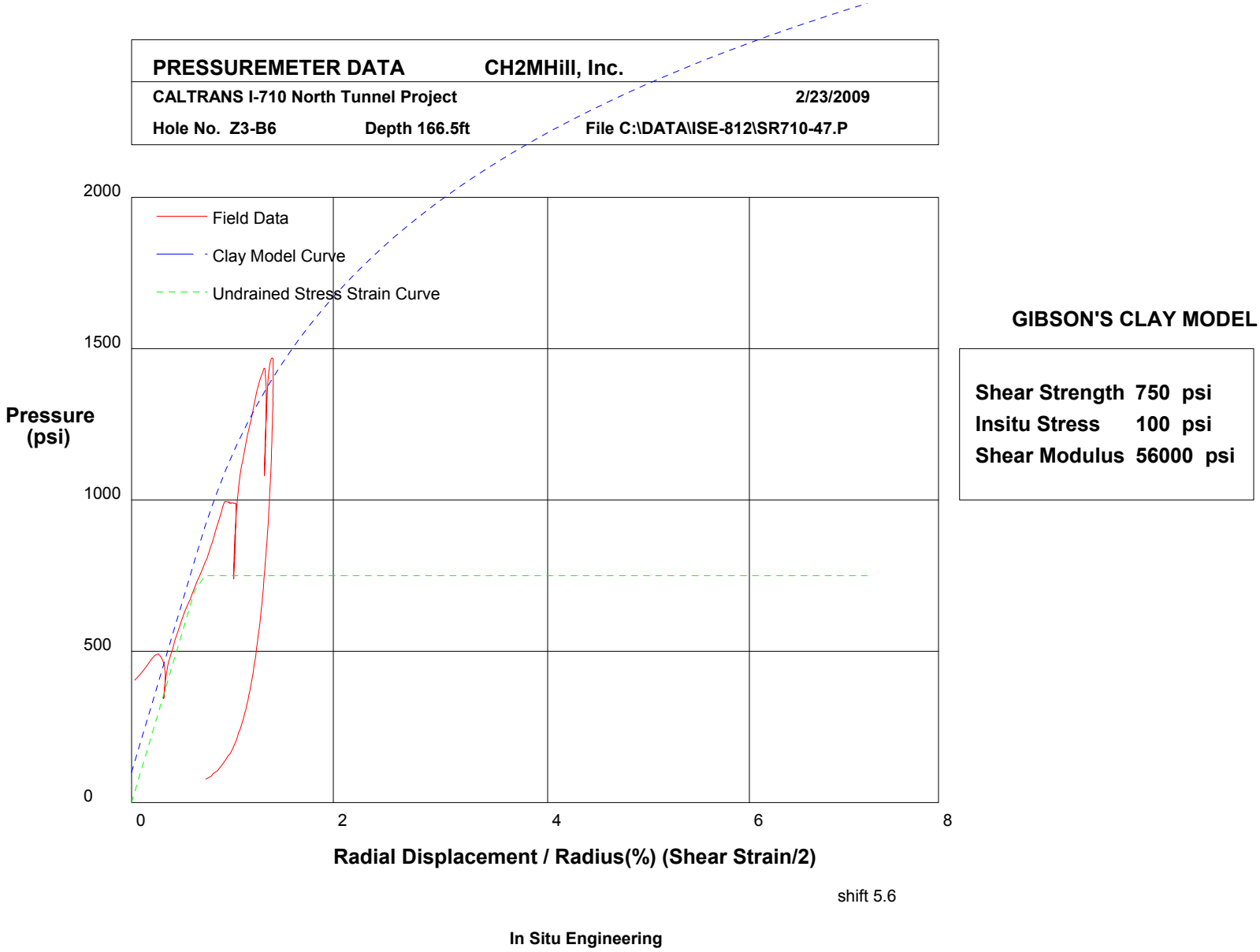

Appendix II - Pressuremeter Model Interpretation

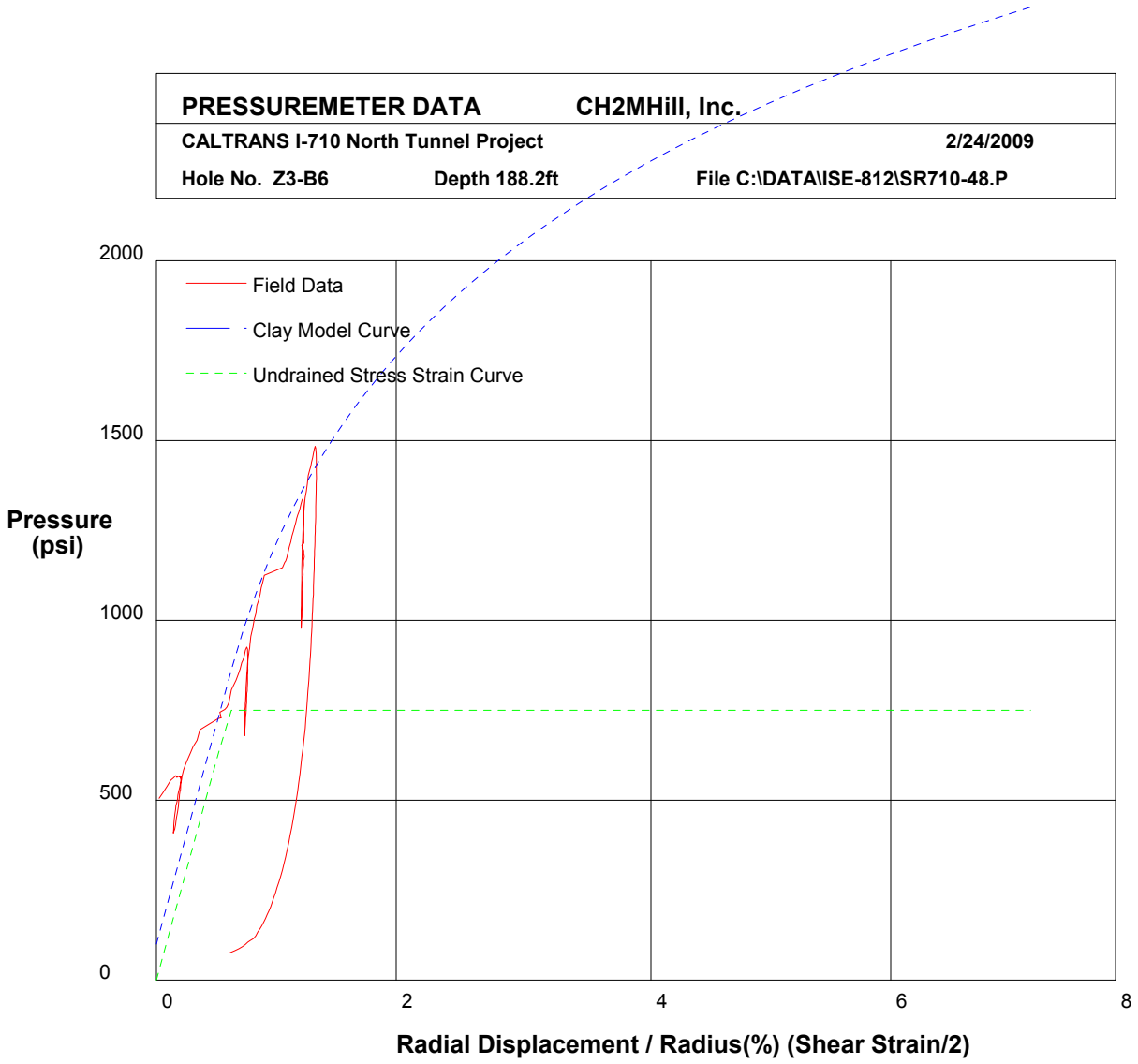

GIBSON'S CLAY MODEL

Shear Strength	**750 psi**
Insitu Stress	**100 psi**
Shear Modulus	**61000 psi**

In Situ Engineering
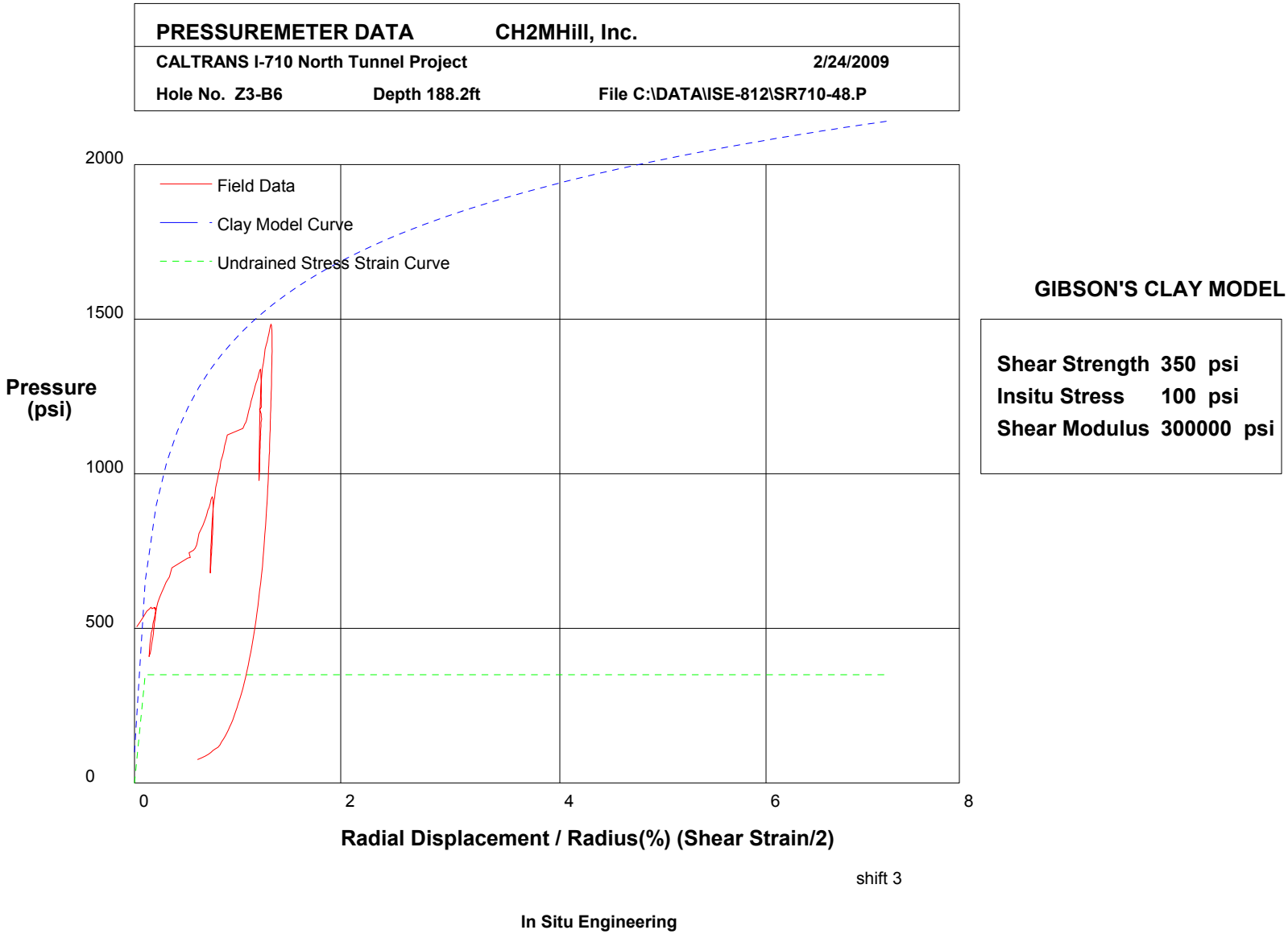
Appendix II - Pressuremeter Model Interpretation